## ABSTRACTS OF THE THIRTIETH ANNUAL MIDWINTER RESEARCH MEETING

## ASSOCIATION FOR RESEARCH IN OTOLARYNGOLOGY



February 10-15, 2007

The Hyatt Regency Denver Denver, Colorado, USA

# Abstracts of the Thirtieth Annual MidWinter Research Meeting of the

### ${f A}_{ m ssociation}$ for

Research in

Otolaryngology

February 10-15, 2007

Denver, Colorado, USA

Peter A. Santi, Ph.D.

Editor

Association for Research in Otolaryngology 19 Mantua Road, Mt. Royal, NJ 08061 USA

ARO Abstracts Volume 30, 2007

#### **CONFERENCE OBJECTIVES**

After attending the Scientific Meeting participants should be better able to:

- Understand current concepts of the function of normal and diseased ears and other head and neck structures.
- Understand current controversies in research methods and findings that bear on this understanding.
- Understand what are considered to be the key research questions and promising areas of research in otolaryngology.

#### ISSN-0742-3152

The Abstracts of the Association for Research in Otolaryngology is published annually and consists of abstracts presented at the Annual MidWinter Research Meeting. A limited number of copies of this CD and previous books of abstracts (1978-2006) are available.

Please address your order or inquiry to:
Association for Research in Otolaryngology
19 Mantua Road
Mt. Royal, NJ 08061 USA

General Inquiry
Phone (856) 423-0041 Fax (856) 423-3420
E-Mail: headquarters@aro.org

Meetings E-Mail: meetings@aro.org

This book was prepared from abstracts that were entered electronically by the authors. Authors submitted abstracts over the World Wide Web using Mira Digital Publishing's PaperCutterTM Online Abstract Management System. Any mistakes in spelling and grammar in the abstracts are the responsibility of the authors. The Program Committee performed the difficult task of reviewing and organizing the abstracts into sessions. The Program Committee Chair, Dr. John Middlebrooks and the President, Dr. Robert V. Shannon constructed the final program. Mira electronically scheduled the abstracts and prepared Adobe Acrobat pdf files of the Program and Abstract Books. These abstracts and previous years' abstracts are available at: http://www.aro.org.

Citation of these abstracts in publications should be as follows: Authors, year, title, Assoc. Res. Otolaryngol. Abs.: page number.

For Example:

Young, Eric, 2007, Circuits and Signal Representations in the Auditory System, Assoc. Res. Otolaryngol. Abs.: **687.** 



#### General Chair

#### Robert V. Shannon, PhD (2006-2007)

Program Organizing Committee

John C. Middlebrooks, PhD, Chair (2005-2008)

John P. Carey, MD (2004-2007)

David P. Corey, PhD (2006-2009)

J. David Dickman, PhD (2005-2008)

Robert Frisina, PhD (2006-2009)

Andrew K. Groves, PhD (2004-2007)

Leonard Kitzes, PhD (2004-2007)

Sharon G. Kujawa, PhD (2005-2008)

Sandra McFadden, PhD (2006-2009)

Joseph R. Santos-Sacchi, PhD (2004-2007)

Karen Steel, PhD (2004-2007)

Xiaoqin Wang, PhD (2005-2008)

Tom C.T. Yin, PhD (2005-2008)

John C. Middlebrooks, PhD, Council Liaison (2006-2007)

Program Publications

Peter A. Santi, PhD, Editor (2000-2009)

Animal Research

Jo Ann D. McGee, PhD, Chair (2001-2007)
Michael Church, PhD (2003-2007)
Elisabeth Glowatzki (2005-2008)
Michael Anne Gratton, PhD (2006-2009)
Cornelis Jan Kros, MD, PhD (2006-2009)
Charles A. Miller, PhD (2006-2009)
Paul Popper, PhD (2005-2008)
Edward J. Walsh, PhD (2006-2009)

Award of Merit Committee

Donata Oertel, PhD, Chair (2006-2009)
Ruth Anne Eatock, PhD (2004-2007)
Robert A. Dobie, MD (2006-2009)
Broyna J. B. Keats, PhD (2004-2007)
Alan R. Palmer, PhD (2004-2007)
William S. Rhode, PhD (2005-2008)
Murray B. Sachs, PhD (2005-2008)
Historian David J. Lim, MD, Council Liaison (2006-2007)

Diversity & Minority Affairs

Vishakha W. Rawool, PhD, Chair (2006-2007)

Henry J. Adler, PhD (2003-2007)

David Z.Z. He, MD, PhD (2006-2009)

Lina A. Reiss, PhD (2006-2009)

Barbara G. Shinn-Cunningham, PhD (2006-2009)

Duane Simmons, PhD (2003-2007)

Ebenezer Nketia Yamoah, PhD (2006-2009) Douglas A. Cotanche, PhD, Council Liaison (2006-2007)

Editor Advisory

Peter A. Santi, PhD, Chair (2000-2009) Gerald Popelka, PhD, Past Editor John C. Middlebrooks, PhD, Program Committee Chair Darla M. Dobson, Executive Director

Education Committee

Alan G. Micco, MD Chair (2005-2008)
Ann Eddins, PhD, Co-Chair (2006-2009)
David J. Brown, MD (2005-2008)
David M. Harris, PhD (2006-2009)
Timothy E. Hullar, MD (2005-2008)
Neil Segil, PhD (2006-2009)
Robert Wickesberg, PhD (2003-2007)
John C. Middlebrooks, PhD, Council Liaison (2006-2007)

Government Relations Committee

Ilsa R. Schwartz, PhD, Chair (2003-2007)

Marian J. Drescher, PhD (2006-2009)

Gay R. Holstein, PhD (2005-2008)

Walt Jesteadt, PhD (2006-2009)

Richard T. Miyamoto, MD (2005-2008)

Jay T. Rubinstein, MD, PhD (2005-2008)

Nigel K. Woolf, ScD (2006-2009)

David J. Lim, MD, Council Liaison, ex officio (2006-2007)

Graduate Student Travel Awards

Douglas A. Cotanche, PhD, *Chair* (2002-2007)
Paul J. Abbas, PhD (2006-2009)
Deniz Baskent, PhD (2006-2009)
Janet L. Cyr, PhD (2006-2009)
Suhua Sha, MD (2006-2009)

Douglas A. Cotanche, PhD, Council Liaison (2006-2007)

#### International Committee

Karen B. Avraham, PhD Chair (2005-2008)
Lin Chen, PhD, China (2006-2009)
Chunfu Dai, MD, PhD, China (2005-2008)
Bernhard Gaese, PhD, Germany, (2005-2008)
Timo Petteri Hirvonen, MD, PhD, Finland (2005-2008)
Philip X. Joris, MD, PhD, Belgium (2006-2009)
Glenis R. Long, PhD, USA (2006-2009)
David McAlpine, United Kingdom (2006-2009)
HongJu Park, MD, Korea (2005-2008)
Nicolas Perez, MD, Spain (2005-2008)
Hiroshi Wada, PhD, Japan (2004-2007)
Shu Hui Wu, MD, Canada (2005-2008)
Karen B. Avraham, PhD, Council Liaison (2006-2007)

#### JARO Editorial Board

Ruth Anne Eatock, PhD, Editor-in-Chief (2011)
J. David Dickman, PhD (2009)
Paul A. Fuchs, PhD (2009)
Matthew C. Holley, PhD (2007)
Gary D. Housley, PhD (2007)
Marci M. Lesperance, MD (2009)
Paul B. Manis, PhD (2009)
Teresa A. Nicolson, PhD (2009)
Andrew J. Oxenham, PhD (2009)
Jay T. Rubinstein, Md, PhD (2007)
Mario A. Ruggero, PhD (2007)
Alec N. Salt, PhD (2009)
Terry T. Takahashi, PhD (2009)
Tom C. T. Yin, PhD (2007)
Fan-Gang Zeng, PhD (2009)

JARO (Publications Committee)

Gerald R. Popelka, PhD, Co-Chair (2004-2007) Arthur N. Popper, PhD, Co-Chair (2004-2007) Monita Chatterjee, PhD (2006-2009) Richard A. Chole, MD, PhD (2005-2008) Charley C. Della Santina, MD, PhD (2004-2007) Richard R. Fay, PhD (2004-2007) Donna M. Fekete, PhD (2006-2009) Keiko Hirose, MD (2004-2007) Marlies Knipper, PhD (2004-2007) Christine Koeppl (2006-2009) Jian-Dong Li, MD, PhD (2005-2008) John Oghalai, MD (2004-2007) Edwin W. Rubel, PhD (2004-2007) Debara L. Tucci, MD (2006-2009) Ebenezer Nketia Yamoah, PhD (2004-2007) Ruth Anne Eatock, PhD, JARO Editor, ex officio Jasmine Ben-Zvi, Springer Representative, ex officio

Peter A. Santi, PhD (2006-2007), Council Liaison

Long Range Planning Committee
Robin L. Davis, PhD Chair (2005-2008)
Barbara Canlon, PhD (2005-2008)
Judy R. Dubno, PhD (2004-2007)
Paul A. Fuchs, PhD (2005-2008)
Steven H. Green, PhD (2005-2008)
Manuel S. Malmierca, MD, (2006-2009)
J. Christopher Post, MD, PhD (2005-2008)
Yehoash Raphael, PhD (2006-2009)
Dan H. Sanes, PhD (2006-2009)
Donna S. Whitlon, PhD (2006-2009)
Amy Donahue, PhD - NIDCD Rep.
P. Ashley Wackym, MD Council Liaison (2006-2007)
Karen B. Avraham, PhD, Chair, International Cmte (2005-2008)

#### Media Relations

Lawrence R. Lustig, MD, Chair (2005-2008)
Ben Bonham, PhD (2006-2009)
Judy Dubno, PhD (2003-2007)
Anil Lalwani, MD (2003-2007)
Daniel J. Lee, MD (2005-2008)
Susan E. Shore, PhD (2003-2007)
Ana Elena Vazquez, PhD (2006-2009)
Edward J. Walsh, PhD (2003-2007)
John Williams, Ex officio AAO-HNS Dir. Congr Rel
Steven Rauch, MD, Council Liaison (2005-2007)

#### Membership Committee

Karen Jo Doyle, *Chair* (2006-2009)
Paul Abbas, PhD (2003-2007)
Jennifer J. Lister (2006-2009)
Diana Lurie, PhD (2003-2007)
Virginia M. Richards, PhD (2006-2009)
Tatsuya Yamasoba, MD, PhD (2006-2009)

#### Nominating Committee

Lloyd B. Minor, MD, Chair (2006-2007) Jay M. Goldberg, PhD, (2006-2007) Donata Oertel, PhD (2006-2007) Donna S. Whitlon, PhD (2006-2007) Eric D. Young, PhD (2006-2007)

Patient Advocacy Group Relations
Charles J. Limb, MD, Chair (2006-2009)
Helen Cohen, EdD (2003-2007)
Sandra Gordon-Salant, PhD (2006-2009)
Kim Gottshall, PhD (2003-2007)
Margaret Kenna, MD (2003-2007)
J. Tilak Ratnanather (2005-2008)
Peter S. Steyger, PhD (2006-2009)
Susan L. Whitney, PhD, PT (2006-2009)
Steven Rauch, MD, Council Liaison (2006-2007)

#### Physician Research Training

David R. Friedland, MD, PhD, Chair (2005-2008)
Marc Coltrera, MD (2003-2007)
Diane Durham, PhD (2003-2007)
Timothy E. Hullar, PhD (2006-2009)
Charles J. Limb, MD (2006-2009)
Saumil N. Merchant, MD (2005-2008)
Yael Raz (2005-2008)
Claus-Peter Richter, MD, PhD (2005-2008)
James F. Battey, MD, PhD, NIDCD Director ex-officio
Maureen Hannley, PhD, Exec VP Rsch, ex-officio
P. Ashley Wackym, MD, Council Liaison (2006-2007)

Research Forum Co-Chairs John S. Oghalai, MD (2005-2008) J. Christopher Post, MD (2004-2007)

#### **President's Message**

Welcome to the mile high city of Denver, Colorado for the 30<sup>th</sup> Annual MidWinter Meeting of the Association for Research in Otolaryngology. This is the first time we've been landlocked for the February meeting; we've moved from the west coast to the east coast of Florida, from the Mississippi delta to Chesapeake Bay. Hopefully, Denver won't be as cold as Baltimore was last year. Denver is a pleasant city with easy access to winter sports activities (hopefully, snowboarding and ski-lodge related injuries will be minimal). The Hyatt Hotel is an excellent facility: it is less that one year old with terrific meeting space and great



views of the city and mountains. Be sure to visit the many shops and restaurants in the LODO district (LOwer DOwntown) and Larimer Square, as well as the new, Daniel Libeskind designed wing of the Denver Art Museum, all within walking distance of the hotel.

Thanks to the good response from our members, we have scheduled many interesting and innovative symposia, including: Neurobiology of Vocal Communication: Beyond Acoustic Features, Specification of the Auditory and Vestibular Hindbrain, Wnt Signaling Pathways and Inner Ear Development, Spatial and Binaural Hearing: Perception and Physiology, Beyond Cochlear Implants: Functional Stimulation and Recording in the Auditory Nervous System, and Ion Transport in the Stria Vascularis: Modeling and Experiment. The short course presented Saturday evening will be Translational Research in Otolaryngology. The presidential symposium on Sunday morning is titled: Ear and Brain: Hearing beyond the Cochlea.

The ARO continues to search for a new meeting venue that will maintain the excellent scientific and social experience of meetings past. Under the constraints of the present economy, the ARO Council and Management Team are working hard to find affordable venues in attractive locations. You may not be aware of the behind-the-scene efforts needed to arrange the MidWinter meeting and run the organization, but thanks are certainly due to the ARO council and to the Talley Management Group for their excellent work in organizing the Denver meeting. In particular, we applaud the hard work of John Middlebrooks (serving double duty as Council member and Program Organizing Committee Chair) and Lisa Astorga (Meeting Coordinator).

This year we have been able to continue to offer travel awards to research trainees, thanks to generous donations from the AAO, DRF, and AAA/AAAF. These funds allow for an important function of the MidWinter meeting: introducing young people to the network of scientists and researchers of the ARO. Young researchers are vital to the health of the organization, as "new blood" invigorates both the scientific and social interactions made possible by the meeting. I vividly remember (well, maybe not vividly) my first scientific meeting and the impact it had on my career (of which the

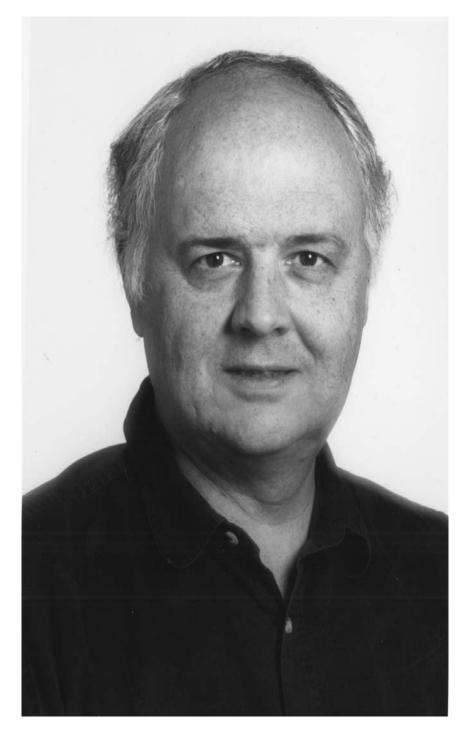
tequila-fueled barn-burners were no small part). We welcome all new attendees and look forward to their ongoing participation in the ARO.

Speaking of "young" researchers, Eric Young has been selected to receive the Award of Merit this year. The title of Eric's Presidential Lecture will be <u>Circuits and Signal Representations in the Auditory System</u>. Many former students and colleagues will participate in this tribute to Eric and his great influence on auditory neuroscience.

Ruth Anne Eatock has assumed editorship of the JARO, while simultaneously moving to a new institution (she is now at the Eaton-Peabody laboratory and the Department of Otology and Laryngology, Harvard Medical School). Anyone who has ever relocated their research lab knows the extra effort required to establish yourself in a new institution. The fact that Ruth Anne has also taken on the JARO editorship deserves our admiration for her commitment to public service.

I expect we will have another fun and productive MidWinter meeting. Attendance and membership in the ARO has remained strong over recent years, despite the difficulties associated with venue changes. The number of registrants and submitted abstracts has been stable over the last 5 years. As the MidWinter Meeting moves to new locations in the future, members remain strongly committed to the meeting and to the organization. It's clear that the ARO is much more than an organization - it's a true community of science. I feel fortunate and look forward to "brainstorming" with colleagues, meeting new people, and relaxing with old friends in Denver.

#### **Bob Shannon**



Eric D. Young, PhD 2007 Award of Merit Recipient

### Eric D. Young, PhD 2006 Recipient of the Award of Merit

The 2007 Award of Merit will be given to Eric D. Young in recognition of his many seminal contributions to our understanding of how the brain enables us to perceive sounds. In many ways Eric's approach to research has set the standard for hearing research throughout the world. Educated with extraordinary depth in engineering, computation and biology, Eric has time and again demonstrated the value of truly integrated experimental and theoretical studies of the nervous system. Eric possesses an unusually independent spirit. He has never hesitated to venture into new territory, whether to adopt new experimental paradigms or cutting edge theoretical constructs.

The source of this independence is undoubtedly to be found in Eric's youth on his family ranch, the Bar-L in Elko, Nevada. By the time he was 12, he was driving hav-cutting machinery as his summer vacation activity. However, early on Eric knew that he was not meant to be a cattle rancher and by the time he reached high school had discovered what would become a life-long passion - building and programming computers. The computer skills he developed at an early age have made him a world leader in innovative neurophysiological data gathering and analysis. Eric left the ranch to study engineering at Caltech where he received his BS in 1967. Having met and married Pamela Perkins, Eric ventured to the East Coast where he earned his PhD in Biomedical Engineering from His thesis, "Recovery from Sound Exposure—A Johns Hopkins in 1972. Comparison of Psychophysics and Physiology" was the first study in what would become one theme in Eric's research career, namely model-driven explorations discharge relationship between auditory-nerve psychophysical performance. Eric's postdoctoral fellowship took him to Jay Goldberg's lab at the University of Chicago in 1972, where he launched his second major research thrust: to understand the function of the dorsal cochlear nucleus. Johns Hopkins was fortunate to be able to convince Eric to return to He is currently Professor of Biomedical Engineering, Baltimore in 1975. Neuroscience and Otolaryngology/Head and Neck Surgery.

Since his postdoctoral days, Eric has led an effort to understand the role of the dorsal cochlear nucleus (DCN) in hearing; he and his colleagues have made a strong case that one of the roles of the DCN is to enable mammals to use spectral cues to localize sound sources. Elegant, direct experimental approaches together with rigorous analyses yield answers to a beautifully logical series of questions. It is revealing to review how the findings unfolded over the past thirty years, both for what has been learned about the DCN and for what it reflects about how a very fine scientist formulated a logical series of questions and developed approaches to address them.

Eric's first paper about the DCN was published in 1976 with Bill Brownell, describing his postdoctoral work. The immediate impetus was a 1973 paper by

Ted Evans and Phil Nelson, who found that anesthesia greatly altered the properties of neurons in the DCN. Accordingly, Eric and Bill decided to work in decerebrate cats. Probing single unit responses with tones and noise revealed consistent patterns. While type II/III units responded with excitation to tones and were unresponsive to broadband noise, type IV units were excited only at low levels and responded vigorously to noise.

The work continued after Eric returned to Hopkins. Which were the cells that produced these responses? He and his colleagues demonstrated that type IV units were principal cells because their axons could be stimulated from the output pathway of the DCN; some type II/III units (now called type II) could be driven antidromically from the ventral cochlear nucleus (VCN) but none could ever be driven by stimulation of the dorsal acoustic stria indicating that they were local neurons. Are these two neuronal types synaptically connected? Herb Voigt and Eric recorded from pairs of neurons in the DCN. The reciprocal response areas together with cross-correlation analysis left no doubt that type II units inhibit type IV units. What is the source of the inhibition that prevents type II units from responding to broadband noise? This question was addressed first by Bill Shofner and Young and revisited by Israel Nelken and Eric; broadly tuned inhibitory neurons in the VCN shape responses to broadband noise. By the 1990s, Eric and his postdoctoral colleagues, George Spirou, Kevin Davis, and Eli Nelken were able to account for all features of the responses of type II and type IV units to sound on the basis of their inputs.

Papers with George Spirou and Lina Reiss showed with startling clarity that type IV units are beautifully suited for encoding the presence of spectral notches, important spectral cues for localizing sounds. Eric recognized that responding to sounds is only a part of the DCN's job, reflecting only the processing carried out in the deep layer of the DCN. A separate system of inputs comes to the DCN through the granule cells in the superficial layer. Granule cells receive input from widespread regions of the brain, including a prominent input from the dorsal column nuclei. How do the dorsal column nuclei influence the principal cells of the DCN? Eric and his colleagues once again approached the question directly. Shocks to the dorsal column nuclei strongly inhibited type IV units. Biomedical Engineering graduate student Patrick Kanold Eric showed that much of the somatosensory information to the DCN reflects proprioceptive information about the pinna. These findings were attractive because information about the position of the pinna has to be taken into account for interpreting spectral cues. Eric's most recent work with Steve Chase addresses the question how information from the DCN is used at the next stage of the auditory pathway, the inferior colliculus.

While pursuing studies of the DCN, Eric managed also to devote a major effort aimed at understanding the relationship between stimulus encoding in the auditory nerve and human perception of complex stimuli like speech. This work first appeared in 1979 in two papers with one of the authors of this citation (MBS)

which demonstrated the power of the population method in which the responses to a stimulus are recorded from a large number of neurons and from these the responses of the whole auditory nerve are inferred. In a tour de force of data analysis, Eric showed how the spectrum of a speech stimulus might be represented in the detailed temporal patterns of auditory nerve discharges. For the past 25 years Eric and his colleagues have continued to detail the auditory nerve encoding of speech in a wide range of circumstances, including background noise and inner ear acoustic trauma. The results of these studies include the need for a reexamination of commonly held ideas about the neural correlates of loudness recruitment and suggestions for the design of new hearing aids based on models for signal processing in the impaired cochlea.

Eric's work is exceptional. In answering a logical series of questions, he has revealed much about how the auditory system works. His papers are a pleasure to read not only for their conclusions but because each is documented meticulously, and analyzed rigorously with sophisticated techniques. His papers are also exceptional in their scholarship. We cannot recall ever thinking that a relevant reference had been omitted. The rigor extends to the way conclusions are drawn in Eric's papers. It was only in the 1990s that his papers began to suggest that the DCN might play a role in making use of spectral cues. Even then, the suggestion served more to provide a framework than to inflate the significance of the work.

Eric is a superb teacher and mentor. For five years he directed the Hopkins Biomedical Engineering graduate Program and has been one of the most active and successful teachers in the Department of Biomedical Engineering. He has been a mentor to a generation of graduate students and postdoctoral fellows who have gone on to successful careers in auditory neuroscience, including Herb Voigt, John White, Kevin Franck, Patrick Kanold, Lina Reiss, Steve Chase, Bill Shofner, George Spirou, Israel Nelken, Roger Miller, Kevin Davis, Ian Bruce, and Michael Heinz.

Eric is also exceptional as a colleague and as an understated but authoritative scientific leader. At meetings it is a pleasure to see his tall frame rise from a seat or appear at a poster to ask a question. Those questions are penetrating, but not aggressive or personal, and they address central issues. They are questions one does not ignore.

For all of his exceptional contributions, Eric Young richly deserves the ARO Award of Merit. On behalf of his many friends and colleagues it is our privilege to congratulate him on this special recognition.

Murray Sachs Donata Oertel Jay Goldberg

#### **Association for Research in Otolaryngology**

Executive Offices 19 Mantua Road, Mt. Royal, NJ 08061 USA Phone: (856) 423-0041 Fax: (856) 423-3420 E-Mail: headquarters@aro.org

Meetings E-mail: meetings@aro.org

#### ARO Council Members 2006-2007

President: Robert V. Shannon, PhD Secretary/Treasurer: Steven Rauch

House Ear Institute Harvard Medical School

Auditory Implant Research Massachusetts Eye and Ear Infirmary

2100 West Third Street
Los Angeles, CA 90057

243 Charles Street
Boston, MA 02114

**President-Elect:** P. Ashley Wackym, MD **Editor:** Peter A. Santi, PhD

Medical College of WisconsinUniversity of MinnesotaDepartment of Otolaryngology &Department of OtolaryngologyCommunicative SciencesLions Research Bldg., Room 121

9000 West Wisconsin Avnenue 2001 Sixth St. SE Milwaukee, WI 53226 Minneapolis, MN 55455

Past President: Lloyd B. Minor, MD Historian: David J. Lim, MD

Johns Hopkins University School of Medicine House Ear Institute

Department of Otolaryngology 2100 W. Third St., Fifth Floor 601 North Caroline Street, Room 6253 Los Angeles, CA 90057

#### Council Members at Large

Douglas A. Cotanche, MD Karen P. Stee Lab for Cellular & Molecular Welcome Tru

Baltimore, MD 21287-0910

Hearing Research

Department of Otolaryngology & Communicative Sciences 300 Longwood Avenue

Boston, MA 02115

Karen P. Steel, PhD, FMed Welcome Trust Sanger Institute Wellcome Trust Genome

Campus Hinxton

Cambridge CB 10 1SA, UK

John C. Middlebrooks, PhD University of Michigan Kresge Hearing Research

Institute

1301 East Ann Street

Ann Arbor, MI 48109-0506

#### Association for Research in Otolaryngology

Executive Offices
19 Mantua Road, Mt. Royal, NJ 08061 USA
Phone: (856) 423-0041 Fax: (856) 423-3420

E-Mail: headquarters@aro.org Meetings E-mail: meetings@aro.org

#### **Past Presidents**

#### **Award of Merit Recipients**

1974-75   Jack Vernon, PhD   1975-76   Robert A. Butler, PhD   1980   Juergen Tonndorf, MD   1976-77   David J. Lim, MD   1981   Hallowell Davis, MD   1982   Hallowell Davis, MD   1983   Ernest Glen Wever, PhD   1980-81   Barbara Bohne, PhD   1984   Teruzo Konishi, MD   1981-82   Robert H. Mathog, MD   1985   Joseph Hawkins, PhD   1982-83   Josef M. Miller, PhD   1986   Raphel Lorente de Nó, MD   1983-84   Maxwell Abramson, MD   1987   Jerzy E. Rose, MD   1984-85   William C. Stebbins, PhD   1986   Robert J. Ruben, MD   1987   Jerzy E. Rose, MD   1987-86   Robert J. Ruben, MD   1998   Åke Flóck, PhD   1988-89   William A. Yost, PhD   1991   William D. Neff, PhD   1988-89   William A. Yost, PhD   1992   Jan Wersäll, PhD   1991-92   Jeffrey P. Harris, MD, PhD   1994-95   Allen F. Ryan, PhD   1995   Kirsten Osen, MD   1995-96   Bruce J. Gantz, MD   1997   Murray B. Sachs, PhD   1996-97   M. Charles Liberman, PhD   1997-98   Leonard P. Rybak, MD, PhD   1998-99   Edwin W. Rubel, PhD   2000-01   Judy R. Dubno, PhD   2001-02   Richard T. Miyamoto, MD   2002-03   Donata Oertel, PhD   2003-04   Edwin M. Monsell, MD, PhD   2004-05   William E. Brownell, PhD   2005-06   Lloyd B. Minor, MD   2005-06		David L. Hilding, MD	1978	Harold Schuknecht, MD
1976-77         David J. Lim, MD         1981         Catherine Smith, PhD           1977-78         Vicente Honrubia, MD         1982         Hallowell Davis, MD           1978-80         F. Owen Black, MD         1983         Ernest Glen Wever, PhD           1980-81         Barbara Bohne, PhD         1984         Teruzo Konishi, MD           1981-82         Robert H. Mathog, MD         1985         Joseph Hawkins, PhD           1982-83         Josef M. Miller, PhD         1986         Raphel Lorente de Nó, MD           1983-84         Maxwell Abramson, MD         1987         Jerzy E. Rose, MD           1984-85         William C. Stebbins, PhD         1988         Josef Zwislocki, PhD           1985-86         Robert J. Ruben, MD         1989         Åke Flóck, PhD           1987-88         George A. Gates, MD         1991         William D. Neff, PhD           1988-89         William A. Yost, PhD         1992         Jan Wersäll, PhD           1999-90         Joseph B. Nadol, Jr., MD         1993         Peter Dallos, PhD           1991-92         Jeffrey P. Harris, MD, PhD         1995         Kirsten Osen, MD           1992-93         Peter Dallos, PhD         1995         Ruediger Thalmann, MD & Isolde Thalmann, PhD           1993-94         Robe			1979	Merle Lawrence, PhD
1977-78         Vicente Honrubia, MD         1982         Hallowell Davis, MD           1978-80         F. Owen Black, MD         1983         Ernest Glen Wever, PhD           1980-81         Barbara Bohne, PhD         1984         Teruzo Konishi, MD           1981-82         Robert H. Mathog, MD         1985         Joseph Hawkins, PhD           1983-84         M. Miller, PhD         1986         Raphel Lorente de Nó, MD           1983-85         William C. Stebbins, PhD         1987         Jerzy E. Rose, MD           1984-85         William C. Stebbins, PhD         1988         Josef Zwislocki, PhD           1985-86         Robert J. Ruben, MD         1989         Åke Flóck, PhD           1987-87         George A. Gates, MD         1991         William D. Neff, PhD           1988-89         William A. Yost, PhD         1992         Jan Wersäll, PhD           1989-90         Joseph B. Nadol, Jr., MD         1993         David Lim, MD           1991-92         Jeffrey P. Harris, MD, PhD         1994         Peter Dallos, PhD           1992-93         Peter Dallos, PhD         1995         Kirsten Osen, MD           1993-94         Robert A. Dobie, MD         1997         Jay Goldberg, PhD           1994-95         Bruce J. Gantz, MD         1		,		
1978-80         F. Owen Black, MD         1983         Ernest Glen Wever, PhD           1980-81         Barbara Bohne, PhD         1984         Teruzo Konishi, MD           1981-82         Robert H. Mathog, MD         1985         Joseph Hawkins, PhD           1982-83         Josef M. Miller, PhD         1986         Raphel Lorente de Nó, MD           1983-84         Maxwell Abramson, MD         1987         Jerzy E. Rose, MD           1984-85         William C. Stebbins, PhD         1988         Josef Zwislocki, PhD           1985-86         Robert J. Ruben, MD         1989         Åke Flóck, PhD           1987-88         George A. Gates, MD         1991         William D. Neff, PhD           1988-89         William A. Yost, PhD         1992         Jan Wersäll, PhD           1999-91         Ilsa R. Schwartz, PhD         1993         David Lim, MD           1990-92         Jeffrey P. Harris, MD, PhD         1995         Kirsten Osen, MD           1992-93         Peter Dallos, PhD         1995         Kirsten Osen, MD           1993-94         Robert A. Dobie, MD         1996         Ruediger Thalmann, MD & Isolde Thalmann, PhD           1995-96         Bruce J. Gantz, MD         1999         Murray B. Sachs, PhD           1996-97         M. Charles Li		•		,
1980-81         Barbara Bohne, PhD         1984         Teruzo Konishi, MD           1981-82         Robert H. Mathog, MD         1985         Joseph Hawkins, PhD           1982-83         Josef M. Miller, PhD         1986         Raphel Lorente de Nó, MD           1983-84         Maxwell Abramson, MD         1987         Jerzy E. Rose, MD           1984-85         William C. Stebbins, PhD         1988         Josef Zwislocki, PhD           1985-86         Robert J. Ruben, MD         1989         Åke Flóck, PhD           1986-87         Donald W. Nielsen, PhD         1990         Robert Kimura, PhD           1987-88         George A. Gates, MD         1991         William D. Neff, PhD           1988-89         William A. Yost, PhD         1992         Jan Wersäll, PhD           1998-90         Joseph B. Nadol, Jr., MD         1993         David Lim, MD           1991-92         Jeffrey P. Harris, MD, PhD         1994         Peter Dallos, PhD           1991-92         Jeffrey P. Harris, MD, PhD         1995         Kirsten Osen, MD           1992-93         Peter Dallos, PhD         1996         Ruediger Thalmann, MD & Isolde Thalmann, PhD           1993-94         Robert A. Dobie, MD         1997         Jay Goldberg, PhD           1995-96         Bru		•		
1981-82         Robert H. Mathog, MD         1985         Joseph Hawkins, PhD           1982-83         Josef M. Miller, PhD         1986         Raphel Lorente de Nó, MD           1983-84         Maxwell Abramson, MD         1987         Jerzy E. Rose, MD           1984-85         William C. Stebbins, PhD         1988         Josef Zwislocki, PhD           1985-86         Robert J. Ruben, MD         1989         Åke Flóck, PhD           1986-87         Donald W. Nielsen, PhD         1990         Robert Kimura, PhD           1987-88         George A. Gates, MD         1991         William D. Neff, PhD           1988-89         William A. Yost, PhD         1992         Jan Wersäll, PhD           1990-91         Ilsa R. Schwartz, PhD         1993         David Lim, MD           1991-92         Jeffrey P. Harris, MD, PhD         1994         Peter Dallos, PhD           1992-93         Peter Dallos, PhD         1995         Kirsten Osen, MD           1993-94         Robert A. Dobie, MD         1997         Jay Goldberg, PhD           1995-95         Bruce J. Gantz, MD         1998         Robert Galambos, MD, PhD           1996-97         M. Charles Liberman, PhD         2000         David M. Green, PhD           1998-99         Edwin W. Rubel, PhD		•		•
1982-83         Josef M. Miller, PhD         1986         Raphel Lorente de Nó, MD           1983-84         Maxwell Abramson, MD         1987         Jerzy E. Rose, MD           1984-85         William C. Stebbins, PhD         1988         Josef Zwislocki, PhD           1985-86         Robert J. Ruben, MD         1989         Åke Flóck, PhD           1986-87         Donald W. Nielsen, PhD         1990         Robert Kimura, PhD           1987-88         George A. Gates, MD         1991         William D. Neff, PhD           1988-90         Joseph B. Nadol, Jr., MD         1992         Jan Wersäll, PhD           1990-91         Ilsa R. Schwartz, PhD         1993         David Lim, MD           1991-92         Jeffrey P. Harris, MD, PhD         1994         Peter Dallos, PhD           1992-93         Peter Dallos, PhD         1995         Kirsten Osen, MD           1993-94         Robert A. Dobie, MD         1997         Jay Goldberg, PhD           1994-95         Allen F. Ryan, PhD         1998         Robert Galambos, MD, PhD           1996-97         M. Charles Liberman, PhD         2000         David M. Green, PhD           1997-98         Leonard P. Rybak, MD, PhD         2001         William S. Rhode, PhD           1998-99         Richard A. Chole	1980-81	Barbara Bohne, PhD		•
1983-84         Maxwell Abramson, MD         1987         Jerzy E. Rose, MD           1984-85         William C. Stebbins, PhD         1988         Josef Zwislocki, PhD           1985-86         Robert J. Ruben, MD         1989         Åke Flóck, PhD           1986-87         Donald W. Nielsen, PhD         1990         Robert Kimura, PhD           1987-88         George A. Gates, MD         1991         William D. Neff, PhD           1988-89         William A. Yost, PhD         1992         Jan Wersäll, PhD           1989-90         Joseph B. Nadol, Jr., MD         1993         David Lim, MD           1990-91         Ilsa R. Schwartz, PhD         1994         Peter Dallos, PhD           1991-92         Jeffrey P. Harris, MD, PhD         1995         Kirsten Osen, MD           1992-93         Peter Dallos, PhD         1996         Ruediger Thalmann, MD & Isolde Thalmann, PhD           1993-94         Robert A. Dobie, MD         1997         Jay Goldberg, PhD           1994-95         Allen F. Ryan, PhD         1998         Robert Galambos, MD, PhD           1995-96         Bruce J. Gantz, MD         1999         Murray B. Sachs, PhD           1996-97         M. Charles Liberman, PhD         2000         David M. Green, PhD           1998-99         Edwi	1981-82	Robert H. Mathog, MD	1985	•
1984-85 William C. Stebbins, PhD 1985-86 Robert J. Ruben, MD 1986-87 Donald W. Nielsen, PhD 1987-88 George A. Gates, MD 1991 William D. Neff, PhD 1988-89 William A. Yost, PhD 1992 Jan Wersäll, PhD 1990-91 Ilsa R. Schwartz, PhD 1991-92 Jeffrey P. Harris, MD, PhD 1992-93 Peter Dallos, PhD 1993-94 Robert A. Dobie, MD 1994-95 Allen F. Ryan, PhD 1995-96 Bruce J. Gantz, MD 1996-97 M. Charles Liberman, PhD 1997-98 Edwin W. Rubel, PhD 1998-00 1998-00 1998-00 1998-00 1998-00 1998-01 1998-01 1998-02 1998-02 1998-03 1998-04 1998-05 1998-06 1998-06 1998-07 1998-07 1998-08 1998-08 1998-09 1998-09 1998-09 1998-09 1998-09 1998-09 1998-00 1998-00 1998-00 1998-00 1998-01 1998-01 1998-01 1998-02 1998-02 1998-03 1998-04 1998-05 1998-06 1998-06 1998-07 1998-08 1998-09 1999-09	1982-83	Josef M. Miller, PhD		± '
1985-86         Robert J. Ruben, MD         1989         Åke Flóck, PhD           1986-87         Donald W. Nielsen, PhD         1990         Robert Kimura, PhD           1987-88         George A. Gates, MD         1991         William D. Neff, PhD           1988-89         William A. Yost, PhD         1992         Jan Wersäll, PhD           1989-90         Joseph B. Nadol, Jr., MD         1993         David Lim, MD           1990-91         Ilsa R. Schwartz, PhD         1994         Peter Dallos, PhD           1991-92         Jeffrey P. Harris, MD, PhD         1995         Kirsten Osen, MD           1992-93         Peter Dallos, PhD         1996         Ruediger Thalmann, MD & Isolde Thalmann, PhD           1993-94         Robert A. Dobie, MD         1997         Jay Goldberg, PhD           1994-95         Allen F. Ryan, PhD         1998         Robert Galambos, MD, PhD           1995-96         Bruce J. Gantz, MD         1999         Murray B. Sachs, PhD           1996-97         M. Charles Liberman, PhD         2000         David M. Green, PhD           1998-99         Edwin W. Rubel, PhD         2001         William S. Rhode, PhD           1999-00         Richard A. Chole, MD, PhD         2003         David T. Kemp, PhD           2001-02         Ri	1983-84	Maxwell Abramson, MD	1987	Jerzy E. Rose, MD
1986-87 Donald W. Nielsen, PhD 1987-88 George A. Gates, MD 1991 William D. Neff, PhD 1988-89 William A. Yost, PhD 1989-90 Joseph B. Nadol, Jr., MD 1990-91 Ilsa R. Schwartz, PhD 1991-92 Jeffrey P. Harris, MD, PhD 1992-93 Peter Dallos, PhD 1993 David Lim, MD 1993-94 Robert A. Dobie, MD 1994-95 Allen F. Ryan, PhD 1995-96 Bruce J. Gantz, MD 1996-97 M. Charles Liberman, PhD 1997-98 Leonard P. Rybak, MD, PhD 1998-99 Edwin W. Rubel, PhD 1999-00 Richard A. Chole, MD, PhD 2000-01 Judy R. Dubno, PhD 2001-02 Richard T. Miyamoto, MD 2002-03 Donata Oertel, PhD 2003-04 Edwin M. Monsell, MD, PhD 2004-05 William E. Brownell, PhD  1998 William D. Neff, PhD 1992 Jan Wersäll, PhD 1993 David Lim, MD 1994 Peter Dallos, PhD 1995 Kirsten Osen, MD 1995 Kirsten Osen, MD 1995 Ruediger Thalmann, MD & Isolde Thalmann, PhD 1996 Ruediger Thalmann, MD & Isolde Thalmann, PhD 1997 Jay Goldberg, PhD 1998 Robert Galambos, MD, PhD 1999 Murray B. Sachs, PhD 1999 Murray B. Sachs, PhD 2000 David M. Green, PhD 2001 William S. Rhode, PhD 2002 A. James Hudspeth, MD, PhD 2003 David T. Kemp, PhD 2004 Donata Oertel, PhD 2005 Edwin W. Rubel, PhD 2006 Robert Fettiplace, PhD 2007 Eric D. Young, PhD 2007 Eric D. Young, PhD	1984-85	William C. Stebbins, PhD	1988	0
1987-88 George A. Gates, MD 1988-89 William A. Yost, PhD 1989-90 Joseph B. Nadol, Jr., MD 1990-91 Ilsa R. Schwartz, PhD 1991-92 Jeffrey P. Harris, MD, PhD 1992-93 Peter Dallos, PhD 1993-94 Robert A. Dobie, MD 1994-95 Allen F. Ryan, PhD 1995-96 Bruce J. Gantz, MD 1996-97 M. Charles Liberman, PhD 1997-98 Leonard P. Rybak, MD, PhD 1998-99 Edwin W. Rubel, PhD 1999-00 Richard A. Chole, MD, PhD 2001-02 Richard T. Miyamoto, MD 2002-03 Donata Oertel, PhD 2003-04 Edwin M. Monsell, MD, PhD 2004-05 William E. Brownell, PhD	1985-86	Robert J. Ruben, MD	1989	Åke Flóck, PhD
1988-89William A. Yost, PhD1992Jan Wersäll, PhD1989-90Joseph B. Nadol, Jr., MD1993David Lim, MD1990-91Ilsa R. Schwartz, PhD1994Peter Dallos, PhD1991-92Jeffrey P. Harris, MD, PhD1995Kirsten Osen, MD1992-93Peter Dallos, PhD1996Ruediger Thalmann, MD & Isolde Thalmann, PhD1993-94Robert A. Dobie, MD1997Jay Goldberg, PhD1994-95Allen F. Ryan, PhD1998Robert Galambos, MD, PhD1995-96Bruce J. Gantz, MD1999Murray B. Sachs, PhD1996-97M. Charles Liberman, PhD2000David M. Green, PhD1997-98Leonard P. Rybak, MD, PhD2001William S. Rhode, PhD1998-99Edwin W. Rubel, PhD2002A. James Hudspeth, MD, PhD2000-01Judy R. Dubno, PhD2003David T. Kemp, PhD2001-02Richard T. Miyamoto, MD2005Edwin W. Rubel, PhD2002-03Donata Oertel, PhD2005Edwin W. Rubel, PhD2003-04Edwin M. Monsell, MD, PhD2006Robert Fettiplace, PhD2004-05William E. Brownell, PhDEric D. Young, PhD	1986-87	Donald W. Nielsen, PhD	1990	Robert Kimura, PhD
1989-90Joseph B. Nadol, Jr., MD1993David Lim, MD1990-91Ilsa R. Schwartz, PhD1994Peter Dallos, PhD1991-92Jeffrey P. Harris, MD, PhD1995Kirsten Osen, MD1992-93Peter Dallos, PhD1996Ruediger Thalmann, MD & Isolde Thalmann, PhD1993-94Robert A. Dobie, MD1997Jay Goldberg, PhD1994-95Allen F. Ryan, PhD1998Robert Galambos, MD, PhD1995-96Bruce J. Gantz, MD1999Murray B. Sachs, PhD1996-97M. Charles Liberman, PhD2000David M. Green, PhD1997-98Leonard P. Rybak, MD, PhD2001William S. Rhode, PhD1998-99Edwin W. Rubel, PhD2002A. James Hudspeth, MD, PhD2000-01Judy R. Dubno, PhD2003David T. Kemp, PhD2001-02Richard T. Miyamoto, MD2004Donata Oertel, PhD2003-04Edwin M. Monsell, MD, PhD2006Robert Fettiplace, PhD2003-04Edwin M. Monsell, MD, PhD2006Robert Fettiplace, PhD2004-05William E. Brownell, PhD2007Eric D. Young, PhD	1987-88	George A. Gates, MD	1991	William D. Neff, PhD
1990-91 Ilsa R. Schwartz, PhD 1991-92 Jeffrey P. Harris, MD, PhD 1992-93 Peter Dallos, PhD 1993-94 Robert A. Dobie, MD 1994-95 Allen F. Ryan, PhD 1995-96 Bruce J. Gantz, MD 1996-97 M. Charles Liberman, PhD 1997-98 Leonard P. Rybak, MD, PhD 1998-99 Edwin W. Rubel, PhD 1999-00 Richard A. Chole, MD, PhD 2000-01 Judy R. Dubno, PhD 2001-02 Richard T. Miyamoto, MD 2002-03 Donata Oertel, PhD 2003-04 Edwin M. Monsell, MD, PhD 2004-05 William E. Brownell, PhD  1994-Peter Dallos, PhD 1995 1995 Kirsten Osen, MD 1996 Ruediger Thalmann, MD & Isolde Thalmann, PhD 1997 Jay Goldberg, PhD 1998 Robert Galambos, MD, PhD 2000 1999-Murray B. Sachs, PhD 1999-Murray B. Sachs, PhD 1999-Murray B. Sachs, PhD 2000 1994 Peter Dallos, PhD 1995 Kirsten Osen, MD 1996 Ruediger Thalmann, MD & Isolde Thalmann, PhD 1997 Jay Goldberg, PhD 2000 1998 Robert Galambos, MD, PhD 2000 1999 Murray B. Sachs, PhD 2000 1999 Murray B. Sachs, PhD 2001 William S. Rhode, PhD 2002 A. James Hudspeth, MD, PhD 2003 David T. Kemp, PhD 2004 Donata Oertel, PhD 2005 Edwin W. Rubel, PhD 2006 Robert Fettiplace, PhD 2007 Eric D. Young, PhD	1988-89	William A. Yost, PhD	1992	Jan Wersäll, PhD
1991-92 Jeffrey P. Harris, MD, PhD 1992-93 Peter Dallos, PhD 1993-94 Robert A. Dobie, MD 1994-95 Allen F. Ryan, PhD 1995-96 Bruce J. Gantz, MD 1996-97 M. Charles Liberman, PhD 1998-99 Edwin W. Rubel, PhD 1999-00 Richard A. Chole, MD, PhD 2000-01 Judy R. Dubno, PhD 2001-02 Richard T. Miyamoto, MD 2002-03 Donata Oertel, PhD 2003-04 Edwin M. Monsell, MD, PhD 2004-05 William E. Brownell, PhD  1995 Kirsten Osen, MD 1996 Ruediger Thalmann, MD & Isolde Thalmann, PhD 1997 Jay Goldberg, PhD 1998 Robert Galambos, MD, PhD 1999 Murray B. Sachs, PhD 1999 Murray B. Sachs, PhD 1999 Murray B. Sachs, PhD 1990 David M. Green, PhD 2000 David M. Green, PhD 2001 William S. Rhode, PhD 2001 William S. Rhode, PhD 2003 David T. Kemp, PhD 2004 Donata Oertel, PhD 2005 Edwin W. Rubel, PhD 2006 Robert Fettiplace, PhD 2007 Eric D. Young, PhD	1989-90	Joseph B. Nadol, Jr., MD	1993	David Lim, MD
1992-93 Peter Dallos, PhD 1993-94 Robert A. Dobie, MD 1994-95 Allen F. Ryan, PhD 1995-96 Bruce J. Gantz, MD 1996-97 M. Charles Liberman, PhD 1997-98 Leonard P. Rybak, MD, PhD 1998-99 Edwin W. Rubel, PhD 1999-00 Richard A. Chole, MD, PhD 2000-01 Judy R. Dubno, PhD 2001-02 Richard T. Miyamoto, MD 2002-03 Donata Oertel, PhD 2004-05 William E. Brownell, PhD  1996 Ruediger Thalmann, MD & Isolde Thalmann, PhD 1997 Jay Goldberg, PhD 1998 Robert Galambos, MD, PhD 1999 Murray B. Sachs, PhD 1999 Murray B. Sachs, PhD 1990 David M. Green, PhD 2000 David M. Green, PhD 2001 William S. Rhode, PhD 2002 A. James Hudspeth, MD, PhD 2003 David T. Kemp, PhD 2004 Donata Oertel, PhD 2005 Edwin W. Rubel, PhD 2006 Robert Fettiplace, PhD 2007 Eric D. Young, PhD	1990-91	Ilsa R. Schwartz, PhD	1994	Peter Dallos, PhD
1993-94 Robert A. Dobie, MD 1994-95 Allen F. Ryan, PhD 1995-96 Bruce J. Gantz, MD 1996-97 M. Charles Liberman, PhD 1997-98 Leonard P. Rybak, MD, PhD 1998-99 Edwin W. Rubel, PhD 1999-00 Richard A. Chole, MD, PhD 2000-01 Judy R. Dubno, PhD 2001-02 Richard T. Miyamoto, MD 2002-03 Donata Oertel, PhD 2003-04 Edwin M. Monsell, MD, PhD 2004-05 William E. Brownell, PhD	1991-92		1995	,
1994-95 Allen F. Ryan, PhD 1995-96 Bruce J. Gantz, MD 1996-97 M. Charles Liberman, PhD 1997-98 Leonard P. Rybak, MD, PhD 1998-99 Edwin W. Rubel, PhD 1999-00 Richard A. Chole, MD, PhD 2000-01 Judy R. Dubno, PhD 2001-02 Richard T. Miyamoto, MD 2002-03 Donata Oertel, PhD 2003-04 Edwin M. Monsell, MD, PhD 2004-05 William E. Brownell, PhD	1992-93	Peter Dallos, PhD	1996	Ruediger Thalmann, MD & Isolde Thalmann, PhD
1995-96 Bruce J. Gantz, MD 1996-97 M. Charles Liberman, PhD 1997-98 Leonard P. Rybak, MD, PhD 1998-99 Edwin W. Rubel, PhD 1999-00 Richard A. Chole, MD, PhD 2000-01 Judy R. Dubno, PhD 2001-02 Richard T. Miyamoto, MD 2002-03 Donata Oertel, PhD 2003-04 Edwin M. Monsell, MD, PhD 2004-05 William E. Brownell, PhD	1993-94	Robert A. Dobie, MD	1997	Jay Goldberg, PhD
1996-97 M. Charles Liberman, PhD 1997-98 Leonard P. Rybak, MD, PhD 1998-99 Edwin W. Rubel, PhD 1999-00 Richard A. Chole, MD, PhD 2000-01 Judy R. Dubno, PhD 2001-02 Richard T. Miyamoto, MD 2002-03 Donata Oertel, PhD 2003-04 Edwin M. Monsell, MD, PhD 2004-05 William E. Brownell, PhD	1994-95	Allen F. Ryan, PhD	1998	Robert Galambos, MD, PhD
1997-98 Leonard P. Rybak, MD, PhD 1998-99 Edwin W. Rubel, PhD 1999-00 Richard A. Chole, MD, PhD 2000-01 Judy R. Dubno, PhD 2001-02 Richard T. Miyamoto, MD 2002-03 Donata Oertel, PhD 2003-04 Edwin M. Monsell, MD, PhD 2004-05 William E. Brownell, PhD	1995-96	Bruce J. Gantz, MD	1999	Murray B. Sachs, PhD
1998-99 Edwin W. Rubel, PhD 1999-00 Richard A. Chole, MD, PhD 2000-01 Judy R. Dubno, PhD 2001-02 Richard T. Miyamoto, MD 2002-03 Donata Oertel, PhD 2003-04 Edwin M. Monsell, MD, PhD 2004 Donata Oertel, PhD 2006 Robert Fettiplace, PhD 2007 Eric D. Young, PhD	1996-97	M. Charles Liberman, PhD	2000	David M. Green, PhD
1999-00 Richard A. Chole, MD, PhD 2000-01 Judy R. Dubno, PhD 2001-02 Richard T. Miyamoto, MD 2002-03 Donata Oertel, PhD 2003-04 Edwin M. Monsell, MD, PhD 2004-05 William E. Brownell, PhD		•	2001	William S. Rhode, PhD
2000-01 Judy R. Dubno, PhD 2001-02 Richard T. Miyamoto, MD 2002-03 Donata Oertel, PhD 2003-04 Edwin M. Monsell, MD, PhD 2004-05 William E. Brownell, PhD	1998-99	Edwin W. Rubel, PhD	2002	A. James Hudspeth, MD, PhD
2000-01 Judy R. Dubno, PhD 2001-02 Richard T. Miyamoto, MD 2002-03 Donata Oertel, PhD 2003-04 Edwin M. Monsell, MD, PhD 2004-05 William E. Brownell, PhD  2004 Donata Oertel, PhD 2005 Edwin W. Rubel, PhD 2006 Robert Fettiplace, PhD 2007 Eric D. Young, PhD	1999-00	Richard A. Chole, MD, PhD	2003	David T. Kemp, PhD
2001-02 Richard T. Miyamoto, MD 2002-03 Donata Oertel, PhD 2003-04 Edwin M. Monsell, MD, PhD 2004-05 William E. Brownell, PhD  2005 Edwin W. Rubel, PhD 2006 Robert Fettiplace, PhD 2007 Eric D. Young, PhD	2000-01	Judy R. Dubno, PhD		± '
2002-03 Donata Oertel, PhD 2003-04 Edwin M. Monsell, MD, PhD 2004-05 William E. Brownell, PhD  2006 Robert Fettiplace, PhD 2007 Eric D. Young, PhD	2001-02	Richard T. Miyamoto, MD		•
2003-04 Edwin M. Monsell, MD, PhD 2004-05 William E. Brownell, PhD 2007 Eric D. Young, PhD	2002-03	Donata Oertel, PhD		, ·
2004-05 William E. Brownell, PhD				<u>.</u>
2005-06 Lloyd B. Minor, MD			2007	Lite D. Tourig, This
	2005-06	Lloyd B. Minor, MD		

#### **Table of Contents**

**Abstract Number** 

Presider	ntial Sym		
	<b>A:</b>	Ear and Brain: Integration of Sensory Cues into Complex Objects	1-7
Symposi	ium		
	<b>B</b> :	Wnt Signaling Pathways and Inner Ear Development	8-13
	<b>C</b> :	Spatial and Binaural Hearing: Perception and Physiology	14-19
Poster			
	D1:	Inner Ear: Hair Cell Genetics	
	<b>D2:</b>	Inner Ear Hair Cells: Prestin	33-41
	D3:	Inner Ear: Anatomy and Physiology 1	42-63
	<b>D4:</b>	Inner Ear Damage and Protection: Clinical Issues	64-73
	<b>D5</b> :	Inner Ear Damage and Protection: Potpourri 1	74-80
	D6:	Inner Ear Damage and Protection: Regeneration, Repair, and Survival	81-96
	D7:	Inner Ear: Hair Cell Mechanics	97-104
	D8:	Auditory Nerve: Anatomy, Chemistry, and Modeling	105-116
	D9	Middle Ear 1	
	D10:	Clinical Audiology 1	
	D11:	Clinical Audiology 2	
	D12:	Clinical Otolaryngology	
	D13:	Clinical Vestibular	
	D13:	Human Genetics	
	D14. D15:	Auditory Prosthesis: Neurotrophic Effects	
	D13.	Speech: Effects of Experience on Reception and Production	
<b>XX</b> 7 ~1 - ~1.		Speech: Effects of Experience on Reception and Production	207-215
Worksh	op E	NIDCD Workshop	216 217
Dottont	_	<u>-</u>	
rauent .	Auvocacy F	y Group Workshop Meniere's Disease - In Search of Answers	218 223
Podium	_	Memere's Disease - In Search of Answers	210-223
Podium	G	Inner Ear: Hair Cells	224 238
Crimmaga	_	IIIICI Edi, IIdii Ceiis	224-230
Symposi	H	Beyond Cochlear Implants: Functional Stimulation and Recording in the Auditory Nervous System	230 244
Worksh		beyond Cochical Impiants. Functional Stimulation and Recording in the Additory Net vous System	237-244
VV OI KSII	op I	Workshop: 3-D Imaging, Modeling, Reconstruction, and Analysis of the Temporal Bone and Brain	245 253
Podium	_	workshop. 3-D imaging, wodering, Reconstruction, and Analysis of the Temporal Done and Drain	243-233
roululli	J	Inner Ear Genetic and Clinical Pathology: Genetics	254 262
Poster	J	milet Eat Geneue and Chineat Lathology. Geneues	234-202
1 USICI	K1:	Regeneration 1	263-278
	K1. K2:	Inner Ear: Hair Cell Synapses and Ion Channels	
	K2: K3:	Inner Ear: Hair Cell Development, Ototoxicity, and Metabolism	
		± ' ' ' ' ' ' ' ' ' ' ' ' ' ' ' ' ' ' '	
	K4:	Development 1	
	K5:	Inner Ear Damage and Protection: Mechanisms of Noise Injury	
	K6:	Aging: Oxidative Stress and Mitochondria	
	K7:	Auditory Nerve: Neurophysiology	
	K8:	Auditory Brainstem: Molecular Aspects	
	K9:	Auditory Brainstem: Physiology A	
	K10:	Auditory Midbrain: Physiology	
	K11:	Auditory Cortex: Structure and Function 1	
	K12:	Sound Localization: Physiology	
	K13:	Psychophysics: Spatial and Binaural Hearing	
	K14:	Psychophysics: Vocalizations	439-445
	K15:	Auditory Prosthesis: Alternatives to Intra-Cochlear Electrodes	446-451
	K16:	Auditory Prosthesis: Current Steering and More	452-458

Animal 1	Researc	h Committee Workshop	
	L:	New Perspectives on Distress in Laboratory Animals	459-460
Podium			
	<b>M</b> :	Auditory Prosthesis	461-473
Symposi			
	N:	Ion Transport in the Stria Vascularis	
	<b>O</b> :	Neurobiology of Vocal Communication: Beyond Acoustic Features	482-486
Podium	_		40- 40-
D 4	<b>P</b> :	Genetics	487-492
Poster	01.	Lucan Fan Machanian	402 507
	Q1:	Inner Ear Mechanics Otoacoustic Emissions 1	
	Q2:		
	Q3:	Middle Ear Models and Measurements	
	Q4:	Regeneration 2	
	Q5:	Development 2	
	Q6:	Inner Ear Damage and Protection: Potpourri 2	
	Q7:	Inner Ear Damage and Protection: Prevention and Treatment of Injury	
	Q8:	Auditory Brainstem: Anatomy and Development	
	Q9	Auditory Brainstem: Physiology B	
	Q10:	Auditory Prosthesis: Probing the Cochlea	
	Q11:	Auditory Prosthesis: Temporal Processing	
	Q12:	Aging: Psychophysics and Speech	
	Q13:	Psychophysics: Pitch and Intensity	
	Q14:	Speech: Effects of Hearing Impairment	
	Q15:	Vestibular Periphery: Receptors	
_	Q16:	Vestibular: Central	674-686
Presiden			<b>40</b> =
	R:	Presidential Lecture and Award Ceremony	
Podium	G.	A. P. Control Charles and F. Control	<b>(99.703</b>
	S:	Auditory Cortex: Structure and Function	
	<b>T:</b>	Inner Ear Damage and Protection: Mechanisms and Treatment of Injury	703-717
Symposi		Consideration of the Auditors and Westingler III. Illusia	710 722
D. 1'	U:	Specification of the Auditory and Vestibular Hindbrain	
Podium	V:	Inner Ear Mechanics	724 726
Poster	٧.	Timer Ear Mechanics	
1 USICI	W1:	Genetics: Animal Models	737-748
	W2:	Aging: CBA Mouse Studies	
	W3:	Inner Ear: Anatomy and Physiology 2	
	W4:	Inner Ear Genetic and Clinical Pathology: Genetically Related Hearing Loss	
	W5:	Inner Ear Damage and Protection: Aminoglycosides	
	W6:	Inner Ear Damage and Protection: Platinum Compounds	
	W7:	Otoacoustic Emissions 2	
	W8:	Auditory Brainstem: Clinical Considerations	
	W9	Auditory Midbrain: Pathways, Plasticity, and Neuroethology	
	W10:	Auditory Cortex: Plasticity, Development, and Hearing Loss	
	W11:	Auditory Cortex: Structure and Function 2	
	W11: W12:	Auditory Cortex: Structure and Function 2  Auditory Cortex: Imaging and Human Studies	
	W12: W13:	Auditory Cortex: Imaging and Human Studies	
		·	
	W14:	Sound Localization: Psychophysics	
	W15	Psychophysics: Streaming and Grouping	
	W16:	Psychophysics: Temporal Processing	
	W17:	Psychophysics: Development and Training	
	W18:	Speech: Reception of Masked or Modified Speech	
D. J.	W19:	Vestibular Periphery: Structure and Signals	941-956
Podium	v.	Development and Degeneration	055 075
	X: v.	Development and Regeneration	95/-90/ 068 076

### 1 Ear and Brain: Integration of Sensory Cues into Complex Objects

Robert Shannon<sup>1</sup>

<sup>1</sup>House Ear Institute, Los Angeles, CA

Patients with auditory implants show large inter-subject variability in speech recognition. Psychophysical studies have demonstrated largely similar basic perceptual abilities across patients and little correlation with speech recognition. Why can some listeners make optimal use of basic sensory information while others apparently cannot? One possibility is that a subsystem of auditory processing is specialized for pattern recognition and selective damage to this subsystem can cause differences in patient performance. The speakers in this session will address this "second" stage of sensory processing in both vision and hearing - how is sensory information assembled into complex sensory objects? And why does this process fail in some pathologies even when basic sensory capability remains intact?

### 2 Optimal Integration of Visual Information Martin S. Banks<sup>1</sup>

<sup>1</sup>UC Berkelev

To achieve coherent and accurate percepts, the nervous system integrates information from various sources. In psychophysical studies, we have examined the integration of visual information from different depth cues and the integration of inter-sensory information from the hand and the eye. One can calculate what the statistically optimal integration would be (in the sense of yielding minimum variance). We find in both cases that the human nervous system integrates information in this optimal fashion. In particular, the nervous system takes into account the relative variances of the sources of information dynamically. As a result, percepts are more precise and accurate than could be achieved from one source of information alone.

## 3 Integration of Visual Information into Objects in Central and Peripheral Vision Bosco Tjan<sup>1</sup>

<sup>1</sup>University of Southern California

Patients with various forms of macular disorders must rely on the peripheral visual fields to recognize objects, identify faces and read. Compared to the fovea, the periphery is far less capable of this type of form vision. Front-end limitations alone, such as spatial resolution and contrast sensitivity, cannot explain the form-vision deficits in peripheral vision. To identify the functional deficits in peripheral vision, we study a phenomenon known as Crowding, which is most severe in the periphery, refers to the marked inability to identify an otherwise perfectly identifiable object when it is flanked by other objects. Using a combination of psychophysical and fMRI techniques, we found that 1) crowding, albeit reduces object-recognition performance severely, does not change the spatial-frequency tuning properties of the visual system; 2) crowding begins with the visual system

extracting erroneous features from wrong spatial locations and ends with inappropriately assembling these features; and 3) the neural origins of the erroneously feature extraction is most likely in V1 and/or V2.

### 4 Failure to Integrate Sensory Cues in Auditory Neuropathy

Fan-Gang Zeng<sup>1</sup>

<sup>1</sup>University of California Irvine

Here I take an analysis-by-synthesis approach to examine perceptual consequences of auditory neuropathy and their implications on normal mechanisms underlying auditory object recognition. I will present psychophysical and speech data to demonstrate that temporal processing deficit is the main reason for the difficulty that individuals with auditory neuropathy have in speech recognition, particularly in noise. I will also contrast neuropathy data with perceptual consequences of sensory hearing loss and electric stimulation. This comparative analysis reveals a practical insight as well as a theoretical insight. The practical one is the need to depart from the traditional approach of emphasizing on audibility in aural amplification and to move towards a balanced approach of compensating for suprathreshold processing deficits. The theoretical insight suggests that the low-frequency temporal fine structure is critical to the segregation and binding of the auditory objects

## 5 Brainstem Encoding of Sound – Implications for Language and Music Nina Kraus<sup>1</sup>

<sup>1</sup>Northwestern University

The auditory brainstem response mimics the acoustic characteristics of the speech signal with remarkable fidelity. The wide array of information simultaneously conveyed by the acoustic structure of speech (e.g. speaker intent/identity, the spoken message), can begin to be disentangled into discrete brainstem response components. Brainstem encoding impacts fundamental auditory cortex activity (signal encoding in noise and hemispheric specialization) and appears to provide early manifestations of cortical 'what' and 'where' pathways, that is, how sensory information is assembled into complex processing streams. Brainstem function is also modulated by reciprocal interactions with higher-level cortical functions subserving language and music.

We are becoming increasingly convinced that the multiple processing schemes inherent in the brainstem play a fundamental role in the normal system, how it breaks down in the impaired system, and how it reacts to differing levels of expertise. For impaired systems (learning and auditory processing disorders), the neural encoding of speech can be used as a biological marker of deficient sound encoding. In contrast, musicians can be used as examples of expert systems to illustrate how extensive auditory expertise can enhance basic sensory circuitry.

Subcortical pre-conscious encoding of sound is more active than previously thought; it is impacted by non-

acoustic factors such as visual stimulation and attention and appears to be "tuned" by life-long, short-term, and real-time experience. Consequently, the wide range of perceptual abilities commonly observed in auditory performance (in music and language-related functions, cochlear implant users, perceptual learning, etc.) can be explained, at least in part, by idiosyncratic (individual-specific) shaping of sensory function mediated by the auditory brainstem.

Supported by: NIH R01 DC01510 and NSF BCS 0544846

## 6 Cortical Areas Specific for Speech Understanding

Sophie Scott<sup>1</sup>

<sup>1</sup>University College, London

In this presentation I will review the evidence for speech specific mechanisms in adult human brains, using PET and fMRI techniques as indices of neural activity. I will outline the hierarchical processing of auditory information relevant to speech, and the extent to which this relates to the early neural processing of speech. I will identify at least two different streams of processing of the speech signal, one associated with the representation of the auditory structure of speech, and one that seems more to link speech perception with speech production. I will address the roles of brain regions beyond primary and secondary auditory cortex, to examine the neural basis for context effects in speech perception. Finally I will outline the roles of hemispheric asymmetry in speech perception.

#### 7 Speech Perception Within a Biologically-Realistic Information-Theoretic Framework Keith Kluender<sup>1</sup>

<sup>1</sup>University of Wisconsin-Madison

During the second half of the 20th century, much research concerning speech perception stood relatively distinct from the study of audition, let alone other modalities of highlevel perception such as vision. Contemporary research, however, is bridging this traditional divide. Fundamental principles that govern all perception, from hair cell to cortex, are shaping our understanding of the perception of speech and other familiar sounds. Information theory and biology of sensorineural systems are emphasized in explanations of classic characteristics of speech perception, including perceptual resilience in the face of degradation. signal variability, segmentation, categorical perception. Multiple experimental findings will be used to illustrate how a series of like processes operate upon the acoustic signal with increasing levels of sophistication on the way from waveforms to words. Common to these processes are ways that perceptual systems absorb predictable characteristics of the soundscape, from temporally local to extended periods (learning), and new information (change) is enhanced. To the extent that this characterization of perception is true, the same principles may be applied to processing of sensory information provided by prosthetic devices such as cochlear implants.

### 8 Wnt Signaling in the Developing Mammalian Cochlea

Alain Dabdoub<sup>1</sup>, **Matthew Kelley<sup>1</sup>**<sup>1</sup>NIDCD/NIH

The development of the cochlea and the organ of Corti entails multiple events including specification of cell fates and the establishment of precise cellular patterns. Although the factors that regulate most of these events have not been identified, the identification of several highly conserved developmental signaling pathways provides a number of strong candidates. Among these is the Wnt signaling pathway, which can mediate diverse cellular events through the activation of at least three separate intracellular cascades.

There are multiple Wnts and Wnt signaling components expressed in the cochlear duct, as a first step we sought to determine the roles of the different Wnt pathways and to identify the specific Wnts mediating each of these events. We report that Wnt4, signaling through the PKC cascade, acts as a potent inhibitor of hair cell development, apparently through direct phosphorylation of Atoh1. Since expression of Wnt4 is restricted to the modiolar region of the cochlear duct, the inhibitory effects of Wnt4 might act to block the formation of hair cells in the greater epithelial ridge. In contrast, activation of the canonical Wnt/β-catenin pathway in the developing organ of Corti by activation of the canonical target TCF induces the formation of ectopic hair cells in the lesser epithelial ridge. However the canonical Wnt regulating this event has not been determined yet. Finally, Wnt7a, which becomes restricted to developing pillar cells, plays a role in the orientation of hair cell stereociliary bundles, presumably through the planar cell polarization pathway. Therefore, different Wnts activate unique intracellular signaling pathways resulting in various cellular events not only within the cochlea but also within the same cochlear cells. How different developmental outcomes are specified will clearly require a thorough understanding of the downstream target genes and intracellular signaling pathways.

### 9 Tracing the Fate of Wnt Responsive Cells in the Inner Ear

Staci Rakowiecki<sup>1</sup>, Martin Riccomagno<sup>1</sup>, **Douglas Epstein**<sup>1</sup>

<sup>1</sup>University of Pennsylvania School of Medicine

Wnt signaling plays a prominent role at multiple phases of inner ear development. In the mouse, Wnt1 and Wnt3a secreted from the dorsal neural tube are required to regulate the expression of genes (*Dlx5*, *Gbx2*) in the dorsal otocyst that are necessary for vestibular morphogenesis. Surprisingly, *Wnt1-/-;Wnt3a-/-* embryos also display a pronounced defect in the outgrowth of the cochlear duct. To better comprehend the cause of this phenotype we used a tamoxifen inducible recombination system (*TopCreER;R26R*) to permanently mark the fate of Wnt responsive cells in the ear. Wnt responsive cells, as measured by X-gal staining, were identified in the dorsal otocyst and thereafter, in most sensory and nonsensory vestibular structures of the mature inner ear upon

tamoxifen administration between embryonic day (E) 8.5 and 10.5. These results are consistent with the spatial and temporal distribution of Topgal reporter expression, an indicator of active Wnt/βcatenin signaling. Remarkably, a population of Wnt responsive cells was also identified in the dorsomedial region of the otic cup that gave rise to Xgal positive cells along the dorsoventral extent of the medial wall of the otocyst at E10.5 and subsequently the sensory epithelium of the cochlea including the inner and outer hair cells and support cells when examined at E18.5. These lineage-tracing experiments identify the origin of sensory cells in the mouse otocyst and suggest that Wnt signaling in these cells is required for both vestibular and cochlear development. To address later functions of Wnt signaling in the inner ear we are currently evaluating the effects of Bcatenin inactivation at specific stages of vestibular and cochlear development.

## 10 Wnt-Frizzled Signaling: the "Ins" and "Outs" of the Hear and Now Craig Malbon<sup>1</sup>

<sup>1</sup>SUNY-Stony Brook

Wnts are secreted, palmitoylated glycoproteins that direct aspects of development, including cell proliferation, fate, and apoptosis. Post -translational modifications, secretion, and gradient formation of Wnt ligands are essential to Wnt function. Wnts exert their effects through binding to members of the superfamily of G protein-coupled receptors termed "Frizzleds", which for some Frizzleds (e.g., Frizzled-1) include the participation of co-receptor proteins LRP5/6. Downstream Wnt signaling events include activation of G proteins (and their effectors) to several read-outs, such as activation of Lef/Tcf-sensitive transcription (canonical pathway), activation of Ca2+ transients and cyclic GMP PDE6 (non-canonical pathway), and activation of JNK (planar cell polarity, PCP). The interactions between G proteins and various effectors are mediated by the unique phosphoprotein Dishevelled (DvI). In worms, zebrafish and mammals, multiple Dvls are expressed and their function(s) remain largely unknown. Far less is known about signaling in the PCP pathway. which appears critical in the proper development of the mammalian cochlea. The major Wnt signaling pathways, signaling elements, and unresolved questions will be updated and discussed.

(Supported by NIH grants DK300111 and DK25410).

## 11 Atypical PKC Mediates Attractive Wnt Signaling in Growth Cone Guidance Yimin Zou<sup>1</sup>

<sup>1</sup>University of California, San Diego

Proteins of the Wnt family are conserved growth cone guidance cues. Given the large number of ligands and receptors, this guidance system is likely to have significant contributions to nervous system wiring. However, the intracellular signaling pathways mediating Wnt dependent axon guidance are unknown. Previously, we reported that Wnt-Frizzled signaling controls the anterior turning of dorsal spinal cord commissural axons after midline crossing. We now show that a novel Wnt signaling

pathway, involving an atypical protein kinase C, PKCζ, mediates Wnt4 attraction and anterior-posterior (A-P) guidance. PKCζ is likely activated by a GPCR - PI3 kinase  $\gamma$  pathway in post-crossing commissural axons, as inhibitors to  $G\alpha_{i/o}$  (pertussis toxin) and PI3 kinase (wortmannin) resulted in A-P randomization and a reduction of Wnt4 stimulated outgrowth. downstream effector of PKC $\zeta$  signaling, is also required as its inhibition by lithium chloride and SB-216763 caused A-P turning defects and blocking of Wnt4 stimulated outgrowth. In addition, a kinase-defective PKCζ mutant caused A-P randomization when expressed commissural axons in an open-book preparation, suggesting that PKCζ functions cell autonomously. PI3 kinase  $\gamma$ , phosphorylated PKC $\zeta$ , and Par-6 are highly enriched in post-crossing commissural axons in vivo, potentially acting as components of the intracellular switch of Wnt responsiveness upon midline crossing.

### 12 Wnt Expression During Inner Ear Development

Ulrike J. Sienknecht<sup>1</sup>, Deborah Biesemeier<sup>1</sup>, **Donna M.** Fekete<sup>1</sup>

<sup>1</sup>Purdue University

Wnt signaling has been implicated in many steps of inner ear formation, including induction, regional patterning, proliferation, cell fate specification and stereociliary bundle orientation. These initial findings have inspired us to undertake a comprehensive spatiotemporal analysis of Wnt ligands, receptors and inhibitors during chicken inner ear morphogenesis. We performed in situ hybridization of 27 probes on cryosections of chicken tissue samples (n=82) at stages ranging from otocyst (embryonic day 3) through early differentiation (embryonic day 13). Results for Wnt ligands and receptors show co-localization or complementary expression patterns that eventually need to be interpreted with respect to the 3 different downstream Wnt signaling pathways: canonical, calcium and planar cell polarity pathways. As a generalization, Wnt signaling to sensory domains appears to be paracrine, with the ligands arising from adjacent non-sensory territories while the receptors are most strongly expressed within the sensory domains. Wnt expression is also associated with the striking morphogenetic event of canal fusion plate formation. Wnt signaling molecules expressed in ganglion neurons during axon outgrowth and synaptogenesis suggest that these processes may also be regulated by Wnt signaling. In cross-section, the cochlear duct is subdivided by partially overlapping gene expression domains. Finally, there are gradients of gene expression across the basilar papilla at the time stereociliary bundles are being polarized. The presence of discrete expression domains of Wnt inhibitors, which are known antagonists for the canonical pathway, raises the possibility that canonical Wnt signaling may be actively downregulated, perhaps to facilitate non-canonical signaling. These observations will influence the design and interpretation of gene misexpression approaches for functional analysis of Wnts in this system.

Supported by NIDCD.

## 13 The Genetic Networks Underlying Wnt Signaling During Early Mammalian Development

Terry Yamaguchi<sup>1</sup>

<sup>1</sup>NCI-Frederick, NIH

Wnts orchestrate the development of the early embryo by regulating several essential processes including cell fate determination, the specification of the body axes, segmentation, and convergent-extension cell movements. How Wnts coordinate the activation of these distinct genetic programs is not well-understood. Understanding how Wnt signaling is regulated in the embryo will provide the foundation for understanding the role of Wnt signaling pathways in cancer, as inappropriate activation of Wnt pathways in adults causes cancer. We are using genetic and molecular tools to define the signaling pathways and transcriptional networks that are activated by Wnts during early mammalian embryogenesis. I will present evidence that graded Wnt signals directly activate multiple transcription factors, and that Wnt-mediated repression, as well as activation, of specific genetic programs is necessary for proper embryogenesis.

## 14 The Role of ITD and ILD in Sound Localization by Cat Cortical Neurons and Human Listeners

Ewan A. Macpherson<sup>1</sup>

<sup>1</sup>Kresge Hearing Research Institute, University of Michigan In the cat, location-sensitive neurons have been found throughout auditory cortex. To determine how this sensitivity is derived from the available acoustical cues, we quantified and compared the contributions of interaural time difference (ITD) and interaural level difference (ILD) to azimuthal location coding for cat cortical neurons in fields A1, AAF, DZ, and PAF and to apparent lateral angle for human listeners. Targets were presented in virtual auditory space, which enabled independent manipulation of ITD and ILD while maintaining an otherwise natural set of binaural and spectral cues. Human listeners weighted ITD highly in stimuli containing low frequencies and weighted ILD highly only in stimuli lacking low frequencies. Paralleling the human psychophysical results, we found significant numbers of ITD-sensitive neurons in cat cortex, but only among cells responsive to low frequencies. ILD sensitivity was rare among cells unresponsive to high frequencies. The balance of ITD and ILD sensitivity in cat auditory cortex neurons appears to depend on the frequency tuning of the individual neuron rather than on its location in a particular cortical field.

15 Enhanced Behavioral and Physiological Processing of Interaural Temporal Disparities Within High-Frequency Auditory Channels

**Leslie Bernstein**<sup>1</sup>, Constantine Trahiotis<sup>1</sup>, Sarah Griffin<sup>2,3</sup>

<sup>1</sup>University of Connecticut Health Center, <sup>2</sup>University

College London, <sup>3</sup>University of Leicester

Our recent behavioral experiments have shown that resolution of interaural temporal disparities (ITDs), extents

of ITD-based laterality, and resistance to binaural interference within high-frequency auditory channels were all enhanced by the use of "transposed" stimuli. working hypothesis is that transposed stimuli provide envelope-based information within high-frequency channels similar to that provided by the waveform within low-frequency channels. The results of recent neurophysiological experiments compliment the behavioral results and bolster the working hypothesis. presentation also reports new findings based on behavioral experiments employing special stimuli that allow for the independent variation of several aspects of the stimulus envelope (modulation frequency, modulation depth, and the "dead-time/relative peakedness"). Taken together, the results reveal important information regarding the particular aspects of the envelopes of high-frequency waveforms that are sufficient for enhanced ITD-processing to occur.

## 16 Towards a Holistic Model of Mammalian ITD Processing David McAlpine<sup>1</sup>

<sup>1</sup>UCL Ear Institute, University College London

Neural mechanisms by which mammals process interaural time differences (ITDs) have been the subject of intense speculation over the last 5 years, since it was first demonstrated that ITD processing is dependent on neural for sound frequency. Neurons with characteristic frequencies (CFs) are preferentially tuned to relatively long ITDs whilst those with higher CFs are preferentially tuned to shorter ITDs. The distribution of preferred ITDs is similar across a range of mammalian species, once appropriate measures of neural filtering for sound frequency are applied. It has recently been suggested that the function of this relationship may be to position the sensitive slopes of ITD functions within the range of ITDs most commonly experienced, and that factors such as head size and the frequency range over which ITDs are processed might influence this. Similar dependence on frequency tuning is observed in high-CF neurons responsive to ITDs with respect to the envelope frequencies present in transposed noise. With respect to mechanisms responsible for generating preferred ITD tuning, evidence from in vivo and in vitro recordings indicate a role for glycinergic inhibition in neurons of the auditory brainstem, supporting the notion that ITD tuning may be implemented by cell biophysics rather than anatomical delay lines. Finally, there appears to be a limit to the explicit representation of ITDs in the mammalian brain. ITDs beyond half the period of the stimulus centrefrequency are not explicitly encoded at the level of single neurons, and this is supported by recent human brain imaging studies using standard psychophysical paradigms. Together, the evidence suggests that ITD processing in mammals is different to that suggested by the classic Jeffress model and text-book versions of ITD processing suggested to date.

### 17 Behavioral and Physiological Studies of the Precedence Effect

Daniel J. Tollin<sup>1</sup>, Tom C.T. Yin<sup>2</sup>

<sup>1</sup>Department of Physiology and Biophysics, University of Colorado Health Science Center, Aurora CO, <sup>2</sup>Department of Physiology, University of Wisconsin, Madison WI
The precedence effect (PE) describes several perceptual phenomena that occur when two sounds are presented from different spatial locations with a variable interstimulus delay (ISD) between their onsets. The neural mechanisms that produce the PE are thought to be responsible for the ability to localize sounds in reverberant environments; yet little is known about these mechanisms in behaving animals. We will show that cats experience the PE phenomena over ranges of ISDs similar to humans and that there is a neural correlate of summing localization, localization dominance and echo threshold in the responses of neurons in the inferior colliculus of cats

Support: NIDCD DC-00116 and DC-02840 (TCTY), and DC-00376 (DJT)  $\,$ 

actively participating in a localization task.

## 18 Neural and Psychophysical Studies of Spatial Hearing in Realistic Acoustic Environments

**Bertrand Delgutte**<sup>1,2</sup>, Barbara Shinn-Cunningham<sup>3</sup>, Sasha Devore<sup>1,4</sup>, Antje Ihlefeld<sup>3</sup>

<sup>1</sup>Eaton-Peabody Laboratory, Massachusetts Eye & Ear Infirmary, <sup>2</sup>Research Laboratory of Electronics, Massachusetts Institute of Technology, <sup>3</sup>Department of Cognitive & Neural Systems, Boston University, <sup>4</sup>Speech & Hearing Bioscience & Technology, Harvard-MIT Division of Health Sciences and Technology

Listeners routinely cope with multiple sound sources and significant acoustic reflections, but most psychophysical and neurophysiological studies have examined processing of simple sources in anechoic space. Here we report results from closely integrated psychophysical and neurophysiological studies focusing on two aspects of hearing in realistic acoustic environments: (1) detection of a target sound embedded in spatially separated masking noise; (2) localization of sounds in rooms. Human measures compared behavioral are measurements from single units in the inferior colliculus (IC) of anesthetized cat. Low-frequency stimuli were used to emphasize interaural time difference (ITD) processing. In both studies, the patterns in human performance closely paralleled quantitative predictions from neural responses. However, the neural codes that predicted these similarities differed in the two tasks. The best neural thresholds in a population of ITD-sensitive IC neurons predicted how behavioral detection thresholds varied with noise azimuth. In the localization task, where both neural and behavioral sensitivity to source azimuth degraded with increasing source distance, localization judgments were predicted by pooling neural responses across the entire population of ITD-sensitive IC neurons. These results suggest that different neural codes underlie detection and localization. A standard interaural cross-correlation model accounted for only some aspects of the data in both studies. In the detection task, amplitude fluctuations in the target enhanced neural signal detection over the model performance. In the localization task, neural responses were more directional than model predictions in reverberant conditions, suggesting that neural processing is influenced by fluctuations in interaural parameters of the stimulus. Thus, both studies point to the importance of temporal factors in binaural processing.

Supported by NIH Grants DC02258, 05778 and 05209.

## 19 Plasticity of Spatial Hearing: from Behavior to Physiology Andrew King<sup>1</sup>

<sup>1</sup>Department of Physiology, Anatomy and Genetics, University of Oxford, UK

As with other perceptual skills, the neural circuits involved in spatial hearing are shaped by experience during development and retain substantial capacity for plasticity in later life. We have shown that ferrets can adapt to altered binaural cue values produced by long-term blocking of one ear during infancy and learn to localize reasonably accurately despite the presence of an earplug. Moreover, this behavioral compensation is mirrored by adjustments to the auditory space map in the superior colliculus. localization accuracy Nevertheless, both and topographic order in the neuronal responses improved immediately following earplug removal, suggesting that adaptation is incomplete and that, even after many months of abnormal acoustical inputs, near-normal responses are observed when a balanced binaural input is provided. Although little evidence for adaptation was observed in mature ferrets that wore a unilateral earplug for several weeks without behavioral testing, these animals can rapidly relearn to localize sounds after occluding one ear in adulthood if they are trained to use their remaining auditory spatial cues in a behaviorally relevant task. Our data suggest that adaptation involves a shift in sensitivity away from the cues that are most affected by the earplug. namely interaural level differences, to other cues that are less affected by the earplug. Auditory localization plasticity in adult ferrets is no longer possible following damage to the primary auditory cortex or elimination of descending cortical inputs to the midbrain, suggesting that both cortical and subcortical processing levels are involved in mediating training-induced adaptation.

# 20 Deciphering the Hair Cell's Transcriptional Code: a Functional Genomics Approach to Understanding the Molecular Constituents of the Hair Cell

Brian McDermott<sup>1</sup>, Jessica Baucom<sup>2,3</sup>, A. J. Hudspeth<sup>2,3</sup>
<sup>1</sup>Case Western Reserve University, <sup>2</sup>The Rockefeller
University, <sup>3</sup>Howard Hughes Medical Institute
In its role as a sensory receptor that represents
mechanical stimuli as electrical responses, a hair cell
contains distinctive structures with specialized molecular
components, including the hair bundle that mediates
mechanotransduction and presynaptic active zones that
permit tonic vesicle release. Because of the paucity of
starting material in each vertebrate ear, on the order of
tens of thousands of hair cells, and the unavailability of a

pure population of hair cells, few of the hair cell's specialized molecular components have been identified and a comprehensive census of the cell's molecular constituents has yet to be accomplished.

As a starting point for an understanding of the molecular constituents of the hair cell, we have used DNA microarray technology to identify the transcripts present in hair cells of the adult zebrafish. Methods have been developed to rapidly isolate small, pure populations of hair cells from the lagena of the inner ear. RNA from these populations has been amplified, labeled, and hybridized to oligonucleotide microarrays. The hair-cell transcriptome of the zebrafish includes genes involved in cytoskeletal function, vesicular fusion, transcription, and ion flow across membranes. Among these are homologs of genes that, when mutated, produce deafness in humans and mice. The transcription profile also encompasses genes of undetermined function. Using the genetic techniques applicable to the zebrafish, we have begun to investigate the roles that some of these genes' products play in hair-cell development and function. This research was supported by grants DC00241 and DC006539 from the National Institutes of Health and the 2006 Annenberg Foundation Grant in Auditory Science from the National Organization for Hearing Research Foundation.

### 21 ZKSCAN1 (a SCAN-KRAB-Zinc Finger Protein) Interacts with Harmonin (USH1C)

**Denise Yan**<sup>1</sup>, Xiao Mei Ouyang<sup>1</sup>, Kazusaku Kamiya<sup>1</sup>, Li Lin Du<sup>1</sup>, Xue Zhong Liu<sup>1</sup>

<sup>1</sup>University of Miami

Usher syndrome (USH) is the most common form of deafblindness. To date, eight causative genes have been cloned. Molecular analysis revealed that the proteins encoded by these genes are integrated in a protein network by binding to protein-protein interaction domains, in particular to the PDZ domains of the USH1C-protein, harmonin. The USH protein complex would be required for the morphogenesis of the stereocilia bundle in hair cells of the inner ear and in the calycal processes of photoreceptor cells of the retina. The domain structure of harmonin suggests that it is involved in binding different proteins, but these vary depending on the tissue and/or cellular context. Here, we have used the yeast two-hybrid system to identify molecular partners for the scaffold protein harmonin, as bait to screen a human cochlear cDNA library. Among 20 primary yeast transformants showing positive interaction, we identified one clone of 1000 bp, which by analysis of the Blast database revealed to be identical to the ZKSCAN1, a SCAN-KRAB-zinc finger protein. Our yeast two-hybrid data are further supported by sequence analysis that revealed a putative PDZ-binding interfaces (PBI) at the C-terminus of ZKSCAN and a stretch of amino acids with significant homology to a protein domain in the adaptor protein Ril, which functions as an internal PBI. Reverse transcriptase-PCR (RT-PCR) of adult mouse cochlear tissues identified two transcripts, suggesting possible dual and perhaps developmentally regulated functions of Zkscan1. Our research findings further confirm the functional versatility of zinc finger proteins that can mediate nucleic acid-binding and protein: protein interactions. Confirmation of the interaction in mammalian cells and characterization of the Zkscan1 transcripts are in process.

The work is supported by NIH DC 05575

# 22 Effects of MDL-28170, an Inhibitor of Notch Signaling Pathway, into the Endolympatic Cavity of Guinea Pig Cochlea After Severe Hair Cell Damage

Ryusuke Hori<sup>1</sup>, Takayuki Nakagawa<sup>1</sup>, Yoshinori Matsuoka<sup>1</sup>, Tomoko Kita<sup>1</sup>, Shinji Takebayashi<sup>1</sup>, Koji Iwai<sup>1</sup>, Tatsunori Sakamoto<sup>1</sup>, Norio Yamamoto<sup>1</sup>, Jyuichi Ito<sup>1</sup> <sup>1</sup>Department of Otolaryngology - Head & Neck Surgery, Graduate School of Medicine, Kyoto University In mammalian cochlea, hair cells and supporting cells originate from the same progenitor cells and Notch signaling pathway plays a role in cell fate determination during development and even after maturation. The inhibition of Notch signaling in the sensory epithelium of cochlea is reported to increase the number of hair cells. For example, genetic deletion of Notch ligand jagged 2 resulted in the increase in the number of hair cells (Lanford PJ et al., 1999). Yamamoto, et al. demonstrated that gamma-secretase inhibitor (GSI), an inhibitor of Notch signaling, induced ectopic hair cells in the cultured cochlea of postnatal mice. In our previous report, two GSIs, DAPT and MDL-28170 (MDL), were injected into the perilymphatic cavity of mature guinea pigs following severe hair cell damage by kanamycin sulfate and ethacrynic acid. MDL, not DAPT, induced a limited number of ectopic myosin VIIa-positive cells in the organ of Corti. This time, we tried to inject MDL into the endolymphatic cavity of one month old guinea pigs. In the first group, MLD was injected once; In another goup, MDL injection was repeated again on the following day. Animals were sacrificed 2 or 4 weeks after MDL injection. Hearing was evaluated by ABR mesurment before and after MDL treatment. To date, no ectopic hair cells were found in animals with single MDL injection. This might result from a limited number of sensory progenitor cells in mature guinea pig cochlea which are expected to respond to Notch signaling inhibition, thus it may not be easy to induce hair cell regeneration simply by modulating Notch signaling pathway in mature guinea pigs. Other conditions of MDL injection are now under investigation.

### 23 Upregulation of Math1 Inhibits Neural Stem Cell Proliferation

**Mark Parker**<sup>1,2</sup>, Brianna Russo<sup>3</sup>, When-Han Tan<sup>3</sup>, Douglas Cotanche<sup>3</sup>

<sup>1</sup>Massachusetts Eye & Ear Infirmary, <sup>2</sup>Emerson College, <sup>3</sup>Children's Hospital-Boston

The upregulation of mammalian homolog of the atonal-1 (Math1) basic helix –loop-helix transcription factor in specific cells of the organ of Corti is sufficient for hair cell genesis. Studies have shown that adenoviral particles that constitutively express Math1 are able to produce novel hair cells when injected into the deafened cochlea (Kawamoto, et. al. 2003; Izumikawa, et. al. 2005). One problem with these and other gene therapy studies is that there is little

control over the cell type infected by the viral particles. A possible means of specifying the location in which a novel hair cell would form would be to engineer a migrating cell to express Math1. The clonal 17.2.neural stem cell (cNSC) exhibits a capacity to migrate to sites of lesion. Our ultimate goal is engineer a cNSC to express Math1 and inject these cells into the deafened cochlea. This data presents a preliminary step in this process.

We transfected (chemical) c17.2 cNSCs with a pCLIG vector consisting of a constitutively expressing Math1 transcript upstream of an enhanced green fluorescent protein (EGFP) by incubation in serum free medium. After 8 hours, the cells were washed and the media was replaced with media containing 15% serum. Viable transfected cells were monitored for up to 72 hours, then either frozen or split for further analysis. Split cells were cultured for an additional 48-72 hours in media containing 10 mM BrdU. Cells were then fixed and processed for immunohistochemistry using polyclonal antibodies directed against either Math1 or BrdU.

Our results indicate that transfected cells overexpress the Math1 protein. In addition, these cells decrease their rate of proliferation compared to non-transfected controls, although they incorporate the BrdU label indicating that they are still capable of entering the cell cycle. These results suggest that the upregulation of Math1 may lead to a decrease the rate of cell proliferation in stem cells.

### | 24 | HES6 Expression is Regulated by MATH1/ATOH1 in Hair Cells

**Deborah Scheffer**<sup>1</sup>, Cyrille Sage<sup>1</sup>, David P. Corey<sup>2</sup>, Veronique Pingault<sup>1</sup>

<sup>1</sup>Inserm, Equipe Avenir, Department of Genetics, Hopital Henri Mondor, Creteil, France, <sup>2</sup>HHMI and Department of Neurobiology, Harvard Medical School, Boston

HES6 is a member of the Hairy and Enhancer of split family of basic helix-loop-helix (bHLH) transcription factors. In contrast to other HES-bHLH factors, HES6 promotes differentiation during neurogenesis, and its expression is upregulated by the proneural bHLH proteins (class I). In the inner ear, *Hes6* is expressed in hair cells (*Qian et al., 2006*) whereas *Hes1* and *Hes5* are expressed in supporting cells. *Hes1*<sup>-/-</sup> and *Hes5*<sup>-/-</sup> mice show a significant increase in the number of hair cells in the cochlea and in the vestibule.

Here, we describe the expression profile of *Hes6* in the mouse inner ear by in situ hybridization, and its transcriptional regulation by the proneural bHLH ATOH1. Hes6 appears to be expressed in the spiral ganglion and in the vestibular and cochlear hair cells. Moreover, Hes6 expression closely follows the expression profile of *Atoh1*. We used a TET-off system allowing inducible ATOH1 expression in osteosarcoma cells. The transcriptome study of these cells with and without the expression of ATOH1 showed that Hes6 expression is upregulated in presence of ATOH1. We confirmed these results by RT-PCR and determined that Hes6 expression is rapidly induced after the beginning of expression of ATOH1. These data, together with its expression profile, suggest that Hes6 is a direct target gene of ATOH1. We confirmed this hypothesis by studying the transactivation capabilities of ATOH1 through the promoter of *HES6*. Luciferase assays showed that ATOH1 activates the promoter of *HES6* through four E-boxes. EMSAs allowed us to confirm that ATOH1 binds these E-boxes with different affinities, further elucidating the consensus and clustering of ATOH1 binding sites.

Our data show that *Hes6* is expressed in hair cells, in contrast to *Hes1* and *Hes5*, and introduce this gene as a direct target gene for ATOH1 in inner ear. These data confirm that HES6 acts in a positive feedback loop with the proneural bHLH proteins during vertebrate neural development.

#### 25 Hearing Loss in Creatine Kinase Knock-Out Mice

**Theo A. Peters**<sup>1</sup>, Jung-Bum Shin<sup>2</sup>, Femke Streijger<sup>3</sup>, Andy J. Beynon<sup>1</sup>, Peter G. Gillespie<sup>2</sup>, Catharina E.E.M. Van der Zee<sup>3</sup>

<sup>1</sup>Department of Otorhinolaryngology, Radboud University Nijmegen Medical Centre, Nijmegen, Netherlands, <sup>2</sup>Oregon Hearing Research Center & Vollum Institute, Oregon Health & Science University, Portland, USA, <sup>3</sup>Department of Cell Biology, Radboud University Nijmegen Medical Centre, Nijmegen, Netherlands

Our demonstration that cytosolic brain isoform creatine kinase (B-CK) is one of the most abundant proteins in the stereocilia of inner ear hair cells motivated us to investigate hearing in mice lacking specific creatine kinase isoforms. As models we studied B-CK single knock-out (B-CK<sup>-/-</sup>) mice and, because the ubiquitous mitochondrial creatine kinase (uMi-CK) isoform can in some cases compensate for the loss of B-CK, we also studied double knock-out mice that lack both B-CK and uMi-CK (CK<sup>=/=</sup>). To assess the hearing, acoustic startle reflex responses and auditory brainstem responses were determined. Both B-CK<sup>-/-</sup> single and CK<sup>=/=</sup> double knock-out mice showed a four-fold lower startle response and prepulse inhibition, suggesting a partial hearing deficit. Auditory brainstem response measurements demonstrated that CK<sup>=/=</sup> double knock-out mice display significantly elevated thresholds in the middle and upper regions of the auditory range of mice (8-32 kHz). The B-CK<sup>-/-</sup> single knock-out animals showed a higher auditory threshold at 32 kHz, but not at the lower range, suggesting compensation by uMi-CK. Initial histological comparisons indicated that CK<sup>=/=</sup> double knock-out inner ears were morphologically normal. Hearing loss in both creatine kinase knock-out mouse models, particularly at higher frequencies, is consistent with the proposed function of B-CK as supplier of ATP for the plasma membrane Ca<sup>2+</sup>-ATPase (PMCA2) in cochlear hair cells. Energy demand by PMCA2 is higher than can be provided for by diffusion from mitochondria and thus the required amounts of ATP may be produced by B-CK.

### 26 Cadherin 23 Alternative Splice Variants – Studying the Molecular Basis of Waltzer

**Ayala Lagziel**<sup>1</sup>, Robert J. Morell<sup>1</sup>, Thomas B. Friedman<sup>1</sup> *NIDCD* 

Mutant alleles of CDH23, the gene encoding cadherin 23, are associated either with deaf-blindness and vestibular

dysfunction (Usher syndrome type 1; USH1D), or isolated deafness (DFNB12). USH1D patients have profound hearing loss, vestibular dysfunction and progressive blindness due to retinitis pigmentosa (RP). A model for mutation in Cdh23 is the waltzer (v) mouse. Waltzer mice are deaf, exhibit vestibular dysfunction but do not develop RP. Cadherin 23 is a single pass transmembrane adhesion protein characterized by cadherin repeat sequences in its extracellular domain. We recently reported immunohistological data that cadherin 23 is associated with transient stereocilia links and we also characterized several short isoforms of Cdh23 (B and C) unaffected by the v6J allele. The absence of a retinal phenotype in homozygous v6J mutants and the expression of certain cadherin 23 isoforms in mutant mice led us to investigate the expression of cadherin 23 isoforms in the cochlea and retina. Using semi-quantitative real time PCR assays on cochlear and retinal RNA from P0 and adult wild type and homozygous v6J mutants, we established that alternatively spliced Cdh23 isoforms differ in their temporal patterns of expression. Moreover, in the retina of v6J homozygous mice a certain alternate transcript (D) is significantly up-regulated relative to its expression level in the retinae of its wild type littermates. We generated antibodies specific to isoform C and confirmed that cadherin 23 isoforms have discrete patterns of expression. particularly in the photoreceptor layer of the retina. Western blot analyses revealed that in the wild type mice, the largest cadherin 23 protein (A) and the only one predicted to be affected by the v6J mutation, is transiently expressed during cochlear development. Our data suggests that the loss of function of the largest cadherin 23 protein variant is responsible for deafness in waltzer mice.

### 27 Otoferlin Interactions at the Synaptic Complex

**Neeliyath A. Ramakrishnan**<sup>1</sup>, Dennis G. Drescher<sup>1</sup> *Wayne State University School of Medicine* 

Mechanoreceptive hair cells lack synaptotagmin and express another C2-domain-containing, calcium-sensing protein, otoferlin. Otoferlin, which in mutated form causes non-syndromic deafness DFNB9 in humans, may substitute for synaptotagmin at the hair-cell synaptic complex. Otoferlin contains six C2, phospholipid/proteininteracting domains, A-F, and a C-terminal transmembrane region. By yeast two-hybrid techniques, we examined the interaction of the C2 domains of mouse otoferlin both with the SNARE protein syntaxin 1A and with the II-III loop of the Cav1.3 calcium channel. We cloned each of the C2 domains in prey vector pGADT7 and cloned the Cav1.3 II-III loop in bait construct pGBKT7. By yeast cotransformation and stringent selective markers, we determined that the otoferlin C2-D domain binds to the calcium channel II-III loop. We also found that otoferlin C2-A and C2-B domains interact weakly with the II-III loop. Otoferlin C2-A interacts strongly with syntaxin 1A. Experiments involving II-III loop deletion mutants identified a SH3 and PDZ domain binding motif that may interact directly with the otoferlin C2-D domain. Reversal of the bait and prey clones yielded similar results. In surface plasmon resonance experiments, Cav1.3 II-III loop and syntaxin 1A peptides were employed as ligands covalently bound to a CM5 sensor chip. Of the six C2 domains, separately, as analytes, C2-D was found to bind strongly to the II-III loop and C2-A to syntaxin 1A. Binding of C2-A to syntaxin 1A was undiminished in the presence of 3 mM EDTA, compared to its binding in 50  $\mu$ M Ca²+ without chelator, suggesting a calcium-independent interaction. Thus, otoferlin interacts with the SNARE protein syntaxin 1A via its C2-A domain and with the Cav1.3 calcium channel via its C2-D domain. Ongoing studies also suggest that otoferlin interacts with VAMP I, Rab 3a, and complexin I. Overall, our results are consistent with a role for otoferlin at the hair-cell synaptic complex.

### 28 A Chimeric Analysis of POU4F3 Function in Hair Cells

Eric Chan<sup>1</sup>, Kwang Pak<sup>2</sup>, Li Yan<sup>2</sup>, Lina Mullen<sup>2</sup>, **Allen F. Ryan**<sup>2,3</sup>

<sup>1</sup>Department of Biology, <sup>2</sup>Department of Surgery/Otolaryngology, <sup>3</sup>Department of Neurosciences, UCSD and VA Medical Center, La Jolla, CA

The POU-domain transcription factor Brn-3.1 (POU4F3. Brn-3c), is selectively expressed in hair cells (HCs) throughout their life, and is required for HC differentiation and survival. The related factors Brn-3.0 (POU4F1) and Brn-3.2 (POU4F2) are expressed in spiral ganglion and other primarily sensory neurons, where they regulate aspects of neuronal differentiation. The DNA binding domains of all three POU4F factors are highly similar and they are thought to bind to the same DNA motifs. Differential function appears to be produced by the remainder of the protein. In order to evaluate the role of different protein domains in the HC specificity of Brn-3.1, we created Brn-3.1/Brn-3.0 chimeric molecules, in which exon 1 (chimera 1), exon 2 (chimera 2) or exon 4 (chimera 4) of Brn-3.0 were substituted for the corresponding region cDNAs encoding the chimeras were of Brn-3.1. ballistically transfected into wild-type (postnatal day 3-5) and Brn-3.1-null (postnatal day 0-1) sensory epithelia. We used epithelia from mice in which HCs expressed GFP under the control of a Brn-3.1 promoter fragment. Chimera 1, which contained 30 amino acids from the amino terminus of Brn-3.0, drastically reduced the survival of HCs in wild-type epithelia, suggesting a dominant negative effect. Epithelia transfected with chimeras 2 or 4 showed HC survival similar to that seen with Brn-3.1 or control (gold particles alone) transfections. When Brn-3.1null HCs were transfected, the highest rate of survival was seen with Brn-3.1 transfection, while Chimeras 1 or 2 produced very low survival. HC survival with Chimera 4 was intermediate. The results suggest that the amino terminus of Brn-3.1 is critical for its survival-promoting function in HCs.

Supported by grant DC00139 from the NIH/NIDCD, by the Research Service of the VA, and by the NOHR.

# 29 Stability Enhancement of the POU4F3 Transcription Factor via the DFNA15 Truncation Mutation: Insights from Molecular Modeling

Christopher Frenz<sup>1</sup>, Philippe Lefebvre<sup>1</sup>

<sup>1</sup>University of Liege

The POU4F3 transcription factor is unique to the cochlea and vestibular hair cells of the inner ear and targeted deletion of POU4F3 results in deafness and balance disorders due to a complete loss of inner ear cells. The DFNA15 mutation, within the gene for the transcription factor, consists of an 8bp deletion. The resultant frameshift from this deletion introduces a stop codon in the first helix of the POUH domain, which results in a loss of transcriptional activity and deafness. One of the interesting consequences of the DFNA15 mutation however, is that leads to an increase in the stability of the truncation mutant above that associated with the wild-type form of the protein. Molecular modeling was utilized to elucidate a potential mechanism for this stability enhancement. Homology models of the Wild-type POU4F3 and the truncation mutant were created via using the EsyPred3D Web Server, which bases its structural predictions on high scoring sequence alignments with proteins of known tertiary structure. The Adaptive Poisson-Boltzmann Solver (APBS) was then utilized to calculate the electrostatic potential surfaces of the models, since the shape and charge distributions of these surfaces implicitly represent a molecules ability to form ionic and covalent bonds, as well as to participate in dipole or hydrophobic interactions. This analysis revealed that the truncation exposes several negatively charged regions within the POUH domain that have the potential to interact with the positively charged cleft present on the POUSD Protein-protein docking calculations, performed on the ClusPro Server, confirmed the feasibility of an intramolecular interaction being present between the two domains of the POU4F3 truncation mutant. It is thereby suggested that the truncation mutation enables the interaction of the two domains, which results in an enhancement of protein stability.

#### 30 Preliminary Characterization of Anti-WDR1 Antibody in the Avian Inner Ear

**Henry J. Adler<sup>1,2</sup>**, Elena Sanovich<sup>1,3</sup>, Kai Yan<sup>1,2</sup>, Robert J. Dooling<sup>1,3</sup>

<sup>1</sup>Center of Comparative and Evolutionary Biology of Hearing, <sup>2</sup>Department of Biology, <sup>3</sup>Department of Psychology, University of Maryland, College Park, MD Studies on hearing loss and recovery in birds and mammals are now identifying, within the ear, protein changes that lead to functional disability. One of the proteins, WD repeat-1 protein (WDR1), contains 11 putative WD40 motifs involved in protein-protein interactions, and demonstrates significant homology to actin-interacting protein-1 (AIP-1) in several species including slime molds. AIP-1 binds cofilin/actin depolymerization factor, suggesting a role of WDR1 in actin dynamics.

The gene encoding WDR1 was upregulated in the acoustically damaged chicken basilar papilla. The shift of WDR1 localization from hair cells in the normal inner ear to both surviving hair cells and supporting cells in a sound-damaged ear suggests a role in inner ear response to acoustic trauma.

Here, we study WDR1 presence in the basilar papillae of chicken and Belgian Waterslager (BWS) canary, the latter of which exhibits high frequency hearing loss. Previous studies reported strong WDR1 identity between chicken and BWS canary. Immunocytochemistry with anti-WDR1 antibody showed staining among the cell bodies of hair cells at least at the luminal surface. However, the antibody may have lost its efficiency over time and distance, and new antibodies were raised against two peptides, which are identical to different WDR1 regions. Western blotting analysis on chicken basilar papilla with affinity purified antibodies yielded a band of roughly 70 kiloDaltons, nearly identical the molecular weight of WDR1. to Immunostaining with the new antibodies, followed by confocal examinations, revealed similar WDR1 distribution among hair cells in the ears of birds with normal (chicken) and abnormal (BWS) hearing. This suggests that WDR1 may not be a significant factor in BWS hearing loss; however, it may be more significant between 7 and 30 days post hatch which corresponds to the time where the BWS canary starts to lose its hearing.

Work supported by NIDCD 000436, NIH DC01372, and NIH P30-DC04664.

### 31 HCN1 Protein Interactions in Saccular Hair Cells

Neeliyath A. Ramakrishnan<sup>1</sup>, **Marian J. Drescher<sup>1</sup>**, Dennis G. Drescher<sup>1</sup>

<sup>1</sup>Wayne State University School of Medicine

HCN1 is the primary HCN isoform underlying  $I_n$  in a model hair cell preparation from the trout sacccule (Cho et al., Neuroscience 118: 525-534, 2003). cAMP-gated  $I_h$  sets the membrane potential for a subpopulation of saccular hair cells, determining spontaneous release of hair cell transmitter for the saccule. In the present study, yeast two-hybrid protocols were used to identify the binding partners for HCN1 associated with physiological function of the channel in vivo. Amino terminus sequence up to the first transmembrane-crossing domain and two carboxy terminus sequences downstream of the cyclic nucleotide binding domain (C1 and C2) in bait construct pGBKT7 were tested in mating protocols with a hair-cell cDNA library in prey construct pGADT7-Rec. Overall, 337 prey clones were sequenced, with 175 clones for the N-terminal bait, 130 for the C1 bait and 32 for the C2 bait. RACK1, the receptor for activated protein kinase C, has been identified as a protein-binding partner for C1 in saccular hair cells. The clone corresponded to ~2/3 of the coding sequence, representing 4 C-terminal WD-40 domains. Cotransformation of the isolated prey RACK1 and the C1 domain of trout HCN1 gave positive results, whereas no colonies were observed in the negative control with empty vector pGBKT7. 5' RACE yielded full-length sequence of RACK1, which for the trout saccular hair cell was 95%

identical in aa to human RACK1. This high homology permitted the use of a primary antibody to human RACK1 to immunolocalize RACK1 in the trout saccule. RACK1 appears to be a hair cell marker, with no immunoreactivity (IR) found in supporting cells or in nerve fibers entering the sensory epithelium. The IR was localized to the base of hair cells, the site of receptor-neural transmission, as well as to supranuclear sites. The interaction of intracellular RACK1 with HCN1 on the basal cell membrane may constitute a mechanism for coordinating efferent regulation of afferent signaling.

## 32 Usher 1 Proteins Function in Developing and Adult Hair Cells: Analysis by Forward and Reverse Genetics

**Ulrich Mueller**<sup>1</sup>, Martin Schwander<sup>1</sup>, Anna Reynolds<sup>1</sup>, Nicolas Grillet<sup>1</sup>, Anna Sczaniecka<sup>1</sup>, Lisa M. Tarantino<sup>2</sup>, Tim Wiltshire<sup>2</sup>, Allen F. Ryan<sup>3</sup>, Elisabeth M. Keithley<sup>3</sup>, Gary D. Housley<sup>4</sup>, Andrea Lelli<sup>5</sup>, Gwenaelle S.G. Geleoc<sup>5</sup>, Jeffrey R. Holt<sup>5</sup>

<sup>1</sup>The Scripps Research Institute, <sup>2</sup>Genome Inst. of the Novartis Res. Foundation, <sup>3</sup>University of California, San Diego, <sup>4</sup>University of Auckland, <sup>5</sup>University of Virginia Through positional cloning efforts, five genes have been linked to Usher Syndrome Type 1 (USH1). These genes encode the cell surface receptors cadherin 23 (CDH23) and protocadherin 15 (PCDH15), the adaptor proteins harmonin and sans, and the molecular motor myosin VIIa (MYO7A). Previous studies have shown that USH1 proteins are expressed in developing hair cells. In vitro studies have provided evidence that USH1 proteins can bind to each other, and functional null alleles of the murine orthologs of human USH1 genes cause defects in hair bundle morphology. Taken together, the findings suggest that USH1 proteins assemble into protein complexes that control hair bundle morphogenesis. Interestingly, some USH1 proteins continue to be expressed in adult hair cells, and two of them, CDH23 and PCDH15, have been shown to co-localize with tip links. The findings suggest that USH1 proteins play important roles in mature hair cells. To distinguish between functions of USH1 proteins in developing and mature hair cells, we have taken a genetic approach. Using gene-targeting strategies, we have generated a panel of mouse lines with subtle mutations in USH1 genes. We have also carried out a large-scale ENU mutagenesis screen and identified 22 mouse lines that inherit hearing defects as recessive traits. Through positional cloning, we have shown that several of the mouse lines carry novel alleles of USH1 genes. We have studied the mice by histology, biochemistry and electrophysiology, and we will provide evidence suggesting that USH1 proteins have distinct functions in developing and adult hair cells.

### 33 Isothermal Titration Calorimetry Study of the Interactions Between Prestin and Anions

#### Withdrawn

## 34 Membrane Cholesterol Concentration Affects Prestin Organization and Lateral Mobility in the HEK Cell Membrane

**Louise E. Organ**<sup>1</sup>, Jennifer N. Greeson<sup>1</sup>, Robert M. Raphael<sup>1</sup>

<sup>1</sup>Rice University

The transmembrane protein prestin is crucial to outer hair cell (OHC) electromotility and is thought to be partially responsible for the sensitivity and frequency selectivity of mammalian hearing. Understanding the mechanisms by which prestin senses transmembrane voltage changes and elicits cellular deformations requires characterizing the organization and mobility of prestin in the plasma membrane environment. To achieve these goals we utilize the quantitative techniques of fluorescence resonance energy transfer (FRET) and fluorescence recovery after photobleaching (FRAP) to show specific prestin-prestin interactions and to study prestin lateral diffusion. Since changes in the membrane composition alter the voltage sensitivity of the displacement current recorded in both OHCs and HEK cells expressing prestin, we examine the effects of membrane cholesterol concentration on prestin association and mobility. Our results suggest the ability of fluorescent fusion proteins to form non-obligate dimers enhances prestin aggregation, and these complexes are degraded when cholesterol is extracted from the plasma membrane via methyl-β-cyclodextrin (MβCD). However, differences due to cholesterol concentration persist in the immobile fraction, IF; the effective diffusion coefficient, D; and in FRET efficiency values when monomeric fluorescent proteins are employed. Membrane loading with cholesterol as well as reloading after depletion also affects the extent of prestin aggregation. These results suggest the temporal and spatial organization of prestin correlate with its function and may underlie the unique electromotile properties of outer hair cells.

#### 35 The Onset and Maturation of Prestin-Associated Charge Movement

**Matthew Volk**<sup>1</sup>, Scott Chaiet<sup>1</sup>, Lavanya Rajagopalan<sup>1</sup>, William Brownell<sup>1</sup>, Fred Pereira<sup>1,2</sup>

<sup>1</sup>Bobby R. Alford Department of Otolaryngology- Head and Neck Surgery, Baylor College of Medicine, <sup>2</sup>Huffington Center on Aging and Molecular and Cellular Biology, Baylor College of Medicine

Prestin is an important component of the membrane-based motor that enhances electromotility in outer hair cells. Its ability to greatly increase charge movement into and out of the lateral wall plasma membrane can be easily measured and has been described as a non-linear capacitance (NLC). Previous experiments have shown that the expression of prestin in the cell membrane of a human embryonic kidney (HEK 293) cell can induce NLC. No studies have fully characterized the time course of NLC onset and progression post-transfection. HEK 293 cells were transfected with an HA-prestin construct and cultured. Capacitance recordings of isolated cells were made at time points between 6 and 48 hours post-transfection, and the prestin-associated charge density

was calculated. All transfected cells (identified by fluorescence from an independently produced GFP encoded in the prestin construct) showed the characteristic bell-shaped NLC. Charge density increased with time post-transfection from a mean of 11.8 fC/pF between 10-20 hours after transfection to 25.0 fC/pF between 36-48 hours after transfection (p<0.001). The presence of a measurable NLC as early as 10 hours post-transfection correlates with immunofluorescence localization of prestin at the plasma membrane. Development of a regulated prestin expression system will allow for a more precise evaluation of prestin membrane expression and NLC.

### 36 Effect of Docosahexaenoic Acid on Prestin-Associated Charge Movement

**John Sfondouris**<sup>1</sup>, Lavanya Rajagopalan<sup>1</sup>, Frederick A. Pereira<sup>1</sup>, William E. Brownell<sup>1</sup>

<sup>1</sup>Baylor College of Medicine

The lateral membrane of the cochlear outer hair cell (OHC) is the site of a membrane-based motor that generates an electromechanical force enabling the OHC to amplify and fine tune sound in the mammalian cochlea. Prestin is a membrane protein that has a central role in OHC electromotility. Its ability to greatly increase charge movement into and out of the lateral wall plasma membrane can be easily measured and has been described as a non-linear capacitance (NLC). We have recently shown that membrane cholesterol content modulates the voltage at peak NLC in OHCs and in prestin-transfected human embryonic kidney (HEK) 293 cells. Interest in the effect of membrane docosahexaenoic acid (DHA) content on the function of prestin was motivated by its effect on rhodopsin function, a membrane protein found in the rod outer segments of the eye. Since rhodopsin and prestin function are both affected by membrane cholesterol content we sought to determine if other changes in membrane composition could also alter prestin function. The present study characterizes the effects of membrane DHA content on prestin function.

HEK 293 cells were transfected with a HA-prestin plasmid construct and cultured. The DHA content of the cell membranes was altered by incubating the cells for a short time in media rich in DHA. The NLC of the cells was then determined using whole-cell patch-clamp and compared to that of untreated HA-prestin transfected HEK 293 cells. Preliminary data shows that in HA-prestin transfected HEK 293 cells to which DHA is added there is a shift in the peak voltage of the NLC in the hyperpolarizing direction (p<0.005). Further characterization of the effects of DHA on NLC in prestin transfected HEK 293 cells should provide a better understanding of the effect of membrane composition on prestin-associated charge movement and on OHC electromotility.

(Supported by NIH-NÍDCD grants R01 DC00354 and T32 DC007367)

### 37 Prestin is Potentially Associated with Proteins Integral to Cellular Polarity

Jing Zheng<sup>1</sup>, Charles Anderson<sup>1</sup>, **Katharine Miller<sup>1</sup>**, Roxanne Edge<sup>1</sup>, Peter Dallos<sup>1</sup>, MaryAnn Cheatham<sup>1</sup> *Northwestern University* 

Prestin is responsible for outer hair cell (OHC) somatic electromotility (Zheng et al., 2000). Hence, prestin knockout mice lose frequency selectivity and sensitivity, as well as somatic electromotility. Interestingly, OHCs from these mice are not only shorter than wild-type OHCs but they also undergo apoptosis at a young age. Why the absence of prestin protein results in cellular death is unknown. Although physiological data suggest that OHC somatic electromotility is modified by other proteins, we know little about the interaction between prestin and its potential partners.

A membrane-based veast two-hybrid approach was used to identify prestin-associated proteins using an OHCenriched cDNA library and full-length prestin as bait. Several proteins were identified as potential prestinassociated proteins including two cellular polarity proteins: Vesicle-Associated membrane associated protein-associated protein (VAPA or VAP-33) and Frizzed3 (FZ3). Because FZ3 is localized asymmetrically at the lateral faces of hair cells, it may be involved in the planar orientation of hair bundles (Wang et al., 2006; Mountcouquiol et al., 2006). VAPA is also an integral membrane protein localized in either intracellular vesicles or at the tight junction in a variety cells and tissues. It is reported to be associated with microtubules and with the endoplasmic reticulum. In order to study the interactions of these two proteins with prestin, expression of VAPA and FZ3 was compared between wild-type OHCs and in OHCs lacking prestin. Additional experiments are conducted to determine if these proteins play important roles in OHC function.

[Supported by NIDCD Grants DC00089, DC006412 and The Hugh Knowles Center Leadership Fund)

### 38 The Roles of a Disorder Motif in the Prestin's C-Terminus

**Michael Podgorski**<sup>1</sup>, Tetsuji Yamashita<sup>1</sup>, Stephen White<sup>1</sup>, Jian Zuo<sup>1</sup>

<sup>1</sup>St. Jude Children's Research Hospital

The prestin's C-terminus is important in self-interaction, non-linear capacitance (NLC), and membrane targeting of prestin in outer hair cells. The STAS domain in prestin's Ctermini contains sequence with abundant non-synonymous substitutions compared to other SLC26 family members and these substitutions are conserved among mammalian prestins. Sequence analysis of mouse prestin's C-terminus using secondary structure and disorder predictive methods suggests a 60-70 residue loop constitutes one of the two discrete motifs in the STAS domain. We therefore hypothesize that this unique loop region serves as a conformational toggle between multiple states when membrane voltage changes. Recombinant proteins containing mouse prestin residues 499-744 (wildtype) or deletions of the loop sequence (negative controls) served to characterize this new motif. Limited proteolysis of the proteins yields peptides that define the loop boundaries as

assessed by MALDI-TOF mass spectrometry. Far UV circular dichroism (CD) of the wildtype protein indicates prevalent disorder in the secondary structure. Further CD studies comparing far UV and near UV CD spectra will discern between random coil and molten globule states. Gel filtration and native gel shift analysis display the dynamic self-interaction and an increased hydrodynamic radius indicative of disorder of the wildtype protein. Subsequent experiments utilizing synthesized 'loop' peptides and various point mutations in the loop region will identify residues key to the protein-protein interface. Western blot analysis and NLC measurements on the wildtype full-length protein and loop-deleted full-length protein will confirm relevance of this activity. The identification of such a disorder region in the C-terminus of prestin will provide insights to the functions of prestin and other SLC26A family members.

## 39 Mutation in the NQE (Saier) Motif in Prestin: Insights into Prestin Structure and Function

**Jun-Ping Bai**<sup>1</sup>, Dhasakumar Navaratnam<sup>1</sup>, Joseph Santos-Sacchi<sup>2</sup>

<sup>1</sup>Department of Neurology, Yale University Medical School, <sup>2</sup>Department of Otolaryngology, Yale University Medical School

SLC26 family of anion transporters has ten members in mammals and is highly conserved in bacteria, fungi, plants and animals. Non-linear capacitance has been established to be the electrical signature of prestins mechanical activity. The relationship between anion transport and NLC is hotly debated. A region that is conserved between all mammalian homologs is the Saier motif. Three residues in this motif (E419, N425 and L483) have been shown to have functional import in the plant (S. hamata) homolog SHST1. Moreover, achondrogenesis type 1b has been linked to two mutations in these residues in SLC26A2. Herein we constructed mutations at invariant residues, E374Q, N382D, L435P and L440P in prestin respectively. Preliminary data show the first three mutations abolished NLC in prestin, which is consistent with the effect on transport of mutating two of these residues in SLC26A2. L440P resulted in NLC with a shifted Vh. These results suggest that these conserved residues likely play important role in prestin's NLC function as well.

## 40 Prestin-Null Ohcs Transduced with Prestin Demonstrate Plasma Membrane Expression and Non-Linear Capacitance

**Anping Xia**<sup>1</sup>, Julian Wooltorton<sup>1</sup>, Donna Palmer<sup>1</sup>, Philip Ng<sup>1</sup>, Fred Pereira<sup>1</sup>, Ruth Anne Eatock<sup>1</sup>, John Oghalai<sup>1</sup>

\*Baylor College of Medicine

Prestin is a motor protein in the outer hair cell lateral wall plasma membrane and is essential for electromotility. The prestin null mouse has a deletion of prestin and results in loss of electromotility. Mammalian cells expressing prestin display a non-linear capacitance (NLC), widely accepted as its electrical signature. We sought to introduce prestin into outer hair cells (OHCs) from the prestin null mouse

using an adenovirus in order to study prestin expression and function. We created a helper-dependent adenoviral virus carrying pCMV-HA-prestin-IRES-hrGFP sequences (HDAd-prestin). We applied the HDAd-prestin to cultured HEK 293 cells and verified that GFP co-expressed with HA-prestin. Patch clamp of infected cells revealed the expected NLC while uninfected cells displayed linear capacitance. We next applied HDAd-prestin to organ of Corti cultures harvested from prestin null cochleae at postnatal day 2 or 3, and studied them 48 hours after infection. Confocal microscopy studies demonstrated that GFP was expressed within outer hair cells, supporting cells, spiral ganglion cells, and fibrocytes. Prestin immunostaining demonstrated that HA-prestin was expressed within the lateral wall of infected OHCs. We also performed patch clamp studies in OHCs from both wild-type and prestin null mice exposed to HDAd-prestin. We found NLC in GFP-positive OHCs, but not in GFPnegative OHCs. Control OHCs from cultures that were not exposed to HDAd-prestin did not demonstrate NLC. This study indicates that neonatal prestin null OHCs transduced with prestin express prestin within the plasma membrane and produce a NLC.

### 41 Modulation of Prestin Function Due to Cysteine Point Mutation

**Ryan M. McGuire**<sup>1</sup>, Fred A. Pereira<sup>1,2</sup>, Robert M. Raphael<sup>1</sup>

\*\*IRICE University, \*\*2Baylor College of Medicine\*\*

Outer hair cell electromotility requires the function of the voltage-sensitive molecular motor protein prestin (Slc26a5). Recently, gel mobility assays and fluorescence resonance energy transfer (FRET) experiments have confirmed the presence of specific prestin-prestin interactions and have implicated intermolecular disulfide bonding in prestin oligomerization. To better understand the nature of these protein interactions we have investigated the consequences of mutating prestin cysteines on complex formation and protein activity. The targeted cysteine residues are predominately clustered in the purported transmembrane domains, but the precise environments of the residues and the specific topology of prestin are currently unknown. Using a gerbil prestineGFP fusion protein as a template, we created several mutant forms with serine replacement of individual cysteine residues and expressed these constructs in human embryonic kidney (HEK) cells. The oligomerization state was investigated using gel electrophoresis and prestin function was analyzed by measuring the nonlinear capacitance using whole-cell patch clamping. Our patch clamp results reveal modulation of the setpoint at which half maximal charge transfer occurs, implying that particular cysteine residues may play a role in tuning the gain of the electromotile response. Further investigation of these residues will contribute to our understanding of the relationship between prestin oligomerization state and function.

## 42 Coherent Hard X-Rays can be Used to Visualize Soft Tissue in the Undisturbed Mammalian Cochlea

Claus-Peter Richter<sup>1</sup>, Chistoph Rau<sup>2</sup>, Ian Robinson<sup>2</sup> <sup>1</sup>Northwestern University, <sup>2</sup>Argonne National Laboratories It is important to examine cochlear morphology from many points of view, including comparative anatomy, cochlear developmental changes, malformation caused by genetic defects, changes related to diseases, sensory physiology, and cochlear modeling. At present, best imaging results were obtained from in situ experiments in the absence of tissue distortion. However, most contemporary imaging methods require invasive specimen preparation, are time consuming, or lack sufficient spatial resolution. Here we demonstrate а method that overcomes shortcomings. This method uses hard X-ray in-line phase contrast imaging. The cochlea is a particularly challenging system because it consists of bony and soft tissues, which are intimately connected. Bone has strong amplitude contrast, which tends to conceal the anatomy of the adjacent soft tissue. Therefore coherent X-rays are used to take advantage of the in-line phase contrast to visualize soft tissues and tomography is used to reduce the contributions from the bone.

Structures with low absorption contrast have been visualized using in-line phase contrast imaging. The experiments have been performed at the Advanced Photon Source (APS), a third generation source of synchrotron radiation at Argonne National Laboratories. The source provides highly coherent X-ray radiation with high photon flux (>10<sup>14</sup> photons/s) at high photon energies (5-70 keV). Thick gerbil cochlear slices have been imaged and were compared with those obtained by light microscopy. Furthermore, intact gerbil cochleae have been imaged to identify the soft tissue structures involved in the hearing process.

Supported by the NSF IBN-415901, DOE DEFG02-91ER45439, DOE DE-AC05-00OR22725, DOE W-31-109-ENG-38

# | 43 | Imaging Inner Ear Organogenesis in Xenopus Laevis and Xenopus Tropicalis with Fourier Domain Optical Coherence Tomography

**Lina Urquidi**<sup>1</sup>, Miranda Salt<sup>1</sup>, Daniel J. Kane<sup>2</sup>, Kristen A. Peterson<sup>2</sup>, Andrei B. Vakhtin<sup>2</sup>, Elba E. Serrano<sup>1,3</sup>

<sup>1</sup>Biology Department, New Mexico State University, <sup>2</sup>Southwest Sciences, Inc., <sup>3</sup>MIT Cell Decision Processes Center

We present results of preliminary efforts to obtain cross-sectional images of the inner ear of larval (stages 45-50) Xenopus laevis and Xenopus tropicalis using optical coherence tomography (OCT). OCT uses light to detect boundaries and interfaces between different materials, as well as differences in absorption or scattering properties. OCT can achieve higher resolution (1-10  $\mu m)$  than ultrasound, MRI or X-ray tomography at depths of up to 4 mm and has the advantage that it can be used to acquire non-destructive optical images in live specimens without

the use of contrast agents such as fluorophores. Additionally, manipulation of image data acquired in one plane allows computational reconstruction of orthogonal image planes. We used Fourier domain OCT with a superluminescent 1300 nm LED source to obtain images with 9 µm resolution along the z axis. An optical scanner was used to acquire 2-D images of the whole animal in the xz (transverse) plane, where z is the depth of the sample, in 4??m increments. These images were compared with brightfield images of paraffin-embedded specimens, sectioned to 10 µm and stained with Harris's hematoxylin and eosin Y or with toluidine blue, and then captured with a Qlmaging digital camera. Orthogonal planes that correspond to coronal (xy) and sagittal (yz) histological sections were computationally reconstructed from the image data. Comparison of OCT inner ear images with brightfield images of the same stage animal demonstrates the feasibility of OCT for imaging the inner ear throughout organogenesis. Results highlight similarities and differences between OCT images and those acquired from stained sectioned specimens. Our long-term goals are to develop OCT applications for continuous studies of organogenesis in individual specimens, and to acquire rapid, real-time in-vivo images of the developing ear in normal and genetically manipulated Xenopus specimens. Supported by NIH S06GM008136, R01DC003292, P50GM068762, R44HL069108.

### 44 Lipid Raft Expression in the Chick Auditory Periphery

**Li Qian Liu<sup>1</sup>**, Andrew Cheng<sup>1</sup>, Chintan Patel<sup>2</sup>, R. Keith Duncan<sup>1</sup>

<sup>1</sup>Kresge Hearing Research Institute, University of Michigan, <sup>2</sup>Division of Biology and Medicine, Brown University

Cellular signaling is often organized into discrete, specialized domains. While this compartmentalization is important for normal cell function, the mechanisms that underlie this structural segregation remain largely unknown. Recent research has revealed specialized areas within the cell membrane called lipid rafts, which have been associated with ion channel signaling and pathways involved in metabolic stress. Our objective was to identify cell types within the chick auditory basilar papilla that expressed lipid rafts and to localize these rafts to specific domains within those cells. Cholera toxin B (CTxB) incorporates into ganglioside GM1 containing lipid rafts. Fluorescently tagged CTxB labeled the cell membranes of isolated auditory neurons and sensory hair cells from the chick basilar papilla. Labeling in hair cells was punctate and localized to the basal pole of the cell body. Based on these observations, we focused attention on caveolae as a subset of lipid rafts, and the caveolin proteins that makeup these specialized structures. Three caveolin genes have been identified in vertebrates (cav1-3). While cav1 and cav2 are ubiquitously expressed, cav3 is specifically expressed in skeletal muscle and glia in the central nervous system. All three caveolin genes were found within the chick basilar papilla and auditory nerve. Semiquantitative PCR showed expression levels similar to

brain. Antibodies to human cav3 cross-reacted with chick tissues, extensively labeling the auditory nerve ganglion and sensory epithelia of the basilar papilla. Experiments with isolated auditory neurons and hair cells confirmed the presence of caveolin based lipid rafts within these cells. This is the first description of cav3 expression in sensory cells.

Supported by NIH P30 DC05188.

## | 45 | Intimate Interaction Between Clc-K and Barttin as Determined by Fluorescence Resonance Energy Transfer (FRET) Analysis

**Karen J. Mu**<sup>1</sup>, Liping Nie<sup>1</sup>, Wei-Nan Lian<sup>1</sup>, Wei-Ping Yu<sup>1</sup>, Ana E. Vazquez<sup>1</sup>, Tsung-Yu Chen<sup>1</sup>, Ebenezer N. Yamoah<sup>1</sup> \*\*University of California, Davis

Barttin is an auxiliary subunit of the CIC-K channel and its functional importance in sound transduction is underlined by the fact that mutations result in Bartter syndrome type IV, of which deafness is a component. Barttin has been identified as crucial for the translocation and function of CIC-K. However, the stoichiometry of the assembly between barttin and the CIC-K dimer is not known.

We employed Fluorescence Resonance Energy Transfer (FRET) technology in order to determine the composition of CIC-K channels on the surface membrane of human embryonic kidney (HEK) cells. CIC-K1-CFP, CIC-K1-YFP, barttin-CFP and barttin-YFP fusion protein constructs were generated using a modified pEGFP-N3 vector. Coexpression of CIC-K1-CFP and barttin-YFP fusion proteins displayed a positive FRET signal, demonstrating that these subunits do indeed form an intimate physical interaction. Interestingly, cells co-expressing barttin-CFP, barttin-YFP and CIC-K1 also displayed a positive FRET signal, implicating the assembly of more than one barttin subunit with the CIC-K1 dimer in the assembly of the functional channel.

A unique property of CIC-K1 channels within the CIC family is the potentiation of current upon increased extracellular calcium, and we have observed this phenomenon in macroscopic recordings from Xenopus laevis oocytes expressing CIC-K and barttin. Upon examination of this effect in HEK cells co-expressing the fusion protein constructs using 1 mM EGTA and 5 and 20 mM of extracellular calcium, we observed that the increase of extracellular calcium has an effect on FRET efficiency, reflecting that the observed potentiation of current upon increasing extracellular calcium may be due to modifiable physical interactions between the CIC-K and barttin subunits. These findings provide a working model to help us better understand the structure and function of CIC-K channels.

This work was supported by the Research Fund of the American Otological Society, Inc.

## 46 Characterization of Mouse Utricle and Saccule Binding Epitopes by M13 Phage Panning

**Peter Gochee**<sup>1</sup>, Susanna Pfannenstiel<sup>2</sup>, Diane Durham<sup>1</sup>, Hinrich Staecker<sup>1</sup>

<sup>1</sup>Department of Otolaryngology, University of Kansas Medical Center, Kansas City, Kansas, <sup>2</sup>Department of Otolaryngology, University of Heidelberg, Germany
One of the challenges of developing specific drugs for the inner ear is targeting individual cell types. Conjugation of drugs or gene therapy vectors directed to cell specific peptides may allow the treatment of individual cell types within the inner ear. We have identified a series of peptides that bind bioavailable epitopes in the mouse inner ear using phage display.

Phage display is a technique in which a library of variants of a peptide is expressed on the outside of a phage virion, while the genetic material encoding each variant resides on the inside. This creates a physical linkage between each variant protein sequence and the DNA encoding it, which allows rapid partitioning based on binding affinity to a given target molecule by an *in vitro* selection process called *panning*.

Three libraries of M13 bacteria phage consisting of 1) 7 random amino acids, 2) 12 amino acids or 3) 7 amino acids flanked by a pair of cysteine residues to create a binding loop, attached to the N-terminus of the minor coat protein pIII were prepared. These libraries were screened against saccule and utricle cultures isolated from C57BI/6 mice. After binding to the tissue in vitro, the phage were and amplified in E. coli. Additional eluted binding/amplification cycles were performed to enrich the pool in favor of binding sequences. After 3 rounds of amplification, individual clones were characterized by DNA sequencing. The sequences were queried against protein databases for homology to known inner ear proteins. Immunofluorescent staining of individual phage clones was performed after binding to macular cultures to localize each clone's binding site.

Our data demonstrates that phage panning of mouse saccule and utricle isolates generates ear specific amino acid sequences and selective binding to specific cell populations within the mouse inner ear. These characterized sequences may allow selective binding and delivery to cells within the inner ear.

# 47 Peripherin Shows Increased Expression in Cultured Rat Spiral Ganglion Neurons, and is Present in all Neuritic Outgrowth from Spiral Ganglion Explants

Jacob Husseman<sup>1</sup>, Allen Ryan<sup>1</sup>

<sup>1</sup>Departments of Surgery/Otolaryngology and Neurosciences, UCSD School of Medicine and VA Medical Ctr

Peripherin is an intermediate filament present in specific neuronal populations. In the cochlea, peripherin is present in type II but not type I spiral ganglion (SG) neurons. We evaluated peripherin expression in cultured SG neurons, with and without the organ of Corti (oC). Intact apical turn, including both SG and oC, as well as isolated SG explants,

were harvested from rat pups from postnatal day 3 (p3) to p10 and cultured for up to 14 days. Immunolabeling was performed for peripherin and neurofilament 200 (NF). Western blotting for peripherin was also carried out on p5 SG explants cultured up to four days. As expected, neurons and fibers of intact apical turns as well as SG explants demonstrated NF labeling in all conditions. Prior to culture, intact apical turns demonstrated peripherin labeling of fibers projecting to the outer hair cells at all ages tested, confirming specificity for type II fibers. After even one day of culture, peripherin labeling in whole mounts appeared to be markedly enhanced in type II fibers, and low levels of expression were observed in type I fibers. In contrast, all neurite outgrowth from cultured SG explants showed strong labeling for peripherin, even though survival of neurons in the explants far exceeded the expected number of type II neurons. Uniform peripherin labeling of neurites persisted for 14 days of culture. Western blotting confirmed up-regulation of peripherin expression after 4 days of culture. The results indicate that culture up-regulates peripherin expression in SG neurons. Despite this upregulation, differential expression in type II neurons is maintained in culture when SG neurons retain contact with the oC. However, SG neurons isolated from the oC uniformly up-regulate peripherin, and differential expression is lost. The data suggest the possibility that contact with hair cells may regulate peripherin expression in SG neurons.

Supported by grant DC00139 from the NIDCD and the Research Service of the VA.

## 48 Role of Membrane Surface Change in Membrane-Based Electromechanical Coupling

**Linda Lee<sup>1</sup>**, Feng Qian<sup>2</sup>, William Brownell<sup>1</sup>, Bahman Anvari<sup>3</sup>

<sup>1</sup>Baylor College of Medicine, Bobby R. Alford Dept of Otolaryngology - Head and Neck Surgery, <sup>2</sup>Rice University, Dept of Bioengineering, <sup>3</sup>University of California Riverside, Dept of Bioengineering

Many cell types, including cochlear outer hair cells, axons, and some cultured mammalian cells, are able to mechanically respond to changes in transmembrane electrical potential. The mechanism responsible for this electrically-induced mechanical force (EMF) generation may reside within the cell's plasma membrane, and result from the interaction between the transmembrane electrical field and membrane surface charge. To investigate the role of membrane surface charge in EMF generation, we expose various cell types to the anionic amphipathic agent salicylate, which is known to reduce outer hair cell electromotility, and measure the EMF and membrane conductance. Using a technique that combines optical trapping with patch-clamping, we form membrane tethers from human embryonic kidney (HEK) cells and prestintransfected HEK cells, and quantify EMF. Our preliminary results indicate that salicylate reduces plasma membrane tether EMF in both normal and prestin-transfected HEK Presence of 10mM salicylate concentration increased the whole-cell membrane conductance in prestin-transfected HEK cells but not in normal HEK cells. To test whether the conductance increase results from the transfection process, GFP-transfected HEK cells lacking prestin were also exposed to salicylate as a control. Initial results show that the conductance of the GFP-transfected cells without prestin is not significantly increased after exposure to salicylate. The increase in membrane conductance of prestin-containing cells is likely caused by a direct interaction of salicylate with the cell's plasma membrane. These experiments help provide insight into the role of membrane surface charge in EMF, and the role of prestin in cell membrane conductance.

Work supported by R01 DC02775, BES-0522862, T32 DC007367 and R90 DK071504.

### **49** Extra-Cochlear Manifestations of the DFNA9 Hereditary Deafness

**Jose Fayad**<sup>1</sup>, Robert Gellibolian<sup>1</sup>, Fred Linthicum<sup>1</sup>

\*House Ear Institute

An autosomal dominant progressive sensorineural deafness. DFNA9, with characteristic inner histopathological changes was described by Khetarpal et al in 1991. The major finding was the replacement of the normal cellulosity of the spiral ligament, limbus, and stroma of the vestibular sensory organs by a homogeneous acidophilic deposit. The deposit in the limbus appeared to have resulted in the disappearance of the peripheral processes that normally connect the hair cells that were present in their specimens with the spiral ganglion cells that were also present, but somewhat reduced in number. These findings were subsequently mapped to chromosome 14q12-13, with the COCH gene being the underlying molecular player. An abundance of cochlin, the product of the COCH gene, is found in the inner ear, particularly in the cochlea. Cochlin is exported from cells in the inner ear and becomes part of the extracellular matrix. Two segments of the cochlin protein, called the LCCL and factor A domains, coordinate interactions with other proteins in the extracellular matrix.

Two temporal bones in our laboratory with the same phenotype found in DFNA9 temporal bones also exhibit similar changes in the incudomalleolar joint and tympanic membrane, when studied under light microscopy. The joint is hypertrophied and the tympanic membrane is thickened by the formation of cartilage within its fibrous layer, a previously undescribed finding. Staining with Alcian Blue shows that the cartilage of the incudomalleolar joint and tympanic membrane is different than the amorphous material seen in the spiral ligament.

PCR-directed DNA mutational analysis of the 5' end of the LCCL domain, which contains the S51P and V66G mutations, from our samples showed none of the aforementioned genetic changes. Further analysis of the 3' end, encompassing the G88E, V104Del, and W117R mutations, is currently underway. Studies are also planned for immunolabeling of the COCH protein product.

## 50 Oxidative and Nitrative Stress Contributes to Hearing Loss in Pendred Syndrome.

**Ruchira Singh<sup>1</sup>**, Nilhan Gunhanlar<sup>1,2</sup>, Philine Wangemann<sup>1</sup>

<sup>1</sup>Kansas State University, <sup>2</sup>Bilkent University

Mutations in the pendrin (Slc26a4) gene cause deafness in Pendred syndrome. Slc26a4 is primarily expressed in the inner ear, thyroid and kidney. Previous studies show hyperpigmentation in stria vascularis (SV) of Slc26a4 mice, implicating oxidative stress. The goal of this study was to determine if increased oxidative stress correlated with the onset of hearing at postnatal day 11 (P11). Slc26a4<sup>-/-</sup>(KO) mice were compared to Slc26a4<sup>+/-</sup>(HET) mice. Studies were focused on four ages: P10 and P15 (before and after the onset of hearing), P30-40 (adolescent) and P75-150 (young adult). Data were obtained from pendrin-expressing tissues, SV, spiral ligament (SL), thyroid and kidney and from non-expressing tissues, liver and spleen. Direct and indirect evidence for oxidative stress was obtained. The presence of oxidized and nitrated proteins (Western blots) served as direct evidence. Indirect evidence included an increase in the transcript (quantitative RT-PCR) or protein expression ratio (Western blots) of transferrin (trf) and transferrin receptor (trfr), a decrease in transcript expression of superoxide dismutase 2 (sod2), metallothionein III (mt3) and an increase in the total iron (Fe) content (ferrozinespectrophotometry). In SV of KO mice, oxidized and nitrated proteins were increased at P10 and P30. Expression of mt3 and sod2 was decreased at P15 and the trf/trfr ratio and Fe content were elevated at all ages. In SL of KO mice, oxidized and nitrated proteins were not seen at P10 but at P30. Expression of mt3 and sod2 was unchanged at P15 and no differences in the trf/trfr ratio and Fe content were observed at all ages. In thyroid of KO mice, an increase in oxidized and nitrated proteins was observed at P30. The trf/trfr ratio was increased at P30 and Fe content was elevated at all ages. In kidney of KO mice, oxidized and nitrated proteins were unchanged at P30. No difference in the trf/trfr ratio was observed at P30. No difference in Fe content was seen at all ages. In liver of KO mice, oxidized proteins were increased and no difference in nitrated proteins was seen at P30. Increased trf/trfr ratio was observed at P30 and Fe content was elevated at all ages. In spleen of KO mice, no difference in oxidized or nitrated proteins or trf/trfr ratio was observed at P30. No difference in Fe content was seen at all ages. In conclusion, these data suggests that oxidative stress in SV of KO mice precedes the onset of hearing and could thereby contribute to hearing loss in KO mice. Further, oxidative stress in the KO mice is not a systemic phenomenon and does not affect all pendrin expressing

Supported by NIH-R01-DC01098, NIH P20 RR017686

51 Acidification and Elevation of the Endolymphatic Ca<sup>2+</sup>, Loss of *KCNJ10* Expression and Loss of the Endocochlear Potential Contribute to the Failure to Develop Hearing in the Pendred Syndrome Mouse Model

**Philine Wangemann**<sup>1</sup>, Tao Wu<sup>1</sup>, Kazuhiro Nakaya<sup>1</sup>, Rajanikanth J. Maganti<sup>1</sup>, Sairam V. Jabba<sup>1</sup>, Donald Harbidge<sup>1</sup>, Joel Sanneman<sup>1</sup>, Daniel C. Marcus<sup>1</sup>

<sup>1</sup>Kansas State University

Pendred syndrome, characterized by childhood deafness and postpuberty goiter, is caused by mutations of SLC26A4, which codes for pendrin. In the present study, mice that lack a complete Slc26a4 gene (KO) were compared to hetero- (HET) or homozygous controls Hearing was evaluated by ABR. (WILD). endocochlear potential (EP), pH and Ca<sup>2+</sup> were measured double-barreled ion-selective electrodes. Degeneration of stria vascularis and the organ of Corti was evaluated by phalloidin-staining and immunolabeling of Kcnj10, Kcng1, calretinin and synaptophysin. At postnatal day 10 (P10), cochlear endolymph of KO was lower in pH (pH 7.1 vs 7.6) and higher in Ca<sup>2+</sup> (0.8 vs 0.08 mM) and apical cell surfaces of strial marginal cells were larger. ABRs were flat and expression levels of Kcng1 and Kcnj10 were similar in KO and HET. Cellular organization of the organ of Corti appeared normal with intact hair bundles and normal-appearing inner and outer hair cells, afferent and efferent innervation. Development of HET from P10 to P15 was associated with an increase in Kcni10 expression in intermediate cells, a growth of the EP from 45 to 80 mV, a reduction in endolymph Ca<sup>2+</sup> from 0.08 to 0.02 mM and an improvement of ABR thresholds from >90 dB to 30 dB. In contrast, in KO Kcnj10 expression in intermediate cells was largely lost while Kcnq1 expression in marginal cells was maintained. The EP decreased from 18 to 9 mV, endolymph Ca<sup>2+</sup> rose from 0.8 to 2.2 mM, ABR thresholds remained at >90 dB and first signs of degeneration appeared in some, but not all, preparations of organ of Corti. Further development of KO from adolescence (P30-P45) to young adulthood (P60-P150) was associated with degeneration of stria vascularis and organ of Corti. Apical surface sizes of marginal cells became uneven. Surface enlargements were associated with a loss of Kcng1 expression and surface reduction with the persistence of Kcng1 expression. Expression of mRNA markers for marginal cells in stria vascularis was reduced but for intermediate and basal cells was unchanged in KO compared to WILD. Degeneration of the organ of Corti progressed from a disorderly appearance of outer hair cell stereocilia to a loss of afferent and efferent innervation. In summary, these data demonstrate that dysregulation of cochlear fluid homeostasis, which is incompatible with the development of hearing, precedes structural degeneration in the organ of Corti. A window of opportunity to restore normal development of cochlear function appears to close early in adolescence with degeneration of stria vascularis and organ of Corti.

Supported by NIH-R01-DC01098, NIH-R01-DC000212 and NIH-P20-RR017686

# 52 Acid Sensitivity of Ca<sup>2+</sup> Absorption in Vestibular System Leads to Increased Endolymphatic [Ca<sup>2+</sup>] in Pendrin Knockout Mice

**Kazuhiro Nakaya**<sup>1</sup>, Donald Harbidge<sup>1</sup>, Philine Wangemann<sup>1</sup>, Bruce Schultz<sup>1</sup>, Daniel Marcus<sup>1</sup>

<sup>1</sup>Kansas State University

The low luminal Ca2+ concentration of mammalian endolymph in the inner ear is required for normal hearing and balance. We recently reported the expression of a Ca<sup>2+</sup> transport system based on the epithelial Ca<sup>2+</sup> channel ECaC1 (trpv5) in primary cultures of rat semicircular canal (SCCD) epithelium [Yamauchi et al., BBRC, 2005]. Transcript expression of several genes of the transport system was under control of vitamin D. These findings were based on the measurements of transport system transcripts and trpv5 protein in these cells. Further, knockout of the CI/HCO<sub>3</sub> exchanger pendrin (slc26a4) in mice was shown to acidify and increase Ca2+ concentration of cochlear endolymph [Wangemann et al., ARO 2007]. In the present study, we tested for functional Ca<sup>2+</sup> transport via the *trpv5* pathway using radiotracer fluxes and tested for homology between the cochlear and vestibular systems for the effects of slc26a4 knockout. Monolayers of SCCD cells were grown on permeable supports and cellular uptake of  ${}^{45}\text{Ca}^{2+}$  was measured individually from the apical and basolateral sides. We found that 1) cellular uptake of radiotracer was greater from the apical than from the basolateral side, consistent with transepithelial absorption of Ca<sup>2+</sup>; 2) absorptive flux was greater after incubation with vitamin D: 3) a cocktail of three *trpv5* inhibitors reduced apical uptake of <sup>45</sup>Ca<sup>2+</sup>; 4) each of the inhibitors was effective by itself (gadolinium, ruthenium red, lanthanum); 5) net 45 Ca2+ absorption was dramatically inhibited by apical acid pH and was stimulated by apical alkaline pH, consistent with the known sensitivity of rabbit *trpv5* to extracellular pH [Yeh et al., JBC, 2003]. The endolymphatic potential, pH and [Ca<sup>2+</sup>] of the utricle were measured in wild type, heterozygous and knockout slc26a4 mice. Absence of slc26a4 drove endolymphatic potential more negative, reduced the pH and increased the [Ca<sup>2+</sup>] of the utricle compared to wild type and heterozygous mice. These data demonstrate that the transcripts and protein found earlier in the SCCD form a functional Ca2+ absorptive mechanism and are consistent with the hypothesis that acidification of endolymph by null expression of the HCO<sub>3</sub> transporter slc26a4 inhibits Ca<sup>2+</sup> absorption via *trpv5*, thus dramatically elevating endolymphatic [Ca<sup>2+</sup>]. Inhibition of the *trpv5* pathway in conditions that acidify endolymph are therefore expected to result in compromised hearing and balance.

Supported by NIH grants R01-DC00212, P20-RR017686 (DCM) and R01-DC01098 (APW) and USDA 2003-35206-14157 (BDS).

### **53** Does Organic Cation Transporter 2 Exist in the Rat Cochlea?

**Victoria Hellberg**<sup>1,2</sup>, Caroline Gahm<sup>1,2</sup>, Hans Ehrsson<sup>3</sup>, Göran Laurell<sup>1,4</sup>

<sup>1</sup>Department of Otorhinolaryngology and Head & Neck Surgery, Karolinska University Hospital, Sweden, <sup>2</sup>Center for Hearing and Communication Research, Karolinska Institute, Stockholm, Sweden, <sup>3</sup>Karolinska Pharmacy, Karolinska University Hospital, Stockholm, Sweden, <sup>4</sup>Department of Clinical Sciences, University of Umeå, Umeå, Sweden

Introduction: Cisplatin is a potent platinum anti-cancer drug used world-wide. Cisplatin has nephrotoxic and ototoxic dose-limiting side effects. Little is known about the mechanisms by which cisplatin enters the inner ear. The basolateral membrane in the kidney and stria vascularis in the inner ear shows some similarities that might influence on the organ specific toxicity. Organic Cation Transporter 2 (OCT2) has been identified in the renal proximal tubules and it plays an important role in the uptake of cisplatin in the kidney. This study was undertaken to investigate if OCT2 can be detected in the rat cochlea. Materials and methods: OCT2 expression was investigated in cochleas from 10 Sprague-Dawley rats. The cochleas were fixed in 4 % paraformaldehyd and paraffin embedded. Sections of the whole cochlea were analyzed immunohistochemistry and immunofluorescens.

Result: The expression of OCT2 in the lateral wall of the cochlea using immunohistochemical methods will be presented. If it turns out that OCT2 is widely present in the cochlea, the next step to be undertaken is to test the hypothesis that OCT2 located in the basolateral membrane of the lateral wall is involved in the uptake of cisplatin.

#### 54 Dexamethason Concentration Gradient Along Scala Tympani of the Guinea Pig Cochlea After Round Window Drug Administration

**Stefan Plontke**<sup>1</sup>, Thorsten Biegner<sup>1</sup>, Bernd Kammerer<sup>1</sup>, Alec N. Salt<sup>2</sup>

<sup>1</sup>University of Tübingen, <sup>2</sup>Washington University School of Medicine

During the last years, the use of intratympanically applied glucocorticoids for the treatment of inner ear disease has become of increasing clinical interest. Although measurements of intracochlear glucocorticoid concentrations after round window (RW) application exist there is very limited information on the distribution of these drugs in the ear. It has been predicted, based on computer simulations, that substantial concentration gradients with lower concentrations in apical turns occur after RW application (Plontke and Salt, Hear Res. 2003;132:34-42). With a recently developed sequential apical sampling method these concentration gradients along the cochlea were confirmed with ionic markers (Mynatt et al. JARO. 2006;7:182-193) and for gentamicin (Plontke et al. 2006; ARO, Abs #611).

Dexamethasone (DEX, 10 mg/ml) was administered to the RW niche of guinea pigs (n=9) in vivo for 2 to 3 hours. Perilymph was then sampled from the cochlear apex using a sequential-sampling protocol. Ten samples (1µl each) were taken into calibrated capillary tubes. Analysis of the samples showed the DEX content of the first sample in each experiment (dominated by perilymph from apical regions) to be substantially lower than that of the third and fourth sample (dominated by basal turn perilymph), qualitatively demonstrating the existence of a concentration gradient along scala tympani (ST). Sample data were then interpreted using a finite element model (http://oto.wustl.edu/cochlea/). This approach permitted the longitudinal gradients of DEX along ST to be quantified. Both, absolute concentration in ST and baso-apical gradient were found to vary substantially. If this variability also occurs under clinical conditions, this may be one explanation for the heterogenity of outcome which is observed after intratympanic therapy for sudden hearing

Work supported by Univ. of Tuebingen fortune grant 1001-0-0 (SP) and NIH/NIDCD grant DC01368 (AS).

### **[55]** Factors Influencing Round Window Membrane Permeability in Guinea Pigs

**Anthony A. Mikulec<sup>1</sup>**, Alec N. Salt<sup>2</sup>

<sup>1</sup>St. Louis University School of Medicine, <sup>2</sup>Washington University School of Medicine

Although the local application of drugs to the inner ear is increasingly being used to treat disorders in the clinic, the drug levels achieved by specific application protocols have not been well established. Recent pharmacokinetic studies (Hahn et al. Hear Res. 212, 2006, 236)(Mynatt et al. JARO 7, 2006, 182) suggest that the perilymph drug levels achieved by drug applications to the round window (RW) niche are highly variable between animals. The main source of variation appears to arise from RW membrane permeability differences in different animals. Studies have also suggested that RW membrane permeability can be influenced by such factors as the background composition of the applied drug solution, by intracochlear pressure and by dehydration of the RW membrane. In the present study we screened the composition (pH and osmolarity) of drugs commonly applied to the RW niche. Drug formulations were often far from physiologic values with pH values ranging from 4.25 to 8.22 and osmolarity varying from 190 mOsm to over 600 mOsm. In other experiments we systematically varied solution osmolarity while monitoring the rate of entry of the marker ion TMPA into perilymph using an ion selective microelectrode sealed into the basal turn of scala tympani. Solution of normal osmolarity (290 mOsm) containing 2 mM TMPA was irrigated across the RW membrane at 5 uL/min to 40-60 mins, followed by 2 mM TMPA solution with lower (190 mOsm) or higher (620 mOsm) osmolarity. TMPA entry was faster for solutions of non-physiologic osmolarity. Computer simulation of the curves of TMPA concentration with time suggested that RW membrane permeability could be increased by up to a factor of two by alterations of solution osmolarity. The influence of other components in commercial drug

formulations, such as the preservatives EDTA and benzyl alcohol, on RW membrane permeability are currently being assessed. Understanding the factors that control the entry of drugs into the cochlea will allow better control of perilymph drug levels to be achieved.

This work was supported by a grant from the American Otological Society (TM).

#### 

**Alec N. Salt**<sup>1</sup>, Jared J. Hartsock<sup>1</sup>, Davud B. Sirjani<sup>1</sup>, Stefan K. Plontke<sup>2</sup>

<sup>1</sup>Washington University School of Medicine, <sup>2</sup>University of Tubingen

Local delivery of drugs to the inner has advantages over systemic delivery and is increasingly being used in clinical practice. In this study, we have investigated the feasibility of performing a single, "one-shot" drug injection into perilymph of the basal turn instead of a commonly used application to the round window membrane. The substance injected trimethylphenylammonium (TMPA) that is detected in low concentrations with ion-selective microelectrodes. Perilymph pharmacokinetics of TMPA following injection was assessed in acute experiments using apical sampling techniques (Mynatt et al. JARO 7, 182-93, 2006). The amount of TMPA retained in perilymph was compared for different injection protocols. In each protocol, 2 mM TMPA was injected at a rate of 100 nl/min for 20 min and perilymph was sampled 10 min after the injection stopped. With the injection pipette sealed into the bony wall of scala tympani in the basal turn, the measured TMPA in samples was close to that predicted by simulations, with 38% of the injected TMPA recovered in the samples. For similar TMPA injections with beveled pipettes (20 µM tip diameter) carefully inserted through the round window membrane, TMPA levels in perilymph were far lower (by a factor of approximately 8) and only 6.6% of the injected TMPA was recovered in the samples. This demonstrates that perilymph leakage around the injection pipette results in loss of TMPA from scala tympani. In a third protocol, a layer of Healon gel (1% hyaluronate; Advanced Medical Optics, Inc) was applied to the round window membrane before it was penetrated by the beveled injection pipette. Measured sample TMPA levels were close to those obtained with the pipette sealed into the bony wall, with 34% of the injected TMPA recovered in the samples. These studies show that in order to perform quantitative one-shot drug applications to the perilymph by injection through the RWM, perilymph leakage must be controlled. In the present study, Healon was able to control the TMPA washout caused by perilymph leakage.

Work supported by NIH/NIDCD grant DC01368 (AS).

## 57 In Vivo Effects of Reduced-Sodium Perilymph Perfusion on Hair Cell and Neural Potentials

Greg A. O'Beirne<sup>1,2</sup>, Robert B. Patuzzi<sup>2</sup>

<sup>1</sup>University of Canterbury, <sup>2</sup>University of Western Australia To determine the functional significance of the sodiumtransport mechanisms of the OHCs in vivo, the effect of reduced perilymphatic sodium on cochlear potentials was investigated by perfusion of scala tympani with a modified artificial perilymph. The Na<sup>+</sup> concentration of the artificial perilymph was reduced by almost 95% (from 150 mM to 8 mM) by substitution with choline, and resulted in an estimated 80% reduction in perilymphatic Na<sup>+</sup> on perfusion through scala tympani. OHC function was assessed using Boltzmann analysis of the low-frequency CM and measurement of the high-frequency summating potential recorded at the round window. Neural thresholds and waveforms were monitored at multiple frequencies. To ensure that the observed effects were due to the reduced Na<sup>+</sup> concentration rather than direct action of choline, experiments were conducted that employed i) pre- and coperfusion with the nicotinic ACh receptor antagonist hexamethonium chloride, and ii) the use of NMDG<sup>+</sup> instead of choline to replace Na<sup>+</sup>.

The >10 minute perfusions caused a transient 2-6% increase in the maximal CM amplitude, a 6-15% increase in MET sensitivity, and a small operating-point shift towards scala tympani that was followed by a larger sustained shift in the opposite direction. These effects were found to be reproducible and reversible, and were largely consistent with an increase in OHC cytosolic Ca<sup>2+</sup> concentration due to a reduction in Ca<sup>2+</sup> efflux through the Na<sup>+</sup>/Ca<sup>2+</sup> antiport (Ikeda et al., 1992). The use of NMDG+ as the Na<sup>+</sup>-substitution ion produced similar effects to the choline, and blockade of the ACh-sensitive Ca<sup>2+</sup> channels of the OHCs by hexamethonium produced no difference in the effects observed. Reductions in the amplitude of the CAP and spontaneous neural noise indicated a distinct neural effect in addition to the hair cell effects. The experimental results from the guinea pig are compared with simulated perfusions carried out in a mathematical model of cochlear regulation.

#### 58 Glycyrrhetinic Acid Activates a Cation Conductance in Dispersed Smooth Muscle Cells of Guinea Pig Mesenteric and Inner Ear Arteries

Zhi-Gen Jiang<sup>1</sup>, Bing-Cai Guan<sup>1</sup>

<sup>1</sup>Oregon Hearing Research Center, Oregon Health & Science University

Gap junctions play a critical role in intercellular electrical and chemical communications and thus in the normal function and development of many organs including the cochlea. Several forms of familial hearing loss result from mutations in connexins, the gap junction building proteins. Glycyrrhetinic acid (GA) compounds are widely used gap junction blockers but often associated with non-junctional membrane actions that are poorly understood. Using whole-cell recording techniques on smooth muscle cells

acutely dissociated from the spiral modiolar artery (SMA) and mesenteric artery (MA), we analyzed membrane actions of the most commonly used 18BGA. We found: 1) With physiological internal and external solutions at room temperature, dissociated smooth muscle cells of the MA showed a resting potential (RP) of  $-16.5 \pm 1.7$  mV (n=5), input resistance ( $R_{in}$ ) of 4.1  $\pm$  0.4  $G\Omega$  (n=8) and input capacitance ( $C_{in}$ ) of 13.1 ± 0.5 pF (n = 8); whereas, in the SMA, they showed  $-20.5 \pm 2.3$  mV (n=5),  $4.7 \pm 0.4$  G $\Omega$ (n=12) and  $6.2 \pm 0.2$  pF (n = 12). The I/V relation of the whole cell current showed a significant outward rectification when the depolarization was beyond -30 mV and inward rectification when the hyperpolarization beyond -40 mV. 2) 18βGA (30μM) caused a small inward current  $(-3.17 \pm 0.98 \text{ pA. ranged 0 to 12 pA. n=18. at a holding})$ potential of -40 mV) associated with an increase in baseline noise in cells of both arteries. The effects are initially small and reversible but accumulative upon long lasting or repeated applications. 3) The net current induced by 18βGA showed an I/V curve with positive slope  $(79.6 \pm 27.8 \text{ pS}, \text{ ranged from 0 to 217 pS})$  between -140and ~-20 mV, while frequently with a negative slope between -20 and +20 mV. Step depolarizations showed an inhibition of the delayed rectifier K<sup>+</sup>-channel (K<sub>V</sub>) in the latter voltage range. 4) When18βGA-induced current showed approximately linear I/V with a positive slope between -140 and -40 mV, the I/V curve had a reversal potential at -13.6 ± 4.6 mV (n=8, ranged between -24 & 9 mV, n=4). We conclude that, in addition to gap junction blockade, 18BGA exerts complex membrane actions including opening of a cation conductance and inhibition of a voltage-gated K<sup>+</sup>-channel, possibly the big conductance Ca<sup>2+</sup>-dependent potassium channel (BK<sub>Ca</sub>).

Supported by NIH NIDCD DC 004716 (ZGJ).

#### 59 Glycyrrhetinic Acids Suppress Ach-Induced Hyperpolarization in Smooth Muscle Cells via Gap Junction Blockade in Guinea Pig Spiral Modiolar Artery

Bing-Cai Guan<sup>1</sup>, Zhi-Gen Jiang<sup>1</sup>

<sup>1</sup>Oregon Hearing Research Center, Oregon Health & Science University

Gap junctions play a critical role in intercellular electrical and certain chemical communications and thus the normal function of the cochlea. Several forms of familial hearing loss result from mutations in connexins, the gap junction building proteins. Glycyrrhetinic acid (GA) compounds are widely used gap junction blockers but their efficacy and side actions are not well determined. Using recently developed whole-cell recording techniques on smooth muscle cells remaining embedded in the spiral modiolar artery, we analyzed membrane actions of two commonly used GAs. We found: 1)  $18\beta$ GA (30  $\mu$ M) caused an increase in membrane input resistance (Rinput) from ~184 M $\Omega$  to ~2.2 G $\Omega$  or a 91 ± 2.1% reduction in the input conductance (G<sub>input</sub>), and resulted in an input capacitance of ~12 pF. In contrast, 30  $\mu$ M 18 $\alpha$ GA reduced the G<sub>input</sub> by only 60% (or  $R_{input}$  increased to ~400 M $\Omega$ ). 2) The inhibition by 18 $\beta$ GA and 18 $\alpha$ GA of the G<sub>input</sub> was

concentration dependent with an IC50 at 2.0 and 4.4  $\mu M$ , respectively. 3) Both drugs (≥30 µM) caused a mild depolarization and a current that had a linear I/V relation with a negative slope and a reversal potential near the 4) Acetylcholine (ACh) induced an resting potential. outward current in SMCs clamped at -40 mV, which showed a positive slope I/V relation and a reversal potential near -85 mV. 5) The ACh-current was concentration-dependently attenuated by 18βGA and  $18\alpha GA$  with an IC<sub>50</sub> of 4.3 & 7.8  $\mu M$ , respectively. We conclude that 18\( \beta \)GA blocks the electro-coupling and could achieve a near complete electrical isolation of the recorded SMC at 30 µM, which was substantially more potent than  $18\alpha GA$ . The I/V relation and sensitivity to  $18\beta GA$  of the ACh-induced current is consistent with a K<sub>Ca</sub>-activation and endothelial origination. Our data indicate that the whole-cell recording from in situ cells combining with the use of 18βGA is a valuable approach to studying vascular intercellular communication mechanisms, which attains better voltage control over the recorded cell than conventional intracellular recording while retains more physiological condition than that of dissociated or cultured

Supported by NIH NIDCD DC 004716 (ZGJ)

# [60] Inhibition of ACh-Induced Hyperpolarization by Dihydropyridines in Cochlear Artery via Blockade of Intermediate Conductance Calcium-activated Potassium Channel

**Yu-Qin Yang**<sup>1</sup>, Xiao-Rui Shi<sup>1</sup>, Bing-Cai Guan<sup>1</sup>, Alfred Nuttall<sup>1</sup>, Zhi-Gen Jiang<sup>1</sup>

<sup>1</sup>Oregon Health & Science University

Using intracellular recording and immunohistochemistry methods, we demonstrated previously that cholinergic fibers innervate the spiral modiolar artery (SMA), the evoked excitatory junction potential is partially sensitive to M3 receptor antagonist, and application of ACh induces a hyperpolarization in SMA cells that have a low resting potential ~-40 mV. The ACh-hyperpolarization originated in the endothelial cells (ECs) by activating a Ca<sup>2+</sup>-activated K<sup>+</sup>-channel (K<sub>Ca</sub>); the hyperpolarization in smooth muscle cells (SMCs) was mainly an electrotonic spread via gap junction coupling. In the present study, using the same methods on *in vitro* SMA preparations, we found that: 1) ACh-hyperpolarization was 95% blocked intermediate conductance  $K_{Ca}$  (IK) blockers,10  $\mu M$ clotrimazole (IC<sub>50</sub> = 116 nM) and 1  $\mu$ M nitrendipine, and by a calmodulin antagonist 100 μM trifluoperazine, but not by the big conductance  $K_{Ca}$  blocker 100 nM iberiotoxin. 2) The protein immunoreactive to anti-SK4/IK1 antibody was clearly localized in all the endothelial cells. 3) The three dihydropyridines, nifedipine, nitrendipine and nimodipine concentration-dependently inhibited the hyperpolarization with an IC<sub>50</sub> of 455, 34 and 3.2 nM, respectively. 3) Among other L-type  $Ca^{2+}$ -channel (I<sub>L</sub>) blockers, verapamil (10 µM) exerted a 20% inhibition on the ACh-hyperpolarization, while diltiazem and the metal ion Ca<sup>2+</sup>-channel blockers Cd<sup>2+</sup> and Ni<sup>2+</sup> had no effect. We conclude that ACh-induced hyperpolarization in the SMA is generated mainly by an activation of the IK in the ECs, and dihydropyridines suppress the EDHF-mediated hyperpolarization by blocking the IK channel, not the  $\rm I_L$  channel.

Supported by NIH NIDCD DC 004716 (ZGJ) and DC00141 (ALN).

## 61 Morphologic and Physiologic Changes of Cochlea after Administration of Plasminogen Activator Inhibitor Type 1 in Guinea Pig

**Beom-Gyu Kim<sup>1</sup>**, Yong-Bok Kim<sup>1</sup>, Hyung-Jong Kim<sup>1</sup>, Hun-Hee Kang<sup>2</sup>, Jong-Woo Chung<sup>2</sup>

<sup>1</sup>Hallym medical center, <sup>2</sup>Asan medical center

Introduction: Plasminogen activator inhibitor type 1 (PAI-1) is an important regulator in the degradation of extracelluar matrix and fibrinolysis which inhibits thrombosis in the vascular system. PAI-1 is normally secreted from endothelial cells, vascular smooth muscle hepatocytes, platelets and adipocytes, with the majority of the circulating PAI-1 from adipose tissue. Many studies, however, have reported that plasma PAI-1 levels are elevated in type II DM, coronary artery diseases and peripheral vascular diseases. In this study, we investigated the physiologic and morphologic changes of cochlea after administration of PAI-1 in guinea pigs to find out the effect of PAI-1 on the microcirculation of cochlea.

Methods and Measures: Guinea pigs with normal Preyer's reflex were divided into a control group and PAI-1 groups. Using auditory brainstem response (ABR), the hearing threshold was measured during the four weeks after placement of saline and PAI-1 (10, 20, and 40 / ) on the round window membrane (RWM). Endocochlear potential (EP) was measured at the 2nd turn of cochlea. At the end of the four weeks, cochleae were harvested and prepared for light microscopy (LM), scanning (SEM) and transmission electron microscopy (TEM).

Results: The ABR threshold was increased from mild to moderate at 30 minutes for the majority of the groups, but they began to recover at 1-3 days (p<0.05). The change of the hearing threshold was not correlated with the concentration of PAI-1. EP decreased significantly in PAI-1 groups comparing with the control group (p<0.05). In the permanent hearing loss group, compressed outer hair cells in the organ of Corti and thinned stria vascularis were observed in the LM study. In the SEM study, stereocilia of outer hair cells were deleted or bent. There was found missing intermediate cells in stria vascularis in TEM study. Conclusions: From these results, we could conclude that PAI-1 may alter the microcirculation of cochlea, and that lead to transient hearing loss and morphological changes. Our studies suggest that PAI-1 is involved in part in the mechanism of inner ear disease that results from the disturbance of microcirculation.

## 62 Can the Effect of High Noise Floor on the Measurement of Low Frequency OAE be Resolved with an Alternative Approach?

**Ming Zhang**<sup>1</sup>, Brianne Davis<sup>1</sup>, Jennifer Holdman<sup>1</sup>, Kelly Morefield<sup>1</sup>, Kristin King<sup>1</sup>, Brenda Flores<sup>1</sup>

<sup>1</sup>Texas Tech University Health Sciences Center

It is known that the low frequency evoked (LFE) ABR is measured to assess neural conditions and the LFE OAE to assess cochlear conditions. However, the high acoustic noise floor in the low frequencies often shadows the OAEs or reduces the signal to noise ratio in the low frequencies such as at 500 Hz. Such acoustic noise can be from ambient environment and also from the subject's respiratory and cardiovascular activities. In addition, measurement of the threshold of LFE OAEs is limited as well due to the acoustic noise. Thus, whether the cochlea can be better assessed with LFE responses or with a new approach becomes an interesting question. Besides LFE OAEs, are there any other tests that can be used? Studies have shown that OAE and cochlear microphonic (CM) are both associated with the function of the hair cells. When hair cells are assaulted, both OAE and CM are compromised. The click evoked (CE) CM was used to assess the cochlear conditions. However, a CE CM represents broadband frequencies, not a specific frequency. The CE CM cannot display a sine waveform either. In contrast, a CM waveform (CMW) can be evoked by a relatively long toneburst. CMW can better represent a single frequency and the response amplitude of a frequency. Therefore, similar to the LFE OAE for cochlea and ABR for neurons, the LFE CMW may be used as an alternative test to assess the cochlea. However, little is known regarding the application of LFE CMW in assessing the cochlear condition. Can CMW be measured noninvasively? Are the measurable responses clear? Do the CMWs have advantages compared with OAE in measuring LFE responses? Is the electric noise level not too high such that it shadows the LFE CMW? Is the threshold of LFE CMWs lower than that of OAEs? Is the signal to noise ratio of LFE CMWs high? To answer these questions, we attempted to measure the LFE CMWs from subjects with normal hearing. Our data suggests that the answers to these questions are generally positive. The advantages, disadvantages, techniques, and artifacts are discussed as

(Authors thank Dr. Dwayne Paschall and Dr. Steven Zupancic for their comments)

## 63 New Approach for Rapid Perfusion Fixation of the Human Inner Ear for CT and MR Microimaging

**Patrick Gannon<sup>1</sup>**, Eric Smouha<sup>1</sup>, Dana Berg<sup>2</sup>, Bradley Delman<sup>1</sup>

<sup>1</sup>Mount Sinai School of Medicine, <sup>2</sup>Columbia University, New York

Hearing and balance organs of the human inner ear are contained within walls of the densest bone in the body, the otic capsule. Due to their conserved location they are difficult to access to conduct prompt post-mortem

preservation. This potential compromise of inner ear tissue viability, compounded by marked friability, is due to factors such as long post-mortem-intervals, and both onset and uniformity of fixation. Here we have dealt with the latter concern by designing new methods to conduct rapid homogeneous fixation by perfusion versus the standard immersion method.

We formulated two methods that will provide reliable and rapid delivery of fixative to the inner ear; perfusion via the arterial and endolymphatic channels. Both conduits are accessible from the outer walls of the petrosal bone. In human cadavers we cannulated tubules of the endolymphatic sac to perfuse, via the vestibular aqueduct, the membranous labyrinth throughout the inner ear. We also cannulated branches of the vertebral / basilar arterial system to perfuse the internal auditory artery which is the only end-artery to the inner ear.

We were able readily achieve both of these goals as indicated by transmission of dye perfusion into endolymph and arterial targets. The arterial perfusion route is an easier and accelerated option that provides a robust rapid solution, with endolymph perfusion acting as a complement. These new methods would provide continued perfusion fixation of the inner ear, commencing in less than 20 minutes. In combination with very short postmortem intervals, we predict premium tissue preservation with high tech imaging and the potential for long-term curation as the primary outcomes.

# 64 Production and Purification of Recombinant Human CTL2 as a Target Protein for Autoantibodies in Autoimmune Hearing Loss

**Pavan K. Kommareddi<sup>1</sup>,** Thankam S. Nair<sup>1</sup>, Mounica Vallurupalli<sup>1</sup>, Melissa Remington<sup>2</sup>, Steven A. Telian<sup>3</sup>, H. Alexander Arts<sup>3</sup>, Hussam K. El-Kashlan<sup>3</sup>, Susan G. Fisher<sup>4</sup>, Vijay Kumar<sup>2</sup>, Thomas E. Carey<sup>1</sup> <sup>1</sup>Kresge Hearing Research Institute, <sup>2</sup>Immco Diagnostics, <sup>3</sup>University of Michigan, <sup>4</sup>University of Rochester

Autoimmune hearing loss (AHL) is poorly understood and lacks a reliable diagnostic test. If identified early AHL can be treated with steroid therapy, but this can lead to severe side effects, and is not warranted in all idiopathic hearing loss patients. The identification of specific autoantigens can lead to diagnostic tests for AHL. Choline transporter like protein 2 (CTL2) is the target antigen of a monoclonal antibody (KHRI-3) that binds to inner ear supporting cells and leads to hair cell death and hearing loss in guinea pigs. Since CTL2 might be an autoantigen in persons afflicted with AHL, the CTL2 ORF was cloned from human inner ear mRNA, fused to an N-terminal 6X His tag and inserted into the pFastBac baculovirus vector that was recombined with a bacmid and transfected into sf9 insect cells. The resulting virus was used to infect logarithmically growing sf9 cells which were harvested at 12, 24, 36, 48, and 72 hours. Protein production was assessed by immunofluorescence and western blotting with optimal expression at 48 hours. The recombinant protein was purified by immunoprecipitation or by nickel or copper affinity columns. The huCTL2 protein produced in sf9 cells

migrates as three bands of 62, 64, and 68 kDa which are detected by antibodies to the His-tag or to CTL2. Digestion with PNGaseF, an enzyme that cleaves N-linked carbohydrate, reduced the protein bands to a single core protein of ~62 kDa. CTL2 protein purified by copper affinity chromatography was used as a substrate in multilane western blots to detect human anti CTL2 antibodies. Of 25 AHL patient sera previously shown to have antibodies to inner ear supporting cells, 18 strongly stained the 62 kDa CTL2 core protein. We conclude that a subset of patients with autoimmune hearing loss have antibodies to CTL2. Additional tests of specificity and sensitivity are underway to determine if this protein will be useful in the diagnosis and treatment monitoring of AHL patients.

### 65 **B-Tubulin Induces Auto-Immune Inner**Ear Disease

**Mohammad Habiby Kermany**<sup>1</sup>, Bin Zhou<sup>1</sup>, Chun Cai<sup>1</sup>, Xiaoping Du<sup>1</sup>, Tai June Yoo<sup>1</sup>

<sup>1</sup>University of Tennessee, Health Science Center, Memphis, TN 38163, USA

Previous studies show that tubulin is a major constituent protein of microtubules, which are prominent structures in the sensory and supporting cells of the inner ear. Our previous study revealed that tubulin is an auto-antigen to the inner ear. In the present study immune-mediated sensorineural hearing loss investigated in Balb/C mice after immunization with purified \( \mathbb{G}\)-tubulin portion. Different concentrations of ß-tubulin were used to immunize Balb/C mice, and the sensorineural hearing loss was determined by far field auditory brainstem responses (ABR) and distortion product oto-acoustic emissions (DPOAE). Sensorineural hearing loss was found in all mice immunized with different ß-tubulin concentrations. Degenerated spiral ganglion and cochlear hair cells were found in the inner ears of higher dose of tubulin immunized groups. The sensorineural hearing loss was correlated with the concentration of ß-tubulin and the sever hearing loss was detected in the higher dose of immunized groups. This study demonstrates that ß-tubulin has the major role of that induces experimental autoimmune hearing loss in mice and supports the conclusion that tubulin is an autoantigen to the inner ear. It also demonstrates that cochlear damages of the spiral ganglion and the Organ of Corti is direct related to the concentration of ß-tubulin.

## 66 Adoptive Immunotherapy of Experimental Autoimmune Hearing Loss via T Cell Delivery of the IL-12 P40 Subunit

**Bin Zhou**<sup>1</sup>, Mohammad Habiby Kermany<sup>1</sup>, Chun Cai<sup>1</sup>, Qing Cai<sup>1</sup>, Tai June Yoo<sup>1</sup>

<sup>1</sup>University of Tenessee

CD4+ T cells are believed to play a central role in the initiation and perpetuation of autoimmune diseases such as autoimmune sensorineural hearing loss (ASNHL). In the murine model for ASNHL, pathogenic T cells exhibit a Th1-like phenotype characterized by heightened expression of proinflammatory cytokines such as IFN-ã.

Systemic administration of "regulatory" cytokines, which serve to counter Th1 effects, has been shown to ameliorate autoimmune responses. However, the inherent problems of nonspecific toxicity limit the usefulness of systemic cytokine delivery as a potential therapy. Therefore, we used the site-specific trafficking properties of autoantigen-reactive CD4+ T cells to develop an adoptive immunotherapy protocol that provided local delivery of a Th1 cytokine antagonist, the p40 subunit of IL-12. Adoptive immunotherapy via T cell delivery of the IL-12p40 subunit was performed by i.v injection of 2x106 Tcell hybridoma cells transfected with IL-12 P40 gene. ABR and DPOAE threshold for â-tubulin immunized mice at 2 weeks and 6 weeks were measured. The distortion product traces of 8, 16, 32 KHz frequency at 80 dB SPL intensity in 300µg â-tubulin immunized were measured. DPOAE shows low responses in immunized groups. Therapeutic groups show restoration of hearing level at 6 weeks after the therapy. In vivo tracking of bioluminescent lymphocytes, transduced to express luciferase, using lowlight imaging cameras demonstrated that transduced CD4+ T cells trafficked to the inner ear, where histological analysis confirmed long-term transgene expression. Thus, we have succeeded to restore the hearing in mice with immunologically induced deafness by adoptive cellular gene therapy.

## [67] Repopulation of Cochlear Macrophage in Mammalian Cochlea after Total Body Irradiation

**Eisuke Sato**<sup>1</sup>, Elizabeth H. Shick<sup>1</sup>, Keiko Hirose<sup>1,2</sup>
<sup>1</sup>Department of Neurosciences, Lerner Research Institute, Cleveland Clinic, <sup>2</sup>Head and Neck Institute, Cleveland Clinic

Recent studies have demonstrated that macrophages are present in normal cochlea and increase in number following acoustic trauma. These cochlear macrophages do not proliferate after noise exposure but migrate into the cochlea through the vasculature.

This study was designed to investigate the cochlear macrophage population by generating bone marrow chimeras. Lethally irradiated 8 week old C57BL/6 mice were transplanted with hematopoietic stem cells from CX3CR1GFP/GFP fetal mice. Donor marrow from CX3CR1GFP/GFP mice is intrinsically fluorescent and donor cells can be easily identified with fluorescent microscopy. Nonirradiated wild type mice and irradiated wild type mice transplanted with wild type bone marrow served as controls. We studied mice at 2, 3, 4, 5, 6, and 8 weeks after transplant to assess hearing and repopulation of cochlear macrophages. A separate group of chimera mice were exposed to octave band noise (8-16 kHz) for 2 hours, 2 weeks after transplantation to evaluate migration of cochlear macrophages, hearing thresholds and hair cell

We found that cochlear macrophages derived from donor bone marrow appeared in spiral ligament 3 weeks after transplant and increased week by week. Noise exposure induced a massive migration of leukocytes, particularly in spiral ligament of the basal turn. There was no difference between CX3CR1 GFP/GFP chimeras and wild type chimeras in hearing threshold, migration of cochear macrophages or tissue injury after noise exposure. These results reinforce the fact that cochlear macrophages are derived from hematopoietic cells and that they are an exchanging and migratory population. Furthermore, CX3CR1 is not necessary for macrophage migration into cochlea and does not appear to play either a protective or destructive role in acoustic injury.

# Role of Bacterial Proteins in the Permeability of Streptococcus Pneumoniae Through the Round Window Membrane and Related Pathological Changes

Patricia Schachern<sup>1</sup>, Vladimir Tsuprun<sup>1</sup>, Sebahattin Cureoglu<sup>1</sup>, Michael Paparella<sup>1,2</sup>, Steven Juhn<sup>1</sup>

<sup>1</sup>University of Minnesota, <sup>2</sup>Minnesota Ear Head and Neck Clinic

The round window membrane (RWM) is the only soft tissue barrier between the middle ear and inner ears and has been shown to be permeable to a variety of substances. An understanding of host and pathogen interactions and bacterial permeability through the RWM are important steps toward the rational design of better treatment for bacterial otitis media (OM) and prevention of inner-ear damage due to OM. There are several pneumococcal proteins, which are involved in direct bacterial adhesion to the host cells or in concealing the bacterial surface from the host defense mechanism. Among these are pneumococcal surface protein PspA and pneumolysin (Ply). PspA is involved in cell adhesion and interactions with the host complement system, and Ply in degradation of the extracellular matrix and lysis of cholesterol-containing membranes. The function of these proteins appears to facilitate significant aspects of pneumococcal colonization and invasion. Compromise of these functions may reduce pathogenicity Streptococcus pneumoniae. We tested the hypothesis that S. pneumoniae mutants, deficient in PspA and Ply, are less virulent and have decreased penetration into the RWM. For these purposes, 10 3, 10 5, 10 6, and 10 7 CFU of wild-type strains and isogenic PspA and Ply mutants of S. pneumoniae serotype 2 strain D39, were inoculated into the middle ear cavities of chinchillas. Two days after inoculation, the bullas were processed for light microscopy and transmission electron microscopy. Our data showed that histopathological changes of the RWM and inner ear and passage of bacteria through the RWM appeared to be less severe for the mutant strain, where PspA was genetically deleted, than for the wild-type strain at all concentrations. Differences between the wild-type and the Ply-deficient mutant were less apparent at concentrations of 10 5 CFU or greater.

Supported by: NIDCD R01 DC006452

# 69 Toll-Like Receptor 2-Dependent NFκB Activation is Involved in Nontypeable Haemophilus Influenzae-Induced MCP-1 UpRegulation in the Spiral Ligament Fibrocytes of the Inner Ear

**Sung K. Moon**<sup>1</sup>, Jeong-Im Woo<sup>1</sup>, Haa-Yung Lee<sup>1</sup>, Jun Shimada<sup>1</sup>, Huiqi Pan<sup>1</sup>, Robert Gellibolian<sup>1</sup>, David J. Lim<sup>1</sup> *House Ear Institute* 

Inner ear dysfunction secondary to chronic otitis media (OM) is not uncommon, which includes high-frequency sensorineural hearing loss or vertigo. Although chronic middle ear inflammation is believed to cause inner ear dysfunction - via entry of OM pathogen-specific molecular signals from the middle to the inner ear - the underlying mechanisms remained unknown, until now. Previously we demonstrated that engineered spiral ligament fibrocyte (SLF) cell lines up-regulate MCP-1 expression after treatment with nontypeable Haemophilus influenzae (NTHi) lysate, one of the most common OM pathogens. We are hypothesizing that the SLF-derived MCP-1 plays a role in inner ear dysfunction secondary to OM. The purpose of this study is to investigate the signaling pathway involved in NTHi-induced MCP-1up-regulation in SLFs. Our results showed that: 1) NTHi induces MCP-1 up-regulation in the SLFs via TLR2-dependent activation of NFκB, which in turn, is mediated by IKKβ-dependent  $I\kappa B\alpha$  phosphorylation, 2) the binding of NF  $\!\kappa B$  to the enhancer region of MCP-1 is involved in this up-regulation, and 3) the identification of a potential NFκB motif, responsive and specific to certain NTHi molecules or ligands. These results may provide us with new therapeutic strategies for prevention of inner ear dysfunction secondary to chronic middle ear inflammation.

#### | 70 | Effects of Gacyclidine Extracochlear Perfusion on Tinnitus in Humans and Intracochlear Perfusion on ABR Thresholds in Guinea Pigs

**Gentiana I. Wenzel<sup>1</sup>**, Hubert H. Lim<sup>1</sup>, Timo Stöver<sup>1</sup>, Thomas Lobl<sup>2</sup>, John Schloss<sup>2</sup>, Burkard Schwab<sup>1</sup>, Thomas Lenarz<sup>1</sup>

<sup>1</sup>Medizinische Hochschule Hannover, <sup>2</sup>NeuroSystec Gacyclidine is a highly specific NMDA receptor antagonist with neuroprotective properties. In guinea pigs, administration of gacyclidine (adsorbed to Gelfoam) into the round window niche or as a bolus injection into the cochlea suppressed salicylate-induced tinnitus. Thus, we investigated in humans and animals if gacyclidine could provide a safe and effective treatment for tinnitus.

We administered gacyclidine as a compassionate treatment in unilateral deaf patients with tinnitus. These patients experienced temporary relief from tinnitus after constant perfusion of gacyclidine into the round window niche for 40-60 hours. This demonstrated that gacyclidine has the potential to suppress tinnitus. However, controlled and long-term delivery of the drug will be necessary for effective treatment. Since the main candidates for this therapy will be hearing patients, we needed to assess whether chronic administration of this drug would compromise hearing performance. Thus, we measured the

effects of chronic intracochlear gacyclidine perfusion on frequency-specific ABR thresholds in guinea pigs.

Guinea pigs were implanted with osmotic pumps that delivered 0.5 µL/h of 0.3 mM gacyclidine for 9 days via a catheter inserted through the round window membrane. The concentration and rate of drug delivery were selected to provide a dose that was substantially higher than is expected for tinnitus control in humans. Frequency-specific ABRs (1-40 kHz, 10-80 dB SPL in 10dB steps) were recorded before implantation and compared with those obtained after drug administration. No significant changes in ABR thresholds were observed suggesting that prolonged administration of gacyclidine for tinnitus treatment should be safe in terms of hearing preservation. Further studies investigating the toxicological effects of different dosages and durations are under way to ensure the safety of the drug for long-term human use and to warrant clinical trials.

### 71 Quinine Induced Tinnitus-Like Behavior Using a Startled Reflex Paradigm

**Edward Lobarinas**<sup>1</sup>, Wei Sun<sup>1</sup>, Lei Wei<sup>1</sup>, Richard Salvi<sup>1</sup> *University at Buffalo* 

The anti-malarial drug, quinine, has been reported to induce tinnitus when administered at high doses and has been used to investigate the neural and biochemical mechanisms underlying tinnitus. Previously, schedule induced polydipsia avoidance conditioning (SIP-AC) was used to evaluate the presence of tinnitus in rats treated with high doses of both salicylate and quinine. Recently, the effects of quinine on tinnitus-like behavior were evaluated using a high-throughput behavioral assay, gap pre-pulse inhibition of acoustic startle (GPIAS), which can be used to estimate tinnitus pitch. GPIAS was used to measure the onset and pitch of guinine-induced tinnitus in rats treated with different doses of guinine. A 50 ms silent gap (gap pre-pulse) in a continuous background noise was used to inhibit the startle reflex elicited by a high level noise burst. The gap was embedded in narrow band noises (NBN) with center frequencies at 6, 12, 16 or 24 kHz. Noise burst pre-pulse inhibition of acoustic startle (NBIAS) was also evaluated to monitor potential changes in hearing following quinine. GPIAS results showed evidence of tinnitus like behavior at frequencies above 6 kHz with no changes in hearing threshold at doses of quinine up to 150 mg/kg. Tinnitus-like behaviors with GPIAS were consistent with previous SIP-AC data, strengthening the use of GPIAS as an animal model of tinnitus.

Supported in part by Tinnitus Research Consortium.

### 72 Differential Gene Expression Profiles in Salicylate Ototoxicity of the Mouse

**Gi Jung IM**<sup>1</sup>, Seo Jin Kim<sup>2</sup>, Sung Won Chae<sup>1</sup>, Jae Hoon Cho<sup>1</sup>, Hak Hyun Jung<sup>1,2</sup>

<sup>1</sup>Department of Otolaryngology, Korea University College of Medicine, Seoul, Korea, <sup>2</sup>Department of Biomedical Sciences, Korea University, Seoul, Korea

Conclusion: This study demonstrated differential gene expression profiles in salicylate ototoxicity with oligonucleotide-microarray. This study may also provide

basic information to candidate genes associated with hearing loss and/or tinnitus or recovery after salicylateinduced cochlear dysfunction.

Objectives: Salicylate ototoxicity is accompanied by temporary hearing loss and tinnitus. The purpose of the present study is to evaluate the gene expression profiles in the mouse cochlea with salicylate ototoxicity using DNA microarray.

Materials and Methods: The subject mice were injected intraperitoneally with 400 mg/kg of sodium salicylate, and an approximate 30 dB threshold shift that was observed by auditory brainstem response was achieved 3 hours after an injection of sodium salicylate and the hearing threshold returned to within normal range at 3 days. Differential gene expression profiles at 3 hours after salicylate injection in comparison to the normal cochlea were analyzed with DNA microarray technology.

Results: The analysis of the ontogenic distribution was performed in up-regulated or down-regulated genes with the Gene Ontology Database system and GFINDer. Microarray revealed that 87 genes were up-regulated two-fold or more in the mouse cochlea with salicylate ototoxicity in comparison to the normal cochlea. Among these genes, increased expression levels of 30 functional genes were confirmed by semi-quantitative RT-PCR.

## 73 MR Imaging of the Ear Following Intratympanic Injection of a Gel Loaded with Gadolinium

**Cecilia Engmér¹**, Andreas Ekborn¹, Tobias Bramer², Katarina Edsman², Allen S. Counter³, Christian Spenger⁴, Tomas Klason⁵, Göran Laurell⁶

<sup>1</sup>Department of Otorhinolaryngology and Head- and Necksurgery, Karolinska Hospital, Stockholm, Sweden, <sup>2</sup>Department of Pharmacy, Uppsala University, Sweden, <sup>3</sup>Neurology Department, Harvard University Biological Laboratories, Cambridge, USA, <sup>4</sup>Depertment of Clinical Neuroscience, Karolinska Institutet, Stockholm, Sweden, <sup>5</sup>Department of Clinical Neuroscience, Karolinska Institutet, Stockholm, Sweden, <sup>6</sup>Department of Clinical Science, Umeå University Hospital

Local drug delivery to the inner ear can be mediated through the use of a slow-release vehicle injected to the middle ear cavity and thereby serving as a reservoir that prolongs drug action. It is generally believed that the injected substance may be distributed to the inner ear through diffusion via the round window membrane. Very little is known about vehicle distribution and elimination after injection. A gel constituting of hyaluronic acid has been identified as a possible vehicle that can be loaded with pharmacological substances for intratympanic administration. The present study was performed on guinea pigs. Using a 4.7 T MRI scanner the anatomical distribution of hyaluronic acid loaded with gadolinium after injection to the middle ear cavity was studied as well as the uptake of gadolinium in the surrounding tissues up to 3 days after administration. It was found that the gel filled up the middle ear cavity exept for a small volume close to apex of the cochlea. The gel was thus in close contact with the round window membrane which allows drug diffusion to the inner ear. Futhermore an uptake of gadolinium into

the inner ear was seen in some of the injected ears. Most of the gel remained in the middel ear cavity for the full duration of the study.

## 74 Effect of Choice of Fixative and Embedding Medium on Immunostaining of the Cochlea

**Jennifer O'Malley<sup>1</sup>**, Saumil Merchant<sup>1,2</sup>, Barbara Burgess<sup>1</sup>, Diane Jones<sup>1</sup>, Joe Adams<sup>1,2</sup>

<sup>1</sup>Massachusetts Eye and Ear Infirmary, <sup>2</sup>Harvard Medical School

The study of proteins by immunostaining is a powerful method to investigate otologic disorders. However, the use of fixatives and embedding media (necessary for preservation of morphology) can obscure antigens, making it difficult to perform immuno assays.

We performed a systematic investigation of effects of (1) three different fixative solutions- 4% formaldehyde (F), 4% formaldehyde + 1% acetic acid (FA), and 4% formaldehyde + 1% acetic acid + 0.1% glutaraldehyde (FGA); and (2) three different embedding media- celloidin, paraffin and polyester wax. Immunostaining of mouse cochlea was studied using a panel of six antibodies.

CBA mice ranging in age from 6 weeks to 2 months were perfused with either F, FA or FGA. Temporal bones were removed, fixed for 25 hours, decalcified in EDTA, embedded, and sectioned at 8-20 micrometers. For each fixative, embedding was done using each of the three media. Prior to immunostaining, celloidin was removed using sodium methoxide, paraffin using xylene, and polyester wax using alcohol. Antibodies to Prostaglandin D Synthase, Aquaporin 1, Connective Tissue Growth Factor, 200 kD Neurofilament, Tubulin and NaKATPase were used.

Immunostaining was successful using all six antibodies in all three fixatives and all three embedding media. While there were differences in strength of signal and localization of antigen between the three fixatives, overall, FA gave the most uniform results. For a given fixative and antibody, there was surprisingly little difference in the quality of immunostaining between celloidin and paraffin, while results in polyester wax were not as good in some cases. Ongoing work is focused on optimizing celloidin processing for immunostaining. Because celloidin gives superb preservation of morphology, these preliminary results suggest that celloidin may be the embedding medium of choice for both morphological and pathological studies, including immunostaining. Supported by NIDCD

## 75 Mefloquine Induced Apoptosis in Hair Cells and Spiral Ganglion Neurons in Cochlear Organotypic Cultures

**Dalian Ding**<sup>1</sup>, Weidong Qi<sup>1</sup>, Haiyan Jiang<sup>1</sup>, Richard Salvi<sup>1</sup> <sup>1</sup>Center for Hearing & Deafness, University at Buffa Mefloquine is a widely used anti-malarial drug. Some clinical reports suggest that it may be ototoxic and neurotoxic; however, there is little scientific evidence from which to draw any firm conclusion. In order to evaluate its ototoxic and neurotoxic potential, we treated cochlear organotypic cultures and spiral ganglion cultures with

mefloquine. Mefloquine caused a dose-dependent loss of cochlear hair cells at doses exceeding 0.01mM. With increasing dose, hair cell loss progressed from base to apex and from outer hair cells. Spiral ganglion neurons and auditory nerve fibers were also rapidly destroyed by mefloquine in a dose-dependent manner. cultures were stained with propidium iodide (PI), to identify morphological changes in the nucleus. carboxyfluorescein FAM-labeled caspase inhibitor 8, 9 or 3. Virtually all the PI-labeled nuclei in hair cells, spiral ganglion neurons and supporting cells were shrunken or fragmented, morphological features characteristic of cells undergoing apoptosis. Both initiator caspase 8 (membrane damage) and caspase 9 (mitochondrial damage), along with executioner caspase 3, were heavily expressed in cochlear hair cells and spiral ganglions after mefloquine. Initiator caspases 8 and 9 and executioner caspase 3 were also expressed in support cells; however, labeling was less widespread and less intense. These results indicate that mefloquine damages both the sensory and neural elements in the postnatal rat inner ear by activating cell death signaling pathways on the cellis membrane and in mitochondria. Work is currently underway to determine if mefloquine is ototoxic when administered in vivo. Supported in part by NIH grant R01 DC06630-01

#### **76** Expression of the Engulfment Protein ELMO in the Mouse Cochlea

Hartmut Hahn<sup>1</sup>, Jochen Schacht<sup>1</sup>

<sup>1</sup>Kresge Hearing Research Institute, University of Michigan, Ann Arbor, MI 48109-0506, USA

The engulfment and degradation of apoptotic cells are important mechanisms to maintain tissue homeostasis during organ development, tissue maturation, cell differentiation and disease. The efficient removal of dying cells from epithelia prevents necrosis, inflammation and an unwanted immunresponse. In the inner ear, apoptotic cell death occurs during development and may also be triggered in the mature cochlea by noise exposure, ototoxic drug challenge and the aging process.

The mammalian proteins Dock180 and ELMO are components of an engulfment machinery in the phagocytosis of apoptotic cells. Both proteins regulate actin-cytoskeleton reorganization and formation of membrane protrusions in the phagocytosis process.

The aim of this study was to analyze the protein expression of ELMO in the inner ear during development and under conditions of kanamycin treatment.

ELMO was expressed in the early postnatal stages of the cochlea (P0 and P2) in Köllikers' organ, a epithelial tissue that gives rise to the organ of Corti. This immunocytochemical staining significantly decreased at later time points (P8) of the postnatal development and in the mature cochlea. In contrast there was no change of ELMO in kanamycin treated cochleae compared to the saline treated controls although hair cell death was induced by this treatment.

The results are consistent with a role of ELMO in an ELMO/Dock180 engulfment pathway during development

of the inner ear but not in the removal of apoptotic cells in the mature organ of Corti.

This study was supported by research grant DC-03685 and core grant P30 DC-05188 from the National Institute on Deafness and Other Communication Disorders, National Institutes of Health.

## 77 Cytotoxic Effects of DMSO (Dimethyl Sulphoxide) on Cochlear Hair Cells in Organotypic Cultures

Weidong Qi<sup>1</sup>, **Dalian Ding**<sup>1</sup>, Richard J. Salvi<sup>1</sup> <sup>1</sup>Center for Hearing and Deafness, University at Buffalo Dimethyl sulphoxide (DMSO) is a widely used vehicle for dissolving water insoluble compounds. DMSO has been reported to have anti-inflammatory and antioxidant properties possibly by scavenging the highly toxic hydroxyl radical. DMSO is often used to dissolve otoprotective compounds applied to the inner ear in vivo and in vitro. However, little is known about its effects on the inner ear. To evaluate it potential impact on the inner ear, we applied DMSO to cochlear organotypic cultures obtained from postnatal day 3 CRL rats. The cochlear basilar membrane containing the organ of Corti was carefully dissected out and placed on collagen gel in serum free medium. The cochlear explants were incubated at 370 C in 5% CO2 for 24 h with DMSO at concentrations of 0%, 0.1%, 0.25%, 0.5%, 0.75%, 1%, 3%, 5%, and 6% (V/V). Specimens were double stained with topro-3, a nuclear stain, and phalloidin to label actin which is heavily expressed in hair cell stereocilia. Caspase-8, caspase-9, or caspase-3 were also evaluated with fluorescently labeled caspase markers. The location and degree of hair cell loss were evaluated by obtaining a cochleogram through entire length of the cochlea. Results show that DMSO concentration exceeding 0.5% resulted in a dose-dependent loss of hair cells. Hair cell damage began in the basal turn and spread towards the apical turn. The hair cells were clearly swollen if DMSO concentration exceeded 2%. Interestingly, most hair cell death was associated with nuclear shrinkage and fragmentation. DMSO treatment activated caspase-9. caspase-8 and caspase-3 indicating that DMSO-induced hair cell destruction occurred through programmed cell death pathways that involved both mitochondrial and death receptors on the cell's membrane. While previous studies indicate that DMSO may antioxidant properties in some system, our results indicate that DMSO is toxic to the postnatal inner ear at concentrations exceeding 0.5%. Research supported by NIH grant R01 DC00630.

# 78 Prenatal Cocaine Exposure Accelerates Morphological Changes and Transient Expression of Tyrosine Hydroxylase in the Cochlea of Developing Rats

Nuno Trigueiros-Cunha<sup>1,2</sup>, Pedro Leão<sup>3</sup>, Nicole Renard<sup>2</sup>, Maria Amélia Tavares<sup>1</sup>, Michel Eybalin<sup>2</sup>

<sup>1</sup>Faculty of Medicine, Porto, Portugal, <sup>2</sup>INSERM U583, Montpellier, France, <sup>3</sup>Faculty of Health Sciences, Braga, Portugal

Prenatal cocaine exposure causes alterations in auditory brainstem response in children and experimental animals

and has adverse effects on auditory information processing and language skills in children. These effects may result from lesions in the cochlea since it is particularly sensitive to chemical insults during the development. We have thus studied here the effect of prenatal cocaine exposure on the maturation of the rat cochlea using the transient non-catecholaminergic expression of tyrosine hydroxylase in spiral ganglion neurons as an index of cochlear maturation, and light microscopy and morphometry to evaluate the maturation of primary auditory neurons and the organ of Corti.

We showed that prenatal cocaine exposure accelerated the cochlear maturation. In the basal coil of cochleas from PND8 cocaine-treated pups, the Kölliker's organ had disappeared, the tunnel of Corti was opened, and the stria vascularis no longer contained undifferentiated marginal cells. The maximum expression of tyrosine hydroxylase in type I primary auditory neurons occurred at PND8 instead of PND12 in pair-fed controls. On the other hand, the prenatal cocaine exposure had no effect on the width and height of the organ of Corti, spiral ganglion volume and number and size of primary auditory neurons.

In conclusion, our data suggest that prenatal cocaine exposure, though not lethal to primary auditory neurons, accelerates aspects of the cochlear sensorineural maturation. This accelerated cochlear maturation in cocaine-treated rat pups could cause auditory dysfunctions by desynchronizing the development of the whole auditory pathway.

#### 79 A Small Animal Device for Delivering Blast Overpressure Exposures

Jianzhong Liu<sup>1</sup>, Ronald Jackson<sup>1</sup>

<sup>1</sup>Spatial Orientation Center

Nearly 50% of all combat injuries in the Middle East are caused by blast explosions. Additionally, 70% of all civilian terrorist attacks in the US and its territories involve bombs and blast injury. Blast injury is a "multidimensional injury" with primary, secondary, and tertiary effects. The overpressure wave resulting from the high explosive energy release produces primary blast effects involving air/fluid-filled spaces such as the lung, head sinuses, middle ear cavities and gastrointestinal tract. Blast injuries are an immediate triage concern but there may be delayed problems for the surviving victims. The lung is a particularly vulnerable organ, and blast injuries in the lung account for the most common immediate fatal injuries. Head injury, both traumatic open and closed, comprises another very important component of blast injuries. Middle and inner ear injuries, such as conductive and high frequency sensorineural hearing loss and vestibular disorders, are also commonly seen after exposure to a blast overpressure wave.

Our laboratory has developed a blast wave generator which can produce blast overpressure waves ranging from 5 to 175 PSI. The blast tube is constructed of one inch thick aluminum walls and can be configured to generate Friedlander waves varying the wave duration as well as wave amplitude. This device uses compressed air introduced into an adjustable volume chamber. When the

chamber pressure exceeds the tensile strength of film diaphragm, the film burst creates a shock wave that travels into an animal holding area. The animal holding area can be configured with the animal in a horizontal (whole body exposure) or vertical (selected body area exposure) position. An attachment will allow for either open-field or closed-chamber exposures. The tube will be utilized to elicit varied degrees of injury including mild, moderate and severe, and then therapy will be applied with agents that can prevent delayed onset metabolic and inflammatory injury.

#### 80 Tonotopic Representation in the Goldfish Saccule

**Julie Schuck<sup>1</sup>**, Reagan Gilley<sup>1</sup>, Brian Rogers<sup>1</sup>, Michael Smith<sup>1</sup>

<sup>1</sup>Department of Biology, Western Kentucky University

Mammalian and avian auditory hair cells display tonotopic mapping of frequency along the length of the cochlea and basilar papilla. It is not known whether the auditory hair cells of fish possess a similar tonotopic organization in the saccule, the primary auditory receptor in many teleosts. To investigate this question, we determined the location of hair cell damage in fish saccules following exposure to specific frequencies. We exposed groups of six goldfish (Carassius auratus) to one of four pure tones (100 Hz, 800 Hz, 2000 Hz, and 4000 Hz) at 176 dB re: 1 µPa for 48 hrs. The left and right saccules of each fish were labeled with phalloidin in order to visualize hair cell bundles. The hair cell bundles were counted at 19 specific points in each saccule to determine the extent and location of hair cell loss. In addition to quantification of anatomical damage, hearing tests (using auditory brainstem response) were performed on each fish immediately following noise exposure. Threshold shifts were calculated by subtracting control thresholds from post-noise exposure thresholds. All noise-exposed fish exhibited significant hair cell and hearing loss following noise exposure. The location of hair cell loss varied along the length of the saccule in a graded manner with the frequency of noise exposure, with lower and higher frequencies damaging the more caudal and rostral regions of the saccule, respectively. Similarly, fish exposed to lower frequency tones exhibited greater threshold shifts at lower frequencies, while higher frequency tone exposure led to hearing loss at higher This data suggests that the frequency frequencies. discrimination ability of goldfish is at least partially driven by peripheral tonotopy in the saccule.

## 81 New Approach for Preserving the Cochlea Function in Cell Transplantation to the Cochlear Modiolus of Guinea Pigs

**Hideaki Ogita**<sup>1</sup>, Takayuki Nakagawa<sup>1</sup>, Kyu Lee<sup>1</sup>, Takayuki Okano<sup>1</sup>, Juichi Ito<sup>1</sup>

<sup>1</sup>Graduate School of Medicine Kyoto University

Several studies have demonstrated the potential of cell transplantation for regeneration of spiral ganglion neurons (SGNs). We have reported that the transplantation of ES cell-derived neurons into the cochlear modiolus rescued

impaired hearing(Okano et al. 2005). However, cell transplantation into the cochlear modiolus requires cochleostomy which can cause severe surgical damage in auditory nerves. In the present study, we refined our surgical techniques for the cell transplantation into the cochlear modiolus. Our new approach is as follows: 1) cochleostomy in the basal turn of cochleae, 2) insertion of a fine glass capillary into the scala tympani, 3) penetration of the bony wall of the Rosenthal canal, 4) injection the material into the modiolus, 5) covering the opening of the cochlear basal turn with a fat graft. Cochlear functional damage caused by this procedure was evaluated by eABR(electrically evoked ABR), and there was no significant elevation of eABR thresholds just after injection of saline.

One week after the transplantation of ES cell-derived neurons, two of the four transplanted cochleae exhibited normal hearing and remaining two showed moderate threshold elevation in ABR measurements. ES cell-derived neurons were identified in the modiolus of all the transplanted cochlea by histological examination.

These findings indicate that our new surgical approach for cell transplantation into the cochlear modiolus has great advantages in preservation of cochlear function and introduction of transplants into the cochlear modiolus.

#### 82 Gene Transfer into Guinea Pig Cochlea via Several Serotypes of AAV Vectors

**Konishi Masaya**<sup>1</sup>, Kawamoto Kohei<sup>1</sup>, Izumikawa Masahiko<sup>1</sup>, Yagi Masao<sup>1</sup>, Asako Mikiya<sup>1</sup>, Kuriyama Hiromichi<sup>1</sup>, Yamashita Toshio<sup>1</sup>

<sup>1</sup>Kansai Medical University

Sensory neural hearing loss (SNHL) is mostly due to degeneration and disappearance of inner hair cells which have mechanosensory functions. The cochlea hair cell loss leads to permanent hearing impairment in mammals and the ability to replace lost hair cells is currently unavailable. Generally, there are two strategies to regenerate lost cells, one is transplanting exogenous cells, the other is manipulating residual cells transform to the desired cells. So far, stem cells are one possibility to use in former technique, and the latter requires a gene transfer system. Several genes have been discovered in mammalian cochlea, some of which are candidates for treating SNHL. To achieve this goal, gene expression must be limited to the specific cells which might be controlled by designing the vector. For clinical application, a minimally invasive approach into the inner ear is desired and a choice of less toxic vector system is needed. With this theory, we used the adeno-associated virus (AAV) as a vector into the inner ear of a guinea pig. Using micro syringe we infused the AAVs into the cochlea via the round window membrane. This approach could also be used in other clinics. Seven days after the injection, cochlea were harvested and the distribution of gene expression was evaluated. To see various biological aspects and tissue tropism, different AAV vector serotypes with the same type of promoter systems (AAV-1, 2, 5, 7, 8 and 9) were used. Additionally, we tried using the same approach inserting adenoviral vector into the guinea pig cochlea and

compared the distribution of gene expression to that of AAVs.

## 83 CAR Distribution in the Auditory Epithelium Does not Reflect Adenovirus Transduction Pattern

**Toru Miyazawa**<sup>1,2</sup>, Shelley A. Batts<sup>1</sup>, Taha Qazi<sup>1</sup>, Donald L. Swiderski<sup>1</sup>, Lisa A. Beyer<sup>1</sup>, Douglas E. Brough<sup>3</sup>, Mark A. Crumling<sup>1</sup>, Yehoash Raphael<sup>1</sup>

<sup>1</sup>Kresge Hearing Research Institute, Univ. of MI, <sup>2</sup>Kanazawa Medical University, Department of Otolaryngology, <sup>3</sup>Department of Vector Sciences, GenVec Inc.

The Coxsackie-adenovirus receptor (CAR) has high affinity to adenoviruses (AV) and is a target for AV binding and entry into cells. Thus efficient AV gene transfer may depend on the distribution of CAR in target organs. We determined which cell types express CAR in cochleae of normal mature guinea pigs and after exposure to ototoxic drugs or intense noise. In normal cochleae, CAR was expressed in hair cells (HC) and all types of supporting cells (SC) except pillars. Expression was strongest in the apical regions of the positive cells. In cochleae deafened with kanamycin or noise, HCs were replaced by scars and all types of SCs, including pillar cells, expressed CAR. In cochleae deafened with neomycin, the organ of Corti was replaced by a flat epithelium composed of polygonal nonsensory cells and distinct cell types could no longer be recognized. Only a small sub-population of cells was CAR positive. Thus the distribution of CAR-positive cells is greatly reduced by neomycin but slightly increased by kanamycin or noise. We then examined the relationship between CAR expression and AV transduction, inoculating Ad. *GFP* into the endolymph of normal and deafened ears. As expected, GFP transduction occurred in most CARpositive SCs. In contrast, CAR-positive HCs were not transduced, but CAR-negative pillar cells were. This pattern was also found in ears deafened with kanamycin or noise. Thus, successful gene transfer in these tissues does not closely reflect CAR expression. In the flat epithelium, gene transfer was limited to a small subset of cells, consistent with the low frequency of CAR-positive cells. This result may indicate that the flat epithelium contains distinct types of cells and that in some inner ear cell types, AV entry may not depend on CAR.

Supported by a gift from Berte and Alan Hirschfield, GenVec, RNID, CHD and NIH/NIDCD Grants R01-DC03389, R01-DC01634, R55-DC007634, R01-DC05401, P30-DC05188, and Research account 2006 in Kanazawa Medical University.

#### 84 HOX-GFP and WOX-GFP Lentivirus Vectors for Inner Ear Gene Therapy

**Laura Pietola**<sup>1</sup>, Antti Aarnisalo<sup>1</sup>, Joonas Joensuu<sup>1</sup>, Jarmo Wahlfors<sup>2</sup>, Jussi Jero<sup>1</sup>

<sup>1</sup>Univ. of Helsinki, Dept. of Otorhinolaryngology, Helsinki, Finland, <sup>2</sup>Univ. of Kuopio, A.I. Virtanen Institute, Kuopio, Finland

The characteristics of two lentivirus vectors, HOX-Ef1a-GFP and WOX-Ef1a-GFP were studied in intracochlear gene delivery. The vectors were microinjected into the mouse cochlea through the round window membrane with the help of micromanipulator. GFP fluorescence of both vectors were seen in the cells lining the scala tympani and scala vestibuli. Hair cells, cells of the stria vascularis and spiral ganglion cells did not show any GFP fluorescence. Peripheral spread of the vector was studied from the brain, heart, lungs, liver, spleen and femoral bone marrow. Only the hepatocytes in the liver of few animals showed GFPfluorescence. Another group of mice were treated with i.p. kanamycin for 15 days where after a microinjection of the vectors into the cochlea were again performed through the round window membrane. Expression pattern of the vectors did not change after kanamycin treatment. Kanamycin caused apoptosis in the inner ear, which was shown with TUNEL staining. Apoptosis was also studied after the lentivirus injection. The studied lentivirus vectors caused only a mild inflammatory reaction in the cochlea, which was studied with CD4 and CD8 antibodies. The expression pattern of these two lentivirus vectors can not be altered by causing aminoglycoside trauma to the organ of Corti.

#### **85** Differentiation of Mouse Embryonic Stem Cells in Guinea Pig Cochlea

**Jeannie Hernandez**<sup>1,2</sup>, Noel Wys<sup>1</sup>, Matt Velkey<sup>2</sup>, Diane Prieskorn<sup>1</sup>, Karolina Wesolwoski<sup>1</sup>, K. Sue O'Shea<sup>2</sup>, Josef Miller<sup>1</sup>, Richard Altschuler<sup>1,2</sup>

<sup>1</sup>KHRI, <sup>2</sup>CDB, University of Michigan

Mouse embryonic stem cells (mESCs) implanted into the guinea pig cochlea can survive and differentiate. Using a mESC line with Doxycline (Dox) inducible expression of Neurogenin 1 (Ngn1) and expression of enhanced green fluorescent protein (eGFP), we observed mESCs in the scala tympani of the deafened guinea pig 4 weeks following their placement. Many cells were immunostained with the neuronal marker TUJ1 but not positive for eGFP, presumably reflecting down-regulation. In situ hybridization for mouse genotype was necessary to demonstrate their stem cell origin. We therefore "re-engineered" this mESC line with eGFP under the control of a different promoter, human ubiquitin ligase C, exons 1-2, as opposed to the original CMV promoter. The eGFP was cloned downstream of the UbC promoter and a hygromycin resistance cassette (driven by the mouse PGK promoter) was inserted into the vector backbone to select for stable cell lines. In vitro studies showed Dox induced differentiation into a neuronal phenotype and the lines continued to express eGFP. For in vivo studies 250,000 -500,000 mESCs were placed in scala tympani / modiolus of guinea pigs, at five weeks after deafening. A miniosmotic pump was used to apply Dox into scala tympani

for 2 days (to transiently induce Ngn1 expression), followed by chronic application of the neurotrophic factors BDNF and GDNF. Cochleae were assessed 4 weeks later (9 weeks after deafening) by immunostaining on paramodiolar cryostat sections. Expression of eGFP. visualized either directly or with immunostaining, remained present both in less differentiated cells as well as TuJ1 immunostained cells with differentiation into a neuronal phenotype. Many TuJ1 immunolabeled fibers in scala tympani were not eGFP positive. These appear to reflect growth of peripheral processes from remaining spiral ganglion neurons, leaving Rosenthals canal and growing towards the stem cells in scala tympani. enhanced spiral ganglion neuron survival and massive growth of peripheral processes into the scar region was also observed even in more apical turns where no stem cells were present. The use of this mESC line in which eGFP expression is well maintained in vivo and in vitro following differentiation allows us to directly show that cells in the scala tympani with a neuronal phenotype are of mESC origin and to identify a robust "bystander effect" on endogenous spiral ganglion neurons. Supported by RO1 DC03820 and P30 DC005188

## 86 Restoration of Balance Sensory Epithelium and Function by Notch Signaling

**Ana H. Kim<sup>1,2</sup>**, Lisa A. Beyer<sup>1</sup>, Tim Buck<sup>1</sup>, W. M. King<sup>1</sup>, Yehoash Raphael<sup>1</sup>

<sup>1</sup>Kresge Hearing Research Institute, Department of Otolaryngology, University of Michigan, <sup>2</sup>New York Eye and Ear Infirmary

Mammals lack hair cell regenerative capacity within the cochlea, and possess very limited regenerative potential within the vestibular end organs. We tested whether manipulating expression of developmental gene cascades can induce transdifferentiation of non-sensory cells to new hair cells in the traumatized vestibular epithelium.  $\gamma$ secretase inhibitors block the Notch signaling pathway. We therefore tested whether inhibition of the Notch signaling with a  $\gamma$ -secretase inhibitor N-[N-(3,5-Difluorophenacetyl-Lalanyl)]-S-phenylglycine t-Butyl Ester (DAPT), would induce a phenotypic transdifferentiation of supporting cells into new hair cells following aminoglycoside ototoxicity. To obtain qualitative measures of the vestibular function, vestibulo-collic reflex (VCR) testing was applied. Vestibular lesions were created by injecting streptomycin through a cochleostomy at the oval window in both ears. By 2 weeks, histologic exam showed complete hair cell loss within the vestibular epithelia. VCR testing showed reduced gain with phase leads consistent with vestibular dysfunction compared to the control group (p=0.00). Two weeks after streptomycin injection, one group received mini-osmotic pump filled with DAPT in the right ear. Two months later, many more immature hair cells were observed in DAPT treated ears compared to the saline treated group. Guinea pigs treated with saline showed continued vestibular dysfunction. In contrast, guinea pigs treated with DAPT showed improvement in gain to both sinusoidal and abrupt step testing, and phase normalization (p=0.00). In conclusion, we have shown that the limited capacity of spontaneous regeneration of mature mammalian vestibular hair cells following aminoglycoside-induced loss is greatly enhanced by Notch signaling inhibition. The DAPT treatment also led to recovery of vestibular function. Supported by NIH/NIDCH Grants R01-DC01634, R01-DC05401, and P30-DC05188.

## 87 Schwann Cells Genetically Modified to Express Neurotrophins Promote Spiral Ganglion Neuron Survival *In Vitro*

Lisa Pettingill<sup>1,2</sup>, Ricki Minter<sup>2</sup>, Robert Shepherd<sup>1,2</sup> <sup>1</sup>The Bionic Ear Institute, <sup>2</sup>The University of Melbourne Spiral ganglion neurons (SGNs) undergo degeneration following sensorineural hearing loss. Their rescue has therapeutic significance as they are the target neurons for cochlear implants. The delivery of exogenous brainderived neurotrophic factor (BDNF) or neurotrophin-3 (NT-3) via an osmotic pump and cannula can have protective effects on SGNs in animal models of deafness, however, issues associated with infection and the limited delivery period of these devices have resulted in the need to develop alternative delivery strategies. Cell transplantation is now considered a potential avenue for neurotrophin delivery in vivo. We genetically modified Schwann cells (SCs) to over-express either BDNF (BDNF-SCs) or NT-3 (NT3-SCs) to determine if neurotrophic support from a cellbased source elicits survival effects on SGNs. SCs from postnatal day (P) 3 rat sciatic nerve were transfected with expression plasmids encoding enhanced green fluorescent protein (EGFP), BDNF-EGFP or NT3-EGFP using Lipofectamine 2000 (Invitrogen). BDNF- and NT3-SCs produced significantly greater amounts of the respective neurotrophin compared with EGFP-SC controls, as determined by ELISA (P<0.05). Genetically modified SCs were then co-cultured with P6 rat SGNs and the survival effects quantified in terms of the number of surviving SGNs after three days in vitro. BDNF- and NT3-SCs significantly enhanced SGN survival in comparison to EGFP-SC controls (P<0.05). BDNF-SCs also provided significantly greater SGN survival in comparison to recombinant human BDNF (P<0.05), while NT3-SCs and recombinant human NT-3 elicited similar survival effects. The transplantation of cells designed to over-express neurotrophins may provide a clinically relevant means of rescuing SGNs in the deaf cochlea.

Supported by the NIDCD (N01-DC-3-1005), the Macquarie Foundation and the Bionic Ear Institute.

## 88 Transgenic Cells Expressing Neurotrophic Factors as a Model for Drug Delivery to the Inner Ear

**Timo Stöver**<sup>1</sup>, Nicola Hofmann<sup>1</sup>, Gerhard Gross<sup>2</sup>, Athanasia Warnecke<sup>1</sup>, Gerrit Paasche<sup>1</sup>, Kirsten Wissel<sup>1</sup>, Thomas Lenarz<sup>1</sup>

<sup>1</sup>Medical University of Hannover, <sup>2</sup>Helmholtz Centre for Infection Research, Braunschweig

It has been shown that the application of neurotrophic factors (NF), e.g. GDNF, BDNF, NT-3 increases the survival rate of spiral ganglion cells in-vitro and in-vivo.

Fluid based delivery systems are mainly used for application of the NF. In our present approach, transfected cells are used for the production of NF. If these cells could be attached to the surface of cochlear implant electrodes, this would provide a new possibility for drug delivery to the inner ear in combination with cochlear implants.

Murine Fibroblasts (NIH-3T3) were transfected via a lentiviral system to generate cell lines expressing neurotrophic factors (GDNF, BDNF) and GFP under the control of a tetracyclin regulated promotor. The genes for the neurotrophic factors were arranged monocistronic or via an IRES-element bicistronic with GFP. As the bicistronic expression of GFP was insufficient we focussed on the monocistronic vectors for further experiments. The expressed and secreted neurotrophic factors were determined in the cell supernatant via an ELISA assay.

Their biological activity was determined by analyzing their potential to induce differentiation in pc-12 cells (rat pheochromocytoma cells). The supernatant of the GDNF producing cells was added to a growing culture of pc-12 cells and the induction of neurites was observed over a period of 10 days. Neurite outgrowth could be seen beginning from day 2. Most of the observed cells showed clear neurite outgrowth till day 10. No outgrowth could be observed when cells were cultured in medium without NF. In the following experimental phases transgenic fibroblasts will be cultivated on the surface of cochlear implant materials and the effect of the emitted NF on spiral ganglion cells in co-culture will be analyzed.

## 89 Combination of Electrical Stimulation and Neurotrophic Factor Treatment in Deafened Guinea Pigs

Verena Scheper<sup>1</sup>, Gerrit Paasche<sup>1</sup>, Josef Miller<sup>2</sup>, Thomas Lenarz<sup>1</sup>, **Timo Stöver<sup>1</sup>** 

<sup>1</sup>Medical University of Hannover, <sup>2</sup>Kresge Hearing Research Institute, Ann Arbor, Michigan

Sensory-neural hearing loss leads to degeneration of spiral ganglion cells (SGCs). Several studies indicate that the SGC degeneration can be reduced by electrical stimulation (ES). Furthermore, treatment with neurotrophic factors (NF) such as GDNF and BDNF provides a protective effect to SGCs. To investigate if the combination of both interventions has a synergistic effect, we investigated the SGC-density in deafened guinea pigs after delayed treatment with GDNF or BDNF and ES.

Pigmented guinea pigs were systemically deafened by a co-administration of kanamycin and ethacrynic acid. Three weeks after deafening the left cochleae were implanted with an electrode/cannula device. The cannula was attached to a mini-osmotic pump (flow rate:  $0.5~\mu$ l/h) filled with GDNF (100 ng/ml), BDNF (100 ng/ml) or artificial perilymph (AP). The drugs were administered into the inner ear for four weeks. In additional groups of animals drug treatment was combined with electrical stimulation via a portable stimulator for 24 days, 24 hrs a day. 48 days after deafening the cochleae were extracted and prepared for histology. The outline of each Rosenthal's canal profile was traced and all SGCs in this area were counted to generate a SGC-density, expressed as the number of SGCs in an area of  $10.000~\mu m2$ .

Our results demonstrate that both, ES and NF treatment caused significant spiral ganglion cell survival when compared to the control group with the effect being more pronounced for the NF. The combination of ES and GDNF application lead to a significant enhancement in SGC survival compared to the application of GDNF or ES alone. We conclude that the combination of local intracochlear delivery of NF and simultaneous electrical stimulation of the inner ear has more potential for SGC-protection than one of the two interventions alone.

#### 90 Inhibition of Spiral Ganglion Neurite Growth by Depolarization Requires Ca2+ Entry Through Multiple Voltage Sensitive Ca2+ Channels and Calpain Activation

**Erika Woodson**<sup>1</sup>, Pamela Roehm<sup>2</sup>, Ningyong Xu<sup>1</sup>, Steven Green<sup>3</sup>, Marlan Hansen<sup>1</sup>

<sup>1</sup>University of Iowa Department of Otolaryngology, <sup>2</sup>New York University Department of Otolaryngology, <sup>3</sup>University of Iowa Department of Biological Sciences

Successful use of a cochlear implant requires a functional auditory nerve, and regrowth of the peripheral processes towards a stimulating electrode would likely enhance performance. We have begun investigating the effects of membrane electrical activity on neurite growth in spiral ganglion neurons (SGNs).

We find that while membrane depolarization with elevated extracellular  $\text{K}^{+}$  promotes SGN survival, it inhibits neurite growth in vitro in a dose dependent fashion. This effect is partially blocked by verapamil,  $\omega\text{-conotoxin GVIA},$  and  $\omega\text{-agatoxin IVA}$  when used separately and is blocked in an additive fashion when the inhibitors are combined, demonstrating the role of multiple voltage-sensitive calcium channels (VSCC) in this process. In support of a role for multiple VSCCs in this response, we find that cultured SGNs express L-, N-, and P/Q-type VSCCs.

We have begun to explore the  $Ca^{2+}$ -activated signals that contribute to reduced neurite growth. Depolarization activates the calcium-dependent neural protease, calpain, in SGNs as demonstrated by increased t-Butoxycarbonyl-Leu-Met-7-amino-4chlorimethylcoumarin (t-Boc-Leu-Met-CMAC) fluorescence, a cell-permanent, fluorescent substrate of calpain. Further, the calpain inhibitors, calpeptin and calpain inhibitor XI, rescue SGN neurite growth under depolarizing conditions. By contrast, the  $Ca^{2+}$ -sensitive kinases protein kinase A and  $Ca^{2+}$ -calmodulin-dependent kinase II, which are required for the pro-survival effects of depolarization, do not contribute to the inhibition of neurite growth.

Thus, membrane electrical activity inhibits SGN neurite growth through different mechanisms than those recruited to promote survival. Identification and manipulation of signals activated by membrane depolarization which inhibit neurite growth may allow elimination of the negative consequences to neurite extension yet permit continued survival benefits to SGNs.

#### 91 Reinnervation of Cochlear Inner Hair Cells by Spiral Ganglion Neuron (SGN) Peripheral Processes Studied in an Organotypic Explant *In Vitro*

Qiong Wang<sup>1</sup>, Daniel J. Denman<sup>1</sup>, Steven H. Green<sup>1,2</sup>
<sup>1</sup>Department of Biological Sciences, University of Iowa, Iowa City, <sup>2</sup>Department of Otolaryngology, University of Iowa, Iowa City

We previously showed that the normal innervation pattern and synaptic interactions between SGNs and hair cells (HCs) are well preserved in vitro in a rat organotypic cochlear culture. Brief exposure to excessive glutamate agonists (NMDA and Kainic acid, NK) in vitro caused the degeneration of type I SGN peripheral processes and loss of IHC-SGN synapses, but HCs and SGN somata remained intact and no increase in SGN cell death was observed. Reinnervation of IHCs occurred and new IHC-SGN synapses formed within 24-48h. However, not all axons regenerate and those that do regenerate innervate multiple IHCs instead of a single one. Also the number of postsynaptic densities (PSDs) does not fully recover to the pre-trauma level. These results mimic aspects of noise induced damage to SGN peripheral processes in vivo described by Pujol and colleagues. We investigated the role of neurotrophin signaling in reinnervation. At 72 h post-NK, both BDNF and NT-3 increased the number of axons regenerating and contacting IHCs to near control no-NK values. We quantified synaptic regeneration by counting the number of PSDs on each peripheral process and on each IHC. At 72 h post-NK, inclusion of neurotrophins significantly increased the number of PSDs, although not to control no-NK values. Also, inclusion of neurotrophins reduced the multiple innervation of IHCs characteristic of post-NK reinnervation. No significant difference was observed between BDNF and NT-3 in any measured parameter. At 2 weeks post-NK, multiple innervation of IHCs by individual SGNs persisted, while inclusion of extraneous NGF could restrict the number of IHCs reinnervated by individual SGN to less than 3. These results could suggest therapeutic interventions to promote recovery from noise damage and may suggest means to facilitate synaptogenesis between SGNs and new HCs as HC regeneration comes into use.

Funded by NIDCD R01 DC02961 (SHG).

#### 92 Depolarization Inhibits the Jun N-Terminal Kinase (JNK)-Jun Proapoptotic Signaling Pathway in Spiral Ganglion Neurons (SGNs) via CaMKII

Jie Huang<sup>1</sup>, Steven Green<sup>2</sup>

<sup>1</sup>Department of Biological Sciences, University of Iowa, <sup>2</sup>Department. of Biological Sciences & Otolaryngology,

University of Iowa

Deafferented SGNs in vivo and SGNs cultured in the absence of trophic factors die. We have previously shown that, like other trophic factor-deprived neurons, SGN death requires the proapoptotic JNK-Jun signaling pathway. Depolarization reduces death of cultured SGNs and we show that depolarization, like peptide neurotrophic factors (NTFs), inhibits JNK activation. Work from other labs has

defined a signaling pathway by which NTFs inhibits JNK activation but, although depolarization is well-known prosurvival stimulus, control of JNK activation by depolarization has not been investigated. We have shown that depolarization (culture in 25 mM K+, i°25Ki±) promotes SGN survival via at least three distinct signaling pathways: Ca2+/Calmodulin-dependent protein kinase II (CaMKII), CaMKIV and cAMP-dependent protein kinase (PKA). We use Jun phosphorylation as an indicator of JNK activity. Transfection of a CaMKII inhibitor (GFP-AIP), but not of a PKA inhibitor nor of dominant negative CaMKIV. prevents inhibition of JNK signaling by 25K. Conversely, transfection of constitutively-active CaMKII is sufficient to inactivate JNK signaling. By transfection of cytoplasmic or nuclear-localized GFP-AIP constructs we showed that CaMKII inhibits JNK activation in the cytoplasm. Depolarization of SGNs induces tyrosine phosphorylation in a CaMKII-dependent manner. Protein tyrosine kinase (PTK) inhibitors (but not selective inhibitors of Src-family PTKs) prevent inhibition of JNK signaling by 25K. Moreover, we have implicated protein kinase B (PKB/Akt) downstream of PTK buy showing that inhibition of Akt activation with LY294002 also prevents inhibition of JNK activation by 25K. These experiments define a signaling pathway CaMKII => PTK => PI-3-OH kinase => Akt => inhibition of JNK activation. In current experiments, we are confirming these key steps and identifying the PTK involved.

## 93 Dexamethasone Treatment of the Cochlea Protects Against Electrode Insertion Trauma-Induced Hearing Loss

**Adrien Eshraghi<sup>1,2</sup>**, Eelam Adile<sup>2</sup>, Arach Esmailzadegan<sup>2</sup>, Reid Graves<sup>2</sup>, Jiao He<sup>2</sup>, Shibing Chen<sup>2</sup>, Fred Telischi<sup>2</sup>, Thomas Balkany<sup>2</sup>, Thomas Van de Water<sup>2</sup>

<sup>1</sup>University of Miami Miller School of Medicine, <sup>2</sup>University of Miami Ear Institute

Corticosteroid (i.e. triamcinolone acetonide) has been demonstrated to protect auditory hair cells from a naturally occurring toxin (HNE) created within cells as a response to excessive levels of oxidative stress. Dexamethasone is a drug used frequently to treat inner ear disorders such as sudden deafness of unknown etiology. Dexamethasone has been demonstrated to be an inhibitor of both the inflammatory process and the MAPK/JNK cell death signal cascade by a series of in vitro and in vivo studies. Because electrode insertion trauma generates oxidative stress and dexamethasone has been demonstrated both in vitro and in vivo to be effective against trauma we have tested this corticosteroid as a hearing conservation therapy in our animal model of cochlear implantation trauma.

Adult pigmented guinea pigs were the experimental animal; dexamethasone was delivered into the scala tympani immediately following insertion and withdrawal of an electrode analog via a cochleostomy at the base of the cochlea; hearing was tested by auditory evoked brainstem responses (ABRs) in response to pure tone stimuli with Intelligent Hearing System hardware and software; the effect of trauma on a cellular level was assessed from stained whole mount preparations of the organ of Corti.

Electrode insertion trauma (EIT) caused both an initial and a progressive loss of hearing. Whole mount preparations showed apoptosis and some necrosis of damaged hair cells in a site distant from the location of insertion trauma. Treatment with high dose dexamethasone (100  $f\acute{Y}g/mL$ ) in artificial perilymph (AP) perfused into the scala tympani immediately after electrode trauma significantly decreased the initial loss and prevented any progressive loss of hearing caused by electrode insertion trauma when compared to the pattern of hearing loss that occurred in both EIT untreated animals and EIT animals that were perfused with AP only.

High dose dexamethasone therapy when delivered directly to the cochlea is an effective otoprotective therapy in our animal model of cochlear implantation induced hearing loss. This therapeutic approach may have clinical application in patients where hearing conservation is important (e.g. hybrid or electro-acoustic stimulation cochlear implant devices).

Supported by grants from MED-EL and Advanced Bionics Corporation.

## 94 Inhibiting JNK Activity Prevents Excitotoxic Cell Death of Neonatal Rat Spiral Ganglion Neurons *In Vitro*

Damon Fairfield<sup>1</sup>, Steven Green<sup>1</sup>

<sup>1</sup>Depts. of Biological Sciences and Otolaryngology, University of Iowa, Iowa City, IA 52242, USA

Spiral ganglion neuron (SGN) death can result from loss of trophic support or from excitotoxic trauma such as noise overstimulation or exposure to elevated [K<sup>+</sup>]<sub>o</sub> as in Meniere's disease. We have shown that chronic depolarization of SGNs in vitro by elevated extracellular K<sup>+</sup> can either promote SGN survival (30 mM K+; "30K") or cause excitotoxic SGN death (80 mM K<sup>+</sup>; "80K") correlated with [Ca<sup>2+</sup>] level. Here we further investigate the mechanisms of excitotoxic SGN death in vitro. Experiments in which SGNs were cultured for various durations in 80K prior to return to 30K show that most SGNs become irreversibly committed to cell death after approximately 8 h in 80K. Cell death is gradual, occurring mainly between 8 h and 24 h after initiation of exposure to 80K. As for SGNs deprived of trophic support in vitro or deafferented in vivo, the pro-apoptotic Jun N-terminal kinase (JNK) pathway is activated in SGNs exposed to 80K, as indicated by increased nuclear immunoreactivity using antibodies specific for Jun phosphorylated (pJun) on Ser63 and Ser73 relative to SGNs maintained in 30K. Elevated pJun immunofluorescence was observed in SGNs by 8 h after culture in 80K, corresponding approximately to irreversible commitment to cell death. Incubation with a cell membrane permeable peptide inhibitor of JNK activation (TI-JIP), but not with a control peptide, reduces SGN death in 80K in a dose-dependent manner. These results indicate that JNK activity is necessary, at least in part, for the death of SGNs under excitotoxic conditions. We are currently examining other pathways which may be involved in regulating SGN survival in response to excitotoxicity and trophic withdrawal.

This research was supported by NIDCD R01 DC002961 (SHG) and an NRSA F32 DC007270 (DF).

#### 95 The Effects of Adenosine Receptor Agonists on Kainic Acid Excitotoxicity in the Guinea Pig Cochlea

**Keiji Tabuchi**<sup>1</sup>, Shuhei Sakai<sup>1</sup>, Isao Uemaetomari<sup>1</sup>, Akira Hara<sup>1</sup>

<sup>1</sup>University of Tsukuba

Previous studies have shown that the application of kainic acid to the round window membrane induces excitotoxicity of cochlear afferent dendrites and decreases the amplitude of the compound action potential (CAP). On the other hand, it is known that adenosine A1 receptor agonists are neuroprotective in excitotoxicity in the central nervous systems. The present study examined whether specific agonists of A1 or A2 adenosine receptors protected the cochlea against excitotoxicity induced by kainic acid. Albino guinea pigs weighing 250g to 300g were used. Kainic acid was dissolved in the artificial perilymph at 10 mM and was applied to the intact round window membrane. 2-chloro-N6-cyclo pentyladenosine (CCPA), a specific A1 adenosine receptor agnonist, or 5-Ncyclopropyl-carboxamidoadenosine (CPCA), a specific A2 adenosine receptor agonist, was intraperitoneally administered immediately before the application of kainic acid. CAP thresholds were examined before, one, three and 7 days after the drug application. CCPA significantly decreased CAP threshold shifts following kainic acid exposure. However, CPCA did not have any effect on the CAP threshold shifts induced by application of kainic acid. These results suggest that activation of A1 adenosine receptors but not A2 adenosine receptors ameliorated cochlear excitotoxicity.

# Mechanisms of Hair Cell Loss and Cellular Re-Organisation in the Organ of Corti of Mice Treated with an Aminoglycoside and Loop Diuretic Combination.

Ruth Taylor<sup>1</sup>, Andrew Forge<sup>1</sup>

<sup>1</sup>Centre for Auditory Research, The Ear Institute, University College London

Sensorineural deafness is typically characterised by a progressive loss of outer hair cells, from base to apex, followed by the delayed loss of inner hair cells. An in vivo mouse model of hair cell loss and epithelial repair has been established that parallels this distinct pattern of loss. An acute dose of kanamycin and bumetanide results in the rapid loss of outer hair cells and subsequent loss of inner hair cells allowing the mechanisms of hair cell death and structural re-organisation of the sensory epithelium to be studied. Examination of tissue at the time of outer hair cell loss suggests no evidence of hair cell nuclei necrotic morphology. However, TUNEL and nuclei morphology indicate that both inner and outer hair cells die via an apoptotic pathway and death of outer hair cells incorporates activation of caspase 3. Thin sectioning reveals that occasionally hair cells rupture before the completion of a normal apoptotic pathway. The delay in loss of inner hair cells in this system allows for the investigation of mechanisms implicated in the extended survival of inner hair cells, such as NF kappa B. Using this model also allows the study of alteration in expression of those supporting cell proteins involved in cochlea homeostasis such as connexins and potassium ion channels during the repair process.

## 97 Hair Bundle Mechanics at High Frequencies: a Test of Series or Parallel Transduction

K. Domenica Karavitaki<sup>1,2</sup>, David P. Corey<sup>1,2</sup>

<sup>1</sup>Harvard Medical School, <sup>2</sup>Howard Hughes Medical Institute

When the tip of a hair bundle is deflected by the force of a sensory stimulus, the stereocilia move as a unit and produce a shearing displacement between adjacent tips. The resulting stimulus could be applied to transduction channels in two different ways: First, if tip links provide the main connection between stereocilia, the opening of one channel reduces the force on others of the series (negative cooperativity). Second, if stereocilia are primarily held together by lateral links, the opening of one channel increases force on other channels, making them more likely to open (positive cooperativity). How the opening and Ca<sup>2+</sup> -dependent closing of transduction channels affects cochlear mechanics depends critically on which model, or how much of each model, dominates the mechanics. To distinguish between the two models we measured the movement of individual stereocilia when pulling on the kinocillium of a bundle using low (<20 Hz) and high (700 Hz) frequencies. Data were collected from two types of preparations: isolated hair cells from the bullfrog sacculus visualized using stroboscopic video microscopy and from whole mounts of the bullfrog sacculus visualized using two-photon microscopy and FM1-43 labeling. For both preparations, within the same column, the shortest and tallest stereocilia moved the same amount suggesting that the bundle moves as a unit. This behavior remained after treating the cells with the Ca2+ chelator BAPTA to cut their tip-links, suggesting that the lateral links are the main links involved in the propagation of stimuli across the bundle. We argue that if the lateral links provide the main connection, transduction channels are mechanically in parallel resulting in positive cooperativity.

### 98 The Mechanotransducer Channels of Mammalian Cochlear Hair Cells

**Robert Fettiplace**<sup>1</sup>, Maryline Beurg<sup>2</sup>, Carole Hackney<sup>3</sup>, Michael Evans<sup>3</sup>

<sup>1</sup>University of Wisconsin-Madison, <sup>2</sup>Université Victor Segalen Bordeaux 2, <sup>3</sup>Keele University

Hair cells detect sound stimuli by vibration of their hair bundles which opens mechanotransducer (MT) channels probably by tensioning tip links between stereocilia in adjacent ranks. The MT channel is one of the few ion channels not to have been identified at a molecular level so it is important to catalog its properties in situ for

comparison with cloned variants. We have therefore measured MT currents and single-channel attributes for inner (IHC) and outer (OHC) hair cells in isolated rat cochleas at positions with different characteristic frequencies (CF). The MT channel is a calcium selective channel (PCa/PNa = 5:1), activated by hair bundle displacements of a few hundred nanometers and displays sub-millisecond adaptation. Calcium influx through the channel is important for triggering adaptation to optimize transducer sensitivity. For OHCs, the peak current size increases with CF but IHCs show little equivalent tonotopic variation. Also the time constant of fast adaptation decreases with CF for OHCs but is invariant for IHCs. To understand the tonotopic variation we isolated single MT channels after brief exposure to BAPTA. MT channels from IHCs are deduced to have a conductance (in 0.02 mM calcium) of 260 pS, but those from OHCs depend on CF, increasing from 140 pS at the apex to 300 pS at the base. The combination of MT channel conductance and tip link number, inferred from scanning electron micrographs, can account for the change in the OHC macroscopic current with CF and its invariance for IHCs. For both cell types we estimate 1 to 2 channels per tip link. The larger channel size in basal OHCs increases sensitivity and, by allowing larger calcium influx, speeds up adaptation. Our results imply the channel has properties possessed by few candidates. Moreover, variation along the tonotopic axis suggests occurrence of multiple channel subunits. A mechanism for varying the unitary conductance will be presented.

Supported by NIDCD grant RO1 DC 01362.

## 99 Evidence that the Membrane Motor of Outer Hair Cells Undergoes Changes in the Bending Stiffness

Jie Fang<sup>1</sup>, Kuni Iwasa<sup>1</sup>

<sup>1</sup>National Institute on Deafness and Other Communication Disorders

Somatic motility (electromotility) of outer hair cells (OHCs) is based on prestin, a membrane protein, and functions analogously to a piezoelectric element, utilizing electric energy available at the plasma membrane. Changes of the membrane area, which results in motile activity, are coupled with transfer of charge, which appears as nonlinear capacitance (NLC) with bell-shaped voltage Here we examined the effects of dependence. amphipathic ions, cationic chlorpromazine (CPZ) and anionic trinitrophenol (TNP), which are thought to change the curvature of the membrane in opposite directions. We found that both chemicals induced positive shifts without changing the steepness or amplitude of the voltage dependence of the NLC. TNP shifted by about 10 mV at 500 microM concentration and CPZ by about 20 mV at 100 microM. These shifts were well correlated with the decrease of cell length by these chemicals at the holding potential of -75 mV. This observation is consistent with the interpretation that increased curvature reduced cell length and shifted the voltage dependence. Furthermore, these voltage shifts did not diminish by removing the cells' turgor pressure or by the digesting the cortical cytoskeleton.

These observations suggest that the effects of these ions on the hair cell motor are not due to changes in membrane tension but changes in membrane curvature. Since the voltage shifts observed were symmetric with respect to the direction of membrane bending, the mechanism for the shifts must be based on bending stiffness and not on shape asymmetry such as splay. Thus our observations suggest that the membrane motor undergoes conformational changes that involve not only displacement of charge and membrane area but bending stiffness as well

#### 100 Slow Motility in Hair Cells of the Frog Amphibian Papilla: Myosin II-Mediated Shape Change

Nasser Farahbakhsh<sup>1</sup>, Peter Narins<sup>1</sup>

<sup>1</sup>UCLA

Using video microscopy, quantitative analysis and modeling, we investigated intracellular mediating the calcium/calmodulin (Ca<sup>2+</sup>/CaM)-dependent slow motility in hair cells dissociated from the rostral region of amphibian papilla, one of the two auditory organs in frogs. The time course of shape changes in these hair cells during the period of pretreatment with several specific inhibitors, as well as their response to the calcium ionophore, ionomycin, were recorded and compared. These cells respond to ionomycin with a tri-phasic shape change: an initial phase of iso-volumetric length decrease (phase 1); a period of concurrent shortening and swelling (phase 2); and the final phase of increase in both length and volume. We found that both the myosin light chain inhibitor, ML-7, and antagonists of the multifunctional Ca<sup>2+</sup>/CaM-dependent kinases, KN-62 and KN-93, inhibit the iso-volumetric shortening phase of the response to ionomycin, while the type 1 protein phosphatase inhibitors, calyculin A and okadaic acid induce minor shortening on their own and potentiate the phase 1 response. Furthermore, blebbistatin, an inhibitor of actin-activated Mg<sup>2+</sup>-ATPase of myosin II, can both shorten the hair cells when applied alone, and convert the response to ionomycin to a purely osmotic one (phase 2). We hypothesize that an active actomyosin-based process mediates the iso-volumetric shortening in the frog rostral amphibian papillar hair cells.

Supported by NIH grant no. DC-00222 to PMN.

### 101 Nonlinearity of the Cochlear Microphonic

**Alfred L. Nuttall<sup>1,2</sup>**, Jiefu Zheng<sup>1</sup>, Yuan Zou<sup>1</sup>, Fangyi Chen<sup>1</sup>, Tianying Ren<sup>1</sup>

<sup>1</sup>Oregon Health & Science University, Oregon Hearing Research Center, <sup>2</sup>Kresge Hearing Research Institute, University of Michigan

The cochlear microphonic (CM) is a field potential that primarily originates from the sound stimulated outer hair cells (OHC) in the cochlea. The CM is readily recorded from the round window niche of the cochlea and can reach 1 mV in magnitude for loud sound at frequencies near 1 kHz. The location of the OHCs generating the CM is

complex, but experimental work has provided evidence that OHCs nearby the round window dominate. The CM waveform has been shown to saturate with high sound levels. This saturation generally has asymmetry such that a spectral analysis shows a dc term as well as even and odd order harmonics. In this study we show that distortion in the CM from the guinea pig takes another form when the cochlea has normal sensitivity. At sound levels of 50 to 90 dB SPL, low frequency pure tones below 2 kHz produced an unusual waveshape characterized by a notch, which occasionally is so prominent to appear as a frequency doubling of the waveform. This CM distortion character was sound level and frequency dependent. Total harmonic distortion (THD) of the CM at 500 Hz had a first peak, as a function of sound level, at about 60-70 dB SPL then became large again as the CM saturated at high sound levels (>90 dB SPL). In addition, the distortion increased (was 'unmasked') when the scala media was perfused with endolymph containing NMGD-CI to replace KCI. The time domain waveform of the CM is related to the ensemble shape of the OHC mechanical transduction function (and any other dynamic conductance changes in the equivalent electrical circuit of the transduction current path). The saturating shape of the Boltzman activation function for stereociliary channels probably accounts for saturation and asymmetry of the CM distortion. To account for the type of distortion seen, having notch and frequency doubling character, requires a nonmonotonic function. These points and data on the origin of the round window recorded CM will be discussed.

Supported by NIH NIDCD DC 00141

## 102 Salicylate Alters the Orientational Order of the Outer Hair Cell Plasma Membrane: A Fluorescence Polarization Microscopy Study

Jennifer Greeson<sup>1</sup>, Robert M. Raphael<sup>1</sup>

<sup>1</sup>Rice University

Prestin is a unique transmembrane protein implicated in the electromotile response of the cochlear outer hair cell (OHC). The activity of prestin is sensitive to salicylate and other lipophilic agents, but the mechanism by which these compounds exert their ototoxic effects is unknown. As prestin is a polytopic protein, there are likely extensive interactions with the surrounding membrane environment. In this study, we are utilizing fluorescence polarization microscopy (FPM), a technique for measuring the orientation of fluorescent membrane markers, in both model systems and living cells. Here, we have extended the FPM theory for use in the cylindrical OHC. A steady state model for the orientation of di-8-ANEPPS, a voltagesensitive membrane probe, predicts the molecule is oriented at 67° with respect to the plane of the membrane. The application of 10mM salicylate induces dramatic changes in the orientational order of the outer hair cell membrane. This effect is not observed in model lipid membranes, indicating that the OHC plasma membrane is particularly sensitive to this non-native amphipath. These findings suggest the organization of the membrane plays a direct role in salicylate-induced reduction of electromotility.

### 103 Stochastic Models for Fast Adaptation and Cochlea Amplfier

Bora Sul<sup>1</sup>, Kuni lwasa<sup>2</sup>

<sup>1</sup>Biophysics Section, NIDCD, NIH, <sup>2</sup>Biophyics Section, NIDCD,NIH

Outer hair cells are critical for the sensitivity and frequency selectivity of the mammalian ear. This function is thought to be achieved by mechanical feedback by those cells that results in amplification (cochlear amplifier). Of the two motile mechanisms in outer hair cells, electromotility in lateral membrane and fast adaptation of hair bundles, we examine the effectiveness of the latter using theoretical models.

Fast adaptation, which leads to fast reduction of transducer current following a peak current, may consist of two main factors: "twitch," a partial closure of channels as the direct effect of Ca influx and "release," a relaxation of intracellular structure that connects the channel with myosin, which is responsible for slow adaptation.

For "release" factor, we constructed a model in which release length is determined by channel gating through Ca with a time delay factor. The model gave reasonable fit with the time course of transducer currents and displacement of the elastic probe for different stimulus levels (Kennedy et. al, 2005). Although our model did not lead to negative stiffness, it was also able to explain the effect of external Ca concentration.

Twitch was examined with a channel gating model, which assumed a single Ca binding site instead of two (Choe et al 1998). As expected, this model can explain bundle movement and force generation (Benser et. al, 1996, Cheung et. al, 2006). The work done by the hair bundle in response to the sinusoidal stimulus showed that this factor indeed contributes to amplification.

The energy source of fast adaptation is changes in intracelluar Ca concentration in the vicinity of the transducer channel, approximated by Ca concentration in the endolymph (~5uM) and in the cytosol (50nM). Thus, if one Ca ion is used per one cycle, energy consumption is (ln 100) kT. Energy loss by viscous drag per cycle, to be counteracted, is proportional to the frequency. If we assume 100% efficiency, 1 nm amplitude, and the viscous drag for the guinea pig cochlea (Ospeck et al, 2003), fast adaptation can support frequency up to 400kHz. However, the real limit must be lower because only twitch contributes to amplification and both gating and release contribute to damping.

## 104 A Nonlinear Multicompartmental Cochlear Model with a Bi-Directional Outer Hair Cell Feedback System

**Shan Lu**<sup>1,2</sup>, David C. Mountain<sup>1</sup>, Allyn E. Hubbard<sup>1,2</sup>

<sup>1</sup>Hearing Research Center, Boston University, <sup>2</sup>Electrical and Computer Engineering

A hydromechanical, multi-compartment model of the cochlea with an outer hair cell (OHC) force generator was able to mimic the physiologically-measured response of the basilar membrane (BM) [Hubbard, A. E., Mountain, D.

C. and Chen, F., "Time-domain responses from a nonlinear sandwich model of the cochlea" in Biophysics of the Cochlea: From Molecule to Model. A.W. Gummer, ed., World Scientific, Singapore]. An improved model that included nonlinear OHC electro-anatomic parameters and scalae electrical parameters was able to mimic cochlear microphonic (CM) data at low frequencies [Lu, S., Spisak, J., Mountain, D. C. and Hubbard, A. E., "A New Multicompartments Model of Cochlea" in Auditory Mechanisms: Processes and Models. A. L. Nuttall, ed., World Scientific, Singapore]. The BM response of this improved model was reduced in the high frequency range because the OHC membrane capacitance severely reduces OHC transmembrane potential when the frequency is high.

In order to overcome this reduced response in the high frequency range, a nonlinear, bi-directional feedback model of the OHC was adopted [Mountain, D. C. and Hubbard, A. E., A Piezoelectric Model of Outer Hair Cell Function. J Acoust. Soc Am. 1994 Jan;95(1):350-4]. Consequently, the mechanical loading of the OHC translates bi-directionally with the electrical impedance of the OHC. The feedback is pseudo-linear in low SPL stimuli and highly nonlinear in high SPL input. This piezoelectrical mechanism allows the energy transferring from the OHC to the mechanics to increase the cycle-by-cycle BM response at high frequencies.

This work was supported by NIH.

# 105 Espin Proteins are Expressed in a Subset of Rat Type-I Spiral Ganglion Neurons and Concentrated in Their Central Projections Innervating Root Neurons and Octopus Cells in the Cochlear Nucleus.

**Gabriella Sekerkova**<sup>1</sup>, Lili Zheng<sup>1</sup>, Enrico Mugnaini<sup>1</sup>, James Bartles<sup>1</sup>

<sup>1</sup>Dept. of Cell and Molecular Biology, Northwestern University Feinberg School of Medicine

The espins are multifunctional actin-cytoskeletal proteins shown previously to be enriched in sensory cells, such as hair cells. Here, we report a novel localization of espins to a subset of spiral ganglion neurons and their central projections in the rat. Affinity purified espin antibody labeled a large subset of type-I spiral ganglion neurons. but not the type II neurons or the vestibular ganglion The espin-positive type-I neurons were neurons. distributed uniformly along Rosenthal's canal, suggesting no correlation with characteristic frequency. The espin antibody also labeled the central processes of type-I neurons, but not their peripheral processes. In the cochlear nucleus (CN), the espin-positive primary acoustic fibers showed a projection pattern typical of type I neurons. Intense immunolabeling was detected in the nerve root region and posteroventral CN (PVCN). The anteroventral CN (AVCN) showed medium staining intensity, while the dorsal CN (DCN) showed a weak labeling that was restricted to deep layers. Espin immunolabeling of the synaptic boutons of the primary fibers was confirmed by confocal imaging, using antibodies to synaptophysin and espin, and by electron microscopy. The espin-positive boutons were especially enriched around the nerve root neurons and the octopus cells in the PVCN. Multiple espin-positive boutons were found on globular bushy cells and giant neurons in the PVCN and AVCN. Small espin-positive terminal and en passant boutons were also identified throughout the neuropil of the CN. Surprisingly, the espin antibody did not label the typical large endbulbs of Held on the spherical bushy cells in the AVCN. Western blot analysis showed that espin 3B and espin 4 isoforms were the dominant espin isoforms in the rat CN. Our results show selective enrichment of espin isoforms in a subset of rat type-I cells, which innervate root neurons and the octopus cells with intermediate modified endbulbs.

(Support: NIH DC004314 to J.R.B.)

#### 106 Differential Regulation of Pre- and Post-Synaptic Proteins by Neurotrophins in the Spiral Ganglion

Jacqueline Flores-Otero<sup>1</sup>, Robin L. Davis<sup>1</sup>

<sup>1</sup>Rutgers University and UMDNJ

Studies from our laboratory have shown that the endogenous firing patterns of spiral ganglion neurons and the underlying voltage-gated ion channels display a tonotopic distribution that is differentially regulated by brain derived neurotrophic factor (BDNF) and neurotrophin-3 (NT-3). Furthermore, the post-synaptic AMPA receptor subunits, GluR2 and GluR3, show a similar type of distribution and regulation. They are enriched in the base and, much like the rapidly activating K+ channel subunits, were up regulated by BDNF and down regulated by NT-3. Based upon these observations, we hypothesized that presynaptic associated proteins would also be differentially distributed and that this distribution would be regulated by BDNF and NT-3.

Quantitative analysis of 5 separate immunocytochemical experiments revealed that anti-synaptophysin antibody labeling was significantly higher in apical (22.7±1.7) compared to basal (13.4±2.2; P<0.01) spiral ganglion neurons. Moreover, the pattern of distribution for a particular protein was predictive of its neurotrophin regulation. We found that NT-3 application significantly up regulated synaptophysin luminance (34.8±3.0; P<0.01 and 22.7±2.2; P<0.05; apical and basal neurons, respectively), whereas BDNF either down regulated or had no effect on synaptophysin luminance (17.5±2.9; P<0.05 and 11.8±1.5; P>0.1, apical and basal neurons, respectively). Experiments evaluating anti-SNAP-25 antibody luminance corroborated these findings.

The results of these experiments show the extraordinarily complex organization of spiral ganglion neurons, extending beyond endogenous voltage-gated ion channels to their interactions with both their peripheral and central targets. Like the AMPA receptors, the pre-synaptic proteins synaptophysin and SNAP-25 were also graded along the frequency map of the cochlea, yet in the opposite orientation with mirror image neurotrophin regulation.

Supported by NIH RO1 DC01856 (RLD) and Gates Millennium Scholarship (JFO).

## 107 Modulation and Modification of Large Conductance Ca<sup>2+</sup>-Activated K<sup>+</sup> Channels in Murine Spiral Ganglia

**Wei Chun Chen<sup>1</sup>**, Mariam Abskharoun<sup>1</sup>, Robin Davis<sup>1</sup> Department of Cell Biology and Neuroscience, Rutgers University

In order to define fully the electrophysiological signature of spiral ganglion neurons, a better understanding of the large conductance  $\text{Ca}^{2^+}\text{-activated}\ \text{K}^+$  (BK) channel is electrophysiological, necessary. Previous pharmacological, and immunocytochemical studies from our laboratory and others have shown that BK channels are present and distributed tonotopically. In both early postnatal and adult mice, anti-BK antibody labeling was enriched in basal neurons compared to their apical counterparts (Adamson et al., JCN, 2002). What is not clear from those studies, however, is whether the differential distribution can be accounted for purely by changes in BK channel density, or whether tonotopic gradations in basic features such as kinetics, calcium sensitivity, and/or voltage dependence are also present.

The hallmark of BK channels is the functional diversity that results from  $\alpha$ -subunit alternative splicing and binding to BK $\beta$ -subunits. To examine this diversity as a function of cochlear location, we have utilized a multifaceted approach. To date we have found that BK $\beta$ 2 and BK $\beta$ 4 subunits are expressed in the ganglion and that anti-BK $\beta$ 4 antibody labeling does not differ between apical and basal spiral ganglion neurons. Initial studies of  $\alpha$ -subunit splice variants, focused on splice site 4, indicate that the prominent BK variant transcript is ZERO, with no evidence of the stress-regulated exon (STREX). Patch clamp electrophysiology is currently under way to characterize the BK single channel profile and to determine whether activity is up-regulated in the presence of cAMP, as would be predicted by the presence of the ZERO transcript.

By applying these basic studies to neurons isolated from known regions of the ganglion, we hope to determine whether BK channel functional diversity is present in the spiral ganglion, and if so, to determine its contribution to the graded firing patterns exhibited by these cells. Supported by NIH RO1 DC01856.

#### 108 BMP4 Maintains Survival but Inhibits Neurite Extension in Dissociated Cultures of Newborn Mouse Spiral Ganglion

**Donna Whitlon**<sup>1,2</sup>, Mary Grover<sup>1</sup>, Jenny Tristano<sup>1</sup>
<sup>1</sup>Department of Otolaryngology, Feinberg School of Medicine, Northwestern University, <sup>2</sup>Hugh Knowles Center, Northwestern University

The mechanisms underlying the development, regeneration and maintenance of bipolar morphology of spiral ganglion neurons has not been well-studied. We previously reported that inclusion of the cytokine LIF or BMP4 in dissociated culture of the newborn mouse spiral ganglion maintained neuronal survival but that survival under the two different conditions was associated with different neuronal morphology. LIF increases the absolute number of bipolar neurons; BMP4 increases the absolute number of monopolar neurons and neurons with no

neurites. Here we measured neurite lengths from control, LIF and BMP4 conditions. We measured the longer neurite (F1) and the shorter neurite (F2) of bipolar neurons and the neurite emanating from monopolar neurons (Fm). The population histograms of neurite lengths demonstrated that the populations of all classes of neurites in the BMP4 conditions were shorter than those of the control or LIF conditions. Further, if BMP4 was present in cultures that also contained LIF, the BMP4 effects predominated: that is, no effect of LIF on bipolar neurons, an increase in neurons with no neurites, and a shortening of neurite lengths as compared to the LIF alone conditions. These experiments emphasize a here-to-fore understudied area of spiral ganglion neurite regeneration: inhibition of neurite outgrowth and length, even in the presence of factors that maintain neuronal survival. The results raise the possibility that inhibitory mechanisms exist in vivo and that regeneration of neurite length will require their inactivation in addition to the presence of growth promoting factors. (Supported by NIH Grant #DC00653)

#### 109 The Role of Transient Receptor Potential Channels in Neural Activation

**Eul Suh<sup>1</sup>**, Agnella Izzo<sup>2</sup>, Joseph T. Walsh<sup>2</sup>, Claus-Peter Richter<sup>1</sup>

<sup>1</sup>Department of Otolaryngology, Feinberg School of Medicine. Northwestern University. <sup>2</sup>Department of Biomedical Engineering, Northwestern University Lasers can be used to stimulate neural tissue such as the sciatic nerve (Wells et al., JBO 2005) or auditory neurons (Izzo et al., LSM 2006). Wells and coworkers suggested that neural tissue is stimulated by heat (SPIE, 2006). Potential ion channels that can be stimulated by heat are the TRPV channels, a subfamily of the Transient Receptor Potential (TRP) ion channels. TRPV channels are nonselective cation channels found in sensory neurons involved in nociception. These channels are activated by various chemical stimuli, particularly by vanilloid compounds such as capsaicin (the ingredient found in hot chili peppers) and resiniferatoxin. Furthermore, TRPV channels can also be thermally stimulated. The activation temperature for the different TRPV channels varies and is 43°C for TRPV1 and 39°C for TRPV3.

Previous studies document the presence of TRPV1 in the rat cochlea. Our study builds upon these findings to show that TRPV1 channels are also expressed in the spiral ganglion cells of the gerbil cochlea. By performing an immunohistochemical staining procedure on frozen 20 um cochlear slices using a primary TRPV1 antibody, we observed specific immunostaining of the spiral ganglion cells. In control experiments, the primary TRPV1 antibody was preadsorbed with synthetic blocking peptide, resulting in the absence of staining. Furthermore, the ability to evoke action potentials using optical radiation were tested before and after the application of resiniferatoxin (TRPV1 channel agonist) and capsazepine (TRPV1 channel antagonist).

Supported by the E.R. Capita Foundation, NIH HHSN260-2006-00006-C, 1R41DC008515-01, F31 DC008246-01.

## 110 A Role for P75ntr in Regulating Spiral Ganglion Schwann Cell Proliferation and Death Following Denervation

**Matthew Provenzano**<sup>1</sup>, Jie Huang<sup>1</sup>, Shaheen Alam<sup>1</sup>, Amanda Nymon<sup>1</sup>, Kaitlin Zander<sup>1</sup>, Ningyong Xu<sup>1</sup>, Marlan Hansen<sup>1</sup>, Steven Green<sup>1</sup>

<sup>1</sup>University of Iowa

Spiral ganglion Schwann cells (SGSCs) myelinate spiral ganglion neurons (SGNs) and are a potential source of neurotrophic support for SGNs. The signals controlling cell cycle and cell death decisions in SGSCs are largely The pro-neurotrophin, proNGF, induces unknown. apoptosis in sciatic nerve Schwann cells following denervation via p75NTR through cleavage of its intracellular domain by a gamma secretase. We have begun to explore the role of p75NTR in cell cycle and cell death regulation of SGSCs. Following aminoglycoside deafening, SGSCs in the osseous spiral lamina and Rosenthal's canal showed an increase in p75NTR expression by immunofluorescence compared to hearing controls. The p75NTR-positive cells colabeled with anti-S100 (a Schwann cell marker), but not anti-neurofilament, antibodies. To further explore the role of p75NTR, we prepared primary cultures of SGSCs devoid of neurons. In these cultures, SGSCs undergoing cell division lose cell surface p75NTR expression and show an increase in nuclear localization of the intracellular domain (ICD), but not extracellular domain (ECD), suggesting that cleavage of p75NTR and nuclear translocation of the ICD regulate SGSC proliferation. To explore p75NTR's role in controlling cell death, we treated cultured SGSCs from with proNGF. The SGSCs express sortilin, a p75NTR coreceptor required for proNGF-mediated cell death. Treatment with proNGF induced apoptosis in a dose dependent manner and was significantly different (p<0.05) than controls or cells treated with mature NGF. These results suggest that p75NTR contributes to regulation of SGSC cell cycle and cell death following hair cell loss and provide a basis for further investigation of Schwann cell function in the deafened cochlea. As SGN viability likely depends on a healthy population of SGSCs, further definition of these mechanisms will contribute to optimizing efforts to maintain or regenerate a functional auditory nerve.

## | 111 | Adaptation Reduces Spike Count Reliability, but not Spike Timing Precision, in Auditory Nerve Responses

Michael Avissar<sup>1,2</sup>, Adam Furman<sup>1</sup>, James Saunders<sup>1</sup>, **Thomas Parsons<sup>2</sup>** 

<sup>1</sup>Department of Otorhinolaryngology - HNS, University of Pennsylvania, <sup>2</sup>Department of Clinical Studies-NBC, University of Pennsylvania

Information can be coded in the nervous system by either a mean firing rate or by the precise timing of spikes. The resultant neural code is constrained by neural noise due to variability in either spike count or spike timing. Adaptation of the firing rate to a constant stimulus is hypothesized to improve the efficiency and reduce redundancy of neural

coding. To better understand the impact of adaptation on neural coding, we made chick single unit auditory nerve recordings and measured changes in the reliability of spike counts and precision of spike timing during short-term rate We found that spike count reliability decreased (increased Fano factor) for all but the lowest frequency cells while the precision of spike timing (temporal jitter) remained steady at all frequencies. Modelina studies suggested that post-synaptic mechanisms reduce the inherent response variability of quantal neurotransmitter release and confer count reliability at sound onset. With adaptation, quantal content diminishes as the readily releasable pool of vesicles depletes and Fano factor increases to approach that predicted by a binomial statistical model. Thus during the course of short-term adaptation, the coding of intensity via a rate code may become constrained by increased neural noise while the coding of frequency and phase via a temporal code is not.

# Temporary Noise Induced Hearing Loss Influences the Post-Stimulus Time Histogram and Single Fiber Action Potential Derived From Human Compound Action Potentials

Jeffery Lichtenhan<sup>1</sup>, Mark Chertoff<sup>1</sup>

<sup>1</sup>University of Kansas Medical Center

The convolution of a post-stimulus time histogram P(t) and a single neuron action potential U(t) models the compound action potential (CAP) (Goldstein and Kiang, 1958, JASA, 30: 107-114). Estimates of in vivo P(t) and U(t) can be acquired by using functional forms in the convolution model, and fitting the solution to physiologically recorded CAPs (Chertoff, 2004, JASA, 116: 3022-30). We have successfully used this procedure to describe P(t) and U(t) in normal and noise-exposed gerbils and subsequently translated this technique to normal-hearing humans (Lichtenhan et al., ARO Abstracts, 2006 and 2007, respectively). Here we determine the influence of temporary noise induced hearing loss on estimates of P(t) and U(t) in humans.

A 115 dBSPL (RMS) narrow band noise centered at 2 kHz was delivered to the right ear of 27 subjects for 15 minutes. Click evoked CAPs were recorded with a tympanic membrane electrode in response to stimuli from 125 to 75 dBpSPL in 10 dB steps. Physiologic CAPs were fit with the analytic CAP using a constrained nonlinear least squares fitting routine (TOMLAB). Hierarchical Linear Modeling provided the intercepts and slopes of P(t) and U(t) parameter-level functions, and determined if hearing loss influenced the growth patterns.

Noise exposure produced a median temporary hearing threshold shift of 15 dB. The profile of P(t) and U(t) parameter-level functions were altered in several ways following noise exposure. As the degree of hearing loss increased, the intercept of the P(t) delay-level function decreased and the intercept of the U(t) decay-level function increased. At 75 dBpSPL P(t) width and number of responding neurons decreased. This shows that during temporary hearing loss less neurons contribute to the CAP

and these neurons have shorter delay, less synchrony and action potentials that decay more rapidly.

Supported by NIH Grant 2 RO1 DC02117 and the KUMC Biomedical Research Training Program.

# 113 The Influence of Hearing Threshold on the Summed Post-Stimulus Time Histogram and Unit Waveform Underlying the Compound Action Potential

**Brandon Tourtillott**<sup>1</sup>, Mark Chertoff<sup>1</sup>, Jeffery Lichtenhan<sup>1</sup>, Katie Esau<sup>1</sup>

<sup>1</sup>Kansas University Medical Center

In 1958, Goldstein and Kiang developed a theoretical model of the Compound Action Potential (CAP) consisting of the convolution of a summed post-stimulus time histogram [P(t)] and a single unit waveform [U(t)]. Previously, Chertoff (2004, JASA 116(5)) derived a solution to the convolution integral and obtained an analytic CAP. The analytic solution was fit to CAPs from normal and noise-exposed gerbils at 100 dBSPL. The results showed an increase in the delay of P(t), and a decrease in the number of nerve fibers contributing to the CAP (Lichtenhan, 2005, ARO Poster 77). In this study we examined the influence of hearing threshold on the *growth* of the parameters of P(t) and U(t) with signal level.

CAPs analyzed in this study were obtained from Mongolian gerbils from the normal and noise-exposed groups used in our previous work (Chertoff et al., 2003, JASA 114(5)). In the present analysis, P(t) and U(t) were obtained by curve fitting the analytic CAP to the physiologic recorded CAPs using a constrained optimization routine. The parameters of P(t) and U(t) were analyzed as a function of signal level and hearing threshold using hierarchical linear modeling.

The results showed that fewer numbers of nerve fibers contributed to the CAP in the noise-exposed animals than in the normal animals. Moreover, the slope of the *growth* functions was directly related to hearing threshold, suggesting a recruitment of nerve fibers in the production of the CAP. In animals with elevated high frequency thresholds, P(t) was shifted to longer delays than the normal-hearing animals. The shift in the delay-level function for high frequency stimuli could be attributed to the temporal integration by auditory nerve fibers.

# 114 A Novel and Simple Explanation for the Non-Poisson Distribution of Interspike Intervals of the Spontaneous Activity of Auditory-Nerve Fibers

**Peter Heil<sup>1</sup>**, Heinrich Neubauer<sup>1</sup>, Dexter Irvine<sup>2,3</sup>, Mel Brown<sup>2</sup>

<sup>1</sup>Dept. Auditory Learning & Speech, Leibniz Institute for Neurobiology, 39118 Magdeburg, Germany, <sup>2</sup>School of Psychology, Psychiatry and Psychological Medicine, Monash University, VIC 3800 Australia, <sup>3</sup>Bionic Ear Institute, East Melbourne, VIC 3002, Australia Auditory-nerve (AN) fibers are thought to code sounds by the timing and/or rate of spikes. Since AN fibers are spontaneously active (some discharge at rates >100 spikes/s in the absence of experimenter-controlled stimulation), it is necessary to characterize this activity as accurately as possible, if the effects of acoustic stimulation on the spiking behavior of AN fibers are to be thoroughly understood. Such a characterization might also provide information about the operation of the ribbon synapses in the inner hair cells (IHCs) from which AN fibers derive their excitation. It could also be useful for the development of more naturalistic stimulation protocols for cochlear implants, and for the refinement of models of the peripheral auditory system.

The distributions of interspike intervals (ISIs) from spontaneous activity of AN fibers appear Poisson-like and are commonly interpreted and modeled to result from a Poisson process providing excitation to the fibers (e.g. exponentially distributed intervals of transmitter release events from the IHC) modified by refractory properties of the fiber itsself.

Here we show, on records of spontaneous activity from barbiturate-anesthetized cat AN fibers, that in combination with a physiologically plausible refractory function an exponential distribution of excitatory events cannot account for the ISI distributions. However, a mixture of an exponential and a gamma distribution with shape factor 2, both with the same scale parameter, provides a superb and physiologically plausible description. The proportion in the mixture and the absolute and relative refractory periods can be considered constant for the vast majority of fibers, whereas the scale parameter varies across fibers. This simple scenario also resolves the enigma of the reported long-term discharge history effects, lasting tens of milliseconds.

Supported by grants of the Deutsche Forschungsgemeinschaft to P.H. (He1721/5-1, 5-2, and SFB-TR 31).

#### | 115 | Effect of Inner Hair Cell Synapse Efficiency on Auditory Brainstem Response Thresholds

**William Krekeler**<sup>1</sup>, Dennis Barbour<sup>1</sup> *Washington University in St. Louis* 

Auditory brainstem responses (ABRs) measured with scalp electrodes increase in amplitude above a detectability threshold as sound intensity is increased. Hearing loss in a subject typically corresponds with a shift in ABR threshold. Pathology of the inner hair cells (IHCs) resulting in diminished synaptic transmission efficiency relative to normal may underlie some forms of hearing loss. In order to better understand the potential contribution of such pathologies to ABR threshold shifts, we adopted a computational model of the auditory periphery that generates simulated auditory nerve (AN) activity. We extended this model to make predictions regarding ABR waveforms and corresponding thresholds as a function of IHC synaptic transmission efficiency. The ABR estimate is generated for an arbitrary auditory stimulus by convolving the AN instantaneous rate response function with that fiber's unitary response function, as calculated from physiologically measured ABR waveforms. A parameter was added to the peripheral nerve response model to alter the effective synapse

transmission efficiency by scaling the release of IHC. neurotransmitter from the pre-synaptic As efficiency is neurotransmitter release scaled ABR logarithmically, modeled thresholds shift approximately linearly on a decibel scale. For global changes in IHC synapse efficiency, frequency-dependent ABR threshold shifts were not observed.

## 116 Efficient, Low Cost, Parallel Processing in the Development System for Auditory Modelling

Lowel O'Mard<sup>1</sup>

<sup>1</sup>University of Cambridge

Efficient, low cost, parallel processing in the Development System for Auditory Modelling

An efficient parallel processing algorithm has been implemented in the Development System for Auditory Modelling (DSAM). The new algorithm is demonstrated by presenting stimuli to a variety of auditory model simulations and determining the increase in speed achieved using multiple processors/cores. The models include auditory-nerve models – both linear and non-linear – in response to simple and complex stimuli.

Physiologically based models perhaps lack the efficiency of models built on a purely functional basis, however, such models serve to avoid introducing problems in later stages by trying to include the subtleties of the physiological processes. Effective physiologically based models of central auditory processing tend to be large in scale. They are made up of many low-level models with multi-channel levels. Small-scale or slow-response simulations can severely hamper research investigations, so efficient computer modelling is a necessity.

Using parallel algorithms is an effective method of increasing the efficiency of computer modelling. Parallel processing is available using various platforms e.g. the fastest super-computers today use multi-computer or "Beowolf clusters". However, such systems are high maintenance and are beyond the costs in time and money for most laboratories. Additionally, the code required for such systems can only run on similar cluster systems. The parallel processing in DSAM has been implemented using "threading". This means that the same code can run on a single processor laptop as on a multi-processor or dual core computing system, all of which are readily available and easily within the budgets for most laboratories. The simulation speed depends only upon the number of separate processors or "cores" available.

The new parallel algorithm implemented in DSAM works by first determining *chains* of processes within the simulation that have similar numbers of best frequency (BF) channels. During processing of a chain the BF channels are distributed equally among the available processors (threads).

The performance of a parallel algorithm is determined by two main measures: *speed-up* and *efficiency*. Speed-up = (N CPU run-time) / (single CPU run-time). The Efficiency = Speed-up / (No. CPU's). The ideal parallel algorithm produces a linear speed-up, i.e. the run time increases linearly with the number of CPU's used, and has an efficiency of 100%. In real-life maximum efficiency is

seldom achieved, however, the new algorithm in DSAM can achieve an efficiency of 93[IMW1]%.

DSAM is available from http://dsam.org.uk.

Acknowledgements

Supported by a BBSRC project grant to Ian M. Winter, The Physiological Laboratory, Cambridge.

#### 117 Theory of Forward and Reverse Middle-Ear Transmission Applied to Otoacoustic Emissions in Infant and Adult Ears

Douglas Keefe<sup>1</sup>, Carolina Abdala<sup>2</sup>

<sup>1</sup>Boys Town National Research Hospital, <sup>2</sup>House Ear Institute

DPOAE input/output (I/O) functions, which differ at f2=6 kHz in human infants relative to adults, were used to nonassess immaturities in forward/reverse transmission through the ear canal and middle ear (Abdala and Keefe, JASA, 2006). The goal of the present study was to understand why DPOAE levels are higher in infants than in adults. Ear-canal reflectance and DPOAE measurements in the same ears were analyzed using a scattering-matrix model of forward and reverse transmission through the ear canal, middle ear and DPOAE levels were larger in infants mainly because the reverse middle-ear transmittance level varied with ear-canal area, which differed by more than a factor of 7 between infants and adults. The forward middle-ear transmittance level was 10 dB less in infants than adults, resulting in poorer conductive efficiency in infants. The reverse middle-ear transmittance level was 7 dB higher in infants, which, with ear-canal effects assessed by reflectance, accounted for the higher DPOAE level in babies.

(Research supported by NIDCD grants DC003784, DC003552 and DC006607, and the House Ear Institute.)

# 118 The Effect of Probe Level on Wideband Energy Reflectance Measurements of the Contralateral Acoustic Stapedius Reflex Threshold

Bethany Kershner<sup>1</sup>, **Patrick Feeney**<sup>2,3</sup>

<sup>1</sup>University of Washington, Speech and Hearing Sciences, <sup>2</sup>University of Washington, Otolaryngology, Head and Neck Surgery, <sup>3</sup>V. M. Bloedel Hearing Research Center Recent studies have suggested that wideband energy reflectance (ER) measurements of the acoustic stapedius reflex (ASR) threshold provide lower estimates of reflex threshold than traditional methods. The present study examined the effect of probe level on the contralateral ASR threshold for the simultaneous presentation of the activator and probe using a wideband ER system. ASR thresholds for a 1000 Hz activator tone were estimated in 20 young adults with normal hearing. A repeatedmeasures design was used in obtaining ASR thresholds for three wideband-chirp levels of 65, 60 and 55 dB SPL, as well as for a standard 226-Hz probe tone. The experimental ASR threshold was determined by examining

shifts in ER across the frequencies 250 to 2000 Hz using the combination of two statistical tests. A magnitude test used an F-ratio to compare baseline variance with that induced by the activator. A correlation test examined the shape of the ER shift across frequency for different activator levels. An additional criterion for the presence of a reflex was that the maximum shift in ER must be 0.01 or higher. A repeated measures ANOVA revealed that there was a significant effect of ASR threshold method. Post hoc analyses revealed that there was no significant difference in ASR threshold between the 65- and 60-dB-probe conditions, however the 55-dB-probe condition resulted in higher ASR thresholds than the other two by 9 and 7 dB, respectively. ASR thresholds obtained using the experimental ER method were significantly lower than those obtained with the clinical system by as much as 18 dB for the 65-dB-probe condition. These results suggest an interaction between the wideband-probe level and the contralateral ASR threshold for simultaneous presentation of the activator and probe. The nature of this interaction is likely a combination of reflex facilitation for higher probe levels combined with decreasing signal-to-noise ratio for the wideband measurements as probe level decreases.

#### 119 Energy Reflectance Tympanometry in Infants

Chris A. Sanford<sup>1</sup>, M. Patrick Feeney<sup>1,2</sup>

<sup>1</sup>University of Washington, <sup>2</sup>Otolaryngology, Head and Neck Surgery

Evidence suggests wideband energy reflectance (ER) is more sensitive to middle-ear disorders than traditional narrowband admittance measurements. ER patterns in adults obtained in the presence of ear canal pressure (ER tympanograms) follow an orderly sequence as a function of frequency across a much broader frequency range than current tympanometric methods. These orderly patterns, if present in young infants and neonates, could be useful in studying infant middle-ear development with potential diagnostic application as well. To investigate the effects of pressure in developing infant ears, wideband ER was obtained at ambient, positive and negative ear canal pressures for 4-, 12-, and 24-week old infants and young adults. Significant findings across age were identified in three frequency regions from .25 to 4.0 kHz. Below .75 kHz there was a progressive increase in ER at ambient pressure with age, as well as an increase in ER with pressure. The magnitude of ER change with pressure decreased with age and was minimal in adults. These low frequency effects in infants are consistent with developmental changes in the infant ear canal wall. From .75 to 2.0 kHz, the effects of pressure for all infants were not significant, suggestive of a developmentally stable frequency range. Above 2.0 kHz, there were differential effects of pressure in infants, with negative pressures causing increases in ER and positive pressures causing decreases in ER; the magnitude of this effect decreased with age. Conversely, the effects of positive and negative pressures were similar for adults. The high frequency effects in infants suggest orderly changes in the effects of middle ear mass, possibly related to the effects of

pressure on immature ossicular joints. These findings show developmental trends in infant wideband ER tympanometry for the ages in this study and provide a basis for additional investigations in young infants.

(Supported by NIDCD: F31-DC007296).

#### 120 Two Novel Methods to Measure Wide-Band Ear Canal Reflectance

Victoria Lee<sup>1</sup>, Jonathan Siegel<sup>2</sup>

<sup>1</sup>Northwestern University; Dept of Communication Sciences and Distorders, <sup>2</sup>Northwestern University; Hugh Knowles Center; Dept. of Communication Sciences and Disorders

Wideband ear canal reflectance measurements typically require an elaborate calibration procedure to measure the source impedance of the reflectance probe. We have evaluated two methods of measuring reflectance with a greatly simplified calibration procedure. The first method is a variant of the commonly used approach of calculating reflectance from the measured ear canal impedance. Pinto and Dallos (IEEE Transactions on Bio-Medical Engineering, BME-15(1), 10-16, 1968) demonstrated that acoustic impedance measured by the probe, the parallel combination of the ear canal and probe source impedances, can be made close to the ear canal impedance alone if the source impedance of the probe is much greater than the ear canal impedance at all A high source impedance probe was frequencies. constructed by using small, highly damped tubes to conduct the excitation sound and to measure the canal pressure frequency response. The second method calculates reflectance from measurements of the standing wave ratio determined by the relative amplitudes of the incident and reflected pressure waves. The ear canal was extended using a brass tube with the end terminated by the high impedance probe described above. The length of the tube greatly reduced the frequency spacing of pressure nodes and antinodes, measured at the terminated end of the tube. After correcting for tube losses, reflectance was calculated at the frequencies of each node and antinode from the standing wave ratio obtained directly from the pressure ratios of adjacent nodes and antinodes. Both methods yield reflectance values consistent with previously measurements, when measured in a group of 29 human Test-retest reliability was best for the reflectances calculated from measured canal impedance. with s.d. averaging 0.1 reflectance unit from 1-8 kHz and 0.16 unit from 8-15 kHz.

Supported by Northwestern University.

## 121 Audiometry with Nasally Presented Masking Noise: Novel Diagnostic Method for Patulous Eustachian Tube

**Yoko Hori**<sup>1</sup>, Tetsuaki Kawase<sup>1</sup>, Jun Hasegawa<sup>2</sup>, Toshinori Sato<sup>1</sup>, Naohiro Yoshida<sup>1</sup>, Takeshi Oshima<sup>1</sup>, Mitsuko Suetake<sup>3</sup>, Toshimitsu Kobayashi<sup>1</sup>

<sup>1</sup>Tohoku University Graduate School of Medicine, <sup>2</sup>Iwaki Kyoritsu General Hospital, <sup>3</sup>Tohoku Rosai Hospital

The Eustachian tube (ET) is a mucosally lined pathway between the nasopharynx and the middle ear. It is normally closed, but temporarily opens as a result of swallowing. Persistently open ET is known as patulous ET. Patulous ET allows sound and/or pressure created on the pharyngeal side to be transmitted to the middle ear cavity with little attenuation. As a result, patients experience and suffer intractable discomfort including aural fullness, autophony and hearing their own breathing. In the present study, the masking noise is presented nasally instead of self-vocalized sound, and the masking effect on the auditory thresholds was measured to assess the sound transmission from nasopharynx to the middle ear, which is objective indicator of the severity of the patulous ET (nasal-noise masking audiometry).

Nasal-noise masking audiometry was examined in 20 ears of 10 normal subjects as well as in 27 ears of 18 patients with patulous ET. Audiometric threshold measurement in response to the test tone presented to the ear was conducted with or without masking noise presented at the nostril on the test side using a special speaker-phone with an olive-shaped tip originally designed for use in sonotubometry. The test tones were presented to the ear through headphones at seven frequencies in the same way as routine audiometry using an audiometer. The band noise centered at the same frequency as the test tone, which is used for the masking noise in routine audiometry, was applied nasally with the special speaker-phone.

The masking effect of nasally presented noise caused elevation of the threshold for the tone presented in the external auditory canal. This threshold elevation was significantly greater in ears with patulous ET (up to about 50 dB), and was decreased to the normal range after obstructive treatment for the patulous ET. These effects were usually remarkable at lower frequency region.

In the present method, the absolute level of the masked threshold during noise presented nasally indicates the degree of the acoustic patency via the ET, and only requires a commercial earphone attached to the nostril and an audiometer. The present method could be another effective tool to assess the severity of the patulous ET, especially in the respect of the acoustic patency.

# 122 Insensitivity of the Transducer-Incus Connection of the Otologics MET<sup>TM</sup> Transducer to Trans - Tympanic Pressure Cycling.

**Hannes Maier**<sup>1</sup>, Stefan Gea<sup>2</sup>, Marcos Sanchez-Hanke<sup>1</sup>, Rudolf Leuwer<sup>1,3</sup>, Willem Decraemer<sup>2</sup>

1 Hamburg University Medical School, <sup>2</sup>University of Antwerp, <sup>3</sup>Klinikum Krefeld

The Otologics "Middle Ear Transducer™" (MET™) is anchored in the temporal bone (TB) with a sound transmitting tip coupled to the incus body. This connection is critical for proper sound transmission and is subject to external forces and movements of the ossicular chain. Pressure differences across the tympanic membrane (TM) are the main source of relative movements and loading, contributing to sound transmission characteristics and theoretically may even damage the transducer.

To investigate the effect on sound transmission, 10 fresh (<48h) human temporal bones were implanted with transducers. Proper coupling of the transducer was achieved by monitoring the vibration response at the incus with a Laser Doppler Velocimeter (LDV). Measurements were performed while applying pressure (0 to  $\pm 80$  hPa) to the external ear canal (EAC). The transfer function across the eardrum was measured using the LDV and an ER-10c probe in the EAC. To monitor relative transducer-ossicle movements, micro CTs of the same TBs were performed at static pressures between 0 to  $\pm 50$  hPa.

Velocity responses to sound stimulation were most affected by pressure at low frequencies. Responses were maximal at 0 hPa while at the highest and lowest pressures tested velocity amplitudes were decreased by ~20dB.

Velocity responses to transducer stimulation had a less pronounced dependency (<10dB) on ear canal pressure than EAC SPL. While velocity responses characteristics in all TBs were homogenous (SD<6dB, 0.125–10 kHz), sound pressure responses were dominated by destructive interferences starting at low frequencies (~ 0.6 kHz).

The application and release of the pressures over the tested range did not result in permanent changes in X-fer function at 0 hPa even after temporal disconnection. Geometry changes in CT reconstructions at all tested pressures did not exceed construction limits. This indicates that moderate pressures do not permanently affect the implant or coupling efficiency.

#### 123 Development of an Aeration Flow Model of the Cadaveric Human Middle Ear.

**David P. Morris**<sup>1,2</sup>, Rene Van Wijhe<sup>1</sup>, Kenneth Valkenier<sup>1</sup>, Manohar Bance <sup>1,2</sup>, Steve Levine<sup>3</sup>, Clarinda Northrop<sup>3</sup> <sup>1</sup>Ear and Auditory Research Laboratory (EAR. Lab) Dalhousie University, <sup>2</sup>Dept. of Surgery, Division of ORL-HNS Capital Health, Halifax Nova Scotia CANADA., <sup>3</sup>The Temporal Bone Foundation, Boston, Mass. USA Aims: Aeration of the human middle ear is a contentious area of study. It is hoped that a better understanding of aeration pathways of the epitympanum will bring insight to atelectasis and retraction pocket formation, the direction of spread of attic cholesteatoma and the development of

recurrent disease after surgical treatment. We have previously proposed the importance of both micro and macro-ventilation pathways to maintain optimal function and aim to illustrate the functional nature of these pathways with dynamic models.

Methods: Histological preparations of serially sectioned human temporal bones were reconstructed in 3-D using the Amira (R) software package. Subsequently Maya (R), a 3D graphics programme, was used to animate the different pathways demonstrated within the middle ear.

Results: Common aeration pathways were identified and animated.

Conclusion: This novel application of existing software products provides a useful tool for the demonstration of middle ear fold anatomy and a dynamic demonstration of micro and macro-ventilation pathways.

Future work will include the virtual modification of fold anatomy and an assessment of its impact on flow pathways.

#### 124 Orientation of the Human Anatomic Axis of Ossicular Rotation

#### N. Wendell Todd<sup>1</sup>

<sup>1</sup>Emory University

Background: Though the orientation of the human anatomic ossicular axis of rotation has rarely been measured, most assume that the axis is reliably set. However, the orientation of the manubrium, as viewed through the external ear canal, has recently been found to vary over a range of 45 degrees.

Hypotheses: The anatomic axis of rotation is quite variable from ear to ear, similar to the variation in manubrium orientation as viewed clinically. Axis orientation is bilaterally symmetrical, and unrelated to mastoid pneumatization.

Methods: 41 bequeathed adult human cranial base specimens (82 temporal bones) were studied in a custom cephalostat. The end of each axis was determined in 3 orthagonal planes.

Results: From the apex of the short process of the incus to the anterior process of the malleus, the direction of the axis was medial (range 5-44, mean 32) degrees, and ranged from 19 degrees above to 27 degrees below (mean 3 degrees below) the Frankfort horizontal plane, left ear. Though bilateral symmetry was found for the anatomic rotational axes, no correlation was found with either the clinical orientation of the manubrium, or the extent of mastoid pneumatization.

Conclusion: The human anatomic axis of rotation is variably oriented, similar to the variability of clinically viewed manubrium orientation.

### 125 3D-CT Imaging in the Sitting Position for the Diagnosis of Patulous Eustachian Tube

**Toshiaki Kikuchi**<sup>1</sup>, Takeshi Oshima<sup>1</sup>, Masaki Ogura<sup>1</sup>, Yoko Hori<sup>1</sup>, Tetsuaki Kawase<sup>1</sup>, Toshimitsu Kobayashi<sup>1</sup> 

\*Department of Otolaryngology-Head and Neck Surgery, Tohoku University Graduate School of Medicine One of the major clinical characteristics of patulous eustachian tube (pET) is the change in severity of symptoms according to the posture. The symptoms are

commonly masked in the recumbent position ,which has detracted from the advantages of modern imaging for the diagnosis of the pET, because computed tomography (CT) and magnetic resonance imaging are performed in the recumbent position.

The present study examined the CT characteristics of the eustachian tube (ET) in patients with pET and normal controls using three-dimensional CT in the sitting position, to assess the clinical usefulness for the diagnosis of pET.

Eighty-seven patients divided into two groups. The patulous ET group consisted of 111 ears of 67 patients with patulous ET. The control group consisted of 30 ears of 20 patients without symptoms characteristic of pET or any abnormal findings in ET function tests.

CT was performed under the resting condition and during Valsalva's maneuver (Valsalva condition). The multiplanar reconstruction technique was used to reconstruct 1-mm-thick gapless images parallel to and perpendicular to the ET long axis. The open tubal distance (OTD) and average ET-gram were examined.

The OTD was significantly longer in the pET group than in the control group under both resting and Valsalva conditions (both p<0.001). The OTD was also significantly longer under the Valsalva condition than under the resting condition in both groups (p<0.01 in the patulous ET group, p<0.001 in the control group). The normal ET lumen was occluded in the cartilaginous portion medial to the isthmus under both the resting and Valsalva conditions in the control group (n=30). However, the occlusive zone could not be observed under either the resting or Valsalva conditions in the patulos ET group (n=111). Completely patent (open) ET was observed with continuous hyperlucency from the pharyngeal to the tympanic orifices in 88 of 111 patients in the pET group, but in none of the control group, indicative of 100% specificity.

We conclude that CT in the sitting position employing Valsalva's maneuver is useful for the diagnosis of patulous ET.

## 126 Using 3D Reconstruction to Demonstrate Anatomy of the Middle Ear Ossicles

**Clarinda Northrop**<sup>1</sup>, Stephen Levine<sup>1</sup>, Collin Karmody<sup>1</sup>

\*\*Temporal Bone Foundation\*\*

Goal: Using computer technology it is possible to make an accurate detailed image of the three middle ear ossicles, details of each ossicle and the relationship of one ossicle to the other. Based on serial histological sections each ossicle was segmented out and rendered into a 3D model where it can be viewed individually or in relation to one another.

Methods: The 20 micron celloidin serial sections of a forty week gestation, 1 day postpartum newborn were scanned into the computer and aligned in Photoshop. Each ossicle was segmented out into an individual layer and using Maya Software made into a 3D model.

Results: From studying our 3D images, we became aware of several anatomical features in the ossicles which have not been well described or described at all. There is a

notch on only the anterior side of the long process of the incus below the level of the pedicle where ligamental fibers are attached. The length and position of the anterior process (processus gracilis) of the malleus can be better appreciated. The curvatures in the cruae of the stapes clearly show the delicate anterior and posterior, superior and inferior arches.

## 127 Mucosa-Associated Lymphoid Tissue in the Middle Ear of Harbour Porpoise, Phocoena Phocoena.

**Susanne Prahl**<sup>1</sup>, Darlene Ketten<sup>2,3</sup>, Andreas Beineke<sup>4</sup>, Markus Sanchez Hanke<sup>5</sup>, Ursula Siebert<sup>1</sup>

<sup>1</sup>Forschungs- und Technologiezentrum (FTZ) Westkueste, <sup>2</sup>Woods Hole Oceanographic Institution (WHOI), <sup>3</sup>Harvard Medical School (HMS), <sup>4</sup>Tieraerztliche Hochschule Hannover, <sup>5</sup>Universitaetsklinikum Hamburg Eppendorf Mucosa-associated lymphoid tissue (MALT) in the middle

Mucosa-associated lymphoid tissue (MALT) in the middle ears have not been previously reported in whales and dolphins. Here, for the first time we present findings of MALT in the submucosal lining of the tympanic cavity of harbour porpoises (Phocoena phocoena). This small cetacean inhabits coastal waters of the northern hemisphere. Tympanic-periotic complexes from stranded or inadvertently by-caught fresh neonate to adult animals originating from German and Danish areas of the North and Baltic were extracted and examined grossly. Middle ears of 31animals considered suitable for histopathologic investigation were decalcified, celloidin-embedded, and sectioned. Every 10th section was H&E stained section and examined. Submucosal rounded aggregations of lymphoid cells with or without germinal centers were identified. These follicles varied in number and size. Primary and secondary follicles could be distinguished from subepithelial lymphatic aggregations. Additionally, follicular and parafollicular areas were present. The occurrence of Stenurus minor, a nematode, in the middle ear and adjacent peribullar regions and sinus of Phocoena phocoena is a common feature in animals from the North and Baltic Seas. Our study shows a significant correlation with the occurrence of MALT. Consequently, we propose that this organism may precipitate the development of MALT in these ears.

### 128 do Pingers Acoustically Impact the Ears of Harbour Porpoises?

**Susanne Prahl**<sup>1</sup>, Jennifer O'Malley<sup>2</sup>, Darlene R. Ketten<sup>3,4</sup>, Julie Arruda<sup>2,3</sup>, Ralf Bechmann<sup>5</sup>, Ursula Siebert<sup>1</sup>

<sup>1</sup>Forschungs- und Technologiezentrum (FTZ) Westkueste, <sup>2</sup>Massachusetts Eye and Ear Infirmary (MEEI), <sup>3</sup>Woods Hole Oceanographic Institution (WHOI), <sup>4</sup>Harvard Medical School (HMS), <sup>5</sup>Roentgenpraxis Heegbarg Hamburg

Acoustic deterrent devices, pingers, are developed to mitigate small cetacean by-catches in European fisheries. However, their effect on the hearing system of harbour porpoises is still unknown. In order to address this relevant concern, it is of major interest to collect morphologic data on the inner and middle ear and consequently an essential precondition to identify general and more specifically,

acoustic pathologies. This study examined the inner ears of Phocoena phocoena for the first time from German and adjacent Danish waters of the North and Baltic Seas.Postmortem examinations of the head were conducted by computerized tomography. The ear region was investigated by means of 20 µm celloidin histology sections with H/E staining. 28 harbour porpoises were sampled, 46.4% of which came from German waters, 53.6% from Danish waters, 71.4% from the Baltic, and 28.6% from the North Sea. Basic morphology data from inner and middle ears of harbour porpoises were collected. None of the fresh animals that were evaluated showed intravital atrophies of organ of Corti sensory cells or signs of neural degeneration. Nevertheless, several pathological changes were found, such as parasitic infestations and inflammatory reactions, each of which can be a cause of the other. Parasites were found in the middle ear, peribullar regions and sinuses, not in the inner ear. The effect of the common finding of parasites on hearing is still unknown. These and additional changes e.g. of the acoustic fat of the lower jaw, reduced 8th cranial nerve and soft tissue deposits will be demonstrated. Since June 2005, the use of pingers has become mandatory in parts of the cod fishery in European waters. Therefore it is even more important to continue the analysis based on a larger sample for comparison with animals not affected by pingers.

### 129 Transduction of PLGa Nanoparticles Through the Round Window Membrane

**Ronald Jackson**<sup>1</sup>, Xianxi Ge<sup>1</sup>, Jianzhong Liu<sup>1</sup>, Elizabeth Harper<sup>1</sup>, Michael Hoffer<sup>1</sup>, Richard Wassel<sup>2</sup>, Kenneth Dormer<sup>2</sup>, Richard Kopke<sup>2</sup>, Ben Balough<sup>1</sup>

<sup>1</sup>DOD Spatial Orientation Center, <sup>2</sup>University of Oklahoma Health Sciences Center

Transduction of PLGA nanoparticles through the round window membrane

This study examined the transportability of polylactic/glycolic acid-encapsulated iron oxide nanoparticles (PLGA-NPs) through cadaver and chinchilla round window membranes (RWM).

Methods: PLGA-NPs were placed on cadaver (ex-vivo) and chinchilla (in-vivo) ears and were exposed with and without magnetic fields for 20 or 40 minutes. 3µl of PLGA-NP suspension (3mg/ml) were placed on all RWMs. Magnetically exposed ears were centered on the pole face of a 4 inch cubic NdFeB48 magnet with the RWM facing up. After exposure time, perilymph was drawn from the scala tympani, placed on formvar grids, and RWMs were dissected and processed for TEM imaging.

Results: The thickness of RWM was  $79\pm12.2\mu$  ranging from  $64-92\mu$  in Cadaver and was  $14.7\pm2.63\mu$  ranging from  $9-19\mu$  in chinchilla. In both models, magnetite nanoparticles were observed after either time points across all 3 layers of the RWM under magnetic force. In cadaver ears, electron-dense deposits were seen (30,000x) in the connective tissue layer, dispersed in radial and longitudinal collagen fiber bundles and in elastic fibers and fibroblasts. In chinchilla RWM, electron-dense deposits were found (12,000x) in the middle ear side

epithelium and within the fibrous layer. At higher magnification (50,000x), magnetite particles appeared as string aggregates ranging from 100 to 300 nm long. Electron Energy Loss Spectrometry (EELS) analysis confirmed the presence of iron. Intense electron-dense deposits were also observed in the perilymph of chinchillas and cadaver ears. At 140K magnification, they appeared as 10-20 nm diameter spherical particles that were embedded in polymer. EELS analysis confirmed the iron makeup of these particles.

Conclusion: Despite the differences in thickness, the PLGA-NPs were transduced through cadaver and chinchilla RWM by external magnetic forces The PLGA-NP groupings were smaller and more dispersed in human RWM than in chinchilla.

#### 130 Identify and Develop Mouse Models for Otitis Media

**Qing Zheng<sup>1,2</sup>**, Yi-Cai Tong<sup>2</sup>, Heping Yu<sup>1</sup>, Shengli Li<sup>1</sup>, Kumar Alagramam<sup>1</sup>

<sup>1</sup>Case Western Reserve University, <sup>2</sup>The Jackson Laboratory

Otitis media (OM), one of the most common human diseases, is affected by multiple factors including Eustachian tube (ET), immune status, innate mucosal defense, pathogens, and genetic susceptibility. The mouse is the premier animal model for human disease research, and mouse models of OM represent powerful tools for advancing the understanding of OM. Resistance to antibiotics has hampered the current management of the disease. In order to develop alternative treatment strategies, identifying the genetic factors underlying the susceptibility to OM, we have developed, and characterized several genetic mouse models of OM with tympanometry and video-otoscopy techniques for the analysis of middle ears in mice. We have tested the sensitivity and specificity of these two tools in mice by matching pathological studies of several potential or known genetic mouse models of OM. We have also developed a pathogen-challenged methodology evaluate genetic mouse models of OM. We will report the details in this meeting.

Supported by NIH grants DC04376 and DC007392 to QYZ

## | 131 | Bisphosphonate Therapy Ameliorates Hearing Loss Due to Osteopenia in Mice Lacking Osteoprotegerin

**Sho Kanzaki**<sup>1</sup>, Yasunari Takada<sup>2</sup>, Kaoru Ogawa<sup>1</sup>, Koichi Matsuo<sup>2</sup>

<sup>1</sup>Department of Otorhinolaryngology,School of Medicine, Keio University, <sup>2</sup>Department of Microbiology and Immunology, School of Medicine, Keio University

Three ossicles the malleus, incus, and stapes conduct sound in the middle ear from the tympanic membrane to the oval window of the inner ear. We analyzed effects of excessive bone remodeling on hearing in mice lacking osteoprotegerin (OPG), a soluble decoy receptor for the osteoclastogenic cytokine, receptor activator of nuclear

κB(RANKL). We previously found that auditory ossicles are massively resorbed by osteoclasts in Opg-/- mice and that nulls exhibit progressive hearing loss beginning as early as 6 weeks of age (Kanzaki et al, 2006). All three ossicles exhibited thinning, especially at the malleal manubrium, and osteoclast numbers increased over controls. The junction between the stapes and the otic capsule was also fixed, as is seen in otosclerosis.

Here, we minimized hearing loss in Opg-/- mice by injecting an inhibitor of bone remodeling, risedronate, 5 times a week for 9 weeks. Radiological analyses revealed that risedronate treatment increased bone mineral density of tibia and auditory ossicles. Auditory brain-stem response (ABR) measurement demonstrated that hearing in such mice was significantly improved by risedronate treatment. Since the stapedial junction remained fused to the otic capsule after treatment, we hypothesize that thickening of the malleal manubrium seen after treatment may facilitate transmission of sound through ossicles.

#### 132 Immunohistochemical Evidence of BMP-2, -4 and -7 and Their Receptors -IB and –II in Otospongiosis

**Goetz Lehnerdt**<sup>1</sup>, Klaus Alfred Metz<sup>2</sup>, Klaus Jahnke<sup>1</sup>, Andreas Neumann<sup>1</sup>

<sup>1</sup>Department of Otorhinolaryngology, University of Duisburg/Essen, <sup>2</sup>Insitute of Pathology and Neuropathology, University of Duisburg/Essen, Germany Hypothesis: Main goal of this study was to perform an immunohistological analysis of bone morphogenetic proteins (BMP)-2, -4 and -7 and BMP receptors(R)-IA, -IB and -II in otoclerosis.

Background: The role of BMP in various tissue growth and repair mechanisms is an ongoing topic in the literature. BMP-2, -4 and -7 are known to be of major importance in bone formation and repair. Their role in otosclerotic bone transformation has not been analysed previously.

Method: Parts of the stapedial footplates, collected during partial stapedectomies in 35 patients with clinical otosclerosis were analysed for histological otosclerotic lesions after hematoxylin&eosin staining. Immunohistochemical analysis was performed using polyclonal IgG antibodies for BMP-2, -4,-7 and the IA-, IB-, II-BMP-receptors as well as biotinylated secondary antibodies, avidin-biotin-peroxidase complex reaction and alkaline phosphatase staining (NBT). Attic bone served as a negative control.

Results: 17 specimens contained otosclerosis, 5 of these were otospongiotic, 9 fibrotic, 2 sclerotic and one both sclerotic and fibrotic lesions, thus in total 17/35 (49%) showed histological otosclerosis. Only in the cases of specimens exhibiting an otospongiotic phase the multiple osteoblasts and osteoclasts showed distinct immunochemical staining for BMP-2, -4 and -7 as well as for R-IB and R-II, whereas R-IA remained negative.

Conclusion: It was shown for the first time that BMP-2, -4 and -7 play a role in the active phase otosclerotic bone remodelling. Their actions are mediated through type-IB and type-II receptors. To determine this role in detail,

further investigations - especially for the phosphorylated Smad proteins within the BMP dependent mediator cascade - will be necessary.

#### 133 Bacteriology of Chronic Otitis Media in C3H/HeJ Mice

**Carol MacArthur**<sup>1</sup>, J. Beth Kempton<sup>1</sup>, Jackie DeGagne<sup>1</sup>, DeAnn Pillers<sup>1</sup>, Dennis Trune<sup>1</sup>

The C3H/HeJ mouse has a single amino acid substitution in its toll-like receptor 4, making it insensitive to endotoxin. As a result, these mice are susceptible to spontaneous chronic otitis media, presumably because they cannot clear gram-negative bacteria. These mice offer a model in which to study middle ear inflammation. However, nothing is known of their middle ear disease mechanisms, particularly the presence and type of invasive bacteria. Therefore, their middle ear infection was characterized by a comprehensive analysis of otoscopy, blood and middle ear cultures, light and electron microscopy, and polymerase chain reaction (PCR).

Otoscopy was performed to confirm middle ear disease in five mice. Cultures of middle ear exudates and blood from all five mice grew Klebsiella oxytoca, a common gramnegative bacterium. Light microscopy of additional middle ears showed intense inflammatory cell infiltrate and the presence of gram-negative bacteria in the middle and inner ears. Electron microscopy revealed abundant rod-shaped bacteria matching published ultrastructural descriptions of K. oxytoca. These bacteria were seen free within the middle ear exudate and being engulfed by neutrophils. The PCR analysis confirmed the presence of K. oxytoca in all infected middle ear exudates tested. No other significant bacteria species were identified in any of the analyses conducted.

This report expands on our previous work of spontaneous chronic otitis media in the C3H/HeJ mouse (MacArthur et al., Laryngoscope, 116:1071-1079, 2006) by confirming the presence and identification of the gram-negative bacteria present in the middle ear. This confirmation of gram-negative K. oxytoca bacteria supports the theory that its middle ear disease arises from bacterial infection. This model of chronic otitis media should therefore serve as a valuable tool for the characterization of middle and inner ear inflammatory disease processes that are induced by middle ear infections.

Supported by NIH-NIDCD R01 DC05593 & DC005593-S1, NIH-NIDCD R21 DC007443, NIH-NIDCD P30 DC005983, and VA RR&D RCTR 597-0160 National Center for Rehabilitative Auditory Research.

### 134 Effects of BCG on Otitis Media with Effusion in Mice

Suling Hong<sup>1</sup>

<sup>1</sup>The Department of Otolaryngology, Chongqing University of Medical Sciences, Chongqing, China

Objective: To study the efficacy and its mechanism of bacilli calmette; aguerin(BCG) for otitis media with effusion(OME) in mice.

Methods: Thirty BALB£¯C mice were randomly divided into 3 groups. Both ovalbumin(OVA)group and BCG group were immunized with OVA£¯alum and challenged with OVA. BCG group was injected with BCG 0.02 mg intracutaneously 3 days before being challenged. The mice were killed 2 days after being challenged. The pathology of the middle ear mucosa were studied and the expression of IL-4 $_{i}$ ¢IL-5 $_{i}$ ¢IFN- $_{i}$ Ã $_{i}$ ¢IL-1 2 were examined with immunohistochemistry method.

Results: Pathological examination showed that middle ear mucosa inflammation and eosinophil infiltration in BCG group were inhibited as compared with that in OVA group. The expression of IFN- $^{1}_{1}$ A $^{1}_{2}$ ¢IL-1 2 were significantly higher in BCG group than that in OVA group.

Conclusion: BCG is an effective immunomodulator, and its treatment effect for OME may be carried out by means of adjustment of the balance of Th1£ Th2.

#### 135 Myd88 and TLR Signaling in Innate Immunity of Otitis Media

**Anke Leichtle**<sup>1,2</sup>, Michelle Hernandez<sup>3</sup>, Jorg Ebmeyer<sup>4</sup>, Kwang Pak<sup>1</sup>, Friedrich Bootz<sup>2</sup>, Stephen Wasserman<sup>3</sup>, Allen F. Ryan<sup>1</sup>

<sup>1</sup>Department of Surgery, Division of Otolaryngology, UCSD School of Medicine, <sup>2</sup>Department of Surgery, Division of Otolaryngology, University of Bonn, Germany,

<sup>3</sup>Department of Medicine, Division of Rheumatology, Allergy & Immunology, UCSD School of Medicine, <sup>4</sup>Department of Surgery, Division of Otolaryngology,

University of Wurzburg, Germany

Introduction: Otitis media (OM), the most common disease of childhood, involves infection of the middle ear (ME) with mucosal hyperplasia and leukocyte infiltration. The interaction between pathogen susceptibility and innate immunity is relevant in OM. We evaluated the role of Toll-like receptor (TLR) signaling, an important mediator of innate immunity, via the myeloid differentiation factor 88 (MyD88) adaptor in OM.

Methods: The MEs of MyD88, TLR2 and TLR4 null mice, control mice (C57BL/6) and rats were inoculated with nontypeable Haemophilus influenzae (NTHi). Animals were sacrificed at various times from 0 hours to 21 days (21d). ME mucosal thickness and cellular infiltration were evaluated histologically. NTHi clearance was assessed by culture of ME effusion. ME mRNA was evaluated by gene chip in control mice, while protein levels were determined by Western blot in rats.

Results: Mucosal thickness and cellular infiltration in MyD88 KO mice inoculated with NTHi are similar to the response in control mice, for the initial period from 0d-3d. However, the ME response is significantly greater at 5d and 10d post-inoculation. TLR2 and TLR4 KO mice also show normal initial ME inflammation. While TLR4 KO mice show incomplete recovery of mucosal thickness at 10d, the mucosal thickness of TLR2 KO mice is significantly higher at 5d and reaches a very high peak at 10d. The protein level of MyD88 and TLR4 in the ME increases strongly from 72 hours to 10d, while TLR2 shows a peak at 3d and decreases at 10d. MyD88 KO mice remain culture positive far longer than control mice.

Conclusion: In NTHi OM, MyD88 and TLR2 and 4 are not essential for the initial ME inflammation. However, for bacterial clearance and subsequent ME recovery, MyD88 and TLR2 signaling are critical. If TLRs contribute to initial ME inflammation in OM, they presumably do so via an alternative linker such as TRIF.

(Supported by grants DC00129 (AR), DC006279 (SW) and Allergy training grant (MH) from the NIH).

## 136 Tissue Remodeling Cytokines in the Middle and Inner Ear During Acute and Chronic Otitis Media

**Dennis Trune<sup>1</sup>**, Beth Kempton<sup>1</sup>, Jacqueline DeGagne<sup>1</sup>, Bobak Ghaheri<sup>1</sup>, De-Ann Pillers<sup>1</sup>, Carol MacArthur<sup>1</sup>
<sup>1</sup>Oregon Health & Science University

Acute and chronic otitis media are significant clinical problems because of uncontrolled inflammation of the middle ear and potential risk to the inner ear. Clinical and experimental efforts focus mostly on the control of inflammatory cells and their related cytokines. However, extensive tissue remodeling occurs in otitis media and little attention is given to those inflammatory cytokines that act primarily on connective tissue and bone. Therefore, the present study characterized those cytokines in otitis media that influence tissue remodeling within the middle and inner ear.

Acute otitis media was induced by transtympanic injection of BALB/c mice with heat-killed H. influenzae according to our standard protocol (MacArthur et al., Hearing Res., 219:12-23, 2006). Chronic otitis media was evaluated in our recently described C3H/HeJ mouse model (MacArthur et al., Laryngoscope, 116:1071-1079, 2006). Inner ear tissues were removed for cytokine gene expression determination by DNA arrays (Ghaheri et al., Laryngoscope, In Press, 2006). Additional animals were used for immunohistochemistry of relevant cytokines identified by DNA array. Histopathology revealed significant remodeling in the chronically inflamed middle and inner ears. DNA array results showed both acute and chronic otitis media altered levels of cytokines relevant to connective tissue and bone. These included bone morphogenetic proteins, fibroblast growth factors, vascular endothelial growth factor, interleukins, tumor necrosis factors. and transforming growth factors. Immunohistochemistry showed positive staining for several of these cytokines.

These findings demonstrate that acute and chronic otitis media induce numerous cytokines related to middle and inner ear tissue reorganization. This parallels published studies of human temporal bones with chronic otitis media showing active fibrosis and bone growth within the middle and inner ear. While inflammatory cell control is critical in suppressing middle ear disease, attention should also be focused on the control of cytokines causing permanent tissue destruction and remodeling. Future studies will help clarify the cytokines most relevant to these disease processes.

(Supported by NIH-NIDCD R01 DC005593 & DC005593S1, NIH-NIDCD R21 DC007443, NIH-NIDCD P30 DC005983, and VA RR&D RCTR 597-0160 National Center for Rehabilitative Auditory Research.)

### 137 Bacteriology of Chronic Suppurative Otitis Media – A Multicenter Study

**Seung Geun Yeo<sup>1</sup>**, Seok Min Hong<sup>1</sup>, Chang II Cha<sup>1</sup>, Dong Choon Park<sup>2</sup>

<sup>1</sup>Kyung Hee University, Seoul, Korea, <sup>2</sup>Catholic University, Suwon, Korea

Objectives: With the development and widespread use of antibiotics, the types of pathogenic microorganisms and their resistance to antibiotics have changed. Knowledge of the species and resistance rates of current pathogens is important for determining the appropriate antibiotics for patients with chronic suppurative otitis media. We investigated the current bacteriology of chronic suppurative otitis media.

Subjects and Methods: A retrospective study of 1102 patients with chronic suppurative otitis media seen at six hospitals in Korea from January 2001 to December 2005. Results. The most commonly identified pathogenic bacterial species was Pseudomonas, with the next most prevalent being methicillin-resistant Staphylococcus aureus (MRSA).

Conclusions: Bacterial predominance and antibiotic sensitivity have changed over time, making continuous and periodic surveillance necessary in guiding appropriate antibacterial therapy.

Key words: Bacteriology, Suppurative otitis media, Multicenter study

#### 138 Long-Term Follow-Up After Laser Myringotomy: Structural and Functional Properties of the Tympanic Membrane

#### Withdrawn

### 139 Chinchilla Middle Ear cDNA Library Investigation

**Joseph Kerschner<sup>1,2</sup>**, Christopher Post<sup>3</sup>, Garth Ehrlich<sup>3</sup> <sup>1</sup>Medical College of Wisconsin, <sup>2</sup>Children's Hospital of Wisconsin, <sup>3</sup>Center for Genomic Sciences, Allegheny-Singer Research Institute

The chinchilla (Chinchilla lanigera) model has been well defined for both in vivo and ex vivo studies of otitis media and has historically been the most widely used animal model in studying the pathophysiology of otitis. Despite this, molecular tools to investigate the pathophysiology of otitis media in the chinchilla model are lacking.

Complimentary deoxyribonucleic acid (cDNA) libraries prepared from the middle ear mucosa (MEM) of the chinchilla were constructed to conduct comparative expression studies between cDNA libraries prepared from uninfected chinchilla MEM, and MEM infected with a low passage clinical isolate of nontypable *Haemophilus influenzae* (NTHi).

Clones randomly selected for DNA sequencing produced ~250,000 nucleotides of almost entirely novel sequence data. BLAST (Basic Local Alignment Search Tool) searches of the GenBank database provided for identification of 22 genes expressed in the chinchilla MEM and not previously described in the chinchilla. In almost all

cases, the chinchilla DNA sequences displayed much greater homology to human or other primate genes than with rodent species.

Based on both phylogenetic comparisons and gene expression similarities with humans the chinchilla MEM appears to be an excellent model for the study of middle-ear inflammation and infection. The cDNA libraries from normal and infected chinchilla MEM will serve as useful molecular tools in the study of otitis media and should yield important information with respect to middle ear pathogenesis.

## 140 Ascorbic Acid Increases Expression of Connective Tissue Growth Factor (CTGF) in Primary Tympanic Membrane Cell Cultures

Robert Marano<sup>1,2</sup>, Emma Brooks<sup>1,2</sup>, Robert Eikelboom<sup>1,2</sup>, Sharon Redmond<sup>1,2</sup>, Marcus Atlas<sup>1,2</sup>, **Reza Ghassemifar**<sup>1,2</sup>

<sup>1</sup>Ear Science Institute Australia, <sup>2</sup>Ear Sciences Centre, The University of Western Australia

Aim: To examine gene expression following the addition of ascorbic acid (Vitamin C) to the media of cultured human tympanic membrane cells.

Methods: Primary human tympanic membrane cells were outgrown from pieces of tympanic membrane tissue in DMEM supplemented with 10% FBS and incubated at 37°C with 5% CO2. Once established the cells were passaged into 12 well culture plates and grown in the same media supplemented with various concentrations of ascorbic acid. Media was changed on daily basis and the cells were used for total RNA extraction upon reaching confluence. The RNA was subsequently used as template in a reverse transcriptase PCR (RT-PCR) reaction. Primers used in the RT-PCR were designed to amplify a 685 bp fragment of CTGF, which were visualised using standard agarose electrophoresis.

Results: Addition of ascorbic acid to the growth media of human tympanic membrane cells resulted in upregulation of CTGF in a dose dependant manner as determined using RT-PCR and semi-quantitative analysis.

Conclusion: The use of supplements such as ascorbic acid in culture media may improve growth and survival of primary cultured cells by increasing the production of extra cellular matrix proteins that are needed for 3 dimensional growth patterns.

## 141 Psoriasin (S100A7), Antimicrobial Peptide, is Increased in Human Middle Ear Cholesteatoma

Jang-Hyeog Lee<sup>1</sup>, Jae-Gu Cho<sup>1</sup>, Kyoung-Min Kim<sup>1</sup>, Gi Jung Im<sup>1</sup>, Jung-Su Woo<sup>1</sup>, Heung-Man Lee<sup>1</sup>, Soon-Jae Ḥwang<sup>1</sup>, Sung Won Chae<sup>1</sup>

<sup>1</sup>Department of otorhinolaryngology-Head and Neck Surgery, Korea University Hospital

Background and Objectives: Cholesteatoma is characterized by an excessive differentiation of keratinocytes that leads to inflammation, granulation tissue, and osteolytic activity with its progression. Psoriasin may also act as a antimicrobial peptide to stimulate the granulocytes and control the differentiation of

keratinocytes. The purpose of this study was to investigate the differential expression pattern and the localization of psoriasin in cholesteatoma and normal external auditory canal skin.

Materials and Methods: The expression levels of psoriasin mRNA were evaluated through real-time PCR and Western blotting. Cholesteatomas and normal external auditory canal skins were immunostained with monoclonal antibody to psoriasin. The localization of immunoreactivity to psoriasin antibody was compared between cholesteatoma and normal external auditory canal skin.

Results: By real-time PCR, the expression level of psoriasin mRNA in cholesteatoma was significantly increased than in normal external auditory canal skins. The psoriasin protein were detected in normal external auditory skins and the dramatically increase of psoriasin in cholesteatomas were also identified in Western blot analysis. In immunohistochemical staining, psoriasin protein was mainly expressed in the granular layer and the upper parts of spinous layer in cholesteatoma epithelium and was expressed in the superficial layer of normal external auditory canal skin.

Conclusion: The increase of psoriasin in cholesteatoma tissues may play a role in inflammatory response and differentiation of epithelium.

## | 142 | Development of Water-Nonsoluble Chitosan Artificial Patches to Repair Traumatic Tympanic Membrane Perforations

**Yun-Hoon Choung**<sup>1</sup>, Jong Hoon Chung<sup>2</sup>, Joon-ho Bae<sup>1</sup>, Jang Ho Kim<sup>2</sup>, Jung-sub Park<sup>1</sup>, Ki Taek Lim<sup>2</sup>, Keehyun Park<sup>1</sup>, You Ree Shin<sup>1</sup>, Seong Jun Choi<sup>1</sup>

<sup>1</sup>Ajou University School of Medicine, <sup>2</sup>College of Agriculture and Life Science, Seoul National University Background and Objectives: Perforated tympanic membranes (TM) and otitis media can be managed with a paper patch or tympanoplasty. However, a paper patch is not bio-compatible and tympanoplasty requires aseptic complex surgical procedures. The aim of this study is to develop new artificial eardrum patches using tissue engineering techniques for the treatment of TM perforations.

Materials and Methods: We made a novel bio-compatible patch of which main component is a water-nonsoluble chitosan. We analyzed the mechanical characteristics (tensile strength, elongation rate, toxicity etc) and surface contour with a scanning electron microscope (SEM). In vivo study, we made about 50% sized perforations in both TMs in adult rats. We covered these patches over the right-sided perforations and considered left TMs without any patches as control. We evaluated the healing state of TM perforations and the change of patches at 7, 10, 14, 21 days after applying patches under a microscope.

Results: Optimal mechanical characteristics of a waternonsoluble chitosan patch scaffold was around 0.04mm in thickness, 6MPa in tensile strength, and 107% in elongation, even though the characteristics was very various depending on the components of chitosan and glycerol. SEM showed very smooth surface of a patch. In vivo study, four (21.1%) and 17 (89.5%) TMs with waternonsoluble patches in 19 adult rats showed no perforations in one and two weeks, respectively. However, left control TMs showed healing of 0 (0%) in one week and 18 (94.7%) in two weeks.

Conclusion: This novel water-nonsoluble chitosan artificial patch is more effective than spontaneous healing to repair traumatic TM perforations.

This study was supported by a grant of the Korea Health 21 R&D Project, Ministry of Health & Welfare, Republic of Korea (A06-00043782)

## 143 Differential Regulation of Allergic Airway Inflammation by Changing Routes of Administration of Lipopolysaccharide in Mice

**Su-Kyoung Park**<sup>1</sup>, Seung-Ha Oh<sup>1</sup>, Kang-jin Lee<sup>1</sup>
<sup>1</sup>Dept. of Otolaryngology, Seoul National University, College of Medicine

Bacterial infection results in the production of inflammatory mediators and may be involved in the pathogenesis of systemic inflammatory response. Endotoxin, a bacterial lipopolysaccharide (LPS), causes systemic inflammation via Toll-like receptor (TLR) 4 on effector cells of innate immunity to induce proinflammatory cytokines. It is well recognized that respiratory infection modulates allergic airway inflammation . However, as for the role for exposure of bacterial components such as LPS in allergic inflammation, there is apparent controversy in animal model.

We evaluated the phenotype and allergic inflammatory degree in murine allergic rhinitis, asthma, otitis media model with changing routes of administration of LPS. BALB/c mice sensitized by intraperitoneal injections of 75 ug of ovalbumin(LPS depleted) and 2 mg of alum in days 1 and 7 were challenged via intranasal, middle ear route with or without anesthesia of 50 ug ovalbumin or 10 ug LPS in days 14, 15, 16, 21, 22 and 23. We studied serum ovalbumin-specific IgE, IgG2a, respiratory parameters with whole body plethymography, cytokines of bronchoalveolar lavage and nasal cavity lavage, TLR4 expression of lung by FACS and histology in normal, allergic rhinitis, asthma model and LPS administration group with different route. Airway eosinophilia, airway inflammation and serum ovalbumin-specific IgE production are more detected in asthma group than only allergic rhinitis group with or without LPS. Membrane TLR4 expression of lung increased in the allergic rhinitis with LPS administration group, which had the highest expression of respiratory obstructive parameter. It is suggested that the regulation of allergic airway inflammation would variable by route of LPS. The up-regulation of TLR4 in the most symptomatic allergic group supports the idea of a role for Toll-like receptors in allergic airway inflammation.

## 144 Factors Predicting Auditory Development in Infants/Toddlers with Hearing Loss

**Yvonne Sininger**<sup>1</sup>, Laurie Eisenberg<sup>2</sup>, Amy Martinez<sup>2</sup>
<sup>1</sup>Division of Head & Neck Surgery, UCLA, <sup>2</sup>House Ear Institute

The value of early identification and intervention for children with hearing loss is still under debate and rigorous

data from prospective studies is sparse. In this study, basic auditory skills, speech and language development data are being been gathered longitudinally on a group of infants and children with hearing loss. Data for this presentation will include parental reports of auditory development milestones gathered using a revised version of the Ling Schedules and expressive and receptive vocabulary development from the McArthur-Bates Communication Development Inventories. Subjects are 64 children with hearing loss identified and fit with amplification between the ages of 1 month and 5 years. Hearing loss ranges from mild to profound. Subjects have been followed at least one year and for as long as 4.5 years. We have conducted preliminary examinations on the relationship between two predictive factors, the age of fitting of appropriate amplification and the degree of hearing loss against several outcome measures. These measures include the age at which a number of key skills emerge, speech and language milestones, and expressive and receptive vocabulary development. The data indicate that these auditory, speech and language skills emerge at a similar age in children fit before a 'critical' age. For example two-syllable babble is seen at about 8 months and two-word utterances at about 20 months for all early-fit infants. Those fit at ages beyond some critical point show a slope of skill emergence related to the delay in fitting. Critical fitting age may vary with each skill or milestone but initial analysis appears to indicate that delays in skill emergence are evident in children fit after 8-10 months of age, regardless of the degree of hearing loss. Vocabulary growth slopes show a negative relationship to age when amplification was fit, and this relationship is also influenced by degree of hearing loss.

## 145 The Prevalence of Tinnitus with Normal Human Aging: A Population-Based Cross-Sectional Study

**SungHee Kim**<sup>1,2</sup>, Jong Heon Shin<sup>1</sup>, Hyung Jun Shim<sup>1</sup>, Soo Chan Park<sup>1</sup>, Dae Keun Song<sup>1</sup>, Soon Suck Jarng<sup>3</sup>, Jung Ki Lee<sup>4</sup>

<sup>1</sup>Department of Otorhinolaryngology, Daegu Fatima Hospital, <sup>2</sup>Daegu Fatima Hospital, <sup>3</sup>Department of Information Control & Instrumentation Engineering, Chosun University, <sup>4</sup>Health Promotion Center, Daegu Fatima Hospital

The natural history and prevalence of tinnitus is still not clear. As both aging and hearing loss are the most important factors for the tinnitus, the prevalence of the tinnitus with aging may provide useful information to clarify the natural history of tinnitus.

We tried to assess the clinical characteristics of tinnitus in healthy population. The subjects were the clients who visited Health Promotion Center of Daegu Fatima Hospital from January 2004 to September 2005 and voluntarily completed hearing questionnaire. We excluded subjects (1) who had past history of ear drainage, usage of known ototoxic drug, such as chemotherapeutic agent, parenteral antibiotics for serious illness such as tuberculosis, and parenteral diuretics, head injury, working in noise environment, attending military service, (2) who tested twice during the period, (3) who aged less than 20 year-old, and (4) who showed asymmetric hearing loss in the

pure tone averages (more than 16 dB average difference of 0.5, 1, and 2 kHz). Finally, 1150 subjects were included. They were 219 men (20 to 78.3 year-old, mean age 48) and 913 women (20 to 83.9 year-old, mean age 46.3). Multivariate logistic analysis was used to evaluate the difference between male and female and the effect of aging and hearing loss. There was no significant difference in gender. Even though the prevalence of tinnitus increased with age, it was not statistically significant. Only the hearing threshold was the factor to affect the presence of tinnitus. The prevalence was increased with hearing threshold, 9.5%, 11.3%, 19.2%, and 40.6% for less than 20dB, 30dB, 40dB and 50 dB by pure tone average of 0.5, 1, 2, and 4 kHz, respectively. Bilateral tinnitus was most common as 62.7%. Remains complained unilateral tinnitus, 22.5 and 14.8% for the right and the left, respectively. According to population based subjects without any significant causes of sensorineural hearing loss, roughly 10% of normal hearing subjects complained tinnitus and it was bilateral in most.

## 146 Different Aspects of Attention and Their Association to Auditory Processing Abilities in Children

**Justin A. Cowan<sup>1</sup>**, David R. Moore<sup>1</sup> MRC Institute of Hearing Research

Considerable variability in performance on perceptual tasks is typical of children relative to adults. It is believed that immature attention abilities underlie this variability. Therefore, attempts to identify auditory processing (AP) impairments in children need to account for the role of This study investigated the relationship of different measures of attention to performance variability on auditory processing tasks. Eight measures of AP (Cowan et al., ARO, 2004) were administered to children aged 6-12 years (N=85) with two consecutive staircase adaptive tracks collected for each task. A measure of performance reliability was determined by the discrepancy between the two threshold estimates. Within AP task indices of attention included track variance, derived from track reversal points, and suprathreshold probe trials, presented for 20 percent of trials. Additional external measures of attention included cognitive tests of verbal memory (Digit Span and Nonsense Words) and attention questionnaires completed by parents and teachers. Developmental effects were observed for both track variance and probe trial errors, with each marker of inattention making unique and significant contributions to explaining threshold variability. There were non-significant relationships between within-task measures of attention and cognitive measures of memory, though probe trial errors were significantly associated to teacher reports of children's attention abilities. These findings show that the alternative methods used to characterise attention have significant consequences for what aspect of attention is captured. Attending to the multifaceted nature of attention is important in understanding children's performance variability on AP tasks.

## 147 Auditory Processing and Cognitive Skills in Typically Developing and Language and Listening Impaired Children

**Melanie A. Ferguson**<sup>1</sup>, Justin A. Cowan<sup>1</sup>, Alison Riley<sup>1</sup>, Emma Booker<sup>1</sup>, David R. Moore<sup>1</sup>

<sup>1</sup>MRC Institute of Hearing Research

Auditory processing (AP) deficits have been identified in children with developmental disorders including dyslexia, ADHD and specific language impairment (SLI). Children may be separately 'diagnosed' as having AP disorder (APD). However, there are currently no standardised and scientifically validated tests of APD. To help identify candidate tests for diagnosing APD, 75 typically developing (TD) children (6-11 y.o.) were examined with a large test battery - audiology, speech perception, AP (spectral, temporal and binaural) and cognitive function (verbal and non-verbal IQ, phonological ability, non-word repetition, memory and reading).14 children (7-11 y.o.) diagnosed with SLI were also tested. In the TD children, there was generally little association between AP and cognitive tests. Frequency discrimination showed significant correlations with IQ (non-verbal, r=-.27; verbal, r=-0.31: p≤0.05) and phonological awareness (r=-0.49: p≤0.001). 8/14 (57%) SLI children performed poorly (> 2 s.d. above the mean for age matched TD children) on at least one AP task and 35% on at least two tasks. Overall AP performance in the SLI group was significantly poorer than the TD group (p≤0.001). However, there was also a significant group difference for non-verbal IQ (p≤0.001). After matching SLI children (n=10) with TD children for age and non-verbal IQ, AP performance remained poorer in the SLI group for backward masking and frequency resolution (p≤0.01). Testing on more challenging AP tasks (e.g. dynamic binaural interaction, spatial unmasking, ordering) and visual spatial frequency discrimination is ongoing in TD, SLI and suspected APD children. A shortened battery of AP tests will be trialled in a large (n~1600) multi-centre study in 2007 to ascertain (i) population norms for AP tests and (ii) prevalence of APD. Data collected to date confirm poorer AP and cognitive performance in SLI children and show that some AP performance deficits remain when non-verbal IQ is controlled.

#### 148 Audiometric and Tympanometric Abnormalities in Osteoarthritis

Vishakha Rawool<sup>1</sup>, Brian Harrington<sup>2</sup>

<sup>1</sup>West Virginia University, <sup>2</sup>Main Line Audiology Consultants, PA

In osteoarthritis, the joint cartilage breaks down. Cartilage exists within the middle ear at the incudomalleolar and incudostapedial joints, the base of the stapes and the rim of the vestibular window. In the current study, tympanometric (admittance, resonance and tympanometric width) and audiometric results were obtained from fifteen participants (10 women and 5 men) diagnosed with osteoarthritis and fifteen, age and gender matched participants without arthritis. The participants ranged in age from 48 to 80 years. Results showed a significantly

higher prevalence of middle ear abnormalities in osteoarthristis. In some cases tympanometeric results suggested loosening pathologies that may arise due to disarticulation of joints. In other cases the results suggested stiffening pathologies that could occur due to ankylosis or due to decreased mobility of one or both ossicular joints following the repair processes that occur after inflammation of the synovial membrane. Since primary osteoarthritis occurs with aging and since the control and arthritic groups were age-matched, age-related sensorineural hearing loss was expected in both the groups included in the current study. The air-conduction thresholds across the two groups did not differ significantly. However, the prevalence of hearing loss was significantly higher in individuals with arthrits. Although osteoarthritis is generally classified as a degenerative condition, some studies suggest that inflammatory events may be involved in its pathogenesis. Systemic inflammation can lead to sensorineural hearing loss. Another possible factor related to hearing loss is immune deregulation, which has been demonstrated in some forms of osteoarthritis. Interestingly, osteoarthritis and hearing loss are considered among the top chronic health conditions in older individuals although the connection between the two has not been previously reported.

#### 149 Auditory Testing Abnormalities of Pelizaeus-Merzbzcher Disease

**Diane Roeder**<sup>1</sup>, Zuliani Giancarlo<sup>1</sup>, James Garbern<sup>1</sup>, Alexander Gow<sup>1</sup>, James Coticchia<sup>1</sup>

<sup>1</sup>Wayne State University

Objectives: To characterize the auditory manifestations of patients diagnosed with Pelizaeus-Merzbzcher Disease (PMD), a rare X-linked disorder of myelin classically characterized by nystagmus, spastic quadriparesis, ataxia, and cognitive delay in early childhood or progressive disease in adulthood.

Study Design/Methods: A prospective case study of 5 pediatric and 3 adult patients diagnosed with PMD who demonstrate varying degrees of abnormal auditory function. These patients underwent comprehensive audiological evaluations, auditory processing tests, and electrophysiological measures. All subjects are male, with an age range from 4 to 42 years of age. The 3 adult subjects were brothers and 2 of the pediatric subjects were first cousins.

Results: Abnormal electrophysiological findings with normal cochlear function were found in all test subjects. Further testing completed on adult subjects revealed further central auditory dysfunction via auditory processing tests. The degree of audiological central dysfunction findings was more severe in subjects with greater symptoms of the disease.

Conclusion: Our findings indicate the need for a full audiological test battery on all patients with Pelizaeus-Merzbacher disease and other severe neurological disorders. Auditory processing test procedures yield functional listening status on subjects with varying stages of the disease and may provide insight into the underlying etiology.

## 150 Restoration of Brainstem Auditory Evoked Potential in Maple Syrup Urine Disease

**Christopher Spankovich**<sup>1</sup>, Lawrence Lustig<sup>2</sup>

<sup>1</sup>Venderbilt University, <sup>2</sup>University of California San Francisco

Objective: The purpose of this study was to report a unique case of reversible brainstem auditory evoked potential (BAEP) involving wave I in maple syrup urine disease (MSUD). The possible mechanism of the hearing loss and reversibility of wave I are proposed based upon the known pathophysiology of MSUD.

Study Design: Retrospective case review.

Setting: Hospital

Patients: Single case report

Intervention: Treatment of MSUD with dialysis and diet

devoid in branched chain amino acids

Main Outcome Measure: brainstem auditory evoked

potentials

Results: Initial presentation of MSUD in a 14 week old child included failure to thrive, present otoacoustic emissions, and an absent BAEPs. Following treatment with dialysis and an MSUD-appropriate diet, the BAEP's gradually recovered.

Conclusion: Appropriate and timely treatment of MSUD can reverse the central neuropathy leading to hearing loss. Because patients with MSUD have elevated levels of glutamate, we propose that the hearing loss in these patients may be related to glutamate excitotoxicity, and that appropriate treatment may lead to normalization of glutamate levels and restoration of hearing in patients with MSUD.

#### 151 A Computer Model of the Audiogram Ray Meddis<sup>1</sup>

<sup>1</sup>University of Essex

Computer models of the auditory periphery have the potential to contribute to the characterisation of individual hearing pathology. However, this implies a minimum requirement that these models are able to represent the audiogram of normal listeners in a manner that is faithful to our understanding of the underlying physiology. If this can be done, it will be possible to represent the audiogram of impaired listeners in terms of the assumed pathology of one or more peripheral organ of hearing. An important feature of the audiogram is the raised absolute thresholds for pure tone stimuli at low and high frequencies. Attenuation of the acoustic signal in the outer and middle ear explains some of the threshold increases at extreme frequencies but other factors are also at work. For example, thresholds are affected by the viability of the mechanical response along the cochlear partition which is. in turn, influenced by outer hair cell responses. The size of the helicotrema is also influential at very low frequencies in Inner hair cell stereocilia contribute a reduced response to the displacement of the basilar membrane at low frequencies while the receptor potential also shows reductions in response at high frequencies. Furthermore, it is possible that the medial and lateral efferent system influence thresholds when we pay close attention to anticipated tones near threshold. A computer model is described that simulates the response of the auditory periphery as a cascade of these individual stages of auditory processing. The parameters of the model have been constrained as far as possible by published empirical measurements made at each stage. The audiogram of the model is determined using psychophysiological procedures for assessing thresholds at different stimulus frequencies and compared with the normal human audiogram.

### 152 Development of a Digitalized Pure Tone Audiometer with Automated Masking

**II-Woo Lee**<sup>1</sup>, Kyong-Myong Chon<sup>1</sup>, Eui-Kyung Goh<sup>1</sup>, Dong-Hoon Lee<sup>1</sup>, Soo-Geun Wang<sup>1</sup>, Jeong-Hwan Ok<sup>2</sup>, Yun-Sung Roh<sup>3</sup>

<sup>1</sup>Dept. of ORL, Pusan National Univ., Busan,Korea, <sup>2</sup>NGC Info Tec Co., Ltd, <sup>3</sup>Roh Yun-Sung ENE Clinic, Seoul,Korea Objective and Background: Recently, internet-based applications are in process of rapid development in human life and the concept of telemedicine and multimedia is important for these applications. Hearing test is one of the essential procedures in otologic field especially in telediagnosis. Current study for tele-hearing test has some limitations in masking problem or making fully automated system. The aim of this study is to develop digital air-conduction pure tone audiometer with automated masking which can be used through wed-based or off-line and to compare the threshold of hearing using conventional and this automated audiometer in both normal and handicapped hearer.

Materials and Methods: To develop automated audiometer system, we prepare test scenario data file according to the pure tone test procedure. This scenario was executed in audiometer main which is supported by sound card and keyboard(mouse) for output and feedback respectively for the examinee. Pure tone for test and white band nose for masking is generated in audiometer sound generation block. To compare this automated audiometer with conventional one, twenty five normal hearer(50 ears) and twenty five handicapped hearer(50 ears) was tested.

Results: Easy Audiometer 1.0 was developed. The difference of hearing threshold between two different systems was 3-6 dB in normal hearer group and 2.5-3.5dB in handicapped hearer group. Scatter plots showed close relationship between these two different systems.

Conclusions: Easy Audiometer 1.0 showed reliable results of hearing threshold in patient with unilateral hearing who needs masking procedure. Screening and basic hearing test may be possible through this Easy Audiometer 1.0 and it could play some role as a part of telediagnosis in otologic field.

## 153 Evaluation of the Antishock Algorithm for Impulse Correction of Transient Signals by the Unitron Element Hearing Aid

**David A. Eddins<sup>1,2</sup>**, Donald Hayes<sup>3</sup>

<sup>1</sup>Deparment of Otolaryngology, University of Rochester, Rochester, NY 14642, <sup>2</sup>Int. Ctr. for Hearing & Speech Res., Rochester Institute of Technology, Rochester, NY 14623, <sup>3</sup>Unitron Hearing Ltd., Kitchener, Ont., Canada

An ideal signal processing strategy for a hearing aid would be one that can minimize the disruption and distraction caused by unwanted sounds and maximize the quality and clarity of desired sounds. Transient sounds such as dishes clanging and doors slamming, when processed by a hearing aid, often are disproportionately loud relative to the surrounding speech environment and can be annoying or uncomfortable. The Unitron Element line of hearing aids introduced the patent-pending antiShock transient correction algorithm designed to quickly detect and attenuate the leading edge of sharp transient sounds to yield proportionate loudness. At the same time, the alogorithm should preserve the awareness of the transient sound and have no effect on the perception of desired sounds such as ongoing speech. AntiShock was evaluated in 40 listeners with moderate to severe sensorineural hearing loss fitted binaurally with the Element 16 behind-the-ear directional hearing aid using a standard prescriptive fitting rule (NAL/NL1). Both pairedcomparison and sound attribute difference rating procedures were used to evaluate the attributes of sound quality, clarity, and annoyance while the antiShock algorithm was either on (mild, moderate, or maximum settings) or off. Stimuli included continuous speech discourse, multi-talker babble, transient noises, or some combination of the three, presented at various sound levels. A total of 44 conditions were evaluated. The results indicated that antiShock substantially reduces the annoying percept associated with sharp transient sounds while preserving speech clarity. In the absence of transient sounds, the antiShock feature had no negative effect on speech quality or clarity. The degree to which annoyance of transient sounds was reduced was graded according to the antiShock setting (mild to maximum) and was greatest when other ongoing sounds were low to moderate in level, reflecting the adaptive nature of the algorithm.

## | 154 | Intervention for Restricted Dynamic Range and Reduced Sound Tolerance: Clinical Trial Update

Monica Hawley<sup>1</sup>, LaGuinn Sherlock<sup>1</sup>, Susan Gold<sup>1</sup>, Allyson Segar<sup>1</sup>, Christine Gmitter<sup>1</sup>, Justine Cannavo<sup>1</sup>, **Craig Formby**<sup>1</sup>

<sup>1</sup>University of Maryland School of Medicine, Baltimore
Hyperacusis is the intolerance to sound levels that
normally are judged acceptable to others. The presence of
hyperacusis (diagnosed or undiagnosed) can be an
important reason that some persons reject their hearing
aids. Tinnitus Retraining Therapy (TRT), originally
proposed for the treatment of persons with debilitating

tinnitus, offers the significant secondary benefit of increased Loudness Discomfort Levels (LDLs) in many persons. TRT involves both counseling and the daily exposure to soft sound from bilateral noise generator devices (NGs). We implemented a randomized, doubleblind, placebo-controlled clinical trial to assess the efficacy of TRT as an intervention for reduced sound tolerance in hearing-aid eligible persons with hyperacusis and/or restricted dynamic ranges. Subjects were assigned to one of four treatment groups: 1) NGs with counseling, 2) placebo NGs with counseling, 3) NGs without counseling, and 4) placebo NGs without counseling. They were evaluated at least monthly, typically for five months or more, on a variety of audiometric tests, including LDLs, the Contour Test for Loudness for tones and speech, word recognition measured at each session's comfortable and loud levels, and on electrophysiological measures. Success for the treatment is defined as a tolerance increase by more than 10 dB as measured by either LDLs or Contour Test for Loudness. For the subjects in Group 1 (NGs and counseling), there was a high rate of success (5/6 subjects). A lower success rate was observed for the partial treatment options: Group 2 (placebo NGs with counseling): 1/5 subjects; Group 3 (NGs without counseling): 4/7 subjects; and Group 4 (placebo NGs without counseling): 0/2 subjects. In some subjects who initially had poor word recognition at comfortable levels, the increased tolerance allowed them to increase the level of their comfortable speech allowing a marked improvement in word recognition at comfortable levels. The interim results are very promising and support the hypothesis of this randomized controlled study that modified TRT appears to offer a new intervention for improving sound tolerance in the general hearing-impaired population, allowing persons with reduced tolerance or limited dynamic ranges to use hearing aids more effectively.

Supported by NIH R01 DC04678.

#### | 155 | Tinnitus and Cochlear Implantation in Adults - A Retrospective Study

**Esma Idrizbegovic**<sup>1</sup>, Anders Freijd<sup>2</sup>, Eva Karltorp<sup>2</sup>, Gerhard Andersson<sup>3</sup>

<sup>1</sup>Department of Audiology, Karolinska University Hospital, Stockholm, Sweden, <sup>2</sup>Department of ENT, section for Cochlea Implant, Karolinska University Hospital, Huddinge, Sweden, <sup>3</sup>Department of Behavioural Sciences, Linköping University, Sweden

Few studies have outlined the temporal association between cochlear implantation and tinnitus onset or changes. The aim of the study was to use validated self-report measures in a consecutive sample of cochlea implant (CI)- patients who reported tinnitus.

Methods: A total of 151 (83% response rate) responded to postal questionnaires, and of these 111 reported that they had tinnitus. Questions regarding tinnitus in relation to CI and the operation were asked. In addition, three established self-report questionnaires were included measuring tinnitus handicap, hearing disability and handicap and finally a measure of anxiety and depression.

Results showed that few patients had permanently worsened tinnitus or got tinnitus following cochlear implantation. However, a fifth did report that their tinnitus was worsened. As many as 25 patients reported that their tinnitus completely disappeared when the processor was turned on and that it returned when the processor was turned off again. Only 4 patients reported that their tinnitus increased when the processor was turned on. A common response (N=31) was that tinnitus was unchanged following the CI operation. Data from established questionnaires showed relatively low levels of tinnitus handicap, moderate levels of hearing disability and handicap, and low scores on the anxiety and depression scales.

Conclusion: Significant amount of patients either experience no change in their tinnitus or a decrease. Level of tinnitus handicap overall is not marked in this population. However, tinnitus could be a significant problem in some CI patients

#### 156 Perceptual Components of Tinnitus Severity

**Mary Meikle**<sup>1</sup>, James Henry<sup>2</sup>, Susan Griest<sup>1</sup>, Barbara Stewart<sup>1</sup>

<sup>1</sup>Oregon Health & Science University, <sup>2</sup>Portland VA Medical Center, Portland, OR

Most existing questionnaires for assessing the severity and negative impact of tinnitus tend to emphasize functional or emotional effects of tinnitus. While such measures are important for diagnostic purposes and as outcome measures, they require time periods of several days to several weeks or longer for observation of meaningful changes following treatment. More rapid evaluation of treatment outcomes can be obtained using patients' reports of the perceptual characteristics of tinnitus such as its loudness, salience, unpleasantness, intrusiveness, and the percentage of time the tinnitus sensations are perceived. However, the extent to which such perceptual attributes of tinnitus are appropriate indicators of the clinical severity of tinnitus has received relatively little systematic attention. To maximize measurement sensitivity, we designed a 43-item questionnaire to quantify patients' responses concerning functional, emotional and perceptual aspects of tinnitus, using a 0-10 point response scale for each guestion. A total of 327 subjects with varying levels of tinnitus, recruited from a diverse group of patients attending clinics in three locations (Oregon, Ohio, Florida), responded to the questionnaires before and after receiving treatment. As expected, the perceptual attributes listed above were positively related to global measures of tinnitus distress, including (1) a Visual Analog Scale and (2) the question "How much of a problem is your tinnitus?" (response levels: 0=Not a problem; 1=Small problem; 2=Moderate problem; 3=Big problem; 4=Very big problem). Effect sizes for the perceptual measures (computed for subjects reporting treatment benefit) ranged from 0.49-1.50. Additional data will be presented concerning the ability of perceptual measures to serve as reliable, sensitive outcome measures for studies that require rapid evaluation

of tinnitus treatments having immediate effects, such as stimulation with electrical, magnetic, or acoustic stimuli.

#### 157 Anxiety and Depressive Symptoms in Tinnitus Patients

Andrea Crocetti<sup>1</sup>, Stella Forti<sup>1,2</sup>

<sup>1</sup>Fondazione Ascolta e Vivi, <sup>2</sup>Fondazione IRCCS Ospedale Maggiore Policlinico, Mangiagalli e Regina Elena

Our clinical knowledge of tinnitus is based on treatment of over 1500 tinnitus patients. We have observed a correlation between tinnitus and symptoms of anxiety and depression which often affect daily life. Patients report that an increasing level of anxiety also exacerbates tinnitus symptoms. This can be explained neurophysiologically by the effect of the limbic system, cortex and peripheral neuropathways in tinnitus.

The aim of this study is to investigate any correlation between tinnitus and anxiety and depressive symptoms.

Materials and methods: The assessment is composed of: Visual Analogical Scales (VAS) for the evaluation of tinnitus induced problems; Tinnitus Handicap Inventory (THI); State and Trait Anxiety Inventory-Y (STAI S-T); Beck Depression Inventory (BDI).

These instruments were chosen based on their psychometric properties, time of administration and validity in many languages; the sample consists of 67 patients.

Results: Correlation between anxiety symptoms and THI score is significant (p<0,01); the same significance was found between depressive symptoms and THI as well as between STAI and BDI. Significant correlation was also found between these questionnaires and the intensity of tinnitus, annoyance and effect on life evaluated by the VAS scale.

23% of the sample had severe tinnitus. Mean anxiety was around the 65th percentile; 35% having an anxiety disorder. 12% of the total sample shows a depressive pathology. 11% of the sample have both anxiety and depression. An inverse correlation between STAI and BDI scores and the duration of tinnitus was observed.

Conclusions: Although about 1/3 of patients are suspected of suffering from anxiety, a pathological level of anxiety and depression was found in only about 10% of the sample. The THI questionnaire is a good predictor for patients with higher levels of depression and anxiety.

## 158 Effectiveness of Unilateral Usage of the Sound Generator for Tinnitus Retraining Therapy

**Nobumichi Maeyama**<sup>1</sup>, Atsuhiko Uno<sup>1</sup>, Miki Okubo<sup>1</sup>, Yuko Takai<sup>1</sup>, Kazuyasu Baba <sup>2</sup>, Seiji Shibata<sup>2</sup>, Kouhei Kawamoto<sup>2</sup>, Hiromichi Kuriyama <sup>2</sup>, Katsumi Doi<sup>3</sup>, Masato Nishimura<sup>1</sup>

<sup>1</sup>Department of Otolaryngology, KKR Otemae Hospital, <sup>2</sup>Osaka Kita Japan Post Hospital, <sup>3</sup>Osaka University

Tinnitus Retraining Therapy (TRT) developed by Jastreboff and his colleagues, is a world-widely spreading treatment for tinnitus. TRT consists of directive counseling and sound therapy that typically the patient uses a sound (noise) generator to reduce awareness of tinnitus distinguished from the background noise. Generally the sound generator is recommended to use on the bilateral ears. However, because of the reasons such as the cost, appearance and difficulty in daily conversation, we usually begin with the unilateral use, following repeated counseling and explanation of TRT itself.

To assess the effectiveness of the sound therapy using the sound generator on one side, we retrospectively examined the results of 27 patients who underwent TRT at KKR Otemae Hospital and at Osaka Kita Japan Post Hospital from November 2004 to April 2006.

Two kinds of questionnaires including Tinnitus Handicap Inventory and Visual Analogue Scale were used to evaluate the results at 6 and 12 months.

Even for the patients complaining of bilateral tinnitus, TRT with unilateral sound therapy showed significant improvements at 6 months. We think that the sound therapy can begin with one sound generator on the one side, then after 6 months, the results should be evaluated. For the patient who did not show clear improvements, bilateral usage of the sound generator may be suggested.

## 159 Clinical Development of SPI-1005, an Otoprotectant for Noise Induced Hearing Loss

**Jonathan Kil<sup>1</sup>**, Bret MacPherson<sup>1</sup>, Carol Pierce<sup>1</sup>, Eric Lynch<sup>1</sup>

<sup>1</sup>Sound Pharmaceuticals, Inc.

Ebselen (SPI-1005), an oral small molecule GPx mimic, has been shown to provide significant protection from TTS and PTS in F344 rats (Lynch et al., 2004, Lynch et al., 2005), Sprague Dawley Rats (Park et al., ARO Abst. 2006) and Guinea Pigs (Pourbahkt and Yamasoba 2003, Yamasoba et al., 2005) when dosed in the range of 8-30 mg/kg. Our current efforts are now focused on translating these pre-clinical findings into a therapeutic for the prevention and treatment of noise induced hearing loss in humans.

We have completed a phase I study of SPI-1005 capsules in 32 normal healthy volunteers to determine the safety, toxicity, ADME, and Pk. Dose escalation was performed in 4 groups ranging from 200 to 1600 mg po. Subjects were followed in house for a period of 72 hours. Multiple EKGs, orthostatic vitals, Chem20, and CBCs were taken during the period of clinical observation. No significant adverse events were noted in 24 drug treated and 8 placebo treated individuals. Pk analysis of ebselen and its metabolites was performed using WinNonlin®5.1 from plasma and urine samples analyzed by LC-MS/MS. These results closely matched the Pk analysis of total selenium in plasma samples by ICP-MS from the same treated individuals. The plasma Pk of ebselen in these human subjects was similar to that in non-human primates dosed with SPI-1005 at comparable levels (10mg/kg).

Phase II safety and efficacy trials will be performed in military populations exposed to noise during weapons training. Historically, a Significant Threshold Shift (STS) occurs even with the use of hearing protective devices. The Clinical trial design for these phase II studies will be discussed along with primary and secondary endpoints using STS and the Tinnitus Handicap Inventory.

## 160 Effect of Round Window Membrane Application of Dornase Alfa on Cochlear Function

Kenny H. Chan<sup>1</sup>, **Jon Zwart<sup>2,3</sup>**, Courntey French<sup>2,3</sup>, Tiffany Lo<sup>2,3</sup>, Chris Le<sup>2,3</sup>, Stanley Allen<sup>2,3</sup>, Choong-Won Lee<sup>2,3</sup>, Tammy Pham<sup>2,3</sup>, Mark Nicosia<sup>2,3</sup>, Derick Ly<sup>2,3</sup>, Jerry Nguyen<sup>2,3</sup>, Dusan Martin<sup>2,3</sup>, You Hyun Kim<sup>2,3</sup>, Earnest O. John<sup>2,3</sup>, Timothy T.K. Jung<sup>2,3</sup>

<sup>1</sup>Children's Hospital, Denver, CO, <sup>2</sup>Division of Otolaryngology-Head and Neck Surgery, Loma Linda University, Loma Linda, CA, <sup>3</sup>Jerry L. Pettis Veterans Medical Center, Loma Linda, CA

Background: Otitis media (OM) is one of the most common diseases. Clinicians have been interested in altering the rheological properties of middle-ear effusion (MEE). Tympanostomy tubes as a treatment of OM are frequently clogged due to thick mucoid MEE. Dornase alfa (Pulmozyme® by Genentech), approved by the FDA since 1994 for treating cystic fibrosis (CF), offers a unique potential for treating OM. It reduces viscoeleasticity of sputum by hydrolyzing DNA released by degenerating leukocytes. Many clinical similarities exist between OM and cystic fibrosis. We strongly believe in its potential efficacy in the treatment of OM. Before it can be implemented for a clinical trial, its ototoxicity potential needs to be ruled out.

Objective: This study evaluates the potential ototoxicity of dornase alfa by monitoring the cochlear function by auditory brainstem response (ABR) before and after its application on the round window membrane (RWM).

Study Design and Methods: A total of 21 adult chinchillas were used for this study. The research design consisted of three groups: control (5 animals), full-strength dornase (8 animals) and dornase [1:10] (8 animals each). Baseline ABR recordings were taken before application of test substances on RWM. RWMs were exposed by posteroinferior approach to the bulla. Saline or test substances were soaked into the Gelfoam and applied on the RWM. Effects on hearing were monitored and recorded hourly by ABR testing for up to 8 hours.

Results: ABR measurements showed that hearing loss was at its maximum six hours after dornase application on the RWM. The mean hearing losses for full-strength dornase and dornase [1:10] were 32±2.9dB and 13±0.32dB respectively. Hearing loss was not significantly different for either dornase [full-strength, p=0.14], or dornase [1:10, p=0.20] when compared to the saline control.

Conclusions: In this study we found that dornase alfa is non-ototoxic, therefore it provides potential therapeutic merits for treating clogged tympanostomy tubes.

#### 161 Ototoxicity of Acetic Acid

**Takafumi Yamano**<sup>1</sup>, Mayumi Sugamura<sup>2</sup>, Tetsuko Ueno<sup>1</sup>, Hitomi Higuchi<sup>1</sup>, Toshihiko Kato<sup>1</sup>, Takashi Nakagawa<sup>1</sup>, Tetsuo Morizono<sup>3</sup>

<sup>1</sup>Fukuoka University, <sup>2</sup>Fukuoka University Chikushi Hospital, <sup>3</sup>Nishi Fukuoka Hospital

Purpose: The bactericidal effect of the acetic acid has been well known. Recently, Burrow's solution has gained popularity as effective ear drops in treating chronic otitis media with methicillin resistant staphylococcus aureus (MRSA). The primary ingredient of this solution is acetic acid, however, no studies have been performed to determine the ototoxicity of acetic acid. The purpose of this study is to study ototoxic effect of acetic acid at various concentration.

Materials and methods: Ototoxicity was evaluated in the guinea pigs by measuring the eights nerve compound action potentials (CAP) using an electrode on the round window. The stimulus consisted of click sounds, and tone burst of 4 and 8 kHz. The middle ears of the animals were filled with acetic acid at several dilutions to give a pH range of 3 to 5. Baseline CAP measurements were first determined, then the middle ears were filled with acetic acid at several dilutions to give a pH range of 3 to 5 and the reduction in the CAP compared to baseline was measured at 30 minutes. The middle ears were drained at 30 minutes then the CAP was collected. The bacteriostatic activity of these solutions against two strains of MRSA, isolated from ears of patients was also studied.

Results: Acetic acid shows a concentration-dependent bacteriostatic activity. A statistically, a significant ototoxic effect was seen for the pH3 acetic acid solution but not at pH4 orpH5. Conclusion:

The guinea pig round window membrane is thinner that in humans and this is likely a factor that could increase the observed ototoxic effects of acetic acid than would be expected to be seen in humans. However, these results warrant caution in the use of acetic acid solutions.

#### 162 Burow's Solution: Concentration-Dependent Ototoxicity and Bacteriostatic Activity.

**Mayumi Sugamura**<sup>1</sup>, Takafumi Yamano<sup>2</sup>, Tetsuko Ueno<sup>2</sup>, Hitomi Higuchi<sup>2</sup>, Toshihiko Kato<sup>2</sup>, Takashi Nakagawa<sup>2</sup>, Tetsuo Morizono<sup>3</sup>

<sup>1</sup>Fukuoka University Chikushi Hospital, <sup>2</sup>Fukuoka University, <sup>3</sup>Nishi Fukuoka Hospital

Purpose: At the previous ARO Meeting in 2006, we reported ototoxic effect of the full-strength Burow's solution for click stimulus. We have new studied the concentration-dependent ototoxicity and bacteriostatic effects of the solution.

Materials and methods: Ototoxicity was evaluated in the guinea pigs using the eights nerve compound action potentials (CAP) using an electrode place on the round window. The stimulus consisted of click sounds, and tone burst of 4 and 8 kHz. The middle ears of the animals were filled with Burow's solution, and the reduction in the CAP was measured at 30 minutes. The bacteriostatic activity of

the solution against two strains of MRSA, isolated from ears of patients in our clinic was also studied.

Results: No ototoxicity was detected when using Burow's solution prepared at half-strength. The bacteriostatic activity of Burow's solution was distinctly concentration-dependent. A white sediment was noticed one month after manufacture, and its gradual increase was followed for 9 months. The pH of the solution was found to drift very slightly in this time, the bacteriostatic effectiveness, studied using the disk method was also found to decrease gradually in this time.

Conclusion: Burow's solution with a half-strength did not show any ototoxic effects, hence we believe this solution can be safely used in the clinical settings. The gradual reduction in the efficacy one month after manufacture appears to be due to the reduced astringency caused by sedimentation of aluminum in the solution rather than due to the change in pH.

## 163 Interactive 3-D Demonstration of Cholesteatoma Extension in the Human Middle Ear and Temporal Bone

David P. Morris<sup>1,2</sup>, Rene Van Wijhe<sup>1</sup>

<sup>1</sup>Ear and Auditory Research Laboratory (EAR. Lab)
Dalhousie University, <sup>2</sup>Dept. of Surgery, Division of ORL-HNS Capital Health, Halifax Nova Scotia CANADA.

Aims: We will demonstrate in an interactive, easy-to-view format the common patterns of cholesteatoma spread in the human middle ear. The patterns will be analysed in light of recent work on epitympanic fold distribution. We will also reconstruct real examples of invasive cholesteatoma where there has been invasion of middle and inner ear structures.

The models allow the operator to "fly through" the temporal bone enabling a true 3-D appreciation of the temporal bone anatomy to become established.

The images will provide a resource for surgical training and are a guide to surgical decision-making. It is also hoped that the models will improve the quality of preoperative counselling offered to our patients in the taking of informed consent prior to otologic surgery.

Methods: High definition computerised tomographic images of temporal bones taken at the pre-operative assessment of patients with cholesteatoma were semimanually segmented using the Amira (R) software package. Important middle and inner ear structures were outlined in addition to the bony anatomy of the skull and the cholesteatoma mass.

Results: Interactive models were made showing several patterns of cholesteatoma extension.

Conclusion: The patterns of cholesteatoma extension were well demonstrated. We have found the models to be useful for both surgical planning and training and in the counselling of our patients prior to surgery.

ARO Abstracts 55 Volume 30, 2007

### 164 Operative Outcome and Audiologic Evaluation of Fat Myringoplasty

Yakout Dogheim<sup>1</sup>, Ossama Sobhy<sup>1</sup>

<sup>1</sup>Faculty of Medicine

Fat myringoplasty are documented to be safe, efficient, with little risk of iatrogenic otologic stroma.

Our aim was to evaluate the procedure of fat myringoplasty as regards operative outcome and audiological evaluation, and to compare ear lobule fat to abdominal fat as grafted material.

We studied two groups A&B, fifteen patients each.Group A undergoing myringoplasty using ear lobule fat,while in group B we used abdominal wall fat. The cases were selected with dry central perforation (30%),with condutive hearing loss and no history of previous myringoplasty.

Our results showed that type of fat did not significantly affect success rate.

Ear lobule is a more convenient source of fat. Post operatively, fat myringoplasty is more appropriate for small perforations with air bone gap. It can be applied as day stay procedure. Proper selection of cases is crutial to achieve satisfactory results.

# 165 Cochlear Implantation in the Presence of Cochlear Nerve Hypoplasia or Aplasia as Suggested by Temporal Bone Magnetic Resonance Imaging

Jong Yang Kim<sup>1</sup>, Kwang-Sun Lee<sup>1</sup>

<sup>1</sup>Asan Medical Center

Background and Objectives: Identifying cochlear nerve hypoplasia or aplasia is dependent on temporal bone magnetic resonance imaging (TBMRI) providing information on the cochlea, internal auditory canal, and the cochlear nerve. The purpose of this study was to review the results of cochlear implantation (CI) in ears with cochlear nerve hypoplasia or aplasia as suggested by TBMRI.

Subjects and Methods: Between April 1999 and April 2005, 321 patients were fitted with cochlear implants by two surgeons in our department. The present study focused on four prelingual patients who underwent CI for cochlear nerve hypoplasia or aplasia as suggested by TBMRI. The perceptive and linguistic results were evaluated based on speech perception and production at pre-implantation and at 1, 3, 6, 9, 12, and 24 months post-implantation.

Results: Pre-operative auditory brainstem responses were absent at 120-dB click stimulation in all patients. At least 10 months after implantation all patients were able to detect 100% of consonants and vowels and their scores in the Categories of Auditory Performance were 4 or above.

Conclusion: We confirmed cochlear nerve presence in cases of cochlear nerve hypoplasia or aplasia as suggested by TBMRI and auditory habilitation was made possible with cochlear implantation. Further studies are needed to confirm cochlear nerve presence before implantation and to predict the outcome of cochlear

implantation in cases of cochlear nerve hypoplasia or aplasia as suggested by TBMRI.

Keywords: Cochlear nerve, Hypoplasia, Aplasia, Cochear implantation.

# 166 Transcranial Magnetic Stimulation for the Treatment of Auditory Phantom Perceptions (Tinnitus) – A Randomized Placebo Controlled Study

**Tobias Kleinjung<sup>1</sup>**, Berthold Langguth<sup>2</sup>, Peter Eichhammer<sup>2</sup>, Michael Landgrebe<sup>2</sup>, Philipp Sand<sup>2</sup>, Juergen Strutz<sup>1</sup>, Goeran Hajak<sup>2</sup>

<sup>1</sup>University of Regensburg, Department of Otorhinolaryngology, <sup>2</sup>University of Regensburg, Department of Psychiatry

Introduction: Repetitive transcranial magnetic stimulation (rTMS) represents a minimal invasive tool for focal brain stimulation. Patients suffering from auditory phantom perceptions (tinnitus) demonstrated focal brain activation within the auditory cortex. Neuronavigated low frequency transcranial magnetic stimulation of the area of increased activity cortex was able to reduce tinnitus perception in first studies.

Methods: Patients suffering from chronic tinnitus underwent a FDG- PET study (positron emission tomography with [18F]deoxyglucose) to detect areas of increased metabolic activity in the cortex. Fusioning of the individual PET scans with structural MRI-scans (T1, MPRAGE) revealed an increased metabolic activation in the primary auditory cortex as target point for rTMS. The exact position of the figure 8-shaped magnetic coil in relation to the target was monitored with a neuronavigational system. The rTMS (110% motor threshold; 1 Hz; 2000 stimuli/ day over 10 days) was performed in a placebo controlled design. For sham stimulation a specific sham-coil system was used. Treatment outcome was assessed over a 3 months period with a tinnitus questionnaire (Goebel and Hiller).

Results: Up to now 60 patients have been included in the trial. In a majority of patients we could localize an increased metabolic activation in the upper dorsal part of the left superior temporal gyrus corresponding to areas of the auditory cortex. Preliminary results indicate that active rTMS results in a significant improvement of tinnitus perception compared to sham rTMS. Treatment effects lasted up to 3 months in some patients.

Conclusion: Neuronavigated low-frequency rTMS seems to represent a promising strategy for the treatment of chronic tinnitus.

#### 167 The History of Serous Otitis Media: Part I of III

#### Robert Ruben<sup>1</sup>

<sup>1</sup>Albert Einstein College of Medicine

Serous otitis media (SOM), which appears to have dogged humankind since the Stone Age, was not generally focused upon as a significant problem until the last half of the 20th century. It has gone by many names, including

middle ear catarrh, catarrhal otitis media, secretory otitis media, and otitis media with effusion, and is characterized by a non purulent fluid in the middle ear clef: the fluid may vary in consistency from thin and watery to a tenacious gel.

Throughout recorded history, although distinctions were not commonly made between SOM and other ear disorders, there are at least two exceptions. The Roman physician Celsus describes what appears to be SOM; the Arabic physician, Albucasis ('Al-Tasrif li man ajaz an-il-talif) recognized the disease and treated it with myringotomy.

The description by Eustachi in 1563 of what subsequently became known as the eustachian tube was a foundation for current understanding of SOM. Du Verney's 17th century developed description and illustration of the eustachian tube, followed by Valsalva's investigation of eustachian tube physiology and function in the 18th was the basis of the first attempt by Guyot, the Postmaster at Versailles, to care for what was probably recurrent SOM means of eustachian tube catheterization. Subsequently, in the late 18th century, several reports appeared on the uses of myringotomy for the care of ear disorders. Cooper starts the 19th Century (1801) by bringing myringotomy into the accepted medical/surgical armamentarium. Soon, however, the procedure became viewed as infective and dangerous.

Deleau (and then Toynbee) in the middle of the 19th century, bypassing myringotomy, developed diagnostic assessments dependent upon eustachian tube function. Deleau popularizes the eustachian tube intubation for the care of middle ear disorders; these appear to include SOM. Meyer's discovery and report of 1868 of the adenoid and use of adenoidectomy to treat middle ear catarrh was rapidly adopted. Politzer, at the end of the 19th century, describes catarrh as SOM and uses a combination of modalities — eustachian tube insufflation (Politzerization), adenoidectomy, and myringotomy — to treat SOM.

### 168 Otitis Media with Effusion Following Head and Neck Surgery

**Rie Kanai**<sup>1</sup>, Ken-ichi Kaneko<sup>1</sup>, Yumi Ito<sup>1</sup>, Shinya Hori<sup>2</sup>
<sup>1</sup>Fukui Red Cross Hospital Department of
Otorhinolaryngology, <sup>2</sup>Kobe City General Hospital
Department of Otolaryngology

Objective: We considered head and neck surgery could be one of the risk factor of otitis media with effusion (OME), therefore we evaluated the incidence of postoperative OME in patients after head and neck surgery.

Methods: The subjects were 48 patients (94 ears without middle ear disease; 22 males, 26 females; mean 42.7 years; range 16°C85 years) who underwent head and neck surgery in our department. The operations were performed under general and local anesthesia in 43 and 5 cases respectively. The regions of the operations were the nose in 10 cases, the throat in 17, the neck in 19, and the middle ear in 2. We examined their ear drums and intratympanic pressure with tympanometry on the day before surgery, 1st°C2nd and 5th°C9th postoperative day,

namely at three stages (preoperative, the first postoperative, the second postoperative) in total.

Results: Middle ear effusion was observed in 6 ears (6.4%) at the first postoperative stage and disappeared in all ears at the second postoperative stage. The preoperative intratympanic pressure was £-22.0¡À29.7 daPa (mean¡ÀSD), while the first postoperative pressure decreased to £-62.9¡À85.1 daPa. Then the second postoperative pressure was recovered up to £-28.0¡À44.0 daPa. There was the significant difference of the average intratympanic pressure between the preoperative and the first postoperative stages (p£½0.01) and between the first and the second postoperative stages (p£½0.01) but there was no significant difference between the preoperative and the second postoperative stages (p=0.14).

Conclusions: We found that intratympanic pressure would change to negative transiently after head and neck surgery, and incidence of postoperative OME was 6.4%. This suggests that head and neck surgery could be one of the risk factor of OME.

### | 169 | Minimally Invasive Endoscope-Assisted | Parotidectomy: A New Approach

Cheng C. Chang<sup>1</sup>

<sup>1</sup>Changhua Christian Hospital

Background: This study evaluates the benefits of a new approach, endoscopic parotidectomy through the post-auricular skin incision, by using an ultrasonically activated scalpel.

Patients and Methods: Fourteen operations for selected patients presenting with benign lower pole parotid disease were performed via minimally invasive endoscopic resection.

Results: All 14 operations were successfully performed endoscopically, and no conversions to conventional open resection were necessary. Of the 14 patients who underwent excision, all of them had benign lesions. The procedures lasted 60 to 150 minutes. Two patients had transient grade II facial paresis. The scar was almost invisible due to its concealed location behind the ear.

Conclusions: Minimally invasive endoscope-assisted parotidectomy is a feasible method for treatment of benign lesions located in the lower pole parotid. The main advantage of this procedure is that the small operative scar is concealed in the post-auricular area resulting in improved cosmetic results.

### 170 Artificial Larynx with Quiet Vibrator and Voice Conversion System

**Takefumi Sakaguchi**<sup>1</sup>, Yoshiki Nagatani<sup>1</sup>, Tomoyuki Kamijo<sup>1</sup>, Takehiko Fukuda<sup>1</sup>, Hiroshi Hosoi<sup>1</sup>

<sup>1</sup>Nara Medical University

We introduce here a new type of artificial larynx, which consists of quiet vibrator and voice conversion system that could provide more naturalness in its produced voice compared to the conventional one.

The basic studies were performed to look into the feasibility of the device. The experiments were performed

under two conditions, i.e., quiet and noisy circumstances. Under 40 dB(A) background noise, the sound pressure level of the point 300 mm distant from the vibrator was 40.2 dB(A) when the input of the transducer was 1 Vpp.

We succeeded to receive the speech sounds which were produced by articulation motion without exhalation through both the normal and the contact-type microphones without any leak of audible sounds to outside. We also performed voice conversion to the recorded voice, and succeeded to improve its naturalness. These results suggest the viability of new type of artificial larynx with quiet vibrator.

### 171 Role of VCAM-1 in Pathogenesis and Recurrence of Diffuse Nasal Polypi

Malak Zoheir<sup>1</sup>, Yakout Dogheim<sup>2</sup>

<sup>1</sup>Medical Research, <sup>2</sup>Ent Dep Alexandria Faculty of Medicine

Nasal polyposis is characterised by accumulation of inflammatory cells particularly eosinophils. Inflammatory cells pass by multistep process at their site of recruitment to undergo adhesion to vascular endothelium followed by extravasation.

Our main objective was to investigate the role of VCAM-1 in selective recruitment of eosinophils in diffuse nasal polypi and to show the effect of quantitative expression of VCAM-1 and number of eosinophils on recurrence of diffuse nasal polypi after treatment.

Our study included 50 randomly selected patients diagnosed to have diffuse polyposis (groupIV) according to Stammberger classification.

Our results showed that there is a significant degree of of eosinophils in polyps compared to inferior turbinate mucosa but both show same VCAM-1 expression. This expression does not correlate with degree of eosinophilia so it cannot be explained on the basis of VCAM-1 expression. Degree of eosinophilia did not differ significantly in cases of recurrence.

But the VCAM-1 expression was significantly higher in these cases.

We concluded that although the degree of VCAM-1 detected in the endothelium vessels does not correlate with the degree of eosinophilia yet, VCAM-1 could be considered as an indictor for high tendency of recurrence...

### 172 Novel Analysis of Olfactory Behavior with Video Cameras and NIH Image Software

**Aigo Yamasaki**<sup>1</sup>, Tsuyoshi Takemoto<sup>1</sup>, Kazuma Sugahara<sup>1</sup>, Hiroshi Yamasita<sup>1</sup>

<sup>1</sup>Yamaguchi university Graduated School of medicin

Current experimental protocols for the analysis of olfactory behavior are complex. We established a simple and reproducible for the evaluation method of olfactory function in mice. We found that mice avoided cotton balls treated with acetic acid and placed in a corner of a square chamber, and we recorded this behavior with a video camera. Videos were analyzed with NIH Image software. The chamber was divided into four areas, and the mean time mice remained in each area was calculated. Before

bilateral olfactory nerve transection, the mean time spent in acetic acid area was significantly less than that in the opposite area (P < 0.05). Eight On to 21 days after transection, mice stayed in each area for a similar period of time. Twenty-eight days after transection, the mean time spent in the acetic acid area was again significantly less than that in the opposite area (P < 0.05). Thus, with this method, we were able to statistically evaluate function and recovery from olfactory nerve transection. This novel method may be useful for the study of olfactory behavior in mice.

# 173 Vestibular Evoked Myogenic Potential (VEMP) Testing: Normative Data with Regulated Sternocleidomastoid (SCM) Tension

Kristen Janky<sup>1</sup>, Neil Shepard<sup>1</sup>

<sup>1</sup>University of Nebraska - Lincoln

Introduction: The literature to date presents conflicting evidence as to the effect of age on the VEMP response. Absent from the literature are normative ranges for VEMP thresholds across test frequencies. Objective: The objective of the current study was to test the hypothesis that significant changes in the VEMP threshold response curve occur as a function of increased age. To test this hypothesis, age related VEMP threshold response curves were generated on a control population utilizing a newly validated means of regulating the amount of SCM muscle tension (Vanspauwen, et al, Laryngoscope, 2006a & 2006b). Vanspauwen et al have demonstrated that monitoring head turn resistance into an inflated blood pressure cuff results in a constant level of SCM contraction throughout testing and smaller variability in VEMP amplitude responses. Methods: Subjects included normal volunteers (n = 40) ranging between 20 and 75 years of age. The healthy subjects completed VEMP testing in response to clicks and 250, 500, 750, and 1000 Hz toneburst stimuli while generating 25 mmHg of resistance above a 20 mmHg baseline against a blood pressure cuff for SCM tension monitoring. Results: Results at the time of abstract submission (n=15) show: (1) lowest response thresholds in dB SPL within the 500 to 750 Hz region, (2) no trend for age effect from 20-56 years, and (3) increases in the latency of the P13/N23 response with decreasing stimulus frequency. The normative thresholds together with characterizing latency and amplitudes of the P13/N23 responses will be presented. The clinical usefulness of these data in the assessment of vestibular disorders; in particular, use of threshold response curves in the identification of Meniere's disease (Rauch, et al., Otology & Neurotology, 2004) will be discussed.

#### 174 Stimulus Repetition Rate on VEMP Thresholds

Chizuko Tamaki<sup>1</sup>, R. Steven Ackley<sup>1</sup>

<sup>1</sup>Gallaudet University

Vestibular-evoked myogenic potentials (VEMP) is a measure of the reflexive contraction of the

sternocleidomastoid muscles (SCM) in response to highintensity acoustic stimulation. Although useful, thresholds are not routinely measured clinically mostly due to its lengthy procedure.

In an effort to reduce effective test time by increasing the stimulus repetition rate, the effects of high stimulus repetition rates on threshold measures were investigated. In twenty (20) otologically and neurologically normal participants between the ages of 20 and 30 years, thresholds were measured at four frequencies (250, 500, 750, and 1000 Hz), using five stimulus repetition rates (5.1/s, 11.1/s, 13.1/s, 15.1/s, and 17.1/s).

Results indicate that the rate of 13.1/s can be used clinically to yield a threshold within 5 dB of that obtained using a commonly used rate of 5.1/s, for 500-, 750-, and 1000-Hz STB. For 250-Hz STB, even the slowest experimental rate of 11.1/s caused excessive shift in threshold.

#### 175 Signal and Noise Characteristics of Vestibular Evoked Myogenic Potentials

**S.R. Prakash**<sup>1,2</sup>, John J. Guinan<sup>2,3</sup>, Barbara S. Herrmann<sup>3,4</sup>, Sharon G. Kujawa<sup>3,4</sup>, Steven D. Rauch<sup>3,5</sup>

<sup>1</sup>Harvard – MIT Division of Health Sciences & Technology, Boston, MA, <sup>2</sup>Eaton-Peabody Laboratory, Massachusetts Eye & Ear Infirmary, Boston, MA, <sup>3</sup>Dept. of Otology and Laryngology, Harvard Medical School, Boston, MA, <sup>4</sup>Dept. of Audiology, Massachusetts Eye & Ear Infirmary, Boston, MA, <sup>5</sup>Dept. of Otolaryngology, Massachusetts Eye & Ear Infirmary, Boston, MA

Clinical measurement of Vestibular Evoked Myogenic Potentials (VEMP) is becoming increasingly popular for diagnostic assessment of vestibular disorders. However, there remain many unanswered questions about the VEMP response. Unlike auditory evoked potentials, the neural response from the vestibular system is measured indirectly as modulation of voluntary neck muscle activation. Depending on the VEMP signal and noise characteristics, the processing schemes required to extract physiologically relevant responses from the surface EMG signals may differ from those commonly used in auditory evoked potential measurements. Earlier studies made direct measurements of muscle fiber and intracellular potentials underlying the VEMP response. Herein we examine how these studies inform our understanding of the signal and noise properties of the VEMP response and explore the importance of these concepts to clinical application of the test.

We define the "signal component" of VEMP as the expected value of the post-stimulus surface EMG signal (or equivalently, the waveform from averaging an infinite number of traces). The "noise component" in the average of a finite number of surface EMG traces arises from additive noise (instrument and physiological), as well as from statistical variation in motor neuron spike timing and motor unit amplitude. We examine the behavior of the noise statistics as a function of the number of averages. We consider the interaction between the vestibular and motor pathways, and analyze the contribution of each to the averaged signal. We find that different features of the

signal waveform depend to different extents on the state of the vestibular periphery, and therefore may have different degrees of clinical relevance. We discuss the implications of this study to the questions, "What features of the VEMP signal are most clinically relevant?" and "Which signal averaging scheme is optimal for estimating these features from finite data?"

### 176 Test-Retest Reliability of Vestibular Evoked Myogenic Potential (VEMP)

**Suwicha Isaradisaikul**<sup>1</sup>, Darcy A. Strong<sup>2</sup>, Sandra A. Gabbard<sup>3,4</sup>, Steven Ackley<sup>2</sup>, Jamie Moushey<sup>2</sup>, Herman A. Jenkins<sup>3,4</sup>

<sup>1</sup>Chiang Mai University, <sup>2</sup>University of Colorado, <sup>3</sup>University of Colorado Health Sciences Center, <sup>4</sup>Marion Downs Hearing Center

Objective: To determine the reliability of VEMP responses with and without the use of electromyography (EMG) monitoring in persons with normal audiovestibular function. Study Design and Setting: VEMP was performed in normal adult volunteers with and without the use of EMG monitoring in two separate sessions. Each session was one to four weeks apart. Threshold repeatability, p13 and n23 latency, p13 and n23 amplitude, p13-n23 interlatency, p13-n23 interamplitude. and interaural differences (IAD ratio) from the first and the second session were assessed by the intraclass correlation coefficient (ICC). Reliability of VEMP responses with the use EMG monitoring was compared to responses without the use of EMG monitoring. Results were interpreted by the same raters. The data was analyzed using SPSS 11.0. Results: VEMP thresholds for conditions with and without the use of EMG monitoring were found to have good reliability. The amplitudes were found to be more reliable in the test condition with the use of EMG monitoring than in the condition without the use of EMG monitoring. The latency and amplitude of n23 were found to be more reliable than p13 latency and amplitude.

Conclusion: Overall, VEMP responses were found to have good test-retest reliability. No apparent differences in response thresholds were observed in the test condition with and without the use of EMG monitoring. Variances in VEMP response parameters may occur over time, which could be attributed either to test-retest variability or progression of pathology. Clinicians should consider these changes when interpreting VEMP responses. EMG monitoring facilitates judgment of the result.

### 177 Vibration-Induced Nystagmus in Patients with Vestibular Disorders

**Hong Ju Park**<sup>1</sup>, JungEun Shin<sup>1</sup>, DaeBo Shim<sup>1</sup>, HyangAe Shin<sup>1</sup>, SangGyun Lim<sup>1</sup>

<sup>1</sup>Konkuk University School of Medicine

It has been reported that vibration applied either to the mastoid or to the sternocleidomastoid (SCM) muscles of subjects after unilateral vestibular deficit induces nystagmus. We recorded horizontal eye movements during unilateral 100 Hz vibration on either mastoid bone

or the SCM muscles in 87 patients with vestibular disorders. Vibration-induced nystagmus (VIN) with slow phase eye velocity > 2 deg/s in more than 3 sites with the same direction was considered pathologic. Patients underwent caloric testing and unilateral weakness (UW) > 25% was considered pathologic. In patients with vestibular neuritis (N=23), 21 patients showed pathologic VIN and the direction of VIN was toward the contra-lesioned side. The degree of the induced-nystagmus on the mastoid showed a significant correlation with the degree of the unilateral weakness on caloric test (p < 0.01). In patients with Meniere disease (N=24), 9 (37.5%) patients showed pathologic UW, 17 (70.8%) showed pathologic VIN and 8 showed pathologic VIN and UW. In patients with migraineassociated dizziness (N=40), 8 (20%) patients showed pathologic UW, 12 (30%) showed pathologic VIN and 4 showed pathologic VIN and UW. VIN testing can enhance sensitivity in detecting vestibular dysfunction in vestibular disorders, especially in recurrent vestibulopathy when combined with caloric test.

## 178 Clinical Characterization and Genetic Analysis of a Large Brazilian Family with Familial Migrainous Vertigo

**Fayez Bahmad**<sup>1,2</sup>, Saumil Merchant<sup>1</sup>, Roberta Bezerra<sup>2</sup>, Jonathan Seidman<sup>3</sup>, Carlos Oliveira<sup>2</sup>

<sup>1</sup>Massachusetts Eye & Ear Infirmary, <sup>2</sup>Brasilia University Hospital, <sup>3</sup>Harvard Medical School

Introduction: Since 1995, we have been studying a large Brazilian family whose members are affected with migrainous vertigo syndrome.

Objectives: The aim of this study is to describe clinical features and the natural history of this symptom complex. We also wish to characterize the genetic basis for this condition in the family.

Methods: A six generation Caucasian family originating from the center of Brazil was followed over ten years and data was collected from 146 members. Clinical data included collected has detailed case histories, and neurological otolaryngological examinations. audiometric evaluation, vestibular testing and imaging studies. Serial clinic and audiometric evaluations were done. We have also undertaken a genome wide linkage analysis in 64 family members and subsequent fine mapping using microsatellite markers.

Results: Our study reveals an autosomal dominant pattern of transmission with incomplete penetrance of the gene and variable expression. Of the 146 members, 32 suffer from migraine with aura. Of these 32 individuals, 10 also suffer from episodic vertigo, tinnitus and/or aural fullness. Audiometric evaluation did not show classic low tone fluctuating sensorineural hearing loss (SNHL). Imaging studies were normal. In this family, migraine preceded the neuro-otological symptoms by 15-20 years on average. Overall, migraine symptoms decreased with time, while the vertigo symptoms had a tendency to get worse. Genetic analysis revealed an area with high lod scores in chromosome 5. Therefore, the genetic locus for this symptom complex in this family appears to be on chromosome 5. Studies are ongoing to investigate candidate genes in this locus.

#### 179 Short-Arm BPPV Revisited: Treatment Outcomes

Neil Cherian<sup>1</sup>, John Oas<sup>2</sup>, Sebastian Cervantes<sup>1</sup>

<sup>1</sup>The Cleveland Clinic, <sup>2</sup>Ohio Head and Neck Institute

Benign paroxysmal positional vertigo (BPPV) is a common yet under recognized otologic syndrome. Controversy exists whether certain subtypes exist. Short-arm BPPV (also referred to as ampullolithiasis) is a phenomenon that has not been widely accepted. Based on our prior work (presented at ARO 2006), short-arm is ultimately a provable subtype of BPPV. A series of ten patients with refractory BPPV was reviewed. This abstract reviews the treatment outcomes of these ten cases.

BPPV is thought to be a consequence of an injured utricular macula (by infection or trauma) or by deranged otoconial metabolism. BPPV is ultimately a disorder of "otoconial destination" and how to return the otoconiae to the utricle. In theory, any area within the endolympathic space of the labyrinth may harbor stray otoconiae. Thus, in short-arm BPPV, it is thought that the otoconiae in short-arm BPPV is located between the utricle and the utricular side of the posterior canal's cupula.

Patients with complaints of positional vertigo were selected. The trend of the symptoms tended to be persistent over the course of weeks to months. Many of these patients failed typical canalith repositioning maneuvers. Dix-Hallpike and supine positional testing were performed. Eye movement data was captured with infrared videonystagmography and analyzed using commercial vestibular laboratory software (Micromedical Technologies). Particle repositioning maneuvers (modified Epley) were attempted for the posterior semicircular canal of interest. A 72 hour vibration-assisted protocol was followed by the patient at home.

Upon review of the eye movement data, the most consistent finding seen in the final position (return to sit) of canalith repositioning maneuvers was a torsional and downbeat nystagmus. Resolution of positional vertigo and the resolution of the susbsequent positional nystagmus were seen. We then postulate that the head vibration stimulus helps to accelerate otoconiae out of the shortarm.

In conclusion, short-arm BPPV of the posterior semicircular canal appears to be a real and treatable form of positional vertigo. Short-arm should be considered in refractory cases of BPPV and may coexist with other variants including that of the same canal.

## 180 Study on Transtympanic Gentamicin Injection in Guinea Pig and Patient with Intractable Vertigo

Chunfu Dai1

<sup>1</sup>Fudan University

Objective: To determine the distribution of gentamicin in the inner ear of guinea pig following local application and explore the efficacy of low dosage intratympanic gentamicin injection on patients with intractable Meniere's disease

Methods and materials: Fifty ul purified GTTR (gentamicin texas red) was injected intratympanically. In group I, just one injection was conducted, In group II, the injection was

conducted once a day, a total four injections were given. In group III, injection was conducted once a week, four injections were completed. The animals were allowed to survive 1, 3, 7, 14, 21, 28 day, respectively. A retrospective study was conducted to investigate the efficacy on intractable Meniere's disease with 30mg/ml gentamicin intratympanic injection during 2003, 5-2004, 5. All patients were asked to observed for three weeks to determine other injection was needed.

Results: Gentamicin accumulated in hair cell with high intensity for 3-4 weeks. Gentamicin distributed in the cochlea in the gradient pattern. More frequency gentamicin injection lead to more gentamicin accumulation.

Nineteen patients with Meniere's disease were treated with intratympanic gentamicin injection. Vertigo control was achieved in 17 patients (89%). Of them, 5 patients were successful only after one injection. Another 8 patients need two injections to control the vertigo, one patient asked endolymphatic sac shunt because he was unable to tolerate the fullness. Vertigo was controlled in 4 patients after 3 injections were performed. Two patients with two injections did show improvement of vertigo. Hearing was improved in two patients following gentamicin injection. Three patients (15%) complained of hearing loss after intratympanic gentamicin injection. The hearing of the other patients did not changed significantly.

Conclusions: Gentamicin was able to accumulated in the hair cell with high intensity for at least 3 weeks following one injection was given. In this case, it is reasonable to wait for 3 weeks to determine another injection was needed in our practice. In fact, Less gentamicin intratympanic injection was applied in our study, Our study showed this approach was able to control vertigo, as well as it reduced the risk of hearing loss following intratympanic gentamicin injection.

Keywords: Meniere's disease, gentamicin, vertigo, therapy

## 181 VOR Gain Reduction and Vertigo Control After Intratympanic Gentamicin for Treatment of Meniere's Disease

Kimanh Nguyen<sup>1</sup>, Lloyd Minor<sup>1</sup>, John Carey<sup>1</sup>

<sup>1</sup>Johns Hopkins School of Medicine

Vertigo control and changes in both horizontal angular vestibulo-ocular reflex (AVOR) gain (measured using magnetic search coils and manual head thrusts) and caloric weakness were assessed in subjects who received intratympanic (IT) gentamicin for unilateral Meniere's disease. A Kaplan-Meier survival analysis allowing inclusion of all subjects to follow up for as long as 8 years demonstrated success in managing vertigo in 96% of 80 subjects; the remainder "failed" and required surgically-destructive procedures. Vertigo control data available for 48 subjects demonstrated an 85.6% decrease in vertigo rates from 12.5  $\pm$  17.1 episodes/mo pre-treatment to 1.8  $\pm$  4.3 episodes/mo post-treatment (p < 0.001). 75% experienced either complete elimination of vertigo or a reduction in vertigo rate of greater than 60%.

AVOR gain decreased 38.2% from  $0.88 \pm 0.15$  to  $0.54 \pm 0.24$  (p < 0.001, n = 46) after the first treatment. Subsequent injections, when required for vertigo control,

did not produce further reductions in gain. Subjects who required only one injection had a pre-treatment gain of  $0.88 \pm 0.12$  and a post-treatment gain of  $0.49 \pm 0.20$  (p < 0.001, n = 22), while those who needed multiple injections had a pre-treatment gain of  $0.88 \pm 0.17$  and a post-treatment gain of  $0.58 \pm 0.26$  (p < 0.001, n = 24).

There were no correlations between AVOR gain reduction or caloric unilateral weakness and vertigo rates after one treatment. There was a trend to more variable vertigo rates among subjects with less AVOR gain reduction. Thus, IT gentamicin treatment was successful in both the management of vertigo and the reduction of AVOR gain in the majority of Meniere's patients, and the greatest effects on AVOR gain were observed after the first injection. However in 49% of cases, vertigo control required multiple injections, suggesting that the salient effects of gentamicin may extend beyond AVOR gain reduction.

## 182 Oculographic Analysis of Induced Nystagmus in Superior Canal Dehiscence Syndrome

Ja-Won Koo<sup>1</sup>, Ji Soo Kim<sup>1</sup>

<sup>1</sup>Seoul National University Bundang Hospital

Sound and pressure induced vertigo are usual manifestations of superior canal dehiscence (SCD) syndrome. However, sound or pressure may not provoke nystagmus in every patient who has dehiscent superior semicircular canal and, if so, the intensity may not be strong enough to identify during the bed side examination under Frenzel glasses. Authors analyzed the characteristics of the nystagmus induced by several kinds of stimuli in three patients who were found to have unilateral dehiscence of the superior semicircular canal on high resolution temporal bone CT.

All patients showed intact stapedial reflex, symmetric caloric responses and lower threshold in VEMP test compared to healthy side by 15 to 20 dB nHL. 500 Hz and 1 kHz short tone burst stimuli (1.1/sec, 2.1/sec, 3.1/sec, respectively), pressure stimuli using politzer bag and vibration stimuli (100 Hz) on the mastoid are delivered. Horizontal, vertical and torsional eye movements were recorded using three dimensional video-oculography system.

Induced eye movement was stronger by 500 Hz tone burst stimulus than 1 kHz in 2 patients. And it was stronger by increasing stimulus rate in one patient but such finding was not consistent in the other 2 patients. Fistula test induced upward and intorsional eye position change in 1 patient. Mastoid vibration induced substantial horizontal nystagmus (3.7-11 deg/sec) with down beating (2.4-6 deg/sec)and extorsional nystagmus (4.3-10 deg/sec) in every patient, which may implicate the excitation of ipsilateral horizontal canal as well.

Intensity and the rotation axis of the induced eye movement showed somewhat different pattern according to the stimuli. However, the induced eye movement was most prominent and easily demonstrated by mastoid vibration.

### 183 Gaze Stabilization and Physical Performance in Vestibular Dysfunction

**Susan Whitney<sup>1,2</sup>**, Miranda Pritchard<sup>3</sup>, Gregory Marchetti<sup>1,4</sup>, Joseph Furman<sup>1,2</sup>

<sup>1</sup>University of Pittsburgh Department of Otolaryngology, <sup>2</sup>University of Pittsburgh Department of Physical Therapy,

<sup>3</sup>University of Pittsburgh Department of Audiology,

<sup>4</sup>Duquesne University Department of Physical Therapy

We sought to assess the relationship between gaze stabilization and physical performance in patients with vestibular dysfunction. The gaze stabilization test (GST) quantifies the functional status of the vestibulo-ocular reflex. Subjects included 41 healthy subjects (n=20: 40-60 years old; n=21: 60-80 years old) and 15 patients with vestibular dysfunction. All subjects were cognitively intact. The GST was performed with subjects seated while viewing a computer monitor. Subjects wore a velocity sensor that quantified the maximum head velocity attainable in the pitch and vaw planes while they accurately identified a briefly illuminated optotype. Subjects completed two physical performance tests prior to the GST: the Functional Gait Assessment (FGA) and the Timed "Up & Go" (TUG). Data analysis: relationship between yaw plane GST velocity and functional gait performance was assessed generalized linear models with adjustment for factors of age group and vestibular disease. Total model and individual factor plus covariate parameter estimates were tested for significance (p < 0.05) and for contribution to variance in functional gait performance (r-squared). Results: Younger subjects demonstrated higher functional gait performance on the TUG and FGA in all subjects. Yaw plane GST velocity, age group, and vestibular disease velocity predicted 35% of the variance in TUG performance (p < 0.01), with yaw plane GST velocity predicting 9% of variance in TUG (p = 0.03). Yaw plane GST velocity, age group, and vestibular disease predicted 49% of the variance in FGA scores (p < 0.01) with yaw plane GST velocity predicting 11% of the variance in FGA scores (p < 0.02). A significant age group and vestibular disease interaction effect was present for both TUG and FGA performance. Conclusion: Gaze stabilization contributes to dynamic gait.

#### 184 Treadmill Walking in a Virtual Grocery

**Susan Whitney**<sup>1,2</sup>, Patrick Sparto<sup>1,2</sup>, James Cook<sup>1</sup>, Redfern Mark<sup>1,3</sup>, Joseph Furman<sup>1,2</sup>

<sup>1</sup>University of Pittsburgh Department of Otolaryngology, <sup>2</sup>University of Pittsburgh Department of Physical Therapy, <sup>3</sup>University of Pittsburgh Department of Bioengineering The purpose of this study was to investigate the test-retest

reliability of normal human behavior while subjects searched for products in a virtual grocery store. The hypothesis was that there would be no difference in subject performance between two visits. Methods: Twelve healthy subjects with no evidence of neurologic disease participated (7 female, 5 male, mean age 38 y, range 21 to 72 y). The single-aisle virtual grocery store was displayed in a full-field of view virtual environment (2.4

m high, 2.4 m wide, 1.5 m deep). The length of the aisle was 120 m, with 2 m breaks placed after every 5 m of products. Subjects were asked to find 2 common cereal boxes placed a total of 20 times along the length of the aisle. The remainder of the products consisted of 30 other types of products. The subjects walked through the store on a custom-made treadmill placed within the environment. The speed of the treadmill and thus the speed of moving through the store was controlled by the amount of force subjects applied to an instrumented shopping cart. The maximum treadmill velocity was limited to 1.2 m/s. Head yaw movement was recorded using an electromagnetic tracker. The outcome measures were the average head vaw velocity, average speed of walking through the store, and number of products found. Nonparametric tests were used to examine if there was a significant difference and significant correlation between values observed on different days. Results: There was no significant difference in the average head yaw velocity (day 1: 29 deg/s and day 2: 25 deg/s, p = 0.31) and average walking speed (day 1: 0.83 m/s and day 2: 0.88 m/s, p = 0.14) from day 1 to day 2. Both head yaw velocity and walking speed from day 1 were significantly correlated with the values from day 2 (Spearman's rho = 0.82 and 0.65, respectively)). Subjects found significantly more products on day 2 than day 1 (median 17 v. 14, p = 0.009). In addition, the number of products located were correlated from day 1 to 2 (Spearman's rho = 0.63). Discussion/Conclusion: Average head velocity and walking speed are repeatable while ambulating on a treadmill in a virtual reality grocery store. changes in these measures noted over the course of rehabilitation in the virtual environment most likely demonstrate change from the intervention, as the measures appear to be relatively stable over time.

#### 185 Mechanism of DVA Recovery with Vestibular Rehabilitation

Michael Schubert<sup>1</sup>, **Amir Allak<sup>1</sup>**, Americo Migliaccio<sup>1</sup>, John Carey<sup>1</sup>, Richard Clendaniel<sup>2</sup>

<sup>1</sup>Johns Hopkins University, <sup>2</sup>Duke University

In vestibular hypofunction, gaze stability during head rotation is reduced because eye and head velocity do not match. Dynamic visual acuity (DVA) involves an active head rotation and is a functional measure of gaze stability. Controlled studies have shown DVA improves in persons with unilateral vestibular hypofunction (UVH), upon completion of vestibular rehabilitation. We were interested in determining how DVA improves. Angular vestibuloocular reflex (aVOR) gains were measured during passive head thrust testing and DVA using magnetic scleral search coils, in four subjects with chronic vestibular hypofunction (n=3 unilateral UVH, n=1 bilateral BVH) and one subject with VOR gain recovery (after vestibular neuritis, VN). Head thrust and DVA testing were performed concurrently before and after DVA scores improved. Comparing preand post-rehabilitation data, there was an increase in aVOR gain during the DVA test in each of the 3 subjects with chronic UVH (mean  $0.75 \pm 0.18$  to  $0.82 \pm 0.21$ , 15%), the subject with BVH (0.48  $\pm$  0.1 to 0.85  $\pm$  0.05, 76%), and the VN subject (0.68  $\pm$  0.04 to 1.02  $\pm$  0.13, 50%). One

chronic UVH and the VN subject had increases in aVOR gain for passive yaw head thrusts (0.41 to 0.45, 9.7% UVH and  $0.25 \pm 0.03$  to  $0.62 \pm 0.08$ , 148% VN). In addition, the UVH and VN subject were noted to have a reduction in the number of compensatory saccades (CS)/head rotation from pre DVA to post DVA (1.9 to 0.7 and 0.45 to 0.38, respectively). For the 2 chronic subjects that did not have any change in passive VOR gain, we found an increase in the ratio of CS/head rotation (mean 0.88 ± 0.09 vs. 1.12 ± 0.08, 28%). Our results suggest DVA recovers as a result of improved VOR gain for active head rotation. The number of CS used per head rotation appears dependent on VOR gain and may be a useful gaze stability mechanism for some people. These data suggest rehabilitation has a mechanistic effect on recovery of gaze stability during active head rotation.

### 186 Training with the Brainport Balance Device Decreases the Risk of Falls

Yuri Danilov<sup>1</sup>, Kim Skinner<sup>1</sup>

<sup>1</sup>Wicab, Inc.

Objective: To investigate the effect of BrainPort balance device training on patients with vestibular disorders who are at a high risk of falls.

Methods: The BrainPort balance device transmits head position information through electrotactile stimulation of the tongue. Subjects use feedback from this stimulus to correct body position to achieve improved balance. Nine subjects ages 59 to 88 years with chronic balance dysfunction due to either peripheral or central vestibulocerebellar pathology completed 6 to 10 BrainPort balance device training sessions over a 5-day period. Training sessions consisted of progressively challenging postural tasks while using the BrainPort, ending with a 20-minute trial. Subjects were tested before the first and after the last BrainPort training session.

Results: At baseline, all subjects scored 19 (out of 24) or lower on the Dynamic Gait Index, indicating that they were at a high risk of falling. After 5 days of training with the BrainPort device, the subjects improved their scores by an average of 4 points. Eight of nine subjects exhibited a more stable gait and improved scores on the DGI, which correlates to a decreased risk of falls. Improvements in balance were supported by other objective measures, such as the Sensory Organization Test and Dizziness Handicap Inventory. Subjects with multiple comorbidities did not improve as much as subjects with a single etiology. Amount of improvement did not correlate to age.

Conclusions: Training with the BrainPort balance device produced improvements in balance, gait and functional activities. This has important potential for decreasing the risk of falls in a broad range of general balance problems. Further studies are warranted.

#### 187 Influence of Electrotactile Tongue Feedback on Controlling Upright Stance During Rotational And/or Translational Sway-Referencing with Galvanic Vestibular Stimulation

Scott J. Wood<sup>1,2</sup>, Mitchell E. Tyler<sup>3</sup>, Paul Bach-y-Rita<sup>3</sup>, Hamish G. MacDougall<sup>4</sup>, Steven T. Moore<sup>5</sup>, Valerie L. Stallings<sup>1</sup>, William H. Paloski<sup>2</sup>, F. Owen Black<sup>1</sup>

<sup>1</sup>Legacy Health System, Portland, <sup>2</sup>NASA Johnson Space Center, Houston, <sup>3</sup>University of Wisconsin, Madison, <sup>4</sup>University of Sydney, Australia, <sup>5</sup>Mount Sinai School of Medicine, New York

Integration of multi-sensory inputs to detect tilts relative to gravity is critical for sensorimotor control of upright orientation. Displaying body orientation using electrotactile feedback to the tongue has been developed by Bach-y-Rita and colleagues as a sensory aid to maintain upright stance with impaired vestibular feedback. MacDougall et al. (2006) recently demonstrated that unpredictably varying Galvanic vestibular stimulation (GVS) significantly increased anterior-posterior (AP) sway during rotational sway referencing with eyes closed. The purpose of this study was to assess the influence of electrotactile feedback on postural control performance pseudorandom binaural bipolar GVS. Postural equilibrium was measured with a computerized hydraulic platform in 10 healthy adults (6M, 4F, 24-65 y). Tactile feedback (TF) of pitch and roll body orientation was derived from a twoaxis linear accelerometer mounted on a torso belt and displayed on a 144-point electrotactile array held against the anterior dorsal tongue (BrainPort, Wicab, Inc., Middleton, WI). Subjects were trained to use TF by voluntarily swaying to draw figures on their tongue, both with and without GVS. Subjects were required to keep the intraoral display in their mouths on all trials, including those that did not provide TF. Subjects performed 24 randomized trials (20 s duration with eyes closed) including four support surface conditions (fixed, rotational sway-referenced, the translating support proportional to AP sway, and combined rotationaltranslational sway-referencing), each repeated twice with and without GVS, and with combined GVS and TF. Postural performance was assessed using deviations from upright (peak-to-peak and RMS sway) and convergence toward stability limits (time and distance to base of support boundaries). Postural stability was impaired with GVS in all platform conditions, with larger decrements in performance during trials with rotation sway-referencing. Electrotactile feedback improved performance with GVS toward non-GVS levels, again with the greatest improvement during trials with rotation sway-referencing. These results demonstrate the effectiveness of tongue electrotactile feedback in providing sensory substitution to maintain postural stability with distorted vestibular input.

### 188 Usefulness of Current Balance Tests for Identifying Balance-Impaired Individuals

**Helen Cohen<sup>1</sup>**, Kay T. Kimball<sup>2</sup>, Ajitkumar P. Mulavara<sup>3</sup>, William H. Paloski<sup>4</sup>, Jacob J. Bloomberg<sup>4</sup>

<sup>1</sup>Baylor College of Medicine, <sup>2</sup>Statistical Design and Analysis, <sup>3</sup>Universities Space Research Association, <sup>4</sup>NASA/ Johnson Space Center

The accuracy (sensitivity and specificity) of many balance tests is unknown. We compared normals to vestibularly impaired patients on some common tests and studied post-flight astronauts. Subjects were adults: 40 normals, 40 patients with vestibular disorders, and 15 post-long duration astronauts. **Patients** were flight computerized dynamic posturography (CDP: Neurocom Equitest), the Berg Balance Scale, the Timed Up and Go test, and the Dynamic Gait Index – and the new Functional Mobility Test (FMT) that we developed: rapidly walking through an obstacle course on compliant foam. Dependent measures are time to complete the course and number of obstacles touched. Astronauts were given CDP and SOT. Scores were examined first using the cut-offs for normal scores described in the literature, and then with Receiver Operating Characteristic (ROC) curves. Using the previously reported norms, no standard test classified more than 77% of subjects as patients or normals correctly. FMT time was most accurate, correctly classifying 95% of patients and 80% of crewmembers. CDP Condition 5 (eyes closed, sway referenced platform motion) correctly classified 80% of patients, and using higher cut-points than the norms classifed 86% of crewmembers. Other tests classified few patients, suggesting they are not accurate. Use of norms based on ROC curves sharpened accuracy. FMT may be even more useful when combined with other measures. With existing norms, no standard tests, including the "gold standard" of CDP, are really useful for determining which individuals have functionally significant balance disorders. Tests of gait often used in balance clinics were the least useful. Improved tests would benefit clinical care and the manned space program. Supported by National Institutes of Health grant DC04167 and the National Space Biomedical Research Institute through NASA NCC 9-58. The staff of the Center for Balance Disorders provided invaluable assistance.

## 189 Exploring Vestibular Responses to High Frequency Stimuli: New Insights into Vestibular Physiology

**Marianne Leveque**<sup>1</sup>, Laurent Seidermann<sup>1</sup>, Erik Ulmer<sup>2</sup>, André Chays<sup>1</sup>

<sup>1</sup>Department of Otolaryngology and ENT surgery, Robert Debre Hospital, Reims, France, <sup>2</sup>Otolaryngology outpatient clinic, Cannes, France

Like cochlea, the vestibular end organs respond to a wide variety of frequencies. Similarly to hearing impairment, a vestibular defect can affect partially the vestibular responses to acceleration and movement in a range of frequencies while preserving the others. Nevertheless, classical vestibular examination realized by videonystagmography (VNG) or electronystagmography (ENG) only explores vestibular responses to kinetic or

caloric stimulations, which represent very low frequencies of 0.5 Hz and 0.0001 Hz respectively. We present here three "high frequencies tests" included in our VNG protocol, which are easy to realize and provide helpful supplemental information on vestibular function.

The Head Shaking Test (HST) represents a stimulation of the lateral semi-circular canal in a 2 Hz frequency. The response is also linked to the central integrator's function. Its realization is manual during VNG.

The Head Impulse Test (HIT) described by Halmagyi and Curthoys provides a 5 Hz stimulus. It can be realized in any of the three planes of each canal in both ears and the head impulse's direction allows differentiating each of the six canals. We have developed a new method based on the video recording of the patient's head connected to a computer for automatical image analysis, which provides an easy and precise way to realize and analyze HIT during VNG.

The Vibration-Induced Nystagmus (VIN) gives data on vestibular responses to frequencies ranging from 30 to 100 Hz. The nystagmus induced reveals a unilateral high frequency vestibular dysfunction. So far, it is unclear whether it is due to the otolithic organs or to the semi-circular canals.

The supplemental data provided by those tests are essential in clinical practice to investigate vestibular pathologies such as vestibular neuronitis and Meniere's disease. Moreover they also give the opportunity to further explore the physiology of the vestibular system.

### 190 The Relationship of the V27I/E114G Genotype to GJB2-Related Hearing Loss

Valentina Pilipenko<sup>1</sup>, Lynne Lim<sup>2,3</sup>, Muhammed Ali<sup>4</sup>, Qing Chang<sup>5</sup>, John Bradshaw<sup>6</sup>, Lee Kenneth<sup>1</sup>, Xi Lin<sup>5</sup>, **John Greinwald**<sup>1,6</sup>

<sup>1</sup>Center for Hearing and Deafness Research Cincinnati, <sup>2</sup>Department of Otolaryngology Head and Neck Surgery, National University Singapore, <sup>3</sup>National University Hospital, Singapore, <sup>4</sup>Dhaka Health Care, <sup>5</sup>Departments of Otolaryngology and Cell Biology, Emory, <sup>6</sup>Department of Otolaryngology, University of Cincinnati

Mutations in the GJB2 gene are a major cause of congenital non-syndromic sensorineural hearing loss (SNHL). The V27I and E114G alleles in GJB2 are reported to be sequence variants that are not associated with hearing loss. However, the combined genotype has been implicated as a cause of hearing loss. We previously reported a higher prevalence of the V27I and E114G genotypes among subjects with SNHL compared to hearing controls in a pilot study in a Bangladeshi population. We hypothesize that V27I and E114G, acting in cis and trans, may result in SNHL.

After appropriate institutional review board approvals, a total of 80 unrelated subjects with idiopathic SNHL (39 from Singapore/41from Bangladesh) and 91 subjects with no SNHL (49 from Singapore/42 from Bangladesh) were enrolled. Most subjects from Singapore were of Chinese ancestry (85.0%). The prevalence of known biallelic hearing loss related GJB2 mutations among the Singaporean and Bangladeshi subjects with SNHL was 17.9% and 2.4%, respectively. There was a high

prevalence of V27I and E114G alleles among the SNHL groups (15.0% and 8.8%, respectively) compared to the hearing controls (8.0% and 3.0%, respectively). A total of 9 (11.3%) SNHL subjects from both groups were identified with the V27I/E114G genotype. Eight subjects had severe-profound SNHL, while 1 other subject had a borderline-mild mixed loss. Genetic analysis confirmed the V27I and E114G alleles acting in cis and possibly trans, contribute to hearing loss.

In-vitro testing of the functional significance of the V27I/E114G genotype was performed using dye transfer and intercellular Ca2+ signaling transfer experiments in a HEK293 cell culture model. Dye transfer and calcium conductance was nil in the homozygous V27I/E114G injected cells, while compound heterozygote, E114G homozygote and E114G heterozygote showed impaired intercellular biochemical coupling. Our data suggest that certain combinations of V27I and E114G mutants contribute to GJB2 related deafness by selectively affecting GJ-mediated biochemical coupling.

#### 191 Functional Analyses of a Deafness-Linked Connexin26 Mutation G45E

**Grace Leu**<sup>1</sup>, Qing Chang<sup>1</sup>, Shoab Ahmad<sup>1</sup>, Xi Lin<sup>1</sup> \*\* Emory University School of Medicine

Mutations in gap junction (GJ) proteins, connexin (Cx) 26 and Cx 30, account for a significant portion of patients with severe sensorineural hearing loss. One Cx26 point mutation, G45E (glycine mutated to glutamate at positon45), is linked to both non-syndromic and syndromic (the Keratitis-ichthyosis-deafness (KID) syndrome) types The mechanism of this Cx26 mutation of deafness. leading to hearing impairment remains unclear. In our previous study, we have found that Cx26G45E mutation causes a gain-of-function defect resulting in leaky GJ hemichannels. Since glycine at this position is conserved in many Cxs (e.g., Cxs30, 32, and 43), we tested the hypothesis that glycine at position 45 is a conserved Ca<sup>++</sup> sensor for the gating of GJ hemichannels.

Using an in vitro expression system, wild type and G45E mutant of Cxs 30, 32, and 43 were transfected in HEK 293 cells. We found that mutational effects of Cx30G45E were similar to that found for Cx26G45E. Cell death resulted within 24hours of transfection, which was rescued by increasing extracellular Ca<sup>++</sup> concentration ([Ca<sup>++</sup>]<sub>o</sub>). Dye loading assay showed Cx30G45E had leaky hemichannels at physiologic [Ca<sup>++</sup>]<sub>o</sub> (1.2mM). Higher [Ca<sup>++</sup>]<sub>o</sub> reduced the dve loading in a dose-dependent manner. These data suggest leaky hemichannels are responsible for cell death caused by Cx30G45E transfections. Our data obtained so far suggested that the glycine at position 45 is a conserved Ca<sup>++</sup> sensor for the gating of GJ hemichannels consisted of Cx26 or Cx30, which are the two most important Cxs for cochlear functions. Further testing of GJ hemichannels consisted of Cx32 and Cx43 is underway to find out whether the function of glycine at position 45 of Cx26 is universally preserved for other Cxs.

## 192 Paucity of Mutations in *GJB2* and *GJB6* in African American and Caribbean Hispanic Populations

**Joy Samanich<sup>1,2</sup>**, Robert Burk<sup>2</sup>, Christina Lowes<sup>2</sup>, Sara Shanske<sup>3</sup>, Alan Shanske<sup>1</sup>, Bernice Morrow<sup>2</sup>

<sup>1</sup>Children's Hospital at Montefiore, <sup>2</sup>Albert Einstein College of Medicine, <sup>3</sup>Columbia University

Approximately 1/1,000 children are born with hearing impairment, half due to genetic and half to environmental causes. Autosomal recessive non-syndromic sensorineural hearing impairment (ARNSHI) comprises 80% of familial cases. Approximately half of familial cases result from coding mutations in the Connexin 26 gene, GJB2, in Caucasian populations. Heterozygous mutations in the single coding exon of GJB2 occasionally co-occur with a deletion in the Connexin 30 gene, GJB6. Few studies have focused on the mutation frequency of these in African American (AA) and Caribbean Hispanic (CH) admixture populations. In this study, we performed bidirectional sequencing of the GJB2 gene and PCR screening for the common GJB6 deletion in 109 predominantly simplex individuals of mostly minority ethnic backgrounds. The hearing impairment ranged from unilateral mild to bilateral profound. None of the AA patients and only one CH patient had a bi-allelic mutation in GJB2. Variations found were T101C (M34T; 1/109), G109A (V37I; 1/109), 35delG (mutation; 6/109, 2/6 CH), 167delT (mutation; 1/109), G139T (mutation; E47V; 1/109 homozygous, CH), C-15T (1/109, AA), G79A (V27I; 10/109, 3/10 CH, 1/10 AA, 1/10 CH/AA), G380A (R127H; 4/109), A670C (Indeterminate; K224Q; 1/109 CH), A503G (novel; K168R; 3/109, 2/3 CH) and C684A (novel; 1/109 CH). None had a GJB6 deletion. Bi-directional sequencing of GJB2 was performed in 187 AA and Hispanic healthy individuals. Our results reveal that GJB2 mutations and GJB6 deletions may not be a significant cause of HI in these minority admixture populations.

#### 193 Functional Classification of Deafness-Linked Connexin26 Mutants

**Qing Chang**<sup>1</sup>, Wenxue Tang<sup>1</sup>, Shoeb Ahmad<sup>1</sup>, Xi Lin<sup>1</sup> Dept of Otolaryngology, Emory University School of Medicine

Mutations in GJB2, which encodes the gap junction (GJ) protein subunit connexin 26 (Cx26), are the major cause of non-syndromic hereditary hearing impairment. To date, more than 100 missense, nonsense, frame-shift, insertion and deletion mutations in the coding sequence of Cx26 have been linked to genetic sensorineural deafness. However, molecular mechanisms underlying Cx26-linked deafness remain unclear.

We generated 40 different Cx26 point mutations associated with human genetic sensorineural deafness, and studied the effect of these mutations on the function of GJs reconstituted in HEK293 cells. We tagged Cx26 and Cx30 with either eGFP or red fluorescent protein (Cxcherry). Therefore, functional tests can be performed from visually identified homomeric or heteromeric GJs consisting of Cx26 and/or Cx30 by the color of GJ plaque fluorescence. Our data suggested that Cx26 mutants

could be functionally classified into at least three major categories: (1) Mutations that affect the membrane trafficking of Cx. No typical GJ plagues could be observed between cell pairs, while co-transfected WTCx30-cherry still forms functional GJs. The mutant Cx26-eGFP showed either even or scattered green fluorescence in the One Cx26 mutation (W77R) apparently cytoplasm. caused a large protein structural change so much that the fluorescence of tagged eGFP protein was affected; (2) Cx26 mutations belonging to the second category were still targeted to the cell membrane for the formation of GJ plaques. They were able to form heteromeric GJs with WTCx30 as well. Depending on their effects on ionic coupling, biochemical coupling, and transdominant effects on WTCx30, these mutations can be further divided into four subgroups; (3) We also identified a novel type of gain-of-function mutation (e.g., G45E), which shifted the Ca<sup>++</sup>-dependent gating of GJ hemichannels such that they are leaky under normal physiological conditions.

These functional classifications should create a better understanding of the molecular mechanisms on Cx26 mutation-associated deafness, which is a necessary first step towards restoration of hearing in patients affected by Cx26 mutations.

#### 194 Evidence for a Mitochondrially Inherited Factor in Human Presbycusis

**Dina Newman**<sup>1</sup>, Sesquile Ramon<sup>1</sup>, Andrea Braganza<sup>1</sup>, Rhea Sanchez<sup>1</sup>, Susan Frisina<sup>2,3</sup>, Frances Mapes<sup>2</sup>, Robert Parody<sup>1</sup>, D. Robert Frisina<sup>2</sup>, David Eddins<sup>2,3</sup>, Michael Osier<sup>1</sup>, Robert Frisina<sup>2,3</sup>

<sup>1</sup>Rochester Institute of Technology, <sup>2</sup>International Center for Speech & Hearing Research, <sup>3</sup>University of Rochester School of Medicine

Presbycusis is a sensorineural hearing loss commonly observed in the elderly. Affected individuals experience a progressive loss of hearing acuity, starting with the highest frequencies. Previous research has shown a strong genetic component to presbycusis susceptibility, with significant mother-child and sibling-sibling (but not fatherchild) correlations. This pattern is consistent with one or more factors on the mitochondrial (mt) genome influencing susceptiblity to presbycusis. Mt haplogroups represent clusters of individuals who share a common maternal ancestor. Approximately 200 human subjects (all >58 years old) were classified into nine common European mt haplogroups (and "other") based on 10 single nucleotide polymorphisms (SNPs). Using pure tone thresholds (PT) ranging from 250 to 14,000 Hz, each haplogroup was tested for differences in hearing ability compared to the other haplogroups. One haplogroup, K, was found to have significantly better hearing than the others. For example, in haplogroup K, PTA1 (ave. PT of 0.25, 0.5 and 1 kHz) of the left ear showed a mean 7.0 dB decrease (p=0.006), while PTA2 (ave. PT of 1, 2 and 4 kHz) of the left ear had a mean 8.4 dB decrease (p=0.02). This difference in hearing ability was gender specific: male left ear showed a mean 11.0 dB decrease (p=0.001) and PTA2 had a mean 15.8 dB decrease (p=0.001); there were no significant differences in females. These data support a sexinfluenced protective allele carried on the mt genome of haplogroup K individuals. Currently we are doubling the sample size in order to improve statistical power and implementing additional statistical methods. Future work will focus on pinpointing the specific genetic difference(s) on haplogroup K chromosomes that influence(s) susceptibility to presbycusis.

## 195 Nonsyndromic Maternally Inherited Hearing Loss Associated with the Mitochondrial Mutation T7510C

**Valentina Labay**<sup>1</sup>, Anne Madeo<sup>1</sup>, Thomas Friedman<sup>1</sup>, Penelope Friedman<sup>2</sup>, Andrew Griffith<sup>1</sup>

<sup>1</sup>National Institute on Deafness and other Communication Disorders, National Institutes of Health, <sup>2</sup>Clinical Center, National Institutes of Health

Sensorineural hearing loss (SNHL) can be inherited as a trait linked to any of the nuclear chromosomes, or the mitochondrial genome. In the latter case, the pattern of inheritance is termed maternal since the mitochondrial DNA (mtDNA) is exclusively inherited from the mother. SNHL is the most common phenotype associated with mtDNA mutations, either as an isolated trait or accompanied by one or more other clinical abnormalities. We ascertained a large North American Caucasian family segregating bilateral SNHL in a pattern consistent with maternal inheritance and complete penetrance. The hearing loss begins during the 1st decade of life and progresses to variable levels of severity. There was no history of aminoglycoside exposure or evidence of associated clinical abnormalities. We sequenced the entire mtDNA in three affected and two unaffected family members. All of the affected, and some unaffected, family members belong to haplogroup H. We identified a previously reported T to C transition at position 7510 in the tRNASer(UCN) gene that co-segregates with SNHL among all family members. The SNHL phenotype in the two previously published families segregating T7510C is also nonsyndromic. T7510C was not detected in control DNA samples in the previous studies, but the associated haplogroups were unknown and it remains possible that T7510C is a haplogroup H-specific polymorphism. We plan to analyze haplogroup H control samples to rule out this possibility. Nevertheless, the pathogenicity of T7510C is supported by a recent study showing that it significantly reduces pre-tRNASer(UCN) processing efficiency. Finally, the SNHL phenotype in our study family is notable for its high penetrance. This could be the result of mitochondrial or nuclear genetic background, environmental factors, or the degree of T7510C heteroplasmy. We are using a Hinfl restriction site created by T7510C as the basis of an assay to determine the presence and degree of heteroplasmy in affected subjects.

196 Absence of Vestibular Symptoms in Two Chinese Families with Novel Mutations in the vWFA2 Domain of COCH: Evidence of Genotype-Phenotype Correlation in DFNA9 Huijun Yuan<sup>1</sup>, Qing Sun<sup>1</sup>, Hanjun Sun<sup>1</sup>, Ran Tao<sup>2</sup>, Wei

**Huijun Yuan**', Qing Sun', Hanjun Sun', Ran Tao<sup>2</sup>, Wei Qin<sup>2</sup>, Denise Yan<sup>3</sup>, Shuzhi Yang<sup>1</sup>, Juyang Cao<sup>1</sup>, Guoyin Feng<sup>2</sup>, Weiyan Yang<sup>1</sup>, Xuezhong Liu<sup>3</sup>, Dongyi Han<sup>1</sup>, Lin He<sup>2</sup>

<sup>1</sup>General Hospital of Chinese PLA, Beijing, <sup>2</sup>Bio-X Life Science Research Center, Shanghai, <sup>3</sup>University of Miami, Miami

Hereditary hearing loss is a heterogeneous condition at both the genetic and clinical levels. Mutations within the LCCL domain of the COCH gene (encoding the cochlin protein) lead to auditory and vestibular impairment in the DFNA9 disorder. In this study, we have recruited a large Chinese family with late onset autosomal dominant nonsyndromic progressive sensorineural hearing loss. Linkage analysis was carried out and a maximum two-point LOD score of 6.69 at theta=0 was obtained for marker D14S1040. Haplotype analysis placed the locus within a 7.6 cM genetic interval defined by marker D14S1021 and D14S70, overlapping with the DFNA9 locus on chromosome 14q12-q13. DNA sequencing of coding exons and exon/intron boundaries of the COCH gene identified a 1625 G>A mutation in exon 12 that cosegregates with auditory dysfunction in the family. The mutation results in a predicted C542Y substitution at an evolutionarily conserved cysteine residue in the vWFA2 domain of cochlin. In addition, we screened the COCH gene for mutation in 26 DFNA Chinese families, 19 small families (the inheritance pattern could not be recognized) and 22 sporadic patients with late onset progressive sensorineural hearing loss. A heterozygous 1535 T>C mutation leading to M512T substitutions was also identified in the vWFA2 domain in a small family. The predominant feature of these Chinese families is that all the affected subjects harboring COCH mutations in the vWFA2 domain do not suffer the vestibular symptoms during their life time and comprehensive vestibular assessment reveals only subtle vestibular hypofunction. Our findings provide the evidence of genotype-phenotype correlation in DFNA9.

The work is supported by NIH DC005575 and NSFC30528025 (China)

### 197 SLC26A4 Gene and Unilateral Hearing Impairement

**Sandrine Marlin**<sup>1,2</sup>, Laurence Jonnard<sup>3</sup>, Delphine Feldmann<sup>2,3</sup>, Sébastien Albert, <sup>4</sup>, Natalie Loundon<sup>5</sup>, Christine Petit<sup>2,6</sup>, Eréa-Noël Garabédian<sup>2,5</sup>, Rémy Couderc<sup>3</sup>, Françoise Denoyelle<sup>2,5</sup>

<sup>1</sup>Service de Génétique, Hőpital d'Enfants Armand-Trousseau, <sup>2</sup>INSERM U587, <sup>3</sup>Service de Biochimie et de Biologie Moléculaire, <sup>4</sup>Service d'ORL et de Chirurgie Cervico-faciale, <sup>5</sup>Service d'ORL et de Chirurgie Cervico-Faciale, <sup>6</sup>Unité de Génétique des déficits Sensoriels Mutations of the SLC26A4 (PDS) gene are involved either in syndromic deafness characterized by congenital sensorineural hearing loss and goitre (Pendred's syndrome), or in congenital isolated deafness (DFNB4). Both, Pendred's syndrome and DFNB4 are autosomal recessive disorders. In a first report, we presented the clinical and genotypic findings of 30 French families, in whom the diagnosis of Pendred's syndrome had been made. In 80% of these families, two SLC26A4 mutations were observed confirming the cause of the disease. In a second report, 112 patients with non syndromic deafness and inner ear malformations (including enlarged vestibular aqueducts), were genotyped for SLC26A4. In this cohort, biallelic mutations were observed in 24% of the patients. In these two cohorts (Pendred and DFNB4) biallelic SLC26A4 mutations were observed in patients with a unilateral enlarged vestibular aqueduct and bilateral hearing impairment. So, we decided to screen SLC26A4 by DHPLC and sequencing in 33 patients presenting with unilateral hearing impairment associated with unilateral enlarged vestibular aqueduct. In none of these patients, biallelic *SLC26A4* mutations were identified. heterozygous SLC26A4 mutation was observed in 4 patients. This study indicates that SLC26A4 is not involved in the unilateral hearing impairment of these patients and is probably not a cause of unilateral hearing impairment.

## 198 Sensorineural Deafness and Male Infertility – A Contiguous Gene Deletion Syndrome

**Yuzhou Zhang**<sup>1</sup>, Mahdi Malekpour<sup>2</sup>, Hossein Najmabadi<sup>2,3</sup>, Richard Smith<sup>1</sup>

<sup>1</sup>Molecular Otolaryngology Research Laboratories, Department of Otolaryngology, University of Iowa, <sup>2</sup>Genetics Research Center, University of Social Welfare and Rehabilitation Sciences, <sup>3</sup>Kariminajan- Najmabadi Pathology and Genetics Center

Syndromic hearing loss that results from contiguous gene deletions is uncommon. Here, we describe three families with a novel syndrome characterized by deafness and infertility. Deafness-Infertility Syndrome (DIS) is caused by large contiguous gene deletions at 15q15.3. These three families do not share a common ancestor and do not share identical deletions. The deleted region is about 100 kb and involves four genes -KIAA0377, CKMT1B, STRC and CATSPER2 - each of which has a telomeric duplicate. This genomic architecture underlies the mechanism by which these deletions occur. CATSPER2 and STRC are expressed in the sperm and inner ear respectively. consistent with the phenotype is persons homozygous for this deletion. A deletion of this region has been reported in one other family segregating male infertility and although deafness sensorineural congenital dyserythropoietic anemia type I (CDAI) was also present presumably due to a second deletion in another genomic region.

# 199 A Novel WFS1 Mutation in a Family with Dominant Low Frequency Sensorineural Hearing Loss Predicts an R685P Amino Acid Change in Wolframin

**Naomi Bramhall<sup>1</sup>**, Jeremy Kallman<sup>2</sup>, Aimee Verrall<sup>2</sup>, Valerie Street<sup>2</sup>

<sup>1</sup>Speech and Hearing Sciences, University of Washington, <sup>2</sup>V.M. Bloedel Hearing Research Center, University of Washington

Low frequency sensorineural hearing loss (LFSHL) is an uncommon clinical finding. Mutations within three different genes (DIAPH1, MYO7A, and WFS1) are known to cause LFSHL. In this report we describe a small American family with dominantly inherited LFSHL that demonstrate linkage to the WFS1 DFNA6/14/38 locus. Sequence analysis of the WFS1 gene reveals a novel heterozygous mutation at c.2054G>C predicting a p.R685P amino acid substitution The c.2054G>C mutation segregates in wolframin. faithfully with hearing loss in the family and is absent in 146 control chromosomes. The p.R685 residue is located with the hydrophilic C-terminus of wolframin and is conserved across species. Functional studies are underway to determine if the mutant WFS1 c.2054C allele is expressed.

#### 200 Mutations of the RDX Gene Cause Nonsyndromic Hearing Loss at the DFNB24 Locus

**Zubair Ahmed**<sup>1</sup>, Shahid Khan<sup>2</sup>, Muhammad Shabbir<sup>2</sup>, Shin Ichiro Kitajiri<sup>1</sup>, Saeeda Kalsoom<sup>2</sup>, Saba Tasneem<sup>2</sup>, Arabandi Ramesh<sup>3,4</sup>, Srikumari Srisailpathy<sup>3,4</sup>, Shaheen Khan<sup>2</sup>, Richard Smith<sup>3</sup>, Saima Riazuddin<sup>1</sup>, Thomas Friedman<sup>1</sup>, Sheikh Riazuddin<sup>2</sup>

<sup>1</sup>National Institute of Deafness and Other Communication Disorders, <sup>2</sup>CEMB, Lahore, Pakistan, <sup>3</sup>Molecular Otolaryngology Research, University of Iowa, <sup>4</sup>Department of Genetics, University of Madras, Madras, India Ezrin, radixin and moesin are paralogous proteins that make up the ERM family and function as cross-linkers between integral membrane proteins and actin filaments of the cytoskeleton. In the mouse a null allele of Rdx encoding radixin is associated with hearing loss as a result of the degeneration of inner ear hair cells as well as with hyperbilirubinemia due to hepatocyte dysfunction. We report that mutant alleles of RDX (p.D578N and p.A469fsX487) are associated with neurosensory hearing loss segregating in two consanguineous Pakistani families. Both of these mutant alleles are predicted to affect the actin-binding motif of the C-terminal actin-binding domain of radixin. Sequence analysis of RDX in the DNA samples from the original DFNB24 family revealed a c.463C>T transition substitution which is predicted to truncate the protein in the FERM domain (p.Q155X). We also report a more complete gene and protein structure of RDX including four additional exons and five new isoforms of RDX that are expressed in human retina and inner ear. Further, high-resolution confocal microscopy in mouse inner ear demonstrates that radixin is expressed along the

length of stereocilia of hair cells from both the organ of Corti and the vestibular system.

#### 201 A Novel Locus for Autosomal Dominant Non-Syndromic Hearing Loss, Maps to Chromosome 2g21.3-Q24.1

**Xiao Mei Ouyang**<sup>1</sup>, Denise Yan<sup>1</sup>, Li Lin Du<sup>1</sup>, Zheng Yi Chen<sup>2</sup>, Xue Zhong Liu<sup>1</sup>

<sup>1</sup>University of Miami, <sup>2</sup>Harvard Medical School and Neurology Service

Hereditary non-syndromic sensorineural hearing loss (NSSHL) is a genetically highly heterogeneous group of disorders. Autosomal dominant form accounts for up to 20% of cases. To date, 54 autosomal dominant deafness (DFNA) loci have been mapped, and 21 genes have been isolated. In this report, we ascertained a four-generation family of Poland-Jewish origin segregating DFNA postlingual deafness. Of the 17 family members in whom DNA was available for genome wide screening and fine mapping, 8 present a bilateral NSHL. The age of onset of HL ranged from 15 years to 30 years. Linkage analysis in this family mapped this novel NSHL locus to a 17 cM region on chromosome 2 between flanking markers D2S442 and D2S1353, with a maximum multi-point lod score of 2.4 at D2S2275. This locus is proximal to the DFNA16 and DFNB27 loci but does not overlap with their genetic intervals. DNA sequencing of coding regions and exon/intron boundaries of 4 cochlear expressed genes (NMI, RND3, TNFAIP6, R1F1), located within the candidate region did not reveal a disease-causing mutation. Four other potential candidate genes (ACVR2A, MBD5, STAM2, GALNT13) are being screened for deafness-causing mutation.

The work is supported by NIH DC 05575

## **202** Effects of Systemic Steroids on Cochlear Morphology After Cochlear Implantation

**Alan Micco**<sup>1</sup>, Anne Hseu<sup>1</sup>, Claus-Peter Richter<sup>1</sup> *Northwestern University* 

Previously, we have shown that systemic steroids have little effect on auditory brainstem responses recorded two weeks after implantation. Thresholds in both experimental groups were similar. However, closer inspection of the spiral ganglion cell morphology revealed differences between the treatment groups. Cochlear morphology seemed to be better preserved with the administration of steroids.

In this experiment we further evaluated the effect of systemic steroids on cochlear morphology after cochlear implantation. Gerbils were implanted with a custom-made implant dummy electrode with and without the administration of systemic steroids. The animals were sacrificed four weeks after implantation to allow enough time for degeneration to occur. Cochlear function was tested using auditory brainstem responses.

After cochlear function was tested and the animals were sacrificed, the cochleae were harvested, fixed dehydrated and plastic embedded. The cochleae were cut using an ultramicrotom at 5  $\mu$ m slices, mounted on glass slides and

stained with toluidine blue. Cochlear morphology, including spiral ganglion survival was compared between the two experimental groups. Systemic steroids appeared to protect cochlear morphology.

Supported by the Silverstein Grant in Neurotology

# 203 Neurotrophic Effects of GM1 Ganglioside and Electrical Stimulation Delivered by a Cochlear Implant on the Cochlear Spiral Ganglion Neurons in Cats Deafened as Neonates

**Patricia Leake**<sup>1</sup>, Gary Hradek<sup>1</sup>, Maike Vollmer<sup>1,2</sup>, Stephen Rebscher<sup>1</sup>

<sup>1</sup>Department of Otolaryngology - Head and Neck Surgery, University of California San Francisco, <sup>2</sup>Department of Otolaryngology, University of Würzburg, Germany

Several previous studies have shown that electrical stimulation delivered by a cochlear implant promotes increased survival of spiral ganglion (SG) neurons in cats deafened as neonates by daily injections of the ototoxic drug neomycin sulfate (Leake et al, 1999, J Comp Neurol 412:543). However, electrical stimulation only partially prevents the progressive SG degeneration following deafness in these animals. Thus, neurotrophic agents that might be used in conjunction with an implant are of interest. GM1 ganglioside is a glycosphingolipid that has been reported to be beneficial in treating stroke, spinal cord injuries and Alzheimer disease. GM1 activates TrkB signaling and potentiates neurotrophins, and exogenous administration of GM1 has been reported to reduce SG degeneration in deafened guinea pigs (Parkins et al, 1999, ARO abstr #660:167).

In the present study, neonatal kittens were deafened (using the same neomycin protocol as in prior studies) and received daily injections of GM1, beginning either at birth or after animals were deafened and continuing until 7-8 weeks of age. GM1-treated animals examined at this age showed a modest improvement in SG density as compared to non-GM1 deafened controls (74% vs 62% of normal). Additional GM1-treated and non-GM1 control groups received a cochlear implant at 7-8 weeks of age, followed by at least 6 months of unilateral electrical stimulation. Electrical stimulation elicited a significant trophic effect in both GM1 and non-GM1 groups as compared to the contralateral, non-stimulated ears. These long-term results also showed that a modest increase in SG density with GM1 treatment was maintained by and additive with the trophic effects of subsequent electrical stimulation (55% vs 46% of normal). However, in the GM1-treated deafened ears contralateral to the implant, SG soma size was severely reduced several months after withdrawal of GM1 in the absence of electrical activation.

Research supported by NIH-NIDCD Contract #N01-DC-3-1006.

## 204 Effects of Different Deafening Protocols and Electrical Stimulation on the Developing Cochlear Nucleus

**Olga Stakhovskaya**<sup>1</sup>, Patricia A. Leake<sup>1</sup>, Gary Hradek<sup>1</sup> Dept. of Otolaryngology-HNS, Univ. of California San Francisco, CA, USA

This study examined the development of the cochlear nucleus (CN) in cats that were deafened using three different protocols. One group of animals was deafened by unilateral cochlear nerve section performed at 2-3 days postnatal (P2-P3), several days prior to the onset of hearing. Two other groups of animals were deafened by daily neomycin injections starting either at P1 or P30. Animals from all groups were examined as juveniles at about 2 months of age. At this age after cochlear nerve section at P2-P3, the CN cross-sectional area (as measured in coronal sections just posterior to the cochlear nerve) was about 35-40% of the normal adult CN. At this same age in animals deafened by neomycin injections starting at P1, the CN was about 58% of the normal adult area. The brief period of normal auditory experience in animals deafened at P30 resulted in a significantly larger CN area (67% of normal adult) as compared to both the other groups (p<0.05) examined at 2 months of age.

To explore the potential role of electrical stimulation in reducing CN degeneration following deafness, additional animals in both the P1 and P30 neomycin-deafened groups received a cochlear implant and were studied after 5-7 months of unilateral electrical stimulation. In both groups, the CN on the non-implanted side exhibited marked growth over several months of further development and reached 75% of normal in P1-deafened animals and 88% in those deafened at P30. Thus, a significant difference was maintained into adulthood in the deafened CN of the 2 groups. Comparison between stimulated and unstimulated CN revealed no difference in overall CN size, but cross-sectional areas of the neurons in the AVCN were larger on the stimulated sides in both neomycin-treated groups. The data suggest that electrical stimulation did not alter the retarded growth of the CN in deaf animals, but could provide a significant trophic effect on the spherical cells of the AVCN.

Supported by NIDCD Contract N01-DC-3-1006 and R01 DC000160

## 205 Chronic Electrical Stimulation Rescues Spiral Ganglion Neurons Following Removal of Exogenous Neurotrophins

Robert Shepherd<sup>1,2</sup>, Anne Coco<sup>1</sup>, Stephanie Epp<sup>1</sup>
<sup>1</sup>Bionic Ear Institute, <sup>2</sup>University of Melbourne
Exogenous neurotrophins (NT) rescue spiral ganglion neurons (SGNs) from degeneration, however, to be effective they must be supplied continuously[1]. We reported a significant rescue advantage when NT administration is combined with chronic electrical stimulation (ES)[2]. Here, we examine whether chronic ES can maintain SGN survival long after cessation of NT delivery. Ten adult guinea pigs were profoundly deafened using ototoxic drugs. Five days later they were unilaterally implanted with a scala tympani electrode array

incorporating a drug delivery system. Brain derived neurotrophic factor (BDNF) was continuously delivered to the scala tympani over a 4 week period while the animal simultaneously received ES via a bipolar electrode array. One cohort (n=5) received ES for 6 weeks, including a 2 week period after the cessation of BDNF delivery (ES6); a second cohort (n=5) received ES for 10 weeks, including a 6 week period following cessation of BDNF delivery (ES10). The cochleae were then harvested for histology and SGN density determined for each cochlear turn for comparison with normal hearing controls (n=4). The withdrawal of BDNF resulted in a rapid loss of SGNs in turns 2-4 of the deafened/BDNF-treated cochleae; this was significant as early as 2 weeks following cessation of the NT when compared with normal controls (p<0.05). Importantly, while there was a small reduction in SGNs in turn 1 (i.e. adjacent to the electrode array) after NT removal, this reduction was not significant compared with normal controls. These results demonstrate that chronic ES can at least partially maintain SGNs after initial rescue using exogenous NTs. This finding has implications for the clinical application of NTs and supports earlier work demonstrating a rapid SGN loss after NT removal[1]. [1] Gillespie et al., 2003 J Neurosci Res 71, 785-790. [2] Shepherd et al., 2005 J. Comp. Neurol. 486, 145-158. Supported by the NIDCD (N01-DC-3-1005), RVEEH and the Bionic Ear Institute

## 206 An Evaluation of Intracochlear New Bone Following Cochlear Implantation in the Human

**Peter Li**<sup>1</sup>, Darren Whiten<sup>1</sup>, Mehmet Somdas<sup>2</sup>, Donald Eddington<sup>1,3</sup>, Joseph B. Nadol Jr.<sup>1</sup>

<sup>1</sup>Department of Otology and Laryngology, Harvard Medical School/Massachusetts Eye and Ear Infirmary, <sup>2</sup>Department of Otolaryngology, Erciyes Medical School, Kayseri, Turkey, <sup>3</sup>Research Laboratory of Electronics,

Massachusetts Institute of Technology

The aims of this study were to evaluate new bone formation in the inner ear following cochlear implantation, to identify factors responsible for inducing new bone formation and to understand the functional significance of new bone in the cochlea.

Thirteen temporal bones from patients who in life had undergone cochlear implantation were prepared for histologic study. The specimens were sectioned in the axial plane and digitally reconstructed in three-dimensions using Amira 4.0 reconstruction and modeling software.

The total volume and distribution of new bone in the cochlea was calculated in these thirteen cases. Factors that may influence the formation of new bone were assessed. The functional effect of new bone was measured by correlating the total amount of new bone with the last-recorded word recognition score.

New bone was found in all thirteen specimens, particularly at the cochleostomy site. In addition, new bone extended variable lengths along the electrode track and in some cases extended beyond the electrode's distal end. Damage to the lateral cochlear wall showed a significant correlation with the total amount of intracochlear new bone

 $(r^2=0.60, p=0.0019)$ . The amount of new bone did not correlate with word recognition scores.

These preliminary results suggest that the degree of damage to the lateral cochlear wall may play an important role in influencing the amount of new bone formation following cochlear implantation. These results also argue for the use of 'modiolar-hugging' electrode designs to minimize this kind of cochlear trauma. Although new bone may not be a determinant of performance as measured by word recognition scores, it may affect the current attempts in cochlear implant surgery to preserve residual hearing.

#### 207 Recognition of Lexical Tone Production by Children with an Artificial Neural Network Xiuwu Chen<sup>1</sup>, Ning Zhou<sup>2</sup>, Yongxin Li<sup>1</sup>, Xiaoyan Zhao<sup>1</sup>,

Demin Han<sup>1</sup>, Li Xu<sup>2</sup>

<sup>1</sup>Beijing Institute of Otorhinolaryngology, <sup>2</sup>Ohio University

Production of accurate pitch contours or tone patterns is important in tone languages such as Mandarin Chinese. Traditionally, tone production is evaluated subjectively using human listeners. The purpose of the present study is to investigate the efficacy of using an artificial neural network as an objective way of evaluating tone production in Mandarin-speaking children. Speech materials were recorded from 61 normal-hearing children with ages between 4 and 9 years old. The fundamental frequency (F0) of each monosyllabic word of the speech data was extracted with an autocorrelation method. The F0 data were the inputs to a feed-forward backpropagation artificial neural network. The number of inputs was experimentally varied from 1 to 12, whereas the number of neurons in the hidden layer was experimentally varied from 1 to 16 in the neural network. The output layer of the neural network consisted of 4 neurons representing the 4 tone patterns of Mandarin Chinese. The recognition performance of the neural network was further compared with that of native-Mandarin-speaking adult listeners. When the number of inputs and number of hidden neurons were  $\geq 3$ , the neural network was able to successfully classify the tone patterns of the 61 children speakers with an accuracy of about 85% correct. This high accuracy was comparable to the tone recognition performance of the native-Mandarin-speaking adults. Individual children speakers showed varied tone production accuracy as revealed in tone recognition by the adult listeners. The neural network also showed sensitivity to the individual differences in tone production. This study demonstrated that the artificial neural network with as few as 3 inputs and 3 hidden neurons can successfully classify tone patterns produced by multiple young children speakers. The neural network can be used as an effective and objective way of evaluating the tone production of children.

[Work supported by NIH/NIDCD grant R03-DC006161.]

#### 208 An Acoustical, Neural-Network and Perceptual Study of Tone Production in Mandarin-Chinese-Speaking Children Ning Zhou<sup>1</sup>, Li Xu<sup>1</sup>

<sup>1</sup>Ohio University

Tone production has great importance for communicating in tone languages such as Mandarin Chinese. Other than perceptual studies, there is a lack of objective means of evaluating the tone production of tone language speakers. In the present study, acoustical, neural-network and perceptual approaches were investigated and applied for evaluating the tone production of Mandarin Chinese speakers. Two subject groups were recruited from Beijing, China, which included 61 normal-hearing children and 14 prelingually-deafened children who had received cochlear implants. The acoustical analysis of tone production was based on the F0 contours of the four lexical tones in Mandarin Chinese. The first measure used in the acoustic analysis examined the statistic distributions of the onset and offset values of a F0 contour represented by tonal ellipses. The size and relative distances of the tonal ellipses that reflect the degree of differentiation among tones were quantitatively measured using three indices. The second measure used in the acoustic analysis was the time sequence correlation that quantifies the deviation of a tone contour from a normative one. The normative contours were derived from the tone production of the 61 normal-hearing Mandarin-Chinese speaking children. The tone contours of the 14 cochlear implant children were evaluated with the time sequence correlation analysis. A feed-forward back-propagation neural network was used for automatic tone recognition. The neural network was trained with the F0 data from the normal-hearing children and used to recognize the tones produced by the cochlear implant children. Tone perception studies were also carried out with 7 normal-hearing human listeners, who were required to identify tones produced by both normalhearing and cochlear implant children. The acoustical, neural-network and perceptual measures were highly correlated with each other in evaluating tone production of children. Tone production in Mandarin-speaking children with cochlear implants showed various degrees of impairment.

#### 209 Effects of Musical Training on the Sound Structure of Speech and Song

Elizabeth Stegemöller<sup>1</sup>, Erika Skoe<sup>2</sup>, Trent Nicol<sup>2</sup>, Catherine Warrier<sup>2</sup>, Nina Kraus<sup>2,3</sup>

Northwestern University, Department of Physical Therapy and Human Movement Sciences, <sup>2</sup>Northwestern University, Department of Communication Sciences,

<sup>3</sup>Northwestern University, Departments of Neurobiology and Physiology; Otolaryngology

Music remains one of the least understood human behaviors. Studying the similarities and differences between speech and song provides an opportunity to examine the role of music in human nature and its biological underpinnings. In this study, 40 subjects grouped as vocalists, instrumentalists, and non-musicians spoke and sang the lyrics to two familiar songs. The acoustic structures of speech and song were compared in

terms of harmonic structure and spectral noise and the effect of musical experience was assessed. Results showed a significant difference between the harmonic structure of speech and song, with song having more precise (simpler) harmonic intervals than speech. This difference was not affected by musical experience. However, higher levels of experience were associated with decreased spectral noise in both signals. Thus, musical training did not affect the harmonic structure of the voice. but did affect the level of spectral noise when both speaking and singing. These results imply the existence of a pervasive biological infrastructure shared by music and language processes, and a link between musical experience and vocal production. Implications for the neural processing of the harmonic structure and spectral noise in speech and song as it relates to preference and learning are discussed.

This work is supported by the National Institute of Health NIDCD R01-01510.

#### 210 Auditory Feedback Affects Vocal **Production in Autistic Children**

Nicole Russo<sup>1</sup>. Charles Larson<sup>1</sup>. Nina Kraus<sup>1</sup>

<sup>1</sup>Northwestern University

Hearing provides important sensory feedback for vocal control. Auditory feedback helps to stabilize voice fundamental frequency (F0), which is a major acoustic cue of prosody. Autistic individuals have problems with prosody perception and production, which is necessary for social and emotional communication. This study draws on studies that have shown that people change their own voice F0 in response to perturbations in pitch of voice feedback. Responses are automatic, as indicated by their latencies (< 200 ms). The present study investigated whether children with autism (AUT) show the same pattern of response to auditory feedback as typically developing (TD) children. Our hypothesis was that abnormalities in the auditory feedback loop would affect AUT responses to vocal feedback. We tested this hypothesis by measuring voice F0 responses to pitch-shifted (- 100 cents, 200 ms) voice feedback while children produced an /a/ vowel into a microphone attached to headphones. Averaged voice F0 responses were calculated from approximately 80 randomly timed pitch-shift stimuli delivered during the vocalizations.

As a group, AUT children produced abnormally heightened responses to pitch perturbations compared to TD children. Furthermore a subset of AUT responses was exaggerated even compared to other AUT responses. Data are being further analyzed with respect to the same children's brainstem responses to speech and behavioral measures of auditory perception. Results may offer some explanation for why AUT children often have difficulty regulating and perceiving pitch; quantifying this deficit may inform the development of training paradigms. Finally, there may be a relationship between hypersensitivity to sound, sensory auditory feedback and vocal control in autism.

[NIH R01 DC01510]

## 211 Musical Experience Shapes Human Brainstem Encoding of Linguistic Pitch Patterns

**Patrick C.M. Wong**<sup>1</sup>, Erika Skoe<sup>1</sup>, Nicole M. Russo<sup>1</sup>, Tasha Dees<sup>1</sup>, Nina Kraus<sup>1,2</sup>

<sup>1</sup>Northwestern University, Department of Communication Sciences, <sup>2</sup>Departments of Neurobiology & Physiology; Otolaryngology

Both music and speech involve the use of functionally and acoustically complex sound. Given that they are cognitively demanding auditory phenomena, music and speech processing are generally attributed to cortical rather than subcortical circuitry, and to cognitive rather than sensory processes. However, less known is how long-term experience using complex sounds shapes subcortical circuitry, the context-specificity, and the reciprocity of this tuning. In the present study, we and nonmusicians' compared amateur musicians' encoding of linguistic pitch patterns at the auditory brainstem. Linguistic pitch patterns involve shifts in pitch over time, and in this study pitch contours were embedded in speech syllables to resemble lexically meaningful pitch patterns, such as those used in Mandarin Chinese. Two measures of neural encoding precision were calculated based on the F0 contours extracted from the frequency following response. First is the stimulus-to-response correlation (Pearson's r between the F0 contour of the stimulus and the subject's response contour), which indicates the faithfulness of pitch-tracking. Second is peak autocorrelation averaged over the entire response, which indicates robustness of neural phase-locking without making reference to the stimulus. We found musicians to show more faithful representation of the stimulus F0 contours and more robust neural phase-locking. These results implicate a common subcortical precursor of two presumed cortical functions, by suggesting that either speech- or music-related experience can tune sensory encoding in the auditory brainstem via the efferent pathway. These results also provide a neurophysiologic explanation for musician's higher-language learning ability, and are directly relevant to policies concerning the funding of music and foreign language education programs.

This work is supported by Northwestern University and the National Institutes of Health grants R03HD051827 and R21DC007468 to P.W. and R01DC001510 to N.K.

# **212** Training Effects on Spectral Shape Discrimination for Speech-Like and Non-Speech Stimuli in Older Hearing-Impaired Listeners

Mini Shrivastav<sup>1</sup>

<sup>1</sup>University of Florida

A previous study (Shrivastav, Humes, and Kewley-Port, 2006)\* found that spectral shape discrimination abilities of older hearing-impaired listeners had a moderate and significant association with their speech-identification scores. In this study, a group of older hearing-impaired listeners and a comparison group of young normal-hearing listeners were tested on speech-identification tests

involving natural and synthesized tokens and a series of spectral shape discrimination tasks involving speech-like and non-speech stimuli. The speech-like stimuli were patterned after the tokens used for the speechidentification task, while the non-speech stimuli consisted of spectrally tilted broadband noise. It was found that young and older listeners performed differently on most of the identification and discrimination tasks. Further, discrimination thresholds for the speech-like and nonspeech stimuli were found to be significantly different, and thresholds for only the speech-like stimuli were found to contribute to speech-identification scores. The present study examined if some of these differences between speech-like and non-speech stimuli could be explained by a difference in the familiarity of the listeners with the two kinds of stimuli. A group of young and older listeners were provided with training to determine if these differences between the two sets of stimuli still persisted. The results of the study provide information on whether these differences can be attributed to familiarity or rather to other factors such as the structure of the two sets of stimuli.

\*Shrivastav, M.N., Humes, L.E., and Kewley-Port, D. (2006). Individual differences in auditory discrimination of spectral shape and speech-identification performance among elderly listeners. J. Acoust. Soc. Am. 119, 1131.

# 213 Perceptual Learning of Spectrally Reduced Speech and Environmental Signals: Effects of Materials and Training on Generalization

Jeremy Loebach<sup>1</sup>, David Pisoni<sup>1</sup>

<sup>1</sup>Indiana University - Bloomington

Adaptation to the acoustic world following cochlear implantation does not, typically, include formal training or extensive rehabilitation. Most hearing-impaired listeners with cochlear implants (CIs) simply rely on experience to teach them how to best use their devices. The question remains, however, whether CI users can benefit from formal training, and if so, what type of training is best? In this study we investigated five different types of training using a pre/post-test design to evaluate the effectiveness of training and generalization of perceptual learning in normal hearing subjects listening to CI simulations.

Five groups of subjects (25 each) were trained on PB words (IEEE, 1969), MRT words (House *et al*, 1965), meaningful sentences (IEEE, 1969), anomalous sentences (Herman & Pisoni, 2000) and environmental stimuli (Marcell *et al*, 2000) using an open-set identification task with orthographic and auditory feedback. CI simulations were made with an 8 channel sinewave vocoder using Tiger CIS software (<a href="http://www.tigerspeech.com">http://www.tigerspeech.com</a>). Each group received training with only one set of materials, but were then tested on all materials.

Pre to post test comparisons demonstrated that all groups showed significant improvement as a result of training. Training successfully generalized to some, but not all stimulus materials. Subjects typically experienced the most benefit for the stimulus set on which they were explicitly trained. Group effects were observed. Subjects who were

trained on words (PB or MRT) did significantly better on all words and subjects who were trained on sentences (anomalous or meaningful) did significantly better on all sentences. Training on speech did not generalize to environmental signals, although training on environmental signals did generalize to all speech materials. These data demonstrate that the type of training and the specific stimulus set that a subject experiences during perceptual learning has a substantial impact on generalization.

### 214 Perceptual Learning of Spectrally-Shifted and Noiseband-Vocoded Speech

**Frank Eisner**<sup>1</sup>, Carolyn McGettigan<sup>1</sup>, Stuart Rosen<sup>1</sup>, Andrew Faulkner<sup>1</sup>, Sophie K. Scott<sup>1</sup>

<sup>1</sup>University College London

We investigated normal-hearing listeners' ability to learn to understand a speech signal that simulates some aspects of the stimulation received from a cochlear implant. Participants were presented with syntactically simple, spoken sentences that were spectrally degraded by noiseband-vocoding. The sentences were also shifted upwards in frequency in order to simulate a shallow insertion of the electrode array in cochlear implantation, and the ensuing misalignment with cochlear tonotopicity. On each trial, listeners were asked to repeat back the sentence they heard, and then received written feedback with a simultaneous repetition of the auditory stimulus. Learning under this feedback condition was relatively fast: Participants in a relatively easy condition (8-band noise vocoding and 4.8 mm shift) reached a performance level of 80% correctly repeated keywords after 30 trials on average, while participants in a more difficult condition (6band noise vocoding and 6.4 mm shift) required approximately three times as much training to reach the same performance criterion. A control condition consisted of stimuli in which the order of bands was inverted in the spectral domain during noiseband-vocoding, and produced no significant learning effect in either group of participants. Future studies will investigate the effects of different types of feedback on the time course of learning.

## 215 Perceptual Adaptation to Spectrally Shifted Vowels: the Role of Shift Type

**Tianhao Li<sup>1</sup>**, Qian-Jie Fu<sup>2</sup>

<sup>1</sup>University of Southern California, <sup>2</sup>House Ear Institute
It has been documented that normal-hearing (NH) listeners
are able to adapt to spectrally shifted speech with only
repeated exposure, as long as the shift is moderate (i.e., <
5 mm along the basilar membrane). However, it remains
unclear whether the degree of adaptation to spectrally
shifted speech is affected by the way how the spectral shift
is performed. Different type of spectral shifts may
introduce different amounts of local or global spectral
mismatch. The present study investigated the effects of
local and/or global spectral shift on the perceptual
adaptation of spectrally shifted vowels. Three kinds of
spectral shifts were tested, including (1) slightly upward
shift with compression to simulate shallow insertion of 16mm-long, 8-electrode array; (2) spatially basal-ward shift

(4mm) on the basilar membrane; and (3) 1-octave upward shift on the frequency domain. One spectrally-matched condition was also examined to check the difference in adapting to spectrally-shifted and -degraded speech. Spectrally-shifted vowels were generated with 8-channel sine-wave vocoder. Five NH subjects were repeatedly tested over 5 consecutive days, with 3 runs for each experimental condition on each day; no training or feedback was provided (i.e., passive learning). Results showed that vowel recognition significantly improved for all three shift conditions over the 5-day study period; there was no change in performance for spectrally-matched speech. While there was some inter-subject variability within the experimental conditions, the mean improvement was comparable across the three shift conditions. These results suggest that the degree of adaptation mainly depends on the extent of spectral shift, rather than the type of spectral shift (local or global spectral shift).

Research is supported by NIH-NIDCD.

#### 216 NIDCD Workshop: Updates From the NIDCD/NIH

**Jim Battey**<sup>1</sup>, Craig Jordan<sup>1</sup>, Amy Donahue<sup>1</sup> \*\*INIDCD/NIH

This session will provide an opportunity for ARO membership to hear updates and learn about recent activities at the NIDCD/NIH. Jim Battey, Director, NIDCD, Craig Jordan and Amy Donahue will present updates on recent activities at the NIDCD/NIH. Topics include NIH and NIDCD budget, NIH Neuroscience Blueprint initiatives, new funding mechanisms [such as the new NIH Pathway to Independence (PI) Award (K99/R00)] as well as ongoing NIDCD and NIH initiatives and funding opportunities. Recent changes in NIH policy, review and grants management will also be highlighted, potentially including electronic submission, electronic review, and shortened review cycles for new investigators. This session will allow time for questions and answers.

### 217 NIDCD Research and Training Workshop for New Investigators

**Roger Miller**<sup>1</sup>, Chris Myers<sup>1</sup>, Daniel Sklare<sup>1</sup>, Melissa Stick<sup>1</sup>, Bracie Watson<sup>1</sup>, Shiguang Yang<sup>1</sup>

\*\*National Institutes of Health\*\*

There will be two concurrent one-hour workshops conducted by NIDCD staff to provide an overview of the NIH funding process for budding and new investigators. One workshop, led by Drs. Sklare and Stick, will provide an orientation to doctoral students, postdoctoral fellows and junior faculty members interested in the junior-level NIH fellowship (F-series) and career development (K-series) awards for basic scientists and clinician-scientists. New training initiatives and directions will be underscored, including the NIH programs providing repayment of educational loans. The NIDCD process for the review and award of F- and K-award applications will be covered in detail.

The second workshop will provide information typically needed to navigate the transition from a trainee into an

independent principal investigator with NIDCD funding. This workshop will start with an overview on how NIH including application timelines. works. submission of the application, peer review assignments, and Advisory Council activities. The roles of NIH program, review, and grants management staff will be described. Since attendees should be planning their transition to independence, issues affecting the decision to apply through the NIH R01 Grant. the Exploratory/Developmental Research Grant, or the R03 NIDCD Small Grant mechanisms will be discussed. NIDCD has a number of special programs to help those seeking an initial award as a principal investigator and encourages the research community to be aware of the special eligibility requirements.

Both sessions will include a discussion of frequently asked questions and mistakes commonly seen during the application process. Time will be provided for questions of general interest.

#### 218 Session Introduction to "Meniere's Disease - In Search of Answers"

**Connie Pilcher**<sup>1</sup>, Dennis Trune<sup>2</sup>, George Gates<sup>3</sup>, Alec Salt<sup>4</sup>, Steven Rauch<sup>5</sup>, Elizabeth Berry<sup>6</sup>

<sup>1</sup>International Meniere Federation, <sup>2</sup>Oregon Health & Science University, <sup>3</sup>Virginia Merrill Bloedel Hearing Research Center, <sup>4</sup>Washington University School of Medicine, <sup>5</sup>Massachusetts Eye & Ear Infirmary, <sup>6</sup>patient

About 50,000 new cases of Meniere's disease (MD) occur annually in the United States, yet there is very little consensus as to what causes the disease. There are undoubtedly several forms of MD or several degrees of reaction to the original insult or dysfunction that affect the subsequent clinical course. Consequently, there are a wide variety of opinions and unresolved clinical issues concerning diagnosis and treatment due to "soft information" from current research and epidemiological data.

This session will enable us to highlight the daily issues of living with MD, to share the latest epidemiologic and etiologic knowledge of this vastly misunderstood disorder, and to articulate the approaches needed that will guide future, essential research by both new and established investigators to better understand, diagnose and treat MD. Speakers will present and discuss with ARO membership:

- 1. The impact of living daily with Meniere's disease.
- 2. The epidemiology of Meniere's disease and the problems of diagnosis.
- 3. Endolymph physiology and dysfunction in Meniere's disease.
- 4. Impact of steroids on ion regulation in Meniere's disease.
- 5. WWMD: What would Meniere do?

## 219 The Impact of Living Daily with Meniere's Disease Elizabeth Berry<sup>1</sup>

<sup>1</sup>Patient

My first symptoms of Meniere's disease occurred while I was on a year's teacher exchange in Adelaide, South Australia. I felt light-headed all the time and I kept hoping it was some kind of weird Australian flu that would subside when I got home. However, I dreaded that it might be chronic and was consumed with worry all year.

Unfortunately dizziness is one of those vague symptoms that can be a part of several illnesses, so it took several doctors before I had a definite diagnosis of Meniere's disease after I returned home.

There are several psychological experiences that I share with anyone with a chronic illness shares. I found that one chooses one's attitude in a given set of circumstances. Looking back, there have been several things that have helped me live with a chronic disease.

In my job as psychotherapist, I have learned that there are many psychological experiences common to people struggling with chronic illnesses. I teach my clients that one chooses his or her attitude in a given set of circumstances. I also share with them some strategies I have used to help me manage my symptoms.

I would like to make some suggestions how I feel physicians can be more helpful in treating patients with a chronic illness. My hope is that as doctors and researchers, you will leave this evening with a better understanding of Meniere's disease from a patient's perspective. I also hope you will accept the challenge to become more involved in finding answers that will alleviate or eliminate its impact on those who suffer with it.

## 220 The Epidemiology of Meniere's Disease and the Problems of Diagnosis George Gates<sup>1</sup>

<sup>1</sup>University of Washington

MD is a common disorder of unknown etiology that causes episodic vertigo with hearing loss, tinnitus, and ear Stress is a commonly cited co-factor in the pathogenesis of MD. MD affects both genders equally and is most common in 40-55 year olds. Some women have symptoms in relation to their menstrual cycle; whether this is hormonal or a reflection of stress is unclear. The overall prevalence of MD is estimated from 17/100,000 population in the U.S. to 46/100,000 in Sweden. The clinical course is variable and unpredictable. About 70% of patients respond to conservative treatment, such as low salt diet, diuretics and symptom suppressants, however 30% get progressively worse and often require surgical therapy. Although the long-term treatment results are acceptable, selection of cases for medical and surgical therapy varies widely.

#### 221 Endolymph Physiology in Meniere's

#### Disease

Alec N. Salt1

<sup>1</sup>Washington University School of Medicine

Understanding the origins of Meniere's disease and developing treatments for the disease requires detailed knowledge of endolymph physiology. The widely accepted, but now discredited dogma that hydrops arises from a failure of the endolymphatic sac to resorb endolymph produced in the cochlea was based on a misinterpretation of results and is now opposed by a substantial body of data. Endolymph flow is not required to maintain endolymph composition. It is now accepted that endolymph composition in the cochlea is maintained predominantly by the local recycling of ions between perilymph and endolymph. Studies of animals with surgically-induced hvdrops show that endolymph composition is near-normal, with only subtle changes of potassium and calcium that progress with time. The endocochlear potential is reduced in the early stages of hydrops and there are cytological changes of fibrocytes in the spiral ligament, both of which suggest that local ion transport processes in the cochlea are disturbed. Both the origins and the results of the ion transport changes remain uncertain. There is also accumulating evidence for the contributions of many structures of the inner ear in endolymph volume regulation. Local volume regulation has been demonstrated to occur in the cochlea and there is good evidence that the endolymphatic sac is also involved in correcting abnormal endolymph volume states. What is lacking is an understanding of the precise roles played by specific processes under normal and volume-disturbed conditions and how the different processes are regulated to achieve a stable state. As a result, there are many factors that can potentially influence endolymph volume In the presence of multiple, competing mechanisms, disturbance of one process may not necessarily result in volume disturbance. Treatment of hydrops in Meniere's patients requires more knowledge of which processes are impaired and which are functional but possibly being regulated inappropriately.

This work supported by NIH/NIDCD grant DC01368.

## **222** Impact of Steroids on Ion Regulation in Meniere's Disease Dennis Trune<sup>1</sup>

<sup>1</sup>Oregon Health & Science University

Although it is generally accepted that Meniere's Disease results from endolymphatic hydrops, the underlying causes of this hydrops may vary. Thus, the effective management of Meniere's Disease is difficult. Glucocorticoids are often recommended to treat this disorder, but results are inconsistent and the steroid-responsive mechanisms are poorly understood. To better understand the potential treatment of this disease, a review will be provided of inner ear ion homeostasis, the natural hormones that control the transport of K<sup>+</sup> and Na<sup>+</sup>, and how therapeutic steroids can influence these processes. Although glucocorticoids are traditionally recommended because of their anti-inflammatory function, they also have a significant influence over cochlear ion homeostatic mechanisms that

may be just as relevant in their control of Meniere's symptoms. There is some clinical and experimental evidence that treatments directly addressing these ion transport dysfunctions may be just as effective.

#### 223 WWMD: What Would Meniere Do? Steven D. Rauch<sup>1,2</sup>

<sup>1</sup>Harvard Medical School, <sup>2</sup>Massachusettse Eye & Ear Infirmary

The hallmark of Meniere's disease is instability of inner ear function affecting both hearing and balance. instability arises from failure of one or more of the many homeostatic systems that regulate inner ear function and Thus Meniere's "disease" is actually a environment. syndrome, with shared presentation but varied cause. This model explains many aspects of clinical experience, including wide variations in severity, diagnostic confusion with other conditions, and mediocre response to current treatments. Consensus clinical diagnostic criteria have been widely accepted, but the actual presentation of MD is highly variable, especially early in the course of the disease before extensive and irreversible inner ear degeneration has occurred. Some patients have severe cochlear symptoms and limited vestibular symptoms, other patients have a vestibular-dominant symptom pattern, and many patients have fairly equal involvement of both hearing and balance. It is logical to believe that this variability arises from differences in underlying pathophysiology and, perhaps, etiology. Patients with shared pathophysiology will exhibit shared patterns of symptoms and test abnormalities. In the mid-19th century all manner of episodic neurological disorders or "fits" were lumped together under the rubric of "apoplectiform cerebral congestion" and attributed to excessive blood pooling in the brain. Prosper Meniere earned his place in medical history in 1861 when he identified a subset of these patients who shared a symptom pattern and a single site of pathology, the inner ear. In the intervening 145 years no one has improved upon his original description of the symptoms. Theories of causation, diagnostic and monitoring approaches, and treatments have not substantially changed in 50 years. However, the last 30 vears have seen dramatic improvements in physiology understanding of inner ear and pathophysiology, our ability to measure inner ear function, and our investigative tools in the clinic and the laboratory. The next great step forward in understanding and managing Meinere's disease will be a replication of Meniere's own achievement: The undifferentiated pool of MD patients must be classified on the basis of shared pathophysiology. Such an objective classification scheme would define subgroups that could be used as study cohorts for investigations of cause, diagnosis, monitoring, and treatment of Meniere's disease.

# 224 Reconstitution of Hair Cell Structures and Functions in Transfected CL4 Epithelial Cells: Targeting and Binding-Site Mapping of the Usher "Interactome" Proteins Cadherin 23 and Harmonin

Lili Zheng<sup>1</sup>, Jing Zheng<sup>2</sup>, Jaime Garcia-Anoveros<sup>1</sup>, **James Bartles**<sup>1</sup>

<sup>1</sup>Northwestern University Feinberg School of Medicine, <sup>2</sup>Northwestern University

We are using LLC-PK1-CL4 epithelial cells as an experimental system in which to reconstitute selected aspects of hair cell structure and function. These cells readily establish apical-basolateral plasma membrane polarity when cultured on glass coverslips and are easy to transfect with multiple expression vector constructs. Moreover, upon transfection with espin, the short brush border microvilli of CL4 cells elongate to yield structures reminiscent of stereocilia. Here, we have used this system to examine the targeting and binding interactions of two stereocilium proteins, cadherin 23 (cdh23), a type-l transmembrane protein that has been implicated in lateral or tip links between stereocilia, and harmonin, a PDZ domain-containing scaffold protein believed to bind the cytoplasmic tail of cdh23. Both proteins are targets of deafness mutations and components of the interacting protein network ("interactome") affected in human Usher syndrome. When expressed in CL4 cells by transient transfection, a FLAG-cdh 23 construct was efficiently targeted to the microvillar plasma membrane. In contrast, GFP-harmonin was present in the cytoplasm and nucleus, but not in microvilli. However, when GFP-harmonin was co-expressed with FLAG-cdh23, the GFP-harmonin efficiently colocalized with the FLAG-cdh23 in CL4 cell microvilli, suggestive of a direct binding interaction. The targeting of FLAG-cdh23 to microvilli and the binding of GFP-harmonin to cdh23 were unaffected by removal of the C-terminal PDZ-binding motif from cdh23. Mutagenesis of harmonin revealed that its PDZ1 domain was necessary and sufficient for binding cdh23, and further mutagenesis of the cdh23 cytoplasmic tail mapped the binding site for the harmonin PDZ1 domain to a peptide in the central region of the tail. These results suggest that co-transfected CL4 cells can be an advantageous system for examining binding interactions among stereociliary proteins in an epithelial cell context.

(Support: NIH DC004314 to JRB)

## **225** Protocadherin-15 is Associated with the Mechanotransduction Machinery of Inner-Ear Hair Cells

**Zubair Ahmed**<sup>1</sup>, Richard Goodyear<sup>2</sup>, Saima Riazuddin<sup>1</sup>, Ayala Lagziel<sup>1</sup>, P. Kevin Legan<sup>2</sup>, Andrew Griffith<sup>3</sup>, Gregory Frolenkov<sup>4</sup>, Inna Belyantseva<sup>1</sup>, Guy Richardson<sup>2</sup>, Thomas Friedman<sup>1</sup>

<sup>1</sup>National Institute of Deafness and Other Communication Disorders, <sup>2</sup>School of Life Sciences, University of Sussex, <sup>3</sup>Otolaryngology Branch, NIDCD, <sup>4</sup>Department of Physiology, University of Kentucky

Inner ear hair cells are the transducers of sound and acceleration. Stereocilia are actin filled protrusions present

on the hair cell's apical surface. Deflection of stereocilia in the direction of the tallest rank leads to opening of mechanotransduction channels, which are presumably imbedded in the stereocilia plasma membrane. The stereocilia, and a kinocilium if present, are interconnected by different filamentous link types. One of these links, the tip link, connects the top of a shorter stereocilium with the lateral membrane of an adjacent taller stereocilium and is thought to gate the hair cell's mechanotransduction channel. The molecular identity of the tip link was previously defined by a monoclonal antibody that recognized an epitope referred to as the tip-link antigen (TLA; Goodyear and Richardson, 2003). We identify the TLA as an avian orthologue of human protocadherin-15, product of the gene for the deafness/blindness Usher syndrome type 1F and nonsyndromic deafness DFNB23 (Ahmed, Goodyear et al. 2006 J Neurosci 26:7022-7034). Mass spectrometry peptide sequencing and western blot analyses revealed that the TLA is protocadherin-15, and thus this adhesion molecule is a constituent of the tip-link complex. There are four distinct isoform classes of Pcdh15 (CD1, CD2, CD3 and SI), three of which encode entirely unique cytoplasmic domains that have distinct spatiotemporal expression patterns within the developing and mature hair bundle. In inner-ear hair cells, protocadherin-15-CD1 is distributed along the side of each stereocilium but is excluded from a region at the very top, while protocadherin-15-CD3 is localized at the tops of the stereocilia where the tip link attaches. Protocadherin-15-CD3 is sensitive to calcium chelation and proteolysis with subtilisin, and reappears at the tips of stereocilia as transduction recovers following the removal of calcium chelators. The extent to which protocadherin-15-CD1 and protocadherin-15-CD3 contribute to the structure of tip-link complex now remains to be determined.

### **226** Auditory Mechanotransduction in the Absence of Functional Myosin-Xva

Ruben Stepanyan<sup>1</sup>, Inna A. Belyantseva<sup>2</sup>, Andrew J. Griffith<sup>3</sup>, Thomas B. Friedman<sup>2</sup>, **Gregory I. Frolenkov**<sup>1</sup> Department of Physiology, University of Kentucky, <sup>2</sup>Laboratory of Molecular Genetics, NIDCD/NIH, <sup>3</sup>Otolaryngology Branch, NIDCD/NIH

In hair cells of all vertebrates, a mechanosensory bundle is formed by stereocilia with precisely graded heights. Unconventional myosin-XVa is critical for formation of this bundle because it transports whirlin and perhaps other molecular components responsible for programmed elongation of stereocilia to the stereocilia tips. A tip of a stereocilium is the site of stereocilia growth and one of the proposed sites of mechano-electrical transduction. adult shaker 2 mice, a mutation that disables the motor function of myosin-XVa results in profound deafness and abnormally short stereocilia that lack stereocilia links, an indispensable component of mechanotransduction machinery. Therefore, it was assumed that myosin-XVa is required for proper formation of the mechanotransduction apparatus. Here we show that in young postnatal shaker 2 mice, abnormally short stereocilia bundles of auditory hair cells have numerous stereocilia links and "wild type"

mechano-electrical transduction. We compared the mechanotransduction current in auditory hair cells of young normal-hearing littermates, myosin-XVa deficient shaker-2 mice, and whirler mice that have similarly short stereocilia but intact myosin-XVa at the stereocilia tips. This comparison revealed that the absence of functional myosin-XVa does not disrupt adaptation of the mechanotransduction current during sustained bundle deflection. Thus, the hair cell mechanotransduction complex forms and functions independently from myosin-XVa-based hair bundle morphogenesis.

## 227 Mosaic Complementation of the Shaker1 Allele Suggests a Novel Role for Myosin VIIa in Hair Cell Stereocilia

**Agnieszka Rzadzinska**<sup>1</sup>, Haydn Prosser<sup>1</sup>, Allan Bradley<sup>1</sup>, Karen Steel<sup>1</sup>

<sup>1</sup>The Wellcome Trust Sanger Institute

A female X-inactivation mosaic strategy was used to study the cellular function of myosin VIIa in auditory sensory hair cells. Mutations in Myo7a cause progressive disorganization of the bundle of mechanosensory stereocilia on the apical surfaces of hair cells and lead to deafness and vestibular dysfunction in mice and humans. BAC clones containing the wild type Myo7a gene were integrated by recombination-mediated cassette exchange (RMCE) into the Hprt locus on the X-chromosome and female mice were generated with one copy of the engineered X chromosome plus one wild type Xchromosome on a background of homozygosity for the mutant Myo7a4626SB allele on chromosome 7. Random X-inactivation of the X-chromosome containing the wild type Myo7a gene led to a fine mosaic of affected and unaffected hair cells, as the X-linked wild type Myo7a gene was able to complement the mutant alleles on chromosome 7 only when the other X-chromosome was inactivated. The ability to compare two interspersed cell populations functionally different only in Myo7a expression revealed abnormal elongation of the mutant stereocilia, suggesting possible involvement of myosin VIIa in turnover of the stereocilia actin.

### 228 Hair Bundles are Specialized for ATP Delivery Via Creatine Kinase

**Jung-Bum Shin**<sup>1</sup>, Femke Streijger<sup>2</sup>, Andy Beynon<sup>3</sup>, Theo Peters<sup>3</sup>, Laura Gadzalla<sup>4</sup>, Debra McMillen<sup>5</sup>, Cory Bystrom<sup>5</sup>, Theo Wallimann<sup>6</sup>, Peter Gillespie<sup>1</sup>

<sup>1</sup>Oregon Hearing Research Center, OHSU, Portland, <sup>2</sup>Department of Cell Biology, NCMLS, Radboud University Nijmegen Medical Centre, <sup>3</sup>Department of Otorhinolaryngology, Radboud University Nijmegen Medical Centre, <sup>4</sup>University of Michigan, <sup>5</sup>Proteomics Shared Resource, OHSU, Portland, <sup>6</sup>Institute of Cell Biology, ETH-Zurich

We have recently adopted proteomic technologies to identify proteins of hair bundles. Bundles from chicken vestibular hair cells were isolated and proteins within were sequenced using shotgun mass-spectrometry methods. Identified proteins were involved in cytoskeletal structure,

Ca2+ regulation, and stress responses. Interestingly, we also identified many proteins involved in ATP metabolism, such as glycolytic enzymes and the brain-type creatine kinase (B-CK). We carried out a more detailed analysis of the role of B-CK in the bundle. B-CK is (after beta-actin) the second most abundant protein in the bundle, present at 0.5 mM; we propose that B-CK is crucial for counteracting ATP consumption by the plasma-membrane Ca2+-ATPase (PMCA). Inhibition of creatine kinase with dinitrofluorobenzene effectively reduced the concentration of ATP in the bundle. ATP depletion should not only affect the plasma-membrane Ca2+-ATPase, but also hair-cell adaptation, which is mediated by the ATP dependent motor activity of myosins. Consistent with this critical role in hair-bundle function, the creatine-kinase circuit is essential for high sensitivity hearing, as demonstrated by hearing loss in creatine-kinase knockout mice (see abstract from Peters et al.).

#### 229 Multi-Isotope Imaging Mass Spectrometry (MIMS) Mapping of Protein Turnover in Hair Cells Reveals Highly Stable Stereocilia

**Valeria Piazza**<sup>1</sup>, Duan-Sun Zhang<sup>1,2</sup>, Greg McMahon<sup>1,3</sup>, Jason Lebeau<sup>1,3</sup>, Adam Cohen<sup>1,3</sup>, Claude Lechene<sup>1,3</sup>, David Corey<sup>1,2</sup>

<sup>1</sup>Harvard Medical School, <sup>2</sup>HHMI, <sup>3</sup>National Resource for Imaging Mass Spectrometry

Hair cells are not replaced during the life of an animal, so they need to degrade and replace their proteins on a regular basis. Tip links, for instance, can be replaced in 5-10 hours, and actin in the bundles of neonatal hair cells in culture is thought to turn over in two days. We have used a new method, multi-isotope imaging mass spectrometry (MIMS), to quantify protein turnover in defined subcellular compartments. This method can detect atoms of specific isotopic mass and has spatial resolution near that of electron microscopy. We fed frogs and mice precursor amino acids labeled with the stable isotope 15N, we sacrificed after times of days to months, and we recorded quantitative images at mass 12C, 13C, 12C14N and 12C15N. The 15N/14N ratios in the inner ear revealed regions of high and low protein turnover.

Adult frogs fed 15N-enriched food were sacrificed at 1, 2, 4, 8, 16, and 32 days. Two control frogs were sacrificed at 1 and 32 days. After a few days, there was a small but statistically significant incorporation of 15N in frog saccular tissue. After 32 days, total protein turnover in hair cells and supporting cells was ~20%, but stereocilia had <10% turnover. Otolithic membrane turnover was very low.

Adult mice were fed 15N food and sacrificed at 1, 2, 4, 8, 16, 22, 32, 50, and 150 days. Cochlear hair cell cytoplasm underwent 100% renewal in 3-5 months but stereocilia had <30% of their protein replaced in 5 months. Other highly stable regions included the shafts of pillar cells, reticular lamina, and tectorial membrane. In both species, small domains of higher turnover appeared towards the tips of stereocilia.

These results, obtained in adult animals in vivo, suggest that the normal turnover of protein in stereocilia may be slower than previously suggested. Indeed, the most stable structures in cochlea are stiff elements carrying the mechanical stimulus: the tectorial membrane, the pillar cells, the reticular lamina and the stereocilia.

## 230 Maturation of Mechanotransduction in Cochlea Outer Hair Cells From Rat Organotypic Cultures

Jessica Waguespack<sup>1</sup>, Bechara Kachar<sup>2</sup>, **Anthony Ricci<sup>1,3</sup>**<sup>1</sup>Louisiana State University, <sup>2</sup>National Institute for Deafness and Communicative Disorders, <sup>3</sup>Stanford University

Mechanoelectric transduction (MET) was investigated in rat organotypic cultures between P0 and P14. Recordings were obtained from outer hair cells (OHCs) at both apical and basal locations to monitor maturation to determine if development occurred tonotopically. In addition, whether tonotopic differences measured in acute preparations (Ricci et al., 2005) developed in culture was also monitored.

Newborn rat pups were sacrificed on the day of birth (P0) and organ of corti was isolated and divided into pieces based on cochlea location and put into culture as previously described (Grati et al., 2006). After at least two hours in culture OHCs were patch-clamped and responses to mechanical stimulation recorded. The whole cell capacitance, zero current potential, and voltage and current-clamp responses to mechanical deflection with a stiff probe were measured to assess maturation of the cultured OHCs.

OHCs responded to mechanical stimulation beginning at (P0) for basal cells, and P2 for apical cells. In each case the currents were small (10s of pA) but rapidly increased over the next 18 hrs to more normal values. Initial MET currents did not show adaptation and the activation curves were shifted to the right so that there was no current on at rest. In contrast to vestibular hair cells (Geleoc and Holt, 2003) but similar to chick auditory hair cells (Si et al., 2003), adaptation matured more slowly than the appearance of MET, taking up to P8 for mature responses to be observed. MET currents were larger and faster in basal cells than in apical cells suggesting tonotopic differences were maintained in the culture system. FM1-43 experiments confirmed the electrophysiological recordings. demonstrating a tonotopic gradient in onset of MET. These imaging experiments also suggested that inner hair cells may mature earlier than OHCs and not tonotopically.

This study demonstrates that in organotypic cochlea cultures the onset of MET occurs tonotopically (between P0-P4) and that tonotopic differences are maintained. The work supports the conclusion that tonotopy is programmed prior to birth and is not dependent on external controls like innervation or endolymph.

Work was supported by NIDCD RO1 to AJR and NIDCD intramural program to BK.

## 231 Calcium-Dependent Inactivation of Calcium Channels in Chicken Auditory Hair Cells

Seunghwan Lee<sup>1</sup>, **Paul Fuchs<sup>2</sup>** 

<sup>1</sup>Hanyang University, <sup>2</sup>Johns Hopkins University School of Medicine

L-type Ca2+ channels control both spontaneous and sound-evoked transmitter release from inner hair cells (Sueta et al., 2004, Hear Res. 188:117). Thus, these channels must have a finite open probability at the hair cells' resting membrane potential, implying weak or incomplete inactivation. Indeed, most reports show little, if any inactivation of hair cell calcium currents; until recently however, when slow, calcium-dependent inactivation (CDI) of calcium current was observed in both mammalian ((Marcotti et al., 2003, J. Physiol. 552:743;; Michna et al., 2003, J. Physiol. 553:747) and reptilian (Schnee and Ricci, 2003, J. Physiol. 549:697) hair cells. Here we report CDI of calcium current after blocking potassium conductances in avian auditory hair cells. CDI was characterized by comparing calcium with barium currents in whole-cell voltage-clamp, and by altering the type (EGTA vs. BAPTA) and amount of cytoplasmic buffer with calcium as charge carrier. The measure of CDI was unchanged by exposure to apamin (1 µM) to rule out potential SK channel contamination. Chicken hair cell calcium channels showed significantly higher levels of inactivation with calcium than with barium as charge carrier under all buffering conditions except the strongest (10 mM BAPTA). Importantly, CDI was significantly reduced with a higher concentration of cytoplasmic buffers. Inactivation time constants (for single exponentials) ranged from 1 to 4 seconds and were slowed in higher buffer. Correspondingly, in 0.1 mM EGTA, the extent of CDI averaged 66%, compared to 48% in 1 mM EGTA, and 37% with 10 mM EGTA. CDI was effectively equivalent with BAPTA, rather than EGTA as buffer. With 1 mM EGTA as internal buffer, CDI was increased when endoplasmic calcium pumps were blocked with thapsigargin or benzo-hydroquinone.

Thus, voltage-gated calcium currents in chicken auditory hair cells can demonstrate CDI. It remains to determine whether CDI plays a role in signaling in vivo, and what factors serve to modulate CDI so that calcium channel gating continues at rest. Supported by NIDCD R01DC000276 and NIDCD P30DC005211.

## 232 Features of a Novel Cav3.1 Calcium Channel Currents in Sensory Cells in the Inner Ear

Jun Zhu<sup>1</sup>, Liping Nie<sup>1</sup>, Rodney Diaz<sup>1</sup>, Ebenezer Yamoah<sup>1</sup>

<sup>1</sup>University of California, Davis, The Center for

Neuroscience/Dept. Otolaryngology, Davis, CA 95618

Voltage-gated Ca currents confer multiple Ca-dependent functions in hair cells. We have cloned a novel Cav3.1 channel from hair cells that may carve their development and regeneration. Using heterologous expression systems, the entire open reading frame of the Cav3.1 channel was cloned into a pNLR-XV vector, in which the channel was flanked by the 5'- and 3'-untranslated regions of a

Xenopus ß-globin gene. From the resulting expression plasmid, cRNAs of the Cav3.1 channel were transcribed in vitro using T7 RNA polymerase and injected into stage V-VI oocytes. Two-electrode voltage clamp experiments were carried out with the oocytes clamp amplifier (OC-725C; Warner Instrument Corp., Hamden, CT). Oocvtes were bathed in a solution that contained (in mM) 96 NaCl, 2 KCI, 5-65 BaCl2, 5 HEPES (N-[2-hydroxyethyl] piperazine-N'-[2-ethanesulfonic acid]), and 1 niflumic acid to block endogenous chloride currents in oocytes (pH adjusted to 7.6 with NaOH). The concentration of NaCl was adjusted accordingly, as the Ba, Ca and Sr concentration was increased from 5 to 65 mM to maintain tonicity of the external solution (300 mosmol). The current was activated using different voltage-clamped protocols. The inward Ba, Sr and Ca currents showed voltagedependent decay. However, startling functional differences appear to exist in the decay of the current when Ba and Ca were used as the charge carriers. The apparent Cadependent relaxation of Cav3.1 may be important in HC functions. The detailed biophysical properties of the Cav3.1 currents will be presented and their functional implications will be addressed.

This work was supported by grants to LN (Deafness Research Foundation), ENY (NIDCD).

### 233 Mechanism Underlying Adaptation at the Inner Hair Cell Ribbon Synapse

Juan Goutman<sup>1</sup>, Elisabeth Glowatzki<sup>1</sup>

<sup>1</sup>Johns Hopkins School of Medicine

Auditory nerve activity shows adaptation in response to prolonged sound stimulation. It has been proposed, that the site of adaptation is the inner hair cell (IHC) afferent synapse, as the IHC receptor potential and the IHC calcium currents do not adapt in a way as the auditory nerve response does.

We studied the role the IHC afferent synapse plays in auditory nerve adaptation by performing simultaneous whole cell recordings from IHCs and corresponding afferent fiber dendrites (AFs) in the postnatal rat organ of Corti (P9-P11). To activate maximal calcium current and transmitter release, IHCs were depolarized with voltage steps from -89 to -29 mV for 1s every 30 s. IHC calcium currents were isolated pharmacologically and excitatory postsynaptic currents (EPSCs) in the AF response were monitored at a holding potential of -84 mV.

The AF responses to IHC depolarization very much resembled auditory nerve fiber responses to sound: The activity dropped to about 10% of the initial response within a second. The decay in activity was fit with two exponentials, the time constants were around 10 ms and 100 ms.

The role of AMPA receptors desensitization was tested by recording in 100 microM cyclothiazide, to remove receptor desensitization. The AF response still adapted but with a slower time course. This remaining adaptation is most likely due to exhaustion of the presynaptic pools of vesicles. The rate of vesicle release (obtained by deconvolution of the AF response with an average EPSC) showed a sharp initial peak (3 ms duration) and a second component that relaxed into a steady state. The recordings

were repeated with different strength of calcium buffering of the IHC, to investigate the role of different vesicle pools in the time course of release.

In summary, both desensitization of AMPA receptors and exhaustion of vesicle release contribute to adaptation at the IHC afferent synapse.

This work was supported by NIDCD DC006476 and HFSP RGY12/2004 grants to EG.

## 234 Calcium Buffering of Vesicle Exocytosis and Electrical Resonance in Chick Auditory Hair Cells

Matthew Giampoala<sup>1</sup>, Thomas Parsons<sup>2</sup>

<sup>1</sup>University of Pennsylvania School of Medicine,

<sup>2</sup>University of Pennsylvania School of Veterinary Medicine Calcium modulates neurotransmitter release and calciumactivated potassium channels responsible for electrical resonance. Intracellular calcium buffers localize calcium signalling within cellular regions and regulate these calcium-dependent processes. We explored calcium buffering in isolated cochlear tall hair cells of White Leghorn chickens (8-21 days old). We approximated endogenous calcium buffering properties by comparing recordings in the presence of endogenous buffer (perforated patch: Nystatin, 200µg/ml) to recordings in the presence of various calcium buffers with known properties and concentrations (whole cell). We monitored both calcium-triggered vesicle fusion and electrical resonance as dependent measures.

Capacitance changes were used as a metric for vesicle fusion. Cells were depolarized with voltage clamp from a holding potential of -81 mV to a testing potential of -21 mV for durations ranging from 50 ms to 500 ms. Endogenous calcium buffering capacity was better mimicked by millimolar concentrations of a fast buffer (1.6mM BAPTA) than by submillimolar concentrations of either BAPTA or the slow buffer EGTA (0.2mM).

Electrical resonance was evoked in current-clamp recordings. Cells were held at a resting potential of -75 mV and then depolarized with current injection steps to elicit characteristic voltage oscillations. Both peak and steady-state voltages of the electrical resonance were measured. Low buffer concentrations of either EGTA or BAPTA (0.2 mM) shifted resonance to lower voltages compared to endogenous buffer conditions while high buffer concentration (1.6 mM) shifted resonance to higher voltages.

Electrical resonance in chick hair cells is most sensitive to the equilibrium properties of calcium buffer, whereas exocytosis depends more on dynamic buffer properties. This suggests that, in these cells, vesicle fusion sites are more closely localized to calcium channels than are BK channels. 235 The Size of Release Quanta at the Hair Cell Ribbon Synapse

Andreas Neef<sup>1,2</sup>, Darina Khimich<sup>1,3</sup>, Primoz Pirih<sup>4</sup>, Fred Wolf<sup>2,5</sup>, **Tobias Moser**<sup>1,2</sup>

<sup>1</sup>University of Goettingen, <sup>2</sup>Bernstein Center for Computational Neuroscience, <sup>3</sup>Center for Molecular Physiology of the Brain, <sup>4</sup>University of Groningen, <sup>5</sup>Max-Planck-Institute for Dynamics and Self-Organization Hair cell ribbon synapses release several vesicles within milliseconds (Fuchs et al., 2003). The mode of exocytosis underlying this behavior remains unknown. Whether it involves statistically independent synaptic vesicle fusion, compound or cumulative fusion likely has a large impact on sound coding. In order to explore the mode of exocytosis we aimed to investigate the size distribution of the exocytic quanta of mouse inner hair cells (IHCs), which should depend on the specific mechanism of synaptic vesicle fusion. Usually the sizes of single vesicles are characterized by their diameter in electron micrographs of fixed tissue. Patch-clamp, on the other hand, allows the measurement of the electrical capacitance added by exocytic fusion at an operating synapse. As the capacitance is proportional to the surface of the vesicle, these measurements provide us with a geometric parameter of the quanta, which are actually released under physiological conditions.

Here, we first used patch-clamp recordings of IHC wholecell membrane capacitance to explore trial-trial fluctuations of exocytosis during repetitive stimulation by short stimuli. The magnitude of these fluctuations is related to the amount of capacitance added by the elementary fusion event (Moser and Neher, 1997) enabling us to estimate the mean apparent size of exocytic quanta to about 80 attofarad (aF) in 15 IHCs. Bootstrapping provided an estimate of the 95% confidence interval of our quantal size estimator of 100 aF. Second, we measured the outer diameter of hair cell synaptic vesicles at and around the ribbon synapses. We observed a narrow normal distribution peaking at 43.7 nm (CV: 0.12). Converting this geometrical estimate (after correction for the bilayer thickness: -5 nm and assuming a specific capacitance of 10 fF\*um-2) yielded a mean vesicle capacitance of 47 aF. Together with our functional apparent quantal size estimate this EM derived single vesicle capacitance indicates that a majority of fusion events comprises statistically independent synaptic vesicle exocytosis. In a third line of experiments we aim at direct investigation of individual fusion events using on-cell patch clamp measurements on IHCs. Towards this end we have established low-noise high resolution on-cell capacitance measurements using a software-lock-in approach.

#### 236 Membrane Tension Alters Anion Binding to Prestin

Joseph Santos-Sacchi<sup>1</sup>, Lei Song<sup>1</sup>

<sup>1</sup>Yale University

The motor protein, prestin, is responsible for our exquisite sense of hearing by providing the basis for cochlear amplification. Chloride is an important modulator of prestin activity since it binds to this molecule and alters characteristics of the motor's displacement charge, or

nonlinear capacitance (NLC; Oliver et al., 2001; Rybalchenko and Santos-Sacchi, 2003; Song et al 2005). Indeed, chloride has been recently shown to directly alter cochlear amplification in vivo (Santos-Sacchi et al, 2006). In addition to prestin's anion sensitivity, motor charge also responds to changes in membrane tension. Here we report on studies to determine whether membrane tension affects prestin's binding affinity for anions. Isolated OHCs were whole cell voltage clamped and NLC was measured under conditions of different intracellular turgor pressure while varying salicylate concentrations, an anion that competes for prestin's chloride binding site. Positive membrane tension induced by turgor pressure was found to shift the dose response curve of salicylate's reduction in NLC, indicating an increase in the IC50 for salicylate. This can be interpreted as a reduction in the affinity of salicylate for prestin, and may account for tension effects on OHC performance. We hypothesize that the conformational changes in prestin which occur during imposed membrane tension, namely a shift from the compact to the expanded motor state, alters the binding site for anions. This reduced binding affinity, and consequent unbinding of anions during the switch is contrary to the extrinsic voltage sensor model of Oliver et al (2001), where anion binding and movement through the membrane field evokes motor expansion.

(Supported by NIDCD grant DC000273 to JSS)

#### 237 Electron Tomographic Analysis of Outer Hair Cell Structure

**William Triffo<sup>1,2</sup>**, Kent McDonald<sup>3</sup>, Manfred Auer<sup>2</sup>, Robert Raphael<sup>1</sup>

<sup>1</sup>Department of Bioengineering, Rice University, <sup>2</sup>Life Sciences Division, Lawrence Berkeley National Laboratory, <sup>3</sup>Electron Microscope Laboratory, University of California, Berkeley

In the mammalian cochlea, the outer hair cell (OHC) is able to generate axial deformations in response to variations in transmembrane potential. The cortex of the OHC, referred to as the lateral wall, can be viewed as a trilaminate composite made up of (1) the plasma membrane, (2) a network of actin, spectrin and 'pillar proteins' termed the cortical lattice, and (3) lamellar stacks known as the subsurface cisternae (SSC).

Previous studies of the cortical lattice using conventional TEM and AFM techniques relied on protocols that removed the lattice from its native environment. Moreover, depending on the fixation method, conflicting depictions of SSC ultrastructure have been reported. We have therefore tested a variety of sample preparation methods, ranging from conventional fixation protocols to high-pressure freezing (HPF) and freeze-substitution (FS). We discuss the usage of cellulose tubing to preserve hair cell architecture during HPF and its potential for correlative light microscopy (LM) and TEM study of OHCs.

Electron Tomography (ET) yields 3D density maps through the use of TEM at a resolution of several nanometers, allowing candidate protein shapes to be screened against the tomogram along with revealing detail in the membranous boundaries of intracellular compartments. Using cochlear samples from mouse and guinea pig, we have employed ET to study the cortical lattice and its structural relationship to the plasma membrane, focusing on the pillar proteins known to span the extracisternal space between the plasma membrane and SSC. Initial results from FS experiments on guinea pig OHC strips 'in tube' yield increased internal membrane contrast, permitting us to address the morphology and substructure of the SSC in HPF/FS samples through ET. We also comment on our progress in the visualization and analysis of rootlet architecture at the junction of the stereocilia bundle and apical region of the cell.

# 238 In Vivo Imaging and Functional Assessment of Mammalian Auditory Hair Cells Using One- and Two-Photon Fluorescence Microendoscopy

**Eunice Cheung**<sup>1,2</sup>, Ashkan Monfared<sup>2</sup>, Gerald Popelka<sup>2</sup>, Nikolas Blevins<sup>2</sup>, Mark Schnitzer<sup>1</sup>

<sup>1</sup>Department of Biological Sciences & Department of Applied Physics, Stanford University, <sup>2</sup>Department of Otolaryngology, Stanford University School of Medicine

Due to its delicacy and deep location within the temporal bone, the mammalian cochlea has largely remained inaccessible to in vivo cellular level imaging. We demonstrate optical imaging of cochlear structures, including auditory hair cells, at micron-scale resolution by using two forms of minimally invasive fluorescence microendoscopy (FME) in live guinea pigs. Both one- and two-photon FME rely on microendoscope probes (350-1000 μm in diameter) that are composed of gradient refractive index (GRIN) micro-lenses. We are developing methods for visualizing and assessing the functional health of auditory hair cells in vivo using FME.

Our assay for hair cell function relies on vital styrl dyes that preferentially label functional hair cells by entering through mechano-transduction channels. Thus, hair cells with functional transduction apparatus are brightly labeled, but those with impaired apparatus are not, allowing an in vivo optical assay of hair cell functionality. After inserting a microendoscope probe into the inner ear via a small cochleostomy in the basal turn, we have imaged rows of brightly labeled inner and outer hair cells that were capable of mechano-transduction at the time of dye injection. Hair cell nuclei and hair bundles are readily apparent in the images.

To test our ability to map cochlear damage at the single cell level, we administered the ototoxin gentamicin into one ear and saline into the opposite ear as a control (N=6 animals). Subsequent in vivo imaging typically revealed brightly labeled rows of inner and outer hair cells in the control ear. In the ears that received moderate doses of gentamicin, microendoscopy revealed a widespread lack of fluorescence labeling in outer hair cells of the basal cochlear turn, as well as lack of labeling in some individual inner hairs cells, consistent with the greater extent of damage caused by gentamicin to outer hair cells. These visual observations were also consistent with our physiological assessments of hearing loss using distortion product otoacoustic emission measurements, which revealed loss of high-frequency auditory function in the

ears to which gentamicin was applied. We anticipate that the ability to image auditory hair cells and cochlear microanatomy in live subjects will lead to advances in both basic and clinically relevant auditory science.

# 239 Beyond Cochlear Implants: Functional Stimulation and Recording in the Auditory Nervous System. Symposium Overview Bryan E. Pfingst<sup>1</sup>

<sup>1</sup>University of Michigan

The need for an auditory prosthesis for patients who cannot benefit from cochlear implants as well as the success of deep-brain stimulation procedures for treatment of various neurological disorders have motivated the development of auditory-prosthetic implants in the central auditory pathway. These new approaches to the auditory prosthesis provide us with the motivation and opportunity to better define the functional characteristics of electrical stimulation within various regions of the auditory nervous system. Recording from chronic implants in these regions also provide the potential for innovative approaches to the treatment of communication disorders. This symposium will explore current research and possible future directions for auditory prostheses based on functional stimulation of, and recording from, peripheral and deep brain structures. Implants placed in neural tissues offer several potential advantages due to the close proximity of the stimulation and recording sites to the neural-activation sites. In the first talk John Middlebrooks will explore some of these advantages by comparing responses to peripheral auditory nerve stimulation using traditional cochlear (scala tympani) implants and responses that are achieved by multicontact electrode arrays inserted directly into the auditory nerve bundle in the modiolus. Warren Grill will then explore the biophysics of deep-brain stimulation, considering how the parameters of electrical stimulation affect the sites and patterns of neural activation. Thomas Lenarz and Hubert Lim, Bryan Pfingst, and Bob Shannon will then review the most current research and clinical data on auditory prostheses which utilize surface and penetrating implants in the cochlear nucleus (CN) and inferior colliculus central nucleus (ICC) for stimulation and recording.

### 240 Enhanced Hearing Replacement Using a Penetrating Auditory Nerve Array

John Middlebrooks<sup>1</sup>, Russell Snyder<sup>2,3</sup>

<sup>1</sup>University of Michigan, <sup>2</sup>UCSF, <sup>3</sup>Utah State University
Conventional cochlear implants can provide excellent
speech reception in the absence of ambient noise, but
implant users experience poor pitch perception and poor
speech reception in noisy environments. These limitations
are due in large part to the remote position of stimulating
electrodes relative to excitable neural elements. That is, a
cochlear implant lies within the bony scala tympani
immersed in electrically conductive perilymph, conditions
which would blunt access of stimulating current to specific
neural populations. Moreover, cochlear implants extend
only to the middle cochlear turn, precluding direct access
to low-frequency fibers from the cochlear apex. As an

alternative, we have tested in anesthetized cats a 16electrode stimulating array that traverses the modiolar trunk of the auditory nerve. We monitor the spread of activation within the ascending auditory pathway by recording at 32 sites along the tonotopic axis of the inferior colliculus. In each animal, we characterize responses to acoustic tonal stimulation and, after deafening the animal, to electric stimulation through conventional scala-tympani electrodes and through electrodes in the intra-neural electrode array. Intra-neural electrodes stimulate specific populations representing throughout the entire audible range. Compared to conventional cochlear implants, intra-neural electrodes show up to 50-fold reduction in threshold and >4-fold increase in the dynamic range of currents over which frequency specificity is maintained. Overlap of activated neural populations is reduced, largely eliminating betweenchannel inference under conditions of simultaneous stimulation using pairs of electrodes. Results obtained in this animal model suggest that intra-neural stimulation implemented in a human auditory prosthesis could improve low-frequency hearing, improve speech reception in ambient noise, and improve pitch perception. Supported by NO1-DC-5-0005

## **241** Biophysics of Deep Brain Simulation: Insights for Central Auditory Prostheses Warren M. Grill<sup>1</sup>

<sup>1</sup>Duke University

Deep brain stimulation (DBS) has emerged rapidly as an effective treatment for movement disorders including Parkinson's disease, essential tremor, and dystonia, and is under investigation for treatment of epilepsy, depression, and obsessive-compulsive disorder. DBS uses an implanted pulse generator connected to a multiple-contact electrode array placed in the thalamus or basal ganglia to deliver continuous stimulation at 130-185 Hz. I will review the parallels between DBS and central auditory prostheses. First, although the clinical benefits of DBS are well documented, the mechanisms of action remain unclear. Mechanistic studies have provided insight into the effects of stimulation on the diversity of neuronal elements in the CNS, and I will present recent evidence suggesting that high-frequency DBS activates the output of the stimulated nucleus and regularizes neuronal firing. Second, the lack of understanding of mechanisms of action makes programming of stimulus parameters a long, ad hoc process that may not result in optimal settings. I will review recent studies on the impact of variations in stimulus parameters on the clinical and side effects produced by DBS. Finally, the experience with DBS demonstrates that chronic stimulation using penetrating electrode arrays into deep brain structures can be well tolerated, and post-mortem materials suggest a relatively benign tissue response. I will review the considerations for non-damaging chronic stimulation of brain tissue. These two approaches to chronic brain stimulation share many similarities, and the development of central auditory prostheses can benefit from the DBS experience.

Acknowledgment: Supported by NIH Grants R01-NS040894 and R21 NS055320.

## **242** Psychophysical and Neurophysiological Studies of Chronic Implants in the Inferior Colliculus: Comparison to Cochlear Implants

**Bryan E. Pfingst**<sup>1</sup>, Deborah J. Colesa<sup>1</sup>, Sanford C. Bledsoe, Jr. <sup>1</sup>, Jennifer M. Benson<sup>1</sup>

<sup>1</sup>University of Michigan

Functional effects of electrical stimulation of the inferior colliculus central nucleus (ICC) were studied using psychophysically-trained guinea pigs with chronicallyimplanted multisite silicon-substrate electrode arrays. Results were compared with those from stimulation of chronic cochlear implants in the same species. Neurophysiological multiunit recordings from the ICC implants in response to contralateral acoustic pure-tone stimulation were used to identify the locus of the implants with respect to the tonotopic axis of the ICC and to monitor the stability of the implants. Psychophysical detection thresholds and neural best frequencies (BFs) were typically stable over time in animals monitored for 1 year or more. However, evidence of implant migration was found in some cases. Psychophysical detection thresholds for ICC stimulation covered the same range as those for cochlear-implant stimulation for some parameters. The range of thresholds was very large for both types of implants. Thresholds did not vary systematically as a function of location along the tonotopic axis of the ICC but they tended to be lower in the rostral regions of the ICC than in the caudal regions. Effects of electrode configuration on detection thresholds were much less pronounced for ICC implants than for cochlear implants, consistent with the close proximity of the ICC implants to the sites of neural activation. Effects of pulse rate on detection thresholds (temporal integration) for ICC implants differed markedly from those for cochlear implants.

Supported by NIH grants R01 DC03389 and P30 DC05188 and NSF grant EEC-9986866.

# 243 The Auditory Midbrain Implant (AMI): Surgical, Psychophysical, and Neurophysiological Results in the First Implanted Patients

**Hubert H Lim**<sup>1,2</sup>, Minoo Lenarz<sup>1</sup>, Amir Samii<sup>3</sup>, Gert Joseph<sup>1</sup>, Joerg Pesch<sup>2</sup>, James F Patrick<sup>2</sup>, Rolf-Dieter Battmer<sup>1</sup>, Madjid Samii<sup>3</sup>, Thomas Lenarz<sup>1</sup>

<sup>1</sup>Hannover Medical University, <sup>2</sup>Cochlear Ltd.,

<sup>3</sup>International Neuroscience Institute

The AMI implanted into the inferior colliculus central nucleus (ICC) is a potential solution for hearing restoration in patients suffering from bilateral neural deafness. The motivation for the AMI stems from the lack of success of the auditory brainstem implant in neurofibromatosis type II (NF2) patients. A human AMI system has been developed with Cochlear Ltd. Through animal and cadaver studies, we have demonstrated that the AMI penetrating array (20 linear sites) can be surgically implanted along the tonotopic gradient of the ICC, and achieves safe and effective stimulation of higher auditory centers. These

studies enabled us to proceed with clinical trials in NF2 patients.

In our first patients, we used a modified lateral suboccipital approach to expose the cerebellopontine angle and internal auditory canal for tumor removal. It was then extended to a lateral supracerebellar infratentorial approach that provided good exposure of the dorsal inferior colliculus and enabled implantation of the AMI along the tonotopic gradient of the ICC with minimal added risk. This approach did not endanger any of the major midline venous structures or the trochlear nerve, and did not result in any apparent postoperative complications. Using the AMI, the patients achieved tonal auditory sensations and could detect different loudness, pitch, and temporal percepts. Although still early in their training, these patients obtained improvements in lipreading capabilities and detecting environmental sounds. Furthermore, consistent electrically-evoked middle latency responses (eMLRs) were recorded even at the first testing session and closely related to psychophysical thresholds and loudness percepts. This suggests that the eMLR may provide an objective measure for AMI fitting.

Overall, these findings confirm that the AMI can safely and effectively elicit specific and distinct auditory percepts. We are currently investigating in human and animals how to stimulate the ICC to combine these different percepts to restore intelligible speech perception.

# 244 Speech Recognition and Psychophysical Results From Electrical Stimulation of the Human Cochlear Nucleus and Inferior Colliculus

**Robert Shannon**<sup>1</sup>, Douglas McCreery<sup>2</sup>, Vittorio Colletti<sup>3</sup>, Minoo Lenarz<sup>4</sup>, Thomas Lenarz<sup>4</sup>, Hubert Lim<sup>4</sup>

<sup>1</sup>House Ear Institute, Los Angeles, CA, <sup>2</sup>HMRI, Pasadena, CA, <sup>3</sup>ENT, University of Verona, Italy, <sup>4</sup>MHH, Hannover, Germany

Cochlear implants are not useful for patients with no remaining auditory nerve, so prosthetic devices have been designed to stimulate the cochlear nucleus in the brainstem and the inferior colliculus in the midbrain, using both surface and penetrating electrodes. We will present psychophysical results and speech recognition results from surface and penetrating electrodes at the level of the cochlear nucleus and inferior colliculus. Surprisinaly. psychophysical measures of temporal, spectral and intensity resolution are similar across stimulation sites and electrode types. Speech recognition and modulation detection are excellent in some patients with stimulation of the cochlear nucleus, but not in patients who lost their auditory nerve from vestibular schwannomas. Quantitative comparison of results from electrical stimulation of the auditory system at different stages of neural processing, and across patients with different etiologies can provide insights into auditory processing mechanisms.

## 245 3D Imaging, Modeling, Reconstruction, and Analysis of the Temporal Bone and Brain

Peter Santi<sup>1</sup>, Alec Salt<sup>2</sup>

<sup>1</sup>University of Minnesota, <sup>2</sup>Washington University School of Medicine

The focus of this workshop is on producing and analyzing 3D reconstruction of cells and structures of the temporal bone and brain. Current methods and results from workshop participants will show that the labor required for producing 3D reconstructions is justified not only for pedagogy, but also for data reduction and visualization of whole organs/structures in multiple subjects. Our keynote speaker is Dr. Arthur Toga, who is the director of the Laboratory of Neuroimaging (LONI) at UCLA. He will describe development of brain atlases and coordinate systems which create a framework for mapping multidimensional data on normal and pathological brain populations. The other workshop speakers will describe 3D reconstructions of the temporal bone from histological sections, block-surface images, optical laser sections (OPFOS), confocal sections, and microCT. Speakers will discuss methods for 3D reconstruction of structures by direct volume rendering and tissue/structure segmentation by outlining and antibody labeling. Visualization of the 3D models will be shown as 2D images, movies, VR movies, solid models (generated by rapid prototyping), virtual orthogonal cross sections, and as stereoscopic projections. Data will be presented on construction of a 3D coordinate system for the mouse cochlea. In addition, normal morphometric data, such as, structure/tissue area and volume, and drug dispersion parameters within inner ear fluids from the 3D models will also be presented.

# 246 Mapping the Structure and Function of Brain: Where We Are and Where We Want To Be Arthur Toga<sup>1</sup>

<sup>1</sup>UCLA School of Medicine

The ability to statistically and visually compare and contrast brain image data from multiple subjects is essential to understanding normal variability and differentiating normal from diseased populations. This talk describes some of these approaches and their application in basic and clinical neuroscience. There are numerous probabilistic atlases that describe specific subpopulations, measure their variability and characterize the structural differences between them. Utilizing data from structural MRI, we have built atlases with defined coordinate systems creating a framework for mapping data from functional, histological and other studies of the same population in several species. This talk describes the basic approach and some of the constructs that enable the calculation of probabilistic atlases and examples of their results from several different normal and diseased populations. The talk will also illustrate some approaches useful in understanding multidimensional data and the relationships between them over time. Finally, there will be challenges identified for future mapping and modeling between modalities, time, subjects and species.

#### 247 OPFOS Imaging of the Cochlea

Arne Voie<sup>1</sup>, Gene Saxon<sup>1</sup>, Mailee Hess<sup>1</sup>

<sup>1</sup>Spencer Technologies

The OPFOS imaging technique was designed to image thin sections of the intact cochlea to gain an understanding of its 3-dimensional anatomy not readily apparent from histological sections. OPFOS enables thin sections from intact specimens to be 1) viewed interactively in real time, or 2) acquired to create a 3D data volume that can be post-processed in a variety of ways, including virtual resectioning, 3D surface rendering, and morphometric analysis of specific structures.

This presentation will cover the fundamentals of the imaging technique and present recent advances in resolution and staining of specific cochlear cells. An example case is presented in which a guinea pig cochlea was harvested and labeled with a rhodamine-conjugated immunolabel specific for Myosin VIIa. Both outer and inner hair cells are successfully stained, (sample preparation and immunostaining provided by Sound Pharmaceuticals, Inc., Seattle, WA) clearly demonstrating that OPFOS can distinguish individual hair cells and can therefore resolve to the cellular level. Stereocilia, visible on the tops of the hair cells, support the assessment that OPFOS has a resolution of less than 5 microns.

The OPFOS technique has been used to image cochleas of the mouse, guinea pig, chinchilla and human. Advances in OPFOS imaging include whole-skull preparations, including the brain, performed on sparrow and mouse specimens. Imaging tissues and individual cells of intact specimens in combination with specific staining makes OPFOS a powerful imaging modality, one that can be applied to a variety of species and anatomical features.

### 248 3D Modeling and Analysis of the Mouse Cochlea

**Peter Santi**<sup>1</sup>, Arne Voie<sup>2</sup>, Tiffany Glass<sup>1</sup>, Ian Rapson<sup>1</sup> *University of Minnesota*, <sup>2</sup>Spencer Technologies, Inc.

Using thin-sheet laser imaging (OPFOS) and digital images from celloidin sections, 3D reconstructions of selected structures of the mouse cochlea were produced. Laser imaging produced a well-aligned stack of images but at a lower resolution compared with digital images obtained from celloidin sections. 3D reconstructions of cochlear structures were produced by direct volume rendering using the Amira (Mercury Computer Systems). In addition, in order to produce 3D reconstructions of individual structures, each structure was manually segmented by outlining structures in selected images and Amira was used to interpolate and generate structure outlines in intervening sections. Amira provided surface and volume calculations for these structures and the 3D models were exported as .stl files to produce solid cochlear models using a rapid prototyping process (fusion deposition). Accuracy of the volume calculations produced by Amira compared favorably with scaled volume displacement determinations of the solid models. Virtual resectioning of the 3D cochlear models were obtained by

fitting a B-spline curve along the length of the basilar membrane to both map the cochlea to a 3D coordinate system and to produce orthogonal cross sections of the scala media along the complete length of the basilar membrane which were morphometrically analyzed. producing advantage in 3D Another cochlear reconstructions, is to visualize and quantitatively assess cochlear structures among different cochleas and animals. 3D reconstructions from different cochleas are first combined, using the Procrustes method, which minimizes the root mean square distance between the points of the polygon on a surface model to corresponding points on a reference surface. The displacement of structures in 3D space was computed (the Hausdorff distance) and represented by a color map on a single, combined 3D cochlear model. Thus, similarities and differences in normal anatomy and in various types of pathology among different cochleas can be visually represented and morphometrically expressed.

Supported by Capita Foundation, Digital Technology Center-UM, and the NIDCD.

## 249 Modeling Drug Dispersion in the Inner Ear Fluids: The Importance of Accurate 3D Anatomical Studies

**Alec N. Salt**<sup>1</sup>, Timothy A. Holden<sup>1</sup>, Ruth M. Gill<sup>1</sup>, Stefan K. Plontke<sup>2</sup>

<sup>1</sup>Washington University School of Medicine, <sup>2</sup>University of Tubingen

Locally-applied drugs are increasingly being used for the clinical treatment of inner ear disorders such as Meniere's disease, sudden hearing loss and tinnitus. Knowledge of the dosages achieved and where in the ear the drugs reach is essential to optimize therapies. In animals, experimental studies have shown that drug spread in the inner ear is dominated by diffusion that takes place slowly along the fluid spaces. Quantitative interpretation of experimental measurements and prediction of the likely drug distribution in humans is only possible through quantitative computer models. Whether the model is a simple 1D representation of a scala or a sophisticated 3D representation of the inner ear, the calculations are highly dependent on the dimensions of the compartments that are used. With more sophisticated models, the interactions of each compartment with adjacent structures also need to be incorporated. At present, models are restricted by the limited availability of anatomic descriptions of the ear. Quantitative anatomic studies have become more feasible with the increased availability of 3D reconstruction programs and the increased capabilities of desktop computers. Data sets for analysis can be obtained from histological sections. magnetic serial resonance microscopy (MRM), computed tomography (CT) and orthogonal plane fluorescence optical sectioning (OPFOS). Each of these methods has different capabilities in terms of which tissues can be detected and at what resolution. As the voxel resolution of the methods increases, the effort required to segment structures increases dramatically, limiting the number of specimens that can be analyzed. Other limitations arise from tissue shrinkage and long

preparation times. In some applications, combining structures segmented from different data sets, such as bone from a CT scan and soft tissues from an OPFOS scan can aid the analysis. The long-term goal of this work is to develop a 3D model of the ear, through which drug dispersal can be calculated based on the anatomic communications present and incorporating the transport and permeability properties of tissue boundaries.

This work supported by NIH/NIDCD grants DC01368 (AS) and DC000581 (TH) and BMBF grant 0313844b (SP).

#### 250 Microct Imaging of the Middle Ear and the Inner Ear

**Sunil Puria<sup>1,2</sup>**, Minyong Shin<sup>3,4</sup>, Jae Hoon Sim<sup>1,4</sup>, James Tuck-Lee<sup>1,4</sup>, Charles Steele<sup>1,3</sup>

<sup>1</sup>Stanford University, Mechanical Engineering,

<sup>2</sup>Otolaryngology-HNS, <sup>3</sup>Aeronautics and Astronautics,

<sup>4</sup>Palo Alto Veterans Adminstration

Our goal is to develop anatomically biomechanical models of middle ears and cochlea for which morphometry data are critical. To obtain morphometry of the ear, histological methods have been the primary technique. However, this technique is destructive and certainly not appropriate for in-vivo imaging of individual subjects. One of the most recent advances for obtaining anatomical information is computed-tomography with um resolutions (microCT). Here we describe methods to determine parameters, needed for computational models, from the microCT imaging modality. MicroCT images, at 10-20 um resolution (both in plane and out of plane), were obtained from cadaveric temporal bone ears of human, cat, chinchilla and guinea pig using a Scanco VivaCT 40 scanner. The high-resolution images (500 to 1500 slices) were used for 3D reconstructions of the ossicles, suspensory ligaments and tendon, tympanic membrane eardrum curvature and its relative position in the ear canal, tympanic membrane thickness, middle ear cavities, scala vestibule and scala tympani area functions, and primary and secondary osseous spiral laminae. Results indicate significant intersubject variability amongst individual subjects and across species. Morphometry measurements will include calculations of: (1) principal axes and principal moments of inertia of the malleus-incus complex and stapes, (2) dimensions and orientation of suspensory ligament and tendon attachments in the principal frame, (3) malleusincus joint spacing, (4) Eardrum thickness as a function of position, (5) middle ear cavity shapes and volumes, (6) location of septa and foreman (if any), (7) 3D reconstruction of the cochlear turns, and (8) 3D reconstruction of the semi-circular canals. The microCT imaging modality offers some distinct advantages over existing histological methods. These include: (1) elimination of stretching distortions commonly found in histological preparations, (2) use of a non-destructive method, (3) shorter preparation time (hours rather than 12-16 months), and (4) results already in digital format.

[Work supported by grant DC 05960 from the NIDCD of NIH.]

### 251 High Resolution Imaging of Mammalian Cochlea by 3D Fluorescent Microscopy

**Glen MacDonald**<sup>1</sup>, Natalie Hardie<sup>2</sup>, Edwin Rubel<sup>1</sup>

<sup>1</sup>University of Washington, <sup>2</sup>University of Melbourne

Fluorescent microscopy can provide 3D images over a range of resolutions from the macroscopic to the subcellular. However, the mammalian cochlea presents challenges, primarily from an optically opaque shell, spherical aberrations and contrast among the tissue components. Traditional microscopic methods for cochlear tissues have relied upon either sectioning or microdissection which impose limitations of time, distortion or serial reconstruction of 2D images. We have been developing an approach to high resolution 3D imaging of fluorescently labeled mammalian Organ of Corti (OC) that routinely yields volumes from 60  $\mu m$  to 400  $\mu m$  in thickness. The cochlear tissues are labeled in situ within the intact cochlea by fluorescent probes selected to survive embedding in epoxy resin. Embedded cochleae are opened by sawing along the modiolar axis for

transverse imaging or by sawing parallel to the basilar

surfaces are optically coupled to coverslips by means of a

film of immersion oil or epoxy and observed by laser

scanning confocal microscopy (LSCM), multi-photon

microscopy (MP) or by widefield epi-fluorescence with

deconvolution. The relative uniformity of the refractive

index through these samples reduces spherical aberration

such that high contrast thick optical volumes are obtained.

Deconvolution is essential for widefield epi-fluorescence to

remove blur and it usually benefits confocal images due to

reduction of residual spherical aberrations from deeper

The sawn

lamina to create 'surface preparations'.

Further improvements are being made in the fluorescent labeling, microscopy and software used for our work. While our initial work was limited to confocal fields of view of 3.05 mm at 5.95 µm/pixel and 202 µm at .396 µm/pixel, using 4X and 60X objectives, respectively, we can now achieve over a 4-fold increase in resolution with greater This method has allowed us to identify the presence and number of inner hair cells within the murine OC after its collapse by presbycusis. Morphometric measurements and spatial relationships in the mammalian OC anatomy may be obtained without serial reconstruction or concern for the angle of sectioning. Visualization and quantitation is possible by commonly available commercial and public domain software application. We will present 3D volumes of the Organ of Corti modeled as QuickTime VR, surface renderings and maximum intensity projections.

This work was supported by NIDCD DC03829, DC04661.

regions.

### 252 3-D Reconstructions of the Human Temporal Bone and Related Structures

**Haobing Wang<sup>1</sup>**, Clarinda Northrop<sup>1</sup>, Mads Sørensen<sup>2</sup>, Barbara Burgess<sup>1</sup>, Saumil Merchant<sup>1,3</sup>, M. Charles Liberman<sup>1,3</sup>

<sup>1</sup>Massachusetts Eye and Ear Infirmary, <sup>2</sup>University of Copenhagen, <sup>3</sup>Harvard Medical School

We have developed three 3-D virtual models of the human temporal bone, in different resolutions and scope, based on serial histological sections or images of tissue-block surfaces. The models are packaged in a cross-platform freeware, the 3-D Surface Viewer, which allows full rotation, visibility and transparency control on Windows, Linux and Mac OSX machines. The virtual models can be "sliced open" at any section, and the appropriate raw histologic image can be superimposed on the cleavage plane. The image stack can also be re-sectioned in three different orthogonal planes. The virtual models, downloadable

https://research.meei.harvard.edu/Otopathology/3dmodels/, are powerful teaching tools for relating 2-D morphology from sections to the complex 3-D anatomy, as well as for surgical training, planning and simulation.

The "Temporal Bone" and "Round Window" Models were created using serial, 20  $\mu m$  thick histological sections from a 14-year old male. The Temporal Bone Model used every fifth section at a resolution of 25.4 x 25.4 x 100  $\mu m$  /voxel, while the Round Window Model utilized every section at a resolution of 12.66 x 12.66 x 20  $\mu m$  /voxel. Both image stacks were imported into Amira® 3.1 (Mercury Computer Systems, San Diego, CA). The sections were aligned and segmented into anatomical structures of interest, and then smooth polygonal surface models were generated. The two models were aligned with each other, and the combination affords an overall view of the human temporal bone, as well as detailed structures in the inner ear related to the round window.

The "Visible Ear" presents the structures of the middle, inner and outer ears in their surgically relevant surroundings. It was created from a digital image library created by Mads S. Sørensen M.D., University of Copenhagen. A fresh-frozen human temporal bone was sectioned at 25  $\mu m$ , and images of the block surface were recorded. The image stack was resampled at a final resolution of 50 x 50 x 50/100  $\mu m/voxel$ . The images were registered in custom software and segmented in PhotoShop® 7.0. The segmented image layers were then imported into Amira® 3.1 to generate smooth polygonal surface models.

Model development supported by a core grant from the NIDCD (P30 DC05209).

## 253 3D Projected Stereoscopic Anatomy of the Temporal Bone

#### Michael Teixido<sup>1</sup>

<sup>1</sup>Jefferson Medical College

Learning temporal bone anatomy is a fundamental part of the Otolaryngology training curriculum. Despite considerable investment of time and effort, confusion about hidden anatomic relationships and forms persist that compromise both our understanding of pathophysiology and our surgical ability. Recent development of digital models of inner ear and cranial base anatomy allow demonstration of complex anatomic relationships and can be enhanced as learning tools using stereoscopic 3D presentation. The ultimate result is faster achievement of accurate insights and better patient care. 3D display of anatomic information can be accomplished using desktop, projected and immersive solutions, and can be shared on the web. Examples of topic- focused teaching materials created for surgical training will be shown using stereo projection with passive stereo allowing a large audience to experience 3D content simultaneously. Demonstrations were created using Amira 3.1.1(Mercury Computer Systems, San Diego, CA). A 3D model for careful examination of current treatments for canalithiasis will also be presented.

This project was supported by NIH Grant Number 2 P20 RR016472-04 under the INBRE Program of the National Center for Research Resources.

## 254 Micrornas in the Auditory and Vestibular System: A New Form of Differential Regulation?

Lilach M. Friedman<sup>1</sup>, Ginat Toren<sup>1</sup>, Hashem Shahin<sup>1</sup>, Eran Hornstein<sup>2</sup>, **Karen B. Avraham**<sup>1</sup>

<sup>1</sup>Dept. of Human Molecular Genetics and Biochemistry, Tel Aviv University, <sup>2</sup>Department of Human Molecular Genetics, Weizmann Institute of Science

MicroRNAs (miRNAs) are small (17-23 nt) double-strand RNAs that can inhibit the translation of target mRNAs and affect, directly or indirectly, the expression of a large part of the protein-coded genes. MiRNAs are encoded by miR genes, and are expressed differentially in different tissues. During the last years, miRNAs have been discovered as having important roles in development and disease of plants and animals. The involvement of miRNAs in the development and function of specific tissues and systems have been focused on only recently, following the development of new and sensitive methods to measure miRNA expression and identify their targets.

Vertebrate ear development may be dependent on miRNAs, as was suggested by recent studies in zebrafish and mice [1-2]. Our goal is to identify miRNAs that contribute to the development and function of the mouse inner ear and may be involved in hearing and deafness in mammals, as well as their target mRNAs. We used bioinformatics and other prediction tools to identify potential miRNAs that may control inner ear development or function. Using expression microarrays to profile the miRNAs of the mouse inner ear, we deciphered the expression of miRNAs in cochlea and vestibule, and compared it to their expression in the brain. The miRNA panel that is expressed in the inner ear is quite different from the panel expressed in the brain. Although most of the inner ear-specific miRNAs are expressed similarly in the cochlea and vestibule (for example, miR-182), some miRNAs have a different expression pattern. The differential expression of miRNAs in the cochlea and

vestibule may be responsible for some of the differences in the cochlear and vestibular transcriptomes and functions.

- 1) Wienholds E et al(2005). MicroRNA expression in zebrafish embryonic development. Science, 309:310-311.
- 2) Weston et al(2006). MicroRNA gene expression in the mouse inner ear. Brain Res, 1111: 95-104.

#### 255 Diminuendo Mutation Affects Hair Bundle Structure

**Agnieszka Rzadzinska**<sup>1</sup>, Elizabeth Quint<sup>2</sup>, Anne Kent-Taylor<sup>3</sup>, Helmut Fuchs<sup>4</sup>, Martin Hrabé De Angelis<sup>4</sup>, Karen Steel<sup>3</sup>

<sup>1</sup>The Wellcome Trust Sanger Institute, Wellcome Trust Genome Campus, Hinxton, Cambridge CB10 1SA, UK, <sup>2</sup>2MRC Institute of Hearing Research, University Park, Nottingham NG7 2RD, UK, <sup>3</sup>Wellcome Trust Sanger Institute, Wellcome Trust Genome Campus, Hinxton, Cambridge CB10 1SA, UK, <sup>4</sup>GSF-National Research Center for Environment and Health, D-85764 Neuherberg Germany

The diminuendo mutation has defined a novel locus involved in hearing and balance on mouse chromosome 6. Mice heterozygous for this mutation show progressive hearing loss, while hearing impairment in homozygotes is profound and combined with severe balance problems. Here we analyzed in detail the surface of auditory epithelia of diminuendo hetero- and homozygotes using field emission scanning electron microscopy. In homozygotes we found that degeneration of hair bundles starts during the first few days after birth and progresses from the basal to apical turn so that by P21 only a few severely degenerate inner hair cells can be found in the apical turn of the cochlea. The organ of Corti of diminuendo heterozygotes shows a lesser degree of hair cell degeneration. The apical surface of outer and inner hair cells is significantly reduced in diminuendo mutants and its shape changed. In misshapen hair bundles of heterozygous animals the staircase-like organization of hair bundle progressively disappears as stereocilia lengths become irregular. Despite morphological changes of the hair bundles, interstereocilial links seem to be unaffected in diminuendo mutants.

### 256 Further Evidence for the Critical Role of Natriuretic Peptides in Hearing

Janet Fitzakerley<sup>1</sup>, George Trachte<sup>1</sup>

<sup>1</sup>University of Minnesota Medical School

Natriuretic peptides (NPs) regulate fluid balance in many tissues, where their actions are mediated by three receptors: NPRA, NPRB and NPRC. NPRA and NPRB are guanylyl cyclases; NPRC acts as a clearance receptor that removes NPs from the circulation. Recent experiments demonstrated that NPRA plays a significant role in the regulation of intracellular cyclic guanosine monophosphate (cGMP) levels in the cochlea, as NPRA knockout mice have lower cochlear cGMP concentrations and exhibit a profound high frequency hearing loss (Fitzakerley and Trachte, Soc. Neurosci. Abstr., 2006). As NPRC is an important regulator of NP concentrations, the

purpose of the current experiments was to assess the effect of eliminating NPRC on auditory function.

Auditory brainstem responses (ABRs) were recorded and cGMP levels determined in NPRC mutant and CBA/J mice that were 24-35 postnatal days of age. The spontaneous mutation used in the current study was found at Jackson Laboratories in the BALB/C strain, and was subsequently crossed with C57BI/6J for embryonic storage.

Homozygous NPRC mutant mice had significantly lower high-frequency thresholds compared to wild-type and heterozygote littermates (approximately 40 dB lower at 32 kHz). ABR thresholds at 12 kHz were not significantly different among any of the mice tested in this study. There were no age-dependent changes in cGMP concentrations among NPRC mutants, as was reported for NPRA knockout mice. Among all mice, animals with the lowest thresholds consistently had the highest cochlear cGMP concentrations, although cochlear cGMP levels tended to be lower in NPRC mutants compared to controls, and were lower in all BALB/C mice than in CBA/J controls.

These data support the hypothesis that NPs are important regulators of cochlear function. Based on these results, it can be hypothesized that increased NP concentrations might preserve auditory function in mouse strains that would normally exhibit early-onset hearing loss.

## 257 TGF-β and Runx2 Control of Bone Matrix Mechanical Properties in Bone Disease-Associated Hearing Loss

Jolie Chang<sup>1</sup>, Delia Brauer<sup>2</sup>, Kristin Butcher<sup>3</sup>, Jacob Johnson<sup>1</sup>, Grayson Marshall<sup>2</sup>, Sally Marshall<sup>2</sup>, Anil Lalwani<sup>4</sup>, Richard Schneider<sup>3</sup>, Lawrence Lustig<sup>1</sup>, Tamara Alliston<sup>3</sup>

<sup>1</sup>University of California San Francisco Department of Otolaryngology - Head and Neck Surgery, <sup>2</sup>UCSF Department of Preventative and Restorative Dental Sciences, <sup>3</sup>UCSF Department of Orthopedics, <sup>4</sup>New York University Medical Center Department of Otolaryngology-HNS

Although several bone diseases have associated hearing loss, the role of bone in hearing is not well understood. Recently, transforming growth factor-beta (TGF-β) was identified as the first known regulator of bone matrix properties, such as elastic modulus and hardness. TGF-β regulates osteoblast differentiation and bone properties by repressing the activity of Runx2, a key osteoblast transcription factor. Mutations in TGF-β cause Camurati Engelmann disease and may play a role in cleidocranial dysplasia (CCD), both bone diseases with associated Runx2 mutations result in CCD. hearing loss. Accordingly, CCD symptoms such as dysplastic clavicles are apparent in Runx2+/- mice and in D4 mice, which overexpress TGF- $\beta$  in bone. We hypothesized that TGF- $\beta$  and Runx2 regulation of bone matrix quality is critical for hearing.

To study the role of TGF- $\beta$  and Runx2 in the ear, we tested hearing in Runx2+/- and D4 mice, examined the cochlea for bony and neural defects, and measured cochlear bone matrix properties. Auditory brainstem response

measurements revealed a significant hearing loss in both Runx2+/- and D4 mice at click, 8, 16, and 32kHz frequencies when compared to wild-type littermates. No structural abnormalities were observed in the otic capsule or the ossicles. Histology and immunohistochemistry showed no apparent defects in the neural structures of the ear. In situ hybridization localized Runx2 expression to the bony cochlear capsule, suggesting a bony defect as the cause of hearing loss. Using atomic force microscopy with nanoindentation, we found that D4 and Runx2+/- cochlear bone, similar to D4 and Runx2+/- tibial bone, exhibited reduced elastic modulus and hardness relative to wild-type cochlear bone. Importantly, crossing Runx2+/- mice with mice that have impaired TGF-β signaling in bone rescued both bone matrix properties and hearing loss in Runx2+/mice. These data show a correlation between hearing loss and reduced bone matrix properties and strongly suggest that hearing loss due to defects in TGF- $\beta$  and Runx2 signaling results from defects in bone matrix properties. These pathways may be therapeutic targets for bone disease and hearing loss.

# 258 Heterozygous Loss of *Chd7* Function in Mice is Associated with Variable and Asymmetric Defects in Vestibular Sensory Epithelia and Innervation

**Meredith E. Adams<sup>1,2</sup>**, Lisa A. Beyer<sup>2</sup>, Elizabeth A. Hurd<sup>3</sup>, Donald L. Swiderski<sup>2</sup>, Yehoash Raphael<sup>1,2</sup>, Donna M. Martin<sup>3,4</sup>

<sup>1</sup>Department of Otolaryngology - Head and Neck Surgery, University of Michigan, <sup>2</sup>Kresge Hearing Research Institute, University of Michigan, <sup>3</sup>Department of Pediatrics, University of Michigan, <sup>4</sup>Department of Human Genetics, University of Michigan

Heterozygous mutations in the novel chromodomain gene CHD7 underlie 60 to 80% of cases of CHARGE syndrome, a multiple congenital anomaly condition associated with defects of the inner ear producing hearing and balance impairments. We have generated a novel Chd7 deficient, gene trapped lacZ reporter allele, Chd7<sup>Gt</sup>. We found that homozygous *Chd7<sup>Gt</sup>* mutations are embryonic lethal. Chd7<sup>Gf/+</sup> mice are viable and display variable degrees of head bobbing and circling, consistent with vestibular dysfunction. Semicircular canal defects were noted in paint-filled labyrinths of e16.5  $Chd7^{Gt/+}$  embryos. The goal of this study was to better characterize the labyrinthine defects and to describe the neuroepithelium and vestibular innervation pattern of early postnatal and adult Chd7Gt/+ mice. Gross morphologic assessment revealed that the lateral and posterior semicircular canals were absent or truncated in all  $Chd7^{Gt/+}$  ears. The extent of canal dysgenesis varied between mice and between right and left ears of the same mouse. Staining for actin and 200 kD neurofilament showed that the posterior ampullary sensory epithelium contained stereocilia but lacked normal innervation, regardless of canal morphology. When the lateral ampulla was present, the epithelium and innervation pattern appeared to be normal. The remaining labyrinthine sensory epithelia appeared normal. These results are consistent with the highly variable and incompletely penetrant phenotype of CHARGE patients and suggest that *Chd7* plays an important role in the development and innervation of the labyrinthine sensory epithelium.

Supported by the National Organization for Hearing Research Foundation (NOHR), the Williams Professorship, a gift from B. and A. Hirschfield, and by NIH grants DC01634, DC05188 and HD40188.

### 259 A Novel Pendrin Mutation in the Recessive ENU Mutant Loop

Amiel A. Dror<sup>1</sup>, Hashem Shahin<sup>1</sup>, Helmut Fuchs<sup>2</sup>, Martin Hrabé de Angelis<sup>2</sup>, **Karen B. Avraham<sup>1</sup>** 

<sup>1</sup>Dept. of Human Molecular Genetics and Biochemistry, Tel Aviv University, Tel Aviv, Israel, <sup>2</sup>GSF Research Center, Institute of Experimental Genetics, Neuherberg, Germany N-Ethyl-N-Nitrosourea (ENU) mutagenesis provide new mouse models for human hearing impairment, a requisite for studying the complexity of inner ear development and mechanisms of human mutations. By utilizing the chemical mutagen ENU, point mutations are randomly generated in mice, leading to a variety of phenotypes. Detailed phenotypic characterization revealed that loop homozygote mice do not respond to a Prever reflex (ear-flick) test and are profoundly deaf according to the auditory brainsteam response (ABR) test. Loop mice exhibit a wide range of vestibular defective behaviors including tilted head, circling, abnormal to total absent of swimming ability and lack of a regular reaching response. A closer look at the vestibular sensory organs, the utricle and saccule, revealed a giant 'stone' structure overlying the vestibular macula instead of the tiny scattered otoconia. Chromosomal mapping, based on polymorphic markers between inbred strains, enabled us to locate the underlying location of the loop mutation to the distal region of mouse chromosome12 where Slc26A4 resides. Sequencing of this gene from loop homozygote cDNA revealed a C to T mutation causing a Ser to Phe amino acid substitution at position 408 within a highly conserved domain of the pendrin protein. SLC26A4 is known to be the gene mutated in human Pendred syndrome (PS), an autosomal recessive disorder characterized sensorineural deafness and goitre. A new mouse model for human PS may help to further elucidate the role of Pendrin in human hearing loss.

### 260 Auditory Development in Progressive Motor Neuropathy (PMN)-Mouse Mutants

**Stefan Volkenstein**<sup>1</sup>, Dominik Brors<sup>1</sup>, Stefan Hansen<sup>1</sup>, Robert Mlynski<sup>2</sup>, Achim Berend<sup>2</sup>, Michael Sendtner<sup>3</sup>, Stefan Dazert<sup>1</sup>

<sup>1</sup>Department of Otolaryngology-Head and Neck Surgery, Ruhr Universitaet Bochum, Germany, <sup>2</sup>Department of Otorhinolaryngology, Universitaet Wuerzburg, Wuerzburg, Germany, <sup>3</sup>Department of Neurobiology, Universitaet Wuerzburg, Wuerzburg, Germany

A missense mutation in the tubulin-specific chaperone E (Tbce) gene in the mouse mutant progressive motor neuronopathy (pmn) is a model of human motoneuron

disease. This recessive inherited disease causes in homocygous mice a degeneration of the first motoneuron beginning in the third week of life and goes on with a progressive weakness of the muscles until it ends up letal due to a paralysis of breathing muscles between fifth/sixth week after birth. The Tbce-gen product is involved in the formation of functional microtubules. This pathomechanism could be involved in inner ear dieseas as well.

Auditory brainstem response audiometry (ABR) was performed in 25 animals from the beginning of hearing (day p12) until their death to analyse their auditory development. In addition histological and histomorphometrical studies of the cochlea were accomplished as well as in vitro investigations for neuritogenesis of spiral ganglion cells and Nucleus cochlearis cells (first and second neuron of auditory pathway).

After a normal development of hearing in the beginning ABR-thresholds in homocygous pmn-mice declined significant in the following period of life until their death.

The proven hearing loss in pmn-mice could be caused by a damage of microtubules in hair cells or spiral ganglion cells. Further in vitro investigations studying the possibility of protection against this hearing loss should be performed as well as scanning electron microscopy to look for damages in these systems.

#### 261 Expression of Ca2+ Currents in Hair Cells During Regeneration

Snezana Levic<sup>1</sup>, Ebenezer Yamoah<sup>1</sup>

<sup>1</sup>Center for Neuroscience, Communication Sceince Center, University of California Davis

Previous studies have suggested that calcium influx through voltage-gated calcium channels may play a role in hair cell development. Here, we have demonstrated the functional expression of transient calcium currents in regenerating hair cells in chicken basilar papilla, following gentamicin-induced hair cell damage. We show that there is transient expression of low voltage-activated (LVA) calcium current that may play a role in regeneration of hair cells. Calcium currents were recorded from hair cells located in the basal aspects of the basilar papilla during 5-45 days post treatment (PT). The composition of extracellular solution were: (in mM) NaCl 110, KCl 6, 4-AP 5, CaCl2 5, TEA-Cl 25, D-glucose 10, HEPES 10; and intracellular solution (in mM) NMG 70, CsCl 75, Na2ATP 5, MgCl2 2, HEPES 10, EGTA 10, D-glucose 10. recorded calcium currents at all post treatment ages examined (PT5-PT45). Calcium currents underwent robust changes from PT5 to 25. The changes in calcium current density were as follows: ~25 pA/pF at PT 5 vs. ~7 pA/pF at PT 40. Furthermore, there was a change in the calcium currents sensitivity to the membrane holding potential during hair cell regeneration (-90 vs. -50 mV; ~90% at PT 5 (n=4), <10% at PT40 (n=3). The transient component, which was activated from a holding potential of -90 mV, was observed only in earlier stages of regenerations (PT5-30). In accordance with this finding, we have observed similar alteration of LVA currents during the development of hair cells. We will present data that demonstrate; 1) The presence of multiple voltage-gated calcium currents during regeneration, 2) Transient upregulation of LVA calcium currents. Thus, expression of LVA channels may be one of the common functional signatures in regeneration and development of hair cells.

This work was supported by grants to ENY (NIDCD)

## 262 GJB2 and GJB6 Mutations in Children with Congenital Cytomegalovirus Infection and Hearing Loss

**Shannon Ross**<sup>1</sup>, Zdenek Novak<sup>1</sup>, Rekha Kumbla<sup>1</sup>, Kui Zhang<sup>1</sup>, Karen Fowler<sup>1</sup>, Suresh Boppana<sup>1</sup>

<sup>1</sup>University of Alabama at Birmingham

Objective: To determine if mutations in connexin genes GJB2 and GJB6 are present in children with hearing loss and congenital CMV infection and to asses the frequency of GJB2 and GJB6 mutations in a predominantly African American newborn population.

Study Design: The study population includes 149 children with congenital CMV infection (19 children with hearing loss and 130 children with normal hearing) and 380 uninfected neonates born at a local hospital in Birmingham, AL. Mutation detection for GJB2 and GJB6 was performed by sequencing and PCR methods.

Results: The study population was predominantly African American (85% of the CMV infected children and 74% of the newborn population). Twenty three (4.3%) of the 529 subjects had CX26 mutations and all mutations were heterozygous. Among the group of children with congenital CMV infection, the overall frequency of GJB2 mutations was significantly higher in the children with hearing loss (4/19, 21%) compared to those with normal hearing (4/130, 3%, p=.017).Four-percent of the control population carried a mutation in GJB2. Among the 530 study children, 8 previously reported mutations (M34T, V27I, R127H, F83L, R143W, V37I, V84L, G160S), and 4 novel mutations (V167M, G4D, A40T, and R160Q), were detected. None of the study children had the 342-kb deletion (delGJB6-D13S1830) in GJB6.

Conclusions: In this predominantly African American population, 4.3% of the subjects were carriers for a GJB2 mutation, most of which have been previously described. The large deletion of GJB6 does not appear to play a role in digenic deafness in the African American population. Although GJB2 mutations were detected in groups of children with and without CMV-related hearing loss, those with hearing loss had a higher frequency of GJB2 mutations. Further studies are needed to determine whether mutations in GJB2 are associated with hearing loss in children with congenital CMV infection.

## **263** LIF Has Multiple Effects on Progenitors Derived From Spiral Ganglion Stem Cells

**Kazuo Oshima**<sup>1</sup>, Dawn Tju Wei Teo<sup>1</sup>, Pascal Senn<sup>1</sup>, Veronika Starlinger<sup>1</sup>, Stefan Heller<sup>1</sup>

<sup>1</sup>Stanford University, Department of Otolaryngology-HNS Leukemia Inhibitory Factor (LIF) has been shown to promote self-renewal of neural stem cells and to support neuronal/glial differentiation. We were interested to

characterize the effect of LIF on cell populations derived from sphere-forming stem cells isolated from the murine spiral ganglion. Spiral ganglion-derived spheres can be propagated in presence of EGF, IGF-1 and bFGF and have the ability to spontaneously differentiate into neural and glial cell types after attaching the spheres to fibronectin-coated surfaces and after withdrawal of growth factors. Initially, we tested whether LIF affected selfpropagation of sphere-forming stem cells by culturing spheres in presence of varying concentrations of LIF. We observed an unexpected dramatic effect of LIF leading to immediate attachment of the floating spheres even to untreated plastic surfaces, a result that made it impossible to determine effects on sphere self-renewal. On the other hand, when we cultured attached spheres in the presence of LIF, we detected a dose-dependent increase of neurons after a two-week differentiation period. Mechanistically we found that LIF increased the number of nestin-positive mitotic cells, which indicates an effect on promoting mitoses of the neural progenitors present in the spheres. We further found that LIF-treated cell populations displayed a reduced number of apoptotic cells when compared with untreated controls indicating an effect on cell survival. Combining LIF with BDNF and NT3 resulted in a significant increase of neurons over treatment with the two neurotrophins alone, which suggests that LIF is an effective reagent to boost neural differentiation from spiral ganglion-derived stem cells, particularly in combination with neurotrophic factors.

### 264 Influence of Non-Neuronal Cells on Spiral Ganglion Neurite Outgrowth

**Stefan Hansen**<sup>1</sup>, Dominik Brors<sup>1</sup>, Christine Grabosch<sup>1</sup>, Stefan Dazert<sup>1</sup>

<sup>1</sup>Department of Otolaryngology/ Head and Neck Surgery, Ruhr-University of Bochum, Germany

The tissue culture system of spiral ganglion explants with projection of neuronal processes is an established model to study a variety of soluble and insoluble factors. There are many of such guidance cues that determine the length and growth behavior of spiral ganglion neurites. Only little is known about the effects of the non-neuronal cells like glial cells and nonglial cells e.g. fibroblasts, that are found in close contact and nearby the neurites of spiral ganglion explants.

In order to study the effects of neurite-accompanying and co-cultivated cells on spiral ganglion neurites, we have used immunohistochemistry and scanning electronic microscopy in spiral ganglion cell cultures of Sprague-Dawley rats.

The distribution of glial and nonglial cells in spiral ganglia cultures and their influence on neurite outgrowth were examined with different culture conditions and different age of the animals.

Our findings suggest an important role of non-neuronal cells in spiral ganglion outgrowth. The results indicate that differentially distributed glial and nonglial cells in the spiral ganglion tissue culture can control the projection of spiral ganglion neurites, as it was described in cultured retinal ganglion cells and neurons of the central and peripheral nervous system before.

Further investigations should also focus on factordependent effects on these cells, moreover this culture model provide a basis on cochlear implant research and improvement of neurite-electrode contact as well as regeneration of spiral ganglion neurites.

## **265** Transplantation of Conditionally Immortal Auditory Neuroblasts to the Auditory Nerve

Ken Kojima<sup>1</sup>, Testuji Sekiya<sup>1</sup>, Matthew Holley<sup>2</sup>, Masahiro Matsumoto<sup>1</sup>, Amanda Nicholl<sup>2</sup>, Richard Helyer<sup>3</sup>, Juichi Ito<sup>1</sup> Department of Otolaryngology\_Head and Neck Surgery, Graduate School of Medicine, Kyoto University, <sup>2</sup> Department of Biomedical Science, The University of Sheffield, <sup>3</sup> Department of PhyPhysiology, University of Bristol

Cell transplantation is a realistic potential therapy for replacement of auditory sensory neurons and could benefit patients with cochlear implants or acoustic neuropathies. The procedure involves many experimental variables, including the nature and conditioning of donor cells, surgical technique and degree of degeneration in the host tissue. It is essential to control these variables in order to develop cell transplantation techniques effectively. We have characterised a conditionally immortal, mouse cell line and have studied its behaviour in vivo following transplantation into the auditory nerve of 14 rats. Structural and physiological markers defined the cells as early auditory neuroblasts that lacked neuronal, voltage-gated sodium or calcium currents and had an undifferentiated morphology. The cells responded appropriately to IGF-1 and FGF-2 in vitro. Following transplantation, they migrated peripherally and centrally and aggregated to form coherent, ectopic 'ganglia'. After 7 days they expressed beta III-tubulin and adopted a similar morphology to native spiral ganglion neurons. They also developed bipolar projections aligned with the host nerves. There was no evidence for uncontrolled proliferation in vivo and hundreds of cells survived for at least 63 days. The surgical technique preserved auditory brainstem responses during and after cell delivery. We have shown for the first time that immortal cell lines can potentially be used in the mammalian ear, that it is possible to differentiate significant numbers of cells within the auditory nerve tract and that surgery and cell injection can be achieved with no damage to the cochlea and with minimal degradation of the auditory brainstem response.

## **266** Neurons Derived From Inner Ear Stem Cells Form Synapses with De-Afferented Hair Cells

**Rodrigo Martinez-Monedero**<sup>1,2</sup>, Eunyoung Yi<sup>3</sup>, Elisabeth Glowatzki<sup>3</sup>, Albert Edge<sup>1,2</sup>

<sup>1</sup>Department of Otolaryngology, Harvard Medical School, <sup>2</sup>Eaton-Peabody Laboratory, Massachusetts Eye and Ear Infirmary, <sup>3</sup>Department of Otolaryngology-Head and Neck Surgery, Johns Hopkins School of Medicine

Regeneration of spiral ganglion neurons and formation of afferent synapses with hair cells would be useful in potential treatments for sensorineural hearing loss in a

patient with surviving hair cells, and could be applied in combination with a cochlear prosthesis or after interventions that regenerate hair cells in the future. We have studied the generation of neurons from inner ear stem cells after in vitro treatment with retinoic acid, noggin or Sonic hedgehog (Shh). The neurons generated have been tested for capacity to form synapses with hair cells in a co-culture system with the de-afferented organ of Corti. Using stem cells isolated from the mouse utricle, neurons were obtained in highest yield by treatment with retinoic acid as compared to noggin and Shh. Based on analysis of expression of neurogenic genes immunohistochemistry, the cells expressed genes involved in the development of the sensory epithelium and auditory neurons, including pax2, GATA3, brn3a and islet1 after 2 to 4 days of differentiation of inner ear stem cells. After 7 to 10 days of differentiation in the presence of retinoic acid, we observed expression of markers consistent with a peripheral or sensory neuron phenotype, including peripherin, calretinin, trkC and trkB. Whole cell patch clamp recordings revealed that the differentiated cells had tetrodotoxin-sensitive sodium currents, further supporting their neuronal nature. They were responsive to glutamate, consistent with expression of GluR2/R3. When placed in culture with the organ of Corti after de-afferentation with βbungarotoxin, the neurons formed new connections with hair cells and expressed markers of synaptic vesicles, SV2 and synapsin. This ex vivo system will allow us to develop the optimal routes for cell engraftment and will increase our understanding of the cell interactions needed to rebuild the damaged inner ear epithelium.

Supported by NIDCD grants DC007174 to AE and DC006476 to EG.

## **267** Transplantation of Auditory-Neuroblast Cells into an Auditory Neuropathy Model: Effects of the Microenvironment

Hainan Lang<sup>1</sup>, John Goddard<sup>2</sup>, Bradley Schulte<sup>1,2</sup>, Matthew Holley<sup>3</sup>, Richard Schmiedt<sup>2</sup> <sup>1</sup>Department of Pathology and Laboratory Medicine, Medical University of South Carolina, <sup>2</sup>Department of Otolaryngology – Head & Neck Surgery, Medical University of South Carolina, <sup>3</sup>Department of Biomedical Science, University of Sheffield, Sheffield, UK Spiral ganglion neurons (SGNs) are the primary afferent neurons of the auditory system, conveying information from cochlear inner hair cells to the central nervous system. The lack of endogenous stem/progenitor cells within the inner ear prevents the regeneration of these SGNs, which can be lost due to genetic mutation, injury, or degeneration secondary to hair cell loss. Transplantation of neural stem/progenitor cells into the inner ear offers a potential strategy for repairing or replacing SGNs and restoring hearing. A recently developed, conditionally immortal cell line, US/VOT-N33 (N33), derived from the ventral region of a mouse otocyst, provides an excellent cell source for transplantation into the inner ear (Nicholl et al., Eur J Neurosci, 2005, 22:343-353). Application of ouabain to the round window of the gerbil ear induces the loss of most SGNs via an apoptotic process following a well-defined time course complete within 2-3 days

(Schmiedt et al., JARO, 2002, 3:223-233). To test the effects of the injured microenvironment of the host inner ear on the survival and differentiation of transplanted cells, N33 cells were pretreated with fibroblast growth factor 2 (FGF-2) and injected directly into Rosenthal's canal, scala tympani or scala media in two groups of gerbils treated with ouabain. The cells were injected 1-3 days after (acute-injury group) or 7 days or longer after (chronicinjury group) ouabain exposure. Histologic examination of the transplanted cochleas was performed 3 to 45 days after N33 transplantation. Survival of N33 cells transplanted into Rosenthal's canal and perilymphatic space was greater in the acute-injury group as compared to the chronic-injury group. However, cell survival following delivery into scala media in both the acute- and chronic-injury groups was poor, indicating that scala media is not an appropriate site for cell transplantation. To better understand the potential role of the injured cochlear microenvironment on the survival of transplanted cells within the inner ear, we are currently examining the expression patterns of selected proteins and genes in ouabain-treated ears.

Supported by NIHDC7506 (H.L.); NIHAG14748 (R.A.S.); NIHDC00713 (B.A.S.)

## **268** Transplantation of Adult GFP Spiral Ganglion Progenitor Cells to *In Vitro* Cultured Cochlear Nucleus

Aleksandra Glavaski-Joksimovic<sup>1</sup>, Malin Anderson<sup>2</sup>, Helge Rask-Andersen<sup>2</sup>, Petri Olivius<sup>1</sup>

Center for Hearing and Communication Research,

Karolinska University Hospital, <sup>2</sup>Department of Otosurgery, Institution of Surgical Sciences, Uppsala University Hospital

Background: It has been shown that certain areas of the mature CNS may undergo self-renewal. Similar observations have recently been made in the auditory system. Isolation of progenitor/stem cells and cell replacement therapy may be a future possibility. In this study we analysed if adult spiral ganglion (SG) progenitor cells could be incorporated in an in vitro rat model consisting of the auditory brainstem slice encompassing the cochlear nucleus and the vestibulocochlear nerve.

Material and Methods: Brains were dissected out from 30 Sprague-Dawley postnatal rats (P12-14) and 300 µm-thick brainstem slices were obtained with a tissue choppingdevice. Brain slices were propagated using membrane interface methods as described by Stoppini (1991). Ten adult transgenic Tau-GFP mice (6-12 months) were used as donor animals for the neuronal progenitor cells. SGs were dissected out from the cochlea, dissociated and cultured in DMEM:F12 medium containing growth factors bFGF and EGF. After 5 (1 days in culture 1µl of progenitor cell suspension in concentration of 1x103/µl was deposited next to cochlear nucleus and vestibulocochlear nerve. Migration, interaction and differentiation of the transplanted cells were documented with fluorescence microscopy and time lapse video microscopy. After 14 days auditory brain slices were fixed and analysed immunohistochemistry using antibodies raised against

neural progenitors (nestin), neuronal (TUJ1) and glia (S-100) markers.

Results: A migration of the transplanted cells into the cochlear nucleus was observed. Immunostaining for TUJ1 and S-100 showed that in co-cultures approximately 60% of the GFP-positive cells were neurons and 40% were glia cells. After two weeks 50% of the cells expressed nestin. Discussion: Survival, migration and differentiation of the transplanted adult progenitor cells as well as interactions with the host cells were observed through immunofluorescence and TLVM. This in vitro-model may be used as a future transplantation model for the inner ear. A prominent number of progenitor-derived neurons were observed in co-cultures suggesting that the host tissue have a stimulatory effect on neural differentiation.

## | 269 | Autologous Transplantation of Olfactory Neural Stem Cells into the Gerbil Cochlea

Fenghe Liang<sup>1</sup>, Bradley Schulte<sup>1,2</sup>

<sup>1</sup>Dept. of Pathology and Laboratory Medicine, Medical University of South Carolina, <sup>2</sup>Dept. of Otolaryngology-Head and Neck Surgery, Medical University of South Carolina

Successful organ/tissue transplantation requires blood type and HLA matching between donors and transplant recipients. This applies also to cell replacement therapy stem cell transplantation because histocompatibility issues compromise cell survival and functional especially long-term recovery, homologous xenotransplants. Autologous or transplantation is an alternative approach that allows engraftment and differentiation of stem/progenitor cells in a setting free from immune system complications and rejection. Stem or progenitor cells derived from nasal olfactory epithelium are an excellent cell source for autologous transplants owing to their ready availability, high rate of self-renewal and pleuropotent properties. Here we report the isolation and characterization of gerbil olfactory neural stem cells and their transplantation into the gerbil cochlea. Cells harvested from olfactory epithelium were cultured in Dulbecco; s modified Eagle; s medium and F12 mixture enriched with fetal bovine serum and the neurosphere-forming cells were characterized by immunohistochemical and electrophysiological analyses. After 10 days in culture, unattached immature stem celllike cells were observed in all olfactory epithelium explants (n=14) and nestin and BRDU positive neurospheres were present in 12 out of 14 (86%) of the cultures. Inactivating outward K currents and inward rectifying K currents, both characteristic of neural cells, were recorded in the neurosphere cells. Neurosphere-forming cells were transfected with yellow fluorescent protein and introduced into perilymph of the animal from which they were obtained through the lateral semicircular canal. Cochlear histopathology was assessed on surface preparations and serial sections. Fibroblast-like new cell growth was observed along the organ of Corti six weeks after transplantation. These results suggest that olfactory epithelium may provide a source of stem cells for use in the treatment of sensorineural hearing loss and other neurodegenerative disorders.

## 270 Developing Stem Cell-Based Therapies for Deafness: Isolation and Differentiation of Human Fetal Auditory Stem Cells (Hfascs)

Wei Chen<sup>1,2</sup>, Stuart Johnson<sup>2</sup>, Walter Marcotti<sup>2</sup>, Peter Andrews<sup>1,2</sup>, Harry Moore<sup>1,2</sup>, **Marcelo N. Rivolta<sup>1,2</sup>** 

<sup>1</sup>Centre for Stem Cell Biology, <sup>2</sup>Department of Biomedical Sciences, University of Sheffield, UK

Hearing impairment is an irreversible condition caused by the loss of sensory hair cells and neurons. The lack of regenerative potential of the human cochlea is due to the fact that progenitors are only produced transiently during embryonic development. There is no cure for deafness although, if neurons are preserved, the sensory function of the ear can be replaced by a cochlear implant.

A potential therapeutic approach could involve the transplantation of appropriate stem cells. Such approach may also provide a mean of delivering neurotrophins to promote the survival of neurons, improving the performance of implanted patients.

Due to the lack of regenerative response in the adult cochlea, we have used the foetal auditory organ as a source for stem cell isolation. By carefully microdisecting the sensory epithelia from 9-11 weeks-old fetuses and using optimized culture conditions including different growth factors we have selectivetly expanded a population of cells that expressed NESTIN, SOX2 and other markers normally associated with the stem cell phenotype. After several months of passaging in vitro, cells remain proliferative and undifferentiated. We have defined culture conditions that induce differentiation into hair cells and neurons. When transferred to neuralizing conditions, cells extend processes and readily differentiate into bipolar auditory neurons that express neurogenin, brn3a, betatubulin III and neurofilaments. They also display typical neuronal potassium and sodium currents. When exposed to hair cell conditions, several hair cell markers as well as potassium and calcium currents are induced.

Experimental work with the human cochlea has been limited to clinical measurements and the analysis of surgical or post-mortem samples. A human in vitro system such as this does not only offers a potential therapeutic application, but it could become a useful model for experimentation and drug testing.

Supported by RNID and Deafness Research UK grants to M. Rivolta.

## **271** Engraftment of Primate ES Cell-Derived Neurons into the Cochlear Modiolus of Deafened Macaques

**Kyu Yup Lee<sup>1,2</sup>**, Takayuki Nakagawa<sup>1</sup>, Shinpei Kada<sup>1</sup>, Yasuko Fujimoto<sup>1</sup>, Harukazu Hiraumi<sup>1</sup>, Ryusuke Hori<sup>1</sup>, Hideaki Ogita<sup>1</sup>, Masahiro Matsumoto<sup>1</sup>, Takayuki Okano<sup>1</sup>, Ken Kojima<sup>1</sup>, Tatsunori Sakamoto<sup>1</sup>, Sang Heun Lee<sup>2</sup>, Juichi Ito<sup>1</sup>

<sup>1</sup>Kyoto University Graduate School of Medicine, Japan, <sup>2</sup>Kyungpook National University Hospital, Korea

We have previously demonstrated functional recovery of cochleae by engraftment of mouse ES cell-derived

neurons into the cochlear modiolus of deafened guinea pigs using measurement of electrically evoked ABRs (eABRs) (Okano et al. 2005). In the current study, we examined time courses of alteration in eABR thresholds following transplantation of macaque ES cell-derived neurons in macaques (Macaca fascicularis). Under general anesthesia, we applied a cisplatin solution onto the round window membrane following posterior hypotympanotomy in both ears of two macaques. ABR recording two or three weeks later demonstrated deafness of macaques. Further 6-8 weeks later, we performed cochlostomy in the basal turn of the left cochlea and injected the medium containing macaque ES cell-derived neurons into the cochlear modiolus. After cell transplantation, an electrode of cochlear implants (CI24M) was inserted into the scala tympani. A receiver-stimulator was placed on the skull. Measurements of eABRs were performed once a month until sacrifice. Improvement of eABR thresholds was observed until 3 months after cell transplantation, and those were saturated. The control ear receiving no transplantation exhibited remarkable elevation of eABR thresholds on 5 months after deafened. These findings indicate that engraftment of ES cell-derived neurons may contribute to the recovery of eABRs in macaques similarly to the results in guinea pigs

## 272 Sensory Neurons Produced by Induction of Human ES Cells with BMP4: Engraftment in the Organ of Corti

**Fuxin Shi<sup>1,2</sup>**, Eduardo Corrales<sup>1,2</sup>, Albert Edge<sup>1,2</sup>
<sup>1</sup>Department of Otolaryngology, Harvard Medical School, <sup>2</sup>Eaton-Peabody Laboratory, Massachusetts Eye and Ear Infirmary

Sensorineural hearing loss can result from degeneration of both hair cells and afferent auditory neurons. Replacement cells for regeneration could potentially be made by directed differentiation of human embryonic stem (hES) cells. In an attempt to generate sensory neurons from hES cells, neuronal progenitors were induced by suspension culture of hES cells in a defined medium in the absence of serum. The cells were positive for nestin, a neural progenitor marker and pax2, an auditory placode marker, and were negative for endoderm markers. The precursor cells could be expanded in vitro in bFGF. Neurons (β-III tubulin positive) and glial cells (glial fibrillary acidic protein positive) differentiated from the neural progenitors after removal of bFGF, but evaluation of neuronal markers indicated insignificant differentiation of sensory neurons. Addition of BMP4 to neural progenitors upon removal of bFGF, however, induced significant numbers of sensory neurons that became positive for peripherin, Brn3a, GATA3, NeuroD, TrkB and TrkC. Addition of hES cell-derived neural progenitor cells to an explant of the organ of Corti after removal of neurons by treatment with β-bungarotoxin gave rise to neurons that contacted hair cells and were positive for synapsin. Differentiated glial cells wrapped the fibers of neurons that contacted hair cells as detected by GFAP staining, mimicking the afferent neurons in the inner ear. To test these cells as possible replacement cells for auditory neurons, they were grafted into the cochlea of a gerbil in

which the spiral ganglion neurons were removed by ouabain. The ES cell-derived neurons that engrafted in the cochlear nerve trunk sent out neurites that had central projections to the brain and peripheral projections to the organ of Corti. Our results suggest that hES cells have the potential to generate sensory neurons that can form synapses with denervated hair cells.

### 273 Differentiation of Human Bone Marrow Stem Cells into Inner Ear Cell Types

Sang-jun Jeon<sup>1</sup>, Albert Edge<sup>1</sup>

<sup>1</sup>Department of Otology and Laryngology, Harvard Medical School, Eaton-Peabody Laboratory

Human mesenchymal stem cells (hMSCs) would be a potential alternative for cell-based treatment of hearing loss if they can be differentiated into inner ear cell types including hair cells or sensory neurons. Human bone marrow cells from healthy adult were harvested and plated on tissue culture plastic for 16 hr, and nonadherent hematopoietic stem cells were aspirated. The adherent cells were cultured in  $\alpha$ MEM containing 9% horse serum and 9% fetal bovine serum and were negative for bloodforming cell markers, CD34 and CD45. They gave rise to chondrocytes expressing type II and IV collagen after culture in the presence of TGFβ, transferrin and insulin. Culture of hMSCs in DMEM/F12 medium containing N2 and B27 without serum in the presence of NT-3, BDNF, Sonic hedgehog and retinoic acid for 10 days gave rise to cells that expressed neurosensory progenitor markers detected by RT-PCR, Musashi, nestin, Pax6, Brn3a, NeuroD, Ngn1, and GATA3, and sensory neuron markers, peripherin and TrkC. The differentiated hMSCs were positive for  $\beta$ -III tubulin (2.1% of the total cells were positive based on immunohistochemistry) and, of these cells, 28% co-stained for peripherin and 31% co-stained For the differentiation to hair cells, we transfected hMSCs with human Atoh1 in an expression vector with a selectable marker for eukaryotic cells. The selected progenitor cells expressed Atoh1 and, after differentiation in DMEM/F12 medium containing N2 and B27 with NT-3 and BDNF for 10 days, expressed hair cell markers, Atoh1, myosin VIIa, p27Kip, Jag2 and espin based on RT-PCR. Co-culture of the Atoh1-transfected cells with an ex vivo organ of Corti from mouse gave rise to cells expressing myosin VIIa and espin that were detected by immunostaining. When the ex vivo mouse organ of Corti was treated with toxins to induce hair cell degeneration, co-cultured bone marrow-derived cells were observed to engraft in the mouse sensory epithelium.

#### 274 Identification and Characterization of Mouse Cochlear Stem Cells

Michael Yerukhimovich<sup>1</sup>, Lianhua Bai<sup>2</sup>, Daniel Chen<sup>1</sup>, Robert Miller<sup>2</sup>, **Kumar Alagramam**<sup>1</sup>

<sup>1</sup>Otolaryngology-HNS, Case Western Reserve University, Cleveland, OH 44106, <sup>2</sup>Department of Neurosciences, Case Western Reserve University, Cleveland, OH 44106 Genetic, noise and drug induced loss of hair cells in the mouse and human cochlea leads to permanent hearing loss due to lack of regeneration of hair cells, which may be due to reduced numbers or loss of regenerative ability of stem cells in the adult cochlea. We hypothesized that the mouse neonate cochlea harbors stem cells capable of differentiating into hair cells. Cells from the primary neonate cochlear culture began to proliferate and formed floating spheres after 14 days in vitro (DIV). comparison, spheres from primary culture of cortex were observed after 7 DIV. Cochlear spheres cells (CSCs) could be passaged and the new spheres were observed after 7 DIV. CSCs were capable of differentiating into astrocytes and oligodendrocytes, but not neurons under the condition tested. CSCs expressed Sox2 and Myo7a, but failed to show markers that are expressed exclusively in mature cochlear tissue, while cells from cortex spheres express Sox2 and Otx2, but not Myo7a. Our results show that cochleae from neonatal mice harbor cells capable of forming spheres and cells from these spheres appear to be better endowed to become hair cells.

## 275 A Targeted Delivery Strategy for the Transplantation of Stem Cells into Rosenthal's Canal

**Bryony Coleman<sup>1,2</sup>**, Steven S. Backhouse<sup>2</sup>, Robert K. Shepherd<sup>1,2</sup>

<sup>1</sup>University of Melbourne, <sup>2</sup>Bionic Ear Institute The delivery of stem cells (SCs) into the mammalian cochlea is a potential strategy to replace degenerating SGNs following a sensorineural hearing loss. Previous attempts to deliver SCs into the cochlea have demonstrated survival of transplanted cells, however, these cells frequently disperse throughout the cochlea and only low numbers have been reported within the target site, Rosenthal's canal. The purpose of this study was to investigate the efficacy of delivering exogenous cells directly into Rosenthal's canal. For comparison we delivered both coloured microbeads (MBs; 20-45 µm in diameter) and live SCs (5-15 µm in diameter) into normal hearing (NH) and aminoglycoside deafened (AD) adult guinea pigs. MBs or SCs were delivered into the left cochlea via a cochleostomy made in the lower basal turn Rosenthal's canal was opened by scala tympani. fracturing the adjacent osseous spiral lamina wall and both MBs (n=4, NH) and SCs (n=5, AD) were then delivered into Rosenthal's canal within a hydrogel (biocompatible 3D matrix) to minimise their dispersal. These groups were compared to animals that underwent surgery alone (n=4, NH). MBs and SCs were observed in the lower basal turn scala tympani and in Rosenthal's canal, and the hydrogel was effective at retaining both the MBs and SCs at the An inflammatory tissue response was implant site. observed in all treated cochleae, however this was localised to the lower basal turn scala tympani. observed decrease in the density of SGNs in the lower basal turn of treated cochleae, was again localised to the surgical site. Although further work is required to optimise the delivery of stem cells into Rosenthal's canal, our findings demonstrate the potential of this approach for the targeted delivery of replacement cells. This will be important for future cell replacement therapies incorporating guided neurite outgrowth in a 3D matrix with electrical stimulation.

### 276 Making Hair Cells From Adult Omental Stem Cells.

**Jianxin Bao**<sup>1</sup>, Jan-Jan Liu<sup>1</sup>, June-Ho Shin<sup>1</sup> Washington Unviersity

Loss of hair cells is one major cause for hearing loss. Embryonic stem cells exhibit tremendous promise to replace cells lost during aging or due to various diseases. However, in consideration of potential clinical allogeneic barriers encountered by these cells, many laboratories have been exploring alternative approaches. Our approach is to examine the feasibility of making hair cells from adult omental stem cells.

We have focused on whether adult omental stem cells have potential to differentiate into hair cells after both intrinsic and extrinsic modifications. Previous work has shown that Mammalian Atonal Homolog 1 (Math1) is necessary for early development of hair cells and is sufficient to convert adult non-sensory cells in the cochlea into hair cells. Our found that over-expression of Math1 in the otic epithelial cell line VOT-E36 made these cells able to sense mechanical vibrations and activate spiral ganglion neurons. However, our preliminary studies demonstrated that single cell-derived adult omental stem cells failed to respond to mechanical stimulations after Math1 overexpression, consistent with previous findings that the ability of Math1 to make hair cells depends on specific cell contexts. To make intrinsic signaling in adult omental stem cells similar to hair cells, we established a novel procedure consisting of VOT-E36 protein transfer, Math1 overexpression, and co-culture with spiral ganglion neurons, which caused modified adult omental stem cells to sense mechanical vibrations. In addition, we found the induction of hair bundles and the mechanotransduction machinery in these modified cells. Furthermore, these modified cells were innervated by spiral ganglion neurons and were able to activate these neurons after mechanical stimulations. The ultimate goal of our research program is to test whether adult stem cells, with both intrinsic and extrinsic modifications, can be differentiated into cells with functional hair cell properties, and subsequently be employed in the reversal of age-related or noise-induced hearing loss.

#### 277 Characterization of Primary Cells Cultured From Human Tympanic Membrane and Surrounding Tissue

**Reza Ghassemifar**<sup>1,2</sup>, Sharon Redmond<sup>1,2</sup>, Natalie Moska<sup>1</sup>, Keith Anandacoomaraswamy<sup>1,2</sup>, Robert Eikelboom<sup>1,2</sup>, Marcus Atlas<sup>1,2</sup>

<sup>1</sup>Ear Science Institute Australia, <sup>2</sup>Ear Science Centre, University of Western Australia

Chronic and non healing tympanic membrane perforations may lead to severe medical complications including meningitis and mastoiditis. Development of an autologous tympanic membrane to repair the clinically impaired membranes relies extensively on understanding its cellular and molecular components and their pathways. In the present study, human tympanic membrane (hTM) and surrounding tissue including human bony canal skin (hBCS), human bony-cartilaginous canal skin (hBCCS) were explanted to cell culture dishes and the outgrown

primary cells were collected, passaged and cryopreserved before characterizing their gene transcripts and protein profiles. During the initial phase of growth, a thin layer of extracellular matrix extending from the explants were always visible prior to cell migration and confluent growth. Second passage primary cells and control cell line (HaCat) were seeded on eight-well chamber slides and grown to confluency before being analysed using RT-PCR, immunoconfocal and flow cytometry for the expression of junctional and cytoskeleton proteins, growth factors and their receptors. Gene transcript analysis revealed that KGF-1 expression was consistently high in all cell types, whilst KGF-2 and its receptor FGFR-2 were more limited in their expression. It was also found that KGFR had consistently greater expression levels than FGFR-2 throughout all samples. Flow cytometry analysis revealed that 98.9% of hTMs, 91.50% of hBCS, 97.36% of hBCCS, and 99.76% of HaCat cells were positive for epitheliumspecific transcription factor ESE-1. Moreover, both immunoconfocal and RT-PCR confirmed that all cell types express polarized epithelial specific cell adhesion molecules including Occludin, ZO-1 and E-cadherin. The results indicate that these primary cells are of epithelial origin and may be used in the development of an artificial tympanic membrane.

#### 278 Expression of Frizzled Genes in the Inner Ear of Adult Mice

**Samit M. Shah**<sup>1</sup>, Barbara L. Christensen<sup>1</sup>, Young-Jin Kang<sup>1</sup>, Mauricio Vieira<sup>1</sup>, Bruce C. Wheeler<sup>1</sup>, Albert S. Feng<sup>1</sup>, Richard Kollmar<sup>1</sup>

<sup>1</sup>Beckman Institute for Advanced Science and Technology, University of Illinois at Urbana-Champaign

The frizzled (FZD) transmembrane receptors of vertebrates and their extracellular 'wingless-related MMTV integration site' (WNT) ligands have been implicated in axon guidance and remodeling, dendrite morphogenesis, and synapse formation. In a microarray-hybridization screen for signaling pathways that are available in spiralganglion neurons, we found that Fzd genes were expressed in the cochlear modiolus of adult mice. Using in situ hybridizations, we confirmed the presence of Fzd mRNAs in spiral ganglia. We are now measuring the abundance of all Fzd and Wnt mRNAs in the cochlea by conducting quantitative RT-PCR experiments. expression of Fzd genes in the spiral ganglia of adult mice suggests that Wnt signaling could be harnessed to stimulate neuronal regeneration in patients with sensorineural hearing loss. By inducing the outgrowth of neurites and attracting them towards the electrodes of a cochlear implant, it may be possible to increase the number of usable frequency channels and thus the fidelity of perceived sounds.

Support contributed by: Sensory Neuroscience Training Program; University of Illinois Campus Research Board, Mary Jane Neer Research Fund, and Beckman Institute for Advanced Science and Technology.

### **279** Voltage Dependence of Transmitter Release at the IHC Ribbon Synapse

Juan Goutman<sup>1</sup>, Elisabeth Glowatzki<sup>1</sup> Johns Hopkins School of Medicine

In the inner ear, hair cells transform sound signals into receptor potentials. The intensity of the sound signal translates into the size of the inner hair cell receptor potential and the rate of action potentials in the auditory nerve fiber response. This relationship should be reflected in the transfer function at the inner hair cell (IHC) afferent synapse.

We studied the voltage dependence of transmitter release at the IHC afferent synapse by performing simultaneous whole cell recordings from inner hair cells (IHCs) and corresponding afferent dendrites (AFs) in the postnatal rat organ of Corti (P9-P11). To exclude AMPA receptor desensitization recordings were done in 100 microM cyclothiazide. IHCs were depolarized with 10 mV steps from -89 to +41 mV for 200 ms every 15 s, or in 2 mV steps from -49 to -29 mV. IHC calcium currents were isolated pharmacologically and the AF response was monitored at a holding potential of -84 mV.

At voltage steps negative to -49 mV, no synaptic activity was found. Around -49 mV, both, calcium current and AF response activated. Between -49 and -29 mV, both calcium current and AF response increased linearly, indicating a linear calcium dependence of vesicle release. A linear calcium dependence was also obtained when the rate of EPSCs (last 100 ms) was measured. However, the average EPSC amplitude stayed constant throughout the voltage range tested, suggesting that the size of the EPSCs, which are thought to activate due to multivesicular release, is calcium-independent.

A linear calcium dependence of transmitter release has also been found in the frog papilla (Keen & Hudspeth, 2006), and may serve for faithful coding of sound intensity. This work was supported by NIDCD DC006476 and HFSP RGY12/2004 grants to EG.

### 280 Slow Inactivation Adjusts Calcium Channel Availability in Rat Cochlear Inner Hair Cells

Lisa Grant<sup>1</sup>, Paul Fuchs<sup>1</sup>

<sup>1</sup>Johns Hopkins University School of Medicine

It is well established that the graded receptor potential of the inner hair cell (IHC) membrane controls the release of neurotransmitter to encode auditory stimuli in the afferent neurone. Calcium entry through Ca<sub>v</sub>1.3 calcium channels activated by the graded depolarisation is a vital step in this process, sensing the voltage change and initiating the fusion of synaptic vesicles to the plasma membrane. The properties of Ca<sub>v</sub>1.3 in mammalian IHCs are strikingly different from those of Ca<sub>v</sub>1.3 expressed in HEK cells (Yang et al 2006, J. Neurosci. in press). In particular Ca<sub>v</sub>1.3 expressed in HEK cells exhibits a marked, relatively rapid calcium-dependent inactivation (CDI) in contrast to the slow and weak inactivation that has been previously reported in auditory hair cells (Marcotti et al. 2003, J. Physiol. 552:743; Michna et al. 2003, J. Physiol. 553:747; Schnee & Ricci 2003, J. Physiol. 549:697). We have further characterised inactivation of calcium channels

in mammalian (rat) neonatal IHCs in the excised organ of Corti preparation using whole-cell voltage-clamp to isolate and record calcium currents (ICa). Long depolarisations (2.5 s @ - 15 mV) consistently evoked a slow decline in ICa amplitude that was significantly reduced with barium as the charge carrier. Depolarisation to + 80mV, which opens channels but opposes the influx of Ca<sup>2+</sup>, did not inactivate the current, providing further evidence for the calcium-dependence of this process. Brief voltage ramps (-75 mV to + 100 mV over 100 ms) applied prior to the depolarising steps, immediately after and at later time points delineated the rate of recovery of inactivation of Ca<sub>v</sub>1.3 under near-physiological conditions (1.3 mM external CaCl, 0.1mM internal EGTA, 35 - 37°C). Complete recovery from inactivation required tens of seconds, providing further insights into the properties and regulation of Ca<sub>v</sub>1.3 in IHCs. Supported by R01 DC000276 to PAF from the NIDCD.

#### 281 K<sup>+</sup> Currents of Adult Mouse Inner Hair Cells Do Not Inactivate

**Mikhail E Bashtanov**<sup>1</sup>, Walter Marcotti<sup>1,2</sup>, Corne J. Kros<sup>1</sup> School of Life Sciences, University of Sussex, Falmer, Brighton, UK, <sup>2</sup>Department of Biomedical Science, University of Sheffield, Sheffield, UK

Activation of  $I_{\rm K,f}$ , a BK current, and  $I_{\rm K,s}$ , a delayed rectifier, largely determines the shape and speed of response of the IHC receptor potential (Kros & Crawford 1990 J Physiol 421:263-291). Knowledge of the kinetics of these currents is helpful in predicting IHC responses in vivo (Lopez-Poveda & Eustaquio-Martin 2006 JARO 7:218-235). We isolated  $I_{\rm K,f}$  or  $I_{\rm K,s}$  from the total outward current directly by blocking most of the other K $^+$  current, using whole-cell patch clamp. Neither of the currents showed inactivation during 50 ms voltage steps from a holding potential of -84 mV to a range of more depolarized potentials, up to -10 mV.

When  $I_{K,f}$  was isolated indirectly, by subtraction, using the BK channel blocker iberiotoxin, the current seemed to inactivate and was sensitive to residual series resistance (R<sub>s</sub>). It has been suggested before that such current traces are distorted due to the varying voltage drop across R<sub>s</sub>, leading to this apparent inactivation (Marcotti et al 2004 J Physiol 557:613-633). A simple program for correction of the current kinetics was developed and tested using a Hodgkin-Huxley model, showing significant reduction in R<sub>s</sub>-induced errors. When using the program to correct experimental data, over- and underestimated values of non-compensated R<sub>s</sub> were deliberately applied as well as the accurate values. When the accurate R<sub>s</sub> values obtained from the experiments were used,  $I_{K,f}$  did not show inactivation. Underestimation of  $R_{\text{s}}$  by as little as 0.5  $\text{M}\Omega$ caused an apparent inactivation of the current similar to that observed in the uncorrected data. The lack of inactivation of  $I_{K,f}$  is consistent with recordings of this current from macropatches, where R<sub>s</sub>-induced errors are very small (Thurm et al 2005 J Physiol 569:137-151). Supported by the MRC

282 The Number of Ribbon Synapses in Mouse Inner Hair Cells Has a Maximum in the Tonotopic Region of Best Hearing and Scales with Exocytosis but not Ca2+ Current

**Alexander C. Meyer**<sup>1</sup>, Alexander Egner<sup>2</sup>, Yuri Yarin<sup>3</sup>, Tobias Moser<sup>1</sup>

<sup>1</sup>University Hospital Göttingen, Germany, <sup>2</sup>Max-Planck-Institute for biophys. Chemistry, Göttingen, Germany, <sup>3</sup>University Hospital Dresden, Germany

The sensitivity of sound perception is highly dependent on the frequency - each detected at a specific tonotopic location in the cochlea. Here, we investigated whether the morphological and physiological properties of the afferent hair cell synapses could contribute to this phenomenon. We found that the number of synaptic contacts per inner hair cell had a maximum in the cochlear region that transmits sounds with highest sensitivity (10-24 kHz). Confocal microscopy of the organ of Corti following immunostaining for RIBEYE, a major component of the synaptic ribbon and for AMPA-receptor subunits GluR2 and 3 was performed to estimate the number of afferent synaptic contacts as colocalized spots of pre- and postsynaptic immunofluroescence.

We then investigated the presynaptic function of inner hair cells at different positions along the apical turn of the cochlea by perforated patch-clamp recordings. Probing exocytosis by measurements of cell capacitance increments after brief depolarizations, we found that hair cells located ~300 µm from the apex released 44% less transmitter than cells located at ~1400 µm from the apex. This functional finding corresponded to a 31% difference in the number of morphologically identified afferent synapses betwen these locations. Interestingly, size, charge and kinetics of the calcium current did not vary with the tonotopic position of the hair cells.

As the IHC Ca2+ influx may not only depend on the synapse number but also on the active zone size we asked whether the size of presynaptic ribbons may vary tonotopically. The Ribbon size distributions at the two tonotopic positions of ~180 and ~1060  $\mu$ m, as estimated by 4Pi high-resolution optical microscopy, were indistinguishable from each other.

In conclusion, the cochlea may use a maximum of neural information channels per hair cells in the range of best hearing. The comparable Ca2+ current despite varying IHC release area might indicate a significant number of extrasynaptic Ca2+ channels.

## 283 Immunogold Localization of BK Calcium Activated Potassium Channels in the Rat Cochlea

**Carole Hackney**<sup>1</sup>, Robert Fettiplace<sup>2</sup>, David Furness<sup>1</sup>, Shanthini Mahendrasingam<sup>1</sup>

<sup>1</sup>Keele University, <sup>2</sup>University of Wisconsin-Madison Large conductance calcium activated potassium (BK) channels are gated by both membrane depolarization and an increase in cytosolic calcium. In lower vertebrate hair cells, BK channels are localized in the pre-synaptic zones near the calcium channels that are believed to regulate neurotransmitter release. These channels have also been

found in mammalian inner (IHCs) and outer hair cells (OHCs), but their precise ultrastructural distribution has not been reported. We have used postembedding immunogold labelling to localize these channels using electron microscopy. Cochleas from post-hearing Sprague-Dawley rats were fixed in 4% paraformaldehyde and 0.1% glutaraldehyde and embedded in LR White resin. Ultrathin sections were immunogold labelled using a polyclonal anti-BKCa channel antibody to the alpha subunit (Alomone Labs) and a secondary antibody conjugated to gold particles. Preadsorption controls were performed by incubating the primary antibody with its antigen overnight at 4oC and then centrifuging the antibody-antigen mixture and the antibody alone at 14, 000g at 4oC before use. In IHCs, plasma membrane labelling was concentrated in patches below the cuticular plate as well as being distributed more evenly elsewhere along the membrane. It may also be associated with the tight junctions between the IHCs and their surrounding supporting cells. Labelling also occurred in the synaptic region between the OHCs and their efferents. Thus, we have found ultrastructural labelling for BK channels in locations reported light microscopically by other groups (Pyott et al. 2004; Hafidi et al. 2005). Preadsorption significantly reduced the labelling especially on the IHC basolateral membrane and the OHC efferent synaptic region. Interestingly these regions also label for ryanodine receptors (Grant et al. 2006). This method will now allow us to determine the quantitative distribution of the BK alpha-subunit along the cochlea.

Supported by NIDCD grant RO1 DC011362 to RF.

#### 284 Localization of BK Channels in Mammalian Vestibular Hair Cells

David Savin<sup>1</sup>, Rebecca Hu<sup>2</sup>, Larry F. Hoffman<sup>2</sup>, **Felix E. Schweizer**<sup>1</sup>

<sup>1</sup>Department of Neurobiology, David Geffen School of Medicine at UCLA, <sup>2</sup>Division of Head and Neck Surgery, David Geffen School of Medicine at UCLA

Voltage and calcium activated potassium channels (BK) are important regulators of neuronal excitability. BK channels are generally thought to be co-localized with calcium channels at presynaptic release sites and seem crucial for frequency tuning in non-mammalian vestibular and auditory hair cells. However, in mammalian auditory hair cells. BK channels have been reported to be localized towards the apical end of the cell, away from release sites (Pvott et al. J Neurosci. 2004). We therefore decided to investigate the localization of BK channels in mammalian vestibular hair cells. Here we report on the distribution of BK channels in the rodent vestibular neuroepithelia using immunohistochemistry and laser scanning confocal microscopy. We used a monoclonal antibody that does not detect a protein in BK-null mutant animals according to Misonou et al. (J. Comp Neurol. 2006). We further confirmed the specificity of the antibody by staining cerebellar and cochlear sections. As previously reported, we find BK immunoreactivity associated with Purkinje cells in the cerebellum. Also in accordance to previous work by others (Pyott et al 2004) we do not detect any labeling of outer hair cells in the rodent cochlea and the staining in inner hair cells appears to be localized towards the apical side. In the rat utricle, we find that the BK-channel antibodies strongly label a subset of both type I and type II hair cells. In individual hair cells, the labeling appears to be fairly uniform and clearly is not restricted to either apical or basal sites, although the staining appears to be enhanced in the very apical portion of the cells. Furthermore, we do not detect any BK-immunoreactivity in the afferent fibers. Taken together, our data indicate that BK channel expression in the mammalian vestibular system differs from the expression pattern in both the mammalian auditory and the non-mammalian vestibular system. Suppported by the NIH/NICDC DC007678 to FES.

#### 285 Protein Partners of Kv and BK Channels in the Cochlea

**Bernd Sokolowski**<sup>1</sup>, Margaret Harvey<sup>1</sup>, Joerg Karolat<sup>1</sup>

<sup>1</sup>University of South Florida

Ion channels in the lateral and basal walls of hair cells modulate signals initiated via transduction and efferent stimulation. Crucial to the development and subsistence of these channels are protein-protein interactions, which regulate different stages in the life cycle of the channel. Characteristics maintained by these interactions include structural modifications via protein folding, shuttling from cytoplasmic organelles to the membrane, and expression at the membrane via regulation of biophysical characteristics and channel number. We have examined two types of K+ channels and their partners in the hair cells of the chick basilar papilla. These channels include the A-type or transient channel found primarily in the short and intermediate cells and the large conductance, calciumactivated or BK channel found largely in the tall hair cells. Previously, we reported that the A-channel interacts with a pentraxin-containing protein, PPTX. Here, we present different functional aspects, including PPTX interactions with ion channels from different voltage-gated K+ channel subfamilies. PPTX interacts with the tetramerization (T1) domain of Kv4 as shown by substitution and deletion mutations. The substitution of charged with neutrally charged amino acids at sites 86, 87, 117, and 118 inhibits PPTX-ion channel interactions. Studies using CHO cells and native tissues show that PPTX coimmunoprecipitates (CoIP) and colocalizes with members of the Kv1, Kv2, and Kv3 subfamilies. These interactions are the result of similar amino acids positioned in the T1 domain of these subfamilies. In comparison, yeast two-hybrid screening, using fragments of the BK channel as bait, isolated interacting partners that include Ca2+sensor/binding proteins and folding proteins. Reciprocal CoIP studies using native inner ear tissues verified interactions that include calbindin, KChIP, and heat shock protein 90. Supported by NIDCD grant DC004295.

### 286 Ryanodine is a Positive Modulator of Acetylcholine Receptor Gating in Cochlear Hair Cells

Javier Zorrilla de San Martín<sup>1</sup>, Jimena Ballestero<sup>1</sup>, **Eleonora Katz**<sup>1,2</sup>, Ana Belén Elgoyhen<sup>1</sup>, Paul Fuchs<sup>3</sup> <sup>1</sup>INGEBI (CONICET), <sup>2</sup>Dept. Physiology, Molecular and Cell Biology (FCEN, University of Buenos Aires), <sup>3</sup>Dept. of Otolaryngology, Head and Neck Surgery, Johns Hopkins School of Medicine

The efferent synaptic specialization of hair cells includes a near-membrane synaptic cistern whose suggests a role for internal calcium stores in cholinergic inhibition. Calcium release channels from internal stores include 'ryanodine receptors' whose participation is usually demonstrated by sensitivity to the eponymous plant alkaloid, ryanodine. However, use of this and other storeactive compounds on hair cells is confounded by the unusual pharmacology of the  $\alpha 9\alpha 10$ -containing hair cell ACh receptor (AChR), which has been shown to be antagonized by a broad spectrum of compounds. Surprisingly, we found that ryanodine is a positive modulator of the hair cell AChR, the first such compound to be found. ACh-evoked currents through the isolated cholinergic receptor of inner hair cells (IHCs) in excised mouse cochleas were enhanced  $\sim 50\%$  by 200  $\mu M$ ryanodine, a concentration that inhibits gating of the ryanodine receptor itself. This facilitatory action appears to be on the AChR itself, since a similar effect was seen for ACh-evoked currents in Xenopus oocytes injected with rat  $\alpha 9$  and  $\alpha 10$  subunit mRNAs, and corresponds to an increase in the apparent affinity for ACh. This unusual positive modulation is not unique to the mammalian receptor. The response of chicken hair cells exposed to ACh is likewise enhanced in the presence of 100 µM ryanodine. This effect can be seen both for currents through AChRs alone, isolated by strong internal calcium buffering; or when the associated SK currents are present in hair cells with weaker calcium buffering. In this latter case, the SK currents become longer-lasting. Finally, the action of ryanodine directly on the hair cell ACh receptor is further supported by the observation of similar effects in hair cells from the crooked neck dwarf chicken, a naturallyoccurring mutant with defective ryanodine receptors.

This novel effect of ryanodine provides new opportunities for design of inner ear therapeutics based on this interaction.

Supported by R01 DC001508 to PAF and ABE from the NIDCD.

# 287 In Vitro Electrophysiology of Hair Cells From Chick Basilar Papilla Suggests that ß Subunits Play a Minimal Role in Electrical Tuning

Mingjie Tong<sup>1</sup>, R. Keith Duncan<sup>1</sup>

<sup>1</sup>Kresge Hearing Research Institute, University of Michigan Large-conductance, Ca<sup>2+</sup>-activated K<sup>+</sup> channels (BK) play an important role in electrical tuning in non-mammalian vertebrate hair cells. The change in BK kinetics along the tonotopic axis has been attributed, in part, to a graded co-expression of β subunits. The β<sub>1</sub> subunit slows channel

kinetics, leading to the hypothesis that  $\beta 1$  subunits are functionally coupled to BK channels in the apical, lowfrequency end of the chick basilar papilla. Tamoxifen (Tx) is a (xeno)estrogen compound that activates BK channels through  $\beta_1$  or  $\beta_4$  subunits. Our prediction was that Tx would facilitate the activation of BK channels in outside-out patches from apical hair cells. In single-channel recordings, Tx decreased the open probabilities (NPo) of most channels, contrary to our hypothesis. A small proportion of patches showed an increase in NPo, but the magnitude was small (< 2 fold), compared to effects in channels known to include  $\beta$  subunits (6-7 fold) (Dick et al. 2002; Dick et al. 2001). Similar results were obtained from ensemble-averaged recordings of multi-channel patches. In most cases, Tx shifted the half-activation potential  $(V_{1/2})$ to more positive voltages. A small proportion of patches showed negative shifts in  $V_{1/2}$ , but the shift was small (< 5 mV), compared to effects in channels known to include  $\boldsymbol{\beta}$ subunits (10-15 mV) (Dick et al. 2001; Duncan 2005). Our data confirmed the presence of  $\beta$  subunits in apical hair cells by showing that some BK channels were activated by Tx. However, the facilitatory effects were insignificant. Moreover, the majority of channels were inhibited by Tx. These data indicate that the distribution of channels with  $\alpha$ +  $\beta$  subunits or the stoichiometric density of  $\beta$  subunits in a single channel is low. Although further study is needed to assess their tonotopic gradients, this study suggests that  $\beta$ subunits play a minimal role in electrical tuning in nonmammalian hair cells. Supported by NIH RO1 051924 and P30 DC05188.

#### 288 Exocytosis in an Auditory Organ of the Frog

**Patricia Quinones**<sup>1</sup>, Peter Narins<sup>1</sup>, Felix Schweizer<sup>1</sup> *UCLA* 

The amphibian papilla (AP) is the auditory organ that is sensitive to the low and mid-frequencies of the frog's hearing range (100-1250 Hz in Rana pipiens pipiens). Although these hair cells show a gradation of properties along the rostrocaudal axis, they can be divided into two subpopulations- rostral and caudal cells- based on their morphology, electrophysiology and innervation patterns. Rostral and caudal hair cells also differ in their synaptic ultrastructure. Low-frequency rostral hair cells are long, cylindrical cells with one large ribbon per synapse while the high-frequency caudal hair cells are shorter and goblet shaped, and tend to have smaller, multiple ribbons per svnapse. Although the exact role of the ribbon in exocytosis is unclear, the fact that rostral and caudal hair cells show disparate numbers of ribbons suggests that their release properties may differ. We tested the hypothesis that differences between rostral and caudal synaptic ultrastructure subserve the differences in vesiclerelease-related capacitance changes, which are an accurate reflection of exocytosis. Using a semi-intact AP preparation, we whole-cell voltage clamped hair cells and measured changes in cell capacitance. Cells were held at -85 mV and depolarized to either -50 mV or -20mV for durations ranging from 5-1000 ms. Our findings show that changes in capacitance were both calcium and voltage dependent, and that there are differences in release

properties between rostral and caudal hair cells. (Supported by NIH grant no. DC-00222 to PMN).

#### 289 Alpha 1 Cholinergic Receptor Subunit in Inner Ear Hair Cells

**Deborah Scheffer**<sup>1</sup>, Cyrille Sage<sup>1</sup>, Paola V. Plazas<sup>2</sup>, A. Belen Elgoyhen<sup>2</sup>, David P. Corey<sup>3</sup>, Veronique Pingault<sup>1</sup> Inserm, equipe Avenir, department of Genetics, hopital Henri Mondor, Creteil, France, <sup>2</sup>Instituto de Investigaciones en Ingeniería Genética y Biología Molecular, Buenos Aires, Argentina, <sup>3</sup>HHMI and department of Neurobiology, Harvard Medicial School, Boston

The mammalian inner ear is innervated by afferent peripheral neurons and by efferent neurons (mostly cholinergic) from the brainstem. Two nicotinic acetylcholine receptor (nAChR) subunits,  $\alpha$ 9 and  $\alpha$ 10, are expressed in inner ear hair cells; in vitro these can form a functional ion-channel receptor with properties similar to hair cells' native acetylcholine receptors. We previously described the expression of a third nAChR subunit in inner ear:  $\alpha 1$  (encoded by *Chrna1*), whose transcription is regulated by the bHLH transcription factor ATOH1. We showed that ATOH1 in vitro activates the CHRNA1 promoter through binding to two E-boxes. In situ hybridization showed that  $\alpha 1$  is specifically expressed in inner and outer hair cells of the organ of Corti, and in type I and type II hair cells of the vestibular epithelia.

Here, we show that the timing of *Chrna1* expression is closely related to that of  $\alpha 9$  and  $\alpha 10$  subunits in the mouse cochlea and vestibule. To determine whether  $\alpha 1$  forms a heteromultimeric receptor with  $\alpha 9$  and  $\alpha 10$ , we analyzed the properties of receptors with subunits expressed in different combinations in Xenopus oocytes. Injections of  $\alpha 1$  cRNA with  $\alpha 9$  and/or  $\alpha 10$  did not change the main electrophysiological properties of the nAChR, suggesting that  $\alpha 1$  does not interact.

Chrna1 is best known as encoding the alpha subunit of the heteromultimeric muscle nAChR. The embryonic  $\gamma$  subunit of that channel, encoded by Chrng is also expressed in hair cells of vestibular sensory epithelia (Z.Y. Chen, personal communication). We therefore tested the expression of all muscle-type nAChR subunits in the cochlea and in the vestibule. Expression data suggest there is another type of nAChR in the inner ear.

#### 290 Colocalization of Prosaposin with nAChR a10 in the OHCs

**Omar Akil<sup>1</sup>**, Christopher Weber<sup>1</sup>, Lawrence Lustig<sup>1</sup> Department of Otolaryngology, University of California San Francisco, San Francisco, CA

Prosaposin, a precursor of four glycoprotein activators (saposin A-D) for lysosomal hydrolases, has been shown to have both lipid transfer properties and neuritogenic activity. Previous studies in our lab have suggested a protein-protein binding interaction between prosaposin and the nAChR a10 subunit (located in the base of the outer hair cells (OHCs)) and have demonstrated that transgenic mice (-/-) lacking prosaposin develop deafness between P19 and P21, suffer a loss of apical OHCs and show abnormal afferent and efferent innervation patterns. These

results suggest that prosaposin or one of its mature cleaved end-products, saposin A-D is involved in the maintenance of normal neural connectivity within the organ of Corti and consequently the maintenance of normal hearing. However, these initial data failed to precisely determine whether prosaposin was located in the base of the OHC, the Deiters' cells (DC), or both. Here we report additional studies undertaken to further refine the location of prosaposin in this region: 1) RT-PCR on a population of microdissected OHCs and DCs; 2) Double-label immunofluorescence with prosaposin antibody and either rhodamin-phalloidin, synaptophysin or choline acetyltransferase (ChAT) and 3) real-time quantitative PCR for characterization of prosaposin and nAChR a9 and a10 in OHCs vs DCs.

Standard RT-PCR on a population of OHCs and DCs demonstrate the presence of both nAChR a9 (a marker of OHCs) and prosaposin but not glutamate aspartate transporter 1 (Glast1), a DC-specific marker. In contrast, DC contains Glast1 cDNA but not nAChR a9, as expected. Double-label immunofluorescence with prosaposin and rhodamin-phalloidin shows that prosaposin predominantly located below the basilar pole of the OHCs, while double labeling with the synaptophysin or ChAT shows that prosaposin is localized either at or below the efferent synaptic cleft below the OHC. To resolve the discrepancy of the presence of prosaposin in OHCs by RT-PCR and DC by immunohistology, quantitative RT-PCR studies in populations of micro-dissected OHCs and DCs was performed, and demonstrate that DCs transcribe a larger amount of prosaposin mRNA than OHCs, though OHCs clearly do express prosaposin mRNA as well.

These results show that prosaposin mRNA is present in both OHCs and DCs, though at higher levels in DCs. In contrast, an antibody directed against saposin D only labels the apical DC and synaptic cleft below the OHC. These finding suggest that one of the other saposins, A-C, but not D is the active form in OHCs.

# 291 Functional Interaction of Ca<sup>2+</sup>-Activated K<sup>+</sup> Channels and α9/α10 ACh Receptors in Hair Cells Involves their Association with Other Proteins

Payam Mohassel<sup>1</sup>, Sabrina Mader<sup>1</sup>, Liping Nie<sup>1</sup>, Jerel Garcia<sup>1</sup>, Ebenezer N. Yamoah<sup>1</sup>, Judilee N. Dinglasan<sup>1</sup>, **Ana E. Vazquez<sup>1</sup>** 

<sup>1</sup>Department of Otolaryngology-HNS and Center for Neurosciences, University of California Davis

The outer hair cells (OHCs) of the mammalian cochlea receive feedback from the brainstem through cholinergic neurons. Previous studies have demonstrated that efferent inputs activate acetylcholine receptors ( $\alpha 9/\alpha 10$  AChR) in OHCs. These receptors are permeable to Ca²+ which gates a small conductance Ca²+ activated K+ current (SK2). Our interest is to understand the molecular mechanisms by which activities of cochlear-specific  $\alpha 9/\alpha 10$  AChRs and SK2 channels confer OHC membrane hyperpolarization. Our previous work demonstrated that reconstitution of cloned SK2 channels and  $\alpha 9/\alpha 10$  AChRs from the cochlea in expression systems was not sufficient to recapture the time course of the ACh-induced efferent

effect in OHCs. Functional interaction between AChRs and SK channels may involve direct association of these channels with other protein(s). We have employed the yeast-two-hybrid technique to identify these proteins. Specifically, using the intracellular amino terminal domain of SK2 as well as the intracellular domain of  $\alpha$ 9 as baits. we isolated isoforms of  $\alpha$  actin as binding partners. An intriguing architecture of proteins association emerges, where SK2 and  $\alpha$ 9 may be held snugly together by binding to different domains of  $\alpha$  actin or to different  $\alpha$  actin isoforms that polymerize together. Other potential partners were also identified. Prosaprosin was identified as a binding partner of  $\alpha 9$ , consistent with previous reports, by others, which showed that prosaprosin is a binding partner of  $\alpha$ 10. Using the  $\alpha$ 9AChR cytoplasmic loop as bait we also isolated partial clones for Giα2. G protein modulator 2. and G protein  $\alpha$ 2. Given that the AChRs in hair cells were demonstrated to have mixed muscarinic and nicotinic pharmacological properties we are investigating the functional significance of these interactions. We are conducting studies that will determine the genuine candidate proteins that associate with AChRs and SK2 channels in the OHCs.

This work was supported by R01-DC006421 to AEV.

# 292 Loss of α9 or α10 Nachr Subunit Induces Changes in Olivocochlear Synaptic Structure: Implications for Cholinergic Activity Mediated Changes in Expression of Cytoskeletal Elements

**Vidya Murthy**<sup>1</sup>, Sevin Turcan<sup>1</sup>, Johnvesly Basappa<sup>1</sup>, Hiren Patel<sup>1,2</sup>, Douglas Vetter<sup>1</sup>

<sup>1</sup>Tufts Univ. School of Medicine, <sup>2</sup>Emory Univ.

Loss of either the  $\alpha 9$  or  $\alpha 10$  genes results in changes in olivocochlear function and synaptic morphology. The abnormal innervation patterns observed in the mutant mice correlate with changes in the expression levels of various adhesion proteins implicated in processes such as target recognition and synaptogenesis (Murthy and Vetter, 2006). We now present data that implicates loss of  $\alpha$ 9 and  $\alpha$ 10 in anterograde changes in cytoskeletal dynamics, and retrograde changes in presynaptic terminal structure, and propose a series of protein:protein interactions to connect these observations. Data from cDNA and Affymetrix chip arrays, ICAT (Isotope Coded Affinity Tag) mass spectrometry based proteomic studies, qPCR, and western blots reveal expression changes in a number of distinct gene/protein classes at early postnatal (P7) and adult ages. Synaptic adhesion proteins such as Dscam, syndecan binding protein, pannexin, connexin 26, as well as neurotrophic factors such as BDNF, netrin and various semaphorins, undergo mis-expression in the null mice. Also, expression of synaptic scaffolding/cytoskeletal proteins are perturbed by the loss of  $\alpha 9$  and  $\alpha 10$  nAChR activity. These include actin, and cytoskeletal interacting proteins such as the catenins, destrin/ADF, N-Wasp, cortactin, decorin, actinin, doublecortin, and tubulin proteins. In addition the loss of nAChR activity also alters the expression of vesicle binding proteins including various VAMPs and synaptobrevin, indicating a bidirectional regulation of synaptic proteins by the nAChRs. These findings provide insights into the molecular mechanisms by which nAChR activity regulates efferent cholinergic synapse formation, maturation and organization in the cochlea. This novel role for cochlear hair cell nAChRs in OC synaptogenesis is tied to its effects on the expression of synaptic adhesion proteins and their interactions with cytoskeleton elements via numerous scaffolding molecules.

Supported by DC006258 (DEV)

#### 293 Peering into the Pore of the Hair-Cell Transducer Channel with Permeant Blockers

Sietse M. van Netten<sup>1</sup>, Corne J. Kros<sup>2</sup>

<sup>1</sup>Department of Neurobiophysics, University of Groningen, The Netherlands, <sup>2</sup>School of Life Sciences, University of Sussex, UK

Recently, pharmacological characterization has been used to infer intrinsic properties of the transducer channel of sensory hair cells, such as pore dimensions (Farris et al 2004 J Physiol 558:769-92). Combining results on the blocking and permeation of channel blockers like dihydrostreptomycin (Marcotti et al 2005 J Physiol 567:505-21), amiloride (Rüsch et al 1994 J Physiol 474:75-86) and FM1-43 (Gale et al 2001 J Neurosci 21:7013-25) we have obtained information on the free energy profile along the transducer channel's pore as sensed by these blocker molecules. In addition to providing information about the position of the binding site, these energy profiles may also indicate sites of positive charges impeding or preventing large blocker molecules with positively charged groups from permeating through the channel. Specifically, a large intracellularly facing energy barrier (15.84 kT) may cause asymmetric entry behaviour of the pore from extraand intracellular sides. This may account for the low potency of the block of intracellular dihydrostreptomycin. Contrary to the intracellular barrier, a barrier located near the extracellular side of the channel appears to be Ca<sup>2+</sup> dependent and, especially at low extracellular Ca2+ concentrations (100 µM), poses a more modest entry barrier to surmount (10.00 kT). This gives rise to a relatively large second-order rate constant (3.52·10<sup>8</sup> s<sup>-1</sup> M<sup>-1</sup> 1), indicative of an almost diffusion-limited influx of extracellular cations.

Taken together, a functional channel pore geometry emerges that consists of a large vestibule that is easily accessible from the extracellular side. The end of the vestibule, located at about 80% of the electrical distance in the pore, as measured from the extracellular side, is lined with negatively charged regions that form a binding site (-8.24 kT). Just behind the binding site, close to the intracellular side of the channel, is a positively charged constriction probably forming the selectivity filter.

Supported by the Netherlands Organisation for Scientific Research and the Medical Research Council

#### 294 Capsaicin Elicited Current in Isolated Outer Hair Cell of Guinea Pig

Tao Wu<sup>1</sup>, Zhi-Gen Jiang<sup>1</sup>, Alfred L. Nuttall<sup>1,2</sup>

<sup>1</sup>Oregon Health & Sciences University, Oregon Hearing Research Center, <sup>2</sup>Kresge Hearing Research Institute, University of Michigan

Capsaicin, heat and change of acidity elicit the sensation of burning pain through selectively activating TRPV1 (transient receptor potential vanilloid) channels on primary sensory neurons. Our previous study has shown that TRPV1 was expressed in outer hair cells (OHCs) and that capsaicin changed the cochlear sensitivity of guinea pigs in vivo (Zheng et al, J Neurophysiol 2003). It was therefore of interest to directly detect the capsaicin-evoked current in isolated OHC in vitro. Here, whole cell recordings were used on isolated OHCs from the 3rd and 4th cochlear turns of guinea pigs with regular NaCl (150 mM) bath and KCI (150 mM) pipette solutions. The average membrane potential was -47.4 ± 3.7 mV (n=19) under current clamp mode. We found that, when OHC was clamped at -70 mV, capsaicin elicited an inward current in a dose-dependent manner:  $8.2 \pm 1.2$  pA at  $0.1 \mu M$  (n=3),  $12.9 \pm 2.3$  pA at 1  $\mu$ M (n=3), 17.5 ± 2 pA at 10  $\mu$ M (n=8), 15.5 ± 1.5 pA at 100  $\mu$ M (n=5) and 15.8  $\pm$  2.1 pA at 1000  $\mu$ M (n=5) (p<0.05 for each group, paired t test), with response saturation concentration around 10 µM. The result is, to some extent, consistent with the findings of TRPV1 expressed in different cells (Caterina et al, Nature 1997). The competitive antagonist, capsazepine (10 µM), and the noncompetitive antagonist, ruthenium red (10 µM), blocked the capsaicin-evoked response by 73% (n=2) and 70% (n=2) respectively. A high concentration of capsaicin (100 and 1000 µM) often evoked a biphasic response; an inward current followed by an outward current that may represent calcium dependent potassium current. These findings support the notion that TRPV1 is present in OHC and plays a role in OHC physiological activities.

Supported by NIHNIDCD grant R01-DC00141.

### 295 Expression of TRPC1 and TRPC3 in Cochlear Hair Cells

Rebecca Miller<sup>1</sup>, Hakim Hiel<sup>1</sup>, Paul Fuchs<sup>1</sup>

<sup>1</sup>Dept of Otlolaryngology - HNS, Johns Hokins University School of Medicine, Baltimore, MD, USA

In OHCs, calcium entry through the nicotinic acetylcholine receptor triggers an efflux of potassium ions through the small conductance potassium channels (SK2) that hyperpolarizes the cell. Recent reports suggest that release from intracellular calcium stores also participates in this process. In other cell types, release from stores is followed by capacitative calcium entry that is believed to replenish store content. This calcium entry is believed to be through transient receptor potential channels (TRPC). In the present work we investigated the expression of two candidate members of this large family of channels, TRPC1 and TRPC3, in adult rat and chick cochlea.

RT-PCR showed that both TRPC1 and TRPC3 mRNA are expressed in rat and chick cochleae. In immunohistochemistry experiments, antibodies against

either choline acetyl transferase (ChAT) or neurofilament 200 (NF 200) were paired with antibodies against either TRPC1 or TRPC3 to highlight any association with auditory nerve inputs onto hair cells. In rat cochlea, immunolabeling revealed that TRPC1 protein is highly concentrated in the cuticular plate area of OHCs; while IHCs had only weak labeling. Similarly in chick basilar papilla, hair cells showed strong labeling at the cuticular plate. In contrast TRPC3 antibodies revealed strong and diffuse labeling of IHCs, while OHCs showed a faint signal. In chick cochlea, both short and tall hair cells showed strong expression of TRPC3 protein throughout the length of the sensory epithelium. However, double labeling with antibodies to ChAT (an efferent synapse marker) showed preferential co-localization with neither TRPC1 nor TRPC3. In addition, there was no gradient of immunolabel for either channel along the tonotopic axis. . These observations indicate that TRPC1 and TRPC3 are not likely to participate in efferent synaptic function, but may play other, as yet unknown roles in cochlear hair cells.

Supported by NIDCD R01 DC001508 and P30 DC005211.

### 296 Molecular Identity of Voltage-Gated Sodium Channel Alpha-Subunits in Mouse Cochlear Inner Hair Cells

**Walter Marcotti**<sup>1</sup>, Ilana Mechaly<sup>2</sup>, Christian Chabbert<sup>2</sup>, Stuart Johnson<sup>1</sup>

<sup>1</sup>Department of Biomedical Science, University of Sheffield, Sheffield, S10 2TN, UK., <sup>2</sup>INSERM U583, Institute of Neuroscience, Montpellier, 34295, France.

Inner hair cells (IHCs) of the mammalian cochlea produce trains of  $\text{Ca}^{2^+}$  action potentials (APs) prior to the onset of sound-induced responses at around postnatal day 12 (Kros et al., 1998, Nature 394:281-284; Glowatzki & Fuchs, 2000, Science, 23:66-68). AP generation by IHCs requires the  $\text{Ca}^{2^+}$  current ( $I_{\text{Ca}}$ ) but not the TTX-sensitive Na<sup>+</sup> current ( $I_{\text{Na}}$ ) (Marcotti et al., 2003, J Physiol 552:743-761). However,  $I_{\text{Na}}$  shapes APs by speeding up the time necessary for the membrane potential to reach threshold thus playing a role in setting their frequency. To date, ten sodium channel subunit isoforms have been characterized (Yu & Catterall, 2003, Genome Biol 4:207). In the present study, using single-cell RT-PCR, we looked for the sodium channel isoforms potentially involved in underlying the sodium current expressed in rat cochlear IHCs.

Experiments were performed on immature rat IHCs (P5-P8) in acutely dissected organs of Corti. Single-cell harvesting and RT-PCR were performed as previously described (Chabbert et al., J Physiol 553:113-123). Briefly, patch pipettes were filled with 8 µl of KCl-based intracellular solution. The cytoplasm of individual IHCs was harvested and RNA was transcribed into cDNA. Amplification was performed in two rounds of PCR. The first round was carried out using a primer matching the five TTX-sensitive Na $^{+}$  channels (Na $_{v}$ 1.1, Na $_{v}$ 1.2, Na $_{v}$ 1.3, Na $_{v}$ 1.6, Na $_{v}$ 1.7) together with primers for  $\beta$ -actin. The second round of amplification was performed to determine the molecular identity of the five isoforms.

The results obtained in this study revealed that different  $\alpha$ -subunit isoforms of the TTX-sensitive Na $^+$  channel could be co-expressed within a single IHC, with a major expression of Na $_v$ 1.1 and Na $_v$ 1.7 subunits. The expression of the Na $_v$ 1.7 subunit agrees with previous electrophysiological observations in mouse cochlear IHCs (Marcotti et al., 2003).

Supported by The Royal Society, Wellcome Trust, Deafness Research UK.

# 297 Pre- and Postsynaptic Changes Underlying the Maturation of Inner Hair Cell Ribbon Synapses do not Depend on the Onset of Hearing

**Michel Eybalin**<sup>1</sup>, Nicole Renard<sup>1</sup>, Annelies Schrott-Fischer<sup>2</sup>, Jean-Luc Puel<sup>1</sup>

<sup>1</sup>INSERM U583, Montpellier, France, <sup>2</sup>ENT Department, Innsbruck, Austria

Inner hair cell (IHC) synapses play a key role in the auditory physiology as they ensure transmission of sound stimuli to first auditory neurons. Glutamate is the neurotransmitter responsible for this fast synaptic transmission which essentially involves AMPA receptors. The glutamate release is dependent on L-type Ca2+ channels with Cav1.3 subunit and occurs at synapses equipped with a dense ribbon thought to mediate the continuous and rapid recruitment of its attached vesicles to the release sites. Despite the importance of the IHC synapse, the cellular and molecular machineries underlying its function are still largely unknown despite their elucidation is of prime importance to gain insight into the occurrence of tinnitus and most forms of deafness.

Using immunocytochemistry, we have studied the expression of a selected set of presynaptic proteins (SNAP25, cysteine-string protein, Rab3 and synaptogyrin) during the postnatal maturation of the rodent cochlea and found that, with the exception of Rab3, they were only detected starting postnatal days 10 and 12, when the first, immature, cochlear potentials can be recorded. During the same postnatal period, we also found that the composition and pharmacological properties of the postsynaptic AMPA receptors changed. GluR2 replaced GluR1 at postnatal day 10, switching the potential composition of AMPA receptors from GluR1/3/4 to GluR2/3/4 and their pharmacology to calcium impermeability.

Finally, we have checked the expression of GluR2 and the 4 presynaptic proteins in the cochlea of the deaf Cav1.3 knock out mice and found that they were all expressed at adult IHC synapses suggesting that their expression was not dependent of the first sound stimuli transduced by IHCs.

## 298 Developmental Expression and Targeting of $\gamma$ - and $\beta$ -Actin Within Stereocilia of Inner Ear Hair Cells

Inna A. Belyantseva<sup>1</sup>, Mei Zhu<sup>2</sup>, Gregory I. Frolenkov<sup>3</sup>,

Thomas B. Friedman<sup>1</sup>, Karen H. Friderici<sup>4</sup>
<sup>1</sup>Section on Human Genetics, LMG, NIDCD/NIH, Rockville, MD, <sup>2</sup>Cell and Molecular Biology Program, Michigan State University, East Lansing, MI, <sup>3</sup>Department of Physiology, University of Kentucky, Lexington, KY, <sup>4</sup>Department of Microbiology and Molecular Genetics, Michigan State University, East Lansing, MI

ACTB and ACTG1 encode  $\beta$ -actin and  $\gamma$ -actin, respectively. These two strikingly similar cytoskeletal proteins differ by only four amino acids in primary sequence at their N-termini. Both  $\beta$ - and  $\gamma$ -actin are ubiquitously expressed in non-muscle cells but  $\gamma$ -actin is the predominant form of actin in cochlear hair cells and in intestinal epithelial cells (Hofer et al., Vandekerckhove et al., 1980). Despite the remarkable similarities between  $\beta$ - and  $\gamma$ -actin (Khaitlina, 2001) and, in certain instances, overlapping localizations, such as in hair cell stereocilia (Furness et al., 2005), genetic data indicate that the function of  $\gamma$ -actin is not compensated for by  $\beta$ actin. Missense mutations of non-muscle ACTG1 are associated with dominantly inherited, nonsyndromic, progressive hearing loss linked to the DFNA20/26 locus (Morell et al. 2000; Zhu et al., 2003; Van Wijk et al., 2003; Rendtorff et al., 2006). Using  $\beta$ - and  $\gamma$ -actin specific antibodies, we compared the localization of these two proteins in mouse hair cells during embryonic and postnatal development. Helios gene gun transfection of postnatal inner ear sensory epithelial explants with GFPand DsRed- tagged  $\gamma$ - and  $\beta$ -actin were used to compare their subcellular targeting. Similar to GFP-β-actin, GFP-γactin appeared at the tips of hair cell stereocilia as soon as 4 hours after transfection of the expression vector. However, the time course of GFP-γ-actin incorporation into the actin core of stereocilia was different from the timing reported for GFP-β-actin (Schneider et al., 2002). To further elucidate the role of γ-actin in stereocilia remodeling or repair, we examined  $\gamma$ -actin expression after acute noise trauma. Our preliminary data suggest that the γ-actin level in guinea pig hair cell stereocilia increases after several hours of noise exposure. A possible role for  $\gamma$ -actin in repair of the actin cytoskeleton of stereocilia will be discussed.

# 299 Neomycin Induces the Rapid Externalisation of Phosphatidylserine on the Apical Surface of Early Postnatal Mouse Cochlear Hair Cells

Richard Goodyear<sup>1</sup>, Jonathan Gale<sup>2</sup>, Kishani Ranatunga<sup>1</sup>, Corne Kros<sup>1</sup>, **Guy Richardson**<sup>1</sup>

<sup>1</sup>University of Sussex, <sup>2</sup>University College London Phosphatidylserine (PS) is a phospholipid that is normally restricted to the inner leaflet of the plasma membrane. During cell death, it becomes externalised and can be labelled with annexin V, a PS-binding protein that does not cross the plasma membrane. In isolated strips of the adult guinea-pig organ of Corti, the apical membrane of hair cells can be labelled with externally applied fluorescent annexin V, as can large membrane blebs that form the apical surface of these hair cells (Shi et al., Am J Physiol, 2005).

Hair cells in cochlear cultures prepared from early postnatal (P0-P3) mice do not label with fluorescent annexin V. However, the addition of 1 mM neomycin induces the rapid (within ~1 min) externalisation of PS, both at room temperature and at 37°C. Annexin V binding is observed first on the hair bundle and then on small, vesicle-filled membrane blebs that form around the perimeter of the hair cell's apical surface. Consistent with this, the membrane capacitance of outer hair cells superfused with 1 mM neomycin increased from 6.1 to 9.3 pF within minutes (n = 5). Neomycin induced PSexternalisation is only observed in hair cells, and is restricted to the apical surface. A basal-to-apical gradient of PS-externalisation is seen along the cochlea that correlates with the ability of the hair cells to load with FM1-43. PS-externalisation could not be blocked by the PI-3 kinase inhibitor LY294002 (10 µM), the adenylate cyclase inhibitor SQ25536 (0.5 mM), or the PI-4 kinase inhibitors, phenylarsine oxide (30 µM) or quercetin (2 mM). Upon neomycin washout, annexin V-PS complexes are rapidly internalised. This process is temperature dependent, failing to occur at 20°C and reaching completion within 2 hours at 37°C.

These results reveal the dynamic behaviour of the hair cell's apical membrane and suggest neomycin may act directly on proteins that normally maintain the orientation of phospholipids in the bilayer.

Supported by the Welcome Trust and the MRC

### 300 Comparison of Activated Caspase Detection Methods in the Chick Cochlea Following Gentamicin Treatment *In Vivo*

Brittany J. Chapman<sup>1</sup>, Jessica L. Guidi<sup>1</sup>, Luke J. Duncan<sup>1</sup>, **Christina L. Kaiser**<sup>1,2</sup>, Caitlin E. Terry<sup>1</sup>, Dominic A. Mangiardi<sup>1,3</sup>, Jonathan I. Matsui<sup>1,4</sup>, Douglas A. Cotanche<sup>1,2</sup> <sup>1</sup>Department of Otolaryngology, Children's Hospital, Boston, MA 02115, <sup>2</sup>Department of Otology and Larvngology, Harvard Medical School, Boston, MA 02214. <sup>3</sup>Department of Biomedical Engineering, Boston University, Boston, MA 02215, <sup>4</sup>Department of Molecular and Cellular Biology, Harvard University, Cambridge, MA 02138 Aminoglycoside antibiotics induce caspase-dependent apoptotic death in cochlear hair cells. Apoptosis, a regulated form of cell death, can be induced by many stressors, which activate signaling pathways that result in the controlled dismantling of the affected cell. The caspase family of proteases is activated in many apoptotic signaling pathways and is responsible for cellular destruction during apoptosis. Two caspases have been identified as being activated in sensory hair cells following aminoglycoside exposure: the initiator caspase-9 (cas-9) and the effector caspase-3 (cas-3). We have analyzed caspase activation in the avian cochlea during gentamicin-induced hair cell death using two techniques: caspase antibody labeling and CaspaTag in situ assay kits. Caspase antibodies bind to the cleaved activated form of cas-9 or cas-3 in specific locations in fixed tissue. Recently, studies have used CaspaTag, a fluorescent inhibitor that binds to a reactive cysteine residue on the large subunit of the caspase heterodimer, in unfixed tissue to examine caspase activation in sensory hair cells (Sugahara et al., Hear. Res. Epub. 2006).

To induce cochlear hair cell loss, 1-2 week-old chickens were given a single injection of gentamicin (300mg/kg). Chicks were sacrificed 30, 42, 48, 54, 72, 96, or 120 hours after injection. Cochleae were dissected and labeled for activated cas-3 or cas-9 using either CaspaTag in situ assay kits or with caspase-directed antibodies. Ears were co-labeled with either phalloidin or myosin VI both to visualize hair cells and to determine the progression of cochlear damage. While the timing of caspase activation was similar using both assays, the CaspaTag method labeled more cells than the antibody labeling, as well as labeling cells at later times following ejection. Additionally, our results show that both cas-3 and cas-9 are activated simultaneously in hair cell death immediately prior to or during their ejection.

Supported by NIH NIDCD grants DC01689 (DAC) DC008235 (CLK).

# 301 Effects of Ototoxic Drugs on Intercellular Communication in Cochlear Cell Line (HEI-OC1) and Preventive Effect of Green Tea and Ginkgo Biloba Extracts

**Yun-Hoon Choung**<sup>1</sup>, Keehyun Park<sup>1</sup>, You Ree Shin<sup>1</sup>, Seong Jun Choi<sup>1</sup>, Hun-Yi Park<sup>1</sup>, Sungook Kang<sup>1</sup>

\*Ajou University School of Medicine

Background and Objectives: The ototoxic mechanisms of cisplatin and aminoglycosides may be related with deterioration of intercellular communication in the cochlea. The objectives of this study are to examine the effect of ototoxic drugs on intercellular communication in cochlear cell line (HEI-OC1) and to evaluate the preventive effect of green tea and ginkgo biloba extracts against ototoxicity.

Methods: To evaluate ototoxicity of gentamicin (GM), streptomycin (SM), and cisplatin, we performed 'neutral red uptake test'. Reverse transcription-polymerase chain reaction (RT-PCR), Western blot, immunocytochemistry staining were done to identify the change of the connexin (Cx26, 29, 30, 31, 43) expression. 'Scrape load dye transfer assay'(SLDTA) was done to evaluate the intercellular communication of HEI-OC1 cells. And we also carried out the above experiments administrating epicatechin (EC), epigallocatechin gallate (EGCG), and ginkgo biloba extracts (GB) to ototoxic drugs in HEI-OC1 cells.

Results: Cx26, Cx30, Cx31, and Cx43 were expressed in HEI-OC1 cells. Through RT-PCR and Western blot, ototoxic drugs down-regulated the expression of Cxs, and EC (50 / ), EGCG (50 $\mu$ M), and GB (300  $\mu$ M) inhibited down-regulation effect of these ototoxic drugs. Immunocytochemistry of HEI-OC1 cells showed the decreased expression and abnormal location of Cxs under ototoxic drugs. SLDTA for functional study showed that GM, SM, and cisplatin down-regulated intercellular

communication, while EC, EGCG, and GB prevented down-regulation effect of these ototoxic drugs.

Conclusion: Gap junctional intercellular communication may play an important role in ototoxic mechanism of aminoglycosides and cisplatin.

This work was supported by the Korea Research Foundation Grant funded by the Korean Government (MOEHRD, Basic Research Promotion Fund) (KRF-2006-E00081)

### 302 Acute Inner Ear Energy Failure Causes Vestibular Hair Cell Damage and Balance Disorder

**Kunio Mizutari**<sup>1,2</sup>, Masato Fujioka<sup>1</sup>, Masato Fujii<sup>2</sup>, Kaoru Ogawa<sup>1</sup>, Tatsuo Matsunaga<sup>2</sup>

<sup>1</sup>Department of Otolaryngology, Keio University School of Medicine, <sup>2</sup>National Institute of Sensory Organs, National Tokyo Medical Center

ATP deprivation in the inner ear caused by decrease of oxygen supply represents a mechanism of some types of inner ear disorders such as inner ear ischemia. Recently, we established a novel animal model of inner ear energy failure using mitochondrial toxin, 3-nitropropionic acid (3-NP)(Hoya et al, 2004). In this animal model, balance disorder was observed in addition to auditory disorder. Auditory disorder was primarily caused by degeneration of cochlear fibrocytes in this model (Okamoto et al. 2005). In the present study, we analyzed time course of vestibular function and structural changes in the peripheral vestibular organs in order to reveal the mechanism of balance disorder in this animal model. SD rats were used. After anesthesia, 3 (I of 3-NP (300 mM or 500 mM) or saline was administered into the round window niche. Then, the spontaneous nystagmus was recorded at several time points using infrared CCD camera. At 7 d after surgery, caloric test using ice water was performed for evaluation of vestibular function. Structural and residual ultrastructural analyses were carried out at 7 d after surgery.

Spontaneous nystagmus reached a peak at 6 h after surgery in both 300 mM and 500 mM 3-NP groups. The nystagmus attenuated gradually and disappeared at 3 d after surgery in both groups. Caloric test was conducted at 1 w after surgery. Nystagmus was induced in 300mM group, but not induced in 500mM group.

SEM study revealed severe loss of stereocilia in 500mM group and disorganized and mildly reduced stereocilia in 300mM group. TEM study revealed severe loss of hair cells in 500mM group, but only slight loss of hair cells in 300mM group. Balance disorder was permanent in 500 mM group while it was reversible in 300 mM group. These findings indicate that balance disorder in the present animal model was caused by damages in the vestibular hair cells. Thus, different pathological mechanisms appear to work for auditory and balance disorders due to acute inner ear energy failure.

### 303 Using Two-Photon, Two-Channel, Metabolic Imaging to Determine the Metabolic Status of the Cochlea

**LeAnn Tiede**<sup>1</sup>, Richard Hallworth<sup>1</sup>, Kirk Beisel<sup>1</sup>, Michael Nichols<sup>1</sup>

<sup>1</sup>Creighton University

Metabolism and mitochondrial dysfunction are thought to be involved in many different hearing disorders including presbycussi and pathological response to disease and injury. Previously, studies of the metabolic status of the organ of Corti. involved usina invasive immunohistochemical studies of mitochondrial enzymes in fixed tissue, with little direct quantification of the metabolic status of mitochondria. Here, we employed two-photon fluorescence imaging of intrinsic fluorophores to study the metabolic capabilities of the different cell types in an excised intact mouse organ of Corti preparation. Reduced nicotinamide adenine dinucleotide (NADH) and the oxidized forms of flavoproteins (Fp) both fluoresce when excited by femtosecond pulses of 740-nm light. Since NADH fluoresces only when reduced and Fp only when oxidized these two intrinsic fluorophores can be used in concert to determine the relative percentages of oxidized and reduced energy equivalents in cells. The results were that inner and outer hair cells both exhibited time dependent changes in the concentrations of oxidized and reduced energy equivalents ranging from 100% reduced to 100% oxidized. This technique is feasible as a means of quantifying the metabolic state of the organ of Corti.

### 304 COUP-TFI Controls Notch-Dependent Hair Cell and Supporting Cell Differentiation

Louisa Tang<sup>1</sup>, Heather Alger<sup>1</sup>, **Fred Pereira**<sup>1,2</sup>

<sup>1</sup>Baylor College of Medicine, <sup>2</sup>Bobby Alford Department of Otolaryngology–Head and Neck Surgery

Orphan nuclear receptor COUP-TFI (NR2F1) regulates many aspects of mammalian development but little is known about its role in cochlear hair cell and Deiter's support cell development. The COUP-TFI knockout (COUP-TFI-/-) has a significant increase in hair cell (HC) number in the mid-to-apical turns: there are frequent inner hair cell (IHC) duplications, 4 rows of outer hair cells (OHC) in the middle turn and up to 6-7 rows of OHCs at the apex, all with an equal number of underlying Deiter's support cells. The total number of hair cells is not increased over wild type, perhaps due to displaced hair cells and a shortened cochlear duct. This implicates a defect of convergent-extension in the COUP-TFI-/- duct. In addition, excess proliferation in the COUP-TFI-/sensory epithelium indicates the origin of the extra HCs in the apex is complex. Since loss-of-function studies of Notch signaling components have similar phenotypes, we investigated Notch regulation of hair cell differentiation in the COUP-TFI-/- mice. In situ hybridization and quantitative real-time PCR analyses confirmed misregulation of Notch signaling components, including Jag1, Hes5 and Lfng, in a manner consistent with reduced Notch signaling and correlated with increases in hair cell and support cell differentiation in COUP-TFI-/- mice.

Disruption of Notch signaling by a ?-secretase inhibitor in an in vitro organ culture system of wild type cochleae resulted in a reduction in expression of the Notch target gene Hes5 and an increase in hair cell differentiation. Importantly, inhibition of Notch activity resulted in a greater increase in hair cell differentiation in COUP-TFI—/—cochlear cultures than in the wild type cultures suggesting a hypersensitivity to Notch inactivation in COUP-TFI—/—cochlea, particularly at the apical turn. Taken together, we present evidence that reduced Notch signaling contributed to increases in hair cell and support cell differentiation in COUP-TFI—/— mice and suggest COUP-TFI is required for Notch regulation of hair cell and support cell differentiation.

#### 305 COUP-TFI Signaling in the Inner Ear

**Celina Montemayor**<sup>1</sup>, Feng Lin<sup>1</sup>, Patricia Pardo<sup>1</sup>, David A. Wheeler<sup>1</sup>, Scott D. Pletcher<sup>1</sup>, Fred A. Pereira<sup>1</sup>

<sup>1</sup>Baylor College of Medicine

The orphan nuclear receptor COUP-TFI (NR2F1) is a member of the nuclear receptor superfamily for which no ligand and precise function are known. The presence of COUP-TF homologues across species and their stunning interspecies similarity indicate that these nuclear receptors play an essential role that has been conserved during evolution. There are two members of this family in mice: COUP-TFI and COUP-TFII, and although they have overlapping expression patterns, knockout studies revealed that each has a vital, specific developmental function. Of particular interest to our lab, COUP-TFI-/mice exhibit an increase in inner ear hair cell numbers, having up to 9 total hair cell rows. To better understand the function of this orphan receptor in the development of mouse inner ear, we seek to define components of the COUP-TFI signaling pathway by identifying in vivo targets. We have obtained microarray gene expression profiles of wild-type and COUP-TFI-/- inner ear tissues. Analysis of identical and experimental replicates revealed a list of 176 genes that are significantly different in expression across genotypes. Gene ontology analysis revealed a significant over-representation of cell cycle, cell adhesion, myeloid cell differentiation, and lipid metabolism-related genes. Real-time RT-PCR confirmed 8 of our top 10 hits, and we describe one such target: Aurora kinase B (Aurkb). We have confirmed in vivo deregulation of Aurkb transcript in P0 and E16 COUP-TFI-/- inner ears, as well as deregulation, at the transcript and protein levels, in HeLa cells over-expressing COUP-TFI. In agreement with these findings, HeLa cells over-expressing COUP-TFI and COUP-TFI-/- MEFs display a cell-cycle arrest phenotype consistent with Aurora B deregulation. These results suggest that regulation of Aurora B expression is a mechanism by which COUP-TFI modulates cell cycle progression during inner ear development. Further analyses will be done to identify the COUP-TFI binding site within the Aurora B promoter and the role of this kinase in the inner ear.

## 306 The Role of EYA1 in Inner Ear Development and Branchio-Oto-Renal Syndrome

Erica LI<sup>1</sup>, Jose Manaligod<sup>1</sup>, **Daniel Weeks<sup>2</sup>** 

<sup>1</sup>Department of Otolaryngology-Head and Neck Surgery, <sup>2</sup>Department of biochemistry

EYA1 mutations result in branchio-oto-renal (BOR) syndrome, an autosomal dominant syndrome that features sensorineural hearing loss. Although knockout mouse models that replicate the BOR phenotype point towards haploinsufficiency as the mechanism for this disease, the possibility of a dominant negative effect has not been explored to date.

We have started to address this question using the embryos of the South African clawed frog, Xenopus laevis, as an animal model to study early ear development.

EYA1 mRNAs encoding known BOR causing mutations were injected into two-cell embryos. We show that expression of these mutations, even in the presence of normal levels of endogenous EYA1, leads to morphologically abnormal ear development as judged by overall size of the otic vesicle and pattern of ear innervation. The molecular consequence of expression of the mutant forms of the EYA1 gene was assessed by quantitative PCR analysis. Embryos expressing mutant EYA1 showed altered levels of several of genes important for normal ear development. These studies lend support the hypothesis that a dominant negative effect may be one of the mechanisms by which EYA1 mutations result in BOR..

### 307 Requirement for Lmo4 in the Vestibular Morphogenesis of Mouse Inner Ear

Min Deng<sup>1</sup>, Ling Pan<sup>1</sup>, Xiaoling Xie<sup>1</sup>, **Lin Gan<sup>1</sup>**<sup>1</sup>University of Rochester

In vertebrate inner ear, auditory and vestibular components are derived from defined compartments within the otocyst. Currently, the molecular mechanisms underlying the otic compartmentalization are largely unknown. Here, we show that the expression of LMO4, a LIM-domain-only transcriptional regulator, demarcates the dorsolateral otocyst. Targeted disruption of Lmo4 results in the vestibular dysmorphogenesis with an absence of three semicircular canals, anterior and posterior cristae, and a loss of the lateral crista and utricular macula with a variable expressivity. In the Lmo4-null otocyst, the formation of canal outpouches is severely impaired and the cell proliferation is reduced in the dorsolateral region. Furthermore. Lmo4-null mutation abolishes dorsolateral expression of Dlx5, an otic patterning gene essential for the development of vestibular structures. Our results demonstrate that Lmo4 is essential for the compartmentalization of the otocyst by regulating the expression of otic patterning genes, revealing a novel role of Lmo4 in developing mouse vestibule.

# 308 Hes1 Cotributes to the Proliferative Capacity of Sensory Precursors in Addition to the Cell Diversification During Mammalian Inner Ear Development

**Junko Murata**<sup>1</sup>, Akinori Tokunaga<sup>2</sup>, Toshiyuki Ohtsuka<sup>3</sup>, Ryoichiro Kageyama<sup>3</sup>, Katsumi Doi<sup>1</sup>, Arata Horii<sup>1</sup>, Manabu Tamura<sup>1</sup>, Takako Iwaki<sup>1,4</sup>, Takeshi Kubo<sup>1</sup>, Hideyuki Okano<sup>2</sup>

<sup>1</sup>Department of Otolaryngology, Osaka University School of Medicine, <sup>2</sup>Department of Physiology, Keio University School of Medicine, <sup>3</sup>Institute for Virus Research, Kyoto University, <sup>4</sup>Department of Communication Disorders and Sciences, Aich Shukutoku University

We reported in the last ARO MWM that Notch1 activation should initially demarcate a prosensory region in the cochlear epithelium and then inhibit progenitor cells from becoming hair cells via classical lateral inhibition during inner ear development by revealing the spatio-temporal pattern of Notch1 activation. A positive feedback loop was assumed to exist between the expression of Jagged1 (Jag1), and Notch1 activation by Jag1 in the earlier stage before hair cell differentiation, is thought to be critical for the maintenance of the sensory precursors. Indeed, other recent papers have shown consistent results mainly by using Jag1-conditional knockout (cko) mice. They showed several types of sensory epithelial defects in the inner ear of Jag1-cko mice (ref. #1, #2).

The maintenance of the sensory precursors includes at least the specification, survival, and the proliferative capacity of them. About the regulation of progenitor cell proliferation, Murata K and their co-researchers indicated that Hes1 directly contributes to the promotion of progenitor cell proliferation through transcriptional repression of a cyclin kinase inhibitor p27Kip1 at least in thymi, livers, and brains (ref. #3).

This time, we investigated the exact expression pattern of Hes1 and Hes5 during the mouse inner ear development, and analyzed Hes1 knockout (KO) mice to clarify the function of Hes1 especially in the proliferative regulation of sensory precursors. Hes1 expression was observed from earlier stage before hair cell differentiation and seemed to depend on the weak Notch1 activation. P27Kip1 was expressed stronger in wider region of cochlear epithelium of Hes1 KO mice as compared with wild type littermates. The number of BrdU-positive proliferating cell was reduced in the KO littermates. These results implicated that Notch-Hes1 pathway may contribute to the adequate proliferation of sensory progenitor cells through the control of p27Kip1 expression.

#### References:

#1 Brooker R et al. Development (2006)

#2 Kiernan AE et al. PLoS Genetics (2006)

#3 Murata K et al. Mol Cell Biol (2005)

#4 Murata J et al. J Comp Neurol (2006)

### 309 Hey Genes Delineate the Sensory Epithelium Lineage in the Developing Inner Ear

**Toshinori Hayashi<sup>1,2</sup>**, Thomas Reh<sup>3</sup>, Hiroki Kokuba<sup>4</sup>, Olivia Bermingham-McDonogh<sup>2,3</sup>

<sup>1</sup>University of Washington, <sup>2</sup>Virginia Merrill Bloedel Hearing Research Center, <sup>3</sup>University of Washington, <sup>4</sup>National Institute of Genetics, Japan

The Notch signaling system is known to be critical for proper inner ear development. Several lines of evidence indicate that Notch is required for at least two phases of development of mouse inner ear. The most well studied role for Notch in cochlear development is in the process of lateral inhibition. In this phase, Delta1 and jagged2 are expressed in the differentiating hair cells and feedback on the Notch expressing supporting cells to inhibit them from differentiating as hair cells. In addition to this function, Jagged1/Notch signaling serves a "prosensory" function earlier in inner ear development. bHLH proteins, Hes1 and Hes5, have been shown to have a role as Notch effectors in the lateral inhibitory phase of cochlear development. However, the Notch effectors for the earlier, prosensory phase of inner ear development are not known.

To investigate this question, we analyzed the expression pattern and function of the Hey genes classified as members of the hairy/enhancer of split family and shown to be important in neural and cardiovascular development. We have found that Hey1 and Hey2 are expressed within the presumptive organ of Corti, as early as cochlear duct formation. The expression of both Hey1 and Hey2 in the developing organ of Corti precedes expression of Math1, which is one of the earliest genes expressed by differentiating hair cells. Their expression pattern coincides both spatially and temporally with Jagged1 expression. By contrast, the Hes genes are expressed only at later stages of development. These expression patterns of Hey1, Hey2 related genes suggest that Hey1/2 has prosensory function for these genes in the developing organ of Corti.

Our analysis of the Hey1 and Hey2 deficient mice failed to show any defects in the development of the hair cells or support cells in the organ of Corti. This may be due to a functional redundancy in these genes, since they are expressed in largely overlapping domains during most of cochlear development.

#### 310 Atoh1 Gene Network in Cochlear Hair Cells

**Kirk Beisel**<sup>1</sup>, Sonia Rocha-Sanchez<sup>1</sup>, Aimee Limpach<sup>1</sup>, Bernd Fritzsch<sup>1</sup>

<sup>1</sup>Creighton University

Members of the basic helix loop helix (bHLH) genes are transcription factors that play pivotal roles in cell fate specification during the development of a variety of tissues and cell lineages. In the inner ear, *Atoh1* is crucial for hair cell differentiation, but is now known to be regulated by other genes in its epithelial and cellular expression. Other bHLH genes, such as *Neurog1*, were identified prior to *Atoh1* expression and contribute to hair cell fate

delineation. The bHLH proteins form an interactome network, a combinatorial complex, that specifics DNA targeting and binding affinities. This complex includes the transducin-like enhancers of split, runt-related transcription factors, forkhead and either activator or repressor bHLH proteins. Heterodimers can bind to *E-box* and *N-box* DNA motifs which should be present in the promoter regions or enhancer elements of downstream genes.

Our goal is to idenify additional bHLH candidates regulating hair cell fate and Atoh1 down-stream genes involved in differentiation. For these transcriptome-based experiments, microarray analyses were performed using several platforms, including the Affymetrix Mouse Expression Set 430 chip, an Agilent Mouse Development 44K Oligo microarray and two custom cDNA arrays, BMAP and CMA-IE1. Dissected organs of Corti (OC) were obtained from E18.5 Atoh1 null and heterozygous littermates and total RNAs were isolated. Comparisons, including dye switching, between the OC from null and heterozygote transcriptomes were done using either amplified or non-amplified labeled probes. Differential expression was observed with 400 or more genes that retain expression in the heterozygous (wild type) OC. Mean intensity and mean fold changes of differences between the heterozygous and null genotypes were based statistical evaluated. As predicted, genes such as Atoh1, Pou4F3, Myo7a, Gfil were absent in the null OC. A number of bHLH genes associated with the Hes subfamily were also differentially expressed. Many of the genes in the Delta-Notch pathway were also down regulated, indicating that Notch signaling and the subsequent lateral inhibition between hair cells and supporting cells was also disrupted. Based on these data, we are constructing an Atoh1-dependent gene regulatory network for the differentiation of hair cells and supporting cells in the cochlea. Downstream genes of this network are being examined for the presence of *E*- or *N*-box motifs in their respective promoter and putative enhancer elements.

## 311 Interdependent Regulation of Ngn1 and Math1 Controls Cell Fate During Inner Ear Development

**Steven Raft**<sup>1</sup>, Herson Quinones<sup>2</sup>, Edmund Koundakjian<sup>3</sup>, Jane Johnson<sup>2</sup>, Lisa Goodrich<sup>3</sup>, Neil Segil<sup>1</sup>, Andrew Groves<sup>1</sup>

<sup>1</sup>House Ear Institute, <sup>2</sup>University of Texas Southwestern Medical Center, <sup>3</sup>Harvard Medical School

Information pertaining to balance and hearing reaches the CNS along a pathway composed of mechanosensory hair cells and cranial sensory neurons. In the embryo, production of hair cells and their associated sensory neurons requires, respectively, the related bHLH genes Math1/Atoh1 and Ngn1/Neurog1. To address the issue of developmental relatedness between these two cell types, we investigated the transition from neurogenesis to hair cell generation during ear development in the mouse, focusing on a heretofore uncharacterized period of temporal overlap between the two processes. Gene expression and Cre-loxP-mediated fate-mapping indicate that a subset of vestibular hair cells is generated from a

region of recent and ongoing neural precursor production. Mutant phenotypes show that the coordinated production of neural precursors and nascent hair cells from this region is regulated by a mutual antagonism between Math1 and Ngn1. We also reveal opposite modes of autoregulation for these two genes in the developing inner ear. These results define genetic regulatory relationships that are essential for converting a neurogenic epithelium into a pair of inner ear sensory epithelia. We propose that neural precursors and a subset of nascent vestibular hair cells are immediate derivatives of a common, multipotent progenitor cell population.

### 312 Expression of Tbx Genes is Regulated by Retinoid Signaling in Mouse Embryonic Stem Cells

**Benjamin Meyer**<sup>1</sup>, Heather Aloor<sup>1</sup>, Rebecca Chan<sup>1</sup>, Eri Hashino<sup>1</sup>

<sup>1</sup>Indiana University School of Medicine

Retinoic acid (RA), the active vitamin A derivative, is a signaling molecule that controls embryonic development through transcriptional regulation of an array of downstream target genes. We previously showed that Tbox family genes, including Tbx1, -2 and -3, are expressed in the embryonic ear. Since Tbx2 was shown to contain a retinoic acid response element in its promoter, we tested in this study whether RA directly or indirectly regulates expression of some of the Tbx genes using mouse embryonic stem (ES) cells as a model system. Incubation of ES cells with RA for 5 days increased Tbx2 by 40-fold, whereas Tbx1 expression was down-regulated to only 11% of the level without RA. Interestingly, Tbx3 was expressed constitutively at a high level in undifferentiated ES cells, but was down-regulated after differentiation. Incubation of differentiated ES cells with RA further reduced the Tbx3 level. These results clearly demonstrate that expression of Tbx1, -2 and -3 is regulated by distinct mechanisms: Tbx2 is positively regulated by RA, whereas Tbx1 and Tbx3 are negatively regulated by RA. To test whether RA-induced upregulation of Tbx2 is mediated by RAR $\alpha$  and/or  $-\gamma$  receptors, we silenced expression of these RAR receptors using the RNA interference technique. ES cells were transfected with anti-RARα and anti-RARy siRNAs in combination and grown in the presence of 1 µM RA for 24-48 h, after which total RNA was isolated for quantitative RT-PCR analysis. transfection efficiency estimated by a GFP reporter assay was approximately 80%. Double transfection with anti-RARα and -y siRNAs resulted in 55% and 64%, respectively, reduction of their targeted receptor gene expression. The Tbx2 mRNA level in double-transfected ES cells was approximately 50% of that in ES cells tranfected with non-targeted siRNA. These results strongly suggest that RA instructively regulates Tbx2 expression in ES cells through constitutive RARα and -y receptors.

#### 313 Spatio-Temporal Expression Patterns of Tlx3 in the Developing Inner Ear

**David Zopf**<sup>1</sup>, Takako Kondo<sup>1</sup>, Heather Aloor<sup>1</sup>, Eri Hashino<sup>1</sup>

Indiana University School of Medicine

Tlx3 is a member of the T-cell leukemia (Tlx) family of homeobox genes. Previous studies have suggested that Tlx3 promotes specification of glutamatergic neurons while inhibiting GABAergic differentiation. Tlx3-deficient mice showed reduced VGLUT2 expression in the dorsal horn and abnormalities in the formation of primary visceral sensory neurons in the brainstem. To begin elucidating novel functions of Tlx3 in auditory/vestibular sensory neuron development, we analyzed spatio-temporal expression patterns of Tlx3 transcripts in the embryonic mouse inner ear. Our quantitative RT-PCR analysis showed that the Tlx3 mRNA level was highest at early embryonic stages (E9-10), after which it declined sharply between E12 and E14. The temporal changes in expression of Tlx3 coincided with those of Neurogenin1 Whole-mount in situ hybridization was and NeuroD. performed with E9 and E10 embryos to reveal gross expression patterns. Tlx3 expression was confined to cranial sensory ganglia, including the trigeminal (V), facioacoustic (VII-VIII), glossopharyngeal (IX) and vagus (X) ganglia, as well as dorsal root ganglia in the spinal cord. In-situ hybridization with transverse cryostat sections cut through the E10 otocyst revealed strong Tlx3 signals in the vestibulocochlear ganglion. Interestingly, only subpopulation of cells in this ganglion was positive for Tlx3, which was in striking contrast with ubiquitous Tlx3 expression in the trigeminal ganglion. No Tlx3 expression was observed in the otic epithelium. Comparison of expression patterns indicated that the Tlx3-positgive domain partially overlaps with the Neurogenin1-positive At E12, strong, but mottled, staining was domain. observed in the vestibulocochlear ganglion. At E16, the vestibular ganglion showed faint staining for Tlx3, whereas the cochlear partition was devoid of Tlx3 expression. These results suggest that Tlx3 might be involved in differentiation of a specific neuronal subtype in the inner ear.

## 314 Forced Expression of Tlx3 Results in Induction of Proneural and Glutamatergic Marker Genes in Embryonic Stem Cells

Takako Kondo<sup>1</sup>, Eri Hashino<sup>1</sup>

<sup>1</sup>Indiana University School of Medicine

The T-cell leukemia 3 (Tlx3) gene has been implicated in specification of glutamatergic sensory neurons. Forced expression of Tlx3 in the dorsal horn of the spinal cord is sufficient to induce ectopic expression of glutamatergic neuron markers, while suppressing **GABAergic** differentiation. Since we found that Tlx3 is highly expressed in the vestibulocochlear ganglion at early embryonic stages, we wanted to test whether Tlx3 plays a role in differentiation of inner ear sensory neurons. A Tlx3 expression vector was constructed by cloning a mouse full-length Tlx3 cDNA into a modified pBud-eGFP vector backbone. Mouse embryonic stem (ES) cells (R1) were transfected with pBud-eGFP-TIx3 or pBud-eGFP control vector using an Amaxa nucleofection kit. After negative selection by Zeocin and expansion, stably transfected ES cells were exposed to neural induction medium containing N2 and BDNF. Microscopic examination revealed that nearly 100% of expanded ES cell clones were eGFPpositive, verifying the transfection efficiency. High Tlx3 expression was detected in ES cells expressing pBudeGFP-Tlx3, but not in untreated ES cells or ES cells expressing pBud-eGFP. Quantitative RT-PCR analysis of undifferentiated ES cells showed that there were no significant differences in gene expression between Tlx3 expressing cells and cells devoid of Tlx3. In contrast, the expression levels of Mash1, Neurogenin1 and NeuroD in Tlx3-expressing ES cells grown in neural induction medium for 4 days were approximately 5-fold higher than those in ES cells expressing the control vector. Moreover, the VGLUT2 mRNA level in Tlx3-expressing ES cells was 30-fold higher than that in control cells. These results strongly suggest Tlx3 as an upstream regulator of the proneural and gultamatergic marker genes. In addition, the differences in effects of Tlx3 overexpression between undifferentiated and differentiated ES cells suggest that Tlx3 exerts context-dependent transcriptional signals on their target genes.

#### 315 FGF Signaling in Otic Development

Ekaterina Hatch<sup>1</sup>, Albert Noyes<sup>1</sup>, Xiaofen Wang<sup>1</sup>, Lisa Urness<sup>1</sup>, Tracy Wright<sup>2</sup>, **Suzanne Mansour<sup>1</sup>** 

<sup>1</sup>University of Utah, <sup>2</sup>University of Edinburgh

Development of the inner ear proceeds through phases of otic placode induction, axis specification, otocyst formation and morphogenesis, and cell type specification. FGF signaling is required during all of these developmental events. In particular, we have shown that Fgf3, Fgf10 and Fgf8 have essential, sequential roles in mouse otic placode induction. These three Fgf genes are also expressed during later phases of otic development, but their later roles are obscured in global knockout mice and particularly in double mutant combinations, by lethality and/or the sequelae to abnormal induction. To achieve temporal and spatial separation of the multiple functions of these signals throughout otic development, we are analyzing embryos carrying various combinations of conditional Fqf alleles inactivated using a variety of CRE drivers. Our analyses show that the endodermal oticinducing FGF signal is provided redundantly by Fgf3 and Fqf8. In contrast, ectodermal expression of these two genes is not required for otic induction. In addition, Fgf3, likely from the hindbrain, is required with variable penetrance and expressivity for otic morphogenesis. Its absence leads to endolymphatic duct/sac and common crus aplasia and cochlear dilation, which are preceded by disturbances of dorsal otic marker genes. In addition, we find that embryos with reduced levels of Fgf10 specifically lack the posterior semicircular canal. We will present these results together with studies of Pax2-Cre- and Foxq1-Cremediated inactivation of Fgf3+Fgf10 and Fgf3+Fgf8.

#### 316 A Zebrafish Mutation Affecting Fibroblast Growth Factor Signaling in the Inner Ear

Yukako Asai<sup>1</sup>, Dylan Chan<sup>1</sup>, Catherine Starr<sup>1</sup>, James Kappler<sup>1</sup>, Richard Kollmar<sup>1</sup>, James Hudspeth<sup>1</sup>

<sup>1</sup>Howard Hughes Medical Institute and The Rockefeller University

A zebrafish mutant line (ru622) identified in our mutagenesis screen displays developmental functional defects of the inner ear. Initially isolated because of their inconsistent startle response at five days post-fertilization, the mutant larvae swim upside-down or in circles, an indication of a vestibular defect. The animals are, however, responsive to touch stimulation and appear grossly normal. In 28% of the mutants, each ear has only one otolith whose shape is often irregular; this phenotype may result from otolithic fusion. The mesenchymal pillars that form the semicircular canals are often abnormal, and fail to elongate and fuse. The morphological and behavioral phenotypes of acerebellar zebrafish, which are defective in the corresponding gene, resemble those of ru622.

Using simple sequence-length polymorphisms and singlenucleotide polymorphisms, we mapped and cloned the gene mutated in ru622. The chromosomal region encompassing the gene displays conserved synteny with human chromosomal region 1p36. Fine-resolution mapping indicated that the mutation occurred at a splicedonor site in a zebrafish homolog of atrophin2.

Atrophin2 has been proposed to serve as a transcriptional co-repressor in the mouse and fly. In keeping with this idea, the expression levels of fqf8 and sef, an antagonist of fgf signaling were examined and found to be overexpressed in ru622 mutants. The larvae whose atrophin2 expression had been diminished with morpholinos were rescued by reducing the expression of Sef. We therefore hypothesized that an excess of Sef. eliminates Fqf signals and produces an fqf8 null phenotype in ru622 mutants: The resultant imbalance of Fgf8 and Sef signals then underlies the abnormal aural development observed in ru622.

#### 317 Disruption of FGFR3 Signaling Results in Defects in Cellular Differentiation, **Neuronal Patterning, and Hearing Impairment**

Chandrakala Puligilla<sup>1</sup>, Feng Feng<sup>2</sup>, Kotaro Ishikawa<sup>3</sup>, Carmen Brewer<sup>3</sup>, Christopher Zalewski<sup>3</sup>, Alain Dabdoub<sup>1</sup>, Bernd Fritzsch<sup>2</sup>, Andrew Griffith<sup>3</sup>, Matthew Kelley<sup>1</sup> <sup>1</sup>National institutes of Health, NIDCD, Section on Developmental neuroscience, <sup>2</sup>Creighton University, <sup>3</sup>National institutes of Health, NIDCD, Otolaryngology

Branch

Fibroblast growth factor receptors (FGFRs) are a family of tyrosine kinases that signal transmembrane interactions with the family of FGFs. Mutations in FGFR genes cause a variety of craniosynostosis and chondrodysplasia syndromes in humans. Our study focuses on FGFR3 as mutations in FGFR3 result in various clinical skeletal disorders including Muenke

Here, we report that Muenke syndrome syndrome. patients also exhibit low frequency hearing loss. Similarly, mice with a targeted deletion of Fgfr3 exhibit significant hearing loss and a complete lack of distortion product otoacoustic emissions. To investigate the basis of this auditory defect, we examined the inner ears of the Fgfr3-/mice. We demonstrate that deletion of Fgfr3 leads to an increase in the number of outer hair cells accompanied by alteration of supporting cell morphology leading to changes in cellular patterning within the sensory epithelium. Furthermore, we observed defects in neuronal innervation that are consistent with changes in the role of supporting cells in the guidance of spiral ganglion fibers. Finally, we show enlarged vessels in the stria vascularis indicating degeneration of the structure. In order to elucidate the mechanisms underlying the effects of Fgfr3 in the cochlea, we examined the expression of Bmp4 and Ihh - known downstream targets of Fgfr3 signaling. Expression levels for both Bmp4 and Ihh were increased in cochleae from Fgfr3-/- mice, suggesting an inhibitory role of Fgfr3. Consistent with these results, exogenous application of localized Bmp4 on wild type cochlear explants induced a significant increase in the number of hair cells while inhibition of Bmp4 resulted in a significant decrease. These results demonstrate that Fgfr3 regulates multiple developmental processes in the cochlea including cellular differentiation, patterning, and innervation.

#### 318 Dynamics of FGF3 Expression in the **Developing Mouse Inner Ear**

Mark Maconochie<sup>1</sup>, Androulla Economou<sup>1</sup>

<sup>1</sup>University of Sussex, UK

The fibroblast growth factors are required for early inner ear development in a number of different vertebrate species. Recent studies have focussed on early inner ear inductive roles, revealing that in the mouse, Fgf3 expression from the hindbrain is required in a redundant manner with additional FGFs to induce the otic vesicle. However, Fgf3 is expressed in additional domains in the developing inner ear. In order to address whether these additional domains of expression have any functional significance, we are using a transgenic mouse carrying regulatory regions of the Fgf3 gene driving a lacZ reporter to investigate the precise details of Fgf3 expression throughout mouse inner ear development.

#### 319 Differential Requirements for FGF3, FGF8 and FGF10 During Inner Ear Development

Elena Dominguez<sup>1</sup>, Laura Zelarayan<sup>2</sup>, Victor Vendrell<sup>2</sup>, Yolanda Alvarez<sup>2</sup>, Mark Maconochie<sup>3</sup>, Thomas Schimmang<sup>1,2</sup>

<sup>1</sup>IBGM, Valladolid, Spain, <sup>2</sup>ZMNH, University of Hamburg, Germany, <sup>3</sup>University of Sussex, Brighton

FGF signalling is involved during multiple steps of inner ear development, including induction of the otic placode, formation and morphogenesis of the otic vesicle and cellular differentiation within the sensory epithelia. Here, we have addressed the role of FGF3, FGF8 and FGF10

during various of these steps in the murine and avian inner ear. In mouse embryos, hindbrain-derived FGF10 ectopically induces FGF8 and rescues otic vesicle formation in Fgf3 and Fgf10 homozygous double mutants. Conditional inactivation of Fqf8 after induction of the murine inner ear placode does not interfere with otic vesicle formation and morphogenesis but affects cellular differentiation in the inner ear. In contrast, inactivation of Fgf8 during induction of the inner ear placode on a homozygous null background for Fgf3 leads to a reduced size otic vesicle or the complete absence of otic tissue. The latter phenotype is more severe than the one observed in mouse mutants with null mutations for Fgf3 and Fgf10 that develop microvesicles. However, FGF3 and FGF10 are redundantly required for morphogenesis of the otic vesicle and the formation of semicircular ducts.

In the chicken embryo, misexpression of Fgf3 in the hindbrain induces ectopic otic vesicles in vivo. On the other hand, Fgf3 expression in the hindbrain or pharyngeal endoderm is required for formation of the otic vesicle from the otic placode. These results provide insights how the spatial and temporal expression of various FGFs control different steps of inner ear formation during vertebrate development.

#### | 320 | Hedgehog Signaling in the Developing Mouse Inner Ear

Dorothy Frenz<sup>1,2</sup>, Wei Liu<sup>1</sup>, Lijun Li<sup>1</sup>

<sup>1</sup>Department of Otorhinolaryngology-Head & Neck Surgery, Albert Einstein College of Medicine, <sup>2</sup>Department of Anatomy & Structural Biology, Albert Einstein College of Medicine

The Hedgehog (Hh) family is comprised of several related proteins, each playing important roles in regulating growth and patterning during development. Previous studies in our laboratory and others (Liu et al., 2002; Riccomagno et al., 2002, 2005; Bok et al., 2005) have shown that morphogenesis of the mouse inner ear is dependent on Sonic hedgehog (Shh). We now investigate whether Indian hedgehog (Ihh) may also function in inner ear development. Our findings show that Ihh mRNA is expressed in the developing mouse otocyst, most notably at 12 days of embryonic development (E12). expression of lhh is not diminished by inactivation of Shh. suggesting that removal of Shh does not abolish all Hh signaling and its influence on inner ear development. Conditional Ihh null mutant mice are currently being generated to ascertain if loss of Ihh function may effect inner ear development. Since Gli3, a downstream effector of Hh signaling, has been hypothesized to act as a negative regulator of inner ear development in the absence of Shh, we questioned whether removal of Gli3 repression is sufficient for normal patterning of the mouse inner ear in the absence of any Hh signaling input. This is now under investigation using mice with a targeted mutation of both Smoothened, which transduces all Hh signaling, and Gli3. Our initial findings suggest that residual Shh-independent Hh signaling may be operant in inner ear development.

#### 321 Hedgehog Signaling Regulates Cell Fate in the Mammalian Cochlear Duct

**Elizabeth Carroll Driver**<sup>1</sup>, Shannon Pryor<sup>2</sup>, Patrick Hill<sup>3</sup>, Joyce Turner<sup>4</sup>, Ulrich Rüther<sup>3</sup>, Leslie Biesecker<sup>4</sup>, Andrew Griffith<sup>2</sup>, Matthew Kelley<sup>1</sup>

<sup>1</sup>NIDCD, NIH, Bethesda, Md., <sup>2</sup>NIDCD, NIH, Rockville, Md., <sup>3</sup>Heinrich-Heine University, Düsseldorf, Germany, <sup>4</sup>NHGRI, NIH, Bethesda, Md.

Mutations in components of the hedgehog signaling pathway can cause a variety of human diseases. Mutations in the transcription factor GL/3, which acts both as an activator and a repressor of hedgehog signaling, result in at least five distinct clinical phenotypes including Pallister-Hall syndrome (PHS). In addition to other defects, some PHS patients exhibit hearing loss, primarily affecting lower frequencies. To explore the basis for this auditory defect, we examined the inner ears of a mouse model of PHS (*Gli3*<sup>4</sup>), which produces only the truncated, repressor form of the Gli3 protein. The cochleae of Gli34 homozygous embryos had a variably penetrant phenotype, with some much shorter and broader than wild-type. There are further defects on a cellular level, most notably large ectopic patches of innervated hair cells in Kölliker's Organ (KO) with vestibular, rather than cochlear, characteristics. We also observed mispatterning of the endogenous hair cells; in strongly affected *Gli3*<sup>4</sup> mutant cochleae, there are as many as seven rows of hair cells, but the rows are disorganized and irregular. As the cellular pattern of hair cells in the cochlea is critical for sensory function, these patterning defects could contribute to auditory deficits. To determine whether hedgehog signaling has a direct effect on cochlear development, we treated cochlear explants with Sonic hedgehog protein (Shh). Consistent with an inhibitory role for hedgehog signaling in hair cell development, we found that Shh treatment inhibits expression of Atoh1 and represses development of hair In contrast, treatment with Shh inhibitors (cyclopamine or Hedgehog interacting protein) results in both ectopic hair cells in KO and an increase in the number of hair cells within the sensory epithelium. These findings are the first to suggest both a direct role for hedgehog signaling in development of the cochlear sensory epithelium, and that hearing loss can result from GLI3 mutations in PHS.

### 322 Signaling of Epithelial-Mesenchymal Interactions by Wnt5a

Dorothy Frenz<sup>1,2</sup>, Wei Liu<sup>1</sup>, Lijun Li<sup>1</sup>

<sup>1</sup>Department of Otorhinolaryngology-Head & Neck Surgery, Albert Einstein College of Medicine, <sup>2</sup>Department of Anatomy & Strucural Biology, Albert Einstein College of Medicine

Interactions between epithelium and mesenchyme are essential to development of the mammalian inner ear. Attention has recently been directed at identifying the signaling molecules that participate in molecular mechanisms of these inductive tissue interactions. Wnt proteins constitute one of the major families of secreted ligands that function in developmental signaling. We

previously reported that Wnt5a is expressed in the developing mouse inner ear and demonstrated the ability exogenous Wnt5a to stimulate otic capsule chondrogenesis in cultured periotic mesenchyme containing otic epithelium (periotic mesenchyme + otic We now show that in the presence of secreted frizzled related protein 3 (sfrp3), a Wnt antagonist expressed in periotic mesenchyme + otic epithelium, or Wnt5a-specific antisense oligonucleotide, diminishes levels of endogenous Wnt5a, otic capsule chondrogenesis is suppressed in culture. In accord with these findings, periotic mesenchyme + otic epithelium harvested from Wnt5a null mutant mice is compromised in its ability to differentiate into cartilage in culture. establish how regulation of chondrogenic differentiation may be disturbed by Wnt5a mutation, expression of stagespecific differentiation markers was examined. embryonic age 14 days (E14), expression of aggrecan protein is reduced in the developing capsule of Wnt5a null mutant mice in comparison to expression in wild-type littermates. Based on the expression patterns of Wnt5a and sfrp3, and the vitro effects of their exogenous proteins, we propose a model of otic capsule formation whereby sfrp3 and Wnt5a act antagonistically to ensure appropriate patterns of chondrogenesis and provide coordinated control of otic capsule development. Our findings support Wnt5a and sfrp3, a counter Wnt, as regulators of otic capsule formation in the developing mouse inner ear.

# 323 Hearing Loss in Noggin Heterozygous Knockout Mice: An Animal Model for Congenital Conductive Hearing Loss in Humans

Chan Ho Hwang<sup>1</sup>, Doris K Wu<sup>1</sup>

<sup>1</sup>NIH/NIDCD

The cochlear duct in the inner ear perceives sounds as vibrations that are generated by the tympanic membrane in the outer ear and further amplified by the three ossicles in the middle ear (malleus, incus and stapes). Conductive hearing loss results from defects in relaying sounds from the outer ear to the cochlear duct. *Noggin* encodes a secreted molecule that antagonizes Bone morphogenetic proteins (BMP). Mutations of the *NOGGIN* gene in humans are associated with several autosomal dominant disorders such as Proximal symphalangism and Multiple synostoses that are characterized by skeletal defects and synostoses. Conductive hearing loss is also a characteristic of these disorders.

We investigated the hearing ability of the *Noggin* heterozygous mice as an animal model for the autosomal dominant hearing disorders associated with *NOGGIN* mutations. Half of the *Noggin* heterozygotes in C57/BL6 background showed unilateral or bilateral hearing loss of 15 to 25 dB threshold shift compared to wildtype littermates (n=11/27). This phenotype is genetic background dependent since heterozygotes of C57/BL6 and FVB hybrids have normal hearing. Even though previous studies from our laboratory showed *Noggin* null embryos have various membranous and bony labyrinth defects that could account for the hearing loss in the

heterozygotes, the analyses of the heterozygous mice with hearing loss all showed ectopic bone formation between the stapes and the surrounding tympanic bone (n=11/11). We conclude from these results that the hearing loss observed in the *Noggin* heterozygous mice is conductive in nature due to the impedance of stapes mobility during sound transmission. Our gene expression analyses indicate that the ectopic bone formation in the mutant middle ear is due to unopposed BMP functions during ossicle formation.

#### 324 Roles of BMP Signaling in Inner Ear Development

**Takahiro Ohyama**<sup>1</sup>, Andy Groves<sup>1</sup>

<sup>1</sup>House Ear Institute

Bone Morphogenetic Protein (BMP) signaling plays crucial roles during embryonic development such as axis formation and neural induction. Several BMPs are known to be expressed in different areas of the inner ear at different times. Previous studies have shown that BMP signaling regulates formation of the otic capsule and the vestibular sensory patches in chick (Chang, W. et al. Dev. Biol. 251, 2002, Liu, W. et al. Dev. Dyn. 226, 2003, Pujades, C. et al. Dev. Biol. 292, 2006). We analyzed the expression pattern of BMP type I receptors (Alk2, 3 and 6) and phosphorylation of Smad 1/5/8 in the mouse inner ear. Although BMP type I receptors are expressed rather ubiquitously in the inner ear, phosphorylation of Smad is localized in unique region such as vestibular sensory hair cells, cochlea duct and neurons. Furthermore, we conditionally disrupted Alk2 or Alk3 in the inner ear epithelium by using Pax2-Cre mice previously generated in our laboratory (Ohyama and Groves, Genesis 38, 2004). We observed subtle, but distinct phenotypes in each mutant allele, suggesting both redundancy and specific roles of the two receptor genes.

### 325 Smad4 Conditional Knockout Result in Hearing Loss in Mice

**Shi-ming Yang**<sup>1</sup>, Zhou-hui Hou<sup>1</sup>, Wei Guo<sup>1</sup>, Jian-he Sun<sup>1</sup>, Yin-yan Hu<sup>1</sup>, Ning Yu<sup>1</sup>, Ji-shuai Zhang<sup>2</sup>, Xiao Yang<sup>2</sup>, David He<sup>3</sup>

<sup>1</sup>Institute of otolaryngology, PLA General hospital, Beijing 100853, China, <sup>2</sup>Genetic Laboratory of Development and Diseases, Institute of Biotechnology, Beijing 10071, China, <sup>3</sup>Dept. Biomedical Science, Creighton University

There were many reports in last decade showed the relative gene for deafness which have been cloned, but the more gratifying result should been focused on the function of the gene. Foremost among the recent advances in genetic manipulation of mouse genome are transgenic and embryonic stem (ES) cell technology. In present experiments, we showed the data from the smad4 conditional knockout mice. Smad4 gene expressed throughout three genotypes cochlea at high level. The smad4 gene expression concentrated on vascular stria, spiral ligament, basal membrane, tectorial membrane, hair cells, supporting cells and spiral ganglion cell. Expressions in vascular stria and organs of Corti were strongest in all

structures. The expression in Smad4+/- were the same as in Smad4 +/+ mice. But Smad4-/- was much weaker than them. Smad4 +/+ and Smad4+/- showed recognizable and reduplicative ABR wave forms in 1 month mice. All the Smad4-/- did not show any recognizable wave forms even with the stimulation of the highest level sound pressures. All the three genotypes mice could be induced normal distortion production otoacoustic emission. Smad4 +/+ and Smad4+/- could be induced normal cochlear microphonics but Smad4-/- could not. Like ABR, Smad4 +/+ and Smad4+/- showed recognizable and reduplicative CAP wave forms. All the Smad4-/- did not show any recognizable CAP wave forms from click and tone burst(4kHz,8kHz,16kHz,32kHz). By light microscope we could see osseous cochlear development deformity in cochlear apex while the other genotypes could not. All three genotypes had not abnormality in middle ear and ossicles. The Smad4 +/+ and Smad4+/- showed normal morphology of inner and outer hair cells and stereocilium. Surface preparation showed that Smad4 +/+ and Smad4+/- had few absence in inner and outer hair cells occasionally while Smad4-/- had also scattered few absence in inner and outer hair cells. All three genotypes showed normal stereocilium. By semi-thinness serial sections we found that Smad4-/- had apparent absence in Deiters cells and spiral ganglion cells compared with the other genotypes. Our present data indicate that homozygotes after Smad4 gene conditional knockout demonstrate severe sensorineural hearing loss and morphological deficient in inner ear.

## 326 Cre-Mediated Conditional Inactivation of BMP Signaling in Otic Mesenchyme Disrupts Cochlear Development

Kyung Ahn<sup>1</sup>, E. Bryan Crenshaw III<sup>1,2</sup>

<sup>1</sup>The Children's Hospital of Philadelphia, <sup>2</sup>Dept. of ORL:HNS, University of Pennsylvania Medical School Epithelio-mesenchymal interactions between the otic mesenchyme and otic vesicle play a critical role in the morphogenesis of the inner ear. Although the importance of mesenchyme in the formation of the cochlea has been established for several years, little is known about the molecular mechanisms that mediate this interaction. To dissect the role of genes during this process, we have developed a strain of mice that can be used to conditionally rearrange genes in the otic mesenchyme, using the Cre/loxP approach. To generate this strain, we have isolated and characterized the otic mesenchymespecific enhancer elements from the mouse Brn4/Pou3f4 gene. Bitner-Glindzicz et al characterized a minimal deletion that inactivated human POU3F4 gene function. resulting in deafness (Bitner-Glindzicz, M., et al., Hum. Mol. Gen. 4:1467, 1995). The region encompassing this deletion, which lies approximately 900 kilobases (kb) from the coding region of the gene, was examined for sequence homology with the mouse gene to identify putative transcriptional regulatory elements. A region within a 1.5 kb DNA fragment showed blocks of >85% evolutionary conservation. We observed that, when placed upstream of the herpes thymidine kinase promoter, these putative transcriptional regulatory elements drive expression of the

Cre recombinase in the otic mesenchyme of transgenic mice. This transgenic strain provides a useful tool for elucidating the role of genes in the otic mesenchyme. Using this strain to induce a conditional knockout of type I BMP receptor signaling in the otic mesenchyme, we have observed that the cochlea is foreshortened in the mutant mice. These data demonstrate that BMP signaling in the otic mesenchyme is necessary for the morphogenesis of the cochlea, and provide insights into the molecular mechanisms that regulate epithelio-mesenchymal interactions during inner ear ontogeny.

### 327 Determining the Rhombemeric Origins of the Murine Auditory Hindbrain

**Peter Mathers**<sup>1</sup>, Warren Morgan<sup>1</sup>, David Howell<sup>1</sup>, Albert Berrebi<sup>1</sup>, George Spirou<sup>1</sup>

<sup>1</sup>Dept. of Otolaryngology, West Virginia University Studies in chick have led to a fate-map for the auditory nuclei of the hindbrain. These structures originate from hindbrain divisions called rhombomeres and maintain the rostral-caudal pattern in which they are born. In these studies, cells populating adjacent nuclei are derived from either the same or an adjacent rhombomere. hypothesize that auditory nuclei of the mammalian hindbrain originate in the rhombomeres and maintain a similar topographic organization as seen in chick. Cremediated recombination lineage-labeling marks developing cells by irreversibly activating reporter gene expression. By employing two rhombomere-specific cre expression lines and comparing labeled regions to known and newly discovered auditory nuclei markers, we have developed a fate-map for several auditory nuclei of the hindbrain. Engrailed-1-cre transgenic mice, where cre expression is restricted to the developing midbrain and rhombomere 1, label several auditory nuclei of the superior olivary complex. These nuclei include the medial, ventral, and lateral nuclei of the trapezoid body (MNTB, VNTB and LNTB, respectively), as well as the intermediate and ventral nuclei of the lateral lemniscus (INLL and VNLL). The Hoxb-1 gene is progressively restricted to rhombomere 4 in the hindbrain of the mouse. Using Hoxb-1-IRES-cre transgenic mice in fate-mapping studies, we have determined that portions of the lateral superior olive (LSO), LNTB, and VNLL originate in rhombomere 4. These results suggest that, as in chick, hindbrain auditory nuclei arise from multiple rhombomeres. However, in contrast to chick, cells born in these rhombomeres do not necessarily seem to maintain a topographic pattern in the mouse. suggesting migration of cells across rhombomeric boundaries. Understanding the normal development of these hindbrain structures may lead to a better understanding of human disease, such as auditory processing disorders.

### 328 A Gal4-Based Gene Trap Screen for Hearing and Balance in Zebrafish

Takunori Satoh<sup>1</sup>, **Donna M. Fekete<sup>1</sup>** 

<sup>1</sup>Purdue University

Gene trapping is a technique to insert a cassette into the genome at random to detect the expression of the endogenous gene located at the insertion site. We are

using this method to screen for genes specifically expressed in otic- or neural-specific cells of the auditory or vestibular systems. Gal4-based cassettes are inserted into the zebrafish germline by injection of pseudotyped retroviral vectors or Tol2 transposases into early embryos. The injected founder fish are crossed to a reporter line carrying a UAS:GAP43-DsRed-Express fusion transgene whose expression requires Gal4 protein. expressing a trapped gene will make Gal4 protein and transactivate the reporter whose presence can be detected by fluorescence screening of live F1 embryos. Fish with relatively specific fluorescence in peripheral or central components of mechanosensory systems will be bred and the trapped genes will be cloned. One major advantage of a Gal4 gene-trap design is its potential for targeting bioactive molecules to specific cells in vivo. This can be accomplished by crossing a particular Gal4-trap line (i.e., the activator line) with a transgenic line carrying a target gene placed downstream of a UAS sequence (i.e., the effector line). A drug-inducible form of Gal4 (GeneSwitch, Invitrogen) will permit even more control over the onset of effector protein expression. As proof-of-principle, we plan to create an effector line with UAS upstream of a toxin gene. When crossed to any of the Gal4 activator lines, we expect the toxin will specifically kill only those cells expressing the trapped gene. This should prove especially powerful for selective ablation of subsets of CNS neurons to assess their role in development and/or in behavior. Finally, we hope to test the trapped genes for possible roles in hearing and balance using loss-of-function approaches, such as morpholino-based gene knockdowns or breeding trapped lines to homozygosity. Supported by NOHR and DRF.

#### | 329 | Death Pathways in Noise-Exposed Outer Hair Cells

**Barbara A. Bohne**<sup>1</sup>, Gary W. Harding<sup>1</sup>, Steve C. Lee<sup>1</sup> *Washington University School of Medicine* 

Using morphological criteria, death pathways in OHCs were determined in organs of Corti (OC) exposed to an octave band of noise (OBN) with a center frequency of either 0.5 or 4 kHz at a moderate sound pressure level (SPL). The specimens were part of our collection of plastic-embedded flat preparations of chinchilla cochleae. Three death pathways were identified: 1) oncosis - OHCs were swollen & pale-staining with a swollen nucleus; 2) apoptosis - OHCs were shrunken & dark-staining with a pyknotic nucleus; & 3) a third death pathway - OHCs had no basolateral plasma membrane, a nucleus deficient in nucleoplasm & cellular debris arranged in the shape of an intact OHC. To minimize the secondary loss of OHCs that occurs post-exposure, the specimens used for quantitative analysis of death pathways had the following characteristics: a) the level to which they were exposed was  $\leq$  95 dB SPL; b) the exposure duration was 6-216 h; c) the cochleae were fixed in-vivo 1-2 h post-exposure; & d) there were no focal OHC lesions in the OC. Fifty-eight noise-exposed cochleae in our collection met these criteria. The specimens had a variable amount of OHC loss, minimal IHC loss, rare pillar loss, & no spiral ganglion cell loss. The cochleae were grouped by total exposure energy  $[E = log_2 (Pa^2 seconds)]$  into 7 Groups with energies ranging from 7.77-17.74 for the 0.5-kHz OBN & 6 Groups with energies ranging from 5.11-14.75 for the 4kHz OBN. In all specimens, degenerating & missing OHCs were classified as to which death pathway the cells were following. Nine non-noise-exposed cochleae were also evaluated for OHC death pathways. The number of OHCs following the third death pathway was significantly greater in the noise-exposed cochleae than the non-noiseexposed cochleae for total exposure energies greater than that produced by a 0.5-kHz OBN at 75 dB SPL for 216 h (i.e., 13.26) or a 4-kHz OBN at 57 dB SPL for 48 h (i.e., 5.11). In cochleae exposed to either octave band, OHCs dying by oncosis or apoptosis were uncommon. Further work must be done on cell-death pathways in the noisedamaged cochlea to determine how the prevalence of the different pathways changes with exposure parameters.

#### 330 High-Frequency Noise-Induced TTS Correlates with Outer-Pillar Pathology

Kristina L. Kluge<sup>1</sup>, **Gary W. Harding<sup>1</sup>**, Barbara A. Bohne<sup>1</sup>

\*\*Mashington University School of Medicine\*\*

Studies have reported a correlation between noiseinduced TTS & structural changes in the organ of Corti such as disarray of stereocilia, swelling of afferent nerve fibers & distortion of supporting-cell bodies. However, no pathological change has been found consistently. & the mechanism of TTS remains unclear. The present study sought to quantify pillar-cell buckling in cochleae fixed when TTS was present & in those fixed after recovery from TTS. Noise-exposed chinchilla cochleae were selected from our permanent collection using the following criteria: a) the exposure was a 4-kHz OBN at 57-86 dB SPL for 24-216 h; b) animals were 1-3-yr-old; c) 34 cochleae were fixed 0-d post-exposure & 12 were fixed after 20-30 d of recovery. Eight control cochleae were also evaluated. All cochleae had been fixed with 1% osmium tetroxide & embedded in plastic. After polymerization, the cochlear ducts were dissected into flat preparations & examined by phase-contrast microscopy. Grade 0 indicated no outerpillar damage. Grade 1 indicated bowing of the outer-pillar bodies. Grades 2, 3 & 4 indicated that the outer pillars slightly, moderately, or severely buckled, respectively. For each cochlea, total exposure energy [E = log<sub>2</sub> (Pa<sup>2</sup> seconds)] was calculated. E ranged from 5.11 (Group 1; 57 dB SPL, 48 h) to 16.92 (Group 6; 86 dB SPL, 216 h). In the apical half of the cochleae, there was little damage to outer pillars in all Groups. In the basal half of the cochleae. little pillar damage was present in Groups 1-Cochleae in Groups 4-6 sustained increasing pillar damage that was concentrated in the base. This damage was significantly different from controls at 78-93% distance from the apex for Group 4; 8-13%, 38%, 53% & 63-88% for Group 5; & 73-83% for Group 6. For the 20-30-d recovery cochleae, the average pillar grades differed significantly from controls for Group 5 at 38%, 53-58% & 78% & for Group 6 at 8% distance. Thus, high-frequency noise exposures that produce TTS also lead to outer-pillar damage, the degree of which increases with E. Recovery from TTS correlates with repair of outer-pillar damage. The data presented here support the hypothesis that outer-pillar damage is a mechanism for TTS.

# 331 Is Plasma Membrane Leakage a Sign of the Shift of the HC Death Pathway From Apoptosis to Necrosis Following Exposure to Intense Noise?

**Bohua Hu<sup>1</sup>**, Donald Henderson<sup>1</sup>, Thomas Nicotera<sup>2</sup>

<sup>1</sup>State University of NY at Buffalo, <sup>2</sup>Roswell Park Cancer Institute

It has been known for years that apoptotic cells preserve their membrane integrity until the late phases of the apoptotic process. Therefore, occurrence of membrane leakage is commonly considered an important sign of cessation of apoptosis or occurrence of necrosis. Here we reported that noise-induced hair cell (HL) apoptosis appear have different pattern of the apoptotic progression. Instead of switching to necrosis, HC apoptosis persist even after the cells lost their membrane integrity. Chinchillas were exposed to an impulse noise (155 dB SPL) or a high level of a continuous noise. Following exposure to the intense noise, nuclear condensation developed rapidly in the center of the cochlear lesion. At the same time, the cells showed the sign of membrane leakage as evidenced by strong uptake of propidium iodide or trypan blue. Although the HCs lost their membrane integrity, the apoptotic phenotypes continue to manifest. SDH activity and mitochondrial membrane potential were preserved in apoptotic HCs until the late phases of apoptosis, suggesting the maintenance of the mitochondrial energetic function. Nuclear condensation continued, leading to generation of small nuclear fragments and, eventually, complete nuclear degradation. More importantly, caspase activity was preserved. Interesting, the HCs with membrane leakage had a relatively intact membrane enclosure as shown by semi-thin sections of the organ of Corti. The plasma membrane of apoptotic HCs confined the cellular organelles within the cells. In contrast, the necrotic cells exhibited the membrane gaps which allow the release of cellular organelles to the extracellular space. Collectively, our observations indicate that loss of membrane integrity did not shift the apoptotic process to necrosis. Apoptotic cells, even with membrane leaks, remain in the apoptotic pathway until complete degradation of the cells.

(Supported by NIDCDP01-DC03600-1A1, NIDCD1R21 DC04984-01 and NIDCD1R03DC006181-01)

### 332 Regulation of Cell Death Pathways Following Exposure to Intense Noise

**Bohua Hu<sup>1</sup>**, Donald Henderson<sup>1</sup>, Wei-Ping Yang<sup>2</sup>

<sup>1</sup>State University of NY at Buffalo, <sup>2</sup>PLA General Hospital, China

The coexistence of apoptotic and necrotic outer hair cell (OHC) death has been found in the organ of Corti following exposure to intense noise. However, the cellular mechanisms that regulate the propensity of cell death

toward apoptosis or necrosis following exposure to intense noise are unknown. The current study was designed to examine the role of energy supply in controlling the cell death propensity toward apoptosis or necrosis following exposure to intense noise. In the first part of the study, the mitochondrial energetic function was compromised by application of 3-Nitropropionic acid (3-NP, 20 mM or 50 mM), an irreversible inhibitor of succinate dehydrogenase (SDH) before or after exposure to an impulse noise at 155 dB SPL. The results showed that inhibition of SDH activity could reduce the rate of the progression of certain apoptotic events, including F-actin cleavage and nuclear degradation, at the early phase of cochlear pathogenesis. However, SDH inhibition could not prevent the initiation of OHC apoptosis. Although SDH inhibition drove a small portion of OHCs to die through secondary necrosis, there was no major shift of cell death pathways from apoptosis to necrosis following the mitochondrial impairment. In the second part of the study, the blood supply to the cochlea was stopped before exposure to the noise. The results showed that complete cessation of the energy supply to the HCs switch apoptosis to necrosis as evidenced by the presence of a large quantity of HCs with swollen nuclei. Although activation of caspases (3, 8 and 9) in dying cells persisted, the level of caspase activity appeared reduced. Collectively, the results of the study suggest that while the mitochondrial energetic function plays an important role in the apoptotic process, it is not an obligatory component for initiation of OHC apoptosis. Other energy sources, such as cytosolic glycolysis, can participant in the regulation of the apoptotic process in the event of mitochondrial dysfunction.

(Supported by NIDCD 1R03DC006181-01)

### 333 The Dynamics of Mitogen-Activated Protein Kinases in the Cochlea After Acoustic Trauma

Inna Meltser<sup>1</sup>, Yeasmin Tahera<sup>1</sup>, Barbara Canlon<sup>1</sup> <sup>1</sup>Physiology & Pharmacology, Karolinska Institutet Mitogen-activated protein kinases, or MAPK (ERK, JNK and p38) are regulators of the intracellular response to different stressors and growth/differentiation factors (Kyriakis and Avruch, 2001). MAPK are expressed in both auditory brainstem neurons (Suneja et al., 2003), as well as in the cochlea (Hess et al., 2002), yet their function is not completely understood. Reductions in hearing thresholds were found after pre-treatment with the inhibitor of JNK (Pirvola et al., 2000) suggesting a protective role in the cochlea. In order to investigate the mechanisms responsible for auditory protection we analyzed the phospho-MAPK expression patterns at different time points after i) a temporary (TTS) or, ii) a permanent (PTS) noise-induced hearing loss. We found the pattern of phospho-MAPK expression after a TTS was different from the expression after PTS. To study the mechanisms underlying the different MAPK expression patterns, we analyzed the total content of several cytokines and BDNF in cochlea tissues using ELISA, and the expression of TNF cochlea receptors and TrkB in the immunocytochemistry and western blot. These findings will help to understand the mechanisms of hearing loss

induced by acoustic trauma and may provide important information that will help prevent or treat acoustic trauma-induced hearing loss using anti-inflammatory drugs including glucocorticoids and MAP kinase inhibitors. Supported by grants from the Swedish Research Council, AMF Trygghetsförsäkring, Tysta Skolan, and the Karolinska Institute.

## Impact of Noise Exposure on Inflammatory Gene Expression in the Guinea Pig and Mouse Cochleas

**De-Ann M. Pillers**<sup>1</sup>, Dennis R. Trune<sup>1</sup>, Jiaqing Pang<sup>1</sup>, Xiaorui Shi<sup>1</sup>, Alfred L. Nuttall<sup>1,2</sup>

<sup>1</sup>Oregon Health & Science University, Oregon Hearing Research Center, <sup>2</sup>Kresge Hearing Res Inst Univ of Michigan

Excessive noise causes significant damage to the inner ear, often involving metabolic, mechanical, vascular, and molecular pathologic mechanisms. Recently it has been determined that inflammatory pathways also are involved, leading to upregulation of numerous genes of the immune system. Nuclear factor – kappa B (NF-kB) is a transcription factor that induces the gene expression of multiple downstream inflammatory cytokines and factors. To better understand the impact of noise on this NFÿB-mediated transduction cascade, guinea pigs and mice were exposed to noise that their cochleas analyzed by DNA arrays. Currently DNA arrays are available only for mice, not for guinea pig. However, the significance of the guinea pig model in noise studies makes its gene expression investigation of great interest. It currently is not known if sufficient homology occurs between the mouse and guinea pig to that the mouse gene array can be employed to evaluate the guinea pig gene expression.

Broad-band noise exposure consisted of 122 dBA for 3 hrs/day for 2 days. Cochleas were harvested and the RNA was extracted for reverse transcription. The cDNA was used in a prefabricated gene membrane array to evaluate the expression of 113 genes related to NF-kB-mediated signal transduction (SuperArray Bioscience Corporation, Frederick, MD). Numerous cochlear genes in both species were upregulated and downregulated by noise exposure. However, there was not a great deal of correlation between guinea pig and mouse. Guinea pigs had 9 genes upregulated while the mouse had 17, with the overlap of only 3 genes. Guinea pig genes centered more on ATP binding, death domain ligands, fos, and nitric oxide biosynthesis. The mouse showed some of these genes, but also much greater expression of transcription factors, apoptosis, and inflammatory processes. The potential reasons for these differences could be related to amount of actual damage to the mouse ear versus the guinea pig, metabolic differences between the species, and of course gene homology differences so that the mouse arrays cannot completely assess guinea pig expression. Further study of the guinea pig will require additional sequence information to take full advantage of it as a model for cochlear gene studies.

(Supported by NIDCD R01 DC005593 and NIDCD R01 DC000105)

#### 335 CCR2 Upregulation in Mouse Cochlea After Acoustic Trauma

**Elizabeth Shick**<sup>1</sup>, Justin Pavlovich<sup>1,2</sup>, Richard M. Ransohoff<sup>1,3</sup>, Keiko Hirose<sup>1,2</sup>

<sup>1</sup>Neuroinflammation Research Center, Lerner Research Institute, Cleveland Clinic, <sup>2</sup>Head and Neck Institute, Cleveland Clinic, <sup>3</sup>Department of Neurology, Cleveland Clinic

CC chemokine receptor 2, CCR2, has recently been demonstrated to exert a protective effect against hair cell loss after acoustic injury. The mechanism of CCR2 neuroprotection is unknown and the cell population that expresses CCR2 in the cochlea has not been identified. CCR2 is known to be expressed by leukocytes and has recently been demonstrated in neurons. It is possible that in addition to recruited hematogenous cells in the ear, sensory cells may express CCR2. Identifying which cells in the ear express CCR2 is an important first step in elucidating the mechanism of its protection. We performed quantitative real time RT-PCR of noise-exposed mouse cochleas to determine the timing of CCR2 upregulation after acoustic trauma. We also performed in situ hybridization with CCR2 digoxigenin-labeled anti-sense probes to identify the cell type responsible for CCR2 expression in the mouse inner ear.

Eight-week-old C57Bl6 mice were exposed to 112dB octave band noise (8-16kHz) for 2 hours, with non-noise exposed littermates as controls. Cochleas were harvested and micro dissected at 0, 1, 2, 3, and 7 days post noiseexposure, and gene expression of CCR2 was analyzed by quantitative real time RT-PCR. There was an 8-fold increase in CCR2 expression 3 days after noise when compared to non-noise exposed controls. In situ hybridization has demonstrated that CCR2 is expressed in both control and noise-exposed cochleas, and that CCR2 positive cells are present in the spiral ligament and the spiral limbus. The number of CCR2 expressing cells is significantly greater after noise when compared to controls. Further identification of these cells will be pursued with double labeling experiments using both in situ hybridization and immunohistochemistry.

#### 336 Noise-Induced Hearing Loss Variation Within and Between Inbred Strains of Mice

**Sharon G. Kujawa<sup>1,2</sup>**, M. Charles Liberman<sup>1,2</sup>, Melissa L. Wood<sup>1</sup>, Bruce L.Tempel<sup>3,4</sup>

<sup>1</sup>Eaton-Peabody Laboratory, Massachusetts Eye and Ear Infirmary, <sup>2</sup>Dept. of Otology and Laryngology, Harvard Medical School, <sup>3</sup>VM Bloedel Hearing Research Center, <sup>4</sup>Dept. of Otolaryngology-Head and Neck Surgery, University of Washington

Vulnerability to acoustic injury varies among inbred strains of mice, and this heterogeneity has been exploited to study genetic contributions to vulnerability differences. Within strains, however, variables such as age and gender can interact with exposure parameters and post-exposure time to shape noise-induced hearing loss (NIHL) and cochlear histopathology among genetically identical individuals. In this study, animals from 2 'resistant' (129S6/SvEvTac,

129S6; MOLF/Ei, MOLF) and 2 comparatively 'vulnerable' (CBA/CaJ, CBA; C57BL/6J, B6) strains were noise exposed (8-16 kHz OBN, 2 hr, 94-112 dB SPL) at different ages (4-64 wk). Age-corrected, noise-induced shifts in ABRs and DPOAEs were calculated 2 wks post exposure by comparison with untreated animals of appropriate age, gender and strain. Three major observations are made: First, age-dependent vulnerability varied among the strains: the dramatic vulnerability shift that occurs between 8-16 wk in CBA is altered or absent altogether in the other strains. Second, gender did not emerge as an important variable influencing NIHL or cochlear histopathology in young-exposed ears. Third, growth of NIHL with increasing exposure level differs greatly among the strains. In young 129S6, it is seen as a remarkably slow growth function (Yoshida et al. 2000). In contrast, NIHL growth functions for young MOLF, B6, and CBA show a clear "critical level" above which NIHL grows steeply with increasing exposure level. Vulnerability differences among these three strains are seen as differences in critical level: the growth function for MOLF (resistant) is right-shifted, whereas B6 is leftshifted along the exposure-level axis compared with CBA. Such inter-strain differences may provide important clues to mechanisms underlying noise vulnerability. As a practical matter, classification of animals from different inbred strains as vulnerable or resistant can be shaped significantly by the age at which the animals are exposed. Research Supported by NIDCD R01 DC0188, R01 DC006305, and P30s DC005209 and DC04661

#### | 337 | Metallothionein I and II Knocked Out Mice of 129 Genetic Background Differ in Their Susceptibility to Noise-Induced Hearing Loss

Jerel Garcia<sup>1</sup>, Esteban Verduzco<sup>1</sup>, Steven P. Tinling<sup>1</sup>, Tejas Patel<sup>2</sup>, Michael Anne Gratton<sup>2</sup>, **Ana E. Vazquez**<sup>1</sup> <sup>1</sup>Department of Otolaryngology-HNS and Center for Neurosciences, University of California Davis, <sup>2</sup>Department of Otorhinolaryngology-HNS University of Pennsylvania Inbred mice strains exhibit widely different susceptibilities to noise-induced hearing loss (NIHL). Inbred substrains of 129 mice have been demonstrated to be highly resistant to NIHL. In contrast, the C57BL/6J is a model for the study of noise susceptibility. In previous work we investigated what molecules might be relevant to the development of NIHL by comparing gene expression levels before and after noise exposure in groups of inbred mice that differ in their susceptibility to NIHL. Higher levels of metallothioneins (MTs) were detected in the 129 mice relative to those in the C57BL/6J mice and upregulation of MT I and II was noted in both strains after noise exposure. MTs are small proteins rich in cysteine and methionine. protective roles against various types of cellular insults in the liver, heart and brain, and are critical to many aspects of cellular biochemistry. For example, they modulate the availability of Zn<sup>2+</sup> to various enzymes and transcription factors. Mice knocked out for the expression of MTI and MTII (MTKO) had comparable baseline auditory brainstem response (ABR) thresholds to mice of their parental strain SvImJ). However, MTKO mice compromised resistance to a 1-h, 105-dBSPL, 10-kHz centered, octave band of noise exposure when compared to mice of the parental strain. ABR recorded 5 days after the exposure revealed that MTKO mice exhibited more threshold shift (TS) than the parental strain mice and a very large variability in the TS was apparent.

Analysis of the ARB TS suggested that at least two populations of MTKO mice exist with respect to their susceptibility to NIHL. Mice that incurred a TS of 10 dB or higher at any of the frequencies tested were classified as "susceptible" while mice that incurred less than a 10 dB TS at all test frequencies were classified as "resistant". Susceptible MTKO mice exhibited an average of 35 dB TS at all test frequencies, significantly larger than the TS incurred by the resistant MTKO mice (p<0.001). The results indicate that there are other, yet to be discovered, modifiers that interact functionally with MT and contribute to the high resistance to NIHL in the 129 SvImJ mice. Supported by R01-DC006442-01 to MAG and R21-

Supported by R01-DC006442-01 to MAG and R21-DC04990 to AEV.

# 338 Deletion of GABA<sub>B1</sub> Receptors From Cochlear Ganglion Cells Leads to Threshold Elevation and Increased Resistance to Permanent Acoustic Injury

**Stéphane F. Maison<sup>1,2</sup>**, Martin Gassmann<sup>3</sup>, Bernhard Bettler<sup>3</sup>, M. Charles Liberman<sup>1,2</sup>

<sup>1</sup>Harvard Medical School, <sup>2</sup>Massachusetts Eye & Ear Infirmary, <sup>3</sup>University of Basel

Despite pharmacologic and immunohistochemical evidence for GABAergic transmission in the cochlea, a clear functional role has not emerged. Recent knockout studies revealed that ionotropic GABA<sub>A</sub> receptor subunits are required for long-term maintenance of cochlear hair cells and neurons [Maison et al, J Neurosci 2006]. To explore the role of metabotropic GABA<sub>B1</sub> receptors, we characterized the cochlear phenotype of mice with targeted deletion of this subunit and its tissue localization using another line with normal GABA<sub>B1</sub> expression coupled to a GFP reporter.

Anti-GFP immunostaining revealed GABA<sub>B1</sub> expression in both type-I and type-II ganglion cells, as well as their synaptic terminals under inner and outer hair cells, respectively. No GFP signal was observed in hair cells. Threshold sensitivity, measured via ABRs and DPOAEs was variable in knockouts, ranging from normal to ~40 dB re wildtypes. In females, mean knockout thresholds were elevated by 5 dB, and, in males, by 15 dB re wildtypes. Threshold shifts were similar whether measured by ABRs or DPOAEs, consistent with an OHC phenotype. Medial olivocochlear function, assessed via DPOAE suppression during efferent electrical stimulation, was unaffected by receptor deletion. GABA<sub>B1</sub> knockouts showed increased resistance to permanent acoustic injury, with mean threshold shifts ~25 dB smaller than wildtypes after exposure to 8-16 kHz noise at 100 dB for 2 hrs. In contrast, there was no vulnerability difference to temporary acoustic injury following exposure to the same noise at 94 dB for 15 min.

GABAergic signaling between OHCs and type-II neurons appears to be required for normal OHC-based amplifier function at low sound level and may also modulate OHC

responses to high-level sound. Both implications are interesting given that type-II / OHC synapses may be reciprocal and that the type-II innervation may mediate local intercellular signaling in the OHC area.

### 339 Activation of Cochlear Innate Immunity by Acoustic Trauma Augments Adaptive Response to Antigen

**Masumichi Miyao**<sup>1</sup>, Peter Billings<sup>1</sup>, Gary S. Firestein<sup>1</sup>, Elizabeth Keithley<sup>1,2</sup>

<sup>1</sup>University of California, San Diego, <sup>2</sup>Veterans Affairs Medical Center, San Diego

Noise-exposure activates an innate immune response with IL-1 $\beta$  expression and infiltration of leukocytes. Previously we showed that activating an innate cochlear immune response with LPS augments an adaptive response to antigen (Ag). To test whether noise exposure could have the same effect, we sensitized Swiss Webster ND4 mice to the Ag, KLH, injected it intrathecally (n=10) and exposed the mice to noise (8-16 kHz, 118 dB for 2 hours) the following day (n=15). Control mice received either noise exposure alone (n=10), Ag challenge alone (n=10) or intrathecal PBS injection alone (n=10). Four hours or 7 days later the mice were sacrificed by intracardiac perfusion with periodate-lysine-paraformaldehyde (PLP) fixative.

We investigated the number and location of cells expressing phospho-NF- $\kappa$ B (Cell Signaling #3037), ICAM-1 (intercellular adhesion molecule, BD Pharmingen 550287) and CD45 (leukocyte common antigen, BD Pharmingen 550539).

Noise exposure resulted in severe hearing loss (>50 dB). Intrathecal Ag injection did not result in hearing loss. Activated NF- $\kappa$ B was identified in the nuclei of hair cells, supporting cells, spiral ligament fibrocytes and neurons 4 hours after noise exposure. ICAM-1 expression was seen in the lower part of the spiral ligament and small vessels within the normal cochlea. It was enhanced following intrathecal Ag injection and acoustic trauma. The number of CD45-positive cells was significantly greater in the Agplus-noise group (71 $\pm$ 52 cells/sec) relative to the Ag-alone group (39 $\pm$ 19 cells/sec) or the noise-exposure group (27 $\pm$ 16 cells/sec)(p<0.001, ANOVA).

These findings indicate that noise exposure activates a cochlear innate immune response, recruits inflammatory cells and, in the presence of Ag, allows for amplification of the adaptive response to that specific Ag.

#### 340 Mitochondrial Mutation and Presbycusis in a Mouse Model

**Brianna Crawley<sup>1</sup>**, Elizabeth Keithley<sup>2</sup>, Peter Billings<sup>2</sup>

<sup>1</sup>UCSD Otolaryngology/Head and Neck Surgery, La Jolla, CA, <sup>2</sup>UCSD and Veterans Affairs Medical Center, La Jolla, CA

Although presbycusis affects more than a quarter of Americas retired population, a century of research efforts has not elucidated its underlying pathophysiology. It is known, however, that degeneration of vital components of the inner ear is associated with age-related hearing impairment, both in animals and in humans. It is

hypothesized that mitochondrial DNA deletions contribute to hearing loss through interference with energy production, resulting in cellular degeneration, as cells involved in sensorineural hearing possess especially high energy requirements. That mitochondrial genomic mutations accrue with age has been well-documented in birds and mammals. Quantification of mitochondrial DNA mutations from human temporal bone correlates with the presence of age-related hearing impairment.

A transgenic mouse, deficient in mitochondrial DNA polymerase gamma activity (Polg<sup>D257A</sup>) and displaying many features of accelerated aging, was used to evaluate the course of hearing loss as determined by DPOAE and ABR. Premature hearing loss has been verified in these animals with worsening of auditory-evoked brainstem response thresholds when compared with their wild-type background at the age of nine months. Though loss of spiral ganglion cells, outer hair cells, and cells of the stria vascularis has been observed, these changes have not been correlated with increased oxidative stress.

We propose that the Polg<sup>D257A</sup> mutant does experience accelerated hearing loss that should be apparent not only in ABR but also in DPOAE measurements, indicating hair cell involvement. We are collecting serial measurements of homozygous mutants, as well as heterozygotes, their wild-type littermates, and wild-type B6 mice without any exposure to maternally derived mutated mitochondria. Preliminary data suggest that homozygous mice experience significant hearing loss at a younger age than wild-type and heterozygous counterparts.

#### 341 Bcl-2 Family Proteins in the Inner Ear of Aged Mice

**Su-Hua Sha<sup>1</sup>**, Andra E. Talaska<sup>1</sup>, M. Angeles Vicente-Torres<sup>1</sup>. Jochen Schacht<sup>1</sup>

<sup>1</sup>Kresge Hearing Research Institute, University of Michigan Mitochondria and mitochondrial dysfunction are key elements in aging and associated cell death and tissue degeneration. Signaling pathways leading to apoptosis are initiated when cytochrome C is released through the outer mitochondrial membrane to the cytoplasm in response to stress stimuli. Mitochondrial Bcl-2 or Bcl-XL can inhibit apoptosis, at least in part, by blocking cytochrome C release. Pro-apoptotic Bcl-2 family members such as BAD, Bid, and Bak block the antiapoptotic effects through heterodimerization with Bcl-2 or Bcl-XL. A nuclear localization of Bcl-2 can be induced by reactive oxygen species which does not play a protective role as mitochondrial localization does.

In this study, we investigate the expression of Bcl-2 family proteins in the inner ear of aged CBA mice. Pro-apoptotic Bcl-2 family members such as Bid, Bim, and Bad increase in the aged cochlea. Bcl-2 also increases with age from 3 months to 18 months in cytosolic, mitochondrial, and nuclear fractions of the cochlea. Specifically, Bcl-2 increases in the organ of Corti and spiral ganglion cells with aging, but not in stria vascularis. Bcl-2 also redistributed to the nuclei of outer hair cells at the age of 18 months. This observation was confirmed in cryosections and surface preparations of the organ of Corti.

Our results suggest that an increase in pro-apoptotic Bcl-2 family members in the inner ear and the redistribution of Bcl-2 to the nuclei of outer hair cells may contribute to outer hair cell loss and presbycusis.

This study was supported by program project grant AG-025164 from the National Institute of Aging and core grant P30 DC-05188 from the National Institute on Deafness and Other Communication Disorders, NIH.

### 342 Mitochondrial DNa Deletion in Presbycusis Development of Fischer 344 Rats

Jian Wang<sup>1,2</sup>, Genliu Sun<sup>3</sup>, Shankai Yin<sup>2</sup>, Zhiping Yu<sup>1</sup>, Ravi Sockalingam<sup>1</sup>, Manohar Bance<sup>4</sup> <sup>1</sup>School of Human Communication Disorders, Dalhousie University, <sup>2</sup>Research Institute of Otolaryngology, JianTong University, Shanghai, <sup>3</sup>Department of Biology, St. Mary University, 4d. Division of Otolaryngology, Department of Surgery, Dalhousie University Aging-related hearing loss, or presbycusis has been associated with large-scale mitochondrial DNA (mtDNA) deletion in previous studies. However, the role of this mtDNA damage in presbycusis is still not clear. This is mainly due to the fact that the deletion is not precisely quantified, nor has it been analyzed with respect to the time sequence of the development of hearing loss with age. The large-scale mtDNA deletion is presumably a cumulative disorder resulting from reactive oxidant metabolite (ROMs) insults. In this study, this deletion was investigated quantitatively and in Fischer 344 Rats of different ages, in an attempt to define the chronological trend of age-related cumulative mitochondrial deletion to the development of hearing loss. The large-scale mtDNA deletion was measured using quantitative real-time PCR and expressed as relative proportion of the copies with deletion in the total mtDNA copies ( $\Delta\Delta$ Ct method). It was found that the copies with deletion increased very quickly during the early stage of rats; life and reached over 60% at the age of 6 months (~1/5 of life span) and the accumulation of the deletion slowed down thereafter. However, a significant hearing loss was not seen until after rats became 12 months old. The results suggest that the existence of the deletion per se does not necessarily imply cochlear damage and hearing loss. If this is a cause of hearing loss, a critical level of the accumulated deletion seems to be needed before cellular malfunction occurs. The long delay between the deletion and the hearing loss indicates the involvement of mechanisms other than mtDNA deletion in the development of presbycusis.

343 Cochlea Structure Differences in Type I and Type II Diabetic Middle Age CBA Mice Olga Vasilyeva<sup>1,2</sup>, Xiaoxia Zhu<sup>1,2</sup>, Susan T. Frisina<sup>1,2</sup>, Robert D. Frisina<sup>1,2</sup>

<sup>1</sup>Univ. Rochester Medical School, <sup>2</sup>Int. Ctr. Hearing Speech Res., Nat. Tech. Inst. Deaf

Recently, our group showed that older diabetic patients exhibited hearing loss compared with age-matched individuals without diabetes. In the current study we hypothesized that experimentally induced diabetes would

accelerate age-related hearing loss in mice compared to controls, as we found in humans. Type I and type II diabetes were induced in middle age CBA mice (12 months old [mon]). Type I: Streptozocin (STZ; 200 mg/kg, i.p., n=8), Type II (high fat diet, 58R3 TestDiet, n=11), and Controls (n=11) were kept for 6 mon. Fasting blood glucose, body weights, Auditory Brainstem Response (ABR), and Distortion Product Otoacoustic Emissions (DPOAE) were evaluated at baseline and every 2 mon. Selected samples of the cochlea were assayed with H and E staining at the end of the experiment. Statistical analysis was performed using Prism 5.1. Body weight of control mice did not change over 6 mon (~30g). There was a significant decline in body weight in the STZ CBA (20%), while high fat mice exhibited ~30% weight gain. In both diabetic groups blood glucose levels significantly increased: 3 fold in the STZ, 1.3 fold in the high fat diet, relative to controls. ABR thresholds were elevated at all frequencies (3-48 kHz) in STZ, while high fat diet mice exhibited ABR thresholds elevations starting at 6 kHz and higher frequencies compared with controls. Similar to ABR thresholds, DPOAE amplitudes declined in both diabetic groups at high frequencies (30-45 kHz) compared to controls. There were no significant differences in spiral cell density or perikaryal size experimental groups. However, a significant atrophy of the stria vascularis in all cochlear turns (~40%) was evident for the high fat diet group only. In summary, a pathogenesis of the accelerated peripheral hearing loss is due to anatomical alterations in stria vascularis in type II compared with type I diabetes, or relative to control mice. Supported by NIH grants NIA P01 AG09524, NIDCD P30 DC05409.

#### | 344 | Effectiveness of Insulin for Treating Hearing Loss in Diabetic Mice

**Brock O'Neil<sup>1</sup>**, Xiaoxia Zhu<sup>1,2</sup>, Olga N. Vasilyeva<sup>1,2</sup>, Susan T. Frisina<sup>1,2</sup>, Robert D. Frisina<sup>1,2</sup>

<sup>1</sup>Univ. Rochester Medical School, <sup>2</sup>Int. Ctr. Hearing Speech Res., Nat. Tech. Inst. Deaf

Type I and Type II Diabetes have been shown to cause a number of metabolic and physiological clinically relevant medical conditions, including hearing loss. For example, we recently reported the nature and extent of peripheral and central hearing loss in aged Type II diabetic human subjects [Frisina et al., Hear. Res. 211: 103-113, 2006]. Aggressive treatment of diabetes through medication, exercise and diet, have proven effective for reducing or slowing the progression of various vascular and metabolic diabetic sequelae in many patients. However, no studies have specifically examined interventions aimed at reducing hyperglycemia in order to preserve hearing in diabetic subjects, or slow down progression of hearing loss due to diabetes. The objective of this study was to examine the effectiveness of insulin treatment in preventing or reversing diabetic induced age-related hearing loss in CBA Auditory brain response (ABR) thresholds and distortion-product otoacoustic emission levels (DPOAEs) were recorded in male streptozotocin treated diabetic mice. Preliminary data suggest that by eight weeks after

induction of diabetes, all mice showed elevated ABR thresholds at 24 and 32 kHz, and reduced DPOAEs between 35 and 48 kHz. Eight weeks after induction of diabetes, mice were implanted with a subcutaneous insulin or palmitic acid control pellet. Although this portion of the investigation is still in progress, there appear to be differences between mice treated with insulin versus control mice as measured by both ABR thresholds and DPOAEs.

Work supported by NIH: Nat. Inst. on Aging, Nat. Inst. for Deafness & Communication Disorders.

### 345 Apoptosis Pathways Change with Age in CBA Mouse Cochlea: A Gene Expression Study

**Sherif F. Tadros**<sup>1,2</sup>, Mary D'Souza<sup>1,2</sup>, Xiaoxia Zhu<sup>1,2</sup>, Emily Pulli<sup>1</sup>, Robert D. Frisina<sup>1,2</sup>

<sup>1</sup>Univ. Rochester Medical School, <sup>2</sup>Int. Ctr. Hearing Speech Res., Nat. Tech. Inst. Deaf

Apoptosis - endogenous programmed cell death (PCD) requires active participation of the cell cycle. Apoptosis is important for regulating inner ear organogenesis and maintaining cellular homeostasis during embryonic development, and participates in crucial cell cycle events in adults. It has been estimated that either too little or too apoptosis contributes to a neurodegenerative conditions, including aging of sensory systems. Apoptosis has different pathways that differ according to tissue type and pathological condition, including extrinsic or intrinsic pathways. The aim of this study is to compare gene expression patterns of different apoptotic pathways as a function of age and hearing loss in CBA mice. Mice were divided into 4 groups based upon age and hearing measurements: young adult control with good hearing (N=8, 4 male, 4 female, age=3.5 +/- 0.4 mon), middle-aged with good hearing (N=17, 8 male, 9 female, age=12.3 +/- 1.3 mon), old with mild presbycusis (N=9, 4 male, 5 female, age=27.7 +/- 3.4 mon) and old with severe presbycusis (N=6, 2 male, 4 female, age=30.6 +/- 1.9 mon). GeneChip expression patterns of 318 apoptosis-related probes were analyzed, and differences in signal-log-ratio and fold changes between subject groups were analyzed. Thirty eight probes showed significant differences in expression. The significant gene families include Caspases, Bcl2, P53, Calpains, MAPK, Jun, Nf-kB-related, and TNF-related genes. These probes were classified according to their expression (up or downregulated) and according to the apoptosis pathway (extrinsic, death receptor pathway and survival factor withdrawal, pathways; intrinsic pathways; and common pathways). It is hoped that increased knowledge of cell death pathways in the aging auditory system may someday lead to interventions to slow or prevent presbycusis – age-related hearing loss.

Supported by the Nat. Inst. on Aging and Nat. Inst. for Deafness and Communication Disorders, NIH.

# 346 Caloric Restriction Suppresses Apoptotic Cell Death in the Mammalian Cochlea and Leads to Prevention of Presbycusis

Shinichi Someya<sup>1,2</sup>, Tatsuya Yamasoba<sup>2</sup>, Richard Weindruch<sup>1</sup>, Masaru Tanokura<sup>2</sup>, Tomas A. Prolla<sup>1</sup> <sup>1</sup>University of Wisconsin-Madison, <sup>2</sup>University of Tokyo Presbycusis is characterized by an age-related progressive decline of auditory function, and arises mainly from the degeneration of hair cells or spiral ganglion (SG) cells in the cochlea. Caloric restriction (CR) extends the lifespan of most mammalian species examined and is the only intervention shown to slow the rate of aging in mammals. Here we report that caloric restriction suppresses apoptotic cell death in the mouse cochlea and prevents late onset of presbycusis (Someya et al., Neurobiology of Aging, 2006). To examine the effects of CR on presbycusis, we reduced the caloric intake of C57/BL6 (B6) mice to 74% of that fed to control animals in early adulthood (2 months of age), and this dietary regimen was maintained until 15 months of age. ABR thresholds measured from 4-month-old young control (YC) and 15-month-old middle-age control (MC) mice revealed that YC mice exhibited normal hearing; however by 15 months, MC mice exhibited significant age-related hearing loss. In contrast, 15-month-old CR mice displayed normal hearing, showing that CR prevented the manifestation of presbycusis to this age. Morphological analysis revealed that MC mice exhibited significant loss of SG cells and hair cells throughout the cochlea. Notably, CR prevented these degenerative changes. To examine the effects of CR on apoptotic cell death in the cochlea, we conducted TUNEL staining and caspase-3 immunostaining. CR mice displayed a significant reduction in the number of TUNELpositive cells and cleaved caspase-3-positive cells relative to MC mice, indicating that apoptosis was suppressed by CR. To examine mRNA expression levels of genes that may be associated with apoptotic cell death and cochlear degeneration in MC and CR mice, we conducted gene expression analysis using high-density oligonucleotide microarrays. A comparison of cochleae from MC and CR mice revealed that CR resulted in down-regulation of 24 programmed cell death-regulating genes out of the 254 genes in this category, including Bak, Bim, Casp6, and II6, indicating that CR suppressed expression of apoptosisrelated genes. Together, our findings suggest that apoptosis is associated with the development of presbycusis, and that CR may prevent presbycusis by inhibiting apoptotic cell death in the cochlea.

# 347 Gene Expression Levels of the Potassium Channel Tetramerization Domain: a Possible Association with Age-Related Hearing Loss in CBA Mice

**Zachary Reese**<sup>1</sup>, Mary D'Souza<sup>1,2</sup>, Marcus Rampton<sup>1</sup>, Xiaoxia Zhu<sup>1,2</sup>, Sherif F. Tadros<sup>1,2</sup>, Robert Frisina<sup>1,2</sup>

<sup>1</sup>Univ. Rochester Medical School, <sup>2</sup>Int. Ctr. Hearing Speech Res., Nat. Tech. Inst. Deaf

The potassium channel tetramerization domain containing (KCTD) gene family contains an N-terminal sequence

homologous to the T1 domain of the Shaker family of voltage-gated potassium channels. However, KCTD proteins lack a transmembrane domain and other aspects of channel proteins. Voltage-gated potassium channels (including the Shaker family) play a critical role in the regulation of the cochlear response to auditory stimuli, and mutations to these channels have been shown to cause hearing loss in mammals, including mice. The role of the "Shaker-related" KCTD gene in auditory function has not yet been outlined. The purpose of this study was to determine the relationship between expression of the KCTD gene within the cochlea and age-related hearing loss (presbycusis) in CBA mice. Four groups of mice were defined based upon their age and hearing levels (as determined by ABR thresholds and DPOAE amplitudes): 1) Young controls, 2) Middle-aged with good hearing, 3) Old with mild presbycusis, and 4) Old with severe presbycusis. DNA-Microarray RMA normalized data yielded 105 potassium receptor probe-sets (22 within the potassium channel subset) in the M430A GeneChip. Log Signal Ratios (LSR) from the probe-sets were subjected to the following statistical analyses: 1) One-way ANOVA, 2) Linear Regression of LSR vs. ABR or DPOAE, and 3) Fold changes in microarray gene expression. Probe sets with expression changes > 1.2-fold over young controls and p values < 0.05 were selected for RT-PCR confirmation of the expression pattern within the subject groups. Four KCTD probe-sets (KCTD7, KCTD9, KCTD10, & KCTD12) met the selection criteria, and RT-PCR validated the microarray results in one (KCTD10) of the four probe-sets. The results suggest that down regulation of the KCTD10 gene may play an important role in age-related hearing loss in the mouse cochlea.

Work supported by NIH: Nat. Inst. on Aging, Nat. Inst. for Deafness & Communication Disorders.

### 348 Age Related Elevation of Catalase and Glutathione Peroxidase Activities in the Rat Cochlea

**Donald Coling**<sup>1</sup>, Max Chen<sup>1</sup>, Donald Henderson<sup>1</sup>

<sup>1</sup>University at Buffalo

Oxidative stress is a pervasive factor in aging. Reactive oxygen species have been implicated as causative factors in cochlear pathology following noise exposure. The inner ear has been shown to combat noise induced hearing loss by upregulation of antioxidant enzymes. The purpose of this experiment is to better understand the role of the antioxidant defense system in the young and aged ear. Specifically, we measured the activities of two enzymes that catalyze the removal of hydrogen peroxide  $(H_2O_2)$ , catalase and glutathione peroxidase (GPx), in 3 month old and 24 month old Fisher-344 rats. Catalase activity was determined by measuring the time-dependent decrease in adsorption of H<sub>2</sub>O<sub>2</sub> at 240 nm. GPx was measured using NADPH-dependent glutathione reductase to regenerate reduced glutathione by measuring the time dependent oxidation of NADPH at 340 nm. GPx activity in 24 month old rats was significantly higher in liver compared to 3 month old rats. There was a tendency for increased GPx activity in brain, lateral wall and sensory epithelium (spiral limbus, organ of Corti and supporting cells of the basilar membrane), but no change in tissue from the modiolus or vestibular organs. Like GPx, catalase activity was elevated in liver. We observed a significant elevation of catalase activity in vestibular tissue, a tendency for age related elevation in the modiolus, but no change in lateral wall or sensory epithelium. In summary, aging inner ear tissues appear to use tissue-selective antioxidant enzymes for detoxifying  $H_2O_2$ . Aging vestibular and modiolus tissues upregulated catalase activity while aging lateral wall and sensory epithelium had elevated levels of GPx. The authors are grateful for funding from NIDCD.

## 349 Chronic Intra-Cochlear Delivery of CGRP, a Lateral Olivocochlear Transmitter, Enhances Auditory Nerve Activity

**Colleen Le Prell**<sup>1</sup>, David Dolan<sup>1</sup>, Karin Halsey<sup>1</sup>, Larry Hughes<sup>2</sup>

<sup>1</sup>University of Michigan, <sup>2</sup>Southern Illinois University Medical School

The lateral olivocochlear (LOC) neurons project from the auditory brainstem to the cochlea, where they synapse on radial dendrites of auditory nerve (AN) fibers. Calcitoningene-related peptide (CGRP) is an LOC transmitter, and auditory brainstem response amplitude is depressed in CGRP-null mice. To test the hypothesis that CGRP plays a key role in AN modulation, we chronically infused CGRP into the guinea pig cochlea for 14 days and evaluated changes in spontaneous and sound-driven activity. When tests were conducted in a quiet background, the amplitude of both round window noise (a measure of ensemble spontaneous activity) and the synchronous whole-nerve response to sound (compound action potential, CAP) were enhanced. No change was noted in onset adaptation of distortion product otoacoustic emissions, indicating that CGRP had no effect on outer hair cells and suggesting the origin of observed changes was neural. When CAP was recorded in the presence of broadband noise (0.5-20 kHz; 8, 16, 24, or 32 dB SPL), we observed a level-dependant reduction in CAP amplitude (i.e., as the noise level was increased, CAP amplitude decreased). This occurs because some auditory neurons respond to the background noise and this suppresses responses to test tones. During CGRP infusion, the noise effects were reduced. All functional measures returned to baseline values post-CGRP. We previously demonstrated that the net effect of disrupting the LOC innervation in the guinea pig is depressed AN activity (Le Prell et al 2003, JARO, 4: 276-290; Le Prell et al 2005, JARO, 6: 48-62). The current results thus suggest CGRP is an LOC transmitter that normally enhances afferent activity. Other preliminary data we have obtained indicate that CGRP antagonists reduce both round window noise and CAP amplitude. Together, these data suggest both tonic and sound-driven release of CGRP by the LOC neurons modulates AN activity in the guinea pig.

Supported by R03-DC007342 (CGL), and P30-DC05188 (DFD).

## 350 Development of Phase Locking in the Barn Owl's Auditory Nerve: The Emergence of Extreme Temporal Precision

Christine Koeppl<sup>1</sup>

<sup>1</sup>University of Sydney

Auditory-nerve fibres in the barn owl phase-lock to frequencies as high as 10kHz. This provides an input of unparalleled temporal accuracy to central circuits comparing the inputs from both ears and deriving interaural time differences for sound localization. Maturation of these central circuits is delayed well into posthatching time, until head growth is completed and physical auditory cues have stabilized. Models have explored the learning rules that may underly synaptic plasticity during those phases and lead to the formation of the map-like representations of ITD found in the adult system. However, nothing is known about the neuronal inputs during that time.

We report recordings from single auditory-nerve fibres of 12 young barn owls, aged between 11 and 63 days posthatching, which is close to fledging. Animals were anaesthetized with isoflurane and artificially respirated. The auditory nerve was exposed at the brainstem level, by aspirating the cerebellum, and recordings were obtained with glass electrodes.

Responses in young owls showed a reduced upper frequency range compared to adults, which gradually expanded and still appeared not fully mature at P63. In the second week posthatching, characteristic frequencies up to 3-4 kHz were found. By P63, this had increased to 7 kHz. In parallel, thresholds showed a dramatic improvement. Phase locking was present from the youngest ages tested and up to the highest frequencies recorded. Like in adults, phase locking began near or below the rate threshold and vector strength rapidly reached a plateau with increasing sound level. However, vector strengths were inferior to those in the adult and scattered over a larger range. This was especially pronounced at the respective upper frequency limits of the different ages and persisted up to P63.

Thus, the very high-frequency phase locking characteristic for the adult owl appears to emerge gradually and over a prolonged period of time, probably continuing after fledging.

Supported by the DFG (Heisenberg fellowship and grants KO 1143/11-1, 2).

## 351 Changes in Multiple Response Parameters of the Chick Cochlear Nerve as a Function of Pure Tone Intensity

Michael Avissar<sup>1</sup>, Shachee Doshi<sup>1</sup>, Adam Furman<sup>1</sup>, Boning Li<sup>1</sup>, Kirin Kennedy<sup>1</sup>, **James Saunders<sup>1</sup>** 

<sup>1</sup>Department of Otorhinolaryngology - HNS, University of Pennsylvania

The chick has been extensively studied as a model for sound-induced acoustic damage to the inner ear, and many parameters of chick cochlear nerve activity have been reported using pure tones at the characteristic frequency (CF) in both control and exposed animals. This has led to a fuller understanding of the effects of acoustic

trauma. Typically these characterizations focus on one response parameter (e.g. discharge rate as a function of stimulus intensity). To better understand how multiple response features change simultaneously, chicks were presented with 100 ms pure tones (at CF), repeated 40 times per intensity at progressively increasing stimulus intensities. The occurrence of action potentials in cochlear nerve units from onset to 20 ms after the offset of the tone was recorded with 30 µs resolution. Thus, all the information available in the spike trains was preserved, permitting a comprehensive view of response dynamics as a function of intensity. A combined raster plot that spanned all intensities was generated for each unit, and this displayed the occurrence time of every discharge during each trial. The combined plot provided a qualitative overview of changes in spike train features with intensity. From these raster displays, quantitative questions about changes in response statistics were formulated. Changes in firing rate, phase-locking, rate-adaptation, and poststimulus suppression as a function of intensity in both control and exposed groups were analyzed. particularly striking result was that the temporal pattern in spike trains emerged at intensities lower than the ratethreshold. This suggested that temporal coding was more sensitive than rate coding, and this may play an important role in detection and discrimination of barely audible sounds. Other results will be summarized at the meeting. [Research supported by NIDCD award DC-00710 to JCS.]

# 352 Dynamic Regulation of Cochlear Surface AMPa Receptor Expression with Physiological Consequences After Acoustic Stimulation in the Mouse

**Zhiqiang Chen**<sup>1</sup>, Sharon G. Kujawa<sup>1</sup>, William F. Sewell<sup>1</sup>
<sup>1</sup>Eaton-peabody Laboratory, Massachusetts Eye and Ear Infirmary, Harvard Medical School

Glutamatergic AMPA receptors mediate fast synaptic transmission between the inner hair cell and the auditory neuron. In cultured auditory neurons, we previously demonstrated that the number of AMPA receptors on the cell surface can be dynamically regulated in response to activation of NMDA and AMPA receptors. We now show a similar dynamic regulation in vivo following acoustic stimulation. A broad-band noise (1 - 40 kHz at 116 dB SPLrms for 10 min) delivered to 5-8 wk old, anesthetized, CBA/CaJ mice produced ABR threshold shifts (~15 dB at 8 kHz, ~20 dB at 20 kHz, and ~30 dB at 45 kHz), which recovered gradually to near pre-exposure levels by 60-70 min. These noise-induced ABR threshold elevations correlated with changes in surface AMPA receptor expression. The surface AMPA receptor was biotinylated from inner ear extracts and quantified by western blot analysis. Two mins following noise exposure, surface AMPA receptor decreased to 49% of control levels, and recovered to 64% at 20 min and to 91% at 1 hr after noise exposure. One interpretation of the data is that acoustic stimulation transiently reduced the number of surface AMPA receptors, which in turn reduced the sensitivity to sound. The robust dynamic regulation of surface AMPA receptor expression in the inner ear following noise

exposure implies a significant role for this process in regulating synaptic strength in auditory function. Research supported by NIDCD.

#### 353 EPSCs in Afferents of the Isolated Frog Sacculus

Mark Rutherford<sup>1</sup>, William Roberts<sup>1</sup>

<sup>1</sup>University of Oregon

Glutamate release from hair cells was monitored with intracellular recordings of EPSCs in the isolated frog sacculus. Whole-cell voltage-clamp and fluorescent labeling confirmed that individual afferent axons can make multiple synaptic contacts with one or more hair cells, as previously shown with dye injection in vivo (Lewis, E.R. et al., 1982). In standard extracellular baseline recording solution (1.8 mM Ca2+/2 mM K+) we observed ongoing EPSCs, with a 10-fold variation in event amplitude and a positively skewed amplitude distribution, even in recordings from axons that appeared to receive only one synaptic input. Most recordings showed frequent multipeaked events suggesting coordinated exocytosis of several synaptic vesicles within a few milliseconds or less, and all showed even larger monophasic events suggestive of synchronous release of many quanta. recordings EPSCs came at regular intervals or in periodic bursts, while in others the intervals between events were distributed exponentially. Depolarization of the hair cells by 40 mM extracellular K+ increased both the frequency and integrated current amplitude of EPSC events, while leaving the peak current amplitudes relatively unchanged.

## 354 Auditory Nerve Responses to Electric Pulse Trains: Rate, Spike-Amplitude, and Temporal Response Adaptation

**Charles Miller**<sup>1,2</sup>, Paul Abbas<sup>1,2</sup>, Fawen Zhang<sup>1</sup>, Barbara Robinson<sup>1</sup>

<sup>1</sup>University of Iowa Dept of Otolaryngology, <sup>2</sup>University of Iowa Dept of Speech Pathology & Audiology

Auditory nerve fiber (ANF) responses to electric stimulation of deaf ears vary in several respects from those elicited by acoustic stimulation of hearing ears. Studies by Javel (1990) and Litvak et al. (2001) have described important steady-state responses of ANFs to running electric pulse trains. Using pulse rates of at least 4800 pps, Litvak et al. (2001) demonstrated that high-rate trains could favorably alter some ANF temporal responses by reducing the high degree of synchrony typical of electric responses. Due, in part, to electrical stimulus artifact issues, previously published efforts did not focus on the nature of the onset responses or short-term changes in ANF responses following onset of the high-rate train.

We have embarked on a systematic study of how ANF responses adapt following the onset of moderate rate (250 pps) and high rate (5000 pps) trains. Work was conducted using chemically deafened acute cat preparations using 40 us/phase biphasic current pulses and standard micropipette techniques.

Rate adaptation was observed to have two time constants (~10 ms and 50-100 ms), consistent with our earlier compound-action-potential findings. This finding suggests

a need to revisit adaptation model assumptions that have been based upon acoustically derived spike data. Rate adaptation was also found to be dependent upon initial spike rate. Additionally, significant reductions in spike amplitude were observed in some fibers, providing a rationale to account for spike amplitude in models of central processing of ANF activity.

Several temporal measures -- jitter, vector strength, and interval histogram (IH) statistics -- were tracked across the 300 ms duration of the pulse trains. At relatively high levels, refractory and adaptation effects could combine to create complex temporal patterns. For example, the IH mode was observed to shift (abruptly, in some cases) from relatively short values to longer ones. In some cases, these increases could persist across long (i.e., several second) time intervals spanning several pulse-train presentations. Other novel temporal responses to high-rate stimuli were observed in post-stimulus-time histograms. They include "build up" responses to 5000 pps stimuli, indicative of integration and, in a relatively small number (5-10%) of fibers "bursting" patterns.

This research is supported by a grant from the U.S. National Institutes of Health (R01DC006478).

### 355 Regulation of Action Potential Firing Threshold by the I<sub>h</sub> Current in Spiral Ganglion Neurons.

Qing Liu<sup>1</sup>, Robin Davis<sup>1</sup>

<sup>1</sup>Department of Cell Biology & Neuroscience, Rutgers University

Spiral ganglion neurons display complex firing properties that differ according to their innervation pattern. Time dependent electrophysiological parameters, such as latency, onset tau, and accommodation are abbreviated in the high frequency regions of the cochlea and become more prolonged and increasingly heterogeneous in the low frequency regions. In contrast, we have found that the threshold voltage for action potential firing, a parameter related to neuronal excitability, has a distinct distribution pattern. Threshold voltage is not graded along the tonotopic axis, but instead is lowest in the mid-frequency range. Thus, neurons with the greatest excitability are those that innervate hair cells within the most sensitive frequency region of the cochlea (Liu & Davis, ARO Abstracts, 2006).

To elucidate the mechanism of this mid-frequency region enhancement of neuronal sensitivity, we are investigating the role of the  $I_h$  current in regulating threshold voltage. Measurements of the magnitude of hyperpolarizing sag, which reflects the activation of the  $I_h$  current in current clamp recording conditions, display a non-monotonic trend similar to that seen for threshold: the highest magnitudes were found in the mid-frequency region. This putative relationship between threshold voltage level and  $I_h$  current magnitude is currently being explored with sequential voltage and current clamp recordings from the same cell. Initial recordings show a strong relationship between measurements of the hyperpolarizing sag magnitude and  $I_h$  current amplitude ( $R^2$ =0.7; -150 mV); thus, validating the rationale for these studies.

The low voltage activation of the  $I_h$  current, its heterogeneous properties (Mo & Davis, *J. Neurophysiol.*, 1997), along with its role in setting the threshold level in other sensory neurons (Doan et al., *J. Neurosci.*, 2004), provides us with a molecular target for studying location-dependent regulation of threshold in the spiral ganglion. Supported by NIH RO1 DC01856.

#### 356 Laser Stimulation of the Auditory Nerve is Possible at High Repetition Rates

**Philip Littlefield**<sup>1</sup>, Agnella Izzo<sup>2</sup>, Jagmet Mundi<sup>2</sup>, Joseph Walsh, Jr. <sup>2</sup>, E. Duco Jansen<sup>3</sup>, Mark Bendett<sup>4</sup>, Jim Webb<sup>4</sup>, Heather Ralph<sup>4</sup>, Claus-Peter Richter<sup>1</sup>

<sup>1</sup>Department of Otolaryngology, Feinberg Medical School, Northwestern University, Chicago, IL, <sup>2</sup>Department of Biomedical Engineering, Northwestern University, Evanston, IL, <sup>3</sup>Department of Biomedical Engineering, Vanderbilt University, Nashville, TN, <sup>4</sup>Aculight Corporation, Bothwell, WA 98011

Stimulation of spatially discrete spiral ganglion cell populations is difficult using electric current. We recently demonstrated that spatially selective stimulation of the cochlea is possible with light. For light being a useful stimulation paradigm for novel interfaces, including cochlear implants, the neurons must be stimulated at high stimulus repetition rates. Here, single fiber recordings were used to show that stimulation is possible at high repetition rates of the light pulses.

A diode laser (Aculight Corporation) was used for the stimulation of auditory nerve. It operates between 1.844 – 1.873  $\mu$ m, with pulse durations of 35-1000  $\mu$ s, and at repetition rates between 1–1000 Hz. The laser was coupled to an optical fiber that was placed against the round window membrane and oriented toward the spiral ganglion cells. The auditory nerve was surgically exposed and single fiber recordings were made.

Results showed that action potentials occurred 2.5-4.0 ms after the laser pulse. Maximum rates of discharge were up to 250 Hz. The action potentials did not respond strictly after the light pulse with high stimulation rates faster than 300 pulses per second.

Supported by the E.R. Capita Foundation, NIH 260-2006-00006-C, 1R41DC008515-01, F31 DC008246-01.

### 357 Characterizing Mouse Models of Neural Hearing Impairment

**Nicola Strenzke**<sup>1</sup>, Anna Bulankina<sup>1</sup>, Darina Khimich<sup>1</sup>, Hauke Werner<sup>2</sup>, Kerstin Reim<sup>2</sup>, Niels Brose<sup>2</sup>, Sandra Lacas-Gervais<sup>3</sup>, Tobias Moser<sup>1</sup>

<sup>1</sup>Inner Ear Lab/Dept. ORL, University of Goettingen and Center for Molecular Physiology of the Brain, <sup>2</sup>Max Planck Institute for Experimental Medicine, Goettingen,

<sup>3</sup>Experimental Diabetology, University of Technology, Dresden

The consequences for human hearing of impaired synaptic transmission and/or neural conduction in the auditory pathway are not well understood. Mouse models may improve our understanding of the mechanisms of neural hearing impairments, as they allow in-depth analysis of pathophysiology and morphology. Here, we tested hearing

in several mouse mutants with genetic defects potentially affecting synaptic transmission and nerve conduction.

Complexins (CPX1-4) are cytosolic proteins involved in synaptic vesicle exocytosis. CPX-1 knockout-mice showed to a progressive, pantonal hearing loss. ABR peaks II-V were increasingly delayed and amplitudes were reduced, while DPOAE appeared normal. Single-cell RT-PCR and immunohistochemistry failed to detect CPX-1 in inner hair cells. Recordings of calcium currents and exocytosis indicated a normal presynaptic function of CPX-1 deficient IHCs. The attractive hypothesis of an impaired synaptic transmission in the auditory brainstem remains to be tested. Single-knockout-mice for Complexins II, III and IV and double-knockout-mice for Complexin III and IV had normal ABR and DPOAE.

Beta-4-Spectrin is required for the clustering of voltagedependent sodium and potassium channels at the nodes of Ranvier and the initial segments of axons. The various beta-4-Spectrin mutants show hearing deficits ranging from severe impairment of neural conduction to mild increases of ABR latency (e.g. Parkinson et al., 2001; Lacas-Gervais et al., 2004). We now show that DPOAE are present and of normal amplitude in beta-4-Sigma1 Spectrin mutant animals, indicating that peripheral sound processing remains intact. In addition, these mice exhibited a temperature-sensitive phenotype with an enhanced conduction delay under hypothermic conditions. Double-knockout mice for PLP and M6B, constituents of myelin in the CNS, develop progressive demyelination and axonal degeneration. We show that these mice are blind due to degeneration of the optic nerve, whereas only a mild hearing loss and a minimal conduction delay was found by ABR testing. DPOAE were normal. Histological analysis revealed only mild degenerative changes in the auditory pathway.

Acknowledgments: This work was supported by a grant of the University of Goettingen to N.S. as well as DFG (CMPB Goettingen), HFSP and EC (Eurohear) grants to T.M.

# 358 Instantaneous Rate Versus Instantaneous Amplitude Curves of Auditory Nerve Fibers with Various Spontaneous Spike Rates

**J. Wiebe Horst<sup>1</sup>**, JoAnn McGee<sup>2</sup>, Edward Walsh<sup>2</sup>
<sup>1</sup>Dept. of Otorhinolaryngology, University Medical Center Groningen, The Netherlands, <sup>2</sup>Boys Town National Research Hospital, Omaha, NE

We collected action potentials from single auditory nerve fibers in cats. Ordering the moments of occurrence of spikes on a time scale of one period of the stimulus yields a period histogram (PH). A PH resembles a filtered and half-wave rectified version of the stimulus waveform. In PHs of complex stimuli, there is a small but definite difference in shape between nerve fibers of high spontaneous (HS) rates and low spontaneous (LS) rates (Horst et al., JASA 88(6) 1990). Near threshold the PHs of HS fibers show fairly linear responses, those of LS fibers show a more expansive character. We checked this quantitatively with pure tones. By relating the

instantaneous discharge rate (IR) bin by bin to the instantaneous stimulus amplitude (IA), we determined instantaneous input-output curves. Such IO-curves turned out to be robust, time-invariant curves for levels ranging at least from synchronization threshold to rate threshold. IRvs-IA curves are fundamentally different from rate-level curves, in which no phase or other instantaneous information is present. IO-curves were determined for nerve fibers with various spike rates. We found that the expansive behavior indeed occurred for pure tones. This was especially clear for average rates up to 10 spks/s as found in responses of LS and MS (medium spont.) fibers. When plotted on a logarithmic vertical scale and linear horizontal scale, the IO-curves become fairly linear, as expected for an exponential relation between IR and IA. HS fibers produce also a more linear curve for the logarithmic vertical scale than for the linear scale. So, PHs can be fairly adequately described by an exponential function independent of the spontaneous rate of the fiber.

The data suggest a parsimonious description for transduction for all fibers: Transduction can be expressed by a single exponential IO-curve, variably attenuated for fibers with different spontaneous rates; i.e., the lower the spontaneous rate, the larger the attenuation.

## The Instantaneous Input/Output Function of Cochlear Transduction Derived From Auditory Nerve (AN) Measurements

Marcel van der Heijden<sup>1</sup>, Philip Joris<sup>1</sup>

<sup>1</sup>K.U.Leuven, Leuven, Belgium

In previous work we measured the amplitude and phase transfer of the cat cochlea from AN responses to tone complexes (van der Heijden & Joris, 2003, 2006). These cochlear transfer functions allow the computation of the "effective stimulus waveform" seen by a hair cell of a given characteristic frequency (CF). This effective waveform is the input to the transduction by a hair cell. On the other hand, the spike trains themselves represent the output of the transducer in terms of instantaneous firing rate. We analyzed the transduction process by comparing input and output.

For CF<500 Hz, I/O functions at low intensities were well described by a linear rectifier. At higher intensities, a sloping saturation occurs. At the highest intensities, saturation becomes abrupt (ceiling effect). The comparison of I/O functions across intensities reveals a gain control process: the output range is adapted to sound intensity.

For CF>500 Hz, lowpass effects blurred the I/O functions, and transduction was well described by a frequency-dependent mixture of fine structure and envelope coding.

Our findings resulted in a heuristic model of the transduction consisting of an intensity-dependent rectifier followed by an intensity-independent lowpass filter. We tested the model on independent responses of the AN to wideband noise. It afforded a good description of the transduction.

Supported by the Fund for Scientific Research - Flanders (FWO G.0392.05) and Research Fund K.U.Leuven (OT/01/42 and OT/05/57).

### 360 Cell-Specific Endocannabinoid Signaling in the Dorsal Cochlear Nucleus

Thanos Tzounopoulos<sup>1</sup>, Larry Trussell<sup>2</sup>, Maria Rubio<sup>3</sup>
<sup>1</sup>Chicago Medical School, Rosalind Franklin University,
<sup>2</sup>Oregon Health & Science University, <sup>3</sup>University of Connecticut

The dorsal cochlear nucleus (DCN), integrates acoustic with multimodal sensory inputs from diverse areas of the brain. Excitatory parallel fibers carry these diverse signals to the apical, spiny dendrites of fusiform cells (FCs) and cartwheel cells (CWCs), while auditory nerve fibers carry acoustic inputs to the basal dendrites of FCs. CWCs form a network of interneurons that directly inhibit FCs. Recordings were made from FCs and CWCs when parallel or auditory nerve fibers were stimulated. In the presence of blockers of glycinergic and GABAergic inhibition, application of the CB1 receptor antagonist WIN 55,212-2 (1µM) resulted in large, similar decrease in parallel fiber EPSCs in FCs and CWCs; When the concentration of WIN-55,212-2 was reduced to 50 nM, a more gradual and limited block of transmission at cartwheel synapses was seen. These data suggest that parallel fiber terminals may differ in their density of CB1 receptors (CB1Rs).

confirmed interpretation was through immunolocalization of CB1Rs. Postembedding immunolocalization was performed using antibodies directed against either the entire C-terminus or a 15-amino acid section of the protein of the CB1R. Parallel fibercartwheel synapses had more membrane labelling than synapses onto fusiform cells, and most of that labelling was facing the postsynaptic density. The functional significance of cell-specific engagement endocannabinoid signaling may be to tune the effect of feed-forward inhibition to the fusiform cells

### 361 Cross-Talk Between GABA<sub>A</sub> and Glycine Receptors in Neurons of Rat Inferior Colliculus

Zheng-Quan Tang<sup>1</sup>, Yun-Gang Lu<sup>1</sup>, **Lin Chen<sup>1</sup>**<sup>1</sup>Auditory Research Laboratory, School of Life Sciences, University of Science and Technology of China

In the inferior colliculus, GABAA and glycine receptors (GABAARs and GlyRs) can be expressed in the same neuron and can be activated simultaneously by the GABAergic and glycinergic neural projections to that neuron. The response of these two inhibitory receptors to the release of GABA and glycine at the same moment may not be equal to the sum of their responses to each neurotransmitter released alone because of the possible interactions between the two types of receptors. In the present study, we investigated the functional cross-talk between GABAARs and GlyRs in cultured neurons of rat inferior colliculus with whole-cell patch-clamp recordings. The total current evoked by co-application of GABA and glycine at saturated concentrations was much smaller than the arithmetic sum of the currents evoked by each neurotransmitter alone, indicating the existance of antagonistic cross-talk between GABAARs and GlyRs in the inferior colliculus. Sequential application of GABA and

glycine revealed that this cross-talk was bidirectional and time-dependent. The GABA-induced current was inhibited by activated GlyRs to a similar extent as the glycineinduced current was inhibited by activated GABAARs. The normal function of GABAARs and GlyRs was required since the cross-talk evoked by co-application of GABA and glyince could be blocked by 30 μM bicuculline, a GABA<sub>A</sub>R antagonist, or by 1 µM strychnine, a GlyR antagonist. Reversal potentials of the current evoked by co-application of GABA and glycine were not significantly different from those of the current evoked by application of either GABA or glycine. Moreover, the cross-inhibition was not blocked by calcium-free external solution or 15 mM BAPTA loaded pipette solution, thereby ruling out extracellular and intracellular calcium as a factor. The results demonstrate a novel pattern of cross-talk, which is a bidirectional, timeantagonistic dependent and interaction, GABA<sub>A</sub>Rs and GlyRs in the inferior colliculus. We suggest that this cross-talk between GABAARs and GlyRs has functional significance for temporal information processing involving inhibitory circuits in the central auditory system. Supported by the National Natural Science Foundation of China (Grant 30470560) and by the National Basic Research Program of China (Grant 2006CB500803).

### 362 Development of Novel Regulators of Calcitonin Gene-Related Peptide (CGRP) Receptor Function

**Rhiannon R. Bussey**<sup>1</sup>, Ian M. Dickerson<sup>2</sup>, Anne E. Luebke<sup>3</sup>

<sup>1</sup>Dept of Biomedical Engineering, <sup>2</sup>Dept of Neurobiology & Anatomy, <sup>3</sup>Dept of Biomedical Engineering, Dept of Neurobiology & Anatomy, University of Rochester Calcitonin gene-related peptide (CGRP) is a neurotransmitter present in the lateral olivocochlear efferent system and inner ear sensory vasculature. Transgenic CGRP knockout mice exhibited no change in their sound thresholds, but had a 20% reduction in suprathreshold sound-evoked cochlear nerve activity. However, the 20% reduction of suprathreshold sound-evoked activity may be due to loss of CGRP signaling either at receptors in the cochlear efferent terminals or in the sensory vasculature.

The CGRP receptor is unique among G protein-coupled receptors because it is a heterotrimeric complex: 1) CLR is the ligand binding G protein-coupled receptor, 2) RAMP1 acts as a molecular chaperone and contributes pharmacological specificity to CLR, while 3) RCP couples the CLR/RAMP heterodimer to the cellular signal transduction pathway. Furthermore, if any component of the CGRP receptor complex is reduced, signaling at the receptor complex is concomitantly reduced.

We have initiated cell culture studies to assess the efficacy of regulating the CGRP receptor proteins as a method to modify CGRP receptor function. We have used a cell line (NIH3T3), which endogenously expresses CLR, RAMP1, and RCP, and has a well characterized CGRP response. We have determined that RCP interacts with the 2nd cytoplasmic domain of CLR and have shown that when this domain of CLR is introduced into cells, RCP/CLR interactions are inhibited in parallel with inhibition of CLR

signaling. We are developing a fluorescence resonance energy transfer (FRET)-based detection of cAMP to supplement standard biochemical detection, which will facilitate *in vivo* non-invasive analysis of CGRP receptor signaling in transgenic mice with altered receptor function. These initial studies will develop technologies to modify CGRP receptor function for use in future gene transfer and transgenic mouse experiments to elucidate the role of CGRP in cochlear function.

(Supported by NIH DC03086, DK052328)

#### 363 Dual Modulation of Gabaergic Transmission by Metabotropic GABa and Glutamate Receptors in a Coincidence Detector

Hongxiang Gao<sup>1</sup>, **Yong Lu**<sup>1</sup>

<sup>1</sup>Department of Neurobiology, Northeastern Ohio Universities College of Medicine

We investigated GABA<sub>B</sub> receptor (GABA<sub>B</sub>R)- and metabotropic glutamate receptor (mGluR)-mediated modulation of GABAergic transmission in neurons of the chicken nucleus laminaris (NL), the third-order avian auditory neurons that detect coincident excitatory synaptic inputs and code timing information of sound. Acute brainstem slice preparations obtained from late embryos (E18-E21) were used. Under whole-cell patch recording configurations, GABA<sub>B</sub>R agonist baclofen (100 µM) significantly decreased evoked inhibitory postsynaptic currents (eIPSCs) in NL neurons, suggesting that GABA release in NL is subject to autoreceptor-mediated feedback regulation. A non-specific mGluR agonist tACPD (100 µM) also significantly suppressed eIPSCs in NL neurons. Furthermore, group II and III mGluRs may be involved in modulating GABA release in NL, because DCG-IV (2 µM), a specific agonist for group II mGluRs, and L-AP4 (10 µM), a specific agonist for group III mGluRs, each significantly reduced eIPSCs in NL neurons. 3,5-DHPG (200 µM), a specific agonist for group I mGluRs, did not affect eIPSCs in NL neurons. Using gramicidin perforated patch recordings, we found that the reversal potential (E<sub>GABA</sub>) of eIPSCs in NL neurons is about -30 mV, suggesting that the GABAergic input to NL can be excitatory (able to generate GABA spikes). Under wholecell recording configurations (with 55 mM Cl in recording pipettes), activation of either GABA<sub>B</sub>Rs with baclofen (100 μM), or mGluRs with tACPD (100 μM), nearly completely eliminated GABA spikes induced by stimulating the GABAergic pathway to NL. We speculate that dual modulation of GABAergic transmission by GABA<sub>B</sub>Rs and mGluRs in NL may play a role in auditory signal processing/temporal coding.

Supported by startup funds from NEOUCOM.

### 364 Auditory Brainstem Responses are Deficient in EphA4 and Ephrin-B2 Mutant Mice

**Ilona Miko<sup>1</sup>**, Mark Henkemeyer<sup>2</sup>, Karina Cramer<sup>1</sup> 
<sup>1</sup>UC Irvine, <sup>2</sup>UT Southwestern at Dallas

Eph proteins are axon guidance molecules that influence the development of auditory circuitry in the chick auditory

brainstem. Our recent investigation of c-fos expression after tone exposure in mice lacking Eph proteins showed that these proteins also affect the distribution of neural activation in the mammalian cochlear nucleus. However, functional deficits in mutant mice have not been assessed physiologically. The present study characterizes neural activation in Eph protein deficient mice with another measure of function, the auditory brainstem response (ABR). We recorded and characterized the ABR of EphA4 and ephrin-B2 mutant mice, aged postnatal day 18-20, and compared them to wild type controls. Over a range of 80 SPL, 12kHz click-tones were presented 10 times/second, and the responses were averaged over 500 trials. The peripheral hearing threshold for EphA4<sup>-/-</sup> mice was significantly higher than controls (63 ± 8.8 dB SPL vs. controls, 41 ± 4.4 dB SPL; t-test, p < 0.05). Waveform amplitudes of peak 1 (P1) were reduced in EphA4-/mutants  $(7.5 \times 10^{-4} \pm 1.8 \times 10^{-4} \text{ microvolts vs. controls}, 15)$  $\times 10^{-4} \pm 4 \times 10^{-4}$  microvolts; p < 0.05). For the ephrin-B2<sup>+/-</sup> mice, peripheral hearing thresholds were also elevated  $(62.8 \pm 3.0 \text{ dB SPL}, \text{ vs. controls}, 55.0 \pm 1.7 \text{ dB SPL}; \text{ p} < 1.0 \text{ dB SPL}; \text{ p} < 1.0$ 0.05). Like the EphA4-/- mice, these ephrin-B2+/- mice showed a reduced P1 amplitude (6.5 x  $10^{-4} \pm 1.2 \times 10^{-4}$ microvolts vs. controls,  $10 \times 10^{-4} \pm 3.2 \times 10^{-4}$  microvolts; p < 0.05). Latency to the P2 peak was shorter in ephrin-B2+1mice  $(2.6 \pm 0.06 \text{ ms vs. controls}, 2.9 \pm 0.07 \text{ ms}; p < 0.05),$ while latency to the P1 peak was unchanged, such that the P1 and P2 peaks were closer in time. These elevated thresholds and reduced P1 amplitudes provide evidence for a hearing deficit in both of these mutant mouse lines, and further emphasize an important role for Eph family proteins in the formation of effective auditory circuitry. Supported by NIH DC005771 (to KSC), T32 NS045540, DC006225 (to MH).

#### 365 Cochlear Nucleus Commissural Neurons Co-Label with Vesicular Glutamate Transporter 2

Jianxun Zhou<sup>1</sup>, Yilei Cui<sup>1</sup>, Susan Shore<sup>1</sup>

<sup>1</sup>University of Michigan

The cochlear nucleus (CN) is the first auditory structure that receives binaural information directly via the CN commissural pathway. Despite evidence that the majority of CN commissural neurons are glycinergic and thus inhibitory, physiological and anatomical evidence suggests that some of the neurons in this pathway are excitatory. We examined the putative excitatory portion of this using anterograde tract tracing pathway immunolabeling of vesicular glutamate transporters (VGLUTs). VGLUTs accumulate glutamate in synaptic vesicles, and are prime markers for excitatory glutamatergic neurons. Consistent with previous observations, injections of anterograde tracers into the CN resulted in terminal labeling in many regions of the contralateral dorsal and ventral CN. The terminal endings of commissural projections were typically en passant or small terminal boutons, but large, irregular swellings were also observed, usually in the granule cell domain. A focused group of labeled CN commissural puncta colabeled with VGLUT2, but co-localization with VGLUT1 was not observed. The commissural puncta that colabeled with VGLUT2 were mostly located in the granule cell domain and were usually large in size, suggestive of mossy fibers. These results provide direct anatomical evidence that the CN commissural projection also contains excitatory neurons that are associated with VGLUT2. Current studies are underway to identify the sources of the double-labeled terminal endings.

Supported by the Royal National Institute for Deaf People (RNID) and NIH P30 05188

### 366 Distribution of Cholinergic Cells in Auditory and Non-Auditory Nuclei of the Guinea Pig Brainstem

Susan D. Motts<sup>1,2</sup>, Brett R. Schofield<sup>1,2</sup>

<sup>1</sup>Northeastern Ohio Univ. Coll. Med., <sup>2</sup>Kent State University

Acetylcholine has been studied in the auditory system primarily at the levels of the cortex and the cochlea/cochlear nucleus. The cholinergic cells that project to these areas are located in the basal forebrain and the superior olivary complex. Other cholinergic cell groups also project to brainstem auditory nuclei (Motts and Schofield, '06, ARO Abstr. 29:42). Identification of those groups was hindered by lack of a systematic description of cholinergic cells in guinea pigs. Here, we use an antibody to choline acetyltransferase (ChAT) to describe the distribution of cholinergic cells in guinea pig brainstem.

ChAT-immunoreactive (ChAT-IR) cells form several prominent groups, including the "named" cholinergic nuclei: pedunculopontine tegmental nucleus (Ch 5), laterodorsal tegmental nucleus (Ch 6), medial habenula (Ch 7) and parabigeminal nucleus (Ch 8), as well as the cranial nerve motor nuclei. Additional concentrations are present in the solitary nucleus, superior colliculus and vestibular efferent group. More cells are scattered in the reticular formation and other nuclei.

Among auditory nuclei, the majority of ChAT-IR cells are in the superior olive, particularly in the lateral superior olive, ventral and lateral nuclei of the trapezoid body and superior paraolivary nucleus. Fewer ChAT-IR cells are found in dorsal and ventral cochlear nuclei. There is a scattering of cells in ventral nucleus of the lateral lemniscus. Another cluster of ChAT-IR cells extends from the lateral edge of PPT to the sagulum, forming a "bridge" that runs dorsal to the dorsal nucleus of the lateral lemniscus.

The results show that the distribution of cholinergic cells in guinea pigs is similar to that of other species. In addition, we note the presence of cholinergic cells in or around a number of auditory nuclei. The results provide a basis for further studies to characterize the connections of these cholinergic groups with auditory nuclei. Supported by NIH DC 04391.

#### 367 Expression Patterns of Kv4.2 and Kv4.3 in the Dorsal Cochlear Nucleus

**Sarah Street**<sup>1</sup>, Karen Montey<sup>2</sup>, David Ryugo<sup>2</sup>, Paul Manis<sup>1</sup> <sup>1</sup> *Univ. of North Carolina at Chapel Hill,* <sup>2</sup> *Johns Hopkins University* 

Transient potassium currents shape many neuronal responses to synaptic input such as firing rate, timing of action potentials, and spread of depolarization throughout the dendritic tree. We have previously shown that a transient potassium current affects the response pattern in DCN pyramidal cells and this channel is probably a member of the Kv4.x family of potassium channels (Kanold and Manis, 1999). In this study, we sought to characterize the identity of the channel responsible for this current in pyramidal cells. To identify pyramidal cells, fluorosceindextran in saline was injected into the inferior colliculus of Sprague-Dawley rats aged postnatal day 28. After 2 weeks, the animals were sacrificed and the brains removed. Cryosections of brainstem and cerebellar tissue (10μm) were then stained with antibodies against Kv4.2 and Kv4.3 and viewed with confocal microscopy. Pyramidal cells stained with fluoroscein-dextran were readily detected because of the bright punctate labeling in cell bodies. Kv4.2 immunostaining was not seen in retrogradely labeled pyramidal cells. However, Kv4.2 was detected in other cell types in the DCN. The majority of these cells, found in all layers of the DCN, were small and round. Based on size and dendritic labeling patterns, and the similarity of the Kv4.2 staining pattern in cerebellar granule cells, these are most likely cochlear nucleus granule cells. In contrast to Kv4.2, Kv4.3 labeling was observed in the soma and dendrites of retrogradelylabelled pyramidal cells, as well as in other processes in the DCN. We suggest that Kv4.3 channels are responsible for some or all of the transient current seen in DCN pyramidal cells.

Supported by NIH Grant R01DC00425 to PBM and F31DC007827 to SES and RO1DC00232 to DKR.

### 368 Deafferentation-Induced DNA Fragmentation in Chick Cochlear Nucleus Neurons

**Hope Karnes**<sup>1,2</sup>, John Tanksley<sup>1</sup>, Doug Girod<sup>1</sup>, Dianne Durham<sup>1</sup>

<sup>1</sup>Department of Otolaryngology-Head and Neck Surgery, University of Kansas Medical Center, <sup>2</sup>Department of Anatomy and Cell Biology, University of Kansas Medical Center

Apoptosis is a strictly regulated cell death process characterized by well-controlled loss of cell volume, condensation of chromatin, fragmentation of DNA, and phagocytosis of cell remnants. Neurons undergo apoptosis during development as well as in response to pathologic stimuli. In the avian cochlear nucleus (n. magnocellularis, NM) cochlea removal results in the death of 20-40% of NM neurons within several days. Wilkinson and colleagues (Neuroscience 120:1071-1079, 2003) demonstrated increased immunoreactivity for cytochromec and activated caspase-9 within 6 hours of cochlea removal, implicating apoptosis in deafferentation-induced NM cell death. Studies in our laboratory (Kaiser, et al.,

ARO Abstracts 2005) demonstrated immunoreactivity for activated caspase-3, an effector protein downstream of caspase-9, beginning 12 hours after cochlea removal. Here we evaluated the time course of nuclear DNA fragmentation in NM, detected via immunofluorescent TUNEL staining, following cochlea removal. Ten day-old birds underwent unilateral cochlea removal and were sacrificed 12 to 48 hours later by overdose of anesthesia and perfusion with avian ringer solution. Brains were postfixed in Carnoy's fixative and embedded in paraffin. Coronal sections were reacted for the presence of cleaved DNA using an apoptosis detection kit (Upstate/Millipore). Little evidence for TUNEL staining was observed at 12 hours after cochlea removal. By 24 hours, TUNEL staining was observed in the nuclei of NM neurons ipsilateral to cochlea removal and was still evident at 48 hours survival. Nuclear DNA fragmentation provides further evidence that apoptotic pathways are involved in deafferentation-induced cell death in NM.

Supported by the Department of Otolaryngology-Head and Neck Surgery and the MRRC Center grant to the University of Kansas (HD02528).

## 369 Kv2.2 Containing Potassium Channels Mediate a Frequency-Dependent Current in the Medial Nucleus of the Trapezoid Body.

**Sarah Griffin**<sup>1</sup>, Jamie Johnson<sup>1</sup>, Anna Skrzypiec<sup>1</sup>, Ian Forsythe<sup>1</sup>

<sup>1</sup>MRC Toxicology Unit, University of Leicester, U.K.

Principal neurons in the Medial Nucleus of the Trapezoid Body (MNTB) are capable of sustaining action potential firing at high-frequencies (≈800 Hz). Potassium current conducted through Kv3 and Kv1 channels rapidly repolarise action potentials and ensure the temporal fidelity of firing. We provide evidence for an additional potassium conductance in these neurons, mediated by Kv2.2 containing channels. Quantitative RT-PCR showed the presence of Kv2.2 mRNA and immunohistochemical labeling confirmed that Kv2.2 protein was expressed in MNTB neurons. In whole-cell patch clamp recording, currents mediated by Kv2.2 containing channels activated at voltages positive to -30 mV and slowly inactivated. In the absence of a specific blocker for this current we investigated its function within a biophysical model implemented using the NEURON simulation software. The magnitude of the Kv2.2 current increased with the firing rate of the model neuron. We conclude that Kv2.2 containing channels provide a hyperpolarizing drive during high-frequency firing which may prevent cumulative inactivation of sodium channels.

#### 370 Differential Expression of HCN Channels in the Cochlear Nucleus

Ana Caban Cardona<sup>1</sup>, Rebecca Eernisse<sup>1</sup>, Paul Popper<sup>1</sup>, **David Friedland**<sup>1</sup>

<sup>1</sup>Medical College of Wisconsin

Hyperpolarization-activated currents (Ih) have been identified in many auditory brain stem neurons including octopus and bushy cells. The channels responsible for

these currents are hyperpolarization-activated cyclic nucleotide-gated potassium channels of which four isoforms are known (i.e., HCN1-4). These channels influence resting membrane potentials, regulate neuronal excitability and likely play important roles in auditory signal used real-time RT-PCR processing. We immunohistochemistry to investigate differential expression of all four HCN channels among the subdivisions of the cochlear nucleus. Higher levels of HCN2 and HCN4 mRNA were detected in the ventral subdivisions of the cochlear nucleus than in the DCN, although this did not reach statistical significance. Realtime RT-PCR results for HCN1 and HCN3, in contrast, showed no differential expression. immunostaining for HCN2 and HCN4 in the DCN but no staining in this region for the other two channels. Our HCN2 labeling was predominantly found in cartwheel cells although previous reports have also shown HCN2 in fusiform cells. We found HCN4 to be most highly expressed in the fusiform cells. HCN4 was also noted among large neurons within the auditory nerve root. We found no neuronal staining for HCN3 in any subdivision and all HCN3 staining appeared localized to fibers in the peri-neuronal spaces. Similar to other studies, we found strong HCN1 staining on octopus cells of the PVCN but in contrast to other studies we did not identify significant staining in bushy cell regions. This study adds to the increasing evidence for differential expression among auditory neurons of the various hyperpolarizationactivating potassium channels. The particular expression of HCN2 and HCN4, which are strongly regulated by cAMP, in the DCN may underlie some forms of neuronal plasticity such as that associated with noise-induced DCN hyperactivity and the generation of tinnitus.

Supported by NIH/NIDCD K08DC006227.

### 371 The Temporal Representation of the F0 of Complex Sounds in the Ventral Cochlear Nucleus Under Reverberant Conditions

Mark Sayles<sup>1</sup>, Neil Ingham<sup>1</sup>, Ian Winter<sup>1</sup>

<sup>1</sup>CNBH, University of Cambridge, UK

Reverberation has a deleterious effect on the intelligibility of complex time-varying stimuli such as speech. Psychophysical experiments have demonstrated that the combination of relatively mild reverberation and modulation of the fundamental frequency (F0) disrupts listeners' ability to perceptually segregate competing speech sounds on the basis of an F0 difference (Culling *et al.*, 1994). As a first attempt to understand the effects of reverberation from a physiological perspective we have recorded the responses to complex time-varying sounds, with and without reverberation, from single neurons in the ventral cochlear nucleus

Stimuli were complex tones containing harmonics 1-20 (summed in cosine or alternating sine-cosine phase) of an F0 with a linear transition ending one octave above the starting frequency. Starting frequencies were spaced at 1/3 octave intervals between 100 and 400 Hz. In order to apply reverberation to these stimuli we convolved the waveforms in the time domain with impulse responses

recorded at source-to-receiver (S-R) distances of 0.32, 0.63, 1.25, 2.5, 5.0 and 10.0m (provided by Dr Tony Watkins). A control stimulus of white noise was also presented. All stimuli were 0.5s in duration, gated on and off with a 1 ms cos<sup>2</sup> window and were presented in random order for typically 25 or 50 repetitions.

To measure the temporal response to the F0 we shuffled all-order inter-spike constructed interval histograms from the recorded spike trains of 95 single units. Most units showed a strong temporal representation of F0 in the dry (no reverberation) condition. However, for many units this representation was degraded with S-R distance. A population analysis increasing demonstrated that the sensitivity of the inter-spike interval representation of F0 to reverberation was dependent on unit best frequency (BF), harmonic spacing and the S-R distance. Increasing harmonic spacing, resulting in fewer harmonics passing through a unit's filter, resulted in a better representation of F0. Our results show that the temporal representation of F0 in frequency regions where harmonics are unresolved is severely affected by reverberation but that when harmonics are resolved the units are relatively resistant to the effects of reverberation.

Acknowledgements: MS is supported by the Cambridge MB/PhD programme.

References: Culling J.F., Summerfield Q., Marshall D.H. 1994. Effects of simulated reverberation on the use of binaural cues and fundamental-frequency differences for separating concurrent vowels. *Speech Commun.* 14: 71-95.

### 372 Bushy Cells in the Ventral Cochlear Nucleus of Mice are of Two Biophysical Types

**Xiaojie Cao**<sup>1</sup>, Matthew J. McGinley<sup>2</sup>, Shalini Shatadal<sup>1</sup>, Donata Oertel<sup>1</sup>

<sup>1</sup>UW-Madison, <sup>2</sup>Oregon Health and Sciences University Bushy cells convey the timing and rate of firing of auditory nerve fibers to the superior olivary complex, where the interaural comparison of time and intensity is the basis for localizing sounds in the horizontal plane. Bushy cells are biophysically distinct from other types of neurons in the VCN. Previous recordings showed that bushy cells (here called bushy I) have a low input resistance in the physiological voltage range and that they fire only at the onset of a depolarization. These features are generated by a low-voltage-activated K+ conductance (gKL) (Manis and Marx, J Neurosci 11: 2865, 1991) and a hyperpolarizationactivated mixed cation conductance (gh). We recently discovered that some anatomically labeled bushy cells differ from those that were described before. Bushy II cells have higher input resistances, a slower and smaller sag in responses to hyperpolarizing currents and can fire even after the onset of a depolarization. To understand what underlies their differences, we made whole-cell recordings in slices from mice. The input resistance of bushy II cells (87±16 MÙ, n=8) is higher than that of bushy I cells (54±11 MÙ, n=11). While the pharmacological properties of gKL and gh are similar in the two populations, the maximum amplitudes of gKL and gh are smaller by a factor of two in

bushy II than in bushy I cells (bushy I gKLmax was  $103.5\pm30.6$  nS n=5, ghmax  $44.5\pm11.2$  nS n=6; bushy II gKLmax  $57.3\pm18.4$  nS n=6; ghmax  $21.1\pm4.7$  nS n=4). The maximum high-voltage-activated (gKH) potassium conductances were of similar magnitude (bushy I  $54.7\pm14.1$  nS n=5; bushy II  $62\pm14$  nS n=6). The biophysical differences result in a sensitivity to slower rates of depolarization in bushy II than bushy I cells. We are testing the hypothesis that bushy I and II cells correspond to globular bushy cells that innervate the contralateral MNTB and small spherical bushy cells that innervate the ipsilateral LSO respectively.

This work was supported by a grant from NIH DC00176.

### 373 Ventral Cochlear Nucleus Responses to Contralateral Sound are Mediated by CN-Commissural and Olivocochlear Pathways

**Seth Koehler**<sup>1</sup>, Sanford Bledsoe<sup>1</sup>, Debara Tucci<sup>2</sup>, Susan Shore<sup>1,3</sup>

<sup>1</sup>Kresge Hearing Research Institute, Dept. of Otolaryngology, University of Michigan, <sup>2</sup>Division of Otolaryngology-HNS, Duke University Medical Center, <sup>3</sup>Dept. of Molecular and Integrative Physiology, University of Michigan

Sound stimulation both inhibits and excites unit activity in the opposite cochlear nucleus. In the normal guinea pig, contralateral sound primarily inhibits ventral cochlear nucleus (VCN) unit activity (Shore et al, Exp. Br. Res.. 2003). However, under conditions of ipsilateral deafening, contralateral stimulation elicits compensatory excitation in VCN units (Sumner et al., J. Neurophysiol, 2005). The inhibitory responses to contralateral sound may be mediated by the CN-commissural pathway, or indirectly via interneurons in the medial nucleus of the trapezoid body (MNTB), both of which are glycinergic. The contralateral excitatory responses may be mediated by cholinergic interneurons in the ventral nucleus of the trapezoid body (VNTB) that enter the CN as collaterals of the olivocochlear bundle (OCB) or via the trapezoid body. Another potential source of contralateral excitation is a glutamatergic component of the CN-commisural pathway (Zhou et al, ARO 2007). We lesioned the putative pathways using lidocaine or the neurotoxin mellitin to elucidate their contributions to activity evoked by contralateral sound in normal and unilaterally deafened preparations.

In the normal guinea pig, lesions of the dorsal and intermediate acoustic striae, as they exit the contralateral CN, eliminated both contralateral inhibition and high threshold excitation. In unilaterally deafened guinea pigs, lesions of the crossed olivocochlear bundle reduced contralateral excitation. These preliminary results indicate that the CN-commissural pathway mediates normal contralateral inhibitory responses. The compensatory contralateral excitation in unilaterally deafened animals appears to be at least partially mediated by olivocochlear neurons. Future studies will determine the contribution of pathways entering the CN via the trapezoid body.

Supported by the Royal National Institute for Deaf People (RNID), NINCD DC-05415 and NIH P30 05188

### 374 Effects of Somatosensory Electrical Stimulation on Neural Activity of the Dorsal Cochlear Nucleus of Hamsters

Jinsheng Zhang<sup>1,2</sup>, Zhenlong Guan<sup>1,3</sup>

<sup>1</sup>Department of Otolaryngology, Wayne State University School of Medicine, <sup>2</sup>Department of Communication Sciences & Disorders, Wayne State Univ College of Liberal Arts & Science, <sup>3</sup>Department of Zoology, Hebei Normal University College of Life Sciences

It has been shown that sound exposure induces hyperactivity in the dorsal cochlear nucleus (DCN) in hamsters, rats and chinchillas. This hyperactivity has been demonstrated to be correlated with the behavioral evidence for tinnitus. It is conceivable that suppression of hyperactivity in the DCN would suppress tinnitus. Somatosensory electrical stimulation (SES) has been used clinically to suppress tinnitus. However, due to a lack of understanding of the mechanisms of tinnitus suppression through SES, this approach has not been developed as an effective and reliable means for treating tinnitus. The current study was to test the effects of SES by delivering electrical current to the basal part of the pinna on DCN activity of both control and tone-exposed animals. Experiments were carried out in 26 adult hamsters, among which 13 were exposed to an intense tone under anesthesia (10 kHz tone, 125-130 dB SPL, 4 hrs) and another 13 age-matched control animals were similarly anesthetized but not exposed to a sound. One to three weeks after sound exposure and control treatment, multiunit activity was recorded at the surface of the left DCN before, during and after electrical stimulation of the left pinna. Electrical stimuli were single biphasic pulses of 200 us duration, delivered at 100-900 uA and 100 pps. The results from both control and exposed groups revealed four response types: S-S, referring to suppression during and after stimulation; E-S, manifesting excitation during stimulation but suppression after stimulation; S-E, showing suppression during stimulation but excitation after stimulation; E-E, representing excitation during and after stimulation. We found that there were more incidences of suppression than excitation during and after stimulation in both control and exposed groups. At higher levels of current, there was a significantly higher degree of suppression after stimulation than during stimulation for both groups, and there was also higher degree of suppression during and after stimulation in exposed animals than in controls. Our results are in line with previous clinical findings and support the view that DCN hyperactivity may be the direct neural correlate of tinnitus and suppression of DCN hyperactivity through SES may be one important approach in tinnitus suppression.

(Supported by ATA).

# 375 The Role of Parallel Fibers in Somatosensory Electrical Stimulation Induced-Effects on Neural Activity of the Dorsal Cochlear Nucleus of Hamsters

Zhenlong Guan<sup>1,2</sup>, Jinsheng Zhang<sup>1,3</sup>

<sup>1</sup>Department of Otolaryngology, Wayne State University School of Medicine, <sup>2</sup>Department of Zoology, Hebei Normal University College of Life Sciences, <sup>3</sup>Department of Communication Sciences & Disorders, Wayne State Univ College of Liberal Arts & Science

It has been shown that somatosensory electrical stimulation (SES) or stimulation of parallel fibers induces both inhibition and excitation in fusiform cells, which are believed to be mediated by inter-inhibitory neurons and fusiform cells. However, it is unclear whether SES-induced inhibitory and excitatory effects on DCN activity would be changed if parallel fibers are transected. Alternatively, it is unknown whether the parallel fiber-inhibitory neuronfusiform cell system is the only mechanism that controls SES-induced effects. Experiments were carried out on 12 previously sound-exposed (10 kHz tone, 125-130 dB SPL, 4 h) and 15 unexposed hamsters. The left DCN was then surgically exposed and multiunit activity was recorded at the DCN surface during and after SES. SES was performed by delivering single biphasic pulses (200 µs pulse width, 100-900 µA, 100 pps) during 30-90 seconds to a pair of electrodes inserted near the left pinna. Following stimulation and recording, micro-sectioning was performed around the recording site to cut off the surrounding parallel fibers. Thirty minutes later, stimulation and recording were repeated. At the end of experiments, the animal was euthanized and its brain was removed, frozen-sectioned and Nissl-stained to verify whether parallel fibers were severed. Our results demonstrated that, before cutting parallel fibers, 81.8% of total trials in control animals manifested changes in activity rates over baseline level following SES whereas 18.2% showed no changes. Similarly in exposed animals, SES induced rate changes in 84.6% of trials and no changes in 15.4% of trials. However, following sectioning of parallel fibers, SES resulted in rate changes in 63.6% of trials and no changes in 36.4% of trials in control animals, while SES caused changes in 53.9% of trials and no changes in 46.1% of trials. Such effects were slightly stronger in exposed animals than in controls. The above results indicate that cutting off parallel fibers only partially affected SESinduced effects on DCN activity. Our data are supported by previous findings that the trigeminal nucleus projects to the granule cell domain and three layers of the DCN, suggesting that the parallel system may not be the only mechanism in controlling somatosensory inputs to the

(Supported by ATA).

# 376 Projections of Low-Frequency Neurons of the Anteroventral Cochlear Nucleus in the Mustached Bat: Precursors to Spectral Integration in the Inferior Colliculus

Asuman Yavuzoglu<sup>1,2</sup>, Jeffrey Wenstrup<sup>1,2</sup>

<sup>1</sup>Northeastern Ohio Universities College of Medicine, <sup>2</sup>Kent State University

Combination-sensitive neurons are facilitated or inhibited when two sounds of different frequencies are presented in a specific temporal relationship. Facilitative combination sensitivity is created in high-frequency regions of inferior colliculus (IC), while some inhibitory combination sensitivity is created in intermediate nucleus of lateral lemniscus (INLL). Both interactions depend on lowfrequency glycinergic inputs, but the origin of these inputs unknown. Here we describe projections physiologically identified low-frequency regions of anteroventral cochlear nucleus (AV), including the specialized marginal zone. In the superior olivary complex, anterograde labeling was located in the lateral part of the ipsilateral lateral superior olive (LSO) and dorsolateral parts of the medial superior olive (MSO) bilaterally. These regions represent low frequencies in the audible range. In the contralateral nuclei of lateral lemniscus, labeled boutons occurred in the medial half of multipolar and columnar divisions of the ventral nucleus (VNLLm, VNLLc) and in INLL. Since the tonotopy in VNLL and INLL is complex, it is unclear whether these regions include highfrequency representations, but the majority of label is consistent with low frequency-regions of these nuclei. Labeling in the dorsal nucleus (DNLL) was only in its lowfrequency, dorsolateral part. In IC contralateral to the tracer deposit, we occasionally observed sparse labeling in high-frequency regions. In contrast, the rostral part of the nucleus, known as a low-frequency region, displayed strong anterograde labeling after low-frequency AV deposits. The results suggest that low-frequency inputs to combination-sensitive neurons do not arise from AV neurons directly. However, AV may contribute to creation of facilitative combination sensitivity by providing input to structures in the ascending auditory pathway that are critical for these interactions.

Supported by NIDCD grant R01 DC-00937 (JJW).

## 377 Synaptic Transmission at AVCN Endbulb Synapses with Poisson Distributed Spike Trains

Yong Wang<sup>1</sup>, Paul Manis<sup>1</sup>

<sup>1</sup>Dept of Otolaryngology, Univ. of North Carolina

The spiking patterns of bushy cells in the mammalian anterior ventral cochlear nucleus (AVCN) are not a carbon copy of the activity in the auditory nerve fibers (ANFs). In vivo recordings from AVCN bushy neurons have shown that a fraction of ANF spikes fail to drive bushy cells. Moreover, recordings from single auditory nerve fibers have revealed high spontaneous firing rates, sometimes exceeding 100 Hz. In addition to the effects of inhibition, synaptic depression during high rates of ANF activity and subsequent recovery during periods of lower activity can

significantly shape the functional relationship between ANFs and the bushy cell. Previously we have shown a rate dependent depression and recovery when ANFs were stimulated with trains of regularly spaced shock stimuli. Here, we recorded AMPA receptor mediated EPSCs in bushy neurons while stimulating ANFs with trains of shocks with Poisson-distributed inter-stimulus intervals. For mean rates of 100Hz and 200 Hz, significant synaptic depression was observed during 500 ms Poissondistributed spike trains. The degree of steady-state synaptic depression with Poisson-distributed spike trains was comparable to that elicited by regularly spaced shocks (~70% at 100 Hz and ~40% at 200 Hz). With regularly spaced shocks, no significant recovery of EPSC amplitude was evident 500 msec after the 100 Hz shock train. However, when stimuli were delivered at 200 Hz, a very synaptic recovery with a time constant τfast=23.3±10.5 ms was followed by a slower recovery τslow=1.5±0.7 sec. The fast phase accounts for about 80% of the total recovery. In contrast, no fast recovery phase was observed following Poisson stimuli at 200 Hz, even though the final synaptic depression was comparable between regular and Poisson stimulus trains. Our data suggest that under normal operating conditions, the endbulb synapse is slightly depressed for those bushy neurons that receive input from auditory nerve fibers with high spontaneous firing rates, and that recovery from synaptic depression depends on the statistical distribution of presynaptic spike times.

(Supported by NIDCD grant DC04551).

## | 378 | Influence of Glycinergic and Gabaergic Inhibitory Inputs on Temporal Responses of Anteroventral Cochlear Nucleus Choppers

Yan Gai<sup>1,2</sup>, Laurel Carney<sup>2,3</sup>

<sup>1</sup>Dept of Biomedical and Chemical Eng, Syracuse University, <sup>2</sup>Institute for Sensory Research, <sup>3</sup>Dept of Biomedical and Chemical Eng, Dept of Electrical Eng and Computer Science, Syracuse University

Chopper response types in the anteroventral cochlear nucleus (AVCN) exhibit distinct temporal response properties to short tones at the neuron's characteristic frequency. Based on the post-stimulus time histogram and regularity analysis of discharge times over the course of the stimulus, AVCN choppers can be characterized into sustained, transient, and slow-adapting choppers. The exact determination of the three sub-categories is still under debate. Although anatomical studies show diversity in the number of auditory-nerve inputs and cell morphologies for AVCN stellate cells, modeling studies suggest that inhibitory inputs might have a substantial effect on the temporal responses of choppers. This study used iontophoretic application of several inhibitory antagonists to block the glycinergic and GABAergic inhibition while recording from AVCN choppers in anesthetized gerbil. In some cases, blocking inhibition changed the temporal responses dramatically, e.g., slowadapting choppers became sustained choppers. For some choppers, the change in the average discharge rate during iontophoretic injection of inhibitory antagonists was a

reflection of a change in regularity or in the chopping frequency. The effects of inhibition on temporal responses to long tones and complex sounds, such as tones in noise and amplitude-modulated stimuli, were also examined with iontophoresis. A multi-compartment integrate-and-fire model was used to simulate the observed temporal changes caused by the blocking of inhibition, and to understand the characteristics of the inhibitory inputs. Since possible inhibitory sources include descending inputs from higher auditory stages, results of this study illustrated possible feedback mechanisms that might be used by the auditory system at the level of cochlear nucleus. Supported by NIH NIDCD-01641.

#### 379 Responses to Long-Duration Tone Sequences in the Cochlear Nucleus.

**Daniel Pressnitzer**<sup>1,2</sup>, Christophe Micheyl<sup>3</sup>, Mark Sayles<sup>4</sup>, Ian M. Winter<sup>4</sup>

<sup>1</sup>Laboratoire Psychologie de la Perception, CNRS - Paris 5, <sup>2</sup>Département d'Etudes Cognitives, Ecole Normale Supérieure, France, <sup>3</sup>Departement of Psychology, University of Minnesota, USA, <sup>4</sup>Centre for the Neural Basis of Hearing, The Physiological Laboratory, University of Cambridge, UK

Recent studies have shown that neural responses in the primary auditory cortex (AI) of anesthetized or awake animals decrease over time upon repeated sound stimulation, with time courses ranging from milliseconds to tens of seconds or more. This multi-second adaptation (MSA) could underlie some important dynamic aspects of the perceptual organization of sound sequences. In particular, the characteristics of MSA have been shown to be quantitatively consistent with the tendency for listeners to hear sequences of tones alternating between two frequencies as a single coherent "stream" at first, but then as two streams after a few seconds of uninterrupted listening - a phenomenon known as "the build up of segregation". However, several important questions remain regarding the origin and the nature of MSA. In particular, little data exists on the responses of single neurons located at lower stages of the auditory pathway to long-duration repeating tone sequences.

In this study, we recorded responses of single units in the cochlear nucleus (CN) of urethane-anaesthetized guinea pigs to repeating tone sequences. In the main condition, the stimuli were ABA triplets, where A and B represent tones of different frequencies. Each tone was 125 ms and triplets were separated by 125-ms silent gaps. Sequences were 10 s or 60 s long. The frequency of the A tones was set at BF, that of the B tones was varied from 1 semitone to 15 semitones above BF. Single units were recorded extracellularly. The results show a gradual reduction in firing rate of single CN units in response to the repeating tones over the course of several seconds after the onset of the stimulus sequence. The general characteristics of this adaptation, including its time course, are similar to MSA in Al. Our results indicate that some form of MSA is already present at the level of the CN and this may play a role in streaming.

#### 380 Mechanisms of Decay of Glycinergic Inhibition in DCN Granule Cells

Veeramuthu Balakrishnan<sup>1</sup>, Larry Trussell<sup>1</sup>

<sup>1</sup>Oregon Health and Science University

Granule cells of the rat DCN and granule cell layer receive strong glycinergic inhibition. We observed that the decay time of glycinergic inhibitory postsynaptic currents (IPSCs) was quite variable, ranging from 7 to over 50 ms. To understand the source of this variability we examined IPSCs in brain slices from P16-20 rats. In voltage-clamp experiments with low-frequency synaptic stimuli, the IPSC amplitude fluctuated widely, presumably reflecting stochastic variation in quantal content. Larger IPSCs had slower decay times, suggesting that removal of transmitter from the cleft was compromised when more vesicles were released. Indeed, the decay time and amplitude also covaried with the concentration of Ca2+ in the bath. The decay time after a stimulus train was strongly dependent on the number and frequency of synaptic stimuli. For example the mean decay time was 39±22 ms for 10 shocks at 20 Hz and 88±31 ms after 10 shocks at 200 Hz We hypothesized that multiple vesicles can be released into the same synaptic cleft, and this abundance of glycine both promotes receptor saturation but also compromises glycine removal, thus slowing the decay. Several observations were consistent with this hypothesis. SR95531, a well-known antagonist of GABA receptors served as a weak antagonist of the glycine receptor. At 300 μM, SR95531 reduced the peak amplitude of IPSCs and accelerated their decay, consistent with the idea that SR95531 reduces rebinding of glycine to its receptors. Moreover, SR95531 reduced depression of IPSCs during a train, consistent with a reduction in receptor saturation. ATX-5407, an antagonist of the GlyT1 glycine transporter, slowed the decay of IPSCs. This intensity-dependence of the glycinergic synaptic decay was studied under currentclamp conditions, and steady spiking was triggered by injection of weak current steps. IPSPs abruptly halted firing and the delay to reestablishment of firing was longer after a train of IPSPs as compared to a single stimulus. These data confirm that glycinergic synapses gate the input to DCN through the granule cell pathway, and show that the duration of inhibition can be regulated through multivesicular release and transmitter pooling.

### 381 Spike Response Mechanisms of Cell Types in the Dorsal Cochlear Nucleus

**Patrick Roberts**<sup>1</sup>, Christine Portfors<sup>2</sup>, Andrew Tolman<sup>3</sup>
<sup>1</sup>Oregon Health & Science University, <sup>2</sup>Washington State University, <sup>3</sup>Portland State University

The dorsal cochlear nucleus (DCN) is a cerebellum-like structure that integrates auditory nerve input with multimodal inputs. There are several morphologically identified cell types in the DCN. We recorded auditory response properties of single DCN units in the awake mouse, and found a variety of physiological response types. The physiological response types were similar to those that have been observed in other preparations, and we could identify each with a corresponding morphological

cell type. We hypothesized that the responses of our DCN units to auditory stimuli could be explained in terms of a combination of membrane properties and synaptic connectivity in the DCN. Therefore, we developed mathematical models based on the known properties of each cell type, then applied synaptic inputs to replicate recordings of spike responses. The combination of modeling with in vivo data allow us to quantify the relative importance of membrane properties and synaptic input in determine the spike patterns generated by auditory stimuli.

### 382 An Electrophysiological Measure of Basilar Membrane Nonlinearity in Humans

Ananthanarayan Krishnan<sup>1</sup>, Christopher Plack<sup>2</sup>

<sup>1</sup>Purdue University, <sup>2</sup>Department of Psychology, Lancaster University, Lancaster, UK

An electrophysiological measure of basilar membrane nonlinearity in humans. Ananthanarayan Krishnan (Dept. of Speech Language Hearing Sciences, Purdue Univ., West Lafayette, IN, 47906) and Christopher J. Plack (Dept. of Psychology, Lancaster Univ., Lancaster, LA1 4YF, England

A behavioral measure of the basilar membrane response can be obtained by comparing the growth in forward masking for maskers at, and well below, the signal frequency. Since the off-frequency masker is assumed to be processed linearly at the signal place, the difference in masking growth with level is thought to reflect the compressive response to the on-frequency masker. The present experiment used an electrophysiological analog of this technique, based on measurements of the latency of Wave V of the auditory brainstem response elicited by a 4kHz, 4-ms pure tone, presented at 65-dB SPL. Responses were obtained in quiet and in the presence of either an onfrequency or an off-frequency (1.8 kHz) pure-tone forward masker. Wave V latency increased with masker level, although the increase was greater for the off-frequency masker than for the on-frequency masker, consistent with a more compressive response to the latter. Response functions generated from the data showed the characteristic shape, with a nearly linear response at lower levels, and 5:1 compression at higher levels. However, the breakpoint between the linear region and the compressive region was at about 60 dB SPL, higher than expected on the basis of previous physiological and psychophysical measures.

## 383 Novelty Responses in the Rat Auditory Midbrain: Evidence From an Oddball Paradigm

**Manuel Malmierca**<sup>1</sup>, Salvatore Cristaudo<sup>1</sup>, David Pérez-González<sup>1,2</sup>, Ellen Covey<sup>2</sup>

<sup>1</sup>Auditory Neurophysiology Unit. Lab Neurobiol of Hearing. Inst. Neurosci. & Univ of Salamanca, Spain, <sup>2</sup>Department of Psychology, University of Washington; Seattle, WA 98195 USA

Stimulus specific adaptation (SSA) has been linked to several perceptual effects including precedence effect,

forward masking and novelty detection (Ulanovsky et al. 2003, Nat. Neurosci. 6:391-398). However, systematic attempts to relate adaptation and responses to novel stimuli are few, especially at subcortical levels.

We recorded the responses of 55 neurons in the rat IC to novel stimuli randomly embedded in a series of standard stimuli. Animals were anesthetized with urethane [1.5 g/kg]. Stimuli were pure tones of 75 ms duration, presented monaurally to the contralateral ear at 10-20 dB above threshold. Two frequencies were chosen, one of which served as the standard and the other as the oddball stimulus. Both frequencies were centered around the neuron's best frequency, and the difference was varied from 0.057-4.1 octaves. The probability of occurrence of the two tones was varied (90/10%, 70/30%, 50/50%, 30%/70%, 10%/90%) so that each frequency served as both the standard and the oddball. We also varied the repetition rate (2/s, 4/sand 8/s).

For 23 neurons (42 %), the response to either tone was stronger when it was the oddball stimulus and weaker when it was the standard at all of the repetition rates tested. The difference between the magnitude of the response to the oddball and the standard was larger for larger  $\Delta f$ . There was also a larger difference between the magnitude of the response to the oddball and standard stimuli at faster repetition rates (8/s vs. 2/s). SSA was also stronger when the oddball was of low probability. According to our criteria (stronger response to the oddball in all conditions tested) these neurons were classified as novelty because of their strong SSA properties. However, most of the remaining neurons (n=28, 51%) showed some degree of SSA at the higher repetition rates, or when using the largest frequency difference between the two tones. Only 4 neurons in our sample (7%) did not showed any SSA properties. These findings suggest that nearly all IC neurons experience some degree of SSA and enhanced responses to novel stimuli under conditions of high contrast and high repetition rate, and that the degree to which they express this characteristic forms a continuum. Supported by NIH DC-00607, DC-00287 to EC and the Spanish DGES (BFI-2003-09147-02-01) and JCYL-UE

## 384 Measurement and Comparison of Bandwidths in the Inferior Colliculus and the Auditory Nerve Using a Spectral Method

(SA084/01 and SA040/04) to MSM. SC held a fellowship

from the USAL.

**Myles Mc Laughlin**<sup>1</sup>, Bram Van de Sande<sup>1</sup>, Marcel van der Heijden<sup>1</sup>, Philip X. Joris<sup>1</sup>

<sup>1</sup>Laboratory of Auditory Neurophysiology, K.U.Leuven, Leuven, Belgium

Auditory filter bandwidth (BW) limits the effect of masking and therefore plays a critical role in tasks such as detecting speech in noisy environments. Psychophysical studies by Jeffress and Bourbon (1965) showed a wider effective critical BW with binaural stimuli than with monaural or diotic stimuli. However, studies by Kohlrausch (1988) found no difference. To our knowledge there have been no physiological studies that directly compare binaurally measured BW with monaural BW. Here we

measure the response of monaural auditory nerve (AN) and binaural inferior colliculus (IC) neurons to the same spectrally manipulated broadband noise in cats. BW and CF were then estimated by fitting filter shapes to the single neuron responses.

In the IC best delay was measured for each neuron and all further stimuli were presented at this best delay. The stimulus consisted of a pair of noise tokens which where interaurally in phase for all frequencies below a certain flip frequency (FF) and had an interaural phase difference of  $\pi$  above FF and visa versa (Kohlrausch 1988). The response as a function of FF was measured. Response as a function of correlation  $(\rho)$  was also measured. In the AN experiments the same stimuli were presented monaurally and autocorrelation analysis was used to simulate a binaural response. To estimate CF and BW a correlation model based on a Gaussian filter shape was fitted to the binaural response. As correlation is not always linearly related to response the  $\rho$  data, when available, were also included in the model.

The main results were as follows: 1) there was no difference in BW measured in the IC compared with that in AN; 2) filter model CF showed a good correlation with threshold curve CF in both IC and AN; 3) filter model BWs in the AN and IC did not show a strong correlation with threshold curve BWs; 4) exclusion of  $\rho$  data in the model lead to a small overestimation of BW.

Supported by the Fund for Scientific Research – Flanders (G.0392.05 and G.0633.07), and Research Fund K.U.Leuven (OT/01/42 and OT/05/57).

## 385 Neural Responses to Amplitude Modulation Using Binaurally Mismatched Carrier Frequencies

**Deidra Blanks**<sup>1</sup>, Logan Foltz<sup>1</sup>, Emily Buss<sup>1</sup>, Douglas Fitzpatrick<sup>1</sup>

<sup>1</sup>University of North Carolina at Chapel Hill

Bilateral cochlear implantation is intended to improve sound localization and speech recognition in noise. In bilaterally implanted subjects the binaural timing cue is carried by the envelope rather than the fine structure. It is not clear to what degree place/pitch matching from the two sides is required to extract the interaural time difference (ITD). To investigate this issue in normal hearing, we measured the neural coding of interaural envelope timing in the rabbit, parametrically adjusting the difference between frequencies at the two ears. Extracellular recordings were made from single neurons in the inferior colliculus of unanesthetized rabbits. The best frequencies of the neurons were above 2 kHz. The stimulus was a binaural beat created using sinusoidally amplitude modulated (SAM) tones with a 1 Hz difference in modulation frequency at the ears. In most cases, the stimuli were presented at the best modulation frequency and intensity as the carrier frequencies at each ear were varied. Results indicated that some neurons could respond to the envelope with carrier frequency mismatches as great as several octaves. In contrast, the behavioral ability in humans to detect ITDs in envelopes is lost for mismatches greater than one octave. The ability of

neurons to detect the presence of an ITD with wide frequency mismatches raises the possibility that subjects may benefit from bilateral stimulation even if the position of stimulation on the two sides is not identical.

This work is supported by NIH T32-DC005360.

### 386 Onset, Repetition, and Envelope Coding in the Auditory Midbrain

Yi Zheng<sup>1</sup>, Heather Read<sup>2</sup>, Monty Escabi<sup>1,3</sup> <sup>1</sup>Biomedical Engineering, <sup>2</sup>Psychology, <sup>3</sup>Electrical Engineering, University of Connecticut, Storrs, CT 06269 The neural representation of single units to sinusoid amplitude modulated (SAM) noise and periodic noise bursts (PNB) were investigated in the inferior colliculus of the anesthetized cat. SAM and PNB were presented at repetition rates ranging from 5 to 500 Hz. Generally, neurons encoded sound information with a temporal code or a rate code or both. Here, we demonstrate and compare the rate and synchrony modulation transfer functions (rMTFs and tMTFs) of SAM and PNB. Both SAM and PNB rMTFs display low-pass or band-pass pattern, or even high-pass pattern, however, the normalized MTFs based on average spikes per stimulus event always exhibit lowpass sensitivity for both. To quantify the temporal precision of spike trains, the spiking reliability and jitter were analyzed at each stimulus condition and plotted as a function of modulation frequency to generate the reliability and jitter MTFs for SAM and PNB. Neural responses to PNB display higher reliability and significantly lower jitter than for SAM. Spike timing jitter for the PNB was in the order of <1 msec and independent of repetition rate while the jitter for SAM covaried with the repetition rate in a manner which resembled the SAM envelope. When we examined the response to one cycle of the sinusoidal onset envelopes we found that the spiking jitter and reliability pattern largely resemble the observed patterns for the SAM sequence. The comparison of all these properties between PNB, SAM onset sinusoid envelopes suggested that neuronal response patterns previously described for SAM sounds are largely dependent on the onset envelope shape (e.g., Heil et al.) and do not properly describe the repetition coding properties of ICC neurons on their own. Alternately, responses to PNB always exhibited a systematic pattern in which the stimulus normalized MTF always exhibited a lowpass function which often matched the vector strength MTF. The results suggest that stimulus repetition and envelope shape are encoded by separate neuronal mechanisms where repetition coding exhibits a lowpass behavior and envelope coding a highpass filter characteristic. Supported by NIDC (R01DC006397-01A1).

#### 387 Time-Frequency Resolution Topography in the Cat Inferior Colliculus

**Francisco Rodriguez Campos**<sup>1</sup>, Eric Flynn<sup>1</sup>, Heather L. Read<sup>1</sup>, Monty Armando Escabi<sup>1</sup>

<sup>1</sup>University of Connecticut

The central nucleus of the inferior colliculus (ICC) has a distinct laminar organization. Previous studies have

characterized the laminar and frequency organizations using pure-tones and modulated signals. Here we hypothesize that STRF neuronal sensitivities obtained with broadband stimuli will be systematically distributed along the rostro-caudal and dorso-medial / ventro-lateral dimensions of the central nucleus, and related to the parameters obtained from the pure tones response. In order to obtain these parameters from the ICC, stimuli consisting of pure tones and dynamic ripple were applied separately; the recording of the neuronal activity within the central nucleus was done using a 16 channel acute recording probe. The probe penetrations are referenced to three specific coordinate axes using a stereotaxic frame assembly and are aligned orthogonal to the ICC isofrequency lamina. Single neurons in the auditory midbrain of mammals exhibit a time-frequency resolution tradeoff in which fast neurons have low frequency resolutions whereas slow neurons are finely tuned. However, neurons with simultaneous high frequency and temporal resolutions are never found. When we examine the three-dimensional organization of the auditory midbrain we find that neurons are systematically organized, in the following way: a continuous gradient for time-frequency resolution is found along the medio-lateral axis. These results offer a neuronal basis for the encoding resolution of the auditory system that could provide clues about perceptual attributes in complex sounds such as timbre and pitch.

(Supported by NIDCD R01DC006397-01A1)

# 388 Relative Importance of Binaural and Monaural Cues to the Directional Sensitivity of Different Unit Types in the Inferior Colliculus.

Oleg Lomakin<sup>1</sup>, **Kevin Davis<sup>1</sup>** 

<sup>1</sup>Department of Biomedical Engineering, University of Rochester, Rochester, NY, 14642

Psychophysical experiments have established that three main acoustic cues contribute to the ability to localize sounds in space: interaural differences in time (ITDs) and level (ILDs), and monaural spectral notches (SNs). Initially, these cues are processed in separate brainstem nuclei, with ITDs in the medial superior olive, ILDs in the lateral superior olive, and SNs in the dorsal cochlear nucleus. It has been hypothesized that each of the three major response types (type V, I, and O units) in the central nucleus of the inferior colliculus (ICC) receives dominant inputs from one of these sources (in order), and thus represents a segregated pathway specialized to process one sound localization cue. To test this hypothesis, the responses of individual ICC units to binaural virtual space (full-cue VS) stimuli were compared to those elicited by a variety of partial-cue VS stimuli. Head-related transfer functions (HRTFs) were used to filter broadband noise spectra to synthesize binaural VS stimuli in the frontal field. In response to full-cue VS stimuli, type I units showed excitatory responses in the contralateral hemifield and inhibitory responses in the ipsilateral hemifield. The responses of type O units were dominated by inhibition except for a tuned excitatory response in the contralateral

hemifield that followed a diagonal contour from low contralateral to high ipsilateral elevations. Manipulations of the binaural cues suggested that ILD, and not ITD, cues were a strong determinant of the directional sensitivity of both of these unit types. Both unit types showed directional sensitivity to monaural VS stimuli. However, type I unit responses were mainly attributable to the effects of sound level (head shadowing), whereas type O units were more sensitive to SNs. These data show that ICC unit types are not sensitive to one sound localization cue alone, but do show different patterns of cue integration.

Supported by NIDCD grant R01 DC 05161-06.

#### 389 Firing Pattern of Neurons From the Tectal Longitudinal Column

**Justin Nichols**<sup>1</sup>, Ankur Patel<sup>1</sup>, Mitali Bose<sup>1</sup>, Antonio Vinuela<sup>2</sup>, M. Auxiliadora Aparicio<sup>2</sup>, Enrique Saldana<sup>2</sup>, Marco Atzori<sup>1</sup>

<sup>1</sup>University of Texas at Dallas, <sup>2</sup>Universidad de Salamanca The tectal longitudinal column (TLC) is a narrow and elongated structure that penetrates the colliculus, differing from its surrounding nuclei by its distinct neural connections and cytoarchitecture. The TLC is present in a large variety of mammals, including rodents, lagomorphs. carnivores, non-human primates and humans. In order to characterize the firing pattern of TLC neurons in Sprague-Dawley rats we used whole-cell current-clamp recordings from visually identified neurons in a brain slice preparation. Electrodes contained a KGluconate based solution with 0.4% biocytin for post-hoc identification reconstruction.

Analysis of the passive properties showed that TLC neurons have a mean input resistance of 344  $\pm$  34 MOhm (n = 9) and a capacitance of 56  $\pm$  7 pF (n = 9), corresponding to a time constant of 17  $\pm$  3 ms. Injections of one-second long square pulses of increasingly large current produced firing patterns with accordingly higher frequency (maximum firing frequency  $50 \pm 7$  Hz, n = 8). Half-height spike width was approximately 1.3 ms. Most recordings displayed a pronounced fast After-HyperPolarization (mean AHP =  $-10 \pm 1$  mV, n = 7). The slope of the frequency-current relationship for a 200-ms long current injection was (188  $\pm$  28 Hz/nA). Some cells had the capability of firing continuously during 1-s long current injections. However, most TLC neurons displayed a "stuttering" firing pattern, showing several intervals of high firing frequency interrupted by silent periods. In order to determine the maximum neuronal firing frequency we stimulated cells with a short but intense current pulse train (thirty 2-ms long pulses, 300 pA) at increasingly higher frequencies. The maximum firing frequency (defined as the maximum frequency at which every pulse produced a spike) was  $108 \pm 8 \text{ Hz (n = 3)}$ .

Altogether, these data suggest that TLC cells are a population of relatively high firing frequency neurons with firing characteristics similar to somatostatin-positive cortical GABAergic interneurons.

#### 390 Local Cooling of Auditory Cortex Alters Responses of Single Neurons in Rat's Inferior Colliculus

Huiming Zhang<sup>1</sup>, Farzaneh Safarpour<sup>1</sup>, **Jack B. Kelly<sup>1</sup>**<sup>1</sup>Institute of Neuroscience, Carleton University, Ottawa, Ontario K1S 5B6 Canada

In addition to receiving ascending projections from the auditory thalamic nucleus, the medial geniculate body, the auditory cortex sends major descending projections back to the medial geniculate and to the inferior colliculus. To gain a better understanding of the functional contribution of descending projections to the auditory midbrain, we recorded responses to tone bursts from single neurons in the rat's inferior colliculus before, during and after local cooling of auditory cortex with a thermal coil placed on the surface of the primary auditory cortex. The cooling coil was constructed from stainless steel hypodermic tubing through which chilled methanol could be circulated to lower the temperature of the underlying cortical tissue according to the procedures described by Lomber et al. (1999). Recordings were made from various locations in the inferior colliculus including both central nucleus (ICC) and dorsal cortex (ICD), which is known to receive direct descending projections from auditory cortex. responses properties of neurons in ICC and ICD were characteristically different before cooling. Most neurons in ICC were strongly driven by tones, were narrowly tuned to sound frequency and had stable responses over time. In contrast, ICD neurons were often not strongly driven by tone bursts and tended to habituate with repeated presentation of the same stimulus. Cortical cooling affected the majority of the neurons tested in both ICC and ICD. Among ICD neurons, a common effect was a decrease in firing rate although increases were found in some neurons. Among neurons in ICC, cortical cooling often resulted in an increase in firing, but decreases were recorded in some neurons. In some cases, ICC neurons with strongly non-monotonic rate-level curves showed an increase in firing during cooling that was apparent only at higher sound pressure levels. Thus, the rate-level curves for these neurons became more nearly monotonic as a result of cooling, suggesting that the deactivation of auditory cortex resulted in a release from inhibition that normally contributed to the shape of the rate-level curve. The results show that descending projections from auditory cortex can modify the level of activity and response properties of neurons in the rat's inferior colliculus.

[Lomber, S.G., Payne, B.R. and Horel, J.A. Journal of Neuroscience Methods 86:179-194, 1999]

Research supported by NSERC of Canada and The Hearing Foundation of Canada.

# 391 Pre-Hyperpolarization Modulates Membrane Excitability and Firing Pattern of Neurons in the Rat's Dorsal Cortex of the Inferior Colliculus

Hongyu Sun<sup>1</sup>, **Shu Hui Wu<sup>1</sup>** 

<sup>1</sup>Institute of Neuroscience, Carleton university, Ottawa, ON K1S 5B6 Canada

The dorsal cortex of the inferior colliculus (ICD) is a pivotal structure in the auditory pathway for integrating ascending and descending auditory inputs. The ICD may play a role in processing specific aspects of auditory information or in regulating the auditory processing by the lower brainstem. Little is known about how intrinsic membrane properties of ICD neurons contribute to the physiological role of the ICD. Our previous results have shown that nearly 80% ICD neurons have a sustained firing pattern in response to depolarizing current iniection. In response hyperpolarizing current injection some of these neurons (55%) exhibited a rebound depolarization upon release of membrane hyperpolarization and the remaining neurons (45%) showed no such rebound after hyperpolarization.

To understand further how ICD neurons process excitatory and inhibitory inputs, we investigated whether the firing behavior and membrane excitability of ICD neuron are influenced by a preceded membrane hyperpolarization. Whole cell patch clamp recordings were made from ICD neurons in brain slices of P9-18 rats. We applied depolarizing current following hyperpolarizing current to ICD neurons, and compared the firing rate and firing pattern while the cell was depolarized with or without prehyperpolarization. For 45 rebound cells, 13 cells showed an increase in firing rate, 8 cells changed their firing pattern to an onset type, 2 cells displayed a pause in their firing and 22 cells had no change in their firing rate, but exhibited irregular firing. For 37 non-rebound cells, 18 cells had no change either in firing rate or firing pattern, 19 cells changed their firing pattern to a pause type (n=8), or a buildup type (n=9) or a buildup/pause type (n=2). The various forms of modification of firing behavior and membrane excitability by pre-hyperpolarization of ICD neurons may provide different mechanisms for processing of auditory signals.

Supported by NSERC of Canada

## | 392 | Intracellular Responses to Pure Tones in Inferior Colliculus Neurons Predict Their Responses to FM Sweeps

Sergiy Voytenko<sup>1</sup>, **Karen Dillard**<sup>1</sup>, Curtis Mortenson<sup>1</sup>, Alexander Galazyuk<sup>1</sup>

<sup>1</sup>Northeastern Ohio Universities College of Medicine
Inferior colliculus (IC) neurons often show response
selectivity to FM sweep direction and/or rate. Our goal was
to determine a neural mechanism(s) underlying response
selectivity to FM sweeps. Intracellular responses were
recorded from neurons in the central nucleus of IC in
awake big brown bats. Each neuron responses were
tested to four different FM sweeps: downward (80 - 20
kHz) and upward (20 - 80 kHz) FM sweeps presented at

two different sweep duration (4 ms and 16 ms). Each recorded neuron was then tested with pure tones 4 ms duration over a wide range of sound frequencies (from 20 kHz to 80 kHz at 4 kHz increment). We found that about 30% of IC neurons showed response selectivity to different FM sweeps. Some of these neurons elicited selective responses to both FM sweep direction and duration (or rate). Postsynaptic responses to pure tones clearly demonstrated that individual IC neurons subthreshold postsynaptic responses (excitatory or inhibitory) to much wider range of sound frequencies than the frequency range over which they exhibited action potentials. It suggests that in response to wide band FM sweeps IC neurons integrate information across wide range of sound frequencies. This integration plays a major role in creation of selective responses to different FM sweeps. Indeed, our data suggest that based on postsynaptic responses of an IC neuron to wide range of pure tones it was possible to predict if this neuron would have response selectivity to FM sweep. For instance, it turns out that neurons exhibiting response selectivity to downward sweep also showed excitatory postsynaptic responses to higher frequency tones whereas they exhibited inhibitory postsynaptic responses to lower frequency tones. Therefore such neurons fired to downward sweep while they showed only subthreshold postsynaptic responses to upward FM sweeps.

Research is supported by grant from the National Institute for Deafness and Other Communicative Disorders (NIH R01 DC005377).

# 393 Time Course of Recovery of Spontaneous Activity (SA) in the Rat Inferior Colliculus (IC) Following Unilateral Acoustic Trauma

**Thomas Imig<sup>1</sup>**, Henry Heffner<sup>2</sup>, Gim Koay<sup>2</sup>, Dianne Durham<sup>1</sup>

<sup>1</sup>Kansas University Medical Center, <sup>2</sup>University of Toledo SA in the IC of rats was measured following unilateral acoustic trauma (isoflurane anesthesia, continuous 16 kHz tone for 60', 115 – 120 dB SPL). At various times following sound exposure, unanesthetized rats were injected with C14 labeled 2 deoxyglucose (2DG) and placed in a quiet sound isolation chamber during uptake. Groups of 4 rats each received 2DG at different times following exposure (4 hour, 1, 2, 4, 8, 16 day, and control). Optical density (OD) measures were obtained from autoradiographs at 10 equally spaced segments that crossed the tonotopic axis of the central nucleus (ICc) and the external nucleus (ICx). OD for corresponding segments of ipsi and contra IC were compared and showed the following results: 1. OD was bilaterally symmetrical in controls. In exposed rats the contra IC showed a decrement in OD with respect to the ipsi IC at each survival time. Acoustic trauma did not cause an increase in OD at any survival time. 2. SA in contra IC showed partial recovery over time. The greatest decrement in OD was seen at 4 hours with lesser decrements at longer times. 3. Recovery of SA followed different time courses in the ICx and ICc. The decrement in OD extended throughout both the ICc and ICx at four

hours. By 2 days, ICx showed full recovery (bilaterally symmetrical OD) but recovery in the contra ICc continued over an 8 day period. 4. Recovery of SA in the ICc showed a low (LF) to high frequency (HF) progression. In 4 h and 1 day groups, SA was decreased throughout the ICc with the greatest decrement in the HF half of the ICc. By 8 days SA recovered to normal levels in LF ICc. The HF half of the ICc showed a decrement in SA, although less so than at earlier times. There was no further change in SA at 16 days.

Supported by the Tinnitus Research Consortium and MRRC Center Grant HD02528.

#### 394 Tonal Patterns Reveal Complex Post-Excitatory Suppression in Mouse Inferior Collicular Neurons

Wm. Owen Brimijoin<sup>1</sup>, Joseph Walton<sup>1</sup>

<sup>1</sup>Department of Otolaryngology, University of Rochester

Post-excitatory suppression (PES) is observed as a decrease in firing rate following an excitatory response. The nature of this suppression is thought of as gaincontrol, correlated to the strength of prior excitation, that uniformly suppresses excitatory responses to subsequent tones. However, we report here that PES has a complex range of effects and sources. Recordings of single-unit and multi-unit clusters were made in mouse inferior colliculus (IC) in response to a patterned tonal DeBruijn sequence using a 16 channel Michigan Probe. The sequence was centered at the neuron's best excitatory frequency (BEF) at 30-50 dB above threshold. It was comprised of an equal number of each of 9 tone frequencies and included an equal number of each possible subsequence of 2, 3, and 4 tones. Tone-triggered averaging was used to create spectrotemporal response maps, which displayed excitatory and inhibitory responses to each tone frequency. Excitatory responses were followed by suppression in ~90% of units. Tone-pairtriggered averaging was used to measure responses to each tone pair. The analysis revealed two findings: 1) PES had differential effects on subsequent responses to excitatory tones in over 60% of units. Tones below BEF tended to suppress excitatory responses to subsequent below-BEF tones, but not to subsequent BEF or above-BEF tones. Similarly, above-BEF tones tended to suppress excitatory responses to subsequent above-BEF tones, but not to BEF or below-BEF tones. BEF tones uniformly suppressed excitatory responses to all subsequent tones. 2) In ~60% of units, suppression following excitatory tones persisted even when the excitatory portion of the response had been masked by a previous tone. These findings argue that PES in the mouse IC does not act as a uniform gain-control and is created by a combination of independent excitatory inputs and spectrotemporallyconcurrent inhibitory inputs.

Research supported by NIH/NIA grant PO1 AG09524 and NIDCD P30 grant DC05409

#### 395 Adaptation to the Statistics of Sound Frequency in Mammalian Inferior Colliculus

**Benjamin Robinson**<sup>1</sup>, Misha Ahrens<sup>2</sup>, Isabel Dean<sup>1</sup>, David McAlpine<sup>1</sup>, Maneesh Sahani<sup>2</sup>

<sup>1</sup>University College London Ear Institute, <sup>2</sup>Gatsby Computation Neuroscience Unit, UCL

Traditional measures of auditory processing isolate successive stimuli in time, thereby deliberately preventing the process of neuronal adaptation, which occurs under natural conditions. By contrast, the present study obtained rate-frequency response curves from the inferior colliculus (IC) of the anaesthetised guinea pig by presenting continuous narrow-band noise with a centre frequency which was varied every 50ms. Each seven-minute stimulus set contained the same range of frequencies, but differed in their statistical distributions, i.e. the average number of times each frequency was presented. Thus, the mean frequency was different for each set.

We found that the rate-frequency curves changed depending on the statistics of the stimulus, and constructed computational models which asked whether simple interactions, such as paired-tone suppression, could explain the complex changes observed.

First we employed a spectrotemporal receptive field (STRF) model. This assumed that current and previous frequency together additively determine a neuron's firing rate. The STRF model failed to capture any of the observed changes in the rate-frequency curves, suggesting that processing in IC is not linear.

We therefore constructed a model which, instead of assuming linear processing, allowed for the most general relationship between the neural response, and the two most recently presented frequencies. This model was more successful at predicting the changes in the rate-frequency curves, and revealed a complex interplay between current and previous frequency.

Looking further back into stimulus history, we found that adding a third frequency improved the model's predictions only minimally. Instead, we hypothesise a cumulative, longer-term dependence on stimulus statistics, in addition to the strong dependence on the two most recent frequencies described above. Elucidation of the time-course of this adaptive process will require further experimentation and modelling.

# 396 Corticothalamic Feedback for the Reshaping of Thalamic Receptive Field by Basal Forebrain Stimulation Incorporated with a Tone Presentation

Yunfeng Zhang<sup>1</sup>, Jun Yan<sup>1</sup>

<sup>1</sup>University of Calgary

Department of Physiology and Biophysics, Hotchkiss Brain Institute, University of Calgary Faculty of Medicine, Calgary, Alberta, T2N 4N1, Canada

Reciprocal interchanges through corticothalamic connections link the cortex and thalamus, the highest sensory processing centers in the brain. Compared with our more thorough understanding of thalamocortical

function, the function of their massive corticothalamic projections is poorly understood. We investigated the receptive field plasticity of the auditory thalamus and the impact of the auditory cortex by using the electrical stimulation of the cholinergic nucleus basalis (NB) of the basal forebrain paired with a tone (tone-ES<sub>NR</sub>). We found that tone-ES<sub>NB</sub> induced robust changes in receptive fields and best frequencies (BFs) of thalamic neurons. tone-ES<sub>NB</sub> shifted thalamic BFs upwards when the frequencies of the paired tones were higher than thalamic BFs. On the other hand, the tone- $ES_{NB}$  shifted thalamic BFs downwards when the frequencies of the paired tones were lower than thalamic BFs. The thalamic BFs were not altered when they were similar to the frequencies of the paired tones. The data suggest that tone-ES<sub>NR</sub> led to a shift of the thalamic BFs towards the frequency of the paired tone. The resulting plastic changes in the receptive fields of the auditory thalamus were markedly similar to those of the auditory cortex but lasted shorter. We also observed that cortical inhibition with muscimol completely abolished these plastic changes in the thalamic receptive fields. Our data strongly suggest that changes in cortical function have a profound impact on the thalamic function, i.e., the auditory cortex instructs the functional alteration of the thalamus.

#### 397 Training with Frequency-Modulated Sweeps Affects Inhibitory Tuning in Primary Auditory Cortex of Common Marmoset Monkeys (Callithrix Jacchus)

**Maike Vollmer**<sup>1,2</sup>, Ralph E. Beitel<sup>2</sup>, Benedicte Philibert<sup>2</sup>, Micheal M. Merzenich<sup>2</sup>, Ben H. Bonham<sup>3</sup>, Steven W. Cheung<sup>2</sup>, Christoph E. Schreiner<sup>2</sup>

<sup>1</sup>Dept. of Otolaryngology, University Hospital Wuerzburg, Germany, <sup>2</sup>Keck Center for Integrative Neuroscience, University of California, San Francisco, <sup>3</sup>Epstein Laboratory, University of California, San Francisco

Frequency-modulated (FM) sweeps are important spectral-temporal cues in animal and human communications. The goal of the present study was to examine the role of learning on the organization of excitatory and inhibitory frequency response areas (FRAs) in a population of direction-selective neurons. Common marmoset monkeys were trained to discriminate the direction of FM sweeps (six up-sweeps vs. six down-sweeps at 8 Hz; 2-18 kHz; 33.2 octaves/s). In anesthetized animals (trained and naïve), the primary auditory cortex was mapped to determine characteristic frequencies (CFs), and a 2-tone simultaneous masking paradigm was used to study excitatory and inhibitory FRAs. Extracellular multineuronal responses to FM sweeps were also recorded.

Preliminary results show that: 1) in all monkeys, FM directional selectivity (DS) changed systematically along the CF axis (low CF sites prefer up-sweeps, high CF sites prefer down-sweeps); 2) however, in behaviorally trained animals, preferred FM-direction was significantly altered by pairing up-sweeps or down-sweeps with reward; 3) in all animals, the bandwidths of both excitatory and inhibitory FRAs decreased with increasing CF; 4) however, in animals for which reward was paired with down-sweeps

during training, the below-CF widths of inhibitory FRAs were consistently enlarged.

The results indicate that FM directional selectivity and the bandwidths of inhibitory FRAs in the primary auditory cortex can be modified by behavioral training in the common marmoset.

Supported by NINDS34835, NIDCD02260 and NS10414.

#### 398 Behavioural and Neural Measures of Pitch Discrimination in Ferrets

**Jennifer Bizley**<sup>1</sup>, Kerry Walker<sup>1</sup>, Andrew King<sup>1</sup>, Jan Schnupp<sup>1</sup>

<sup>1</sup>University of Oxford

Investigating the cortical basis of sound perception requires a stimulus set that allows the perceptual attributes of the sound to be systematically and independently manipulated in a fully parametric fashion. In order to investigate the neural basis of pitch, timbre and location judgements we have used a set of 'artificial vowel' stimuli consisting of band-pass filtered click trains. The band-pass filters were used to impose peaks ('formants') in the energy spectrum of the stimuli, which determine the stimulus timbre. Altering the click rate allowed us to vary the pitch of the sound while leaving the timbre unchanged. Here we compare behavioural and neural measures of pitch discrimination. Water-restricted ferrets were trained in a two-interval, two-alternative-choice paradigm. Upon licking a central 'start' spout, the ferret was presented with two short consecutive sound bursts. The first sound was a reference, with the second, target, sound having either a higher, or lower, pitch than the reference. The ferret indicated the direction of the pitch change by responding at one of two spouts located to either side of the start spout. A correct trial was rewarded with a small amount of water. Incorrect trials elicited negative feedback in the form of a "time-out" during which the ferret was unable to initiate a new trial. Psychometric functions were obtained from a minimum of 25 trials per stimulus with a total of 30 different target frequencies centred about the reference frequency. Psychometric functions had a mean slope of 72% (±14%) per octave. Single unit recordings were also made in both anaesthetised and awake, passively listening, ferrets. Stimuli used in neural recordings were identical to those used in behavioural testing allowing us to compare directly neural and behavioural pitch discrimination abilities.

## 399 Cortical Representation of Natural and Altered Vocalizations in Primary and Non-Primary Auditory Areas of the Cat

Boris Gourévitch<sup>1</sup>, Jos Eggermont<sup>1</sup>

<sup>1</sup>University of Calgary

We investigated the neural representation in the cat's auditory cortex of its conspecific vocalization, the "Meow". A typical Meow is highly tonal and is mainly composed of a fundamental frequency around 570 Hz, with harmonic components having the highest intensity between 1.5 and 2.5 kHz and extending to 5.2 kHz. We recorded multi-unit responses of anaesthetized cats to a natural Meow, as

well as time reversed and altered in carrier frequency or time envelope, in four auditory cortical areas: Primary Area (AI), Anterior Auditory Field (AAF), Posterior Auditory Field (PAF) and Posterior Ectosylvian Gyrus (EP). 243 recording sites in 16 adult cats were used, and frequency of highest activity for each of them was called best frequency (BF). In AI, the multi-unit activity mainly revealed onset activity, crucial for discrimination of vocalizations, or responses with a few peaks occurring at the onset of those tonal components related to the BF of the sites. Significant inhibition was observed during the stationary course of the stimuli. Other areas showed more sites responding with a sustained activity, especially EP area where no onset neurons were found at all. Spatial maps of activation revealed: 1) a possible role of the dorsal part of Al in discrimination of carrier-altered meows; 2) a clear role of ventral AI, posterior AI and EP area in discrimination between forward and time-reversed Meows. Firing rate, type of temporal response, and neural synchrony all allowed discrimination of the different meow alterations, while local field potentials were not. This result suggests local neural characteristics, and combinations of them, are crucial for vocalization processing.

## 400 Responses to Species Specific Communication Calls in Guinea Pig Auditory Cortex

**Jasmine Bailey**<sup>1</sup>, Alan Palmer<sup>1</sup>, Mark Wallace<sup>1</sup>

\*\*MRC Institute of Hearing Research\*\*

Species specific communication calls provide ecologically relevant stimuli for investigating how the brain processes complex acoustic stimuli. Guinea pigs (GPs) are very vocal animals having at least 13 identifiable calls, most of which are associated with specific behaviours. From the 13 we identified 2 calls that appear to encode information in their repetition rate (tooth-chatter), or in changes in their fundamental frequency (F0) (Drrr). Tooth chatter consists of trains of brief broadband clicks that are produced prior to an aggressive encounter, the click rate increases (from 9-16 Hz) with the level of the GP's aggression. The Drrr is a tonal alarm call that prompts surrounding GPs to freeze. The F0 of this call decreases (from 429-296 Hz) with the animals' age.

The responses to these 2 communication calls and to click trains (2.5-160 Hz) of cells in both core and belt regions of the auditory cortex of the anaesthetised GP, were recorded with multielectrodes. In the primary auditory area (AI) 50% of units (n=257, CF<1.2 kHz) responded to the multiple syllables in the *Drrr* call, whereas none of the units in the dorso-caudal belt responded to more then two syllables (n=35). Locking to the click train fell off with increasing click rate, but 45% of our sample locked well to 10 Hz clicks with 10% showing a preference for 10 Hz. When the *tooth chatter* was used as a stimulus a similar picture emerged with different cells showing preferences for different click rates within the call.

Identifying cells with particular sensitivities to the systematic changes within these calls may provide a

method to identify cortical areas that extract information about size and emotional state from vocalizations.

#### 401 A Neurophysiological Study of Auditory Stream Segregation in Ferret Auditory Cortex

**Ling Ma**<sup>1</sup>, Pingbo Yin<sup>1</sup>, Mounya Elhilali<sup>1</sup>, Jonathan Fritz<sup>1</sup>, Christophe Micheyl<sup>2</sup>, Andrew Oxenham<sup>2</sup>, Shihab Shamma<sup>1</sup> *University of Maryland at College Park*, <sup>2</sup> *University of Minnesota* 

Auditory stream segregation is a fundamental aspect of whose hearing perception neurophysiological underpinnings remain largely unknown. All previous investigations have employed animals in anesthetized, or awake but non-behaving situations, leaving open the guestion of whether attention to the stimuli could affect the responses and their interpretations. To address these concerns, we explored streaming in one of its simplest forms - using two alternating tones (ABAB...). In one task, the A tone is roved in frequency from one trial to the other while the animal listened for a change in the frequency of a B-tone (B'); Roving the Atone encouraged the animal to focus its attention on the Btone stream. Recordings in the primary auditory cortex (AI) were then made while the animal detected the B' target, and were then compared to responses while the animals listened passively (without behavior) before and after the task. Response strengths and rate of adaptation from onset to both the A and B tones were measured and compared before and after the task. Changes were systematic and included enhancement of the B-tone responses relative to the A, as well as a faster adaptation rate after the behavior. None of these changes occurred in a naive animal listening passively to the same stimuli. In a second set of recordings, we tested the hypothesis that spatial separation of the A and B tone responses is the primary factor in mediating streaming by comparing responses in a naive animal to alternating versus simultaneous A-B sequences. While the percepts in these two conditions are very different, being much more "segregated" in the alternating case, responses to the tones did not differ significantly enough to explain this change in percept. We shall discuss this case further in light of other psychoacoustical and physiological data.

### | 402 | Neuronal Adaptation to Sound Level in Auditory Cortex

Paul V. Watkins<sup>1</sup>, Dennis L. Barbour<sup>1</sup>

<sup>1</sup>Department of Biomedical Engineering, Washington University, St. Louis, MO, USA

Cortical and subcortical sensory neurons in many species have been found to alter their tuning characteristics on short time scales as a function of the recent history of stimulus attributes—a characteristic typically referred to as adaptation. Such strategies can function to improve neuronal coding efficiency. In particular, a sequence of short-duration sounds having intensities drawn randomly from a nonuniform distribution has been shown to elicit substantial neuronal adaptation in anesthetized guinea pig inferior colliculus. This adaptation leads to a mapping

between sound level and spiking rate such that the maximum coding efficiency occurs for the most commonly occurring sounds in the distribution. The neuron's input/output function is thus shifted from its static rate-level curve (i.e., rate responses to stimuli presented singly and in silence). We found that most neurons in awake monkey auditory cortex do not adapt to sound level history in such a way as to improve coding efficiency. The level adaptation we observe appears to manifest primarily as a scaling of the overall response rate, such that a neuron will respond more to a particular sound level when adapted to a distribution containing predominantly lower sound levels than when adapted to a distribution containing predominantly higher sound levels. We demonstrate this scaling effect for neurons with monotonic rate-level curves similar to those of the subcortical neurons studied previously as well as for neurons with non-monotonic ratelevel curves, which represent a substantial proportion of cortical neurons. Although this result describes the majority of neurons studied, a subset of neurons demonstrating onset-only responses may adapt in such a way as to improve coding efficiency. The magnitude of this effect, however, appears to be smaller than for subcortical neurons.

#### 403 Behavioural and Neural Measures of Pitch Discrimination in Ferrets: Part II

**Kerry Walker**<sup>1</sup>, Jennifer Bizley<sup>1</sup>, Andrew King<sup>1</sup>, Jan Schnupp<sup>1</sup>

<sup>1</sup>University of Oxford

Investigating the cortical basis of sound perception requires a stimulus set that allows the perceptual attributes of the sound to be systematically and independently manipulated in a fully parametric fashion. In order to investigate the neural basis of pitch judgments we have used a set of "artificial vowel" stimuli consisting of bandpass filtered click trains. The band-pass filters were used to impose peaks ("formants") in the energy spectrum of the stimuli, which determine the stimulus timbre. Altering the click rate allowed us to vary the pitch of the sound. Here we compare behavioural measures of pitch discrimination in ferrets across two 2-interval, 2-alternative-choice paradigms. In the first task, the ferret initiated each trial by licking a centre spout, and two short consecutive artificial vowel sounds were then presented. The first sound was a reference, with the second, target, sound having either a higher or lower pitch than the reference. The ferret indicated the direction of the pitch change by responding at one of two spouts located to either side of the start spout. The resulting ferret psychometric functions were similar in shape but much shallower in slope (mean slope of 72% ±14% per octave) than human psychometrics measured on a similar task. To lower the cognitive demands of the pitch discrimination paradigm, a separate group of ferrets were trained on a same/different version of the task in which they were not required to report the direction of pitch difference between the target and reference sounds. Here, ferrets' spout choice indicated whether the target and reference sound on each trial were of the same pitch or different pitches. In addition, local field

potentials were recorded in an awake ferret while artificial vowels of varying pitch were presented in an oddball paradigm. Thresholds based on the evoked neural responses are compared to behavioural thresholds for the same stimuli.

### 404 Cortical Forward Suppression: Does Probe Frequency Matter?

**Chris Scholes**<sup>1</sup>, Sylvie Baudoux<sup>1</sup>, Alan Palmer<sup>1</sup>, Chris Sumner<sup>1</sup>

<sup>1</sup>MRC Institute of Hearing Research

Physiological forward masking is measured as a decrease in neuronal response to a probe tone when preceded by a masking tone. At the level of the auditory nerve the amount of masking depends on the number of spikes elicited by the masker. Thus, the frequency dependence of the masking follows closely the tuning of the nerve fiber regardless of probe frequency. In central neurons, masking tuning curves can be different from excitatory tuning curves, probably influenced by inhibition. Nevertheless, it is usually assumed that the choice of probe frequency is not critical.

Recently, Ulanovsky et al. (Nat Neurosci, 2003) showed that adaptation to long sequences of tones in cortical neurons is 'frequency specific': adaptation occurs independently for different frequency regions within a receptive field. Also, two-tone forward masking can be frequency specific in the inferior colliculus (Bonham and Snyder, pers. comm., 2004), where forward masking tuning curves are dependent on the probe frequency. Calford and Semple (J Neurophysiol, 1995) also found frequency specific effects in 7 cortical neurons with wider tuning. In this study, we expand these results to investigate the extent to which forward masking is frequency specific in the cortex.

We collected unit responses in Al in response to forward masking stimuli. We varied the masker across a range of levels and frequencies, followed by probes of 2 or 3 different frequencies.

The frequencies at which masking was most sensitive and at which masking was strongest were both correlated with the probe frequency and not the CF of the neuron. Also, the tuning of the masking was similar to the tuning of the neuron pointing to an architecture of broadly tuned overlapping inputs to the cortical neuron.

In conclusion, forward masking is frequency specific in many cortical neurons. Frequency specificity might be a fairly general characteristic of adaptation and suppression in cortical responses at all time scales.

## 405 Parameters Influencing Neuronal Adaptation to Pure Tone Stimuli in the Awake Rat Auditory Cortex

**Wolfger von der Behrens**<sup>1</sup>, Manfred Kössl<sup>1</sup>, Bernhard Gaese<sup>1</sup>

<sup>1</sup>JW Goethe-University, Frankfurt

Clear representation of behaviorally relevant stimuli in a noisy environment is one of the major challenges for the auditory system. One possible solution to this problem are differentiated responses according to stimulus statistics. In this respect, rare sounds (deviants) are more effective in directing attention and processing resources than more frequent ones (standards). This effect is paralleled by the well established 'mismatch negativity' in event-related potentials (Näätänen et al. 2001) when stimuli are presented in an 'oddball' stimulation paradigm. Only few studies have investigated adaptation under such conditions at the single neuron level (e.g. Ulanovsky et al. 2003) and most of them were done under anaesthesia.

We examined how low probability sounds are represented by single neurons in awake rats. Chronically implanted animals with up to 4 movable electrodes (SE and tetrodes) in both hemispheres of the auditory cortex were tested with sequences of pure-tones (duration 100-200 ms, 50 dB SPL) under free field conditions. Sequences of repetitive standard stimuli were randomly interspersed with low probability deviants (10% to 30%) of different sound frequency (up to 1 octave).

A high percentage of neurons showed clear effects of adaptation. A stimulus specific adaptation index (SI) (after Ulanovsky et al. 2003) was calculated for analyzing the neuronal response to a tone as standard compared to as deviant. The magnitude of the effect depended on stimulus statistics. Adaptation increased with lower deviant probability (and higher standard probably) significantly. Additionally, the adaptation index was computed for different time windows after stimulus onset and, as a control, 100 ms before stimulus onset. Most significant adaptation effects were present in the phasic On-response of neurons. Integrated over the whole stimulus duration, the adaptation effect decreased rapidly.

(This work was supported by the German National Academic Foundation and DFG)

#### 406 Laminar Differentiation in the Mouse Auditory Cortex: A Histochemical Comparison with Visual and Somatosensory Cortices

**Lucy A. Anderson**<sup>1</sup>, Jennifer F. Linden<sup>1,2</sup>

<sup>1</sup>UCL Ear Institute, <sup>2</sup>Department of Anatomy & Developmental Biology, University College London Reliable histochemical analysis of cortical lamination is required for the investigation of laminar differences at either a physiological or an anatomical level. Such analysis is also interesting for what it can reveal about cell, myelin, and enzyme distributions across the cortical layers. For these reasons, we examined laminar differentiation in the mouse auditory cortex by staining for Nissl, myelin, acetylcholinesterase and cytochrome oxidase. compared the patterns of staining to those observed in visual and somatosensory cortices, using qualitative and quantitative analyses. Dense cytochrome oxidase staining was evident primarily in layers I and IV of the auditory cortex, but also in lower layer V of visual and somatosensory cortices; these laminar patterns were clearly localised within distinct areal boundaries for all three sensory modalities. Acetylcholinesterase staining was dark and homogeneous in the auditory cortex, but more localised to middle and superficial layers in the visual and somatosensory cortices. As previously documented in

the mouse, NissI staining revealed subtle patterns of cell body distribution across the layers in all three cortical areas. Myelin staining was not effective for differentiating the layers, but a dense plexus of fibres was a useful marker of the tangential extent of auditory cortex and other sensory cortices. We concluded that cytochrome oxidase and Nissl stains are the most useful for differentiating layers in the mouse auditory cortex; cytochrome oxidase and myelin stains are most effective for distinguishing areal boundaries. We also observed that laminar distributions of cytochrome oxidase acetylcholinesterase expression varied between auditory cortex and other sensory cortices. Thus, our results suggest that laminar patterns of cell activity and neuromodulatory influences differ between the auditory cortex and other sensory cortices in the mouse.

#### 407 Can Ferrets Perceive Relative Pitch?

Pingbo Yin<sup>1</sup>, Jonathan Fritz<sup>1</sup>, Shihab Shamma<sup>1</sup> <sup>1</sup>Institute for System Research, University of Maryland Unlike humans, relative pitch perception is difficult to demonstrate in animals, which often attend to absolute properties of the sound elements rather than to the relationships between them. In the present study, we demonstrate that ferrets could be trained to discriminate between rising and falling tonal patterns based on relative pitch. Three ferrets were trained using a positivereinforcement paradigm in which a sequence of reference (1-5 repeats) and target stimuli was presented and animals were rewarded when responding correctly to the target. The training procedure consisted of 3 phases: (I) animals were trained on the basic rule, by learning to discriminate a rising from a falling sequence, consisting of one fixed tone pair. Animals could solve the task either by attending to the absolute pitch of the two individual components in the sequence or by attending to the pitch contour. (II) To emphasize the contour cue, rising and falling sequences were randomly chosen on each trial from a list of 5-17 tone pairs over a range of 1-4 octaves. The tone separation in each tone pair was fixed at 1/3 octave. Hence, pitch contours were constant across trials, but absolute pitch changed on each successive trial. (III) In the final phase, rising and falling sequences were randomly chosen from the list of tone pairs for each reference repeat and target, and hence varied within as well as between trials. Thus, the absolute pitch cue was no longer available, and the ferret could use only the pitch contour cue to solve the task. Two ferrets were trained on rising (as reference) vs. falling pattern (as target) and one ferret was trained on the reverse pattern. All 3 ferrets met performance criterion in the three training phases, and performed the task based on pitch contour over a 4-octave range. These results suggest that ferrets, like humans, can extract the relative pitch relationship of sequential components of complex sounds.

# 408 Disentangling the Contribution of Intracortical and Thalamo-Cortical Projections to the Generation of Subthreshold Spectral Receptive Fields in the Auditory Cortex

**Marcus Jeschke<sup>1</sup>**, Matthias Deliano<sup>1</sup>, Frank W. Ohl<sup>1,2</sup>
<sup>1</sup>Leibniz Institute for Neurobiology, <sup>2</sup>Otto-von-Guericke-University Magdeburg

The receptive field of neurons is a classical concept in the neurosciences that describes the responses of neurons to the variation of stimulus parameters. Studies of the visual system that could show that the responses of cortical neurons can be modified by stimuli outside the receptive field led to the distinction of classical receptive fields from subthreshold receptive fields. Recent studies in the somato-sensory and visual system are putting the role of intracortical interactions for the generation of the subthreshold receptive field into the focus of research. In the auditory domain it has been hypothesized that intracortical connections contribute especially to the border areas of spectral receptive fields. These connections were also implicated for the generation of the preference for spectral and temporal modulations.

Hence our goal was to investigate the contribution of different projection systems to subthreshold receptive fields using one-dimensional current source density analysis in anesthetized Mongolian gerbils (Meriones unguiculatus) to gain further insights into the generation of such fields. As has been hypothesized, best frequency and non best frequency evoked current source densities exhibit a different laminar pattern. By taking advantage of the fact that neuronal activities that occur along the recording axis must lead to a balanced current source density pattern we could show that the additional sink after non best frequency stimulation can only be explained by activities outside the recording axis. To directly test this explanation we cut the auditory cortex along the isofrequency axis. This procedure led to the total abolishment of the additional sink after non best frequency stimulation and also to a more balanced current source density pattern. Preliminary data indicate that the tuning of the initial sink around layer 3 and 4 did not change after cutting the cortex. This finding is in alignment with the general assumption that the early layer 3 and 4 sink is caused by the activity of thalamo-cortical projections. However, the overall amplitude of the evoked current source density was decreased. This result suggests that intracortical processing e.g. by local feedback loops is necessary to generate the observed macroscopic current source density pattern under normal conditions.

### 409 Binaural Characterization of Core and Belt Regions of the Macaque Auditory Cortex

**C.R. Camalier**<sup>1,2</sup>, William R. D'Angelo<sup>1</sup>, Susanne J. Sterbing-D'Angelo<sup>1</sup>, Yoshi Kajikawa<sup>3</sup>, Troy A. Hackett<sup>1,4</sup>, Jon Kaas<sup>1,2</sup>

<sup>1</sup>Ctr Integrative and Cognitive Neuroscience, Vanderbilt Univ., <sup>2</sup>Vanderbilt Brain Institute, <sup>3</sup>Nathan Kline Institute, <sup>4</sup>Dept Speech and Hearing Sciences; Vanderbilt Univ Our current working model of primate auditory cortex designates three interconnected regions (core, belt, and parabelt) which are thought to represent different levels of processing. Each region is comprised of multiple areas, or subdivisions, which are distinguished by unique anatomical and physiological profiles. With respect to the binaural inputs to cortex, studies are lacking, but it is generally assumed that the subcortical pathways are similar to those described for other mammals. In cortex. interhemispheric connections between homotopic areas are dense for areas in all three regions, including those in the core. Therefore, on the basis of known anatomical features, binaural processing in primate auditory cortex is expected to be comparable to that of other mammals, such as the cat or guinea pig. Unfortunately, such studies are rare. Thus, a general goal of the current study was to expand our understanding of binaural processing in primates by recording neuronal activity in auditory cortex to monaural and binaural acoustic stimulation. Single-unit responses were obtained from neurons in both the core and belt regions. We delivered ipsilateral, contralateral, and binaural clicks through headphones to a passively listening macague monkey. The discrete nature of the click stimulus makes it optimal for determining response latencies, and its broad spectrum reliably drives auditory neurons in both regions of cortex. Distributions of response latencies and firing rates were analyzed with respect to presentation condition. In addition, we evaluated the degree to which cortical responses to binaural stimuli can be characterized by the responses to stimuli presented to each ear separately. These data were then used to evaluate whether the strength and timing of binaural integration differs across levels of processing, i.e., the core and belt regions.

#### 410 A Temporal Processing Pathway Along the Rostral Axis of the Superior Temporal Gyrus in Marmosets

**Daniel Bendor**<sup>1</sup>, Xiaoqin Wang<sup>1</sup>

<sup>1</sup>Johns Hopkins University

Primate auditory cortex is composed of a core region of auditory fields that are tonotopically organized, receive inputs from the lemniscal pathway, and respond to narrowband sounds such as pure tones. Anatomical data has delineated three distinct fields within this core region: AI (primary auditory cortex), R (rostral field), and RT (rostral temporal field). Physiologically, only AI and R have been mapped in awake primates, and studies in the rostral field have been limited to pure-tone evoked neural response properties. We have investigated spectral and temporal response properties of single-units recorded from AI, R, and RT in two awake marmoset monkeys. Here we

show that RT contains a tonotopic map that is the mirror reversal of the tonotopic map in R. We also observe a stimulus-locked discharges decrease in (stimulus synchronization) along the rostral axis of the superior temporal gyrus, with RT neurons showing the weakest stimulus synchronization. In addition, the discharge rates of RT neurons are more narrowly tuned to temporal features in the acoustic signal than neurons in R or Al. These data suggest that the temporal representation of time-varying acoustic signals (in the form of stimulus synchronization) is transformed into a rate code along the rostral axis of the superior temporal gyrus. We propose a model of information flow in auditory cortex in which, originated from AI, temporal and spectral information is processed along the rostral and lateral axis of the superior temporal gyrus, respectively.

### 411 Coding of Interaural Time Delays in the Macaque Auditory Cortex

**William D'Angelo**<sup>1</sup>, Susanne Sterbing\_D'Angelo<sup>1</sup>, Corrie Camalier<sup>1</sup>, Troy Hackett<sup>1</sup>, Jon Kaas<sup>1</sup>

<sup>1</sup>Vanderbilt University

Six decades ago, the Jeffress model of interaural time difference (ITD) processing introduced the idea that ITDs are coded by a continuum of cells tuned to different delays. Recordings in the auditory cortex of the unanesthetized rabbit have indeed revealed tuning to a broad continuum of delays, including sensitivity to ITDs from both ipsilateral and contralateral space. However, as theorized by von Bekesy, and addressed by recent neurophysiological studies, the encoding of ITDs might occur simply through a comparison of the activity of the neural populations in the two hemispheres. With this in mind, we investigated how ITDs are represented within the auditory cortex of the awake macague monkey. Sensitivity to ITDs of single neurons and multi-neuron clusters was measured using static ITDs in noise and with dynamic ITDs using binaural beats imposed on narrow-band noises. To distinguish between the models mentioned above, the data were evaluated for the distribution of best ITDs and for evidence of ITD coding of both ipsilateral and contralateral delays within a single hemisphere. We further evaluated whether ITDs are processed differently between the core and belt regions of the auditory cortex.

## | 412 | The Formation of the Auditory Space Map in the Midbrain Pathway of the Mongolian Gerbil

Katuhiro Maki<sup>1</sup>, Shigeto Furukawa<sup>1</sup>

<sup>1</sup>NTT Communication Science Labs

The midbrain pathway runs from the central nucleus of the inferior colliculus (ICc), through the external nucleus of the inferior colliculus (ICx), to the superior colliculus (SC). This pathway plays an important role in auditory space processing, especially in forming the auditory space map. This study compared the three nuclei of anesthetized gerbils as to the rigorousness of topographical representation of the auditory space. The stimuli were 50-ms wide-band noise bursts with various sound levels that

varied in terms of the azimuth on the horizontal plane in a virtual acoustic space. Generally, the SC units exhibited sharper spatial tuning than the ICc and ICx units. The spatial tuning of the IC units broadened more rapidly with increasing sound level than that of the SC units. The best azimuth, defined as that where the unit exhibits its maximum firing rate, was calculated for the units that exhibited significant spatial selectivity. Consistently in the three nuclei, azimuths contralateral to the recording site were more heavily represented than ipsilateral azimuths. In the SC, the unit's best azimuths were arranged topographically so that the front to rear stimulus directions were represented rostro-caudally over a wide range of sound levels (5-60 dB re. threshold). In the ICx, there was a topographical gradient of the best azimuths, which was apparent only for low sound levels (5-15 dB re. threshold), and the topographical arrangement was opposite to that in the SC (rostral units preferred rear stimulus). The spatial sensitivities of the ICx units could be accounted for partly by the interaction between the direction-dependent stimulus spectrum and the units' spectral sensitivities, although the tonotopy in the ICx is generally not well defined. In the ICc, we failed to find the topographical distribution of the best azimuths. The results indicate that in mammals such as gerbils, the formation of a rigorous auditory space map is incomplete until the SC level.

# 413 Effect of Roving Overall Stimulus Level on Interaural Level Difference Discrimination Thresholds of Neurons in the Lateral Superior Olive

Jeffrey J. Tsai<sup>1</sup>, Daniel J. Tollin<sup>2</sup>

<sup>1</sup>Department of Neurology, University of Colorado Health Sciences Center, Denver, CO USA, <sup>2</sup>Department of Physiol and Biophys, University of Colorado Health Sciences Center, Aurora, CO USA

Interaural level differences (ILDs) are a cue to sound location. Humans can discriminate ILDs of ~1-2 dB, a threshold not degraded by roving the overall level of the stimuli presented to the two ears. Although the neural basis for ILD discrimination is unknown, neurons in the lateral superior olive (LSO) are the most peripheral in the auditory pathway to be sensitive to ILDs. But unlike the psychophysics, LSO responses to ILDs are not invariant to changes in overall stimulus level. Here, we examine single unit responses to ILDs in the LSO of anesthetized cats as stimulus level is roved. For characteristicfrequency tones, ILDs were manipulated by fixing the signal level to the ipsilateral ear and varying the signal level at the contralateral ear. ILD selectivity was examined for 2-4 overall levels spanning 6-20 dB. For each neuron, roving was effected by randomly and equally sampling from the responses at each overall level, and ILD discrimination thresholds were calculated using detection theory. ILD thresholds at a pedestal ILD of 0 dB did not change significantly with roving in 4/8 neurons studied. When roving did affect ILD thresholds, they increased by 57% (range 50-64%) relative to the mean threshold obtained across the range over which level was roved. A model that differenced the empirical rate-ILD responses of

a neuron and an "anti-neuron", one with a mirror-symmetric response about the 0 dB ILD axis, reduced the threshold increase due to roving to 10% (0-25%). Moreover, the best ILD threshold of a neuron was often obtained at a pedestal ILD other than 0 dB, and could be as good as behavioral thresholds (~1-2 dB). Thus, although responses of LSO neurons conflate overall level and ILD of the stimulus, roving stimulus level does not always degrade the neurons' ILD discrimination thresholds. We suggest that a difference model of ILD discrimination that incorporates the LSO and its contralateral counterpart may play a role in reducing the response variance imparted by unknown overall stimulus level.

Support: NIDCD R01-DC6865

#### 414 Temporal Processing in Binaural Neurons

Jason Roberts<sup>1</sup>, Emily Buss<sup>1</sup>, Douglas Fitzpatrick<sup>1</sup>

<sup>1</sup>University of North Carolina at Chapel Hill, Department of Otolaryngology / Head and Neck Surgery

An important binaural cue is the interaural time difference (ITD), or difference in the time of arrival of sounds at the two ears. The encoding of ITDs has been well-studied both behaviorally and physiologically. However, there has long-standing discrepancy between physiological and behavioral studies regarding the ability to track moving sources based on dynamic changes in the ITD. Behaviorally, sensitivity to ITD modulation falls off precipitously with increasing modulation rate; this decline begins at rates an order of magnitude smaller than those observed for comparable monaural tasks, a result that has been termed "binaural sluggishness". In contrast to these behavioral results. physiological studies demonstrated that brainstem neurons can follow dynamic changes in the ITD at relatively high rates. It has therefore been proposed that the physiological source of binaural sluggishness is central to the brainstem. However, these physiological and behavioral studies characterize sensitivity in different ways. Behavioral studies estimate threshold ITD sensitivity, while physiological studies characterize the neural representation using large ITD excursions. The discrepancy between the physiology of brainstem neurons and behavior may therefore be due to these differing approaches. To test this, we recorded from ITD sensitive neurons in the inferior colliculus in unanesthetized rabbits and estimated the threshold ITD for a range of modulation rates and peak ITDs. Most neurons showed a threshold for detection of a moving stimulus that increased with increasing modulation rate. The thresholds obtained were often similar to those observed in the comparable behavioral experiment (Grantham and Wightman, J. Acoust. Soc. Am. 63:511-523, 1978). Thus, at least some aspects of binaural sluggishness are displayed in brainstem neurons, and do not depend on higher order processing.

This work is supported by NIH T32-DC005360 N1 DCD.

### 415 Synaptic Inhibition in MSO Neurons: A Cellular Mechanism for ITD Tuning

Roberta Donato<sup>1</sup>, David McAlpine<sup>1</sup>

<sup>1</sup>UCL- EAR Institute

We have developed a brainstem slice preparation from juvenile guinea pigs to study the role of synaptic inhibition in the cellular mechanisms of sound localization. Electrical responses of neurons located in the medial superior olive (MSO) were examined in response to train of stimuli applied at the contralateral trapezoid body fibres at various frequencies in the patch clamp-current clamp configuration under control conditions, or when glycinergic inhibition was blocked with strychnine. With an intracellular solution containing a low concentration of CI-, excitatory or inhibitory synaptic events displayed an opposite polarity at resting potential (~-60mV). Whereas pharmacological block of inhibition left the conductance of MSO cells at rest unchanged, the decay time of synaptically-evoked EPSPs was significantly increased. The short PSPs decay time could be due either to a 'phasic' decrease in the cell membrane time constant occurring during the synaptic event, or to the algebraic summation of a precisely-timed and relatively fast EPSP or a relatively slow IPSP of opposite polarity. To test between these possibilities, neurons were held at a potential more negative than the chloride reversal potential, so that EPSP and IPSP were of the same sign. In these conditions, applying strychnine had the opposite effect on the decay time of the EPSP. suggesting that algebraic summation of well timed synaptic events plays a major role in shortening the decay time of PSPs, and hence in establishing a precise short time window for membrane depolarization. This can have a profound impact for coincidence detection. Moreover, the coefficient of variation of the interevent intervals, which was very low in control conditions, was systematically higher when inhibition was blocked, suggesting that the precision of the timing of the synaptic responses deteriorates when synaptic inhibition is absent. Preliminary data indicate stimulation of bilateral inputs to MSO neurons to be effective in facilitating responses evoked at particular delays between the two set of stimuli.

## 416 Non-Linear Coding of Sound Spectra by Discharge Rate in Neurons of the Medial Nucleus of the Trapezoidal Body (MNTB)

Kanthaiah Koka<sup>1</sup>, Daniel J. Tollin<sup>1</sup>

<sup>1</sup>Department of Physiology & Biophysics, University of Colorado Health Sciences Center, Aurora, CO
Neurons in the MNTB are important for encoding the interaural level difference (ILD) cue to sound source location because they provide the inhibitory input to the lateral superior olive (LSO) from the contralateral ear. In order for a neural correlate of ILD to be computed accurately by LSO, it is critical that MNTB neurons reliably encode the spectral characteristics of sounds. Here, the Random Spectral Shape (RSS) method was used to examine the ability of MNTB neurons to encode sound spectra via discharge rate. The RSS technique allows estimates of how spectral level is weighted, both linearly

and non-linearly, across a wide band of frequencies.

Here, rate responses to an ensemble of 100 noise-like RSS stimuli were used to estimate the first (linear) and second (non-linear) order spectral weighting functions for 15 MNTB neurons with characteristic frequencies from 300 Hz to 35 kHz. Weighting functions were measured at several stimulus levels spanning the dynamic range of each neuron. The validity of the estimated weighting functions was tested for each neuron by predicting the rate responses to arbitrary RSS stimuli. Here, 80 of the 100 RSS stimuli were used to estimate the first and second order weights, from which the responses to the remaining 20 RSS stimuli were then predicted. A goodness-of-fit metric (Q), ranging from 0 (poor fit) to 1 (perfect fit), was used to assess the quality of the model predictions for two cases: 1) the first-order weights only; and 2) the first- and second-order weights. By including the second order (non-linear) terms the average Q value, computed across all neurons and all stimulus levels, increased significantly (p<0.0001) to 0.49±0.019 from 0.30±0.019. The significant improvement in Q value observed by adding the secondorder weights suggests that spectral level is combined across frequencies in both a linear and a non-linear manner.

Support: NIDCD R01-DC6865

### 417 Reversible Plasticity in the Auditory Brainstem Induced by Noise Exposure

Ida Siveke<sup>1</sup>, Evelyn Schiller<sup>1</sup>, Benedikt Grothe<sup>1</sup>
Ludwig Maximilians University Munich

Neuronal plasticity is an important mechanism for learning and adaptation to environmental changes. Plasticity in the auditory system of mammals, however, has almost exclusively been investigated with invasive or damaging techniques. In the present study we investigate the plasticity of sound localization mechanism using a non-invasive approach. In mammals, interaural time differences (ITDs) and interaural level differences, the major cues for sound localization, are encoded in the superior olivary complex (SOC) by a complex temporal interaction of binaural excitatory and inhibitory inputs. Various developmental studies have shown that in the SOC several types of experience dependent plasticity occur. Here, we investigated the influences of noise in adult animals with presumably normal ITD tuning.

The SOC projects directly to the dorsal nucleus of the lateral lemniscus (DNLL). We compared ITD and IID sensitivity of DNLL neurons which are getting direct projections from the SOC from three groups of adult gerbils. All animals were raised in a normal acoustic environment. A control group was never exposed to noise, a second group was exposed to omnidirectional white noise for 14 days as adults and then tested within 7 days after exposure, and a third group exposed to the same noise but recovered for at least 14 days after exposure. Exposure to omnidirectional noise changed the ITD and IID coding of the neurons. The changes of the ITD and IID coding have to result from changes of the complex binaural interactions in the SOC and can be explained by an increase of the inhibitory input. These effects, however, were not visible anymore, when animals were allowed to recover for more than 14 days.

These experiments show a quantifiable, reversible plasticity in sound localization mechanisms, which can be used as a model-system to investigate adult plasticity in the auditory brainstem, without damaging or invasive treatment.

### 418 Dynamics of ITD Sensitivity in the IC: Adaptive Coding?

**Julia K. Maier<sup>1,2</sup>**, Isabel Dean<sup>2</sup>, Nicol S. Harper<sup>2</sup>, Georg M. Klump<sup>1</sup>, David McAlpine<sup>2</sup>

<sup>1</sup>Zoophysiology and Behaviour Group, Carl-von-Ossietzky University Oldenburg, <sup>2</sup>UCL Ear Institute, Centre for Auditory Research, 332 Gray's Inn Road, London WC1X 8EE

Interaural time differences (ITDs) are the main cue for localising azimuthal position of a sound source in hearing. mammals adapted to low frequency Electrophysiological recordings demonstrate sensitivity to dynamic spatial cues is a general property of neurons in the inferior colliculus (IC) (Spitzer & Semple 1993; McAlpine et al. 2000). Further, IC neurons show adaptive coding for sound intensity that extends the dynamic range of IC neurons, improving coding for the most commonly-encountered sound intensities (Dean et al. 2005). Here, we investigate whether adaptive coding in the IC extends to ITD. Unlike sound intensity there is not considered to be a dynamic range problem in the ITD domain. Further, binaural integration, a necessary step in ITD sensitivity, excludes contributions from mechanisms below this level of the pathway. Single-neuron recordings were made in the IC of anaesthetised guinea pigs to white noise stimuli of 5s duration, repeated 75 times. Within each 5s presentation the ITD, randomly chosen from a defined distribution, was changed every 50ms. ITDs presented ranged over a full cycle re. neuronal bestfrequency. Distributions were chosen with a high probability (80%), remaining ITDs were presented with a 20% probability. IC neurons showed a range of adaptive changes to different ITD distributions, from those showing evidence of a change in neural gain, to those in which ITD functions were inverted relative to baseline functions (i.e. from "trough-type" to "peak-type"). Preliminary analysis using signal-detection-theory indicates some neurons respond to changes in ITD distributions by shifting the most sensitive portions of their functions towards the high probability region. This adaptive behaviour must reside at or above the level of the medial superior olive (MSO).

Supported by MRC, the SFB/TRR31 "Aktives Gehoer" and the InterGK "Neurosensory Science, Systems and Applications", Oldenburg, Germany.

#### 419 Neural Correlates of the Precedence Effect in the Barn Owl's Auditory Midbrain are Determined by Proximity to the Inhibitory Regions of Spatial Receptive Fields

Brian Nelson<sup>1</sup>, Terry Takahashi<sup>1</sup>

<sup>1</sup>University of Oregon

The precedence effect (PE) describes how direct sound dominates perception in an echoic environment. Neural

responses to leading and lagging stimuli in the external nucleus of the barn owl's inferior colliculus (ICx) are diminished when these stimuli are superposed because cues to both locations are altered. Under certain conditions, however, responses to lagging sounds are suppressed in relation to those of leading sounds, providing a possible neural correlate for the PE (asymmetric suppression). Ongoing time delays do not drive this form of suppression because responses to correlated 100 ms stimuli are identical to those of uncorrelated stimuli. Onset delay also does not drive suppression because responses to lagging stimuli are unaltered when the onsets of stimuli are synchronized. Spatial receptive fields in ICx are produced by both excitation and inhibition. We mapped excitatory regions with a single sound source and then the presumptive 'inhibitory' regions with two sources, where one source was positioned at each single unit's best excitatory location and the second was roved across numerous frontal locations (10° staggered locations). Spike rates within the troughs of inhibited regions approached zero or were lower than spontaneous. Using lead and lag stimuli, we demonstrate that asymmetric suppression is predicted by the leading source's proximity to an inhibitory trough. A burst of spike rate occurs at the offset of the lead stimulus, suggesting recovery from asymmetric inhibition. This burst strengthens with the duration of the lag's trailing segment (i.e., delay), and is robust when the lead is placed near an inhibitory trough. Results indicate that cells rebound rapidly from this form of inhibition and that the locations of lagging stimuli should become discriminable as delay increases. Lagging stimuli positioned outside of these presumptive inhibitory regions may also become discriminable as delay increases due to the phasic nature of responses in ICx.

### 420 Responses to Virtual Space Stimuli in the Auditory Cortex of the Cat

Liora Las<sup>1</sup>, Ayelet Shapira<sup>1</sup>, Israel Nelken<sup>1,2</sup>

<sup>1</sup>Dept. of Neurobiology, Hebrew University, <sup>2</sup>ICNC, Hebrew University

The Anterior Ectosylvian Sulcus (AES) contains auditory neurons whose activity is believed to be important for sound localization. However, the response properties of neurons in AES have not been characterized in detail. In particular, the location of the relevant auditory field in AES has been under some debate. We recorded neuronal activity in AES and in A1 of halothane-anesthetized cats in response to pure tones and to virtual acoustic space (VAS) stimuli that mimicked sound sources from the frontal hemisphere. Most of the neurons in A1 and in AES responded to both pure tone and VAS stimuli. The majority of neurons that had significant response to VAS stimuli showed significant association between sound location and elicited spike counts, and sometimes also with 1st spike latency. Space-selective neurons were preferentially located in the posterior AES (pAES) where their proportion among all auditory-sensitive neurons was higher than in anterior AES (aAES) or in A1. Most A1 neurons responded preferentially to contralateral sounds. Neurons in AES had their spatial selectivity distributed more homogenously than neurons in A1, with 25% of the space selective neurons tuned to central locations, three times more than in A1. Furthermore, the proportion of neurons preferring frontal locations was somewhat higher in pAES compared to aAES. Thus, pAES may show a specialization for representing frontal space.

#### 421 Anatomy and Physiology of Binaural Neurons in the Brain Stem of Lizards

**Jakob Christensen-Dalsgaard**<sup>1,2</sup>, Yezhong Tang<sup>2</sup>, Catherine Carr<sup>2</sup>

<sup>1</sup>Inst. Biology, University of Southern Denmark, <sup>2</sup>Dept. Biology, University of Maryland

Lizard ears are highly directional, and the directionality is created by acoustical coupling of the eardrums (Christensen-Dalsgaard and Manley, J Exp Biol 208:1209-1217, 2005). Therefore, effectively every neuron in the lizard auditory pathway is directional, a property very different from the situation in birds and mammals with uncoupled ears, where sound direction is computed by specialized neural circuits in the central nervous system. Another property of the lizard directionality is that it is highly asymmetrical across the midline and therefore could be sharpened by binaural interactions. We have studied the neural processing of these binaural neurons in the Tokay gecko (*Gekko gecko*) combined with anatomical characterization of the recording sites.

We anesthetized gekkos by isoflurane inhalation (3%) and removed a part of the skull overlying the brain stem. We sealed the exposure with a gelatine sponge and allowed the animal to recover for two days. On the day of experiment, we re-anesthetized the animal with isoflurane and reexposed the brain. We stimulated the lizards dichotically using two earphone couplers sealed over the eardrum. We recorded first when the interaural transmission was not impeded, and then recorded after inserting a mold blocking the mouth cavity. Neural responses were recorded extracellularly using metal electrodes or dextran amine-filled glass micropipettes, allowing iontophoretic injections and subsequent anatomical tracing.

We found the binaural neurons in two different sites in the gecko brain stem. The most caudal of these sites was in the vicinity of the nucleus magnocellularis. Here, we found predominantly low-frequency cells (BF around 400 Hz) with a complex response showing both excitation and inhibition. Another site was more ventral and rostral in the brain stem, in and around the superior olive. This region was characterized by both contralateral monaural and binaural responses to higher best frequencies.

#### 422 Do Elevation-Sensitive Neurons in Cat Auditory Cortex Encode Space or Merely Spectrum?

**Ewan A. Macpherson**<sup>1</sup>, Ian A. Harrington<sup>2</sup>, G. Christopher Stecker<sup>3</sup>, Chen-Chung Lee<sup>1</sup>, John C. Middlebrooks<sup>1</sup>

<sup>1</sup>Kresge Hearing Research Institute, University of Michigan, <sup>2</sup>Department of Psychology, Augustana College, <sup>3</sup>Department of Speech & Hearing Sciences, University of Washington

Human vertical-plane sound localization is disrupted for ripple-spectrum stimuli with ripple densities in a sensitive band of 0.75—2 ripple/oct, but is accurate for stimuli with higher or lower ripple densities. A cortical correlate of this would be a neuron whose spatially-varying firing pattern was resistant to the presence or absence of sourcespectrum features outside the sensitive band. We have shown that the spatial tuning of most elevation-sensitive neurons in A1 and AAF, but not most of those in DZ and PAF, can be predicted by a linear model of the interaction of the spatially varying directional transfer functions with neurons' weighted integration of energy across frequency. We hypothesized that that nonlinear spectral processing in DZ and PAF neurons might support robust spatial coding despite source-spectrum variation (outside the sensitive band), whereas the linear processing in A1 and AAF would simply reflect the spectrum at the eardrum, and thus lead to disruption of coding at all ripple densities. We recorded from neurons in fields A1, AAF, DZ, and PAF in anesthetized cat while varying the elevation and ripple density (from 0.25-8 ripples/oct) of wideband noise-burst stimuli. We measured the elevation-related information (in bits) transmitted by each unit by training artificial neural networks to categorize spike patterns from flat-spectrum trials. Networks were tested with other flat-spectrum or ripple-spectrum trials. The difference between the flat- and ripple-spectrum results was compared between cortical fields at each ripple density. In support of our hypothesis, at 0.25 and 0.5 ripple/oct (for which human localization is hardly disrupted), we observed the smallest loss of transmitted information in PAF, and significantly greater loss in A1 and AAF. DZ results were intermediate. Above 2 ripples/oct, all fields exhibited similar, mild information loss.

#### 423 Neuro-Magnetic Indices of Auditory-Perceptual Segregation of Mistuned and Delayed Tones by Adults and Children

**A. Quentin Summerfield**<sup>1</sup>, Isabella Paul<sup>1</sup>, Pádraig T. Kitterick<sup>1</sup>, Joel R.A. Burton<sup>1</sup>, Paul M. Briley<sup>1</sup>, Peter J. Bailey<sup>1</sup>

<sup>1</sup>Department of Psychology, University of York, York YO10 5DD, UK

A perturbed component of a harmonic complex may be heard as a separate source of sound from the other components. We used magneto-encephalography (MEG) to study the role of attention when listeners segregate and spatially localise perturbed components.

The 3rd component of a 24-tone complex with a fundamental frequency of 200Hz was not perturbed in the *In-tune* condition, was raised in frequency by 8% in the

Mistuned condition, and started 160ms after, but ended with, the other components in the Delayed condition. Components were played through a circle of 24 loudspeakers arranged around an acoustic manikin; the 3rd component came from 45° to the left or right or straight ahead. Recordings made with the manikin were presented binaurally to 16 adults and 16 pre-adolescent children with normal hearing, while brain activity was recorded with a 248-channel whole-head neuro-magnetometer. Subjects either reported whether the 3rd component came from the left or right (Attended conditions) or ignored the acoustical stimuli and performed a visual discrimination task (Unattended conditions).

Compared with the *In-tune* condition, delay and mistuning were associated with a reduction in the magnitude of the MEG signal over the temporal lobes about 400 ms after stimulus onset. In attended conditions, this reduction was related to accuracy of localisation: the reduction was significant only in those conditions where accuracy also increased significantly compared with the *In-tune* condition (*Delayed* and *Mistuned* for adults; *Delayed* for children). In unattended conditions, the reduction was significant only for adults and only for delay.

These results suggest that: (1) the reduction reflects a modulation of activation by detection of a perturbed component; (2) a delayed component can grab attention automatically, while active attention is required to detect a mistuned component; and (3) both automatic and active attention are immature in some pre-adolescent children.

## 424 The Role of the Olivocochlear Bundle in Azimuthal Localisation and Auditory Plasticity

**Samuel Irving**<sup>1</sup>, M. Charles Liberman<sup>2</sup>, Christian J. Sumner<sup>1</sup>, David R. Moore<sup>1</sup>

<sup>1</sup>MRC Institute of Hearing Research, Nottingham, UK, <sup>2</sup>Eaton Peabody Laboratory, Boston, USA

Unilateral and asymmetric conductive hearing losses lead to immediate impairments in the ability to localise sound. Azimuthal sound localisation in ferrets can return almost to pre-plug levels within a few weeks of unilateral ear plugging with frequent training (Kacelnik et al, PLoS, 2006). Little is currently known about the mechanisms involved in this adaptation. Xiao and Suga (Nature Revs Neurosci, 2002) suggested that efferent pathways from the higher auditory system to the periphery are implicated in plasticity. The final common pathway to the cochlea is the olivocochlear bundle (OCB). To ascertain whether the OCB is involved in localisation and the adaptation observed after conductive hearing loss, ferrets were trained in an absolute localisation task where they approached one of 12 speakers (30° intervals) producing a noise (40-1000ms; 56-84 dB SPL). The OCB was unilaterally lesioned (lateral floor of 4th ventricle) and localisation was reassessed before and after unilateral plugging ipsilateral to the lesion. No significant change in localisation was found pre- to post-lesion, prior to plugging. Plug insertion caused a large deficit in localisation (from 3.2° to 43.5° mean error) as previously found, but further training failed to show significant improvement in the lesioned ferrets. Removal of the plug immediately returned

performance to pre-plug levels. The results suggest a role for the OCB in this form of experience-dependent plasticity, but not in azimuthal localisation.

## [425] Task-Dependence of Spatial Sensitivity in the Dorsal Zone (Area DZ) of Cat Auditory Cortex

**Chen-Chung Lee**<sup>1</sup>, Ewan Macpherson<sup>1</sup>, Ian Harrington<sup>2</sup>, John Middlebrooks<sup>1</sup>

<sup>1</sup>Kresge Hearing Research Institute, University of Michigan, <sup>2</sup>Department of Psychology, Augustana College Previous studies from our lab have shown that the neurons in cortical area DZ have higher spatial sensitivity than neurons in A1 of anesthetized cats. This suggested that area DZ may play important roles in the processing of auditory spatial information. In the current study we investigated the spatial sensitivity of DZ in awake animals. We recorded extracellular spike activity with chronically implanted 16-channel probes. In all conditions, probe stimuli were 80 ms broadband noise bursts from free field speakers in the horizontal plane, spaced in 20 degree increments. We compared three behavioral conditions: 1) Idle: Cats were exposed to the probe stimuli but did not perform any behavioral tasks. 2) Detection: Cats were trained to detect a change from the probe stimulus to a click train, regardless of the location of the sound. 3) Localization: Cats were trained to distinguish a shift in stimulus elevation to 40 degree above horizontal plane. All three conditions were compared within single 1-hr sessions. Our sample of DZ neurons contained many units sharply tuned to the frontal midline. Other units with preference either for contralateral or ipsilateral location also showed sharper azimuth tuning than typically is observed for units in awake A1 or in anesthetized DZ. The effects of task on overall spike rate did not differ systematically among three conditions. However, about half of the units showed task-dependent modulations of spike-rate-azimuth function. Spatial selectivity, represented by the tuning width and the modulation depth of the spike-rate-azimuth function, increased from Idle to Detection to Localization tasks. The enhanced selectivity usually resulted from increased suppression of responses to non-favored locations. We interpret these taskdependent changes in spatial sensitivity as a top-down modulation of the spatial sensitivity of auditory cortical neurons.

Supported by RO1-DC-00420

# A Physiologically-Based Population Rate Code for Interaural Time Differences (ITDs) Predicts Bandwidth-Dependent Lateralization

Kenneth E. Hancock<sup>1,2</sup>

<sup>1</sup>Massachusetts Eye & Ear Infirmary, Eaton-Peabody Laboratory, <sup>2</sup>Harvard Medical School, Department of Otology and Laryngology

ITDs are encoded centrally in the medial (MSO) and lateral (LSO) superior olives. It is a longstanding view that these neurons are conceptually arranged in an array with

characteristic frequency (CF) on one axis and best ITD (BD) finely distributed on the other to form a labeled-line code of ITD. One important perceptual aspect of binaural hearing that has been explained using labeled-line models is the dependence of lateralization on stimulus bandwidth.

The labeled-line model has been challenged by physiological data from the guinea pig, confirmed in the cat and gerbil, showing there is not a full complement of BDs for all CFs. It has been suggested that ITD may be represented by a rate code, in which the activity of many neurons pool to form a single ITD channel on each side of the brain.

We demonstrate the ability of such a model to predict bandwidth-dependent lateralization. Each channel comprises 625 model neurons, whose CFs and BDs are distributed to mimic physiological data from the cat inferior colliculus. Each neuron cross-correlates the bandpass-filtered stimuli to the two ears, and the channel output is simply the summed firing rate of its neurons.

The model predicts lateralization as a function of bandwidth, if four channels are used, one representing each MSO and one each LSO. The lack of need for labeled lines minimizes the precision required in the BD array and may explain how a viable ITD representation is formed despite the existence of several factors that determine the BD of individual neurons. Finally, the outputs of the population rate model are appropriate for controlling muscle movements that orient the head toward a sound source. Thus, it is conceivable that the neural ITD code is an evolutionary remnant of a primitive coupling between sensory stimulation and motor response.

# 427 Biophysical Mechanisms for Forming Sound-Analogue Membrane Potentials by Phase-Locked Synaptic Inputs in Owl's Auditory Neuron

**Go Ashida<sup>1,2</sup>**, Kousuke Abe<sup>2</sup>, Kazuo Funabiki<sup>1,3</sup>

<sup>1</sup>Graduate School of Medicine, Kyoto University, <sup>2</sup>Graduate School of Informatics, Kyoto University,

<sup>3</sup>Systems Biology, Osaka Bioscience Institute

Owls use internaural time difference (ITD) to locate a sound source. In the avian auditory system, the second order station, nucleus magnocellularis (NM), providing axonal delay lines and the third order station, nucleus laminaris (NL) providing coincidence detectors are known to be involved in ITD encoding. Electrophysiology has revealed that presynaptic NM fibers generate spikes in a phase-locked manner and postsynaptic membrane potential of a NL neuron shows sinusoidal waveforms (Sound Analogue Potential; SAP). Although the formation of SAPs by the convergence of phase-locked inputs from NM neurons can be expected qualitatively, the parameter dependence of those waveforms is still a subject of quantitative study. We performed a computer simulation of the synaptic inputs from the bilateral NM neurons to create SAPs in the NL neuron and investigated its parameter dependence. Parameters such as the degree of phaselocking, the number of convergence and the time course of a unitary synaptic input affect the amplitude of SAP, the

amplitude of DC depolarization and the spectral features of synaptic noise in a complex manner. When we chose a proper set of parameters, calculated amplitudes of SAP and DC depolarization are similar to those observed in vivo. These results imply that simulational recreation of the SAPs observed in in vivo experiments of owl's NL is feasible with biophysical components reported in auditory coincidence detector neurons. However, low frequency noise still remained several times larger than that observed in experiments. We will also discuss how the owl's auditory system reduces noise.

### | 428 | Rate Representation of HRTF Spectral Shapes in the Inferior Colliculus

Brad May<sup>1</sup>, Michael Anderson<sup>1</sup>, Matthew Roos<sup>1</sup>

<sup>1</sup>Johns Hopkins University

This presentation describes the auditory coding of spectral cues for sound localization in the inferior colliculus of unanesthetized, decerebrate cats. Single-unit responses were characterized with closed-field noise bursts that conveyed the monaural spectral shapes, binaural level differences (ILDs), and binaural time differences (ITDs) of the head-related transfer function (HRTF: the external ear's transformation of a free-field sound as it propagates to the eardrum). The relative importance of monaural versus binaural processing was evaluated by comparing responses to monaural versus binaural simulations of the frontal sound field. Our current measures focus on neurons whose spatial tuning was largely dictated by monaural spectral cues. To a first approximation, the responses of monaurally tuned (MT) neurons were predicted by the local gain of the HRTF. That is, lowest and highest discharge rates correlated with sound levels at the neuron's excitatory best frequency (BF: the most sensitive frequency). Strong inhibitory effects surrounded the excitatory field of most MT neurons at low stimulus levels and often expanded across BF at high levels. This broad inhibitory tuning exerted a powerful modulatory effect on the dynamic range of responses to broadband sounds. Noise bursts with the same local gain elicited different response magnitudes depending upon the extent to which global inhibitory patterns were activated or attenuated by directionally dependent peaks and nulls (notches) in the HRTF spectrum. From the perspective of sound localization, the spectral selectivity of MT neurons provides a rate representation of source location that is tuned in both azimuth and elevation.

This research was funded by NIDCD grant DC000954.

# | 429 | Detection of Combined Changes in Interaural Time and Intensity Differences: Comparison Between Low and High Frequency Signals

Shigeto Furukawa<sup>1</sup>

<sup>1</sup>NTT Communication Science Laboratories

The major models of lateralization implicitly assume that information about interaural time and intensity differences (ITD and IID, respectively) is processed by a common

binaural mechanism, which is isomorphic across the frequency ranges. The present study attempted to test this assumption of isomorphism using an approach based on the signal detection theory (SDT).

The stimuli were a 500-Hz tone (low frequency signal) and a "transposed" stimulus, which was a 4-kHz tone amplitude-modulated with a half-wave-rectified 125-Hz sinusoid (high frequency signal). The stimuli were 200 ms long, and were presented dichotically with various combinations of baseline ITDs and IIDs. The detectability of the ITD and/or IID change from the corresponding baseline values was measured with the method of constant stimuli. A two-alternative forced-choice method was used, and the subject's task was to indicate the stimulus interval that contained the ITD and/or IID change. The ITD and IID changes, when combined, were always consonant in terms of direction. The percentage of correct responses was converted to the detectability index, d'.

According to the SDT, the detectability index of combined ITD and IID changes,  $d'_{C}$ , is predicted by an equation: d $'_{C}^{2} = d'_{T}^{2} + d'_{I}^{2} + 2 r d'_{T} d'_{I}$ , where  $d'_{T}$  and  $d'_{I}$ , respectively, are the detectability indices when the ITD and IID changes are presented alone, and *r* is the correlation coefficient for the internal noises that limit ITD and IID performance, respectively. We estimated the *r* values from the detectability indices obtained in the experiment. The r values were generally greater for the high frequency signal  $(r = \sim 1.0)$  than for the low frequency signal  $(r < \sim 0.5)$ , although they varied markedly depending on subjects and stimulus conditions. This indicates that for high frequency signals, the performance for ITD and IID discrimination is limited mainly by a common noise source (implying a common mechanism for ITD and IID), whereas the internal noises that limit ITD and IID discrimination are more or less independent (implying separate mechanisms). The results suggest that the mechanisms that process ITD and IID are qualitatively different for different frequency ranges.

## 430 The Relative Contribution of Interaural Cues to Binaural Detection at High Frequencies

Tracy Pogal-Sussman<sup>1</sup>, H. Steven Colburn<sup>1</sup>

<sup>1</sup>Department of Biomedical Engineering and Hearing Research Center, Boston University

This study compares the relative contributions of interaural cues to binaural unmasking at high frequencies in conditions with a diotic masker and a phase-reversed signal, NoSπ. We used a 128-Hz sinusoidal signal and 25-Hz low-pass noise multiplied by a 128-Hz carrier to control the fine-structure phase  $\alpha$  between the multiplied noise masker and signal [Breebaart et al, J Acoust Soc Am 106 (1999)]. Waveforms were then transposed to 4 kHz so that the envelopes of the high frequency stimuli contained the interaural information [van de Par and Kohlrausch, J Acoust Soc Am 101 (1997)]. We manipulated α to create four  $NoS\pi$  conditions with time-varying interaural differences: interaural time differences (ITDs), interaural intensity differences (IIDs), combinations of ITDs and IIDs which reinforce (same sign), and combinations of ITDs and IIDs which conflict (opposite signs). In addition, we

examined the relative effect of both static and time-varying interaural differences. The task is to discriminate between the diotic NoSo reference intervals and a phase-reversed NoSπ interval [Bernstein and Trahiotis, Hearing Res, 62 (1992)]. Performance is defined by the threshold signal-tonoise ratio (SNR) for discrimination, and is analyzed in terms of the distributions of time-varying ITDs and IIDs corresponding to the SNR at threshold. Our initial results suggest that performance is better when the interaural cues are in conflict than when they reinforce. In the condition with conflicting interaural cues, the perceptual width of the  $NoS\pi$  stimulus is broader than in the condition with reinforced interaural cues. The broader stimulus is easier to discriminate from the compact, diotic reference stimulus. This result is suggestive of a perceptual "width" cue being used for the task.

[Supported by NIH grant DC 00100.]

### 431 Combination of Monaural and Binaural Masking Release

Jesko Verhey<sup>1</sup>, Bastian Epp<sup>1</sup>

<sup>1</sup>Institut f. Physik, Universität Oldenburg

Thresholds of a sinusoidal signal in the presence of a broadband masker are markedly lower when the masker has the same envelope fluctuations in different frequency regions, i.e. is comodulated (CM), compared to a masking condition with uncorrelated masker envelope fluctuations (UN). This threshold difference is commonly referred to as comodulation masking release (CMR(UN-CM)). A masking release is also observed when an interaural phase difference (IPD) is introduced for the signal but not for the masker. This threshold difference is commonly referred to as binaural masking level difference (BMLD). The present study investigates, if the auditory system can benefit from both, monaural and binaural cues, when a signal with an IPD is masked by a CM masker. Thresholds are measured for a sinusoidal signal with a frequency of 700 Hz and IPDs in the range from 0 to 180 degrees. Three different maskers are used: In the UN and the CM condition, the masker consists of a 20-Hz wide noise band centred at the signal frequency (on-frequency masker, OFM) and four 20-Hz wide flanking bands (FB) centred at 300, 400, 1000. and 1100 Hz. The masker in the third condition consists of the OFM only. The condition is commonly referred to as reference (RF) condition, since it was also used as a reference for the calculation of CMR (CMR(RF-CM)). Thresholds for all conditions decrease as the IPD increases. The CMR(UN-CM) is independent of the IPD, i.e. the combined monaural and binaural masking release is the sum of the BMLD and the CMR. The CMR(RF-CM) decreases as the phase increases. This probably results from the different masker bandwidth in the two conditions rather than reflecting a reduced ability of the auditory system to benefit from comodulation. The data of an additional experiments with partially comodulated maskers further support the hypothesis that the combined masking release is simply the sum of CMR(UN-CM) and the BMLD.

#### 432 A Model for Predicting Binaural Loudness of Spatial Sounds

Ville Sivonen<sup>1</sup>, Wolfgang Ellermeier<sup>1</sup>

<sup>1</sup>Aalborg University

The location of a sound source relative to the listener greatly affects the physics of binaural stimulation: Depending on the angle of incidence, the transfer of sound from the source to the ears changes dramatically. As a consequence of these dependencies, which can be described by head-related transfer functions (HRTFs), the sound signals reaching the two ears often differ from one another, both in terms of their time of arrival and their spectral characteristics.

In order to predict the loudness of spatial sounds, it is thus important to know how the two, often different signals reaching the listener's ears are integrated into a single binaural percept. Current loudness models [e.g., Moore et al., J. Audio Eng. Soc., 45, 224-239, (1997)] assume "perfect summation" of loudness across the ears, that is, binaural loudness being a simple sum of the monaural loudnesses in sone units. This assumption, however, is based on headphone studies quantifying the binaural effect on loudness, in which the effects of HRTFs and the spatial aspects are being disregarded.

The present paper summarizes results from a series of experiments reporting on (1) how the spatial location of a sound affects its perceived loudness, and (2) how the binaural summation of the at-ear signals should be modeled to predict the loudness of sounds from various locations. The results provide evidence for less-than-perfect summation of loudness when truly spatial sound stimulation is used. More specifically, a power summation of at-ear spectra makes fairly accurate predictions of the mean data obtained.

#### 433 Predicting Thresholds for Echo Detection and Localization From Speech Onset Characteristics

**Scott Miller**<sup>1</sup>, Ruth Litovsky<sup>1</sup>, Keith Kluender<sup>1</sup> *University of Wisconsin - Madison* 

This study examined how the acoustic characteristics of speech sound onsets can account for echo thresholds and lag discrimination thresholds, phenomena that are often used to investigate the precedence effect. Past efforts to predict these and other precedence effect thresholds from auditory stimulus characteristics have used artificial stimuli, such as short clicks and noise bursts that, unlike speech, typically do not have multiple spectral transients and do not overlap at the inter-stimulus intervals that correspond to psychophysical thresholds. In the current study, four CV stimuli were selected as pairs, "buh" vs. "wuh" and "duh" vs. "yuh," which would differ respectively in the abruptness vs. gradualness of the onset of the waveform envelope but would otherwise have highly similar spectral and temporal characteristics. thresholds and lag discrimination thresholds were measured psychophysically (N = 9), and repeatedmeasures ANOVAs confirmed that thresholds for the abrupt onset stimuli were significantly lower on both tasks. Results were then compared with two prediction algorithms adapted from perceptual center (p-center) models found in the speech perception literature: a frequency dependent center of gravity (FCoG) model and a frequency-dependent amplitude increase (FAIM) model. Bivariate correlations confirmed the predictive validity of the FCoG model for both kinds of thresholds, while FAIM correlations failed to reach statistical significance. To our knowledge this is the first demonstration of systematic variability in precedence effect thresholds among speech sounds. Discussion will focus on the limitations of these two prediction algorithms and on efforts to extend physiologically plausible computational models of monaural onset detection and binaural localization to account for these data.

# 434 Modeling Spatial Release From Masking in a Cocktail Party Environment with Multiple Maskers and Multiple Masker Types: Angular Separation, Asymmetry and Interaural Statistics

**Gary Jones**<sup>1</sup>, Ruth Litovsky<sup>1</sup>

<sup>1</sup>University of Wisconsin-Madison

Spatial release from masking (SRM) in a cocktail party environment has proven quite difficult to model. Part of the reason for this is that speech intelligibility depends on multiple features of maskers and the masker array. A model proposed by Bronkhorst breaks SRM into two components that are roughly equated with the contributions to release from masking of 1) angular separation of maskers from the target, and 2) the asymmetry of the masking array. While this model has produced good fits to data for masking of speech targets by noise maskers, attempts to apply it to more recent data from experiments in which both targets and maskers are speech have yielded mixed results. An alternative model tested here is based on the interaural statistics of the combined maskers. In the current study the contributions of angular separation and asymmetry to SRM were measured psychophysically and compared with the predictions of both models.

We examined SRM for several two-masker conditions in the frontal hemifield using spondees as targets and steady-state noise, modulated speech-shaped noise (MSSN), and speech as maskers. The results of these experiments were as follows: 1) the contribution of angular separation to SRM was greater than predicted by the Bronkhorst model across masker locations and across masker types, 2) SRM was greater for speech maskers than for noise maskers, 3) growth of the angular separation component with increasing angle did not match predictions of the Bronkhorst model, and 4) the pattern of measured values was not consistent with an interaural statistics account of SRM. These results suggest that modeling SRM is complicated, in particular when speech sources are used. There is a need to reconsider how to best describe the components of SRM and how to incorporate different components within the model to account for speech and noise maskers.

#### 435 Informational Masking in Children: Failures of Early Selection

Frederic Wightman<sup>1,2</sup>, Doris Kistler<sup>1,2</sup>

<sup>1</sup>University of Louisville, <sup>2</sup>Heuser Hearing Research Center Informational Masking in Children: Failures of Early Selection

Segregating a target speech signal from a background of interfering sounds is fundamental for successful communication in everyday acoustical settings. The task is made more difficult by the impact of informational masking, a central auditory system effect whereby sounds that are similar to a target sound interfere with processing of the target. Children demonstrate much more informational masking than normally hearing adults and do not reach adult levels of performance until the mid-teenage years. One of the most important stimulus factors that mitigate informational masking is spatial separation of target and distracter. In normally hearing adults, spatial separation can reduce informational masking by as much as 18 dB. In children, however, this effect is much smaller. Even when a speech target is presented to one ear and a speech masker is presented to the other ear, children demonstrate as much as 15 dB of informational masking. Considered in the context of theories of selective attention, this result suggests that children have immature "early selection" skills that might allow them to segregate a target from a distracter on the basis of physical differences (e.g., talker gender, spatial location).

#### 436 Spatial Release From Speech-On-Speech Masking with Symmetrically-Placed Maskers

**Nicole Marrone**<sup>1</sup>, Christine Mason<sup>1</sup>, Gerald Kidd Jr<sup>1</sup>

\*Boston University\*

Spatial release from masking was studied in a three-talker soundfield listening experiment. The target talker was presented at 0° azimuth and the maskers were presented either from the same loudspeaker as the target (colocated) or from loudspeakers located symmetrically around the target. The symmetric placement of the maskers greatly reduced any "better ear" listening advantage. The targetto-masker ratio (T/M) for 50% correct identification was measured by adapting the masker level against the fixedlevel target. When the maskers were separated from the target by only ±15°, a spatial release from masking of about 8 dB was found. Wider separations increased the release to more than 12 dB. This large effect was eliminated when binaural cues were degraded by covering one ear with an earplug and earmuff. Increasing reverberation in the room increased T/M for the separated, but not colocated, conditions reducing the release from masking. Time-reversing the masker speech improved performance for both colocated and spatially separated conditions, but lowered T/M the most for the colocated condition again resulting in a reduction in the spatial release from masking. Overall, the results were interpreted as evidence supporting a "spatial filter" thought to reflect the focus of attention at a point along the horizontal

[Work supported by AFOSR and NIH/NIDCD].

#### 437 Binaural Release From Masking for a Tone in Noise and in Multitone Maskers

**Frederick J. Gallun**<sup>1</sup>, Nathaniel I. Durlach<sup>1,2</sup>, H. Steven Colburn<sup>1</sup>, Barbara G. Shinn-Cunningham<sup>1</sup>, Virginia Best<sup>1</sup>, Antje Ihlefeld<sup>1</sup>, Christine R. Mason<sup>1</sup>, Gerald Kidd, Jr. <sup>1</sup>Boston University, <sup>2</sup>MIT

Variations in the detection threshold of a 500-Hz target tone masked by random noise and by sets of ten masker tones (with a "protected region" from 400-600 Hz) were studied as a function of simultaneous shifts in the interaural amplitude ratio and interaural time delay of the target tone. For both masker types, the reduction in threshold observed when the time and amplitude differences favored the same ear was not significantly different from the reduction observed when the differences favored opposite ears, as found with a noise masker by Colburn and Durlach (JASA, v.38, 1965). That this pattern held for both types of maskers argues against a simple position variable explanation for binaural release from maskers that fall either in near or in distant frequency regions. While there are similarities in binaural unmasking for the two masker types, at least for simple detection tasks, correlations between release for noise and multitone maskers for individual listeners accounted for only 15% of the variance, while correlations within each masker type for different sized interaural differences accounted for 60% of the variance. Thus, the seemingly similar patterns of binaural release from masking for the two masker types may come about by different mechanisms.

# Age on Speech Intelligibility and Spatial Release From Masking in Child and Adult Listeners

Patti Johnstone<sup>1</sup>, Ashley Eisen<sup>2</sup>, Ruth Litovsky<sup>3</sup> <sup>1</sup>University of Tennessee - Knoxville, <sup>2</sup>State University of New York at Buffalo, <sup>3</sup>University of Wisconsin - Madison Spatial release from masking (SRM) refers to the finding that speech intelligibility improves when interfering speech is spatially separated from the target speech. This has been studied by the authors under a number of conditions in the sound field. The purpose of the present study was to examine the effect of the content and talker type of the interferer. Two interferer topics (Harvard IEEE sentence materials; child-relevant social topic) were each recorded with two different talkers (adult woman, girl). Speech intelligibility thresholds were compared in guiet, and with interferers that were spatially near the target speech (at 0°) or separated from the target by 90° to the right. Participants with normal hearing included 20 adults and 20 typically-developing, 6-7 year-old children.

Results show that interferer topic had a significant effect. The child-relevant social topic produced significantly higher SRTs and greater amounts of masking for both children and adults. Interferer topic did not affect SRM in either group. The age of the talker also affected performance. Overall, the voice of the adult woman produced higher SRTs and more masking than the voice of the young girl but SRM was not affected by the differences in voice characteristics. Finally, when

compared to adults, children demonstrated higher SRTs for both talkers and greater amounts of masking for the adult woman talker but no significant difference in the amount of SRM. These findings suggest that interferer topic and voice type are both important factors to explore in studies of informational masking, but may not be relevant to spatial configurations of talker and interferer.

# 439 Antibiotic Injections (Hair-Cell Death and Regeneration) Delay Development of High Frequency Sensitivity and Vocal Behaviors in Hatchling Chicks

**Lincoln Gray**<sup>1</sup>, Brenda Ryals<sup>1</sup> *James Madison University* 

Randomly selected chicks from three batches were injected with 400mg/kg Gentamycin within a few hours of hatching. Subjects were tested approximately every other day between post-natal days 4 and 11 (51 tests of 10 control birds; 81 tests of 14 antibiotic-injected birds). Peep suppression was recorded in response to 1500, 1800, 2000, 3800, 4100, 4400, 4600, 4800, and 5000 Hz pure tones presented at 75, 70, 55, 59, 74, 79, 80, 82, and 85 dB SPL respectively (louder tones or tones closer to 3kHz would be recorded as if they were vocalizations, yielding false negative results in this paradigm). Duration of delays in the subjects' vocalizations was the dependent variable (pooled over subjects to form ROCs). The antibioticinjected animals showed no responsiveness to any of the high-frequency tones between 4 to 7 days of age. The treatment is expected to kill hair cells in the proximal 25% of the basilar papilla resulting in a significant hearing loss at frequencies above 1500 Hz, as observed. At older ages responsiveness returned to normal, suggesting hair-cell regeneration. The group-by-age interaction was highly significant ( $F_{1,124}=6.7$ , p=.01). Thus the normal development of high-frequency hearing sensitivity was delayed by approximately one week. The development of the central and peripheral auditory systems in these subjects was desynchronized. Since both simple and complex auditory processing can be measured with the peep-suppression method, this animal model appears relevant to developmental processes in children with early cochlear implants, as their brain could also be developing slightly ahead of their peripheral sensitivity. Finally, there were some indications that the antibiotic-injected birds maintained immature vocal behaviors into older ages. Thus, antibiotic-injected chicks could also be a useful animal model of early vocal behaviors relevant to humans with early hearing loss.

Supported by NIDCD R01DC1372 to BR and DC4303 to LG.

#### 440 the Influence of Species-Specific Vocalizations on Rhesus' Reward Choices

**Yune-Sang Lee<sup>1</sup>**, Brian Russ<sup>1</sup>, Ashlee Ackelson<sup>1</sup>, Allison Baker<sup>1</sup>, Yale Cohen<sup>1</sup>

<sup>1</sup>Department of Psychological and Brain Sciences, Dartmouth College

Adaptive behavior requires that animals form decisions that optimize potential rewards and minimize potential

punishment. To form these decisions, animals must consider previous knowledge or experience, the current context, and other factors. One of the more important factors is how social information is integrated into the decision-making process. For instance, rhesus monkeys will forego the opportunity to receive a larger juice reward when given the opportunity to view pictures of high-status male or female perinea (Deaner et al., 2005). Here, we extended this observation and tested how rhesus monkeys integrate species-specific vocalizations (auditory stimuli) into their decision-making process. In the first phase of the experiment, after fixating a central LED, an LED to the left of the monkey; s fixation (T1) and an LED to the right of the monkey; s fixation (T2) were presented. Monkeys were free to shift their gaze to either T1 or T2 to receive a juice reward. However, the amount of juice that the monkeys received depended on their choice. The monkeys rapidly identified the target that provided the larger juice reward. In the next phase, when monkeys chose T2, a species-specific vocalization was presented concurrently with juice. The acoustic class and the amount of juice at T1 and T2 changed on a block-by-block basis. Data to date suggest that monkeys, independent of acoustic class, are not willing to forego juice rewards to hear vocalizations. Instead, one monkey needed to be j°paidj± (i.e., receive more juice) in order to hear the vocalizations, whereas a second monkey; s choices were independent of the presentation of the vocalizations. These data suggest that monkeys integrate auditory stimuli into their decisional processes differently than they do visual stimuli.

This research was supported by NIH.

### 441 Effective Envelope Modification by Coherent Demodulation

**Kaibao Nie**<sup>1</sup>, Les Atlas<sup>2</sup>, Pascal Clark<sup>2</sup>, Bishnu S. Atal<sup>2</sup>, Jay T. Rubinstein<sup>1</sup>

<sup>1</sup>VM Bloedel Hearing Research Center, University of Washington, Seattle, <sup>2</sup>Dept. of Electrical Engineering, University of Washington, Seattle

Acoustic signals can be decomposed into slowly-varying temporal envelopes and fast-changing temporal fine structure. The Hilbert transform approach has been widely used to perform this decomposition. Envelopes from the Hilbert transform are usually filtered to study how envelope modification could affect speech intelligibility with psychoacoustic experiments. Ghitza (JASA, 2001) demonstrated that this approach of envelope modification is ineffective, since the Hilbert fine structure interacts with the filtered Hilbert envelope and the reconstructed envelope is not distortion-free after modification and combination. In this study, we propose an effective approach of acoustic signal decomposition by coherent demodulation. Amplitude modulations (AM) of an acoustic signal are coherently extracted by tracking the sub-band carriers of the signal. Preliminary experiments have shown that this approach can produce distortion-free and desirable AM filtering. The coherent demodulation approach can potentially provide a new tool to conduct psychoacoustic studies on the contributions of amplitude

modulation and frequency modulation to speech recognition.

(Supported by NIH R01 DC007525)

# 442 Discrimination of Natural and Acoustically Altered Song Syllables of Normal-Hearing and Hearing-Impaired Canaries

**Amanda Lauer**<sup>1</sup>, Robert Dooling<sup>1</sup>, Michelle Eisenberg<sup>1</sup>

\*\*University of Maryland\*\*

A strain of canary bred for a distinct low-pitched song, the Belgian Waterslager (BWS), has been used in many studies of song learning and production. These birds have a hereditary high-frequency hearing loss linked to inner ear abnormalities that develop before the song learning period. There are known auditory perceptual differences between BWS and normal-hearing non-BWS canaries. instance, BWS show reduced frequency resolution and discrimination at high frequencies and enhanced temporal resolution at high sound levels. Whether these perceptual differences influence vocal communication in these birds is an open question. Here, we investigated discrimination of natural and acoustically altered BWS and non-BWS song syllables in both strains. We also tested discrimination of natural canary song syllables in three other species: zebra finches, budgerigars, and humans. BWS canaries were equally good at discriminating among BWS and non-BWS syllables, but were better than non-BWS canaries at discriminating among BWS syllables. Zebra finches, budgerigars, and humans performed equally well when discriminating among BWS and non-BWS syllables. However, all three of these species were slightly faster than canaries when making the discriminations. enhanced performance could be due to differences in auditory perceptual abilities or in motor capabilities.

[Supported by NIH DC01372, DC05450, and DC04664].

### 443 Auditory Memory for "Meaningful" and "Meaningless" Signals in a Songbird

**Melanie A. Zokoll<sup>1</sup>**, Ulrike Langemann<sup>1</sup>, Georg M. Klump<sup>1</sup> *<sup>1</sup>University of Oldenburg* 

Experiments in humans suggest that auditory memory persistence varies with the meaning attached to the stimuli presented (e.g., Peterson et al. 1961, Canad J Psychol 15:143-147). In the present study we investigate in songbirds whether the persistence of the birds' auditory memory differs between "meaningless" stimuli (sinusoids, noise bursts) and "meaningful" stimuli (song motifs).

Five European starlings (Sturnus vulgaris) were trained in a Go/NoGo procedure and a delayed non-matching-to-sample (DNMTS) paradigm was used to estimate the persistence of the auditory memory store. In each trial of a session, a series of up to 6 identical sample stimuli and a final test stimulus were presented with random inter stimulus intervals (range 1-27 s). The test stimulus was either the same as (NoGo-Stimulus) or was different (Go-Stimulus) from the sample. Auditory memory persistence was measured as a function of the delay between the last sample and the test. Tested parameters were differences

in either the frequency (6 tonal stimuli in the range of 1100 to 3492 Hz, 400 ms, step size was 1/3 octave) or in the amplitude modulation rate of broadband noise stimuli (range 20 to 113 Hz, 400 ms, step size was a Weber fraction of 1.41) or differences between song motifs (600 ms). Test stimuli became sample stimuli in the following trial. All stimuli were randomly varied in level (61 dB±3 dB SPL). Memory performance was expressed as the proportion of correct responses in relation to the total number of pairs of sample and test stimulus that were presented with a specific delay. Auditory memory persistence of our animal model did not differ substantially between the stimulus types. Persistence was rather long (up to 26 s) but showed distinct individual variation. Increasing the number of samples presented before the test stimulus improved performance. Performance was also improved for more salient differences between samples and test.

Supported by the DFG, InterGK 591 and SFB/TRR 31.

## 444 Vocal Communication and Social Learning in Juvenile and Adult Eptesicus Fuscus

#### Withdrawn

#### 445 Auditory-Category Perception in Rhesus Macagues

Yale Cohen<sup>1</sup>, Brian Russ<sup>1</sup>, Lauren Orr<sup>1</sup>, Lauren Wool<sup>1</sup>, Farshad Chowdhury<sup>1</sup>

<sup>1</sup>Dartmouth College

Categorization is a natural and adaptive process that is seen in all animals. While there is a great deal of variability within and across stimuli, animals typically ignore some sources of variation while attending to others to guide behavior. By categorizing or grouping together previously known stimuli, humans and animals can begin to interpret novel ones. In the present study, we trained rhesus macaques to categorize artificial auditory stimuli based on their acoustic structure. The monkeys were trained to differentiate between two spoken words: /bad/ and /dad/. For each word, we created prototypes that were presented at three different pitches. We also created acoustic morphs of these prototypes; in morphing, two prototypes (i.e., the two phonemes) are chosen and then a (linear) mapping based on the physical features of the prototypes is calculated. Categorical perception was tested using a delayed match-to-category task. In this task, one of the six prototypes was chosen as the sample stimulus. The sample stimulus was repeated two to four times, with a delay of 500 msec between presentations. After another 500 msec, a choice stimulus was presented. The choice stimulus was either a prototype stimulus or one of the morphed stimuli. Following choice-stimulus offset, the monkey shifted their gaze to a leftward target if they thought that the sample and choice stimulus was a match. The monkey shifted their gaze to a rightward target if they thought the sample and choice stimulus were different. We found that rhesus macaques reliably perceived and

discriminated between auditory categories regardless of the pitch of the prototypes. Similar to humans, our monkeys showed a sharp category boundary in perception of the morphed stimuli. These results show that rhesus macaques can discriminate artificial auditory stimuli, and lays the groundwork for further investigation into the neural correlates of categorical perception.

Support contributed by the NIH.

## 446 Tone-On-Light Masking Reveals Spatial Selectivity of Optical Stimulation in the Gerbil Cochlea

**Agnella Izzo<sup>1</sup>**, Alice Lin<sup>1</sup>, Monica Oberoi<sup>1</sup>, Claus-Peter Richter<sup>1</sup>

<sup>1</sup>Northwestern University

Light can artificially stimulate nerve activity in vivo. A significant advantage of optical neural stimulation is the potential for higher spatial selectivity when compared with electrical stimulation. An increased spatial selectivity of stimulation could improve significantly the function of neuroprosthetics, such as cochlear implants. Cochlear implants restore a sense of hearing and communication to deaf individuals by directly electrically stimulating the remaining neural cells in the cochlea. However, performance is limited by overlapping electric fields from neighboring electrodes. Here, we report on the spatial selectivity of optical stimulation in the cochlea with a novel method: tone-on-light masking.

For the measurements, the probe response was evoked with light and was masked with a continuous acoustic tone. The placement of the optical fiber determined the probe frequency and was fixed for each trial. When the acoustic tones activated a cochlear segment that was also stimulated by the laser pulses, the laser evoked CAP decreased. In a similar manner to tone-on-tone masking, the masker level was determined such that it reduced the laser evoked CAP by a constant fraction. From this method, we constructed tone-on-light masking curves to indicate the corresponding region of the cochlea that the laser is stimulating.

Tone-on-light masking studies revealed tuning curves of optically stimulated cochleae that exhibit best frequencies between  $6-11\,$  kHz and Q10dB ratios between  $2-7.\,$  Tone-on-tone masking data and tone-on-electric masking data will be provided for comparison.

Supported by the E.R. Capita Foundation, NIH HHSN260-2006-00006-C, 1R41DC008515-01, F31 DC008246-01.

# 447 Behavioral and Physiological Determinations of Threshold to Electrical Stimulation of the Inferior Colliculus in Rabbits

**Douglas Fitzpatrick**<sup>1</sup>, Charles Finley<sup>1</sup>, Michael Ingraham<sup>1</sup>, Jason Roberts<sup>2</sup>, Oliver Adunka<sup>1</sup>, Harold Pillsbury<sup>1</sup>

<sup>1</sup>Univ. of North Carolina at Chapel Hill, <sup>2</sup>East Carolina

In patients lacking a viable auditory nerve, functional hearing may be provided using an implant at a central

University

brain site. The inferior colliculus (IC) is an attractive choice because of its central role in auditory pathways, relatively homogeneous cellular structure and accessible tonotopic organization. The feasibility of an IC implant is being addressed using behavioral and electrophysiological measures in an unanesthetized rabbit preparation. Here we report the threshold to electrical stimulation using intra IC field recordings for comparison with the threshold measured behaviorally.

The implant was a Michigan-style chronic electrode with 16 contacts that spanned a 3 mm distance (NeuroNexusTech, Inc). The 1250 µm<sup>2</sup> iridium contacts were activated by cyclic voltammetry to achieve final impedances of ~100 kOhms. The electrodes were inserted through a cannula placed in the dorsal skull to a position just overlying the IC. The location for implantation was selected based on prior single-unit recordings to ensure that the array would span a wide range of characteristic frequencies in the central nucleus. This was confirmed subsequently by multi-unit recordings from the implanted array's contacts. Intra IC neural field recordings were obtained from unstimulated contacts of the electrode while selected contacts were electrically stimulated with biphasic pulses. Electrical artifact was isolated using highbandwidth stimulation and recording to prevent temporal smearing of the artifact and neural response. Behavioral threshold was determined in the same animal used for the physiological measurements. The behavioral task was conditioned avoidance.

The thresholds for detection of implant stimulation were comparable in the physiological and behavioral experiments. For 60  $\mu s/phase$  biphasic pulses the lowest current level yielding a consistent neural response was about 15  $\mu A,$  and the lowest current level yielding behavioral responses that were above chance was about 20  $\mu a.$  Both the physiological and behavioral thresholds have been stable for several months. These results show that measurements of the physiological efficacy of IC stimulation made within the IC itself show a close correlation with behavior.

This work was supported through a contract with the Advanced Bionics Corporation.

### | 448 | Identifying Effective Stimulation | Parameters for an Auditory Midbrain Implant

**Hubert H Lim**<sup>1,2</sup>, Minoo Lenarz<sup>1</sup>, Anke Neuheiser<sup>1</sup>, Uta Reich<sup>1</sup>, Guenter Reuter<sup>1</sup>, Thomas Lenarz<sup>1</sup>

<sup>1</sup>Hannover Medical University, <sup>2</sup>Cochlear Ltd.

The auditory midbrain implant (AMI) is now in clinical trials. Although the first implanted patients achieve different loudness, pitch, and temporal percepts using the AMI, it is still not clear how to stimulate the inferior colliculus central nucleus (ICC) to achieve intelligible speech perception. As an initial step towards identifying effective stimulation strategies, we investigated the effects of different ICC stimulus parameters (i.e. phase duration, pulse rate, amplitude modulation depth and frequency) on auditory cortical activity in a guinea pig model. Multi-site silicon probes were used to record from different layers and isofrequency regions within the primary auditory cortex

(A1) in response to stimulation (monopolar, cathodicleading pulses) of different isofrequency locations within the ICC using our human AMI penetrating array. As expected, A1 neural thresholds decreased as the phase duration (41-984 µs) increased where the lowest charge per phase was observed at 41 µs. However, the threshold versus phase duration curves varied across different stimulation locations along the ICC laminae suggesting that different population of neurons within the ICC and higher auditory regions may be activated. depending on stimulation location, cortical neurons exhibited different synchronization properties that could span a wide range of pulse rates (~10 to 70 pps) and modulation frequencies (~20 to 60 Hz). For higher pulse rates and modulation frequencies, cortical neurons usually ceased firing after the onset response and exhibited larger rebound activity. Furthermore, different cortical neurons responded optimally to different combinations of pulse rate, modulation depth, and modulation frequency. Overall, these findings demonstrate that location of implantation within the ICC and selection of certain stimulus parameters can affect the extent and effectiveness of auditory cortical activation. Different combinations of stimulus parameters identified in this study will be implemented in our AMI patients and hearing performance will be assessed.

# 449 Tonotopic Representations in the Inferior Colliculus Following Multichannel Electrical Stimulation of the Dorsal Cochlear Nucleus of Guinea Pigs

**Michael Hoa**<sup>1</sup>, Zhenlong Guan<sup>1,2</sup>, Gregory Auner<sup>3</sup>, Jinsheng Zhang<sup>1,4</sup>

<sup>1</sup>Dept of Otolaryngology, Wayne State Univ, <sup>2</sup>Dept of Zoology, Hebei Normal Univ, <sup>3</sup>Dept of Electrical and Computer Engineering, Wayne State Univ, <sup>4</sup>Dept of Communication Sciences & Disorders, Wayne State Univ Auditory brainstem implants (ABI) are used to stimulate the cochlear nucleus (CN) to recover hearing for patients who cannot benefit from cochlear implants. Although patients with ABI have demonstrated speech perception. large variability in speech perception across individuals exists. One of the factors that contribute to such variability may be the limited access to tonotopic gradients in the CN. Of the three subdivisions of the CN, the dorsal cochlear nucleus (DCN) is the best known tonotopic structure. Electrical stimulation of the DCN has been clinically shown to induce speech perception (Soussi and Otto, 1994). However, the physiological mechanisms underlying such speech perception have not been delineated. The current study sought to characterize the tonotopic representation in the inferior colliculus (IC) in response to multichannel stimulation of the DCN in guinea pigs. Prior to electric stimulation, tuning curves in the right IC were obtained in response to tone sweeps delivered to the left ear. Implantation of stimulation electrodes was performed by inserting a 16 channel microwire array in the left DCN. Recording of single- and multi-unit activity in the right IC at different depths was performed with a 16-channel NeuroNexus probe. Electrical current (pulse width 82-245

us, 10 pps, 0-80 uA at steps of 1 uA) was delivered to stimulate different tonotopic loci of the DCN along its mediolateral axis. Offline data analysis was performed to construct electrical spatial tuning curves, reflecting activity rate as a function of the current level and depth of recording sites. Our results demonstrated that stimulation of a lower frequency domain of the DCN evoked stronger activity in a lower frequency domain of the IC. Similarly, stimulation of a higher frequency domain of the DCN yielded more activation in a higher frequency domain of the IC. The tonotopic representations to electrical stimulation were verified by comparison with the tuning curves. Our results suggest that the DCN may be a promising target for hearing recovery and that the tonotopic map in the DCN may be useful for developing more effective electrode arrays and stimulation strategy.

## 450 Auditory Brainstem Responses to Multichannel Electrical Stimulation of the Dorsal Cochlear Nucleus of Rats

**Edward Pace**<sup>1</sup>, Zhenlong Guan<sup>1,2</sup>, Gregory Auner<sup>3</sup>, Jinsheng Zhang<sup>1,4</sup>

<sup>1</sup>Dept of Otolaryngology, Wayne State University, <sup>2</sup>Dept of Zoology, Hebei Normal University, <sup>3</sup>Dept of Electrical and Computer Engineering, Wayne State University, <sup>4</sup>Dept of Communication Sciences & Disorders, Wayne State University

Auditory brainstem implants (ABI) have been developed to stimulate the cochlear nucleus (CN) to recover hearing for patients with cochlear abnormality that prevents successful hearing rehabilitation through cochlear implants. The current study explored the possibility of multichannel electrical stimulation of the dorsal cochlear nucleus (DCN), one of the three subdivisions of the CN. Electrically evoked auditory brainstem response (EABR) is frequently used method for examining neural activation along the auditory pathways following electrical stimulation. In this study, we characterized EABRs in response to multichannel electrical stimulation of the DCN. Experiments were carried out in eight adult Long-Evans rats. A 16 microwire array was placed on the surface and implanted acutely at different depths of the left DCN. Single biphasic electrical pulses of 40 us duration were delivered at intensities of 0-100 uA and at a rate of 100 pps. EABR responses were recorded from a vertex electrode that was placed subdurally near the right inferior colliculus. The waveform morphology of EABR was analyzed by comparing the amplitudes, latencies and thresholds obtained at different insertion depths of the stimulation array in the DCN, at different tonotopic loci along the DCN, and at different stimulation intensities. Our results demonstrated that, at a given insertion depth, the amplitudes of waves I-V were increased while their latencies were shortened as the intensities of current were increased. We also found that the thresholds of EABR responses from stimulation at the DCN surface were higher than those from a subsurface stimulation. The amplitudes of these waves were larger when stimulating subsurface tissues than stimulating the surface. In addition, EABRs obtained when stimulation electrodes were at 0-50 um below the DCN surface had similar waveforms. EABRs with other waveform morphology obtained when stimulation electrodes were at 150-250 um also had similar waveforms. Finally we also observed different waveform morphology of EABRs when different tonotopic loci along the DCN were stimulated. Our results suggest that stimulation strategies need to be further explored to optimize the current ABI system.

#### 451 Anatomical Attachments of the Otologics MET™ Transducer

**James Kasic<sup>1</sup>**, Nicholas Pergola<sup>1</sup>, James Easter<sup>1</sup>, William Simms<sup>1</sup>, Herman Jenkins<sup>2</sup>

<sup>1</sup>Otologics, LLC, <sup>2</sup>University of Colorado Health Sciences Center

The standard Otologics "Middle Ear Transducer™" (MET™) attaches to the ossicular chain via a ceramic probe tip inserted into a laser-ablated hole in the incus. This method has been used in both the semi- and fully-implantable devices. The laser ablation procedure is time consuming and requires expensive equipment not readily available in every surgical setting. Precise alignment of the probe tip with the hole is required to function appropriately. Apparatuses that would permit attachment of the transducer to the incus or other middle ear structures without the use of a surgical laser would simplify the surgical procedure and allow treatment of conductive and mixed hearing loss.

To investigate the effect of "laserless" energy transmission to the middle ear, 10 fresh temporal bones were implanted with transducers coupled to the ossicles. These included 1) laserless V tip and saddle tip to the incus; 2) standard laser-drilled ceramic probe tip insertion; and 3) direct connection to the capitulum of the stapes, via a commercially available ossicular prosthesis. Coupling was measured by monitoring the vibratory response of the lateral crux of the stapes with a Laser Doppler Velocimeter Equivalent transducer loading was achieved through monitoring the electrical properties of the transducer. Velocity responses were greatest for the V tip connection to the incus and the prosthetic connected to the stapes, which were 10 dB mm/S/V greater than the saddle tip which was, in turn, 10 dB mm/S/V greater than that of the standard tip attachment.

Despite its field tested robustness, the standard "laser" tip attachment may not represent the most efficient way to stimulate the ossicular chain for this implanted hearing device. Alternate ossicular attachment mechanisms show promise for better ossicular coupling and new indications, while also simplifying the surgical procedure.

## 452 Inferior Colliculus Response to Monopolar and Bipolar Dual-Channel Cochlear Implant (CI) Stimulation

**Ben H. Bonham<sup>1</sup>**, Russell L. Snyder<sup>1,2</sup>, Olga Stakhovskaya<sup>1</sup>

<sup>1</sup>Epstein Laboratories, Dept of OHNS, Univ of Calif San Francisco, <sup>2</sup>Utah State Univ

Current steering, or division of a fixed total stimulating current between adjacent CI electrodes, has recently gained attention as a means to increase the number of perceptually independent stimulating channels available to

implant users. Programming strategies based on current steering are attractive to both CI users and manufacturers because they provide a way to increase the frequency resolution of CIs without requiring physical modification or redesign of the implanted devices.

We examined the distribution of neuronal activity in the guinea pig inferior colliculus central nucleus (IC) evoked by stimulating current that was divided between two CI channels. Single current pulses or pulse trains were applied to adjacent or nearby monopolar CI electrodes, or to overlapping bipolar electrode pairs. Neuronal activity was measured using a 16-site recording probe inserted to an acoustically-calibrated depth along the IC tonotopic axis.

By choosing two CI channels that evoked unique distributions of activity, we were able to examine the change in distributed activity as current was gradually redirected from the first to the second channel. When current was divided between two channels, the minimum (threshold) current required to elicit a response was higher than when the current was applied to only one. When stimulating current was divided between two interdigitated bipolar channels the region of highest activity was usually narrow and shifted gradually along the tonotopic axis. When current was divided between two monopolar channels, the region of highest activity shifted gradually along the tonotopic axis in some cases, but in others exhibited a quantal change in location, and ectopic regions of activation were frequently observed.

On average, CI users are able to distinguish several "virtual" channels between adjacent monopolar channels (Litvak, ARO 2005). Our results may explain the poorer performance experienced by some users.

Support by NIDCD N01-DC-2-1006

#### 453 Loudness and Perceptual Dimensions of Current Steered Electrodes

**Filiep Vanpoucke**<sup>1,2</sup>, Peter-Paul Boermans<sup>3</sup>, Jeroen Briaire<sup>3</sup>, Patrick Boyle<sup>1</sup>, Johan Frijns<sup>3</sup>

<sup>1</sup>Advanced Bionics, <sup>2</sup>Universiteit Antwerpen, <sup>3</sup>Leiden University Medical Center/ENT

Objective: Simultaneous stimulation of multiple electrodes causes their individual electrical fields to sum within the cochlea. One application of this field superposition principle is to redistribute a given current pulse over two electrodes, and continuously vary the current fraction. This likely causes the peak of the electrical field to continuously shift between the two electrodes, since this technique is able to elicit multiple pitch percepts [1]. Therefore, current steering may provide an improved site-of-excitation cue, and eventually lead to better frequency resolution, speech understanding and music appreciation. psychoacoustic evaluations concentrated on loudness and intermediate pitch [1]. This study investigates whether different hearing sensations are produced by pulse trains delivered sequentially, than by simultaneous current steering on adjacent electrode contacts.

Methods: N=10 adult CII/HR90K subjects listened to pairs of stimuli differing only in their current steering coefficient or stimulation mode (simultaneous or sequential). First all

stimuli were loudness balanced. Next a multidimensional scaling experiment was performed. Subjects indicated on a continuous scale how different each pair sounded. The resulting dissimilarity numbers were interpreted as distances in 2D space.

Results: During loudness balancing a consistent and stable percept was found for simultaneous stimulation. For sequential stimulation loudness was highly dependant on the current fraction applied, differences of up to 100% in EDR being required to restore equal loudness. The multidimensional scaling experiment was found to be difficult and needs further refinement. In approximately half of the subjects a pitch dimension could be found. Timbre differences were present, but did not result in systematically different trajectories in perceptual space. References: [1] G. Donaldson, H. Kreft, L. Litvak, "Placepitch discrimination of single- versus dual-electrode stimuli by cochlear implant users", Jasa, Aug 05.

## 454 An Alternative Filterbank of Speech Processing in Cochlear Implants for Better Melody Recognition Bomjun Kwon<sup>1</sup>

<sup>1</sup>University of Utah

Cochlear implant (CI) users may perceive intermediate place-pitches between those elicited by the individual electrodes when two electrodes are stimulated simultaneously (Donaldson et al., J. Acoust. Soc. Am. 118:623-626, 2005). Similar results were obtained with sequential dual-electrode stimulation (Kwon and van den Honert, J. Acoust. Soc. Am. 120:EL1-EL6, 2006), where the discriminability of adjacent electrodes (the apical pair in the study), specified by cumulative d', was 7.3, on average, measured from 12 subjects. The result potentially presents a high performance of pitch discrimination, sufficient to judge the smallest musical interval (a ratio of 6% in frequency); yet CI users do not reliably recognize musical excerpts accurately, regardless of their speech recognition performance (Gfeller et al., Ear Hear. 26(3):237-250, 2005). One possible explanation is that, unlike dual-electrode stimulation examined in those pitch studies above, three or more electrodes (or channels) are stimulated even when a pure tone input is processed by current speech processing strategies, due to overlapping bands from wide filter skirts; thus making the discrimination of tones (and the identification of musical intervals) more difficult in real life. The present study proposes an alternative filterbank with less overlapping bands, where no more than two channels are stimulated from a pure tone input so that CI users could better perform a frequency discrimination task, possibly to the similar level reported in the above dual-electrode studies. A preliminary experiment reveals similar word recognition scores with an experimental MAP based on the alternative filterbank, to those with a CIS MAP. Further investigation would be necessary to examine melody recognition with the proposed filterbank, to validate the expected benefit.

### 455 Improving Frequency Discrimination in Cochlear Implant Users

**Ginger Stickney<sup>1,2</sup>**, Peter Nopp<sup>2</sup>, Andrea Nobbe<sup>2</sup>, Peter Schleich<sup>2</sup>, Clemens Zierhofer<sup>3</sup>

<sup>1</sup>Hearing Instrument Consultants, <sup>2</sup>MED-EL Corporation, <sup>3</sup>University of Innsbruck

Two methods for potentially improving frequency discrimination were investigated in MED-EL cochlear implant users. The first utilizes a temporal fine structure coding method in the low frequency bands, called Channel Specific Sampling Sequences (CSSS), where a series of pulse packets are modulated by temporal fine structure and combined with traditional envelope coding. The CSSS are applied to two most-apical electrodes in a frequency range up to 320 Hz. The resulting speech processing strategy is called Fine Structure Processing (FSP). Comparisons were made between FSP and Continuous Interleaved Sampling (CIS) at 150, 180, 200, and 250 Hz. Results showed that just noticeable differences were better with FSP than CIS for standard frequencies up to 200 Hz, indicating that low frequency temporal coding provided by FSP helps users detect smaller changes in the lower frequencies.

The second method investigated the use of virtual channels, where intermediate frequencies can be perceived by varying relative amplitudes of adjacent Comparisons were made between virtual electrodes. channels created by simultaneous stimulation of electrode pairs (parallel virtual channels) and by sequential stimulation (sequential virtual channels) for an electrode pair in the apex, middle, and base of the cochlea. Bellshaped filters were used in all conditions. Results showed slightly better discrimination with sequential than parallel virtual channels, however this was not statistically significant. Discrimination also varied greatly across subjects and electrode pairs. In sum, both methods could improve frequency discrimination beyond that found with traditional speech processing strategies. With further research it should be possible to identify the method best suited for each user, the listening conditions in which this type of coding proves most beneficial, and how these two methods might be combined for improving frequency resolution in both high and low frequencies.

### 456 Increased Spectral Resolution Enhances Listening Benefit in Cochlear Implant Users

**Dawn Burton Koch<sup>1</sup>**, Mary Joe Osberger<sup>1</sup>, Andrew Quick<sup>1</sup> \*\*Advanced Bionics Corporation

In 2003, Advanced Bionics released HiResolution® (HiRes®) Sound, a sound-processing algorithm that implemented more channels and higher rates of stimulation than previous-generation methods. The goal of HiRes Fidelity 120 is to build on the strengths of original HiRes by improving representation of the stimulus spectrum in the electrical stimulation pattern. HiRes Fidelity 120 first analyzes the incoming sound signal using a 256-bin Fast Fourier Transform. The algorithm then processes the temporal and spectral information in parallel. Temporal detail is extracted using a Hilbert

transform while a navigator determines the energy maximum for each electrode pair. The estimated frequencies of the spectral maxima are used to compute the rate of the pulse train and to continuously select the optimal locations for delivering stimulation. The 120 spectral bands are created by precisely varying the proportion of current delivered simultaneously to adjacent electrodes in each electrode pair using active current steering. For each electrode pair, eight real and "steered" bands are available, thereby creating at total of 120 separate spectral bands (15 electrode pairs x 8 spectral bands).

This multi-center clinical study documented the listening benefits of HiRes sound processing with Fidelity 120 in adult Bionic Ear users. Benefit with original HiRes was assessed at a baseline visit and compared with HiRes Fidelity 120 benefit after one and three months of use. Then subjects were refit with standard HiRes and tested again. Outcome measures included speech perception in quiet and noise, music and sound quality ratings, self-reported benefits, and a preference questionnaire. To date, results show that HiRes 120 is a viable sound-processing option that improves benefit appreciably for some CII and HiRes 90K recipients in a variety of listening environments. The reported benefits extend beyond speech perception, and encompass everyday sounds and music appreciation.

### 457 Mapping the Place and Rate Induced Pitches Across a Cochlear Implant Array

**Joshua Stohl**<sup>1</sup>, Chandra Throckmorton<sup>1</sup>, Leslie Collins<sup>1</sup> Duke University

There is evidence that while speech recognition by cochlear implant users is relatively good, speech recognition in noise and the ability to identify musical patterns is still poor (Gfellar et al., 2003). One possible strategy for improving speech recognition scores in noise and music appreciation is to use variable stimulation rates to convey more pitch information to implant users (Nie et al., 2005; Throckmorton et al., 2006). It has also been suggested (Throckmorton et al., 2006) that these strategies may be most effective when algorithms are tuned to each cochlear implant user. Specifically, if the rates that can be discriminated are known for each electrode, this information could be used to determine the best set of presentation rates in a multi-rate algorithm. A SPEAR3-based psychophysical environment has been developed by modifying an assembly language program provided by HearWorks Pty Ltd and constructing Visual Basic graphical user interfaces. In this study, data was collected from cochlear implant users with the SPEAR3 to determine the number of discriminable rates on electrodes at various locations on the cochlea. The series of JNDs was measured on five electrodes, including one apical, three middle and one basal electrode. A reference rate of 100 pulses per second (pps) was presented and an adaptive two-interval, forced-choice Levitt procedure was used to determine the next discriminable rate, or the justnoticeably-different (JND) rate. The resulting JND rate was then used as the reference rate in the subsequent experiment, and this procedure was repeated until the

reference rate was approximately 500 pps. Discriminable rates were then pitch ranked to provide an estimate of the pitch structure as a function of place and rate across the entire array.

#### 458 Developing a SPEAR3-Based **Experimental Psychophysics Environment**

Joshua Stohl<sup>1</sup>, M. Selin Kucukoglu<sup>1</sup>, Chandra Throckmorton<sup>1</sup>, Leslie Collins<sup>1</sup>

<sup>1</sup>Duke University

In the past, experimental interfaces for cochlear implants have been used to perform psychophysical experiments. adjust user MAPs, and have allowed researchers to make changes to available speech processing algorithms including filter parameters and update rate (e.g., Hirshorn, et al, 1986; Shannon, et al 1990). HearWorks Pty Ltd has recently released the SHARP/SPEAR Programming System (SPS) that may be used in the same manner as previous experimental interfaces but also allows researchers to access the digital signal processor and upload assembly language programs that support development of unique psychophysical experiments and the implementation of new sound processing algorithms. The SPS is capable of interfacing with a SPEAR3 (Sound Processor for Electrical and Acoustic Research, revision 3) sound processor and Nucleus Cl22 and Cl24 cochlear implants. In this work, a SPEAR3-based environment for implementing psychophysical experiments that uses an assembly language program modified from the version provided by HearWorks as well as a graphical interface developed in Visual Basic will be presented. Data taken in psychophysical tasks such as threshold, maximum comfortable loudness level, loudness balancing and rate discrimination will also be presented. The data are then compared with data reported in the cochlear implant literature to validate the use of the SPEAR3-based environment for continuing psychophysical experiments.

#### 459 Animal Research Committee Workshop: **New Perspectives on Distress in Laboratory** Animals

JoAnn McGee<sup>1</sup>

<sup>1</sup>Boys Town National Research Hospital

A principal function of the Animal Research Committee is to provide the membership at large with an opportunity to participate in the discussion of special interest topics related to the care and use of animals in biomedical research. One of the most important issues confronting the biomedical research community is the assessment, alleviation and prevention of pain and distress in laboratory animals. In addition to the desire and ethical responsibility of scientists to reduce pain and distress in research animals to a minimum, biomedical scientists must also comply with legislative regulations and policies concerning laboratory animals. Currently, efforts are underway to modify the guidelines pertaining to pain and distress in research animals, and the importance of sound, objective scientific input to the policy-making process cannot be overstated. This year, we are pleased that Dr. William J. Martin, an expert on the subject of pain and suffering and

a scientist who has played a prominent role in the development of regulations and guidelines relating to pain and distress in laboratory animals, has agreed to discuss present-day efforts in this area. Dr. Martin is the Senior Director in the Department of Pharmacology at Theravance Inc. and has studied the physiology and pharmacology of pain transmission and modulation for over fifteen years. Before joining Theravance, Dr. Martin led a team of scientists at the Merck Research Laboratories in an effort to develop novel analgesics. He currently serves as a member of the Animal Care and Experimentation Committee of the American Physiological Society for which he leads a working group on pain and distress.

#### 460 New Perspectives on Distress in **Laboratory Animals**

William Martin<sup>1</sup>

<sup>1</sup>Theravance, Inc.

The purpose of this presentation is to update the membership on potential changes to federal regulation or policies pertaining to the use of animals in research. Biomedical researchers who conduct studies involving animals carry unique obligations to the animals in their care, to the scientific community and to society at large. The NASA Principles for the Ethical Care and Use of Animals provide one framework within which these obligations can be considered. Specifically, the ethics of using animals in research require: (a) Respect for Life; (b) Societal Benefit, and; (c) Non-maleficence. According to the NASA Principles, "non-maleficence" entails that the minimization of distress, pain and suffering is a moral imperative. To guide biomedical researchers in this arena, the Institute for Laboratory Animal Research (ILAR) issued a report in 1992 entitled "Recognition and Alleviation of Pain and Distress in Laboratory Animals." In 2005, ILAR stated its intention to update and supplement its 1992 report in two separate reports, one on pain and the other on stress and distress. Similarly, this presentation will be in two parts. The first will discuss the definitions of stress and distress, including a review of the scientific understanding of causes and functions of stress and distress, with an emphasis on determining when stress becomes distress and how the latter can be prevented or managed. The second part of the presentation will discuss the physiology and pharmacology of pain within the context of laboratory animal care, including a review of current approaches to the management of pain as well as the challenges that some of these approaches present to the conscientious researcher and IACUC member.

#### 461 Intensity Dependence of Binaural Sensitivity in Field A1 of Hearing and Congenitally Deaf Cats

**Andrej Kral**<sup>1</sup>, Jochen Tillein<sup>1</sup>, Silvia Heid<sup>2</sup>, Rainer Hartmann<sup>2</sup>

<sup>1</sup>Laboratory of Auditory Neuroscience, <sup>2</sup>Institute of Sensory Physiology and Neurophysiology

Congenitally deaf white cats are a model of human congenital deafness. In their auditory system effects of

auditory deprivation on auditory functional properties can be studied. Numerous functional deficits in the auditory system of these animals have been demonstrated (Kral et al., Cereb Cortex 10: 714). These deficits were the consequence of an altered developmental sequence and additional degenerative processes (Kral et al, Cereb Cortex 15: 552). However, some features are at least rudimentary preserved. The present investigation was aimed at intensity dependence of sensitivity of cortical units to interaral time difference (ITD). Hearing controls were deafened at the beginning of the experiment. Both groups of animals were stimulated through cochlear implants in wide biopolar configuration. Mapping of the field A1 using microelectrode-recorded local field potentials with stimulation at the ipsilateral and contralateral ear was performed in anaesthetized animals using biphasic pulses (200µs/phase). Single and multiunits were recorded during binaural stimulation at different over-threshold intensities. For each unit, first thresholds to stimulation at ipsilateral and contralateral ears were determined with pulsatile stimulation. Sensitivity to interaural time difference in the range of -600 µs (ipsilateral ear leading) to 600 µs (ipsilateral ear lagging) was tested with single pulses and pulse trains (500 Hz, 3 pulses) at intensities of 0 – 10 dB over unit's threshold. Afterwards, at 2-6 dB over threshold, sensitivity to interaural level differences were tested with constant average binaural intensity at different interaural time differences (-400, -200, 0, 200, 400 µs). Time-intensity trading was evaluated. Hearing controls showed a large range of intensities (10 dB) where sensitivity for ITD was increasing, whereas in deaf animals highest sensitivity was also observed around threshold intensities. The results demonstrate that despite some rudimentary sensitivity for ITDs, field A1 of naive animals shows functional differences compared to controls.

Supported by Deutsche Forschungsgemeinschaft (KR 3370/1-1).

## 462 Cochlear Implantation Influences the Cochleotopic Organisation of the Primary Auditory Cortex in the Deafened Cat

James Fallon<sup>1,2</sup>, Dexter Irvine<sup>1</sup>, Anne Coco<sup>1</sup>, Lauren Donley<sup>1</sup>, Rodney Millard<sup>2</sup>, Robert Shepherd<sup>1,2</sup>

<sup>1</sup>The Bionic Ear Institute, <sup>2</sup>Department of Otolaryngology, The University of Melbourne

The cochleotopic organisation of the primary auditory cortex (AI) can be altered by changes in output from the cochlea. In the extreme case of congenitally- or neonatally-deafened animals, where there is no output from the cochlea, AI has a 'rudimentary' cochleotopic organisation. The effects of chronic intra-cochlear electrical stimulation (ES) on the cochleotopic organisation of AI in long-term deafened animals are not clear. Therefore, two months after neonatal deafening, four profoundly deaf cats were implanted with a multi-channel scala tympani electrode array and received unilateral ES (up to 200 days) to a restricted section of the basal turn from a Nucleus® CI24 cochlear implant and Nucleus® ESPrit 3G speech processor. An additional four animals

served as age-matched unstimulated deaf controls. Recordings from a total of 389 multi-unit clusters in Al were made using a combination of single tungsten and multi-channel silicon electrode arrays. Significant cochleotopic organisation of AI was observed in all but one of the chronically stimulated animals (Pearson correlation; all p < 0.01), while only one unstimulated control animal exhibited cochleotopic organisation (Pearson correlation; p < 0.01). Additionally, stimulation at 3 dB above minimum cortical threshold resulted in a significantly greater area of activation in the chronically stimulated animals than in the unstimulated controls (t-test; p = 0.04). These results indicate that chronic ES can result in i) a more defined cochleotopic organisation of AI than is present in the longterm deaf; and ii) an increase in the area of activation produced by supra-threshold stimuli. Maintenance or reestablishment of a cochleotopically organised Al by activation of a restricted sector of the cochlea may contribute to the improved clinical performance observed among subjects implanted at a young age.

Work funded by NIDCD (NO1-DC-3-1005) and The Bionic Ear Institute.

# | 463 | Measuring Psychometric Functions for Detection in Electric Hearing Infants and Toddlers Using the Observer-Based Psychoacoustic Procedure

**Vasant K. Dasika**<sup>1</sup>, Lynne A. Werner<sup>1</sup>, Kaibao Nie<sup>1</sup>, Susan J. Norton<sup>1,2</sup>, Jay T. Rubinstein<sup>1,2</sup>

<sup>1</sup>University of Washington, <sup>2</sup>Children's Hospital & Regional Medical Center, Seattle, WA

Few behavioral measures exist to test and optimize signal processing strategies in preverbal infants and toddlers who use cochlear implants. One goal of this work is to investigate approaches to better fit cochlear implants in young children. In this study, the observer-based psychoacoustic procedure (OPP) was used to measure both psychometric functions for detection and response latency functions in electric hearing infants, toddlers, and adults. Preliminary data have been collected from three electric hearing toddlers (ages 15, 25, and 26 months) and two postlingually deafened electric hearing adults. Stimuli were either current pulse trains delivered to one or a few of the electrodes in a subject's electrode array or acoustic free-field pure-tones. All subjects successfully met an 80% correct response criterion in detecting signals and correctly rejecting no-signals when clearly-detectable-signal trials and no-signal trials were randomly presented during training. In the subsequent testing phase, the amplitude of the signal was varied. Both toddlers and adults generally showed an increasing likelihood of detecting signals as a function of signal level. Moreover, the time that it took the observer to decide that a signal had been presented on the basis of the child's behavior, the response latency, generally decreased as a function of signal level. These observations are consistent with published findings from the auditory development literature. Our findings suggest that: 1) OPP holds promise in measuring the hearing capacity of infants and toddlers who use cochlear implants, and 2) the psychometric function measured via OPP will be sensitive enough to reflect changes due to

signal processing strategy modifications in this often difficult-to-assess population.

[Supported by NIH 5 T32 DC 000018 and 2 T32 DC000033-16, the estate of Verne Wilkins, and the National Organization for Hearing Research Foundation.]

## 464 Emergence of Localization Abilities in Children with Sequential Bilateral Cochlear Implants

**Tina M. Grieco**<sup>1</sup>, Shelly P. Godar<sup>1</sup>, Patti M. Johnstone<sup>2</sup>, Gongqiang Yu<sup>1</sup>, Ruth Y. Litovsky<sup>1</sup>

<sup>1</sup>Waisman Center, University of Wisconsin-Madison,

<sup>2</sup>University of Tennessee-Knoxville

Bilateral cochlear implants (CIs) are becoming more prevalent in children who are deaf. One of the motivating factors for this trend is the interest in providing these children with spatial hearing abilities. Our previous work has shown that localization acuity in a right/left discrimination task develops during the first two years following bilateral activation. The present study examined performance during that same two-year period on a more complex sound localization task involving a multiplesource speaker array spanning +/- 70°. Subjects (N=15), ranging in age from 5 to 14 years, were asked to locate sound sources that were either 10° apart (15-AFC) or 20° apart (7-AFC), depending on their age and right/left discrimination ability. Stimuli consisted of speech or pink noise at 60 dBA with or without +/- 4 dB roving. All subjects completed the task twice, first using their bilateral Cls and subsequently using only their first Cl, which allowed us to test the hypothesis that children localize better when using bilateral CIs versus their first CI. In addition, some children participated in the experiment at multiple time intervals post-bilateral activation to test the hypothesis that auditory experience plays an important role in the development of localization abilities. Our results show that despite large inter-subject variability in performance, the majority of children locate sound sources better in the bilateral condition compared with the first-CI condition. In addition, in subjects who participated in the experiment at multiple time intervals, localization acuity improved with longer bilateral CI experience. These findings suggest that localization with multiple sources is an important measure of the emergence of spatial hearing abilities in a new but growing population of children who are deaf. In addition, there may be important implications to the finding that localization is possible in a person whose auditory system was never acoustically activated.

## 465 Development and Validation of the University of Washington (UW) Music Test for Cochlear Implant Users

**Robert Kang**<sup>1</sup>, Grace Liu<sup>2</sup>, Ward Drennan<sup>1</sup>, Jeff Longnion<sup>1</sup>, Bevan Yueh<sup>1,3</sup>, Jay Rubinstein<sup>1,4</sup>

<sup>1</sup>University of Washington, <sup>2</sup>Columbia University College of Physicians and Surgeons, <sup>3</sup>VA Puget Sound Health Care System, <sup>4</sup>Virginia Merrill Bloedel Hearing Research Center Introduction: Assessment of cochlear implant outcomes centers around speech recognition. Despite improvements in speech recognition, music perception remains a

challenge. No standardized test exists to quantify music perception in a clinically practical manner. This study presents the UW Music Test as a reliable music perception test for implant users.

Methods: A test was developed to examine 3 specific aspects of music perception: pitch direction discrimination, melody recognition and timbre recognition. The pitch subtest utilized an adaptive procedure to determine just noticeable differences (JNDs) for complex tone pitch direction discrimination. The melody and timbre subtests assessed recognition of 12 common isochronous melodies and 8 musical instruments playing an identical 5-note sequence. Testing was repeated for each subject to evaluate test-retest reliability.

Results: Twenty-seven cochlear implant users were tested. Pitch direction discrimination JNDs ranged from 1 to 5.8 semitones (Mean=2.6, SD=1.6). Melody and timbre recognition ranged from 2.8% to 80.6% correct (Mean=21.9%, SD=17.7) and 20.8% to 70.8% (Mean 41.8%, SD=13.8), respectively. Pearson correlation coefficients with CNC word scores for pitch, melody and timbre were -0.66 (p<0.001), 0.39 (p<0.063) and 0.41 (p<0.052), respectively. As a measure of test-retest reliability, intraclass coefficients correlating scores between each subject's test instances for pitch, melody and timbre were 0.85, 0.86 and 0.63, respectively.

Conclusions: The UW Music Test discriminates a wide range of music perceptual ability. Subjects performed best on pitch direction discrimination, but were least accurate on melody recognition. Moderate correlations were seen between CNC word scores and music test results. Testretest reliability was moderate to strong. The UW Music Test provides a reliable metric for a standardized evaluation of music perception in cochlear implantees.

Acknowledgments: NIDCD, NOHR, Cochlear Corp.

## 466 Speech Recognition as a Function of the Number of Channels in the Hybrid Cochlear Implant: Quiet and Background Noise

**Lina Reiss**<sup>1</sup>, Christopher Turner<sup>1</sup>, Sheryl Erenberg<sup>1</sup>, Jessica Taylor<sup>1</sup>, Bruce Gantz<sup>1</sup>

<sup>1</sup>University of Iowa

The Hybrid (short-electrode) cochlear implant is designed to provide high-frequency information while preserving residual low-frequency acoustic hearing. Long-term speech recognition scores in Hybrid patients are comparable to those of traditional long-electrode patients, ranging as high as 70-75% (vowel-consonant-vowel) with the implant alone, despite the use of fewer electrodes (5 or 6) and a shorter segment in the cochlea (10 mm). Would increasing the number of channels along this 10 mm implant improve performance?

We investigated speech recognition in quiet and background noise as a function of number of channels (electrodes) for 6 Hybrid subjects. Subjects were tested using the implant only (direct electric stimulation) with a speech processor providing 6, 3, 2, and 1 channels. Three subjects were also tested with 5 and 4 channels. In quiet, the 3 best subjects showed no significant improvements

beyond 4 channels; the rest used <4 channels. The 3 best subjects were also tested in steady background noise (0, +5 dB SNR), and showed slight improvements with 5 or 6 channels over 4. These results are similar to previous studies of channel use in long-electrode subjects who plateaued at 4 electrodes spaced 2-3 times farther apart in quiet (Shannon et al., 1995) but used more electrodes in noise (Fu et al., 1998; Friesen et al., 2001). This implies that electrode interactions may not be the limiting factor for channel benefit, at least in quiet.

Normal hearing subjects were also tested using simulations of the Hybrid implant. In quiet and in noise, subjects performed similarly to the best Hybrid subjects, suggesting that the best Hybrid patients maximize use of the channels available. Overall, these results suggest that increasing the number of electrodes in the Hybrid implant will not improve speech recognition in quiet, but may improve recognition in noise.

Funding for this research was provided by NIDCD grants RO1DC000377 and 2P50 DC00242 and GCRC/NCRR grant RR00059.

#### 467 Channel Interactions in Cochlear Implants

**Qing Tang**<sup>1</sup>, Raul Benitez<sup>2</sup>, Fan-Gang Zeng<sup>1</sup>

<sup>1</sup>University of california, Irvine, <sup>2</sup>Technical University of Catalonia

Multichannel cochlear implants have been successfully but seem to reach a performance plateau possibly due to channel interaction. Better understanding of channel interactions can potentially increase the number of independent electrodes and improve cochlear implant performance. Here we examined the effects of channel interaction at the physical, neural, and behavioral level in five Clarion cochlear implant users. Electric field imaging (EFI) revealed similar intracochlear electric field patterns among all subjects, with its width being wider and its slope being shallower at apex than at base. Evoked compound action potentials (ECAP) and behavioral threshold detection data showed much greater individual variability than the EFI data, reflecting possibly different degrees and patterns of nerve survival among these implant subjects. The present results suggested that perceptual changes in threshold were related to the summation of electric fields in the cochlea, whereas the neural masking functions were strongly determined by the individual nerve survival distribution among subjects. Our findings complemented many of the results obtained by previous studies, motivating the future work on exploring channel interaction using non-simultaneous stimulation.

## 468 Auditory Stream Segregation Using Temporal Periodicity Cues in Cochlear Implants

Robert Hong<sup>1</sup>, Christopher Turner<sup>1</sup>

<sup>1</sup>University of Iowa

Auditory stream segregation involves the ability of a listener to perceptually segregate two rapidly alternating

sounds into different perceptual streams. By studying auditory streaming in cochlear implants (CI), we can obtain a better understanding of the cues that CI recipients can use to segregate different sounds, which may have relevance to such everyday activities as the understanding of speech in background noise. In this study, we focus on the ability of CI users to use temporal periodicity cues to perform auditory stream segregation. A novel rhythmic discrimination task involving sequences of alternating amplitude-modulated (AM) noises is used to assess this ability. Preliminary results suggest that most CI users can stream AM noise bursts at relatively low AM center frequencies (near 80 Hz AM), but that this ability diminishes at higher AM center frequencies. Additionally, the ability of CI users to perform streaming using temporal periodicity cues appears to be comparable to that of normal-hearing listeners. These early results imply that CI subjects may in certain contexts (i.e. when one of the talkers has a relatively low fundamental frequency) be able to use temporal periodicity cues to segregate and thus understand the voices of competing talkers. These results thus provide theoretical support for how signal-processing strategies with rates of stimulation able to encode fundamental frequencies may lead to the better speech perception in competing talker backgrounds.

Funding for this research was provided in part by research grants RO1DC000377, 2P50 DC00242, and 5T32 DC000040-13 from National Institutes on Deafness and Other Communicative Disorders, National Institutes of Health.

## 469 Discrimination of Schroeder-Phase Harmonic Complexes by Cochlear Implant Users

**Jeff Longnion**<sup>1</sup>, Chad Ruffin<sup>1</sup>, Ward Drennan<sup>1</sup>, Jay Rubinstein<sup>1</sup>

<sup>1</sup>University of Washington

Temporal fine-structure contributes significantly to the perception of music and speech in noise [Smith et al. 2002, Kong et al. 2005]. Thus, improved delivery of finestructure in cochlear implantees could improve their ability to discriminate these difficult stimuli. Successful evaluation of the ability of new stimulation strategies to deliver finestructure relies upon tests that can demonstrate sensitivity to fine structure. Toward this goal, we have evaluated the ability of listeners to discriminate positive and negative Schroeder-phase harmonic complexes (SPHCs), a timereversed pair of harmonic complexes with identical longterm spectra and minimal envelope modulation. The ability of 22 cochlear implant (CI) users and 7 normal-hearing (NH) listeners to discriminate positive and negative SPHCs was evaluated using a 4-interval, 2AFC paradigm at four fundamental frequencies: 50, 100, 200 and 400Hz. Results in NH listeners showed average percent correct scores of 97, 97, 96, and 66% at each respective frequency, consistent with results reported by Dooling et al. [2002]. CI users, however, had significantly lower average scores of 86, 82, 68 and 59% (p < 0.05). The 18 CI users who repeated the test did not show a significant learning effect at any fundamental frequency, suggesting

good test, retest reliability. Correlation analyses revealed that the 200Hz score was significantly correlated (p < 0.05) with CNC words (R=0.52), SRT in babble and noise (R=0.49), avg. pitch difference limen (DL) (R=0.46), and timbre recognition (R=0.47). Avg. SPHC score was correlated with CNC (R=0.64), avg. pitch DL (R=-.47) and timbre (R=0.49). Furthermore, single channel tests in one listener revealed better performance with analog than with pulsatile stimulation. The results merit further study of the utility of SPHC discrimination as a measure of phasesensitivity. Work supported by NIH grants T32-GM07266 and R01-DC007525.

## 470 Effects of High-Rate Pulse Trains on Modulation Detection in Cochlear Implant Users

**Christina Runge-Samuelson**<sup>1</sup>, Jamie Jensen<sup>1</sup>, P. Ashley Wackym<sup>1</sup>

<sup>1</sup>Medical College of Wisconsin

STUDY AIM: Psychophysical modulation detection thresholds (MDTs) have shown correlations with phoneme recognition scores in cochlear implant users. Random electrical stimulation paradigms designed to increase neural noise have been shown to improve MDTs and vowel discrimination, as well as vowel encoding in auditory nerve fibers. High-rate constant-amplitude electrical pulse trains have been found to elicit stochastic response behaviors apparent in auditory nerve and psychophysical threshold measures. The study aim was to investigate the effects of constant-amplitude high-rate pulse trains on MDT. HYPOTHESIS: High-rate pulse trains will improve cochlear implant users' sensitivity to modulations (i.e., decrease MDT). METHODS: Subjects were users of the Advanced Bionics Clarion CII or HiRes 90K cochlear implant. MDT was measured by adaptively modulating "low-rate" 1000 Hz (75 μs/phase) pulses to various depths of 100 Hz sinusoid using a three-down, one-up, 3-AFC procedure. MDTs were measured with and without 5000 Hz pulses on adjacent electrodes. RESULTS: The presence of high-rate pulse trains decreased MDT by ≥ 4 dB on at least one electrode for 5 of 6 subjects, and MDT decreases of up to 14 dB were observed. In addition, nonmonotonic effects across high-rate pulse level were evident, consistent with stochastic resonance.

Sponsored by the NIH/NIDCD R03 DC006361-01 and intramural funds from the Department of Otolaryngology and Communication Sciences, Medical College of Wisconsin

# 471 Cochlear Implant Gap-Detection Thresholds in Primary Auditory Cortex Depend on Pulse Rate and Lead Burst Duration

Alana E. Kirby<sup>1</sup>, John C. Middlebrooks<sup>1</sup>

<sup>1</sup>University of Michigan

Although adaptation at the inner hair cell synapse almost certainly plays a role in acoustic forward masking, the observation of forward masking in cochlear-implant users who lack hair cells indicates an additional central processing component. We examined a related measure, gap detection threshold, for acoustic noise-burst and electrical pulse-train stimuli in the guinea pig primary auditory cortex. We measured neural multi-unit responses while varying lead burst durations (10-600 ms) and electric pulse rates (254-4096 pps). When lead bursts were short (10-50 ms), gap thresholds were substantially longer that those measured psychophysically, perhaps due to anaesthesia-induced potentiation of intra-cortical inhibition. Consistent with that explanation, gap thresholds varied across cortical laminae in short-lead conditions. When lead bursts were long (?100 ms), thresholds were similar in magnitude to published psychophysical data. In long-lead conditions, gap thresholds varied little across cortical lamina, indicating that gap detection thresholds reflect subcortical processing. Gap thresholds were roughly equal for acoustic and 254 pps electrical stimulation. Electric thresholds showed a striking decrease, by as much as a factor of eight, with increasing pulse rate. The present results support the hypothesis that central processing plays a major role in gap detection. Moreover, the observation that gap thresholds shorten with increasing pulse rate has important implications for design of speech processors.

Supported by R01 DC04312

### 472 Optimizing Electric Stimulation to Suppress Tinnitus

**Fan-Gang Zeng**<sup>1</sup>, Qing Tang<sup>1</sup>, Jeff Carroll<sup>1</sup>, Andrew Dimitrijevic<sup>1</sup>, Arnold Starr<sup>1</sup>, Leonid Litvak<sup>2</sup>, Jannine Larky<sup>3</sup>, Nikolas Blevins<sup>3</sup>

<sup>1</sup>Unversity of California Irvine, <sup>2</sup>Advanced Bionics Corporation, <sup>3</sup>Stanford University

Here we reported psychophysical, electrophysiological, and clinical results from a unique subject, CINH001, who received a Clarion HiRes90k cochlear implant to control debilitating tinnitus in his right ear. CINH001 had essentially normal hearing in his left ear, so that he could match both tinnitus and electric stimulation in the right ear to acoustic stimulation in the left ear. CINH001 matched his tinnitus to an acoustic stimulus of 4000-8000 Hz and at 70-90 dB SPL. The effect of electric stimulation on tinnitus was evaluated as a function of pulse rate from 25 to 5000 Hz, pulse duration from 10 to 500 uS per phase, electrode position from apex to base, and stimulation configuration from monopolar to bipolar mode. Different from previous studies showing a suppressive effect of high-rate stimulation on tinnitus, only stimuli with low rates (40-100 Hz), short pulse duration, the most apical electrode, and monopolar mode could suppress his tinnitus. Objective measures in both spontaneous and event-related evoked potentials also showed a difference related to the presence and absence of tinnitus. An innovative acoustic waveform employing a Gaussian-enveloped sinusoid and optimized programming of electric parameters allowed CINH001 to use his behind-the-ear processor to suppress tinnitus effectively at home. These results underscore the need to customize electric stimulation for tinnitus suppression and suggest that complementary stimulation,

rather than masking, is the brain mechanism underlying the present surprising finding.

(Supported by NIH RO1 DC002267)

## 473 Audiometric Results From the Otologics Fully Implantable Hearing Device Phase I Clinical Trial

**Virginia Lupo**<sup>1</sup>, James Kasic<sup>2</sup>, Alan Franklin<sup>2</sup>, Herman Jenkins<sup>1</sup>

<sup>1</sup>University of Colorado Health Sciences Center,

<sup>2</sup>Otologics, LLC

Audiometric results of the Otologics Fully-Implantable Hearing Device were assessed in 20 adult patients with bilateral moderate to severe sensorineural hearing loss, Subjects were required to have a pure tone average of 40 – 80 dB in the ear to be implanted, and unaided NU-6 scores greater than 40% at 80 dB HL or 40 dB SL in the ear of implantation. Other selection factors included post lingual onset and a stable, non fluctuating hearing loss. Subjects all had normal middle ear anatomy and had used appropriately fitted hearing instruments for at least 3 months. The transducer was attach to the body of the incus via insertion into a laser drilled hole and provided direct mechanical stimulation of the middle ear ossicles.

A repeated-measures within-subjects design assessed aided sound field thresholds, speech performances and subjective patient benefit scales (APHAB, device usage, and implant vs. aid usability) with the subject's own, appropriately fitted, walk-in hearing aid(s) and the fully-implantable prosthesis.

Results demonstrated 10 to 20 dB of functional gain across audiometric frequencies at two and three months post implantation and increased by 5 to 10 dB at six months with improved fitting algorithms. Pure tone averages and monaural word recognition scores were slightly better for the walk-in-aided condition at two and three months post implantation (p < 0.05) but were similar at six months post implantation. Mean APHAB scores indicate that patients overall perceived better benefit from the implant device when compared to their own aid, with the exception of aversiveness to sound, where their own aid was perceived slightly better. The patient's subjective evaluations indicated that the implant was exceptional in expected areas, such as visibility to others and occlusion and performed at least as well as their aid in all other measures.

Although monaural word scores and aided thresholds favored the walk-in-aided condition, preliminary results of the Otologics MET Fully-Implantable Hearing Device Phase I trial provide evidence that this fully implantable device may be a desirable alternative to currently available hearing aids in patients with sensorineural hearing loss.

### 474 Ion Transport in the Stria Vascularis: Modeling and Experiment

Robert M. Raphael<sup>1</sup>

<sup>1</sup>Rice University

Many types of genetic deafness are due to mutations in ion channel and transporters expressed in the stria vascularis that maintain the endocochlear potential and

endolymphatic potassium concentration. These recent genetic advances are consistent with the emerging view that disorders of ion homeostasis are the final common pathway in a variety of inner ear diseases, including Meniere's disease. Presently, the precise nature of the contributions of individual ion channels and transporters to ion homeostasis and transport in the stria are poorly understood. However, electrophysiologists have recently made progress characterizing the ion conductances and transporters expressed in the different specialized cells of the stria. Additionally, more accurate electron microscopic images of the stria have been obtained and a mathematical model of ion transport in the stria has been constructed. A particular challenge in understanding strial function is the small volume and inaccessibility of strial fluids, especially the intrastrial space, which may be met with new technological advances in electrical recording techniques. This symposium aims to bring together anatomical. electrophysiological and computational modeling approaches to studying ion transport in the stria. The goal will be to exchange ideas and increase our appreciation of the normal function of the stria in the hopes of deepening our understanding of various clinical manifestations of hearing loss and deafness associated with disorders of ion homeostasis.

#### 475 Inner Ear K+ Recycling Pathways Bradley Schulte<sup>1</sup>

<sup>1</sup>Medical University of South Carolina

Mechanoelectrical transduction by sensory hair cells (HCs) is dependent on the development of a large transcellular K<sup>+</sup> gradient. Generation of the endocochlear potential by the stria vascularis also depends on maintaining a substantial K<sup>+</sup> gradient between intermediate cells and the intrastrial space. The formation of inner ear K<sup>+</sup> gradients is a complex process requiring the cooperation of numerous ion channels, pumps and exchangers in multiple cell types. Alterations in any of these ion transport mediators can disrupt K<sup>+</sup> homeostasis and lead to hearing and balance disorders. It is now generally accepted that K<sup>+</sup> leaked or effluxed through HCs into perilymph, is recycled back to endolymph via multiple pathways. The main objective of the lateral recycling pathway in the cochlea, is to deliver K<sup>+</sup> into the intrastrial space for return to endolymph by marginal cell Na.K-ATPase activity. This involves the movement of K<sup>+</sup> through a syncytial network composed of four types of lateral wall fibrocytes and strial basal and intermediate cells, all of which are connected by gap iunctions. Three of these fibrocyte populations are enriched in Na,K-ATPase and strategically situated to resorb K<sup>+</sup> from perilymph in the scala tympani (type IV), the scala vestibuli (type V) and the spiral ligament near the outer sulcus (type II). Each of these cell types is coupled to type I fibrocytes which serve as the final common pathway for moving the resorbed K<sup>+</sup> into the stria vascularis. The K<sup>+</sup> effluxed from outer sulcus cells is thought to be derived from perilymph surrounding outer HCs, where it is taken up by Deiters and tectal cells and transported intracellularly through a second gap junctionally-coupled network of epithelial supporting cells in the organ of Corti. This process would prevent K<sup>+</sup> build

up in the fluid surrounding outer HCs, where it could compromise repolarization and become cytotoxic. A similar system is thought to recycle  $K^{+}$  effluxed from inner HCs medially through inner sulcus cells and limbal fibrocytes for return to endolymph by interdental cells. Elucidation of the specific cellular and molecular alterations underlying disturbances in inner ear  $K^{+}$  homeostasis offers the prospect of greatly enhancing the diagnosis and treatment of certain hearing and balance disorders.

#### 476 Expression of Proteins Contributing to Strial Function

#### Michael Anne Gratton<sup>1</sup>

<sup>1</sup>University of Pennsylvania

The presence of a strongly positive endocochlear potential in scala media is crucial to hair cell transduction. This potential is due to isolation of intrastrial space by tight junctions of marginal and basal cells at the apical and basal surfaces of the stria vascularis respectively, high potassium throughput across the intermediate cell membrane, and extremely high potassium concentration in the intrastrial space with active secretion of potassium from marginal cells into endolymph. The active secretion of potassium relies on energy sources supplied by strial vasculature. The use of animal models in conjunction with immunohistochemistry and immunoelectron microscopy is developed to understand how dysregulation of ion flux across marginal and intermediate cell membranes impacts auditory function.

#### 477 The Composition of K+ Channels in the Strial Vascularis.

#### Ebenezer N. Yamoah<sup>1</sup>

<sup>1</sup>University of California, Davis

The endocochlear potential (EP), ~80 mV, is an upshot of the intricate K<sup>+</sup> regulation in the cochlear duct that augments the sensitivity of transduction of auditory signals. Yet, the detailed molecular mechanism for the generation of the EP is unclear. Among the unknowns are the candidate K<sup>+</sup> channels that establish the high throughput of K<sup>+</sup> in the intermediate and basal cells of the strial vascularis. We predict that a plethora of K<sup>+</sup> channels are assembled to establish the high throughput of K<sup>+</sup> ions across cells in the strial vascularis. Using tissue-specific libraries, we have cloned the genes encoding specific outward and inward rectifier K+ channels. Functional expression of the channels suggests that there is an orchestra of K<sup>+</sup> channels that operate closely together to establish and maintain the EP. We propose that while the inward rectifiers may stabilize the membrane potential of cells in the strial vascularis, outward rectifiers may promote K+ flux to confer EP. Because these channels function in multicomponent systems, it is difficult to determine several things: first, the precise contribution of each channel to the EP in vivo or 2) the compensatory mechanisms that occur in response to perturbations in the activity of a given channel. We are developing and

analyzing functional knockout and cell-specific gene knockout mouse models for a number of these channels. This approach will provide novel insights concerning  $K^{\dagger}$  channels functions and their physiological processes, which would be difficult to obtain by other means. We will discuss the advances we have made in these studies.

This work was supported by grants to ENY (NIDCD).

#### 478 A Mathematical Model of Ion Transport in the Stria Vascularis

Imran Quraishi<sup>1</sup>, Robert M. Raphael<sup>1</sup>

<sup>1</sup>Rice University

The stria vascularis contains a complicated network of transport proteins that operate synergistically to establish the endocochlear potential and transport potassium into the endolymph. We have constructed a computational model of ion transport in the stria vascularis based on available experimental data. We first consider an isolated layer of marginal cells and find that they do not make a significant direct contribution to the endocochlear potential but are capable of sustaining considerable potassium flux into the endolymph. Next, we expand the model and show that the inclusion of the channels and transporters expressed in the intermediate and basal cells is sufficient to generate the endocochlear potential. A particularly interesting prediction is the sensitivity of strial function to the potassium concentration in the intrastrial space. The model is useful for determining the dependence of the system on the properties and expression levels of different ion transporters and channels, which can be used to predict the effects of genetic mutations and drug interactions. For example, we examine the mechanisms of loop diuretic ototoxicity and genetic deafness due to potassium and chloride transport deficiencies, such as Jervell and Lange-Nielsen syndrome and Bartter's syndrome, type IV. Such simulations demonstrate the utility of compartmental modeling to investigate the role of ion homeostasis in inner ear physiology and pathology.

### 479 Contributions by Extra-Strial Epithelial Cells to Endolymph Homeostasis

Daniel Marcus<sup>1</sup>

<sup>1</sup>Kansas State University

Although this symposium focuses on function of the stria vascularis. other epithelial cells bordering endolymphatic space actively contribute to regulation of the levels of potassium, sodium, chloride and calcium in endolymph. Sodium and potassium transport and cell signaling mechanisms in Reissner's membrane and outer sulcus cells will be reviewed. Recent findings on calcium absorptive mechanisms and chloride secretory mechanisms will also be described in (homologous) vestibular epithelia (vestibular transitional semicircular canal). The study of ion transport processes and their regulation in the inner ear require special methods and experimental strategies. Transport has been studied at the whole organ, epithelial domain, cellular and single-membrane levels with electrophysiologic and molecular biologic techniques. Several of the most powerful techniques and experimental strategies used will be summarized within the context of the cell physiology. Transport by extra-strial cells contributes importantly to endolymph homeostasis and thereby to hearing and balance.

Supported by NIH grants R01-DC000212 and P20-RR017686.

#### 480 Profiling Electrochemical Microdomains in Extracellular Space

Peter Smith<sup>1</sup>, Robert Raphael<sup>2</sup>

<sup>1</sup>MBL, <sup>2</sup>Rice University

The importance of chemical profiles in the extracellular space is clearly understood by those in hearing research. It is, however, less well appreciated by biologists in general where functional considerations frequently stop at the plasma membrane. Inevitably though the spatial tortuosity inherent to extracellular compartments, their confined diffusional space, and complex chemical composition, make for interesting questions on how these factors feedback on cell function. Such feedback is clearly relevant in the auditory system, as with regulation of K<sup>+</sup> in the lateral wall of the cochlear duct, and [H<sup>+</sup>]<sub>o</sub> has been proposed to play a role in visual off-center on-surround. The problem, however, is how to make measurements in these extracellular spaces without disturbing the very actions one is trying to study. This is not a simple matter to solve and indeed there is no one solution. presentation brings together a number of approaches, some traditional, some more recent and others speculative, which address the problem of chemically sampling extracellular microdomains. Broadly, techniques available fall into the classes of optical and electrochemical.

Optical sensing based on fluorescent reporters is well established in their free form. Protein reporters, both fluorescent and luminescent, are of more interest for their ability to be specifically targeted to cellular regions – luciferase (ATP) and the pH sensitive Green Fluorescent Proteins are examples. Encapsulated nanoparticles with fluorescent, chemically selective properties are an exciting new development not yet applied to this field.

Electrochemical detection systems are showing a renaissance in the field of microdomain analysis. Capillary electrophoresis in the micron dimension, coupled to microfabricated samplers and electrode arrays, are challenging but rewarding. New approaches to enhance signal to noise detection, along with millisecond response times, has brought back conventional potentiometric and amperometric sensors as powerful tools, with the promise of more from innovative applications of activated nanotube arrays.

# 481 The Generation of the Endocochlear Potential – A Perfect Collaboration Within Stria Vascularis and Spiral Ligament Philine Wangemann<sup>1</sup>

<sup>1</sup>Kansas State University

The exquisite sensitivity of the cochlea, which mediates the transduction of sound waves into nerve impulses,

depends on the endocochlear potential. Recent advances have led to a detailed understanding of the mechanisms involved in K<sup>+</sup> secretion and the generation of the endocochlear potential. The endocochlear potential is essentially a K<sup>+</sup> equilibrium potential that is generated by the K<sup>+</sup> channel Kcnj10 (Kir 4.1) in conjunction with a very low K<sup>+</sup> concentration in the intrastrial fluid and a high K<sup>+</sup> concentration in the cytosol of intermediate cells. Consequently, the endocochlear potential is sensitive to conditions that affect the K<sup>+</sup> concentrations on either side of the K<sup>+</sup> channel or the K<sup>+</sup> channel itself. Pharmacological evidence and data obtained in a broad variety of transgenic mice has contributed to our understanding of the mechanisms involved in K<sup>+</sup> secretion and generation of the endocochlear potential. Supported by NIH-R01-DC01098.

## 482 A Mouse Model for the Cortical Processing of Natural Communication Sounds

Robert Liu<sup>1,2</sup>

<sup>1</sup>Emory University, <sup>2</sup>Center for Behavioral Neuroscience One of the ultimate goals of auditory systems research is to understand how the auditory cortex learns to process socially-acquired communication sounds to functions such as detection, discrimination categorization. The mouse presents an exciting opportunity to investigate this by combining behavioral, electrophysiological and computational methods. In this talk, I describe a comprehensive approach that utilizes well-characterized mouse vocalizations to study how auditory cortical neurons convey information for vocalization detection and discrimination. In particular, the contrast between pup call coding in mothers and pupnaïve females reveals how the communicative significance of a vocalization type is correlated with its cortical representation. As research into mouse models of hearing expand, this neuroethological paradigm adds a new dimension for the dissection of mechanisms underlying communication sound processing.

This work is supported by NIH DC08343, and the Center for Behavioral Neuroscience (NSF IBN-9876754).

#### 483 Cues for Call Recognition by Cortical Neurons

Jagmeet Kanwal<sup>1</sup>

<sup>1</sup>Georgetown University

Mustached bats, Pteronotus parnellii, employ a complex repertoire of calls for social interactions among conspecifics. We are using multiple approaches to understand the neural coding and representation of communication signals within the auditory cortex of mustached bats. Behavioral studies show that the usage and meaning of different call types follows Morton's Motivation-Structure hypothesis. According different hypothesis, acoustic features convey motivationally distinct signals. For example, harsh, broadband calls signal aggression and tonal sounds with relatively shallow frequency modulated patterns signal affiliative interaction. Tuning to acoustic features,

therefore, may serve the purpose of both call discrimination and perception of their emotional content or significance. Our electrophysiological motivational recordings from different regions of the auditory cortex (AC) suggest that different cortical neurons may be tuned to one or more acoustic features that allow them to discriminate between different call types and their variants. Neural activity distributed across different cortical areas and determined by complex acoustic features may constitute the functional unit for mapping a call type within the cortex of mustached bats. Neural activity indicating consensus among a distributed set of neurons may underlie recognition of call type or the mood (emotional/motivational status) of the emitter. elaborate this hypothesis and present neurophysiological data on responses of cortical neurons to basic acoustic patterns, call features and whole calls in awake mustached bats.

### 484 Neural and Behavioral Correlates of Functionally Meaningful Auditory Categories Yale Cohen<sup>1</sup>

<sup>1</sup>Dartmouth College

A ubiquitous feature of abstract categorization systems is that they ignore psychophysically distinctive functionally meaningless variation. The variation that is ignored, though, is dependent on the level of categorization. For example, at one level of categorization, the unique facial features that identity a person are ignored when the sex of a person is determined. At a different level, however, the variation between the sexes is ignored when the individual is categorized as a human or nonhuman. While analogous categorical processing levels are also observed in language and non-human vocalizations. we have relatively little understanding of the neural circuitry subserving this type of acoustic categorization, especially when it involves the categorization of vocalizations at different semantic levels. In this talk, we are going to discuss how rhesus monkeys "spontaneously" categorize vocalizations based on the referential information and discuss the role of the ventrolateral prefrontal cortex as part of a circuit involved in this categorization process.

## 485 Neural Correlates of Vocal Behavior in Marmosets Xiaoqin Wang<sup>1</sup>

<sup>1</sup>Johns Hopkins University

The common marmosets exhibit a wide range of vocalizations and remain highly vocal in captivity. The rich vocal behavior of this non-human primate species makes it an ideal model to study neural basis of vocal communication. Our quantitative analyses show that marmoset vocalizations contain exquisite information on call type and caller identity and the highly structured vocalizations emerge from postnatal development. Using functional neuroanatomy and neurophysiological recording techniques, we have studied cortical regions in both temporal and frontal lobes that are activated when marmosets listen to vocalizations or engage in vocal

exchanges with conspecifics. Our experiments show that cortical responses to vocalizations are shaped by the statistics of acoustic structures of vocalizations and modulated by vocal control signals, indicating the role of auditory-vocal interactions in cortical processing of vocalizations. These studies point to the importance of studying vocal processing in proper behavioral context and pave the way to understand the neural circuitry underlying primate vocal behavior.

### 486 Modulation Information in Human Speech Perception

David Poeppel<sup>1</sup>

<sup>1</sup>University of Maryland College Park

The mechanisms underlying the analysis of speech dynamics in human auditory cortex remain largely unknown. One possibility is that information on specific time scales is preferentially extracted. Human speech contains rich dynamics in the amplitude and frequency domains - both of which contribute to comprehension – and one hypothesis is that specific time scales (modulation frequencies commensurate with processing syllabic versus segmental representations) are privileged with respect to their contribution to comprehension.

Psychophysics has shown that modulation frequencies below 16 Hz play a crucial role for intelligibility. Based on psychophysical, MEG, and fMRI data, we support and extend these observations. In particular, our work argues for a multi-time resolution model of speech perception: Low-modulation frequencies characteristic of syllabic-rate processing are complemented by information at higher modulation rates typical of segmental modulation.

Intelligibility data suggest that both low and high modulation frequencies contribute to successful perception, specifically that modulation frequencies from 25-40 Hz contribute significantly, contrary to the conjecture that modulations below 16 Hz suffice. The central role of low modulation frequencies remains: MEG data show that the phase pattern of theta band (~4-8 Hz) responses recorded from human auditory cortex reliably tracks and discriminates spoken sentences. and that discrimination ability is correlated with speech intelligibility. fMRI recordings suggest that there may be cortical specializations and some degree of lateralization at these modulation rates. Cumulatively, our data are consistent with the view that there are (at least) two concurrently processed time scales critical to the analysis of speech: temporal integration at the segmental scale with ~20-50 ms temporal windows and at the syllabic scale with ~150-300 ms windows.

#### 487 Noise Resistance Mapped to Four Loci in 129S6 Mice

B.L Tempel<sup>1,2</sup>, K.W. Broman<sup>3</sup>, V.A. Street<sup>1,2</sup>, J.C. Kallman<sup>2</sup>, D.J. Shilling<sup>2</sup>, M.C. Liberman<sup>4,5</sup>, S.G. Kujawa<sup>4,6</sup> <sup>1</sup>Dept. of Otolaryngology-HNS, University of Washington, Seattle, <sup>2</sup>The V.M. Bloedel Hearing Research Center, University of Washington, Seattle, 3Dept of Biostatistics, Johns Hopkins University, Baltimore MD, <sup>4</sup>Eaton-Peabody Laboratory and, <sup>5</sup>Department of Otology and Laryngology, Harvard Medical School, Boston, <sup>6</sup>Department of Audiology, Massachusetts Eye and Ear Infirmary, Boston Toward understanding the biological basis of noise resistance and eventual formulation of therapies to prevent noise-induced hearing loss (NIHL), the identification of specific genes contributing to noise resistance is a critical step. To simplify this search across the whole genome, we chose to study isogenic, inbred strains of mice. Both physiological and anatomical work suggests that 129S6 (129S6/SvEvTac) mice are highly resistant to noise exposure and that this resistance is intensity independent (Yoshida et al., 2000; Kujawa et al., ARO 2007). When exposed to noise (octave band 8-16kHz, 103 dB SPL, two hours) the good hearing CBA/CaJ (CBA) strain showed ~50 dB threshold shift measured 2 weeks post-exposure; in contrast 129S6 mice showed ~10 dB shift. Through directed breeding schemes we showed that the noise resistance trait in 129S6 is recessive to CBA. Screening N2 backcross animals for noise resistance suggested a multigenic pattern of inheritance with 3 to 5 genes contributing. Quantitative Trait Locus (QTL) mapping in 234 N2 animals at 15 to 20 centiMorgan (cM) resolution reveals four chromosomal regions - on Chrs. 4, 11, 14 and 17 - that contribute significantly to the resistance. In this cross, the maximum LOD score was 6.0 detected at 12 kHz on Chr 17. Reanalysis at 5 cM resolution refines the QTL regions on Chrs. 4 and 17. Congenic and consomic strains carrying only one of these QTL regions are being isolated, with the expectation that these strains will show partial noise resistance. An integrative multi-step genomic approach, including gene expression microarray studies, quantitative PCR analysis, ancestral single nucleotide polymorphism analysis and gene sequencing, is being used to identify candidate genes in the QTL regions (Shilling et al., ARO 2007). Functional complementation of the noise resistant phenotype will be required to provide the final identification of specific noise reisistance genes. Research Supported by grants from NIDCD.

# 488 Nuclear Modifier Gene for the Phenotypic Expression of the Deafness-Associated Mitochondrial 12S Rrna Mutations

Min-Xin Guan<sup>1,2</sup>

<sup>1</sup>Cincinnati Children's Hospital Medical Center, <sup>2</sup>University of Cincinnati College of Medicine

Human mitochondrial 12S rRNA A1555G and C1494T mutations have been associated with aminoglycoside-induced and nonsyndromic deafness in many families worldwide. However, matrilineal relatives of intra-families or inter-families carrying the A1555G mutation exhibited a

wide range of penetrance and expressivity including severity and age-of-onset in deafness. Our previous investigation revealed that the A1555G mutation is a primary factor underlying the development of deafness but is not sufficient to produce a deafness phenotype. Thus, nuclear modifier genes have been proposed to modulate the phenotypic manifestation of the A1555G mutation. Here we identified the nuclear modifier gene TRMU encoding a highly conserved mitochondrial protein related to tRNA modification. Genotyping analysis of TRMU in 613 subjects of an Arab-Israeli kindred and 210 Italian/Spanish families and 31 Chinese pedigrees carrying the A1555G or C1494T mutation revealed a missense mutation (G28T) altering an invariant amino-acid residue (A10S) in the evolutionarily conserved N-terminal region of Trmu protein. Interestingly, all eighteen Arab-Israeli/Italian/Spanish matrilineal relatives carrying both the TRMU A10S and 12S rRNA A1555G mutations exhibited congenital profound deafness. Functional analysis showed that this mutation did not affect importing of Trmu precursors into mitochondria. However, the homozygous A10S mutation leads to a marked failure in mitochondrial tRNA metabolisms, specifically reducing the steady-state levels of mitochondrial tRNAs. As a consequence, these defects contribute to the impairment of mitochondrial protein synthesis. Resultant biochemical defects aggravate the mitochondrial dysfunction associated with the A1555G mutation, exceeding the threshold for expressing the deafness phenotype. These findings indicate that the mutated TRMU, acting as a modifier factor, modulates the phenotypic manifestation of the deafness-associated 12S rRNA mutations.

## 489 Old Genes, New Functions – Insights into the Role of Myosin VI Through the *Tailchaser* Mouse Mutant

Ronna Hertzano<sup>1,2</sup>, Ella Shalit<sup>1</sup>, Agnieszka K. Rzadzinska<sup>3</sup>, Tamar Tenne<sup>1</sup>, Uri Ron<sup>4</sup>, Joshua T. Tan<sup>5</sup>, Helmut Fuchs<sup>6</sup>, Tama Hasson<sup>5</sup>, Nir Ben-Tal<sup>4</sup>, Mireille Montcouquiol<sup>7</sup>, Martin Hrabe de Angelis<sup>6</sup>, Karen P. Steel<sup>3</sup>, Karen B. Avraham<sup>1</sup>

<sup>1</sup>Dept. of Human Molecular Genetics and Biochemistry, Tel Aviv University, Israel, <sup>2</sup>Department of Otorhinolaryngology, University of Maryland, Baltimore, MD, <sup>3</sup>The Wellcome Trust Sanger Institute, Wellcome Trust Genome Campus, Hinxton, Cambridge, UK, <sup>4</sup>Department of Biochemisry, George S. Wise Faculty of Life Sciences, Tel Aviv University, Israel, <sup>5</sup>Section of Cell and Developmental Biology, University of California, San Diego, La Jolla, CA, <sup>6</sup>Research Center for Environment and Health, Institute of Experimental Genetics, Neuherberg, Germany, <sup>7</sup>Developmental Neurosciences, Neuroscience Institute François Magendie, Bordeaux, France

Myosin VI (*Myo6*) is one of the first identified and best studied inner ear hair cell-specific genes. Mutations in *Myo6* underlie human and mouse autosomal recessive hearing loss and cause vestibular dysfunction in zebrafish. We now present *Tailchaser*, an autosomal dominant auditory and vestibular ENU-induced mouse mutant with a

newly discovered D179Y mutation in myosin VI. Tailchaser mice hair cells harbor multiple defects ranging from kinocilium mislocalization, bundle disorganization and stereocilia fusion to stereocilia bifurcation and branching. Despite the early expression of myosin VI, structural defects in the hair cells could only be observed after E18.5, similar to what was observed in the original *Snell's waltzer Myo6*-null mutant mice.

We describe the mapping and cloning of the D179Y mutation, and show that myosin VI protein localization and expression levels are unchanged in the *Tlc/*+ and *Tlc/Tlc* mice. We extend our initial structural analysis of the *Tailchaser* inner ears by high resolution scanning electron microscopy and immunohistochemistry. By using ARPE-19 cells expressing GFP-Myo6 or GFP-Myo6(D179Y) we demonstrate that while the myosin VI (D179Y) mutation does not interfere with recruitment of the protein to GIPC-associated uncoated vesicles, it inhibits the delivery of endocytic vesicles to the early endosome. Finally, we show that the original *Snell's waltzer* mutants have stereocilia bifurcation and branching, further supporting the association between the D179Y mutation and the *Tailchaser* phenotype.

## 490 Mutations of TRIC, Encoding a Novel Tight Junction Protein, are Associated with DFNB49 Nonsyndromic Hearing Loss.

**Saima Riazuddin**<sup>1</sup>, Zubair Ahmed<sup>1</sup>, Alan Fanning<sup>2</sup>, Ayala Lagziel<sup>1</sup>, Shinichiro Kitajiri<sup>1</sup>, Khushnooda Ramzan<sup>3</sup>, Shaheen Khan<sup>3</sup>, Parna Chattaraj<sup>1</sup>, Penelope Friedman<sup>4</sup>, James Anderson<sup>2</sup>, Inna Belyantseva<sup>1</sup>, Andrew Forge<sup>5</sup>, Sheikh Riazuddin<sup>3</sup>, Thomas Friedman<sup>1</sup>

<sup>1</sup>NIDCD/ NIH, <sup>2</sup>University of North Carolina, <sup>3</sup>Centre of Excellence in Molecular Biology, <sup>4</sup>Clinical Center/ NIH, <sup>5</sup>University College London

Profound congenital deafness segregating in two families was mapped to chromosome 5q12.3-q14.1 (Ramzan et al 2005). The meiotic information from six additional families refined the disease linked haplotype to 2.4 megabases. One of the genes in the refined interval is TRIC which encodes tricellulin, a tetraspan integral-membrane tight junction (TJ) protein. Tricellulin is localized at the tricellular attachment points of most epithelial cells. Antibodies generated to the N-terminus of tricellulin show that tricellulin is concentrated at the tricellular TJs in epithelial cells of the inner ear including hair cells, their supporting cells, reissner's membrane and the stria vascularis. In the organ of Corti tricellulin is localized along the structurally complex junctions between supporting and neurosensory hair cells. Given the expression of Tric in a variety of tissues, the deafness phenotype caused by these mutations is surprising. In eight DFNB49 families we found four different mutations of TRIC including a nonsense and three splice site mutations. Exon trapping and RT-PCR data using RNA from lymphocytes of DFNB49 subjects show that the splice site mutations cause aberrantly spliced mRNA, resulting in frameshifts and premature truncations of the protein. These mutations remove a conserved domain of this protein, which is predicted to bind the cytosolic scaffolding protein ZO-1. We provide data showing the affect of these mutations on the binding ability to ZO-1. There are some isoforms of tricellulin which remain unaffected by the mutant alleles and, we predict play a role in maintaining the epithelial barrier of other tissues. Mouse models of mutant Tric will allow us to test this hypothesis and answer the question as to why DFNB49 mutant alleles of TRIC selectively affect inner ear function

#### 491 The Effects of Human Espin Deafness Mutations on Espin Targeting and on Actin Bundle Organization and Length Regulation

Lili Zheng<sup>1</sup>, Kirstin Purdy<sup>2</sup>, Gerard Wong<sup>2</sup>, **James Bartles**<sup>1</sup>

<sup>1</sup>Northwestern University Feinberg School of Medicine,

<sup>2</sup>University of Illinois, Urbana-Champaign

Espins are actin-bundling proteins present at high concentration in hair cell stereocilia and are the target of deafness mutations. Espins contain a 116-amino acid Cterminal actin-bundling module (ABM), which is necessary and sufficient for their actin-bundling and parallel actin bundle-elongating activities. Mutagenesis of the ABM has identified two F-actin-binding sites, abs1 and abs2, disposed at either end of the ABM. We have compared the effects of recessive (2469delGTCA) and dominant (2543delAAG) mutant alleles of the espin gene that affect abs2 and are associated with severe hearing loss in humans. Wild-type espin potently bundles F-actin in solution and is efficiently targeted to, and dramatically elongates, microvilli in transfected CL4 epithelial cells. By small-angle x-ray scattering (SAXS), wild-type espin forms highly organized actin bundles, with hexagonally packed filaments that are slightly over-twisted and show an interactin spacing of 12.6 ± 0.2 nm, even at low espin:actin ratios. In contrast, 2469delGTCA-espin, which is missing abs2, does not bundle F-actin well in solution, poorly targets and elongates microvilli in transfected CL4 cells and, when analyzed by SAXS, yields a poorly organized, loosely spaced, nematic network with an inter-actin spacing of 21.3 ± 2.5 nm over a wide range of espin:actin ratios. The 2543delAAG-espin, which is missing a K residue from abs2, can bundle actin filaments in solution and is slightly more active than 2469delGTCA-espin at targeting and elongating microvilli in transfected CL4 cells. By SAXS, 2543delAAG-espin forms actin bundles at high espin:actin ratios, but with larger and more variable interactin spacing (12.6-14.6 nm), and, with decreasing espin:actin ratios, shifts to a poorly organized, nematic network with an inter-actin spacing of 19 ± 1.5 nm. Thus, abs2 plays critical roles in espin targeting and in actin bundle organization and length regulation (NIH DC004314 to JB, NSF DMR-0409769 to GW)

ARO Abstracts 169 Volume 30, 2007

#### 492 Mutations in the Gene Encoding Pejvakin, a Novel Protein Expressed in the Afferent Auditory Pathway, Cause DFNB59 Auditory Neuropathy in Man and Mouse

Sedigheh Delmaghani<sup>1</sup>, Francisco Del Castillo<sup>1</sup>, Vincent Michel<sup>1</sup>, Michel Leibovici<sup>1</sup>, Asad Aghaie<sup>1</sup>, Uri Ron<sup>2</sup>, Lut Van Laer<sup>3</sup>, Nir Ben-Tal<sup>2</sup>, Guy Van Camp<sup>3</sup>, Francina Langa<sup>1</sup>, Dominique Weil<sup>1</sup>, Mark Lathrop<sup>4</sup>, Paul Avan<sup>5</sup>, **Christine Petit**<sup>1</sup>

<sup>1</sup>Institut Pasteur, <sup>2</sup>University of Tel Aviv, <sup>3</sup>University of Antwerp, <sup>4</sup>Centre National de Génotypage, <sup>5</sup>Faculté de Médecine. Clermont-Ferrand

Most forms of inherited sensorineural hearing impairment are due to cochlear cell defects. However, up to 10% of all cases of permanent hearing impairment in children, is caused by a lesion located beyond the cochlea. Auditory neuropathy is a type of sensorineural hearing impairment in which neural transmission of the auditory signal is impaired, while cochlear outer hair cells remain functional. Here we report on DFNB59, a novel gene on chromosome 2q31.1-q31.3 mutated in four families segregating autosomal recessive auditory neuropathy. DFNB59 encodes pejvakin, a paralog of DFNA5 which is a protein of unknown function also involved in nonsyndromic hearing impairment. Pejvakin is expressed by neurons of the afferent auditory pathway. Furthermore, Dfnb59 knockin mice, homozygous for the R183W mutation identified in one DFNB59 family, display abnormal auditory brainstem responses indicative of neuronal dysfunction along the previously pathway. Unlike described sensorineural deafness genes, all of which underlie cochlear cell pathologies, DFNB59 is the first human gene implicated in nonsyndromic deafness due to a neuronal defect. Dfnb59 knockout mice which are in progress should help clarify the role of pejvakin.

### 493 The Stability of Cochlear Models Assessed Using a State Space Formulation.

Stephen Elliott<sup>1</sup>, Emery Ku<sup>1</sup>, Ben Lineton<sup>1</sup>

<sup>1</sup>University of Southampton

Linear models of cochlear dynamics are generally formulated in the frequency domain. Predictions generated by such models are used to compare with direct measurements. They are also the basis for more realistic nonlinear models. The results of such frequency domain models are not valid, however and can be misleading, if the system is not stable. The stability of such a model can be difficult to unambiguously determine from the calculated multichannel frequency response alone. In contrast the stability of a state space model can be readily established, by examining the eigenvalues of a single matrix. The stability of a state space model can thus be checked before the frequency response is calculated, in order to verify its validity. A state space model has been formulated for the discretised macromechanics and a generalised lumped active micromechanical model of the cochlea. A specific micromechanical model is used to illustrate this formulation, which is due to Neely and Kim (JASA 79 pp1472-1480, 1986), and for their assumed parameters the state space model is seen to be stable and to give frequency responses identical to those previously published. The stability of the model is found to be robust to smooth spatial variations of these parameters, but extremely sensitive to abrupt changes in the distribution of parameters along the cochlea. Random spatial variations also give rise to instabilities, even if they are smooth and very small, and these instabilities evolve into limit cycle oscillations if a compressive nonlinearity is introduced into the active feedback loops. These simulated oscillations have a distribution of frequency spacing that is similar to that observed in SOAEs.

### 494 Comparing Time Domain Simulations of Different Nonlinear Models of Cochlear Micromechanics

Emery Ku<sup>1</sup>, Stephen Elliott<sup>1</sup>

<sup>1</sup>University of Southampton

The cochlea exhibits many phenomena which are believed to be the result of a nonlinear active mechanism. Examples of nonlinear behaviour include the production of Spontaneous Otoacoustic Emissions (SOAEs), suppression of an SOAE with the introduction of a second tone, and entrainment of an SOAE with a closely-placed tone.

Isolated Van der Pol oscillators have previously been proposed as a model of such cochlear activity. Some of the properties this nonlinear system shares with the cochlea include the ability to reach limit cycle oscillations, entrain frequencies near resonance, and suppress the natural frequency response with the introduction of a second tone.

In this study, an isolated nonlinear version of Neely and Kim's (1986) active micromechanical model of the cochlea was implemented in the time domain using a 4<sup>th</sup> order Runge-Kutta approach. A saturating nonlinearity was imposed upon the feedback force, so that a limit cycle arose when the gain was increased past the point of instability. It was demonstrated that the response of the limit cycle resonance can be suppressed with the introduction of another tone, and entrained if the tone gets very close in frequency to the limit cycle. These simulations are shown to be qualitatively similar to those produced by both a time domain formulation of a Van der Pol oscillator and clinical measurements of SOAEs in live cochleae.

These results show that a number of nonlinear models can produce responses that are similar to observed cochlear phenomena. In order to distinguish between these formulations, current work is focused on developing a time domain simulation of a complete, coupled cochlea model which includes a saturating nonlinearity in each of the 500+ active micromechanical systems.

#### 495 Asymmetry of Wave Travel in a Three-Dimensional Cochlear Model

**Egbert de Boer<sup>1</sup>**, Alfred Nuttall<sup>2,3</sup>, Jiefu Zheng<sup>2</sup>

<sup>1</sup>Academic Medical Center, <sup>2</sup>Oregon Health & Science University, <sup>3</sup>Kresge Hearing Institute

In classical models of the cochlea the mechanical properties of the cochlear partition (in which the basilar membrane plays a dominant role) are functions that depend only on the local longitudinal coordinate. Wave propagation in such models is symmetrical, i.e. the same for both directions, for waves traveling towards the apex and towards the base. Not all recently discovered phenomena of cochlear responses can be explained on that basis. 'Non-classical' models contain mechanical properties that depend on variables at more than one location. In such models wave propagation may well be asymmetrical. In this poster a primitive model with feedforward is studied, with particular emphasis on symmetry and asymmetry of wave travel. It is found that the velocity of propagation is essentially symmetrical, but that power amplification for waves in one direction may turn into power dissipation for waves in the other direction. Experimental evidence for asymmetrical wave propagation can, in principle, be explained by this mechanism. The findings of this study point toward a generic property of non-classical models, and they encourage deeper study of un-orthodox types of cochlear model.

## 496 Motion of the Tectorial Membrane in the Basilar Papilla of the Northern Leopard Frog, Rana Pipiens

**Richard L.M. Schoffelen<sup>1,2</sup>**, Johannes M. Segenhout<sup>1</sup>, Pim van Dijk<sup>1,2</sup>

<sup>1</sup>Department of Otorhinolaryngology / Head and Neck Surgery, University Medical Center Groningen, <sup>2</sup>Fac. of Medical Sciences, School of Behavioral and Cognitive Neurosciences, University of Groningen

The inner ear of the frog is unique among vertebrates. It contains two auditory end organs, both of which lack a basilar membrane (BM). The lack of this structure in the auditory receptors of the frog implies that the frequency selectivity of these organs must be entirely due to the mechanical and electrical properties of the hair cells and the tectorial membrane (TM). Despite the absence of a BM, the sensitivity and tuning characteristics of the frog ear are similar to those of other vertebrates.

We obtained stroboscopic confocal-microscope images of the TM in the intact basilar papilla (BP) of a freshly killed northern leopard frog, in response to sinusoidal stimulation of the oval window. The TM's low opacity allows 'optical sectioning', in order to create a 3D image of the TM motion under stimulation, without damaging the supporting structure. To our knowledge, this is the first publication of recordings of the TM response in the frog inner ear.

Earlier anatomical reports suggest that the TM in the BP is a thin sheet suspended from the sides of the BP's lumen. Our recordings indicate that its dimensions are of the same order of magnitude in all three directions. Preliminary results from two specimens give average values of  $113\mu m$  (height),  $193\mu m$  (width) and  $49\mu m$  (depth).

Qualitative analysis shows that the movement of the TM has a component along the excitation direction of the hair cells. Additionally, there appears to be a perpendicular component of motion along the direction of the hair bundle, i.e. to and from the hair cell body. The TM movement is not uniform: the amplitude appears to be larger close to the hair cells than near the 'upper' rim of the TM.

These results show that measuring TM motion in the frog ear is feasible. The TM in the BP appears to have a relatively simple response to sinusoidal stimuli.

#### 497 Basilar Membrane and Tectorial Membrane Stiffness in CBA/Caj Mice

Ingo Teudt<sup>1</sup>, Scott McCusker<sup>2</sup>, Claus-Peter Richter<sup>3</sup>

<sup>1</sup>Northwestern University; University of Hamburg, Dep Oto/HNS, <sup>2</sup>Northwestern University, <sup>3</sup>Northwestern University, Dept Oto/HNS

The past decade has brought remarkable advances in the understanding of the auditory system and its components. However, it still remains unclear how structures of the organ of Corti and the tectorial membrane move in detail and by what mechanism their patterns of vibration contribute to the cochlear amplifier. By investigating physical and dynamical properties of the basilar membrane (BM) and the tectorial membrane (TM), better understanding of their influence to the cochlear amplifier can be accomplished. So far stiffness measurements of the BM and TM have been performed in multiple mammals but little data is available on mice.

In this study we determined the BM and TM stiffness in CBA/CaJ mouse strains. Measurements were performed in hemicochlea preparations using a 12  $\mu$ m tip sensor, driven by an electric bimorph. The Young's modulus of the BM was 5.79, 2.77 and 0.93 KPa at the basal, middle and apical cut edge. For the TM, we determined a Young's modulus of 1.06, 0.94 and 0.31 KPa, respectively. Both structures yielded a decrease in stiffness towards the apex.

For mice, no BM and little TM stiffness data are available in the literature. Therefore our values in the CBA/CaJ mouse provide important default data to be compared with stiffness data in other mouse strains, particularly for knockout mice with impaired hearing ability.

Supported by the NSF IBN-415901

# 498 Basilar Membrane Response to Electrical Stimulation in Mice with and Without Tectorial Membrane Loading

Marcia Mellado<sup>1</sup>, Markus Drexl<sup>1</sup>, Ian Russell<sup>1</sup>
<sup>1</sup>School of Life Sciences, University of Sussex, Falmer, Brighton Sussex, BN1 9QG, UK

The large dynamic range, sensitivity and frequency selectivity of the cochlea are due to amplification of responses at low level sounds and compression at high levels by the outer hair cells (OHC). Two mechanisms have been proposed as a basis for cochlear amplification:

active bundle movement and OHC motility, but their relative contributions are unclear in the mammalian cochlea. We have stimulated mice cochleae with AC current using a metal electrode on the round window and an Aq/AqCl pellet on the neck. Currents of different frequencies and levels were injected and a laser interferometer was focused on the high frequency region of the basilar membrane (BM) to obtain tuning curves of the mechanical response. Experiments were conducted on wild type and Tecta mice. Tecta mice contain a mutation of the tectorial membrane (TM) glycoprotein, alpha-tectorin. In homozygous mice, lacking alpha-tectorin, the TM is detached from the organ of Corti. Heterozygous mice have a normal TM (Legan et al., 2000). The electrically evoked BM tuning of wild type and heterozygous mice cochleae resemble acoustic tuning previously reported for the same region, with a tip and a second threshold minimum about half an octave below it. BM responses to electrical stimulation from homozygous, heterozygous and wild type mice are similar in tuning and sensitivity. This differs from previous acoustic tuning curves where homozygous mice were less sensitive and without the second peak. Both peaks are associated with cochlear amplification at low levels and compression at high levels. BM displacements in response to electrical stimulation are blocked by salicylate applied via the round window membrane. Sharp and sensitive frequency tuning can, therefore, be electrically elicited from the cochleae of Tecta mice in which somatic motility is present but the TM load required for any possible hair bundle force to be feedback into the system is missing.

Research supported by MRC, IBRO / FENS and DFG.

#### 499 Estimation of Anisotropic Properties of Tectorial Membrane in the Cochlea

**Zhijie Liao**<sup>1</sup>, Emilios Dimitriadis<sup>1</sup>, Richard Chadwick<sup>1</sup> *National Institutes of Health* 

The relative motion between the mammalian tectorial membrane (TM) and reticular lamina, caused by the incoming sound wave, bends the outer hair cell (OHC) bundles to open ion channels, whereby the mechanical energy is transduced into electrical currents that are required for proper function of the inner ear. The TM is an anisotropic and heterogeneous acellular matrix where the collagen fibrils run predominantly in the radial direction. Understanding the critical role of TM in hearing, and even in hearing loss, requires the determination of its intrinsic mechanical properties. In this study, based on the displacement measurement experiment on mouse TM using magnetic beads (Abnet and Freeman, 2000), a mathematical model (Chadwick et al. 2004) is employed to estimate the TM shear moduli, which are independent of the measurement instrumentation and experimental methodology. It is found that the shear moduli along and normal to the collagen fibrils are 6.7 kPa and 0.14 kPa respectively. Incorporation of these data into quantitative models of cochlear mechanics could help better understand the underlying mechanism of hearing.

## 500 Stiffness Modulation in the Organ of Corti Induced by Chlorpromazine and Salicylate

**Jiefu Zheng**<sup>1</sup>, Niranjan Deo<sup>2</sup>, Yuan Zou<sup>1</sup>, Karl Grosh<sup>2</sup>, Alfred Nuttall<sup>1,3</sup>

<sup>1</sup>Oregon Hearing Research Center, Oregon Health & Science University, <sup>2</sup>Department of Mechanical Engineering, The University of Michigan, <sup>3</sup>Kresge Hearing Research Institute, The University of Michigan Outer hair cell (OHC) electromotility, which provides mechanical force to the basilar membrane (BM), is essential to sound amplification in the mammalian cochlea. In this process, proper OHC stiffness is required to maintain normal electromotility. To investigate the in vivo role of OHC stiffness in cochlear amplification, chlorpromazine (CPZ) and salicylate (SAL), drugs that alter OHC lateral wall micromechanics and electromotility, were infused into the cochleae in living guinea pigs. The effects of these drugs on acoustically and electricallyevoked BM velocity measured with a laser Doppler vibrometer were observed. CPZ significantly reduced cochlear amplification as measured by a decline of the acoustically-evoked BM velocity response near the best frequency (BF) accompanied by a loss of nonlinearity and broadened tuning. A phase lead of BM velocity above the BF and a phase lag below the BF were observed, which indicate a putative stiffness increase due to CPZ. CPZ also substantially reduced the overall magnitude of the electrically-evoked BM. Importantly, the high-frequencynotch (near 50 kHz) in the electrically-evoked BM velocity response shifted towards higher frequency with a corresponding phase change. In contrast, SAL resulted in a shift of the notch frequency in an opposite direction. Through modeling, we propose that with a combined OHC somatic and hair bundle forcing, the shift of the notch in the electrically-evoked BM motion at high frequencies may indicate stiffness alteration of the OHCs that is responsible for the alterations in cochlear amplification. These results also indicate that CPZ and SAL have different effects on OHC stiffness.

Supported by NIH NIDCD R01 DC00141 (ALN), DRF (JZ) and NIH NIDCD R01 DC004084 (KG)

#### | 501 | In Vivo Imaging and Vibration | Measurement of Guinea Pig Cochlea and | Through Bone Imaging

**Fangyi Chen**<sup>1</sup>, Niloy Choudhury<sup>2</sup>, Jiefu Zheng<sup>1</sup>, Scott Matthews<sup>1</sup>, Alfred L. Nuttall<sup>1,3</sup>, Tianying Ren<sup>1</sup>, Yuan Zou<sup>1</sup>, Steven L. Jacques<sup>2,4</sup>

<sup>1</sup>Oregon Health & Science University, Oregon Hearing Research Center, <sup>2</sup>Biomedical Engineering, Oregon Health & Science University, <sup>3</sup>Kresage Hearing Research Institute, The University of Michigan, <sup>4</sup>Dermatology, Oregon Health & Science University

An optical coherence tomography (OCT) system was built to acquire in vivo, both images and vibration measurements of the organ of Corti of guinea pigs. The organ of Corti was viewed through a ~500-µm diameter hole in the bony wall of the scala tympani of the first cochlear turn. In imaging mode, the image was acquired

as reflectance. In vibration mode, the basilar membrane (BM), reticular lamina (RL) or other structures were selected based on the image. Under software control, the system would move the scanning mirrors to bring the sensing volume of the measurement to the desired tissue location. To address the gain stability problem of the homodyne OCT system, a vibration calibration method is developed by adding a vibrating source to the reference arm to monitor the operating point of the interferometric system. Vibrations of ±2 nm and ±22 nm were recorded in the BM in response to low and high sound levels at 14 kHz above a noise floor of 0.2 nm.

In vivo images of the organ of Corti at the basal turn clearly indicate reflectance signals from the BM, RL, tectorial membrane, and Reissner's membrane. The vibration spectra measured at those locations demonstrated the optical sectioning capability of the OCT system and the typical frequency tuning expected from the traveling wave. From the image at the basal turn, the tunnel of Corti and the inner sulcus are also visible. To test the capability for image quality, the organ of Corti was imaged from an isolated cochlea at the apical turn. This image clearly shows the outer hair cells, Hensen's cells and other supporting cells. To test the potential of the OCT system to conduct vibration measurement on an intact cochlea, an image was also acquired without opening the apical bony wall of the cochlea. The shape of the organ of Corti is clear and the tunnel of Corti is recognizable, which demonstrates the penetrating capability of this far infrared OCT system.

Supported by NIDCD DC 00141 and DC 006273.

#### 502 Similarity Between the Otoacoutic Emissions and Basilar Membrane Vibration

**Wenxuan He<sup>1,2</sup>**, Alfred L. Nuttall<sup>1,3</sup>, Tianying Ren<sup>1,2</sup>
<sup>1</sup>Oregon Health and Science University, <sup>2</sup>Xi'an Jiaotong University, <sup>3</sup>The University of Michigan

The basilar membrane (BM) vibration at otoacousticemission frequencies, such as 2f1-f2 for the cubic distortion product otoacoustic emission increases as the frequency increases, when the f2/f1 approaches one, while the emission in the ear canal decreases and forms a bell-shape response curve. A number of theories have been developed to account for difference between the BM and emission measurements. However, the BM data showing the above feature were mostly measured from the longitudinal location at or near the generation site of the emissions. In order to obtain a more complete view on the relationship between the otoacoutstic emissions and corresponding BM vibrations, the cubic DPOAE was evoked by two primary tones f1 and f2 (f1<f2) in sensitive gerbil ears. Sound pressure in the ear canal, the vibration of the stapes footplate, and the BM vibration were measured as a function of the emission frequency, which was varied by changing f1 when f2 was constant. Measurements were taken from the 16 kHz longitudinal location and the emission generation site was varied by using different f2 frequencies. It was found that when the measurement location is at or near the DPOAE generation sites, i.e., the f1 and f2 overlap place, the BM response is dominated by cochlear tuning, which is significantly different from the emission in the ear canal. However, as the emission-generation site moved away from the measured site and toward the apex by using low-frequency f2 (below 8 kHz), the frequency response of the BM vibration became similar to that of DPOAE in the ear canal. A transition pattern of BM responses was observed when the 12 kHz f2 was used. The possible underlying mechanisms that could account for these results will be discussed. Supported by NIH-NIDCD.

#### 503 A Live Demonstration of an Active Physical Model of the Cochlea

Tina Jovic<sup>1</sup>, Curtis King<sup>1</sup>, Richard Rabbitt<sup>1,2</sup> <sup>1</sup>University of Utah, <sup>2</sup>Marine Biological Laboratory Following in the spirit of Georg von Bekesy, we have constructed a physical model of the cochlea but this time incorporating active elements to demonstrate the cochlear amplifier. The work builds on the model of R. Keolian which mimics the passive traveling-wave frequency decomposition carried out by the elastohydrodynamics of the cochlea (J. Acoust. Soc. Am., 101(2): 1199-1201). We have constructed a similar model, but augmented with hair-cell cilia like sensors to measure the local velocity of the fluid and electromagnetic actuators to actively feed energy locally into the model. The actuators are powered by feedback from the velocity sensors to generate a viscosity canceling effect. Our model is also outfitted with an electromagnetic shaker capable of delivering complex waveforms to the model oval window. Since the model is much larger than the cochlea its best frequencies are shifted down to the range from 5 to 80 Hz. Music played into the model demonstrates the complex response of the cochlear partition and the kinds of behaviors that can result from active amplification. The most interesting responses are obtained when music is recorded in stereo. digitally processed and replayed. One channel is frequency shifted using a wavelet transform to match the best frequencies of the model while the other channel is played without modification. This allows the listener to

observe the motion of the cochlear partition in temporal

synchrony with hearing the original soundtrack. A live

demonstration of the apparatus in response to pure tones,

speech, and music will be presented under both passive

[Supported by NIDCD R01 DC04928]

and active conditions.

#### | 504 | Modeling Membrane-Cytoskeleton Interaction in the Cochlear Outer Hair Cell Tether Pulling Experiment

**Kristopher Schumacher**<sup>1</sup>, Aleksander Popel<sup>1</sup>, Bahman Anvari<sup>2</sup>, William Brownell<sup>3</sup>, Alexander Spector<sup>1</sup>

<sup>1</sup>Johns Hopkins University, <sup>2</sup>University of California, Riverside, <sup>3</sup>Baylor College of Medicine

The mechanics of cochlear outer hair cells is important to the sound amplification in the inner ear. The outer hair cell's plasma membrane is the site of the cell's active properties and is part of the tri-layer lateral wall, where the membrane is attached to the cytoskeleton by a system of radial pillars. Membrane tether pulling is an experimental manipulation that provides insight into properties of the membrane (e.g., bending and membrane reservoir) and its interaction with the cytoskeleton. Here, we present a modeling study to simulate the outer hair cell plasma membrane deflection and bending and its interaction with the cytoskeleton during tether pulling experiments. In our analysis, three regions of the membrane are considered: the body of a cylindrical tether, the area where the membrane is attached and interacts with the cytoskeleton, and the transition region between the two. By using a computational method, we estimate the shape of the membrane in all three regions, as well as the distributions of the bending moment and shear force over a range of tether lengths and forces observed in experiments. The modeling results allow a characterization of the experimentally unobservable sub-nanometer membrane deflections within the attachment zone with strong membrane-cytoskeleton bonds. The results contribute towards a better understanding of the mechanics of this cell critical to active hearing. Further, the geometry and membrane-cytoskeleton adhesion properties of the attachment zone can be modified to model the mechanics of different cells such as HEK cells used to study the properties of the membrane protein prestin.

## 505 Reduced Traveling Wave Propagation and Endocochlear Potential in a Mouse Model of Mondini Cochlear Dysplasia

Anping Xia<sup>1</sup>, Ann Marie Visosky<sup>1</sup>, Jang-Hyenon Cho<sup>1</sup>, Ming-Jer Tsai<sup>1</sup>, Fred Pereira<sup>1</sup>, **John Oghalai**<sup>1</sup>

<sup>1</sup>Baylor College of Medicine

A common type of inner ear malformation found in humans is Mondini dysplasia in which cochlear coiling is disrupted. There is an incomplete partition between the cochlear turns and the cochlear duct is shorter than normal. The BETA2/NeuroD1 null mouse cochlea has a similar histologic appearance and we used this mouse model to better understand the pathophysiology of this condition. Laser doppler interferometry studies in excised cochleae revealed that tuning in the null mouse was broadened compared to wild-type and heterozygote mice in the apex. Additionally, null mice had significantly reduced phase lag accumulation with increasing stimulus compared to wild-type and heterozygote mice. A large phase lag is considered characteristic of traveling wave propagation. In vivo studies demonstrated that the null mouse lacked auditory brainstem responses and distortion product otoacoustic emissions, and had severely reduced cochlear microphonic responses and endocochlear potentials. Fluorescence microscopy showed that hair cell stereocilia had a normal pattern of FM 1-43 dye uptake and that the electromotility motor protein prestin was expressed normally within the outer hair cell lateral wall. Electrically-evoked otoacoustic emissions could be elicited in null mice, although the amplitudes were lower than those of wild-type mice. These data indicate that traveling wave propagation is reduced in the BETA2/NeuroD1 null mouse cochlea, and suggest that the Helmholtz independent resonator model may more accurately

represent the passive cochlear mechanics of Mondini dysplasia. Additionally, even though the reduced endocochlear potential inhibits forward transduction, reverse transduction may still be functional.

#### 506 Postnatal Alterations in Ohc Stiffness and Protein Distribution

Heather Jensen-Smith<sup>1</sup>, Richard Hallworth<sup>1</sup>

<sup>1</sup>Creigton University

Outer hair cells (OHCs) in the organ of Corti exhibit nonlinear, mechanical responses to auditory stimulation that increase hearing sensitivity 100-fold (40 dB). Effective force transmission to the organ of Corti requires OHCs to possess a specific amount of stiffness. Maturation of stiffness in OHCs may therefore be an important factor in mammalian hearing development. The mechanical properties of developing and mature OHCs were compared using calibrated glass fibers. OHC specific compliance increased immediately before the onset of hearing. By hearing onset, OHC compliance dramatically OHCs have a specialized lateral wall decreased. consisting of a plasma membrane, in which the motor protein prestin is densely packed, an actin-spectrin cortical lattice and subsurface cisternae. Developmental alterations in protein distribution and localization of each of these structures were correlated with alterations in OHC Lateral wall F-actin content was highly compliance. correlated with OHC compliance before the onset of hearing. Prestin incorporation at the onset of hearing was negatively correlated with compliance. These results suggest that F-actin and prestin modulate the passive mechanical properties of OHCs before and after the onset of hearing, respectively. Furthermore, these dramatic alterations in OHC mechanics clearly indicate that the OHC must acquire specific mechanical properties in concert with electromotility to generate a sharply tuned

Supported by N.I.H. (N.I.D.C.D) grant DC02053, N.C.R.R C06 RR17417-01, NSF EPSCoR EPS-0346476 (CFD 47.076), and the Deafness Research Foundation.

### 507 Modeling Superior Canal Dehiscence: Predictions of the Air-Bone Gap in Humans

**Jocelyn Songer**<sup>1,2</sup>, Michael Ravicz<sup>1</sup>, Wade Chien<sup>1,3</sup>, Saumil Merchant<sup>1,3</sup>, John Rosowski<sup>1,3</sup>

<sup>1</sup>Massachusetts Eye and Ear Infirmary, <sup>2</sup>Massachusetts Institute of Technology, <sup>3</sup>Harvard Medical School

A superior semicircular canal dehiscence (SCD) is an inner ear lesion that affects both the auditory and vestibular systems. In humans, an SCD can cause both a decrease in sensitivity to air-conducted sound and an increase in sensitivity to bone-conducted sound, resulting in an air-bone gap. This air-bone gap is typically largest at frequencies below 1000Hz and has been reported as 24  $\pm$  7dB between 250 and 4000Hz (Minor et al, 2003) and 37dB at 500Hz (Mikulec et al, 2004). Previous acoustomechanical measurements in human temporal bones using air-conducted sound have demonstrated that an SCD causes a decrease in round window velocity consistent with a shunting of acoustic energy away from

the cochlea (Chien et al, In Press). These changes in mechanics can be predicted using a lumped-element model of SCD in the human ear. Further, a lumped-element model of the effect of SCD on bone-conducted sounds has been created and used to predict measurements of increased bone-conduction sensitivity post-SCD in chinchillas.

The goal of this work is to update the model of the effect of SCD on air-conducted sounds in humans and adapt the chinchilla model of SCD to appropriate human parameters. The two models will then be combined to predict the airbone gap associated with an SCD. These predictions will then be compared to measurements of air- and bone-conduction thresholds in a collection of over 20 SCD patients. Preliminary model results predict an air-bone gap that is largest at frequencies below 1000Hz. The model of air-bone gap in SCD can be an important predictive tool for determining the effects of dehiscence size, location, and middle-ear mechanics on auditory symptoms in patients with SCD.

### 508 Bias Due to Noise in Otoacoustic Emissions Measurements

Bradford Backus<sup>1</sup>

<sup>1</sup>University College London

Measurements of otoacoustic emission (OAE) magnitude are often made at low signal/noise ratios (SNRs) where measurement-noise generates bias and variability errors that have led to the misinterpretation of OAE data. To gain an understanding for these errors and their effects, a two part investigation was carried out. First, the nature of OAE measurement-noise was investigated using human data from 50 stimulus-frequency OAE experiments involving medial olivocochlear reflex (MOCR) activation. The noise was found to be reasonably approximated by circular Gaussian noise. Furthermore, when bias errors were taken into account, measurement variability was not found to be affected by MOCR activation as had been previously reported. Second, to quantify the errors circular Gaussian noise produces for different methods of OAE magnitude estimation for distortion-product, stimulus-frequency and spontaneous OAEs, simulated OAE measurements were analyzed via 4 different magnitude estimation methods and compared. At low SNRs (below ~6 dB), estimators involving Rice probability density functions produced less biased estimates of OAE magnitudes than conventional estimation methods, and less total rms error—particularly for spontaneous OAEs. They also enabled the calculation of probability density functions for OAE magnitudes from experimental data.

### 509 Transient Otoacoustic Emissions Measured with a Highly Linear System

Jill Placek<sup>1</sup>, Jonathan Siegel<sup>2</sup>

<sup>1</sup>Northwestern University; Dept. of Communication Sciences and Disorders, <sup>2</sup>Northwestern University; Hugh Knowles Center; Dept. of Communication Sciences and Disorders

Measuring transient otoacoustic emissions using linear signal averaging has proven difficult due primarily to the relatively poor linearity and frequency response of the sound source transducers used to evoke emission from the ear. We report measurements of transient emissions evoked from the ears of humans using clicks and tone pips generated using transducers that have better bandwidth and much better linearity than those commonly used. Residual stimulus ringing can be separated from overlapping early components of the emission by scaling down and subtracting the pressure response to the stimuli measured at sound pressure levels as much as 60 dB above those used to evoke emsissions, (the reference and probe stimuli, respectively). These measurements reveal early components of the emissions that appear to exhibit less saturation than later components. These earliest components are thus selectively removed by typical nonlinear extraction techniques in which the difference in level between the probe and reference stimulus is less. For tone-pips, the spectral responses of both early and late components of the emssion were centered on the frequency of the pip, showing some evidence of dispersion. Using low-level, variable frequency suppressor tones, we found that the earliest part of the emission was suppressed most effectively by tones as much as an octave above the frequency of the probe, indicating an origin basal to the location peak for the probe. Suppressors closer to the probe frequency selectively suppressed the later components of the emission. We conclude that a relatively larger region of the cochlea than expected generates the emission.

Supported by Northwestern University.

#### 510 Low-Frequency Modulation of Dpoaes in Humans

**Lin Bian**<sup>1</sup>, Kelly Watts<sup>1</sup>

<sup>1</sup>Arizona State University

Distortion product otoacoustic emissions (DPOAEs) are useful indicators of inner ear function since they are generated from the hair cell transduction processes. Recently, we have explored a new way of measuring DPOAEs as a measure of the dynamic changes in cochlear transduction. In this method, a low-frequency tone was introduced to bias the cochlear partition and in turn to modulate the gain of cochlear transducer. Previous results in rodents showed that the bias tone can modulate the DPOAEs in a way that its temporal patterns resemble the nonlinear transfer characteristics of the cochlear transducer. Therefore, in this study, the feasibility of this technique was tested in humans. Low-frequency modulations of DPOAEs were measured from subjects with normal hearing thresholds and middle ear functions. The magnitude of the bias tone was descended from 20 to 0 Pa in multiple steps while the levels of the primary tones were fixed. Effects of these bias tones were examined by comparing the DPOAE responses with and without the bias tone in frequency domain. The amplitudes of the DPOAEs showed great variability indicating possible involvement of other mechanisms. Spectral difference could eliminate the DPOAEs generated through other mechanisms to preserve the nonlinearly generated DPOAEs. The relative amplitudes of the multiple sidebands around the DPOAEs determine the modulation patterns of the distortion products. DPOAE modulation

sideband amplitudes grew with both primary and bias levels. The sideband magnitude also showed limits of growth that indicate the preferred modulation signal conditions. Low-frequency modulation of DPOAE thus could be used as a clinical measure of inner ear transduction if the recording and analyzing methods can be optimized.

Supported by NIH/NIDCD grant: R03 DC006165

#### | 511 | Level Dependence of Distortion-Product Otoacoustic Emissions (DPOAEs) Using the Scissor and Equal-Level Paradigms

Changmo Jeung<sup>1</sup>, Glenis R. Long<sup>1</sup>

<sup>1</sup>Program in Speech and Hearing Sciences, Graduate Center of the City University of New York, New York We explored the dependence of DPOAE amplitudes when the level of L2 was varied in 5dB steps. The level of L1 was determined either by using the scissor paradigm (L1=0.4\*L2+39 dB SPL) claimed to generate the largest DPOAE amplitude at low L2 levels, or by using the equal level paradigm in which L2=L1. The level dependence of the DPOAEs was evaluated in normal hearing subjects using logarithmically sweeping tones (2s/octave) which maintained a constant frequency ratio (f2/f1= 1.22). F2 ranged from 1000 to 8000 Hz. Wide-band analysis permitted examination of the DPOAE fine structure because both the generator and reflection components fell within the filter. Narrow-band analysis permitted examination of the generator component alone. When both components were present, the DPOAEs collected using the scissor procedure always showed less DPOAE fine structure than when the DPOAEs were collected with equal level primaries. Greater changes in the frequency of the DPOAE fine structure were also seen when equal level primaries were used. Narrow-band analysis provides a rapid tool for evaluating the generator component uncontaminated by the reflection component, therefore reducing the variance of input/output (I/O) functions. DPOAE I/O functions obtained using the scissor paradigm were characterized by compressive growth at moderate levels and more linear growth at higher levels. This pattern is similar to basilar membrane input/output functions. The equal-level paradigm gave more linear growth at lower levels. We applied Inverse Fast Fourier Transform (IFFT) and time windowing to extract both the generator and the reflection components based on the two-source model of DPOAE fine structure. While the growth of the generator component was greater for the scissors paradigm, the magnitude of the reflection component was similar for both paradigms. Consequently, the difference in the magnitude of the generator component appears to be mainly responsible for the changes in the magnitude of DPOAE fine structure in the different paradigms.

### 512 Quantitative Features of DPOAE I/O Functions in Normal and Impaired Human Fars

**Stephen T. Neely**<sup>1</sup>, Tiffany A. Johnson<sup>2</sup>, Judy G. Kopun<sup>1</sup>, Connie Converse<sup>1</sup>, Elizabeth Kennedy<sup>1</sup>, Darcia M. Dierking<sup>1</sup>, Michael P. Gorga<sup>1</sup>

<sup>1</sup>Boys Town National Research Hospital, <sup>2</sup>University of Kansas

product otoacoustic emission (DPOAE) Distortion input/output (I/O) functions were measured in 322 ears of 176 human subjects at as many as 8 f<sub>2</sub> frequencies per ear. The f<sub>2</sub> frequencies ranged from 707 Hz to 8 kHz in half-octave steps. Behavioral thresholds (BT) at the f<sub>2</sub> frequencies ranged from -5 to 60 dB HL. Quantitative features of more than 1700 I/O functions were analyzed. DPOAE thresholds were estimated by two different methods. First, a linear function was fit to distortion pressure (in micropascal) versus L2 (in dB SPL) in the manner suggested by Boege and Janssen (2002). Second, a nonlinear function was fit to the same data. The nonlinear function was based on the idea that cochlear mechanics are linear near the threshold of hearing and that cochlear responses become gradually more compressive as stimulus level is increased above threshold. DPOAE thresholds estimated by both methods were used to predict BTs. Results of preliminary analysis showed that most of the I/O functions were better fit by the nonlinear method, especially at higher frequencies. Predictions of BT based on DPOAE thresholds were slightly improved by the nonlinear method; however, the DPOAE thresholds observed at any given BT were still widely distributed. An advantage of the nonlinear method may be that it provides an estimate of compression growth rate (CGR). At most frequencies, the median CGR (across I/O functions of the same f<sub>2</sub>) decreased as BT increased, consistent with the loss of cochlear compression that is often associated with moderate hearing loss. The I/O functions at 8 kHz differed (from the I/O functions at other frequencies) in exhibiting an increase in CGR between 0 and 40 dB HL. The observation that CGR properties differ across frequency suggests that nonlinear response growth in the cochlea may differ between basal and apical locations.

[Work supported by NIH/NIDCD grants R01 2251 and P30 4662.]

# **513** Cochlear-Source Contributions and Distortion Product Otoacoustic Emission (DPOAE) Test Performance in Humans

**Tiffany A. Johnson**<sup>1</sup>, Stephen T. Neely<sup>1</sup>, Judy G. Kopun<sup>1</sup>, Darcia M. Dierking<sup>1</sup>, Connie Converse<sup>1</sup>, Elizabeth Kennedy<sup>1</sup>, Hongyang Tan<sup>1</sup>, Michael P. Gorga<sup>1</sup>

\*\*Boys Town National Research Hospital\*\*

DPOAEs contain contributions from a distortion and a reflection source. It has been proposed that the interaction of these sources affects the accuracy of clinical applications of DPOAEs (e.g., Shera, 2004). Here, we evaluate changes in dichotomous-test performance while controlling cochlear sources that contribute to the DPOAE. Data were obtained from 98 normal and 107 hearing-

impaired ears with f<sub>2</sub>=2 and 4 kHz and L<sub>2</sub> ranging from 0 to 80 dB SPL, with L<sub>1</sub> chosen to optimize L<sub>dp</sub> (Neely et al., 2005; Johnson et al., 2006a). These data were collected for a control condition (no suppressor, f<sub>3</sub>) and with f<sub>3</sub> presented at 3 levels that previously had been shown to reduce the reflection-source contribution (Johnson et al., 2006b). ROC curve area (AROC) was computed for each of the 4 conditions. Regardless of L<sub>2</sub>, AROC observed for the conditions that included a suppressor was ≤ AROC for the control condition. This suggests that reducing the contribution from the reflection source by presenting a suppressor did not result in more accurate identification of auditory status. A subset of ears for which the largest errors were made (i.e., normal ears with the smallest DPOAEs and impaired ears with the largest DPOAEs) returned for additional data collection. For this subset, a larger AROC (by 12- 15%) was observed for f<sub>2</sub>=2 kHz in 2 of 3 suppressor conditions and when a frequencysmoothing approach was used to control source contribution. No differences were observed at 4 kHz. In light of the smaller AROC observed for the larger sample, these results should be viewed cautiously. While the results in the small sample (N=26 ears) revealed increases in AROC when the reflection source was controlled, results from the larger sample (N=205) showed an opposite effect, suggesting that controlling cochlear-source contribution with a suppressor may introduce diagnostic errors for a more general population of patients.

[Work supported by the NIH - NIDCD F32-DC007536, R01-DC02251, P30-DC04662.]

### 514 DPOAE Mechanisms and the Estimation of Hearing Thresholds

**Tracy Fitzgerald**<sup>1</sup>, Marquitta Merkison<sup>1</sup> *University of Maryland College Park* 

The 2f1-f2 DPOAE measured in the ear canal is a combination of energy from two mechanisms, nonlinear distortion and linear reflection (e.g., Shera & Guinan, 1999). Several researchers, such as Shera (2004), have suggested that isolating the nonlinear distortion component may reduce intra-subject variability in DPOAE levels and improve diagnostic tests using DPOAEs. In the present study, we tested this hypothesis by measuring 2f1f2 fine structure from individuals with normal-hearing thresholds or mild hearing impairment and using inverse fast Fourier transform (IFFT) analysis to separate the contributions from the nonlinear distortion and reflection components. 2f1-f2 DPOAE fine structure was measured in 10 Hz steps using the OpenDP system (Smith et al., 2005) with f2/f1 = 1.2 for all measurements. Fine-structure was measured using L1= 65 and L2 = 55 dB SPL from f2 = 1500-4500 Hz. Fine structure was also measured from a more limited frequency range (typically f2 = 1500-2500 Hz or 3750-4500 Hz) for different primary levels [L2 = 20-65 dB SPL in 5 dB steps; L1 = 0.4 L2 + 39 dB (Kummer et al., 1998)]. IFFT analysis was accomplished using the NIPR program developed by Dr. Carrick Talmadge. The levels and thresholds of the nonlinear distortion and reflection components will be compared with hearing levels to evaluate whether better prediction of hearing levels is possible using the individual components.

(This research was supported by an American Speech-Language-Hearing Foundation 2005 New Century Scholars Research Grant.)

# 515 Slow Oscillatory Cochlear Adaptation to Brief Low Frequency Over Stimulation: The Human OAE 'Bounce' Effect Revisited

David T. Kemp<sup>1</sup>, Oliver J. Brill<sup>1</sup>

<sup>1</sup>Ear Institute, University College London

Human hearing sensitivity can increase in the minute following brief intense low frequency sound exposure (Hirsh and Ward 1955). Kemp (1986) reported a corresponding biphasic bounce in OAE suggesting a second order system regulating OHC 'energy levels'. More recently Kirk and Patuzzi (1997) investigated the post exposure bounce of CM, CAP, SP, EP and DPOAE in guinea pig. Cochlear effects persisted with TTX ruling out neural involvement in the bounce. They proposed a mechanism in which OHC operating point was shifted due to sound induced ionic changes, the components of which decayed exponentially at differing rates causing a biphasic change in sensitivity. In our study the OAE bounce effect was recorded in (initially) 9 human subjects after a 150Hz, 100dBSPL tone applied for up to 2m. TEOAEs were recorded at 10s intervals before and for up to 5m after exposure. OAE intensity typically was unchanged just after the exposure but was enhanced by 1dB at 50s and depressed by 1dB at 140s. A similar time course was found in all subjects but the relative size of the bounce differed being larger in subjects with larger OAE. This relationship did not apply across frequency within subjects. Continuous activation of the cochlear reflex by contralateral white noise did not alter the time course or magnitude of the bounce suggesting no efferent involvement but it did depress the OAE level. A damped oscillator model fitted the bounce data better than the double exponential passive depletion model suggested by Kirk et al. No ear showed depression without also showing enhancement and we propose that LF over-stimulation excites a compensatory mechanism that ensures cochlear amplifier gain is normal after brief over-stimulation. We don't think just a shift in OHC operating point would explain our data.

Kemp DT (1986) Hearing Research, 22:95-104. Kirk DL and Patuzzi RB (1997) Hearing Research 112:49-68. Kirk DL, Moleirinho A and Patuzzi R B (1997) Hearing Research 112:69-86.

# 516 Group Delay Contour Plots Derived From DPOAE Level/Phase Maps in Normal Hearing and Noise-Damaged Humans

**Barden Stagner**<sup>1</sup>, Deanna Meinke<sup>2</sup>, Brenda Lonsbury-Martin<sup>1</sup>, Glen Martin<sup>1</sup>

<sup>1</sup>Jerry Pettis Memorial Veterans Medical Center,

<sup>2</sup>University of Northern Colorado

Distortion-product otoacoustic emission (DPOAE) level/phase maps were obtained with an extended DPOAE low-frequency range in 20 normal-hearing subjects (10 females, 10 males) and 10 males with noise-induced hearing loss (NIHL). To construct the DPOAE ratio vs

level/phase plots, DPOAEs were measured in DPOAE frequency steps of approximately 44 Hz (0.5-6.0 kHz) in response to primary-tone sweeps at 3 levels (80,80; 75,75; 65,55 dB SPL), using constant f<sub>2</sub>/f<sub>1</sub> ratios incremented in 0.025 steps (1.025-1.5). DPOAE level was directly plotted while phase was corrected for primary-tone phase variation and unwrapped before plotting. The  $2f_1-f_2$ DPOAEs showed 'wave-fixed' phase patterns at standard f<sub>2</sub>/f<sub>1</sub> ratios of 1.21 and 'placed-fixed' phase behavior for closely spaced  $f_2/f_1$  ratios. When present, the  $2f_2-f_1$  DPOA showed place-fixed behavior. To further analyze these data, group delays (GDs) were computed for derived f<sub>1</sub> sweeps for constant f2 frequencies across the entire response area. Delays were based upon 9 data points and processed as a running least-squares fit. resulting GDs were then contour plotted as a function of  $f_2/f_1$  ratio and  $f_2$  frequency. This procedure resulted in cochlear delays of approximately 6 ms at f<sub>2</sub>=1 kHz, decreasing to around 1.5 ms at f<sub>2</sub>=5 kHz. Algorithms were also developed so that GDs could be derived for constant f<sub>1</sub> with swept f<sub>2</sub>, or constant ratio trajectories through the data. These procedures clearly illustrated the well-known effects of sweep method on GDs. Average GDs of normal males as compared to normal females were not remarkably different. Although primary-level dependent, at primary-tone levels of 65,55 dB SPL, average GDs were longer for NIHL males than for normal males at the same level.

(Supported by NIDCD: DC000613, DC003114).

#### 517 A Study of Human DPOAE Fine Structure

Karen Reuter<sup>1</sup>, Dorte Hammershøi<sup>1</sup>

<sup>1</sup>Aalborg University

Otoacoustic emissions (OAEs) are a promising method to monitor early noise-induced hearing losses. When distortion product otoaocustic emissions (DPOAEs) are obtained with a high frequency resolution, a ripple structure across frequency can be seen, called DPOAE fine structure. In this study DPOAE fine structures are obtained from 74 normal-hearing humans using primary levels of L1/L2=65/45 dB. The subjects belong to groups with different age and exposure history. A classification algorithm is developed, which quantifies the fine structure by the parameters ripple place, ripple width, ripple height and ripple prevalence. Temporary changes of the DPOAE fine structure are analyzed by measuring DPOAE both before and after exposing some of the subjects to an intense sound. The characteristic patterns of fine structure can be found in the DPOAE of all subjects, though they are individual and vary from subject to subject within groups. The results do not indicate that the DPOAE fine structure alters in a simple way with the state of hearing.

### 518 Distortion-Product Otoacoustic Emissions in a Nonlinear Traveling Wave Model

Xuedong Zhang<sup>1</sup>, David C. Mountain<sup>1</sup>

<sup>1</sup>Hearing Research Center and Biomedical Engineering Department, Boston University

Recent studies (Knight and Kemp, 2000, JASA 107:457; Kalluri and Shera, 2001, JASA 109:622) suggest that distortion-product otoacoustic emissions (DPOAE) have at least two generation regions which involve different generation mechanisms. This study explores the generation and propagation of DPOAEs within the cochlea using numerical simulation.

A multi-mode active traveling model (Hubbard et al., 1997, Diversity in Auditory Mechanics, World Scientific) was modified to include nonlinear active outer hair cell force generation. The numerical implementation of the model was validated by comparing the numerical responses with the analytical solution. We evaluated the model distortion product responses both at the stapes and at various locations within the simulated cochlea. The distributions of distortion product magnitude and phase along the basilar membrane were a complex function of primary frequency and level suggesting that more than two generation sites are involved in the production of DPOAEs.

[Funded by NIDCD grant R01-DC29]

### 519 Otoacoustic Estimates of Cochlear Tuning: Validation in the Chinchilla

**Christopher A. Shera**<sup>1</sup>, John J. Guinan, Jr. <sup>1</sup>, Andrew J. Oxenham<sup>2</sup>

<sup>1</sup>Eaton-Peabody Laboratory, <sup>2</sup>University of Minnesota Otoacoustic and behavioral measurements independently suggest that the quality factors (Q<sub>ERB</sub>) of human peripheral auditory filters are both larger (sharper tuning) and more strongly dependent on frequency than previously believed (Shera, Guinan & Oxenham, PNAS, 2002; Oxenham & Shera, *JARO*, 2003). The otoacoustic evidence for sharper tuning stems from the empirical correlation between physiological Q<sub>FRB</sub> measured in auditory-nerve fibers (ANFs) and the group delays of stimulus-frequency otoacoustic emissions (SFOAEs). Correlations between the sharpness of cochlear tuning and basilar-membrane (BM) group delay are expected from filter theory, and a proportionality between BM and SFOAE delay is predicted by coherent-reflection models of SFOAE generation (e.g., Zweig & Shera, JASA, 1995; Shera & Guinan, JASA, 2003; Shera, Tubis & Talmadge, ARO, 2006). We test these predicted correlations in chinchilla by analyzing published measurements of ANF Wiener kernels (Recio-Spinoso et al., J Neurophys, 2005; Temchin et al., J Neurophys, 2005) and SFOAEs (Siegel et al., JASA. 2005). Contrary to recent suggestions (Siegel et al., JASA, 2005; Ruggero & Temchin, PNAS, 2005), all predicted relationships hold at least in the base and middle of the cochlea, and perhaps throughout. In particular, the otoacoustic measurements accurately predict sharpness and frequency dependence of chinchilla cochlear tuning.

Supported by NIH R01 grants DC03687 (CAS), DC00235 (JJG), and DC03909 (AJO).

# 520 The Relationship Between DPOAE Suppression Tuning and Acoustic Reflectance/Admittance in Human Infants Carolina Abdala<sup>1</sup>, Sandy Oba<sup>1</sup>, Ellen Ma<sup>2</sup>, Douglas Keefe<sup>3</sup>

<sup>1</sup>House Ear Institute, <sup>2</sup>University of Southern California, School of Medicine, <sup>3</sup>Boystown National Research Hospital Human newborns show immaturities in DPOAE suppression that can partially be explained by immaturities in middle ear transmission (Abdala and Keefe, 2006 JASA) The present study assessed whether acoustic reflectance and admittance measured in the ear canal further explain these immaturities. DPOAE suppression tuning curves (STCs) at f2 = 6000 Hz and reflectance/admittance were measured in the same infants at birth and through 6 months of age (5 test sessions). DPOAE STCs remained immature throughout the 6 month test period: STCs were excessively narrow and steep on the low-frequency flank and the tuning curve tip was at lower levels in infants. Consistent with previous reports, reflectance and admittance features changed from birth through 6 months of age. In contrast, most STC features (Q10, tip-to-tail, slope on low-frequency flank and tip level) were relatively constant during this same timeframe, suggesting an apparent dissociation between DPOAE suppression and reflectance/admittance. Correlations between infant STC and reflectance/admittance accounted for < 10% of the variance in nearly all cases. Thus, reflectance/admittance explained relatively little of the variance in DPOAE suppression features from birth through 6 months of age. When adult data were added, correlations improved significantly, e.g., admittance magnitude at mid-to-high frequencies accounted for 47-65% of the variance in STC tip-to-tail ratio and Q10. This finding suggests that acoustic reflectance and admittance mav be useful in understanding changes in DPOAE suppression that occur from infancy through young adulthood.

(Research supported by NIDCD grants DC003552, DC006607 and the House Ear Institute.)

# | Frequency Dependence of the Spectral Period and Depth of DPOAE Fine Structure in Normal Hearing Subjects

Lauren Shaffer<sup>1</sup>, Jennifer Hill<sup>1</sup>

<sup>1</sup>Department of Speech Pathology & Audiology, Ball State University

Fine structure is a normal feature of evoked otoacoustic emissions that are recorded with fine frequency resolution. While this pattern exists to some extent in most subjects with normal hearing, the frequency range over which fine structure is observed and the depth of fine structure varies significantly between individuals. Sources for the variation in fine structure pattern amongst individuals remain largely unidentified, although suppression or damage to the reflection component of distortion product otoacoustic emissions (DPOAEs) has been shown to reduce or abolish the fine structure pattern (Mauermann et al., 1999, Talmadge et al., 1999). The spacing between adjacent amplitude maxima or minima in the fine structure has been referred to as the spectral period of otoacoustic

emissions (Zwieg and Shera, 1995). We report measures of fine structure spacing and fine structure depth from a group of normal hearing subjects. Specifically we recorded the 2f1-f2 DPOAE for the frequency range of 1000-6000 Hz using a frequency ratio of 1.22, with two different level conditions (L1=60, L2=45; L1=55, L2=40). Preliminary results suggest frequency dependence for both measures. We discuss the frequency dependence of these measures, comparing our results to theoretical predictions and other recently published data.

### **522** A Non-Linear Finite-Element Model of the Newborn Tympanic Membrane

**Li Qi**<sup>1</sup>, W. Robert J. Funnell<sup>1</sup>, Sam J. Daniel<sup>1</sup> \*\*McGill University

The tympanic membrane (TM) in newborns is significantly different from that in adults. Understanding the behaviour of the newborn TM, including its response to high static pressures, is important for interpreting tympanometric measurements in newborn hearing screening and diagnosis. Here we present a three-dimensional non-linear finite-element model of a 22-day-old newborn TM. The geometry is based on a clinical X-ray CT scan and on the published literature, supplemented by histological images. A polynomial hyperelastic constitutive law is used and large deformations of the TM are simulated. Plausible ranges of material properties are explored. The volume displacement of the TM under high static pressures is calculated and compared with available tympanometry results.

### 523 Modeling the Incudo-Malleal Joint and Its Mechanical Properties

**Minyong Shin**<sup>1,2</sup>, Jae Hoon Sim<sup>2,3</sup>, Charles Steele<sup>3</sup>, Sunil Puria<sup>3,4</sup>

<sup>1</sup>Stanford University, Department of Aeronautics and Astronautics, <sup>2</sup>Department of Veterans Afairs, <sup>3</sup>Stanford University, Department of Mechanical Engineering, <sup>4</sup>Stanford University, Department of Otolaryngology-HNS Modeling middle ear ossicles dynamics is essential in order to elucidate structure and functional relationships of the middle ear and to develop prostheses. One of the difficulties in developing ossicles model is the joint between the incus and the malleus (IM). Since this connection occurs over a wide area, a simple spring-dashpot model cannot reflect its functional properties. The goal of this research is to develop a mathematical model of the IM joint and perform a parametric study to estimate its mechanical properties.

We present a mathematical model of the IM joint based on lubrication theory. Parameter estimation proceeds by comparing the simulation result with 3-D motion measurements. The experiment for the measurements is carried out by fixing the malleus and exciting the incus with a magnetic force and moment motor developed for small biological structures. The response of the incus is measured at 4 points in 3 directions, using a Laser Doppler Vibrometer. 3-D reconstruction of microCT scan images of the IM complex provides morphometry of the IM joint with approximately 10  $\mu m$  resolution. As shown previously (J.Marquet,1981) the IM joint forms an articular

capsule which has viscous fluid surrounded by an articular ligament (elastic wall) between incus and malleus at the outer boundary of the joint. Considering its thin geometry and capsular structure with the elastic wall around to confine the viscous fluid, lubrication theory and an elastic wall boundary condition are used in the mathematical model. The viscosity of the fluid inside the capsule and Young's modulus along the elastic wall are the unknown parameters for the calculation. Results show 1) measured x, y, z velocity in local coordinates in frequency domain, 2) 3-D geometry of IM joint, 3) pressure distribution when motion is applied to the surfaces, 4) mechanical property estimation including viscosity of the fluid inside the joint and Young's modulus distribution along the articular ligament.

#### 524 Multi-Field Coupled Finite Element Analysis for Sound Transmission in Otitis Media with Effusion

Rong Gan<sup>1</sup>, Xuelin Wang<sup>2</sup>

<sup>1</sup>School of Aerospace & Mechanical Engineering and Bioengineering Center, University of Oklahoma, <sup>2</sup>School of Aerospace & Mechanical Engineering, University of Oklahoma

Otitis media with effusion (OME) as a middle ear disease is diagnosed with fluid in the middle ear cavity and commonly has the middle ear pressure differing from atmospheric pressure. These mechanical changes in the ear result in conductive hearing loss which was characterized by a reduction of the movement of the tympanic membrane and stapes footplate in cadaver ears or human temporal bones in our lab. In this paper, we report a newly constructed 3-D finite element (FE) model of human ear based on a set of histological sections of a human temporal bone. This model not only adds another individual model into our ear model data base, but also extends the FE analysis into a new dimension for multifield FE analysis of pathological ears. The OME was first simulated in the model with variable fluid levels in the middle ear cavity. The interfaces between the air, structure, and viscous fluid in the ear canal and middle ear cavity were identified, respectively. The acoustic-structurefluid coupled FE analysis was conducted in the model under 90 dB SPL input sound in the ear canal as the middle ear fluid level was varied from zero to a full fill of the cavity. The results include the model-predicted displacements of the tympanic membrane and stapes footplate when fluid in the cavity was varied. The FE results were compared with the data obtained in human temporal bones. Finally, the change of middle ear transfer function induced by fluid variations in the cavity was derived. This study provides a new method to evaluate the effect of OME on middle ear function for sound transmission. (Supported by NIH/NIDCD and NSF/CMS)

## 525 A Finite Element Model for the Coupled Middle Ear of the Domestic Cat From Mct Imaging Data

James Tuck-Lee<sup>1,2</sup>, Peter Pinsky<sup>1</sup>, **Sunil Puria<sup>1,2</sup>**<sup>1</sup> Stanford University, <sup>2</sup> Veterans Affairs Palo Alto Health Care System

Physics-based models of the middle ear enable the vibrational response to be computed over the physiological frequency range of hearing, given accurate anatomical geometry, mesh resolution, meaningful material properties, and model assumptions. We have developed a fully coupled finite element model of the middle ear of the domestic cat towards this goal, using computed tomography (CT) imaging of cadaver specimens. The geometries of the ear canal, eardrum, and middle ear cavities were determined, including the overall thickness of the eardrum, from the µCT data. The microstructure of the eardrum is taken from Fay et al. (2005, J Biomech), modeling the eardrum as a composite, and using the same thickness properties for the two separate layers of aligned collagen fibers. Unlike Fay's model, however, this is a fully coupled three dimensional acoustic model for the ear canal and middle ear cavities, and we do not make any assumptions regarding axisymmetry for the local drum elements. We add prestress of the eardrum via loading at the tensor tympani attachment to the malleus, and use a circuit model representation of the ossicles and cochlear load (Puria and Allen, 1998, JASA) attached at the umbo. Finally, we have added mass moment of inertia terms for the ossicles, based on mass estimates and calculations from µCT data, on the hypothesis that these rotational terms become significant at higher frequencies.

The finite element model response is compared in both open and closed-cavity situations to existing experimental data, using a radiating boundary condition for the open cavity. We also observe the behavior of different points on the eardrum at to study the apparent mistuning effect of multiple resonances. Modifications are then made to the geometry and properties of the model, including changing levels of prestress, the added rotational inertia of the ossicles, and the removal of the septum. These help us to better understand the structure-function relations in the eardrum and middle ear cavities, and its behavior at higher frequency ranges.

### **526** The Effects of Complex Stapes Motion on the Cochlear Response in Guinea Pigs

**Alexander Huber**<sup>1</sup>, Damien Sequeira<sup>1</sup>, Christian Breuninger<sup>2</sup>, Albrecht Eiber<sup>2</sup>

<sup>1</sup>University Hospital Zurich, <sup>2</sup>University of Stuttgart According to the classical theory of hearing, only piston like movements of the stapes cause hearing sensations. On the other hand, rocking like stapes movements, with no net volume flux through the oval window, that occur naturally at higher frequencies are no stimulus to the cochlea.

It was the goal of this study to test this hypothesis.

In anesthetized guinea pigs a custom-built, three-axis piezoelectric actuator, capable of eliciting any desired vibration mode, was coupled to the stapes superstructure. The produced different movement patterns were controlled

by laser Doppler vibrometry and electrophysiological measurements of the cochlear potentials were simultaneously recorded.

The results of the present study show a cochlear excitation in all distinct movement patterns of the stapes, including rotational movements that could not be explained by the prevailing theory of hearing. Hence, the hypothesis was not verified.

#### 527 A Gear in the Middle Ear

**Sunil Puria**<sup>1,2</sup>, Jae Hoon Sim<sup>1,3</sup>, Minyong Shin<sup>3,4</sup>, Charles Steele<sup>1</sup>

<sup>1</sup>Stanford University, Mechanical Engineering,

<sup>2</sup>Otolaryngology-HNS, <sup>3</sup>Palo Alto Veterans Adminstration,

<sup>4</sup>Aeronautics and Astronautics

The malleus, incus and the coupling joint between them are unique to mammals and what role they play in sound transmission to the stapes is not well understood. At high frequencies, middle ear dynamics is determined by threedimensional inertial properties of the ossicles, which depends on their mass distribution. To better understand the dynamics of the malleus and incus we used the microCT imaging modality to scan cadaveric temporal bones of human, cat, chinchilla and guinea pig ears and reconstructed the volumes of their ossicles. The volume reconstruction of the malleus indicates that it has a solid rod-like shape in human, is a hollow elliptical cylinder in cat, and has an I-beam like shape in guinea pig and chinchilla. By contrast the long process of the incus has a solid rod-like shape. From the ossicle volumes, principal axis of rotation and pricipal moments of inertia, around the center of gravity, were calculated.

In both human and cat, the minimum moment of inertia is for rotational vibration along the long axis of the malleus (inferior-superior axis). The rotational moment of inertia for the two other orthogonal directions is higher by a more than a factor of 5. How is the torsion motion of the malleus coupled to the stapes, which lies in an orthogonal plane? The malleus-incus joint (MIJ), which is mobile in human and cat, provides the needed angle change for the torsion motion of the malleus to be transferred to rotation of the incus in a direction perpendicular to the stapes axis. One can think of the malleus-incus joint in a manner analogous to bevel gears and helical gears found in machinery. Both the mobile MIJ and bevel gears allow a change in the operating angle of two linked rotational shafts. Consistent with this view, the malleus is cylindrically shaped which is strong against torsion. Asymmetrical anatomy and material properties of the eardrum can result in assymetrical motions at high frequencies, which in turn lead to rotational motion of the manubrium. In contrast to the human and cat, both guinea pig and chinchilla have a fused MIJ. And their minimum moment of inertia is through the fused anterior-posterior axis, which indicates that the classical axis of rotation is maintained at low and high frequencies in these species. This is consistent with the I-beam like malleus shape that is better suited for bending rather than

[Work supported by grant No. 05960 from the NIDCD of NIH.]

### 528 Non-Middle Ear Causes of Air-Bone Gaps

**Saumil Merchant<sup>1,2</sup>**, Chris Halpin<sup>1,2</sup>, Wade Chien<sup>1,2</sup>, John Rosowski<sup>1,2</sup>

<sup>1</sup>Massachusetts Eye and Ear Infirmary, <sup>2</sup>Harvard Medical School

The majority of cases of an air-bone gap (as determined by audiometry) result from disorders affecting the external or middle ears. This presentation will review our clinical experiences with (1) inner ear lesions and (2) audiometric artifacts that can lead to an air-bone gap. These patients usually have a normal tympanic membrane and an aerated middle ear, thus mimicking middle ear pathology such as otosclerosis. Accurate diagnosis is important to avoid unnecessary middle ear surgery.

Audiometric artifacts with spurious air-bone gaps include leakage of sound around head phones, collapse of the ear canal and impedance mismatch with a large mastoid cavity. These may be suspected when tuning fork tests do not match the audiogram. Repeat audiometry with proper technique is helpful in the diagnosis.

Inner ear lesions that can present with an air-bone gap without vestibular symptoms include dehiscence of the superior semicircular canal, enlarged vestibular aqueduct, Paget's disease of the temporal bone, intralabyrinthine schwannoma, and occlusion of the round window from the cochlear side by otosclerosis. Such lesions comprised 13% of a series of 117 consecutive cases with an air-bone gap greater than or equal to 20 dB and a healthy, intact tympanic membrane. Diagnostic clues include presence of the acoustic reflex, bone conduction thresholds better than 0 dB, presence of the VEMP response with abnormally low thresholds, hypermobility of the umbo on laser Doppler vibrometry, and imaging studies in selective cases. These inner ear disorders can be considered as experiments of nature, and investigation of their mechanics can provide insight into pathways of sound transmission in the middle and inner ears. Research into their mechanics can also lead to better diagnostic tests, such as measurement of umbo motion by laser vibrometry.

The presentation will also review appropriate nomenclature with respect to air bone gaps and conductive hearing loss.

Supported by NIDCD

# | 529 | High Resolution Heterodyne | Interferometry Measurement of Middle Ear | Ossicle Displacement Under Quasi-Static | Pressure Changes

Joris Dirckx<sup>1</sup>, Jan Buytaert<sup>1</sup>, Wim Decraemer<sup>1</sup>

<sup>1</sup>University of Antwerp

We developed a setup to measure displacement of middle ear ossicles with high resolution using a heterodyne interferometer with position decoder. The setup was used to investigate the response of the middle ear to slowly varying pressures by measuring the displacement of the umbo and the stapes in rabbit. Displacement versus pressure curves were obtained at linear pressure change rates of 200Pa/s, 300Pa/s, 500Pa/s, 1kPa/s and 1.5kPa/s, with amplitude ±2.5kPa. We found that stapes amplitude is independent of pressure change rate (34ìm±5ìm, n=6). The stapes displacement versus pressure curves are highly non-linear and level off for pressures beyond ±1kPa. Stapes motion shows no measurable hysteresis at 1.5kPa/s, which demonstrates that the annular ligament has little visco-elasticity. Hysteresis increases strongly at the lowest pressure change rates. Stapes motion is not a simple lever ratio mimic of umbo motion, but is the consequence of complex changes in ossicle joints and ossicle position. Umbo amplitude increases a little from (118ìm±15ìm n=6) at 1.5kPa/s to (165ìm±19ìm, n=6) at 200Pa/s. At 1.5kPa/s, the ratio of stapes and umbo amplitude is (0.29±0.02, n=6), at 200Pa/s this ratio decreases to (0.21±0.02, n=6). Umbo motion already shows significant hysteresis at 1.5kPa/s, but hysteresis increases further as pressure change rate decreases. We conclude that in the quasi-static regime ossicle movement is not only governed by visco-elasticity, but that other effects become dominant when pressure change rate decreases below 1kPa/s. The increasing hysteresis can be caused by increasing friction as speed of movement decreases, and incorporating speed depending friction coefficients will be essential to generate realistic models of ossicle movements at slow pressure change rates.

### 530 Exploring Sound Transmission Through the Middle Ear by Tracing Middle Ear Delay

Ombeline de La Rochefoucauld<sup>1</sup>, Elizabeth Olson<sup>1</sup>

<sup>1</sup>Columbia University

Based on comparisons of ear canal and intracochlear pressure (measured in scala vestibuli just behind the footplate), the gerbil middle ear transmits sound with a gain of  $\sim 20 - 25$  dB that is almost flat with frequency (up to at least 45 kHz), and a delay-like phase corresponding to a 25 - 30 μs delay (Olson, 1998, JASA; Dong and Olson, 2006, JASA). The relationship between ear canal pressure and stapes velocity is similarly delay-like (e.g., Olson and Cooper, 2000, ARO). In a different study, Puria and Allen (1998, JASA) measured and modeled a ~36 μs tympanic membrane acoustic delay in the cat middle ear. Just how the middle ear is able to transmit sound with such high temporal and amplitude fidelity is not known, and is particularly mysterious given the complex motion the ossicles and tympanic membrane are known to undergo (e.g. Decraemer, Khanna and Funnell, HR, 1989). In this study we explore middle ear sound transmission by looking within the middle ear transmission path for sources of the delay. Experiments are performed in vivo on gerbils using a heterodyne interferometer. Velocity of the middle ear components is measured and phases are compared in order to trace the delay. Based on ear canal length, acoustic delay can account for  $\sim$  10  $\mu s$  of the delay. Within the ossicular path at frequencies up to ~ 25 kHz we find that the stapes motion (along the piston axis) is delayed by  $\sim 7 \mu s$  relative to the umbo, and the amplitude ratio (stapes/umbo) is relatively flat. At higher frequencies this relationship seems to become more complex.

By tracing the middle ear delay and identifying mechanical sites where delay occurs, we hope to better understand how acoustic signals in the ear canal are transformed to the mechanical signals that are transmitted by the ossicles and finally excite the cochlea.

# [531] The Pedicle of Lenticular Process in Gerbil, Cat and Human Does not Produce a Boost at the High Frequency Limit of the Audible Range

**Willem Decraemer**<sup>1</sup>, Ombeline de La Rochefoucauld<sup>2</sup>, Shyam Khanna<sup>2</sup>, Joris Dirckx<sup>1</sup>

<sup>1</sup>Univ. of Antwerp, <sup>2</sup>Columbia University

In a recently reopened discussion on the factors that limit the bandwidth of hearing in mammals, a new finding, a boost across the pedicle, was described by Robles et al. (ARO 2006, abstract 639). Based on measurements on chinchilla they concluded that at the high frequency end of the audible range (above 32 kHz in chinchilla) the amplitude of ossicular vibration is increased up to 20 dB between the long process of the incus (LPI) and the head of the stapes while the phase accumulates an extra phase lag. From measurements at the LPI and lenticular plate of the incus (LenPI), in a first series of measurements, they had already drawn the same conclusion. The effect was seen as nature's way to widen the bandwidth of middle ear transfer further.

We have performed experiments and reanalyzed some of our older ossicular vibration data to verify whether we can find a similar boost in a few species: gerbil, cat and human.

When opening the pars flaccida in gerbil the view allows a direct measurement of the component of vibration of the LPI and the LenPI along the piston direction of the stapes. LPI and LenPI vibration measured in direct succession in several animals, in an anesthetized or fresh cadaver condition, do not show a significant amplitude boost or phase lag across the pedicle as described in chinchilla.

Three-dimensional vibration measurements of the entire ossicular chain in cat and human do not show large differences in vibration amplitude or phase between the LPI and stapes head at high frequencies.

Chinchilla could have a specific comportment or else methodological difference in measuring the vibration velocity (at an angle with the piston direction?) may be the cause of the discrepancy with our findings.

# | 532 | Analysis of Stapes Three-Dimensional Motion: Effects of Modifying Malleolar and Incudal Ligaments

**Hideko Heidi Nakajima**<sup>1</sup>, Saumil N. Merchant<sup>1</sup>, John J. Rosowski<sup>1,2</sup>, William T. Peake<sup>1,2</sup>

<sup>1</sup>The Eaton-Peabody Lab, Mass. Eye & Ear Infirmary, Dept Otology & Laryngology, Harvard Med School, <sup>2</sup>Research Lab. of Electronics, Mass. Institute of Technology

With low-frequency acoustic stimuli in normal human ears, piston-type motion of the stapes is thought to be the dominant mode of motion; however, existing descriptions

of the spatial components of stapes motion are not definitive. The stapes is assumed to be driven by rotational motion of the malleus-incus complex with the anterior malleal ligament (AML) and posterior incudal ligament (PIL) defining the axis of rotation. We have measured the 3-D motion of the head of the stapes and how it is affected by modification of AML and PIL.

Laser Doppler velocity measurements were made on the

head of the stapes from 3 directions to resolve 3 piston-type orthogonal components: (medial-lateral) motion, superior-inferior motion (perpendicular to the long axis of the stapes footplate), and anterior-posterior motion (perpendicular to the short axis of the stapes footplate). We determined the effects on these components of manipulations such as stiffening and cutting the axial ligaments in three fresh human cadaveric temporal bones. The superior-inferior motion of the stapes head in the normal middle ear was found to be similar in magnitude to the piston-type motion, presumably a consequence of stapes rotation around the footplate's long axis,. The anterior-posterior motion, perhaps associated with rotation around the short axis of the stapes footplate, was significantly (~20 dB) smaller than the other two components. These findings have implications regarding the coupling of rotational motion of the incus to the stapes. Stiffening the axial ligaments generally had little effect on stapes motion. Cutting the AML resulted in small effects in the piston-type and superior-inferior motion (~2 dB), but more in the anterior-posterior (~5 dB). Cutting both the AML and PIL resulted in increased velocities (~10 dB) in the anterior-posterior direction. At high frequencies (generally between 1-2 kHz), there were sometimes narrow-band changes in all directions with most manipulations.

#### 533 Measures of Middle-Ear Mechanics in a Retinoic Acid Receptor Alpha Mutant Mouse

John Rosowski<sup>1</sup>, Melissa Wood<sup>1</sup>, Raymond Romand<sup>2</sup>

<sup>1</sup>Massachusetts Eye & Ear Infirmary, <sup>2</sup>Institut de
Génétique et de Biologie Moléculaire et Cellulaire,
Strasbourg, France

Retinoc acid receptors play a significant role in the development of the mammalian fetus, including the development of ear structure and sensory mechanisms. Recently a retinoic acid receptor alpha knockout mouse (RARalpha-/-) has been demonstrated to exhibit significant 30-40 dB hearing loss in its adult stage (Romand et al. unpublished observations). The inner-ear sensory and neural structures in these RARalpha-/- mutants seem to be normal, though there are mild structural abnormalities in the ossicular chain. In order to test whether the hearing loss in these mutants had a conductive component, we measured sound-induced umbo velocity in a group of RARalpha-/- and in a group of age-matched RARalpha+/+ non-mutants. Umbo velocity was measured with a laser-Doppler vibrometer in response to frequency-modulated sound signals containing frequencies from 1 to 50 kHz. The sound pressure of the stimulii was monitored by a probe-tube microphone positioned just at the opening of the bony ear canal. The umbo-velocity in the control population of RARalpha+/+ mice is similar to velocities measured in other strains of mice of similar age. The magnitude of the umbo-velocity in the mutant RARalpha-/-population was on average 10-15 dB lower than in controls, with the largest differences occurring at frequencies < 10 kHz. However, the responses in the mutant ears were quite variable, with some mutants having velocities of near normal magnitude and others in which the velocities were hidden in the vibrometer noise. The ears of several control and mutant mice have been embedded in celloidin and are being prepared for sectioning and morphometric analyses of the middle ears.

#### 534 Preliminary Analyses of Tympanic-Membrane Motion From Holographic Measurements

**John Rosowski**<sup>1,2</sup>, Matthew Rodgers<sup>3</sup>, Michael Ravicz<sup>1</sup>, Cosme Furlong<sup>3</sup>

<sup>1</sup>Eaton-Peabody Lab., Dept. of Otolaryngology, Mass. Eye & Ear Infirmary, Boston MA, <sup>2</sup>Harvard-M.I.T. Div. of Health Sciences and Technology, Cambridge MA, <sup>3</sup>Dept. of Mechanical Engineering, Worcester Polytechnic Institute, Worcester MA

A new system for the rapid holographic measurements of the sound-induced displacement of the surface of the tympanic membrane (TM) [Furlong et al., ARO 2006 #644] has been used to quantify the pattern of TM motion in post-mortem cat and chinchilla heads. First, high-speed time-averaged holography, which provides full-field-of-view identification of the nodal patterns of TM motion at video rates while a stimulus tone is swept in frequency, was used to determine the natural frequencies of the TM. Second, stroboscopic holography was used to determine the absolute positions of >60,000 points on the eardrum surface in response to tonal sound stimuli at the natural frequencies and other frequencies of interest at 4 to 8 instants per stimulus period. These measurements allow us to reconstruct the magnitude and phase of soundinduced TM motion.

In this presentation we address several issues in the analysis of holographic data: (1) An automatic procedure to isolate the TM within the hologram. We have developed techniques that evaluate (a) the magnitude of motion, (b) the gradient of motion, and (c) spatial correlations in reflectivity to mask the non-moving surroundings from the image, leaving only the TM. The resulting TM data are then used to quantify the volume displacement of the membrane with sound stimuli of known level, where the ratio of the time-rate of change of volume to the sound pressure is the acoustic admittance. measurements suggest admittance values that are similar to admittances quantified by acoustic techniques. Quantification of wave motion on the TM. The masked patterns are analyzed by 2-dimensional Fast-Fourier transforms, which reveal the primary components of wave motion in various directions across the TM surface. Such transforms describe radial waves of motion on the surface of the chinchilla TM at frequencies as low as 5 kHz and demonstrate that the wavelength of TM wave motion decreases as frequency increases.

### 535 Variations in Static Pressure in Chinchilla Middle Ears with Blocked Eustachian Tube

**John Rosowski<sup>1,2</sup>**, Michael Ravicz<sup>1</sup>, Saumil Merchant<sup>1,2</sup>, Michael McKenna<sup>2</sup>

<sup>1</sup>Eaton-Peabody Lab., Massachusetts Eye & Ear Infirmary, Boston MA USA, <sup>2</sup>Dept. of Otology & Laryngology, Harvard Medical School, Boston MA USA

Fluid accumulation in the middle ear is frequently seen in otitis media. The accumulation of middle-ear fluid can cause hearing loss and may be associated with infection that damages middle-ear structures and imperils health. The trigger for generation of fluid in the middle-ear is believed to be negative middle-ear pressure caused by absorption of middle-ear gas by a combination of metabolic processes and net gas transfer from the middle ear to the blood. Normally, periodic openings of the Eustachian tube allow middle-ear pressures to equilibrate. Therefore, negative pressure and middle-ear fluid are linked to Eustachian tube dysfunction.

We are developing a chinchilla model of Eustachian tube dysfunction in order to test possible therapies. In chinchilla, the normal Eustachian tube is semi-patulous [Doyle, Arch Otolaryngol. 1985; 111:305-8] and allows easy equilibration of middle-ear pressure, even when the animal is anesthetized. Blocking the Eustachian tube by silicone injections resulted in a transient increase in middle-ear static pressure that reversed after several hours and eventually led to the development of a negative middle-ear pressure relative to ambient. The rate of pressure decrease suggests that 1) gas is absorbed from the middle ear and 2) the rate is substantially lower than the 2-4 microliter per minute uptake estimated for human ears [Elner, Acta Otolaryngol 1977;83: 25-8].

## 536 Investigation of the Mechanics of Type III Stapes Columella Tympanoplasty Using Laser Doppler Vibrometry

**Wade Chien<sup>1,2</sup>**, John Rosowski<sup>1,2</sup>, Saumil Merchant<sup>1,2</sup>

<sup>1</sup>Massachusetts Eye & Ear Infirmary, <sup>2</sup>Harvard Medical School

The type III stapes columella tympanoplasty procedure involves placing a fascia graft directly onto the stapes head. Postoperative hearing results vary widely, with airbone gaps ranging from 10 to 60 dB.

Our goal was to investigate structure-function correlations after this procedure and understand its mechanics. We used laser Doppler vibrometry to measure velocity of the tympanic membrane (TM) graft in 22 patients (23 ears). Measurements were made at three locations: over the stapes, round window and protympanum. These velocity measurements were correlated with stapes mobility (judged at surgery), post-operative aeration status (assessed by autoinflation or by postoperative CT scan), and the postoperative audiometric result.

The 23 ears were divided into three groups: 1) Non-aerated ears, n=2. The air-bone gaps were 40-60 dB. TM velocities over all three locations were 20-40 dB lower than normal umbo velocity in normal hearing subjects. 2) Fixed

stapes with an aerated middle ear, n=2. The air-bone gaps were 40-60 dB, and TM velocities were equivalent to normal umbo velocity in one case, and lower by 15-20 dB in another case. 3) Mobile stapes and aerated middle ear, n=19. There were two subgroups: small air-bone gaps ≤ 30 dB (n=7) and large gaps > 30 dB (n=12). There were significant differences in TM graft velocities over the stapes between these two subgroups. At low frequencies (300 Hz), graft velocity over the stapes was 3-5 dB higher in patients with large gaps (p < 0.05), suggesting inadequate coupling between the graft and the stapes. At frequencies above 1000 Hz, graft velocity over the stapes was 5-10 dB higher in patients with small gaps (p < 0.05). In conclusion, in addition to stapes mobility and middle-ear aeration, other important determinants of hearing may include how well the TM graft moves with sound and how well it couples to the stapes. Also, laser Doppler vibrometry has utility in post-operative diagnosis of nonaeration of the middle ear.

#### 537 Viral Gene Expression in the Mouse Inner Ear, *In Vitro* and *In Vivo*

Clifford Hume<sup>1,2</sup>, Ming Xiao<sup>1</sup>, Hsin-Pin Lin<sup>1</sup>, Debbie Bratt<sup>1</sup> <sup>1</sup>University of Washington, Dept of Oto HNS, <sup>2</sup>VMBHRC Gene therapy for hearing loss and balance disorders will require delivery vehicles that can efficiently and specifically target the appropriate cell types in the inner ear. In other organ systems, this has required careful matching of nonreplicating, non-disease causing viruses with gene control elements active only in the target cells. This "doubletargeting" maximizes the safety and specificity of each therapy. For each particular molecular or cellular defect, the required temporal and spatial specificity of gene expression will be unique. Because of the availability of models of human hearing loss, we have focused on identifying the cellular targets of viral infection in the mouse inner ear. In the current studies, we compared the targets of Type 5 Adenovirus (E1-/E3-/polymerase-) and AAV6 infection in vitro and in vivo in normal hearing mice. In vitro cultures were established from neonatal Swiss Webster mice (P0-P5), infected with viruses after one day of culture and analyzed after three days. For the vivo studies, viruses were injected into the inner ears of adult Swiss Webster mice either through a posterior semicircular canalostomy or a basal turn cochleostomy. Two weeks after injection, ears were analyzed by frozen section immunohistochemistry. Using hCMV-GFP reporters, we find that both of these viruses target dramatically different cell types in vitro and in vivo at these ages. dependence on site of inoculation also varies depending on the virus. While the reporters in both of these viruses are strongly expressed in auditory and vestibular hair cells in vivo, the predominant targets of infection in the neonatal organ of Corti are non-sensory cells.

# 538 Superparamagnetic Iron Oxide Incorporated into PLGa Nanoparticles as a Potential Non-Viral Vector for Inner Ear Therapy

Ronald Wassel<sup>1</sup>, Richard Kopke<sup>1,2</sup>, Kejian Chen<sup>1</sup>, Brian Grady<sup>3</sup>, Angelica Vasquez<sup>4</sup>, Kenneth Dormer<sup>1,2</sup>

<sup>1</sup>Hough Ear Institute, <sup>2</sup>University of Oklahoma Health Science Center, <sup>3</sup>University of Oklahoma, <sup>4</sup>Oklahoma Medical Research Foundation

Hearing loss affects ~39 million Americans, noise-induced hearing loss for example, being a major cause of hair cell loss and disability. Hair cells neither naturally repair nor regenerate in mammals. Restoration of hearing through regeneration of cochlear hair cells from remaining supporting cells by gene therapy with Math-1 using viral vectors has become a distinct possibility recently. Nevertheless, a non-viral, non invasive approach would be preferable in a clinical setting for reasons of safety and efficacy.

Superparamagnetic iron oxide nanoparticles (SPIONs) were coated with oleic acid then encapsulated into poly(D,L-lactide-co-glycolide) (PLGA) particles using an oil-in-water-in-oil emulsion technique. Size of the composite particles, as determined by dynamic light scattering, could be varied from 160 nm to 280 nm by varying either power or time of sonication while the zeta potential remained near -20 mV. Transmission electron microscopy showed SPIONs ranging in diameter from 5 to 15 nm encapsulated inside the polymer and indicated that they were uniformly dispersed within the PLGA particles.

SPIONs, multiply encapsulated into PLGA formed composite nanoparticles (SPN's) that were moved across the RWM in guinea pigs and cadavers, as well as into various cell cultures. These results have been confirmed by either transmission electron or confocal microscopy. When a large concentration of nanoparticles was directly injected into the cochlea SPN's were found in the organ of Corti. The SPNs have been shown to have enhanced transport across the round window membrane by magnetic targeting. In this case the SPN's were observed in the RWM, in the perilymph and tissue of the basal turn (basilar membrane, and stria vascularis).

The results suggest that SPN's can be used to deliver therapeutic biomolecules into perilymphatic fluid via transport across the cochlear round window membrane (RWM) using an external magnetic field.

### 539 Coxsackie Adenovirus Receptor and ανβ3/ανβ5 Integrins in Adenovirus Gene Transfer of Rat Cochlea

**Frederic Venail**<sup>1,2</sup>, Jing Wang<sup>1</sup>, Jerome Ruel<sup>1</sup>, Guy Rebillard<sup>1</sup>, Michel Eybalin<sup>1</sup>, Jean Luc Puel<sup>1</sup>

<sup>1</sup>INSERM U583, <sup>2</sup>ENT department - University Hospital Gui de Chauliac - Montpellier

This study was designed to determine whether Coxsackie adenovirus receptor (CAR) and alphavbeta3/alphavbeta5 integrin co-receptors are involved in adenovirus gene transfer in the rat cochlea. We find that CAR and integrin

co-receptors are expressed in every cell subtype transduced by the adenoviral vector Ad5 DeltaE1-E3/cytomegalovirus/green fluorescent protein (GFP) on cochlear slices in vitro. The spiral ganglion neurons, which do not express CAR, were not transduced by the virus. Blocking these receptors by monoclonal antibodies decreased transgene expression, whereas disrupting tight junctions with ethylenediaminetetraacetic acid led to an increased transgene expression. However, sensory hair cells and strial cells also expressing CAR and alphav integrins were not transduced by the vector. GFP expression was also studied in vivo. Perilymphatic perfusion of adenovirus in vivo did not affect hearing and only cells lining the perilymphatic spaces were transduced. Endolymphatic perfusion resulted in low-frequency hearing loss and although some cells of the organ of Corti were efficiently transduced, the sensory and the strial cells were not. Transduced sensory and strial cells were occasionally observed in cochleas after single shot of adenovirus. Pretreatment with anti-CAR and anti-alphav antibodies decreases GFP expression in vivo, suggesting that the CAR/alphav integrin pathway is involved in adenovirus transduction in the cochlea.

### 540 The Effect of Age of Injury on the Efficacy of Math1 Mediated Hair Cell Restoration *In Vitro*

Kim Baker<sup>1</sup>, Chi Hsu<sup>2</sup>, Douglas E. Brough<sup>2</sup>, Mark Praetorius<sup>3</sup>, **Hinrich Staecker**<sup>4</sup>

<sup>1</sup>Univ. of Maryland, <sup>2</sup>GenVec Inc., <sup>3</sup>Univ. Heidelberg, <sup>4</sup>Univ. Kansas School of Medicine

Delivery of the atonal homolog math1 has been demonstrated to result in the generation of hair cells after aminoglycoside damage. To study the dynamics of hair cell regeneration we treated adult mouse macular organ cultures with neomycin followed by an advanced generation adenovector carrying math1 driven by the human CMV promoter, the chicken beta actin promoter or the glial fibrillary acidic protein promoter. These promoters differ both in strength of expression, expression kinetics and cell specificity. Total dose of vector was varied as was the time post neomycin treatment that vector was administered to the explants. At 5 day intervals explants were fixed and either whole mount stained for myosin VII or serially sectioned and stained for myosin VII. Total hair cell counts were obtained for each culture condition. The choice of promoter was found to significantly affect the math1 expression levels and the effect of math1 on damaged tissue. In vitro restoration of hair cells could be seen by 5 days post math1 delivery. Efficacy of math1 mediated hair cell restoration declined with progressive delay post injury. This corresponded to tissue changes in the expression of regulators of math1.

## 541 Comparative Analysis of Chick Sensory Epithelium Viability When Cultured on Artificial Matrices

**Nathaniel Spencer**<sup>1,2</sup>, Luke Duncan<sup>2</sup>, Catherine Klapperich<sup>1</sup>, Douglas Cotanche<sup>2</sup>

<sup>1</sup>Boston University, <sup>2</sup>Children's Hospital of Boston

The chick sensory epithelium regenerates in response to damage in vivo. In this study, a technique was developed for preserving the chick auditory organ in vitro for physiological, pharmalogical and future applications. The sensory epithelia were isolated from the chick, and the distal-mid sections were attached to artificial extracellular matrices. Puramatrix, collagen, collagenchondroitin sulfate and matrigel are soft substrates that were chosen for the broad range of signaling features presented to the sensory epithelia. Puramatrix was used both in and without tension. The stiffnesses of the matrices at time zero was characterized. Dimensional analysis of the epithelia was conducted, and stereocilia density quantified, for 24h, 48h and 72h time points on each matrix. It was determined that while all four matrices were suitable for three days of culture, the collagenchondroitin sulfate substrate was the most consistent in promoting hair cell survival. This may indicate a prosurvival feature of the inclusion of glycosaminoglycan chains in the culture system.

### 542 Sox2 and Jagged1 Expression in Adult Mouse Inner Ear Sensory Epithelia

**Elizabeth Oesterle**<sup>1</sup>, Sean Campbell<sup>1</sup>, Ruth Taylor<sup>2</sup>, Andrew Forge<sup>2</sup>, Clifford Hume<sup>1</sup>

<sup>1</sup>Department of Otolaryngology-HNS, VMBHRC, University of Washington, <sup>2</sup>Center for Auditory Research, UCL Ear Institute

In humans and other mammals, significant hair cell (HC) loss leads to irreversible hearing and balance deficits. whereas HC loss in non-mammalian vertebrates is repaired by spontaneous generation of replacement HCs. Research in HC regeneration has been hampered by the lack of in vivo damage models for adult mouse inner ear and a paucity of cell-type specific markers for non-sensory supporting cells in the sensory epithelium (SE). The present study had 2 purposes: To develop a protocol to damage adult mouse organ of Corti in vivo, and to investigate Sox2 and Jagged1 expression in adult mouse inner ear SE. Sox2, a transcription factor of the SRYrelated HMG box (SOX) family, is involved in proliferation and/or maintenance of neural stem cells and in Jagged1 is a member of the Notch neurogenesis. signaling pathway, a pathway thought to contribute to the regeneration of some mature tissues after damage. Sox2 and Jagged1 are known to be expressed in developing inner ear SE, but their expression in the adult ear remains to be delineated.

We report on a non-surgical approach for inducing HC damage in vivo in adult mouse organ of Corti by a single high-dose injection of the aminoglycoside kanamycin coupled with a single injection of the loop diuretic furosemide. This protocol results in outer hair cell (OHC)

lesions throughout virtually the entire length of the cochlea by 3 days after the injections. Using immunocytochemical techniques, Sox2 is shown to be expressed in supporting cells in normal and damaged adult mouse inner ear SE. Sox2 is also expressed in Type II vestibular HCs. Supporting cells in mature vestibular, but not auditory, SE express Jagged1. In sum, these results show that kanamycin with furosemide kills OHCs throughout the adult mouse cochlea and suggest Sox2 and Jagged1 are involved in the maintenance of some supporting cells in adult mouse ear.

Supported by: NIDCD R01 DC03944; NIDCD P30 DC04661, NICHHD P30 HD002274; Oberkotter Foundation

#### 543 Up-Regulation of Notch Signaling Following Ototoxic Deafening

**Shelley A. Batts**<sup>1</sup>, Christopher Shoemaker<sup>1</sup>, Yehoash Raphael<sup>1</sup>

<sup>1</sup>University of Michigan

During development, the mammalian cochlea is specified into heterogeneous cells types under the direction of Notch signaling system. Notch activity confers a prosensory character on groups of cells by "lateral induction", and subsequently establishes a fine-graded pattern of hair cells and supporting cells by "lateral inhibition." regenerative process of hair cells in non-mammalian vertebrates includes changes in Delta-Notch signaling. Such changes have not been reported in the mammalian ear. We tested whether differences in Notch expression (in comparison to birds) following ototoxicity are responsible for mammals' inability to produce hair cells postembryonically. Pigmented adult male guinea pigs deafened systemically with kanamycin and were ethacrynic acid, and then sacrificed either 24 hours, 3 days, 5 days, or 7 days later. Immunohistochemistry of cochlear whole mounts were performed using primary antibodies to Notch1, Jag1, Delta1, and activated Notch1 Results showed an up-regulation of Notch1 receptor expression in inner hair cells at 1 day, which was stable until 7 days. Jag1 expression was up-regulated in the Pillars and Deiters cells; expression peaked at 1 day and gradually decreased over the remaining time periods examined. NICD expression was widespread and peaked after 1 day post deafening, slightly decreasing at 3 days and remaining stable until 7 days. Delta1 expression at all time points was nonexistent. Therefore, we conclude that in mammals the pro-supporting cell ligand Jag1 is activated, in contrast to birds where the pro-hair cell ligand Delta1 is activated following ototoxicity. This reduces and impedes the chances of pre-existing progenitors in the organ of Corti from spontaneously differentiating into hair cells following ototoxic insults and subsequent Notch activation.

Supported by the Williams Professorship, by a gift from B. and A. Hirschfield, and by NIH/NIDCD Grants DC01634, DC05401, DC007634, DC05188.

### 544 Determination of Mechanotransduction and Prestin Immunoreactivity in the P27-/Mouse Cochlea

**Rende Gu<sup>1</sup>**, Carol Pierce<sup>1</sup>, Huy Tran<sup>1</sup>, James LaGasse<sup>1</sup>, Eric Lynch<sup>1</sup>, Jonathan Kil<sup>1</sup>

Previous reports from p27 knock-out (KO) mice indicate an increase in supporting cell and hair cell numbers (hyperplasia), the presence of supporting cell and hair cell regeneration, and a reduction in hearing sensitivity as measured by ABR (Lowenheim et al., PNAS 1999, Chen and Segil Dev 1999, Kanzaki et al., Hear Res 2006). We postulated that the loss of function in these mice is due to an alteration in the cytoarchetecture of the organ of Corti versus a loss of function that was cellular and or molecular in origin.

To hypothesis, test our we examined mechanotransduction ability of auditory hair cells using AM1-43, a fixable mechanotransduction dye analogous to FM1-43 (Gale et al., J Neurosci 2001, Geleoc and Holt, Nat Neurosci 2003). Results indicate that one month old p27 KO mice display the same ability to uptake AM1-43 as heterozygote and wild type littermates when evaluated in whole mount and cross section. We further determined the presence of prestin (the outer hair cell motor protein responsible for cochlear amplification) by using a prestin antibody under immunofluorescence. Whole mount and cross sectional analyses reveal equivalent prestin staining in p27 KO when compared to heterozygote and wild type littermates.

These data indicate that hair cells within the organ of Corti of the p27 KO mice possess the critical proteins necessary for mechanotransduction and electromotility found in normal hair cells. These data further support the hypothesis that the loss of hearing sensitivity in the p27 KO is not due to a defect at the cellular or molecular level, but an alteration of tissue cytoarchitechture.

#### 545 Towards Hair Cell Regeneration Through Manipulation of Retinoblastoma (pRb)

Sang Goo Lee<sup>1</sup>, Chandra Vargeese<sup>2</sup>, Pamela Pavco<sup>2</sup>, Roberto Guerciolini<sup>2</sup>, Zheng-Yi Chen<sup>1</sup>

<sup>1</sup>Massachusetts General Hospital and Harvard Medical School, <sup>2</sup>Sirna Therapeutics, Inc.

Previously we have established that retinoblastoma is a key gene controlling cell cycle exit, maturation and survival of inner ear sensory epithelia. In the cochlea, permanent deletion of pRb leads to cell cycle reentry of both hair cells and supporting cells in postnatal mice. Proliferating sensory epithelia ultimately undergo apoptosis, due to failure to mature properly. However, vestibular pRb-null hair cells survive and function in adult inner ear. Thus, it is postulated that the role of pRb in the cell cycle exit control can be separated from its functions in other aspects of development. Furthermore, it is hypothesized that transient and reversible block of pRb function may facilitate the production of functional hair cells that can mature and survive.

Our goal is to develop a strategy for transient and reversible inhibition of pRb functions using RNA interference (RNAi) and to identify a route for efficient delivery of small interfering RNAs (siRNAs) into hair cells and supporting cells. The RNAi approach will be used to block pRb function, as RNAi has been shown to be effective in reducing the targeted mRNA level. Our RNAi strategy is based on the use of chemically modified siRNAs that are targeted to the Rb gene sequence. Although chemically modified for stability, these siRNAs will ultimately be cleared from the cells, thus making the effect transient and reversible. This strategy has a distinct advantage in that it circumvents the undesirable effects of long-term reduction of Rb. We screened multiple Rbtargeted siRNAs with homology to both human and mouse Rb genes as such Rb siRNAs have potential for future use in human. We have identified two Rb siRNAs that can robustly knockdown Rb mRNA levels in both human and mouse cells in vitro within 5 days of incubation. The duration of knockdown effect and recovery of the endogenous Rb mRNA level is being evaluated. Separately, we have investigated a wide-range of delivery formulations for efficient hair cell/supporting cell delivery. We have identified one delivery formulation that shows rapid uptake by both hair cells and supporting cells in inner ear organ culture. The combination of the use of potent Rb siRNA with delivery formulations for efficient cellular delivery should pave the way for manipulation of pRb for hair cell regeneration. Also importantly, the delivery formulation discovered should have broad implications for investigating gene functions in hair cells and supporting cells.

# 546 FLIVO - A Novel Technique for Identifying Caspase-Mediated Cell Apoptosis in the Chick Cochlear Nuclei After Deafferentation

**Yuan Wang**<sup>1</sup>, Christopher K. Thompson<sup>2</sup>, Edwin W. Rubel<sup>1</sup>

<sup>1</sup>Dept of Oto-HNS and Virginia Merrill Bloedel Hearing Research Center, University of Washington, <sup>2</sup>Neurobiol & Behav Prog, Virginia Merrill Bloedel Hearing Research Center, University of Washington

The avian nucleus magnocellularis (NM) receives direct input from the auditory nerve. This projection is critical to the survival of NM neurons; following cochlea removal, about 30% neurons in the ipsilateral NM die. In vitro immunocytochemical studies have suggested that deafferentation of NM neurons results in caspase activation, an important component of programmed cell death. To test whether deafferentation-induced cell death in vivo is mediated by caspases, we used FLIVO, a novel in vivo fluorescent probe that specifically binds active caspases. We performed unilateral cochlea removal on 5-10 day old chicks and then injected FLIVO intracardially at intervals from 6 to 114 hours later. Tissue was fixed 30 minutes after the FLIVO injection and histologically processed. Positive staining was verified in the liver and gut. Six hours after cochlea removal, nearly every neuron in the ipsilateral NM displayed an increase in FLIVO staining. By 65 hours, the intensity of FLIVO labeling in

<sup>&</sup>lt;sup>1</sup>Sound Pharmaceuticals, Inc.

some neurons did not appear to be different from contralateral NM neurons, whereas other neurons still maintained a high level of staining. Many of these FLIVOpositive cells exhibited apoptotic morphology. By 114 hours, FLIVO in the surviving NM neurons returned to control levels. In addition, we detected FLIVO staining in the dorsal portion of the ipsilateral nucleus laminaris (NL) and the ventral portion of the contralateral NL, both of which receive inputs from the deafferented NM neurons. FLIVO staining in these regions was strong but diffuse at 6 hours, specific and punctate at 65 hours, and not present at 114 hours. Our results support FLIVO as a useful tool for identifying caspase-mediated programmed cell death. We observed caspase activation not only in the cell body but also in the axonal terminals or/and dendrites of deafferented neurons. This is the first observation that either axonal and/or dendritic degeneration in NL may be mediated by caspase activation.

Supported by grants DC03829, DC04661, and GM07108 from NIH/NIDCD

### 547 Preservation, Synaptic Plasticity and Regeneration of Adult Target Deprived Spiral Ganglion Neurons

**Dongguang Wei<sup>1,2</sup>**, Zhe Jin<sup>2</sup>, Leif Järlebark<sup>2</sup>, Eric Scarfone<sup>2,3</sup>, Mats Ulfendahl<sup>2</sup>

<sup>1</sup>Center for Neuroscience, University of California Davis, <sup>2</sup>Center for Hearing and Communication Research, Karolinska Institutet, <sup>3</sup>CNRS

Most forms of sensorineural hearing loss result from irreversible loss of cochlear hair cells (HC) and the following degeneration of target deprived spiral ganglion neurons (SGN). Secondary degeneration of SGNs could severely compromise the efforts to rehabilitate the hearing impaired patients with cochlear implants or hair cell regeneration. To identify the trophic factors that enhance the survival and promote neurites regrowth of target deprived adult SGNs, adult mouse SGNs were separated from hair cells and studied in vitro in the presence of neurotrophins and growth factors. administration of fibroblast growth factor 2 (FGF-2) and glial cell line-derived neurotrophic factor (GDNF) provided support for long-term survival, while FGF-2 alone could strongly promote neurite regeneration. Fibroblast growth factor receptor FGFR-3-IIIc was found to up-regulate and translocate to the nucleus in surviving SGNs. Isolated adult SGNs projected neurites to cocultured HCs. However, when they were deprived from HCs, the surviving SGNs displayed synaptic plasticity by establishing various synaptic contacts with other SGNs. Cells from adult mouse spiral ganglion were pooled and promoted to re-enter cell cycle with the help of epidermal growth factor (EGF) and FGF-2. After induced differentiation, they could carry out both symmetric and asymmetric cell division and gave birth to new neurons. In summary, we established a long term in vitro culture system of adult SGNs and demonstrated that coadministration of FGF-2 and GDNF could be an efficient route to preserve target deprived SGNs. FGF-2 could strongly promote neurite regrowth. After loss of HCs, SGNs displayed synaptic plasticity by establishing various

synaptic contacts with other SGNs. The observation of dividing neurons in vitro indicates the possibility of progenitor or stem cell residents within adult spiral ganglion, which may contribute to neurogenesis.

## 548 Non-Syndromic Hearing Loss with Vestibular Dysfunction Caused by Espin Mutations is Rare

**Sandrine Marlin**<sup>1</sup>, Isabelle Rouillon<sup>2</sup>, Delphine Feldmann<sup>3</sup>, Laurence Jonard<sup>3</sup>, Natalie Loundon<sup>2</sup>, Christine Petit<sup>4</sup>, Eréa-Noël Garabédian<sup>2</sup>, Rémy Couderc<sup>3</sup>, Françoise Denoyelle<sup>2</sup>

<sup>1</sup>Service de Génétique, Hôpital d'Enfants Armand-Trousseau, <sup>2</sup>Service d'ORL et de Chirurgie Cervico-faciale, Hôpital d'Enfants Armand-Trousseau, <sup>3</sup>Service de Biochimie et de Biologie Moléculaire, Hôpital d'Enfants Armand-Trousseau, <sup>4</sup>unité de Génétique des déficits Sensoriels, Institut Pasteur, Paris, France

Sensorineural hearing loss due to a genetic cause is the most frequent sensory deficit in children and is considered to affect one in 1000 newborns. A significant research effort has been led over the last decade to identify the genes involved in non-syndromic hearing loss (NSHL). Except for connexin26 which is frequently mutated in NSHL and a few others genes, the prevalence of the other genes is not known. Espin mutations were described for the first time in 2004 in two families with NSHL with autosomal recessive transmission and vestibular dysfunction.

The purpose of our study was to select patients with the rare phenotype consisting in congenital and isolated NSHL associated with vestibular areflexia from a large population of deaf patients (1500), and to study the ESPN gene in these patients.

Thirteen unrelated patients and four patients from two families presenting a congenital NSHL associated with vestibular hyporeflexia or areflexia were selected. The deafness was congenital, profound and sporadic in all cases. Retinopathy was investigated by fundoscopy and electroretinography in order to exclude Usher syndrome type 1. Six patients where originally from Indian Ocean. The 13 exons of ESPN gene were studied by sequencing in the 13 unrelated patients and markers mapped to the ESPN locus were analysed in the 2 families.

No deleterious mutation was found in the 13 selected patients, and the ESPN gene was excluded in the two families. We conclude that this rare phenotype is genetically heterogeneous and that the ESPN gene is not frequently implicated in this phenotype.

#### 549 Immune Cells in the Cochlea of the Amikacin Treated Rat

Sabine Ladrech<sup>1</sup>, Jing Wang<sup>1</sup>, Lionel Simmoneau<sup>1</sup>, **Jean Luc Puel**<sup>1</sup>, Marc Lenoir<sup>1</sup>

<sup>1</sup>INSERM U.583

Recent studies have proven the capacity of supporting cells to trans-differentiate into new hair cells in the mammalian cochlea (Izumikawa et al., Nat Med 11, 2005; White et al., Nature 44, 2006). This makes the supporting cells potential targets for therapeutic manipulation.

However, damage to hair cells caused by noise or ototoxic exposure is generally followed by supporting cell disappearance. Understanding the reasons for supporting cells degeneration may help to promote the success of potential therapies.

Scavenger cells may have positive effects on tissue reparation through cell residues elimination and cytokine release, but they could have deleterious effects on remaining epithelial structures via autoimmune and inflammatory responses. In the noise or ototoxic exposed cochleas, they could exacerbate the initial damage.

The goal of this study was to investigate the organ of Corti of amikacin treated rats for the presence of macrophages. The density of macrophages was assessed from the end of the amikacin treatment until the complete degeneration of the organ of Corti using specific markers of leukocytes (anti-CD45 and anti-ED1 antibodies).

Very few macrophages were seen in the cochleas of the non-treated rats. In the amikacin damaged organs of Corti, a peak in macrophage density (around 20 fold the normal value) occurred during the week post-treatment when hair cells died through apoptosis. Surprisingly, after complete hair cell disappearance, the density of phagocytes remained very high during one additional month coinciding with the progressive degeneration of the remaining nonsensory epithelial cells. Density of phagocytes did not return to normal value even after 10 weeks (almost 5 fold normal values).

These results suggest that macrophages mediate clearance of the hair cell apoptotic corpses but a subsequent chronic inflammation may contribute to induce secondary degradation of the supporting cells.

# | 550 | Quantitative Evaluation of the Progression of Mitotic-Based Hair Cell Regeneration in the Avian Cochlea Using a Novel Watershed-Based Nuclear Segmentation Protocol

**Dominic Mangiardi<sup>1,2</sup>**, David Mountain<sup>1</sup>, Douglas Cotanche<sup>2</sup>

<sup>1</sup>Boston University, Dept of Biomedical Engineering, <sup>2</sup>Childrens Hospital Boston, Dept of Otolaryngology

Sound pressure waves generated in the environment are converted into fluid movement inside the cochlea, the organ of hearing. Inner ear sensory hair cells are responsible for detecting this fluid movement and are vital for the production of neural signals that provide the brain with auditory information. Damage to these sensory receptors can result in permanent hearing and balance disorders in humans. However, other vertebrate species, such as the chicken, have the capacity to regenerate lost sensory hair cells via induction of quiescent neighboring supporting cells in the sensory epithelium to re-enter the cell cycle and produce daughter cells that repopulate the damaged sensory epithelium. Understanding the mechanisms of hair cell regeneration in these systems could potentially lead to the development of therapies for sensory hair cell loss in humans. In this study, a quantitative analysis of the progression of mitotic-based hair cell regeneration in the avian cochlea following gentamicin-induced hair cell loss was performed. Twoweek old chicks were administered a single injection of gentamicin (300 mg / kg) to induce hair cell loss and a separate injection of BrdU (100 mg/kg) to label progenitor cells passing through DNA synthesis. Chicks were sacrificed and the cochleae dissected at specific times relative to BrdU injection. Immunohistochemistry was used to label whole-organ preparations for BrdU, myosin-VI and -VIIa, and cellular nuclei. Confocal microscopy was combined with a novel watershed algorithm-based nuclear segmentation protocol to determine the position of nuclei in the regenerating area of the epithelium as well as characterize the cells as BrdU- or myosin-positive. The time of BrdU injection relative to gentamicin treatment and length of time prior to sacrifice were varied to examine the timing and location of S-phase induction and the initiation of hair cell-specific gene expression in daughter cells.

### Vestibular Hair Cells Following Aminoglycoside Toxicity

**Ivo Prigioni**<sup>1</sup>, Giancarlo Russo<sup>1</sup>, Daniela Calzi<sup>1</sup>, Luciana Gioglio<sup>2</sup>

<sup>1</sup>Department of Physiological and Pharmacological Sciences, University of Pavia, Italy, <sup>2</sup>Department of Experimental Medicine, University of Pavia, Italy

Aminoglycoside antibiotics, including gentamicin (GM), are known to induce severe degenerative effects in both cochlear and vestibular organs. The discovery that hair cells readily regenerate in fish, amphibians, reptiles and birds after antibiotic treatment has stimulated the study of the mechanisms of repair and regeneration of the hair cells in different inner ear organs. The present investigation was designed to elucidate the morphological and functional recovery of hair cells in frog semicircular canals. GM was administered intraotically close to the perilymphatic cisterna at the concentration of 5 mM (15 µl volume). Frogs were sacrificed at post-injection times ranging from 1 to 20 days. Degenerative changes at hair cell level started 1-2 days after GM treatment and were severe in the intermediate regions of the crista and then involved the central and peripheral regions. Hair cell degeneration in the three crista regions appeared complete after 6-8 days. Damaged hair cells showed stereocilia loss together with a swelling of cell bodies and nuclei. Partially extruded hair cells from the epithelium were also observed together with large epithelial holes. Regenerating hair cells were often seen 6 day after GM treatment. They were identified based on their small cell bodies and nuclei as well as their small immature hair bundles. From this stage, hair cells density increased and the sensory epithelium recovered a normal appearance within 15 days. The functional recovery of hair cells during the regenerative period was studied by using whole cell patch recordings in crista slice preparations up to 20 days from gentamicin treatment. Passive and active electrical properties of hair cells from control animals have been compared with those of regenerating hair cells. Regenerating cells showed patterns of responses qualitatively similar to those of normal hair cells. However, the magnitude of the ionic currents increased during recovery suggesting that new hair cells came from precursors which reacquired progressively their complement of ionic channels. We found that the complement of K+ channels were completely functional in regenerated hair cells at 15 days post-treatment with gentamicin. Moreover, the regenerated cells in each region of the crista neuroepithelium reacquired the same complement of channels of normal preparations.

# Sensory Regeneration in the Avian Inner Ear: Evidence for the Involvement of JNK Signaling

Mark Warchol<sup>1</sup>

Washington University School of Medicine

Sensory hair cells in the avian ear can quickly regenerate after acoustic trauma or ototoxic injury. During regeneration, hair cells recover the same phenotypic features and innervation as their counterparts in the undamaged ear. The present study used organ cultures of the mature chick utricle to investigate the signaling pathways that are involved in the re-establishment of hair cell phenotype and orientation.

Utricles from chicks (P7-21) were placed in organ culture and treated for 24 hours with 1 mM streptomycin, which killed nearly all hair cells. Utricles were then maintained in culture for an additional 7-10 days, in order to permit regeneration. After 10 days recovery, hair cell density had returned to about 30% of control values. Treatment with the JNK inhibitor SP600125 for the final 3-6 days in vitro resulted in no detectable changes in hair cell numbers, as determined by immunoreactivity for calretinin, acetylated tubulin or PAX2. However, JNK inhibition did reduce the number of recovered stereocilia bundles, to about 50% of control levels.

Additional experiments examined the recovery of stereocilia orientation in this culture system. An antibody against acetylated tubulin was used to label the apical surfaces and kinocilia of all regenerated hair cells. Kinocilia were typically found at one edge of the apical surface, which defined the hair cell's polarization vector. After 7-10 days of regeneration, hair cells in randomlyselected regions within the extrastriolar (cotillus) portion of the utricle all possessed similar orientation vectors to those of their nearest neighbors. In addition, most hair cells were correctly oriented with respect to the striolar reversal zone. Treatment for the final 3-6 days in vitro with the JNK inhibitor SP600125 resulted in impaired formation of kinocilia. When fully-formed kinocilia were observed, they were randomly oriented with respect to the striolar reversal zone. These results suggest that the cues for bundle orientation are maintained within the sensory epithelium of the isolated utricle. In addition, it appears that JNK activation is required for normal stereocilia formation and orientation, perhaps acting as a downstream signal in the noncanonical Wnt pathway (e.g., Montcouquiol et al., Ann Rev Neurosci 29:363, 2006). Supported by R01 DC006283

#### 553 Developmental Changes in Responsiveness of Rat Spiral Ganglion Neurons to Neurotrophins: Differential Regulation of Survival and Neuritogenesis in Explant Culture

**Kenji Kondo**<sup>1,2</sup>, Kwang Pak<sup>1</sup>, Eduardo Chavez<sup>1</sup>, Lina Mullen<sup>1</sup>, Sara Euteneuer<sup>1,3</sup>, Allen Ryan<sup>1</sup>

<sup>1</sup>University of California, San Diego School of Medicine, and Veterans Administration Medical Center, <sup>2</sup>University of Tokyo, Graduate School of Medicine, <sup>3</sup>Ruhr-University Bochum, School of Medicine

The developmental changes in responsiveness of rat spiral ganglion neurons (SGNs) to neurotrophin-3 (NT-3) and brain-derived neurotrophic factor (BDNF) were examined using an explant culture system. SG explants at embryonic day 18 (E18), postnatal day (P) 0, P5, P10 and P20 were cultured with the addition of either NT-3 or BDNF at different concentrations (0.1-100 ng/ml) and analysed for three parameters: SGN survival, the number of neurites emanating from the explants and the length of neurite extension. In E18 cultures, survival and neurite number were enhanced more strongly by NT-3 than BDNF, while neurite extension was unaffected by NT-3 and only weakly enhanced by BDNF. SGNs began to lose dependence on NT-3 at P0. In contrast, BDNF became a more potent stimulant of survival, neurite number and neurite extention in P5 and P10 culture. Although the intrinsic capacity of SGNs to produce and extend neurites declined considerably by P20, they still retained the capacity to respond to both NT-3 and BDNF. These temporal patterns in responsiveness of SGNs to neurotrophins correspond well to the expression pattern of the two neurotrophins in cochlear sensory epithelium in vivo, and also correlate with the time course of developmental events in SGNs such as cell death and the rearrangement of hair cell innervaion.

### 554 Neonatal Auditory Neurons Respond to an Otocyst-Derived Neurotrophic Factor

Kavitha Challagulla<sup>1</sup>, Annette Vu<sup>1</sup>, Heather Nardone<sup>2</sup>, Lynne Bianchi<sup>3</sup>, Kate Barald<sup>4</sup>, **John Germiller**<sup>1,2</sup>

<sup>1</sup>The Children's Hospital of Philadelphia, <sup>2</sup>University of Pennsylvania, <sup>3</sup>Oberlin College, <sup>4</sup>University of Michigan Beginning at its earliest stages, auditory nerve development depends on diffusible signals secreted by its peripheral target, the inner ear. Functional assays have identified one of the earliest of these signals, termed otocyst-derived factor (ODF), which is secreted by the otocyst and stimulates primitive neurons of the early cochleovestibular ganglion (CVG). Although presently ODF remains poorly characterized, it does not appear to contain any of the known neurotrophic factors, including the neurotrophins. Our laboratories aim to identify the active components of ODF, define its role in development, and explore its potential applications in maintenance and regeneration of auditory neurons. However, at present it is not known whether ODF retains its potent trophic effects on neurons beyond early development. Therefore, we tested whether ODF could stimulate neurite outgrowth in auditory neurons from late fetal mice (16.5 dpc) and

neonates (P0-P1). Dissociated spiral ganglion neurons were incubated for 48 h in supernatants from otocystderived cell line IMO-2B1. This cell line was previously shown to secrete a functionally-identical neurotrophic activity as the mouse otocyst in vivo. Results were compared with control media, and with neurotrophins BDNF and NT-3, alone or in combination. assessment was done blinded to treatment group, and from 8 independent harvests of IMO-2B1 media. Exposure to IMO-ODF media resulted in robust outgrowth of long neurites at both stages of development, considerably greater than that observed with either control media or the neurotrophins. These data suggest that the otocyst secretes a potent neurotrophic activity, that remains stimulatory for spiral ganglion neurons well beyond early development. Currently, we are determining whether this responsiveness to ODF persists in later postnatal and adult neurons.

# 555 Interactive Roles of Fibroblast Growth Factor 2 and Neurotrophin 3 in the Sequence of Migration, Process Outgrowth, and Axonal Differentiation of Mouse Cochlear Ganglion

Waheeda Hossain<sup>1</sup>, **Chrystal D'Sa<sup>1</sup>**, D. Kent Morest<sup>1</sup>

Dept. of Neuroscience, University of Connecticut Health Center

The same growth factors appear to have different actions depending on the stage of development. We investigated this phenomenon in the mouse by testing the interaction of fibroblast growth factor 2 (FGF2) and neurotrophins on cochlear ganglion (CG) development with an in vitro model. The portions of the otocyst fated to form the CG and cochlear epithelium were co-cultured at embryonic day 11 (E11). Cultures were divided into groups fed with defined medium, with or without FGF2 and neurotrophin supplements, alone or in combination, for 7 days. We measured the number of migrating neuroblasts and distances migrated, neurite outgrowth, and axon-like processes. We used immunohistochemistry to locate neurotrophin 3 (NT3) and its high affinity receptor (TrkC) in the auditory system, along with FGF2 and its R1 receptor, at comparable developmental stages in vitro and in situ from E11 until birth (P1) in the precursors of hair cells, support cells, and CG cells. Potential sites for interaction were localized to the nucleus, perikaryal cytoplasm, and cell surfaces, including processes and growth cones. In mutants overexpressing FGF2, there were significant increases in migration and proliferation of CG neurons in vitro, compared to wildtype. Time-lapse imaging and quantitative measures support the hypothesis that FGF2 alone or combined with neurotrophins promotes migration and neurite outgrowth. Synergism or antagonism between NT3 and other factors suggest interactions at the receptor level. Formation of axons, endings, and synaptic vesicle protein 2 were increased by interactions of NT3 and FGF2. Similar experiments with a mutant overexpressor for FGF2 suggest that endogenous FGF2 supports migration and neurite outgrowth of CG neuroblasts as well as proliferation, leading to accelerated development. The

findings suggest interactive and sequential roles for FGF2 and NT3. (Supported by NIH grant DC006387 and a UCHC fellowship (CD)).

# 556 Auditory Circuit Assembly: Development of Spiral Ganglion and Cochlear Nucleus Neurons and Their Connections

**Jessica L. Appler<sup>1,2</sup>**, Edmund J. Koundakjian<sup>1,2</sup>, Lisa V. Goodrich<sup>2</sup>

<sup>1</sup>Program in Neuroscience, <sup>2</sup>Department of Neurobiology-Harvard Medical School

Sensory information from the ear is processed in the brain by neurons that are organized tontopically and that transmit auditory information remarkably quickly, features that are essential for comparison of sounds between two ears. Key to the proper perception of sound are spiral ganglion neurons, which receive input from hair cells in the cochlea and communicate all aspects of complex sound stimuli to bushy cells and other neurons in the cochlear Hair cells and spiral ganglion neurons are nucleus. tonotopically organized in the cochlea, with neurons carrying information about neighboring frequencies located near each other and organized in a gradient from base to apex. In addition, both spiral ganglion neurons and bushy cells make unusually large synapses called calyces, which permit the rapid transmission of synaptic signals. Proper assembly and function of auditory circuits therefore involves both the development of tonotopic projections and the formation of specialized synaptic connections between spiral ganglion neurons and bushy cells.

We are using genetic tools to study the development of connections between spiral ganglion neurons and bushy cells. To begin, we examined spiral ganglion development using the Neurogenin 1-CreERT2 transgenic mouse line. This line allows for tight spatial and temporal control over the developing spiral ganglion. Initially, we crossed Ngn1-CreERT2 to the Z/EG and Z/AP reporter lines to visualize spiral ganglion neuron projections, including calyceal endings. We then labeled small, isolated populations of neurons located in either the base or the apex of the cochlea and examined their projections into the developing cochlear nucleus. These experiments revealed that the projections are organized tonotopically as early as E15.5. Finally, we screened 1200 transcription factors in the murine genome to identify factors that may regulate aspects of auditory circuit assembly. We found an initial group of 75 transcription factors that may be involved in cochlear nucleus neuron type specification and spiral ganglion neuron guidance and synaptogenesis. Further studies are aimed at both identifying early markers of individual populations of cochlear nucleus neuron types and pinpointing the function of candidate transcription factors in the development of auditory circuitry.

## 557 Robo Protein is Expressed in the Developing Spiral Ganglion During Neurite Outgrowth

Alyssa Hackett<sup>1,2</sup>, Wei Gao<sup>1,2</sup>, Yael Raz<sup>1</sup>

<sup>1</sup>University of Pittsburgh Medical Center, <sup>2</sup>These authors contributed equally to this research.

Robo protein is expressed in the developing spiral ganglion during neurite outgrowth.

Background: The spiral ganglion neurons must connect the cochlear sensory epithelium with higher auditory centers while conserving a precise tonotopic organization. Several axon guidance cues have been implicated in regulating topographic innervation of sensory organs. The three slits genes and their corresponding robo receptors have been shown to play a major role in neuronal guidance in the brain as well as the developing visual, olfactory and somatosensory systems. The functional role of the slit/robo signaling pathway in the inner ear is unknown. Detailed expression of the slit and robo genes in the inner ear during the period of neurite outgrowth has been previously described. The focus of this study is the expression of robo protein in the developing mouse cochlea.

Methods: Immunohistochemistry was performed on tissue sections from 13 and 16 day old mouse embryos using antibodes for robo 1 and 3. Stained sections were photographed using confocal microscopy.

Results: At E13 expression robo 1 expression was noted in the cochleovestibular ganglion. This expression persisted at E16 but by P0 to P5 expression was negative in the cell body and persisted in the neurites. Curiously, in the adult, expression was again noted in the soma. The robo 3 antibody revealed weak staining in the cochleovestibular ganglion at E13. At E16, robo expression is clearly defined along the length of the spiral ganglion as well as the processes extending to the organ of Corti.

Discussion: Expression of robo protein in the developing auditory neurons suggests a role for slit/robo signaling in neurite guidance. The epitope used to generate the robo3 has potential for significant crossreactivity with robo1 and robo2. Further studies will be directed at determining the specificity of this antibody for the three robo homologs.

# **558** Expression of *Slits* and *Robos* During Chick Inner Ear Development Suggests Dual Roles in Axon Guidance and in Epithelial Boundaries

Andrea M. Campero<sup>1</sup>, **Donna M. Fekete**<sup>1</sup>

<sup>1</sup>Purdue University

The mechanosensory hair cells in the chicken inner ear are innervated by bipolar afferent neurons. During development each neuron migrates to its final position in either the auditory or vestibular ganglion while it simultaneously sends a peripheral process to navigate into only one of the 8 distinct sensory organs. Little is known about whether auditory and vestibular axons respond to different attractants and/or repellents as they explore the periphery. The presence of repellants in the otic epithelium is suggested by our unpublished data which

show that auditory axons avoid ectopic vestibular patches induced experimentally in the embryonic cochlear duct.

In order to test the hypothesis that repellants influence inner ear axons, we have examined the expression of slits and robos during development of the chick inner ear. We performed in situ hybridizations during ear morphogenesis (E3-E11) on sections using antisense RNA probes directed against chicken slit1, slit2, slit3, robo1 or robo2 (gift of Ed Laufer, Univ. Columbia). Otic ganglion neurons express robo2 on E4, during peripheral axon outgrowth. At the same time, *slits* are strongly expressed in the region of the ear immediately adjacent to the ganglion, suggesting that slits may act to divert axons to more distant sensory primordia. Curiously, several of these undifferentiated sensory primordia also express robos. By E6, robo transcripts in the innervated sensory organs are flanked by slit2 in the adjacent non-sensory epithelium. This juxtaposition of slit and robo domains could reveal a new role for these molecules in establishing or maintaining sensory/nonsensory boundaries. Alternatively, slits may be playing a more traditional role by either channeling axons towards the hair cells or by restricting them from entering non-sensory territory. We are currently conducting overexpression experiments by electroporating slits into the developing otocyst to differentiate between these hypotheses.

#### **559** A Disorganized Innervation of the Inner Ear Persists in the Absence of ErbB2

**Bernd Fritzsch<sup>1</sup>**, Jackie Morris<sup>2</sup>, Laura Hansen<sup>1</sup> \*Creighton University, <sup>2</sup> \*Baldwin College

ErbB2 protein is essential for the development of Schwann cells and for the normal fiber growth and myelin formation of peripheral nerves. We have investigated the fate of the otocyst derived inner ear sensory in the absence of ErbB2. Afferent innervation of the ear sensory epithelia shows numerous fibers overshooting the organ of Corti, followed by a reduction of those fibers in near term embryos. This suggests that mature Schwann cells do not play a role in targeting or maintaining the inner ear innervation. Comparable to the overshooting of nerve fibers, sensory neurons migrate beyond their normal locations into unusual positions in the modiolus. They may miss a stop signal provided by the Schwann cells that are absent as revealed with detailed histology. Reduction overshooting afferents may be enhanced by a reduction of the neurotrophin Ntf3 transcript to about 25% of wildtype. Ntf3 transcript reductions are comparable to an adult model that uses a dominant negative form of ErbB4 expressed in the supporting cells and Schwann cells of the organ of Corti. ErbB2 null mice retain afferents to inner hair cells possibly because of the prominent expression of the neurotrophin Bdnf in developing hair cells. Despite the normal presence of Bdnf transcript, afferent fibers are disoriented near the organ of Corti. Efferent fibers do not form an intraganglionic spiral bundle in the absence of spiral ganglia and appear reduced and disorganized. This suggests that either ErbB2 mediated alterations in sensory neurons or the absence of Schwann cells affects efferent fiber growth to the organ of Corti.

#### 560 Medial-Lateral Positioning of Superior Olivary Complex Neurons

**David Howell**<sup>1,2</sup>, Warren Morgan<sup>1,2</sup>, George Spirou<sup>1,3</sup>, Albert Berrebi<sup>1,4</sup>, Peter Mathers<sup>1,2</sup>

<sup>1</sup>Sensory Neuroscience Research Center, Dept. of Otolaryngology, WVU School of Medicine, <sup>2</sup>Dept. of Biochemistry and Molecular Pharmacology, WVU School of Medicine, <sup>3</sup>Dept. Physiology and Pharmacology, WVU School of Medicine, <sup>4</sup>Dept. of Neurobiology and Anatomy, WVU School of Medicine

Migratory neurons reach their adult position through the use of guidance cues. Although cues necessary for neuronal positioning along the anterior-posterior and dorsal-ventral axes are known, the signals positioning nuclei along the medial-lateral axis are not well characterized. Developing medial nucleus of the trapezoid body (MNTB) and other superior olivary complex (SOC) neurons express RNAs for DCC, robo1 and robo2 receptors that mediate axon guidance and neuronal migration through binding netrin and slit ligands, which are expressed at the brainstem midline. Combinations of these receptors are expressed in longitudinal tracts of cells that extend caudally to the SOC. A high-medial to low-lateral gradient of DCC expression is observed in the MNTB at E17.5, suggesting a potential mechanism for establishing the medial-to-lateral frequency organization of this nucleus. The utilization of netrin-DCC signaling in MNTB migration is supported by the absence of MNTB neurons in netrin1- and DCC-deficient mice and the presence of a laterally displaced MNTB in mice heterozygous for a netrin1- or DCC-mutant allele. Stereologic estimates indicate the total number of MNTB neurons is similar in wild-type and DCC heterozygous animals. The tonotopic organization of the MNTB is preserved in the laterally displaced MNTB, as determined by pure-tone-stimulated cfos immunoreactivity. In DCC heterozygous animals, the ventral tegmental nucleus is laterally displaced, whereas the trochlear nucleus, whose axons are repelled by netrin, is medially displaced. We propose that brainstem nuclei require dose-dependant netrin-DCC and slit-robo signals for medial-lateral positioning.

Supported by NIH/NCRR grant P20 RR15574 and R01 EY012152.

## 561 Lrig3: A Novel Ig Superfamily Protein Regulates Fusion During Lateral Canal Morphogenesis

**Victoria E. Abraira**<sup>1</sup>, Hannah Keirnes<sup>1</sup>, Andrew Tucker<sup>1</sup>, John Slonimsky<sup>2</sup>, Lisa V. Goodrich<sup>1</sup>

<sup>1</sup>Harvard Medical School, Department of Neurobiology, Boston MA, <sup>2</sup>Novartis, Boston MA

Morphogenesis of the complex labyrinths of the inner ear involves precisely regulated cell proliferation, cell death, and cell-cell interactions in the epithelium and mesenchyme of the otic vesicle (OV). In developing semicircular canals, defined regions of the otic epithelium grow towards each other and meet to form the fusion plate. In the fusion plate, the epithelium thins and the basal lamina breaks down. Subsequently, the epithelium disappears and the region is filled with mesenchyme, thereby forming a canal out of an initial pouch structure.

Little is known about the molecules that control the behavior of cells in discrete regions of the otic vesicle. Here we report that a novel Ig superfamily protein, Lrig3, acts during morphogenesis to regulate fusion of the lateral semicircular canal.

Lrig3 is disrupted in the genetrap line LST16 in which the wild type transcript is truncated and replaced with reporter genes. Lrig3LST16 homozygotes exhibit circling and head tossing behavior, suggestive of inner ear defects. Consistent with the behavioral phenotype, lateral semicircular canals are truncated in Lrig3LST16 mutant inner ears. Prior to canal morphogenesis, Lrig3 is expressed in the lateral domain of the OV, which gives rise to the lateral semicircular canal. Although Lrig3 expression is detected in the early OV, mouse mutants show normal expression of all marker genes examined and canal formation is grossly normal until embryonic day E12. At this stage, the posterior portion of the lateral pouch undergoes an early fusion event over a much larger area than normal. This is accompanied by expansion of the fusion plate marker Netrin-1 in the epithelium of Lrig3LST16 homozygotes. Moreover, mutants show a larger area of epithelial thinning accompanied by ectopic regions of basal lamina breakdown, as determined by antilaminin staining and electron microscopy. We conclude, that Lrig3 normally influences lateral canal morphogenesis by modulating the timing and extent of fusion in the lateral canal pouch. Lrig3 is a single pass transmembrane protein with 16 leucine rich repeats and 3 lg domains in the extracellular region, and a short cytoplasmic tail with not known motifs. Current studies are aimed at understanding the molecular functions of Lrig3 and further elucidating the effect of Lrig3 mutations in the fusion plate.

### **562** Comprehensive Analysis of Expression Profiles of the Life Cycle of Mouse Utricle

**Mingqian Huang**<sup>1</sup>, Albena Kantardzhieva<sup>1</sup>, Sang Goo Lee<sup>1</sup>, Kambiz Karimi<sup>2</sup>, Zheng-Yi Chen<sup>1</sup>

<sup>1</sup>Massachusetts General Hospital and Harvard Medical School, <sup>2</sup>Ingenuity Systems

Detailed knowledge of gene expression throughout inner ear development is essential for the characterization of their roles at molecular, cellular and systems levels. We conducted Genechip microarray analysis of gene expression in developing mouse utricle from progenitor stage to matured and aged utricles. In addition, we performed expression analysis with purified sensory epithelia and FACS sorted hair cell and supporting cell populations. Our study has uncovered virtually all the genes expressed in the life cycle of mouse utricle development, and identified the genes whose expression is developmentally regulated in the hair cells, supporting cells and stroma/neuron, respectively. The analysis showed that the overall gene expression profiles can be grouped into eight distinct stages, corresponding with progenitor cell population, cell fate determination, initiation of differentiation, maturation, and aging. In situ hybridizations generally confirmed the expression results. We have systematically mapped all the signaling pathways at cell subtype resolution, using the cluster analysis and

the Ingenuity Pathway Analysis. We showed that Notch signaling pathway is mediated through interactions of at least 17 molecules with distinct hair cell or supporting cell distribution. One of the prominent pathways identified is the Wnt/beta-catenin signaling. Over 42 Wnt/beta-catenin signaling genes are identified with hair cell or supporting cell specific expression patterns. The pathway network showed that the Wnt/beta-catenin pathway is activated in supporting cells and is suppressed in hair cells. The analysis of aging utricle showed the upregulation of genes involved in protein folding, apoptosis, lipid metabolism, calcium signaling and molecular transporters. Therefore, the increased stress response and elevation of expression of transporters and calcium pumps are likely important in maintaining homeostasis of aging utricle. Finally, we have used the expression data to screen for stem cell target genes that are expressed in the inner ear progenitor cells. We identified the inner ear progenitor genes that showed altered expression when progenitors are differentiated, suggesting their roles in progenitor cell specification. Our data will serve as a valuable resource for research in the cloning of genes involved in deafness, genes of the complex transduction and genes essential regeneration.

## and KCNQ4 Currents in the *Pit1*<sup>dw</sup> Model of Secondary Hypothyroidism

Mirna Mustapha-Chaib<sup>1</sup>, Qing Fang<sup>1</sup>, Sally Camper<sup>1</sup>, David Dolan<sup>2</sup>, **R. Keith Duncan<sup>2</sup>** 

Department of Human Genetics, University of Michigan, <sup>2</sup>Kresge Hearing Research Institute, University of Michigan Thyroid hormone (TH) is essential to normal hearing in humans and rodents. Other studies have established potassium currents (BK and KCNQ4) and the outer hair cell motor protein (PRESTIN) as TH-sensitive (Rüsch et al., 1998, 2001; Weber et al., 2002; Winter et al., 2006). Molecular and physiological data show that BK channel expression in TH receptor knockouts is delayed by 6 to 8 weeks (Rüsch et al., 1998, 2001). It remains unclear whether outer hair cell motility and KCNQ4 currents follow a similar developmental delay. Our morphological data indicate delayed maturation and altered expression of KCNQ4 and PRESTIN in Pit1<sup>dw</sup> mice, which is a model of secondary hypothyroidism. To investigate this further, we measured nonlinear capacitance (NLC) and KCNQ4 currents throughout development in wild-type and Pit1<sup>dw</sup>mice. Nonlinear capacitance increased with age in both wild-type and Pit1<sup>dw</sup>mice, but the timescales for acquiring NLC were dramatically different. The NLC of 6 week old Pit1<sup>dw</sup>mice was similar to that from 2 week old wild-type mice, indicated a developmental delay of at least Similarly, we found evidence of delayed 4 weeks. maturation of KCNQ4 currents in *Pit1*<sup>dw</sup>mice. As wild-type mice mature in age, the voltage-dependence of OHC potassium currents shifts substantially to negative voltages, with half-activation (V<sub>1/2</sub>) reaching approximately -85 mV. This negative activation range is dominated by the effects of KCNQ4. Preliminary data from Pit1<sup>dw</sup>mice showed that young mutant mice (2 weeks of age) were similar to neonatal wild-type mice with a  $V_{1/2}$  of about -35 mV. However, as the mutant mouse matures to 6 weeks of age, total potassium currents appear to be a mixture of KCNQ4 and the neonatal current. As with PRESTIN, the question remains whether KCNQ4 currents reach mature wild-type levels and exhibit the same biophysical features in *Pit1*<sup>dw</sup> mutants as they do in normal mice. Supported by NIH R01 DC05053 and P30 DC05188.

# | 564 | Developmental Expression of Osteoprotegerin, Matrix Metalloproteinase-13 and Sclerostin in the Postnatal Murine Otic Capsule

**Argyro J. Bizaki**<sup>1</sup>, Konstantina M. Stankovic<sup>1</sup>, Joe C. Adams<sup>1</sup>, Arthur G. Kristiansen<sup>1</sup>, Michael J. McKenna<sup>1</sup> Department of Otolaryngology, Massachusetts Eye and Ear Infirmary, Boston, Massachusetts, USA.

Studies of otic capsule development may provide insights into the pathophysiology of otosclerosis, a leading cause of acquired hearing loss, which is histologically characterized by abnormal bone remodeling. Following development, the otic capsule undergoes very little remodeling compared to other bones. Recent studies from our lab have shown that osteoprotegerin (OPG) is a potent inhibitor of otic capsule remodeling, and that its absence leads to pathologic remodeling that closely resembles otosclerosis. To examine this further, we have undertaken studies in the murine otic capsule and cochlea to determine postnatal developmental expression of OPG, and two other genes that control bone remodeling: matrix metalloproteinase-13 (MMP-13), a collagenase involved in turnover of the extracellular matrix, and sclerostin (SOST), a negative regulator of bone formation.

Using quantitative RT-PCR, we found substantial changes in mRNA levels as the otic capsule matured from the cartilaginous anlage at postnatal day 2 (P2) to the adult pattern of ossification at P16: a 35.6+/-3.6 fold increase in OPG, a 7.5+/- 3.7 fold increase in SOST, and a 8.3+/-0.5 fold decrease in MMP13. The mRNA changes were reflected in the intensity of immunostaining for the corresponding proteins. Using immunostaining, OPG intensely localized to fibrocytes of the spiral ligament and weakly to lacunae of osteocytes in the otic capsule, SOST localized to osteocytes of the otic capsule, and MMP13 localized to the endosteal layer of the otic capsule adjacent to the cartilaginous rests. Taken together, dynamic patterns of expression of OPG, SOST and MMP13 in the developing otic capsule correlate with increasing inhibition of bone remodeling.

### Frenatal Dioxin Exposure is Dependent Upon Mouse Strain

**Theresa M. Safe**<sup>1</sup>, Lisa A. Opanashuk<sup>2</sup>, Anne E. Luebke<sup>1,3</sup>
<sup>1</sup>Dept. of Biomedical Engineering, <sup>2</sup>Dept. of Environmental Medicine, <sup>3</sup>Dept. of Neurobiology and Anatomy, University of Rochester Medical Center

2,3,7,8-tetrachorodibenzo-*p*-dioxin (TCDD), a ubiquitous and persistent environmental contaminant, is a potent teratogen. Whereas developmental TCDD toxicity is mediated by the aryl hydrocarbon receptor (AhR), the

normal function of the AhR is poorly understood. Interestingly, adult AhR knockout (AhR KO) mice have elevated auditory thresholds when compared to their wildtype (WT) littermates. The mouse Ahr locus exists as four alleles:  $Ahr^{b1}$ ,  $Ahr^{b2}$ ,  $Ahr^{b3}$ ,  $Ahr^{d}$ . Previous studies have suggested that polymorphisms at loci other than Ahr may have a significant impact on dioxin sensitivity following prenatal exposure. Therefore, this study tested whether dioxin exposure during a critical period of hair cell development disrupts auditory system function in two mouse strains that contain  $Ahr^{b}$  alleles, which encode a high affinity receptor isoform.

C57B6 and CBA dams were exposed to 500 ng/kg TCDD or olive oil (vehicle) on embryonic day 12 by gavage. Cochlear function was analyzed at 1.5 months of age by measuring 1) auditory brainstem response (ABRs ) to tone pips from 5.6 to 30 kHz, and 2) distortion-product otoacoustic emissions (DPOAEs) evoked by primaries with f<sub>2</sub> at the same frequency values. The experimental groups were: 1) TCDD-exposed compared to vehicle-exposed CBA mice, and 2) TCDD-exposed compared to vehicleexposed C57B6 mice. Because prenatal TCDD exposure has been associated with sexually dimorphic effects, males and females were analyzed separately. Cochlear threshold sensitivity was significantly elevated in both female and male mice in the C57B6 strain but not significantly elevated in the CBA strain following TCDD exposure. The differential sensitivity in two mouse models containing Ahr<sup>b</sup> alleles is consistent with the notion that genetic polymorphisms in addition to AhR could mediate the adverse effects of TCDD on cochlear function following exposure.

(Supported by NIH: DC03086, ES013512, ES01247)

#### 566 Establishing an Animal Model of Embryonic Iron Deficiency

Camelia N. Mihaila<sup>1</sup>, **Adam C. Dziorny**<sup>2</sup>, Anne E. Luebke<sup>2,3</sup>, Margot Mayer-Pröschel<sup>3,4</sup>

<sup>1</sup>Dept. of Pharmacology & Physiology, <sup>2</sup>Dept. of Biomedical Engineering, <sup>3</sup>Dept. of Neurobiology & Anatomy, <sup>4</sup>Dept. of Biomedical Genetics, University of Rochester Medical Center

Iron deficiency is the most prevalent nutritional deficiency in the world, affecting 25% of the world's infants. In addition to hematological consequences, perinatal iron deficiency can lead to blood-brain barrier alterations, longterm cognitive abnormalities, learning impairments, and hypomyelination. The pathology of hypomyelination has been confirmed in anemic children, who exhibit slower auditory nerve conduction velocities when compared to non-anemic children. While it is not clear how iron deficiency affects gliogenesis, we recently discovered that iron deficiency disrupts glial precursor cell function during embryogenesis as early as E13.5, a developmental window that had not been considered in previous studies on the possible causes of dysmyelination associated with iron deficiency. Our data are consistent with the observation in children that months of postnatal iron replacement do not correct the conduction velocity defect. Taken together our data suggest that hypomyelination resulting from iron-deficiency might be a precursor cell disorder.

In order to further define the window of vulnerability and timepoints that would be relevant for therapeutic interventions, we established a rodent model in which we can analyze the effects of embryonic iron-deficiency to hypomyelination in a non-invasive manner. We provide data showing that the duration of iron deficiency prior to mating determines the onset of embryonic iron deficiency. In addition, we show that offspring from iron-deficient rat dams exhibited significantly slower auditory nerve conduction velocities as assessed by auditory brainstem response (ABR) latency measures. Work is ongoing to establish a similar model in the CBA mouse, which would allow future studies of central auditory temporal processing to be performed. Such studies are necessary to determine if there is a link between embryonic iron-deficiency and language learning impairment.

(Supported by NIH DC003086, NS044374, and GM007356)

#### 567 Is the Pathology of Endolymphatic Duct and Sac Caused by Genetic Aberrations of Their Two Normal Developmental Phases? Leslie Michaels<sup>1</sup>, Sava Soucek<sup>2</sup>, Tao Upile<sup>1</sup>, Anthony

**Leslie Michaels**', Sava Soucek<sup>2</sup>, Tao Upile', Anthony Wright<sup>1</sup>

<sup>1</sup>University College London, <sup>2</sup>St. Mary's Hospital, London Two forms of major pathologic change affect the endolymphatic duct and sac (EDS): a) enlarged EDS (enlarged vestibular aqueduct), often associated with sensorineural hearing loss and b) primary endolymphatic "sac" tumor, a malignant neoplasm commencing in duct or sac or both. We studied the development of the human EDS in temporal bones ranging from 8 weeks gestation through fetal life and childhood into adulthood to seek a possible developmental basis for these pathologies. At 8 weeks the EDS form a blind-ended duct, lined by a simple flat epithelium showing papillary ingrowths towards the lumen at the saccular end. The EDS steadily elongate and widen throughout the whole of fetal life, but maintain their character as a simple tube, with patches of papillae. During fetal life small tubules begin to grow out from the epithelium of parts of the EDS. This process slowly extends to the whole of the EDS and is completed by about 4 years postpartum (Ng and Linthicum. Laryngoscope. 1998;108:984-987/ 2000;110:1452-1456). The whole EDS now manifest narrow, often multiple, tubules and zones of papillae, polypoid protrusions of hyaline material, probably collagen, into the lumen and psammoma bodies. Surrounding the duct are numerous blood vessels penetrating into the lumen of the vestibular aqueduct from the surrounding bone. We suggest that pathological enlargement of the EDS may take place as a result of failure of development from the earlier phase of a single, wide tube to the later multitubular phase, e.g. from genetic changes of the type associated with Pendred syndrome. Breakdown of the normal homeostatic mechanisms of the EDS would occur, but normal endolymph production would continue in the cochlea and widen the EDS. Endolymphatic "sac" tumor could result from mutation of genes, e.g. those responsible for von

Hippel Lindau disease, activating neoplastic proliferation in the already hyperplastic, multitubular EDS.

#### 568 Developmental Expression of Spiral **Ligament Fibrocyte Type Marker Molecules in Rodents**

#### Withdrawn

#### 569 Phylogenetic Conservation and **Expression of Neurosensory Micrornas in Mechanosensory Organs**

Marsha Pierce<sup>1</sup>, Michael Weston<sup>1</sup>, Bernd Fritzsch<sup>1</sup>, **Garrett** Soukup<sup>1</sup>

<sup>1</sup>Creighton University

MicroRNAs have been indicated to play crucial roles in development of the vertebrate ear. In analogy to other systems, they likely contribute to cellular proliferation, differentiation, and fate specification to establish the neurosensory epithelia that comprise the auditory and vestibular systems. Analysis of miR-183 expression demonstrates mechanosensory hair cell-specific expression in mouse and zebrafish ear, suggesting its importance in hair cell specification and function. To further explore the function of miR-183, we have examined the phylogenetic conservation of miR-183 family members among bilaterian organisms. We find that homologous sequences are widely distributed among invertebrates including chordate, hemichordate, echinoderm, arthropod, and nematode species. Using in situ hybridization, we have examined the expression of miR-183 family members among various vertebrate and invertebrate organisms. Results demonstrate that miR-183 family members are expressed in hair cells of vertebrates organisms including embryonic chicken ear, lamprey ear, and neuromasts and electroreceptors of salamander skin; in hair cells of the invertebrate hagfish ear; in epithelial cells of the hemichordate acorn worm; and most strikingly in mechanosensory neurons and hair cells in the Johnston's organ and haltere of *Drosophila*, the fruit fly's respective auditory and vestibular organs. The presence of homologous neurosensory microRNAs in organisms diverged by ~600 million years of evolutionary history supports the view that mechanosensory cells share a common ancestry and developmental mechanisms. Moreover, our results strengthen prospects for determining miRNA function in vertebrate ear development through scrutiny of predicted homologous miRNA target genes.

570 Neurosensory Microrna Expression in the Developing Mouse Inner Ear and Dependence on Sensory Cell Specification Michael Weston<sup>1</sup>, Marsha Pierce<sup>1</sup>, Bernd Fritzsch<sup>1</sup>,

Garrett Soukup<sup>1</sup>

<sup>1</sup>Biomedical Sciences, School of Medicine, Creighton University

Numerous studies have established the significance of miRNAs in cellular differentiation and specification in neurogenesis and epithelial morphogenesis. We are using the mammalian inner ear as a model system for investigating miRNA directed molecular processes and have previously used miRNA microarrays, RT-PCR, northern blot analysis and in-situ hybridization to show that miRNAs 96, 182 and 183 are expressed specifically in sensory hair cells and spiral and vestibular neurons. To gain insight into the role these miRNAs might play in lineage determination of these cells, we used whole-mount in situ hybridization using DIG labeled LNA probes to detail the temporal and spatial expression of miR-183, 96 and 182 as a function of mouse inner ear development, maturation and homeostasis in CD-1 (wt), Neurog1 and Atoh1 deficient mice. miRNA expression was below readily detectable levels in the E10.5-11.5 otocyst. By E12.5, miR-183. 96 and 182 expression was evident in the statoacoustic ganglia and the otic epithelium. By E14.5, miR-183, 96 and 182 expression is concentrated in inner ear ganglia and sensory regions within the otic epithelium. These data establish miR-183, 96 and 182 as markers for sensory and neuronal cell fate commitment in the developing ear. By E18.5, miR-183, 96 and 182 expression in the organ of Corti is consistent with being limited to differentiated hair cells. This pattern persists well into adulthood but displays both radial and lateral expression gradients as a function of age. While sensory neurons are absent in Neurog1 null mice, they still develop sensory epithelia, including hair cells that express miR-183. However, miRNA expression is undetected in *Atoh1* null mice, which lack morphologically distinct hair cells but retain sensory neurons. These data suggest that neurosensory miRNA 183, 96 and 182 expression is perpetuated only in conjunction with epithelial hair cell specification and that specific miRNAs may influence the differentiation of complex sensory epithelia from the primitive otic neuroepithelium. The topographic expression pattern of miR-96, 182 and 183 during mouse inner development/maturation/stasis suggests that these small RNAs may participate to enforce neuronal and sensory cell fates by blocking gene programs which promote supporting cell differentiation. The elucidation of specific miRNA-regulated cellular pathways that intersect normal ear development and hearing disease etiologies may provide novel avenues for future therapeutic intervention. supported by Grant NIH/NCRR work is

5P20RR018788-03.

#### 571 Clarin-1 in the Developing and Mature Cochlea

#### Withdrawn

### 572 Whirlin Complexes with P55 at the Stereocilia Tip During Hair Cell Development

Philomena Mburu<sup>1</sup>, Yoshiaki Kikkawa<sup>2</sup>, Stuart Townsend<sup>1</sup>, Rosario Romero<sup>1</sup>, Hiromichi Yonekawa<sup>2</sup>, **Steve D.M. Brown<sup>1</sup>** 

<sup>1</sup>MRC Mammalian Genetics Unit Harwell, <sup>2</sup>Department of Animal Science, The Tokyo Metropolitan Institute of Medical Science

Hearing in mammals is dependent upon the proper development of actin-filled stereocilia at the hair cell surface in the inner ear. Whirlin, a PDZ domain-containing protein, is expressed at stereocilia tips and by virtue of mutations in the whirlin gene is known to play a key role in stereocilia development. We have shown that whirlin interacts with the MAGUK protein p55. p55 is expressed in outer hair cells in long stereocilia that make up the stereocilia bundle as well as surrounding shorter stereocilia structures. p55 interacts with protein 4.1R in erythrocytes and we found that 4.1R is also expressed in stereocilia structures with an identical pattern to p55. Mutations in the whirlin gene (whirler) and in the myosin XVa gene (shaker2) affect stereocilia development and lead to early ablation of p55 and 4.1R labelling of stereocilia. The related MAGUK protein CASK is also expressed in stereocilia in both outer and inner hair cells where it is confined to the stereocilia bundle. CASK interacts with protein 4.1N in neuronal tissue and we found that 4.1N is expressed in stereocilia with an identical pattern to CASK. Unlike p55, CASK labelling showed little diminution of labelling in the whirler mutant and is unaffected in the shaker2 mutant. Similarly expression of 4.1N in stereocilia is unaltered in whirler and shaker2 mutants. p55 and protein 4.1R form complexes critical for actin cytoskeletal assembly in erythrocytes and the interaction of whirlin with p55 indicates it plays a similar role in hair cell stereocilia.

### 573 Non-Muscle Myosin II Regulates Cochlear Elongation Through a Convergent Extension Mechanism

**Norio Yamamoto**<sup>1</sup>, Xuefei Ma<sup>2</sup>, Robert Adelstein<sup>2</sup>, Matthew Kelley<sup>1</sup>

<sup>1</sup>NIDCD, <sup>2</sup>National Heart, Lung, and Blood Institute/NIH The presence of an elongated cochlea plays a key role in both the ability to perceive high frequencies and in frequency discrimination. The developmental and evolutionary mechanisms that directly regulate this elongation are largely unknown although it has been suggested that planar cell polarity (PCP) pathway might affect this regulation through a convergent extension mechanism (Montcouquiol, M et al. 2003, Wang, J et al. 2005).

Non-muscle myosin II is a conventional myosin found in non-muscle cells and is involved in cytokinesis, cell motility and cell polarization including the process of convergent extension as it occurs, for example, in Drosophila germ band elongation. Three different non-muscle myosin IIs (II-A, II-B and II-C) have been reported in mammals. Mutations in human non-muscle myosin II heavy chain genes can cause hereditary deafness but the basis for the auditory defect is unknown. To begin to determine the role

of myosin II genes in auditory function, the activity of myosin II was inhibited using two specific myosin II inhibitors, Blebbistatin and Y27632. Treatment of embryonic cochlear explants with either inhibitor disrupted the elongation of cochlear sensory epithelium, resulting in a shorter and wider sensory epithelium compared to control cochlear explants. Moreover, knock-in mice expressing an apparent dominant negative form of nonmuscle myosin II-B (R709C) that appears to inhibit the function of other myosin II molecules have shortened cochlea with a broadened width that appears similar to the cochlea from inhibitor experiments. These results suggest that convergent extension is an important process in cochlear development and elongation and that myosin II plays an analogous role in both the germ band elongation in Drosophila and cochlear extension in mammals. The results also suggest that the basis for the auditory defects in humans with myosin II gene mutations may be related to defects in cochlear elongation.

# 574 The Distribution of the Planar Cell Polarity Molecule Prickle-Like 2 Reveals an Additional Patterning Mechanism that Generates the Line of Reversal in Vestibular Epithelia

**Michael Deans**<sup>1</sup>, Dragana Antic<sup>2</sup>, Matthew Scott<sup>2</sup>, Jeffrey Axelrod<sup>2</sup>, Lisa Goodrich<sup>1</sup>

<sup>1</sup>Harvard Medical School, <sup>2</sup>Stanford University School of Medicine

Hair cells in the utricle and saccule are patterned in an orderly array that enables the detection of linear motion in all directions. This patterning coordinates stereociliary bundle polarity between adjacent cells and ensures that deflections of the stereocilia generate similar physiological responses within them. In addition, hair cells are divided into two functional groups with opposing bundle polarities that are separated by a line of reversal located within the These two groups generate complimentary striola. excitatory and inhibitory responses to motion that further facilitates the perception of linear acceleration. patterning the utricle and saccule is critical for vestibular function and presents a unique challenge during development because most hair cells share the polarity of their neighbors, but there is an abrupt change in orientation at the line of reversal.

The organization of hair cell stereociliary bundles parallel to the plane of the sensory epithelia is called planar cell polarity (PCP) and is regulated in part by a protein network specialized for PCP signaling that includes Frizzled 3/6, Disheveled 1/2 and Vangl2. We have evaluated the distribution of an additional PCP molecule, Prickle-like 2 (Pk2) to determine when PCP signaling might be acting during vestibular development, and whether PCP is modulated locally at the line of reversal. We find Pk2 asymmetrically localized and enriched at hair cell to support cell boundaries. Pk2 enrichment is initiated at E13.5, before stereocilia can be visualized with phalloidin, and concurrent with migration of the kinocilia to one edge of the cell. We also report the novel finding that the distribution of Pk2 is not altered at the line of reversal. As a result, in utricle hair cells located medial to the line of reversal, Pk2 is located opposite of the kinocilium, while in hair cells located lateral to the line of reversal, Pk2 and the kinocilium are adjacent. Similarly within the saccule, Pk2 distribution remains constant across the line of reversal. We propose that the patterning mechanism generating the line of reversal does not require a change in the distribution of PCP molecules. Instead, the final position of the kinocilium may be determined cell intrinsically and guided by the polarity axis established by the PCP proteins.

### 575 Cochlear Morphology is Delayed in Tshr(hyt) Mutant Hypothyroid Mice

**Edward Walsh<sup>1</sup>**, W. Bruce Warr<sup>1</sup>, Jo Ellen Boche<sup>1</sup>, JoAnn McGee<sup>1</sup>

<sup>1</sup>Boys Town National Research Hospital

Morphological changes that accompany the final stages of cochlear development during which responses to airborne sounds first appear and mature have been described in a relatively wide range of vertebrates. Among mammals, a widely recognized pattern of inner ear developmental events has been established, although the timing of specific features of maturation appears to vary in a species and strain specific manner. Among altricious mammals including the mouse, explicit morphological features of the organ of Corti are poorly defined in the immediate postnatal period. Although sensory cells are identifiable. the organ appears as a compact mass of epithelial cells with little or no evidence of Corti's tunnel or the spaces of Nuel. The inner spiral sulcus is fully occupied by a deep pseudostratified epithelium and a primordial tectorial membrane (TM) exists as a relatively thin layer contiguous with the surface of this apparently secretory tissue commonly known as Kolliker's organ. The lesser TM extends as a slip that covers the lesser epithelial ridge into which stereociliary bundles of both inner (IHC) and outer hair cells (OHC) extend. On the first postnatal day, fibers of the olivocochlear bundle (OCB) can be identified in the inner spiral bundle (ISB), particularly in basal and middle turns of the cochlear spiral, but not in the immediate vicinity of sensory cells generally. There is a clear absence of OCB fibers in apical regions of the end organ. In neonatal hypothyroid Tshr(hyt) mutant mice, organ of Corti development is notably delayed. The differentiation of sensory cells is less evident, TM thickness is diminished and the OCB is identifiable in the ISB of the basal turn only, although projection magnitude appears diminished relative to normal animals. The maturation of end organ features will be discussed, emphasizing differences in the rate and extent of development between normal and profoundly hypothyroid mice.

Supported by NIH-NIDCD DC00982, DC04566, DC04662

### 576 Computational Model of Ion Transport Pathology in the Stria Vascularis

Imran Quraishi<sup>1</sup>, Robert M. Raphael<sup>1</sup>

<sup>1</sup>Rice University

The stria vascularis contains a complicated network of transport proteins that operate synergistically to establish the endocochlear potential and transport potassium into the endolymph. We have constructed a computational model of ion transport in the stria vascularis based on available experimental data. We first consider an isolated layer of marginal cells and find that they do not make a significant direct contribution to the endocochlear potential but are capable of sustaining considerable potassium flux into the endolymph. Next, we expand the model and show that the inclusion of the channels and transporters expressed in the intermediate and basal cells is sufficient to generate the endocochlear potential. A particularly interesting prediction is the sensitivity of strial function to the potassium concentration in the intrastrial space. The model is useful for determining the dependence of the system on the properties and expression levels of different ion transporters and channels, which can be used to predict the effects of genetic mutations and drug interactions. For example, we examine the mechanisms of loop diuretic ototoxicity and genetic deafness due to potassium and chloride transport deficiencies, such as Jervell and Lange-Nielsen syndrome and Bartter's syndrome, type IV. Such simulations demonstrate the utility of compartmental modeling to investigate the role of ion homeostasis in inner ear physiology and pathology.

### 577 Role of Fibrocytes in Glutamate Homeostasis and Presbyacusis

David Furness<sup>1</sup>, Maxwell Lawton<sup>1</sup>

<sup>1</sup>Keele University

The spiral ligament contains several types of fibrocyte that express proteins involved in homeostasis. These include a glutamate transporter, GLAST. Fibrocytes show early degeneration in some animal models of presbyacusis (Hequembourg and Liberman, 2001; J Assoc Res Otolaryngol. 2, 118-129). Fibrocyte degeneration may thus lead to a degradation in the composition of cochlear fluids that contributes to presbyacusis.

We tracked how the number of fibrocytes changed with age in CD-1 mice. In 5-week mice we investigated distributions of GLAST and glutamate in fibrocytes using immunogold electron microscopy, and examined glutamate transport in excised live lateral wall by tracking uptake of the glutamate analogue D-Aspartate by immunofluorescence. Physiological responses to glutamate were investigated by incubating lateral wall in a fluorescent sodium-sensitive dye and monitoring changes in dye-marked fibrocytes in response to a brief exposure to 1 mM glutamate.

CD-1 mice lose significant numbers of type II, III, IV and V fibrocytes with age. Type V and type II fibrocytes contain the most GLAST and Type V fibrocytes contain the most glutamate, implying a correlation between GLAST expression and glutamate uptake. Fibrocytes expressing GLAST in the lateral wall showed uptake of D-Asp, confirming that they have a functional glutamate transport process. Application of glutamate to sodium-sensitive dyelabelled cells in the type V fibrocyte region elicited a decrease in fluorescence intensity a few seconds after exposure, implying that physiological changes accompany the uptake of glutamate.

These data suggest that fibrocytes play a role in glutamate homeostasis and that degeneration could be involved in presbyacusis. Since fibrocytes are mesenchymal in origin and can be maintained in proliferating cultures, we are exploring the possibility of a regenerative or replacement cell therapy designed to restore a degenerating fibrocyte population.

### | 578 | Heptanol Application to the Gerbil Round Window: A Model of Fibrocyte Apoptosis

**John Goddard**<sup>1</sup>, Hainan Lang<sup>1</sup>, Bradley Schulte<sup>1</sup>, Richard Schmiedt<sup>1</sup>

<sup>1</sup>Medical University of South Carolina

Fibrocytes of the spiral ligament are intricately linked through a network of gap junctions and are thought to play a pivotal role in K+ homeostasis within the mammalian cochlea. In the present study, heptanol, a gap junction uncoupler, was applied to the round window (RW) of gerbils for two mins and subsequently removed. The gerbils were allowed to recover for various time intervals. ranging from 12 hrs to several weeks. Histopathologic studies of the basal and middle turns 24 hrs after heptanol exposure revealed reductions in immunostaining intensity for connexins 26 and 30 and the Na-K-Cl cotransporter within the lateral wall. This was accompanied by apoptosis in type II and type IV fibrocytes as revealed by terminal deoxynucleotidyl transferase biotin-dUTP nick end labeling (TUNEL) and confirmed by electron microscopic analysis. Edema was evident in the stria vascularis at 24 hrs, one week and two weeks post-exposure, with recovery to relatively normal morphology by four weeks. Compound action potential (CAP) thresholds were significantly increased with a near-total loss of the endocochlear potential (EP) at 24 hrs. By four weeks both the CAP thresholds (4.0 to 0.5 kHz) and the EP showed partial recovery. Finally, a scattered loss of outer hair cells was observed in the basal turn. These data suggest that heptanol application to the RW, although not limited to effects on the cochlear lateral wall, could serve as a unique model of fibrocyte apoptosis. Such a model is critical to the understanding of lateral wall physiology as it would allow examination of fibrocyte function, repair, and repopulation from several potential sources, including exogenous stem or progenitor cells.

### 579 The Etiology and Pathophysiology of Post-Traumatic Endolymphatic Hydrops

**Michael Hoffer**<sup>1,2</sup>, Kim Gottshall<sup>1,2</sup>, Ben Balough<sup>1,2</sup>, Derin Wester<sup>1</sup>, Robert Moore<sup>1</sup>

<sup>1</sup>Spatial Orientation Center, <sup>2</sup>Naval Medical Research Center

Endolymphatic hydrops and its pathologic correlate Meniere's disease has been ascribed to multiple different etiologies including autoimmune, viral mediated and genetic pre-disposition. Despite a great deal of study the vast majority of cases remain classified as idiopathic. One speculated etiology of endolymphatic hydrops, trauma, remains somewhat controversial. While post-traumatic

Meniere's disease has been reported in the literature there are few formal studies of the relationship of the trauma to Meniere's disease and even less evidence that the trauma is truly etiologic. We report on 254 individuals who initially presented to our center with the post-traumatic dizziness. We have divided this group into those who suffered blunt closed head injury (198 patients) and those who suffered purely blast injury (56 individuals). Twelve percent (7/56) of the blast injury patients were diagnosed with Meniere's disease as compared to only three percent (6/198) of those in the closed head injury group. In addition, the blast injury group of patients presented significantly earlier as compared to the closed head injury group. Given the higher percentage of blast injury patients who suffer Meniere's disease we developed an experimental model to examine the effects of blast on the inner ear and to definitely demonstrate that blast injury can be etiologic in producing endolymphatic hydrops. This study has implications regarding the basic cause of endolymphatic hydrops and provides an improved basic science and clinical understanding of Meniere's disease.

#### 580 JNK-1 Inhibitor May Reduce Hearing Loss in Acute Labyrinthitis

**Gregory Barkdull<sup>1</sup>**, Yannick Hondarrague<sup>2</sup>, Elizabeth Keithley<sup>1,3</sup>, Jeffrey Harris<sup>1,3</sup>, Thomas Meyer<sup>2</sup>

<sup>1</sup>UCSD Oto/HNS, <sup>2</sup>Laboratoires Auris SAS, France,

<sup>3</sup>Veterans Affairs Medical Center, SD

Cochlear inflammation is linked to the hearing loss caused by viral labyrinthitis, autoimmune inner ear disease and bacterial meningitis. Previous histopathologic studies have demonstrated loss of both inner and outer hair cells. Over weeks to months, new bone forms within the labyrinth. These events are irreversible. The present study investigates the potential otoprotective properties of the JNK-1 inhibitor, AM-111, in an experimental model of acute labyrinthitis.

Sterile labyrinthitis was generated by injection of antigen into the scala tympani of sensitized guinea pigs (n=8). In the experimental group (n=10), AM-111 in a hyaluronic acid gel formulation was delivered to the round window membrane at the same time as antigen challenge. Cochlear function was then monitored over the course of 3 weeks with serial ABR and DPOE exams. Guinea pigs were sacrificed by intracardiac perfusion and their cochleas processed for histological examination on day 21.

Untreated animals developed severe to profound hearing loss by day 3 and this persisted until day 21. Four of the animals receiving AM-111 however, had some preservation of hearing on day 3, and their hearing benefit was maintained through day 21. Histology confirmed the presence of inner and outer hair cells at day 21 in animals receiving AM-111. These preliminary results suggest that inhibition of the JNK signaling pathway may prove to be a useful treatment strategy for sensorineural hearing loss due to inflammation.

This study was supported by Auris Medical, Lohn-Ammannsegg, Switzerland, under a Cooperative Research

and Development Agreement with the Medical Research Service of the Department of Veteran Affairs.

The lead author was supported by the NIH training grant, NIDCD DC-000028

#### 581 TNF α is Ototoxic to Auditory Hair Cells In Vitro and Treatment with Dexamethasone Protects These Hair Cells

**Thomas Van De Water**<sup>1</sup>, Adrien Eshraghi<sup>1</sup>, Shibing Chen<sup>1</sup>, Scott Haake<sup>1</sup>, Korey Jaben<sup>1</sup>, Xiaoyun Nong<sup>1</sup>, Thomas Balkany<sup>1</sup>

<sup>1</sup>University of Miami Ear Institute, University of Miami Miller School of Medicine, Miami, FL

TNF alpha plays a major role in endoplasmic reticulum stress-induced cell death (Yang et al. 2006). Dexamethasone can inhibit TNF alpha-induced cell death (Udo et al. 2001). TNF alpha and its receptor is expressed in the cochlea following vibration damage induced hearing loss (Zhou et al. 2005). There is at present no direct proof that TNF alpha is ototoxic to auditory hair cells (HCs).

To explore the effect of TNF alpha on auditory HCs and the protective effect of dexamethasone (DXM), we used P-4 rat organ of Corti explants, a series of TNF alpha concentrations(i.e. 25 to 1000 ng/mL) and a series of DXM concentrations (i.e. 25 to 250 micrograms/mL) in the cell culture medium. After 4 days in vitro, explants were fixed, stained with FITC-phalloidin and examined with fluorescence microscopy. Cuticular plates with intact stereocilliary bundles were counted as viable HCs and expressed as HC density for the base, middle and apical areas of the explants. Hair cell counts were expressed as mean values +/- SD,n=20 explants/condition. Statistical analysis was performed with a Students t test and ANOVA; significance was set at p < 0.05.

Loss of auditory HCs in the TNF alpha exposed explants occurred in a dose dependent manner with the loss of HCs expressed in a characteristic base to apex pattern. Loss of HCs in the explants began at a TNF alpha conc. of 50 ng/mL. The viability of both inner (IHCs) and outer (OHCs) hair cells was affected by ototoxic levels(e.g. 250 ng/mL) of TNF alpha. The presence of DXM in the medium containing an ototoxic dose of TNF alpha (i.e. 1000 ng/mL) protected both IHCs and OHCs in a dose dependent fashion.

TNF alpha is ototoxic to the auditory HCs in the organ of Corti explants and dexamethasone protects the explant's HCs from TNF alpha's ototoxicity. Based on these in vitro results and those of the vibration-induced hair cell death study (Zhou et al. 2005), TNF alpha appears to be involved in the loss of HCs that are subjected to a physical trauma such as can occur during skull base surgery and cochlear implantation. Locally delivered dexamethasone may be an effective therapy for the conservation of hearing when subjecting the cochlea to the physical forces generated during the full insertion of an electrode array.

Supported by Advanced Bionics Corporation, Valencia, CA, USA

### 582 Dynamic Mobilization of Microglia/Microphage in the Mouse Inner Ear

**Takayuki Okano**<sup>1</sup>, Takayuki Nakagawa<sup>1</sup>, Tomoko Kita<sup>1</sup>, Shinpei Kada<sup>1</sup>, Juichi Ito<sup>1</sup>

<sup>1</sup>Graduate School of Medicine, Kyoto University

In the last meeting, we reported that certain cell populations in the inner ear are derived from bone marrows (BMs), which showed phenotype of microglia or macrophage expressing Iba-1 or F4/80. Previous studies have indicated that BM-derived cells are involved in the maintenance of auditory function. Yagihashi et al. have reported that macrophage macrophage colony stimulating factor (M-CSF) possesses neuroporotective effects in a rat model of auditory nerve injury. A series of studies from Iwai et al. have demonstrated acceleration of senorineural hearing loss by immune dysfunction and its prevention by BM transplantation. These findings indicate that BMderived cells in the inner ear contribute to the maintenance of inner ear homeostasis. Thus, we investigated dynamics of microglia/macrophage in inner ears under pathological conditions of inner ears. First, we examined alteration in numbers of cochlear microglia/macrophage following systemic application of M-CSF. M-CSF application induced increase of such cell populations in the cochlea, indicating that cochlear microglia/macrophage are continuously supplied from BMs. We also examined response of microglia/macrophage under two different pathological conditions, local surgical stress and age-related degeneration. Both pathological conditions resulted in increase of microglia/macrophage. These findings indicate that microglia/macrophage in the inner ear are dynamically supplied from BMs according to conditions of inner ears.

# 583 Toll-Like Receptor Signaling Pathways in the Neonatal Mouse Cochlea: Activation by Murine Cytomegalovirus (MCMV) Infection

**Nigel Woolf<sup>1,2</sup>**, Dawn Jaquish<sup>1,2</sup>, Fred Koehrn<sup>1,2</sup>

<sup>1</sup>UCSD Medical School, <sup>2</sup>VA San Diego Healthcare System

The innate immune system provides the first line of defense against invading pathogens. The family of Toll-like receptors (TLRs) recognizes conserved pathogenassociated molecular patterns (PAMPS) and activates a variety of signaling pathways that induce target genes that mediate inflammation and direct antimicrobial activity. At present little is known about the role of TLRs in inner ear immunity. This study investigated the expression of TLR1-TLR9 and the TLR downstream adaptor protein MyD88 in cochleae from control and murine cytomegalovirus (MCMV) infected C.B-17-SCID mice. Previously we reported (Woolf et al., ARO, 29:485, 2006) that newborn (P0) mice IP inoculated with recombinant MCMV (rMCMV: Smith strain MCMV expressing an EGFP reporter gene) developed, for the first time in an animal model, the endolabyrinthis characteristic of congenital human cytomegalovirus (HCMV) cases. Control C.B-17-SCID P14 mice were untreated; and experimental mice IP inoculated with 0.1 PFU of rMCMV and sacrificed at P14. Oligo GEArray Microarrays (OMM-052: SuperArray, Frederick,

MD) identified 31 genes significantly upregulated by MCMV infection, including TLR3 and MyD88. Microarray results were validated by RT-PCR: end-point RT-PCR amplified TLR1-TLR9 and MyD88 mRNA in both control and rMCMV infected inner ears. Immunohistochemistry confirmed that rMCMV infection significantly upregulated TLR3 and MyD88 protein expression in the cochlea. Double-label immunohistochemistry demonstrated that TLR3 and MyD88 expression was present in rMCMV infected (EGFP expressing) cells within stria vascularis, spiral ligament, modiolus, and inflammatory infiltrates in scala tympani and the spiral modiolar vein. Notably, no TLR3 or MyD88 immunostaining was observed in control cochleae. Our data confirm TLR signaling pathways are present in uninfected mice cochleae, and rMCMV endolabyrinthitis upregulates inner ear TLR3 and MyD88

Support: NIH DC00386, NIH DC02666 & VA Research Service.

#### | 584 | Cisplatin Induces Cytoplasmic to Nuclear Translocation of Nucleotide Excision Repair Factors Among a Proportion of Spiral Ganglion Neurons

O'neil Guthrie<sup>1</sup>, Carey Balaban<sup>1</sup>

<sup>1</sup>University of Pittsburgh

Genomic DNA is a high-affinity target for the antineoplastic molecule cisplatin. Cellular survival from cisplatin DNA damage is dependent on removal of cisplatin-DNA adducts by DNA nucleotide excision repair (NER) pathways. The rate-limiting steps in the NER reaction pathways are DNA damage identification and verification. These steps are accomplished by the proteins xeroderma pigmentosum complementation group C and A (XPC & XPA) and RNA polymerase II. Unlike RNA polymerase II, XPC and XPA have no known cellular function beyond DNA repair. Cisplatin is known to damage spiral ganglion neurons at the basal coil of the cochlea therefore we suspected that it may target their DNA and activate XPC and XPA. Female Fisher344 rats were given two, four day cycles of 2 mg/kg cisplatin (or saline), separated by a 10 day rest period. A 2 x 3 x 2 factorial design, consisting of two treatment conditions (cisplatin and saline treatment), three survival times (5, 19 and 22 days) and two analysis methods (quantitative PCR and immunohistochemistry) was employed to evaluate the expression and distribution of XPC and XPA. Quantitative PCR revealed statistically significant differences (almost 2-fold) in cochlear XPC and XPA mRNA levels after cisplatin treatment at all times except day 22 for XPA. Immunohistochemistry revealed that 50% of spiral ganglion neurons in control rats showed cytoplasmic expression of XPC and XPA. After cisplatin treatment, 50% of spiral ganglion neurons showed increased nuclear expression of XPC and XPA, which appears to represent translocation from the cytoplasm. Basal coil spiral ganglion neurons translocated XPC and XPA at later treatment cycles and with less magnitude than apical coil neurons after cisplatin treatment. Therefore, it is suggested that cisplatin treatment induces nuclear translocation of DNA NER proteins among spiral ganglion neurons and that this nuclear translocation is more effective at the apex than the base.

This work was supported by an NRSA [F31 DC05757-03] award.

#### 585 Engineered Interface for Intracochlear Infusions in Small Rodents

**Dean G. Johnson<sup>1</sup>**, XiaoXia Zhu<sup>1,2</sup>, Robert D. Frisina<sup>1,2</sup>, David A. Borkholder<sup>1,2</sup>

<sup>1</sup>Rochester Institute of Technology, <sup>2</sup>University of Rochester School of Medicine and Dentistry

Inner ear disease therapy research involving cochlear infusions in mice is challenging due to anatomical size, and the lack of commercially available cannulae with integrated insertion stops. Historically researchers have created custom cannula by insertion of micro-tubing into larger tubing to create a stepped profile, or by manually applying a small volume of silicone Silastic® a fixed distance from the tip of the micro-tubing. These approaches rely on the effective change in tubing diameter to provide an insertion stop to limit cannula intrusion into the intracochlear space. The profile also facilitates bonding the cannula to the bony tympanic bulla for long term infusion studies. While successful in some applications, the methods of construction make consistency and reliability difficult to achieve, particularly for mice. In the present investigation, a method has been developed to facilitate controlled interfaces for intracochlear infusions. Using microfabrication technologies, precision molds have been created that allow control of the size and shape of a Silastic® insertion stop molded around capillary tubing. The insertion depth is controlled by mold design. The approach allows consistent manufacture of micro-cannulae of varying tubing size specifically designed for intracochlear infusions in mice or other small rodents. Details of the mold fabrication process, molding techniques, and data on dimensional consistency of produced micro-cannulae are presented. Preliminary results of intracochlear infusions in the mouse using microcannulae designed specially for the surgical approach and anatomical limitations are analyzed and discussed. This approach has the potential to enhance infusion consistency, and mitigate complications associated with variable insertion depths and leakage at the cochleostomy site.

Supported by the Nat. Inst. for Deafness & Communication Disorders and Nat. Inst. on Aging, NIH.

### 586 Extrapolated Recovery Curves for Noise-Exposed Animals

**Marco A. Ayala**<sup>1</sup>, John K.M. Coleman<sup>1</sup>, Robert H. Riffenburgh<sup>1</sup>, Ronald L. Jackson<sup>1</sup>

<sup>1</sup>Naval Medical Center San Diego

Certainly, the military qualifies for a very noise hazardous work environment. Loss of hearing degrades the soldier's war fighting ability and places an enormous economic drain on the US government as well as having a detrimental affect on the quality of life for the noise-injured

individual. In light of this, we have been studying in a chinchilla model both pre- and post-noise treatment strategies utilizing several different compounds, including: two glutathione precursors and reactive oxygen species scavengers (methionine and L-N-acetylcysteine), a mitochondrial protectant (acetyl-L-carnitine), a glutamate antagonist (Carbamathione), and a novel peptide with antiapoptotic properties (AM-111) for continuous and impulse exposure conditions. Previously, extrapolated recovery curves for noise-exposed salinetreated animals and noise-exposed experimentally treated animals (Kopke et al, 2002) at the tested frequencies of 2, 4, 6, and 8 kHz. Recovery curves were derived using a curvilinear regressional analysis which was based on four separate threshold shift measurements. extrapolated recovery curves indicated that experimentally treated animals continued to recover hearing, as measured by ABR, far longer than saline-treated animals, with treated ears reaching asymptote at almost 5 weeks while control ears reach asymptote by week three. The current study was undertaken a) to refine the recovery curve by increasing the number of post-noise threshold shifts observations, b) by investigating any differences in recovery between pharmacological agents, c) by determining if recovery varies by experimental design (with-in and between group models), and d) to determine if a difference exists between recovery times for the impulse and continuous noise groups.

### 587 Protective Effects of Calcium Blockers in Acoustic Injury of the Cochlea

**Isao Uemaetomari**<sup>1</sup>, Keiji Tabuchi<sup>1</sup>, Hidekazu Murashita<sup>1</sup>, Akira Hara<sup>1</sup>

<sup>1</sup>University of Tsukuba

Voltage gated calcium channel (VGCC) blockers have neuroprotective effects and prevent cell death of central nervous system (CNS) in various kinds of CNS injuries. However, only a few VGCC blockers have been tested for inner ear injuries such as ototoxicity and the acoustic injury. VGCC blockers are divided into 5 subtypes including L-, N-, P-, Q- and T-types. The purpose of the present study was to examine which type of VGCC blockers could ameliorate the acoustic injury. Female ddY mice of 8 weeks of age were used in this study. Animals were subjected to a 4 kHz pure tone of 128 dB SPL for 4 hours through an open field system inside a soundexposure box. Auditory brainstem response (ABR) was examined before, one and two weeks after acoustic overexposure. After final ABR measurements at two weeks after acoustic overexposure, surface preparations are prepared for a morphological study. Whole mounts of organ of Corti were stained for the nucleus with propidium iodide, and missing hair cells (missing of staining with propidium iodine) were counted. L-type VGCC blockers, administrated immediately before acoustic overexposure, significantly improved the ABR threshold shifts and decreased hair cell loss two weeks after acoustic overexposure although other types of calcium channel blockers tested did not have any protective effect. The

present findings suggest that L-type VGCC blockers have protective effects against acoustic injury of the cochlea.

# Signalling Molecules as Therapeutic Targets for Hair Cell Death in the Injured Inner Ear

**Jing Wang**<sup>1</sup>, Jérôme Ruel<sup>1</sup>, Sabine Ladrech<sup>1</sup>, Jean-Luc Puel<sup>1</sup>

<sup>1</sup>INSERM

The therapeutic value of round window membrane delivered (RWM) D-JNKI-1 peptide against acoustic trauma-induced hearing loss is tested and characterized. Morphological characteristics of sound-damaged hair cell nuclei labeled by Hoechst staining show that apoptosis is the predominant mode of cell death following acoustic trauma. Analysis of the events occurring after acoustic trauma demonstrates that JNK/SAPK activates a mitochondrial cell death pathway (i.e. activation of Bax, release of cytochrome c, activation of procaspases and cleavage of fodrin). FITC-conjugated D-JNKI-1 peptide applied onto an intact cochlear RWM diffuses through this membrane and penetrates cochlear tissues with the exception of the stria vascularis. A time-sequence of fluorescence measurements demonstrate that FITC labeled-D-JNKI-1 remains in cochlear tissues for as long as 3 weeks. In addition to blocking JNK-mediated activation of a mitochondrial cell death pathway, RWM delivered D-JNKI-1 prevents hair cell death and development of a permanent shift in hearing threshold that is caused by acoustic trauma in a dose-dependent manner  $(EC_{50} = 2.05 \mu M)$ . The therapeutic window for protection of the cochlea from acoustic trauma with RWM delivery of D-JNKI-1 extended out to 12 hours post- noise exposure. These results show that the MAPK/JNK signaling pathway plays a crucial role in acoustic trauma-initiated hair cell death. Blocking this signaling pathway with RWM delivery of D-JNKI-1 may have significant therapeutic value as a therapeutic intervention to protect the human cochlea from the effects of acoustic trauma.

This work was supported by Auris Medical (Contract n°03233A20).

# 589 Protective Effect of Coenzyme Q10 in Noise-Induced Hearing Loss in the Guinea Pig

Yoshinobu Hirose<sup>1</sup>, Kazuma Sugahara<sup>1</sup>, Makoto Hashimoto<sup>1</sup>, Takefumi Mikuriya<sup>1</sup>, Hiroshi Yamashita<sup>1</sup>

'Yamaguchi University, Graduate School of Medicine
Substantial evidences suggest that reactive oxygen species are producted in cochlear after acoustic overstimulation trauma and cause cochlear damage. Therefore noise-induced hearing loss can be reduced by treatment with antioxidants.

Coenzyme Q10 is one of the antioxidants and vitamin-like substance. The reagent is used for the treatment of disorders of oxidative injury, such as Parkinson fs disease, stroke, and ischemic heart disease.

In the present study, we investigated the effect of Coenzyme Q10 on acoustic trauma in guinea pigs. Animals were divided into two groups. All animals were exposed to intense band noise centered at 4 kHz for 3 h (130 dB sound pressure level). In the CoQ10 group (n=10), Coenzyme Q10 (20 mg/kg) was administrated i.p. two hours before noise exposure. In the control group (n=10), same dose of the solvent was given i.p.. Seven days after noise exposure, we assessed auditory brainstem response (ABR) threshold. In addition we observed the cochlear hair cell damages.

The ABR threshold shift was significantly less in CoQ10 group than in control group. Also, the proportion of defective outer hair cells was less in CoQ10 group than in control group.

In the previous study, it was reported that coenzyme Q10 protected neuronal cell death caused by oxidative stress in vitro. The other researcher reported that, coenzyme Q10 protected rat brain cell caused by ischemia in vivo.

These facts suggest that coenzyme Q10 reduces the cochlear oxidative stress caused by acoustic over stimulation.

# 590 Administration of Amitriptyline Attenuates Noise-Induced Hearing Loss Via Glial Cell Line-Derived Neurotrophic Factor (GDNF) Induction

**Seiji Shibata**<sup>1</sup>, Yasunori Osumi<sup>1</sup>, Masao Yagi<sup>1</sup>, Seiji Kanda<sup>2</sup>, Kohei Kawamoto<sup>1</sup>, Hiromichi Kuriyama<sup>1</sup>, Toshimasa Nishiyama<sup>2</sup>, Toshio Yamashita<sup>1</sup>

<sup>1</sup>Dept. Otolaryngology Kansai Medical University, <sup>2</sup>Dept. Public Health Kansai Medical University

Antidepressant treatments have been described to induce neurotrophic factors (NTFs) and reverse the cell loss observed in rodent stress models. Amitriptyline (AT), a tricyclic antidepressant agent, has been reported in recent studies to induce glia cell line-derived neurotrophic factor (GDNF) synthesis and release in rat C6 glioblastoma cells. GDNF with other neurotrophic factors have shown protective effects in the inner ear against ototoxic and acoustic trauma by chronic infusions in the cochlea. Therefore we investigated whether AT could induce endogenous GDNF synthesis in the cochlea and attenuate cochlea damage against acoustic trauma. In the previous Mid Winter Meeting 2 years ago, we showed the presence of GDNF in the rat cochlea by RT-PCR. At this meeting we detected GDNF protein in the cochlea by additional experiments. We used Hartley guinea pigs and injected AT (30mg/kg) or saline into the peritoneum. Subjects were exposed to 117dB SPL octave band noise centered at 4kHz for 24h. Noise-induced hearing loss (NIHL) was assessed with auditory brain stem response (ABR) at 4, 8 and 16kHz measured prior to the injection, 3 days, and 7 days after noise exposure. For histological assessment we observed the sensory epithelium using a surface preparation technique and assessed the quantitative hair cell (HC) damage. We evaluated GDNF synthesis with or without intense noise exposure at 3, 12 and 24h after the administration of AT in the cochlea using Western blot analysis. GDNF expression was shown 3h and 12h after the injection without noise, whereas with noise the GDNF expression lasted for 24h. The AT-administrated group showed significantly reduced ABR threshold shift and significantly less HC damage in the inner HCs and in the 3rd row of OHCs than the saline-administrated group. These findings suggest that the administration of AT induced GDNF levels in the cochlea and attenuated cochlea damage from NIHL.

#### 591 Effects of NAC and ALCAR on Noise-Induced Hearing Loss in Rats

**Kejian Chen<sup>1</sup>**, Jianzhong Liu<sup>2</sup>, Ronald Jackson<sup>2</sup>, Kenneth Dormer<sup>3</sup>, Richard Kopke<sup>1</sup>

<sup>1</sup>Hough Ear Institute, <sup>2</sup>Naval Medical Center, San Diego, <sup>3</sup>University of Oklahoma Health Sciences Center

Acoustic trauma is a common cause of sensorineural hearing loss both in military and civilian work environments. It is generally accepted that acoustic injury leading to hearing loss is caused by an overproduction of cellular reactive oxygen species (ROS) and free radicals. Evidence suggests that ROS and free radicals are produced in the mitochondria and mitochondrial damage is related to noise-induced hearing loss (NIHL).

This study employed a combined approach to combat NIHL. N-acetylcysteine (NAC), a powerful scavenger of oxygen free radicals also enhances the synthesis of the key normally-occurring cellular antioxidant glutathione. Acetyl-L-carnitine (ALCAR) helps protect mitochondria from oxidative stress. We have compared the effects of each drug applied alone with those of their combination.

Rats were randomized into 5 groups: a, controls with no treatment, n=2; b, exposed to noise and administered saline, n=6; c, exposed to noise and administered ALCAR (100 mg/kg), n=6; d, exposed to noise and administered NAC (200 mg/kg), n=6; and e, exposed to noise and administered both ALCAR (100mg/kg) and NAC (200mg/kg), n=6.

Animals were exposed to a 105 dB octave band noise centered at 13.6 kHz for 80 minutes. Drugs were injected 2 days before, 1 hour after and twice a day for 2 more days. Auditory brainstem responses were measured before and weekly after noise. Mean ± SD dB threshold shifts at 4, 8, 15, and 30 kHz were compared between groups. Two-way ANOVA was used in statistical analysis.

After 3 weeks controls with no treatment showed no threshold shift. In the noise-exposed, saline-injected group, 30-50 dB threshold shifts were found. NAC or ALCAR alone reduced the threshold shifts by 44% and 45%, respectively, while the 2-drug combination reduced the threshold shift by 71%. The differences were significant in higher frequency domains.

The results suggest that a combined approach with drugs having different mechanisms may be more effective in hearing protection.

#### 592 Effects of 4-OH-PBN on Noise Induced Hearing Loss in Chinchillas

**Kejian Chen<sup>1</sup>**, Chul-Hee Choi<sup>1</sup>, Lisa Kite<sup>2</sup>, Angelica Vasquez<sup>3</sup>, Ronald Jackson<sup>4</sup>, Robert Floyd<sup>3</sup>, Richard Kopke<sup>1</sup>

<sup>1</sup>Hough Ear Institute, <sup>2</sup>University of Oklahoma Health Sciences Center, <sup>3</sup>Oklahoma Medical Research Foundation, <sup>4</sup>Naval Medical Center, San Diego

Acoustic trauma is a common cause of sensorineural hearing loss both in military and civilian work environments. It is generally accepted that acoustic injury leading to hearing loss is caused by an overproduction of cellular reactive oxygen and free radical species. Evidence suggests that antioxidants are neuroprotective and can reduce the damage from acoustic over exposure.

This study tested a hydroxylated alpha-phenyl-tert-butylnitrone (4-OH-PBN), a nitrone-based free radical trap, on noise induced hearing loss.

Chinchillas were randomized into 5 groups of 6 animals each. Animals were all exposed to noise and administered drug with different doses: a, administered carrier solution only; b, administered 4-OH-PBN (10 mg/kg); c, administered 4-OH-PBN (20 mg/kg); d, administered 4-OH-PBN (50 mg/kg); e, administered 4-OH-PBN (75 mg/kg).

Chinchillas were exposed to a 105 dB narrow-band noise centered at 4 kHz for 6 hours. Four hours after noise exposure 4-OH-PBN with different doses or carrier solution was injected intraperitoneally. Animals received the same injections twice a day for 2 additional days.

The auditory brainstem response (ABR) was tested at 0.5, 1, 2, 4, 6, and 8kHz, before, immediately after, and 3 weeks after noise exposure. Mean  $\pm$  SE ABR threshold shift was calculated and two-way ANOVA was used in statistical analysis.

For the controls there was an increasing threshold shift from lower to higher frequencies ranging from 10 to 40 dB SPL. For the 4-OH-PBN treated animals ABR tests demonstrated protective effects in a dose-dependent fashion. There were 32, 44, 58, and 74% threshold shift reductions with 10, 20, 50, and 75 mg/kg drug injections, respectively. The differences between the controls and treated groups were more significant at higher frequencies and with higher drug doses.

The results suggest that 4-OH-PBN is effective in hearing protection, even administered 4 hours after noise exposure.

Supported by a grant from Office of Naval Research

#### | 593 | Long-Term Pretreatment by Geranylgeranylacetone Upregulates Heat Shock Proteins and Ameliorates Noise Injury in the Guinea Pig

**Takefumi Mikuriya**<sup>1</sup>, Kazuma Sugahara<sup>1</sup>, Tsuyoshi Takemoto<sup>1</sup>, Kenji Takeno<sup>1</sup>, Makoto Hashimoto<sup>1</sup>, Yoshinobu Hirose<sup>1</sup>, Hiroaki Shimogori<sup>1</sup>, Hiroshi Yamashita<sup>1</sup> *Yamaguchi University, Graduate School of Medicine* It is known that heat shock response is necessary for cochlea function and hair cell survival when the mammalia

is exposed to intense noise. Previously, we reported that Geranylgeranylacetone (GGA) which is accepted as an inducer of the heat shock proteins (Hsps) at gastric mucosa, liver, heart, and brain, etc could induce Hsps in the guinea pig's cochlea and attenuate the cochlear damage functionally and histologically. However, the effect is not unsatisfactory yet. At this meeting, we show more effective method of GGA treatment against noise trauma. We used male Hartley guinea pigs in this study. All animals were administered GGA (100 mg/kg) or same dose of vehicle orally once a day. For western blotting assay, we used whole cochlea and the primary antibody against Hsp 70(inducible Hsp70), Hsp 40, Hsp 27,βactin(as internal control). One or seven days after the administration, we assessed the induction of Hsps in the cochlea. For functional assessment, we measured thresholds of the auditory brain stem response (ABR). For histological assessment, we observed the sensory epithelium using surface preparation technique. animals that were administered GGA or vehicle orally once a day for 1- 4 weeks were exposed to intense noise for three hours (octave band noise with a center frequency of 4 kHz). Seven days after the noise exposure, we assessed ABR examination and histological examination. After the single oral dose of GGA, western blot analysis showed that the expression of Hsp 70 was increased compared with vehicle's. Moreover, repetitive administrations for 7 days could enhance the upregulation of Hsp70. These results indicate that the long-term administration of GGA may have a stronger protective effect than short-term administration by the function of Hsp 70. To demonstrate the postulation, we assessed ABR and histological examinations 7 days after the noise exposure among the groups that were given some dose of GGA daily for 1-4 weeks or vehicle. Drastically there were most protective effects on ABR thresholds and the loss of outer hair cells in the longest administration of GGA group. These results suggest that long-term administration of GGA can be an effective method of otoprotection against noise injury.

#### | 594 | The Effects of Systemic or Topical Administration of Edaravone on Attenuating Noise Induced Hearing Loss

**Makoto Hashimoto**<sup>1</sup>, Kazuma Sugahara<sup>1</sup>, Yoshinobu Hirose<sup>1</sup>, Takefumi Mikuriya<sup>1</sup>, Kuniyoshi Tanaka<sup>1</sup>, Hiroaki Shimogori<sup>1</sup>, Hiroshi Yamashita<sup>1</sup>

<sup>1</sup>Yamaguchi University Graduate School of Medicine

Noise exposure leads to increased level of reactive oxygen species in the cochlea, and noise-induced hearing loss can be reduced by treatment with antioxidants. We reported the effects of the antioxidant edaravone, the free-radical scavenger used clinically to treat acute cerebral infarction, against acoustic trauma in guinea pigs. In this study we investigated the effects of topical or systemic administration of edaravone on attenuating noise induced hearing loss. After 3-h exposure to 130-dB noise, edaravone or saline was injected intraperitoneally once a day for 3 days (systemic administration) or edaravone-soaked Gelform was placed on the round window before wound closure (topical administration). Seven days after

noise exposure, we examined the shift in auditory brain stem response thresholds. On systemic administration, the significantly smaller shift in auditory brain stem response threshold was observed in the edaravone group; on the contrary on topical administration, no significant difference was observed in auditory brain stem response threshold between the edaravon and control group. These data may support the importance of the reduced cochlea blood flow and ischemia/reperfusion injury in the cochlea, especially stria vascularis. Our results suggest that systemic injection of edaravone may be clinically effective in the treatment of acoustic trauma.

## 595 Retinoic Acid Can Rapidly Resuscitate Hearing in Noise-Induced Temporary Threshold Shift in Mice

**Joong Ho Ahn**<sup>1</sup>, Hun Hee Kang<sup>2</sup>, So Young Kim<sup>2</sup>, Cahng Gun Cho<sup>3</sup>, Jong Woo Chun<sup>1</sup>

<sup>1</sup>Asan Medical Center, <sup>2</sup>Asan Institute for Life Sciences, <sup>3</sup>Dongguk University International Hospital

Backgrounds: Exposure to loud noise can induce temporary or permanent hearing loss; however, the mechanism underlying the death or recovery of hair cells after acoustic trauma remains unclear. 1-cys peroxiredoxin (1-cysPrx), a member of the peroxiredoxin family with a single conserved cysteine residue, reduces a broad spectrum of hydroperoxides. All-trans retinoic acid (ATRA) is an active metabolite of vitamin A with antioxidant and free-radical scavenging properties.

Objective: To evaluate the effects of ATRA for noise-induced temporary threshold shift (NITTS) in mice.

Materials and Methods: We assessed auditory brainstem response (ABR) thresholds to evaluate cochlear function. ABR of the 15 ears of mice were measured before and right after noise exposure, then measured at 1st, 3rd, 5th, 7th, 2nd weeks, 3rd weeks, and 4th weeks after noise exposure. ATRA (1mg/kg, oral injection) were fed before or right after noise exposure.

Results: After noise exposure (120 dB SPL, 3 hours), ABR thresholds showed an increase of approximately 55 dB SPL that returned to normal after 21 days. Cochlear function in both pre- and post-ATRA treated groups recovered more quickly than in control. Immunohistochemistry and Western blot showed elevated 1-cysPrx in both pre- and post-ATRA treated groups.

Conclusion: These results showed that ATRA activated 1-cysPrx, inducing rapid resuscitation of hearing after NITTS in mice through antioxidant effects.

#### 596 Effect of Retinoic Acid Administered After Noise-Exposure in Mice

**Hyun Joon Shim**<sup>1</sup>, Hun Hee Kang<sup>2</sup>, Joong Ho Ahn<sup>2</sup>, Jong Woo Chung<sup>2</sup>, Sang Won Yoon<sup>1</sup>

<sup>1</sup>Dept. of Otolaryngology, Eulji Hospital, University of Eulji, College of Medicine, <sup>2</sup>Dept. of Otolaryngology, Asan Medical Center, University of Ulsan, College of Medicine Objectives: One of the mechanism by which intense noise exposure induces apoptosis of cochlea hair cells is the C-Jun NH2-terminal kinase (JNK) pathway. All-trans retinoic acid (ATRA) is a potent inhibitor of activator protein 1, a

transcription factor of the JNK pathway. In this study we evaluated the time course of JNK expression after noise exposure, and the effect of post-exposure treatment of ATRA on noise induced hearing loss (NIHL). Moreover, we determined a window of time for effective post-exposure treatment of ATRA.

Methods: We compared the expression of JNK immediately after and 2 weeks after noise exposure in the cochleae of mice fed only rat chow by immunohistochemistry. We measured the threshold shifts of mice fed with ATRA starting various onset times after noise exposure.

Results: Our assays for JNK immunoreactivity showed results indicating that the JNK pathway, which induces apoptosis, continues for a minimum of 2 weeks after noise exposure. Mice fed with ATRA beginning within 2 days after noise had more preserved hearing threshold than mice fed sesame oil or only rat chow.

Conclusion: Early treatment with ATRA, within 2 days of exposure to noise, reduced hair cell loss and decreased JNK expression, indicating that ATRA can alleviate NIHL by these mechanisms.

## **[597]** The Effect of Retinoic Acid and Beta Carotene in the Mouse Inner Ear with Noise-Induced Hearing Loss

**Grace Jung Eun Shin**<sup>1</sup>, Jong Woo Chung<sup>2</sup>, Dae Bo Shim<sup>1</sup>, Hun Hee Kang<sup>3</sup>

<sup>1</sup>Department of Otolaryngology and Head & Neck, Konkuk University Hospital, <sup>2</sup>Department of Otolaryngology, Asan Medical Center University of Ulsan College of Medicine, <sup>3</sup>Asan Institue for Life Sciences

Background: This study was designed to find out the preventive role of all trans retinoic acid (ATRA) and Betacarotene on mice with experimentally triggered noise induced hearing loss and to compare the effects of both. Material and Methods: BALB/c mice, age of 4 weeks, with normal hearing on auditory brainstem response (ABR) was chosen for the investigation. For retinoic acid study, experimental group (n=4) had ATRA Pellet inserted subcutaneously on their neck before the noise exposure. Control group (n=4) had no pellet inserted while noise exposure. All mice were exposed to broadband white noise of 120 dB SPL for 3 hours per day for 5 days. Then their hearing was measured immediately after and hearing loss was confirmed. Month later their hearing was measured again. In the beta-carotene experiment, experimental group (n=5) had beta-carotene pellet inserted subcutaneously on their neck before the noise exposure. Same noise exposure schedule and hearing measuring method was used for this study group. Mice which completed the hearing follow-up had their cochlear extracted for tissue confirmation. And they were stained with hematoxyline & eosin stain and c-jun n-terminal kinase (JNK) stain for observation.

Results :In the retinoic acid experiment, average hearings for both control and the experimental group were 21.25  $j^3/4$  2.7 dB HL. After the noise exposure, control group showed 80.00  $j^3/4$  2.3 dB HL and the experimental group showed 52.50  $j^3/4$  1.75 dB HL. Hearing thresholds had improved to 76.25  $j^3/4$  1.2 dB and 46.25  $j^3/4$  1.8 dB after 1 month,

respectively. The threshold of both group showed a statistically significant difference (p < 0.05). In the beta-carotene experiment, both control and studied group showed 21.66  $i^3/4$  3.23 dB on their hearing. After the noise exposure, the control group showed 85.00  $i^3/4$  3.41 dB HL and experimental group showed 61.00  $i^3/4$  2.34 dB HL. After one month their hearing thresholds were 80.00  $i^3/4$  3.4 dB HL and 62.00  $i^3/4$  1.2 dB HL, respectively. The threshold of both group showed a statistically significant difference (p < 0.05).

Conclusion: From these experiments we can see that retinoic acid and beta-carotene helped to prevent the hearing loss partially, when introduced to the mice before the noise exposure. The preventive effect of these two substances differs by about 15 dB.

### 598 History of Hearing and Hearing Loss Research at NIOSH

Rickie Davis<sup>1</sup>

<sup>1</sup>NIOSH

The Occupational Safety and Health Act of 1970 created two new agencies, the National Institute for Occupational Safety and Health (NIOSH) in the Centers for Disease Control and Prevention (CDC) and the Occupational Safety and Health Administration (OSHA) in the Department of Labor. NIOSH's mission is to protect the American worker from occupational illness, injury and death through research and education.

Since its inception, NIOSH has been actively involved in hearing research. NIOSH wrote the first criteria document for Noise Induced Hearing Loss which became the bases for the Occupational Noise Exposure Standard (1971) and the Hearing Conservation Amendment (1983).

In 2006, the Institute of Medicine of the National Academies of Science was contracted to do a peer review of the NIOSH Hearing Loss Prevention Program. This required the program to organize past and present research efforts into a coherent body of knowledge. We found that our research clustered around four themes: 1) Contribute to the development, implementation and evaluation of effective hearing loss prevention programs; 2) Reduce hearing loss through interventions targeting personal protective equipment; 3) Develop engineering controls to reduce noise exposures; 4) Improve understanding of occupational hearing loss through surveillance and investigation of risk factors.

This presentation will highlight some of the hearing research efforts and partners over the 30+ years of its history.

#### 599 Diverse Synaptic Terminals on Rat Stapedius Motoneurons

**Thane E Benson**<sup>1</sup>, M Christian Brown<sup>1,2</sup>, Daniel J Lee<sup>1,2</sup>
<sup>1</sup>Eaton Peabody Laboratory, Massachusetts Eye and Ear Infirmary, <sup>2</sup>Department of Otology and Laryngology, Harvard Medical School

The middle ear muscle (MEM) reflex is a major efferent system to the auditory periphery and, in humans, is mediated primarily by contraction of the stapedius muscle. This reflex protects the ear from acoustic injury and

reduces the masking effects of background noise. Although the afferent and efferent pathways of the MEM reflex are well characterized, the central pathways are poorly understood. To elucidate the central reflex circuitry and other inputs, we characterized the synaptic profile of stapedius motoneurons (SMNs). Horseradish peroxidase labeled perifacial neurons ventromedial to the facial motor nucleus were selected for EM analysis (3 SMNs from 2 rats). Several types of terminals were found to synapse on SMNs. One type has oval-to-round vesicles filling the terminal, occasional dense core vesicles, and a markedly asymmetric synapse. This terminal type is small, 0.5-1 µm. Some of them may be serotoninergic (Thompson and Thompson, 1998, Brain Res. 787:175-178). Another terminal type has round vesicles clustered near the asymmetric synapse. This type is larger, e.g., abutting the SMN along 10 µm of proximal dendrite and 1.75 µm at its widest. It makes intermittent contacts with the SMN separated by small (less than 1 µm) discontinuities including minute glial processes. This type of terminal may be from globular bushy cells of the cochlear nucleus (Smith, P. H. et al., 1991, J. Comp. Neurol. 304:387-407). Surprisingly few synapses from these large terminals may explain the high threshold of the stapedius reflex driven by an otherwise low-threshold source. Other terminals include small ones with pleomorphic vesicles and symmetric active zones, a terminal with large, round vesicles and a subsynaptic (?) cistern rather than a flocculent postsynaptic density, and a terminal with round vesicles of bimodal sizes. A diversity of terminal types suggests a relatively large amount of synaptic integration in SMNs.

Supported by: NIDCD RO1 DC01089 and KO8 DC06285

# 600 Gene Expression in the Cochlear Nucleus: Microarray Analysis of Multipolar and Spherical Bushy Cells Isolated by Laser Capture Microscopy

**David Friedland<sup>1</sup>**, Rebecca Eernisse<sup>1</sup>, Nicole Lenihan<sup>2</sup>, John Doucet<sup>2</sup>

<sup>1</sup>Medical College of Wisconsin, <sup>2</sup>Johns Hopkins University The cochlear nucleus is the only central nervous system region receiving direct input from the auditory nerve. Primary auditory signals are processed within the cochlear nucleus and relayed to higher auditory centers for interpretation of sound location, pitch and intensity. Distinct processing tasks are addressed by specific types of neurons such as spherical and globular bushy cells, multipolar cells, octopus cells and several classes of neurons in the dorsal cochlear nucleus. electrophysiological and morphological studies have helped to define some of the features sub-serving the unique response properties of these cells, the genetic determinants of these phenotypes have not been delineated. We performed microarray analysis on RNA extracted from spherical bushy and multipolar cells within the rat ventral cochlear nucleus. Multipolar cell bodies were retrogradely labeled with BDA conjugated Alexa-488 by stereotactic injection of tracer into the inferior colliculus. Spherical bushy cells were labeled by Nissl stain and selected from the rostral most portion of the AVCN based

upon a large, round cell body and the absence of BDA-Alexa-488 label. Cells were individually selected by lasercapture microscopy, RNA was extracted and samples were run on the GE Whole Rat Genome MicroArray. Biological replicates were performed and data analyzed for consistency of expression results across different animals. Microarray data were mined for the expression of genes important for signal transduction including neurotransmitters. receptors and ion channels. Comparison was made between multipolar and bushy cell arrays to identify differentially expressed transcripts that may underlie the unique physiological properties of these neurons. Over 100 transcripts and genes showed greater than 2-fold expression difference between spherical bushy and multipolar cells.

This work was supported by NIH/NIDCD K08DC006227, R01DC006268 and P30DC05211.

#### 601 Opioid Receptor Expression in the Major Nuclei of Brainstem Auditory Pathway

**Nopporn Jongkamonwiwat**<sup>1</sup>, Pansiri Phansuwan-Pujito<sup>2</sup>, Stefano O. Casalotti<sup>3</sup>, Andrew Forge<sup>3</sup>, Hilary Dodson<sup>3</sup>, Piyarat Govitrapong<sup>4,5</sup>

<sup>1</sup>Faculty of Health Science, Srinakharinwirot University, <sup>2</sup>Department of Anatomy, Faculty of Medicine, Srinakharinwirot University, <sup>3</sup>UCL Centre for Auditory Research, University College London, <sup>4</sup>Neuro-Behavioural Biology Center, Inst. of Sci. and Tech. for Res. and Dev. Mahidol University, <sup>5</sup>Center of Neuroscience and Department of Pharmacology, Faculty of Science, Mahidol University

There are numbers of evidence have indicated the existence of opioid peptides in the major nuclei in the auditory pathway. Opioid peptides are known to act as a neurotransmitter or neuromodulator and they have been involved in variety function such as pain cardiovascular functions, but their roles in audition are still in limitation. Recently, we have identified and localized the mu-(MOR), delta-(DOR) and kappa-(KOR) opioid receptor subtypes within the rat and guinea pig cochlea. In the present study we have extended our studied to the expression of opioid receptors in the major brainstem auditory nuclei of guinea pig. The expression of opioid receptor subtypes has been determined by reverse transcriptase-polymerase chain reaction (RT-PCR). Amplification of RNAs from cochlear nucleus and inferior colliculus with MOR, DOR and KOR primers resulted in products of the predicted lengths 217, 356 and 397 bp, respectively. All three receptor subtypes were further localized by immunocytochemical study. The main finding is that we found all types of opioid receptor virtually in most of the nuclei of brainstem auditory pathway. The immunoreactivities of opioid receptors were strongly expressed in the cochlear nuclear complex, superior olivary complex and inferior colliculus. This suggests that the opioid receptors are widely distributed through the major nuclei of auditory pathway. Our results can be implicate that opioids possibly function in the central auditory pathway and may play a role in regulation of the auditory perception. However, the role of opioid receptors in the auditory system remains unclear and further studies are necessary to characterize the opioid mechanisms in the auditory pathway.

### 602 The Effect of Slice Orientations on Auditory fMRI at the Inferior Colliculi Level

**Lavinia Slabu**<sup>1</sup>, Remko Renken<sup>1</sup>, Hans Hoogduin<sup>1</sup>, J.Esther C. Wiersinga-Post<sup>1</sup>, Hendrikus Duifhuis<sup>1</sup>

\*\*University of Groningen, Neuroimaging Center\*\*

In spite of a great amount of research dealing with activation of the auditory cortex, little information exists on functional imaging of subcortical auditory pathway [1]. Functional imaging of the brainstem is complicated due to heart beat related motion, blood flow, cerebrospinal fluid movement, tissue deformation and small size of the auditory nuclei. From literature it is reported that the brainstem motion is related to the heart beat in the rostrocaudal and ventro-dorsal directions [2]. The aim of this study is to investigate the effect of the slice orientation on auditory fMRI measurement in the inferior colliculi.

Sparse sampling was used (TR=12 s) to minimize the influence of the echoplanar noise. The stimuli consisted of pink noise modulated in the temporal and spectral domain [3]. BOLD contrast images were acquired at a 3 T MRI system with gradient echo planar imaging, without cardiac gating [2, 3, 4]. Three different slice orientations were used: approximately parallel, at 45 degrees, and orthogonal to the brainstem.

Fourteen healthy volunteers participated for this study. Four data sets were excluded due to excessive head motion. We calculated standard deviation (SD), normalized standard deviation (NSD) of the residuals, effect size, median t-values, signal intensity and number of active voxels to quantify variability in activation between orientations and subjects [5].

T-values are not significantly different for the three orientations. Therefore, their sensitivity is approximately equal. Inter-orientation differences are highlighted in the SD, the NSD and the effect size. The orthogonal slice orientation offers the highest effects size, but also results in the highest SD and NSD. The 45 degrees slice orientation offers the highest spatial accuracy and show the smallest SD and NSD values. We assume that these effects are due to the brainstem motion and less macrovascular artifacts.

#### Reference:

- [1] Heßelmann et al. (2001). Hearing Research 158: 160-164.
- [2] Enzmann DE and Pelc NJ (1992). Radiology 185: 653-660.
- [3] Langers et al. (2005). Neurolmage 20: 265-275.
- [4] Yetkin et al. (2004). The Laryngoscope 114: 96-101.
- [5] Chen N-K et al. (2003). NeuroImage 19: 817-825

## 603 Maturation of MNTB Neurons Parallels Growth of the Calyx of Held Prior to the Onset of Hearing

Brian Hoffpauir<sup>1</sup>, George Spirou<sup>1</sup>

<sup>1</sup>WVU School of Med

We have previously shown that, in mice, formation of immature calyces of Held begins on postnatal day 2 (P2) and can occur in as few as 48 hours. By P4, immature calyces can cover nearly half of their postsynaptic targets, the principal cell of the medial nucleus of the trapezoid body (MNTB). Postsynaptic currents mature in concert with calyx growth, increasing from 0.44 nA to 6.71 nA from P2-P4. The rapid increase in current amplitude led us to hypothesize that the MNTB cell likely reduces its input resistance during this period of growth to prevent overstimulation. Using current clamp recordings and following animals from the same litter (P0 - P8), we find that the firing properties of MNTB cells begin maturing during the stages of protocalyx growth. From P0-P2, MNTB cells produce trains of action potentials during single depolarizing current steps. Beginning at P3-P4, some cells produce a single spike in response to current injection at or just above threshold, although most fire multiple spikes or trains of spikes in response to suprathreshold current steps. Beginning at P6, most MNTB cells produce only 1-3 spikes in response to current steps. The resting input resistance shows a large decrease from 607  $\pm$  40 M $\Omega$  to 241  $\pm$  34 M $\Omega$  over P0-P4. For the same time period we also observe a 2.3-fold decrease in action potential halfwidths and a 3-fold increase in the threshold for action potential generation. The maturation of these properties continues from P4-8, but at a slower rate. The most rapid change for all of these parameters occurs between P2-P4. a time that corresponds to the emergence and growth of the protocalyx. Voltage clamp recordings, performed in the presence and absence of Dendrotoxin I, show increases in both the low-threshold and high-threshold K<sup>+</sup> channel currents. Together, these data suggest that developmental changes in the biophysical properties of the MNTB cell coincide with the rapid growth of the presynaptic calyx before the onset of hearing.

# [604] The Neural Source of Commissural Connections Between the Cochlear Nuclei: Distinct Components Revealed by Axonal Trajectory

John Doucet<sup>1</sup>, Nicole Lenihan<sup>1</sup>

<sup>1</sup>Johns Hopkins University

Of the two major classes of multipolar neurons in the ventral cochlear nucleus (VCN), D-stellate cells are thought to be the neural source of the CN commissural pathway. D-stellate cells have large somata covered with synaptic terminals and axons that exit the nucleus via the dorsal or intermediate acoustic stria (DAS/IAS). At the ARO last year, we presented a study of VCN commissural neurons that combined retrograde labeling of these cells in rats with immunocytochemical detection of synaptic vesicles. Confocal microscopy was employed to quantify the size of the labeled cell bodies and the percentage of

the soma apposed by synaptic terminals. Consistent with prior descriptions of D-stellate cells, many labeled neurons had large somata (soma area > 350 µm²) and percent appositions greater than 80%. But surprisingly, more than 70% of the labeled cells had a soma < 350 µm<sup>2</sup> and a percent apposition < 50%. In the experiments presented here, we followed up on this work by studying how the axons of VCN commissural neurons exit the CN. In rats, we made a large injection of Flurogold (FG) in the left CN and surgically cut the DAS/IAS of the right CN - severing the axons of D-stellate cells in the right CN that project their axons across the brain stem and into the FG injection site. Using the same analyses described above, we made the following observations: (1) hundreds of FG-labeled neurons were observed in the right VCN, (2) none of these neurons had a soma > 350 µm<sup>2</sup> and a percent apposition > 60%, consistent with transection of all D-stellate axons, and (3) all the FG-labeled neurons had somata < 350 µm<sup>2</sup> and the majority (83% of cells) had percent appositions < We conclude that D-stellate cells are a small component of the commissural pathway linking the cochlear nuclei. Instead, the neural source of this pathway is primarily small and medium-sized cells that have relatively few synaptic terminals on their soma and appear to project their axons out of the nucleus via the trapezoid body.

This work was supported by NIH/NIDCD grants R01DC006268 and P30 DC05211.

## 605 Transneuronal Analysis of the Middle Ear Muscle Reflex Pathways Using Pseudorabies Virus

**Alanna Windsor**<sup>1</sup>, Botond Roska<sup>2</sup>, M. Christian Brown<sup>3,4</sup>, Daniel J. Lee<sup>4,5</sup>

<sup>1</sup>Harvard College, <sup>2</sup>Friedrich Miescher Institute for Biomedical Research, <sup>3</sup>Department of Otology and Laryngology, Harvard Medical School, <sup>4</sup>Eaton Peabody Laboratory, Massachusetts Eye and Ear Infirmary, <sup>5</sup>Dept. of Otolaryngology, UMass Memorial Medical Center

The middle ear muscle (MEM) acoustic reflex is a major efferent system to the auditory periphery and is thought to protect the ear from acoustic injury and reduce the masking effects of background noise. Sound presented to one ear can trigger the contraction of the MEMs in the same ear (uncrossed reflex) and opposite ear (crossed reflex). The afferent pathway, passing from nerve fibers in the cochlea to the cochlear nucleus, and the efferent pathway, passing from motoneurons in the brainstem to the MEMs, are well described. However, the interneurons and central pathways that mediate the MEM reflexes are poorly understood. The aim of this study was to localize and characterize the interneurons of the stapedius and tensor tympani reflex in rats using Bartha pseudorabies virus (PRV). PRV is a retrograde neurotropic viral tracer that labels neurons in a trans-synaptic fashion. We performed time-graded survival experiments and fluorescence immunohistochemistry for both pathways following MEM injection. At 24-hour survival periods, MEM motoneurons were labeled, followed at successive time intervals by superior olivary complex (SOC), cochlear

nucleus, locus coeruleus, and inferior colliculus neurons. Notably, tensor tympani injections revealed PRV-labeled neurons in the anteroventral cochlear nucleus, and PRV-labeled neurons in the posteroventral cochlear nucleus following stapedius injection at 72-120 hour survival times. These data provide valuable clues about the inputs to MEM motoneurons and the circuitry of the reflex pathways. Supported by the NIDCD 1 K08 DC06285-01 and the American Hearing Research Foundation.

## 606 Characterization of the Superior Paraolivary Nucleus in the Unanesthetized Mouse

Richard A. Felix, II<sup>1,2</sup>, Albert Berrebi<sup>1,2</sup>

<sup>1</sup>West Virginia University School of Medicine, <sup>2</sup>Sensory Neuroscience Research Center

The superior paraolivary nucleus (SPON) is a prominent cell group of the mammalian auditory brainstem. However, the functional role of the SPON in hearing remains unclear. Previous investigations of SPON physiology have produced conflicting results. In the gerbil, SPON neurons show both monaural and binaural responses, have a wide range of spontaneous activity rates and display onset and offset discharge patterns (Behrend et al., 2002; Dehmel et al., 2002). In contrast, rat SPON responses are exclusively monaural, show low rates of spontaneous activity and respond overwhelmingly to the offset of stimuli (Kulesza Jr. et al., 2003). In this study, we examined responses of SPON neurons from unanesthetized mice. We obtained single-unit responses to noise, pure tones and sinusoidally amplitude modulated tones. All SPON neurons were driven exclusively by stimuli presented to the contralateral ear and the vast majority of responses showed offset discharge patterns and had low rates of spontaneous activity. Most units displayed little or no activity during the presentation of noise or tone stimuli, but a subset of SPON neurons showed substantial chopper-like activity during presentation of broad-band noise stimuli. Compared to pure offset responders, this subset of neurons was capable of phase-locking to higher modulation rates of SAM tones. Other characteristics of SPON neurons in the mouse, including offset response latency, thresholds and sharpness of frequency tuning were similar to those reported in the rat (Kulesza Jr. et al., 2003). The subtle differences observed between mouse and rat response properties may be due to genuine species differences, or to the use of anesthetics in previous in-vivo rat experiments.

Supported by DC-06626 to ASB.

## 607 The Role of GABAB Receptors in Development of Inhibitory Projections to the MSO

**R. Michael Burger<sup>1,2</sup>**, Olga Alexandrova<sup>2</sup>, Benedikt Grothe<sup>2</sup>, Achim Klug<sup>2</sup>

<sup>1</sup>Lehigh University, <sup>2</sup>Ludwig Maximilians Universität München

Interaural time disparities are processed over networks of auditory neurons that derive their response properties by virtue of intrinsic and network properties. The network devoted to processing ITDs must develop a precise synaptic architecture in order to compute ITDs on the usecond scale. Indeed, previous studies indicate inhibitory inputs to the MSO exhibit an experience dependent remodeling resulting in a biased distribution of inhibition to MSO neuron somas. Disruption of normal auditory experience prevents this remodeling and results in receptors more broadly distributed over somas and dendrites. Recent studies have shown that GABAB receptors mediate a developmentally restricted plasticity in the LSO, a nucleus that shares some of its inhibitory input with the MSO. We aimed to examine the role of GABAB receptors in the development of inhibitory input to the MSO. We used whole cell recordings from MSO neurons to evaluate GABAB influences on synaptic transmission during the critical period. Second we manipulated GABAB signaling in vivo and then evaluated the distribution of inhibitory receptors in adult MSO neurons using immunohistochemical methods. We draw three main conclusions from our data; 1) GABAB activation provides a strong suppression of synaptic transmission at both excitatory and inhibitory MSO synapses 2) MSO neurons show a GABAB receptor dependent long term depression similar to LSO neurons 3) Preliminary data suggests that blocking GABAB receptor signaling in vivo results in a redistribution of glycine receptors. These data taken together demonstrate for the first time that GABAB receptors may underlie both developmentally and physiologically important functions in the MSO.

### 608 Dendrites of Medial Olivocochlear (MOC) Neurons

M. Christian Brown<sup>1,2</sup>, Jessica Levine<sup>1</sup>

<sup>1</sup>Mass. Eye & Ear Infirmary, <sup>2</sup>Harvard Medical School Frequency tuning curves of MOC neurons are sharp, indicating that sound-evoked input that drives these neurons occurs within restricted CF bands. Although input to MOC neurons is mainly onto their dendrites, the patterns of dendritic orientation and extent have not been systematically investigated. The dendrites of MOC neurons were studied by staining for acetylcholinesterase in CBA mice. Darkly AChE-stained large periolivary neurons were presumed to be MOC neurons. numbers and distribution were generally similar to those reported using retrograde labeling in mice (Campbell and Henson, 1988, Hearing Res. 35: 271-274) although a few AChE-stained neurons were also seen dorso-medial to the In contrast, numbers of AChE-stained neurons within the LSO (presumably lateral (L) OC neurons) were somewhat smaller than with retrograde labeling, possibly indicating some non-cholinergic LOC neurons were missed with the AChE stain.

MOC dendrites were thick and tapered gradually with distance from the soma. Some dendrites could be traced up to 0.3 mm and some ended in swellings. The dendrites mingled with fibers of the trapezoid body. Most dendrites from neurons ventral to the LSO were oriented medially or laterally. These dendrites were constrained ventrally by the ventral surface of the brainstem and dorsally by the LSO, which they did not invade. For MOC

neurons in more rostral areas (rostral VNTB / RPO), some dendrites also coursed dorso-ventrally. In sagittal sections, some dendrites were observed to run rostro-caudally. Although most MOC neurons had dendrites that were intertwined with those of other neurons, a few isolated neurons at the edges of the periolivary regions were reconstructed to all of their dendrites. All dendrites of these single MOC neurons could be contained within a single plane. These varying patterns of MOC dendrites suggest varying patterns of synaptic input that drive the sharply tuned responses.

(Supported by NIDCD grant 01089).

### 609 Alterations in Kinesin Expression Following Lead Exposure in the Developing Murine Brainstem

**Sunyoung Park**<sup>1</sup>, Diane Brooks<sup>1</sup>, Diana Lurie<sup>1</sup>

<sup>1</sup>Dept. of Biomedical and Pharmaceutical Sciences, The University of Montana, Missoula MT

Lead exposure during development is associated with learning disabilities such as dyslexia, and has also been found to result in auditory temporal processing deficits. We have found that Pb exposure during development alters the expression of three kinesin motors (kif1A, kif5A, kif17), and their cargos specifically within the murine auditory brainstem. The kinesin superfamily of proteins are motor proteins that serve to transport various organelles and macromolecules along microtubules. Pb-induced changes in kinesin expression could modulate auditory temporal processing because the cargos of these kinesins are molecules that can regulate synaptic transmission. These cargos include the structural protein neurofilament, the synaptic protein synaptophysin, and various glutamate have previously observed receptors. We expression of phosphorylated neurofilament synaptophysin in the auditory brainstem of Pb-exposed mice, implicating kinesin proteins as a target of Pb. In this study, CBA/CaJ mice were chronically exposed to 0 mM (control), 0.01 mM (very low), 0.1 mM (low), and 2 mM (high) Pb-acetate (n=4) from gestation through postnatal day 21. Our very low levels of Pb produce an extremely low blood Pb level of 11 ug/dl, close to blood Pb levels that are considered to be safe in children (10 ug/dl). Immunoblot analysis of the auditory brainstem demonstrates that very low levels of Pb exposure increases the expression of kif5A, and decreases the expression of kif1A, and kif17. Very low levels of Pb also result in changes in immunoreactivity for synaptophysin and increased expression of phosphorylated neurofilament within auditory nuclei. Our results demonstrated that exposure to even very low levels of Pb results in significant changes in the expression of kinesins and their cargos within the auditory brainstem. Such alterations may contribute to deficits in auditory temporal processing in children exposed to lead.

Supported by NIH P20 RR17670 and RR015583.

## GABA-Evoked Responses in Developing Spherical Bushy Cells of Gerbil

**Thomas Reinert**<sup>1</sup>, Mirko Witte<sup>1</sup>, Ivan Milenkovic<sup>1</sup>, Rudolf Rubsamen<sup>1</sup>

<sup>1</sup>Institute of Biology II, University of Leipzig

Spherical bushy cells (SBC) of the mammalian cochlear nucleus (CN) contain the first central synapses of the afferent auditory pathway and compute signals that contribute to sound localization based on interaural time differences. SBC integrate excitatory inputs from few auditory nerve terminals (endbulbs of Held) with acoustically driven, GABA- and glycine-mediated inhibition. We recently showed a switch from depolarizing to hyperpolarizing E<sub>GABA</sub> in SBC between postnatal days 5 and 7 (P5-7) which is mediated by the CI-extruding cotransporter KCC2. Here we utilized Ca<sup>2+</sup> imaging, Cl<sup>-</sup> imaging, gramicidin-perforated patch clamp, immunohistochemistry to address the basis depolarizing EGABA in early developing SBC. The GABAA receptor-mediated Ca2+ signals were evoked in P3-5 but not in P15 gerbils and Ca<sup>2+</sup> transients were dependent on the Cl gradient. Consistent with this finding is a gradual decrease in [CI], in developing SBC, as indicated by the MEQ fluorescence imaging. The depolarizing gradient for  $Cl^{-}$ , as revealed by  $E_{GABA}$  and by GABA-evoked  $Ca^{2+}$ signals, was maintained by a bumetanide-sensitive CIaccumulating mechanism. This suggests a possible action of a Na+-K+-Cl cotransporter (NKCC). This notion is supported by CI-imaging data which indicate an involvement of a Na<sup>+</sup>-dependent Cl<sup>-</sup> accumulation in SBC was independent of the animals Immunohistochemical staining of the anteroventral CN revealed expression of NKCC1 in SBC even after the switch from depolarizing to hyperpolarizing action of GABA. Taken together, these experiments indicate a possible role of NKCC1 in transient maintainance of depolarizing GABA effect on developing SBC.

## 611 The Effect of Pb on Pathfinding Genes Within Auditory Nuclei in the Developing Murine Brainstem

**Linda Jones**<sup>1</sup>, Diane Brooks<sup>1</sup>, Corbin Schwanke<sup>1</sup>, Mark Pershouse<sup>1</sup>, Diana Lurie<sup>1</sup>

<sup>1</sup>Dept. of Biomedical and Pharmaceutical Sciences, The University of Montana, Missoula MT

The developing brain is very susceptible to the toxic effects of Pb, and Pb exposure in children is a known risk factor for learning disorders, IQ reduction, hyperactivity and dyslexia. Auditory pathways appear to be particularly vulnerable to Pb, and children with learning disorders such as dyslexia have been shown to have deficits in central auditory processing. Of particular concern is chronic exposure to Pb during early neural development, a period of neuronal differentiation, migration, axonal pathfinding and synapse formation. The current study utilized microarray analysis of gene expression in the auditory brainstem at postnatal days 14 (P14) and 21 (P21) to identify targets of Pb toxicity among developmental genes.

Balb/c mice were exposed to 0 mM or 0.1 mM Pb acetate from gestation through P14 or P21. RNA samples (n=4/group) were used to probe microarray chips using the NIEHS Toxchip v1.0 and the mouse MWG set A 10K oligo chip. Significantly, several neuronal pathfinding genes were altered in response to Pb exposure, particularly at P14 when the auditory system first responds to sound and becomes activity-dependent. Included in the altered genes are those that are involved in the Wnt signaling pathway (e.g. Wnts, APC, Axin, LRP6) as well as neuronal guidance proteins (e.g. RhoA, Merlin, Slit 1, Robo-1). Of particular interest is the increase of robo-1, a regulator of midline crossing of axons in the brain and a candidate gene for dyslexia (Hannula-Jouppi, et al. PLoS Genetics 1(4):467, 2005). Using immunohistochemistry, we have confirmed increases in the proteins Merlin and Robo-1 in The establishment of appropriate neural circuitry during development is fundamental for sensory function, learning, and behavior. That Pb promotes alterations in pathfinding genes suggests its effect on auditory temporal processing may include changes in the establishment of appropriate neuronal circuitry.

Supported by NIH P20 RR17670 and P20 RR15583.

## 612 The Role of Hair Cell and Afferents in Shaping Central Auditory Connections as Studied in the Atoh1 and Pou4f3 Ddl Mutation

Feng Feng<sup>1</sup>, Bernd Fritzsch<sup>1</sup>

<sup>1</sup>Creighton University

Hair cells are essential for mechanoelectric transduction, but also provide trophic support of sensory neurons during development. Thus, viability of sensory neurons and the quality of their interaction with cochlear nuclei neurons (second order auditory neurons) depends on proper activity and trophic input from hair cells into spiral sensory neurons. In the absence of an ear (and sensory neurons), neonatal cochlear nucleus neurons are not viable. Today, the effect of the absence of hair cells alone, combined with the presence of spiral ganglion neurons, throughout embryonic development on auditory nucleus has not been assessed. Atoh1 and Pou4f3 null mice initially develop hair cell precursors, but lose them rapidly in late embryonic and early neonatal development. However, many (Atoh1) or most spiral neurons (Pou4f3) initially survive this loss until birth, and many spiral neurons even survive until 6 months of age in Pou4f3 null mice. In addition, Atoh11 is expressed in most cochlear nucleus neurons and the cochlear nuclei are absent at birth in Atoh1 null mice. These mice therefore are unique models to study the effect of simple absence of hair cells combined with a progressive reduction of spiral sensory neurons on the development of cochleotopic afferent projection and cochlear nucleus neurons.

Hypothesis: Correct afferent targeting and a crude topographic map of cochlea to cochlear nuclei connections can develop in mouse independently of cochlea hair cell maturation. We used the LacZ reporter of the hair cell specific *Atoh1* gene and positively identify undifferentiated hair cells even in *Atoh1* null mice. We show the topological progression of loss of spiral neurons in

neonates (both genes) and 7, 14, 21 day old and 4 month old animals (*Pou4f3*). The central projection of the cochlea is targeted and topologically specific in both lines, suggesting neither hair cell nor differentiated cochlear nucleus neurons playing any role in formation of a crude topology. In adult *Pou4f3* null mice we find considerable development of cochlear nucleus neurons, suggesting that the afferent fibers, even with a delayed loss in the absence of hair cells, can suffice to rescue a substantial number of cochlear nucleus neurons.

#### 613 Serotonergic Projections From the LSO to the IC in the Neonatal Mouse

Ann Thompson<sup>1</sup>

<sup>1</sup>University of Oklahoma Health Sciences Center

Serotonin (5-HT) is expressed by "non-serotonergic" thalamic, noradrenergic, and auditory brainstem neurons mouse<sup>1,2</sup>. In somatosensory perinatal of the thalamocortical projections, 5-HT and it's interaction with the 5-HT 1B receptor regulates the pattern and size of afferent terminal arborizations in an activity-dependent manner<sup>3</sup>. One of the two auditory brainstem nuclei that atypically express 5-HT, the lateral superior olive (LSO) contains neurons that project to the inferior colliculus (IC) and the cochlea, as well as neurons that form intrinsic connections. In the current study, we sought to determine if the neurons in the LSO that express 5-HT in the neonate projected to the IC. The retrograde tracer wheat germ agglutinin apo-horseradish peroxidase-Au (WGAapoHRP-Au) was injected into the IC of 4 and 5 day old pups (monoamine oxidase A knockouts). One to two days later, the brains were collected and then sections cut and the simultaneous detection processed for WGAapoHRP-Au and 5-HT. As viewed under the light microscope, 5-HT-immunoreactive neurons in the LSO contained WGAapoHRP-Au, indicating that LSO neurons exhibiting the serotonergic phenotype postnatally project to the IC. This suggests that if it has the same function in LSO afferents as in somatosensory afferents, 5-HT may mediate the formation of the fibrodendritic laminae in the IC.

<sup>1</sup>Cases, et al. (1996) Lack of barrels in the somatosensory cortex of monoamine oxidase A-deficient mice: role of a serotonin excess during the critical period, Neuron, 16:297-307.

<sup>2</sup>Thompson, A.M. (2006) "Non-serotonergic" lateral superior olivary neurons of the neonatal mouse contain serotonin, Brain Res., doi:10.1016/j.brainres.2006.08.126.

<sup>3</sup>Laurent, et al. (2002) Activity-dependent presynaptic effects of serotonin 1B receptors on the somatosensory thalamocortical transmission in neonatal mice, J. Neurosci., 22:886-900.

Supported by the Oklahoma Center for the Advancement of Science and Technology (HR05-118).

#### 614 Development of Glutamatergic Neurotransmission in Auditory Neurons is Partially Dependent on Excitatory Input: Lessons From Organotypic Cultures

Juan R Martinez-Galán<sup>1</sup>, Carmen Diaz<sup>1</sup>, **Jose Juiz<sup>1</sup>**<sup>1</sup>Universidad de Castilla-La Mancha/Medical School

To what extent the arrival of synaptic inputs affects the normal development of synaptic receptor function is a matter of debate. The question is relevant to understand the processing abilities of auditory neurons deprived of afferent connections early in development. We analyzed the function of ionotropic (AMPA and NMDA) and metabotropic (mGLUr) glutamate receptors in developing auditory neurons of the brain stem using optical recordings of intracellular calcium dynamics after bath-application of AMPA, NMDA and mGluR agonists and corresponding antagonists to organotypic chicken embryo cultures of the auditory brain stem, containing nucleus magnocellularis (NM) and nucleus laminaris (NL). We used organotypic cultures from five days embryos kept in culture from two days (d5+2d, beginning of identifiable synaptogenesis) to 13 days (d5+13d). Explants at five days rendered neurons deprived of peripheral input. Calcium dynamics through glutamate receptors were compared with control brain stem slices of comparable developmental stages. time course of activation of AMPA/kainate receptors was similar in both cases, with calcium increases peaking at d5+10d. However, the strength of the response was significantly reduced in organotypic cultures. responses to NMDA application were significantly increased in d5+2d cultures compared to controls, with no differences at later stages. More complex responses were found after application of t-ACPD. These findings support that the development glutamate receptor function is partially indepedent of synaptic input. However, normal synaptic input is needed for fine tuning of receptor activity. particularly in the case of mGLUrs.

Supported by BFI2003-09147CO2-02 and GC-02-018.

#### 615 Probability Density Functions of Neural Coincidence Detectors in the Brainstem

Ram Krips<sup>1</sup>, Miriam Furst<sup>1</sup>

<sup>1T</sup>el Aviv University

Probability Density Functions of Neural Coincidence Detectors in the Brainstem

Auditory neural activity in the periphery is usually described as non homogeneous Poisson process (NHPP). It is characterized by either Excitatory- Excitatory (EE) or Excitatory-Inhibitory (EI) coincidence detectors. The stochastic properties of the axons that exit the EE and EI nuclei are essential in order to analyze that brainstem nuclei activity.

The probability density functions of EE and EI outputs were analytically derived. We proved that for an EE nucleus that receives two NHPP inputs with instantaneous rates  $\lambda_1$  and  $\lambda_2$ , the output is also a NHPP with an instantaneous rate

$$r(t) = \lambda_1(t) \int_{t-\Delta}^{t} \lambda_2(\zeta) d\zeta + \lambda_2(t) \int_{t-\Delta}^{t} \lambda_1(\zeta) d\zeta \quad \text{where } \Delta \text{ is}$$

the coincidence window which is smaller than the refractory period ( $\tau_R$ ). For an EI nucleus whose instantaneous rates NHPP inputs are  $\lambda_E$  and  $\lambda_I$  for the excitatory and inhibitory input respectively, the output is also NHPP with instantaneous rate

$$r(t) = \lambda_e(t) \left[ 1 - \int_{t-\Delta}^t \lambda_i(\zeta) d\zeta \right], \text{ for } \Delta < \tau_R.$$

Following those derivation it is possible to estimate thresholds for interaural level difference and interaural time delays.

#### 616 Processing of Amplitude Modulated Tones in the Medial Nucleus of the Trapezoid Body and the Superior Paraolivary Nucleus of the Rat

Alexander Kadner<sup>1</sup>, Albert S. Berrebi<sup>1</sup>

<sup>1</sup>West Virginia University, Dept. Otolaryngology

We previously described a neural circuit, consisting of the Medial Nucleus of the Trapezoid Body (MNTB) and Superior Paraolivary Nucleus (SPON), that generates responses to the offset of sound stimuli.

We assessed the responses of this circuit to amplitude modulated sound. We recorded from 26 MNTB units and 14 SPON units. Stimuli were amplitude modulated tones presented 20 dB above threshold. The carrier frequency was the neuron's characteristic frequency and the modulation rates (MRs) ranged from 40 to 1200 Hz. We calculated the vector strength for each MR presented and considered a neuron's response phase locked to the stimulus if its vector strength reached 0.3 or higher.

Comparison of vector strengths between MNTB and SPON units showed that at MRs of 80 Hz or lower, SPON units achieved higher vector strengths than MNTB neurons (p<0.05), whereas at MRs of 520 Hz or higher, vector strengths of MNTB units were greater than those of SPON units (p<0.05). On average, MNTB units synchronized to MRs up to 780±62 Hz, whereas SPON units synchronized only to MRs of 389±88 Hz (p<0.01). On average, the highest vector strength observed in MNTB was 0.71±0.03 whereas the average highest vector strength in SPON was 0.92±0.02 (p<0.001). MNTB units on average reached their highest vector strength at a MR of 227±30 Hz, whereas SPON units reached their highest vector strength at a MR of 91±21 Hz (p<0.01).

This suggests that at low MRs SPON neurons show higher temporal acuity than can be explained from their known synaptic inputs. Previous anatomical studies from our laboratory have suggested that SPON neurons provide GABAergic inhibition of one another via axonal collaterals (Kulesza and Berrebi, 2000). Such self-inhibition might cause transient responses to each modulation cycle at low MRs. However, at high MRs this self-inhibition might

outlast a modulation cycle, suppress spiking and, consequently, synchronization. Supported by DC-06626 to ASB.

#### 617 Determination of Glycinergic Synaptic Decay Time in the MNTB

Tao Lu<sup>1</sup>, **Larry Trussell<sup>1</sup>** 

<sup>1</sup>Oregon Health and Science University

Neurons of the rat MNTB receive fast, glycinergic transmission (Awatramani et al, 2004). The decay time of miniature IPSCs (mIPSCs) are 2-3 ms at room temperature and less than 1 ms in mature MNTB at physiological temperature. What factors cause such rapid glycinergic responses? We hypothesized that rapid receptor kinetics could account for fast synaptic decay. However, responses of glycine receptors to rapid application of glycine were several-fold slower in decay time than mIPSCs. This difference did not seem to be an artifact of patch excision, such as damage to receptors or selective sampling of non-synaptic receptors. Glycine responses in patches and whole cells had similar decay times. Receptors in patches and at synapses had similar conductance and a low sensitivity to picrotoxin, consistent with heteromeric receptors. Synaptic release of Zn2+ did not account for the difference, since chelation of Zn2+ did not alter mIPSCs. We did find that the decay of the patch responses was sensitive to the duration of application, and this relation suggested that synaptic glycine might decay in much less than 1 ms in the MNTB. To explore this idea further, we investigated the effect of SR95531, a weak antagonist of the glycine receptor, on response amplitude and risetime. Comparing the response of patches and mIPSCs to SR95531 also suggested that synaptic glycine must decay within 1 ms. Recent experiments are also exploring the possibility that other compounds might be coreleased with glycine and regulate the receptor.

#### 618 Binaural Responses Match the Cross-Correlation of Monaural Inputs

Philip Joris<sup>1</sup>, Marcel van der Heijden<sup>1</sup>

<sup>1</sup>Laboratory of Auditory Neurophysiology, K.U.Leuven, Leuven, Belgium

The medial superior olive (MSO) is the main site for binaural interaction of low-frequency signals. Its neurons function as coincidence detectors which compare the temporal structure of their monaural inputs at an internal delay. The output of one neuron as a function of ITD, or the output at a given ITD of an array of MSO neurons with different internal delays, can be described as a crosscorrelation of the monaural input signals. Although it is known that, to a first approximation, the monaural inputs from the two ears to a given binaural neuron are matched (e.g. in characteristic frequency CF and bandwidth), the degree of matching has not been examined in detail. Some features of binaural responses suggest mismatches in the CFs of the monaural inputs from the two ears (Yin and Kuwada, 1983; Joris et al., 2006).

We recorded from low-CF, ITD-sensitive neurons in the inferior colliculus (IC) of pentobarbital-anesthetized cats

and monkeys and used two stimulus paradigms to retrieve the monaural tuning of binaural neurons. The first method consisted of delivering broadband noise and reconstructing the reverse correlation filters for each ear. In the second method we used a low-frequency version (van der Heijden and Joris, 2006) of the zwuis stimulus (van der Heijden and Joris, 2003), allowing reconstruction of amplitude and phase spectra for each ear. Because both methods require phase-locking of the responses to stimulus fine-structure, only neurons with very low BFs were tested.

The results show that 1) IC neurons differ considerably in the frequency-extent of phase-locking, 2) this extent is often different for contra- and ipsilateral ear, 3) monaural filters of the two ears can differ in amplitude and phase spectra, 4) cross-correlation of the impulse responses derived from monaural filters are in good agreement with the binaural responses at different ITDs.

Supported by the Fund for Scientific Research – Flanders (G.0392.05 and G.0633.07), and Research Fund K.U.Leuven (OT/01/42 and OT/05/57).

#### [619] Interaction Between the Anterior Auditory Cortical Field and External/Dorsal Cortex of the Inferior Colliculus: Responses to Synthesized Spices-Specific FM Tones

**Takashi Doi**<sup>1</sup>, Hiroshi Riquimaroux<sup>1,2</sup>

<sup>1</sup>Graduate School of Engineering, <sup>2</sup>Bio-navigation Research Center, Doshisha University

In this study, we investigated neural responses in the inferior colliculus (IC) of Mongolian gerbils (Meriones unguiculatus) to frequency modulated (FM) tones related to their spices-specific sounds. Gerbils vocalize various types of FM sounds for communication. Subjects were lightly anesthetized during the experiment. Enamel coated Elgyloy microelectrodes penetrated IC from dorsal to ventral direction, and neural activities were extracellularly recorded contralaterally to the ear of stimulation. Several types of upward and downward FM tones were systematically synthesized around a neuron's best frequency (BF) and presented via an earphone. Each FM tone had different time-frequency course with the same duration (150 ms). Features of neural responses in IC changed along the dorsoventral penetration tracks. In the dorsal sites, latencies were long (~50 ms), and the neurons tended to have high selectivity to FM rates and directions. In contrast, advancing in the ventral direction, latencies were getting shorter (~20 ms), and the selectivity to FM rates and directions were getting lower. In our previous study, we found that neurons in the anterior auditory field (AAF) tended to have high selectivity to FM signals. The latencies of the AAF neurons were ~30 ms. According to previous studies, strong descending connections from AAF to ventral division of the medial geniculate body (MGBv) were reported (Budinger et al., 2000), and descending connections from MGBv to mainly external nucleus of the inferior colliculus (ICx) were found (Kuwabara & Zook, 2000). These results indicate that the outputs of processed FM signals in AAF are sent back to IC. In order to process or to represent FM signals, IC may not work by itself, but may collaborate with AC. [This research was supported by a grant to RCAST at Doshisha Univ. from MEXT, Innovative Cluster Creation Project by MEXT.]

#### [620] Synaptic Mechanisms Underlying Temporal Characteristics of Responses of Neurons in the Rat's Ventral Nucleus of the Lateral Lemniscus to Repetitive Stimulation of Afferent Inputs

Huiming Zhang<sup>1</sup>, Nashwa Irfan<sup>1</sup>, **Shu Hui Wu**<sup>1</sup>

<sup>1</sup>Institute of Neuroscience, Carleton university, Ottawa, ON K1S 5B6 Canada

The ventral nucleus of the lateral lemniscus (VNLL) is suggested to be involved in encoding and processing of temporal acoustic cues. Our previous studies show that VNLL neurons generate excitatory and/or inhibitory postsynaptic potentials (EPSPs and/or IPSPs) in response to electrical stimulation of the lemniscal fibers. The EPSPs are mediated mainly by AMPA receptors, and the IPSPs are mediated by glycine and/or GABA<sub>A</sub> receptors. The purpose of this study was to explore further the synaptic mechanisms that underlie the processing of temporal characteristics of afferent inputs to VNLL.

Intracellular recordings were made from VNLL neurons in brain slices of 14-21 day old rats. Suprathreshold responses (spikes) and EPSPs were evoked by stimulation of the lemniscal fibers with 20 electrical pulses at interpulse intervals (IPIs) of 5-200 ms. Antagonists of GABA<sub>A</sub> and glycine receptors were applied to examine the effects of synaptic inhibition on responses to repetitive stimulation. Most VNLL neurons tested were able to follow repetitive stimulation with a probability of firing greater than 0.9 at IPIs of 100-200 ms. However, as the IPI was shortened to 10 or 5 ms, the firing probability was reduced to 0.69 or 0.41 respectively. There was a trend of progressive prolongation of spike latencies over the spike train. The shorter the IPI, the more evident the prolongation of the spike latencies. The occurrence time of spikes within a train displayed little fluctuation, i.e., small latency jitter. Similar temporal characteristics of the responses were observed when synaptic inhibition was removed. Analyses of amplitude, rise time and latency of the EPSPs revealed that progressive reduction in amplitude of the EPSPs over the train of stimulus pulses may account for the decrease in firing rate at short IPIs. The spike latency shift over the train may be attributed to a slower rising phase of the EPSP underlying the spike. Supported by NSERC of Canada

## 621 Tonotopic Variation in the Temporal Filtering Properties of Nucleus Laminaris Neurons

**Sean Slee**<sup>1</sup>, Matt Higgs<sup>1</sup>, Adrienne Fairhall<sup>1</sup>, William Spain<sup>1,2</sup>

<sup>1</sup>Univesity of Washington, <sup>2</sup>VA Puget Sound Health Care System

Auditory brainstem neurons in the Nucleus Laminaris (NL) encode interaural time difference (ITD), a cue used to localize low frequency sounds. NL is tonotopically

organized; characteristic frequencies of neurons vary linearly from the caudo-lateral to rostro-medial pole of the nucleus. In the present study we measured the tonotopic variation of intrinsic temporal filtering underlying spike generation in NL neurons. We made whole cell current clamp recordings from NL neurons in slices of chicken brainstem (T = 35°C, age E21-P1). Neurons were stimulated with 250 seconds of Gaussian distributed noise (stdev. / mean = 0.5) scaled in each neuron to produce an average membrane potential of around -45 mV. We used the resulting spike train to compute the spike triggered average (STA) current that drove spikes in each neuron, giving a linear estimate of its intrinsic temporal filtering. We measured the STA of neurons across the tonotopic axis and grouped them into high frequency (2.5-3.3 kHz), middle frequency (1-2.5 kHz), and low frequency (0.2-1 kHz) ranges. We further divided the low frequency neurons into two subsets based on single or multiple firing to direct current input. We found significant differences in intrinsic temporal filtering between the 4 groups of cells as measured by the time course of the STAs. The temporal filters had a broad band pass spectral profile. We found the fastest temporal filtering in the middle frequency neurons (peaking at 273 Hz), slightly slower filtering in the high frequency neurons (253 Hz), and the slowest temporal filtering in low frequency neurons (137 and 98 Hz, single and double spiking respectively). We also tested the affect of physiological temperature (40°C) and synaptic conductance on temporal filtering. We found a small increase (~5%) in filtering speed due to temperature and a larger increase (~35%) due to artificial synaptic conductance delivered using dynamic clamp.

# 622 Contribution of Resting Conductances and Voltage-Gated Na<sup>+</sup> Channel Gating to Action Potential Initiation and Propagation in MSO Principal Neurons

**P. J. Mathews**<sup>1,2</sup>, L. L. Scott<sup>1</sup>, N. L. Golding<sup>1,2</sup>
<sup>1</sup>University of Texas at Austin, Section of Neurobiology,
<sup>2</sup>Institute for Neuroscience, Austin, TX 78712

The time-coding neurons of the medial superior olive (MSO) modulate their firing rate as a function of interaural timing differences, submillisecond cues azimuthal sound location. Previously we found small action potentials (APs) at the soma of mature principal MSO neurons and small resting input resistances largely shaped by low-voltage activated potassium currents and Ih. One possibility is this large resting conductance shunts the amplitude of somatic APs. To test this hypothesis, we altered the properties of MSO neurons in brainstem slices from P14 gerbils using a digital dynamic clamp system (50 kHz sampling). A large ohmic conductance with a reversal potential at rest (-61±1.2 mV at 35°C) was introduced through a whole-cell somatic patch pipette. The additional resting conductance reduced the time constants of the neurons 2-3 fold (730 $\pm$ 35 to 290 $\pm$ 39  $\mu$ s, n=3), but somatic AP amplitudes did not decrease substantially (40±1.0 to 37±0.88 mV at 400 pA above threshold). Thus, a large resting conductance at the soma is not sufficient to cause small somatic APs. Next, we turned to Na<sup>+</sup> channel kinetics, since these typically shape the rising phase of APs. A nucleated-patch, voltage-clamp technique was employed to study Na $^+$  currents at the soma of 11 MSO neurons in brainstem slices from P13-18 gerbils (at 25 $^{\circ}$  C). Na $^+$  currents peaked at -10 mV with an average of -372±73 pA, and exhibited a voltage-dependent activation similar to that found in other brain areas (V<sub>1/2</sub> = -30±1.3 mV, k=8±0.1 mV). In contrast, the steady state inactivation of somatic Na $^+$  channels was surprisingly hyperpolarized (V<sub>1/2</sub> = -77±1.4 mV, k= -7±0.5 mV, n=6) such that at rest (-61mV) only ~10% of somatic Na $^+$  channels are available to contribute to the somatic AP. Together these findings suggest that the depolarized resting potential mediated by the large resting conductance limits the availability of Na $^+$  channels, and in turn the backpropagation of the axonal AP into the soma and dendrites.

### 623 Neural Representation of the Pitch of Iterated Rippled Noise in the Human Brainstem

Ananthanarayan Krishnan<sup>1</sup>, **Jayaganesh Swaminathan**<sup>1</sup> *Purdue University* 

Physiological and perceptual studies have shown differences in the representation of pitch of iterated rippled noise (IRN) stimuli with positive and negative gain. With positive gain, the pitch corresponds to  $1/\tau$  ( $\tau$  = delay in ms) and with negative gain, the pitch corresponds to  $1/2\tau$ . This study evaluates whether these encoding differences are preserved in the scalp recorded human frequency following response (FFR) which represents sustained phase-locked neural activity among a population of neurons in the rostral brainstem. FFRs were recorded to IRN stimuli with positive and negative gains at low and high iteration steps (n=4 & n=64) for delays ( $\tau$ ) of 2, 4 and 8 ms. Pitch strength and accuracy of pitch tracking were measured from the FFR's using autocorrelation analysis. Our preliminary results reveal autocorrelation peaks corresponding to time lag  $\tau$  for both positive and negative gain conditions with the FFR's being more robust for high iteration step. These findings suggest that pitch extraction is accomplished by an autocorrelation analysis at the brainstem level and the temporal response pattern of FFR reflects stimulus envelope condition. The FFR pitch representation at the level of brainstem appears to be similar to that observed for chopper units in the cochlear nucleus.

#### 624 A Brainstem Vocoder Based on a Model of the Ventral Cochlear Nucleus

Stefan Bleeck<sup>1</sup>. Ian Winter<sup>2</sup>

<sup>1</sup>Institute of Sound and Vibration Research, Southampton, <sup>2</sup>Institute of Physiology and Anatomy, Cambridge

Significant parallel processing occurs at the level of the ventral cochlear nucleus (VCN). It is believed that underlying this processing are discrete cellular response types which have a unique signature in their temporal adaptation patterns. However, in reality it is often difficult to define response types as discrete. Here we demonstrate that a large sample (n=648) of VCN neurons can be accurately modelled as belonging to a continuous

parameter space, even if they were not classifiable using traditional methods (Blackburn and Sachs, 1988).

We constructed first order interspike interval distributions (FOIDs) from the responses to 50ms best-frequency tone bursts. FOIDs were then plotted on a logarithmic time axis and fitted with an "extreme value distribution" (EVD). The EVD is a variation of the statistical "central limit theorem" that states that the distribution of the extreme values of arbitrary populations has a defined EVD. EVDs predict the probability of the occurrence of rare events independently of the underlying probability function. Therefore the probability for spike generation can be described statistically without knowing the exact underlying mechanism. The two parameters of the fitted FOID (mean and variance) uniformly fill a well defined area of the parameter space. Single unit types recorded from the VCN occupy different, slightly overlapping areas of this parameter space. An "automatic classification" scheme (measuring the distance to population means) closely matches the classification schemes traditionally used by physiologists.

The statistical properties of the EVD allows accurate simulation of all major VCN response types, e.g. Onsets, primary-like and choppers, as well as many units usually identified as unclassifiable. We suggest that the EVD provides a useful way of describing temporal responses of units in the VCN and could be incorporated in models of signal processing.

Using these principles we developed a VCN-vocoder analogous to a cochlear implant vocoder working along the principle that external stimulation of neurons in the VCN are perceived as sounds. How these stimuli might be perceived can be explored by reconstructing the sound of the simulated response of a population of neurons. The properties of the neuron population can be controlled (e.g. only Chopper neurons). The vocoder might become a tool for cochlear and brainstem implant research.

## 625 3-Dimensional Organization of Frequency in the Cochlear Nucleus of the CBA/J Mouse

**Michael A. Muniak**<sup>1</sup>, Alejandro Rivas<sup>1</sup>, Karen A. Montey<sup>1</sup>, Bradford J. May<sup>1</sup>, Howard W. Francis<sup>1</sup>, David K. Ryugo<sup>1</sup>

\*\*Johns Hopkins University\*\*

The inescapable relationship between structure and function has proven an important approach for exploring biological mechanisms of hearing. The orderly representation of frequency originates in the cochlea and is retained throughout most of the central auditory system. Because the cochlear nucleus initiates the ascending auditory pathways, knowledge of its tonotopic organization will provide clues to how frequency becomes established in central auditory system. Prior reports have explored general features of tonotopy in the cochlear nucleus (eg., Ehret & Fischer, 1991), but a complete 3-Dimensional (3-D) anatomical description of frequency representation in the mouse is lacking. We made dye injections into specific frequency regions of the cochlear nucleus. These data revealed a frequency map of the CBA/J mouse cochlea (Rivas et al., ARO Abst., 2005) that was essentially

identical to a map obtained with similar methods (Mueller et al., 2005). The place-frequency map indicated a logarithmic distribution of frequencies along the length of the cochlea. These injections also produced robust labeling of auditory nerve fibers and neurons in the dorsal and ventral cochlear nuclei. We have created a 3-D tonotopic map of the cochlear nucleus based on this Reconstructions of individual cases were manipulated via software (Amira) to achieve positional congruence within the virtual space. This map is being analyzed to determine whether the frequency organization of the cochlea is modified by the projections of the auditory nerve to the cochlear nucleus. Such data could indicate how frequency specializations become determined in the central nervous system.

Supported by NIH/NIDCD grants DC00232, DC00023, DC05909, DC05211, and DC00143.

#### 626 Nonzero Mean Input Processes in Volterra Series Analysis

**Bernhard Englitz<sup>1,2</sup>**, Sandra Tolnai<sup>2</sup>, Rudolph Rübsamen<sup>2</sup>, Jürgen Jost<sup>1</sup>

<sup>1</sup>Max-Planck-Institute of Mathematics in the Sciences, Leipzig, Germany, <sup>2</sup>Institute of Biology II, University of Leipzig, Germany

The experimental identification of a nonlinear system is often studied within the framework of functional expansions, i.e. Volterra or Wiener Series. In the auditory domain it has become common to consider the spectrogram of the stimulus as the input domain rather than the time-varying sound-pressure. The spectrogram represents the volume of the stimulus, hence only assumes positive values and consequently exhibits a positive mean. If in this case the cross-correlation method is used for identification of the coefficients of the Wiener Series, each kernel-estimate will be systematically influenced by the presence of other kernels in the system. The exact form of this influence is derived for arbitrary input distributions, especially gaussian, white noise with mean. The effectiveness of empirical orthogonalization of basis functionals is demonstrated on the basis of linear regression and the exact orthogonal algorithm. Simula-

tions and experiments from the early auditory system are presented to illustrate the improvements in kernel estimation and response prediction.

#### 627 Refinement and Verification of the Four-Electrode Reflection Coefficient Technique

**Alan Micco**<sup>1</sup>, Mulan Choski<sup>1</sup>, Gagan Kumar<sup>1</sup>, Claus-Peter Richter<sup>1</sup>

<sup>1</sup>Northwestern University

Cochlear implants electrically stimulate residual spiral ganglion cells to restore hearing sensation in severe to profound hearing-impaired individuals. The patterns of cochlear current flow can be determined by measuring the impedances of cochlear structures. In previous studies, we presented the four-electrode reflection coefficient technique, which we used to measure tissue resistivities

for selected cochlear structures. In this series of experiments, we refined and verified this technique.

Several series of measurements were carried out in homogeneous materials, such as potatoes, chicken and red meat. Measurements were made with the four electrode probes. The measurements were made for fresh materials and after the objects were placed in parformaldehyde for 24 hours. The results obtained with the four-electrode coefficient technique were verified using a second technique.

For the second technique, tissues were placed in a cylinder shaped chamber of given volume. The small sides of the chamber served as contacts to inject current with a given amplitude. The voltage difference between two electrodes, which were separated by a given distance, was measured at several locations between the current injecting electrodes. The measurements gave the resistance for a "cylinder section". By knowing the tissue volume of the cylinder section and the resistance between the measuring electrodes, the tissue resistivity could be calculated.

Resistivity values obtained with the two different methods were similar for the same tissue, thus verifying the fourelectrode reflection coefficient technique. Fixation changed the tissue resistivity.

Supported by a grant from Silverstein Grant in Neurotology

#### 628 An Electro-Anatomical Model of the Gerbil Cochlea

Matthew Crema<sup>1</sup>, David Mountain<sup>1</sup>

<sup>1</sup>Boston University

To convey the spectral information in an acoustic signal to a cochlear implant (CI) listener it is highly desirable that stimulating current excite only local populations of auditory nerve fibers. A commonly implicated factor in the poor performance of some CI listeners is the effect of current spread from the stimulating electrodes; both longitudinally along the length of the scala tympani, and radially into the modiolus. This effect can produce broad activation patterns, resulting in the excitation of undesired populations of auditory nerve fibers. To aid in our understanding of current spread in the cochlea and to electrophysiological experiments, developed an anatomically correct volume conduction model of the gerbil cochlea, where Poisson's equation for electrical conduction is solved using the finite element method. The three dimensional geometry of our model is constructed by segmenting images obtained via magnetic resonance microscopy (MRM). Voxels representing bone, fluid, and tissues of differing conductivity (ie. Reissner's Membrane, organ of Corti, Stria Vascularis, etc.) are assigned different conductivities. The resulting model can be used to predict the potential field resulting from a wide range of electrode configurations. Application areas include not only cochlear implant research but also studies of cochlear potentials as well as electrically-evoked potentials and electrically-evoked outer hair cell motility and otoacoustic emissions. Our procedure can be used to rapidly construct anatomically correct patient and species specific models.

Funded by NIDCD grant R01-DC29

#### [629] Identifying Spiral Ganglion Dead Regions with the Tripolar Electrode Configuration: A Practical Model of Cochlear Implant Stimulation

**Steven Bierer**<sup>1</sup>, Julie Bierer<sup>1</sup>

\*\*Inversity of Washington\*\*

The restricted electrical field afforded by the tripolar (TP) electrode configuration, should provide better resolution of tonotopic cochlear implant (CI) information than the more commonly used monopolar (MP). However, our lab has previously demonstrated that a subset of TP channels within a CI subject can exhibit relatively high thresholds and limited loudness growth. This finding implies 1) the existence of discrete regions of spiral ganglion "dead regions"; or 2) a greater radial distance from the electrodes to the spiral lamina. In this study, we explore the contributions of these elements to CI perception with a simple computational model.

The model consisted of 3 parts. The first part modeled the static electrical potential produced by a linear array of electrodes surrounded by concentric volumes of different conductivities. The second part modeled the activation of 20,000 spiral ganglion neurons, evenly spaced in clusters. The neurons were positioned in the outer conductive shell at a specified distance, d, from the electrode array. Dead regions were simulated by effectively removing entire clusters of neurons. The probability of a neuron firing an action potential was derived from published activation properties of nerve fibers. Finally, perceptual threshold and loudness were inferred from the total number of active neurons across the cochlea.

Current spread was varied by changing the fraction of current, f, flowing from the active electrode to two flanking return electrodes. Consistent with psychophysics, thresholds were highest and growth of loudness most shallow when f = 1 (TP). In addition, the impact of dead regions on both threshold and loudness became progressively more evident as f varied from 0 to 1. Overall, the findings suggest that TP is most effective for imaging dead regions, which may benefit the development of patient-specific CI mapping strategies, while partial-TP (f<1) configurations may be most appropriate for practical use.

## | 630 | Effect of Cochlear Implant Stimulation | Parameters on Stapedius Muscle EMG | Recordings

**Ryan Clement**<sup>1</sup>, Daniel Gilbert<sup>1</sup>, Natasha Tirko<sup>1</sup>, Oneximo Gonzales<sup>1</sup>, Jon Isaacson<sup>2</sup>

<sup>1</sup>Department of Bioengineering, The Pennsylvania State University, <sup>2</sup>Department of Otolaryngology, The Pennsylvania State University

The electrical stapedius reflex (ESR) threshold, detected by acoustic impedance, has been shown to be highly correlated with behavioral comfort levels established by cochlear implant recipients. However, reports suggest acoustic impedance changes are typically not detectable in 30-40% of patients. The objectives of this study were to develop an animal model and investigate the

characteristics of the stapedius muscle electromyogram (stEMG) signal elicited by a cochlear implant, as an alternative measure of ESR activation. Tungsten bipolar microwire electrodes were placed into the stapedius muscle cavity of rats to record the stEMG, during stimulation of the auditory nerve with an intracochlear electrode. Maximum stEMG potentials ranged from 20 µV to greater than 500 µV with a mean value of 174 µV (8 -42 dB SNR; mean: 24 dB). The dynamic ranges of the responses that reached saturation were approximately 10 dB, with lowest thresholds observed for wider pulse-widths and greater electrode separations. Post-operative stEMGs were also successully recorded in several animals. In the future the stEMG signal could expand the clinicians toolset for ensuring proper device fitting. It could also serve as a feedback signal for better integration of the device with the auditory system.

This work was supported in part by a Grace-Woodward Grant in Medicine and Engineering from Penn State's College of Engineering and College of Medicine and by National Institute for Deafness and Communication Disorders (NIDCD; R21DC007227).

## 631 The Dependence of Vestibular Function After Cochlear Implantation on the Location of Cochleostomy

Ingo Todt<sup>1</sup>, Dietmar Basta<sup>1</sup>, Arne Ernst<sup>1</sup>

<sup>1</sup>Unfallkrankenhaus Berlin

Vestibular dysfunction and dizziness are known complications after cochlear implantation. Dizziness after implantation is often described, but the frequency in the literature is quite variable. Less is known about the function of the vestibular receptors after cochlear implantation. Because the location of cochleostomy can be assumed to be a central factor, it's role for the preservation of vestibular function needs to be further investigated.

The aim of the present study was to compare the location of cochleostomy with vestibular function and subjective complaints.

Therefore we observed pre- and postoperative vestibular receptor function (saccule, vestibular evoked myogenic potentials; semicircular canal, caloric testing) and the dizziness handicap inventory (DHI) in 78 CI patients, which have been implanted through a modified round window approach or anterior to the round window.

Beside a high frequency of preoperative dizziness of 54 % (DHI), we observed a preoperative loss of VEMP in 29 % CI patients and in 20 % a pathologic caloric testing.

We observed a correlation between preservation of vestibular function, DHI scores and the location of cochleostomy.

Looking at the preservation of vestibular receptor function in cochlear implantation the modified round window approach has to be recommended.

#### 632 Human Auditory Steady-State Responses and Cochlear 'Dead Regions'; Part I - Normally Hearing People.

**Karolina Kluk**<sup>1</sup>, M. Sasha John<sup>2</sup>, Terence W. Picton<sup>2</sup>, Brian C. J. Moore<sup>3</sup>

<sup>1</sup>The University of Manchester, UK, <sup>2</sup>Rotman Research Institute, Toronto, Canada, <sup>3</sup>Department of Experimental Psychology, University of Cambridge, UK

A dead region (DR) is a region of the cochlea with no functioning inner hair cells and/or neurones. A DR can be detected by measuring; (1) masked thresholds in threshold equalizing noise (TEN) and (2) psychophysical tuning curves (PTCs). Both methods require behavioural responses from the patient. An early diagnosis of DRs is very important for hearing-aid fitting and for assessing a child for a cochlear implant. This study was intended as a first stage in developing an objective method of diagnosing DRs that would eliminate the requirement of behavioural responses from the patient, thus making it useful for detecting DRs in young children. The auditory steady-state response (ASSR) could provide the basis for such objective test. The ASSR is an evoked potential that closely follows the time course of the stimulus modulation; the evoked-response is specific to the frequency of the carrier. Using normally hearing adults we investigated: (1) the effect of TEN on the amplitude of ASSRs; (2) the effects that using notched-TEN stimuli had on the accuracy of TEN-test results (3) the ways of reducing the time necessary for conducting the ASSR test and increasing the frequency resolution of such test; and (4) the possibility of measuring electrophysiological tuning curves (ETCs) using amplitude-modulated frequencyswept carrier frequencies. The results show that: (1) TEN has a greater masking effect on the threshold measured electrophysiologically than on the threshold measured behaviourally: (2) the introduction of the narrow-band notches does not significantly reduce the masking effect of the noise on the amplitude of ASSRs; (3) good ASSRs can be recorded in a reasonably short time with fine frequency steps over a wide range of frequencies for signal that sweeps in carrier frequency; (4) It is possible to obtain reliable ETCs using ASSRs in normally hearing people.

Supported by Deafness Research UK, Pauline Ashley Award 2006. Rotman Research Institute, Toronto, Canada. Audiology and Deafness Research Group. The University of Manchester.

## 633 Effect of Inter-Channel Temporal Offset on Channel Interactions in Cochlear Implant Users

**Ashmita Gaur<sup>1,2</sup>**, Robert V. Shannon<sup>1</sup>, John Galvin<sup>1</sup> House Ear Institute, <sup>2</sup>University of Southern California, Los Angeles

High stimulation rates have been shown to produce greater channel interactions in the guinea pig auditory cortex at threshold levels (Middlebrooks 2004, in J Acoust. Soc. Am.). In the Nucleus cochlear implant (CI), multielectrode stimulation requires pulse trains to be interleaved in time. At high stimulation rates (eg. 2000

pulses per second per channel or pps/channel), the delay between interleaved pulses can be as small as 500 µs. The threshold measured in the auditory cortex is determined largely by the integration of cochlear stimuli within the first ~1ms of stimulation. It is unclear how the temporal offset between interleaved pulses may affect channel interaction at suprathreshold levels. In the present study, intensity difference limens (DLs) were measured for two simultaneously interleaved channels each stimulated at 250 pps/channel at 200 µs/phase and 50 µs inter-phase delay, using BP+1 stimulation mode. The masker-probe pair was spatially separated by 2.35-3 mm. The temporal offset between the masker and the probe was varied from 50µs to 1500µs and intensity DLs were measured for a number of masker and probe levels. Preliminary results show that DLs are elevated for short temporal offsets and were reduced as the temporal offset was increased to half the stimulation period.

# 634 Modulation Detection and Intensity Discrimination in Cochlear Implant Users: Effects of Modulation Rate, Stimulation Rate and Stimulation Level

John Galvin<sup>1</sup>, Qian-Jie Fu<sup>1</sup>

<sup>1</sup>House Ear Institute

Modulation sensitivity across the entire dynamic range (DR) has been strongly correlated with cochlear implant (CI) users' phoneme recognition performance [Fu (2002), in Neuroreport]. Previous normal-hearing and CI studies [e.g., Donaldson and Viemeister (2000), in J. Acoust. Soc. Am.] suggest that a similar decision variable may support both modulation detection and intensity discrimination. It is unclear how intensity resolution may contribute to modulation sensitivity when the dynamic range (DR) is expanded with relatively high stimulation rates. In the present study, we measured CI users' amplitude modulation detection thresholds (MDTs) at loudnessbalanced stimulation levels that spanned the electrode DR; MDTs were measured for carrier pulse train stimulation rates of 250, 500, 1000, and 2000 Hz and for modulation frequencies of 5, 20, 50 and 100 Hz. We also measured amplitude intensity difference limens (DLs) for the same stimulation rates and levels used for modulation detection. For all modulation frequencies, modulation sensitivity was generally poorer at low stimulation levels and at higher modulation frequencies; mean MDTs were generally better for low stimulation rates, especially at low presentation levels (< 35 % DR), similar to previous findings of Galvin and Fu (2005; in JARO). Similar to MDTs, intensity DLs were significantly lower for lower stimulation rates at low presentation levels (< 35 % DR). Thus, for a range of modulation rates and stimulation levels, high stimulation rates provided no advantage for modulation detection or intensity discrimination. MDTs were correlated with intensity DLs. While the mean slope was comparable to that found by Donaldson and Viemeister (2000), there were significant differences in slope values across subjects and across different ranges of presentation level. In general, the slope was shallower for the upper portion of the DR than for the lower portion, suggesting that modulation sensitivity for the upper portion of the DR was

better than predicted by intensity resolution. The slope was also affected by interactions between modulation rate and stimulation rate; lower stimulation rates generally produced shallower slopes, suggesting that, at low stimulation rates, modulation sensitivity was better than predicted by the intensity resolution.

#### 635 Responses of Inferior Colliculus Neuronal to SAM Tones and Electrical Pulse Trains

Russell Snyder<sup>1,2</sup>, Ben Bonham<sup>2</sup>

\*\*Utah State University, \*\* University of California Contemporary cochlear implants (CIs) encode speech using several strategies. To examine the neural encoding of acoustic and electric signals relevant to speech, we compared responses of guinea pig inferior colliculus (IC) neurons to sinusoidally modulated (SAM) tones and SAM electrical pulse trains. We inserted a 16-site recording probe along the IC tonotopic axis in normal hearing animals and recorded responses to acoustic tones to estimate threshold, CF, and Q of neurons at each site. We fixed the recording probe in place and recorded responses to one or two simultaneously presented SAM tones of various carrier frequencies, intensities, modulation frequencies (30-200Hz) and depths (0-100%).

We then deafened the cochlea, inserted a CI electrode custom-designed for guinea pigs, and recorded responses to single and two channel monopolar and bipolar pulse trains (20-1000pps). We systematically varied stimulus channel, intensity, and modulation frequency and depth.

At stimulus onset, unmodulated stimuli evoked activity across a relatively broad region of the IC tonotopic axis. Subsequent activity diminished rapidly but selectively. After 10-30ms, activity at locations remote from the best (strongest responding) location for a given tone or pulse train on a given channel decreased to near spontaneous levels, whereas neurons at the best location continued to respond. This remote decrease enhanced the selectivity of steady state responses and strongly influenced response to modulated signals. The remote decrease was greater for electric than for acoustic stimulation. SAM stimuli evoked progressively less remote decrease as modulation depth increased.

Our results suggest that 1) the response to speech sound transients is more broadly distributed across the tonotopic axis of the auditory CNS than would be predicted by acoustic spectra, and 2) the amplitude compression of Cl-processed speech favors activation selectivity. Supported by NIDCD N01-DC-2-1006.

## 636 Cochlear Implantation Influences the Temporal Responsiveness of the Primary Auditory Cortex in the Deafened Cat.

**James Fallon**<sup>1,2</sup>, Dexter Irvine<sup>1</sup>, Anne Coco<sup>1</sup>, Lauren Donley<sup>1</sup>, Rodney Millard<sup>2</sup>, Robert Shepherd<sup>1,2</sup>

<sup>1</sup>The Bionic Ear Institute, <sup>2</sup>Department of Otolaryngology, The University of Melbourne

Chronic intra-cochlear electrical stimulation (ES) is known to increase the temporal responsiveness of the auditory system in long-term deaf animals. Specifically, chronic ES

results in increases in the maximum following frequency and decreases in the latency and temporal jitter of neurons in the inferior colliculus. However, the effect of long-term deafness and chronic ES on the temporal responsiveness of neurons in the primary auditory cortex (AI) is not clear. Therefore, two months after neonatal deafening, four profoundly deaf cats were implanted with a multi-channel scala tympani electrode array and received unilateral ES (up to 200 days) to a restricted section of the basal turn from a Nucleus® Cl24 cochlear implant and Nucleus® ESPrit 3G speech processor. An additional four animals served as age-matched unstimulated deaf controls. Recordings from a total of 389 multi-unit clusters in Al were made using a combination of single tungsten and multi-channel silicon electrode arrays. The maximum rate at which units could be driven from chronically stimulated cochlear regions was significantly higher than that at which units could be driven by stimulation of the corresponding regions in unstimulated deaf control animals (Mann-Whitney; p = 0.04). However, chronic ES resulted in no significant change in temporal jitter (Mann-Whitney; p = 0.2) and a small but significant increase in the first spike latency at a supra-saturation current (Mann-Whitney; p = 0.04) of the responses of units in AI. These findings indicate that chronic ES can produce changes in the temporal responsiveness of AI, with increases in both the maximum following frequency and latency of responses. These changes in the temporal responsiveness of Al have implications for the methods used to encode the fine temporal structure of stimuli used in modern cochlear

Work funded by NIDCD (NO1-DC-3-1005) and The Bionic Ear Institute.

# 637 Evidence for Temporal Fine Structure Encoding by Cochlear Implant Subjects Using Envelope-Modulated Speech Processing Strategies

**Chad Ruffin**<sup>1,2</sup>, Grace Liu<sup>1,2</sup>, Ward Drennan<sup>1,2</sup>, Jong Ho Won<sup>1,2</sup>, Jeff Longnion<sup>1,2</sup>, Jay Rubinstein<sup>1,2</sup>

<sup>1</sup> Virginia Merrill Bloedel Hearing Research Center,

<sup>2</sup>University of Washington

The extent to which temporal fine structure contributes to sound perception by cochlear implantees using envelopemodulated speech processing strategies is not well understood. We have developed a technique to vary the amount of fine structure present in acoustic stimuli from 0% to 100%. Stimuli were processed using a 12-channel vocoder in which the Hilbert envelope from each band was used to modulate the fractionally randomized Hilbert phase. If cochlear implant sound processing strategies do not encode fine structure, equal performance on psychoacoustic tasks would be expected whether they were tested with 0 or 100% randomization of the fine structure. Our tasks included a complex tone pitch discrimination task tested using 3 fundamental frequencies (130,164 and 233 Hz) and measurement of the speech reception threshold (SRT) for a closed set of 12 spondees presented in two-speaker babble. Both tasks were done with 0 and 100% randomization of fine structure. For 12 listeners, complex tone discrimination was better with no

fine structure randomization; the difference between 0 and 100% fine structure randomization increased for each frequency, becoming significant at 233 Hz (DL 130Hz = 1.1 semitones (p=0.08), DL 164Hz = 1.4 semitones (p=0.07), DL 233Hz = 2.3 semitones (p=0.03). The spondee reception threshold of the cohort was 3.6 dB higher (p = 0.003) with 100% fine structure randomization. The regression coefficients of performance vs. time for both tasks were negative and parallel, indicating that learning occurred equally in both conditions. These results were correlated with other tasks benefiting from fine structure perception, e.g. melody discrimination. The results suggest that temporal information beyond envelope is accessible to implantees with envelope-modulated strategies. [Work supported by: University of Washington; NIH R01 DC007525; Ruffin is a Howard Hughes Medical Institute Medical Research Training Fellow]

### 638 Effect of Channel Interactions on ITD Sensitivity in Bilateral Cochlear Implant Users

Gary Jones<sup>1</sup>, **Smita Agrawal**<sup>1</sup>, Ruth Litovsky<sup>1</sup>, Richard van Hoesel<sup>2</sup>

<sup>1</sup>University of Wisconsin-Madison, USA, <sup>2</sup>CRC HEAR, Melbourne, Australia

Previous work in our lab has shown that ITD sensitivity can be within normal limits with 100 pps pulse trains for some adult bilateral cochlear implant users (BICI) whose onset of deafness was in mid-childhood or later. However, this work was done using single-electrode stimulation, and channel interactions have been shown to elevate probe and modulation detection thresholds in unilateral adult CI users. Thus, it is important to establish how ITD sensitivity is affected by multi-channel stimulation. Findings in this area can influence decisions about incorporating ITD cues in speech processing strategies for BICI users.

We examined ITD sensitivity in Nucleus-24 BICI users with binaural pairs of pitch-matched electrodes at 100 pps (25 or 50 us/phase) in monopolar stimulation mode. A probe signal and an accompanying signal were temporally interleaved so that the accompanying signal led the probe by one-half interpulse interval. ITD JNDs for a probe in the middle of the electrode array presented at 90% of the dynamic range were measured while varying the accompanying signal's: a) place of stimulation relative to the probe from -8 to +8 electrodes, b) level from 20% to 90% of the dynamic range, and c) ITD (matched to probe, fixed at 0-ITD, fixed at one ear). Results of these experiments are as follows: 1) presence of the accompanying signal influences ITD sensitivity across accompanying signal locations; 2) JND may either increase or decrease relative to single-electrode JNDs when the accompanying signal's ITD is matched to probe; 3) JND is highest when the accompanying signal's ITD is not matched to probe; and 4) these effects disappear as the level of the accompanying signal is reduced. These results suggest that stimulation on multiple electrodes can result in a range of interaction effects that may make both positive and negative contributions to binaural sensitivity, and highlight potential difficulties in coding multiple ITDs using present stimulation methods.

#### 639 Electrically Evoked Auditory Steady-State Responses in a Guinea Pig Model

**Fuh-Cherng Jeng**<sup>1</sup>, Paul J. Abbas<sup>2</sup>, Carolyn J. Brown<sup>2</sup>, Charles A. Miller<sup>2</sup>, Barbara K. Robinson<sup>2</sup>, Kirill V. Nourski<sup>2</sup> School of Hearing, Speech and Language Sciences, Ohio University, <sup>2</sup>Department of Speech Pathology and Audiology, The University of Iowa

Most cochlear implant systems available today provide the user with information about the envelope of the speech signal. The goals of this study were to explore the feasibility of recording the electrically evoked auditory steady-state response (ESSR), to investigate the latency estimates — indicative of the generator site(s) of the response, and to examine the characteristics of the response.

Sinusoidally amplitude-modulated electric stimuli with alternating polarities were used to elicit responses in adult guinea pigs. Separation of the stimulus artifact from evoked neural responses was achieved by summing alternating polarity responses or by using spectral analysis techniques. The recorded responses exhibited physiological response properties including a pattern of non-linear growth. The responses were also not recordable using stimuli with 0% modulation depth, following administration of TTX or after euthanasia. These findings are all consistent with a hypothesis that the electrically evoked steady-state response is an evoked potential generated by the auditory system and can be effectively separated from electric stimulus artifact.

Latency estimates derived from the slope of modulation transfer function of the response revealed at least two distinct generators of the scalp recorded potential. One that has about 22 ms latency and is evoked by the lower (13.1-55.1 Hz) modulation frequencies and the other has a shorter latency of approximately 2 ms and is evoked by higher modulation frequencies (65.1-320.1 Hz). The response latency estimates were not dependent on stimulus level either at the lower or the higher modulation frequency regions. Because the response was elicited using a stimulus that shares important features with that cochlear implant users listen to on an everyday basis, this potential might be useful in clinical or basic research efforts.

#### 640 Discrimination of Temporal Intervals by Young and Elderly Listeners

**Peter Fitzgibbons**<sup>1</sup>, Sandra Gordon-Salant<sup>2</sup>, Jessica Barrett<sup>2</sup>

<sup>1</sup>Gallaudet University, <sup>2</sup>University of Maryland, College Park

The study measured listener sensitivity to increments in the inter-onset interval (IOI) separating pairs of successive 20-ms 4000-Hz tone pulses. A silent interval between the tone pulses was adjusted across conditions to create reference tonal IOI values of 25-600 ms. For each condition, a duration DL for increments of the tonal IOI was measured in listeners comprised of young normal-hearing adults and two groups of elderly adults with and without high-frequency hearing loss. Discrimination performance

of all listeners was poorest for the shorter reference intervals, and improved to stable levels for longer intervals exceeding about 200 ms. Temporal sensitivity of the young listeners was significantly better than that of the elderly listeners in each condition, with the largest agerelated differences observed for the short stimulus intervals. For comparison purposes, duration DLs were also measured for filled stimulus intervals using 4000-Hz tone bursts at three reference durations in the range 50-200 ms. Discrimination measured with these filled intervals was better than that observed for the corresponding unfilled intervals, but age-related performance differences remained at each reference duration. There were no significant performance differences observed between the elderly listeners with and without hearing loss.

## 641 Correlates of Frequency Discrimination in Cortical Evoked Potentials of Younger and Older Adults

**Kelly C. Harris**<sup>1</sup>, John H. Mills<sup>1</sup>, Judy R. Dubno<sup>1</sup> \*\*Medical University of South Carolina\*\*

As part of an ongoing study of age-related changes in auditory processing, frequency discrimination thresholds were measured using the cortical auditory evoked potential, N1-P2, in younger and older adults with normal hearing. Behavioral measures have shown age-related differences in intensity and frequency discrimination that are larger at lower than higher frequencies, which may be associated with age-related declines in temporal processing. However, substantial individual differences and equivocal results among studies have been reported. Behavioral measures may be affected by age-related changes in auditory processing, changes in cognitive processes, such as attention, and by task and response criteria. As such, electrophysiologic measures, such as the N1-P2, may be a more reliable method of assessing age-related changes in auditory processing. In a previous study from our lab, the N1-P2 was used to assess intensity discrimination at 500 and 3000 Hz in younger and older normal hearing adults. N1-P2 intensity discrimination thresholds were consistent with behavioral measures of intensity discrimination, and showed a similar frequencydependent age-related effect. In the current study of frequency discrimination, subjects were 10 younger and 10 older adults with normal hearing. The N1-P2 was elicited by a 150-ms change in frequency in otherwise continuous 500-Hz and 3000-Hz pure tones presented at 70 dB SPL. Frequency discrimination threshold was defined as the smallest change in frequency needed to evoke an N1-P2 Frequency discrimination thresholds were significantly higher for older than younger subjects at 500 Hz and 3000 Hz and age-related differences were larger at 500 Hz than at 3000 Hz, consistent with previous behavioral measures of frequency discrimination.

[Supported by NIH/NIDCD]

# 642 Effect of Age on Tolerance of Background Noise as Characterized by Acceptable Noise Level and the Speech-Spatial-Quality Scale

**Robert C. Nutt**<sup>1</sup>, Chandler Marietta<sup>1,2</sup>, D. Robert Frisina<sup>1,2</sup>, David A. Eddins<sup>1,2</sup>

<sup>1</sup>International Center for Hearing and Speech Research, Rochester Institute of Technology, <sup>2</sup>Department of Otolaryngology, University of Rochester School of Medicine

Numerous useful tools have been developed to quantify hearing aid benefit and to predict hearing aid success. The Acceptable Noise Level (ANL) test was developed in this context and appears to be a promising tool with clinical applications. In studies relating to background noise and hearing aid benefit, several factors contributing to intersubject variability (including age) have been reported to be unrelated to ANL by previous investigators. To date, published reports have not considered the effect of age, independent of hearing loss, on the measures comprising the ANL test. The present study explores the effect of age on ANL and the relation of both to the perception of communication abilities assessed by the Speech-Spatial-Quality Scale. A sample of 36 individuals with normal hearing (defined as pure tone threshold < 25 dB HL at octave frequencies from 250 to 8000 Hz) was divided into three groups according to age: younger (18-27 years), middle-aged (40-49 years) and older (61-72 years). Acceptance of background noise was measured using male running speech as the primary stimulus presented with and without 12-talker babble (Arizona Travelogue, Stimuli were presented through a Cosmos Inc.). loudspeaker located at 0° azimuth and testing was performed in a double-walled audiometric booth. The ANL test was administered on two separate days for each subject. The Speech-Spatial-Quality Scale was completed by each subject to assess the perception of hearing ability. Preliminary results indicate little effect of aging on the ANL score and a systematic decline in the most comfortable level (MCL) and the tolerance of competing background level (BNL) with increasing age. The reduced tolerance of sound level, including target and background sounds, may be one element of the ANL test that provides relevant predictive information regarding communication ability with or without amplification via hearing aids.

Supported by NIH NIA P01 AG09524, NIDCD P30 DC05409

### **[643]** Hearing in Noise Test – HINT and Aging Patricia Guimaraes<sup>1,2</sup>, David A. Eddins<sup>1,2</sup>, D. Robert Frisina<sup>1,2</sup>

<sup>1</sup>Department of Otolaryngology, University of Rochester, Rochester, NY 14642, <sup>2</sup>Int. Ctr. for Hearing & Speech Res., Rochester Institute of Technology, Rochester, NY, 14623

The ability to understand speech in background noise is a problem encountered by many hearing impaired listeners, including those with mild-to-moderate hearing loss, hearing aid users, and also listeners with cochlear

implants. This study focuses on characterizing abilities to understand speech in background noise and its relation to aging. We used the Hearing in Noise Test - HINT, administered in a sound-field environment. The HINT sentences were presented from a speaker in front of the listener and consisted of four background conditions: quiet, noise at 0 degrees (front), noise at 90 degrees (right), and noise at 270 degrees (left). Advantages of the HINT relative to other measures of speech perception in noise include an indication of central binaural processing and a measure of the spatial release from masking (RFM) in addition to providing a general measure of speech recognition in noise. Human subjects (N=818) were divided into five groups according to their age: Young (18-37 yr, N=96), Middle-Aged (38-57 yr, N=92), and Young-Old (58-68 yr, N=233), Middle-old (69-81yr, N=346) and Elderly-Old (82+ yr, N=51). Auditory testing included a hearing test battery comprised of tympanometry, pure tone audiometry (air and bone conduction), and oto-acoustic emissions testing. The results indicated increase in pure tone thresholds with age, especially at higher frequencies, consistent with many previous investigations. The HINT revealed an increase in sentence threshold in noise with age, indicating that the older subjects needed a higher signal-to-noise ratio to achieve 50% correct detection. The HINT also revealed a binaural benefit for speech-in-noise. with thresholds being lower for noise sources located at 90 degrees or 270 degrees than a noise source located at 0 degrees. The RFM declined systematically with age. The onset of this decline was evident in the middle-aged group and increased with increasing age.

Supported by NIH grants NIA P01 AG09524, NIDCD P30 DC05409 and the Int. Ctr. Hearing & Speech Res.

## 644 The Effects of Age on the Spatial Release From Informational and Energetic Masking

**Chandler Marietta**<sup>1,2</sup>, Robert C. Nutt<sup>2</sup>, D. Robert Frisina<sup>1,2</sup>, David A. Eddins<sup>1,2</sup>

<sup>1</sup>Deparment of Otolaryngology, University of Rochester, Rochester, NY 14642, <sup>2</sup>Int. Ctr. for Hearing & Speech Res., Rochester Institute of Technology, Rochester, NY 14623

Informational masking and the spatial release from informational masking provide useful measures for investigating the "cocktail party" phenomenon. present study was designed to determine the degree to which aging, in the absence of hearing loss, mitigates informational and energetic masking and the spatial release from both. Subjects performed a closed-set, adaptive speech identification task adapted from Arbogast, Mason, and Kidd (2002; J. Acoust. Soc. Am. 112, 2086-2098). Stimuli from the Coordinate Response Measure (CRM) Corpus were pre-processed by a sine wavevocoder-based cochlear implant simulation algorithm that separated sentences into 15 distinct frequency bands. Signal sentences consisted of 8 randomly-selected frequency bands. Masker sentences were processed in three ways: 1) different-band sentence (i.e. informational masking), comprised of 6 of the remaining 7 bands; 2)

different-band noise, also comprised of 6 of the remaining 7 bands; and 3) same-band noise (i.e. energetic masking), comprised of the 8 bands corresponding to the signal sentence. Different-band noise and same-band noise masker sentences were created by multiplying the longterm spectra of the masker sentence bands and broadband noise. Signal stimuli were presented from a speaker at 0° (front) azimuth. Masker stimuli were presented simultaneously from either 0° or 90°(right) azimuth. Adult subjects with normal hearing were separated into three groups of 12: younger (18-27), middle-aged (40-49) and older (61-72). All subject groups benefited from spatial separation of the masker, showed significant informational masking, and significantly greater spatial release from informational compared to energetic masking. Analyses revealed age-dependent changes in spatial release of both informational and energetic masking where the younger group benefited most and the older group least.

Supported by NIH NIA P01 AG09524, NIDCD P30 DC05409, and the Int. Ctr. for Hearing & Speech Res.

#### 645 Mechanisms of Age-Related Hair Cell Death

**Donald Henderson**<sup>1</sup>, Bohua Hu<sup>1</sup>, Eric Bielefeld<sup>1</sup>, Weiping Yang<sup>2</sup>, Guang-Di Chen<sup>1</sup>

<sup>1</sup>SUNY at Buffalo, <sup>2</sup>PLA General Hospital, China The Fischer 344 rat has been used as a model of agerelated hearing loss (ARHL). At 24 months, the Fischer 344 typically has a high-frequency hearing loss, greatly suppressed DPOAE and a cochleogram with 60-80% missing outer hair cells (OHC) in the basal and apical region and scattered losses through the middle of the cochlea. When the OHC are examined more closely, the OHC appear to be dying by both apoptosis and necrosis by a ratio of 8:1. The apoptotic cells have been shown to express caspase 3 and may express both the initiator caspase 8 and 9, as well as, cytochrome C. The structural protein F-actin begins to depolymerize as the cell starts the apoptosis cycle. BCH is upregulated in OHC throughout cochlea. The discrepancy between the magnitude of hearing loss and population of OHC can be partially explained by changes in mitochondria. example, remaining OHC throughout most of the organ of Corti have reduced SDH staining which implies attenuated mitochondrial function which would lead to reduced DPOAE and shifted evoked potential thresholds.

[Research supported by grant #1R01DC00686201A1]

## 646 Behavioral and Physiological Correlates of Temporal Pitch Perception in Electric and Acoustic Hearing

**Robert Carlyon**<sup>1</sup>, Suresh Mahendran<sup>1</sup>, John Deeks<sup>1</sup>, Stefan Bleeck<sup>2,3</sup>, Ian Winter<sup>2</sup>, Patrick Axon<sup>4</sup>, David Bagulev<sup>4</sup>

<sup>1</sup>Medical Research Council, <sup>2</sup>University of Cambridge, <sup>3</sup>University of Southampton, <sup>4</sup>Addenbrooke's NHS Trust A series of experiments investigated "purely temporal" pitch perception by normal-hearing ("NH") and cochlearimplant ("Cl") listeners, and compared the NH results with

recordings of auditory-nerve (AN) activity to the same stimuli. Experiment 1 presented bandpass filtered (3900-5400 Hz) acoustic pulse trains to NH listeners. Such stimuli convey pitch via AN phase-locking, and do not produce reliable place-of-excitation cues to pitch. In the "4-6" condition, listeners compared the pitch of a train in which the inter-pulse intervals (IPIs) alternated between 4 and 6 ms to that of isochronous pulse trains having a range of IPIs, and a point of subjective equality (PSE) was derived from the underlying psychometric function. Consistent with previous results obtained at a lower signal level, the PSE was on average 5.7 ms - longer than the mean IPI of 5 ms. In other conditions the IPI alternated between 3.5-5.5 ms and 4.5-6.5 ms. As the overall IPI increased, the PSE became more similar to that of the mean IPI in the alternating-interval stimulus. Experiment 2 was similar but presented electric pulse trains to one channel of a CI. The results were similar to those obtained with NH listeners. Experiment 3 measured Compound Action Potentials (CAPs) to the "4-6" stimulus in anaesthetised guinea pigs and in two NH listeners. The CAP to pulses occurring after a 4-ms interval was smaller than that to those occurring after 6-ms intervals. This refractory effect was independent of overall stimulus level, consistent with the level-independence of the behavioral pitch judgements. The behavioral results are discussed in terms of a simple model in which an array of more-central neurons fire when the CAP exceeds a threshold that differs across neurons. This leads to a small number of high-threshold neurons firing only on every other pulse. Pitch is then derived from the mean 1<sup>st</sup>-order inter-spike intervals derived from this more-central array.

### 647 A Combinatorial Neural Mechanism Related to Subjective Pitch Perception

Daryl Wile<sup>1,2</sup>, Evan Balaban<sup>2</sup>

<sup>1</sup>University of Calgary, <sup>2</sup>McGill University

The mechanism by which the brain derives a sensation of pitch, an attribute of sounds by which they can be arranged on a scale from low to high, is contentious. Spectral pitch theories assign a major role to the pattern and position of peaks and valleys in the activity sounds induce along the hair cell array in the cochlea, while temporal theories assign a major role to repeating patterns of neural activity over time. Neither is sufficient to explain all pitch perception phenomena, which has led to a search for mechanisms which combine these types of information. By recording an auditory brainstem-evoked potential called the frequency-following response (FFR), it is possible to examine the characteristics of neural activity in the early auditory pathway evoked by sounds.

Here, subjective pitch percepts and patterns of neural activity evoked by auditory stimuli were compared in the same individuals. It is demonstrated that a weighted sum of two kinds of timing information (evident in the FFR and originating in higher-frequency regions of the cochlea) accurately predicts subjective pitch perception. By combining patterns of lower-frequency timing information originating in higher-frequency regions of the cochlea, this mechanism may reconcile place- and timing-related theories of pitch perception.

#### 648 Is the Pitch of Low-Frequency Pure Tones Based on Spectral Information After All? Evidence From Experiments Using Binaural Masking Release

**David Magezi**<sup>1</sup>, Rosanna Moore<sup>1</sup>, Sarah Ponting<sup>1</sup>, Katrin Krumbholz<sup>1</sup>

<sup>1</sup>MRC Institute of Hearing Research

The ability to detect frequency changes in pure tones has traditionally been explained by two broad classes of theory. According to "spectral" theories, frequency discrimination is based on changes in the spatial distribution of activity along the tonotopic array. In contrast, "temporal" theories assume that frequency discrimination involves analysing the temporal information in the phaselocked auditory-nerve firing patterns. Previous studies have shown that performance in frequency discrimination and frequency or mixed modulation (FM, MM) detection decreases rapidly for frequencies above about 4 kHz, and the fact that this decrease coincides with the assumed limit of phase locking in humans has been interpreted as indication that pitch perception in low-frequency pure tones is based on temporal mechanisms. In order to avoid comparing performance across frequency, we performed a series of similar tasks with low-frequency tones in conditions of binaural masking release (BMR). Due to binaural sluggishness, phase-locked temporal information would be expected to be absent in BMR. We found that FM detection thresholds were much higher in BMR ( $S_{\Pi}N_0$ condition) than in an appropriately matched control condition  $(S_0N_0)$ , whereas frequency discrimination performance in static tones was similar between the two masking conditions. The results suggest that, while binaural sluggishness smoothes the pitch estimate over time, it does not obliterate the information that the pitch analysis is based on, as would be expected if binaural sluggishness acted on the input to the pitch processor, and the input to the pitch processor were phase-locked temporal information. Moreover, no significant difference was found between the two masking conditions for 1) the effect of relative modulator phase on detection of combined AM and FM (MM), and 2) performance in FM detection with and without random-phase AM of equal detectability. This suggests that the previously reported differences between high- and low-frequency tones in these tasks may result from differences other than the availability of phase-locked temporal information. The current results would appear to have important implications for the development of models of pitch perception and auditory temporal processing.

## 649 Frequency Discrimination Thresholds for Pure Tones and Mistuned Components in Harmonic Complexes in Mongolian Gerbils

Astrid Klinge<sup>1</sup>, Georg M. Klump<sup>1</sup>

<sup>1</sup>Department of Biology and Environmental Sciences, Zoophysiology & Behaviour Group

Frequency is a major cue exploited by the auditory system to segregate sounds. Frequency discrimination of pure tones can on the one hand rely on place mechanisms (i.e., a change of the cochlear excitation pattern with a change

in frequency) and on the other hand rely on temporal mechanisms (i.e., on processing of time intervals between neuronal responses). Special processing mechanisms may be used in the analysis of harmonic tone complexes (for a review see Hartmann 1996, JASA 100: 3491) and mistuned harmonics (e.g., Moore et al. 1985, JASA 77: 1861).

Frequency difference limens (FDL) for pure tones and for mistuned components in harmonic tone complexes are determined in behavioural experiments with Mongolian gerbils (Meriones unguiculatus). The gerbils are trained in an operant procedure with food rewards using a Go/NoGo paradigm. Signals of a constant frequency composition are provided as a reference and target signals with a change in frequency presented at random intervals have to be detected. FDLs for pure tones are determined for frequencies ranging from 200 to 6400 Hz. Detection of mistuning (i.e., a frequency shift) of single components is tested presenting harmonic complexes consisting of the fundamental frequency (200 and 800 Hz) and the next 11 harmonics. The minimum frequency shifts necessary for detection of a change are determined for the first, second and eighth harmonic.

Previous studies in humans and birds (e.g., Moore et al. 1985; Lohr & Dooling 1998, J Comp Psych 112: 36) have demonstrated a much better frequency discrimination in the case of mistuned harmonics than in the case of pure tones. Birds appear to be superior compared to humans in detecting mistuning. Here we will test whether gerbils show the pattern that is typical for humans and discuss the results in relation to possible perceptual mechanisms for detecting frequency changes of pure tones and components of harmonic tone complexes.

Supported by the DFG (InterGK 591, SFB/TRR 31)

# 650 An Exploration of the Spectral Envelope Space of Musical Instruments Using Envelope Morphing Permutation Strategies David Gunawan<sup>1</sup>, D Sen<sup>1</sup>

<sup>1</sup>The University of New South Wales

The spectral envelope is known to be a salient parameter of musical instrument timbre perception. This study explores the spectral envelope space by measuring the perception of a number of different linear-log morphing permutations between the trumpet and the clarinet using 2AFC experiments. The contrasting envelopes of these two instruments allow for the investigation of the prominent parameters of the spectral envelope which dominate timbre classification. The results show that the spectral envelopes of what is perceived to be a trumpet even at 95% probability for the various morphs contain a large proportion of the clarinet resonances. Psychometric functions for the different morphing permutations are calculated and the data is analysed against a number of timbre classification models and masking models, revealing that there may be a need to incorporate masking models into timbre classification systems. The results also highlight the dominance of the lower frequencies in timbre perception as found in other studies.

#### 651 Temporal Integration in a Titmouse Species (Aves, Paridae, Parus Major)

**Nina U. Pohl<sup>1</sup>**, Georg M. Klump<sup>1</sup>, Hans Slabbekoorn<sup>2</sup>, Ulrike Langemann<sup>1</sup>

<sup>1</sup>University of Oldenburg, <sup>2</sup>Leiden University

The ability of the auditory system to integrate acoustic information over time affects signal detection, signal discrimination and detecting signal changes over time. For relatively long-lasting signals (several hundreds of milliseconds), thresholds for signal detection are roughly independent of signal duration. For brief acoustic signals, however, detection threshold is a function of signal duration. In addition, signal detection depends on the frequency of the signal. Great tits (Parus major) communicate with calls and song elements of short duration and show unusually high frequency resolution for signals above 4 kHz (Langemann et al. 1998, Anim Behav 56: 763). In this study we are interested in this species' ability for temporal integration.

Five great tits were trained in a Go/NoGo paradigm to report the detection of sinusoidal signals of different duration in silence or in a continuous noise background. The background matched the natural sound pressure level and spectral distribution of either urban or woodland environmental noise. Test frequencies were 2, 4, and 6.3 kHz, signal duration was 30, 100, 300, and 1000 ms. Signal detection theory was applied to determine the level of the test signal at detection; threshold criterion was a d' of 1.8. The time constant of the temporal integration function was derived using the model of Plomp and Bouman (1959, JASA 31: 749).

A repeated measures ANOVA of preliminary data showed significant differences in detection thresholds for signal frequency and signal duration. Thresholds for 30 ms signals were about 4 dB, 5 dB, and 7 dB less sensitive than at 100, 300 and 1000 ms, respectively. Time constants calculated from these detection thresholds decreased with increasing signal frequency and were on average 120, 80, and 70 ms for signal frequencies of 2, 4, and 6.3 kHz, respectively. The integration constants of the great tit are thus slightly shorter than those observed in other bird species.

Supported by the DFG, SFB/TRR 31

### | 652 | Threshold as a Function of Duration in Normal and Impaired Listeners

Wendy Lecluyse<sup>1</sup>, Ray Meddis<sup>1</sup>

<sup>1</sup>University of Essex

Florentine, Fastl and Buus (1988) found threshold decreased continuously with increasing duration up to 500 ms with a typical slope of 2-3 dB/decade. Their slopes did not differ significantly across frequencies but were shallower for hearing impaired listeners. We replicated this study for normal listeners. Thresholds were measured in 6 normal listeners using stimuli with durations from 8 to 512 ms at 0.25, 1, 4 and 12 kHz. Functions relating threshold to duration typically consisted of an initial slope followed by a horizontal platform. We found that the sloping section of the function ended at durations much shorter than 500 ms. Average slopes were in the range of 3-5 dB/octave and

decreased significantly with increasing frequency. Tests with hearing impaired listeners show a similar pattern.

Reference: Florentine M., Fast H., Buus S. (1988). "Temporal integration in normal hearing, cochlear impairment, and impairment simulated by masking." J. Acoust. Soc. Am., 84(1), 195-203.

#### 653 Prediction of Behavioral Thresholds Using a Model of Partial Loudness

Walt Jesteadt<sup>1</sup>, Samar Khaddam<sup>1</sup>, Hongyang Tan<sup>1</sup>, Lori J. Leibold<sup>1</sup>

<sup>1</sup>Boys Town National Research Hospital

Moore, Glasberg and Baer ( "A model for the prediction of thresholds, loudness, and partial loudness," J. Audio Eng. Soc. 45, 224-237, 1997) describe use of a model of loudness, recently adopted as the ANSI standard (ANSI S3.4-2005), to predict masked thresholds and they compare their estimates to results reported in several published studies. They assume that masked threshold represents the level of a signal that has a constant low partial loudness, typically 2 phons. The partial-loudness model uses only spectral information, with no assumptions about the temporal properties of stimuli. Although the model is not intended to provide a complete description of masking, it can be used to predict the thresholds that would be expected on the basis of the power spectrum model, taking into account changes in spread of excitation with level. These predictions provide a useful reference for interpreting results that deviate from the power spectrum model as a result of temporal cues, uncertainty or other factors. Moore et al. focused on predicting masking for broadband maskers and signals, but their model also makes reasonable predictions for many stimulus configurations with narrowband maskers or These include detection of tones in noise, signals. auditory filter conditions, masking patterns, and intensity discrimination as a function of level. Applications and limitations of the partial-loudness model of masking will be discussed.

[Supported by NIH grants DC 006648 and DC 000013.]

### [654] Revisiting the Mid-Level "Hump" in Auditory Intensity Discrimination Martin Pienkowski<sup>1</sup>

<sup>1</sup>Karolinska Institutet

Weber's (and Fechner's) 19th century "law of sensation" purports that the just noticeable difference in stimulus intensity ( $\Delta I$ ) is directly proportional to the baseline or "pedestal" intensity (I); that is, the Weber fraction,  $\Delta I/I$ , is constant with I. In psychoacoustic experiments,  $\Delta I$  has typically been measured using adaptive procedures that require many stimulus trials at a fixed (or slightly "roved") pedestal intensity; the procedures are repeated successively with other pedestals to obtain  $\Delta I/I$  vs. I. Weber's law is then observed to hold for broadband noise stimuli. For tones, a "near-miss" is usually seen:  $\Delta I/I$  is not constant but decreases with I, perhaps due to the "spread of excitation" to additional cochlear frequency channels. If, however, I is roved (i.e., randomly varied, trial-to-trial) over a large range (> 30 dB at least), ΔI/I vs. I has been reported to be non-monotonic (e.g., Berliner et al., 1977,

JASA 61, 1577-85): as I increases,  $\Delta I/I$  increases to peak at mid-SPLs before decreasing again to near-miss proportions. This mid-level "hump" or deterioration in intensity discrimination performance has also been observed under standard, fixed-level procedures, but only for very brief (< a few 10s of ms) stimulus sounds.

Here the effects of both wide-range roving and short stimulus duration on the intensity dependence of the Weber fraction were investigated concurrently. Standard adaptive methods were used in both slightly- and fully-roved paradigms (i.e., across the entire audible range) for both 300 and 4 ms-long, 4 kHz tones. In all 8 normal-hearing subjects tested, the near-miss observed with 300 ms tones in slightly-roved mode gave way to a significant mid-level hump in fully-roved mode. With 4 ms pips, a hump was not always present under slight roving, and if present, not always accentuated under full roving. Notably, in 4 subjects with mild HL, the hump was reduced, or not present, under all conditions.

It is speculated that the mid-level hump could reflect the well-known compressive nonlinearity in cochlear mechanics. Under typical experiment conditions, the central auditory system might compensate for the presumed peripheral mid-intensity information-deficit, thereby producing Weber's law or the near-miss. For example, it has recently been shown that guinea pig inferior colliculus neurons can quickly adjust their operating points (i.e., the steep parts of their rate-intensity functions) to the prevailing stimulus intensity range (Dean et al., 2005, Nat Neurosci 8, 1684-9). This adjustment will not occur when stimuli vary randomly and uniformly across the entire audible range, nor perhaps when their durations are too short to trigger sufficient activity in the auditory nerve (to effect such plasticity), thus exposing the mid-level hump.

#### 655 Consonant Profiles for Hearing-Impaired Listeners

**Sandeep Phatak**<sup>1</sup>, Yang-Soo Yoon<sup>1</sup>, Jont Allen<sup>1</sup> *University of Illinois at Urbana-Champaign* 

The effect of hearing loss on speech recognition in noise by hearing-impaired (HI) listeners is generally measured in terms of SNR-Loss. However, SNR-Loss, which is an average measure, fails the provide information about the HI listener's loss of performance on different consonants and vowels. This information would be very useful in customizing the hearing aids as well as the rehabilitation therapy for individual HI listener. We propose an analysis technique that provides the 'Consonant Profile,' i.e. a comparison of individual HI listener's performance with that of an average normal hearing (NH) listener, on consonantby-consonant basis. A Miller-Nicely(1955) [1] type closedset recognition experiment was conducted with young NH listeners and elderly HI listeners. The listeners were asked to recognize the consonant in nonsense CV-syllables with 16 consonants and 1 vowel, presented in a white noise masker at different signal-to-noise ratios (SNRs). The consonant scores of HI listeners were found to be related to their audiograms [2]. We will verify whether the consonant profiles of individual listeners can be explained using their audiograms and the SNR-spectra of the

consonants. An SNR-spectrum of a consonant is the SNR for that consonant, plotted as a function of frequency, for a given spectrum of masking noise.

References:

[1] Miller, G. A. and Nicely, P. E. (1955) ``An analysis of perceptual confusions among some English consonants," J. Acoust. Soc. Am., 27(2) 338-352.

[2] Yoon, Yang-soo, Allen, J. B. and Gooler, D. M. (2006) "Signal-to-noise ratio loss and cosonant perception in hearing impairement under noisy environment," IHCON 2006.

## 656 Effects of Cochlear Hearing Loss on the Ability to Use Temporal Envelope or Fine Structure Cues in Speech Identification

**Christian Lorenzi**<sup>1,2</sup>, Gaetan Gilbert<sup>1</sup>, Heloise Carn<sup>1,2</sup>, Stephane Garnier<sup>2,3</sup>, Brian Moore<sup>4</sup>

<sup>1</sup>LPP - FRE CNRS 2929, Univ. Paris 5, DEC, Ecole Normale Supérieure, <sup>2</sup>GRAEC GDR CNRS 2967, <sup>3</sup>Laboratoire Entendre, <sup>4</sup>Departement of Experimental Psychology, University of Cambridge

The present study investigated the effects of cochlear damage on the ability to identify speech using either envelope (E, the relatively slow variations in amplitude over time in each of several frequency bands) or temporal fine structure information (TFS, the rapid oscillations with rate close to the center frequency of each band). To address this issue, vowel-consonant-vowel stimuli were processed by filtering them into 16 adjacent frequency bands. The signal in each band was processed using the Hilbert transform so as to preserve either the envelope or the temporal fine structure. The band signals were then recombined and the stimuli were presented to subjects for identification. After training, normally hearing listeners scored perfectly with unprocessed speech, and about 90% correct with E and TFS speech. Both young and elderly listeners with moderate flat hearing loss (n=7 in each group) performed almost as well as normal with unprocessed and E speech, but performed very poorly with TFS speech, indicating a greatly reduced ability to use TFS. For the younger hearing-impaired group, scores were highly correlated with the ability to take advantage of temporal dips in a background noise when identifying unprocessed speech. The results suggest that the ability to use TFS may be critical for "listening in the background dips".

## 657 Predictions of Speech Intelligibility with a Model of the Normal and Impaired Auditory Periphery

Muhammad Zilany<sup>1</sup>, Ian Bruce<sup>1</sup>

<sup>1</sup>McMaster University

A fall-off in speech intelligibility at higher-than-normal presentation levels has been observed for listeners with and without hearing loss (e.g., Studebaker et. al., JASA, 1999). Speech intelligibility predictors based on the acoustic signal properties, such as the articulation index and speech transmission index, cannot directly account for the effects of presentation level and hearing impairment.

Recently, Elhilali et. al. (Speech Communication, 2003) introduced the spectro-temporal modulation index (STMI), a speech intelligibility predictor based on a model of how the auditory cortex analyzes the joint spectro-temporal modulations present in speech. However, the auditory-periphery model used by Elhilali et al. is very simple and cannot describe many of the nonlinear, level-dependent properties of cochlear processing, nor the effect of hair cell impairment on this processing.

The goal of our study is to quantify the effects of speech presentation level and cochlear impairment on speech intelligibility using the STMI with a more physiologicallyaccurate model of the normal and impaired auditory periphery (Zilany and Bruce, JASA, 2006). This model features a number of important effects seen in auditory nerve fiber responses at high presentation levels, such as the elevation, broadening and frequency-shift in tuning, the component-1/component-2 transition, and peak splitting. Additionally, outer and inner hair cell impairment can be incorporated. Preliminary results show that the model is able to predict the fall-off in speech intelligibility at high presentation levels for normal hearing listeners. Predictions of the effects of presentation level in unaided and aided conditions for listeners with hearing loss will be described.

[This work was supported by NSERC Discovery Grant 261736 and the Barber-Gennum Chair Endowment.]

# 658 Spectral Shape Discrimination for Speech-Like and Non-Speech Stimuli and Their Contribution to Speech Understanding in Older Hearing-Impaired Listeners Mini Shrivastav<sup>1</sup>

<sup>1</sup>University of Florida

Speech-understanding difficulties observed in elderly hearing-impaired listeners are clearly associated with recognition and discrimination of consonants, particularly within consonants that share the same manner of articulation. Spectral shape is an important acoustic cue that serves to distinguish such consonants. The present study examined whether individual differences in speech identification among older hearing-impaired listeners could be explained by individual differences in spectral-shape discrimination ability. The study also examined differences in discrimination thresholds for speech-like and nonspeech stimuli. Regression analyses revealed moderate predictive relationships between some of the spectralshape discrimination thresholds and speech-identification performance. The results indicated that when all stimuli were at least minimally audible, some of the individual differences in the identification of natural and synthetic speech tokens by elderly hearing-impaired listeners could be attributed to the differences in their spectral-shape discrimination abilities for similar sounds. Further, significant differences were found between performance for speech-like and non-speech stimuli, such that only speech-like discrimination thresholds for stimuli contributed toward individual differences in speechidentification.

#### 659 Microrna Expression Profiling in Vestibular Schwannomas Using Microarrays

Joseph Cioffi<sup>1</sup>, **Sabrina Mendolia-Loffredo<sup>1</sup>**, Martin Hessner<sup>1</sup>, Lisa Meyer<sup>1</sup>, P. Ashley Wackym<sup>1</sup>

\*\*Medical College of Wisconsin\*\*

Vestibular schwannomas are slow growing, benign tumors that arise from Schwann cells of the eighth cranial nerve. They are usually unilateral and sporadic but can occur bilaterally in association with the autosomal dominant genetic disorder neurofibromatosis type 2 (NF2). Vestibular schwannomas often exhibit phenotypic Growth rate, morphology, and degree of variability. vascularity can vary widely. The molecular basis for NF2 and sporadic development of vestibular schwannomas is not completely understood. Furthermore, the relationship between NF2 gene mutations and tumor phenotype remains to be clarified; monozygotic twins with NF2 show some variability in disease manifestations. MicroRNAs may play a role in tumorigenesis and/or phenotypic heterogeneity in these tumors. MicroRNAs are evolutionarily conserved, small (~22nt), non-coding RNA molecules that regulate gene expression at the level of translation and have recently been implicated in development, differentiation, and cancer. We developed microRNA microarrays that enable the simultaneous detection of 377 unique microRNAs. MicroRNA from two vestibular schwannomas was isolated, fluorescently labeled, and used to probe these microarrays. TIGR Spotfinder 3.1.1 software was used to quantitate signal Approximately 50 microRNAs exhibited intensity. moderate to high levels of expression in each tumor, with 84% of these common to both. Real-time PCR was used to confirm expression levels for a subset of expressed microRNAs. Some of these have been shown to be preferentially expressed in brain and other neural tissues while others are predicted to target messenger RNAs which encode proteins, such as merlin, important in the development of vestibular schwannomas. expression profiling in vestibular schwannomas and normal Schwann cells may provide further insight into the molecular pathways associated with the growth of these tumors.

## 660 Rat Vestibular Periphery cDNA Library Analysis Using in Silico Protein and cDNA Sequence Prediction

Christy Erbe<sup>1</sup>, Joseph Cioffi<sup>1</sup>, Joseph Roche<sup>1</sup>, Paul Popper<sup>1</sup>, Tina Samuels<sup>1</sup>, Rebecca Eernisse<sup>1</sup>, Sarah Edmiston<sup>1</sup>, P. Ashley Wackym<sup>1</sup>

<sup>1</sup>Department of Otolaryngology, Medical College of

Wisconsin, Milwaukee, WI 53226

In an effort to comprehensively characterize the rat vestibular transcriptome, we sequenced 22,080 randomly selected cDNA clones from a normalized Rattus norvegicus vestibular (Scarpa's ganglia and end organs) cDNA library. These were then systematically analyzed and parsed into the following categories: named genes, predicted genes, matched genes with no description, and new ESTs with no UniGene ID. After discarding the sequences from 3,583 clones due to poor quality or empty vector, the sequences from 18,497 clones were

categorized and represented a total of 8,289 unique UniGene clusters. Clones that did not have homology to any known UniGene clusters were aligned to the rat genome and may represent novel ESTs or previously unknown 3' untranslated regions of known ESTs. To characterize this last group of clones we developed a method to predict upstream cDNA sequence using online alignment and gene prediction programs. Clones were first aligned to the rat genome (UCSC BLAT) to replace any ambiguous bases with genomic sequence. corrected cDNA sequences were aligned to the rat genome (NCBI) and the exon-intron structures were identified with GENSCAN (MIT). The GENSCAN output gives a predicted gene as well as an amino acid sequence corresponding to our cDNA that can be either backtranslated to give predicted cDNA sequence, or aligned using the BLASTp algorithm to search for protein homology. Finally, the predicted cDNA was used to design upstream primers that enabled us to "walk" up the sequence using PCR. We tested this method on four cDNA clones from our library and, on average, we were able to identify >900 bp of upstream sequence in one round of PCR. Three out of the four clones we analyzed were highly homologous to previously identified proteins (BLASTp), indicating that our cDNA sequence may represent 3' untranslated region for these proteins. The protein sequence for the final clone did not have any significant homologies using the BLASTp algorithm indicating that it may be a novel cDNA. We have used this method to rapidly and efficiently screen these cDNAs for useful sequences. Continued analysis of these previously unidentified EST's from rat vestibular periphery transcriptome may provide new insights into vestibular function.

Supported by NIDCD grants R01DC02971 and R03DC006571.

#### 661 Neuropeptides and Neuropeptide Receptors in the Rat Vestibular Periphery

Paul Popper<sup>1</sup>, Wolfgang Siebeneich<sup>1</sup>, Christy Erbe<sup>1</sup>, Tina Samuels<sup>1</sup>, Alexandra Lerch-Gaggl<sup>2</sup>, P. Ashley Wackym<sup>1</sup> Department of Otolaryngology, Medical College of Wisconsin, Milwaukee, WI 53226, <sup>2</sup>Department of Cell Biology, Neurobiology Anatomy, Medical College of Wisconsin, Milwaukee, WI 53226

Microarray analysis of gene expression indicated that neuropeptides and neuropeptide receptors previously not reported were expressed in neurons of Scarpa's ganglia. We used RT-PCR to confirm the expression of galanin, galanin receptor 1, cholecystokinin (CCK), CCK B receptor, vasoactive intestinal polypeptide (VIP), VIP receptor 1, Neuropeptide Y and orphanin FQ in Scarpa's ganglia and to show that they are also expressed in the cristae ampullares. Immunohistochemistry was used to study the distribution of the molecules in the rat vestibular Galanin immunoreactivity was observed in ganglion cells but not in calretinin immunoreactive cells. In the crista galanin immunoreactivity was colocalized with tubulin and in hair cells. Galanin receptor 1 immunoreactivity was detected in calretinin positive and negative neurons and in hair cells. CCK immunoreactivity

was colocalized with tubulin and in type II hair cells. CCK B receptor was observed in boutons in the crista epithelia and in a few hair cells. VIP immunoreactivity was observed in fibers along blood vessels and in a few type II hair cells and VIP receptor 1 immunoreactivity in blood vessels and in typel and II hair cells. Orphanin FQ immunoreactivity was observed in type II hair cells and in calretinin immunoreactive fibers. These data indicates a reciprocal interaction between vestibular hair cells and vestibular afferent neurons.

Supported by NIDCD grants DC02971 and DC006571.

## 662 Distribution of Two Pore-Domain Potassium Channels in the Adult Rat Vestibular Periphery

John Winkler<sup>1</sup>, P. Ashley Wackym<sup>1</sup>, Christy Erbe<sup>1</sup>, Alexandra Lerch-Gaggl<sup>2</sup>, Paul Popper<sup>1</sup>

Department of Otolaryngology, Medical College of Wisconsin, Milwaukee, WI 53226, <sup>2</sup>Department of Cell Biology, Neurobiology Anatomy, Medical College of Wisconsin, Milwaukee, WI 53226

Constitutively active background or "leak" two-pore-domain potassium (K) channels (Kcnk family), as defined by lack of voltage and time dependency are central to electrical excitability of cells by controlling resting membrane potential and membrane resistance. Inhibition of these channels by several neurotransmitters (eg, glutamate, or acetylcholine) induces membrane depolarization and subsequent action potential firing as well as increases membrane resistance amplifying responses to synaptic inputs. In contrast, their opening contributes to hyperpolarization. Because of their central role in determining cellular excitability and response to synaptic stimulation these channels likely play a role in the differential effects of vestibular efferent neurons on afferent discharge. Microarray data from previous experiments showed KCNK 1,2,3,6,12 & 15 mRNA in Scarpa's ganglia. Real-time RT-PCR showed KCNK 1,2,3,6,12 & 15 mRNA expression in Scarpa's ganglia and KCNK 1,2,3,6,12 but not 15 mRNA expression in the crista ampullaris. A differential distribution of the two-poredomain potassium channels  $K_{2P}1.1$ , 2.1, 3.1 and 6.1 like immunoreactivity in the vestibular periphery was seen (corresponding to KCNK genes 1,2,3 & 6). K<sub>2P</sub>1.1i (TWIK 1i) was detected along nerve terminals, hair cells, supporting cells, and blood vessels of the crista ampullaris and in the cytoplasm of neurons of the Scarpa's ganglia. K<sub>2P</sub>2.1i (TREK 1i) was detected in nerve terminals of the crista ampullaris, and in neuronal fibers and somata of neurons of Scarpa's ganglia. K<sub>2P</sub> 3.1i (TASK 1i) was detected in nerve terminals, in the apical portion of supporting cells, and in the hair cells and vestibular dark cells of the crista ampullaris, and in neuron cytoplasm in Scarpa's ganglia. K<sub>2P</sub> 6.1i (TWIK 2i) was detected in the hair cell stereocilia, hair cell and supporting cell membrane, vestibular dark cells, blood vessels, and nerve fibers of the crista ampullaris. K<sub>2P</sub> 6.1i was mainly in neuron fibers of Scarpa's ganglia and minimally in the somata.

## 663 Amiloride-Sensitive Epithelial Sodium Channel (β-ENaC) Immunolocalization in Human Vestibular Endorgans.

**Gail Ishiyama**<sup>1</sup>, Ivan Lopez<sup>2</sup>, Robert W Baloh<sup>1</sup>, Akira Ishiyama<sup>2</sup>

<sup>1</sup>Neurology Dept UCLA School of Medicine, <sup>2</sup>UCLA School of Medicine, Surgery Dept Div Head & Neck

The epithelial sodium channel (ENaC) is a highly sodiumselective amiloride-sensitive cation channel, belonging to the degenerin/ENaC gene superfamily (Sagnella and Swift, Current Pharm Des 2006, 12, 2221-2234). In the adult rat vestibule, ENaC subunit mRNA expression was detected in the apical membrane of the sensory epithelia and the stroma (Gründer et al., Eur J Neurosci 13, 641-2001) and immunohistochemical localization 648. corresponded with these findings (Zhong and Liu, Hear Res 193, 1-8, 2004), and semicircular canal duct epithelial monolayers from rat demonstrate sodium absorption with physiological characteristics of ENaC (Satyanarayana et al. Am J Physiol Renal Physiol 286:F1127-1135, 2004). There are no previous studies on ENaC localization in the human vestibular endorgans. Vestibular endorgans were microdissected from human temporal bones 3-5 hours post-mortem from individuals with no history of vestibular problems (age ranging from 75-99 years old; n=6). Cryostat sections were incubated with a rabbit b-ENaC antibody (1:1000 in PBS, Alomone, Israel), and analyzed using fluorescent microscopy. In the crista ampullaris and macula utricle, b-ENaC immunoreactivity localized to the transitional epithelial cells at the periphery of the vestibular sensory epithelia and to the epithelial cells of the membranous labyrinth and semicircular canal duct epithelium. Hair cells and supporting cells were nonimmunoreactive. Colocalization of b-ENaC Na+K+ATPase corroborates the exclusive localization of b-ENAC in non-sensory epithelial cells. b-ENaC immunoreactivity was also observed in fibroblasts within the crista and utricular stroma. The high degree of conservation of b-ENaC expression in the vestibular endorgans of human suggests that ENaC plays a critical role in inner ear ionic homeostasis, and may lead to therapeutic strategies for inner ear pathologies.

Funded by NIDCD-NIH grants DC005028-01, AG09693-10, DC005187.

#### [664] Is Anti-Ctbp2 a Marker for Synaptic Ribbons in Vestibular Organs?

**lain Miller**<sup>1</sup>, David Sams<sup>1</sup>, Mark Berryman<sup>2</sup>, Ellengene Peterson<sup>1</sup>

<sup>1</sup>Neuroscience Program, Department of Biological Sciences, Ohio University, <sup>2</sup>Department of Biomedical Sciences, Ohio University

We are attempting to develop a light microscopic marker for synaptic ribbons in turtle utricle. Previous investigators employed electron microscopy of serial-sectioned material to visualize ribbons. This time- and labor-intensive method makes it difficult to analyze the spatial variation in synaptic organization that may contribute to spatial variation in afferent responses to head movement. Thus, a light microscopic marker for ribbon synapses would facilitate analysis of their spatial patterning.

The "ribbon" of ribbon synapses is composed of a unique ~120 kDa structural protein, RIBEYE, which is a splice variant of the CtBP2 gene. Another splice variant, CtBP2, is a ~50kDa nuclear transcription co-repressor protein. Both RIBEYE and CtBP2 share an identical C-terminal B domain of 420 residues, and each has a unique N-terminal A domain of 565 and 20 residues, respectively. A mouse monoclonal antibody generated from an 84 residue fragment of the B domain is available commercially; it identifies CtBP2 and RIBEYE. Western blot immunoassay of this CtBP2 antibody against turtle vestibule extract identifies bands at ~50 (CtBP2), ~110 and ~120 kDa (RIBEYE). The ~110 kDa band is interpreted as a RIBEYE breakdown product (tom Dieck et al. 2005).

Confocal microscopy of anti-CtBP2-labelled utricular neuroepithelia reveals diffuse staining of supporting cell nuclei and intensely stained puncta along the basolateral membranes of type I and type II hair cells. In electron microscopic material, the antibody labels dense bodies at ribbon synapses. Preliminary results suggest that there are significant differences in the size and density of labeled puncta at different macular loci. Our data suggest that CtBP2 may be a light microscopic marker for ribbon synapses in turtle utricle and that there are zonal variations in the synaptic linkages between utricular hair cells and afferents.

Support by the Deafness Research Foundation (IMM) and DC05063 (EHP)

### 665 Neurotransmission in Calyx-Bearing and Bouton Afferents in the Turtle Posterior Crista

Jay M. Goldberg<sup>1</sup>, Shilpa Chatlani<sup>1</sup>, J. Christopher Holt<sup>2</sup>

<sup>1</sup>Univ Chicago, <sup>2</sup>Univ Texas Med Branch

We recorded synaptic activity in current clamp from calyxbearing (CD) and bouton (B) afferents near their peripheral termination in the posterior crista, while the canal duct was stimulated with an indenter. Both quantal and non-quantal activity was recorded from both types of fibers, but CD afferents required much more intense stimulation to produce comparable effects. Power spectra were used to deduce mEPSP shape (qshape) and duration (qdur), while quantal size (qsize) and quantal rate (qrate) were estimated by shot-noise theory. gshape usually consists of a depolarization described by an alpha function, f(t) = t exp(-at), a = 500-1500/s. In some units, more commonly in CD units particularly during excitation, depolarization is followed by a small hyperpolarization. Both monophasic and biphasic mEPSPs are blocked by CNQX. compared to B units, CD units had the following characteristics: gdur is slightly smaller, gsize is 2.5-5x grate is comparable. and non-quantal transmission is proportionately larger and is less susceptible to CNQX block. These comparisons have implications for quantal release from hair cells, for the clearance of glutamate and K<sup>+</sup> from the synaptic cleft, and for postsynaptic current flow from inner-face synapses to the spike generator.

#### 666 Diminution of Quantal Size in Calyx-Bearing Afferents and the Potential Role of Postsynaptic Active Conductances

**J. Christopher Holt**<sup>1</sup>, Shilpa Chatlani<sup>2</sup>, Jay Goldberg<sup>2</sup>
<sup>1</sup>Univ Texas Med Branch, <sup>2</sup>Univ Chicago

Quantal size (gsize) is much smaller in calvx-bearing (CD) units than in bouton (B) units. By monitoring activity immediately after the impalement of CD units, we find that following a transient depolarization and a high-frequency burst of spikes, there can be a large (3 - 5x) diminution in gsize taking place in the next 20 - 120 s and continuing well after the initial depolarization and spike burst. There is no accompanying decline in quantal rate. A similar decline in gsize is not seen in B units. These results argue that the small gsize of CD units seen during prolonged impalements is an artifact triggered by the initial penetration. A persistent drop in terminal impedance cannot explain the gsize decline, as the fall in gsize is not associated with a decline in efferent-mediated responses. Extracellular recordings of stimulated spike discharge are consistent with this conclusion. We suggest that the transient depolarization, taking place during the initial impalement, alters active postsynaptic conductances. Consistent with the hypothesis, gsize is markedly reduced when a persistent Na<sup>+</sup> current is blocked by TTX and is similarly enhanced by the KCNQ blockers, linopirdine and XE 991. Active conductances may be necessary so that synaptic currents arising on the inner face of the calyx ending can reach the outer face and the spike generator.

# Localization of the Potassium-Chloride Cotransporters, KCC3 and KCC4, and the Glutamate Transporter, Glast, in the Peripheral Vestibular Epithelium

Edmund Ho<sup>1</sup>, Jay M. Goldberg<sup>2</sup>, **Anna Lysakowski**<sup>1</sup> \* Univ Illinois Chicago, <sup>2</sup>Univ Chicago

Receptor currents are carried out of hair cells by K<sup>+</sup> ions. In addition, neurotransmission involves the release of glutamate from hair cells. Homeostatic regulation of the extracellular concentrations of K<sup>+</sup> and glutamate is important in the maintenance of function. In most hair-cell systems, there is a close relationship between hair cells (HCs) and supporting cells (SCs). SCs contain much of the homeostatic machinery, including the glutamate transporter, GLAST, as well as the K-Cl co-transporters, KCC3 and KCC4. The same may be true for vestibular type II, but not type I HCs. In the latter case, the calyx ending separates the HC from the SC, effectively preventing SCs from regulating ion concentrations in the synaptic cleft. For this reason, we became interested in the distributions of GLAST and the KCCs in vestibular neuroepithelia. Sections of vestibular endorgans were stained with antibodies and viewed in a confocal microscope. Antibodies were obtained from Chemicon and diluted 1:200 to 1:400. Calretinin-immunoreactivity identified calyx afferents and most type II HCs. Positive control tissues were kidney and cochlea. previously reported (Takumi et al. 1997), GLAST is confined to SCs, including their basal portions and their extensions towards the top of the neuroepithelium. Unlike

the situation in the cochlea, where KCC3/4 are found exclusively in SCs (Boettger et al. 2002), there is intense KCC3/4 staining of vestibular calyx endings and less intense staining of SCs and cells in the transitional epithelium. The localization of KCC4 in calyx endings was confirmed by immunogold EM. KCCs could help clear  $K^{\!\!\!+}$  from the cleft between the type I HC and its afferent. A glutamate transporter other than GLAST could remove neurotransmitter from the cleft, but the molecular identity of that transporter is unknown.

Supported by NIH DC-02058.

## 668 Are Outer-Face Synapses Needed for Quantal Synaptic Transmission at the Calyx Ending?

Jay M. Goldberg<sup>1</sup>, Anna Lysakowski<sup>2</sup>

<sup>1</sup>Univ Chicago, <sup>2</sup>Univ Illinois Chicago

The question of quantal transmission from type I hair cells to calyx endings has remained controversial. In the chick, Yamashita and Ohmori (1991) failed to record quantal activity from morphologically identified calyx afferents. Intracellular recordings from lizard afferents were interpreted as indicating the presence of quantal transmission in calyx endings (Schessel et al. 1990). Unfortunately, calyx fibers were identified based on an assumption questioned by subsequent work in turtle. Intracellular recordings near the turtle posterior crista show that calyx-bearing afferents have both quantal and nonquantal transmission (Holt et al., this meeting). But in most preparations, even pure calyx afferents receive synaptic inputs on their outer faces from type II hair cells. Could the quantal transmission arise solely from outer-face synapses? Stated another way, is the type I hair cell capable of quantal transmission? In this paper, we present 3 lines of evidence supporting such transmission: 1) The type I hair cell has the morphological machinery to support quantal transmission. To cite one example, type I hair cells in the central zone of the chinchilla crista have, on average, more than 20 ribbon synapses (Lysakowski & Goldberg 1997). 2) Recordings from solitary type I hair cells and calyx endings provide evidence of quantal transmission in the absence of outer-face ribbons (Rennie & Streeter 2006). 3) Because of the preponderance of type I hair cells in the central zone of the squirrel-monkey crista, there are few opportunities for type I to type II contacts. Ultrastructural examination, summarized here, shows that only 1 in 5 central type I hair cells is contacted by an outer-face synapse. Yet, the discharge of all afferents in the central zone is irregular. As argued by Holt et al. (2006), irregular discharge is based on guantal noise since the only other source of irregularity, channel noise, is much too small. Supported by DC-2058 and DC-2521.

## 669 The Topographic Distribution of Calretinin-Positive Calyces in Otoconia-Deficient Utricles

**William Yao<sup>1</sup>**, Rebecca Hu<sup>2</sup>, Timothy Jones<sup>3</sup>, Larry Hoffman<sup>2</sup>

<sup>1</sup>University of Colorado School of Medicine, <sup>2</sup>Geffen School of Medicine at UCLA, <sup>3</sup>East Carolina University Calyx-only afferent neurons projecting to the utricle exhibit unique characteristics with respect to dendritic morphology (they possess only calyces), cell biology (they uniquely express calretinin), and physiology (they exhibit lower sensitivities than afferents with comparable projection loci and spontaneous discharge). Recent evidence suggests that they project predominantly to the medial striola (Xue et al. SFN Abs. 2005). Hair cells in this region exhibit similar morphologic (and, therefore, physiologic) polarization vectors (MPVs), raising the possibility that the dendritic specialization of this subpopulation may somehow depend upon natural stimulation. We tested this possibility by investigating the distribution of calretininpositive (CAL+) afferents in otoconia-deficient (OTO-) mutant mice. Neuroepithelia from confirmed head tilt (het-Nox3) mutant mice, as well as from control heterozygous animals in which otoconia develop normally, were dissected free and immunocytochemically processed for calretinin expression within the calyces and parent axons of afferent neurons. Stereocilia bundles were also labeled with phalloidin. These double-labeled specimens were analyzed via confocal microscopy, whereby CAL+ calyces could be directly associated with the MPV of the enclosed hair cell. These methods also enabled a detailed analysis of the striolar region and MPV reversal line in normal and OTO- utricles. We found the distribution of hair cell MPVs in the striolar region of OTO- utricles to be similar to normal specimens, including the presence of "displaced" hair cell MPVs. CAL+ calyces predominantly projected onto hair cells of the medial striola in OTO- utricles, similar to that confirmed for control utricles. We have not observed CAL+ calvces associated with hair cells with displaced MPVs. These data demonstrate that the distribution of calyx-only afferents is not critically dependent upon natural stimulation-evoked activity modulation.

Supported by DC005776 (TAJ, LFH).

#### 670 Dendritic Arbor Architectures Within the Murine Utricle

**Larry Hoffman**<sup>1</sup>, Rebecca Hu<sup>1</sup>, Timothy Jones<sup>2</sup>
<sup>1</sup>Geffen School of Medicine at UCLA, <sup>2</sup>East Carolina University

To investigate the role of natural stimulation in the maturation of utricular afferent neuron dendritic architecture, we are comparing arbor morphologies in utricles from otoconia-deficient mice to those in their heterozygote, otoconia-containing littermates. We have previously reported our findings on *calyx-only* arbors, which project to the striolar region of the utricle. In this presentation we focus upon afferent arbors with *dimorphic* architectures, which project throughout the utricle. Following intracranial exposure of the left vestibular nerves in anesthetized adult mice, extracellular injections of

fluorophore-conjugated biocytin were made. postinjection period allowed for centrifugal transport of the label, after which the anesthetized animals were rapidly decapitated and fixative was infused into the vestibule. The temporal bones were removed and immersion-fixed for 3 hours. The vestibular neuroepithelia were dissected free and histochemically processed with phalloidin to label hair cell stereocilia. Afferent arbors and stereocilia were imaged into separate channels via confocal microscopy to analyze the association between dendritic architecture, terminal field locus, and hair cell morphologic polarization vectors (MPVs). Dimorphic afferent dendritic morphologies appeared to be distinguished on the basis of four general regions of the utricular neuroepithelium. This included the perimeter extrastriola, striola, lateral extrastriola (region lateral to the striola but medial to the perimeter), and medial extrastriola. In the arbors analyzed to date, it appears that the dimorphic afferents in OTOutricles exhibit larger terminal field areas compared to dimorphic afferents projecting to comparable areas in normal utricles. This may be due to enhanced dendritic arbor refinement associated with the presence of natural stimulation in animals with otoconia-containing utricles. Supported by DC005776 to LFH and TAJ.

### 671 Nitric Oxide Inhibits Ca<sup>2+</sup> Current in Hair Cells Via a Cgmp-Dependent Mechanism

**Enrique Soto**<sup>1</sup>, Angélica Almanza<sup>1</sup>, Francisco Navarrete<sup>1</sup>, Rosario Vega<sup>1</sup>

<sup>1</sup>Instituto de Fisiologia, Unversidad Autónoma de Puebla, México.

The structural elements of the NO-cGMP signaling pathway have been described in the vestibular peripheral system. In different cell types NO markedly affects intracellular Ca2+ homeostasis by influencing release of Ca2+ from intracellular stores and its inflow through membrane Ca<sup>2+</sup> channels. By using the whole- and perforated-cell patch-clamp technique we evaluated the action of NO on Ca<sup>2+</sup> currents in type I hair cells isolated from the semicircular canal crista ampullaris of the rat (P14 -18). The NO donors 3-morpholinosydnonimine (SIN-1), sodium nitroprusside (SNP), and (±)-(E)-4-Ethyl-2-[(Z)hydroxyimino]-5-nitro-3-hexen-1-yl-nicotinamide (NOR-4) inhibited in a voltage-independent manner the Ca<sup>2+</sup> current in type I hair cells. The NO scavenger 2-(4carboxyphenyl)-4,4,5,5-tetramethylimidazoline-1-oxyl-3oxide (CPTIO) prevented the inhibitory effect of SNP on the Ca<sup>2+</sup> current. The selective inhibitor of the soluble form enzyme guanylate cyclase (sGC) [1,2,4]Oxadiazolo[4,3-a]quinoxalin-1-one (ODQ) decreased the SNP-induced inhibition of the Ca<sup>2+</sup> current. The membrane-permeant cGMP-analogue 8-Br-cGMP mimicked the SNP effect. KT-5823 a specific inhibitor of cGMP-dependent protein kinase (PGK) prevented the inhibition of the Ca<sup>2+</sup> current by SNP and 8-Br-cGMP. These results demonstrated that NO inhibits in a voltageindependent manner the voltage-activated Ca2+ current in rat vestibular-type-I hair cells via the activation of a cGMPsignaling pathway. The inhibition of the Ca<sup>2+</sup> current by NO may contribute to regulate intracellular Ca<sup>2+</sup> concentration and hair-cell synaptic transmission.

Financed by SEP-CONACyT 46511 grant to ES and BUAP-VIEP 20/SAL/06-G grant to RV.

## 672 Differential Lipid Raft Localization of ErbB2 in Vestibular Schwannoma Cells and Schwann Cells

Kevin Brown<sup>1</sup>, Jason Clark<sup>1</sup>, Marlan Hansen<sup>1</sup>

<sup>1</sup>University of Iowa - Department of Otolarynology - Head and Neck Surgery

Objective: To evaluate differential lipid raft localization of the growth factor receptor erbB2 in Schwann cell (SC) and vestibular schwannoma (VS) cells.

Study Design: Lipid raft and non-lipid raft cell fractions were probed for erbB2 in fresh VS tissue and fresh peripheral nerve (proliferating or quiescent SC). Colocalization studies were also performed to evaluate erbB2 localization.

Methods: Fresh VS tissue or rat peripheral nerve (proximal or distal to a crush injury) was isolated into Triton X-100 (TX-100) soluble (non-raft) and sodium dodecyl sulfate (SDS) soluble fractions (lipid raft fraction). Extracts were separated and blotted with antibodies against erbB2 and phosphorylated (activated) erbB2. Separately, VS cells were probed with anti-erbB2 and cholera toxin B (CTB, a raft marker) to evaluate co-localization. Levels of activated Erk1/2 were also evaluated by western blot and the requirement of MEK and PI3 kinase to VS proliferation evaluated by inhibitors *in vitro*.

Results: We demonstrate constitutive raft localization of erbB2 in VS cells, and phosphorylation of erbB2 in that fraction. We also demonstrate inducible lipid raft localization of erbB2 in rat peripheral nerve distal to a crush injury (proliferating segment). Furthermore, erbB2 is phosphorylated in raft fractions of the distal proliferating segment. Co-localization studies on VS cells in culture demonstrates co-localization of erbB2 with CTB confirming localization to lipid rafts. We also explored the contribution of downstream signals activated by erbB2 including MEK/ERK1/2 and PI3-K/Akt to VS growth. We find high levels of activated Erk1/2 constitutively expressed in human VSs *in vivo* and that inhibitors of MEK and PI3-K both inhibit VS proliferation in vitro.

Conclusions: These data demonstrate erbB2 constitutively localized to lipid rafts in VS in both whole tissue and cell culture. ErbB2 is also inducibly localized to rafts in denervated sciatic nerve (undergoing SC proliferation) suggesting a critical role for erbB2 in SC proliferation. ErbB2 is phosphorylated in raft fractions, and phosphorylated erbB2 activates downstream signaling cascades which ultimately promote proliferation. Constitutive lipid raft localization and phosphorylation of erbB2 in VS cells likely contributes to the increased proliferative potential of VS cells in an erbB2/Erk/Akt dependent fashion.

## 673 Efferent-Mediated Rotational Responses in Superior-Canal Afferents of the Alert Monkey

Soroush Sadeghi<sup>1</sup>, Jay M. Goldberg<sup>2</sup>, Lloyd B. Minor<sup>3</sup>, **Kathleen E. Cullen**<sup>1</sup>

<sup>1</sup>McGill Univ, <sup>2</sup>Univ Chicago, <sup>3</sup>Johns Hopkins Med Sch In decerebrate chinchillas (Plonik et al. 2002), rotational responses could still be obtained from semicircular-canal fibers in the vestibular nerve after conventional afferent responses were nulled by placing the corresponding canal orthogonal to the plane of motion. Responses were type III, i.e. were excitatory for both rotational directions and were efferent -mediates as they were abolished when the vestibular nerve was sectioned central to the recording electrode. Here we show that similar type III responses can be obtained from superior-canal afferents in the alert monkey when the horizontal canals are selectively stimulated. As in the chinchilla, the responses require large rotational velocities (320 deg/s), are larger in irregular than in regular afferents, consist of both fast and slow response components, and are seldom larger than After destruction of the contralateral 10-15 spikes/s. labyrinth, excitatory responses can be obtained by either excitatory or inhibitory rotations of the remaining horizontal The vestibular source of the responses was confirmed bv their abolition after contralateral labyrinthectomy followed by the plugging of the ipsilateral horizontal canal. Although canal plugging eliminated responses in horizontal-canal afferents to the relatively low-frequency trapezoidal rotations used to test efferent function, responses of presumed afferent origin were still seen to high-frequency (4 - 8 Hz) sinusoidal rotations. These last results confirm observations of Rabbitt et al. (1999) in the toadfish.

# 674 Evaluation of Phosphorylated Form of Camp/Calcium Response Element Binding Protein Expression in the Guinea Pig Brainstem in Unilateral Vestibular Re-Input Model Using Tetrodotoxin with Osmotic Pump

**Kenji Takeno**<sup>1</sup>, Hiroaki Shimogori<sup>1</sup>, Kazuma Sugahara<sup>1</sup>, Takefumi Mikuriya<sup>1</sup>, Hiroshi Orita<sup>1</sup>, Yoshinobu Hirose<sup>1</sup>, Hiroshi Yamashita<sup>1</sup>

<sup>1</sup>Yamaguchi University Graduate School of Medicine We reported the process of vestibular function in the unilateral vestibular re-input model using tetrodotoxin (TTX) with osmotic pump in the guinea pig. This model has the unique character so that directional preponderance of nystagmus (DP) to the TTX-treated side was observed on VOR examination at 7 days after vestibular re-input and was not observed at 14 days after vestibular re-input. These results suggest that the neural plasticity caused by the unilateral intracochlear administration of TTX is similar to that caused by the unilateral labyrinthectomy (UL) and may remain after vestibular re-input. However, the process of neural plasticity in our model is unknown. Several reported that phosphorylated studies cAMP/calcium response element binding protein (pCREB) was used as a marker of neural activation and expressed

in the brainstem after UL. The aim of this study is to clarify the process of the neural plasticity in our model by evaluation of the pCREB labeling neurons in the brainstem.

Hartley white guinea pigs with normal Preyer's reflexes and tympanic membranes were used in this study. Two groups (TTX group and UL group) were made. In TTX group, TTX administration to unilateral inner ear was performed for 3 days with osmotic pump. In UL group, UL was performed by surgical and chemical method. We operated on the right ear in all animals. We observed the pCREB labeling neurons in the brainstem at several post-operative intervals in both groups.

In both groups, the pCREB labeling neurons were detectable in both sides of the vestibular nucleus at 1h post-operation. These results suggest that pCREB may be a marker of neural activation in our model.

#### [675] Quantitative Changes in Calcium-Related Molecules in the Rat Vestibular Nucleus Complex Following Unilateral Vestibular Deafferentation

**Chisako Masumura**<sup>1</sup>, Arata Horii<sup>1</sup>, Kenji Mitani<sup>1</sup>, Tadashi Kitahara<sup>1</sup>, Atsuhiko Uno<sup>1</sup>, Takeshi Kubo<sup>1</sup>

<sup>1</sup>Department of Otolaryngology, Osaka University School of Medicine

Inquiries into the neurochemical mechanisms of vestibular compensation in animal models of lesion-induced neuronal plasticity reveal the involvement of both voltage-gated Ca<sup>2+</sup> channels (VGCC) and intracellular Ca<sup>2+</sup> signaling. We, previously, used microarray analysis to examine genes that show asymmetrical expression between the bilateral vestibular nucleus complex (VNC) 6 h following unilateral vestibular deafferentation (UVD), and it showed an upregulation of some calcium-related genes such as  $\alpha 2$ subunit of L-type calcium channels, calcineurin, and plasma membrane Ca2+ ATPase 1 (PMCA1) in the ipsilateral VNC. To further elucidate the role of calcium related molecules in vestibular compensation, we used a quantitative real-time PCR method to confirm the microarray results and investigated changes in expression of these molecules at various stages of compensation (6 h to 2 weeks after UVD). In addition, we also investigated the changes in gene expression during Bechterew's phenomenon and the effects of calcineurin inhibitors on the vestibular compensation. Accordingly, real-time PCR showed that α2 subunit of VGCC, PMCA2, and calcineurin genes were transiently up-regulated 6 h after UVD in ipsilateral VNC. A subsequent UVD, which induced Bechterew's phenomenon, reproduced a complete mirror image of the changes in gene expressions seen in the initial UVD, which corroborates the above results. Pretreatment by FK506, a calcineurin inhibitor, decelerated the vestibular compensation. This observation suggests that after increasing the Ca2+ influx into the ipsilateral VNC neurons, calcineurin may be involved in their synaptic plasticity. Conversely, an up-regulation of PMCA2, a brainspecific Ca<sup>2+</sup> pump, would increase an efflux of Ca<sup>2+</sup> from those neurons and thus prevent cell damage following UVD.

#### 676 Electrophysiological Properties of Rat Vestibulocerebellum Interneurons

Luisa Botta<sup>1</sup>, Egidio D'Angelo<sup>1</sup>, **Sergio Masetto<sup>1</sup>**<sup>1</sup>Dip. Scienze Fisiologiche Farmacologiche, University of Pavia, Italy

Acceleration produced by head movement in space is transduced by vestibular hair cells, and transformed into frequency modifications of primary vestibular afferents (PVAs) action potentials discharge. This signal is relayed by PVAs to the vestibular nuclei (VN) and to the cerebellar neurons. Unipolar brush cells (UBCs) and granule cells (GCs) are interneurons of the granular layer of the vestibulocerebellum that receive signals from PVAs and VN. We have investigated the electrophysiological properties of UBCs and GCs located in the vestibulocerebellum lobi I (lingula) and X (nodulus), by combining the patch-clamp technique in ruptured wholecell configuration with the slice preparation of the rat cerebellum (postnatal day 17-23). UBCs showed a mean membrane capacitance (Cm) of 9.8 pF (± 3.2; n = 13), a mean input resistance (Rm) of 0.81 GOhm (± 0.41), and a mean resting potential (Vz) of -54.4 mV (± 7.5). GCs had a mean Cm of 3.3 pF (± 0.9; n = 21), a mean Rm of 3.3 GOhm ( $\pm$  0.5), and a mean Vz of -55.9 mV ( $\pm$  8.7). The voltage responses of UBCs and GCs was significantly different: when depolarized from -70 mV by current steps large enough to elicit an action potentials discharge, UBCs showed a transient (phasic) discharge of action potentials. lasting less than 50 ms, whereas GCs showed a sustained (tonic) discharge of action potentials, lasting for the whole current step duration (1000 ms). These differences accompanied to different patterns of ion currents recorded in voltage-clamp mode: UBCs showed a slow inward rectifying current (Ih), with or without an anomalous K<sup>+</sup> rectifying current (IK1). Conversely, all GCs expressed IK1, whereas none expressed Ih.

Since the afferent activity of PVAs differs in response dynamics, with purely phasic and tonic discharges at the two extremes of a broad dynamics range, present results suggest that UBCs intrinsic properties would match phasic PVAs, whereas GCs would match tonic PVAs.

## 677 Low-Threshold K<sup>+</sup> Currents Underlie the Firing Characteristic of Vestibular Ganglion Neurons

**Shinichi Iwasaki**<sup>1</sup>, Yasuhiro Chihara<sup>1</sup>, Ken Ito<sup>1</sup>, Yoshinori Sahara<sup>2</sup>

<sup>1</sup>Department of Otolaryngology, Faculty of Medicine, University of Tokyo, <sup>2</sup>2Department of Biochemistry & Cellular Biology, National Institute of Neuroscience, National Center

Vestibular afferents are classified as regularly or irregularly discharging patterns, and use their characteristic firing patterns to encode vestibular information and carry them to the brain. To elucidate the major factors responsible for the discharge regularity of vestibular primary afferents, we examined the intrinsic firing properties of isolated rat vestibular ganglion cells (VGCs) and explored contributions of K<sup>+</sup> channels to the discharge regularity.

Three classes of VGCs were distinguished on the basis of a degree of spike frequency adaptation observed during sustained membrane depolarization: most neurons exhibited a strong adaptation generating just a single spike or short bursts of spikes, and the others showed moderate adaptation or tonic firing. A degree of spike frequency adaptation in a neuron did not correlate with the cell size. Considerable variation in K<sup>+</sup> currents was present in the class of VGCs. In the presence of 4-aminopyridine or  $\alpha$ dendrotoxin ( $\alpha$ -DTX), selective blockers of Kv1  $\alpha$  subunits, phasic firing turned into sustained firing, indicating that Kv1 channel control the firing characteristic of the pahsic VGCs. In tonic VGCs, tetraethylammonium decreased the frequency of discharges at membrane potentials above threshold while  $\alpha$ -DTX lowered the threshold for initiation of discharge in response to depolarizing current steps. Blockade of Ca<sup>2+</sup> activated K<sup>+</sup> channels and H- currents also had some effects on the firing pattern of the tonic VGCs. Our results indicate that **VGCs** heterogeneous intrinsic firing properties, and that lowthreshold K<sup>+</sup> channels are critical to determining a pattern of spike discharges that optimize the responsiveness of the vestibular neurons, thereby contributing to the timing of VG inputs.

### 678 Effect of Age on Post-Rotatory Nystagmus Following OVAR

Joseph Furman<sup>1</sup>, Robert Schor<sup>1</sup>

<sup>1</sup>University of Pittsburgh

The aim of this study was to assess the influence of age on the spatial characteristics of the vestibulo-ocular reflex (VOR). We assessed the amount of reorientation of the axis of eye velocity, i.e., "revectoring", following cessation of constant velocity off-vertical axis rotation (OVAR). The subject population consisted of 19 normal older persons between the ages of 66 and 76 (mean 70.2) and 26 younger persons between the ages of 20 and 30 (mean 23.5). OVAR was performed using a rotate-then-tilt paradigm with an off-vertical tilt of 30 degrees and a rotational velocity of 90 deg/sec. Each subject underwent as many as eight OVAR trials with two possible directions of rotation (clockwise and counterclockwise) and four possible stationary post-rotatory orientations with respect to gravity: nose-up, nose-down, right-ear-down, and leftear-down. Eye position was measured using threedimensional scleral search coils. Eye positions were expressed as rotation vectors using a reference position of straight ahead. We obtained the orientation of the slow component eye velocity directly from the corresponding velocity rotation vector. These orientations were averaged over three five-second epochs centered at 5, 10, and 15 seconds following cessation of rotation. When the orientation of eye velocity changed from head-vertical toward earth-vertical, we considered this evidence for revectoring. We found that all of the younger subjects and all but one of the older subjects showed revectoring in at least one trial. However, when the data were examined on a trial-by-trial basis, more of the trials in the younger subjects (64%) showed revectoring compared to the older subjects (50%). For both the older and younger subjects,

revectoring was more evident when the subjects were stopped ear-down than nose-up or nose-down. Our data suggest that there is a small but measurable influence of age on the three-dimensional characteristics of the VOR.

#### 679 Response Vector Orientation (RVO) of **Central Otolith-Related Neurons**

Sergei B. Yakushin<sup>1</sup>, Julia N. Eron<sup>1</sup>, Bernard Cohen<sup>1</sup>, Theodore Raphan<sup>2</sup>

<sup>1</sup>Mount Sinai School of Medicine, <sup>2</sup>Brooklyn College, **CUNY** 

Central neurons that have otolith sensitivity may receive input from primary otolith afferents, the semicircular canals, and body proprioceptors. Moreover, some of these neurons may be part of the network that implements velocity storage. In this study, we determined the otolith polarization vectors of two classes of central otolithrecipient neurons: pure-otolith neurons and canal-otolith convergent, vestibular-only (VO) neurons in alert cynomolgus monkeys. Units with significant proprioceptive input were excluded. We determined the response vector orientation (RVO), which is the projection of otolith polarization vectors to the horizontal plane, based on two methods. In one, the head was statically tilted about a spatial horizontal axis by 30° while the head orientation was varied in yaw. In the second, the RVO was calculated based on the unit responses obtained during steady state off-vertical vaw axis rotation (OVAR) at velocities from 30-120°/s and tilt angles up to 90°. RVO's determined for CW and CCW rotations were averaged. The RVO determined by static tilt and OVAR for pure-otolith neurons were within 80° (range 0-80°). However, the RVO in the VO neurons determined by tilt and OVAR differed by more than 90° (range 90-180°). OVAR in the steady state produces continuous nystagmus with a bias velocity through activation of velocity storage (Kushiro et al., 2002), and there is no canal activation. We postulate that these differences in RVO determined by the two methods may be due to the relationship of the VO neurons to velocity storage (Reisine and Raphan 1992).

Supported by NIH Grants: DC04996, DC05204, EY11812, EY04148, and EY01867

#### 680 Otolith Response Vector Orientation (RVO) of Central Vestibular Neurons Can Be Altered by Adaptation in Tilted Positions

**Julia Eron**<sup>1</sup>, Bernard Cohen<sup>1</sup>, Theodore Raphan<sup>2</sup>, Sergei Yakushin¹

<sup>1</sup>The Mount Sinai Medical School, <sup>2</sup>Brooklyn College, **CUNY** 

Primary otolith afferents have polarization vectors that remain invariant under a wide range of head movements and sustained orientations (Fernandez and Goldberg 1976a,b,c). It has been assumed that central neurons also have invariant otolith polarization vectors. We recently showed (Eron et al., 2006; SFN) that vestibular-only (VO) and vestibular-plus-saccade (VPS) neurons altered their otolith response vector orientation (RVO) after the angular vestibulo-ocular reflex (aVOR) gain was decreased in sidedown position for two hours. After adaptation the maximal aVOR gain changes were observed in the position of adaptation. The RVO's also tended to align with interaural axis, which is the axis of gravity sensed in the position of adaptation. Whether observed changes in RVO were specific to the process of aVOR gain adaptation or were the results of keeping the head in one orientation for a prolonged time in not known and was investigated in the present study. Neurons that received semicircular canal and otolith-related convergent inputs were recorded in two monkeys (Macaca fascicularis) in the vestibular nuclei. Some neurons were tested before and after decreasing the aVOR gain for 2 hr in an on-side position. The response vector orientation was changed in most of tested neurons after gain adaptation. Other neurons were tested before and after animals were statically tilted side-down and kept in this position for 2 hrs. The majority of tested units changed their RVO similarly to that described after aVOR gain adaptation. Thus, our data suggests that otolith polarization vectors of the central vestibular neurons can be altered by orienting the head in side-down position. Supported by NIH Grants: DC04996, DC05204, EY11812,

EY04148, and EY01867

#### 681 Compensatory Head Movement Produced by the Angular Vestibulo-Collic Reflex (aVCR) During Quadrupedal **Locomotion of the Monkey**

Yongqing Xiang<sup>1</sup>, Padmore John<sup>2</sup>, Sergei B. Yakushin<sup>2</sup>, Mikhail Kunin<sup>1</sup>, Theodore Raphan<sup>1</sup>, **Bernard Cohen<sup>2</sup>** <sup>1</sup>Dept. of CIS, Brooklyn College, CUNY, <sup>2</sup>Mount Sinai School of Medicine

Relatively little is known about how well the aVCR provides head stabilization in three dimensions during quadrupedal locomotion. To determine this, we recorded angular head, body and limb movement of cynomolgus and rhesus monkeys with a motion detection system (Optotrak) while animals walked on a treadmill from 0.45 to 1.2 m/s. Estimates of head and body yaw around the spatial vertical, pitch around the interaural axis, and roll about the naso-occipital axis were computed relative to space. Body rotations were periodic, in phase with the stride cycle in yaw and roll, but with the step frequency in pitch. Cycle-averaged head movements were largest in yaw, and smaller in roll and pitch, although there was variation in amplitude with walking style. The range of head rotation (h) relative to the range of body rotation (b) in space, expressed as a stabilization ratio (Sr=h/b) was used as a measure of how well the head was stabilized in space. A small value of Sr indicated good stabilization with little head movement in space. In typical animals, the head was well stabilized in space by the aVCR against large perturbations of the body in yaw Sr=0.17 (2.9\overline{\pi}/24.8\overline{\pi}) and for roll Sr=0.05 (1.7œ/36.8œ). Head and body pitch were small and of the same amplitude giving an Sr=0.99 (3.5\omega/3.6\omega). This indicated that the pitch component of head movement was not stabilized in space by the aVCR. In other animals, head and body yaw rotation was smaller and not stabilized Sr =1.47 (6.9æ/4.7æ). There was no constant head fixation point in pitch, possibly because the monkeys were untrained to watch forward visual targets.

Thus, the aVCR provided significant head stabilization for roll and for larger yaw head movements than 5-10œ, but did not compensate for smaller body movement in yaw and pitch during normal locomotion. The angular vestibulo-ocular reflex (VOR) is likely, to provide the additional compensation necessary to stabilize gaze in space in every dimension.

Support: EY11812, DC05204, EY04148, EY01867

## 682 Sensory Modality of a Dual-Task Influences Standing Postural Sway Response to Moving Visual Environments

Mark Redfern<sup>1</sup>, Mark Musolino<sup>1</sup>

<sup>1</sup>University of Pittsburgh

Postural sway response to optic flow (i.e. moving visual environments) is influenced by many factors including vestibular health, age, and duration of exposure. We investigated the role of attention in the postural response to optic flow. We used a dual-task paradigm with the secondary task being a choice reaction time (CRT) task. Two studies were conducted. In the first study, six healthy adults were exposed to visual scene movement of 5 deg. peak-to-peak and 0.25 Hz in the antero-posterior direction. Exposure was no movement for 30 s, followed by 60 s of a An auditory CRT task was sinusoidal movement. performed concurrently during different periods of the visual motion. The conditions included: C1) no CRT task, C2) CRT task concurrent with scene movement throughout, C3) CRT task for the first 30 s of the scene movement, C4) CRT task for the last 30 s of the scene movement, and C5) CRT task for the entire stance time. The sway data were analyzed by performing a timefrequency analysis and computing the power in a frequency band (0.2-0.3 hz.) over time. Results showed that without a concurrent CRT task, sway rose when the scene movement began, and then there was a reduction over time (adaptation). When the auditory CRT task was included, there was a reduction in the magnitude of response compared to the no-task condition during the first 30 s of the stimulation. Thus, performing the auditory CRT task during exposure to a moving visual environment causes a reduction in the magnitude of sway during the initial motion of the scene when movement is usually strongest. A follow-up study included a visual CRT as well as an auditory CRT under fixed and moving scene conditions for 12 healthy adults. This study showed again that subjects swayed less during the auditory CRT task compared to no task. During the visual CRT task, however, there was no reduction in sway. Taken together, these two studies suggest that the sensory modality of a secondary task during exposure to moving visual environments influences the sway response. We propose that the auditory task focuses attention away from the visual sensory channel, and thus reduces the impact of The visual task, however, vision on postural sway. maintains attention in the visual stream, and thus does not have an impact on postural sway.

#### 683 Foot Dynamics During Walking on Upward Inclines

**Koji Kudo**<sup>1</sup>, Yasuhiro Osaki<sup>2</sup>, Mikhail Kunin<sup>3</sup>, Catherine Cho<sup>1</sup>, Bernard Cohen<sup>1</sup>, Theodore Raphan<sup>3</sup>

<sup>1</sup>Mount Sinai School of Medicine, <sup>2</sup>Osaka University Graduate School of Medicine, <sup>3</sup>City University of New York During natural walking on a treadmill, foot dynamics are determined by walking velocity and frequency of stepping (Osaki et al, 2006). Specifically, the foot follows characteristic phase plane trajectories along the forward (X-axis) direction, and is governed by a linear main sequence relationship between peak forward velocity and foot position while vertical (Z-axis) foot movement is related to specific toe clearance from the ground. We questioned whether the dynamics of foot movement along the X- and Z-axes and toe clearance would be affected by walking on an incline. Foot and leg movements were monitored in three dimensions with a motion detecting system (Optotrak) while subjects walked on linear treadmill (Quinton). Phase plane plots of the forward toe velocity vs. forward toe position while walking on grades from 0-10° were independent of angle and followed the same circular trajectory as when walking on level ground. Phase plane trajectories in the lateral (Y-axis) direction were also indistinguishable from those determined when walking on level ground. The Z-axis phase plane plots in spatial coordinates were markedly different, however, in that the foot did not drop to the same downward level during the swing as when walking on the level. However, when the toe Z position was computed relative to the extrapolated height of the treadmill, the toe Z trajectory was not significantly different from that determined during level walking at all velocities. These data support our state theoretic model, which postulates that there is active feedback control that determines the forward foot dynamics. Thus, the state of the foot and control signals that govern the swing must embed the angle of the incline so that toe clearance relative to the walking surface is independent of the grade.

Supported by NIDCD grants DC 05222 and DC 05204

#### 684 Influence of Visual Optokinetic Stimuli on Stationary Stepping

**Alejo Suarez<sup>1,2</sup>**, Teresa A. De Aragaveytia<sup>2</sup>, Mariana Arocena<sup>1,2</sup>

<sup>1</sup>British Hospital, <sup>2</sup>Otoneurology Lab

Objective: The aim of this study was to evaluate the influence of an optokinetic (OK) visual stimulation, when a stationary gait exercise is performed.

Methods: 50 healthy subjects were tested (16 males and 34 females), with a mean age of 29.1 years old (ranging from 18 to 54). The subjects were asked to step in the place for 30 seconds, while they were in the center of a drum with wide black and white stripes that covers all the visual field of the patient, spinning at a speed of 36°/s. First the drum spins 30 seconds in clockwise (CW) direction (left to right from the observer point of view) and after repositioning of the subject, 30 seconds in counterclockwise (CCW) direction (right to left). At the beginning of the test, they stood at a mark on the floor that

was taken as 0°, measuring the degrees of deviation from the original position at the end of the test.

Results: From the 50 subjects, only 1 did not deviate in either direction when it was tested in CW or CCW direction.

There were no deviation toward the opposite direction of the sense of optical flow, so when there was a deviation, all were to the right when the OK stimuli was in CW sense and to left in CCW sense (in the direction of the slow phase of the OK nystagmus).

There was a significant deviation toward the optical flow sense in both directions of OK stimulation (p < .001, Student t test,  $\alpha$ =.025), with a mean deviation of 38.44° to the right in CW direction and 53.76° to the left in CCW direction.

Discussion: There are a large number of studies about the influence of different visual cues effects or after-effects on posture and gait. We present a dynamic postural response to optokinetic visual stimulation, in healthy subjects. The potential use of this test in daily clinical practice to asses an aspect of sensory integration of the balance system is discussed.

## 685 Postural Sway Velocity, Analysis of the Peak Values in Aged Patients with Instability. Preliminary Report

**Alejo Suarez**<sup>1,2</sup>, Dario Geisinger<sup>3</sup>, Ximena Carrera<sup>3</sup>, Hamlet Suarez<sup>1,2</sup>

<sup>1</sup>British Hospital, <sup>2</sup>Otoneurology Lab, <sup>3</sup>Medicaa Research Deparment

Objective: The aim of this study was the analysis of postural sway peak velocities (PSPV) under different visual frame reference in aged patients with instability.

Methods: 12 aged patients (≥ 65 years) with instability and/or falls. A clinical evaluation was made, and also an electronystagmography and CT scan. 25 healthy subjects (mean age 31 years) were studied as controls.

Postural responses were obtained through a force platform, recording the center of pressure (COP) during 60 sec, and calculating its distribution area by a 95% confidence ellipse (CE). The five higher PSPV were chosen and plotted. Peak velocity was defined as the distance between two points of the COP divided by the sampling period.

COP displacement was recorded under two different visual frame reference: With a still visual frame reference (no specific stimuli).

Optical flow with a retinal stimulus. Horizontal optokinetic (OK) stimulation at a speed of 60°/s. This visual stimulation was generated by a software and delivered to the patient through virtual reality goggles.

The higher five PSPV were plotted and referenced to the 95%, 75% and 50% CE.

Results: PSPV showed stochastic behavior, without any significant direction of movement (from the periphery to the center of the CE or from the center to the periphery of the CE).

Normal and elderly patients with instability showed PSPV out of the ellipse, but elderly patients had significant higher values and also in the context of the higher CE values and therefore closer to the base of support limits.

Discussion: The usefulness of the information obtained from PSPV in order to a risk of fall analysis in elderly patients with instability is discussed.

### 686 Effect of Head Tilt on Learning a Finger Pointing Task

John Anderson<sup>1</sup>

<sup>1</sup>University of Minnesota

The ability to adapt movements to changes in the environment and patterns of sensory inputs is important for motor control. This involves learning visuomotor transformations. Gravity plays a role in establishing an inertial reference frame that could influence the motor learning. In this study adaptations to rotations of the visual representation of a finger's position in space were examined for pointing movements in spinocerebellar ataxia (SCA) 6 and 8, genetic subtypes wherein the clinical manifestations indicate that primarily the cerebellum is affected, although other regions of the brain can be involved later in the disease process. The questions addressed were whether (a) learning the visuomotor transformations would be affected to a greater extent than the accuracy of the pointing movement and (b) gravity stimulation due to a head tilt would change the rate of learning. The subjects sat on a chair in front of a computer monitor with the head upright or tilted laterally. Five visual targets were shown on the screen, one at a time. There was a central reference target and four others, equally displaced along the four diagonals. The position and of the index finger and the orientation of the head in space were recorded with three-dimensional Polhemus sensors. The position of the finger in a certain region of the frontal or sagittal plane was mapped onto the screen, so that both the representation of the finger position, "cursor", and the visual target could be seen. The task was to move the finger in space so that the cursor was superimposed on the target. Finger path length, direction, speed, and end point error were calculated. Patients with early or mild disease had normal or mildly to moderately abnormal endpoint errors under control conditions. However, the ability to adapt to 90 degree rotations and large head tilts was severely affected. Adaptations to smaller rotations and head tilts were affected, but to lesser amounts.

### 687 Circuits and Signal Representations in the Auditory System

Eric Young<sup>1</sup>

<sup>1</sup>Johns Hopkins University

The brainstem auditory system consists of a number of different neural circuits, each of which contains a processed version of the neural representation of the acoustic environment. Most of these have not been studied extensively. Among the well-studied parts of this system are the cochlear nucleus and the inferior colliculus. In this talk, the representation of sound in these nuclei will be discussed, with reference to their known wiring diagrams and suggestions about their functional roles in hearing.

Research supported by the NIDCD

## 688 Frequency-Modulated Sweep Speed and Direction Selectivity in Primary Auditory Cortex of Awake Squirrel Monkeys

**Marc Heiser**<sup>1,2</sup>, Ralph Beitel<sup>1</sup>, Maike Vollmer<sup>1</sup>, Steven Cheung<sup>1</sup>, Christoph Schreiner<sup>1,2</sup>

<sup>1</sup>Coleman Memorial Laboratory, Department of Otolaryngology, U.C.S.F., <sup>2</sup>W.M. Keck Center for Integrative Neuroscience, U.C.S.F.

Frequency-modulated (FM) sweeps are important components of animal communication sounds including human speech. We measured the response selectivity of single neurons in primary auditory cortex (AI) of awake squirrel monkeys for the speed and direction of FM sweeps. Many of these neurons are direction selective and there are more neurons with greater direction sensitivity than in the anesthetized squirrel monkey. Al neurons in the awake squirrel monkey are more speed selective than in anesthetized animals although the range of best speeds is similar. In addition, we compared FM sweep responses to pure tones responses and demonstrate that neurons with sustained responses to pure tones also have sustained FM sweep responses. Tonal receptive field edge frequencies and bandwidth can be predicted from the FM sweep responses of these sustained neurons but not from neurons with onset-only FM responses. While our results and those of others demonstrate that Al neurons are sensitive, on average, to FM sweep parameters, they do not address the trial-bytrial reliability of these responses. In order to determine more specifically the discriminative power of single neurons we calculated ideal observer performance and the mutual information between neuronal responses and FM sweep parameters. This analysis quantifies the limitations of single neuron responses for decision making. Supported by NIH DC02260 and NS34835

## 689 Auditory Spectrotemporal Receptive Fields in the Superior Temporal Gyrus of Rhesus Macaques

**Brian Russ**<sup>1</sup>, Patrycja Olsynski<sup>1</sup>, Ashlee Ackelson<sup>1</sup>, Allison Baker<sup>1</sup>, Frederic Theunissen<sup>2</sup>, Yale Cohen<sup>1</sup>

<sup>1</sup>Dartmouth College, <sup>2</sup>University of California at Berkeley Auditory communication signals (i.e., vocalizations) are important to the socioecology of several species of nonhuman primates such as rhesus monkeys. Vocalizations are hypothesized to be processed preferentially in a ventral pathway that includes the belt and parabelt region (BPR) of the auditory cortex and the prefrontal cortex. We are interested in determining which acoustic features of vocalizations are coded by neurons in this ventral pathway, and how features are represented in different areas of this ventral pathway. In this study, we investigated the coding properties of neurons in the BPR of two rhesus calculated macaques. Specifically, we their spectrotemporal receptive fields (STRF) of neurons in the BPR; a STRF is a linear filter that transforms a representation of an auditory stimulus into a prediction of a neuron's firing rate. The STRFs of BPR neurons were generated from data collected while rhesus fixated a central light and passively listened to exemplars from ten

classes of species-specific vocalizations. Neurons in the belt and parabelt region responded robustly to the species-specific vocalizations. One population of neurons responded to all of the exemplars, whereas a second responded to only a subset of the exemplars; these neurons were also sensitive to the temporal qualities of the vocalizations. The STRFs were consistent with these observations: the STRFs of one population were not structured in that they did not show filter properties consistent with feature selectivity, whereas a second demonstrated selectivity to certain combinations of acoustic features. These results will be compared and contrasted with previous results from the ventrolateral prefrontal cortex, an area that receives input from the BPR

Support Contributed by the NIH.

## 690 Sound Level Dependence and Thalamocortical Input Differentiate Two Rat Auditory Cortices

Heather Read<sup>1</sup>, Douglas Storace<sup>1</sup>, Daniel Pollev<sup>2</sup> <sup>1</sup>University of Connecticut, <sup>2</sup>Vanderbilt University Rat primary auditory cortex (AI) and the ventral auditory field (VAF) share a common topographic organization for characteristic frequency (CF) sensitivity (i.e. cochleotopy). Mirror reversals in CF organization have been used to distinguish between AI and belt regions; however, this method is not useful for distinguishing between AI and VAF. The goal of this study is to quantify functional and structural differences between these regions using electrophysiological, hemodynamic, and anatomical methods. A border between AI and VAF was identified as drop optical response magnitudes. in Electrophysiological recordings confirmed significant differences in spectral tuning bandwidth, threshold and a marked difference in intensity-response functions such that approximately 80% of recording sites were non-monotonic in VAF compared to approximately 15% In Al. retrograde tracer injections into frequency matched regions of AI and VAF revealed significant differences in the distribution of afferent input from the medial geniculate These data strongly suggest that AI and VAF should be regarded as distinct fields in the rat and that VAF might be specialized to process acoustic inputs embedded in greater levels of masking noise. Supported by: National Institute of Child and Health Development: HD2080

## Tonotopy in Primary Versus Secondary Human Auditory Cortex

**Dave Langers**<sup>1,2</sup>, Walter Backes<sup>3</sup>, Pim van Dijk<sup>1,2</sup>
<sup>1</sup>Dept. of Otorhinolaryngology, University Medical Center Groningen, <sup>2</sup>School of Behavioural and Cognitive Neurosciences, University of Groningen, <sup>3</sup>Dept. of Radiology, Maastricht University Hospital
The human cerebral auditory cortex can be subdivided into

primary and secondary regions on the basis of cytoarchitectonic features. In addition, functional differences between these areas exist. In this study, the

cortical representations of sound frequency and lateralization were mapped using functional magnetic resonance imaging (fMRI), by measuring the responses to narrowband stimuli centered at 125, 500, 2000 or 8000 Hz that were delivered diotically, or monotically left or right. In spite of considerable inter-subject variability, tonotopic progressions in optimal stimulus frequency were observed along the Heschl's gyrus, where primary auditory cortex is located. In addition, responses in the primary auditory cortex were strongly lateralized to the hemisphere contralateral to the stimulus presentation. This is in good accordance with various reports on humans and other mammals. However, in the secondary auditory cortex, which comprises the planum polare and planum temporale, frequency preferences were erratic and no tonotopic organization was found. Also, these areas did not show a systematic preference for contralateral stimulation. We interpret this as evidence for differences in the neural representation of sound. Possibly, acoustic sound features are encoded in primary auditory cortex, while in secondary cortex object-related features are extracted. We were also able to establish that frequency mappings in the cortex did not depend upon the side of stimulus presentation, and lateralization preferences did not depend upon stimulus frequency.

## 692 Contrasting Effects of Cortical Inactivation on Medial Geniculate Body and Inferior Colliculus

**Simon Jones**<sup>1</sup>, Kyle Nakamoto<sup>1</sup>, Alan Palmer<sup>1</sup> \*\*MRC Institute of Hearing Research

To investigate the function of the profuse descending projections from auditory cortex (AC) we have reversibly inactivated Guinea pig AC under urethane anaesthesia. Inactivation was achieved using a cryoloop whilst recording from AC, Inferior Colliculus (IC) and Medial Geniculate Body (MGB) with microelectrodes.

One confounding factor in interpreting any changes in recorded responses is the number of routes through which the AC can exert its effects. However, any effect of AC inactivation seen at the level of the MGB, but not the IC can be attributed to the corticothalamic pathway.

Post-Stimulus Time Histograms (PSTHs), Inter-Spike Interval Histograms (ISIHs) and Cross-Correlograms (CCs) have been compared for MGB neuron and IC responses elicited using 50ms clicks. Responses were classified using a hierarchical clustering analysis.

Some MGB PSTHs (55/145) show a late (>200ms) peak that is absent in the responses of IC neurons and that is suppressed by AC inactivation. Other MGB neurons (37/145) showed facilitation of responses to one ear while the responses to the other were suppressed (a type of change not evident in IC responses to single clicks). IC PSTHs typically showed two short-latency peaks the later of which was suppressed by AC inactivation. ISIHs for MGB neurons had a peak at longer ISIs that became broader during AC inactivation. IC neuron ISIHs often showed multiple peaks and only the peaks at longer ISIs were suppressed during AC inactivation. Peaks at shorter ISIs in IC ISIHs typically became narrower during AC inactivation. Stimulus driven correlation between MGB

neurons (assessed from CCs) is lower during AC inactivation, whilst the CCs of IC neurons were unaffected. By contrasting changes observed in MGB with those observed in IC specific effects of the corticothalamic pathway can be determined. These can be ear specific, occur at specific times or effect the degree of correlation between MGB neurons.

# 693 Hemispheric Comparison of Responses in Primary Auditory Cortex (AI) to Frequency Modulated Sweeps in the Common Marmoset (Callithrix Jacchus)

Ralph E. Beitel<sup>1</sup>, Maike Vollmer<sup>2</sup>, Benedicte Philibert<sup>1</sup>, Ben H. Bonham<sup>3</sup>, Steven W. Cheung<sup>1</sup>, Christoph E. Schreiner<sup>1</sup>, Michael M. Merzenich<sup>1</sup>

<sup>1</sup>W.M. Keck Center for Integrative Neuroscience, University of California, San Francisco, CA, <sup>2</sup>University Hospital Wuerzburg, Department of Otolaryngology, Wuerzburg, Germany, <sup>3</sup>Epstein Laboratory, Otolaryngology-HNS, University of California, San Francisco, CA

Our recent study of frequency receptive field (FRF) parameters (characteristic frequency, threshold, sharpness of tuning and minimum response latency) using pure tones reported that the functional organization of Al is not lateralized in the common marmoset (Philibert et al., J Comp Neurol 487:391-406: 2005).

In the present study, neuronal responses in AI evoked by FM sweeps were compared between hemispheres within individual monkeys (n=5). Three monkeys were trained to discriminate FM sweep direction (six sequential upward or downward sweeps; 125 ms ISI; 2-18 kHz; 33.2 octave/s) and were rewarded with a drop of juice for correct discrimination. Ten hemispheres in anesthetized monkeys (3 trained, 2 naïve) were densely mapped using metal microelectrodes.

The results show that: 1) both the proportion of neurons that preferred downward FM sweeps and the magnitude of neuronal responses to downward versus upward FM sweeps were significantly different in trained compared with naïve animals; and 2) hemispheric comparisons of directional preference or magnitude of response to downward versus upward FM sweeps were significantly different in only one of the five monkeys (binomial test: p=0.376). The hemispheric comparisons together with the results from our FRF study indicate no evidence for lateralization of Al in the common marmoset for representation of simple (pure tone) or relatively complex stimuli (FM sweeps).

Supported by NS10414, NINDS34835, NIDCD02260

# 694 Effects of Iontophoretical Application of GABA and Gabazine Remote From the Application Site in Gerbil Primary Auditory Cortex

**Christoph Möller**<sup>1</sup>, Simone Kurt<sup>2</sup>, Henning Scheich<sup>1</sup>, Holger Schulze<sup>1</sup>

<sup>1</sup>Leibniz Institute for Neurobiology, Magdeburg, Germany, <sup>2</sup>Dept. Neurobiology, University of Ulm, Germany

Throughout the literature the effects of iontophoretically applied neurotransmitter-agonists or -antagonists on the local activity of neurons are typically studied at the site of drug application. Here we report the effects of the inhibitory neurotransmitter GABA and the GABA<sub>A</sub>-antagonist gabazine (SR 95531) on neuronal activity at locations that are remote from the application site, that is, that are beyond the diffusion radius of the applied drug.

Neuronal responses to pure tone stimulation were recorded from a total of 250 single or multi-units in primary auditory cortex (AI) of 13 adult male Mongolian gerbils (1) at the application site and (2) at four additional recording sites, in distances between 300 and 1350 µm from the application site. We found that whereas application of GABA in general led to a decrease and gabazine to an increase in neuronal activity at the application site, a certain number of units at remote recording sites showed effects opposite to these local, drug-induced effects: After application of GABA, 21% of the units recorded at sites remote to the application site showed increases in neuronal activity. Such an opposite effect to the direct drug effect was even more pronounced after application of gabazine: Here, the majority of units recorded at remote sites (56%) showed a decrease of neuronal activity. These effects were seen both in spiking activity and amplitudes of local field potentials.

As a diffusion of the applied drug to the remote recording sites could be excluded, these data demonstrate the existence of long range, inhibitory interactions within gerbil AI. These interactions could be realized either by long range inhibitory projections or by long range excitatory projections to local inhibitory interneurons.

## 695 Effects of Salicylate on Spontaneous Activity in Brain Slices of Different Central Auditory Structures

**Dietmar Basta<sup>1,2</sup>**, Romy Goetze<sup>2</sup>, Magdalena Sliwowska<sup>2</sup>, Arne Ernst<sup>1</sup>

<sup>1</sup>Dept. of ENT at ukb, University of Berlin, Germany, <sup>2</sup>Institute of Biology Humboldt-University of Berlin, Germany

Salicylate is well known to produce tinnitus in humans and animals as well. It has been shown that systemic application of salicylate primarily changes outer hair cell electromotility and can influence neuronal activity in several parts of the auditory system. A direct action of salicylate on neurons of the inferior colliclus has been shown earlier in brain slice preparations. However, such an effect cannot be excluded for other parts of the central auditory pathway. The present study therefore investigated

the in-vitro-effect of salicylate application on the single unit spontaneous activity in brain slices of the cochlear nucleus, medial geniculate body and primary auditory cortex

Single unit responses were extracellularly recorded in 200 µm thick slices of the related deafferentiated brain area. During the measurement of spontaneous activity, 1.4 mM sodium salicylate (corresponding to tinnitus related serum levels in rats (Cazals, 2000, Prog. Neurobiol. 62, 583-631)) were added by superfusion.

Sixty seven percent of the neurons in the cochlear nucleus, 76 percent of the neurons in the medial geniculate body and 64 percent of the neurons in the primary auditory cortex responded with a significant and reversible change in firing rate during superfusion with salicylate. The mean value of absolute changes in neuronal firing rate was significantly lower in the cochlear nucleus and primary auditory cortex than in the medial geniculate body. The response of neurons within the medial geniculate body was not significantly different to those obtained earlier from the inferior colliculus.

The present data suggest that the auditory midbrain and thalamus plays a key role in the salicylate-induced tinnitus generation.

Supported by the Sonnenfeld Foundation, Berlin, Germany

## 696 Fitting Linear Models to Non-Linear Spectrotemporal Response Functions: Consequences for STRF Analysis

**G. Bjorn Christianson**<sup>1,2</sup>, Jennifer F. Linden<sup>1,3</sup>, Maneesh Sahani<sup>2</sup>

<sup>1</sup>UCL Ear Institute, <sup>2</sup>Gatsby Computational Neuroscience Unit, <sup>3</sup>Department of Anatomy and Developmental Biology, University College London

Neurons in the central auditory system are often described by the spectrotemporal receptive field or response function (STRF), conventionally defined as the best linear fit between the spectrogram of a sound and the spike-rate it evokes. Unfortunately, the true stimulus-response relationships of auditory neurons are commonly non-linear, and this makes interpretation of the best linear fits difficult. An STRF is assumed to provide an estimate of the receptive field of a neuron, i.e. the spectral and temporal range of stimuli that affect the response and whether the effects are excitatory or inhibitory. However, when the true response function is non-linear, the STRF will be stimulusdependent, and changes in the stimulus properties can alter estimates of the polarity and spectrotemporal extent of receptive field components. We demonstrate through simulations that these effects can be dramatic. Even when uncorrelated stimuli are used, simple and biologically plausible neuronal non-linearities can produce STRFs with spurious receptive field elements, indicating contributions from time-frequency combinations to which the neuron is actually insensitive. Only when the distributions of the stimulus values are statistically independent does the STRF reliably indicate features of the underlying receptive field, and even then it gives only a conservative estimate of its spectrotemporal extent. One consequence of these observations is that any stimulus-induced change in an STRF could arise, at least in part, from a consistent but non-linear neuronal response to stimulus ensembles with differing higher-order dependencies, rather than from stimulus-driven adaptation in response properties. Thus while auditory cortical neurons may well adapt to the statistics of different stimulus ensembles, stimulus-dependence of STRFs alone is not sufficient proof of this. This work was supported by the Gatsby Charitable Foundation.

#### 697 The Interaction Between Attention and Auditory Pop-Out

**Juanjuan Xiang**<sup>1</sup>, Mounya Elhilali<sup>1,2</sup>, Shihab Shamma<sup>1,2</sup>, Jonathan Simon<sup>1,3</sup>

<sup>1</sup>Department of Electrical and Computer Engineering, <sup>2</sup>Neural Systems Laboratory, <sup>3</sup>Biology Department, University of Maryland, College Park

The auditory pop-out phenomenon is argued to arise from the presence of salient acoustic cues that become perceptually more detectable from an interfering background. In this study, we focus on the interplay between this pop-out effect and the attentional focus of subjects due to different auditory task demands. We use a stimulus consisting of a repeating tone target in a background of random notes, based on a design commonly used in informational masking experiments. The detectability of the target tone depends on various parameters, including the size of the spectral separation between target and masker frequencies. We adapted these IM stimuli to the purposes of this study by randomly desynchronizing all background maskers throughout the duration of the stimulus, making the target tone the only regular frequency channel in the sequence. We contrast the subjects' performance complementary tasks: (1) a "target task", consisting of detecting changes along the spectral dimension, where subjects are asked to detect a frequency shift of the target signal; and (2) a "background task", consisting of detecting changes along the temporal dimension, where subjects are asked to detect a change in the duration of the masker tones. Using this design, we first confirm the previous findings with the 'classical' IM stimuli; namely the dependency of the target unmasking on the size of the protection zone. We also explore the interaction between the pop-out effect of the target and the attentional focus of subjects, as measured by the performance of both target and background tasks. By combining both spectral (target) and temporal (masker) changes in the stimulus, we are able to use identical stimulus sets for both tasks; hence manipulating a single free parameter in the experiment: the attentional state of subjects. In addition, we complement the psychophysical results of this study with a physiological investigation of the neural basis of this phenomenon. We use the high temporal resolution of magnetoencephalography (MEG) to explore whether the 'pop-out' of the target signal is reflected in the cortical responses of human subjects, by contrasting physiological measurements under both target and background attentional states, again with identical stimulus sets for both tasks.

### 698 Cortical Mechanisms of Speech Perception in Noise

#### Withdrawn

# 699 Primary and Non-Primary Cortical Encoding of the Speech Envelope: Implications for Neural Representation and Perception in Humans

**Daniel A. Abrams**<sup>1</sup>, Trent Nicol<sup>1</sup>, Steven G. Zecker<sup>1</sup>, Mitra J. Hartmann<sup>2</sup>, Nina Kraus<sup>1,3</sup>

<sup>1</sup>Communication Sciences, Northwestern University, <sup>2</sup>Departments of Mechanical and Biomedical Engineering, Northwestern University, <sup>3</sup>Departments of Neurobiology, Physiology and Otolaryngology, Northwestern University Previous evidence indicates that slow temporal information (<20 Hz) is encoded differently between primary and nonprimary auditory cortex and that non-primary cortex is specifically tuned to encode these low stimulus frequencies. Thus far, simple acoustic stimuli have been used to characterize these tuning properties. investigated whether non-primary cortex might also be tuned to encode the low-frequency temporal information present in speech known as the speech envelope. We measured local field potentials (LFPs) in the auditory cortex of guinea pigs to a number of speech sentences. These responses were quantitatively compared to cortical evoked potentials measured in both non-disabled and learning-disabled children, a population that has demonstrated abnormal auditory perception and central encoding of speech. A primary goal of this cross-species comparison is to extrapolate the relative contributions of primary and non-primary auditory pathways from the guinea pig LFP responses to the human brain responses. These data may provide insight into the nature of the auditory system in learning disabled individuals, and whether abnormal auditory encoding is specific to primary or non-primary components of the response.

Supported by National Institutes of Health grant R01 DC01510-10 and National Organization for Hearing Research grant 340-B208.

#### | 700 | Latency of the Neuromagnetic Pitch Response Depends on Fundamental Frequency and Spectral Envelope

**Steffen Ritter**<sup>1</sup>, Hans Guenter Dosch<sup>2</sup>, Hans-Joachim Specht<sup>3</sup>, André Rupp<sup>1</sup>

<sup>1</sup>Section of Biomagnetism, Dept. of Neurology, University of Heidelberg, <sup>2</sup>Institute for Theoretical Physics, University of Heidelberg, <sup>3</sup>Institute of Physics, University of Heidelberg

A generally accepted and clear definition of pitch and timbre is still an open discussion and often both terms are mixed up in investigations of tone height. However, fundamental frequency and spectral envelope of a sound play a major role in the perception of tone height. Electrophysiological experiments showed that one sub-

component of the complex N100-signal, called pitch onset response was found to be highly correlated with the perceived tone height. In the present investigation tone height of harmonic complex tones was varied by independently changing the fundamental frequency and the spectral envelope. In a psychoacoustic test, relative tone height was determined using a two alternative forced choice task. For the neuromagnetic investigation, the psychoacoustically tested tones were balanced in energy and presented in a continuous stimulation with abrupt pitch changes to isolate the pitch specific responses. Auditory evoked fields were recorded with a 122-channel magnetoencephalograph (MEG).

Perceived tone height increased with both, an increase of the fundamental frequency as well as with an increase of the center frequency of the passband. A high correlation between the latency of the evoked pitch change response (PCR) and the psychoacoustically derived relative tone height was found. However, the results show that an increasing fundamental frequency shortens the latency of the PCR. In contrast, moving the center frequency of the spectral envelope to higher frequencies affects the latency of the PCR in opposite direction.

Our findings demonstrate that the known relation between the perceived tone height and the latency of the pitch sensitive component of the N100-complex has to be considered in further experiments in view of fundamental frequency and spectral envelope of a presented sound.

## 701 The Development of Sound-Induced Obligatory Responses at Different Stimulus Rates in Human Cortex

**Elyse Sussman**<sup>1</sup>, Valia Gumenyuk<sup>2</sup>, Julia Grushko<sup>1</sup>, Katherine Lawson<sup>1</sup>

<sup>1</sup>Albert Einstein College of Medicine, <sup>2</sup>Henry Ford Hospital This study assessed the normal development of soundinduced cortical responses in humans (children ages 8-16 years, and adults). Auditory evoked brain responses were used as an index of cortical maturation. The obligatory auditory responses (P1-N1-P2-N2 components) are known to have different cortical generators within auditory cortices. This allows us to assess different phases of the auditory response. A few studies have assessed these cortical components developmentally, however, in most studies data were collapsed across age groups obscuring any year-to-year morphological changes. In the current study, we examined the effect of temporal rate on the elicitation of the P1-N1-P2-N2 components to unattended sounds at four levels of inter-stimulus interval (150, 350, 550, and 750 ms) in children grouped separately by year (ages 8, 9, 10, 11 years), in adolescents (age 16 years) and one group of young adults (ages 22-40 years). We found both age and stimulus rate effected changes in the morphology of the waveforms. Notably, in adolescents, although the P1-N1-P2 components were more adult-like than child-like, the N2 component, which is a hallmark of the child obligatory response, was still present. These results indicate that cortical maturation continues through adolescence.

## 702 Effects of Tinnitus Laterality on Brain Activity – A Positron Emission Tomography Study

**Berthold Langguth**<sup>1</sup>, Tobias Kleinjung<sup>2</sup>, Juergen Strutz<sup>2</sup>, Goeran Hajak<sup>1</sup>, Peter Eichhammer<sup>1</sup>

<sup>1</sup>Department of Psychiatry, University of Regensburg, <sup>2</sup>Department of Otorhinolaryngology, University of Regenburg

Modern brain imaging methods including functional magnetic resonance imaging (fMRI) and positron emission tomography (PET) afford unprecedented opportunities for the in vivo study of central auditory system function. With the advent of these mapping techniques new insights into the etiology of chronic tinnitus could be gained. Particularly, PET studies have contributed to a paradigm shift, demonstrating that the actual generator of chronic tinnitus is central in most cases. In detail, using [18F] deoxyglucose (FDG) as a radiotracer our group could replicate and confirm previous findings pointing to a significantly increased metabolic activity in the left primary auditory cortex (PAC, Brodmann area 41) in patients suffering from permanent tinnitus complaints. These imaging results have also build the rationale basis to use low-frequency PET-guided repetitive transcranial magnetic stimulation as a causally orientated treatment option for tinnitus.

This finding of unilaterally increased metabolic activity in the left auditory cortex independently of tinnitus laterality contrasts with findings in animal models of tinnitus where increased activity has been detected in the auditory cortex contralateral to the tinnitus side.

To further investigate the effect of tinnitus laterality on brain activation patterns we compared FDG PET data from patients with different tinnitus laterality (unilateral left, unilateral right, bilateral predominantly left, bilateral predominantly right, bilateral).

Results have shown that differences in tinntus laterality are reflected by different metabolic activity patterns in distinct nonauditory cortical regions. These results may help to develop new treatment targets for chronic tinnitus and to further individualize treatment strategies.

## 703 The Good, Bad and Ugly Effects of Acute and Chronic Stress on the Auditory System

**Peter Johansson**<sup>1</sup>, Yeasmin Tahera<sup>1</sup>, Saïda Hadjab<sup>1</sup>, Barbara Canlon<sup>1</sup>

<sup>1</sup>Department of Physiology and Pharmacology, Karolinska Institutet

Stress is an experience common to all organisms and the auditory system is particularly sensitive to physical, as well as psychological stress. Different acute stressors that are documented to affect the auditory system include acute restraint stress and sound conditioning. Both of these stressors have been shown to provide physiological and morphological protection against a subsequent acoustic trauma. These protective effects are mediated by an activation of the hypothalamic-pituitary-adrenal axis (HPA

axis) and glucocorticoid receptors (GR). However, a more clinically important paradigm would be to study the effects of chronic stress on the auditory system. At present, there is little information regarding chronic stress effects on the adult auditory system.

Our hypothesis is that chronic stress does not protect against acoustic trauma due to de-sensitization of HPA axis. To test this hypothesis CBA mice were subjected either chronic stress (4 hours of restraint stress for five consecutive days) or acute stress (4 hours of restraint stress for one day). Control mice were kept individually in their ordinary cages during these 4-hour periods. All experiments were performed during the same time of the day to minimize circadian rhythm influences. Auditory brainstem responses (ABR) were measured to establish the effects of acoustic trauma. Analyses of serum corticosterone (CORT) and adrenocorticotropic hormone (ACTH) as well as of GR in the paraventricular nucleus of the hypothalamus and the cochlea were conducted in order to assess changes in the hormonal regulation.

The effects of chronic stress on the auditory system will be discussed in neuroendocrinological terms. Preliminary findings indicate that chronic stress has a negative effect on the auditory system compared to the positive effects of acute stress. The implications of these findings will also be discussed.

# 704 Chronic Oxidative Stress (Injury) From Mild Carbon Monoxide Exposure (25 ppm) During Development of the Cochlea and Cerebellar Cortex

**Ivan A Lopez**<sup>1</sup>, Dora Acuna<sup>2</sup>, Douglas Webber<sup>2</sup>, Luis Beltran-Parrazal<sup>1</sup>, Araceli Espinosa-Jeffrey<sup>2</sup>, John Edmond<sup>2</sup>

<sup>1</sup>Surgery Dpt Div head & Neck UCLA School of Medicine, <sup>2</sup>MRRC UCLA School of Medicine

We have determined whether chronic mild exposure to carbon monoxide (CO) at 25 ppm in air over the gestational period, interferes with the normal development of the cochlea and cerebellar cortex. Pregnant rats were exposed chronically to CO from gestational day 5 to 20. Pups with their mother were exposed again to CO from postnatal 6 to 20. Comparisons immunohistochemical methods were made with age matched rat pups from pregnant rats not exposed to CO. The whole organ of Corti of CO exposed pups stained with Phalloidin, myosin VIIa and calbindin antibodies showed no hair cell loss; however, at P20 there was alteration in the morphology of inner hair cells at the basal region of the cochlea. Synapsin-1 was decreased in nerve terminals that innervated inner hair cells from P3 to P20. HSP-32 and SOD-1 were high in the stria vascularis from P6 to P20. At P3 inducible nitric oxide synthase (iNOS) was high in blood vessels of the cochlea in CO exposed pups. In the cerebellar cortex, synapsin-1 and neurofilament were decreased. HSP-32 and SOD-1 were upregulated at P12 and P20. At P20, iNOS remains up-regulated in the inner ear and cerebellar vasculature as well as in Purkinje neurons. Nitrotyrosine accumulates in blood vessels of the inner ear. In conclusion chronic mild CO concentrations supplied exogenously in air to the developing rat causes

vulnerable regions of the inner ear (hair cells, auditory neurons and the stria vascularis) and brain (cerebellum) to produce CO endogenously (HSP32 is upregulated) within nerve cells and at the same time promotes the endogenous production of nitric oxide (NO) within neurons and blood vessels. The persistent production of NO promotes the production of reactive oxygen species generating sustained oxidative injury that results in impaired auditory and neuronal function.

Funded by TRDRP grants 14RT0043 (IA Lopez) and 14RT0068 (J Edmond).

#### 705 Decreased Neuroglobin in the Rat Cochlea After Prenatal Mild Carbon Monoxide Exposure

**Ivan A Lopez**<sup>1</sup>, Dora Acuna<sup>2</sup>, Luis Beltran-Parrazal<sup>1</sup>, John Edmond<sup>2</sup>

<sup>1</sup>Surgery Dpt Div head & Neck UCLA School of Medicine, <sup>2</sup>MRRC UCLA School of Medicine

Neuroglobin (Ngb) is a respiratory protein that plays an essential role in oxygen homeostasis in neuronal tissue (Burmester and Hankeln, New Physiol Sci, 19:110-113, In the present study we determined first by immunohistochemistry whether Ngb is present in the adult rat cochlea using antibodies specific to Ngb. Second, we determined whether chronic mild carbon monoxide (CO) exposure at 25 ppm in air over the gestational period alters the expression of Ngb. Pregnant rats were exposed chronically to CO from gestational day 5 to 20. Rat pups were grouped as follows: Group-A: prenatal exposure only and were not CO-exposed postnatally; group B: Prenatal exposure followed by postnatal exposure from P6 to P20; group-C: Pregnant rats not CO-exposed then CO-exposed as in group B; Group-D: Pregnant rats not CO-exposed and not CO-exposed postnatally. In the organ of Corti of normal adult rats and in air-exposed pups (group-D) Ngb was present in supporting cells that surround nonimmunoreactive inner and outer hair cells. Ngb was found in fibrocytes of the spiral ligament, but not in the stria vascularis. Ngb was present in spiral ganglia neurons. A dramatic decrease in Ngb was observed in group-B. Group-A, showed also a considerable decrease in Ngb. Group-C showed almost normal level of Ngb. By contrast Ngb is reported to be up-regulated by hypoxic conditions (Li et al Brain Res 1096:173-9, 2006). The association of Ngb expression with high metabolic activity in neuronal, retinal (Hankeln et al IUBMB Life, 56:671-9, 2004) and cochlear cells (present study), possibly coupled to a subcellular co-localization to mitochondria, suggests a function for Ngb in either oxygen homeostasis, or detoxification of reactive oxygen species. A decrease of Ngb in rat pups exposed to CO supports the idea that mild chronic exposure to CO exerts detrimental effects on cochlear development.

Funded by TRDRP grants 14RT0043 (IA Lopez) and 14RT0068 (J Edmond).

#### 706 Effects of Acoustic Trauma in the Spiral Ligament

Joe Adams<sup>1</sup>, Sarah McCaffery<sup>1</sup>, Sharon G Kujawa<sup>1</sup> <sup>1</sup>Mass. Eve & Ear Infirmnary

Previous work has shown that acoustic trauma can have profound effects upon the spiral ligament. Type IV fibrocytes in the spiral ligament are 24 dB more vulnerable to loss following acoustic trauma than hair cells but little is understood regarding deficits that may result from such losses. Immunocytochemical evidence indicates that unlike type II fibrocytes, type IV fibrocytes probably have little to do with K+ ion recirculation. Type IVs are positive for the Na+. K+, 2Cl- co-transporter NKCC1 but not for Na+, K+-ATPase, which suggests that they may be subject to osmotic stresses but do not actively accumulate K+ ions like type IIs. In mice type IVs stain weakly or not at all for Cx26 and Cx30 and they lack the membrane amplification that characterizes type IIs. Instead, type IVs are positive for connective tissue growth factor (CTGF), a cytokine that has been widely studied in its role controlling production of extracellular matrix components, including collagens and glycoproteins. Even after long survival periods following acoustic trauma that results in type IV cell loss there is little or no change evident in the composition of nearby collagen bundles, as assayed by aniline blue staining. This suggests that control of collagen bundle composition may be controlled by root cells, which are also positive for CTGF. In contrast to the lack of effects upon collagen, fuchsin staining shows a clear loss of the staining of the extracellular ground substance around sites of type IV cell loss early after acoustic trauma with no signs of recovery after prolonged survivals. Cell loss after prolonged survivals may also include type II and type III fibrocytes. How these changes may contribute to continuing deterioration of the cochlea following acoustic trauma remains a subject for further study.

#### 707 Neuroprotection Against Acoustic Trauma by Estrogen & Receptors

Yeasmin Tahera<sup>1</sup>, Inna Meltser<sup>1</sup>, Margaret Warner<sup>2</sup>, Malou Hultcrantz<sup>3</sup>, Agneta Viberg<sup>1</sup>, Jan-Åke Gustafsson<sup>2</sup>, Barbara Canlon<sup>1</sup>

<sup>1</sup>Physiology & Pharmacology, Karolinska Institutet, <sup>2</sup>Biosciences & Nutrition, Karolinska Institutet, <sup>3</sup>Clinical Neuroscience, Karolinska University Hospital Estrogens and their receptors, ERα and ERβ, have been shown to have multiple roles in the nervous system, yet their function in the auditory system is unknown. To explore the specific roles of each receptor subtype in estrogen-associated auditory function, intact and knockout male and female adult mice (aromatase KO, ARKO; ERa KO, ERKO; ERβ KO, BERKO) were used as models. Auditory brainstem response thresholds after acoustic trauma was exacerbated in male and female BERKO and ARKO mice compared to wild type. After acoustic trauma ERKO mice had similar thresholds as the wild type mice. Pre-treatment with the ERa-selective agonist propyl pyrazole triol (PPT) before acoustic trauma partially protected ARKO mice but had no effect in wild type mice. In contrast, the ERβ-selective agonist diarylpropionitrile (DPN) protected auditory thresholds in both wild type and ARKO mice. The expression of ERα and ERβ in the inner ear was partially overlapping. ERB was localized to the inner hair cells, spiral prominence and the spiral ganglion neurons. ERa was found in the inner hair cells, the external sulcus cells and the stria vascularis. Basal ERB protein levels from wild type female mice were higher than in males, and there was an increase in ERB protein expression after trauma. Investigations into mechanisms underlying the different responses to acoustic trauma revealed that a BDNF mediated protection via MAPK (ERK) is apparent in the wild type mice while the ARKO mice show a reduced expression of BDNF that is concomitant with the increased damage induced by acoustic trauma. The data demonstrated a considerable ERβ mediated neuroprotection in the auditory system. Supported by grants from the Swedish Research Council, AMF Trygghetsförsäkring, Tysta Skolan, and the

Karolinska Institute.

#### 708 Therapeutic Effect of IGF-1-Hydrogel Therapy on Noise-Induced Hearing Loss in **Guinea Pigs**

**Takayuki Nakagawa**<sup>1</sup>, Kyu Yup Lee<sup>1,2</sup>, Takayuki Okano<sup>1</sup>, Masahiro Matsumoto<sup>1</sup>, Harukazu Hiraumi<sup>1</sup>, Kazuya Ono<sup>1</sup>, Yasuhiko Tabata<sup>1</sup>, Juichi Ito<sup>1</sup>

<sup>1</sup>Kyoto Univ., <sup>2</sup>Kyungpook National University Hospital The biodegradable gelatin hydrogel is a suitable material for local inner ear delivery of neurotrophins or growth factors via the round window membrane (Endo et al. 2005). We have reported the efficacy of pre-treatment with IGF-1 locally applied via a biodegradable gelatin hydrogel for prevention of noise-induced hearing loss (Iwai et al. 2006). IGF-1 is a clinically applicable growth factor, and a hydrogel is a non-toxic material. In addition, clinical trials of use of a hydrogel in other fields have begun in Japan. Such backgrounds encourage us to realize clinical application of IGF-1-hydrogel therapy for the treatment of inner ears. We thus examined therapeutic effects of local IGF-1 application by hydrogels after onset of noiseinduced hearing loss in this study. Adult guinea pigs were used as experimental animals. At 5 h after noise exposure (4 kHz octave band noise at 120 dB SPL for 5 h), a piece of hydrogels immersed with IGF-1 was placed on the round window membrane of the left ear. The right cochleae treated with a hydrogel immersed with saline were used as controls. ABR recording was performed on days 3, 7, 21 after the treatment. Temporal bones were collected on day 21 and provided for histological analysis. ABR measurements demonstrated significant effects of IGF-1-hydrogel treatment on preservation of hearing. Histological analysis demonstrated significant protection of outer hair cells by IGF-1-hydrogel treatment. These findings indicate that IGF-1-hydrogel therapy has the potential for the treatment of noise-induced hearing loss.

## | 709 | D-Methionine (D-Met) Rescue From Noise-Induced Hearing Loss: Post-Administration Intervals

**Kathleen Campbell**<sup>1</sup>, Robert Meech<sup>1</sup>, Deb Larsen<sup>1</sup>, Diana Mitchell<sup>2</sup>, Larry Hughes<sup>1</sup>

D-met protects against cisplatin-induced, aminoglycoside-induced and noise-induced hearing loss. However, many noise exposures cannot be fully anticipated in advance (ie .military and emergency personnel). Therefore an otoprotective agent that could be administered after the noise exposure and still prevent permanent noise induced hearing loss (NIHL) would have great clinical applicability. Because the otoprotective/rescue agent may not be immediately available to someone suddenly exposed to noise, it is of clinical interest to determine how long after the noise exposure D-met can be administered and still protect against NIHL.

In this study, 5 groups of male chinchillas Laniger were individually exposed to a 105 dB SPL narrow band of noise centered at 4 kHz for 6 hours. In the 4 experimental groups, D-met (200 mg/kg per dose) was initially administered at 1, 3, 5 or 7 hours hour post noise exposure plus 4 additional doses BID (5 doses) at 12 hour intervals. The control group received equivalent volume saline injections.

Auditory brainstem response testing (ABR) was performed just prior to the noise exposure and again on post-exposure days 1, 14 and 21. ABR thresholds were measured in response to tone bursts centered at the frequencies of 2, 4, 6, and 8 kHz. An intensity series was obtained for each animal from 100 to 0 dB peak sound pressure level (SPL) for tone bursts in 10 dB decrements. Threshold was defined as the lowest intensity capable of eliciting a replicable, visually detectable response.

Data collection is ongoing. Based on results to date, at 21 days after the noise exposure

D-met significantly reduced noise-induced ABR threshold shifts when administered starting at 1, 3 or 5 hours after the cessation of the 6 hour noise exposure. At the time of abstract submission, we have data on only 3 animals at the 7 hour post administration interval which appears to reduce the ABR threshold shift but has not yet reached significance.

## 710 Cochlear Injuries After Exposure to a Kurtotic Noise and Styrene and Its Protection

**Guang-Di Chen**<sup>1</sup>, Donald Henderson<sup>1</sup>

<sup>1</sup>SUNY at Buffalo

Combined exposure to both noise and aromatic solvents such as styrene is common in many industries. In this study, cochlear electrical responses and injuries of auditory hair cells as well as supporting cells (including cell death) were determined in rats after exposure to a high kurtotic noise and styrene. Protection against the cochlear injuries by antioxidants (N-Acetyl-L-cysteine and idebenone) was also investigated.

The noise exposure (10-20 kHz, at a level of 100 dB SPL with 110-dB impact noise [40-ms duration, 1-ms rise and 30 ms fall time, 1/s], 6 hrs per day for 5 days a week for 3 weeks) induced a frequency-dependent permanent threshold shift (PTS) with a maximal level of about 30 dB at 12 kHz. Morphologic examination in some individuals with severe functional loss showed no sign of damage to auditory hair cells (stereocilia) or supporting cells. The styrene exposure attacked Deiter; s cells first. For a shortperiod styrene exposure (7 days, 1/d at a dosage of 800 mg/kg by gavage), the majority of Deiter; s cells in the middle turn showed condensed nuclei, but the outer hair cells (OHCs) looked normal. The 3-week styrene exposure (at 400 mg/kg) destroyed almost all of the 3rd row OHCs and some in the 2nd and 1st rows in the middle turn. Surprisingly, there was only a slight PTS (<5 dB) observed at middle frequencies. The combined exposure showed potentiative effect in the middle frequency region where both the noise and styrene showed toxic effects, functionally or structurally. Treatment with N-acetyl-Lcysteine and idebenone significantly protected against the functional loss induced by the noise and styrene.

The results indicate that styrene exposure may cause a severe cochlear injury before a hearing loss can be detected. Risk of noise exposure may be significantly increased in the styrene-exposed individuals. The cochlear damage can be partially protected with application of antioxidants.

This study was supported by NIOSH grant 1R010H008113-01A1.

## 711 Free Radical Scavengers, Vitamins A, C, and E, Plus Magnesium Reduces Noise Trauma

**Colleen Le Prell**<sup>1</sup>, Larry Hughes<sup>2</sup>, Josef Miller<sup>1</sup>

<sup>1</sup>University of Michigan, <sup>2</sup>Southern Illinois University Medical School

Free radical formation in the cochlea plays a key role in the development of noise-induced hearing loss (NIHL). The amount, distribution, and time course of free radical formation have been defined, including a clinically significant formation of both reactive oxygen species and reactive nitrogen species 7-10 days following noise exposure. Noise-induced reduction in cochlear blood flow, now known to reflect free radical formation, has also been described. Here we report that the antioxidant agents, vitamins A, C, and E, act in synergy with magnesium to effectively prevent noise-induced trauma in the guinea pig. Neither the antioxidant agents nor magnesium reliably reduced NIHL or sensory cell death when these agents were delivered alone, at the doses we used. combination, however, they were highly effective in reducing both hearing loss and cell death. preventions of noise-induced trauma was clinically significant, and statistically reliable, even with treatment initiated just one hour prior to noise exposure. This study supports roles for both free radical formation and noiseinduced vasoconstriction in the onset and progression of NIHL. Identification of this safe and effective antioxidant intervention that attenuates NIHL provides a compelling

<sup>&</sup>lt;sup>1</sup>Southern Illinois University School of Medicine,

<sup>&</sup>lt;sup>2</sup>University of Chicago

rationale for human trials in which micronutrient agents are used to eliminate this major cause of acquired hearing loss.

Acknowledgments. Support for this research was provided by the National Institutes of Health (NIH-NIDCD R01 DC03820 and P30 DC005188), the General Motors Corporation/ United Automotive Workers Union, and the Ruth and Lynn Townsend Professor of Communication Disorders.

## 712 Regional Distribution of Superoxide Dismutase 2 (SOD2) in the Spiral Ganglion of Rats and Monkeys

Yu-Lan Mary Ying<sup>1</sup>, Carey Balaban<sup>1</sup>

<sup>1</sup>Department of Otolaryngology, University of Pittsburgh Hair cells and spiral ganglion cells appear to be more vulnerable to toxins at the base of the cochlea than at the For example, aminoglycosides and cisplatin produce hearing loss in a high to low frequency gradient, and sensorineural damage in a base-to-apex gradient. Furthermore, age-related hearing loss begins with the high frequencies represented at the base of the cochlea. Sha et al. (Hearing Res., 155, 2001, 1-8) reported that the differential vulnerability of basal and apical hair cells coincided with a significantly lower level of antioxidant glutathione in basal outer hair cells. However, there are no previous reports of a similar gradient in ROS mechanisms in the spiral ganglion. This study examined expression of the superoxide dismutase (SOD) family in the cochlea. Immunohistochemical methods were used to identify the distribution of Copper/Zinc SOD (SOD1) and Manganese SOD (SOD2) in paraffin embedded sections of paraformaldehyde fixed, formic acid decalcified temporal bones from rats and macaques. Binding sites of primary rabbit polyclonal antibodies to superoxide dismutase 2 (Abcam Inc., ab13534) and Cu/Zn superoxide dismutase (Abcam Inc, ab13498) were visualized with standard ABC methods and a diaminobenzidine chromogen. Both the proportion of SOD2 immunopositive spiral ganglion cells and the intensity of immunoreactivity were greater in the apical turn than in the basal turn in both species, but there was no corresponding gradient in the distribution of SOD1. Because SOD2 activation is an upstream event for reduction of mitochondrial ROS production via activation of mitochondrial uncoupling proteins, this finding suggests that spiral ganglion cellular responses to ROS exposure vary along the cochlear spiral, with a lower response capacity in the basal turn. In particular, the results raise the broader question of how the regional distribution of multiple ROS metabolic pathways may contribute to agerelated and toxin-induced patterns of hearing loss.

## 713 Using the Zebrafish Lateral Line to Screen an FDA Library for Compounds that Protect Hair Cells

Henry Ou<sup>1,2</sup>, David Raible<sup>3,4</sup>, Edwin Rubel<sup>1</sup>

<sup>1</sup>University of Washington, Dept. Otolaryngology-HNS, VM Bloedel Hearing Research Center, <sup>2</sup>Children's Hospital and Regional Medical Center, <sup>3</sup>University of Washington, Dept. Biological Structure, <sup>4</sup>VM Bloedel Hearing Research Center

The zebrafish lateral line is a powerful tool for studying hair cells and hair cell loss. Using a high-throughput screening protocol developed previously by Santos et al. (2005), we screened a library of 1,040 FDA-approved compounds (NINDS Custom Collection) for protection against neomycin-induced hair cell death. Five days postfertilization zebrafish with hair cells labeled with fluorescent dye were pretreated for 1 hour with FDA library compounds at 100 µM concentration, and then treated for 1 hour with 200 µM neomycin. Hair cell death was then assessed using in vivo fluorescence microscopy. Using this method, seven new compounds were identified that conferred strong protection against neomycin-induced hair cell death. The dose-response curve for each of the 7 drugs was assessed in response to 200 µM neomycin. Hair cell loss with increasing doses of neomycin was then determined using the optimal dose for each protective drug. Hair cell survival was maintained between 60% and 100% even at high doses of neomycin. Our work demonstrates the utility of the zebrafish system for rapidly identifying and obtaining quantitative data for protective compounds. We are currently testing the protective compounds in mammalian systems.

This work is supported by NIDCD grants DC04661 and DC05987 and NICHHD grant HD002274

#### 714 Phosphoinositide Signaling in the Organ of Corti

Su-Hua Sha<sup>1</sup>, Hong-Yan Jiang<sup>1</sup>, Jochen Schacht<sup>1</sup>

<sup>1</sup>Kresge Hearing Research Institute

Phosphatidylinositol (4,5)-bisphosphate (PIP2) phosphatidylinositol (3,4,5)-trisphosphate (PIP3) play a crucial role in various cellular processes. These lipids direct two major independent signaling cascades in the cytoplasm and in the nucleus. PIP3 affects multiple downstream targets of the phosphoinositide 3-kinase pathway, including Akt and NF-fÛB. Nuclear PIP2 may influence pre-mRNA splicing and chromatin structure. Aminoglycosides strongly bind to phosphoinositides and alter their membrane distribution and metabolism. Here, we investigate phosphoinositide signaling in the mouse inner ear in vivo with chronic systemic administration of kanamycin as a probe. Immunoreactivity to PIP3 decreased in the organ of Corti, especially in outer hair cells, while PIP2 increased. In agreement with reduced PIP3 signaling, phosphorylated Akt1/2 decreased in both the cytoplasm and nuclei of outer hair cells after kanamycin treatment. PIP2 was initially present at the apical poles of outer hair cells but appeared in their nuclei

after drug treatment. Nuclear PIP2 formed a complex with histone H3 and attenuated its acetylation.

These findings suggest that kanamycin disturbs the balance between PIP2 and PIP3, consequently modifying gene transcription via histone acetylation and diminishing the PIP3/Akt survival pathway. These reactions may contribute to the loss of outer hair cells through programmed cell death induced by aminoglycosides.

This study was supported by research grant DC-03685 and core grant P30 DC-05188 from the National Institute on Deafness and Other Communication Disorders, National Institutes of Health.

# | 715 | Inhibition of Transient Receptor Potential Vanilloid Receptor 1(TRPV1) | Expression or Function in the Cochlea Attenuates Cisplatin Induced Hearing Loss

**Debashree Mukherjea**<sup>1</sup>, Sarvesh Jajoo<sup>1</sup>, Debra Larsen<sup>1</sup>, Craig Whitworth<sup>1</sup>, Leonard Rybak<sup>1</sup>, Vickram Ramkumar<sup>1</sup>

\*Southern Illinois University School of Medicine\*

Previous studies have demonstrated the presence of transient receptor potential vanilloid-1 (TRPV1) channels in the rat cochlea. However, the role of these channels in the cochlea is not clear. Using an organ of Corti derived cell line (UB/OC-1), we demonstrate the presence of TRPV1 and show its induction within 24 h by the chemotherapeutic agent, cisplatin (2.5 μM). The induction of TRPV1 was associated with an increase in reactive oxygen species (ROS) generation, an increase in the NADPH oxidase isoforms Rac1 and NOX3, increased intracellular Ca2+ release and induction of apoptosis in UB/OC-1 cells. Interestingly, inhibition of TRPV1 by ruthenium red (20µM) and capsazepine (10µM) attenuated cisplatin-mediated apoptosis of UB/OC-1 cells, as evidenced by TUNEL assays and production of proapoptotic proteins, such as Bax and p53. Depletion of TRPV1 by short interfering (si)RNA abrogated the increase in ROS generation, NOX3 expression, intracellular Ca<sup>2+</sup> release and apoptosis of UB/OC-1 cells. Furthermore, in vivo (round window) application of a single concentration (1 ug) of siRNA against TRPV1 to rats for 48 h reduced cisplatin (13mg/kg, i.p)-induced ototoxicity, as measured by auditory brainstem responses (ABRs). ABRs were determined 72 h following cisplatin administration. These results implicate TRPV1 in cisplatin cytotoxicity and ototoxicity and demonstrate the potential utility of targeting this channel (using siRNA or TRPV1 antagonists) for treating hearing loss produced by chemotherapeutic agents. This work was supported by SIU School of Medicine Excellence in Academic Medicine award to VR and NIH RO1-DC02396 grant to LPR.

### 716 Heat Shock Inhibits Neomycin-Induced JNK Activation

**Mona Taleb**<sup>1</sup>, Carlene S. Brandon<sup>1</sup>, Lisa L. Cunningham<sup>1</sup>

\*\*Medical University of South Carolina\*\*

Death of sensory hair cells can be induced by a number of stressors, including age, noise trauma, and therapeutic drugs such as aminoglycosides and cisplatin.

Aminoglycoside-induced hair cell death is mediated by c-Jun N-terminal kinase (JNK) and caspases. The induction of HSPs is a ubiquitous and highly-conserved stress response which serves to protect cells from death by inhibiting apoptotic proteins. In many systems, HSP induction can inhibit the activation of both caspases and JNK. In the in vitro adult mouse utricle preparation, we have previously shown that heat shock (43°C for 30 minutes) results in rapid and robust transcriptional upregulation of heat shock proteins (HSPs). Heat shock inhibits both neomycin- and cisplatin-induced hair cell death in the adult mouse utricle. The most stronglyinduced HSP in this system is HSP-70, which is upregulated over 250-fold 2 hours after heat shock. In order to determine whether HSP-70 alone is sufficient to protect hair cells from aminoglycoside-induced death, we utilized transgenic mice that constitutively overexpress rat HSP-70. HSP-70 overexpression protects the utricular hair cells against neomycin-induced cell death, and the protective effect of HSP-70 overexpression alone accounts for most of the protective effect of heat shock. We now have begun to examine the molecular mechanism(s) by which heat shock inhibits neomycin-induced hair cell death. Utricles from CBA mice were cultured under four different conditions: 1) No heat shock/ no neomycin; 2) Heat shock/ no neomycin; 3) No heat shock/ neomycin treated (2 mM for 12 hours); 4) Heat shock/ neomycin treated. Utricles were prepared for quantitative Western blot analysis using a phospho-specific antibody that is specific for JNK that is dually phosphorylated at thr 183 and tvr185. Heat shock alone (group 2) resulted in moderate activation of JNK compared to the control (group 1). Neomycin exposure alone (group 3) resulted in robust activation of JNK, and this neomycin-induced JNK activation was significantly inhibited by heat shock (group 4). These data suggest that the protective effect of heat shock may be via inhibition of neomycin-induced JNK phosphorylation. Experiments are currently underway to determine if overexpression of HSP-70 also inhibits JNK phosphorylation.

## | 717 | Inhibiting Neomycin-Induced ERK Activation Delays IHC Death in Neonatal Rat Cochlear Cultures

Manuela Lahne<sup>1</sup>, Jonathan Gale<sup>1</sup>

<sup>1</sup>UCL EAR Institute

Cellular stress results in the activation of various members of the Mitogen Activated Protein Kinase (MAPK) family including c-Jun N-terminal kinase (JNK), p38 kinase and Extracellularly Regulated Kinases 1 and 2 (ERK1/2). In the cochlea, research has focused on the role of JNK during acoustic and ototoxic insults. Recently, we showed that following mechanical damage ERK1/2 are transiently and specifically activated in cochlear supporting cells (SCs) surrounding damaged hair cells (HCs). Here, we investigated whether ERK1/2 are activated during exposure of HCs to the aminoglycoside antibiotic neomycin.

Cultures of basal and middle turn P1 rat cochleae were treated with 1 mM neomycin for 8 or 24 hrs and ERK1/2 activation was assessed using an antibody directed to the

dually-phosphorylated form of ERK1/2. Eight hrs after neomycin ERK1/2 was activated in clusters of SCs that in the majority of cases surrounded pyknotic HC nuclei. Pyknotic nuclei were observed first in inner hair cells (IHC) and subsequently in outer hair cells (OHC). The activation of ERK1/2 in surrounding SCs followed this pattern. At 8 hrs middle turns typically exhibited only a few pyknotic HC nuclei coinciding with less or no activation of ERK1/2 in SCs. The function of activated ERK1/2 in neomycininduced HC death was investigated using U0126, an inhibitor of MEK1/2, the MAPK kinase. HC loss was determined as the sum of both pyknotic and extruded nuclei in DAPI stained specimens. At 8 hrs IHC loss was significantly decreased in neomycin-treated cultures exposed to U0126 (10 µM) compared to neomycin treatment alone. However, at 24 hrs U0126 treatment failed to prevent IHC loss. There was also a reduction in OHC loss at both 8 and 24hrs in the presence of U0126; however the effect was not statistically significant.

In summary, we suggest that neomycin induced HC damage triggers ERK1/2 activation in the surrounding SCs and this activation contributes to the subsequent HC loss.

## 718 Specification of the Auditory and Vestibular Hindbrain

Karina Cramer<sup>1</sup>

<sup>1</sup>University of California, Irvine

During embryogenesis, the ear begins to differentiate and send projections into the hindrain. Auditory and vestibular nuclei aggregate and the neurons in these nuclei form connections with their targets. These developmental events culminate in circuitry that is precisely wired for the perception of auditory and vestibular stimuli. The embryonic origins of these structures and developmental mechanisms that orchestrate the differentiation of this system are beginning to be identified. Breakthroughs in methodological approaches, including molecular genetics and imaging methods, have led to an improved understanding of this system. In our previous studies we used lipophilic dyes to map cell fates in the hindbrain. In addition, we have identified the roles of several genes in avian auditory circuit formation using in ovo electroporation to transfect the hindbrain and neuronal tracing to assess subsequent changes in axonal trajectories. We are currently examining functional changes in mice lacking these genes. This symposium will examine how new approaches have been applied to auditory and vestibular brainstem development. Recent advances have led to the characterization of processes underlying formation of auditory and vestibular nuclei, regulation of neuron number and type, and specification of appropriate connections.

Supported by NIH DC005771.

## 719 Local Degradation Shapes the Retinoic Acid Morphogen Gradient in Hindbrain and Ear Development

Richard White<sup>1</sup>, Angela Linville<sup>1</sup>, Arthur Lander<sup>1</sup>, **Thomas** Schilling<sup>1</sup>

<sup>1</sup>University of California, Irvine

Positional identities along the anterior-posterior axis of the vertebrate nervous system are first assigned during gastrulation by multiple posteriorizing signals, including retinoic acid (RA), Fgfs, and Wnts. RA is produced just posterior to the hindbrain by retinaldehyde dehydrogenase 2 (raldh2) in paraxial mesoderm, and degraded anteriorly by cyp26 enzymes, suggesting that it forms a gradient across the hindbrain and placodal fields and acts as a morphogen. Consistent with this idea, RA is required during gastrulation for the specification of posterior hindbrain segments (rhombomeres) as well as the auditory and lateral line placodes in a dose-dependent manner in all vertebrates that have been examined. We used cell transplantation and implantation of RA-coated beads into RA-deficient zebrafish embryos to assess the range of RA signaling. Consistent with its proposed role as a morphogen, we find that RA signals directly over many cell diameters rather than being relayed through intervening cells, and activates distinct hox genes depending on its concentration. We demonstrate that these long-range aspects of RA signaling are modulated by local degradation, primarily through the activity of cyp26a1, which we show is RA-dependent and suppressed by Fgf signaling. Computational analyses suggest that this arrangement creates a much more robust axial patterning system, in which the RA gradient can compensate both for fluctuations in availability of its precursor, vitamin A, and for the continuously increasing length of the anteriorposterior axis during gastrulation. These results provide insights into the mechanisms that create stable gradients in tissues and the need for multiple interacting signals. They also help explain how global RA administration can rescue RA-deficient embryos.

# | 720 | Assembly of the Brainstem Cochlear Nuclear Complex as Revealed by Intersectional and Subtractive Genetic Fate Maps

Susan Dymecki<sup>1</sup>

<sup>1</sup>Harvard Medical School

Molecular approaches to fate mapping offer new views of the developing nervous system. In vivo studies can be performed in mice, wild-type or genetically altered, and, by defining molecularly the embryonic cells initially labeled, genetic homologies between structures can be revealed. Here, we add to the genetic fate-mapping arsenal a new tool that permits improved molecular selection of cells under study by offering "intersectional" and "subtractive" capabilities. Applying this approach to study brainstem progenitors, they find that the cochlear nuclear complex, the entry point for all central auditory processing, is assembled in a modular fashion from molecularly distinct subpopulations arrayed as rostrocaudal microdomains

within and outside the hindbrain rhombic lip. The authors further uncover surprising parallels and distinctions between the development of the brainstem auditory and cerebellar systems.

## 721 Regulation of a Unique Physiological Phenotype and Neuron Number in Developing Cochlear Nucleus

**Edwin W. Rubel**<sup>1</sup>, Julie A. Harris<sup>2</sup>, MacKenzie A. Howard<sup>3</sup>, R. Michael Burger<sup>1</sup>

<sup>1</sup>Dept of Oto-HNS and Virginia Merrill Bloedel Hearing Research Center, University of Washington, <sup>2</sup>Neurobiol & Behav Prog, Virginia Merrill Bloedel Hearing Research Center, University of Washington, <sup>3</sup>Physiol & Biophysics, Virginia Merrill Bloedel Hearing Research Center, University of Washington

Specification of the auditory and vestibular hindbrain includes determination of the correct number and phenotypes of neurons that are required for processing and integrating information arising in the inner ear and efferent CNS circuits. This process requires physiological and anatomic specializations that are unique to each neuronal network. We will discuss two examples of this process that occur relatively late in ontogeny of the cochlear nuclei. In the first example, we will describe the ontogeny of a unique depolarizing GABAergic inhibitory process in the avian auditory hindbrain. This process requires coupling development of a low voltage activated (LVA) K+ conductance that underlies the conversion of GABAergic stimulation from excitatory to inhibitory with maintenance of a neonatal-like depolarizing response to activation of GABA A receptors. The second example involves the final determination of neuron number in the mammalian cochlear nucleus. Research from our laboratory and others has revealed a sharply defined critical period during postnatal development of the mammalian cochlear nucleus. During the first postnatal week in the mouse or gerbil, deprivation of afferent input from the eighth nerve results in massive apoptotic-like neuron loss. Following this critical period, there is no apparent neuronal cell death following the same treatments. We have conducted a series of experiments aimed at determining candidate molecules underlying this dramatic change in trophic regulation. experiments have yielded complicated but surprising results suggesting: 1) a shift in gene expression that favors more plasticity of the developing brain and more stability of the maturing brain; and 2) rapid and dramatic transcriptional changes occur in deafferented tissue at all ages, but the groups of transcripts upregulated and downregulated due to deafferentation are strikingly different during and after the critical period.

Supported by grants DC03829, DC00395 and DC04661 from NIH/NIDCD

## **722** The Formation of Functional Circuitry in the Vestibular and Auditory Pathways

Joel Glover<sup>1</sup>

<sup>1</sup>University of Oslo

Using voltage-sensitive and calcium-sensitive recording, the development of functional circuitry in central auditory and vestibular pathways has been charted in the chicken embryo. Appropriately specific functional connections, detected as optical responses in central nuclei following stimulation of peripheral afferents, form in a characteristic sequence starting at around 7 days of embryonic development. Pharmacological manipulation allows identification of the functional sign of the connections, and in the vestibular system demonstrates excitatory and inhibitory connections form contemporaneously in the appropriate patterns for reflex activation of motoneuron targets. The specificity of these premotor connections develops in the presence of chronic NMDA blockade and spontaneous synchronous activity, suggesting that activity is not a critical factor in establishing the proper synaptic connectivity in the vestibular pathways. The development of functional connections revealed by optical recording will be related to anatomical and genetic studies of axon pathfinding and the neuroepithelial origin of nuclear groups.

### 723 A Genetic Dissection of Auditory Circuit Assembly and Function

Lisa Goodrich<sup>1</sup>

<sup>1</sup>Harvard Medical School

The proper perception of sound depends on the precise wiring of spiral ganglion neurons to hair cells in the ear and target neurons in the the cochlear nucleus complex of the auditory brainstem. The spiral ganglion develops in parallel with the vestibular ganglion in a common anlage, but auditory and vestibular neurons are ultimately incorporated into separate circuits that mediate distinct perceptions. To understand how neurons of the inner ear acquire unique wiring specificities, we have performed genetic fate mapping to pinpoint when auditory and vestibular neurons segregate during development and to follow the subsequent emergence of auditory circuits. Using Cre-lox technology to follow the fates of Neurogenin-1 (Ngn-1) expressing precursors through development, we labelled small clusters of cells and visualized the complete trajectories of individual cells, down to the level of the endbulb of Held. We have found evidence that vestibular and spiral ganglion neurons derive from two overlapping waves of neurogenesis, with early precursors contributing predominantly to the vestibular system and not producing precursors that will later populate the spiral ganglion. Within the spiral ganglion, Type I and Type II neurons appear to arise from a common precursor. In addition, axonal projections are tonotopically organized in the cochlear nucleus as early as E15, while the cochlear nucleus is still developing and before peripheral processes have reached the organ of Corti.

We used a similar genetic fate mapping strategy to demonstrate that *Math1*-expressing precursors in the rhombic lip are a major source of cochlear nucleus neurons, and are currently examining whether different subsets of cells arise at different stages of development. Finally, we found that rhombic lip progenitors are exposed to FGF ligands early in development and can activate the MAP kinase pathway. Blocking FGF signaling by overexpression of the FGF antagonist Sef inhibits auditory nucleus development in the chick, while excess FGF signaling in *Sef* mutant mice causes anatomical and physiological defects in cochlear nucleus function, providing new insights into the development of the cochlear nucleus from the rhombic lip.

## 724 Piezoelectricity Increases Outer Hair Cell High Frequency Response

Ning Yu<sup>1</sup>, Hong-Bo Zhao<sup>1</sup>

<sup>1</sup>University of Kentucky Medical Center

Outer hair cell (OHC) electromotility is a cochlear amplifier and can actively boost the basilar membrane vibration to enhance auditory sensitivity and frequency selectivity. OHC electromotility is membrane-potential dependent and driven by cross-membrane voltage. Although the conformation of prestin motor proteins can be rapidly changed up to 100 kHz, its driving force (cross-membrane voltage) would be dramatically attenuated at high frequency by membrane capacitance, which forms a lowpass filter with cut-frequency less than 1 kHz. Outer hair cells also have remarkable piezoelectricity. Mechanically elongating and compressing OHC can produce electric currents. Here, we report that OHC piezoelectricity can overcome membrane capacitance damping to improve OHC high frequency responses. The OHC piezoelectric response showed a high-pass property and was increased as the stimulus frequency was increased. The cutfrequency was 70-90 kHz, mainly limited by the recording system. Simultaneous administrations of electronic and mechanical (piezoelectric) stimulation to the OHC, which mimics the OHC suffered electronic (receptor current through transduction channels) and mechanical (the vibration of the basilar membrane) stimulations in vivo, generated the flat response up to 80 kHz. Abolishment of eliminated piezoelectricity this high frequency enhancement. Like a regular cell, the sole electronic frequency response of the OHC was low-pass; the cutfrequency was ~1 kHz. Finally, as computer modeling expected, the resonant peaks were also visible in the responses to electronic-mechanical stimulation. Our results indicate that OHC electromotility can perform at high frequency effectively to contribute active cochlear mechanics in whole mammalian auditory frequency range. Supported by NIH DC05989 and the Research Foundation of American Tinnitus Association.

#### 725 The Outer Hair Cell's Active Force Production in the Cochlear Environment

Bill Liao<sup>1</sup>, Aleksander Popel<sup>1</sup>, William Brownell<sup>2</sup>, **Alexander Spector**<sup>1</sup>

<sup>1</sup>Johns Hopkins University, <sup>2</sup>Baylor College of Medicine Cochlear outer hair cells amplify and sharpen acoustic signals, and they are crucial to active hearing in mammals. It has been demonstrated that isolated outer hair cells produce electromotility-based active forces at frequencies up to several tens of kilohertz. It is of key importance to understand how the outer hair cell generates physiologically significant active forces under highfrequency conditions in the cochlear environment. In the cochlea, the cell's active behavior is modulated by mechanical (surrounding viscous fluid, deformable basilar and tectorial membranes) and electrical (cell's membrane and intracochlear potentials) factors. We present computational modeling of the outer hair cell active force production that takes into account the electrical, electromechanical (prestin-related piezoelectricity, mechanosensitive channels), and mechanical (stiffness and viscosity) properties of the cell's composite membrane as well as the cell interaction with the cochlear fluid and solid components. Our analysis also includes the effect of the intracochlear electric potentials measured under highfrequency conditions in the vicinity of outer hair cells. The parameters of our integrative model are based on available experimental data. We have shown that an individual outer hair cell can overcome the high-frequency electrical and mechanical modulation and produce an active force of several tens of pN for frequencies up to tens of kilohertz. The obtained results are important for a better understanding of the role of outer hair cells in the cochlear amplifier mechanism.

#### **726** Cholesterol Modulates Prestin Function

**Lavanya Rajagopalan**<sup>1</sup>, Haiying Liu<sup>1</sup>, Angela Sturm<sup>1</sup>, Amy Davidson<sup>2</sup>, Fred Pereira<sup>1</sup>, William Brownell<sup>1</sup>

<sup>1</sup>Baylor College of Medicine, <sup>2</sup>Purdue University

The motor mechanism that underlies outer hair cell (OHC) electromotility resides in the lateral wall plasma membrane. In the mature OHC, this membrane domain has a lower concentration of cholesterol than the apical and basal regions of the cell, and contains the membrane protein prestin. Here we show a dynamic and reversible relationship between membrane cholesterol levels and prestin-associated charge movement in both OHCs and prestin-transfected HEK 293 cells. Prestin exists in distinct membrane foci in association with lipid rafts in HEK 293 Depletion or loading of cholesterol causes a redistribution of prestin within the plasma membrane and influences prestin self-association in HEK 293 cells. The results provide evidence for lipid-protein interactions in prestin function and an explanation for the low cholesterol in the adult OHC lateral wall membrane.

## 727 Absent Voltage-Dependent Stiffness in Basal Turn Outer Hair Cells

Richard Hallworth<sup>1</sup>
<sup>1</sup>Creighton University

Outer hair cell electromotility is proposed to be the source of cochlear mechanical amplification. The axial stiffness of outer hair cells essential for communication of force to the organ of Corti, and any modulation of stiffness should have a significant effect on inner ear function. Outer hair cell stiffness has been shown to be a function of membrane potential, but has only been demonstrated for apical lowfrequency cells, whilst cochlear amplification is arquably more important in the basal, high-frequency cochlea. The voltage-dependent stiffness of basal turn outer hair cells was investigated by two methods. In contrast to previous reports, no evidence was found for voltage-dependent changes in outer hair cell stiffness. The results call into question the importance of outer hair cell voltagedependent stiffness as a component of cochlear amplification.

Supported by N.I.H. (N.I.D.C.D) grant DC02053 and N.C.R.R C06 RR17417-01.

## | 728 | Evidence for Prestin in 10 Nm Particles in the Lateral Membrane of Outer Hair Cells: an Atomic Force Microscopic Study

**Ghanshyam Sinha**<sup>1</sup>, Firouzeh Sabri<sup>1</sup>, Emilios Dimitriadis<sup>2</sup>, Kuni Iwasa<sup>1</sup>

<sup>1</sup>Biophysics Section, NIDCD, NIH, <sup>2</sup>DBEPS, ORS, OD, NIH

Electromotility is based on prestin, a member of the SLC26 family of membrane transporters, and harnesses electrical energy available at the lateral plasma membrane of outer hair cells for cochlear amplifier that contributes to the exquisite sensitivity and frequency specificity of the mammalian ear. Because electron microscopy (EM) shows that the site of this motile activity is densely packed with10 nm particles, it has been assumed that 10 nm particles contain prestin. Here we tested this assumption by using atomic force microscopy (AFM).

We used "cell-free" preparation in which the lateral plasma membrane is firmly mounted on glass, exposing the cytoplasmic surface of an outer hair cell (from guinea pigs) for raster scanning by an AFM tip. This preparation showed densely packed membrane particles with diameter of about 10 nm after correcting for the geometry of the cantilever tip. The particles were arranged in a rectangular lattice with small correlation length but predominately aligned in one direction at 37 nm spacing. The particle density and heights were around 850  $\mu m^{-2}$  and 8-12 nm respectively. Specimens labeled with antiprestinsecondary antibody complex showed larger antibody particles with comparable alignment and density. Specimens labeled with non-specific antibodies showed randomly distributed antibody complexes at a lower density.

The dimension, density, and alignment of the membrane particles in unlabeled specimens were consistent with the 10 nm particles observed with EM. The density and alignment of antiprestin labeled specimens indicated that prestin antibodies had specific interaction with those

particles. Based on these observations we suggest that 10 nm particles are either made of prestin or contain prestin. Additionally, we noticed that the anisotropic packing pattern of the particles would require a certain symmetry on 10 nm particles, Such a requirement can lead to models for 10 nm particles. For example, we found that a model for prestin tetramer, which consists of two disulfide bond based prestin dimers as suggested by biochemical studies [Zheng et al, J Biol Chem 281 (2006) 19916], can have a symmetry consistent with our observation.

#### 729 Effects of Electrical Stimulation of Efferent Fibers on OHC Function

#### Withdrawn

#### 730 Interferometric Measurement of Coherent Stereociliary Motion

**Andrei Kozlov**<sup>1</sup>, Thomas Risler<sup>1,2</sup>, Armin Hinterwirth<sup>1,3</sup>, A. J. Hudspeth<sup>1</sup>

<sup>1</sup>Rockefeller University, <sup>2</sup>Institut Curie, <sup>3</sup>University of Washington

Mechanical force is thought to gate the mechanoelectrical-transduction channels of a hair cell by exerting tension through tip links. A hair bundle's sensitivity is determined by the relation between the applied force and the number of channels opened: the narrower the force range over which gating occurs, the greater the sensitivity. Theoretical studies suggest that the concerted gating of transduction channels mediates gating compliance, which in its most extreme form yields negative hair-bundle stiffness. In conjunction with the activity of myosin-1c, negative stiffness contributes to active hair-bundle motility, an active process that amplifies and tunes the responses of hair cells in at least some species.

The extent to which the gating of independent transduction channels is concerted depends on how strongly the individual stereocilia are constrained to move as a unit. To assess the degree of common motion among stereocilia, we developed a dual-beam laser interferometer that measures simultaneously the displacements of two stereocilia with a sub-nanometer spatial resolution and a sub-millisecond temporal precision. For either a quiescent or a spontaneously oscillating hair bundle, the thermal movements of stereocilia located on the bundle's opposite edges show a cross-correlation near unity, an indication that these processes display almost identical motions. The signals from the opposite sides of a hair bundle exhibit high coherence and zero phase lag over the frequency range from 100 Hz to more than 10 kHz. The mechanical degrees of freedom of stereocilia are thus strongly constrained, indicating that a force applied anywhere in the hair bundle deflects the structure as a unit. This feature favors the concerted gating of transduction channels that maximizes the sensitivity of mechanoelectrical transduction and enhances the hair bundle's capacity to amplify its inputs.

This research was supported by NIH grant DC00241 and by HHMI.

#### 731 Structure and Biochemical Properties of CDH23

**Piotr Kazmierczak<sup>1</sup>**, Elisabeth Wilson-Kubalek<sup>1</sup>, Ron Milligan<sup>1</sup>, Ulrich Mueller<sup>1</sup>

<sup>1</sup>The Scripps Research Institute

CDH23 is a cell surface receptor and member of the cadherin superfamily. Genetic studies have demonstrated that mutations in the human CDH23 gene cause Usher Syndrome Type 1 and nonsyndromic deafness. Studies in animal models have provided evidence that CDH23 is a component of extracellular linker filaments that connect the stereocila and kinocilium of a hair cell into a bundle. In developing hair cells, CDH23 is localized at lateral links between stereocilia, and at kinociliary links between the kinocilium and the longest stereocilia. In functionally mature hair cells, CDH23 is localized at tip links. To gain further insights into the biochemical feature and physical properties of extracellular linker filaments in hair cells, we have expressed the extracellular domain of CDH23 as a soluble fragment using eukaryotic expression systems that allow for the formation of disulfide bonds and glycosylation of the expressed proteins. We have successfully purified the entire recombinant CDH23 extracellular domain consisting of 27 cadherin repeats, and we have purified fragments containing only some of the cadherin repeats. We have obtained structural information indicating that CDH23 molecules form a rod like helical filament. Similar to what has been observed for other members of the cadherin superfamily, formation of a rigid and organized structure is strictly dependent on Ca2+. We will present the structural data, provide information on the cadherin repeats in CDH23 that mediate interactions between CDH23 molecules, and compare the CDH23 structure to the features of extracellular linker filaments in hair cells as determined by high-resolution electron microscopy. We are currently extending our studies to other extracellular linker proteins in hair cells and analyze the physical properties of these molecules (such as their elasticity) to gain insights into the mechanisms by which the filaments regulate the cohesion, growth, and movement of the hair bundle.

### 732 Hydrodynamics of an Inner Hair Cell Stereocilia Pair with Tip Links

Sonya Smith<sup>1</sup>, Richard Chadwick<sup>2</sup>

<sup>1</sup>Howard University, <sup>2</sup>NIDCD

Inner hair cell (IHC) stereocilia deflection is traditionally thought to be the result of its interaction with the surrounding oscillatory endolymphatic flow. However recent experiments using time-resolved confocal imaging indicate that this deflection, at least in the apical turn, is out of phase with the maximum displacement of the reticular lamina which suggests an additional influence [1]. Hensen's stripe may play a role altering the fluid flow in this region due the close proximity of IHC stereocilia to this part of the tectorial membrane. Additionally results of Cai et al. [2] show velocity vectors in the tunnel of Corti that coincide with the radial motion of the IHC body. The complex relationship between IHC stereocilia deflection reticular lamina and tectorial membrane displacements directly affects mechano-transduction and

thus understanding the physical mechanisms involved in this process is important. We have developed a computational model of IHC stereocilia deflection using the immersed boundary method that includes tip links. We present results that show the effect of fluid flow stimulus and Henson stripe proximity on the deflection and subsequent mechano-transduction of an IHC stereocilia pair at various locations of the cochlea. The results are compared with the optical Lagrangian flow method of Cai et al. and the confocal imaging of Friedberger et al. References:

- 1. Fridberger, A., et al. Imaging hair cell transduction at the speed of sound: Dynamic behavior of mammalian stereocilia. PNAS 103:1918-1923, (2006)
- 2. Cai, H., et al., Motion analysis in the hemicochlea. Biophys. J. 85:1929-1937, (2003).

# | 733 | Distortion Products Measured Simultaneously in Basilar-Membrane Vibrations and Ear-Canal Otoacoustic Emissions

**Hongxue Cai<sup>1</sup>**, Shyamla Narayan<sup>1</sup>, Alberto Recio-Spinoso<sup>1</sup>, Mario Ruggero<sup>1</sup>

<sup>1</sup>Northwestern University

Narayan et al. (ARO MWM Abst. 21: 181, 1998) reported on distortion-products (DPs) simultaneously recorded as otoacoustic emissions (DPOAEs) and basilar-membrane (BM) vibrations in chinchilla. Here we present more results from the same study. Stimuli were tone pairs ( $f_1$  and  $f_2$ ,  $f_1 < f_2$ ), presented at equal levels (L<sub>1</sub> = L<sub>2</sub>, 30 – 80 dB SPL in 10-dB steps), using 3 paradigms: BM characteristic frequency (CF,  $\sim$  9 kHz) = 2f<sub>1</sub> - f<sub>2</sub>, f<sub>2</sub>, or the geometric mean ( $f_{GM}$ ). In some experiments,  $f_1$  and  $f_2$  were started at the same time with the same phase. In others, stimuli consisted of 3 epochs (10, 30 and 10 ms): f<sub>1</sub> alone, f<sub>1</sub> and f<sub>2</sub> together, and f<sub>2</sub> alone, respectively. BM vibrations were recorded with a laser velocimeter. Regardless of paradigm, low- (e.g.,  $2f_1$ - $f_2$ ) and high-sideband (e.g.,  $2f_2$ - $f_1$ ) BM DPs or DPOAEs varied continuously with frequency across CF, so that their amplitudes and phases were the same at CF and the group delays were the same on either side of CF. With the  $2f_1-f_2 = CF$  paradigm, the amplitudes of the low-sideband BM DPs vibrations and DPOAEs varied nonmonotonically with frequency, with a notch at  $f_2/f_1 \cong 1.05 - 1.1$ . [For BM vibrations, this behavior contrasts with the findings of Robles et al., J. Neurophysiol. 77: 2385-2399, 1997 but agrees with results of Cooper and Rhode, J. Neurophysiol. 78: 261-270, 1997]. The notch was highly correlated with significant suppression of the  $f_1$  BM responses by the presence of  $f_2$ . Also with the  $2f_1-f_2$  = CF paradigm and stimulus SPLs 30-60 dB, there was a high correlation (coefficients of determination: 88-96%) between the phases of DPOAEs and BM DPs. Post-mortem magnitude changes were mildest for DPOAEs and most pronounced for BM DPs, especially with the  $2f_1-f_2 = CF$  paradigm. The present results extend those of Narayan et al., who stated that at the BM site with  $CF = f_2$ , DPOAE "group delays were similar to those measured at the BM for responses to tones" (implying that DPOAEs do not propagate to the middle ear via reverse BM traveling waves). Our findings

suggest that DPs generated by stimulus levels 60 dB SPL or lower are principally generated at the cochlear region where  $f_1$  and  $f_2$  interact and then directly propagate to the middle ear *via acoustic waves in the cochlear fluids*, emerging from the ear canal as the dominant components of DPOAEs. This conclusion is consistent with the results of Ren (*Nature Neurosci.* 7: 333-334, 2004), Ruggero (*ARLO* 5: 143-147, 2004) and Gong et al. (*ARO MWM Abst.* 28: 113, 2005). Supported by NIH grant DC-00419.

## 734 Three-Dimensional Vibration of the Basilar Membrane in Living Cochlea

Tianying Ren<sup>1,2</sup>, Wenxuan He<sup>1,2</sup>

<sup>1</sup>Oregon Health and Science University, <sup>2</sup>Xi'an Jiaotong University

Sound-induced basilar membrane (BM) vibration has traditionally been described as a transverse wave. The complex three-dimensional (3-D) structures and the active forces generated by the outer-hair-cell somatic motility and/or active hair bundle motion may, however, introduce non-transverse vibrations. The auditory bulla and round window of young healthy gerbils with normal hearing were opened under anesthesia and the BM was optically accessed through the enlarged round window. Acoustic tones at different frequencies and intensities were delivered into the external ear canal. Tone-induced BM vibrations in transverse, longitudinal, and radial directions were measured using interferometric methodology. We observed vibrations in the longitudinal and radial direction in addition to those in the transverse direction. Relative vibration magnitude of the longitudinal and radial components with respect to the transverse vibration decreases as stimulus intensity increases. The orientation of the vibration path in 3-D plots changes with stimulus frequency. The longitudinal and radial components decrease as the frequency decreases from the characteristic frequency (CF). The 3-D BM vibration also depends on cochlear sensitivity. Intravenous application of furosemide resulted in significant changes in magnitude and orientation of the BM vibration. These data demonstrate that the BM vibration at the CF location is three-dimensional rather than the one-dimensional in the transverse direction. Vibration in the radial direction, which excites the hair cells by opening and closing transduction channels, is an inherent property of the BM vibration in sensitive animals. These results and the data describing the spatial pattern of BM vibration (Ren, 2002), token reveal a three-dimensional mechanical together. mechanism responsible for cochlear sensitivity. nonlinearity, and frequency selectivity in sensitive cochleae.

Supported by NIH-NIDCD.

#### 735 Relating Intracochlear Pressure to Cochlear Emissions

Wei Dong<sup>1</sup>, Elizabeth Olson<sup>1</sup>

<sup>1</sup>Columbia University

We recently observed that under some conditions we could relate distortion product (DP) pressure measured at a localized longitudinal position in the cochlea to DP oto-acoustic emissions (DPOAEs). The pressure sensors

have been used in past measurements to study cochlear wave mechanics and nonlinearity. Pressure responses were recorded simultaneously in scala tympani (ST) close to the basilar membrane (BM) in the basal turn of gerbil cochlea, and in the ear canal (EC). The presence of the intracochlear pressure sensor appeared to change the emissions and enhance our ability to correlate the emissions to the localized pressure. This finding led us to suppose that the sensor could act as a localized reflector for the cochlear traveling wave. In the present study we pursued this further, and show that the sensor did not change the DPOAEs as it approached the basilar membrane, even at distances as close as 7 μm. However, if the sensor was used to locally damage the organ of Corti, for example by distending it, the emissions were In these cases, the local DPs became changed. correlated with the DPOAEs over a relatively wide frequency range, either because of a 'reflector' effect, or because the region of the cochlea that remained healthy and nonlinear was restricted to apical regions. In cochleae in which local damage was not done, the DPs and DPAOAEs were also correlated, in both amplitude fine structure and phase delay, but only at frequencies well below the local best frequency. The phase relationship between DPs and DPOAEs favors a reverse traveling wave as the predominant mode of travel out of the cochlea.

#### 736 Intracochlear Pressure and Derived Quantities From a Three-Dimensional Linear Model

Yong-Jin Yoon<sup>1</sup>, Sunil Puria<sup>1,2</sup>, Charles R. Steele<sup>1</sup>
<sup>1</sup>Department of Mechanical Engineering, Stanford
University, <sup>2</sup>Department of Otolaryngology-Head and Neck
Surgery, Stanford University

The measurements of gerbil intracochlear pressure (Olson, 1998, 2001) offer an unusual opportunity for validation of model calculations. Presently, we extend the macro-mechanical cochlear model for the chinchilla anatomy (Yongjin et al, 2006 ORL) to the the gerbil anatomy. The BM properties are physical, with orthotropic elastic properties and no fictitious mass or damping. Hence there are no free unjustified parameters for adjustment to fit experimental results.

Intracochlear pressure in the ST is obtained by adding the fast wave to the traveling pressure wave. From the intracochlear pressure simulation, derived quantities including (i) BM velocity, (ii) pressure difference across OC, and (iii) the OC impedance in the base are calculated by following Olson's procedure (1998; 2001). These quantities are compared with animal measurements and show excellent agreement. By comparing exact and estimated OC impedances, we find that the fast wave component in the estimated OC impedance causes phase fluctuation out of the reasonable range (negative real part even for the passive cochlea).

The comparison of animal measurements and model results of derived quantities (i-iii) is promising, but not fully satisfactory. The CF-to-place map in the passive model and frequency responses of BM velocity magnitude and intracochlear pressure are in close agreement with those

observed in animal measurement. The feed-forward linear active model shows excellent agreement with experimental data in the BM relative velocity magnitude. However, the calculated phase shows a larger roll-off at the CF by two and half cycles for the frequency dependence at a fixed point for both the active and passive cases. Several parameter variations were explored to determine the cause of this discrepancy. This includes scala area and duct area tapering rate variations.

#### 737 Characterization of Human Neural Stem Cells

**Andrew Kamien**<sup>1</sup>, Lulu Wang<sup>2</sup>, Wen-Hann Tan<sup>1,3</sup>, Douglas Cotanche<sup>1,4</sup>

<sup>1</sup>Dept. of Otoloaryngology, Children's Hospital Boston, <sup>2</sup>Program in Neuroscience, Harvard Medical School,

<sup>3</sup>Division of Genetics, Children's Hospital Boston, <sup>4</sup>Dept. of Otology & Laryngology, Harvard Medical School

The overall aim of our research is to regenerate inner ear hair cells that have been damaged or lost. As the neural tube secretes many of the transcription and growth factors required by the developing otocyst in embryonic and fetal life, we believe neural stem cells (NSC) have the potential to develop into inner ear hair cells under the appropriate environmental signals. Moreover, NSC retain the capacity to differentiate into all types of neuronal cells appropriate to the local environment and demonstrate the capacity to migrate to the site of neuronal injury. Human NSC would be the preferred source of cells for the regeneration of inner ear hair cells due to the reduced risk of crossspecies reactivity. There is very little data on the development of human **NSC** in different performed initial microenvironments. We have characterization of a human NSC line derived from the premature postnatal newborns immunocytochemistry. When grown under differentiating conditions, these NSC upregulated Connexin 45, Myosin 6 and  $\beta$ -III tubulin, which are seen in a variety of differentiated cells including cochlear hair cells, and downregulated the stem cell marker SOX2. In addition, we will present data on the different patterns of gene expression using cDNA microarrays of the differentiated and non-differentiated cells.

## 738 Phenotypic Changes Precipitated by Altered MYH9 Expression in Cultured Hela Cells

**Yan Li<sup>1,2</sup>**, David R. Friedmann<sup>1,2</sup>, Anand N. Mhatre<sup>2</sup>, Anil K. Lalwani<sup>1</sup>

<sup>1</sup>Laboratory of Molecular Otology, <sup>2</sup>Laboratory of Molecular Genetics, Department of Otolaryngology, NYU School of Medicine

Mutations within the nonmuscle myosin heavy chain type IIA have been linked to an autosomal dominant disorder characterized by platelet macrocytosis, thrombocytopenia and leukocyte inclusions, with or without additional clinical features that include sensorineural deafness, cataracts and nephritis. From studies of type II myosin in invertebrates and analogy with the skeketal and smooth muscle myosin II, MYH9 was considered to be involved in

cellular functions. However, the specific diverse contribution of MYH9 in a number of diverse cellular functions remains largely unknown. We address the biological role of MYH9 by assessing the effects of altered MYH9 expression in cultured HeLa cells. Altered expression of MYH9 was accomplished by transfection of HeLa cells with siRNA or expression vectors carrying mutant MYH9 alleles. MYH9 siRNA down-regulated MYH9 protein expression within the trasnfected HeLa cells, transiently, i.e., complete suppression of protein was observed at 3 days post transfection. Transient suppression of MYH9 induced the following changes: reduced cell proliferation, about 50% relative to controls at 96 hours after transfection, alteration in cell morphology and actin distribution within the cytoplasm and disruption of focal adhesions. The decreased cell numbers was not due to apoptosis as assessed by flow cytometry and apoptosis assay. Also, transient reduction in MYH9 did not yield multinucleated cells suggesting that cell division was not affected and thus indicating that MYH9 function is not critical for cytokinesis. The physical and functional alterations induced by transient MYH9 suppression were also observed in HeLa cells transfected transiently or stably with MYH9\(\triangle C594\), MYH9 allele carrying a deletion of its C-terminal coding region. However, transfection with MYH9<sup>R705H</sup> or MYH9<sup>R702C</sup>, naturally occurring mutant alleles of MYH9, or MYH9∆N592, a MYH9 allele carrying a deletion of its N-terminal coding region did not induce a phenotypic alteration. Thus, the results of these in vitro studies identify and clarify the specific contributions of MYH9 in cell structure and function. Moreover, these studies also suggest that MYH9<sup>R705H</sup> or MYH9<sup>R702C</sup> do not disrupt basic processes that include maintenance of cell structure and cell adhesion.

### 739 Conservation of the Prestin, *Slc26a5*, Gene in the Monotreme

Divvya Sanjeevi<sup>1</sup>, Remen Okoruwa<sup>1</sup>, Michael Weston<sup>1</sup>, Richard Hallworth<sup>1</sup>, **Kirk Beisel**<sup>1</sup>

<sup>1</sup>Creighton University

Prestin mediates and allows for shape changes of outer hair cells (OHCs) in response to sound waves at particular frequencies, thereby functioning as the mammalian cochlear amplifier. Use of electromotility as a mechanism for sound amplification is only found in extant eutherian mammals (marsupials and placentals). The monotremes (echidna and platypus) are unique among vertebrates by sharing many features common to the eutherian mammals and to ancestral mammals, birds and reptiles. monotremes use electromotility as a mechanism for cochlear amplification? Experimental data suggest that echidnas exhibit otoacoustic-like emissions, indicative of cochlear amplification. Although the monotreme middle ear is typically mammalian, the cochlea is not, having multiple rows of inner hair cells (IHCs), OHCs, and supporting cells in a comma shaped cochlea that contains at its end a lagenar macula. Extra rows of hair cells are not unique to monotremes, but are found in engineered mutants affecting delta/notch/hes signaling pathway, the PCP pathway for convergent extension, Neurog1, and Foxq1. This suggests that the underlying genetic

mechanism for formation of cochlear morphology was already present in the monotremes.

Protein homology of Slc26a5 orthologs among eutherian mammalian species, including the opossum, is >85% identical overall. In contrast, non-mammalian vertebrates share strong homology in only the sulfate transporter, SUL, and STAS domains which are also shared by all other Slc26a paralogs. Genomic BAC libraries of Tachyglossus aculeatus (echidna) and Ornithorhynchus anatinus (platypus) were screened. Southern analysis was done on the positive BAC clones genomic fragments identified and subclones. Sequence and genomic analysis of the platypus found an identical exon-intron organization and 80-85% similarity in protein sequence with the eutherian mammals. These data suggest that monotreme Slc26a5 ortholog was already evolved to possibly function as the electromotility motor prior to the evolution of the eutherian cochlea architecture (one IHC row, 3 OHC rows and 2 pillar cells). In vitro and in vivo experiments are still needed to determine the localization and functional properties of monotreme prestin.

#### 740 Cloning and Characterization of Xenopus Inner Ear Calcium-Activated Potassium Channel α and β-1 Subunits

**David R. Sultemeier<sup>1</sup>**, Casilda Trujillo-Provencio<sup>1</sup>, Elba Serrano<sup>1</sup>

<sup>1</sup>Biology Department, New Mexico State University, Las Cruces NM

Differential expression of large conductance calciumactivated potassium channel (BK) α-subunit splice variants and the  $\beta$ 1-subunit across the tonotopic axis of peripheral auditory organs gives rise to channels with different gating kinetics, and Ca<sup>2+</sup> and voltage sensitivity. This differential expression has been shown to facilitate the establishment of resonant frequency and electrical tuning in vertebrate hair cells of several species (rev. Fettiplace and Fuchs 1999). As part of our interest in understanding gene expression in the inner ear and to further establish Xenopus spp. as model organisms for inner ear developmental studies, we present preliminary data describing the genomic organization, conservation, and electrophysiological characteristics of X. laevis and X. *tropicalis* BK channel  $\alpha$  and  $\beta$ 1 subunits. Computational analysis of public domain *X. tropicalis* genomic sequence (http://genome.jgi-psf.org)suggests that the X. tropicalis BK  $\alpha$ -subunit gene comprises 27 constitutively expressed exons, and contains 7 putative exons that are homologous to alternatively expressed exons in mammals and chick. Additionally, a single locus containing a gene with homology to human KCNMB1 was identified in the X. tropicalis genome. Using RT-PCR we have isolated and cloned full length BK  $\alpha$  and  $\beta$ 1 subunits from *X. laevis* and X. tropicalis inner ear total RNA. The Xenopus  $\alpha$ -subunit cDNAs code for proteins that share above 91% amino acid identity with mammalian and chick  $\alpha$ -subunits. Conversely, the Xenopus β1-subunit cDNAs code for proteins that share below 47% amino acid identity with mammalian and avian β1-subunits. Hydrophobicity plots of isolated Xenopus β1-subunits suggest the proteins have two transmembrane domains, in agreement with β1-subunits in other species. Functional characterization of isolated  $\alpha$  isoforms and  $\beta$ 1-subunits are underway using electrophysiological approaches.

Supported by NIH S06GM008136, R01DC003292.

## 741 Gene Expression Profiling of *Xenopus*Organs Yields Insight into the Inner Ear Transcriptome

**TuShun Powers**<sup>1</sup>, Casilda Trujillo-Provencio<sup>1</sup>, Charlie Whittaker<sup>2</sup>, Elba E. Serrano<sup>1,3</sup>

<sup>1</sup>Biology Department, New Mexico State University, <sup>2</sup>MIT Center for Cancer Research, <sup>3</sup>MIT Cell Decision Processes Center

We are interested in the emergence of auditory and vestibular endorgans from the otic vesicle of the amphibian, Xenopus. As part of this effort we aim to identify genes essential for inner ear function and development. Xenopus is an attractive organism for these investigations because unlike *Homo sapiens*, *Xenopus* can regenerate and replace sensory hair cells in response to damage. Results presented here use microarray analysis to compare the transcriptional profiles of inner ear tissue with those of brain and kidney. Our goals are to identify candidate genes for hereditary disorders of hearing and balance, and to determine genetic similarities and differences between the organ systems. RNA (RIN  $\geq$  8.0) isolated from juvenile *Xenopus* (inner ear, brain, kidney) and larval inner ear was processed and hybridized to the Affymetrix Xenopus genome array. We determined that optimization of stringent RNA isolation procedures was essential before cRNA labeling to ensure production of high quality microarray data. Curation of the 15,503 probe sets was necessary in order to functionally characterize features of the microarray transcriptional profiles. Microarray data were normalized with the GCRMA summarization method. Box and RNA degradation plots of the data showed experimental procedures were consistent and reproducible among arrays (performed in triplicate). Hierarchal clustering uncovered tissue specific expression patterns among the organ arrays. When transcriptional profiles of the three organs were examined using k-means clustering, over 400 genes were found to have higher expression in inner ear tissues as compared to brain and kidney. Moreover, this global analysis uncovered differences between larval and juvenile inner ear transcriptional profiles that are being analyzed in order to identify genes that that may be essential for directing development of the inner ear.

Supported by NIH S06GM008136, R01DC003292, P50GM068762.

## 742 Gene Expression Profiling of the Inner Ear in the Adult Zebrafish with Massively Parallel Signature Sequencing (MPSS)

Jin Liang<sup>1,2</sup>, Arthur N. Popper<sup>2,3</sup>, Shawn M. Burgess<sup>1</sup>
<sup>1</sup>National Human Genome Research Institute, National Institutes of Health, Bethesda, MD, <sup>2</sup>Neuroscience and Cognitive Science Program, University of Maryland, College Park, MD, <sup>3</sup>Department of Biology, University of Maryland, College Park, MD

The inner ear is a highly specialized compartment with uniquely differentiated cell types for the auditory and vestibular functions. Thus, we assume that there are genes that are specifically expressed in the inner ear and are critical for the auditory and vestibular functions. Here we used a relatively new technique. Massively Parallel Signature Sequencing (MPSS), to study the gene expression profile of the inner ear in adult zebrafish. Using MPSS, we profiled gene expression of both the zebrafish inner ear and the zebrafish brain. We generated 45,259 unique transcription tags with a sensitivity to detect the level of transcription as low as 3 transcripts per million (tpm). By comparing the inner ear MPSS tags to the brain MPSS tags, we were able to identify tags that 1) are mapped to genes already known to be expressed in the inner ear, 2) are mapped to transcripts previously identified, but with no known expression or function in the inner ear, and 3) can not be mapped to any currently known or predicted transcript. RT-PCR results have verified the tissue-specific expression of some candidate genes in our MPSS data. The preliminary analysis of our data suggests that the MPSS is a powerful technique for large-scale and in-depth gene expression profiling of the inner ear in the adult zebrafish, which will allow us to identify new and potentially exciting genes expressed specifically in the inner ear.

### 743 Characterization of Pcdh15<sup>av-6J</sup>, an Allele of Mouse Protocadherin 15 Gene

Qing Zheng<sup>1</sup>, Heping Yu<sup>1</sup>, Lauren Kisley<sup>1</sup>, Yayoi Kikkawa<sup>2</sup>, Karen Pawlowski<sup>2</sup>, Charles Wright<sup>2</sup>, **Kumar Alagramam**<sup>1</sup>

Otolaryngology-HNS, Case Western Reserve University, Cleveland, OH 44106, Otolaryngology-HNS, University of Texas Southwestern Medical Center, Dallas, TX 75390

We have characterized a new allele of the protocadherin 15 gene (designated  $Pcdh15^{av-6J}$ ) that arose as a spontaneous, recessive mutation in the C57BL/6J inbred strain at The Jackson Laboratory. Analysis revealed an inframe deletion in Pcdh15, which is predicted to result in partial deletion of cadherin domain (domain 9) in Pcdh15. Morphologic study revealed normal to moderately defective cochlear hair cell stereocilia in *Pcdh15*<sup>av-6J</sup> mutants at postnatal day 2 (P2). Stereocilia abnormalities were consistently present at P5 and P10. Degenerative changes including loss of inner and outer hair cells were seen at P20, with severe sensory cell loss in all cochlear turns occurring by P40. The hair cell phenotype observed in the 6J allele between P0 and P20 is the least severe phenotype yet observed in Pcdh15 alleles. However, young  $Pcdh15^{av-6J}$  mice are unresponsive to auditory stimulation and show circling behavior indicative of vestibular dysfunction. Since these animals show severe functional deficits but have relatively mild stereocilia defects at a young age they may provide an appropriate model to test for a direct role of Pcdh15 in mechanotransduction.

## 744 Mineralocorticoid Treatment Partially Compensates for Strial Dysfunction in *Kit<sup>w</sup>/Kit<sup>w-V</sup>* Mutant Mice

Dennis Trune<sup>1</sup>, Beth Kempton<sup>1</sup>

<sup>1</sup>Oregon Health & Science University

Steroid therapy is recommended for acquired hearing loss, such as sudden hearing loss, autoimmune inner ear disease, and Meniere's disease. However, no effort is made to treat the hearing deficits in genetic disorders, such as connexin and stria vascularis mutations. We are learning more of cochlear ion homeostasis and the redundancy in ion transport channels, particularly those involving  $K^{\dagger}$ . It is possible that the loss of some ion flow due to a gene mutation may be partially overcome by enhancement of other ion transport processes with overlapping functions. If partial compensation of lost homeostatic mechanisms can be achieved, it could lead to therapies for genetic hearing disorders that currently have no effective treatment.

The KitW/KitW-v mutant mouse suffers from lack of stria vascularis intermediate cells due to impaired neural crest cell migration into the inner ear. Their endocochlear potentials fail to develop because of severely impaired ion transport into the endolymph. A potential parallel is seen between this mouse mutation and human disorders of endolymph production. Although the intermediate cell is the final cellular mediator of endolymph K<sup>+</sup> and Na<sup>+</sup> concentrations, other cells in the stria and lateral wall also have channels and transporters for these ions. Therefore, the objective of this study was to determine if partial compensation of hearing deficits in these mice can be achieved by enhancing other ion transport processes through treatment with the mineralocorticoid aldosterone. Kit<sup>W</sup>/Kit<sup>W-v</sup> mutant mice were obtained from Jackson Laboratories and tested by ABR audiometry at 2 months of age. Half of the mutant mice were then given aldosterone (15 µg/kg) in their drinking water for 4 months. Posttreatment ABR thresholds showed steroid treated mice did not develop as severe of hearing loss as the untreated mutants. Although both groups still showed severe hearing loss due to absence of intermediate cells, the partial compensation by steroid therapy indicated control of this hearing loss was possible. These preliminary findings suggest the medical management of genetic hearing loss is potentially feasible and warrants further investigation. (Supported by NIH-NIDCD R01 DC05593, NIH-NIDCD P30 DC005983, and VA RR&D RCTR 597-0160 National Center for Rehabilitative Auditory Research.)

ARO Abstracts 255 Volume 30, 2007

# 745 Abnormal Cochlear Dystrophin Proteins in Muscular Dystrophy Mice. Do They Explain the Cognitive Defects Seen in Human Duchenne Muscular Dystrophy?

**De-Ann Pillers**<sup>1</sup>, Beth Kempton<sup>1</sup>, Bojan Malmin<sup>1</sup>, Jiaqing Pang<sup>1</sup>, Dennis Trune<sup>1</sup>

<sup>1</sup>Oregon Health & Science University

Dystrophin is a cytostructural protein in muscle that links the actin cytoskeleton to a transmembrane cluster of proteins known as the "dystrophin-associated protein complex". Dystrophin RNA is differentially spliced to form transcripts that encode several different sized isoforms, and their defective production in Duchenne muscular dystrophy (DMD) underlies the many muscle, eye, brain, and heart pathologies of that disease. Recent studies have suggested inner ear function is impacted by dystrophin mutations in  $mdx^{Cv3}$  mice (Pillers et al., ARO 2005), potentially explaining the cognitive defects commonly associated with this disease. To better characterize the potential role of dystrophin in hearing, ABR audiometry was used to evaluate auditory function in the mdx,  $mdx^{Cv3}$ , and age-matched C57BL controls. Dystrophin gene expression in the ear was evaluated to identify the isoforms normally present and potentially defective in muscular dystrophy mice.

Both mdx and  $mdx^{Cv3}$  mice demonstrated normal ABR thresholds, but  $mdx^{Cv3}$  mice had shorter ABR waves and interpeak intervals. Western blot analysis of the wild type C57BL/6J cochlea showed expression of isoforms Dp427, Dp116, and Dp71. However, none of these dystrophin proteins were detected in the cochlea of  $mdx^{Cv3}$ , suggesting they are absent when defective gene expression occurs. RT-PCR analyses of the normal cochlea showed the most common isoforms (Dp427m, Dp140, Dp116, and Dp71) were present. quantitative RT-PCR was performed using probes and primers specific for these various isoforms, as well as a probe and primer generic to the conserved carboxyterminus of dystrophin to serve as a marker for total dystrophin isoform expression. This demonstrated the cochlear expression of alternate forms of Dp427, including Dp427c (cortex) and Dp427p (Purkinje). The sum of the expression of Dp427m, Dp427c, Dp427p, Dp140, Dp116, and Dp71 appeared to account for all cochlear isoforms.

A subset of patients with Duchenne muscular dystrophy has cognitive defects ranging from dyslexia to mental retardation. Genotype-phenotype correlations in man have shown that 3' DMD mutations, such as that found in the  $mdx^{Cv3}$  mouse, are predominantly associated with the cognitive defects. We speculate abnormal auditory processing may be one physiologic basis for these cognitive defects.

(Dickinson Foundation, Oregon MRF, NEI EY10084, NIDCD DC05593 & DC005983, and VA RCTR 597-0160)

### 746 A Dominant and Recessive Sensory Screen for New Deaf Mouse Mutants

**Emma L. Coghill<sup>1</sup>**, Sue J. Young<sup>1</sup>, Andrew Parker<sup>1</sup>, Richard B. Gale<sup>1</sup>, Steve D. M. Brown<sup>1</sup>

<sup>1</sup>Mammalian Genetics Unit

A dominant and recessive sensory screen for new sensorineural deafness mutants is underway utilising the Harwell Mutagenesis program. ENU (N-Ethyl-Nnitrosourea), a powerful chemical mutagen, is injected into C57BL/6J males creating point mutations in their germline. Following a period of sterility, mutagenised mice are mated to C3H/HeH females and progeny enter a broad phenotype driven screening programme for both dominant and recessive mutations. A monthly average of 220 G1 mice and 200 G3 mice (across 5-6 recessive pedigrees) undergo a primary sensory screen at 7 weeks. This protocol is derived from "The European Mouse Phenotyping Resource of Standardised Screens" (EMPReSS). Hearing impaired G1 mice are re-tested followed by inheritance testing and the hearing impaired phenotype of mutant progeny from inherited G1 and G3 pedigrees further confirmed by an auditory brainstem response (ABR) test. Genome scans are carried out on confirmed mutant lines to determine chromosomal map position. The broader phenotype of each mutant line is also investigated using additional behavioural tests, histological and histochemical analysis, SEM and 3D reconstructions of the inner ear of mutants from MRI data. A number of new G1 and G3 lines that display hearing impairment, with variable elevated auditory thresholds, alone and in combination with circling, headbobbing and pigmentation defects, are presented.

## 747 Effects of PMCA2 Mutations on Auditory Sensitivity in Neo-Natal Deafwaddler Mice

Sarah M. Lies<sup>1,2</sup>, Bruce Tempel<sup>2,3</sup>

<sup>1</sup>Dept. of Speech and Hearing Sciences, University of Washington, Seattle, WA. USA, <sup>2</sup>The V.M. Bloedel Hearing Research Center, University of Washington, Seattle, WA. USA, <sup>3</sup>Dept. of Otolaryngology-HNS, University of Washington, Seattle, WA. USA

The Atp2b2 gene encodes the plasma membrane calcium ATPase, isoform 2 (PMCA2) which plays a significant role in regulating and maintaining low Ca2+ in stereocilia of the auditory hair cells. Here we examine the role of PMCA2 in hearing sensitivity of neonatal mice. We also ask if homozygous mutants display sensitivity to sound at ages as young as postnatal day (P) 16. Auditory brainstem responses (ABRs) were collected and compared between age-matched littermate controls (+/+) and two alleles of deafwaddler: a hypomorphic allele,  $Atp2b2^{dfw}$ , with 30% function and a null allele,  $Atp2b2^{dfw2J}$ . ABRs were evoked at 5.6, 8, 11.3, 16, 22.6, 32, and 40 KHz and collected at P16, 3, 4, 5, 7, and 9 weeks of age. At 5 weeks results showed thresholds similar to those reported by McCullough and Tempel (ARO 2005) for heterozygotes (+/-) of both strains. As previously shown for adults, neonatal homozygotes (-/-) of both alleles showed no response at any test frequency even when auditory stimuli were delivered at the sound intensity limits of our equipment. At P16, heterozygotes of both strains showed

similar responses as their respective +/+ littermates when averages of mid-frequency thesholds (8, 11.3, and 16 KHz) are compared (+/dfw) and controls, 44 + 1.9 dB; +/dfw2J and controls, 39 + 2.4 dB SPL). In contrast, at 3 weeks of age +/dfw2J and +/+ looked dissimilar with midfrequency average thresholds of 55 + 2.4 dB SPL and 32 + 3.1 dB SPL (respectively) while the +/dfw and +/+ look similar with thresholds of 30 + 2.9 dB SPL. At 4 weeks, thresholds were similar in +/dfw2J, +/dfw and +/+ with midfrequency averages at 30 + 2.4 dB SPL for all. These data show that ABR thresholds are worse in +/dfw2J at 3 weeks than in +/dfw or in +/+ controls from either strain. Thus, PMCA2 expression in +/dfw2J but not in +/dfw has a transient functional consequence at 3 weeks, possibly inducing a compensatory response by 4 weeks of age. Research Supported by RO1 DC002739.

## | 748 | Candidate Gene Analysis in *nihl-1*, a Noise Resistance Locus on Chromosome 17 in 129S6 Mice

**D.J. Shilling**<sup>1</sup>, R.S. Silverstein<sup>1,2</sup>, S.G. Kujawa<sup>3,4</sup>, V.A. Street<sup>1,5</sup>, B.L Tempel<sup>1,5</sup>

<sup>1</sup>The V.M. Bloedel Hearing Research Center, University of Washington, Seattle, <sup>2</sup>Program in Neurobiology and Behavior, University of Washington, Seattle, <sup>3</sup>Eaton-Peabody Laboratory and Massachusetts Eye and Ear Infirmary, <sup>4</sup>Dept. of Otology and Laryngology, Harvard Medical School, <sup>5</sup>Dept. of Otolaryngology-HNS, University of Washington, Seattle

Noise-induced hearing loss (NIHL) is a widespread and growing health problem. We have used inbred strains of mice to identify quantitative trait locus (QTL) regions that contribute to noise resistance in 129S6 (Tempel et al., ARO 2007). Here we report on candidate genes in the nihl-1 QTL defined on proximal Chromosome 17 as an example of the integrative multi-step genomics approach being used. In parallel with the whole genome phenotypic QTL analysis, we examined differential gene expression in isolated cochlea of 129S6 and CBA strains using 30,000+ gene arrays (Codelink). We found 1691 genes that were differentially expressed genome-wide at a fold difference of >1.50 and a p value of <0.05; of these, 52 genes localized to Chr 17. To refine the nihl-1 region we examined single nucleotide polymorphism (SNP) databases available from the Broad Institutue and Wellcome Trust Oxford Genome Center and found that SNPs differed between 129S6 and CBA proximal to 34 Mb on Chr 17, but did not differ distally. Since we predict noise resistant genes will differ in ancestral inheritance, we restricted our examination of candidate genes to Chr 17 proximal to 34 Mb. We compiled a list of all genes or gene family members implicated in auditory function and aligned this list with differentially regulated genes on proximal Chr 17. We performed qPCR analysis on the 6 genes emerging from this alignment; 2 genes were confirmed as having >2 fold over/under expression between strains. We are currently studying the adjacent and virtually identical Hspa1a and Hspa1b genes, encoding the inducible heat shock 70 proteins, which have been linked to noise and aminoglycoside resistance (Yoshida et al,

Cunningham, 2006). We will report whether one or both are differentially regulated and whether sequence variations in these genes or their promoters might correlate to differential expression levels in 129S6 vs CBA. Eventually, candidate SNPs will be transferred between strains to test for functional effects on the *nihl-1* related phenotype.

Research Supported by Grants from NIDCD.

## 749 Divergence of Hearing Sensitivity and Endocochlear Potential (EP) in CBA/J and CBA/CaJ Mice After 12 Months of Age

Kevin K. Ohlemiller<sup>1</sup>, Patricia M. Gagnon<sup>1</sup>

<sup>1</sup>Washington University Dept. of Otolaryngology

CBA/J and CBA/CaJ inbred mice are often used as standard 'good hearing' strains, and treated as equivalent in hearing ability and aging characteristics. To test this assumption we compared round window CAP thresholds and basal turn EPs in the two strains at 6 mo intervals from 6-24 mos. The number of mice compared at each age ranged from 12-26, mixed by gender. CAP thresholds were obtained at 2.5, 5, 10, 20, 28.3, 40, and 56.6 kHz.

At 6 and 12 mos of age CBA/J and CBA/CaJ hear similarly and show EPs ranging 100-120 mV. By 18 mos, however, thresholds diverge (2-way ANOVA, p=.001), with CBA/CaJ exhibiting ~10 dB higher thresholds at high frequencies. By 24 mos, thresholds above 10 kHz in CBA/CaJ are ~20 dB higher than in CBA/J. Pearson correlation on EP versus age in CBA/J indicated no relation. By contrast, the EP progressively decreases in CBA/CaJ after 12 mos (p<.001), and averages significantly lower than in CBA/J (94.2 mV vs. 105.9 mV; t-test, p<<.001). EPs in old CBA/CaJs were marked by scatter, with values as low as 30 mV. The fraction of animals with EPs above 110 mV fell to 2% (vs. 27% in CBA/J). Conversely, the fraction of animals with EPs below 90 mV rose to 24% (vs. 0% in CBA/J), with no effect of gender.

CAP thresholds and EP were not significantly correlated (p=.08). Thus we speculate that age-related threshold shifts and EP reduction in CBA/CaJ mice reflect other factors, and are not directly related. EPs in old CBA mice have not been extensively examined. We recently reported that BALB/cJ mice >19 mos of age tend toward EP reduction that correlates with strial marginal cell density (Ohlemiller et al., HR 2006). BALB mice show an initial EP that is somewhat lower than most strains, while the upper range of EPs appears stable with age. Since aging trends in the EP differ between CBA/CaJ and BALB, cellular correlates of EP decline may also differ. Morphological assessments are underway.

(Supported by WUSM Dept. Otolaryngology and NIH P30 DC04665)

### 750 CBA/J Mice as a Model for Sensorineural Presbycusis

Su-Hua Sha<sup>1</sup>, Jochen Schacht<sup>1</sup>

<sup>1</sup>Kresge Hearing Research Institute

In sensorineural presbycusis, the mammalian inner ear loses its hair cells with advancing age, accompanied by a functional decrease in balance and hearing. In the organ of Corti, the number of outer hair cells decreases initially in the basal region, leading to high-frequency hearing loss. Male CBA/J mice show significantly elevated auditory thresholds at 24 kHz at 12 months or older (p < 0.05) compared to younger animals of 1.5 to 8 months. Thresholds at 12 kHz are significantly elevated by 18 months. There was no significant difference between the thresholds of the right and left ears at any frequency After 18 months, high-frequency thresholds tested. showed a bimodal distribution. A cluster of animals maintained nearly normal thresholds near or below 40 dB and another cluster had significant threshold elevations with thresholds of 60 dB and above. Almost all 26 monthold mice (9 out of 10) had severe hearing deficits at all frequencies tested, with 6 out of 10 showing no response (thresholds >100 dB). The functional loss at high frequencies correlated with the loss of hair cells in the basal turn of the cochlea. Density of spiral ganglion cells significantly decreased by age 22 months in all turns of the cochlea. In contrast, the endocochlear potential was still stable at 26 months.

Our results suggest that CBA/J mice provide a suitable model for research on sensorineural presbycusis. This species possesses the ahl (age related hearing loss)-resistant allele, and therefore is not prone to premature hearing loss as is, for example, the C57/BL strain. The choice of a single sex (in this case, male) is demanded by the fact that the rate of age-related hearing loss differs between male and female (Guimares et al., 2004). Importantly, the progressive morphological changes in the basal turn accompanied by high frequency hearing loss are typical features of age-related hearing loss in humans. This study was supported by program project grant AG-025164 from the National Institute of Aging and core grant P30 DC-05188 from the National Institute on Deafness and Other Communication Disorders. NIH.

## | 751 | Increasing GABA Alters Receptive Field Properties in the Inferior Colliculus of Old CBA Mice

**Joseph Walton**<sup>1</sup>, Paul Allen<sup>2</sup>, Nicholas Schmuck<sup>1</sup>, Kathy Barsz<sup>1</sup>

<sup>1</sup>Dept of Otolaryngology University of Rochester Medical Center, <sup>2</sup>Brain and Cognition University of Rochester
Inhibitory neurosignalling plays a critical role in shaping neuronal responses to sound. Age-related alteration in the interplay between excitatory and inhibitory neurotransmission has been postulated to underlie temporal processing disorders in elderly listeners. Vigabatrin (VGB) irreversibly inhibits GABA transaminase, the main transporter of GABA from the synaptic cleft, leading to increased levels of GABA in nerve terminals and

increased GABA availability for synaptic transmission. Gleich et al. (1999) reported that old gerbils which displayed elevated gap thresholds significantly improved after VGB administration. In the current study we show that VGB can also alter receptive field (RF) properties of inferior collicular neurons in old CBA mice.

VGB was taken from commercially available sachets which contain only 500 mg pure VGB powder. VGB was administered to >24 month old CBA mice (N=4) via an IP injection (50 mg/kg). In six >24 month old control mice (C) a saline injection was administered. MUA was acquired using a 16-channel vertically oriented Michigan Probe. RFs were measured using 25 ms pure tones, presented contralaterally at frequencies between 2 & 64 kHz, and from 0 to 80 dB SPL. For each RF the best frequency (BF), minimum threshold (MT), bandwidth at 10 (Q10) and 40 dB (Q40) above MT, maximum driven rate and spontaneous rate were computed. The data set comprised 418 units from VGB mice and 550 units from control mice. VGB had no effect on BF (mean=27.7 kHz) but did significantly improve MTs (C=39.5 dB, VGB 31.3 dB, p<.001). The Q10 bandwidth (M= 3.16) was not affected by VGB, but the Q40 bandwidth was widened (C 1.4, VGB 1.1, p<.001). While VGB did not affect the spontaneous rate, it did reduce the maximum rate (C=24.1 spk/sec, VGB=7.9 spk/sec, p<.001). findings suggest that increasing GABA, via VGB administration, alters the neural coding of simple sounds and may form the basis of improved temporal processing, reported previously, by sharpening the temporal filter.

Research supported by NIH/NIA grant PO1 AG09524 and NIDCD P30 grant DC05409

# 752 Aging Reduces the Effect of Spatially Separating the Markers on the Gap Thresholds of Inferior Collicular Neurons in CBA Mice

**Kathy Barsz**<sup>1</sup>, Paul D. Allen<sup>2</sup>, Nicholas Schmuck<sup>1</sup>, Joseph P. Walton<sup>1</sup>

<sup>1</sup>University of Rochester Medical Center, <sup>2</sup>University of Rochester

Behaviorally, minimal gap thresholds (MGTs) increase when the pre- and post-gap markers are located in different spatial channels. Although aging impairs monaural gap detection, age-related loss of spatial sensitivity may decrease the distinction between different spatial channels and thus maintain cross-channel gap detection. This study explored cross-channel gap detection in inferior collicular neurons of young (1-4 month) and old (25-27 month) CBA mice. Noise bursts were used to separate gaps of 1-96 ms. The pre-gap burst was contralateral to recording site and the post-gap burst was either contralateral or ipsilateral. Multiunit activity (MUA) was recorded using a vertically oriented 16-channel Michigan probe. In the young mice, MGTs were expected to be longer when the post-gap burst was ipsilateral. We predicted that age-related differences would be found when the post-gap marker was contralateral, but not when the post-gap marker was ipsilateral.

The MGT was defined as the shortest gap that elicited a just noticeable increase in activity relative to a 0-ms-gap control stimulus. When both markers were contralateral, 79% of the units recorded from young mice had MGTs <5 ms as compared to 59% in old mice (p<.05). When the post-gap marker was moved to the ipsilateral hemi-field, the number of units with MGTs <5 ms dropped to 32% in the young mice (p<.05), and 25% in the old mice (p>.05). In this condition, there was no age-related difference in the number of units with MGTs <5 ms (p>.05) because young mice lost more units with good temporal sensitivity as compared to old mice. The same pattern of results was found when MGT was defined as 25% recovery on the gap function.

Our interpretation of this result is that, because of reduced spatial sensitivity in the aging auditory system, the gap markers are treated as arriving from similar spatial channels, thus preserving temporal encoding for the old mice when the gap markers are spatially separated.

## The IGF-Receptor Pathway Associated Gene Expression Levels: Links with Age-Related Hearing Loss in CBA Mice

Mary D'Souza<sup>1,2</sup>, Amulya Penmetsa<sup>1</sup>, Xiaoxia Zhu<sup>1,2</sup>, Martha L. Zettel<sup>1,2</sup>, D. Robert Frisina<sup>1,2</sup>, Robert D. Frisina<sup>1,2</sup> <sup>1</sup>Univ. Rochester Med. School, <sup>2</sup>Int. Ctr. Hearing Speech Res., Nat. Tech. Inst. Deaf

This study's objective was to find the relationships of insulin growth factor (IGF) receptor expression levels in the cochlea and inferior colliculus (IC) and age-related hearing loss in CBA mice. Four groups of mice were included, defined by age and neurophysiological data, namely ABR thresholds and DPOAE amplitudes. The four subject groups were: Young Adult Controls, Middle aged with good hearing, and Old mice (>22 mon) with either Mild or Severe Presbycusis. The MOE430A Affymetrix GeneChip, comprised of 22,600 probe-sets for RMA analysis, yielded 38 probe-sets related to IGF-receptors. The 38 probe-sets in this family were furthermore subjected to statistical analysis: ANOVA, Linear regression of Gene chip data and DPOAE or ABR Threshold and GeneChip expression levels. Gene expression changes with a cut-off of above 2-fold change showed that IGFbinding protein 7 and IGF-2 receptor were statistically significant and revealed higher levels of expression with age and hearing loss. To date, the roles of these proteins in the aging auditory system have not been studied, although the IGF-1 null mouse model has been reported to have sensorineural hearing loss. We have also analyzed our GeneChip data expression profiles for a focused gene panel from a particular biological pathway, namely the IGF-receptor metabolic pathway. Genes coding for casein kinase, trafficking proteins, glutamine receptors, Jun and fos family members, transporters for sodium and chloride, the oncogene family ELK, MAP-kinase, SHC binding proteins, GRB and Sos family homolog show interesting age-related expression profiles. Our ongoing analyses include validating the pathway focused gene panel expression changes with quantitative real-time PCR data. A greater understanding of gene expression changes linked to age-related hearing loss allow for a better conceptualization of the molecular underpinnings of Presbycusis.

Supported by the Nat. Inst. on Aging and Nat. Inst. for Deafness and Communication Disorders, NIH.

## 754 Correlations Between ABR Thresholds and DPOAE Amplitude Level Shifts in CBA/CaJ Mice Become Stronger with Age

**Xiaoxia Zhu<sup>1,2</sup>**, Robert D. Frisina<sup>1,2</sup>
<sup>1</sup>Univ. Rochester Medical School, <sup>2</sup>Int. Ctr. Hearing

Speech Res., National Tech. Inst. Deaf Precise relations between age-related changes in auditory peripheral sensitivity, as measured by auditory brainstem response thresholds (ABRs) and the health and well-being of the outer hair cell system, as determined by distortion product otoacoustic emission levels (DPOAEs) remain elusive. For example, it is usually assumed that changes in the outer hair cell system precede overall sensitivity declines. This study's goal was to compare ABR threshold shifts (ABR TS) and DPOAE amplitude level shifts (DPOAE ALS) for young adult, middle-aged and old CBA/CaJ (CBA) mice. Young adult mice (N = 115, 1.5-4 month old [mo] ) had their hearing measured by ABRs (3-48 kHz) and DPOAEs (Geometric means: 5-45 kHz). These measurements served as baselines for comparison to each individual middle-aged (N = 126, 11-16 mo) and old (N = 86, 22-34 mo) mouse. Linear regressions (GraphPad Prism 4.0) were conducted to analyze the correlations between ABR TS and DPOAE ALS in different frequency bands for different ages. Results: significant correlation were observed between ABR TS and DPOAE ALS across all frequency ranges in middle-aged (F (1,124) = 4.219, p = 0.0421,  $r^2$  = 0.0329) and old CBAs (F (1,84) = 18.43, p < 0.0001,  $r^2$  = 0.1799). A significant correlation  $(F(1,124) = 5.319, p = 0.0228, r^2 = 0.04113)$  was present in the high frequency range (40-50 kHz) in middle-aged CBA mice. There were also significant correlations for all of the frequencies ranges covering the mouse audiogram in the old animals. This study demonstrates that the correlations between ABR TS and DPOAE ALS change with age becoming stronger in old age. In clinical diagnoses of age-related hearing loss - presbycusis, DPOAE level may be a useful diagnostic test, particularly for early detection of presbycusis in middle age subject groups.

Supported by the Nat. Inst. on Aging and Nat. Inst. for Deafness and Communication Disorders, NIH.

#### 755 F1 (CBA X C57) Mice Maintain Auditory Afferent Function with Age Despite Rapid Loss of MOC Efferent Feedback System Functionality

Matthew Bak<sup>1</sup>, Xiaoxia Zhu<sup>1,2</sup>, Robert Frisina<sup>1,2</sup>

<sup>1</sup>Univ. Rochester Medical School, <sup>2</sup>Int. Ctr. Hearing Speech Res., Nat. Tech. Inst. Deaf

Presbycusis – age-related hearing loss - is a ubiquitous problem affecting the majority of our elderly population. A similar age-related deterioration in hearing has been demonstrated in various strains of mice. Specifically, we

have discovered that CBA mice develop a functional decline in the medial olivocochlear (MOC) system prior to the classic worsening of auditory sensitivity, and deficits in outer hair cell function, that approximate age-related changes seen in many humans [Jacobson et al., Laryngoscope 113: 1707-1713, 2003]. The auditory functions of F1 mice, a hybrid between CBA and C57 mice, which undergo a rapid age-dependent hearing loss, were studied at three different ages: 3, 15 and 27 months. The MOC system was evaluated by recording distortionproduct otoacoustic emission amplitudes (DPOAEs) with and without contralateral suppression, OHC function was measured by recording DPOAEs, and the overall sensitivity of the afferent auditory system was assessed by ABR thresholds. Results demonstrated that F1 mice have early loss of function in the MOC system, like C57s, when compared to CBAs of equivalent age. However, F1 mice maintain auditory sensitivity with age and have superior ABR thresholds in old age compared to CBA mice. This is unlike previous CBA and C57 findings which suggested that declines in the MOC system precede ABR threshold and DPOAE deficits with age. The F1 data suggest that there may be less dependency of these processes in F1s, i.e., F1 mice maintain noteworthy afferent auditory function in old age despite early deficits in the MOC system. This makes the F1 strain a unique mouse model for presbycusis, but one that may be used to evaluate auditory efferent feedback system aging declines in the presence of good peripheral sensitivity.

Work supported by NIH: Nat. Inst. on Aging, Nat. Inst. for Deafness & Communication Disorders.

## | 756 | Exposure to an Augmented Acoustic Environment Alters GABA (GAD67) Levels in the IC and Al of Aged Mice with Presbycusis

Jeremy Turner<sup>1,2</sup>, Jennifer Parrish<sup>1</sup>, Loren Zuiderveld<sup>1,3</sup>, Stacy Darr<sup>1,2</sup>, Larry Hughes<sup>1</sup>, Donald Caspary<sup>1</sup>

<sup>1</sup>SIU School of Medicine, <sup>2</sup>Illinois College, <sup>3</sup>University of Illinois College of Medicine

Age-related hearing loss, presbycusis, is one of the most common ailments of the elderly. Presbycusis is often treated with hearing aids which serve to amplify some or all sound frequencies lost to peripheral hearing loss. However, hearing aids have mixed results in the elderly population because presbycusis, in addition to the peripheral hearing loss, involves age and deprivationinduced plastic changes to the central auditory system. As a result, reintroducing sound with a hearing aid does not necessarily (or immediately) restore normal hearing to the elderly listener. This delay in the effectiveness of hearing aids after fitting patients is frustrating for many hearing aid users and may result in rejection of the device in a subset of elderly patients. How this acclimatization process works is poorly understood, but it is likely that central plastic changes resulting from wearing hearing aids are involved. The current study examines neurochemical changes occurring in aged animals when exposed to an augmented acoustic environment (AAE). Aged CBA mice (22 mo, n=26) with presbycusis were either exposed to 6 weeks of low-level (70 dB SPL), broad-band noise stimulation (12 hrs/night) or normal vivarium conditions. The effects of the treatment were assessed by immunohistochemistry of GAD67 in the inferior colliculus (IC) and primary auditory cortex (AI). AAE treatment increased GAD67 levels in the IC of both male and female mice. However, in AI, AAE increased GAD67 labeling in females and decreased GAD67 in males. IC upregulation of GAD67 levels in response to increased acoustic input suggests that IC changes are consistent with what would have been predicted from previous aging studies. Neurochemical changes in Al are more complex. Nevertheless, these findings suggest that the aged auditory system retains neurochemical plasticity of the GABA system, suggesting that environmental stimulation might have significant affects on system function.

Supported by NIH grants AG023910 (JGT), DC00151 (DMC)

## | 757 | Muscarinic Signaling in Cochlear Function: Insight From Mice with Targeted Deletion of Receptor Subtypes

**Stéphane F. Maison<sup>1,2</sup>**, Jürgen Wess<sup>3</sup>, Neil M. Nathanson<sup>4</sup>, M. Charles Liberman<sup>1,2</sup>

<sup>1</sup>Harvard Medical School, <sup>2</sup>Massachusetts Eye & Ear Infirmary, <sup>3</sup>NIH-NIDDK, <sup>4</sup>University of Washington

Acetylcholine (ACh) is the major neurotransmitter of olivocochlear (OC) efferent neurons. OC effects on outer hair cells (OHCs) are mediated by  $\alpha 9/\alpha 10$  nicotinic ACh receptors (nAChRs). Mechanisms of OC effects on cochlear nerve fibers are less well characterized. Pharmacological, immunohistochemical and RT-PCR studies suggest that muscarinic (m) AChRs are present in both OHCs and cochlear ganglion cells, however, their in vivo function remains unclear. To assess the role of mAChRs, we are studying cochlear phenotypes in mice with targeted deletion of each mAChR (M1, M2, M3, M4 or M5, and a double knockout for M2/M4).

Cochlear thresholds and suprathreshold responses were normal in all knockouts, via ABR and DPOAE amplitude-vs-level functions. Cochlear histology was also normal, as assessed by light-microscopic evaluation of plastic-embedded sections. Medial OC function, assessed by measuring DPOAE suppression with OC electrical stimulation, was unaffected by loss of any receptor subunit. Correspondingly, the distribution of efferent terminals was normal in the knockouts, as assessed by immunostaining of cochlear whole mounts for the cholinergic marker, VAT.

The most striking phenotype was a significant reduction in acoustic injury observed in the M2/M4 double knockout, following exposure to either moderate noise levels, causing temporary threshold shifts, or to more intense levels causing permanent deficits, in wildtype littermates. The vulnerability differences were seen in both DPOAE and ABR metrics, suggesting that OHCs may be involved. Acoustic vulnerability is being assessed in all 5 single-knockout lines.

The suggestion that mAChR signaling increases noiseinduced damage is interesting given that nAChR signaling reduces acoustic injury [Maison et al, J Neurosci 22:10838, 2002], yet OC-mediated effects may include both protective and anti-protective components [Rajan, J Neurophysiol 86:3073, 2001].

Research supported by RO1 DC00188 and P30 DC05209.

#### | 758 | A Novel, Strychnine-Resistant, Cochlear Response Enhancement Evoked by Efferent Stimulation

**Stéphane F. Maison<sup>1,2</sup>**, Douglas E. Vetter<sup>3</sup>, M. Charles Liberman<sup>1,2</sup>

<sup>1</sup>Harvard Medical School, <sup>2</sup>Massachusetts Eye & Ear Infirmary, <sup>3</sup>Tufts University School of Medicine

The well-studied suppressive effects of efferent-mediated ACh release on cochlear responses such as DPOAEs or CAPs are mediated by  $\alpha 9/\alpha 10$  ACh receptors and are potently blocked by strychnine. Here, we report a novel, strychnine-resistant, efferent-mediated enhancement of CAPs and DPOAEs in anesthetized mice that is elicited by shock-evoked activation of the efferent bundle at the floor of the IVth ventricle.

In control experiments, efferent-mediated response enhancement is seen as a slow rise of DPOAE or CAP amplitudes to supranormal levels after recovery from the classic suppressive effects seen during a 60-sec epoch of efferent stimulation. The magnitude of enhancement could be as great as 10 dB, and tended to be greater for high-frequency stimuli. Post-shock enhancements have been observed, but were assumed to be an "overshoot" of the suppressive "slow" effect [Sridhar et al. 1995, J Neurosci 15:3667].

To assess the pharmacology of efferent-mediated enhancement, strychnine was injected and shock-evoked effects were monitored 5, 20, 35 and 50 min post injection. Strychnine at 3 mg/kg could eliminate suppressive efferent effects without affecting the slow response enhancement. After strychnine suppression blockade, DPOAE amplitudes rose to a peak within 5 sec after efferent-stimulation onset, maintained a constant level through the stimulation epoch and then slowly decayed back to baseline in ~100 sec.

Dose-response curves (data from 23 mice at 8 strychnine concentrations) suggest that suppression and slow enhancement arise from different mechanisms: the EC50 for blockade of suppressive effects was  $\sim 0.8$  mg/kg, 1.5 orders of magnitude lower than that for blockade of slow enhancement ( $\sim$ 20 mg/kg). Slow enhancements could be seen in mice with targeted deletion of the  $\alpha$ 9 ACh receptor subunit, further suggesting that nicotinic ACh receptors are not involved in this novel efferent effect.

Research supported by RO1 DC 188 (MCL), RO1 DC 6258 (DEV) and P30 DC 5029 (MCL).

### 759 Lateral Olivocochlear Efferents: ARole in Balancing Interaural Neuronal Excitability

**Keith Darrow**<sup>1</sup>, Stephane Maison<sup>2</sup>, Charles Liberman<sup>2</sup>

<sup>1</sup>MIT - Harvard Medical School, <sup>2</sup>Department of Otology and Laryngology, Harvard Medical School

Principal cells of the lateral superior olive (LSO) compute sound location based on interaural level differences that are initially coded as response-rate differences in fibers of the left and right auditory nerves. The LSO complex is also the origin of lateral olivocochlear (LOC) efferent neurons that innervate auditory nerve dendrites in the ipsilateral cochlea. LOC activation can either enhance or inhibit auditory nerve output, suggesting the LOC system may adjust neural excitability in the two cochleas to maintain the accuracy of sound localization [Groff and Liberman, J Neurophysiol 2003;90:3178-200].

Here, we explore LOC function *in vivo* via bilateral measurement of cochlear function after selective, unilateral destruction of LOC cell bodies by stereotaxic injection of neurotoxin. Lesion success was assessed histologically by bilateral analysis of brainstem sections and cochlear whole-mounts immunostained or histochemically reacted for cholinergic markers. Cochlear function was assessed by bilateral measurement of amplitude-vs.-level functions for ABRs and DPOAEs at 7 log-spaced frequencies.

Mice with successful LOC lesions showed selective loss of efferent terminals in the inner hair cell area, without change in the efferent innervation of outer hair cells. Physiologically, lesioned mice showed enhanced ABR amplitudes ipsilaterally and reduced ABR amplitudes contralaterally, without any interaural asymmetries in DPOAE thresholds or suprathreshold amplitudes. Whereas animals with intact LOC showed a tight interaural correlation in Wave-1 ABR amplitudes at all stimulus frequencies, cases with LOC destruction showed large interaural variability in neural response amplitudes. A simple model is presented to explain the results, whereby LOC neurons sample, with a slow integration time, the same ascending inputs contacting LSO principal cells, and send feedback signals to the auditory nerve to maintain an interaural balance in afferent excitability.

Research supported by T32 DC 00038, RO1 DC00188 and P30 DC05209.

## 760 Dual Function of the Lateral Olivocochlear Efferent Pathway in the Mammalian Cochlea

**Jerome Ruel<sup>1</sup>**, Regis Nouvian<sup>1</sup>, Guy Rebillard<sup>1</sup>, Michel Eybalin<sup>1</sup>, Jean-Luc Puel<sup>1</sup>

<sup>1</sup>INSERM U 583, INM, Hopital Saint Eloi, Montpellier, France

The efferent lateral olivocochlear (LOC) system, originating from the lateral superior olive, modulates the activity of afferent dendrites of primary auditory neurons below the sensory inner hair cells. The LOC innervation may use several neuroactive substances such as acetylcholine (ACh), GABA, dopamine (DA), enkephalins, dynorphins and calcitonin gene-related peptide. Most of

the data dealing with LOC efferent physiology come from the lesioning of the entire olivocochlear bundle or electrical stimulation of the inferior colliculus. The difficulty in interpreting these experiments led some authors to use a selective pharmacological approach to study LOC efferent function. Here, we demonstrated that LOC system can both excitate and inhibit the activity of auditory nerve fibers. In a first set of experiments, we analyzed the role of ACh which is present both in the LOC and medial olivocochlear (MOC) systems. Perilymphatic perfusions of ACh in presence of strychnine, which blocks the effect of the MOC system, increased the spontaneous and sound driven activities of single auditory nerve fibers showing that ACh has an excitatory role. In contrast, perilymphatic perfusions of DA, which is only present in the LOC system, has inhibitory effect on both spontaneous and sound driven activity of single auditory nerve fibers. In addition, perilymphatic perfusions of eticlopride, a selective D2 receptor antagonist, increased the spontaneous firing of auditory nerve fibres suggesting that the inhibition exerted by DA is tonic. Finally, perilymphatic perfusions of the selective DA transporter (DAT) inhibitors, i.e. nomifensine and BTCP, abolished the spontaneous and sound evoked activity of auditory nerve fibers while increasing the endogenous level of extracellular DA. In conclusion, ACh and DA may constitute a gain control acting at the initialization site of action potential to maintain the adequate firing of the auditory nerve fibers.

## | 761 | A Computer Model of Medial Efferent Activity in the Auditory Periphery

Robert Ferry<sup>1</sup>, Ray Meddis<sup>1</sup>

<sup>1</sup>Univeristy of Essex

At present little is known about how the efferent system modifies the response of the auditory system. To aid our understanding of the role the medial efferent system plays in auditory perception we extended the functionality of an existing computer model of the mammalian auditory periphery to include the effect of stimulating descending fibers of the olivocochlear bundle (OCB). To implement this effect we improved upon the architecture of an existing phenomenological model of basilar membrane mechanical filtering. The modified model simulates the effect of efferent suppression by applying a level attenuation to the signal in only the nonlinear path of the system. Signals that pass predominantly through the linear path of the system are not subject to this attenuation.

The model was evaluated using two different sets of physiological data; one at the level of the basilar membrane (Russell and Murugasu, 1997, JASA 100:1680) and the other at the level of the auditory nerve (Guinan and Stankovic, 1996, JASA 102:1734). It is demonstrated that the improved model reliably simulates the main effects observed in these physiological measurements. These model results, and hence, the physiological data are consistent with the hypothesis that a given level of medial efferent activity results in a fixed attenuation of the input signal in the nonlinear path irrespective of the signal level. As a consequence, tuning curves become shallower when the medial efferent system is stimulated.

### 762 Kir5.1 Channels in the Stria Vascularis of the Mouse Inner Ear

**Liping Nie<sup>1</sup>**, Amy Liao<sup>2</sup>, Michael Anne Gratton<sup>2</sup>, Jun Zhu<sup>1</sup>, Ebenezer N Yamoah<sup>1</sup>

<sup>1</sup>University of California, Davis, The Center for Neuroscience, 1544 Newton Ct, Davis,CA 95618, <sup>2</sup>University of Pennsylvania, Department of

Otorhinolaryngology-HNS 3400 Spruce St. Philadephia The endocochlear potential (EP) is indispensable for normal sound transduction. The cochlear hair cells utilize the EP to overcome intrinsic membrane noise to obtain their exquisite sensitivity. It is generally believed that the stria vascularis (StV) plays a fundamental role in the generation of EP. Here, we demonstrate that Kir5.1 is expressed abundantly in the mouse StV. Using customdesigned antibodies, we show that Kir5.1 channels are highly expressed in the basal cells of the StV as well as in the intermediate cells, where they are co-expressed with Kir4.1 channels. Overall, the expression level of Kir5.1 in the intermediate cells is much lower than that in the basal cells and than that of Kir4.1 in the intermediate cells. Since Kir4.1 channels play a role in the generation of the EP and because the channel forms a functional heteromeric channels with Kir5.1, the co-localization of these Kir4.1 and Kir5.1 channels in the intermediate cells suggests that Kir5.1 may contribute towards the generation of EP in the mouse inner ear. In addition, our results showed robust expression of Kir5.1 channels in the basal cells of the StV. where they may play a unique role in the K+ cycling. Furthermore, we have cloned the gene encoding Kir5.1 in the cochlea (Genbank accession # AY377989) and the functional study of Kir5.1 and Kir4.1/5.1 in the heterologous expression systems has been performed. We will discuss the detailed biophysical properties of Kir5.1 current and their regulation by Kir4.1. Our finding suggests that specific K+ channels operate intimately together to confer their roles in the StV.

This work was supported by grants to LN (NOHR Foundation), to ENY NIH-DC03828, DC04523 and to MAG NIH-DC 006442.

### Ganglion Neurons

Sara Euteneuer<sup>1,2</sup>, Kuo-Hsiung Yang<sup>3</sup>, Kwang Pak<sup>1</sup>, Stephen Fausti<sup>4</sup>, Stefan Dazert<sup>2</sup>, Allen F. Ryan<sup>1,5</sup>

<sup>1</sup>UCSD, Department of Surgery/Otolaryngology and VA Medical Center, La Jolla, CA, USA, <sup>2</sup>Department of Otolaryngology, Ruhr-University Bochum, School of Medicine, Germany, <sup>3</sup>UCSD, Department of Biology, La Jolla, CA, USA, <sup>4</sup>National Center for Rehabilitative Auditory Research, Portland VA Medical Center, Portland, OR, USA, <sup>5</sup>UCSD, Department of Neurosciences, La Jolla, CA, USA

Introduction: Glial cell line-derived neurotrophic factor (GDNF) has been shown to protect mammalian spiral ganglion (SG) neurons in vivo after loss of inner hair cells, as well as to support SG neuron survival in vitro. GDNF binds to a co-receptor, GFRa1, which lacks an intracellular signaling domain and therefore must partner with a transmembrane receptor. One such partner is Ret (rearranged during transformation). However NCAM

(neuronal cell adhesion molecule) has more recently been identified as an alternate GDNF receptor. We are studying the potential roles of Ret and NCAM in cochlear GDNF signaling.

Methods: Inner ear morphology was evaluated in newborn Ret and adult NCAM knock-out mice. ABRs were measured in NCAM knockouts. Western blotting was used to evaluate phosphorylation of Fyn, a downstream adaptor of NCAM, in adult rat SG explants exposed to GDNF. GDNF interaction with GFRa1 was evaluated in neonatal and adult rat SG explants.

Results: Preliminary results suggest normal development of the cochlea in both Ret and NCAM knockout mice, at the ages studies to date. Western Blotting indicated that Fyn is activated by GDNF. Addition of exogenous GFRa1 enhanced the effects of GDNF on both neonatal and adult SG neurons.

Discussion: The results to date are consistent with GDNF signaling via GFRa1 and NCAM in SG neurons,but they also indicate that NCAM is not necessary for normal cochlear development. Evaluation of SG explants from Ret and NCAM knockout mice will help to elucidate the roles of each receptor in GDNF signaling.

Supported by NIH/NIDCD grant DC00139 (AR), the Medical Research (AR) and Rehabilitation Research and Development Services of the VA (AR, SF), and the German DFG grant EU 120/1-1(SE).

### 764 P2X Receptor Knockout Mice Exhibit Altered Hearing Function

**Gary D. Housley**<sup>1</sup>, Srdjan M. Vlajkovic<sup>1</sup>, Peter R. Thorne<sup>1</sup>, Rachel T. Morton-Jones<sup>1</sup>, Baljit S. Khakh<sup>2</sup>, Debra A. Cockayne<sup>3</sup>, Allen F. Ryan<sup>4</sup>

<sup>1</sup>University of Auckland, New Zealand, <sup>2</sup>University of California, Los Angeles, <sup>3</sup>Roche, Palo Alto, <sup>4</sup>University of California, San Diego

P2X receptor subunits assemble as homomeric or heteromeric trimers to form ATP-gated ion channels. These ion channels can be activated via ATP release involving autocrine/paracrine P2X<sub>2</sub> neurotransmission/neuromodulator signaling. receptor subunit expression in the cochlea is known to be broadly distributed to the hair cells, other epithelial cells lining the cochlear partition, as well as the spiral ganglion neurons. In contrast P2X3 receptor expression in the cochlea is primarily neuronal. In order to investigate the functional significance of these purinoceptor signaling pathways on cochlear function in vivo, we have utilized transgenic mouse null and double null mutations for the P2X<sub>2</sub> and P2X<sub>3</sub> receptors. Auditory brainstem responses (ABR) and distortion product otoacoustic emissions (DPOAE) revealed differences in integrated cochlear performance under ambient sound conditions and with noise-induced threshold shifts, compared with wildtype controls, which varied for the three different mouse lines. Cellular electrophysiology of epithelial cells and spiral ganglion neurons obtained from the cochlear tissue of the null mutant mice showed differences in membrane conductances to application of ATP and P2X receptorselective agonists compared with wildtype controls, which may reconcile the alterations in ABR and DPOAE

responses of the P2X receptor null mice. The study provides physiological evidence for intrinsic purinergic regulation of hearing under normal and noise-stress conditions.

Support: Health Research Council of New Zealand, U.S. Dept of Veterans Affairs – Medical Research Service, Marsden Fund and James Cook Fellowship (Royal Society NZ).

### 765 Localization of Alpha 1 Adrenergic Receptors in the Gerbil Inner Ear

**Claudius Fauser**<sup>1</sup>, Andrea Lohner<sup>1</sup>, Simone Kaiser-Moore<sup>1</sup>, Heike Weikhardt<sup>1</sup>

<sup>1</sup>Klinik of the Technical University Munich

The inner ear has an extended sympathetic innervation and appears to be influenced by sympathetic stimulation. In a previous study we demonstrated that the beta 1 and 2 adrenergic receptors are located in various cells of the inner ear (Fauser et al., J.Membr.Biol. 201, 25-32, 2004).

The objective of the present study was to localize the alpha 1 adrenergic receptor ( $\alpha_1$  AR) in inner ear tissues. Therefore, immuno-histochemical-staining and RT-PCR were performed.

Paraffin sections were prepared from decalcified, formalin perfusion-fixed gerbil temporal bones.  $\alpha_1$  AR were detected by a polyclonal anti- $\alpha_1$  AR-antibody and visualized with biotinylated secondary antibody. RT-PCR for the three subtypes A, B, and D of the  $\alpha_1$  AR were performed on four complete inner ears.

Light microscopy examination revealed prominent and consistent immunostaining for  $\alpha_1$  AR in type I and II spiral ganglion cells, the organ of Corti. Weaker staining was found in the stria vascularis as well as sensory cells of the untricle and the ampullas. RT-PCR demonstrated the presence of  $\alpha_{1A}$  and  $\alpha_{1D}$  AR, but not  $\alpha_{1B}$  AR RNA in inner ear tissue

In a previous study functional  $\alpha_{1A}$  AR were found to be the cause of vasoconstriction in the spiral modiolar artery.

Our data revealed  $\alpha_1$  AR localized in sensory and non-sensory cells of the cochlea and the vestibular organ. Their function remains unknown.

Supported by KKF 8758168

## 766 Adrenergic Innervation of the Organ of Corti: Expression of Adrenergic Receptor Transcript and Protein

Ryan Berecky<sup>1</sup>, Marian J. Drescher<sup>1</sup>, Dennis G. Drescher<sup>1</sup>, Khalid M. Khan<sup>2</sup>, James S. Hatfield<sup>3</sup>

<sup>1</sup>Wayne State University School of Medicine, <sup>2</sup>Kuwait University, <sup>3</sup>John D. Dingell VA Medical Center

The existence of adrenergic pathways subserving the organ of Corti (OC) was suggested by immunostaining for dopamine  $\beta$ -hydroxylase (DBH), the enzyme of synthesis of norepinephrine (Drescher et al., Neuroscience 142:139-164, 2006). Adrenergic receptors (AR), mediating the response to adrenergic input, are present within the OC as defined by immunoreactivity (Khan et al., ARO Abstr. 29: 300, 2006). The immunoreactivity can derive from both

receptor protein expressed by cells comprising the OC as well as from neural receptor protein transported to the OC from distant cell bodies of putative adrenergic, afferent or efferent pathways. Indeed, new immunocolocalization studies from our laboratory suggest overlap of AR receptor protein and DBH within the OC for the apical and upper middle turns of the rat cochlea. Further, β1 and β2 ARimmunoreactive nerve fibers have been traced from the spiral limbus, a putative source of DBH-positive nerve fibers, to the habenula perforata. We have now applied RT-PCR to microdissected cochlear subfractions to unequivocally determine whether transcripts for ARs are expressed by cells comprising the OC. Transcripts for β1 and  $\beta 2$  ARs were detected in the OC subfraction, which has been morphologically documented as containing primarily hair cells and supporting cells. In addition, \( \beta 1 \) and  $\beta 2$  AR transcripts were found in spiral ganglion and lateral wall cochlear subfractions. Transcript for  $\alpha$ 1 AR was not found in either the OC or spiral ganglion subfraction, but  $\alpha$ 1 AR cDNA was amplified from the lateral wall subfraction. These results are consistent with a postsynaptic presence of  $\beta 1$  and  $\beta 2$  AR on hair cells/supporting cells and a presynaptic expression of  $\alpha 1$  AR by adrenergic nerve fibers within the OC. Apical synapses on the outer hair cells, observed for the apical and upper middle turns in non-primates and in all cochlear turns for primates, are hypothesized to be a site of adrenergic input.

## 767 Effect of Estrogen Substitution on Estrogen Receptors in the Inner Ear

**Rusana Simonoska**<sup>1</sup>, Annika Stenberg<sup>1</sup>, Lena Sahlin<sup>2</sup>, Malou Hultcrantz<sup>1</sup>

<sup>1</sup>Dept of Otorhinolaryngology, KNV, Karolinska University Hospital and Institute, <sup>2</sup>Dept of women and child health, Karolinska Institute

Background: Older women in the normal population, tend in menopause to develop more severe hearing loss compared to males. In Turner Syndrome (loss of one X chromosome), ear and hearing problems are common among these patients and affects outer, middle and inner ear. Middle-aged Turner women frequently complain of a rapid onset of social hearing problems, due to pre-aging of the ear (presbyacusis).

In our previous study done on pregnant rats we showed that estrogen receptors vary during different stages of pregnancy and maturation.

Can substitution with estrogens have an impact on the estrogen receptors in the inner ear?

Aim: The effect of selective and non-selective estrogen substitution on estrogen receptors in the inner ear in rats. Methods: Four different groups of rats have been substituted with different substances: non-selective estrogen agonist, selective estrogen agonists (alpha and beta respectively) and saline (for control). All specimens were stained immunohistochemically for estrogen receptors, both alpha and beta.

Results: Estrogen receptors content and localisation differ in these 4 groups.

Conclusion: Estrogen receptors are present in the inner ear and are up- or down regulated depending on the type of estrogen the rats received.

#### 768 Expression of KCNQ1/KCNE1 K+ Channels and P2Y4 Receptors in Strial Marginal Cells During Development

**Jun Ho Lee**<sup>1</sup>, Dong-Gu Hur<sup>2</sup>, Jeong-Hwa Heo<sup>2</sup>, Ja-Won Koo<sup>1</sup>, Sun O. Chang<sup>2</sup>, Chong-Sun Kim<sup>2</sup>

<sup>1</sup>Seoul National University Bundang Hospital, <sup>2</sup>Seoul National University Hospital

This study was conducted to investigate expression of KCNQ1/KCNE1 K+ channels and P2Y4 receptors in the developing rat strial marginal cells (SMCs) using a voltagesensitive vibrating probe and immunohistochemistry. The chromanol 293B, a blocker of KCNQ1/KCNE1 K+ channel, inhibited short-circuit currents (Isc) from postnatal day 1 (P1) to P21 SMCs. Similarly, the lsc were found to be decreased by uridine 5'-triphosphate at all ages. The ineffectiveness of suramin and pyridoxalphosphate- 6azophenyl-2',4'-disulfonic acid to block the action of UTP indicated that the apical P2Y receptor is P2Y4. The immunoreactivity for KCNQ1, KCNE1, and P2Y4 was found at P1 stria vascularis, respectively. In conclusion, KCNQ1/KCNE1 K+ channels are expressed before achievement of the adult-like endolymphatic ion composition, and the coincidence of P2Y4 receptors might have a role in protection for immature hair cells against noise exposure.

### 769 TRPA1 in Supporting Cells of Inner Ear Epithelia

**Andrew Castiglioni**<sup>1</sup>, Anne Duggan<sup>1</sup>, Jaime Garcia-Anoveros<sup>1</sup>

<sup>1</sup>Northwestern University

TRPA1 is expressed in sensory epithelia of the inner ear and in nociceptive neurons. Despite similar biophysical properties between heterologous TRPA1 channels and the hair cell transducer, as well as functional evidence from TRPA1 knockdown experiments (Corey et al, 2004; Nagata et al, 2005), mice with a pore domain deletion in TRPA1 have altered nociception but no defects in hearing or hair cell transduction (Bautista et al, 2006; Kwan et al, 2006). Therefore, the functional role of TRPA1 in cells other than somatosensory neurons remains unclear. Previous experiments reported low levels of TRPA1 mRNA and TRPA1 protein in auditory and vestibular hair cells (Corey et al, 2004; Nagata et al, 2005). These experiments also show TRPA1 mRNA expressed at higher levels in the surrounding support cells. Here we characterize the expression pattern of TRPA1 protein in auditory and vestibular sensory epithelia of mouse as well as mechanosensory organs of nematodes. Using our antibody raised against the N-terminus of mouse TRPA1, we find TRPA1 protein expressed in support cells of vestibular epithelia as well as in supporting Deiters' and pillar cells of the organ of Corti. Expression in support cells is greater than in hair cells and is restricted to lateral apical regions closest to adjacent hair cells. TRPA1 is highly conserved across species and C. elegans express their TRPA1 ortholog in mechanosensitive and nociceptive organs. Interestingly, ciliated sensory neurons and their associated support cells as well as support cells of the mechanosensory male tail express ceTRPA1. The

expression of TRPA1 in supporting cells of mechanosensory organs appears conserved and may be ancient.

Supported by DC006089, NS044363 (JGA), and NS041234 (AJC).

## 770 Differential and Developmental Expression of Potassium Currents in Deiters Cells of the Gerbil Cochlea

Xiang Wang<sup>1</sup>, David He<sup>1</sup>

<sup>1</sup>Department of Biomedical Sciences, Creighton University School of Medicine, Omaha, NE 68178

Supporting cells in the organ of Corti of mammalian cochleae are thought to play an important role in maintaining cochlear homeostasis for the normal functioning of sensory hair cells and auditory neuronal terminals. It was proposed that cochlear supporting cells could take up potassium ions released from the hair cells during mechanosensory transduction process and recycle them back to the endolymph through gap junctional systems in the cochlea. Recent studies indicate that supporting cells can be transformed into hair cells through transgenic manipulations. Thus, understanding the physiological function of supporting cells has become essential for elucidating the cochlear homeostasis as well as the hair cell regeneration. In this study, we investigated the electrical properties of the isolated Deiters cells (DCs) from both adult and neonatal gerbil cochleae using wholecell voltage clamp techniques. We tried to determine whether the potassium conductance is differentially expressed along the cochlea. We also wanted to determine whether the potassium conductance undergoes developmental changes before and after the onset of hearing. Gerbils ranging in age from 4 and 30 days after birth were used for the experiments. Our results show that the maximum currents of the Deiters' cells are uniform along the cochlea. Potassium conductance also underwent significant changes between 4 and 10 days after birth. The Deiters' cells reached adult-like responses at 10 days after birth, just before the onset of hearing. (Supported by NIH grant DC 004696).

# 771 Pattern of Connexin26 Expression in the Cochlea Demonstrated by Transgenic Expressions of Egfp From a Modified Bacterial Artificial Chromosome (BAC)

**Shoeb Ahmad**<sup>1</sup>, Wenxue Tang<sup>1</sup>, Yan Qu<sup>1</sup>, Jones Chonnettia<sup>2</sup>, Ping Chen<sup>2</sup>, Xi Lin<sup>1</sup>

<sup>1</sup>Department of Otolaryngology, Emory University School of Medicine, <sup>2</sup>Department of Cell Biology, Emory University School of Medicine

Genetic studies reveal vital roles for gap junctions (GJs) in the cochlea. However, the pathogenesis of deafness due to mutations in connexins (Cxs, which is the building block of GJs) remains obscure. We and others have shown that most cochlear GJs are formed from heteromeric assemblies of Cxs26 & 30. Similar to phenotypes found in human, absence of either Cx26 or Cx30 gene in mice

results in deafness. Our previous work showed that restoring protein level of Cx26 by a genetic approach to its wild type level rescued the hearing sensitivity of Cx30 knockout mice, indicating Cx26 expressed along at appropriate levels is sufficient for normal hearing.

We are currently pursing the rescue of hearing in Cx26 conditional knockout mice by genetically over expressing the Cx30 gene through transgenic expressions of extra copies of Cx30 from a modified bacterial artificial chromosome (BAC) containing genes for both Cxs 26&30. To avoid over-expressing Cx26, we replaced its coding sequence in the BAC with a reporter gene (eGFP). Pronuclear injections of the modified BAC in oocytes of FVB mice resulted in 5 founder mice (BAC<sup>Cx26/eGFF</sup> that carried extra copies of Cx30 gene. Since eGFP in the BAC is under the control of Cx26 specific regulatory mechanisms, the eGFP fluorescence in BAC<sup>Cx26/eGFP</sup> mice is expected to be an indicator of the temporal and spatial patterns of Cx26 expression. Our preliminary data showed developmentally-regulated expression fluorescence in the cochlea, liver, skin and kidney. In the skin of neonate mouse pups, brightest fluorescence was observed in tail tips and body extremities. In cochlear sections, eGFP expression showed a developmentallyregulated pattern consistent with our previous data obtained by immunolabeling (Sun et al., 2005, Am J Physiol). These  $BAC^{Cx26/eGFP}$  mice will be used to cross with the Cx26 conditional knockout mice to test whether their hearing could be rescued by genetically overexpressing Cx30. Permanent cell lines derived from the cochleae of BAC<sup>Cx26/eGFP</sup> mice will also help us studying the molecular mechanisms regulating the cochlear expression of Cx26.

## 772 Sole and Concerted Performances of Cx26 and Cx30 in the Cochlear Sensory Epithelium

Hong-Bo Zhao<sup>1</sup>, Ning Yu<sup>1</sup>

<sup>1</sup>University of Kentucky Medical Center

Gap junctional coupling in the cochlea is crucial for mammalian hearing. Connexin26 (Cx26) and Cx30 are predominant isoforms of gap junction channels in the cochlear sensory epithelium. In this study, the cellular distributions of Cx26 and Cx30 in the cochlear sensory epithelium of guinea pigs were examined immunofluorescent staining and confocal microscopy in whole-mount of the cochlear sensory epithelium and dissociated cell preparations. The expression of Cx26 and Cx30 demonstrated a longitudinal gradient distribution in the epithelium and was reduced 3-fold from the cochlear apex to base. The reduction was more pronounced in the Deiters cells and pillar cells than in the Hensen cells. Cx26 was expressed in all types of supporting cells, but little Cx30 labeling was seen in the Hensen cells. Cx26 expression in the Hensen cells was mainly concentrated in the 2nd and 3rd rows, forming a distinct band along the sensory epithelium at its outer region. In the dissociated Deiters cells and pillar cells, Cx30 showed dense labeling at the cell bodies and processes in the reticular lamina. Cx26 labeling largely overlapped that of Cx30 in these regions. Cx26 and Cx30 were also co-expressed in the gap junctional plaques between Claudius cells. Neither Cx26 nor Cx30 labeling was seen in the hair cells and spiral ganglion neurons. These observations demonstrate that Cx26 and Cx30 have a longitudinal gradient distribution and distinct cellular expression in the auditory sensory epithelium. This is in consistence with patch clamp recording and dye uptake assay that Cx26 and Cx30 can solely and concertedly perform different functions in the cochlea.

Supported by NIH DC05989

## 773 Quantitative Analysis of Connexin26 and Connexin30 Expressions in the Lateral Wall of the Mammalian Cochlea

Ying-Peng Liu<sup>1</sup>, Hong-Bo Zhao<sup>1</sup>

<sup>1</sup>University of Kentucky Medical Center

Gap junction is crucial for hearing function. Connexin26 (Cx26) and Cx30 are the major isoforms of gap junction channels in the cochlea. Gap junctional coupling extensively exists in non-sensory cells in the cochlea and forms two gap junctional systems: the epithelial gap junctional network between the cochlear supporting cells in the auditory sensory epithelium, and the connective tissue gap junctional network between the stria vascularis (SV) and spiral ligament (SPL) in the cochlear lateral wall. In this study, the expressions of Cx26 and Cx30 in the connective tissue gap junctional network in different species (mouse, rat, and guinea pig) were examined by Western blot analysis and immunofluorescent staining. We found that the expressions of Cx26 and Cx30 in the SPL were higher than in the SV in all three-examined species. The expression of Cx26 in the SPL was 1.81±0.45, 1.88±0.3, and 7.86±1.82-fold higher than in SV in mouse, rat and guinea pig, respectively. The ratio of Cx30 expression at the SPL to the SV was 2.87±0.59, and 3.43±0.58-fold. Immunofluorescent staining of SV and SPL for Cx26 and Cx30 showed that Cx26 and Cx30 were strong and co-expressed in the SV and SPL. However, sole expression of Cx26 and Cx30 was also visible. In the SPL, the staining showed that Cx26 and Cx30 were almost uniformly distributed over the epithelium. Our date indicate that Cx26 and Cx30 have distinct expressions at the SV and the SPL in the cochlear lateral wall. The data also reveal that the expressions of Cx26 and Cx30 in the cochlea have differently expressive levels in different species.

Supported by NIDCD DC 05989.

# 774 Molecular and Functional Characterisation of Connexin 26 and Connexin 30 Gap Junctions in the Avian Inner Ear

**Regina Nickel**<sup>1</sup>, Daniel Jagger<sup>1</sup>, Andrew Forge<sup>1</sup>
<sup>1</sup>Centre for Auditory Research, UCL Ear Institute, University College London

Supporting cells in the avian inner ear are extensively coupled by gap junctions, which are permeable for large

anionic fluorescent tracers, such as calcein (MW 623, -4). This is in contrast to the hearing cochlea, in which the presence of heteromeric Cx26/Cx30 gap junction channels impairs the transfer of such molecules. Here, we have examined the expression patterns and functional properties of the inner-ear specific chicken connexin 30 (cCx30) and a newly identified chicken connexin with a predicted molecular weight of 26 kDa, called cCx26.

In situ hybridisation showed that cCx30 and cCx26 transcripts were both widely expressed in the cochlear duct and utricle in an overlapping pattern, suggesting coexpression of these isoforms similar to that in the mammalian inner ear. To verify the presence of both connexin proteins in inner-ear gap-junction plaques, isoform-specific antibodies for cCx30 and cCx26 were generated. Immunohistochemistry confirmed the presence of cCx30 and cCx26 in supporting cells of the auditory and vestibular sensory epithelium, and in the ion-transporting epithelia of the chick inner ear.

The functional properties of cCx26 and cCx30 gap junctions were examined in HeLa cells expressing cCx26-GFP and cCx30-DsRed constructs. The fluorescently tagged connexins were transported to the cell membrane and formed functional gap junction as demonstrated by a dye coupling assay, in which Lucifer yellow (LY; MW 457, -2) and Neurobiotin (NB; MW 323, +1) were co-loaded into single HeLa cells during whole-cell patch recordings. Preliminary results showed that cCx26-GFP gap junctions were permeable for NB but not LY. Unlike mammalian Cx30, cCx30-DsRed gap junctions transferred both LY and NB and may thus account for the diffusion of large anionic molecules among the supporting cell syncytium in the avian inner ear. The dye coupling properties of HeLa cells co-expressing cCx26 and cCx30 are currently being investigated.

Supported by the BBSRC and the Royal Society.

# T75 Unitary Permeability of Cochlear Gap Junction Channels to Second Messengers Measured by FRET Microscopy and Dual Whole-Cell Current Recordings

**Victor Hernandez**<sup>1</sup>, Mario Bortolozzi<sup>1</sup>, Vanessa Pertegato<sup>1</sup>, Martina Beltramello<sup>1</sup>, Manuela Zaccolo<sup>1,2</sup>, Sergio Pantano<sup>1,3</sup>, Fabio Mammano<sup>1,3</sup>

<sup>1</sup>Padova University - V.I.M.M., <sup>2</sup>Dulbecco Telethon Institute, <sup>3</sup>CNISM

In the inner ear, gap junction channels composed of proteins from the connexin (Cx) family connect the cytoplasm of adjacent cells to allow for intercellular transfer of ions and metabolites. Abnormal or impaired connexin function has been linked to several diseases, including skin disease, cataracts and peripheral neuropathies. In particular, defective permeation of cAMP through gap junctions has been hypothesized to underlie certain forms of X-linked Charcot-Marie-Tooth (CMTX) disease, whereas InsP3 permeability defects have been recently implicated in genetic deafness. We have developed a new, fast and accurate method to estimate quantitatively the permeability of single human connexin

26 wt gap junction channels (HCx26wt) to these second messengers. The method is based on combined measurements of junctional conductance by dual patch clamp recordings and FRET microscopy of biosensors selective for cAMP and InsP3. Measurements of unitary permeability to Lucifer Yellow (LY), a fluorescent tracer widely used to assay the permeability of gap junction channels, gave permeability ratios 6.7 for cAMP/LY and 8.1 for InsP3/LY . The results are analyzed in terms of an all-atom model of the wild type human connexin 26 connexon, suggesting that permeation of InsP3 is facilitated by specific interaction with pore-lining residues.

# | 776 | Characterization of Cochlear Pericytes and Effects of Loud Sound on the Expression of Contractile Proteins in the Guinea Pig Lateral Wall

**Xiaorui Shi**<sup>1</sup>, Dennis R. Trune<sup>1</sup>, Alfred L. Nuttall<sup>1,2</sup>
<sup>1</sup>Oregon Health & Sciences University, Oregon Hearing Research Center, <sup>2</sup>Kresage Hearing Research Institute, The University of Michigan

Vascular pericytes express various proteins, including contractile and non-contractile filaments play important roles for many organs in the regulation of local blood perfusion. We sought to clarify the role of pericytes in cochlear blood flow, and its involvement in noise induced hearing loss. Using the nitric oxide probe, DAF-2DA and immunohistochemistry, we identified and characterized pericytes in the cochlear lateral wall microvasculature of the guinea pig. Three types of pericytes are distributed at lateral wall vessels. Type I pericytes, with fusiform shape and a few long processes along the capillary, were found on the capillaries of both the spiral ligament (SL) and stria vascularis Type II pericytes had (SV). circumferential band-like processes encircling vessels. They were found in the pre-capillary arterioles near scala vestibuli. Type III pericytes had a flattened cell body and short, irregular processes and were found at the venular cochlear side of the lateral wall. immunohistochemically detected the change in expression of alpha-smooth muscle actin (á-SMA) and desmin under unstimulated and loud sound stimulated (LSS) conditions. á-SMA and desmin immunolabel was strong for Types II and III. Type I pericytes in the SL labeled for desmin and á-SMA. Type I pericytes in the SV, only weakly labeled for desmin and not á-SMA at all. Pericyte-related, noncontractile proteins NG2 and calcitonin gene-related peptide, were seen on all types of pericytes. LLS was 3 hours/day to broadband noise at 122 dB SPL for 2 consecutive days. Increased immunoreactivity for desmin was seen on the vessels of the SL and the SV. Detachments of the pericyte long processes were frequently seen on some vessels of the SL. RT-PCR analysis showed mRNA expression for desmin was significantly increased after LSS. Results indicate that the function or sensitivity of pericytes may be heterogeneous in the two vascular systems and they have the molecular components for contraction and mechanical support. Changes of pericyte contractile intermediate filaments may indicate an active part in LSS cochlear pathology.

Supported by NORH 2005 and NIH NIDCD grant R01 DC00105.

### 777 Application of Proteomics to Human Temporal Bone Research

**Saumil Merchant**<sup>1,2</sup>, Bryan Krastins<sup>2</sup>, Darryl Erik Palmer-Toy<sup>3</sup>, Jennifer O'Malley<sup>1</sup>, Joe Adams<sup>1,2</sup>, Joseph Nadol Jr. <sup>1,2</sup>, David Sarracino<sup>2</sup>

<sup>1</sup>Massachusetts Eye and Ear Infirmary, <sup>2</sup>Harvard Medical School, <sup>3</sup>Kaiser Permanente

Proteomic assays, which enable the rapid identification of hundreds of proteins from extremely small tissue samples such as histological sections, offer great potential for improving our understanding of otologic disorders. However, proteomic studies have thus far been conducted on unfixed (frozen) sections. We recently described a protocol to successfully retrieve proteins from the cochlea from paraffin-embedded human temporal bones (Palmer-Toy et al, J Proteome Research, 2005;4:2404)

We have since extended our technique to bones embedded in celloidin or polyester wax. Cochlear tissue was first manually microdissected. Celloidin was removed using ether-alcohol, and polyester wax using ethanol. Proteins were digested with trypsin, followed by liquid chromatography and mass spectrometry to generate peptide fragmentation patterns. Proteins were identified by matching the peptide fragmentation patterns with on-line databases of human proteins. Experiments were performed on 30 unstained archival sections that had been stored in alcohol up to 4 years.

Proteins were successfully retrieved from sections embedded in celloidin, polyester wax or paraffin. Over 230 unique proteins were identified from a normal cochlea, including cochlin, vimentin, cytokeratins, neurofilaments, tubulin, collagens, myosin, cadherin, and ion channel proteins. The protocol enabled retrieval of proteins from tissue comprising only 2-3 histological sections. Future studies will focus on understanding sources of variability and improving on current rates of retrieval.

In summary, proteomic analysis can be performed successfully on fixed and embedded archival human temporal bone sections. Proteomic approaches hold promise to advance our understanding of the normal and the diseased ear. Our method is non-proprietary, and can be applied to any fixed and embedded tissue contained in collections of departments of pathology.

Supported by NIDCD

### | 778 | Molecular Mechanisms of Cell Death in the Cochlea of Connexin30 Knockout Mice

**Wenxue Tang<sup>1</sup>**, Yan Qu<sup>1</sup>, Qing Chang<sup>1</sup>, Shoeb Ahmad<sup>1</sup>, Ping Chen<sup>1</sup>, Xi Lin<sup>1</sup>

<sup>1</sup>Dept of Otolaryngology, Emory University School of Medicine

Mutations in connexin30 (Cx30) gene are linked to human inherited non-syndromic deafness. The most commonly found Cx30 mutation is deletion mutation (e.g., GJB6-D13S1830) that effectively eliminate gene expression.

Targeted deletion of Cx30 coding sequence in mice (Cx30 mice) results in a total loss of endolymphatic potential (EP), hair cell loss and deafness (Teubner et al., 2003). We have used this mouse model to investigate the molecular mechanisms of cell death in the cochlea.

Whole-mount cochlear preparations immunolabeled with myosin6 made at various postnatal stages indicated little hair cell death at P18 when hearing loss was significant enough to prevent these animals from hearing most of the ambient noises. TUNEL staining, however, showed apoptosis in many supporting cells at P18. The time course of hair cell death in individual Cx30<sup>-/-</sup> mouse was highly variable. In general, complete hair cell loss took at least 4 months starting from basal and spreading to the apical regions. These data suggested that hair cell death in the cochlea of Cx30<sup>-/-</sup> mice happened largely in the absence of any sound-driven transducing activities. In searching for underlying molecular mechanisms responsible for hair cell death, we have examined expressions of a family of 14 facilitative glucose transporters (GLUTs) in the cochlea by microarray, quantitative PCR, Western blotting and immunolabeling approaches. Results showed that GLUT1 and GLUT10 had the highest expressions in the cochlea. immunostaining localized GLUT 10 to the reticular lamina of both inner and outer hair cells, GluT1 was highly expressed in endothelial cells lining microvessels and some fibrocytes near stria vascularis. Cells depend on a constant supply of glucose to serve as the predominant source of ATP generation, which is the major cellular energy source. Failure to detect major GLUT combined with data showing high-density expression of connexins in supporting cells suggested that glucose transport in supporting cells critically depends on normal function of gap junctions (GJs). Comprises to GJ-mediate intercellular glucose transport towards supporting cell may starve these cells of energy supply, ultimately result in cell death in the cochlea of Cx30<sup>-/-</sup> mice.

## | 779 | Investigation of the Pattern and Time Course of Vestibular Hair Cell Death in Connexin30 Knockout Mice

**Yan Qu<sup>1</sup>**, Wenxue Tang<sup>1</sup>, Xi Lin<sup>1</sup>

<sup>1</sup>Dept of Otolaryngology, Emory University School of Medicine

Mutations in connexin26 (Cx26) and Cx30 genes are most common genetic defects responsible for about half of inherited prelingual non-syndromic deafness cases. The most commonly found human Cx mutations in either Cx26 (e.g., 35delG) and Cx30 (e.g., e.g., GJB6-D13S1830) effectively eliminate gene expression. Animal models for these Cx mutations are available now, as targeted deletion of either Cx26 or Cx30 coding sequence in mice results in non-syndromic hearing loss similar to symptoms found in human. Cochlear hair cells die gradually in Cx30 knockout (Cx30-/-) mice in a period of about 4 months after birth, and animals are totally deaf after hair cell death. It is known that both Cx26 and Cx30 are highly expressed in the auditory and vestibular supporting cells. Therefore it is puzzling why Cx30-/- mice do not show any obvious

vestibular symptoms. To investigate whether vestibular hair cells survival in Cx30<sup>-/-</sup> mice, we labelled them with hair cell markers (Myosin6 or 7a) in either whole-mount samples or sections obtained at various time points after births. Comparing to time-matched wild type mice, our data showed significant and gradual vestibular hair cell and hair bundle loss in Cx30<sup>-/-</sup> mice. We are currently quantifying results obtained from saccule, utricle and crista ampulla regions. In summary, our data suggested that vestibular hair cell death in Cx30<sup>-/-</sup> mice was probably masked by adaptation of the animal to a degree they failed to show any obvious symptomatic vestibular defects.

### 780 Characterization of Knockout Mouse Model for Usher Syndrome Type 1C

**Xue Zhong Liu**<sup>1</sup>, Denise Yan<sup>1</sup>, Heping Yu<sup>2</sup>, Chantal Longo-Guess<sup>3</sup>, Xiao Mei Ouyang<sup>1</sup>, Li Lin Du<sup>1</sup>, Kazusaku Kamiya<sup>1</sup>, Qing Yin Zheng<sup>2,3</sup>

<sup>1</sup>University of Miami, <sup>2</sup>Case Western Reserve University, <sup>3</sup>The Jackson Laboratory

Usher syndrome (USH) is an autosomal recessive disorder characterized by combined hearing loss and retinal degeneration. USH is clinically and genetically heterogeneous with at least 11 chromosomal loci mapped and eight causative genes cloned. In hair cells of the inner ear, the proteins encoded by these genes are part of a protein complex, in which, the actin bundling and PDZdomain containing protein, harmonin might coordinate the activities of the USH proteins and bridge them to the cytoskeleton of the hair cell. Disruption of the USH protein network would lead to stereociliary disorganization, as observed in mouse models, and is thought to be responsible for congenital deafness in patients with USH. To further understand the role of harmonin in the pathogenesis that leads to USH1, we have used the technique of gene targeting by homologous recombination to generate Ush1c knockout mice. In embryonic and postnatal mice heterozygous Ush1c+/-, LacZ expression was detected in both the inner and outer hair cells of the cochlea. Homozygous mutant mice (Ush1c-/-) exhibit the hyperactivity and head-tossing typical behavior associated with inner ear defects and are completely deaf. Inner ear morphology analysis by light microscopy and scanning electron microscopy (SEM) revealed that, at three weeks of age, outer hair cells of Ush1c-/- mice showed disorganized stereocilia compared to the well-organized pattern and rigid structure observed in Ush1c+/littermates. Sub-cellular localization of the known USH 1 proteins in Ush1c-/- cochleas are currently investigated. The work is supported by NIH DC05575 and DC007392

#### | 781 | Mitochondrial Mutations in Maternally-Inherited Non-Syndromic Deafness: Prevalence of Known Mutations and Whole Mitochondrial Genome Screening Using a Microarray Resequencing Mitochondrial DNA Chip

Marianne Leveque<sup>1</sup>, Sandrine Marlin<sup>2</sup>, Laurence Jonard<sup>1</sup>, Vincent Procaccio<sup>3</sup>, Pascal Reynier<sup>4</sup>, Sylvain Baulande<sup>5</sup>, Remy Couderc<sup>1</sup>, Eréa-Noël Garabédian<sup>6</sup>, Christine Petit<sup>7</sup>, Delphine Feldmann<sup>1</sup>, Françoise Denoyelle<sup>6</sup>

<sup>1</sup>Department of biochemistry and molecular biology, Armand Trousseau Children Hospital, Paris, France,

<sup>2</sup>Department of medical genetics, Armand Trousseau Children Hospital, Paris, <sup>3</sup>Center for Molecular and Mitochondrial Medicine and Genetics, University of California, Irvine, USA, <sup>4</sup>INSERM U688, Angers, France, <sup>5</sup>PartnerChip, Evry, France, <sup>6</sup>Department of ENT surgery, Armand Trousseau Hospital, Paris, France,

<sup>7</sup>21Department of Sensorial Disease Genetics, Pasteur Institute, Paris

Mitochondrial DNA (mtDNA) mutations have been implicated in non-syndromic hearing loss either as primary or as predisposing factors. As only a part of the mitochondrial genome is usually explored in deafness, its prevalence is probably under-estimated. Among 1350 families with sensorineural deafness collected through a French collaborative network, we selected 29 large families with a clear maternal lineage and screened them for the known mtDNA mutations in 12S rRNA, tRNAser(UCN) and tRNAleu(UUN) genes. When no mutation could be identified, a whole mitochondrial genome screening was performed, using a microarray resequencing chip: the MitoChip version 2.0 developed by Affymetrix, Inc. Known mtDNA mutations was found in 9 of the 29 families: five with A1555G, two with the T7511C, one with 7472insC and one with A3243G mutation. In order to estimate the prevalence of these mutations in the French population, we screened 71 additional families with 2 deaf maternal relatives and 95 sporadic cases, but did not find any of these mtDNA mutations. In the remaining 20 families, the resequencing Mitochip detected 258 mitochondrial homoplasmic variants and 107 potentially heteroplasmic variants. Controls were made by direct sequencing on selected fragments and showed a high sensibility of the MitoChip but a low specificity, especially for heteroplasmic variations. An analysis on the basis of species conservation, frequency and phylogenetic analysis was performed to select the more probably pathogenic variants. The entire genome analysis allowed us to identify additional families with a possibly pathogenic mitochondrial variant: T669C, C1537T, G8078A, G12236A and G15077A. These results indicate that the new MitoChip platform is a rapid and valuable tool for identification of new mtDNA mutations in deafness.

## 782 Molecular Analysis of Netrin-1 and Nkx5-1 in Patients with Superior Semicircular Canal Dehiscence

**Nicolas Gürtler**<sup>1</sup>, Nicolas Roknic<sup>2</sup>, Alexander Huber<sup>3</sup>, Rudolf Häusler<sup>4</sup>

<sup>1</sup>Dept. of ENT, Cantonal Hospital Aarau, Switzerland, <sup>2</sup>Dept. Oto/HNS, University Hospital Basel, Switzerland, <sup>3</sup>Dept. Oto/HNS, University Hospital Zürich, Switzerland, <sup>⁴</sup>Dept. Oto/HNS, University Hospital Bern, Switzerland Superior semicircular canal dehiscence has only been discovered in 1998. This syndrome includes vertigo and oscillopsia induced by loud stimuli or changes of middle ear or intracranial pressure. The dehiscent bone has been identified on computed tomography scans and confirmed by intraoperative findings. The etiology of this syndrome is not clear. Findings from both temporal bone CT and histologic study suggest a congenital or developmental origin. In the last years, a couple of genes involved in inner ear morphogenesis have been described. Specifically, Netrin-1 (NTN1) and Nkx5-1 (HMX3) have been shown to regulate the formation of the superior semicircular canal. Mutations in these genes might lead to a disturbed development of this canal and might eventually represent novel diagnostic and therapeutic approaches in the management of this disease.

10 patients with superior semicircular canal dehiscence were included in the study. DNA was extracted from venous blood. The coding sequences of NTN1 and HMX3 were amplified by PCR and sequenced on an ABI-analyzer. The results are presented. The discussion is focused on a possible molecular origin of this syndrome.

## **T83** Bmp4 Gene Expression Analysis in the Murine Inner Ear Using LCM

**Denise White<sup>1</sup>**, Valentina Pilipenko<sup>2</sup>

<sup>1</sup>University of Cincinnati College of Medicine/ Cincinnati Children's Hospital Medical Center, <sup>2</sup>Cincinnati Children's Hospital Medical Center

Bmp4 (bone morphogenic protein 4) is a member of the TGF-ß family that has been demonstrated to play a role in the regulation of inner ear development. There are three different Bmp4 transcripts, 1A, 1B and intron 2. Varied transcript expression of Bmp4 has been reported for the inner ear and other organs in the mouse model. We hypothesize that at least two of the known isoforms of Bmp4 in the inner ear are tissue specific (epithelial vs. mesenchymal). LCM (Laser Capture Microdissection) was used to procure cells from inner ear cryosections of CD1 E10.5 mouse embryos that were fixed in 70% ethanol. The otocyst epithelial and mesenchymal cells expressing Bmp4 were identified using In-situ hybridization on corresponding inner ear cryosections of mice from the same litter that were fixed in 4% Paraformaldehyde. Bmp4 isoform expression was determined by RT-PCR analysis of RNA obtained from LCM. At E10.5, only transcript 1A not the 1B transcript was detected, in both the epithelial and mesenchymal tissue. By studying the tissue expression of Bmp4 isoforms in the inner ear at different embryonic stages, the molecules involved in inner ear

development can be elucidated. Further studies are currently underway to delineate the Bmp4 regulation in inner ear development at different embryonic stages.

#### 784 Functional Analysis of ChM-I Knock-Out Mouse

**Katherine McLaughlin**<sup>1</sup>, Omar Akil<sup>1</sup>, Christopher Weber<sup>1</sup>, Lawrence Lustig<sup>1</sup>

<sup>1</sup>Department of Otolaryngology; University of California, San Francisco

Chondromodulin-I (ChM-I) is a cartilage-specific matrix protein that has been found to be a potent inhibitor of angiogenesis, a suppressor of T-cell responses and of synovial cell proliferation and a promoter of proteoglycan synthesis and growth of chondrocytes. Its expression has been identified in rat articular cartilage and eyes, in the mouse thymus, in developing chick hearts and eyes, and in human intervertebral discs and tumors such as salivary pleomorphic adenomas and chondrosarcomas. Previous studies in our lab (Vakharia et al 2006, ARO) have demonstrated expression of ChM-I in rat cochlear lateral wall, spiral limbus, tectorial and Reissner's membranes, spiral ganglion cells, and inner and outer hair cells. Here we report additional studies undertaken to characterize the function of ChM-I within the mouse cochlea.

Studies exploring the function of ChM-I in the mammalian cochlea were performed on ChM-I knock-out (KO), heterozygous (HT), and wild type (WT) C57BL/6 mice at 6 weeks of age. Studies included auditory brainstem response (ABR), distortion product otoacoustic emission (DPOAE), and DPOAE with contralateral suppression (CS-DPOAE). ABR, DPOAE and CS-DPOAE studies showed no significant differences in hearing thresholds between the WT, HT and KO mice, indicative of normal hearing and normal efferent auditory function. Histologic analysis of permanent cochlear sections also shows no apparent difference in cochlear structures, with a normal organ of Corti and hair cell counts for all three groups of mice.

These results demonstrate that knocking out ChM-I does not affect mammalian hearing. It also suggests that ChM-I function may be redundant with other proteins in the cochlea, accounting for normal function in the KO mouse. Further, the role of ChM-I in the cochlea has yet to be elucidated.

### 785 Cochlear Anatomy and Physiology in the Re-Derived Prestin Knockout Mouse

**Charles T. Anderson**<sup>1</sup>, Roxanne Edge<sup>1</sup>, Christina Georgopoulos<sup>1</sup>, Peter Dallos<sup>1</sup>, Mary Ann Cheatham<sup>1</sup> *Northwestern University* 

It is now well established that prestin knockout mice lack frequency selectivity and exhibit reduced sensitivity (Liberman et al., 2002; Cheatham et al., 2004). Because these animals are useful for studying cochlea processing, they were cryopreserved at the Mutant Mouse Regional Resource Center at the University of North Carolina. The mice were re-derived by mating founders obtained through in vitro fertilization using B6129SF1/J oocyte donors and sperm from prestin knockout mice. Because the hybrid

mice used to generate oocyte donors were created by mating a C57BL6 (hereby abbreviated BL6) female with a 129S1 male, the re-derived mice are on a mixed 129S7/129S1/BL6 background. The latter contrasts with the original knockout, which is simply 129S7/BL6. In order to assist ourselves and others who might use these animals, both anatomical and physiological experiments were performed on F2 and F3 generation re-derived mice confirm phenotype. Cytocochleograms constructed to document the degree of apoptosis observed for both inner and outer hair cells. Cell status was determined using MicroSuite™Five (Soft Imaging System, Corp.), which allows users to create a single in-focus image from several images taken at different focal planes. The sharpest pixels are then used to form the final image. This feature is especially useful for quantifying thick and unevenly mounted cochlear segments. physiological experiments, compound action potential (CAP) thresholds, input-output functions and tuning curves were collected to document changes in sensitivity and tuning. Data indicate that this re-derived prestin knockout mouse exhibits an ~50 dB threshold shift and shows no frequency selectivity. Hence, this re-derived prestin knockout mouse can be used in studies of cochlear amplification. (Supported by NIDCD grant DC00089).

#### | 786 | Small Molecule Screen to Identify Compounds that Attenuate Aminoglycoside Induced Hair Cell Death

**Felipe Santos**<sup>1,2</sup>, Julian Simon<sup>3</sup>, David Raible<sup>2,4</sup>, Edwin W. Rubel<sup>1,2</sup>

<sup>1</sup>Dept of Oto-HNS, University of Washington, <sup>2</sup>Virginia Merrill Bloedel Hearing Research Center. <sup>3</sup>Fred Hutchinson Cancer Research Center, <sup>4</sup>Department of Biological Structure, University of Washington Sensory hair cell death in the inner ear is observed in the majority of vestibular disorders and hearing loss. The aminoglycoside antibiotic neomycin induces lateral line sensory hair cell death in wildtype zebrafish in a manner analogous to aminoglycoside-induced sensory hair cell toxicity in the inner ear of mammals. We developed an in vivo drug toxicity-interaction screen of over 10,000 small molecules from a chemical library and identified two druglike small molecules with shared structural similarity that prevent aminoglycoside induced sensory hair cell death in the zebrafish lateral line. These compounds, F5 and H10, did not inhibit the antimicrobial (bactericidal or bacterialstatic) activity of neomycin. These methods and the identified compounds may define druggable targets or drug leads for vestibular and auditory sensory hair cell protection.

Supported by grants DC 05987,04661, F32 DC 007244-01 and AAO-HNSF Resident Research Grant

## 787 Response of Hair Cells in the Zebrafish Lateral Line to Acute and Chronic Aminoglycoside Exposure

**Kelly N. Owens**<sup>1,2</sup>, Lisa S. Ness<sup>3</sup>, Keri O'Connell<sup>3</sup>, David W. Raible<sup>1,2</sup>, Edwin W Rubel<sup>1,4</sup>

<sup>1</sup>V.M. Bloedel Hearing Research Center, <sup>2</sup>Dept. of Biological Structure, <sup>3</sup>Dept. of Speech and Hearing Sciences, University of Washington, <sup>4</sup>Dept. of Otolaryngology-HNS

One of the more experimentally tractable causes of inner ear hair cell loss is exposure to aminoglycoside antibiotics. Different aminoglycoside are known to differentially kill hair cells, although the underlying cause is poorly understood. We use the lateral line of zebrafish, Danio rerio, as a model system to understand biological processes and genetic variation in hair cell loss. In wildtype zebrafish, lateral line hair cells are killed by aminoglycosides in a dose-dependent manner. Here, we examined the response of lateral line hair cells to acute and chronic gentamicin and neomycin exposure. We immersed 5 day post-fertilization larvae in 0-400 µM gentamicin or neomicin for 30 min, rinsed, and counted hair cells 60 min later. Many more hair cells were retained in animals treated with higher doses (100-400 µM) of gentamicin compare to neomycin. This observation may reflect a difference in maximal hair cell loss inducible by the drugs in this model or, alternatively, in the time required for hair cell loss. To address this idea, fish exposed to varying doses of either gentamicin or neomycin for 30 min and examined after 1, 11 or 24 hr. By 24 hr post-treatment, there were no significant differences in the number of hair cells in animals treated with neomycin and gentamicin, indicating that both aminoglycosides can induce the same eventual degree of hair cell loss but that gentamicin acts more slowly. To assess chronic aminoglycoside exposure, larvae were exposed to drug 0-24 hrs prior to fixation and hair cell counts. Chronic neomycin exposure produced maximal hair cell loss by 3-6 hr of exposure. In contrast, chronic gentamicin exposure produced increased hair cell loss with time. We hypothesize that differential kinetics of hair cell loss induced by neomycin and gentamicin reflects an underlying two-step mechanism of aminoglycosideinduces hair cell death with a rapid phase and a longer cumulative phase.

Supported by DC05987, DC006998, DC04661 and HD002274.

# | 788 | Increased Susceptibility of Aminoglycosides in Cochlear Mitochondrial Dysfunction\The Interaction of Kanamycin with 3-Nitropropionic Acid in Guinea Pigs

Chia-Der Lin<sup>1,2</sup>, **Kiyoshi Oda**<sup>2</sup>, Daisuke Yamauchi<sup>2</sup>, Takeshi Oshima<sup>2</sup>, Toshimitsu Kobayashi<sup>2</sup>

<sup>1</sup>China Medical University Hospital, <sup>2</sup>Tohoku University Graduate School Of Medicine

The present study was designed to investigate the interaction of aminoglycoside in cochlear mitochondrial dysfunction. We mimicked cochlear mitochondrial dysfunction by administrating a mitochondrial toxin, 3-nitropriopionic acid (3-NP) into the cochlea via the round

window menbrane. Guinea pigs treated with 150mM of 3-NP exhibited significant temporary threshold shifts in auditory brainstem response (ABR). The animals with normal thresholds of ABR were administered with 150 mM of 3-NP and/or 400 mg/kg of kanamycin (KM), followed by consecutive ABR measurements and their cochlear hair cell counting at sacrifice. Significant ABR threshold shifts were observed in the animals treated with 3-NP alone and 3-NP/KM at 14 days after administration. The threshold shifts were greater in the animals with 3-NP/KM than those with 3-NP alone. The recovery was observed in the animals treated with 3-NP alone. Significant loss of outer hair cells in the cochlear basal and second turns was observed in the 3-NP/KM-treated group but not in the other alone, KM alone or control). A aroups (3-NP straightforward relationship between aminoglycoside ototoxicity and mitochondrial dysfunction could be revealed in this study.

### 789 TRPV4 Enhances Cytoplasmic Uptake of Aminoglycosides

Takatoshi Karasawa<sup>1</sup>, Qi Wang<sup>1</sup>, Peter Steyger<sup>1</sup>

<sup>1</sup>Oregon Health & Science University

We have previously demonstrated that cytoplasmic uptake of aminoglycosides is modulated by regulators of the transient receptor potential vanilloid (TRPV) receptors, a subgroup of the TRP channel family. TRP channels are non-selective channels that conduct cations and aminoglycosides, including gentamicin. If aminoglycosides enter enter sensory hair cells via the stereociliary mechanoelectrical transduction channels (or via apical endocytosis) to induce cytotoxicity and deafness, how do aminoglycosides enter the endolymph? We hypothesized that a TRP channel enables gentamicin to be transported from serum through the stria vascularis into the endolymph, where the drug can then access hair cell apices. Since a member of TRP family, TRPV4, is abundantly expressed in the stria vascularis, we hypothesized that TRPV4 plays a role in the intra-cochlear transport of aminoglycosides.

To determine if TRPV4 is permeable to aminoglycosides, cells that stably express TRPV4 were generated from AML12 mouse hepatocyte cells by retroviral gene delivery. TRPV4-expressing and vector-only (control) cells were incubated with a gentamicin-Texas Red conjugate (GTTR) for 30 seconds under a variety of conditions known to regulate TRPV4 channels, and cytoplasmic GTTR uptake was analyzed by confocal microscopy.

Enhanced GTTR uptake was observed in cells treated in  $Ca^{2^+}$ -free buffer during GTTR incubation, a condition that opens TRPV channels. At physiological extracellular (1.25 mM)  $Ca^{2^+}$  levels, AML12-derived, TRPV4-expressing cells showed enhanced GTTR uptake over vector control cells. The TRPV4 agonists PMA and  $4\alpha$ -PDD further enhanced GTTR uptake over similarly-treated vector control cells at both 37°C and at room temperature, while a non-specific TRPV4 inhibitor Ruthenium Red blocked GTTR uptake in the cells.

The data indicate that heterologous expression of TRPV4 enhances cytoplasmic uptake of aminoglycosides. Thus

TRPV4 may play a role in aminoglycoside transport across the stria vascularis that forms a part of the blood-labyrinth barrier.

Funded by NIDCD R01 04555 (PSS), F32 DC008465 (TK), P30 05983, and the Medical Research Foundation of Oregon.

### 790 Intracellular Modulation of Aminoglycoside Uptake

Qi Wang<sup>1</sup>, Takatoshi Karasawa<sup>1</sup>, Peter Steyger<sup>1</sup>

<sup>1</sup>Oregon Health & Science University

Aminoglycosides enter cells through both endocytosis and via more rapid non-endocytotic mechanisms. Non-endocytotic uptake of aminoglycosides can be altered by manipulating the extracellular or intracellular environment (pH, [Ca<sup>2+</sup>], and voltage), conditions that also regulate transient receptor potential vanilloid channels (TRPV). If non-endocytotic uptake occurs principally through the non-selective cation channels, can intracellular signalling pathways that regulate ion channels and transporters also modulate aminoglycoside uptake?

Confluent MDCK cells were incubated with gentamicin-Texas Red (GTTR) for 30 seconds under conditions known to acutely modulate expression or activity of ion channels or transporters. Chronic drug treatment (10 or 30 minutes) was also examined. Cytoplasmic GTTR uptake was analyzed by confocal microscopy.

Lanthanum-induced internalization of cation channels reduced GTTR uptake levels that returned to control levels within 30 minutes. The K<sup>+</sup> transport-inhibiting loop diuretics (bumetanide, ethacrynic acid and furosemide) all increased GTTR uptake in MDCK cells regardless of incubation time. The anti-diuretic vasopressin acutely reduced GTTR uptake. However, sustained vasopressin incubation did not significantly alter GTTR uptake. Forskolin (which elevates cAMP levels) increased GTTR uptake. The non-steroidal, anti-inflammatory drug flufenamic acid also acutely decreased GTTR uptake but not after chronic incubation.

Pharmaceutical agents that rapidly enhance GTTR uptake do not lose their effect with chronic treatment. However, pharmaceutical agents that acutely inhibit GTTR uptake may lose their efficacy during chronic treatment. Chronic treatment with vasopressin increases cAMP levels and protein kinase A activity that phosphorylates TRP channels, potentiating their activity. Similarly, flufenamic acid is a cyclooxygenase inhibitor enhancing the generation of eicosanoids that potentiates TRP channels. Thus, understanding the intracellular mechanisms that modulate aminoglycoside uptake is required to develop pharmaceutical methods to reduce cellular uptake of aminoglycosides *in vivo*.

Funded by NIDCD R01 04555, and P30 05983.

## 791 Adenovector Mediated Delivery of Bcl-2 in a Mouse Model of Aminoglycoside Ototoxicity

**Susanna Pfannenstiel<sup>1,2</sup>**, Mark Praetorius<sup>2</sup>, Peter K. Plinkert<sup>2</sup>, Hinrich Staecker<sup>1</sup>

<sup>1</sup>KUMC, <sup>2</sup>University of Heidelberg Medical Center

Overexpression of bcl-2 has been demonstrated to prevent hair cell death in an in vitro ototoxicity model. To evaluate the protective effects of bcl-2 in vivo, we have developed an in vivo model of gentamicin ototoxicity in the mouse using transtympanic delivery of gentamicin. Adult C57BI/6 mice were anesthetized and the round window niche exposed. Gentamicin 40 mg/ml was applied to the round window using a microsyringe to prevent air bubbles blocking contact of gentamicin with the round window. After 30 minutes the gentamicin was removed and mice allowed to recover. At 6 and 12 hours as well as 1, 2, 5 and 10 days post gentamicin treatment the inner ear was examined by serial sectioning. Histology, expression of apoptosis markers and hair cell counts were determined for the cochlea and for the macular organs. A second group of mice was pretreated with an advanced generation adenovector expressing human bcl-2 driven by the CMV promoter delivered via the posterior semicircular canal. Forty eight hours after vector delivery mice were treated with intratympanic gentamicin and evaluated at 10 days post ototoxicity as described. Results were compared to mice pretreated with a control vector expressing green fluorescent protein.

### 792 The Roles for IGFPBs on the Neomycin Treated Immortocells

**Jee Young Park**<sup>1</sup>, Dong Hoon Shin<sup>2</sup>, Seung Ha Oh<sup>1</sup> Seoul National University Hospital, <sup>2</sup>Seoul National University, Department of Anatomy

IGFBPs are important for the survival of the damaged cells and believed to modulate the function of IGF-1 at their site of action. In contrast to the well known protective effect of IGF-1, the function of IGFBPs in the inner ear cell survival is not demonstrated yet. In this study, we could demonstrate that the endogenous IGFBP-4 was increased following the neomycin treatment in the inner ear cell lines [HEI-OC1 (cochlea origin), UB/UE-1 (utricle origin)] by immunocytochemistry and Western blot analysis. Exogenous IGF-I, IGFBP-4, or -5 alone and mixtures (10 ng/ml) showed positive effects on the cell viability, in both neomycin treated and non-treated group. Down-regulation of endogenous IGFBP-4 by using siRNA (small interfering RNA) diminished the cell viability and addition of exogenous IGF-I, IGFBP4, or IGFBP5 could rescue the cell survival. The increased expression of mitogen activated protein kinases (MAPKs) following neomycin treatment was confirmed and the MAPK inhibitors could enhance the cell viability, indicating that the MAPK activity is responsible for the cell survival. Neomycin treatment also could increase the metalloproteinases (MMPs) secretion which was known to modify IGFBP activity. In summary, inner ear cells showed the increased production

of IGFBP in response to the neomycin treatment and this endogenous IGFBP has a function of cell survival.

Keywords: IGFBP, neomycin, HEI-OC1, UB/UE-1

#### 793 Protective Effect of Pifithrin-Alpha Against Gentamicin-Induced Vestibular Hair Cell Loss

Mei Zhang<sup>1</sup>, Michelle Levin<sup>1</sup>

<sup>1</sup>University of Florida

Recently, blocking critical steps in the cell death pathways has been suggested as a useful strategy to prevent druginduced ototoxicity. P53 is a key regulator in the programmed cell death process. We previously discovered that pifithrin- $\alpha$  (PFT) blocked cisplatin-induced apoptosis and protected both cochlear and vestibular hair cells (Zhang et al., 2003). In this project we carry out experiments to determine if PFT also protects vestibular hair cells from gentamicin-induced damage. Utricular cultures were obtained from P3 Sprague-Dawley rats. Two groups of cultures were treated with gentamicin alone  $(500\mu M$  or  $1000\mu M$ , n=5) to obtain a gentamicin dose response curve. Another two groups of cultures were treated with 500µM or 1000µM gentamicin plus 100µM PFT (n=5) to study the protective effect of PFT. Untreated control cultures were run in parallel. After 48 hours of treatment, the cultures were fixed with 10% formalin and stained with fluorescent labeled-phalloidin. Then the tissues were mounted and observed under fluorescence microscopy. The images were processed with Adobe Photoshop5.5 software. The numbers of vestibular hair cells per 0.05 mm<sup>2</sup> were counted from three representative regions of each explant and the mean number was determined for each specimen. Data were analyzed by The results showed that gentamicin caused significant hair cell loss and induced a dose-dependent damage in the vestibular cultures of P3 rat utricles. PFT showed partial protection against 500μM or 1000μM gentamicin-induced vestibular damage (P<0.05).

Supported by Deafness Research Foundation

## 794 Coenzyme Q10 Protects the Vestibular Hair Cells Against the Ototoxicity of Aminoglycoside

**Kazuma Sugahara**<sup>1</sup>, Takefumii Mikuriya<sup>1</sup>, Tsuguyuki Arai<sup>1</sup>, Tsuyoshi Takemoto<sup>1</sup>, Makoto Hashimoto<sup>1</sup>, Hiroaki Shimogori<sup>1</sup>, Hiroshi Yamashita<sup>1</sup>

<sup>1</sup>Department of Otolaryngology, Yamaghichi University, Graduate School of Medicine

It is well known that the production of free radicals is associated with the sensory cell death induced by aminoglycoside. Many researchers reported that antioxidant reagents could protect sensory cells in the inner ear. Coenzyme Q10 (CoQ10) is one of the antioxidants which can be used as the health food in many countries. The purpose of this study was to investigate the role of CoQ10 in mammalian vestibular hair cell death induced by aminoglycoside. Cultured utricles of CBA/CaN mice were used. In this study, the reagent Water-soluble

Q10 was used as an antioxidant. Cultured utricles were divided to three groups (Control group, Neomycin group, Neomycin + CoQ10 group). In the Neomycin group, utricles were cultured with neomycin (1 mM) to induce hair cell death. In Neomycin + CoQ10 group, utricles were cultured with neomycin and CoQ10 (30|0.3 fÊM). Twenty-four hours after exposure to neomycin, the cultured tissues were fixed with 4% paraformaldehyde. To label hair cells, immunohistochemistry were performed using anticalmodulin antibody. The rate of survival vestibular hair cells was evaluated with the fluorescence microscope. The survival rate of hair cells in Neomycin + CoQ10 group was significantly more than that in Neomycin group.

These data indicated that CoQ10 protects sensory hair cells against neomycin-induced death in mammalian vestibular epithelium. These results show that CoQ10 can be used as the protective drug in the inner ear.

#### | 795 | Effect of Low Level Laser on Ototoxicity Prevention of FM1-43 in Postnatal Organotypic Culture of Rat Utricles Yong Won Chung<sup>1</sup>

<sup>1</sup>Dankook Univ. Hosp.

was investigated.

Backgrounds and Objectives: The styryl pyridinium dye FM1-43 has been widely used to observe synaptic vesicle recycling. It is a nontoxic, fluorescent, cationic dye whose fluorescence markedly increases after partitioning into membrane. FM1-43 quickly fills the cytoplasm of hair cells, but labels only the plasma membrane of adjacent supporting cells. Rapid entry of FM1-43 is inhibited by drugs that block the mechanically gated transduction channels, suggesting the dye can itself act as a permeant blocker of the channels. In this study, the effects of low level laser and FM1-43 on ototoxicity induced by gentamicin in postnatal organotypic culture of rat utricles

Materials and Methods: An organotypic culture of 2-7-day-old rat utricular maculae was established. In a series of experiments utricles were exposed to either irradiation of low level laser(LG group)or 10  $\mu$ M FM1-43(FG group) or both(LFG group) followed by 1mM of gentamicin treatment for 12 hrs. The results of experimental groups were compared with the control group by confocal laser scanning and scanning electron microscopy.

Results: Rapid incubation with FM1-43 dye protected vestibular hair cell damage induced by gentamicin treatment. Moreover, substantial effect of low level laser on ototoxicity prevention of FM1-43 in postnatal organotypic culture of rat utricles was found. There were statistical significant differences among all groups but between control and LFG group by both confocal laser scanning and scanning electron microscopy. In addition, caspase-3 activity was hardly found in LFG group after double staining with Phalloidin-FITC by confocal laser scanning microscopy.

Conclusion: These results suggest that there is a additive protection effect of low level laser and FM1-43 against gentamicin ototoxicity in postnatal organotypic culture of rat utricles

#### 796 Early Changes in the Organ of Corti After a Severe Ototoxic Insult

Young Ho Kim<sup>1,2</sup>, Yehoash Raphael<sup>1</sup>

<sup>1</sup>University of Michigan, <sup>2</sup>Seoul Municipal Boramae Hospital, Seoul National University College of Medicine Kanamycin and ethacrynic acid can be used in combination to induce a severe ototoxic lesion. Typically, hair cells degenerate whereas supporting cells remain in the auditory epithelium. The early sequence of degenerative changes in the auditory epithelium is not well characterized. The goal of this study was to characterize the first changes that can be identified in the morphology of hair cells and supporting cells after the insult. Mature pigmented guinea pigs were given systemic kanamycin (400 mg/kg) followed two hours later by ethacrynic acid (40 mg/kg). Five hours after the ethacrynic acid injection, cochleae were harvested and labeled for actin, S100, acetylated tubulin, prestin, KHRI-3, or DNA. Cochleae of normal guinea pigs were used as controls. Five hours after the insult, many outer hair cell nuclei contained irregular chromatin staining consistent with degenerative changes. Prestin staining showed that the cell membrane of some outer hair cells was distorted. Using the markers listed above we determined that at this time there was no noticeable change in the apical surface of the epithelium. The only change seen in supporting cells at this time point was irregular and slightly disorganized array of microtubules at the apical domain. The data suggest that the degeneration of outer hair cell nuclei is under way at five hours after the insult and may precede changes of supporting cells. The appearance of early changes under the surface implies that surface analysis may fail to detect initial changes in the epithelium. The data indicate that attempts to rescue hair cells may need to occur before or very early after an ototoxic insult and that the (yet to be discovered) signal for initiation of the scarring process may be transmitted around this early time point.

Supported by the Williams Professorship, by a gift from B. and A. Hirschfield, and by NIH/NIDCD R01 Grants DC01634, DC05401, DC007634, and P30 Grant DC05188.

### 797 A New Model of Early Onset Deafness in the Rat

**Julia Grushko<sup>1</sup>**, Dorothy Frenz<sup>1</sup>, Elyse Sussman<sup>1</sup>

\*Albert Einstein College of Medicine

Several different animal models have been established to study hearing loss. These models have relied on complete sectioning of auditory afferents or on genetic knockout methods. The purpose for developing a new model is to mimic early onset deafness in a rat but cause no damage to the eighth nerve and no systemic side effects. Rats were deafened on postnatal day 12, prior to the opening of the ear canal. The surgical deafening procedure used an ototoxic drug applied directly to the round window. We found that the application of the ototoxic drug led to cochlear hair cell death as evaluated with auditory brainstem response. This new animal model of early onset deafness will be useful for characterizing plastic changes of the brain that result from sensorineural hearing loss.

### 798 Using the Zebrafish Lateral Line to Screen for Ototoxicity

**Lynn L Chiu**<sup>1</sup>, Edwin W Rubel<sup>1</sup>, David W Raible<sup>2</sup>, Henry Ou<sup>1,3</sup>

<sup>1</sup>Department of Otolaryngology - HNS and VM Bloedel Hearing Research Center, University of Washington, <sup>2</sup>Department of Biological Structure and VM Bloedel Hearing Research Center, University of Washington, <sup>3</sup>Childrens Hospital and Regional Medical Center, Seattle.

The zebrafish has emerged as a valuable model for studying hair cell development, structure, genetics and behavior. Like all aquatic vertebrates, zebrafish have hair cells on their body surface organized into a sensory system called the lateral line. These hair cells are highly accessible and easily visualized using fluorescent dyes. Morphological and functional similarity to mammalian hair cells of the inner ear make the zebrafish a powerful tool for studying drug ototoxicity.

The ototoxic potential of certain drugs has historically been uncovered by anecdotal reports that have lead to more formal investigation. Currently, no standard screen for ototoxicity in drug development exists. Thus, for the vast majority of FDA approved drugs, the ototoxic potential remains unknown. In this study we used 5 day old zebrafish larvae to screen a library of 1,040 FDA approved drugs for ototoxic effects on hair cells of the lateral line. Hair cell nuclei were selectively labeled using YOPRO-1, a fluorescent vital dye. One fish was placed into each well of a 96 well plate and one drug from the FDA library was introduced into each well at a concentration of 100  $\mu$ M. Hair cell viability was visualized in vivo using fluorescence microscopy. Using this method, all 1,040 drugs were rapidly screened for ototoxic effects. All screening was done blinded to the identity of the drugs. Known ototoxic drugs, such as neomycin, cisplatin and carboplatin, were positively identified using these methods, as proof of concept. Several compounds were discovered to be selectively toxic to hair cells, and dose-response curves were determined by quantifying hair cell loss as a function of drug concentration. This study demonstrates the potential for the zebrafish lateral line for screening for drug ototoxicity, and sets the stage for a standardized scale by which the ototoxicity of drugs can be easily compared.

Supported by grants DC04661, DC05987, T32-DC00018, HD002274, and Amer Soc Ped Oto.

### 799 Cisplatin Uptake into Mammalian Cochlear Hair Cells *In Vitro*

Dalian Ding<sup>1</sup>, Haiyan Jiang<sup>1</sup>, **Richard Salvi**<sup>1</sup>

\*\*University at Buffalo\*\*

Cisplatin is a widely used anti-cancer drug that is known to be both ototoxic and nephrotoxic. Cisplatin preferentially damages the hair cells in the inner ear and to a lesser extent the supporting cells and spiral ganglion neurons. The mechanisms that result in cisplatin-induced hair cell loss are not well understood; however, one factor that may play a role is the rate of uptake of cisplatin into hair cells versus supporting. To address the issue, we treated p3-5 rat cochlear organotypic cultures with cisplatin conjugated

to the fluorescent probe, Alexa 488 (0.25 mM) (Cis488), and examined the time course of Cis488 uptake using confocal microscopy. Very little Cis488 was found in the organ of Corti 6 h post-treatment. However, at 12 h post-treatment, Cis488 was selectively taken up by hair cells, slightly more in OHC than IHC. At 18 h post-treatment, heavy Cis488 labeling was seen in the hair cell region, but some labeling was also seen in the supporting cell region. At 24 h post-treatment, when there was significant damage to the hair cells, strong Cis488 labeling was seen in both the hair cell and supporting cell regions. These results suggest that the initial influx of cisplatin into hair cells may explain why hair cells are damaged prior to supporting cells. We are grateful to D. Bharali for conjugating Alexa488 to cisplatin.

Supported by NIH grant R01 DC06630-01

### 800 Cisplatin-Induced Changes in Apoptotic Gene Expression in Sensory Versus Neural Subdivisions of Rat Cochlear Cultures

**Haiyan Jiang**<sup>1</sup>, Dalian Ding<sup>1</sup>, Weidong Qi<sup>1</sup>, Richard Salvi<sup>1</sup> Center for Hearing & Deafness, University at Buffa

Cisplatin is both ototoxic and neurotoxic; however the cell signaling pathways leading to the destruction of hair cells and spiral ganglion neurons are not well understood. To identify some of the early events leading to cisplatininduced apoptosis in the inner ear, we treated postnatal rat cochlea cultures with 0.2 mM cisplatin for 3 h and then used focused gene microarrays (SuperArray) containing 128 apoptosis related genes to identify the early changes in gene expression in cochlear regions containing mainly the basilar membrane or spiral ganglion neurons. In the basilar membrane fraction containing the hair cells, 12 genes showed a large increase in expression. These included 3 members of the Bcl-2 family (bcl2a1, Bok, Mcl1), 2 in the CARD family (Cradd, Birc3), 2 in the p53/DNA damage family (Casp3, Gadd45), 2 in the TNF Receptor family (Tnfrs12a, Tnfrsf1a), 1 in the Death Effector Doman family (Cflar), 1 in the Death Domain family (Myd88) and 1 in the TRAF family (Traip). Three of these genes are also classified as anti-apoptotic (Mcl1, Birc3, and Cflar). In the spiral ganglion neuron fraction, 11 genes showed a large increase 3 h after cisplatin treatment. These included 3 in the TNF Receptor family (Tnfrsf11b, Tnfrsf1a, Tnfrsf1b), 2 in the Bcl-2 family (Bcl2a1, Mcl1), 1 in the CARD family (Bcl10), 1 in the Death Domain family (Bcl10), 1 in the Death Effector Domain family (Fadd), 1 in the IAP family (Birc2), and 1 in the p53/DNA damage family (Gadd45), and Rrad. Two of the genes, Mcl1 and Birc2, are members of the antiapoptotic family. These results indicate that during the early stages of cisplatin induced damage to the organ of Corti and spiral ganglion both apoptotic and anti-apoptotic genes are upregulated in response to stress and DNA damage. While there was overlap in gene expression in basilar membrane and spiral ganglion, some differences were observed which may reflect the unique response of each tissue.

Supported by NIH R01 DC06630-01.

## 801 Cisplatin Treatment *In Vivo* Induces Nuclear Expression of the Nuclear Excision Repair Protein XPD in Rat Spiral Ganglion Cells

Audra Webber<sup>1</sup>, Carey Balaban<sup>1</sup>

<sup>1</sup>University of Pittsburgh

DNA adduct formation is a major cytotoxic action of cisplatin in cancer cells. Nuclear excision repair (NER) is a primary cellular mechanism for repairing DNA adducts. This study tests the hypothesis that NER is activated by cisplatin damage in the mammalian cochlea. Female Fisher 344 rats were exposed to two cycles of cisplatin (4 days each, 2 X 1 mg/kg i.p.), separated by a 10 day rest period (Minami et al. Hearing Res. 198, 2004, 137-143). The expression of XPD, a helicase crucial for NER, was examined via immunohistochemistry in cochleae from cisplatin treated and control (saline treated) rats on days 5, 19, and 22 of the protocol. Spiral ganglion cell (SGC) XPD expression could be either cytoplasmic or within and apposed to the nucleus. Cisplatin treatment resulted in an increase in the total proportion of SGCs expressing XPD across days 5 and 19 (p<0.05, ANOVA main effect). This difference reflected a significant increase in the proportion of SGCs with nuclear staining on day 19 (p<0.05), with a particularly prominent increase in the basal cochlear turn. These findings are consistent with the hypothesis that cisplatin induced DNA damage results in XPD translocation to the nucleus. The greater response in the cochlear base is consistent with reported gradients of cisplatin cytotoxicity in the cochlea, suggesting that DNA damage may contribute to cisplatin ototoxicity.

### 802 Preventive Effect of Procaine HCL on Cisplatin Induced Ototoxicity in Guinea Pig

Yong Ho Park<sup>1</sup>, Ah Young Kim<sup>1</sup>

<sup>1</sup>Chung Nam National University

Aims: The use of cisplatin is limited by dose-dependent nephrotoxicity, ototoxicity. Some papers demonstrated that procaine HCI(P.HCI) increases the therapeutic index of cisplatin, reducing nephrotoxicity, improving antitumor activity. There is no paper to evaluate the effect of P.HCI on ototoxicity, the purpose of study was to evaluate the preventive effect of P.HCI on cisplatin induced ototoxicity. Methods: Twenty guinea pigs were used and divided into 4 groups. In normal control group(n=5), saline was injected intraperitoneally. In positive control cisplatin(14 mg/kg) dissolved in saline was injected. In experimental group(n=5), P.HCl(50 mg/kg) in water at 0.5 hour before injection of cisplatin. Last group was injected by P.HCI. Before and after 10day, ABR threshold shifts were evaluated. The effect of P.HCl on ototoxicity was evaluated with ABR threshold changes and histologic examination Results and Conclusion: After injection of cisplatin, ABR indicated that P.HCl reduced threshold shift significantly. The cochlear hair cells, especially outer hair cells in basal turn, were severely damaged in cisplatintreated group comparing to P.HCI/cisplatin-treated group. In P.HCI/cisplatin-treated cochlea, the number of apoptotic cells was markedly reduced comparing to only cisplatin treated group. Procaine hydrochloride might protect cisplatin induced ototoxicity in guinea pig.

### 803 Protective Effect of Minocycline on Cisplatin-Induced Ototoxicity

**Chi-Kyou Lee**<sup>1</sup>, Yang-Sun Cho<sup>2</sup>, Ki Ryung Kim<sup>2</sup>, Hee-Yeon Shim<sup>2</sup>, Sung Hwa Hong<sup>2</sup>, Won-Ho Chung<sup>2</sup> <sup>1</sup>Dept.of ORL-HNS, Soonchunhyang University Cheonan Hospital, <sup>2</sup>Dept. of ORL-HNS, Samsung Medical Center, Sungkyunkwan University

Objectives: Cisplatin(CDDP) is widely used chemotherapeutic agent which is known to be highly ototoxic. Previous studies have shown that minocycline, a tetracycline derivative, is neuroprotective and it can protect against aminoglycoside ototoxicity *in vivo* and *in vitro*. This study investigated the protective effect of minocycline *in vivo* against cisplatin-induced ototoxicity.

Study design: Prospective experimental morphological and functional study.

Methods: Fifteen Hartley albino quinea pigs were used. The animals were treated for 7 consecutive days with normal saline + cisplatin, minocycline + normal saline or minocycline + cisplatin. Minocycline groups were pretreated with 45 mg/kg minocycline intraperitoneally 12 hours before cisplatin injection, and then 45 mg/kg minocycline was injected daily for 7 days. In cisplatin groups, single dose of 15 mg/kg cisplatin was injected intraperitoneally on first day. After treatment, the changes in hearing were evaluated by means of auditory brain stem response (ABR) using click and tone burst at 8, 16 and 32 kHz. The changes in hair cell morphology of basal turn were evaluated by scanning electronic microscopy (SEM). Results: Animals that received cisplatin and normal saline showed a click ABR threshold shift by a mean of 48 dB. Minocycline followed by normal saline did not cause an ABR threshold shifts. The animals that received minocycline followed by cisplatin showed a threshold shift on click ABR by a mean of 30 dB with significantly less frequency of shift. These findings were closely supported with morphological study with SEM.

Conclusion: The study supports the hypothesis that minocycline may protect cisplatin-induced ototoxicity. Further investigation on the mechanisms of protection will enhance the possibility of minocycline as a new otoprotective agent.

# 804 Characteristics of Normal Newborn Transient-Evoked Otoacoustic Emissions. Ear Asymmetries and Gender Effects Erik Berninger<sup>1</sup>

<sup>1</sup>Karolinska Institutet

Analysis was performed on all transient-evoked otoacoustic emissions (TEOAEs) obtained in newborns who passed bedside universal hearing screening during a six-year period, to characterize normal TEOAEs and to study ear and gender effects (n=60,431). 0.18% of the screened newborns revealed subsequently bilateral hearing losses exceeding 30 dB HL. Short recording times

(median=33 s) was observed in combination with high entire TEOAE level (median=18.8 dB SPL, @ 81.8 dB SPL peak), and high reproducibility (median=86%). Signal-tonoise ratio (S/N) in TEOAE was highly frequencydependent, poor at low frequencies. Prolonged averaging increased median reproducibility to 97%, but the minor S/N-improvement at low frequencies did not justify the longer test time. Highly significant mean lateral asymmetries (right > left) and gender differences (female > male) existed in entire TEOAE level, S/N TEOAE, and in half-octave frequency bands (700-4,000 Hz). Mean lateral and gender entire TEOAE level differences were 1.1 dB and 1.3 dB, respectively. At high frequencies, the gender effect exceeded the ear effect. Stimulus levels were not affected by ear or gender. Hence, physiological differences at the level of organ of Corti were demonstrated in newborns.

### 805 The Effect of Posture on Otoacoustic Emission Fine Structure

**Robert Risley**<sup>1</sup>, Sumit Dhar<sup>1</sup>, Timothy Hain<sup>1</sup> *NorthWestern University* 

### Withdrawn

# 806 Compensating for Deviant Middle Ear Pressure in Otoacoustic Emission Measurements, Data and Comparison to a Middle Ear Model

**Janny Hof**<sup>1</sup>, Lucien Anteunis<sup>1</sup>, Paul Avan<sup>2</sup>, Emile de Kleine<sup>3,4</sup>, Pim van Dijk<sup>3,4</sup>

<sup>1</sup>Academic Hospital Maastricht, Otolaryngology - Head and Neck Surgery, The Netherlands, <sup>2</sup>Labatory of Sensory Biophysics, School of Medicine, Clermont-Ferrand, France, <sup>3</sup>Dept. of Otorhinolaryngology/Head and Neck Surgery, University Medical Center Groningen, <sup>4</sup>Fac. of Medical Sciences, School of Behavioral and Cognitive Neurosciences, University of Groningen

Transient evoked otoacoustic emissions (TEOAEs) are generated within the cochlea and their detection is influenced by the transmission through the middle ear. Deviant middle ear pressure has an effect on the forward and retrograde transmission of emissions. We investigated the effect of compensation of a deviant middle ear pressure on amplitude and phase of TEOAEs. We measured TEOAEs at ambient- and at compensated middle ear pressure in 59 children. The middle ear pressure was determined by tympanometry.

Compensation of middle ear pressure resulted in higher emission amplitudes. This increase was significant for the 1 and 2 kHz frequency bands. We found a negative correlation between amplitude increase and middle ear pressure for these low-frequency bands.

The TEOAE at compensated middle ear pressure showed a phase lag with respect to the ambient measurement.

The changes of TEOAE amplitude and phase were modeled with Zwislocki's lumped-element model of the middle ear. We assumed that compensating for middle ear

pressure changes the stiffness of the tympanic membrane. The amplitude and phase changes were consistent with the model for middle pressures in the range of -200 daPa to +40 daPa.

### 807 Real Time Contralateral DPOAE Modulation Via the Olivocochlear Pathway

**Alok Sharma<sup>1,2</sup>**, Adrian L. James<sup>1,2</sup>, Richard J. Mount<sup>1,2</sup>, Robert V. Harrison<sup>1,2</sup>

<sup>1</sup>Auditory Science Laboratory, Dept of Otolaryngology Head & Neck Surgery, Hospital for Sick Children, <sup>2</sup>University of Toronto, Toronto, Canada

Outer haircell activity is influenced by the descending neurons of the olivo-cochlear efferent pathway, which can be activated by acoustic stimulation of the opposite ear. This response is often referred to as the contralateral suppression reflex. We question whether the term reflex is appropriate, and hypothesize that contralateral cochlear connections (via the olivocochlear efferent pathway) operate as a continuously modulating control system.

Aims: to test the hypothesis that activity from one ear can continuously modulate (not just suppress) the sensitivity of the opposite ear; and to determine the characteristics of this modulation.

Method: In an animal model (chinchilla), distortion product otoacoustic emissions (DPOAE; 2f1-f2) were recorded in real time (Vivo 6-00 DPR device) from one ear during presentation of an acoustic stimulus to the opposite ear. All recordings were made in a sound attenuated booth in awake, non-anaesthetised animals. Broadband noise was applied to the contralateral ear (Etymotic Research ER-2 transducer), and its amplitude was modulated at various levels and rates about a resting state. DPOAE amplitudes were recorded continuously during the contralateral sound stimulation, and observed in real time, as well as stored for subsequent signal averaging as required.

Results: The recorded amplitude of the DPOAE directly varies, with an inverse relationship, to the amplitude of sound stimuli in the opposite ear. In the time domain, DPOAE changes mirror sound stimuli variations after a latency period of approximately 25ms, consistant with a neural pathway delay across the brainstem. A change in amplitude of contralateral stimulus of 10dB results in an inversely modulated 2.1dB change in DPOAE.

Conclusion: Noise stimuli to one ear continually modulate DPOAEs of the contralateral ear, via the olivocochlear pathway. The term "reflex" cannot be applied to this system because it is a continuous response rather than an all or none phenomena.

# 808 A Study on Improving the DPOAE Contralateral Suppression Test in Human Ears: Effect of Middle-Ear Muscle Reflex and Measurement of Phase Change Xiao-Ming Sun<sup>1</sup>

<sup>1</sup>Wichita State University

Distortion product otoacoustic emissions (DPOAEs) can be altered in amplitude by contralateral sound stimulation (CAS), conventionally called DPOAE contralateral suppression because the DPOAE amplitude is reduced in most cases. This phenomenon has been generally accepted to be a reflex mediated by the medial olivocochlear (MOC) system. Many efforts were made to use the DPOAE contralateral suppression measurement in assessing functional status of the efferent system. However, concerns arose from previous studies regarding the confounding effects of the sound-induced middle-ear muscle (MEM) reflex so that the CAS was always cautiously chosen at low levels, which in turn limited the dynamic range of the test. As a step to improving the DPOAE contralateral suppression test, this study was designed to investigate the extent to which the MEM reflex contributes to the alteration of DPOAE amplitude by CAS. The DPOAE amplitude-frequency functions measured with high resolution, which showed fine structure (see Sun, 2005 ARO), in the absence and presence of CAS. Broadband noise was presented as the CAS at low and high levels, 20 dB below and above the MEM reflex threshold, respectively. DPOAE time course was also measured at the frequencies corresponding to the peaks and troughs in the fine structure. The preliminary analysis revealed that the high-level CAS did not dramatically reduce the DPOAE amplitude. In the cases that the DPOAEs were enhanced by the low-level CAS at the peak frequencies, the enhancement was usually increased in the presence of the high-level CAS. While precise contribution of the MEM reflex could not be elucidated with a simple approach, the high-level CAS evidently caused substantial alteration of DPOAE amplitude via the MOC reflex. It seems that the phase changes of DPOAEs in the presence of CAS at low and high levels may provide indication concerning the activation of the MOC reflex. Details on the results will be presented and discussed.

### 809 Otoacoustic Emissions in the Common Marmoset (*Callithrix Jacchus*)

Michelle Valero<sup>1</sup>, Edward Pasanen<sup>2,3</sup>, Donna Layne<sup>4</sup>, Suzette Tardit<sup>4</sup>, Dennis McFadden<sup>2,3</sup>, Rama Ratnam<sup>1</sup>

Department of Biology, University of Texas at San Antonio, <sup>2</sup>Department of Psychology, University of Texas at Austin, <sup>3</sup>Center for Perceptual Systems, University of Texas at Austin, <sup>4</sup>Southwest Foundation for Biomedical Research, San Antonio

The common marmoset (*Callithrix jacchus*) is emerging as an attractive model for hearing research in non-human primates. However, almost no data exist on the peripheral hearing in this species. As a first step in this direction we measured distortion product (DP), click-evoked (CE), and spontaneous (S) otoacoustic emissions (OAEs) in this species. DPOAEs were readily measured from left and right ear canals of 10 marmosets (age ranging from 1.5 – 12 years). Using equilevel primaries ( $f_2/f_1$  = 1.21), we determined both DPOAE input/output functions and DPOAE audiograms ('DPgrams'). The input/output functions were generally monotonic and similar to those observed in rhesus monkeys. DPgrams were obtained for  $f_2$  frequencies extending from 3 – 13 kHz. In general, the

DPgrams were bandpass in characteristic with a peak observed at an f<sub>2</sub> of about 8 kHz (DP: 5 kHz). Based on this small sample of 10 individuals, we observed that: (1) compared to younger animals, older animals' DPOAEs at the high frequencies were absent or significantly weaker; (2) mean amplitudes were weaker than observed for Rhesus monkeys (about 75 dB below primary levels); and (3) surprisingly, the left-ear responses were generally slightly larger than the right-ear responses, which is opposite to the typical findings for humans. No SOAEs were observed in any of these individuals. CEOAEs were obtained for several click-levels, permitting extraction of the nonlinear component of the response in various frequency bands, comparable to the frequency ranges where DPOAEs were measured. Our findings demonstrate the feasibility of carrying out OAE studies in the common marmoset, and suggest that it is a useful model for research into the mechanisms of peripheral hearing in primates.

### 810 Pygopod Lizards are not Deaf

**Geoffrey Manley<sup>1,2</sup>**, Johanna Kraus<sup>1</sup>, Ulrike Sienknecht<sup>3</sup>, Christine Koeppl<sup>1</sup>

<sup>1</sup>Technische Universitaet Muenchen, <sup>2</sup>University of Western Australia, <sup>3</sup>Purdue University

In his 1978 book "The Reptile ear", Wever reports the recording of microphonic potentials from one individual Lialis burtonis, a legless lizard of the family Pygopodidae which occur almost exclusively in Australia. The 1 microvolt "threshold" he used indicated a best hearing sensitivity of about 65dB SPL. This was a very surprising finding, given that pygopods are classified as close relatives of the geckos, which are at least 50dB more sensitive. In combined field and laboratory studies of hearing in pygopods, we examined whether these animals really are so hard of hearing. We concentrated on the same species as Wever, but also examined several others using CAP measurements in the lab and spontaneous otoacoustic emission (SOAE) measurements in the lab and the field.

Although it proved difficult to record SOAE in these species, spectra were obtained in a minority of individuals with frequencies up to 8.25kHz, the highest SOAE frequency ever recorded in lizards. A suppression tuning curve of an emission at 6.3 kHz had a minimal threshold near the emission of 19dB SPL, easily comparable to similar data from geckos. CAP audiograms were also easily recordable in all cases. It thus appears that Wever's data are erroneous and that pygopod hearing is comparable to that of other sensitive lizard groups such as geckos and skinks. Pygopods can, as Wever reported, close their ear canal and it is possible that his specimen was measured in this condition. However, his drawing of the middle ear of his specimen differs substantially from those we studied and he may have had an animal with a malformed auditory system, emphasizing the danger of using one single specimen in such studies.

Supported by a grant to GAM from the Deutsche Forschungsgemeinschaft. We thank CALM of Western Australia for permission to work in National Parks.

### 811 Otoacoustic Emissions in Humans, Birds, Lizards, and Amphibians: A Comparative Study Reveals Differences in Emission Generation Mechanisms

**Christopher Bergevin**<sup>1</sup>, Dennis M. Freeman<sup>2</sup>, Christopher A. Shera<sup>3</sup>

<sup>1</sup>Speech and Hearing Biosciences and Technology Program, MIT, Cambridge, MA, <sup>2</sup>Dept. of Electrical Engineering and Computer Science, MIT, Cambridge, MA, <sup>3</sup>Eaton-Peabody Laboratory of Auditory Physiology, MEEI, Boston, MA

Much of what is known about the generation of otoacoustic emissions (OAEs) derives from mammals and takes account of relevant mammalian anatomy and physiology. Since non-mammals have OAEs, but lack some mammalian features, such as basilar-membrane traveling waves and hair-cell somatic motility, our goal is to learn more about OAE generation through a systematic study of evoked OAEs at lower stimulus levels. We examined four species with very different inner-ear anatomies: humans, chickens, geckos, and frogs. In mammals, the phase gradients (slope of emission phase with respect to frequency) indicate that there are at least two fundamentally different generation mechanisms. Here, the specific question we aim to answer is: In light of anatomical and physiological differences, is there evidence for multiple generation mechanisms in the non-mammalian vertebrates? Our results show many similarities among the four species in emission properties, such as significant level-dependent SFOAE phase gradients on the order of at least 1 ms (significantly larger in humans), non-linear (and sometimes non-monotonic) emission growth with stimulus level for both DPOAEs and SFOAEs, and the presence of spontaneous OAEs. A key difference in our data among species, however, stems from the relation between SFOAE and DPOAE phase gradients as well as gradients between lower (2f1-f2) and upper-sideband (2f2-f1) DPOAEs. Unlike the data in humans and chickens, the gradients provide no evidence of multiple generation mechanisms for lower versus upper-sideband DPOAEs in geckos and frogs. In addition, chickens have a frequencyindependent lower side-band DPOAE phase (similar to humans), supporting the presence of a scaling-symmetric traveling wave in the avian ear, in agreement with previous mechanical measurements.

Supported by NIH grants T3200038, R01 DC0023821 (DMF), and R01 DC03687 (CAS).

# Rate-Intensity Functions of Ventral Cochlear Nucleus Neurons in Normal and Hearing-Impaired Cats and Their Possible Relationships to Loudness Recruitment

**Shanqing Cai<sup>1</sup>**, Wei-Li Ma<sup>1</sup>, Benjamin Letham<sup>1</sup>, Eric D. Young<sup>1</sup>

<sup>1</sup>Center for Hearing and Balance, Johns Hopkins University, Baltimore, Maryland

Loudness recruitment, an abnormally rapid increase in loudness with sound intensity, is commonly seen in

sensorineural hearing loss. Its physiological mechanism remains obscure. Previous research in our lab revealed that auditory nerve fiber (ANF) population rate responses in cats with noise-induced hearing loss (NIHL) did not show recruitment, suggesting that recruitment reflects changes in central neurons.

The current study examined rate-intensity relationships of ventral cochlear nucleus (VCN) neurons in normal-hearing and deafened cats. Cats were deafened with exposure to 2-kHz noise bands (50 Hz wide, 111-112 dB SPL for 4 hours). Peripheral hearing thresholds were measured with the compound action potential. Simple and complex stimuli, including tones, broadband noise and speech tokens, were presented to construct rate functions ipsilateral to the site of recording. A pseudo-population approach was used to address the problem of limited data yield. Rate functions were analyzed by a linear spline regression algorithm.

Noise exposure caused 30-50 dB threshold shift in a range of frequencies surrounding 2-kHz. VCN units showed elevated thresholds and broadened tuning. Generally, the slopes of individual rate functions were not significantly different in normal and impaired ears. But NIHL caused decreased occurrence of non-monotonic rate functions. On the population level, NIHL reduced the range of unit thresholds and led to a larger degree of overlap between the dynamic ranges of different neurons. Similar effects were also observed in archived ANF data, though to a lesser degree. As a result, the population average rate functions showed steeper slopes and compressed dynamic ranges in the deaf ear. Simulated loudness matching between the normal and deaf populations produced curves with slopes greater than 1 dB/dB, consistent with recruitment. Full recruitment (rate catchingup at 80-90 dB SPL) was observed in a number of situations.

(Supported by NIH grant DC00109)

### 813 Cortical and Subcortical fMRI of Unilateral Tinnitus

**Cris Lanting**<sup>1,2</sup>, Emile de Kleine<sup>1,2</sup>, Hilke Bartels<sup>1</sup>, Dave Langers<sup>1,2</sup>, Pim van Dijk<sup>1,2</sup>

<sup>1</sup>Department of Otorhinolaryngology / Head and Neck Surgery, University Medical Center Groningen, <sup>2</sup>Fac. of Medical Sciences, School of Behavioral and Cognitive Neurosciences, University of Groningen

The current understanding of possible mechanisms of tinnitus generation is still poor. Our goal is to find a possible neural correlate of tinnitus, using fMRI.

In this work we used 10 patients (5 male) with unilateral tinnitus (5 left sided, 5 right sided) and 9 healthy subjects (4 male). Subjects had no or minor hearing deficits in both ears (max. 30 dB HL). Experiments were performed on a 3T Philips Intera scanner. 41 coronal slices (2 mm) were acquired using a matrix of 128x128 voxels (1.75 x 1.75 mm²) using sparse sampling (TR=10 s). Stimuli consisted of right and left stimulation with levels of 40 and 70 dB (SPL) of rippled noise.

Data were realigned and normalized to a custom made template using SPM5. First level analysis was performed using multiple regression and regions of interest (ROI) of the auditory pathway were defined (cortex, MGB, IC, SOC and CN). Percent signal changes were obtained for each condition for each region and symmetry indices were obtained. A second level analysis was performed using an ANOVA design to assess group differences and group-by-level interactions.

Results from the ROI analysis indicate that for the control group the cortex and inferior colliculus responded strongest to contralateral stimuli. A difference was observed between the two tinnitus patient groups. The left sided tinnitus group showed a predominant response towards ipsilateral stimuli at the cortex while the right sided tinnitus group responded more like the control group. A general trend of higher activation in the inferior colliculus as response to stimuli was observed in tinnitus patients compared to controls.

Our data suggest that there are differences in activation on cortex level and inferior colliculus level between the control group and the patient groups. Analysis of other nuclei will be performed.

### 814 Laminar Organization of the MSO in Autism

#### Randy Kulesza<sup>1</sup>

<sup>1</sup>Lake Erie College of Osteopathic Medicine

Autism is a psychosocial disorder clinically characterized by social difficulties, impairment in verbal and non-verbal communication skills and other typical repetitive behaviors. Despite the increasing number of individuals diagnosed with autism, the neurobiology of this condition is poorly understood. However, researchers have uncovered numerous structural anomalies in the brainstem, cerebellum and forebrain of autistic individuals. Further, there is substantial support in the literature for functional alterations involving the auditory system in autism, including an increased sensitivity to sound intensity, a decreased auditory dynamic range and impaired perception of speech and other social sounds, but an enhanced perception of pitch and music (Kellerman et al., 2005). Additionally, it has been observed that autistic individuals have difficulty detecting speech in noise, specifically when the background noise contains complex temporal features (Alcantara et al., 2004). These findings taken together with reported brainstem anomalies, suggest a disruption in the lower auditory brainstem, namely the superior olivary complex (SOC), a group of brainstem nuclei that function in sound source localization and descending modulation of the cochlea.

In an effort to find an anatomical correlate to the functional auditory deficits found in autistic individuals, we examined the SOC in post-mortem brain tissue from autistic individuals obtained from the Autism Tissue Program. The neurons of the human medial superior olive (MSO), an SOC cell group, have been shown to display a precise geometric organization and it has been suggested that this laminar organization is essential for sound source

localization. We have examined the neuronal architecture of the MSO in three age-matched control and autistic specimens. Preliminary results indicate a significant disruption of the laminar organization of the MSO.

# 815 Conductive Hearing Loss Leads to Changes in the Expression of Excitatory and Inhibitory Neurotransmitter Receptors in Cochlear Nucleus Neurons

Keith Dlugolenski<sup>1</sup>, Rebecca Finco<sup>1</sup>, Lina Patel<sup>1</sup>, Andrew Moiseff<sup>1</sup>, **Maria Rubio<sup>1</sup>** 

<sup>1</sup>University of Connecticut

This study focuses on determining whether conductive hearing loss affects the general and synaptic expression of excitatory and inhibitory receptors in cochlear nucleus neurons. We performed unilateral ear plugging and after 1week of survival, we analyzed the expression of AMPA and NMDA glutamate receptor subunits, and the glycine receptor  $\alpha 1$  subunit (GlyR  $\alpha 1$ ) at the light microscopic level. Our quantitative analyses revealed a significant increase in the general expression of GluR3 AMPA subunit in fusiform and cartwheel cells in the dorsal cochlear nucleus (DCN). Furthermore, the expression for GlyR $\alpha$ 1 decreased significantly in fusiform cells but not in cartwheel cells. These results indicate that a relatively short 1-week exposure to 30 dBA attenuation of sound is sufficient to result in up-regulating excitatory and downregulating inhibitory neurotransmitter receptors in DCN projection neurons. Next, we investigated whether hearing reduction also redistributed synaptic AMPA receptors in cochlear nucleus neurons receiving auditory nerve input, and whether these changes occurred in a relatively short time after unilateral earplug. Therefore, we performed postembedding immunogold labeling after freezesubstitution following 1-day of unilateral earplug. The quantitative analysis of the gold labeling for AMPA receptor subunits showed significant changes in the synaptic expression of specific AMPA receptor subunits at the synapse formed by the auditory nerve on projection neurons in the anteroventral and dorsal cochlear nuclei. These results indicate that hearing reduction affects the general and/or synaptic expression of AMPA and glycine receptors in cochlear nucleus neurons. Further, our data show that these changes occur rapidly. Therefore, our studies revealed that under circumstances of sound reduction, neurons in the brainstem are capable of modulating their synaptic strength by regulating the number of glutamate receptors at the synapse.

Funding: NIH/NIDCD RO1 DC006881-01A2 to M.E.R. and NSF DBI-0420580 for funds to purchase the Tecnai 12 Biotwin.

## 816 The Effects of Increasing Rates of Stimulation in Pediatric Cochlear Implant Users

**Taryn Davids**<sup>1</sup>, Jerome Valero<sup>2</sup>, Blake Papsin<sup>2</sup>, Robert Harrison<sup>2</sup>, Karen Gordon<sup>2</sup>

<sup>1</sup>University of Toronto Department of Otolaryngology-Head and Neck Surgery, <sup>2</sup>Department of Paediatric Otolaryngology – Head & Neck Surgery, Sick Kids

We examined the electrically evoked effect of increasing rates of stimulation on the auditory system. Our hypothesis was that increasing rates of electrical stimulation would impact central auditory activity as measured by evoked potential waveform latency, amplitude and thresholds for both evoked potentials of the auditory brainstem (eABR) and middle latency responses (eMLRs) (reflecting thalamo-cortical activity).

Electrically evoked responses were recorded in 11 N24 RE cochlear implant users aged 5- 17 years. Electrical stimulation was delivered at 11 Hz as single pulses, or pulse bursts at 500, 900, or 3600 pulses per second (pps). Response thresholds were determined. Significance was defined as p<0.05.

Latencies of brainstem responses were not significantly affected by rate of pulse presentation within a pulse burst. The eABR ellI wave amplitude was significantly higher in responses evoked by the 500 pps pulse burst than by the single pulse (p<0.01), however, wave eV showed a decrease in amplitude when evoked by the 500 pps burst compared to the single pulse (p<0.01). Further increases in pps (rate) within a pulse burst resulted in decreased amplitude of ellI with no significant changes in eV amplitude. EMLRs showed no statistically significant change in amplitude or latency with increased stimulation rates.

We conclude that auditory brainstem responses in children evoked by a single electrical stimulus differ from those evoked by electrical pulse bursts. The increased wave elll amplitude evoked by a 500 pps pulse burst suggests a summation effect of eABR amplitude responses from the initial pulses within the pulse burst sequence. This does not occur in responses evoked by either 900 or 3600 pps pulse bursts, suggesting adaptation effects of the auditory brainstem with higher rates of stimulation. More central areas appear more resilient to high rates of stimulation.

## 817 Pathological Effect of Auditory Nerve Demyelination on Cochlear Nucleus in Human

**Bappaditya Ray**<sup>1</sup>, Saroj Sharma<sup>1</sup>, Amit Kumar Dinda<sup>2</sup>, Shashi Wadhwa<sup>1</sup>, Tara Sankar Roy<sup>1</sup>

<sup>1</sup>Department of Anatomy, All India Institute of Medical Sciences, <sup>2</sup>Department of Pathology, All India Institute of Medical Sciences

Auditory neuropathy is a well-known cause of sensorineural hearing loss following cardiopulmonary bypass procedures in adults. The present study was performed on cochlea, auditory nerve (AN) and cochlear nucleus (CN) retrieved from a 40-day-old female infant

who underwent reparative procedure for her congenital cyanotic heart disease and expired in the early postoperative period. The AN and CN were processed for light electron-microscopic observations. Segmental demyelination in the fascicles of the transitional zone of the AN arising from the basal and some middle turns of the cochlea was noted. The distal most portion of the nerve did not reveal any features of degeneration, except some dilated endoneurial capillaries containing monocytes. Ultrastructural findings conformed to the diagnosis of acute myelinopathy. The cochlear nucleus (CN) was studied using various immunocytochemical markers microtubule-associated-protein-2 (MAP-2), synaptophysin (SYN), parvalbumin (PA) and calbindin (CB). The anterior portion, especially the nerve root portion of the nucleus (VCN) revealed strong expression of MAP-2 while the posterior regions showed decreased immunostaining indicating down-regulation of cytoskeletal proteins in the affected neurons. The anterior and anteromedial portions of both VCN and dorsal cochlear nucleus (DCN) showed strongly immunostained SYN positive perisomatic terminals while decreased immunoreactivity on the lateral and posterolateral regions. PA and CB expression revealed an increased immunostaining of AN fibers entering the nuclear complex as compared to the contralateral side. The affected neurons showed increased PA and CB immunoreactivity in a pattern as opposed to MAP-2 and SYN. The spiral ganglion neurons were normal histologically and did not reveal any features of degeneration. The results provide a possible cochleotopic innervation of the VCN in human that might be helpful while placing electrodes during invasive brainstem implants.

### 818 Effect of Vagal Nerve Stimulation on a Rat Tinnitus Model

**Joseph Ursick**<sup>1</sup>, Dianne Durham<sup>1</sup>, Hinrich Staecker<sup>1</sup>, Phillippe Lefebvre<sup>2</sup>, Jean Schoenen<sup>3</sup>, Martin Scholsem<sup>4</sup>, Thomas Imig<sup>5</sup>

<sup>1</sup>Department of Otolaryngology Head and Neck Surgery, Kansas University Medical Center, <sup>2</sup>Department of Otolaryngology, University of Liege, Belgium, <sup>3</sup>Department of Neurology, University of Liege, Belgium, <sup>4</sup>Department of Neurosurgery, University of Liege, Belgium, <sup>5</sup>Department of Molecular and Integrative Physiology, Kansas University Medical Center

Vagal nerve stimulation (VNS) has been used to treat a variety of disorders including epilepsy and depression. Recently, VNS has been shown to decrease neuronal spontaneous activity (SA) associated with chronic facial pain in a rat model. Several animal models suggest that tinnitus may be associated with changes in SA in the dorsal cochlear nucleus (DCN), inferior colliculus, and auditory cortex. Using a rat model of noise-induced tinnitus (Durham and Imig, JCN 490:391-413, 2005), we examined the effects of VNS on 2-deoxyglucose (2DG) uptake in the DCN of three groups of Long Evans rats. Rats were anesthetized and exposed to 15-20 kHz band pass noise at 115 dB SPL for one hour. Five days later, the VNS group (n=4) was implanted with a vagal nerve stimulator (Cyberonics, Inc.). On day 6, the stimulators

were activated and on day 7, 2DG was injected. A non-VNS group (n=8) received acoustic trauma and 2DG injection after 7 days, but no VNS stimulation. A control group (n=9) received neither noise exposure nor VNS. Animals were placed in a quiet sound attenuated chamber for 45 minutes during 2DG uptake. Rats were sacrificed and brainstem sections were prepared for 2DG film Optical density (OD) measurements autoradiography. were used to determine 2DG uptake in the high frequency (HF) and low frequency (LF) regions of the DCN. These OD values were used to calculate a symmetry ratio (ipsi HF/LF)/(contra HF/LF). In the control group, the symmetry ratio was near one. Noise exposure decreases 2DG uptake in the high frequency region of the ipsilateral DCN. Thus, both noise trauma groups showed a decreased symmetry ratio. However, the VNS group had a symmetry ratio that was intermediate to those in control and non-VNS groups. VNS stimulation may reduce the alteration of SA caused by noise trauma and thus warrants further study as a potential tinnitus therapy. Supported by the Tinnitus Research Consortium and the Dept. of Otolaryngology Head and Neck Surgery, KUMC

### 819 Acoustic Trauma Induces Long-Term Temporal Correlations in DCN

**Benjamin Letham**<sup>1</sup>, Wei-Li D. Ma<sup>1</sup>, Shanqing Cai<sup>1</sup>, Eric D. Young<sup>1</sup>

<sup>1</sup>Center for Hearing and Balance, Department of Biomedical Engineering, Johns Hopkins University
Changes to the functional properties of the dorsal cochlear nucleus (DCN) that follow acoustic trauma are not well understood. Past studies (e.g. Kaltenbach et al.) have reported an increase in mean spontaneous firing rates following acoustic trauma. However, recent work from our lab in DCN principal cells has found no change in mean spontaneous firing rate. This finding has led us to study temporal patterns in DCN spontaneous activity that may change independent of the mean rate. One pattern of specific interest is long-range dependence (LRD). LRD is an effect of fractal rate fluctuations, where rate fluctuations have weak correlations on the scale of minutes.

Cats were acoustically traumatized by exposure to 10kHz noise at 107dB SPL for four hours. Compound action potentials showed a >60dB threshold shift at and above 10kHz. Ten minutes of spontaneous activity were recorded from isolated single DCN units in these deaf cats as well as a group of normal hearing cats. LRD can be quantified by computing the Fano factor for a range of counting times. The Fano factor has a power-law dependence on counting time, and the exponent of the power-law is called the fractal dimension. This dimension is a measure of the spike count variance and LRD.

The average fractal dimension of the 10kHz-exposed DCN units is significantly higher than that of normal DCN units. Surprisingly, there is no correlation between higher fractal dimension and the degree of threshold shift (or spontaneous activity). The increased fractal dimension implies that neurons in exposed cats have more long-term correlations and higher spike count variance. Increased spike count variance could contribute to tinnitus by

providing a fluctuating rate signal that would be interpreted as resulting from a fluctuating sound.

(Supported by NIH grant DC00109 and the Tinnitus Consortium).

### 820 Auditory Brainstem Response in Otsuka Long-Evans Tokushima Fatty Rats, a Model of Obese Type II Diabetes Mellitus

Ken Uehara<sup>1</sup>, Mikio Suzuki<sup>1</sup>

<sup>1</sup>University of the Ryukyus

Although clinical observations about relationship between diabetes and sensorineural hearing loss were pronounced, the detail pathophysiology in inner ear and central auditory pathway remain obscure. In animal studies with alloxan- or streptozotocin-induced type I diabetic rat models, an increase in the latency of ABR and deterioration of hearing threshold has been reported. In order to evaluate the audition of Otsuka Long-Evans Tokushima Fatty (OLETF) rats at the age 50 weeks, a model of spontaneous obese type II diabetes, we measured ABR and compared the results with those in control Long-Evans Tokushima Otsuka (LETO) rats.

Latencies of individual waves and hearing thresholds for clicks were measured under pentobarbital sodium anesthesia. The latencies for wave III and IV were significantly prolonged in OLETF rats compared with those in LETO rats. However, there was no significant difference in hearing levels for clicks between two groups. There was no statistical significance in caudal motor nerve conduction velocity between OLETF and LETO rats. These results suggest that central auditory pathway is more sensitive to diabetic condition than inner ear. Further pathologic study is needed to clarify the lesions in inner ear and central auditory pathway.

## 821 The Dorsal Cochlear Nucleus as a Contributor to Auditory and Non-Auditory Components of Tinnitus

James Kaltenbach<sup>1</sup>

<sup>1</sup>Waynes State University

The dorsal cochlear nucleus (DCN) has been modeled in numerous studies as a possible source of tinnitusgenerating signals. This hypothesis was originally developed on the basis of evidence that the DCN becomes hyperactive following exposure to intense noise. Since these early observations, evidence that the DCN is an important contributor to tinnitus has grown considerably. In this paper, the available evidence to date will be summarized. In addition, the DCN hypothesis of tinnitus can now be expanded to include possible involvement in other, non-auditory components of tinnitus. It will be shown by way of literature review that the DCN has direct connections with non-auditory brainstem structures, such as the locus coeruleus, reticular formation and raphe nuclei, that are implicated in the control of attention and emotional responses. The hypothesis will be presented that attentional and emotional disorders, such as anxiety and depression, which are commonly associated with tinnitus, may result from an interplay between these nonauditory brainstem structures and the DCN. Implicit in this hypothesis is that attempts to develop effective antitinnitus therapies are likely to benefit from a greater understanding of how the levels of activity in the DCN are influenced by different states of activation of these nonauditory brainstem structures and vice versa.

## 822 Auditory Temporal Processing in the Guinea Pig Measured with Reflex Modification Audiometry

**Paul Allen**<sup>1</sup>, Nathaniel Housel<sup>1</sup>, Alaina Muldrow<sup>1</sup>, Peter Rivoli<sup>1</sup>, Stephanie Yee<sup>1</sup>, James Ison<sup>1</sup>

<sup>1</sup>University of Rochester

We sought to determine basic parameters of auditory temporal acuity in guinea pigs (N=4, males) using prepulse inhibition (PPI) of the acoustic startle response (ASR) as an objective index of sensory reception. The prepulse stimuli were silent gaps in otherwise continuous noise or the onset of sinusoidal amplitude modulation (SAM) of otherwise featureless noise. These stimuli provide standard measures of temporal acuity in other species, including humans, but they may be of particular relevance for guinea pigs because their vocal repertoire includes sounds that are comprised of periodic amplitude modulated noise varying in modulation frequency and duration. ASR magnitudes for startle eliciting stimulus (ES) levels of 80 to 130 dB SPL presented in quiet did not increase between P14 to P72, even with a 300% weight gain over this period. However, the ASR did increase with age when the ES was presented in a continuous noise background (70 dB SPL), this suggesting a maturation of their arousal response to noise. The effects of brief gaps in noise were similar to those found in mice, rats, and gerbils. When a 10 ms gap preceded the ES at intervals of 10 to 300 ms two separate phases of inhibition emerged, the first with maximum inhibition at 10 to 20 ms followed by a recovery of the ASR, then a second less powerful phase of inhibition with its maximum at about 100 ms, followed by a final recovery. When quiet gaps of 1 to 15 ms immediately preceded the ES, inhibition was evident at 1ms and was significant in 3 subjects at just 2ms. When quiet gaps of 1 to 15 ms preceded the ES by 100 ms, inhibition developed more slowly, reached a lower asymptote, and was more variable across subjects. The effects of SAM stimuli were unique compared to mice and gerbils. The onset of 100% SAM 100 ms prior to the ES completely inhibited the ASR for modulation frequencies (MF) of 30 to 150 Hz, with recovery at higher SAM frequencies. However, for 50% and 25% SAM modulation depths all animals showed very large facilitation of the ASR for MF less than 60 Hz. These novel SAM phenomena may result from common modulation features in these SAM stimuli and conspecific vocalizations.

## 823 Salicylate-Induced Tinnitus: Effects of Salicylate on Neurons in Dorsal Cochlear Nucleus

**Lei Wei**<sup>1</sup>, Wei Sun<sup>1</sup>, Dalian Ding<sup>1</sup>, Matthew Xu-Friedman<sup>1</sup>, Richard Salvi<sup>1</sup>

<sup>1</sup>University at Buffalo

The neural mechanisms for tinnitus are not well understood, but one hypothesis is that it originates from high rates of spontaneous activity in the dorsal cochlear nucleus (DCN). Support for this hypothesis has come from studies showing elevated spontaneous rates in the DCN following noise and cisplatin-induced hearing loss. High doses of sodium salicylate reliably induce tinnitus, but it is unclear what effects salicylate has on spontaneous activity in the DCN. To test this hypothesis, we prepared brain slices of the DCN from p13-20 rats and recorded the spontaneous firing rate of individual neurons before, during and after treatment with 1.4 mM salicylate. This concentration of salicylate in CSF has been shown to induce behavioral manifestations of tinnitus in rats. Recordings were obtained from three cell types, fusiform, cartwheel and giant cells, with identifications based on their morphological and/or physiological characteristics. The spontaneous spike rate of cartwheel and giant cells remained unchanged or increased slightly after salicylate perfusion. In contrast, the spontaneous spike rate of most fusiform cells decreased significantly after salicylate treatment. The results indicate that the effects of salicylate are specific to fusiform cells. Spontaneous spike rate partially recovered following brief (3-5 min) salicylate perfusion and wash-out. The recovery of spontaneous spike rate in fusiform cells was inversely related to perfusion duration and salicylate concentration. To determine if the decrease in spontaneous rate was induced by changes in synaptic activity, we recorded spontaneous post-synaptic currents in voltage clamp. No significant change was seen after salicylate treatment. These results suggest that the salicylate-induced decrease in spontaneous rate in fusiform cells is unlikely to be due a change in synaptic input, but may involve changes in the cell's intrinsic properties.

Supported in part by Tinnitus Research Consortium.

### 824 Alterations in Spontaneous Discharge Rates of Single Units in the Dorsal Cochlear Nucleus Induced by Intense Sound Exposure

Paul Finlayson<sup>1</sup>, James Kaltenbach<sup>1</sup>

<sup>1</sup>Wayne State University

Hyperactivity in the dorsal cochlear nucleus (DCN), characterized by increases in spontaneous activity, has been implicated as a possible factor contributing to tinnitus following noise exposure. Evidence for the phenomenon of noise-induced hyperactivity in the DCN has been obtained mostly using methods that examine activity of neural clusters (multiunit recordings) or populations of neurons (cfos, 2-deoxyglucose), an exception being a study by Brozoski et al., 2002, demonstrating noise-induced increases in single unit spontaneous discharge rates in the chinchilla DCN. Evidence for noise-induced hyperactivity

from our laboratory has been based almost entirely on multiunit recordings, raising the question of whether these increases reflect increased discharge rates at the single unit level, or instead, might be due to some other change. Increased multiunit activity could result from increases in extracellular voltages caused by increases in single unit spike amplitude, increased synchronous discharges, increases in the number of active units, or breakdown in intercellular insulation (demyelination). The present study was undertaken to determine whether intense sound exposure causes increases in the discharge rates of single units in the DCN. We performed three separate experiments, each comparing spontaneous discharge rates of single units in the DCNs of tone-exposed and control hamsters. In each experiment, a different combination of electrode impedance, electrolyte solutions, exposure conditions and recovery times were used. Animals were exposed to an intense (115-127 dB SPL) 10 kHz tone for 4 hours, either while anesthetized or while awake and freely mobile. Post-exposure recovery times were varied from 5 to 30 days. Recordings were obtained from more than 200 units at varying depths below the DCN surface. The results from all three experiments revealed considerable overlap in the range of spontaneous rates recorded in the two animal groups. Despite this overlap, the mean single unit discharge rates from exposed animals were consistently higher than those from control animals and were statistically significant. These results make it likely that multiunit hyperactivity reflects, at least in part, increases in single unit discharge rate. The possibility that one or more other factors might also contribute to multiunit hyperactivity cannot be ruled out.

(Supported by NIH grant DC003258).

## 825 Molecular Correlates of Noise-Induced Tinnitus: Alterations in Gene Expression Influencing Inhibition in the Dorsal Cochlear Nucleus

**Avril Genene Holt**<sup>1</sup>, Catherine Lomax<sup>2</sup>, Susan Land<sup>1</sup>, James Kaltenbach<sup>1</sup>

<sup>1</sup>Wayne State University, <sup>2</sup>University of Michigan

Noise-induced tinnitus can be a debilitating condition that decreases quality of life. A hallmark of noise-induced central tinnitus is thought to be a change in the balance between inhibition and excitation with sustained increases in spontaneous neuronal activity that begin in the dorsal cochlear nucleus (DCN). To explore mechanisms involved in this imbalance we screened nine genes influencing inhibitory neurotransmission in the DCN for changes in expression at different times following noise exposure. Animals were divided into ten groups: half were exposed to an intense (125-130 dB SPL) 10 kHz tone for 4 hours, and half were age matched unexposed controls. Exposed animals were assessed at each of 5 different postexposure recovery times: 0d, 2d, 5d, 14d and 29 days. The expression of nine genes, four glycine receptor genes (glyR1a, glyR2a, glyR3a, glyRb), four muscarinic receptors (muscR2, muscR3, muscR4, muscR5), and ChaT were assessed across groups. Each experimental group consisted of 3 RNA pools for each time-point, comprised of the DCN from three rats. Real time RT-PCR indicates that the DCN has some normal level of expression for each gene examined. In exposed animals, most glycine receptor subunits showed a trend towards an initial increase in expression followed by a decline in gene expression; however only glyR2a showed statistically significant increases in expression at the 0 (p  $\leq$  0.035) and 5 (p  $\leq$ 0.020) day time points with a return to normal expression levels by 29 days. A similar trend was seen among muscarinic receptors with increased expression immediately after exposure, followed by decreased expression at later time points. Again, only one of the receptors showed a statistically significant change in expression with muscR4 having decreased levels two (p < 0.025) and five (p  $\leq$  0.033) days after exposure. Compared with age-matched controls, ChAT expression after noise exposure showed a different temporal pattern from those of glycine and muscarinic receptors, with no change in gene expression at the 0 day time point, a sustained increase in expression that was statistically significant by the 14 day time point (p  $\leq$  0.038) and a 65% decrease in expression at the 29 day time point (p  $\leq$  0.084). These results suggest that alterations in the expression of neurotransmitter receptors influencing inhibition are among the changes occurring in the DCN that are thought to underlie noise-induced tinnitus.

(Supported by R01 DC003258 to JAK)

### 826 Using Earlab to Simulate Diagnostic and Prosthetic Systems

**David Mountain**<sup>1,2</sup>, David Anderson<sup>1</sup>, Glenn Breshanhan<sup>3</sup>, Andrew Brughera<sup>1</sup>, Socrates Deligeorges<sup>4</sup>, Viktor Vajda<sup>1</sup>, Allyn Hubbard<sup>1,5</sup>

<sup>1</sup>Boston University Hearing Research Center, <sup>2</sup>Boston University Dept. of Biomedical Engineering, <sup>3</sup>Boston University Scientific Computing and Visualization Group, <sup>4</sup>Biomimetic Systems, Inc., <sup>5</sup>Boston University Dept. of Electrical and Computer Engineering

Large-scale simulations of physiological systems hold great promise for integrating experimental data, and for predicting the outcomes of experimental and therapeutic manipulations. We believe that, for simulation to become more widely used, simulation systems should be designed to mimic both the biological system and the diagnostic and therapeutic devices that may be used to study and/or treat the biological system.

We have developed a modular software system for use by auditory scientists and clinicians called EarLab <a href="http://earlab.bu.edu">http://earlab.bu.edu</a>. The underlying software architecture is designed to be able to represent any physiological system or group of systems using interchangeable modules. Simulation parameters are loaded at runtime which facilitates species specific and patient-specific modeling.

To facilitate a wide range of simulation goals, EarLab modules have been developed that mimic the auditory periphery and brainstem nuclei. Additional modules have been developed to simulate data obtained through electrocochleography and to simulate cochlear prosthetics. The system also allows the user to simulate impaired auditory systems as well as the normal auditory system.

Examples will be shown that demonstrate how the modular approach facilitates rapid modification and extension of existing models to simulate new experimental and clinical paradigms.

Funded by NIH grant DC04731

## | 827 | Vesicular Glutamate Transporters 1 and 2 Immunolabel Distinct Subsets of Terminals in the Rat Inferior Colliculus

Ling Tong<sup>1</sup>, Douglas Oliver<sup>2</sup>, Avril Genene Holt<sup>3</sup>, Mike Ross<sup>4</sup>, Susan Shore<sup>4</sup>, Yilei Cui<sup>4</sup>, Richard Altschuler<sup>4</sup> <sup>1</sup>KKRI, University of Michigan, <sup>2</sup>University of Connecticut, <sup>3</sup>Wayne State University, <sup>4</sup>KHRI, University of Michigan Glutamate is a major excitatory transmitter in both ascending and descending auditory pathways, particularly for the pyramidal component of the ascending pathways. Vesicular glutamate transporters (VGLUT) 1 and 2 can label different and distinct subsets of glutamatergic terminals. The present study examined the distribution of VGLUT1 and 2 in the central nucleus, dorsal cortex and lateral cortex of the rat inferior colliculus (IC). VGLUT1 and VGLUT2 immunolabeling occurred in different terminals across each IC division, with no overlap. VGLUT1 terminals were larger than VGLUT2 labeled terminals in all divisions. In the central nucleus there were many VGLUT1 and VGLUT2 immunolabeled terminals. The VGLUT1 terminals were predominantly axo-dendritic and were relatively evenly distributed among central nucleus neurons. In contrast, the VGLUT2 terminals had a more limited distribution, but they blanketed the somata and proximal dendrites of medium-to-large (20 - 28 micron long diameter) neurons. VGLUT2 was infrequent around the somata of smaller neurons but made scattered contacts throughout the neuropil. In the dorsal cortex, VGLUT2 immunolabeled terminals were more numerous than VGLUT1 terminals. The VGLUT2 terminals in dorsal cortex made axo-somatic contacts on small dendrites and a sub-population of medium-to-large neurons showed prominent axo-somatic and proximal dendritic contacts. In the lateral cortex there were also more VGLUT2 than VGLUT1 immunolabeled terminals. The VGLUT2 labeled terminals in lateral cortex were found on most neurons. contacting dendrites in layer 1 and both somata and dendrites in layers 2 and 3. However prominent axosomatic or proximal dendrite contacts were not seen as in the central nucleus and dorsal cortex. VGLUT1 terminals made predominantly axo-dendritic contacts, a pattern consistent across the IC. These findings therefore identify distinct population of glutamatergic inputs to the rat IC with different patterns of distribution and suggest they originate in different types of neurons providing inputs to the IC. Supported by NIDCD RO1 - DC00383

## 828 Blocking Spontaneous Activity in Postnatal Rat Inferior Colliculus Perturbs Development of Afferent Compartments

**C.K.** Henkel<sup>1</sup>, D.A. Agee<sup>1</sup>, S.R. Franklin<sup>1</sup>

<sup>1</sup>Wake Forest University

Afferent projections to the central nucleus of the inferior colliculus (IC) distribute in a banded pattern along IC layers. Previous studies have shown that this pattern of afferent compartmentalization develops between postnatal day 4 and postnatal day 8 in rat pups. Unilateral cochlear ablation at postnatal day 2 or 9, presumably altering spontaneous activity asymmetrically in ascending brainstem pathways, disrupts segregation of the DNLL afferent distribution. The present study was undertaken to determine more directly if blockade of spontaneous activity in the IC perturbs development of DNLL afferent bands. An Elvax polymer was prepared with 0.5 mg/ml dose of tetrodotoxin (TTX) or a GABA agonist, muscimol. Postnatal day 4 or 5 rat pups were operated to expose the dorsal surface of the midbrain and an Elvax-TTX or muscimol patch was implanted over the IC. At postnatal day 12, the treated and control rat pups were sacrificed by perfusion with paraformaldehyde. A glass pin coated with carbocyanine dye, Dil was inserted into the dorsal tegmental commissure of Probst to label the crossing axons of the DNLL projection to the IC. After 6 weeks incubation, the brains were sliced and sections mounted for microscopic analysis of labeled axons in IC. Dil labeled fibers in the untreated IC were distributed in distinct bands along IC layers. Dil labeled fibers in the treated IC exhibited only modest segregation. Preliminary statistical evaluation indicated that the banded distributions on the treated and untreated side were significantly different. The findings support a permissive role for spontaneous activity in development of afferent compartments in IC.

Supported by NIH grant DC004412 and in part by Mr. and Mrs. A. Tab Williams, Jr. and Family Neuroscience Research and Program Development Endowment

### 829 Patterns of Convergence for Multiple Afferent Projections to the Central Nucleus of the Inferior Colliculus Prior to the Onset of Hearing

**Robert Fathke, Jr.** <sup>1</sup>, John McHaffie<sup>2</sup>, Craig Henkel<sup>2</sup>, Mark Gabriele<sup>1</sup>

<sup>1</sup>James Madison University, <sup>2</sup>Wake Forest University School of Medicine

The central nucleus of the inferior colliculus (IC) is a laminated structure that receives multiple converging afferent projections. Although specific patterns of convergence for several of these inputs have been recently described in the adult, little is known about the ontogeny of these projections. The present study used the carbocyanine dyes Dil, DiA, and DiD concurrently to determine the development and spatial relationships of various combinations of these converging inputs within the central nucleus of the IC. Fixed brain preparations in the early postnatal rat and cat were examined at various developmental stages prior to hearing onset. Double- and triple-labeling studies facilitated the visualization of layered

inputs arising from various subdivisions of the cochlear nuclei (CN), the lateral and medial superior olivary nuclei (LSO, MSO), and the dorsal nucleus of the lateral lemniscus (DNLL). Layered afferent patterns from each of these sources were localized and terminated within appropriate sublayers of the central nucleus prior to experience. While certain inputs filled the extent of the laminae, exhibiting a more band-like morphology in coronal sections, other inputs exhibited a greater degree of specificity, terminating within target sublayers as a series of afferent patches. Cases labeling inputs arising from opposite sides resulted in layered arrangements that targeted adjacent sublayers and interdigitated within the IC. Conversely, inputs sharing source laterality targeted similar sublayers, thereby exhibiting varying degrees of projection overlap. The early appearance of these afferent patterns suggest that distinct synaptic domains within the IC are largely defined prior to experience. It remains unclear whether these projections initially target specific sublayers, or whether they are sculpted from a preexisting diffuse projection distribution. Embryonic experiments are planned and mechanisms that may shape these patterns are discussed.

## 830 Early Sound Exposure Alters Frequency Coding in the Inferior Colliculus (IC) of the Rat

Marco Izquierdo<sup>1</sup>, Manuel Malmierca<sup>1</sup>, Douglas Oliver<sup>2</sup>
<sup>1</sup>Auditory Neurophysiology Unit. Lab Neurobiol of Hearing.
Inst. Neurosci. & Univ of Salamanca, Spain, <sup>2</sup>; Dept.
Neuroscience, Univ. Connecticut Health Center,
Farmington CT.

The IC is a convergence centre for most of the auditory information en route to the cortex. Postnatal sound exposure leads to changes in the tonotopic map in the auditory neocortex, but its role in the IC is unknown. Therefore, we studied the IC in adult rats following postnatal sound exposure (14kHz 60-70dB pure tone pips, from P9-P28, Zhang et al., 2001). In the central nucleus of IC, recordings after P49 show that the early sound exposure modifies the size of the 14 kHz frequency lamina when compared to the control. The length of the frequency step that included 14 kHz in exposed animals was significantly different (p<0.001) from the 14kHz step in the control, as well as different from the adjacent frequency laminas within exposed animals. Nevertheless, there were no differences in the steps to either side of 14 kHz or the mean step size between exposed animals and controls. In three cases, there was a significant decrease in the size of the 14kHz lamina instead of an increase. Over the entire IC including dorsal and lateral cortex, the total number of multi-unit recordings at the exposed frequency showed a small, consistent increase (p<0.07) that suggests an influence of the early sound exposure even outside of the central nucleus. To investigate these changes further, we recorded 51 frequency response areas from well isolated single units. The four units with a BF at 14 kHz were similar to control in threshold and bandwidth near threshold. However, 68% of the units (19/28) with BF above 14 kHz had a peak of higher activity around 14 kHz. Two-tone suppression in 28 single units showed that the

secondary peak of activity around 14 kHz may be due to increased excitation because inhibition was absent. In contrast, 2/28 cases with BF > 14kHz showed a distinct island of inhibition at 14kHz.

In summary, early sound exposure alters the tonotopic map in the central nucleus of IC. Most often, it increases the size of the frequency-band lamina and increases the number of neurons responding to the frequency of the early sound exposure. This alteration may be the result of frequency-specific synaptic changes.

Supported by the NIH grant R01 DC00189 (DLO) and Spanish DGES (BFI-2003-09147-02-01) and JCYL-UE (SA084/01 and SA040/04) to MSM. MAI held fellowships from the MEC and JCYL.

### 831 Commissural Projections of the Inferior Colliculus

Manuel Malmierca<sup>1</sup>, Olga Hernández<sup>1</sup>, Adrian Rees<sup>2</sup>
<sup>1</sup>Auditory Neurophysiology Unit. Lab Neurobiol of Hearing.
Inst. Neurosci. & Univ of Salamanca, Spain, <sup>2</sup>School of
Neurology, Neurobiology and Psychiatry, The Medical
School, Newcastle upon Tyne, UK.

The commissure of the IC (CoIC) is a distinctive fibre tract connecting the ICs. It represents a significant afferent input to the IC and provides the last opportunity for interaction between the left and right sides of the auditory pathway at the subcortical level. Recently, we reported that the commissural projection modulates spectral and temporal neuronal responses in the IC (Malmierca et al. 2003, 2005). Early anatomical studies suggest that the projections from one IC to the other were densest in the dorsomedial region of the IC (Aitkin et al. 1984; Coleman and Clereci, 1987). More recent studies (Malmierca et al. 1995; Saldaña and Merchán, 1992) have demonstrated that these projections extend over the whole IC, but could not distinguish whether each neuron projected only to a corresponding point in the contralateral side, or whether its area of influence extended more widely. To address this question in rat, we have injected a mixture of BDA fluorescein-dextran and tetramethyl-rhodamine-dextran into physiologically defined regions of the IC in the same animal (n=4), and made computer-assisted reconstructions of all labelled neurons in the contralateral side. Our results reveal that neurons in a frequency band lamina in the CIC make a divergent projection that encompasses the whole of the equivalent lamina in opposite side, but the density of this projection is weighted towards a point matching the position of the injection. In the dorsal cortex there are two populations of neurons projecting across the commissure. One projects to the frequency-band laminae in the central nucleus, while the other projects exclusively and diffusely within the dorsal cortex. Such connections could facilitate processing within the ICs: the point-to-point pattern permits interactions between specific regions of corresponding frequency-band laminae, whereas the divergent projection would subserve integration across the lamina.

This study was supported by DGES (BFI-2003-09147-02-01) and JCYL-UE (SA040/04) to MSM, TheWellcomeTrust (066348) to AR and Spanish MCYT (FP-2000-5811) to OH.

## 832 Neural Responses to Ultrasonic Vocalizations in the Inferior Colliculus of the Awake Mouse

Christine Portfors<sup>1</sup>, Patrick Roberts<sup>2</sup>, Kreg Jonson<sup>1</sup> <sup>1</sup>Washington State University, <sup>2</sup>Neurological Sciences Institute, Oregon Health & Science University Ultrasonic vocalizations are commonly emitted by mouse adults and pups. These vocalizations often contain energy between 50-80 kHz with some pup calls containing energy up to 100 kHz. It is unclear how these ultrasonic vocalizations are encoded by neurons in the auditory system because frequencies greater than 50 kHz are not well represented in the mouse cochlea. To determine whether auditory neurons respond to these natural sounds, we examined responses of single units in the inferior colliculus (IC) of the awake mouse to adult and pup ultrasonic vocalizations. Responses to single tones and combinations of tones were recorded and used to predict responses to vocalizations. Responses to ultrasonic vocalizations were not always explained by single tone frequency tuning curves, but were sometimes explained by responses to combinations of ultrasonic frequencies. Neurons in IC responded to the combination of two ultrasonic frequencies if the difference between the frequencies was near the neuron's characteristic frequency. Responses to ultrasonic difference frequencies may be a mechanism by which low frequency neurons in the mouse's auditory system are able to respond to ultrasonic vocalizations. This mechanism would enable a reduced frequency representation in the cochlea while maintaining neural responses to natural ultrasonic vocalizations.

#### 833 Accounting for Complex Frequency Interactions in Predictions of Neural Responses to Social Vocalizations in the IC of the Mustached Bat

**Lars Holmstrom**<sup>1</sup>, Patrick Roberts<sup>2</sup>, Christine Portfors<sup>3</sup>
<sup>1</sup>Portland State University, <sup>2</sup>Oregon Health & Science University, <sup>3</sup>Washington State University

The inferior colliculus (IC) of the midbrain is believed to be sensitive to complex features of auditory stimuli. Neurons in the IC of the mustached bat integrate sensory input from multiple frequency bands in a complex and often nonlinear fashion. These neurons are important for encoding the mustached bat's echolocation and social vocalizations. The purpose of this study was to quantify the contribution of complex frequency interaction effects on the responses of these neurons to social vocalizations. Neural responses to synthetic single and two tone stimulus protocols were recorded for a population of neurons. In addition, neural responses to social vocalizations of the mustached bat were recorded. Many of the neurons sensitive to combinations of tones were found to have tuning characteristics that fall within behaviorally relevant frequency bands found in the bat's own vocalizations. A minimum mean squared error (MMSE) linear model integrating both frequency and temporal features of the stimulus was designed to predict the response of a given neuron to novel vocalizations not used in the design of the

model. This model was then extended to include a corrective term accounting for the complex two tone frequency tuning characteristics of the neuron. It was found that the model with the corrective term improved predictions of the neural response when compared to predictions made by the simpler model.

## 834 Comparison of Frequency Tuning in Inferior Colliculus Obtained with Extracellular and *In Vivo* Whole Cell Recordings

**Ruili Xie**<sup>1</sup>, Josh Gittelman<sup>1</sup>, George Pollak<sup>1</sup>

<sup>1</sup>University of Texas at Austin

Neurons in the inferior colliculus (IC) express a wide variety of tuning curves, including narrow or broad classical V-shaped tunings, O-shaped tuning curves in which neurons only respond at low intensities, and null tuning curves where neurons do not respond to tones at any frequency-intensity combination. Here we compare the tuning of IC neurons recorded with extracellular electrodes to both the tuning of synaptic inputs and discharges obtained with in vivo whole cell recordings. We were especially interested in inhibition, and the degree to which excitatory tuning was flanked by inhibitory surrounds. With extracellular recordings, excitation was monitored as discharges and inhibition was inferred by the increased discharges that were evoked while inhibition was blocked by local application of inhibitory channel blockers. With in vivo whole cell recordings, excitation and inhibition were visualized as depolarizing hyperpolarizing membrane potentials.

The same types of tuning described above that were observed with extracellular recordings were also seen with in vivo whole cell recordings. This included cells whose synaptic and discharge tuning were both V shaped and were dominated by excitation with little evidence of inhibition. These cells apparently correspond to narrow Vshaped tuning obtained with extracellular recordings that did not expand when inhibition was blocked. Other cells had V-shaped excitatory synaptic and discharge tuning but surrounding frequencies evoked combined IPSP-EPSPs in which inhibition suppressed the excitation. These cells most likely correspond to those cells with V-shaped tuning curves recorded extracellularly where tuning expanded when inhibition was blocked. The third types of cells had synaptic responses dominated by broadly tuned inhibition. EPSPs were only evoked by a limited range of frequencies, and spikes were evoked only by an even narrower range of frequencies and only at low intensities. The discharge tuning features of these neurons were similar to O-shaped tuning curves that were recorded extracellularly. Finally, yet other neurons with tuning dominated by inhibition did not fire any action potential to any tone burst, and apparently correspond to neurons with null tuning curves obtained with extracellular recordings. Supported by NIH grant DC00268.

# 835 Mechanisms of FM Sweep Directional Selectivity Revealed by Whole-Cell Recordings in the Inferior Colliculus of Awake Bats

**Joshua Gittelman**<sup>1</sup>, Ruili Xie<sup>1</sup>, George Pollak<sup>1</sup> *UT Austin* 

Many neurons in the inferior colliculus (IC) express directional preferences for FM sweeps. The dominant model (Suga, '65) holds that directional preferences are created by asymmetries of sideband inhibition. The model predicts that FM signals sweeping in the preferred direction activate excitatory frequencies first, evoking spikes. FMs that sweep in the non-preferred direction first activate inhibitory sidebands, which then suppress the following excitation. Thus, FMs in the preferred direction should first depolarize the cell, whereas FMs in the non-preferred direction should evoke hyperpolarization first.

To directly observe membrane potential changes evoked by FM sweeps, we made whole-cell current-clamp recordings from IC cells. We found neurons that were FM directionally selective and cells that were non-selective. In some directionally selective cells, the temporal order of hyperpolarization and depolarization changed with sweep direction, consistent with Suga's model. directionally selective cells, however, the temporal order did not change with sweep direction; inhibition led excitation in response to both upward and downward sweeps. In one cell, we estimated inhibitory and excitatory conductances (g<sub>e</sub> and g<sub>i</sub> respectively) and the inhibitory and excitatory currents evoked by FM signals. The cell strongly preferred upward sweeps, yet both upward FM and downward FM evoked the same latency difference between g<sub>i</sub> and g<sub>e</sub>, where g<sub>i</sub> latency was always shorter than g<sub>e</sub>. The direction selectivity was therefore not created by differences in excitatory and inhibitory latencies, but rather was created by a greater relative change in ge than in gi; comparing responses to upward FMs with downward FMs, the increase in ge was proportionately larger than the increase in gi, yielding a net increase in excitation to upward FMs. These data suggest that direction selectivity is created by more than one mechanism in the IC.

Supported by NIH grant DC 00268.

### 836 Neural Selectivity for Spectral Motion in Conspecific Vocalizations

Sari Andoni<sup>1</sup>, Na Li<sup>1</sup>, George Pollak<sup>1</sup>

<sup>1</sup>University of Texas at Austin

Frequency-modulated (FM) signals are a prominent feature of both human and animal vocalizations. When FM stimuli sweep upward or downward in frequency they create a movement of mechanical energy across the sensory surface of the cochlea. In humans, this movement results in the perception of motion across successive pitches termed spectral motion. Spectral motion cues, such as the direction and velocity of motion, could provide the auditory system with the necessary elements that lead to the perception of an auditory object. Here we analyzed spectrotemporal features of conspecific communication calls used by the Mexican free-tailed bat and show that

these features are in agreement with tuning properties reflected in receptive fields of auditory neurons in the inferior colliculus (IC). By decomposing conspecific vocalizations into their spectral and temporal modulations, i.e. moving ripples, we were able to determine the FM direction and average velocity present in each call. Comparing spectral and temporal modulation rates present in bat calls with those modulation rates that evoked neural responses showed that IC neurons, by means of full spectrum-time inseparability, are tuned for the FM direction most prominent in their conspecific vocalizations. Additionally, directional (quadrant) inseparability enabled IC neurons to be tuned for the velocity of spectral motion, where the FM velocities present in bat communication signals corresponded strongly with the range of sweep velocities to which IC neurons are best tuned. This shows that auditory neurons in the IC are optimally tuned for spectral motion cues found in their conspecific vocalizations.

# 837 Current Injection Evoked Responses with *In Vivo* Whole Cell Recordings Mimic the Response Features of *In Vitro* Recordings but do not Correlate with the Sound Evoked Responses in the Inferior Colliculus

Ruili Xie<sup>1</sup>, George Pollak<sup>1</sup>

<sup>1</sup>University of Texas at Austin

Response features of inferior colliculus neurons to both current injections and tone bursts were studied with in vivo whole cell recordings in awake Mexican free-tailed bats. Three types of temporal discharge patterns evoked by depolarizing current injections were obtained in 44 IC neurons, including onset, sustained adapting, and sustained non-adapting firing patterns. In response to hyperpolarizing current injections, nearly 50% of the neurons showed initial hypepolarization followed by a depolarization sag as well as rebound depolarization and/or spikes, which suggests the presence of I<sub>h</sub> current. Similar response features to both de- and hyperpolarizing current injections were also reported in previous in vitro studies with rats and mice, which indicates that in vitro recordings reveal the true intrinsic properties of the neurons.

Three types of responses were also obtained from these neurons evoked by 50ms tone bursts that were presented at 50dB SPL at various frequencies. The averaged resting potential of all the neurons was –61mV. At rest, 45% of the neurons responded to tones across multiple frequencies with excitation-dominant responses. In comparison, inhibition dominated the responses of 50% of the neurons. Only 5% of the neurons responded to tones with dominant excitation at middle frequencies and dominant inhibition at surrounding frequencies.

The current evoked response features, however, did not correlate with the response features evoked by tone bursts. In each type of the current evoked discharge patterns, there were neurons that responded to tones with either excitation-dominant responses or inhibition-dominant responses. We conclude that the intrinsic

properties of IC neurons shape their sound evoked response features, but intrinsic properties alone cannot predict how these neurons respond to auditory stimuli. Supported by NIH grant DC00268

## 838 Mapping the Neuronal Response Properties in the Inferior Colliculus of Mexican Free-Tailed Bats

Na Li<sup>1</sup>, Sari Andoni<sup>1</sup>, George Pollak<sup>1</sup>

<sup>1</sup>Institute of Neuroscience, University of Texas at Austin

This study evaluated how different neuronal response properties evoked by a set of downward and upward frequency modulation sweeps (FMs) are organized in the inferior colliculus (IC) of Mexican free-tailed bats. Multi-unit recordings were used to map the IC and obtain an overall view of how response features evoked by FM sweeps are topographically arranged. The results obtained with multiunit recordings were subsequently confirmed with single-unit recordings.

Multi-unit recordings showed that direction selective cells, cells that prefer FMs that sweep in one direction over FMs that sweep in the other direction, are especially prevalent in two regions of the IC. Direction selective cells dominate the posteromedial and anterolateral regions of the IC, whereas non-selective cells are most prevalent in the rest of the IC. While neurons in the anterolateral and posterolateral regions of the IC express directional preferences, cells that prefer downward FM sweeps are far more prevalent in the posteromedial region. Most cells in the anterolateral region prefer upward FM sweeps.

The findings based on multiunit recordings were then confirmed with single unit recordings. Single-unit recordings showed that 63% of cells in the posteromedial region are downward selective and 67% of cells in the anterolateral region are upward selective. In addition, single-unit recordings also showed that cells in the posteromedial region prefer different FM rates than cells in the anterolateral region. About 60% of the cells in the posteromedial region responded most strongly to FMs sweeping at fairly fast velocities, from ~ 25-75 oct/sec. In contrast, over 70% of the cells in the anterolateral region responded most strongly to slower FMs with velocities of about 12.5 oct/sec.

Previous studies showed that different aural response properties are clustered in the IC of bats and other mammals. Here we show that different FM response properties are also segregated in the IC.

Supported by NIH grant DC 00268.

## 839 The Strength of Auditory-Cued Associative Learning Reflects the Level of Nicotinic Receptor Function in the Auditory Cortex

**Kevin Liang**<sup>1</sup>, Bonnie Poytress<sup>1</sup>, Norman Weinberger<sup>1</sup>, Raju Metherate<sup>1</sup>

<sup>1</sup>UC Irvine

Recently, we showed that nicotinic acetylcholine receptors (nAChRs) in adult auditory cortex (ACx) enhance physiological processing of acoustic stimuli, but neonatal nicotine exposure impairs both physiology and auditory-cued behavior (Liang et al., Eur. J. Neurosci., 2006). To better understand the relationship between nAChR function and behavior, here we correlate the degree of physiological enhancement with behavioral performance in individual animals.

Adult rats learned an auditory-cued active avoidance task over 4 days of training with varying degrees of success, and were classified as "good," "intermediate" or "poor" performers (n=4 for each group). After training, rats were anesthetized and tone-evoked local field potentials (LFPs) were recorded in layer 4 of ACx before and after delivery of nicotine (0.7 mg/kg, s.c.) or saline. Nicotine effects differed significantly among the three groups. In "good" performers, nicotine enhanced LFP amplitude and decreased response threshold to characteristic frequency (CF) stimuli, but had opposite effects on responses to spectrally-distant stimuli (i.e., auditory filters narrowed). In contrast, nicotine had no effect on LFPs in "poor" performing animals, and weak effects (not significant) in "intermediate" performers. We then conducted similar experiments in rats (n=11) that were exposed to nicotine neonatally, a treatment that leads to adult nAChR dysfunction (Liang. et al. 2006). Behavior of the treated animals resembled that of "poor" performing controls, and did not correlate with any physiological effects of nicotine.

Our findings suggest that nAChRs are required for "good" learning of auditory-cued active avoidance, further supporting an important role for the neurotransmitter acetylcholine in auditory learning.

### 840 Environmental Noise Delays Temporal Auditory Processing Development

**Wei Sun**<sup>1</sup>, Liyan Zhang<sup>1</sup>, Anna Hansen<sup>1</sup>, Daniel Stolzberg<sup>1</sup>, Richard J. Salvi<sup>1</sup>

<sup>1</sup>University at Buffalo

The processing of complex sounds such as language requires rapid temporal information processing at multiple stages along the auditory pathway, including the auditory cortex (AC) where rapid temporal cues are decoded and interpreted. Recent studies suggest that impoverished auditory experiences can lead to profound and potentially long lasting deficits on function and structure of the AC. For example, when rodents were raised in constant, broad band noise environment during the critical developmental period, neurons in the AC neurons showed poor neural tuning, abnormal tonotopic organization and sluggish temporal responses. It is unclear whether the sluggish neural responses observed in the AC leads to an auditory

temporal processing deficit that be read out in an observable behavioral response. To determine if postnatal noise rearing during the critical period leads to perceptual deficits in auditory temporal processing, we measured prepulse inhibition of the acoustic startle reflex using a silent gap in a continuous background noise to suppress the startle response. The minimum gap duration needed to suppress the startle reflex to a criterion amount was defined as the gap detection threshold (GDT). groups of new born rats were used (1) a control group raised in a normal quiet environment, or two groups raised in moderate noise environment (70 dB SPL, white noise), (2) one group raised from P12-P53 and another (3) raised from P12-P90. GDT were tested at different postnatal ages. Rats raised in a quiet environment showed a rapid decrease of GDT from P27-P45; the average GDT reached a plateau of less than 4 ms (n = 5) after P45. In contrast, the average GDT was  $16 \pm 7$  ms (n = 3) in the P12-P53 group and  $8.7 \pm 1.1 \text{ ms (n = 3)}$  at P12-P90 group; the GDT of the both noise raised groups were significantly different from the GDT of the control group. After noise raised rats were returned to a normal, quiet environment, their GDT rapidly dropped to less than 4 ms in 5-7 days. Our results provide the first behavioral evidence showing that noise-rearing during the critical period leads to an impairment in auditory temporal resolution as reflected in the startle reflex read out. However, the deficits in startle reflex GDT quickly recovered to normal when the rats were returned to their quiet environment. Research supported in part by grants from NIH and DRF

## 841 Neonatal Nicotine Exposure Delays Development of Auditory Temporal Resolution

**Anna Hansen**<sup>1</sup>, Liyan Zhang<sup>1</sup>, Daniel Stolzberg<sup>1</sup>, Richard Salvi<sup>1</sup>, Wei Sun<sup>1</sup>

<sup>1</sup>University at Buffalo

Maternal smoking leads to cognitive and learning deficits in children and adolescents. Moreover, neonatal nicotine exposure has been found to impair cell proliferation and synaptic developments in the central nervous system. In the auditory system, chronic exposure of nicotine to newborn rats impairs auditory cortex (AC) function. Recent studies suggest that AC impairments lead to deficit in auditory learning in adult rats. Since the AC plays a crucial role in auditory learning and the processing complex signals, we hypothesized that neonatal nicotine exposure might lead to deficits in auditory temporal acuity. To test this hypothesis, we exposed neonatal rats to nicotine and assessed auditory temporal acuity by using a gap detection paradigm to assess pre-pulse inhibition of the acoustic startle reflex. The minimum gap duration (silent interval) in a continuous background noise needed to suppress the acoustic startle reflex was defined as the gap detection threshold (GDT). Three groups of neonatal rats were used: (1) a control group, injected with saline from P8-P12, (2) a low dose nicotine group (1 mg/kg) and (3) a high dose nicotine group (5 mg/kg) both injected with nicotine from P8-P12 (twice a day). GDTs were tested at P20, P28, P35, P45, P60 and P120. In the control group,

GDT showed a rapid developmental decrease from P28 to P45. In contrast, GDT declined more slowly in the nicotine treated groups compared to the control group during the developmental period. GDT in the nicotine groups were significantly different from the control group at P35. However, the GDT differences between nicotine groups and control group decreased from P45 to P60 suggesting a transitory rather than permanent effect. These results suggest neonatal nicotine exposure delays, but not permanently impair auditory temporal acuity.

Research supported in part by grants from NIH and DRF.

### 842 Stress Response in Rat Brain After Different Durations of Noise Exposure

**James Samson**<sup>1</sup>, Rathinasamy Sheeladevi<sup>2</sup>, Rajan Ravindran<sup>2</sup>, Manohar Senthilvelan<sup>2</sup>

<sup>1</sup>Nofer Institute of Occupational Medicine, Lodz, Poland, <sup>2</sup>University of Madras, Chennai, India

The auditory effects of noise exposure and its implications have been widely studied and documented. However, the non-auditory effects of acoustic stimuli, particularly the stress response of the brain to noise exposure is quite complex. Therefore, this study attempts to determine the relationship between the major factors involved in the brain's stress response and noise exposure.

The alteration in the levels of plasma corticosterone, brain norepinephrine, and expression of brain heat shock proteins (Hsp70) after different durations of noise exposure (acute - 1 day, sub acute - 15 days and chronic - 30 days) has been studied to analyze their role in combating time dependent stress effects of noise. Broadband white noise exposure (100 dB SPL for 4 hours per day) to male wistar albino rats significantly increased the levels of plasma corticosterone and norepinephrine in all three durations of noise exposure.

The increased levels observed after chronic noise exposure suggests that animals are not adapting to noise even after 30 days of exposure. The important role of Hsp70 in combating noise induced stress is evident from the significant increase in its expression after chronic exposure, while there was a reciprocal decrease in the norepinephrine and corticosterone when compared with their levels after acute and sub acute noise exposure. This indicates that the time dependent stress response to noise exposure is а complex mechanism interconnected systems such as hypothalamo-pituitaryadrenal axis, heat shock proteins and may have implications in the brain when there is a prolonged noise exposure.

### 843 Hypoxic Changes of Central Nervous System in Noise-Exposed Mouse

**Young-Jin Kim<sup>1</sup>**, Hun Hee Kang<sup>2</sup>, Joong Ho Ahn<sup>2</sup>, Kwang-Sun Lee<sup>2</sup>, Jong Woo Chung<sup>2</sup>

<sup>1</sup>daejin medical center, <sup>2</sup>asan medical center

Background and objectives: When noise-induced hearing loss occurs, hypoxia is detected in inner ear tissues. In previous study noise-induced inner ear hypoxia was

proved by the increase of HIF-1a, which is expressed? in the nucleus under hypoxic condition. Another hypoxic marker, pimonidazole is also widely used to see the hypoxic area by injection from outside. Existence of tinnitus or hyperacusis with noise-induced hearing change may suggest the change of central nervous system, but no exact site or timing of change is alleged until now. The study is designed to investigate the site-specific hypoxic change in central auditory pathway during noise induced threshold shift.

Materials and Methods: Fifty six BALB/c hybrid mice with normal hearing were exposed to 120 dB SPL broad band noise for 3 hours. Immediately after noise and 7 days after noise exposure, the brains of mice were extracted. They were cryosectioned by 15 (m thickness and examined by immunofluorescence using monoclonal antibody of HIF-1a and pimonidazole HCL (hypoxyprobe(-1).

Result: After noise, the hearing thresholds of mice decreased to 49.5 ( 8.0 dB HL and the hearing were recovered to 27.9 ( 4.3 dB HL in 7 days. In the coronal section of brain, HIF-1a was detected immediately after noise in the auditory cortex, hippocampus and inferior colliculus. At least for 7 days, these signals persisted although without additional noise exposure. When the same slides were double stained by hypoxyprobe(-1, auditory cortex, hippocampus and inferior colliculus showed more localized hypoxic signals. The uptake of pimonidazole increased after 7 days.

Conclusion: In noise-induced transient threshold shift, hypoxia occurred in central nervous system and it persisted until 7 days, even though hearing was recovered. These changes were sensitive in auditory cortex and hippocampus.

Keywords: Noise-induced hearing loss, Central nervous system, Hypoxia, Hypoxia-inducible factor 1a, Pimonidazole

### 844 Gap Processing Across A1 Layers in Young and Aged Rats

**Larry Hughes**<sup>1</sup>, Loren Zuiderveld<sup>2</sup>, Jeremy Turner<sup>1,3</sup>, Jennifer Parrish<sup>1</sup>, Donald Caspary<sup>1,2</sup>

<sup>1</sup>Department of Surgey/Otolaryngology, Southern Illinois University School of Medicine, <sup>2</sup>Department of Pharmacology, Southern Illinois University School of Medicine, <sup>3</sup>Department of Psychology, Illinois College

Age-related hearing loss affects approximately 30% of the population over the age of 65. Presbycusis can be considered a slow central and peripheral deterioration of auditory function which manifests itself as deficits in speech comprehension, especially in noisy environments. Speech comprehension requires the processing of rapidly changing sounds and silent intervals. Gap detection has been used as a simple measure of auditory temporal acuity. The present study examined age-related gap detection in rat primary auditory cortex (A1). Unit responses were simultaneously recorded from all layers of the left A1 of 15 young and 13 aged FBN rats using a 16-channel electrode (Neuronexus single shank, Technologies, Ann Arbor, MI). Three A1 penetrations were attempted on each rat. Broadband Noise was presented

to the contralateral ear at 60 dB SPL with a variable silent interval embedded within the stimulus. Gap widths of 0ms, 2ms, 4ms, 8ms, and 16ms were presented in a pseudorandom order and spontaneous activity was recorded for 2 min before and after the Gap protocol. Acoustic protocols were executed by custom software (Hancock & Voigt) and data recorded on a Plexon system. A mixed model repeated-measures analysis of variance was evaluated for sorted responses on each channel to determine neural responses to the various gap presentations. Superficial lavers (I-III)significantly higher stimulus driven firing rates than deeper layers for both young and aged animals. Aging was associated with increased stimulus driven firing in the superficial but not deeper layers of A1. Superficial layers increased firing rate in response to the gap while neurons in deeper layers appeared insensitive to the gap. Finally, there was a tendency for the change in firing rate in response to the gap, in superficial layers, to be greater in young rats than aged.

Supported in part by (SIU Excellence in Academic Medicine, LFH; NIH DC00151, DMC; and NIH AG023910, JGT).

# 845 Correlations Between Intrinsic Optical Signals and Unit Response Properties in Rat Auditory Cortex Following Altered Developmental Trajectories

Nathan Higgins<sup>1</sup>, Heather Read<sup>1</sup>

<sup>1</sup>University of Connecticut

Altered cortical development due to genetic or environmental factors can shift auditory representations, however it is not always clear what auditory regions or what specific response property may change. Previously, we described reduced spike-rate responses to pure-tone and periodic noise bursts in A1 of rats that had parietal freeze-lesions induced the first day after birth (P1). In the present study, the Fourier intrinsic imaging and multi-unit recording techniques were used to map best frequency (BF) responses across five cochleotopic areas in rat auditory cortex (Kalatsky et al, 2005). Transient pure-tones were presented to both ears via hollow earbars for imaging and unit recording. Puretones were presented as a train in ascending and descending frequency order. Tone trains contained 16 (2-32 kHz) or 2 tones (8, 16 kHz) for measuring intrinsic response BF and magnitude, respectively. Multi-unit activity was recorded in layer IV with tungsten electrodes; optical activity was recorded at the same cortical depth. High correlations were found for optical map and unit activity BF estimates across multiple sound levels. Optical magnitude was correlated with spike rate measured at the same cortical site. Spike rate-level functions and BF correlations were reduced in animals with parietal microgyri versus controls. This data suggests that fourier intrinsic imaging can be used to successfully compare BF, cochleotopy, and rate-level sensitivities across different auditory cortical areas and animals.

Research supported by NICHD: HD2080

## 846 Neural Circuits for Silent Speechreading in Postlingual Deaf: Activation Pattern and Correlation with Speechreading Fluency

**Hyo-Jeong Lee<sup>1</sup>**, Eric Truy<sup>2</sup>, Dominique Sappey-Marinier<sup>3</sup>, Anne-Lise Giraud<sup>1</sup>

<sup>1</sup>Inserm U742, University of Pierre and Marie Curie (Paris 6), Paris, France, <sup>2</sup>Departement d'ORL, Hopital Edouard Herriot, Lyon, France, <sup>3</sup>CERMEP, Hospital Neurologique, University of Claude Bernard, Lyon, France

Speechreading is a major communication mean in postlingually deafened patients. Activation of superior temporal auditory areas during silent speechreading is observed in normal hearing subjects (Calvert et al., Science 1997), while different neural circuits are implicated in born deaf (MacSweeney et al., Neuropsychologia 2002). In this present study, neural networks associated with silent speechreading were investigated in postlingual deaf. Functional MRI data were collected in 9 postlingually deafened adults and 15 normal hearing controls while they speechread numbers or counted meaningless lip movements (gurning).

Both groups engaged common neural circuits during silent speechreading, encompassing bilateral posterior superior temporal gyri (STG), inferior parietal lobule and bilateral inferior prefrontal cortex. Contrary normal subjects who presented higher activation levels for speechreading than counting in bilateral anterior insula, left prefrontal and anterior cingulate cortices, deaf subjects activated the same network for both conditions. This reflects that deaf subjects are proficient speech-readers, and have an increased sensitivity to face motion, even during meaningless mouth movements. In patients, the left posterior STG region positively correlated with speechreading fluency assessed pre-scanning during clinical tests.

This study shows that neural networks normally dedicated to auditory speech are re-wired to process visually-presented speech following auditory deprivation in postlingually deafened adults. Speechreading fluency correlates to the activation in left posterior STG region (Area Spt; Hickok and Poeppel, Cognition 2004), which is supposed to be critical interface between sensory- and motor- based representations of speech.

## **847** Prenatal Alterations to the HPA Axis Induces Gender-Related Dysfunction in Adult Life to Acoustic Trauma.

**Saïda Hadjab**<sup>1</sup>, Amzad Hossain<sup>1</sup>, Nenad Bogdanovic<sup>2</sup>, Agneta Viberg<sup>1</sup>, Barbara Canlon<sup>1</sup>

<sup>1</sup>Physiology & Pharmacology, Karolinska Institutet,

<sup>2</sup>Neurobiology, Karolinska University Hospital, Huddinge

Prenatal stress results in long-term disruption of neuronal function and persistent behavioral disorders. In the present study we used prenatal exposure to dexamethasone (DEX, a synthetic glucocorticoid), and adult exposure to an audiogenic stressor in the offspring, to investigate i) the effects on behavior, using the elevated plus maze, and ii) responsiveness of the hypothalamic-pituitaryadrenocortical (HPA) axis to acoustic trauma.

Stereological quantification of neuronal protein expression (glucocorticoid receptor, GR) and corticotrophin releasing hormone (CRF) in the paraventricular nucleus (PVN) demonstrated gender-related differences in the basal protein expression, as well as its responsiveness to acoustic stress. Acoustic trauma caused a robust and nuclear responsiveness of GR expression translocation in DEX females. The present data exemplify the differential sensitivity of the developing nervous and endocrine systems to stress, depending not only on gender but also on the nature of the stressful experience endured by the mother during pregnancy and the offspring in adult-life.

Supported by grants from the Swedish Research Council, AMF Trygghetsförsäkring, Tysta Skolan, and the Karolinska Institute.

### 848 Early Metabolic Responses of Auditory and Visual Cortex in Deaf Cats Measured by FDG-PET

**Min-Hyun Park**<sup>1,2</sup>, Jin-Su Kim<sup>3</sup>, Hyo-Jeong Lee<sup>1</sup>, Jae Sung Lee<sup>3</sup>, Dong Soo Lee<sup>3</sup>, Seung-Ha Oh<sup>1</sup>

<sup>1</sup>Department of Otolaryngology, Seoul National University College of medicine, Seoul, Korea, <sup>2</sup>Boramae Municipal Hospital, Seoul, Korea, <sup>3</sup>Department of Nuclear Medicine, Seoul National University College of Medicine, Seoul, Korea

The resting cerebral glucose metabolism has been reported to show deafness-related cortical plasticity in deaf patients. Auditory cortical plasticity by deafness has been reported in deaf rat models by glucose metabolism using 2-deoxyglucose autoradiographic methods. In this study we examined cerebral metabolic activity pattern in deaf cats in auditory and visual cortex and then compared with that of normal hearing controls using FDG-PET scanning.

Eleven FDG-PET images of cat brain were obtained using a microPET R4 scanner (Concorde Microsystems Inc., Knoxville, TN) in 7 domestic cats. Four scans were collected in normal hearing status and 7 scans following deafening procedure by intravenous ethacrynic acid. The mean duration of deafness was 7.4 months. During FDG uptake and scanning, the cats were laid in the scanning room with ambient noise and illumination under anesthesia by ketamine (100mg/kg) and xylazine (10mg/kg). The emission images were acquired after injection of 2.8;3/40.1 mCi FDG following the transmission scan using 68Ge line source. Metabolic activity was measured in three regions of interest (ROIs), which were drawn on primary auditory cortex, visual cortex, and cerebellum in both hemispheres and compared between two status (normal hearing vs. deaf). To standardize metabolic activities, the mean count ratios of each ROI to the mean count of cerebellum were calculated.

The glucose metabolic ratio decreased in deaf status compared to hearing status in bilateral auditory cortex (p = 0.006 for left side, p = 0.109 for right side), showing decreased neural activity in auditory cortex by deprived sensory input. In contrary, visual cortex showed higher metabolism (p = 0.012 and 0.006 for left and right visual cortex) in deaf status compared to hearing status,

suggesting compensatory visual hyperactivity of deaf cats. This preliminary results show early metabolic response following deafness in cat deaf model using FDG-PET analysis method.

## 849 Sensorineural Hearing Loss Disrupts Inhibitory Short-Term Plasticity in the Developing Auditory Cortex

**Anne Takesian**<sup>1</sup>, Vibhakar Kotak<sup>1</sup>, Dan Sanes<sup>1</sup>

New York University

Much of auditory perception relies upon temporal processing, and deficits arising from developmental hearing loss may perturb the underlying synaptic mechanisms. While sensorineural hearing loss (SNHL) has been shown to weaken GABAergic inhibition in the auditory cortex (Kotak et al., 2005), the extent to which developmental SNHL affects the temporal properties of inhibitory connections has not been explore. In this study, we assessed the affect of developmental SNHL on inhibitory short-term plasticity using a paired-pulse ratio (PPR) paradigm. SNHL was induced in gerbil pups at postnatal (P) day 10 and the animals were raised for 6-11 days. Using whole-cell voltage-clamp recordings in auditory cortex layer 2/3 pyramidal neurons, GABAA receptor-mediated inhibitory postsynaptic currents (IPSCs) were elicited by extracellular intracortical stimulation in the presence of ionotropic glutamate receptor antagonists. The results showed that IPSCs in control gerbils generally displayed paired-pulse facilitation (PPF), and this was significantly reduced in SNHL neurons PPR=2.7±0.4, N=14; SNHL PPR=1.2±0.4, N=12, p=0.03). Inhibitory short-term plasticity is known to be variable, with individual neurons exhibiting both facilitation and depression, and our recordings also displayed this characteristic. In control neurons, IPSCs showed a high incidence of PPF and a low incidence of paired-pulse depression (PPD) (82% PPF, 11% PPD, N=14). However, IPSCs in SNHL neurons showed a low incidence of PPF and a high incidence of PPD (32% PPF, 58% PPD, N=12). Preliminary recordings in pre-hearing gerbils (P9-11) suggest that PPD predominates (N=6), which resembles the induced bias towards PPD observed in SNHL neurons. Together, these results suggest that hearing loss perturbs the maturation of mechanisms underlying inhibitory shortterm facilitation, which may impact temporal processing by the auditory cortex.

(This study was supported by NIH DC6864 to DHS and VCK)

### 850 Effects of Deafening on Dendritic Spine Formation in the Rat Auditory Cortex

**Scott Schachtele**<sup>1</sup>, Joseph Losh<sup>1</sup>, Michael Dailey<sup>1</sup>, Steven Green<sup>1</sup>

<sup>1</sup>University of Iowa

Rat auditory cortical pyramidal neurons rapidly develop dendritic spines, the primary location of excitatory synapses in the central nervous system, between the ages of postnatal day (P)11 and P21 (<0.1 spine/µm and >1 spine/µm, respectively). This increase in spine density correlates temporally with both the establishment of mature auditory hair cell thresholds and hearing-evoked activity in central auditory neurons, suggesting a correlation between hearing onset and synaptic reorganization in the auditory cortex. The goal of this research is to investigate the role of early auditory afferent input on the patterning of dendritic spine development in neonatal rats from P4, prior to hearing onset, through P42 when hearing is mature. In vivo dendritic spine density was assessed using the lipophilic dye 1,1'-dioctadecyl-3,3,3',3'tetramethylindocarbocyanine perchlorate (Dil) in P4, P9, P11, P14, P19, P21 and P42 rats. Interestingly, early postnatal deafening via kanamycin-induced hair cell toxicity (P8-P15) does not significantly alter the rate of spine formation in layer 2/3 and 5 auditory cortical pyramidal neurons compared to control hearing rats. To further examine this lack of an effect from deafening, we analyzed (1) spine density variability (2) difference in dendritic arborization and (3) growth of new projections from other sensory cortices (cross-modal sensory plasticity). Our results show no significant difference in spine density variability, complexity of the dendritic arborization or in cross-sensory plasticity between hearing and deafened animals. Currently we are combining Dil labeling with immunohistochemistry for Bassoon, a presynaptic scaffold protein, to enable visualization of synapses on dendritic spines. Using this technique we will be able to determine if early postnatal deafening results in a change in synapse occupancy of dendritic spines in vivo.

## 851 Long-Term Synaptic Plasticity in the Intact Auditory Cortex is Enabled by Nucleus Basalis Stimulation

**Robert Froemke**<sup>1</sup>, Michael Merzenich<sup>1</sup>, Christoph Schreiner<sup>1</sup>

<sup>1</sup>UCSF

Receptive fields of the adult sensory cortex are plastic, capable of a high degree of reorganization. In most cases, plasticity requires activation of subcortical neuromodulator nuclei such the nucleus basalis (NB), the primary source of cortical acetylcholine (ACh). However, the relation between forms of synaptic plasticity such as long-term potentiation (LTP) and depression (LTD) with receptive field plasticity is unknown.

We made whole-cell recordings in vivo from neurons in the primary auditory cortex of adult anesthetized rats. After mapping receptive fields with tone pips, we repetitively paired tones at a certain frequency, the conditioned stimulus (CS), with electrical stimulation of NB. This NB pairing procedure led to LTP of excitation evoked by the

CS. Conversely, LTD of excitation to the best frequency (BF) was observed after pairing. NB pairing also induced LTD of inhibitory current evoked by the CS. These changes persisted for >20 minutes and were frequency-specific; aside from changes to CS and BF, responses to all other frequencies were generally unaltered. Excitatory and inhibitory plasticity were coordinated together, as both effects were prevented when either NMDA receptors or ACh receptors were blocked. Moreover, excitatory LTP could be induced by repetitive presentation of the CS alone, when inhibition was blocked via intracellular dialysis with picrotoxin. Finally, recordings made in serial over a period of hours indicated a slower time course for eventual retuning of cortical inhibition.

This shift in the balance of excitation and inhibition might alter the firing mode of cortical neurons. After NB pairing, neurons that originally fired relatively sparsely fired in a more tonic manner. These results demonstrate that long-lasting modifications of excitatory and inhibitory inputs are rapidly induced in vivo, and can be used to control the spectrotemporal structure of cortical receptive fields.

## 852 Gene Expression and Plasticity of Rat Auditory Cortex After Bilateral Cochlear Ablation

**Seung-Ha Oh<sup>1</sup>**, Jae-Jun Song<sup>2</sup>, Chong-Sun Kim<sup>1</sup> Seoul National University, <sup>2</sup>Dongguk University International Hospital

Sensoroy deafferentiation affects the development of the cetnral nervous system. It is reported that auditory cortex is rewired after deafening and the plastic change is more prominent in prelingual deafness.

In this study, we made prelingual deaf rat model and used DNA microarray to analyze the differential gene expression in the primary auditory cortex between the deaf and age matched normal control groups. The cochlea was ablated bilaterally at a postnatal 10-14 days in the deaf groups. The gene expression of auditory cortex was compared at 2, 4, and 8 weeks after ablation.

In deaf groups, the expression of immediate early genes (EGR1, 2, 3, 4, c-fos, ect.) and neural plasticity related genes (ARC, syngr1, BDNF, ect.) was decreased at 2 weeks and increased at 4 weeks. L-type voltage dependent calcium channel alpha 1c subunit (Cacna1c) was upregulated at 2 weeks and L-type voltage dependent calcium channel alpha 1s subunit (Cacna1s) was upregulated at 4 weeks. The expression neurotransmitter related genes (Gabra5, Chrnb3, Chrne, ect.) were decreased at 12 weeks. For selected genes the changes in gene expression were confirmed by real-time PCR.

These findings indicate that the plastic change of synaptic connectivity induced by the immediate early genes and the plasticity related genes plays an improtant role in the eraly change of auditory cortex after deafening during the critical period. Also, we believe that decreased expression of neurotransmitter related genes is the result of long term change by the cross-modal plasticity.

### 853 Auditory-Visual Processing in Children with Cochlear Implants

**Phillip Gilley**<sup>1</sup>, Anu Sharma<sup>1</sup>, Michael Dorman<sup>2</sup>

<sup>1</sup>University of Colorado at Boulder, <sup>2</sup>Arizona State University

Our sensory systems typically process multimodal information with great frequency and efficiency. This study was designed to investigate whether the late introduction of auditory stimulation would affect the integration of information from the auditory and visual modalities. We examined unimodal and bimodal stimulus processing in a group of congenitally deaf children who received cochlear implants as a means of introducing input to the central auditory system at different ages. The children participated in a reaction time task that compared detection and reaction times for auditory alone, visual alone, and combined auditory-visual stimuli. Event-related potentials were recorded during the task to index differences between neural responses to unimodal and Preliminary results indicate that bimodal stimulation. children who received a cochlear implant late in childhood show deficits in the processing of combined auditory-visual stimulation when compared to children implanted early in childhood or when compared to normally hearing children. These results suggest that integration of auditory and visual stimuli is dependent upon early sensory experience. Some reorganization of the central pathways may occur after a period of early sensory deprivation, allowing the development of integrative processing of auditory-visual input.

# 854 Nicotinic Activation Facilitates Thalamocortical Transmission by Enhancing Excitability and Spike-Timing Precision in Myelinated Thalamocortical Axons

Hideki Kawai<sup>1</sup>, Ronit Lazar<sup>1</sup>, Raju Metherate<sup>1</sup>

<sup>1</sup>University of California, Irvine

Auditory information reaches primary auditory cortex (A1) via axons of ventral medial geniculate (MGv) neurons that project to cortical layers 3-4. The information is carried by action potentials (APs) initiated in MGv axons following synaptic integration in dendrites and the soma. Thus, thalamocortical axons provide a potentially powerful locus for regulation of information transfer; however, to date there has been no evidence for such a regulatory mechanism.

Using the auditory thalamocortical brain slice from adult mice, we found that nicotine, an agonist of nicotinic acetylcholine receptors (nAChRs), enhanced thalamocortical axon excitability as reflected in increased probability of AP induction at stimulus sites in the superior thalamic radiation (STR, through which thalamocortical axons course). The effect was blocked by the nAChR antagonist dihydro- -erythroidine (DH E). Nicotine also decreased the onset latency of axon spikes in the white matter and monosynaptic EPSCs in A1, especially when using weaker, prolonged stimuli that mimic near-threshold inputs to MGv axons. Spike-timing variability also decreased, indicating that nicotine may further enhance

thalamocortical transmission by synchronizing APs. Consistent with increased AP probability and timing precision, nicotine increased the initial slope of STR-elicited local field potentials (LFPs) recorded in A1. Finally, in preliminary *in vivo* studies, we found that DH E injected near STR in anesthetized mice reduced the initial slope of tone-evoked LFPs in A1, indicating tonic nicotinic control of thalamocortical axons by ACh.

Our results demonstrate, for the first time, that a neurotransmitter can regulate conduction along thalamocortical axons. Control of axon excitability and spike timing may contribute to nicotinic enhancement of auditory processing in A1.

# B55 Differential Effects of Iontophoretic Application of the GABA<sub>A</sub>-Antagonists Bicuculline and Gabazine on Tone-Evoked Local Field Potentials in Primary Auditory Cortex

**Simone Kurt**<sup>1</sup>, Christoph Möller<sup>2</sup>, Holger Schulze<sup>2</sup>
<sup>1</sup>Department of Neurobiology, University Ulm, <sup>2</sup>Leibniz Institute for Neurobiology, Magdeburg

 $\gamma$ -aminobutric acid (GABA) is one of the main inhibitory transmitters in the central nervous system. In a recent study we have demonstrated differential effects of two iontophoretically applied GABAA-blockers, bicuculline (BIC) and gabazine (SR 95531), on neuronal responses in primary auditory cortex (AI) (Kurt et al., Hear. Res. 212, 224-235, 2006): Whereas the only effect of gabazine was to block GABA<sub>A</sub>-mediated inhibition, BIC-application additionally induced dose-dependent side-effects, probably on calcium-dependent potassium channels. As both the blocking of GABA<sub>A</sub>-mediated inhibition as well as the mentioned side-effects lead to an increase in overall neuronal activity and excitability, the increase of neuronal spiking activity was stronger after BIC than after gabazine application. Here we investigated the effects of the two drugs on pure tone evoked local field potentials (LFPs) in AI.

LFPs were recorded from the left AI of anaesthetized and unanaesthetized Mongolian gerbils before, during and after microiontophoretic application of BIC and gabazine using multi-barrel glass electrodes (5-6  $\mu$ m tip diameter).

After the application of both drugs, a significant (paired ttest) increase of the N1-component of the LFP was observed in both anaesthetized (BIC: control: 480.2  $\mu V$ ; drug: 849.8  $\mu V$ ; P = 1.8E-5; gabazine: control: 333.5  $\mu V$ ; drug: 505.9  $\mu V$ ; P = 0.0002) and unanaesthetized animals (BIC: control: 185.5  $\mu V$ ; drug: 458.4  $\mu V$ ; P = 3.3E-7; gabazine: control: 438.4  $\mu V$ ; drug: 706.0  $\mu V$ ; P = 0.04), but this increase was much more pronounced after BIC than after gabazine application (over all animals: BIC: 310.3  $\mu V$ ; gabazine: 194.6  $\mu V$ ; ANOVA: P = 0.05). Furthermore, after application of BIC a prolongation of LFPs was observed that was not seen after gabazine application.

We conclude from these results that the secondary BIC effects seen in neuronal spiking responses can also be demonstrated in LFP data.

## 856 GABA<sub>a</sub> Receptor Subunit Changes in a Noise-Exposure Model of Tinnitus: Rat Medial Geniculate Body

**Donald Caspary**<sup>1,2</sup>, Danyelle Martin<sup>3</sup>, Lynne Ling<sup>1</sup>, Hongning Wang<sup>1</sup>, Pete Hutson<sup>4</sup>, Jeremy Turner<sup>2,5</sup>, Emma Reuschel<sup>6</sup>, Larry Hughes<sup>2</sup>

<sup>1</sup>Department of Pharmacology, Southern Illinois University School of Medicine, <sup>2</sup>Department of Surgery/Otolaryngology, Southern Illinois University School of Medicine, <sup>3</sup>Department of Microbiology, University of Illinois at Chicago, <sup>4</sup>Department of Sleep and Schizophrenia Research, Merck Inc., <sup>5</sup>Department of

Psychology, Illinois College, <sup>6</sup>Department of Chemistry and Biology, Illinois College

The medial geniculate body (MGB) is the major auditory thalamic nucleus. MGB receives segregated ascending inputs from the inferior colliculus and descending cortical inputs from auditory cortex and nonauditory cortices. Previous studies have reported noise-induced evidence of tinnitus in the central auditory system. The present study examined selective GABA<sub>A</sub> receptor subunit changes three months following a 16kHz octave-band, 115dB noiseexposure, thought to induce tinnitus in rats. Two non "wild-type" GABA receptor subunits, the  $\alpha_4$  and  $\delta$  subunits appear to be concentrated in synaptic and extra-synaptic Subunit message levels were constructs in MGB. quantified using in situ hybridization and subunit proteins were visualized using fluorescent immunocytochemistry in young and aged noise-exposed rats compared to young and aged unexposed controls. Young noise-exposed rats showed significant upregulation of the  $\alpha_4$  subunit in both ipsi- and contralateral MGB (>50% increase), while aged rats showed α<sub>4</sub> subunit upregulation in the contralateral MGB (>100%increase). Young and aged noise-exposed rats showed significant δ subunit upregulation in the MGB (dorsal, young>48%; aged>103%; ventral, young>84%; aged>170%) contralateral to the noise exposure.

It has been proposed (Sur et al., 1999) that upregulation of a  $\alpha_4\beta\delta$  GABA<sub>A</sub> receptor construct may be a compensatory plastic change to offset hyperactive neuronal networks. The present GABA<sub>A</sub> receptor subunit changes suggest that noise-exposure related changes in MGB may, in part, subserve the percept of tinnitus. Age-related differences in subunit plasticity associated with noise-exposure might provide insights into the increased incidence of tinnitus in the elderly.

Supported in part by American Tinnitus Association, NIH DC00151, and Merck Inc.

## 857 Effects of Sodium Salicylate Induced Tinnitus on Auditory Cortex Local Field Potentials in Awake Rats

**Daniel Stolzberg**<sup>1</sup>, Wei Sun<sup>1</sup>, Guang Yang<sup>2</sup>, Edward Lobarinas<sup>1</sup>, Richard Salvi<sup>1</sup>

<sup>1</sup>University at Buffalo, <sup>2</sup>Yueyang Hospital of Shanghai Traditional Medical and Pharmacy University

Sodium salicylate (aspirin), a well known inducer of tinnitus in both humans and animals, has been used extensively to investigate the neurophysiological correlates of tinnitus in animal models. Despite the fact that tinnitus is only perceived when subjects are conscious, nearly all of the neurophysiological studies of tinnitus carried out to date have been carried out under anesthetics which disrupt or alter the neural process that give rise to this phantom auditory sensation. To avoid the confounding effects of anesthetics, we carried out a series of experiments in which we measured the tone-burst evoked, local field potential from the auditory cortex (AC) of conscious rats before and after administering a high dose (250 mg/kg, i.p.) of salicylate known to produce behavioral signs of tinnitus around 16 kHz. A chronic, electrode implanted on the AC was used to record the cortical evoked potential in response to tone bursts presented at 4, 8, 12, 16, 24 and 32 kHz. Sound level was increased from the animal's threshold up to 90 dB SPL. Preliminary recordings showed that salicylate caused an increase in the peak-topeak amplitude of the AC evoked response at 2 h and 6 h post-treatment. The largest amplitude increase, on the order of 80%, occurred at 16 kHz around 90 dB SPL (p<0.05). The salicylate-induced amplitude enhancement was noticeably less at frequencies below 16 kHz (45-55%, 4-12 kHz) and above 16 kHz (35-55%, 24-32 kHz). The AC amplitude enhancement was greatest at 2 h postsalicylate and decreased slightly at 6 h post-treatment, except at 16 kHz where there was a slight amplitude increases.

Supported in part by grant from the Tinnitus Research Consortium

## 858 Cooling Auditory Cortex Alters the Interaural Level Difference Sensitivity of Neurons in the Inferior Colliculus

Kyle Nakamoto<sup>1</sup>, Alan Palmer<sup>1</sup>

<sup>1</sup>MRC-Institute of Hearing Research, Nottingham, U.K.

The descending projections from the cortex were studied in anaesthetized guinea pigs by cooling the cortex and measuring the changes in the response of inferior colliculus (IC) neurons. Responses to tones, clicks, broadband and sinusoidally amplitude modulated (SAM) noise at different ILDs were measured before, during and after the auditory cortex was cooled. The responses to clicks consisted of a transient onset response followed by a second response ~10-30 ms later. In the majority of IC cells ( ~60%), when the cortex was cooled, the second peak was severely reduced ( >50%). The responses to the SAM stimuli consisted of an initial response, and a later more sustained response. The initial response consisted of two distinct peaks, and the primary effect of cooling was a reduction of the second peak, similar to the response to clicks. This resulted in an overall suppression of the ILD functions during cooling and had little effect on their shape. The effect of cooling on the later responses was more complex. In approximately half of the cells the peak of the ILD function shifted during cortical cooling. Additionally, cooling altered the ILD at which the maximum locking of the spikes to the envelope of the SAM stimulus occurred. Overall these results suggests that the descending projections from the cortex modulate the values of ILD to which cells in the IC are sensitive. Such

a role for the cortico-collicular projection is consistent with recent studies that indicate that it is necessary for plastic changes to altered binaural localization cues.

## 859 Mechanisms of the Auditory Thalamocortical Transformation: Dual Projections Via Branched Axons

Amar Kishan<sup>1</sup>, Charles Lee<sup>2</sup>, David Larue<sup>1</sup>, Jeffery Winer<sup>1</sup> <sup>1</sup>University of California, Berkeley, <sup>2</sup>University of Chicago How do thalamic projections influence the neocortex? The cat medial geniculate body (MGB) projects to 13 areas of auditory cortex (AC), five of which are tonotopically organized. To study how the two frequency maps within the MGB might create these spectral maps in the AC, we injected two sensitive retrograde tracers, the beta fragment of the cholera toxin (CT?) and its gold conjugate (CT?G), at mapped and unmapped AC loci and counted the proportions of MGB neurons labeled by each tracer and by both. In one experiment, wheat germ agglutinin apo-HRP conjugated to gold (WAHG) was used with CT?. Matchedfrequency deposits in primary auditory cortex (AI) and in the anterior auditory field (AAF) were compared to unmapped cases with deposits in tonotopic and nontonotopic fields.

Following matched-frequency deposits, fewer than 5% of double-labeled cells were found in every MGB division. Interestingly, the tonotopically organized ventral division did not have a significantly different percentage of double-labeled cells than the other divisions. The highest mean values were seen in the rostral pole nucleus: 2.7% compared to 1.8% elsewhere.

Surprisingly, there were no significant differences between the results from mapped cases and unmapped ones involving tonotopic and non-tonotopic fields. Branched axons are thus a small but consistent part of the thalamocortical (TC) projection and are equally common in all MGB divisions. Whether these collateral projections are developmental remnants that escaped axonal pruning remains unknown. In light of the relative paucity of TC branching, more robust mechanisms for effecting the TC transformation could be heterotopic projections (Lee et al., *Neuroscience*, 2004, **128**:871-887) and the massive divergence of MGB axons in AC (Huang and Winer, *J. Comp. Neurol.*, 2000, **427**:302-331).

We thank Prof. S.K. Upadhyaya for statistical assistance. Supported by USPHS grant R01 DC02319-27.

## 860 Functional- and Cytotoxicity of Copper on Spontaneously Active Auditory Cortex Networks *In Vitro*

Kamakshi Gopal<sup>1,2</sup>, Guenter Gross<sup>1,2</sup>

<sup>1</sup>University of North Texas, <sup>2</sup>Center for Network Neuroscience

Copper is critical for energy production in the cells; however, excess copper leads to impairment of energy metabolism. Copper toxicity has been linked to the pathogenesis of neurodegenerative disorders such as Alzheimer's disease, Parkinson's disease, and

amyotrophic lateral sclerosis. Auditory dysfunctions such as hearing loss and auditory processing disorders are commonly observed in the above disorders.

This study characterized the toxicity of copper in auditory cortex networks (ACN). Functional toxicity was defined as cessation of electrophysiologic activity within ACNs in the presence of copper. Auditory cortex neurons dissociated from auditory cortices of 15-16 day old mouse embryos were grown on photoetched multielectrode arrays, containing 64 transparent indium-tin oxide electrodes. Mature ACNs (at least 21 days in vitro) that were spontaneously active were coupled to a multichannel recording system for continuous extracellular monitoring of multisite action potentials before and during exposure to CuCl2.

Results from acute experiments with serial additions of 1-100 micM CuCl2 produced inhibition of spike and burst activity. Sub-chronic experiments with single dose exposures of 25, 100 and 200 micM CuCl2 resulted in cessation of electrophysiologic activity within 1 - 4 hours, followed by extensive cell death by 12 hrs. The inhibitory effects from copper exposure in acute and sub-chronic experiments were irreversible with complete medium replacement. Initial analysis indicated a power function relationship between the concentration of copper applied and time required to reach 90% activity reduction. With 200 micM CuCl2, 90% activity cessation was reached approximately an hour after application.

## 861 Cerebral Activity in Response to a Masking Sound in Patients with Intractable Tinnitus

**Mikio Suzuki<sup>1</sup>**, Hideaki Kouzaki<sup>2</sup>, Minao Tamaki<sup>1</sup>, Ken Uehara<sup>1</sup>

<sup>1</sup>University of the Ryukyus, <sup>2</sup>Shiga University of Medical Science

Functional magnetic resonance imaging was performed in twelve patients with intractable tinnitus and normal subjects to determine the tinnitus-related regions where cerebral activity showed a positive or negative correlation to monaural masking noise stimulus. A blood oxygenation level-dependent (BOLD) signal increase was observed in the exclusive contralateral auditory cortex. There was no significant difference of the BOLD signal increase between normal subjects and patients in the conjunction analysis using random effect model. Cerebral regions that showed a BOLD signal decrease in normal subjects were the cuneus, cingulate gyrus, and paracentral lobule. In the patients f group, the cerebral regions that showed a BOLD signal decrease were the postcentral gyrus, bilateral thalamus, and bilateral lingual gyrus. A conjunction analysis using random effect model was performed to compare the decrease in BOLD signals between the tinnitus patients and controls, and revealed that the only significant difference in BOLD decrement was in the bilateral thalamus. Although the relationship between tinnitus and thalamic activity is not fully understood, such thalamic activity is consistent with the findings about other peripheral neural injuries.

# 862 Metabolic Activation of Auditory Cortex and Inferior Colliculi During Salicylate-Induced Tinnitus in Rats: A Micropet Imaging Study

**Asit Paul**<sup>1</sup>, Edward Lobarinas<sup>1</sup>, John Luisi<sup>1</sup>, Richard Simmons<sup>1</sup>, Hani Nabi<sup>1</sup>, Richard Salvi<sup>1</sup>

<sup>1</sup>University at Buffalo

The purpose of this study is to investigate the metabolic activities in central auditory structures in vivo during salicylate-induced tinnitus in rats. The behavioral induced paradigm, schedule polydipsia-avoidance conditioning (SIPAC), was first used to determine if tinnitus was present in rats treated with a high dose of salicylate. Following verification of salicylate induced tinnitus, a dedicated, high resolution animal positron emission tomography system (microPET Focus 120) was used to image the changes in brain metabolic activities associated with a high-dose of salicylate (250 mg/kg, i.p). In both the baseline and salicylate condition, rats were placed in a sound attenuating cubicle for 60 min after the injection of a radiolabeled glucose analog, F-18 labeled fluorodeoxyglucose (FDG, ~74 MBg, i.p). Thereafter, microPET scans of the rat brains were performed for 60 min in the prone position under isoflurane gas anesthesia. The frontal pole was considered as reference (control) area; FDG counts in frontal pole were expressed as a fraction of injected FDG dose per unit volume. Counts ratio between central auditory structures (auditory cortices, thalami and inferior colliculi) and frontal pole was used to compare between baseline and post-salicylate metabolic activity. The results show that the frontal pole FDG activity did not change between baseline and the post-salicylate condition, suggesting it as a metabolically inert area during tinnitus. During salicylate induced tinnitus, inferior colliculi (P=0.03) and auditory cortices (P=0.003) showed significant increase in FDG activities, whereas there was no significant difference in thalamic activity (P=0.07) from the pre-salicylate, baseline state. Our study shows increased metabolic activity consistent with neuronal activation in inferior colliculi and auditory cortices during salicylate-induced tinnitus in rats. Supported by Tinnitus Research Consortium.

# 863 Neural Activity Correlating with Consonance and Dissonance of Musical Chords in Monkey Primary Auditory Cortex (A1)

Yonatan Fishman<sup>1</sup>, Mitchell Steinschneider<sup>1</sup>

<sup>1</sup>Albert Einstein College of Medicine

Previous studies have shown that perceived dissonance of musical chords correlates with the magnitude of oscillatory activity in auditory cortex of both monkeys and humans that is phase-locked to the waveform envelope of the chords (Fishman et al., 2001). However, these studies left several questions unanswered: Does the amount of neural activity correlate with perceived dissonance, irrespective of whether or not that activity displays a periodic oscillatory pattern? Is dissonance-related activity restricted to transient or to sustained portions of responses to the

musical chords? These questions are examined by reanalyzing data obtained from A1 of awake macaques. Stimuli were dyads commonly used in Western music. Dyad tones were each composed of 10 consecutive harmonics. Base tones corresponded to middle C (256 Hz) and an octave above: duration of stimuli was 450 ms. Spectra of chords overlapped the best frequency of the recorded neural populations. Neural activity in middle laminae of A1 was examined using two response measures: multiunit activity (MUA) and net current flow at the location of the initial current sink identified by current source density (CSD) analysis. Two time windows were analyzed, corresponding to the transient (0-100 ms poststimulus onset) and sustained (100-445 ms) portions of the chord-evoked responses. The magnitude of sustained, but not transient, neural activity as reflected by both MUA and CSD measures was significantly correlated with perceived dissonance of the musical chords. Specifically, dissonant chords such as minor 2nds and major 2nds evoked significantly greater sustained activity than consonant chords such as octaves and perfect 5ths. These findings are consistent with fMRI data showing enhanced responses to dissonant chords in emotion-related brain areas (Pallesen et al., 2005) and suggest that temporal information reflecting dissonance is converted into a rate code at later stages in the processing of musical chords.

## 864 Development of Amplitude Modulation Processing in Auditory Cortex of Awake Gerbils

**Merri Rosen**<sup>1</sup>, Maria Ter-Mikaelian<sup>1</sup>, Malcolm Semple<sup>1</sup>, Dan Sanes<sup>1</sup>

<sup>1</sup>New York University

The emergence of mature temporal processing is essential for a broad range of auditory tasks, from sound localization to speech recognition. Surprisingly, development of the neuron coding properties that support these tasks has never been assessed in awake animals. Thus, the extent which anesthetics have contributed understanding of functional development remains unclear. We have addressed this issue by recording from single neurons in the auditory cortex of awake restrained gerbils prior to sexual maturation (postnatal days 30-38) and in adults (>P50). We presented sinusoidally amplitude modulated (SAM) stimuli monaurally while recording extracellularly from single units in auditory cortex, and measured both the neural synchrony (i.e., vector strength) and the response strength (i.e., discharge rate) to variations in modulation frequency and modulation depth. Neurons recorded in young animals displayed lower vector strength and discharge rate in response to the SAM frequencies that best activated adult neurons. For example, the average vector strength at 2 Hz was 0.48 ± 0.03 in young animals and 0.68  $\pm$  0.03 in adults, and average discharge rate was 5.9 ± 0.6 in young and 3.4 ± 0.5 spikes/sec in adult animals. SAM depth functions generally increased for both young and adult animals between 5 to 40%. However, for a given increase in modulation depth, adult neurons displayed a much greater change in both temporal and rate coding measures. While

general features of temporal processing are clearly present, both the synchrony and the response magnitude are relatively meager during this late period of development. Therefore it is plausible that these changes reflect the gradual developmental emergence of AM depth resolution observed in children.

Supported by NIH DC6864 to DHS

# 865 Conductive Hearing Loss Induces Opposing Effects on Spike Frequency Adaptation and Synaptic Depression in Auditory Cortex

**Han Xu**<sup>1</sup>, Vibhakar Kotak<sup>1</sup>, Dan Sanes<sup>1</sup> New York University

Conductive hearing loss (CHL), as observed during otitis media, is common in children. While CHL may affect language acquisition, it is not known whether it disrupts central auditory function, as does sensorineural hearing loss (SNHL). In this study, bilateral CHL or SNHL was produced surgically in gerbils at postnatal (P) day 10 and animals were reared for 8-13 days. The short-term plasticity (STP) of thalamus-evoked postsynaptic potentials (PSP) and spike frequency adaptation were examined in auditory cortex layer 2/3 pyramidal neurons with whole-cell recordings. To study STP of thalamusevoked PSPs, the medial geniculate was stimulated with current pulse trains at 2 to 40 Hz. PSP amplitude displayed depression during the train at each frequency, and the depression increased with higher stimulus frequency. Compared to controls, CHL neurons displayed greater short-term depression (STD) at each frequency. For example, the normalized steady-state amplitude at 20 Hz was significantly smaller for CHL neurons (control: 0.39  $\pm$  0.02; CHL: 0.31  $\pm$  0.03; p < 0.02). Spike frequency adaptation was examined by injecting neurons with a train of 50 successive 5 ms current pulses at rates from 5 to 100 Hz. In CHL neurons, spike adaptation was significantly less than observed for controls. For example, the firing probability of CHL neurons at 40 Hz stimulation was higher than controls (control: 76 ± 4%; CHL: 89 ± 3%; t-test; p=0.03). CHL neurons also displayed a depolarized resting potential (control:  $-64.2 \pm 0.4$  mV; CHL:  $-62.6 \pm 0.4$ ; p = 0.01) and an increased input resistance (control:  $165 \pm 8.5$ MOhm; CHL: 216 ± 9.3 MOhm; p<0.001). SNHL neurons displayed a similar but more severe change in synaptic depression and spike frequency adaptation. These results demonstrate that moderate hearing loss development (CHL) alters central auditory function and suggests that perceptual impairments associated with CHL are due, in part, to central alterations.

### 866 Auditory Responses in the Amygdala of Awake Mustached Bats

**Diana Coomes**<sup>1</sup>, Donald Gans<sup>1,2</sup>, Jeffrey Wenstrup<sup>1</sup>

<sup>1</sup>Northeastern Ohio Universities College of Medicine, <sup>2</sup>Kent State University

The amygdala is an important center for processing emotion, learning, and memory. Although it is not typically thought of as an auditory structure, the amygdala receives input from the medial geniculate body and auditory cortex and has projections to the inferior colliculus and auditory cortex. The influence of these projections on auditory processing has yet to be determined. To begin to identify auditory functions of the amygdala, we examined multiunit amygdalar responses after a variety of auditory stimuli presented to the contralateral ear broadband/narrowband noise, tones, upward/downward frequency modulated sweeps, and communication calls). Responsive and non-responsive areas were marked with a neural tracer. Of the areas that did respond (primarily basolateral), four response types were observed: locked tonic (9/47), locked phasic (19/47), prolonged firing (22/47), and inhibitory (4/35). We hypothesized that the amygdala would respond primarily to auditory signals relevant to the animal (e.g., communication calls). As expected, a majority of responses (40/47) were elicited by communication calls. A smaller number of units responded to downward frequency modulated sweeps (2/47), tones (2/47), and broadband noise (2/47). No responses were observed to upward frequency modulated sweeps. Some of the responses habituated after several presentations for varying amounts of time (few seconds-10 minutes). The results support our hypothesis that significant stimuli evoke amygdalar responses more than other auditory stimuli and that amygdalar units have a variety of excitatory and inhibitory responses to auditory stimuli.

Communication calls were provided by J. Kanwal (Georgetown U.) and C. Portfors (Washington State U.). Supported by NIDCD R01 DC 00937 (JJW), F32 DC007786 (DLC)

### 867 Towards an Awake Auditory Cortex Electrophysiology Preparation in the Mouse

**Edgar Galindo-Leon**<sup>1</sup>, Brian Kocher<sup>1</sup>, Yongkui Zhang<sup>1</sup>, Robert Liu<sup>1,2</sup>

<sup>1</sup>Emory University, <sup>2</sup>Center for Behavioral Neuroscience

There is a growing interest in using the mouse as a neuroethological system for investigating communication sound processing. While earlier electrophysiological studies of this have utilized anesthetized preparations, an awake model is clearly preferred. Towards this end, we developing been a head-restrained, anesthetized mouse preparation to examine single unit auditory cortical activity. One difficulty, though, is consistently targeting desired auditory cortical regions, since the relatively short duration of such recordings limits the ability to obtain full maps of the auditory cortex. To overcome this, we use a combination of methods to (1) more reliably position recording electrodes (4-6 MOhm tungsten), and (2) more quickly estimate characteristic frequencies. For the former, we performed a series of anesthetized experiments to test whether the tonotopic reversal between the primary and anterior auditory fields can be stereotaxically determined. Using a grid of holes covering the presumptive auditory cortex, our preliminary data indicates that a coordinate system scaled to the bregma-lambda distance on the skull can achieve this. For the latter, we used the local field potential (LFP) as a way to estimate the tone-frequency tuning of a recording site in

the absence of well-isolated single units. For both anesthetized and non-anesthetized animals, the LFP shows significant auditory-evoked power above the spontaneous LFP power in the 5-20 Hz range. However, the ratio of the evoked versus spontaneous power spectrum appears to be sensitive to the anesthetic level, thereby reinforcing the necessity of non-anesthetized preparations. These methods should now enable us to sample from similar locations within the auditory cortices of different animals, and facilitate the study of cortical sound processing in non-anesthetized mice.

Supported by NIH DC08343, and the Center for Behavioral Neuroscience (NSF IBN-9876754).

## 868 Effect of Auditory Task on the Expression of the Immediate-Early Gene C-Fos in the Ferret Cortex

**Victoria Bajo**<sup>1</sup>, Fernando Nodal<sup>1</sup>, Tobias Overath<sup>1</sup>, Andrew King<sup>1</sup>

<sup>1</sup>Department of Physiology, Anatomy and Genetics, University of Oxford

Immediate-early genes represent the first wave of gene expression that is triggered by cellular stimulation and their proteins' immunoreactivity can be used as an index of functional activity. Here we mapped the expression of c-Fos in the cortex of ferrets trained either to localise broadband noise bursts in the horizontal plane or to detect 1 kHz tones embedded in noise. The animals were housed in silence and darkness 1 hour after the final training session and then overdosed with pentobarbital and perfused with fixative. The brains were dissected and immunoreactions carried out on tangentially-flattened sections of the cortex using a rabbit primary antibody. Stereological analyses were performed with the optical fractionator using Neurolucida software. stimulation always induced c-Fos expression in the auditory cortex, which is located in the ectosylvian gyrus (EG), and the overall amount of activation was independent of the task performed. However, a different pattern of activation within the EG was observed for the localisation and tone-in-noise tasks. In the middle EG, where the primary auditory fields are located, sound localisation training resulted in homogeneous activation. By contrast, in ferrets trained to detect tones in the presence of a noise masker, activity was observed mainly in the anterior part of MEG, where the anterior auditory field has been described. In the anterior EG, where higherlevel auditory fields are found, anterior to posterior differences in c-Fos expression were observed for the two tasks. In the posterior EG, most activation was found dorsally and no differences were apparent between the tasks. In the orbital gyrus, where prefrontal cortex is located, auditory training induced c-Fos expression, mainly in ventral areas and particularly when the tone-in-noise detection task was performed. These results suggest that sound-evoked c-Fos expression can be used to identify the cortical areas involved in task-specific processing.

### 869 Encoding of Phonemes in the Neuronal Population Responses to Continuous Speech

**Nima Mesgarani**<sup>1</sup>, Stephen David<sup>1</sup>, Jonathan Fritz<sup>1</sup>, Shihab Shamma<sup>1</sup>

<sup>1</sup>University of Maryland

Animal behavioral studies suggest that the neural mechanisms underlying speech perception are based upon common mammalian mechanisms of auditory processing. In order to explore the contributions of innate auditory versus learned mechanisms to the neural encoding of speech, an important step is to determine the representation of phonemes in the auditory cortex of naive non-human animals.

In this study, we examined the responses of single neurons in the primary auditory cortex of naive awake ferrets to various American-English phonemes in the TIMIT corpus. The TIMIT corpus is a widely used continuous speech database spoken by multiple male and female speakers which includes a time-aligned phonetic transcription. Speech samples from TIMIT were chosen to represent a diversity of male and female speakers. We presented these stimuli to head-restrained awake ferrets and recorded the responses of 79 primary auditory cortical neurons.

For analysis, we segmented the continuous speech samples into sequences of phonemes, which represent the smallest significant units of speech. We characterized the response properties of each neuron as the average peristimulus time histogram response to each phoneme (across multiple exemplars of each phoneme). We then computed the extent to which these phonemes are distinguishable based on the neural responses of a population of cortical cells. Across a population of A1 neurons, we observed distinct patterns of phoneme selectivity that may provide a bottom-up neural basis for low-level phoneme discrimination.

Finally, we also computed a distance-matrix between all phoneme pairs, and compared it to the well-known analogous confusion matrix measured in humans (Miller and Nicely, 1955; Allen, 2005). This comparison provides insight into the relationship between the neural representation and perception of speech sounds and other complex natural stimuli.

### 870 Neural Substrates of Musical Creativity: a Functional MRI Study of Jazz Improvisation

Charles Limb<sup>1,2</sup>, Allen Braun<sup>2</sup>

<sup>1</sup>Johns Hopkins Hospital, <sup>2</sup>National Institutes of Health

In order to investigate the neural substrates of musical creativity, we examined spontaneous musical improvisation in six professional jazz pianists using functional MRI. Musicians participated in two functional imaging paradigms of low and high musical complexity, both of which required spontaneous musical improvisation using a non-ferrous MIDI piano keyboard in either highly constrained or entirely unconstrained formats. Overlearned musical passages matched for complexity served as the control condition in each paradigm. In both paradigms, widespread changes were seen throughout the

brain during improvisation, when compared to over-learned musical performance. Improvisation was associated with a dissociated pattern of activity in the prefrontal cortices—focal activation of the medial prefrontal (frontal polar) cortex coupled with broad deactivation of dorsolateral prefrontal and lateral orbital regions—and concomitant increases in sensorimotor and decreases in limbic activity. These findings suggest a model in which a uniquely distributed neural state provides a cognitive context that enables spontaneous artistic creativity.

## 871 Functional MRI Connectivity of Frontal – Temporal Lobe Interactions in Demanding Word Recognition Conditions

**Mark Eckert**<sup>1</sup>, Adam Walczak<sup>1</sup>, Stewart Denslow<sup>1</sup>, Jayne Ahlstrom<sup>1</sup>, Amy Horwitz<sup>1</sup>, Judy Dubno<sup>1</sup>

<sup>1</sup>Medical University of South Carolina

Recognizing spoken words in complex and demanding environments can require the allocation of considerable attentional resources. The interaction between frontal lobe attention and central auditory systems is poorly understood. This fMRI study examined the interaction between medial frontal and temporal lobe regions during a demanding word-recognition task in 7 normal hearing adults. The listening conditions in this sparse sampling experiment (TR=8s) were rendered demanding by using a parametric design in which words were degraded by lowpass filtering. Medial frontal cortex exhibited increased activity with decreasing word intelligibility. Functional connectivity analyses demonstrated that medial frontal activity exhibited coupled activity with bilateral anterior temporal and inferior frontal regions. These results suggest that challenging listening conditions engage a frontal-to-temporal network. This network may support the identification of spoken words in complex and demanding listening conditions and may fail in older adults who have difficulty understanding speech.

Work supported by NIH/NIDCD

### 872 Lexical Demands Assessed with Functional MRI

**Eric B. Ortigoza**<sup>1</sup>, Mark A. Eckert<sup>2,3</sup>, Chris Rorden<sup>3,4</sup>, Amy R. Horwitz<sup>2,3</sup>, Jayne B. Ahlstrom<sup>2</sup>, Judy R. Dubno<sup>2,3</sup>

<sup>1</sup>Medical University of South Carolina, College of Medicine, <sup>2</sup>Medical University of South Carolina, Department of Otolaryngology - Head and Neck Surgery, <sup>3</sup>Medical University of South Carolina, Center for Advanced Imaging Research, <sup>4</sup>University of South Carolina, Department of Communication Sciences and Disorders

Several models attempt to describe the complex processes involved in spoken-word recognition. The Neighborhood Activation Model suggests that neural representations of words are organized into neighborhoods of similar-sounding words and that listeners select the target from competing words in the same neighborhood. This model predicts that words in dense neighborhoods are hard to recognize and elicit greater activation throughout a neighborhood as listeners

search their lexicon for the target word. In this study, functional MRI (fMRI) was used to determine whether hard-to-recognize words elicit greater activation in language-related cortex than easy-to-recognize words. Sixteen right-handed, normal-hearing adults (8 males and 8 females with a mean age of 23) whose native language was American English listened to a list of easy words, hard words, or silence. To limit brain activation due to the 3T MR scanner noise, a sparse temporal sampling paradigm was used. Results of a behavioral task conducted following brain scanning confirmed that recognition of easy words was significantly better than recognition of hard Random effects analyses of the fMRI data confirmed predictions that left inferior frontal gyrus and superior temporal sulcus regions would show elevated activation for hard words compared to easy words (p<0.01, cluster extent p<0.01). These results support the neighborhood activation hypothesis and confirm evidence that processing lexically complex words engages inferior frontal cortex.

Work supported by NIH/NIDCD

### 873 Neuromagnetic Responses to Binaural Beat in Human Cerebral Cortex

**Shotaro Karino**<sup>1</sup>, Masato Yumoto<sup>2</sup>, Kenji Itoh<sup>3</sup>, Sotaro Sekimoto<sup>3</sup>, Kimitaka Kaga<sup>1</sup>

<sup>1</sup>Department of Otolaryngology, Faculty of Medicine, University of Tokyo, <sup>2</sup>MEG Lab, Department of Clinical Laboratory, Graduate School of Medicine, University of Tokyo, <sup>3</sup>Department of Cognitive Neuroscience, Graduate School of Medicine, University of Tokyo

The dichotic presentation of two sinusoids with a slight difference in frequency elicits subjective fluctuations called binaural beat (BB). BBs provide a classic example of binaural interaction considered to result from neural interaction in the central auditory pathway that receives input from both ears. To explore the cortical representation of the fluctuation of BB, we recorded magnetic fields evoked by slow BB of 4.00 or 6.66 Hz in nine normal subjects. The fields showed small amplitudes; however, they were strong enough to be distinguished from the noise accompanying the recordings. Spectral analyses of the magnetic fields recorded on single channels revealed that the responses evoked by BBs contained a specific spectral component of BB frequency, and the magnetic fields were confirmed to represent an auditory steady-state response (ASSR) to BB. The analyses of spatial distribution of BB-synchronized responses and minimumnorm current estimates revealed multiple BB ASSR sources in the parietal and frontal cortices in addition to the temporal areas, including auditory cortices. The phase of synchronized waveforms showed great variability, suggesting that BB ASSR does not represent changing interaural phase differences (IPD) per se, but instead it reflects a higherorder cognitive process corresponding to subjective fluctuations of BB. Our findings confirm that the activity of the human cerebral cortex can be synchronized with slow BB by using information on the IPD.

### 874 Intracranial Cortical Auditory Responses in Normal and Impaired Listeners

**Dana Boatman**<sup>1</sup>, Alon Sinai<sup>1</sup>, Nathan Crone<sup>1</sup>

<sup>1</sup>Johns Hopkins School of Medicine

To investigate cortical response patterns in normal and impaired listeners, auditory evoked potentials were recorded intracranially from eight right-handed patients with subdural electrodes implanted over left lateral temporal and parietal cortex. All had normal hearing and were left-hemisphere dominant for language. Speech recognition abilities were evaluated behaviorally using degraded speech (low-pass background noise). Stimuli were digitized syllables (/ba/, /da/) and tones (steady-state, frequency-modulated) matched to syllable formant frequencies. The 300-msec stimuli were presented (40 dB SL) sequentially in a passive oddball paradigm (82% standard, 18% deviant). Recordings were blocked by stimulus type, with 300 trials per block. For each stimulus condition, N1-P2 latencies and amplitudes were measured on the averaged waveform. Difference waveforms were computed to identify later mismatch negativities. The spatial-temporal distribution of evoked responses across electrode sites co-registered was to each patient's 3D-MRI reconstructions.

For normal listeners (4), early N1 responses to steadystate tones were maximal at electrodes located on the inferior parietal operculum, immediately superior and slightly posterior to maximal N1 responses for speech and frequency-modulated tones on the posterior superior temporal gyrus. Normal listeners also showed larger cortical spatial distributions for mismatch negativities for speech than tones. Conversely, impaired listeners (4) showed more variability and overlap in the cortical distributions of N1 responses and mismatch negativities than normal listeners. Group comparisons showed additional differences in the spatial-temporal distributions of high-frequency gamma activity. Our results suggest that individual differences in speech recognition abilities are reflected in the underlying spatial-temporal distribution of cortical auditory responses.

Funded by R01-DC005645

## 875 A Cortical Network and Effective Connectivity for Human Auditory-Object Analysis

**Timothy Griffiths**<sup>1</sup>, Sukhbinder Kumar<sup>1</sup>, Lauren Stewart<sup>2</sup>, Klaas Stephan<sup>2</sup>, Jason Warren<sup>2</sup>

<sup>1</sup>Newcastle University, <sup>2</sup>University College London

This work examines the cortical analysis of cues to auditory-object identity in humans using functional MRI. The concept of auditory object is controversial [Griffiths and Warren: Nature Reviews Neuroscience 5(2004) 887-892]: the critical process that we address here is the abstraction of features from the spectrotemporal acoustic structure that might be used to generalize between similar objects with different fine structure.

Previous work [Warren, Jennings and Griffiths: Neurolmage 24(2005) 1052-57] examined the analysis of spectral envelope and demonstrated a network for the

analysis of spectral envelope independently of fine-spectral structure including bilateral planum temporale (PT), and right superior temporal sulcus (STS). Further analysis of the network in the right hemisphere using dynamic causal modelling [Friston Harrison and Penny: Neurolmage 19(2003) 1273-1302] demonstrates serial effective connectivity from Heschl's gyrus (HG) to PT to STS and modulation of connectivity between HG and PT during the analysis of spectral envelope.

We have also carried out an experiment where subjects are presented with a 'timbral texture' comprising randomly placed frequency ramps in log-frequency time space where a proportion of the ramps are constrained to move in the same direction. Systematic increase of the proportion of coherent ramps produced a systematic change in the perceived acoustic object and a systematic increase in the BOLD activity in bilateral PT and right STS. The network shows a high degree of similarity to the network for spectral-envelope abstraction.

The results support the existence of a similar right-hemisphere system for the analysis of two different acoustic cues to auditory-object identity, and suggest a common system for the abstraction of higher-order object properties. Data from cognitive neuropsychological studies [Samson, Zatorre and Ramsay: Brain 125(2002) 511- 23] are congruent with this view.

### 876 Dynamics of Electrophysiological Responses in Human Auditory Cortex Assessed Through High-Density Subdural Grid Recordings

**Mitchell Steinschneider**<sup>1</sup>, Hiroto Kawasaki<sup>2</sup>, Hiroyuki Oya<sup>2</sup>, Matthew Howard<sup>2</sup>

<sup>1</sup>Albert Einstein College of Medicine, <sup>2</sup>University of Iowa College of Medicine

Multiple methodologies are being used to identify informational flow in human auditory cortex. Intracranial recordings obtained from patients undergoing evaluation for surgical treatment of epilepsy offer unique opportunities to evaluate auditory cortical activity at high spatial and temporal resolution. We are examining the reliability and sensitivity of spatial, temporal, and spectral patterns of EEG and auditory evoked potentials (AEPs) in assessing informational flow in auditory cortex. Protocols are IRB and NIH approved, and all patients gave informed consent prior to their participation.

AEPs recorded from grid electrodes located over the lateral surface of the temporal lobe contain reliable, large amplitude positive and negative components with an onset latency of about 20 ms that localize in a distributed manner across the posterior portion of the superior temporal gyrus (STG). These components are followed by lower amplitude waves that localize to areas beyond the regions of initial activation. The reliability of these later waves, whose generators include portions of the middle temporal gyrus (MTG), is being assessed.

Spectral analysis of stimulus-evoked changes in EEG power offers a complementary view of auditory cortical activity. The largest relative changes occur in very high

gamma frequencies (> 70 Hz) that are maximal initially in a distributed manner along the posterior portion of the STG. These changes are paralleled by less pronounced and shorter duration increases in the low frequency EEG. These patterns of activity are reliably observed across subjects and stimuli. Later power increases, especially those at high gamma frequencies, are seen at multiple loci on the MTG and supramarginal gyrus. Their reliability and stimulus specificity are being evaluated.

We conclude that analysis of EEG and AEP spectrotemporal dynamics is a promising method to assess informational flow in human auditory cortex. Supported by DC042890 and DC000657.

### 877 Morphometrics of the Superior Temporal Gyrus in the General Population

**Dominic V. Pisano<sup>1</sup>**, Patrick E. Barta<sup>1,2</sup>, J. Tilak Ratnanather<sup>1</sup>

<sup>1</sup>Center for Imaging Science, Johns Hopkins University, <sup>2</sup>Dept of Psychiatry, Johns Hopkins University School of Medicine

Recent neuroimaging studies of the primary auditory cortex have focused on morphometry, gender and laterality of the planum temporale and Heschl's gyrus that form part of the superior temporal gyrus (STG). In a neuroimaging study of 20 healthy subjects (10 male, 10 female), we studied the effect of gender and laterality on morphometric properties of the grey matter of the STG. Surface area, volume, and cortical thickness of each subject's left and right STGs were obtained from triangulated gray/white surfaces reconstructed from MRI subvolumes of the STG using computational anatomy methods including dynamic programming (DP) delineation of gyral and sulcal curves (Ratnanather et al., 2003). DP was initiated with several landmarks. The posterior landmark of the STG boundary begins at the intersection of the angular gyrus (AG) and the STG at the most posterior extent of the lateral fissure (LF). The anterior landmark of the STG boundary is located at the superior portion of the temporal pole at the ascending ramus of the LF. The inferior extent of the STG boundary follows from the posterior landmark along the superior temporal sulcus (STS) all the way to the anterior landmark. The superior extent of the STG boundary follows from the anterior landmark along the LF to the posterior landmark. Surface area was calculated by summing the areas of all the triangles constituting the STG. Cortical thickness map was calculated by associating a distance to each grey-matter voxel closest to the STG surface (Miller et al., 2003). Volume was calculated by summing the histogram of the cortical thickness map. It was necessary to separate the supramarginal gyrus from the MR images to remove voxels miscalculated in the cortical thickness maps. Preliminary MANOVA analysis suggests effect of gender for surface area and volume (p<0.02) and effect of laterality on thickness (p=0.0002) indicating possible functional differences in the STG.

Supported by R01-MH064838, P41-RR15241

# 878 FMRI Evidence for Spatial Dissociation of Changes of Overall Level and Signal-To-Noise Ratio in Auditory Cortex for Tones in Noise Maskers

**Stephan M.A. Ernst<sup>1</sup>**, Jesko L. Verhey<sup>1</sup>, Stefan Ulppenkamp<sup>1</sup>

<sup>1</sup>Institut für Physik, Universität Oldenburg

The phenomenon of masking has been widely used in auditory research to study both peripheral and central auditory processing in human listeners. Masked thresholds are often expressed as a ratio of signal intensity and masker intensity indicating the importance of the sensation correlated to sound intensity. It is, however, still not completely understood how the physical parameter sound intensity is exactly transformed into the sensation which is usually referred to as loudness and the partial loudness/audibility of a signal in the presence of a masker. In the present study we used functional MRI to investigate the representation of changes of level and signal-to-noise ratio (S/N) in human auditory cortex. Five-note tonal melodies with frequencies from 440 to 587 Hz were presented in a masking noise for signal-to-noise ratios from -18 dB to 24 dB in 6 dB-steps. For small S/N (-18, -12, -6 dB) the overall level of the sound is nearly constant, but the audibility of the tone varies with S/N. For S/N of 0 dB and above, the tone is always clearly audible, and the perceived change is mainly the increase of overall level. This clear perceptual separation of two effects is reflected by a spatial dissociation of the respective activation in auditory cortex. Brain regions mainly sensitive to level changes were found in Planum temporale, while those regions mainly sensitive to S/N changes were located in lateral Heschl's gyrus. There is almost no overlap between these two regions. The data indicate a different coding mechanism for the overall loudness and the audibility of periodic signals. The region sensitive to the S/N largely overlaps with the pitch-sensitive regions in lateral Heschl's gyrus found in previous studies. This suggests that the audibility of a tone in noise is determined by the overall pitch strength.

Supported by DFG, UP 10/2-2

### 879 The Processing of Phase Modulation: An MEG Study

**Rebecca Millman**<sup>1</sup>, Garreth Prendergast<sup>1</sup>, Will Woods<sup>1</sup>, Gary Green<sup>1</sup>

<sup>1</sup>York Neuroimaging Centre, The Biocentre, York Science Park, Heslington, York, YO10 5DG

Biologically relevant sounds contain patterns of changes in loudness (amplitude modulation) and pitch (frequency modulation). The aim of this study was to investigate the mechanism/s involved in the perception of perceptually salient phase modulation (PM) using magnetoencephalographic steady-state responses (SSRs).

Neuromagnetic SSRs phase lock to the modulation frequency of modulated sounds. SSRs to amplitude modulation (AM) have been recorded for a wide range of modulation frequencies. A recent study using frequency-

modulated AM stimuli [Luo et al., (e-published). Concurrent encoding of frequency and amplitude modulation in human auditory cortex: MEG evidence. J. Neurophysiol.] suggested that a phase modulation encoding mechanism exists for low (<5 Hz) frequency modulation (FM) modulation frequencies but additional AM encoding is required for faster FM modulation frequencies. Phase-modulated stimuli were created with raised-cosinusoidal pulses. The stimulus was either an unmodulated 1-kHz tone or a 1-kHz carrier frequency that was phase-modulated with a modulation frequency of 4, 8 or 12 Hz. The PM depth for each modulation frequency corresponded to a frequency sweep of 158 Hz. The stimulus duration was 240 s.

The FFT of each MEG channel was calculated to obtain the phase and magnitude of the SSR. The SSRs to 4-Hz PM were more robust than the SSRs to either 8-Hz or 12-Hz PM, indicating that the encoding mechanism may depend on the modulation frequency (Luo et al., 2006). The neural sources of the SSRs were analysed with a beamformer.

These results suggest that differences exist in the ability of auditory cortex to phase lock to modulated sounds; different mechanisms may operate depending on the modulation frequency. Whereas previous studies showed that a wide range of AM modulation frequencies are encoded by phase-locked activity, the present data suggest that PM is only encoded by phase-locking for modulation frequencies less than about 8 Hz.

## 880 Influence of Music Specialty on Pitch Production and Perception: Psychoacoustic and Electrophysiologic Measures

**Dee Nikjeh**<sup>1</sup>, Jennifer Lister<sup>1</sup>, Stefan Frisch<sup>1</sup>

<sup>1</sup>University of South Florida

Neurological evidence suggests that instrumental musicians experience changes in the auditory system related to their musical training; yet, little is known about such changes in formally-trained vocal musicians. Auditory pitch discrimination and laryngeal control are recognized as essential skills for vocal musicians; however, the relationship between the two skills is unclear.

Vocal pitch production accuracy, behavioral pitch discrimination, and cortical representation of pitch were examined among 40 formally-trained musicians (19 vocalists/21 instrumentalists) and 21 non-musician controls. All were right-handed young adult females with normal hearing. Stimuli were harmonic tone complexes approximating the physical characteristics of piano tones in the mid-frequency range of the untrained female vocal register extending from C4 to G4 (F0 = 262-392 Hz). Vocal pitch recordings were spectrally analyzed to determine pitch production accuracy (PPA). Difference limens for frequency (DLFs) were measured using an adaptive psychophysical paradigm. Cortical auditory evoked potentials (CAEPs), including the MMN and P1-N1-P2 response, were used to assess neural representation of pitch at the level of the auditory cortex.

All musicians demonstrated significantly better PPA and DLFs than the non-musicians; the two musician groups did not differ significantly on these measures. PPA and DLF

results were significantly correlated for the instrumentalists only. The PPA and DLFs of the vocalist group showed remarkably minimal inter-subject variability. Significantly larger P1 amplitudes were found for non-musicians than musicians, but the P1 amplitudes of the two musician groups did not differ. In contrast, significantly shorter MMN latencies were found for the vocalists. CAEP results suggest that some auditory neural responses may be sensitive to the type of formal music training received.

## 881 Stimulus Presentation Methods for the Acoustic Change Complex: Averaging Efficiency

**Tiffany Leach-Berth**<sup>1</sup>, Dassan Ali<sup>1</sup>, Brett Martin<sup>2</sup>

<sup>1</sup> *Montclair State University,* <sup>2</sup> *Graduate Center of CUNY*The purpose was to determine whether continuously alternating stimulus presentation is more efficient than the typical interrupted stimulus presentation for eliciting the cortical auditory P1-N1-P2 acoustic change complex (ACC) in adults and children. Continuously alternating the stimulus eliminates the silent period between stimuli, and takes less time. It is possible, however, that the increased rate of presentation will result in decreased response amplitudes due to neural refractory effects, thereby canceling any advantage in terms of test time and signal-to-noise ratio.

The ACC was elicited using a 75 dB SPL synthetic vowel containing a change of second formant frequency at midpoint (/ui/) in a group of adults (22 to 31 y.o.) and a group of children (6 to 9 y.o.). Recordings were obtained from 32 surface electrodes in four stimulus presentation conditions: interrupted presentation of the /u/-/i/ change using a 2 second stimulus onset asynchrony (SOA), interrupted presentation using a 1 second SOA, interrupted presentation of /uiu/ using a 2 second SOA, and continuous alternation between /u/ and /i/.

Continuous stimulus presentation was more efficient than conventional interrupted stimulus presentation for both adults and children. It took half as long as the interrupted method while presenting the same number of sweeps and twice the number of change events. The benefits of continuous presentation were not offset by a serious reduction in response amplitude. This study supports the conclusion that the ACC could be used as a clinical index of auditory speech discrimination capacity in adults and children.

### 882 How Many Talker-Specific Tokens are Needed to Reduce Talker Variability Effects?

Yi-ping Chang<sup>1</sup>, Qian-Jie Fu<sup>1,2</sup>

<sup>1</sup>Department of Biomedical Engineering, University of Southern California, <sup>2</sup>Department of Auditory Implants and Perception, House Ear Institute

For cochlear implant (CI) patients and normal-hearing (NH) subjects listening to acoustic CI simulations, speech recognition significantly worsens when the speech tokens from multiple talkers are randomly mixed within a stimulus set, relative to performance for individual talkers tested in succession. However, it remains unclear how many speech tokens from individual talkers are needed to

extract talker-specific characteristics and reduce these talker variability effects. In the present study, multi-talker vowel recognition was measured while varying the number of talker-specific speech tokens tested in succession. Six NH subjects were tested while listening to a 4-channel sine-wave vocoder. Stimuli included 12 vowels presented in /h/V/d/ context, produced by 2 male and 2 female talkers; the stimulus set contained 384 vowel tokens (12 vowels\*4 talkers\*8 repeats). For all experimental conditions, the entire stimulus set was tested. The presentation of vowel tokens was organized in blocks with different sizes: 1 (randomly mixed), 8, 16, 32, 48, and 96 (individual talkers tested in succession); vowel tokens in each block were spoken by the same talker. Results showed that mean vowel recognition scores gradually increased from 74 to 80 % correct as the number of tokens in each block was increased from 1 to 48, beyond which no further improvement was observed. These results suggest that NH listeners need only minimal exposure to a talker to extract talker-specific characteristics and reduce talker variability effects.

Research is supported by NIH-NIDCD.

## 883 Spectral Ripple Resolution and Speech Perception in Babble and Speech-Shaped Noise by Cochlear Implant Listeners

**Jong Ho Won<sup>1,2</sup>**, Ward Drennan<sup>1</sup>, Jay Rubinstein<sup>1,2</sup>

<sup>1</sup>VM Bloedel Hearing Research Center, University of Washington, Seattle, WA, <sup>2</sup>Dept of Bioengineering, University of Washington, Seattle, WA

The present study examined spectral resolution capability using spectral ripples and evaluated speech reception thresholds (SRTs) for spondees in two-speaker babble and speech-shaped noise in 25 cochlear implant users. Previous experiments have shown a correlation between spectral ripple discrimination ability and vowel and consonant recognition in quiet (r =0.52, p=0.01 for vowel; r =0.60, p=0.003 for consonant) [Henry et al., 2005]. This study extends this finding to common practical problem of speech understanding in noise. A 3-alternative forced choice, two-up and one-down adaptive procedure was used to determine the minimum ripple spacing that subjects could discriminate between standard and inverted ripple sounds [Henry et al., 2005]. Within-trial roving was used to control for level cues. A 12-alternative forced choice, one-up and one-down adaptive procedure was used to determine the SRTs for spondees at 50% correct [Turner et al., 2004]. There was a significant correlation between spectral resolution and SRT in both types of noise (r =-0.52, p=0.0073 for babble; r =-0.63, p=0.0008 for speech-shaped noise). This result shows that good spectral resolution is significantly correlated with good speech perception in noise. Thus, current data reveal that the spectral resolution test with ripple sounds can partially predict the speech perception abilities in noise of cochlear implant listeners. (Supported by NIH R01 DC007525)

# 884 Simulating Consonant and Vowel Recognition Rates in Cochlear Implantees for Varying Comression Ratios and Number of Electrodes Using Normal Listeners

**D. Sen<sup>1</sup>**, W. Li<sup>1</sup>, D. Chung<sup>1</sup>, P. Lam<sup>1</sup> *University of New South Wales* 

We explore two parameters in cochlear implant processors in terms of their effect on consonant and vowel recognition rates. The final goal is to evaluate the values of these parameters required to match the performance of acoustic resynthesis models to that of actual cochlear implant recipients. While there have been reports on the effect of each of the single parameters in isolation, our work attempts study the effect of the two parameters jointly.

The resynthesis models that we have used are very much like that of others in the literature [1,2]. In addition to these models however, we add the effect of compression and the effect of choosing only a few of the total twenty two possible electrodes in the implant processor. The first of this two, compression, is used in cochlear implants to account for the fact that the dynamic range of the implant electrodes is only of the order of 6-10 dB, to which has to be mapped the 110 dB or so of acoustic dynamic range that normal listeners can hear. Each electrode output was thus modified by a simple exponent > r, as follows >  $E_o$  =  $(E_i - k)^r$ , where  $E_i$  is the output of the Nucleus front end processor for a certain electrode,  $E_0$  is the result of the dynamic range mapping, k is constant to ensure threshold levels of hearing and *r* is the compression factor that was being investigated. The second parameter being investigated jointly along with r is the N of the "N of M" SPEAK strategy where only the *N* most salient electrodes are chosen to excite the nerves in the cochlea. Since we were using Nucleus front end software from Cochlear Ltd., we had 22 electrodes to choose from (i.e M=22). It was necessary to model the SPEAK strategy since the recipient data (from University of Melbourne) were from patients using the SPEAK strategy and Nucleus processors. Initial tests where we only modified the compression factor failed to match both the vowel and consonant scores. Only by adding a second degree of freedom and changing N along with r, could we match both vowel and consonant scores simultaneously.

[1] Shannon, R. V., Zeng, F. G., Kamath, V., Wygonski, J., & Ekelid, M., "Speech recognition with primarily temporal cues", Science 270, pp 303-304, 1995.

[2] Spahr, A., Dorman, M. & Loizou, P., "Effects on performance of partial misalignments of spectral information in acoustic simulations of cochlear implants", JASA, 112, 2002.

## 885 Processing Fundamental Frequency Contrasts with Cochlear Implants: Psychophysics and Speech Intonation

Monita Chatterjee<sup>1</sup>, Shu-Chen Peng<sup>1</sup>

<sup>1</sup>Department of Hearing and Speech Sciences, University of Maryland, College Park, MD 20742

Although fundamental frequency (F0) is not explicitly encoded by present-day cochlear implant speech (CI) processors, F0 information is available to CI listeners

through the temporal envelope. Multiple studies have shown that a salient F0 cue is critical for separating speech from competing backgrounds. In this presentation we will report on experiments investigating the ability of CI listeners to discriminate between SAM signals modulated at different rates in the voice pitch range. Stimuli are presented on a single channel as well as in the presence of competing SAM on other channels. In a parallel experiment on intonation processing by the same listeners, we quantify their ability to utilize F0 cues to recognize speech intonation contrasts. In this experiment, the F0, intensity, and duration properties of a bisyllabic word are systematically manipulated, resulting in 360 resynthesized stimuli. Listeners identify each stimulus as question- or statement-like. Preliminary results suggest that i) CI listeners vary in their psychophysical ability to detect differences in temporal envelope; ii) modulation frequency discrimination thresholds increase with increasing modulation frequency; iii) modulation frequency discrimination is impaired in the presence of off-channel, competing SAM; iv) when the carrier frequency is less than 4 times the modulation frequency, CI listeners are quite sensitive to aliased cues and v) CI listeners' psychophysical modulation frequency discrimination thresholds are predictive of their ability to utilize F0 cues in recognizing speech intonation contrasts of acoustic stimuli through their speech processor.

[Work supported by NIDCD R01 04786]

## 886 Perceptual Cue Weighting by Cochlear Implant Listeners Who Wear a Hearing Aid in the Unimplanted Ear

Shu-Chen Peng<sup>1</sup>

<sup>1</sup>University of Maryland at College Park

Current cochlear implants (CIs) are limited in coding voice pitch, which is important for listeners' speech intonation recognition. However, perception of intonation contrasts involves multiple acoustic dimensions, i.e., fundamental frequency (F0), intensity, and duration patterns. It is unclear how CI listeners who wear a hearing aid (HA) in the unimplanted ear would benefit from multiple acoustic dimensions via electrical vs. acoustic hearing. The purpose of this study is to determine implant listeners' perceptual weighting of different cues via a CI vs. HA. In ongoing experiments, adult CI recipients who use a HA in the nonimplanted ear performs a perceptual cue weighting task in CI alone, HA alone, and CI & HA conditions. Stimuli comprise resynthesized bisyllabic words where F0, intensity, and duration properties are manipulated orthogonally. Each listener identifies question vs. statement contrasts of stimuli in a two-alternative forcedchoice task. Preliminary results with one listener indicates that she exploited all F0, duration, and intensity cues to identify intonation contrasts via a CI, but she relied exclusively on F0 information via a HA. Findings of this study will help improve our understanding of the perceptual basis of implant listeners' speech intonation recognition via electrical vs. acoustic hearing.

[Work supported by NIDCD R01 04786]

## 887 Acoustic Correlates of Vocal Emotion Recognition by Normal-Hearing and Cochlear Implant Listeners

Xin Luo<sup>1</sup>, Qian-Jie Fu<sup>1</sup>

<sup>1</sup>Department of Auditory Implants and Perception, House Ear Institute

Our previous study has shown that vocal emotion recognition performance of cochlear implant (CI) users was much poorer than that of normal-hearing (NH) listeners, but was significantly better than chance level. The present study attempted to identify acoustic correlates of vocal emotion recognition by NH and CI listeners. The House Ear Institute emotional speech database was used; one female and one male talker each produced 10 simple, everyday English sentences according to 5 target emotions (i.e., neutral, anxious, happy, sad, and angry). First, acoustic cues such as fundamental frequency (F0), duration, and overall amplitude were extracted from each sentence. Acoustic analyses showed that, happy sentences have the highest mean F0 values and the largest F0 variation ranges, while sad sentences have the lowest mean F0 values and the smallest F0 variation ranges for both talkers. The female talker produced neutral sentences with the shortest durations, while producing sad sentences with the longest durations. However, there is no significant difference in durations among different emotions produced by the male talker. Angry sentences have the highest overall amplitudes, while sad sentences have the lowest overall amplitudes for both talkers. Second, vocal emotion recognition was tested in NH and CI listeners listening to original speech, speech without overall amplitude cues, or speech without duration cues. Perceptual results showed that, removing duration cues did not affect vocal emotion recognition by both NH and CI listeners. However, removing overall amplitude cues had more disruptive effects on vocal emotion recognition in CI users than in NH listeners, and such disruptive effects were mostly on the recognition of angry and neutral emotions by CI users. These results suggest that when spectral details are greatly reduced as in CI users, overall amplitude cues contribute more strongly to vocal emotion recognition.

## 888 Melody Perception Using a Novel Harmonic Spacing Filtering Scheme in Cochlear Implant Sound Processing

Weiqi Wei<sup>1</sup>, Li Xu<sup>1</sup>

<sup>1</sup>Ohio University

One of the greatest challenges the researchers are facing today is to improve music perception in cochlear implant users. We proposed a novel filtering scheme using harmonic spacing instead of the traditional filtering scheme using the Greenwood formula. We tested this novel scheme by using a tone-excited vocoder to simulate the cochlear implant stimulations. Thirty-two piano melodies with all rhythmic information removed were used in this study. Two experiments were carried out. In Experiment I, 5 normal-hearing subjects participated in the music score recognition test. A 5-consecutive-notes segment was

selected from each melody at a randomly-selected starting point. Subjects listened to 10 segments each processed with the harmonic-spacing or Greenwood filtering scheme and wrote down the corresponding numbered musical notation. In Experiment II, 15 normal-hearing subjects participated in the quality judgment test. Twelve melodies were selected randomly from the group of 32. Each melody was processed using the two filtering schemes. All subjects listened to the processed melody pairs and decided the naturalness of the melodies using a scrolling bar scaled between 0 and 10. The results showed that the harmonics-spacing scheme yielded a music score recognition performance of 40-62% (52% on average) correct whereas the Greenwood scheme produced a performance of around 14-34% (25.5% on average) correct. The differences were statistically significant (p<0.05). All subjects indicated that the processed sounds were more natural when using the harmonics-spacing scheme than using the traditional Greenwood filtering scheme. Thus, a better representation of the harmonics in the music sounds by choosing a filter spacing scheme that is more tuned to the acoustic features of the music sounds may provide cochlear implant recipients better melody perception.

### 889 Blind Signal Processing for Improved Speech Recognition in Bilaterally Implanted Users

Kostas Kokkinakis<sup>1</sup>, Philipos Loizou<sup>1</sup>

<sup>1</sup>Department of Electrical Engineering, University of Texas at Dallas

Bilateral cochlear implantation seeks to restore the advantages of binaural hearing by improving access to binaural cues. Still, many bilaterally implanted users experience difficulties in communicating in background noise.

In this context, bilateral devices can benefit from the integration of a novel processing strategy, known as blind source separation (BSS). BSS is a statistical technique that can process multi-sensory observations of an inaccessible set of signals (sources) in a manner that reveals their individual form. More importantly, it can do so without assuming any prior knowledge about the mixing structure or the source signals themselves. Noisy speech information captured from the microphones located behind each ear can be perceptually enhanced with the use a single speech processor. Hence, unlike existing bilateral cochlear implant processors that operate independently of one another, the BSS algorithm presupposes the existence of a single processor driving two implants. As such, the BSS algorithm capitalizes on the ILD and ITD information present in the mixtures of signals received by the two microphones, and uses that information to separate the target from the masker signals.

This initial study focused on assessing the potential of the BSS algorithm for improving speech recognition in adverse conditions wherein the target and masker are spatially separated. To evaluate the performance of the BSS method, binaural open-set recognition experiments were carried out with pre-measured head-related transfer

functions using the SPEAR3 processor. The target signal was assumed to be directly in front of the user, while the masker signal (competing speech or speech-weighted noise) was placed at different angles. Sentence recognition tests with Nucleus-24 bilateral users revealed that the BSS algorithm produced large improvements in intelligibility, irrespective of the temporal or spectral characteristics and position of the masker signal.

### 890 Improved Speech Intelligibility by Spectral Contrast Shaping

Paul V. Watkins<sup>1</sup>, Nathan J. Killian<sup>1</sup>, **Dennis L. Barbour**<sup>1</sup> *Washington University* 

Some neurons in auditory cortex exhibit a substantial dynamic response range at intermediate spectral contrast values. Spectral contrast represents variance in sound energy distribution across frequency. Previous studies using spectral contrast enhancement to improve the intelligibility of noisy speech have demonstrated some benefit for normal listeners and cochlear implantees. We reasoned that filtering or shaping the contrast of noisy speech to match the contrast tuning of these auditory cortex neurons may prove to be a useful strategy for improving speech intelligibility in noisy situations. Such a strategy may by particularly useful for cochlear implantees, whose native contrast filtering circuitry is likely to be nonfunctional. We decomposed noisy speech into frequency and contrast components, applied exponential weighting to randomly selected contrast values, and finally reconstructed a time-domain signal by summing across the individual filters. The normalized correlation metric (NCM)—verified previously to be an accurate predictor of noisy speech intelligibility for cochlear implantees—provided quantitative estimates of intelligibility changes. Signal components of intermediate contrast (4-8 dB) were found to be more important for increasing speech intelligibility than were high- (8-20 dB) or low-contrast (0-4 components. When preferentially emphasizing contrast values in the intermediate range, we found NCM score increases of 10-20% for speech+white noise having signal-to-noise ratios of -5, 0, and 5 dB. Preferentially enhancing the highest contrast values resulted in substantially decreased NCM scores. These observations agree with neurophysiological expectations and imply that contrast shaping may be a useful noise-reduction algorithm for improving noisy speech intelligibility in normal-hearing listeners and/or hearing-impaired listeners such as cochlear implantees.

## 891 Biologically-Inspired Spectral Enhancement to Improve Speech Recognition in Hearing-Impaired Listeners

Joshua Alexander<sup>1</sup>, Keith Kluender<sup>1</sup>, Rick Jenison<sup>1</sup>

<sup>1</sup>University of Wisconsin - Madison

One consequence of sensorineural hearing loss (SNHL) not overcome by conventional amplification is a smearing of spectral detail resulting in part from a reduction in adaptation and suppression- neuroprocesses that serve to selectively enhance onsets and spectral contrast in

normal-hearing (NH) listeners. Kluender and Jenison (2004; U.S. Patent No.: 6732073B1) describe a method of enhancing spectral contrasts via a real-time DSP implementation that mimics these neuroprocesses. Gain is determined by the time-varying history of energy across a bank of narrow filters. The greatest gain is assigned to channels where preceding energy is lowest and where energy is greatest in a local neighborhood. features that change over time are enhanced at the expensive of those that are relatively static. NH listeners with simulated spectral smearing and listeners with SNHL identified nonsense syllables with vCv and hVd structures and sentences with background babble. recognition for processed speech was variable compared to unprocessed speech. In some cases, recognition with processing was the same or better than without processing and in others it was worse. Research is ongoing to search for ways the processing can be improved by customizing it to individual patterns of hearing loss.

[Supported by NIDCD.]

## 892 Nonlinear Distortion in Hearing Aids: Relating Signal Characteristics to Auditory Perception

**James Kates**<sup>1,2</sup>, Kathryn Arehart<sup>1</sup>, Ramesh Muralimanohar<sup>1</sup>

<sup>1</sup>University of Colorado, <sup>2</sup>GN Resound

Speech intelligibility and sound quality in hearing aids are affected by the distortion and unintended nonlinear signal effects within the device. mechanisms in a digital hearing aid include saturation, numeric underflow, and the signal and noise modulation introduced by algorithms such as dynamic-range compression and noise reduction. The relationship between nonlinear distortion and intelligibility and sound quality is unclear. In a recent experiment, Arehart and Kates (2006) found that audibility could explain some aspects of quality judgments for speech subjected to noise and distortion, but multi-dimensional scaling indicates that more aspects of the degraded signal are processed by the listeners in formulating their quality judgments. This presentation investigates the relationship between the signal properties of the degraded speech and the perceptual dimensions underlying the quality judgments by normal-hearing and hearing-impaired listeners. The signal analysis procedures include spectra of the signals and the distortion products, envelope modulation spectra, and correlations between the time-frequency representations of the distortion products and the underlying speech signal.

## 893 Benefits of High-Frequency Amplification: Spectral Shaping Under Earphones and with Hearing Aids

**Amy R. Horwitz**<sup>1</sup>, Jayne B. Ahlstrom<sup>1</sup>, Judy R. Dubno<sup>1</sup> *Medical University of South Carolina* 

A widely debated issue concerning auditory function and its relation to hearing aids is the benefit and optimal degree of high-frequency amplification for individuals with high-frequency hearing loss. Some studies report improved speech recognition with increased speech audibility in the higher frequencies, whereas other studies report that speech recognition remains constant or deteriorates as amplification is added in the higher frequencies. In the first of two experiments, older adults with moderate to severe high-frequency hearing loss listened monaurally under earphones to speech that had been spectrally shaped according to the NAL-R prescriptive target. Recognition of nonsense syllables in quiet and in noise was measured as a function of lowpass-filter cutoff frequency. Incrementally increasing the cut-off frequency in third-octave steps between 2.2 and 5.6 kHz revealed the extent to which increases in amplified speech cues helped or hindered listeners' speech recognition. Results suggested that speech recognition generally improved with increasing high-frequency audibility. In the second experiment, ten subjects who participated in the first study were fit with bilateral in-thewide-dynamic-range-compression hearing according to the NAL-NL1 prescriptive target (similar to NAL-R in the first experiment). Aided recognition of nonsense syllables was measured in the sound field in noise at identical low-pass cutoff frequencies as in the first study and in guiet for the broadband condition. Speech was presented from a loudspeaker in front of the listener with noise at a +5-dB signal-to-noise ratio. Speech recognition in quiet was similar with hearing aids and under earphones. In contrast, speech recognition in noise was poorer with hearing aids than under earphones, although improvements in recognition with additional highfrequency speech bands were similar for hearing-aid and earphone listening. [Supported by NIH/NIDCD]

### 894 Localization of Pure Tones by Cats

Janet Ruhland<sup>1</sup>, Tom Yin<sup>2</sup>

<sup>1</sup>Dept. of Physiology, Univ. of Wisconsin, <sup>2</sup>Dept. of Physiology and Neuroscience Training Program, Univ. of Wisconsin

Sound azimuth is based on two binaural cues, interaural differences in the time of arrival (ITD) and level (ILD) of the sounds at the ears. Because of head size, cats use ITD's for localizing sounds with frequencies below about 3000 Hz, and ILD's for higher frequency sounds. Sound elevation is based on patterns of the broadband power spectra at each ear that result from the directiondependent acoustic filtering properties of the head and pinnae. We hypothesized that localization of pure tones in azimuth would be nearly as accurate as localization of broadband noise, but localization of pure tones in elevation would be more difficult. In some studies human subjects localize pure tones at idiosyncratic elevations depending on frequency and individual bias. We wanted to see if cats also show these characteristics in localizing pure tones in azimuth and elevation. Cats were trained using operant conditioning to indicate the apparent locations of sounds via gaze shift (combined eye and head movements). Targets consisted of 1000 ms broadband noise bursts and 500 ms tones (500, 1000, 2500, and 6000 Hz). Targets were presented at locations between ± 40° in azimuth along the horizontal plane and between ± 30° in elevation

along the median plain. For each frequency, localization performance was summarized by the slope (or gain) of the linear regression relating the localization responses of the cats to the target positions. Although cats were accurate localizing noise targets in elevation, they were unable to localize tones in elevation. Rather than having unique responses to tones of different frequencies the cats appeared to respond with a "default" location to all frequencies and target positions presented in elevation; a location that was unique to each individual cat. Localization of tone targets in azimuth is possible because ITD and ILD cues are available. Poor localization of source elevation is consistent with the hypothesis that broadband spectral information is critical for sound localization in elevation.

Supported by grants DC02840 and DC07177.

### 895 Localizing Bioacoustic Sources with a Microphone Array

Kimberly Walsh<sup>1</sup>, Rama Ratnam<sup>1</sup>

<sup>1</sup>University of Texas at San Antonio

Many vocally communicating species such as songbirds and frogs congregate in dense noisy choruses. An important ecological and ethological problem is to determine the spatial and temporal structure of such choruses. Male frogs and toads in particular, congregate around bodies of water, establish territories, and vocalize to announce their sexual readiness to females. Our longterm goal is to develop techniques to determine the distribution and identity of species, the numbers of participating individuals and their locations, and the spatial and temporal correlations in the vocalizations. The use of a microphone array to localize individual sources is one possibility, and is investigated here. An array of microphones formed an enclosed rectangular arena in a sound chamber, and the task was to determine the location of sounds originating within this arena. The impulse responses for sounds originating from a number of locations within the arena were first determined, and these impulse responses were convolved with vocalizations from several species of frogs and toads. A sound localization algorithm operating in the frequency domain was used to determine the direction of arrival (DOA) of sounds for pairs of microphones. Using a triangulation procedure, these DOAs were then used to estimate the location of the individual sources. We investigated the effect of a number of important bioacoustical parameters on the performance of the localization algorithm. These included spectral bandwidth of calls and background noise, and the temporal overlap and duration of calls. When signal-tonoise ratio was high, localization acuity was fairly robust to a reduction in bandwidth and increase in temporal overlap. But in the presence of noise, broad-band sounds such as the trills of Ranid frogs were more easily localized than were narrow-band sounds produced by Bufonid toads. The performance of the algorithm is discussed with respect to these findings.

## 896 Auditory Distance Coding: Candidate Acoustic Cues in Binaural Room Impulse Responses of Barn Owls

**Duck Kim<sup>1</sup>**, Andrew Moiseff<sup>2</sup>, J. Bradley Turner<sup>1</sup>, Justin Gull<sup>1</sup>

<sup>1</sup>University of Connecticut Health Center, <sup>2</sup>University of Connecticut

Neural mechanisms for localizing sounds in azimuth and in elevation have been studied extensively. In contrast, mechanisms responsible for auditory localization of distance are poorly understood. The present study is the first step toward filling this gap of knowledge. Candidate cues for auditory distance are: 1) ratio of direct-toreverberant (D/R) signal amplitudes, 2) interaural level difference (ILD), 3) interaural time difference (ITD), 4) spectral patterns, and 5) direct signal level. We measured individual barn owl's binaural room impulse responses (BRIRs) with microphones embedded in ear molds that blocked the ear canals with sounds at various distances and azimuths within a radius of 80 cm from the owl's head. We presented maximum length sequence stimuli and recorded BRIRs at 98 kHz sample rate in two conditions: 1) a sound-absorbent environment where the walls of an acoustic chamber were lined with Sonex foam (Ilbruck). and 2) a sound-reflective environment where hard boards were placed on the walls of the chamber.

Based on our observations, we conclude that: 1) D/R ratio is the most effective candidate cue for coding auditory distance because it systematically changes with distance not only for 45° and 90° azimuths but also for 0° azimuth; and 2) ILD is a useful, but less effective cue for auditory distance because it systematically changes with distance only when a sound source is located closer than 40 cm and at an azimuth away from the mid-sagittal plane. Although ITD is accepted as the primary cue for azimuth, it also changes with sound-source distance particularly when the source is located closer than 40 cm and away from the mid-sagittal plane. Spectral patterns and direct signal level also change with distance. Thus, a comprehensive theory of 3-dimensional auditory localization must incorporate the fact that all of the major acoustic cues change with distance particularly when a sound source is close to a listener (< 40 cm in the barn owl).

### 897 The Auditory "Franssen Effect" Illusion in Zebra Finches and Budgerigars

**Thomas Welch**<sup>1</sup>, Elizabeth McClaine<sup>1</sup>, Micheal Dent<sup>1</sup>

1 University at Buffalo

The properties of the auditory illusion known as the Franssen Effect (FE) have been characterized in humans and also more recently in cats. It was not known, however, whether this illusion would occur in non-mammals, and if it did occur, if the characteristics would be similar. Here, we examined the FE in two species of birds: budgerigars and zebra finches. To elicit the FE, listeners are presented with a signal which has been split into a transient component, carrying an abrupt onset and ramped offset and separated in space from the sustained component which has a slowly rising onset and longer overall duration. When these two signals are played to human and cat listeners

simultaneously, under certain conditions (where the listening environment is difficult), the perception is that of a long-duration steady state tone being played at the location of the transient source even though the stimulus has ended. The birds in the following experiments were trained using operant conditioning methods on a categorization task to peck a left key when presented with a stimulus from a left speaker and to peck a right key when presented with a stimulus from a right speaker. Once training was completed, FE stimuli were presented during a small proportion of trials for each experimental session. We measured the FE at speaker separations of 60 and 180 degrees in both echoic and echoic-reduced conditions. Both species of birds exhibited the FE, although to varying degrees, across conditions. The birds performed equally in echoic and echoic-reduced conditions, but exhibited a stronger FE with 180 degrees of speaker separation. With this separation, the lowest and highest frequency stimuli elicited the strongest illusory FE. These results show that non-mammalian species also experience the FE illusion in confusing listening situations in a manner similar to mammals, suggestive of more general auditory processing mechanisms.

## 898 Free-Field Localisation of Speech and Speech-in-Noise Signals by Normally Hearing and Cochlear Implanted Children and Adults

**John Murphy**<sup>1,2</sup>, Gerry O'Donoghue<sup>2</sup>, Quentin Summerfield<sup>3</sup>, David Moore<sup>4</sup>

<sup>1</sup>MRC Institute of Hearing Research, <sup>2</sup>ENT Directorate, Queen's Medical Centre, Nottingham, <sup>3</sup>Department of Psychology, University of York, <sup>4</sup>MRC Institute of Hearing Research, Nottingham

Spatial hearing makes a significant contribution to communication by enhancing the perception of target sounds in noisy environments. Consequently, poor spatial hearing is a major contributor to auditory handicap. Our aim is to investigate the spatial hearing abilities of bilateral cochlear implant users, relative to those of unilateral users and typically hearing people. Here, we report initial results from typically hearing children (6-16 y.o.) and adults. We have implemented a series of spatial hearing tests (A.Q. Summerfield, unpublished) that use the McCormick Toy Discrimination Test, presented via a 24 loudspeaker ring (MRC Institute of Hearing Research). Initially, a free-field threshold (speech-in-quiet; front loudspeaker - 0° azimuth) was obtained. The Toy Test was then repeated with a pink noise masker (60 dBA) (speech 0° azimuth; noiseloudspeakers -90°(left), +90° and 0°). These tests measured spatial release from masking (SRM). Finally, we assessed absolute localisation. Five video monitors were paired with five loudspeakers ( 30° or 15° separation). The monitors each displayed a talker saying "Hello, what toy is this?" A discrete image of a Toy was shown in the top left corner of the monitor screens. The task of the listener was to say the name of the toy displayed with the talker whose image was co-located with the sound. Adult listeners (n = 6) achieved masked thresholds of 42.2 dBA(Left), 48.6(Centre) and 42.7(Right), giving SRM of 6.2 (s=2.9). Children tested to date (n = 40) could perform the tasks with considerable ease. Mean masked thresholds were 45.3 dBA(L), 51.5(C) and 45.4(R). SRM was 6.1(2.1). Ceiling or near ceiling performance in the localisation tasks was reached by all listeners. Our results indicate that masked thresholds and SRM do not change within the tested age group, and the localisation tasks produced ceiling performances from typically hearing groups. Further work will examine SRM and localisation in CI users.

### 899 Monaural Virtual Localization: Implications for Bilateral Cochlear Implants

**Daniel Shub<sup>1,2</sup>**, Suzanne Carr<sup>2</sup>, Yunmi Kong<sup>2,3</sup>, H. Steven Colburn<sup>1,2</sup>

<sup>1</sup>Harvard-MIT Health Sciences and Technology, <sup>2</sup>Boston University Hearing Research Center and Department of Biomedical Engineering, <sup>3</sup>Princeton University

This work explores the ability of normal-hearing and of unilateral subjects to identify the location of a sound source when listening with a single ear. Measurements with a virtual 13-speaker array (spanning the frontal hemifield) were made for each subject. The stimulus was a tone complex with 20 components logarithmically spaced between 0.5 and 8 kHz. Before spatial processing, the spectral profile was flat. Spectral shaping was imposed using head-related transfer functions (CIPIC database). The overall level was randomized to reduce loudness cues while preserving the spectral profile. The stimuli were presented over a single headphone to the right ear of the normal-hearing listeners and to the normal-hearing ear of the unilateral listeners. Subjects were instructed to identify the simulated location, not report the perceived location, of the source. Both subject populations had similar performances on these monaural tasks, suggesting that prolonged monaural is not more helpful than binaural experience for monaural localization. The average rootmean-squared and mean unsigned differences between the source and reported locations were 34° and 24°. respectively. Subjects demonstrated little bias; the maximum bias was 8.2° towards the ear to which the stimuli were presented. The slopes of the best fitting lines were between 0.69 and 0.97. This level of performance is substantially better than reports of monolateral cochlear implant (CI) performance and roughly matches bilateral CI performance on similar tasks (B. Poon, Ph.D. thesis, MIT HST, 2006). The results suggest that current bilateral CIs preserve a similar amount of useful localization information as the theoretically ideal monolateral CI. Bilateral CI performance (where interaural cues especially level may be useful) is about the same as differences performance of unilateral listeners (where no interaural cues are available) with a fixed-spectrum stimulus.

[Supported by NIH DC00100 and DC05775]

### 900 Measurements of Acoustic Characteristics of Pulse-Echo Pairs in FM Echolocating Bat (*Pipistrellus Abramus*) During Flight Using by a Telemetry Microphone System

**Shizuko Hiryu**<sup>1</sup>, Tomotaka Hagino<sup>1</sup>, Hiroshi Riquimaroux<sup>1,2</sup>, Yoshiaki Watanabe<sup>1,2</sup>
<sup>1</sup> *Graduate School of Engineering,* <sup>2</sup> *Bio-navigation Research Center, Doshisha University* 

The possibility of compensation mechanism, in which pulse intensity is adjusted in relation to the distance to a target resulting in maintenance of a constant intensity of the echo (echo-intensity compensation) were acoustically examined for Japanese house bats (P. abramus; an FM bat). We developed a small telemetry microphone (Telemike) that was light enough (0.6 g including a battery) to be carried by the animals (P. abramus weighs 5 g). Further, the Telemike set at the bat's head allowed us to observe not only the emitted pulses, but also the returning echoes to which the bat listened during flight. We analyzed the signal characteristics of pulse-echo pairs combined with a high-speed video camera system as a bat flying toward the wall (target wall) on which a landing mesh was attached in the laboratory. The maximum SPL (peak-topeak) of emitted pulse at the microphone above the bat's head during flight was approximately 130 dB (re 20 µPa), which was almost 20 dB higher than when the bat was at rest. Pulse intensity in bats intending to land exhibited a marked decrease by approximately 30 dB within 2 m of distance from the target wall, and the mean reduction rate was 6.5 dB per halving of distance (21.6 dB per decade) for the three bats. We found that the intensity of echoes returning from the target wall measured at the head of the flying bat indicated a nearly constant intensity (-42.6  $\pm$  5.5 dB weaker than the pulse emitted in search phase). These findings may provide direct evidence that bats adjust pulse intensity to compensate for changes in echo intensity to maintain a constant intensity of the echo returned from the approaching target within the range necessary for optimal signal processing.

[The research supported by a grant to RCAST at Doshisha Univ. from MEXT, Special Research Grants for the Development of Characteristic Education from the Promotion and Mutual Aid Corporation for Private Schools Japan, Innovative Cluster Creation Project by MEXT.]

# 901 Echolocation Behavior of a CF-FM Bat (*Rhinolophus Ferrumequinum Nippon*), Recorded with a Telemetry Microphone System During Flight

**Yu Shiori**<sup>1</sup>, Shizuko Hiryu<sup>1</sup>, Tatsuro Hosokawa<sup>1</sup>, Hiroshi Riquimaroux<sup>1,2</sup>, Yoshiaki Watanabe<sup>1,2</sup>

<sup>1</sup>Graduate School of Engineering, <sup>2</sup>Bio-navigation Research Center, Doshisha University

We observed the echolocation behavior of CF-FM bats (*Rhinolophus ferrumequinum nippon*) during landing to the target wall in the laboratory. Changes in acoustic characteristics such as interpulse interval (IPI), pulse duration, and frequency of the second harmonic CF

component (CF2) of pulses were examined by using a telemetry microphone (Telemike) set on the bat's head. The echolocation pulse of the bats consists of an upward initial FM, a long CF and a downward terminal FM components. The second harmonic is emitted with the greatest energy. Pulse CF2 frequency emitted at rest is about 69 kHz. Once in flight, the bats decreased pulse duration and IPI within 1-2 m from the target wall (target distance). Using the flight speed measured by the highspeed video cameras, we estimated pulse CF2 frequency to maintain the echo CF<sub>2</sub> frequency at constant (Dopplershift compensation, DSC). The estimated frequencies showed good agreement with the measured values within the target distance of 1-2 m. These findings indicate that bats started the approach phase within 1-2m of the target distance, exhibiting DSC for the echo from the target wall. Since pulse duration of the bats ranged between 10 and 70 ms, echoes observed by the Telemike were occasionally overlapped with the next outgoing pulse. However, we found that the next outgoing pulse never overlapped with the echo from the target wall during the approach phase. This suggests that the bats start to adjust IPI and pulse duration so that the echo from the attended target (i.e. the target wall) can be received without overlap with the next outgoing pulse, which may be necessary to detect information about the attended target in this bat species.

[The research supported by a grant to RCAST at Doshisha Univ. from MEXT, Special Research Grants for the Development of Characteristic Education from the Promotion and Mutual Aid Corporation for Private Schools Japan, Innovative Cluster Creation Project by MEXT.]

### 902 Sequential Grouping Influences Binaural Interference

**Virginia Best**<sup>1</sup>, Laura Stupin<sup>1</sup>, Frederick J. Gallun<sup>1</sup>, Simon Carlile<sup>2</sup>, Barbara G. Shinn-Cunningham<sup>1</sup>

<sup>1</sup>Boston University, <sup>2</sup>University of Sydney

Binaural interference describes a phenomenon where binaural judgments of a high-frequency target stimulus are disrupted by the presence of a simultaneous lowfrequency interferer. Many previous studies have shown that binaural interference is reduced when simultaneous grouping cues such as synchronous onsets and harmonicity, which encourage the grouping of target and interferer, are eliminated. These findings are consistent with the idea that binaural interference is related to auditory object formation, although this relationship has not been fully explored. In this study, we show that perceptual organization based on sequential grouping cues can also affect binaural interference. Subjects used a matching task to indicate the perceived lateral position of a high-frequency sinusoidally amplitude-modulated (SAM) tone containing an interaural time difference. Lateral extents were reduced significantly by the presence of a simultaneous diotic low-frequency SAM tone, but were largely restored when the interferer was 'captured' in a stream of identical tones. A control condition confirmed that the effect was not due to peripheral adaptation. The data lend further support to the idea that binaural

interference is a product of processes related to the perceptual organization of auditory information.

[Work supported by R01 DC05778-02 and F32 DC006526 from NIDCD]

### 903 Precedence Effect Buildup in a Simulated Reverberant Room

Pavel Zahorik<sup>1</sup>, Devan Haulk<sup>1</sup>

<sup>1</sup>University of Louisville

Previous research has demonstrated that listeners' abilities to detect or discriminate changes in a single echo are diminished after repeated presentations of both source and echo. This buildup of echo suppression (precedence effect buildup) along with the release from suppression when dramatic changes are made to the spatial relationship of source and echo is taken as evidence of a complex neural process that adapts and suppresses the acoustical contributions of the echo. Here we demonstrate that precedence effect buildup generalizes to a more natural listening environment with multiple echoes and reverberation. The listening environment was a moderately reverberant rectangular room (5.7 × 4.3 × 2.6 m; broadband  $T_{60} \approx 0.4$  s) simulated using high-quality virtual auditory space (VAS) techniques. abilities to discriminate spatial changes in ensembles of early reflections were evaluated both with and without previous listening exposure to the room. distribution of early reflection ensembles was manipulated by imposing a shift factor to the natural distribution along the left-right spatial dimension. The number of shifted reflections in the ensemble was varied to include the first 2 to 512 reflections, in doubling increments. corresponded to a range of maximum delay values for the reflection ensembles of 4 to 52 ms for this simulated room. In a single interval task, listeners were asked to report the direction of the shift, either left or right of midline. Although performance in task depended on the number of reflections in the ensemble and the corresponding maximum delay for both conditions, performance was generally impaired under conditions of prior listening exposure to the room: a result that is consistent with a buildup of echo suppression.

## 904 Head-Related Transfer Functions Obtained Psychoacoustically

Nelson Pak Hung Wong<sup>1</sup>, **Torsten Marquardt<sup>1</sup>** 

<sup>1</sup>University College London

We investigated the possibility of simulating a virtual loudspeaker location whilst listening with headphones using filter functions derived from the difference between auditory threshold curves measured using (a) the loudspeaker and (b) the headphone. Rather than measuring sound pressure level at the ear drum using miniature microphones under known stimulus power, we adjusted the stimulus power to obtain a measure of threshold in sound pressure level at the ear drum. As a function of stimulus frequency, the differences in stimulus power between the two audiograms give the transfer function required to filter headphone sounds such that they

are judged to originate from the loudspeaker location. Six auditory thresholds were obtained for four subjects in the range of 2 - 14 kHz using Bekesy tracking (median of three tracks): (1) left/right headphone, (2) left/right ear with loudspeaker straight in front of subject (2 m distant), (3) left/right ear with loudspeaker positioned 1.3 m lower (in the medial vertical plane) than in (2). All measurements took place in an anechoic chamber. The four filter functions (left and right ear for upper and lower loudspeaker) were then derived and applied to a 2-14 kHz band of flat-spectrum noise. Three of the four subjects reported good externalization of these two test stimuli and were able to distinguish the HRTF for the upper loudspeaker, the lower loudspeaker and an average HRTF (average of all subjects for both loudspeaker locations) in a 3AFC task with more than 90% correct. The audiograms of the forth subject were of the lowest quality, and the method apparently was ineffectual for this listener. The ability to localize the two real loudspeakers was 100% for all subjects.

## 905 The Influence of Aging on Interactions Between Eye Position and Human Sound Localization

**Qi N. Cui<sup>1</sup>**, Babak Razavi<sup>1,2</sup>, William E. O'Neill<sup>1</sup>, Gary D. Paige<sup>1</sup>

<sup>1</sup>Dept. of Neurobiol. & Anat., Centers for Navig. & Communic. Sci., and Visual Sci., <sup>2</sup>Dept. of Biomed. Eng., Univ. of Rochester, Rochester, NY USA

Vision and audition provide the brain with spatial information to guide natural activities. Input conveying eye position in the head is required to maintain spatial congruence since the retinae move with the eves while the ears remain head-fixed. Interestingly, eye movements shift sound localization relative to the head. We have reported that the shift is spatially broad and uniform, develops exponentially (minutes) in the direction of ocular gaze, and approaches ~40% of eye eccentricity in young subjects. Age-related effects on human sound localization include poorer accuracy in elevation but not azimuth, presumably due to degraded high-frequency hearing and the associated loss of spatial cues required for vertical localization. In this study we examined whether age alters the interaction between eve position and sound localization. Young (18-44yo), middle-aged (45-64yo), and elderly (65-81yo) subjects were tested in a dark echoattenuated room with their heads fixed and facing the center of a cylindrical screen (2m distance). A non-visible speaker on a robotic arm behind the screen presented auditory targets in a random sequence across the frontal field (±50° Az x ±25° El). Subjects fixated 1 of 3 visual spots (Ctr., L&R20°) while localizing targets using a laser pointer guided by peripheral vision. Results demonstrate a reduced shift of auditory space toward eccentric gaze in the elderly but only for peripheral space (>±20° re-head). In young subjects, the eye position-dependent shift was comparable for stimuli limited to high- and low-frequency bands, suggesting that the effect spans auditory spatial channels (interaural intensity and time differences). Thus, its attenuation in the elderly cannot be due simply to peripheral presbycusis. Results quantify an eye position-,

time-, and age-dependent adaptation of auditory space. This adaptation declines in the eccentric auditory space with advancing age, suggesting a central etiology of spatial hearing.

### 906 The Role of Attention in the Spatial Perception of Speech

**Pádraig T. Kitterick**<sup>1</sup>, A. Quentin Summerfield Department of Psychology. University of York

This study examined the role of attention in a multi-talker 'cocktail-party' listening task. Uncertainty was varied by manipulating three aspects of a target phrase: who said it, when it occurred, and where it was spoken from. We expected that participants would find it more difficult to hear out information within the target phrase when there was more uncertainty about it. We aimed to quantify the benefits of constraining who, when, and where.

Normal-hearing adults sat in the centre of a ring of 24 loudspeakers. Phrases were presented in a sequence. Participants were instructed to listen out for a target phrase, identified by a unique call sign. Their task was to report two further key-words in that phrase. In Condition 1, a new phrase started every 800ms, so that at any moment three talkers were speaking simultaneously. In Condition 2, phrases started in pairs, with a 10dB level difference within each pair. We measured the target-masker ratio at which both key-words were identified with an accuracy of 71% correct.

In Condition 1, thresholds averaged -12.9dB. Knowing *who* would speak improved thresholds significantly by 2.2dB. Improvements from knowing *when* (0.2dB) or *where* (0.9dB) were not significant. Performance was about 9dB poorer in Condition 2, but the advantages from reducing uncertainty were greater. Knowing *who, where, or when* improved thresholds significantly by 3.2dB, 5.1dB and 0.3dB, respectively.

Subjectively, attention is grabbed involuntarily by the onset of each new phrase. When the phrases start in pairs, attention is drawn to the more intense phrase. Reducing uncertainty about the target makes it easier for participants to focus and sustain attention on the target phrase.

These results demonstrate that attention plays a significant role in spatial listening for speech, and that knowledge about the location and voice of a talker is beneficial in coping with demanding listening environments.

PTK is supported by a studentship from RNID.

## 907 The Effects of Optokinetic Stimulation and Eye Position on Orientation of Sound Lateralization

Rika Otake<sup>1,2</sup>, **Akinori Kashio<sup>2</sup>**, Mitsuya Suzuki<sup>1,2</sup>
<sup>1</sup>Department of Otolaryngology, Tokyo Metropolitan Police Hospital, <sup>2</sup>University of Tokyo

Objective: Using dichotic sound, the effect of optokinetic stimulation and eye position on the orientation of sound lateralization was investigated in humans.

Experiment 1: 12 subjects were studied by testing the interaural time difference (ITD) and interaural intensity difference (IID) discriminations during optokinetic (OK) stimulation. At 90"¬/sec of the light stripes angular velocity

the amplitudes for the ITD discrimination tests during OK stimulation were significantly greater compared to those either before the beginning of OK stimulation or at that of 30"¬/sec (p<0.05). No significant difference was observed in the amplitude for the IID discrimination test was observed between before and during OK stimulation. During OK stimulation, all subjects felt that their perceptual body axes shifted toward the quick phase of OK nystagmus, and the median line of amplitude for the ITD discrimination test significantly shifted to the quick phase side of the optokinetic nystagmus.

Experiment 2: 10 subjects were studied by testing the interaural time difference (ITD) discrimination under different conditions of visual fixation. The amplitudes obtained during the ITD discrimination tests during eccentric fixation were significantly greater than those obtained while gazing straight ahead (P < 0.05). The median line of amplitude obtained during the ITD discrimination test shifted toward the direction of the gaze. Conclusions: The current study demonstrates that sound lateralization sensitivity during ITD discrimination may be altered by OK stimulation and eccentric gaze. These data suggest that nystagmus or the sensation of self-rotation or the gaze direction influences auditory afferent information such as sound lateralization.

### 908 The Effect of Vestibular Stimulation on Orientation of Sound Lateralization

**Mitsuya Suzuki**<sup>1,2</sup>, Rika Otake<sup>1,2</sup>, Tatsuya Yamasoba<sup>1</sup>

<sup>1</sup>Department of Otolaryngology, University of Tokyo,

<sup>2</sup>Department of Otolaryngology, Tokyo Metropolitan Police Hospital

Using dichotic sound, the effect of vestibular stimulation, consisting of caloric stimulation for lateral semicircular canal fs ampulla and gravity acceleration for the utricular macula, on the orientation of sound lateralization was investigated in 10 subjects. The interaural time difference (ITD) discrimination test was performed in a dark room while caloric nystagmus was induced by iced water irrigated into the external auditory canal or while the gravity acceleration for utricular macula changes between a seat title and a decubitus position. The amplitudes for the ITD discrimination tests after caloric stimulation were significantly greater than those before caloric stimulation (P<0.05). During caloric stimulation, all subjects reported that their perceptual body axes shifted toward the slow phase side of nystagmus, and the median line of amplitude for the ITD discrimination test shifted to the slow phase side of the nystagmus. In contrast, when subjects were gazing a visual target fixed straight ahead of subjects, no significant difference in the amplitudes or the median line shift of amplitude was observed between before and after caloric stimulation. On the gravity acceleration for utricular macula, no significant difference in the amplitudes for the ITD discrimination tests was observed between seat title and a decubitus position. In 8 subjects, the median line in amplitude for the ITD discrimination test shifted to the slow phase side of the nystagmus. In contrast, when subjects were gazing a visual target fixed straight ahead of subjects, no significant difference in the median line shift of amplitude was observed between seat title and a

decubitus position. The current study suggests that sound lateralization sensitivity during ITD discrimination may be altered by vestibular stimulation such as caloric stimulation or gravity acceleration.

909 Spatial Unmasking of Birdsong by Budgerigars and Zebra Finches

**Micheal Dent**<sup>1</sup>, Elizabeth McClaine<sup>1</sup>, Barbara Shinn-Cunningham<sup>2</sup>, Virginia Best<sup>2</sup>, Erol Ozmeral<sup>2</sup>, Rajiv Narayan<sup>2</sup>, Frederick Gallun<sup>2</sup>, Kamal Sen<sup>2</sup>

<sup>1</sup>University at Buffalo, <sup>2</sup>Boston University

For animals to communicate effectively in noisy environments, they must be able to segregate an important signal from irrelevant background sounds (interferers). In humans, this ability is increased when the signal can be spatially separated from the interferers. This same ability has been found in animals using pure-tone signals in broadband noise interference, but studies using biologically relevant stimuli are less common. Here, using operant conditioning techniques, we tested budgerigars and zebra finches on their ability to identify a zebra finch song in the presence of a background masker emitted from either the same or a different location as the signal. Three types of maskers were used, which differed in their spectro-temporal characteristics: broadband modulated noise, and choruses of zebra finch songs. These stimuli were presented at different signal-to-noise ratios according to the method of constant stimuli and thresholds for correctly identifying the zebra finch songs were calculated. Thresholds were generally lower for the zebra finches than for the budgerigars, and there were only minor differences in thresholds between the three masker types for both species of birds. In addition, for the zebra finches but not for the budgerigars, thresholds for the spatially separated signal and masker conditions were lower than those for the spatially coincident signal and masker, suggestive of spatial unmasking. This may indicate a species-specific advantage for listening to complex acoustic stimuli in noisy environments.

## 910 Lateralization of Dynamic Interaural Time and Level Differences in High-Frequency Click Trains

G. Christopher Stecker<sup>1</sup>

<sup>1</sup>University of Washington

Localization and lateralization of amplitude-modulated, high-carrier-frequency sounds is relatively impaired---and dominated by information contained in the sound onset--when modulation rates exceed approximately 100 Hz. While several recent studies have focused on the processing of envelope ITD cues in such stimuli, past studies demonstrated similar binaural adaptation regardless of binaural cue type, suggesting a rate limitation in high-frequency inputs to binaural processing rather than envelope ITD processing per se. In this study, we compared ILD and envelope-ITD thresholds for trains of band-limited 4000 Hz Gaussian impulses across rates of 100, 200, and 500 pps. Right-favoring interaural differences were static (condition RR), increased linearly from diotic (condition 0R), or decreased linearly toward diotic (condition R0). Thresholds were calculated from the largest interaural difference in each stimulus (i.e. the onset of R0 or offset of 0R trains). Overall, thresholds were strongly dependent on pulse rate, worse at 500 than 200 or 100 pps. ILD and envelope ITD thresholds were especially impaired in condition 0R at 500 pps, consistent with lateralization dominance of the onset at high rates for both interaural cue types.

## 911 From Tone to Complex: Generalization of the Effects of Spatial Cues and Attention on Grouping and Streaming

**Adrian KC Lee<sup>1</sup>**, Steve Babcock<sup>2</sup>, Barbara Shinn-Cunningham<sup>1,3</sup>

<sup>1</sup>Harvard-MIT Health Sciences and Technology, Speech and Hearing Bioscience and Technology, <sup>2</sup>Department of Biomedical Engineering, Boston University, <sup>3</sup>Hearing Research Center and Department of Cognitive Neural Systems, Boston University

Previous experiments showed that the apparent perceptual organization of a scene containing two simultaneous streams depends on which stream is being attended. With appropriate manipulation of the spatial cues, a clearly detectable target (which could logically belong to either of the streams) was "orphaned," in that it was never perceived as part of the foreground stream, regardless of which stream was attended.

The current experiment uses a similar paradigm to measure directly the contribution of an ambiguous target to each of two ongoing streams. Slowly repeating (SR) and fast repeating (FR) harmonic complexes were presented with different, but related fundamental frequencies. An ambiguous target complex was presented simultaneously with the SR complex, but consisted of the same harmonics as the FR complex. In different blocks, subjects attended either to the SR or the FR stream. In each block, they adjusted the target-complex intensity presented in a single-stream control stimulus (SR or FR) to match the perceived timbre / pitch of the SR or FR stream in the mixture.

Results are compared with those of the previous experiment to confirm that spatial cues play a subtle but important role in how listeners segregate ambiguous spectro-temporal elements over time scales of tens of milliseconds.

[Supported by ONR N00014-04-1-0131]

### 912 Auditory Grouping in Gray Treefrogs Mark Bee<sup>1</sup>

<sup>1</sup>University of Minnesota

Auditory scene analysis refers to processes that parse the complex acoustic waveform generated by multiple sound sources into coherent perceptual representations. While auditory scene analysis remains an influential paradigm for understanding human hearing and speech perception, students of animal behavior have devoted little attention toward investigating auditory scene analysis in the context of acoustic communication in non-human animals. This is

surprising given that the communication behavior of many non-human animals also relies on an ability to perceptually organize complex acoustic scenes. One important aspect of auditory scene analysis is the perceptual grouping of the simultaneously and sequentially produced sounds from a common source. In this study of the gray treefrog (Hyla chrysoscelis), I used female phonotaxis behavior to test the hypothesis that common spatial origin promotes the perceptual integration of the simultaneous (harmonics) and sequential (pulses) sound elements of male mating calls. The call consists of a series of discrete sound pulses (50 pulses s<sup>-1</sup>) with a fundamental frequency of about 1.1 kHz and a dominant second harmonic of about 2.2 kHz. Females exhibit strong pulse-rate selectivity and prefer with both harmonics over single-harmonic alternatives. When given a choice between a spatially coherent call (both harmonics originating from the same speaker) and a spatially incoherent call (each harmonic from different speakers separated by 7.5°, 15°, 30°, or 60°), females preferentially chose the spatially coherent call. When I presented females with two interleaved pulse sequences (each presented at half the normal rate), phonotactic responses increased linearly as the angular separation between the two pulse sequences decreased from 180° to 0°. Together, these results suggest that common spatial origin functions as an auditory grouping cue for simultaneous and sequential perceptual integration in frogs and plays a potentially important role in auditory scene analysis in this group of lower vertebrates. This work serves to highlight frogs as one potentially important group of vertebrates for integrating behavioral and neurophysiological studies of the mechanisms and evolution of auditory scene analysis.

This work was supported by a Grant-in-Aid from the Dean of the Graduate School of the University of Minnesota and NIDCD 1R03DC008396-01.

## 913 Effects of Context on Auditory Stream Segregation

**Joel Snyder**<sup>1</sup>, Olivia Carter<sup>1</sup>, Suh-Kyung Lee<sup>2</sup>, Erin Hannon<sup>1</sup>, Claude Alain<sup>3</sup>

<sup>1</sup>Harvard University, <sup>2</sup>Harvard-MIT Health Sciences and Technology, <sup>3</sup>Baycrest Centre for Geriatric Care Perceptual organization in naturalistic settings typically occurs within a rich context that includes the individual's recent history of perceptual experiences. We carried out a series of experiments examining the influence of preceding context on auditory stream segregation (or "streaming"). We presented low tones (A), high tones (B), and silences (-) in a repeating ABA- pattern to young adults, who indicated whether they perceived one stream of tones with a galloping rhythm (ABA-ABA-...), or two streams of tones with metronome rhythms (A-A-A-... and B---B--...). On each trial, the A tone had a fixed frequency and the B tone either had the same frequency as the A tone or one of three higher frequencies. Listeners were more likely to perceive streaming on the current trial when the previous trial had a smaller frequency separation between A and B tones, and when they had not perceived streaming at the end of the previous trial. Effects of the previous trial appeared even when listeners deliberately tried to

perceive a specified organization in the current trial (i.e., one stream or two streams). The effect of the previous trial on the current trial diminished when we increased the inter-trial intervals from 1.44 sec to 5.76 sec. This time course of context effects suggests that sensory or perceptual adaptation with a time constant in the range of seconds plays an important role in streaming. Overall, these findings demonstrate that context is important for understanding the mechanisms underlying perceptual organization of auditory sequences.

#### 914 Detection of Delayed Tones in Auditory Streaming Sequences: An Objective Measure of the Build-Up of Auditory Stream Segregation

**Sarah Thompson**<sup>1</sup>, Bob Carlyon<sup>1</sup>, Rhodri Cusack<sup>1</sup>

\*\*MRC Cognition and Brain Sciences Unit

Sequences of the form ABA-ABA- etc., where A and B stand for pure tones of different frequencies, can be heard in either of two ways: as an integrated single stream with a galloping rhythm, or as two separate streams of regularly repeating high or low tones. In the latter case, the ability to compare timing information between the two streams is lost. When the frequency separation between the A and B tones is large, or the repetition rate is fast, the likelihood of hearing segregation increases. However, the percept can also vary in sequences where these parameters are held constant. The probability of hearing two streams increases with sequence duration, and this build-up is typically measured with a subjective rating task. Since it is not always desirable to have a participant's attention focused on assessing their own perception, we sought a simple behavioural measure which would provide an objective correlate of stream segregation.

Our first experiment included a 'delay' condition in which participants were asked to detect, within a 12.5 s sequence, a signal consisting of 4 ABA- triplets in which the B tone had been delayed relative to the A tones. Performance improved with increasing delay (15 - 40ms). deteriorated with increasing frequency separation between the A and B tones ( $\Delta f = 4$  or 8 semitones), and was better when the signal occurred early (2.0 s) compared to late (9.5 s). These last two findings are consistent with this task being hardest in those conditions which produced a twostream judgment in subjective rating experiments. It was concluded that the delay condition indexed stream segregation in an objective manner, without requiring explicit streaming judgments. Further experiments used this measure to investigate the relationship between subjective and objective judgements in the same participants. We also discuss the implications of these results in terms of previously-reported effects of attention on the build-up of streaming.

### 915 Effects of Auditory Grouping on Phonemic Restoration

**Dali Wang**<sup>1</sup>, Barbara Shinn-Cunningham<sup>1</sup>
<sup>1</sup>Boston University

When speech is interrupted by silences, speech intelligibility is enhanced when broadband noise occurs in

the silences, a filling-in process is known as "phonemic restoration." If the broadband envelope of the missing speech is imposed on the noise (speech-modulated noise), intelligibility is further enhanced. We presented diotic, interrupted speech with unmodulated and speechmodulated noise whose interaural time differences were either 0 or 300 µs. We expected the perceived location of the noise to have no effect on performance with unmodulated noise. However, we expected improvement in performance with speech-modulated noise to be reduced when the noise was perceived from a different direction than the speech. Specifically, we expected spatial separation of the interrupted speech and noise to promote hearing the two sources as distinct perceptual streams, which should interfere with the integration of the partial speech information from the modulated noise with the information in the interrupted speech. As expected, spatial configuration has no effect on intelligibility for unmodulated noise. For speechmodulated noise, performance is best when speech and noise are from the same location, and is equivalent to that of unmodulated noise when speech and noise are from different directions. Results show that perceptual organization of the scene affects how information is combined across auditory streams.

Supported by grants from the National Science Foundation.

## 916 The Use of Two Different Paradigms in Studying Comodulation Masking Release in the Mouse (Mus Musculus)

**Karin B. Klink**<sup>1</sup>, Verena N. Weik<sup>1</sup>, Georg M. Klump<sup>1</sup> \*\*University of Oldenburg\*\*

Signal detection threshold in noise with correlated amplitude fluctuations over a range of frequencies is generally lower than the threshold for signal detection in noise without such a correlation. This effect has been termed comodulation masking release (CMR), and has been attributed to auditory processing within one auditory channel (within-channel cues) and/or across several auditory channels (across-channel cues). Two different paradigms have been used to study CMR: the bandnarrowing paradigm and the flanking-band paradigm (for a review see Verhey at al. 2003, Exp Brain Res 153: 405).

We determined psychophysical thresholds for detecting an 800-ms 10-kHz tone in noise in the house mouse (NMRI strain) which has its best hearing between 10 to 20 kHz and an auditory-filter bandwidth of 3.3 kHz at a center frequency of 10 kHz (Weik et al., ARO 2006). In the bandparadigm, we used comodulated unmodulated noise with a bandwidth ranging from 0.1 to 20 kHz, and mice showed a considerable CMR (up to 12.8 dB) for masker bandwidth of 0.4 kHz and above. This shows that in the mouse a large amount of CMR can be attributed to within-channel cues only. To test whether across-channel processing can also contribute to CMR, we also determined thresholds using the flanking-band paradigm. We used two noise maskers with a bandwidth of 25 Hz each that were either correlated or uncorrelated. While one masker was always centered at 10 kHz, the other was centered at a frequency in the range from 5 kHz to 15 kHz. In this experiment, the amount of CMR appeared to be lower than in the band-narrowing experiment.

Supported by the DFG and the Joint Niedersachsen – Israel program

### 917 A Unified Approach to the Detectability of Signals in Comodulated Noise

**Michael Buschermöhle**<sup>1</sup>, Ulrike Feudel<sup>1</sup>, Jan A. Freund<sup>1</sup>
<sup>1</sup>Carl-von-Ossietzky University Oldenburg

Experimental paradigms like comodulation detection difference (CDD) or comodulation masking release (CMR) show that the detectability of signal sounds in the presence of comodulated noise can be improved compared with the presence of unmodulated noise. Comodulated noise here is defined as noise having common amplitude modulations in different frequency regions, which is a typical property of natural sounds like animal vocalizations. In the present study, general aspects of signal detectability in comodulated noise and in noise are investigated theoretically, unmodulated especially considering compression, which is an essential signal processing step in the auditory system. The theoretical results are supplemented with simulations for possible neuronal responses in which the signal detectability is also examined.

Specifically, one can find that the signal-to-noise ratio (SNR) for small signal amplitudes in a compressed stimulus with comodulated noise is enhanced relative to the SNR for small signal amplitudes in a compressed stimulus with unmodulated noise. The auditory system may take advantage of this property of the compressed stimulus. A possible exploitation of this feature of compressed stimuli via spike mechanisms is discussed.

Experimental results [1] which indicate that under certain conditions the presence of comodulated noise may lower the detection thresholds for sine tones to values below the absolute threshold while unmodulated noise has a masking effect are discussed in the light of our theoretical considerations.

(Supported by DFG)

### 918 Amplitude-Modulation Detection in Rabbit: Behavioral and Physiological Results

**Laurel Carney**<sup>1</sup>, Paul Nelson<sup>2</sup>, Yan Gai<sup>1</sup>, Kristina Abrams<sup>1</sup>, Fabio Idrobo<sup>3</sup>

<sup>1</sup>Syracuse University, <sup>2</sup>Johns Hopkins University, <sup>3</sup>Boston University

Statistical analyses of the responses of single cells in the inferior colliculus of rabbit suggest that changes in average firing rate are not sufficient to explain human thresholds for sinusoidal amplitude modulation (AM) detection (Nelson, 2006). However, temporal (envelope-locked) aspects of neural responses provide cues for modulation at significantly lower modulation depths that are more consistent with human psychophysical performance. To test the generality of these conclusions across species, we compared behavioral AM detection thresholds in the rabbit to the previously reported physiological results. Rabbits were tested using a two-alternative-choice operant-

conditioning paradigm. In preliminary measurements, rabbit AM detection thresholds for a 5-kHz-tone or wideband-noise carrier and sinusoidal modulation frequencies of 4- or 60-Hz were considerably less sensitive than those in human listeners and were more consistent with single-unit physiological thresholds based on rate. (It is possible that the behavioral results in rabbit improve somewhat with extended Implications and puzzles raised by these results for neural coding of amplitude modulation in humans and rabbits will be discussed. For example, if neural rate and temporal response properties to AM are qualitatively similar in rabbit and human, then humans may achieve their enhanced sensitivity to AM by making use of temporal information that rabbits do not use. Alternatively, if humans use ratebased coding strategies, then neural rate responses in humans must be significantly more sensitive to AM than they are in rabbit.

[Supported by NIH NIDCD-01641.]

### 919 Internal Representations of Amplitude Modulation Revealed by Reverse Correlation

Marine Ardoint<sup>1</sup>, Pascal Mamassian<sup>1</sup>, Christian Lorenzi<sup>1</sup>
<sup>1</sup>Laboratoire de Psychologie de la Perception FRE CNRS-Paris 5 #2929, ENS-DEC

Recent work suggests that listeners achieve amplitudemodulation (AM) detection by computing the cross correlation between the outputs of hypothetical AM channels and memory stored templates according to an "optimal detector" scheme. The present study aimed to assess the validity of such a template matching process by applying the reverse correlation technique to an AM detection task performed in the presence of masking noise. A constant stimuli, two-interval, two-alternative forced-choice procedure was used. Each listener completed 100 sessions of 100 trials. In each trial, the listener's task was to identify the interval containing a 4-Hz sinusoidal AM applied to a 1-kHz sine carrier. All stimuli were presented in a gaussian white noise at a fixed, +6-dB signal-to-noise ratio. All noise maskers were stored and bandlimited by auditory filters with center frequencies between 0.57 and 1.66 kHz. For each frequency band, the filtered noises that influenced the detection or the nondetection of the 4-Hz AM target were averaged and combined to obtain a so-called "classification image" (or template) reflecting the characteristics of the noise that biased the listener's decision.

In 4 listeners out of 10, the classification images computed for the audio-frequency bands centered between 1.3 and 1.5 kHz showed a clear, 4-Hz AM component. These results provide direct evidence for (i) off frequency listening, and (ii) the involvement of a template matching process in the present AM detection task.

The ability to discriminate changes in the starting phase of a 4-Hz sinusoidal AM target was measured in a second experiment using a constant stimuli, three-interval, three-alternative forced-choice procedure. The results indicate that the 6 listeners showing no 4-Hz AM component in their classification images also show the poorest AM phase discrimination performance. This shows that the

reverse correlation technique is intrinsically limited by the listeners' phase uncertainty.

# 920 Forward Masking in the Amplitude Modulation Domain: Further Psychophysical Observations and Potential Physiological Correlates

**Magdalena Wojtczak**<sup>1</sup>, Paul C. Nelson<sup>2</sup>, Laurel H. Carney<sup>2</sup>, Neal F. Viemeister<sup>1</sup>

Department of Psychology, University of Minnesota, <sup>2</sup>Institute for Sensory Research, Syracuse University Recently, Wojtczak and Viemeister [2005, J. Acoust. Soc. Am. 118, 3198-3210] demonstrated forward masking in the amplitude modulation (AM) domain. The present study examined whether this effect has correlates in physiological responses to AM at the level of the auditory midbrain. The human psychophysical experiment used 40-Hz, 100% AM (masker AM) that was imposed on a 5.5kHz carrier during the first 150 ms of its duration. The masker AM was followed by a 50-ms burst of AM of the same rate (signal AM) imposed on the same (uninterrupted) carrier. The time course of recovery was longer for the tonal carrier than that observed with the noise carrier in the previous study by Woitczak and Viemeister. Gating the carrier for the duration of the masker and signal AM with a silent gap in between revealed even more forward masking and longer recovery times. In the physiological experiment, single-unit extracellular recordings in the awake rabbit inferior colliculus (IC) were obtained for stimuli designed to be similar to the uninterrupted-carrier conditions used in the psychophysics. The masker AM was longer (500 ms compared with 150 ms in the psychophysical experiment), and the carrier and modulation rate were chosen based on each neuron's audio- and envelope-frequency selectivity. Although a small subset of the population of IC cells did exhibit some degree of AM forward masking, most of the responses to the signal AM were unaffected by the presence of a preceding masker AM. This was true for analyses based on both average spike count and temporal correlation between the responses to masked and unmasked signal AM. Unless the physiological observations were caused by species differences, they suggest that higher stages of processing must be considered to account for the effectively longer AM processing time constants measured perceptually in humans.

[Supported by NIDCD/NIH grants DC00683, DC006804, DC7268, and DC01641)].

# 921 Preliminary Data Evaluating the Effect of Gabapentin on Auditory Temporal Resolution Characterized by a Gap Detection Task in Gerbils

Otto Gleich<sup>1</sup>, **Juergen-Theodor Fraenzer<sup>1</sup>**, Jürgen Strutz<sup>1</sup> *University of Regensburg* 

Impaired auditory temporal processing is improved by the drug  $\gamma$ -vinyl-GABA (Sabril) that increases GABA levels in the brain (Gleich et al., 2003, Neuroreport 14:1877-1880). However, Sabril can reduce the visual field. Thus we

began evaluating the anticonvulsant Gabapentin (GP). GP was effective in the treatment of certain forms of tinnitus, where GABA mechanisms have repeatedly been implicated (Bauer and Brozoski, 2001, JARO 2:54-64; 2006, Laryngoscope 116: 675-681).

In each animal threshold for an 800 ms broad band noise pulse was determined. The noise pulse was subsequently used as a carrier for the gap with a level set 30 dB above each individual's threshold. GP was administered in the drinking water at a dose of 350 mg/kg/day. Testing was performed 1-2 hours after GP intake. Gap detection thresholds were determined, before, during and at least two weeks after cessation of GP administration for 5 young (8-13 months) and 10 old (27-37 months) gerbils.

A two way repeated measure ANOVA using age and treatment as factors revealed a significantly higher mean gap detection threshold for old (3.1 ms) as compared to young (2.0 ms) gerbils (p = 0.019). Mean gap detection threshold during GP treatment (2.9 ms) was slightly higher compared to thresholds determined before (2.5 ms) and after GP treatment (2.3 ms), however, these differences were not significant (p = 0.212) and there was no interaction between age and treatment (p = 0.923).

These preliminary data provide no evidence for a beneficial effect of GP on temporal resolution, if anything, the group mean data suggest that performance may deteriorate during GP treatment. In contrast to initial expectations, GP has no effect on GABA receptors, enzymes or transporters (Errington et al., 2005, Curr. Top. Med. Chem. 5, 15-30) and consequently cannot compensate age dependent declines in the GABA system. We thank S. Kopetschek and C. Wögerbauer for help with the behavioral experiments. Supported by the DFG Str275/4-5.

## 922 Perception and Processing of Ramped and Damped Complex Echoes in the Bat *Phyllostomus Discolor*

**Sven Schoernich**<sup>1</sup>, Frank Borina<sup>1</sup>, Gerd Schuller<sup>1</sup>, Lutz Wiegrebe<sup>1</sup>

<sup>1</sup>Ludwig-Maximilians-University Munich

Through echolocation, bats are not only able to detect an object in the darkness, but also to gather information about its structure. It has been shown that the bat *P. discolor* is able to use the echo roughness (i.e. the amount of the envelope fluctuation) to classify complex natural objects like trees or bushes. Recent recordings showed that echoes from those objects often possess a ramped or damped overall envelope, depending on the object's structure and the echolocation call's penetration depth.

In the current psychoacoustical and neurophysiological experiments, we investigate the effect of a ramped or damped overall envelope on the bats' sensitivity to echoroughness changes. The psychoacoustical experiments were implemented as a 2AFC, virtual-object playback paradigm with positive reinforcement. Preliminary results indicate that with a ramped overall envelope, roughness sensitivity is better than with a damped or a flat overall envelope.

In the neurophysiological experiment, 81 neurons in the inferior colliculus of 2 P. discolor were tested for their ability to capture the perceptual effect of the overall envelope on echo roughness. About 70 % of all tested neurons encoded echo roughness significantly in their response rate: If the spike rate increased with increasing roughness, the neuron was classified as rough-encoding (ca. 36 %); if the spike rate decreased with increasing echo roughness, the neuron was classified as smoothencoding (ca. 33 %). Interestingly, neither a ramped nor a damped overall envelope improved roughness sensitivity in rough-encoding units. In smooth-encoding units, however, the perceptual effects were mirrored in that roughness sensitivity was best with a ramped envelope, intermediate with a damped envelope and worst with a flat envelope.

#### 923 The Effect of a Precursor on Growth-of-Masking Functions

Vidya Ganesh<sup>1</sup>, Elizabeth Strickland<sup>1</sup>

<sup>1</sup>Purdue University

An ongoing series of experiments in this laboratory have examined the temporal effect in simultaneous masking, also known as overshoot. This refers to the fact that a higher signal-to-masker ratio is needed to detect a short-duration signal at the onset of a masker if it is preceded by silence as compared to being preceded by a precursor (either a separate sound or a continuation of the masker). The temporal effect is of interest because it seems to be consistent with a decrease in the gain of the active process in the cochlea with acoustic stimulation. This is the type of effect that might be expected from activation of the medial-olivocochlear bundle reflex (MOCBR).

The present study extends examination of the temporal effect to forward masking. The objective of this study was to examine the effect of precursor level and duration on the temporal effect in subjects with normal hearing. Growth-of-masking functions were obtained using a short-duration 4 kHz signal and an off-frequency masker with and without a 4 kHz precursor. Precursor duration and level were varied.

Preliminary results show a compressive GOM function for the no-precursor condition, as has been found in previous studies. The addition of a precursor shifts the GOM function to the right, consistent with a decrease in gain at the signal frequency. This shift increases with precursor level. Surprisingly, the short-duration precursor has a greater effect than the long-duration one. This may reflect aspects of the time course of onset of the MOCBR.

# 924 Right-Left Hemispheric Asymmetry in Sensitivity to Slow but not Fast Frequency Modulations as Revealed in Ear Differences as a Function of Rate

**Manon Grube**<sup>1</sup>, Timothy Griffiths<sup>1</sup>, Adrian Rees<sup>1</sup> Auditory Group, Newcastle University

The present study aimed to test the hypothesis that auditory cortices of the two hemispheres differ in their sensitivity to frequency modulations by looking at ear differences as a function of sweep rate. Hemispheric lateralization has been postulated in the form of a left- vs. right-hemisphere specialization in fast temporal, speechrelated vs. spectral processing (Schwartz & Tallal, 1980; Zatorre & Belin 2001), as well as in the form of preferred window lengths of analysis (Boehmio et al. 2005). Under the assumption of contralaterally dominant projections, postulated leftand righthemispheric specializations would be expected to yield right- and leftear discrimination advantages for fast and slow changes in frequency, respectively. Psychometric functions for the sensitivity to rates of change were determined using a 3 interval, 2 alternative forced-choice dichotic stimulation paradigm (Kimura, 1967). Frequency sweeps to be discriminated were presented to one, competing noise stimuli to the other ear; measurements for right and left ear were interleaved. Frequency sweeps extended from 1.0 to 1.5 kHz; sweep durations were 50, 100, 200 and 400 ms. Data were drawn from a sample of 44 subjects. Partly contrasting hypothesized predictions, no significant rightear advantage for the shorter durations was found at group levels but a left-ear advantage for the longer sweep duration was (p=.026 for 400 ms, single sample t-test). The results are in good agreement with functional data from Boehmio et al. (2005) and point to faster changes being processed to equal extent by both hemispheres' auditory cortices, and to slower changes over window sizes beyond about 300 ms tapping into right-lateralized mechanisms of contour analysis critical in music as in speech perception.

### 925 Auditory Processing Performance of Preschool Children

**David Moore**<sup>1</sup>, Sally Hind<sup>1</sup>, Katie Dangerfield<sup>1</sup> *MRC Institute of Hearing Research* 

Psychoacoustic studies in children often focus on ages 0-1 and 6+ years, but major developmental milestones related to listening occur in the 1-6 range. We ask here whether computer-based measures of auditory processing (AP) used in 6-12 v.o. children may be used with typically developing preschool children (PSC) aged 3-5 years. Piloting of our AP test battery ('CAPE'), presented via a laptop PC and headphones led to inclusion of a systematic pre-test practice period. The final battery comprised 7 core AP tasks (backward and simultaneous masking, notched noise masking, frequency modulation (2 Hz, 2 kHz carrier), tone detection (1 kHz; 20 and 200 ms), frequency discrimination) and 2 derived measures (temporal integration, frequency resolution). Each task used a 3I-2AFC 3-down, 1-up adaptive response paradigm. Standardised cognitive measures were also obtained. 57 PSC were tested in a guiet area of the child's nursery. All children met the pre-test practice criteria, were willing to wear headphones, and successfully completed all tasks with the exception of frequency discrimination. Threshold analysis to date for the PSCs (n=30) on the other 8 measures showed more inter-listener variability than in older people. Statistical comparisons across all ages (3.5 y.o. - adult) found significant improvements with increasing age for backward masking (Z = -3.27, p<.001) and frequency resolution (Z = -3.91, p<.001), but not for

simultaneous masking (Z=-0.43), frequency modulation (Z=-.28) or temporal integration (Z=-1.26). Absolute thresholds were higher in the PSCs (due to poor test acoustics?), but comparable simultaneous masked thresholds (medians: 3-5y.o: 51.4dB, 6-7: 50.5dB, 8-9: 50.0dB, 10-11: 49.4dB, Adult: 48.5 dB; all groups n>20) gives confidence in the ability of the PSCs to perform these AP tasks. These data open the way to early identification of hearing and listening difficulties and the ability to partial out AP contributions to learning problems.

## 926 Frequency Discrimination Learning in Children: Effects of Age and Intelligence

**Lorna F. Halliday**<sup>1</sup>, Jenny L. Taylor<sup>1</sup>, David R. Moore<sup>1</sup> <sup>1</sup>MRC Institute of Hearing Research

Children usually perform more poorly than adults on auditory perceptual tasks, particularly those that are thought to carry a high cognitive load and/or that are heavily dependent on central auditory processing. However, the question of whether perceptual training can improve children's auditory performance to adult levels has not been previously assessed. We examined the effects of age and intelligence on learning on an auditory frequency discrimination task. Four groups of normally-hearing children (6-7 years, 8-9 years, 10-11 years) and adults (18-40 years) performed a 3I-3AFC adaptive (3D:1U) frequency discrimination task (600 trials in 8 x 75-trial blocks), using a fixed standard stimulus (1 kHz). Results for the child participants showed a main effect of training, with frequency discrimination limens (DLF) decreasing from 14.9±1.6% in the first block to 12.7±1.5% in the eighth block. However, in general, this improvement was confined to the first three blocks. Throughout the training session, DLFs for the 6-7- year group were significantly poorer but parallel to those of the older children and adults. However, by the end of training, some individual 6to 7-year-olds produced DLFs that were close to the mean of the adult group. Significant correlations were found between DLFs obtained at the beginning of training and performance on a measure of nonverbal ability - these correlations were confined to the older (10-11+ years) groups. Nonverbal ability was not significantly associated with degree of improvement in DLFs with training for any of the groups. These results suggest that children learn following training on a simple psychoacoustic test during a relatively short session and that the shape of the learning curve does not change with age within the range examined. However, age-related improvements frequency discrimination may involve high level cognitive processes which need to be in place before adult levels of ability can be achieved.

## 927 Infants' and Adults' Thresholds for a Tone Masked by Constant, Remote-Frequency Maskers

**Lynne Werner**<sup>1</sup>, Lori Leibold<sup>1</sup>

<sup>1</sup>University of Washington

In an experiment examining informational masking in infants, Leibold (2004) reported that infants and adults exhibited masking of a tone by two tones of constant,

remote frequencies. Neither informational nor energetic masking would be expected for adults under these conditions. In the present experiment, infants' and adults' detection of a tone masked by two constant frequency tones or two narrow bands of noise were compared. The target tone was 1000-Hz, 300-ms duration with 16-ms rise/fall. Unmasked and two masked thresholds were estimated using an observer-based procedure. The maskers were either tones of 581 and 2920 Hz or 50-Hzwide noise bands centered at 556 and 2895 Hz. The duration of the maskers was 300 ms with 16-ms rise/fall. A one-interval adaptive procedure was used to estimate thresholds. The maskers repeated at 600-ms intervals. The target tone was presented simultaneously with the maskers on signal trials. Listeners received feedback whenever they correctly detected the target. About 75% of the adults demonstrated 3-5-dB of masking in both conditions, but the threshold in the two-noise condition was generally higher than in the two-tone condition. Nearly all infants demonstrated 5-15-dB of masking in both conditions, but the threshold in the two-tone condition was generally higher than in the two-noise condition. Thus, introducing a timbre difference between the target and masker reduced the amount of masking for infants, but not for adults.

#### 928 The Development of Sensitivity to Amplitude and Frequency Modulation Follow Distinct Time Courses

**Karen Banai**<sup>1,2</sup>, Andrew T. Sabin<sup>1</sup>, Nina Kraus<sup>1,2</sup>, Beverly A. Wright<sup>1,2</sup>

<sup>1</sup>Department of Communication Sciences and Disorders, Northwestern University, <sup>2</sup>Northwestern University Institute of Neuroscience

Adequate sensitivity to ongoing changes in auditory signals such as amplitude modulation (AM) and frequency modulation (FM) is important for normal speech and language skills. However, relatively little is known about the normal development of AM and FM sensitivity in school-age children and adolescents. In the current experiment we evaluated the developmental time course of sensitivity to sinusoidal AM (carrier: 1-s white-noise; modulation rates: 8, 64 and 125 Hz) and FM (carrier: 1.5-s 1-kHz tone; modulation rates: 2, 20 and 240 Hz) across children aged 8-10 and 11-12 y/o and adults. For FM, both average performance (mean) and performance consistency (within-listener standard deviation) were adult like in the 8-10 y/o for all three rates. On the other hand, for AM, average performance was still not adult-like in the 10-12 y/o for any rate. However, poorer AM sensitivity in children could not be attributed to poorer performance consistency in this group because standard deviation stayed stable across the three age groups. The different developmental time courses of average sensitivity and performance consistency for AM suggests that these two measures of performance may be governed by separate mechanisms developing at different rates. Furthermore, the presence of developmental improvement in average sensitivity in AM but not FM suggests that, at least during development, sensitivity to AM and FM may be limited by different neuronal bottlenecks that mature at different rates. This suggestion brings to question the idea that AM and FM are processed through a similar neural code starting at low levels of the auditory pathway. Supported by NIH/NIDCD.

### 929 Development of Perceptual Correlates of Reading Performance

**Kerry Walker**<sup>1</sup>, Susan Hall<sup>2</sup>, Raymond Klein<sup>2</sup>, Dennis Phillips<sup>2</sup>

<sup>1</sup>University of Oxford, <sup>2</sup>Dalhousie University

Performance on perceptual tasks requiring discrimination of brief, temporally proximate or temporally varying sensory stimuli (temporal processing tasks) is impaired in some individuals with developmental aphasia and/or dyslexia. Little is known about how these temporal processes in perception develop and how they relate to language and reading performance in the normal population. The present study examined performance on 8 temporal processing tasks and 5 language/reading tasks in 120 unselected readers who varied in age over a range in which reading and phonological awareness were developing. Performance on all temporal processing tasks except coherent motion detection improved over ages 7 years to adulthood (p < .01), especially between ages 7 Independent of these age effects, and 13 years. performance on all 8 temporal processing tasks predicted phonological awareness and reading performance (p < .05), and three auditory temporal processing tasks predicted receptive language function (p < .05). Furthermore, all temporal processing measures except within-channel gap detection and coherent motion detection predicted unique variance in phonological scores within subjects, whereas only within-channel gap detection performance explained unique variance in orthographic reading performance. These findings partially support Farmer and Klein's (1995) notion of there being separable perceptual contributions to phonological and orthographic reading development. The data also are compatible with the view that the umbrella term "temporal processing" encompasses fundamentally different sensory or cognitive processes that may contribute differentially to language and reading performance, which may have different developmental trajectories and be differentially susceptible to pathology.

## 930 Different Daily Training Requirements for Learning Versus Generalization on Duration Discrimination

Beverly Wright<sup>1</sup>, Andrew Sabin<sup>1</sup>

<sup>1</sup>Northwestern University Department of Communication Sciences and Disorders

Listeners can improve their ability to discriminate between sounds with multiple-session practice, and often generalize that learning to untrained stimuli on the trained discrimination task. However, it is not known whether the same daily training requirements apply to both learning and generalization. To investigate this question, we compared stimulus generalization on a duration-discrimination task across listeners who were trained with one of three regimens that differed 1) in the number of

trials per session and 2) in whether or not each session also included training on a task other than duration In all cases, the training consisted of discrimination. repeated threshold measurements, over 6 to 10 daily sessions, using an adaptive (3-down/1-up), two-interval forced-choice procedure. All three trained groups learned more than untrained controls on the standard stimulus used in training (100 ms, 1 kHz), and none generalized that learning to an untrained standard duration (50 ms) at the trained frequency (1 kHz). However, while listeners (n=6) who practiced only duration discrimination for 360 trials per session showed no generalization to the trained duration (100 ms) at an untrained standard frequency (4 kHz), listeners (n=6) who practiced for 900 trials per session did, as did listeners (n=8) whose training alternated between duration and frequency discrimination every 120 trials for a total of 720 trials per session (360 trials per discrimination task). These results suggest that, for multiple-session training on duration discrimination, more practice per session is required for generalization to an untrained stimulus than for learning on the trained stimulus. However, not all of the practice in each session need be on duration discrimination: Practice on a different task (frequency discrimination) actually appears to facilitate generalization, at least when the standard stimulus is the same. [Supported by NIH.]

### 931 The Time Course of Auditory Generalization

Roselyn M. Wilson<sup>1</sup>, **Beverly A. Wright<sup>1</sup>** 

<sup>1</sup>Northwestern University

Training on an auditory discrimination task often leads not only to learning on the stimulus used during training, but also to the generalization of that learning to untrained However, it is not known whether this generalization follows the same time course as the initial learning itself. To investigate this question, we trained listeners for either two (n=9), four (n=10), or ten (n=14) days on a duration-discrimination task with a single standard stimulus and compared learning on the trained stimulus (100 ms, 1 kHz) as well as generalization to an untrained stimulus (100 ms, 4 kHz) across the groups. In all cases, the daily training consisted of 15 threshold measurements (900 trials), using an adaptive (3 down/1 two-alternative forced-choice procedure. up), Generalization to the untrained stimulus did not occur until after learning on the trained stimulus had begun. Two-day trained listeners improved only on the trained stimulus (100 ms, 1 kHz), while four- and ten-day trained listeners improved not only on the trained stimulus, but also on the untrained stimulus, which had the same duration as (100 ms), but a different frequency from (4 kHz) the trained one. Thus, generalization to the untrained stimulus lagged behind learning on the trained stimulus. This result implies that the present training affected a neural circuit that was initially tuned only to the trained stimulus, but that became more broadly tuned after extended training, or that it different affected circuits, with different characteristics, either sequentially or simultaneously, but that, of the two circuits, modification of the circuit governing generalization always required more practice. As to the design of perceptual training regimens, the observation of delayed generalization suggests that maximal generalization to untrained stimuli may require continued practice even after some learning on the trained stimulus has occurred.

[Supported by NIH.]

#### 932 Informational Masking Measured in Young and Elderly, Hearing-Impaired Listeners Using a 'Two-Channel' Speech-in-Speech-in-Noise Design

Trevor Agus<sup>1,2</sup>, Michael Akeroyd<sup>1</sup>

<sup>1</sup>MRC Institute of Hearing Research Scottish Section, <sup>2</sup>University of Strathclyde, Glasgow

The term 'informational masking' refers to masking effects additional to simple energetic considerations, such as would be predicted by the power-spectrum model. We measured informational masking for speech in young, elderly and elderly hearing-impaired listeners, using a 'speech-in-speech-in-noise' design based on Kidd et al. [2005, J. Acoust. Soc. Am., 118, 982-92], by comparing speech identifiability in a condition with a static-noise masker to a condition with a competing-speech-and-noise masker. All the stimuli were filtered into seven half-octavewide, half-octave-separated frequency bands with center frequencies between 256 Hz and 8194 Hz. Alternate bands (i.e. #1, 3, 5, 7 and #2, 4, 6) were then grouped into two 'channels'. One channel consisted of a target sentence at 52 dB, masked by a speech-shaped noise whose level was varied to form psychometric functions. The second channel was either a speech-shaped noise ('N'), competing sentences added to that noise ('SN'), a more-intense speech-shaped noise ('N+'), or a competing sentence with that more-intense noise ('SN+'). Because the second channel was in alternate bands to the target, the 'leakage' of energy from one to the other will be minimal, and so the energetic masking of the N and SN maskers should be equal. Thus any difference between the effects of the N and SN maskers may represent informational masking.

Fourteen participants were tested: five young, five elderly, and four elderly listeners with mild hearing-impairments. The results showed informational masking, in that the SN masker was more effective than the N masker: the mean shifts in psychometric functions from the N condition to the SN condition were 4 dB, 5 dB and 6 dB for the three groups respectively. Both the SN+ and N+ maskers were generally less effective than the SN masker for both normal-hearing groups, with mean shifts in psychometric functions of -2 to -3 dB relative to the SN condition. This effect may be due to the more-intense noise energetically masking the competing speech, so reducing its ability to informationally mask the target speech in the other channel. However, the SN+ and N+ maskers were more effective than the SN masker for the elderly, hearingimpaired group by up to 2 dB, which is consistent with a broadening of their auditory filters.

# 933 Human Speech Detection Thresholds and Pitch Discrimination Thresholds for Narrow Bands of Speech in White Masking Noise

**Nadeeka Yapa**<sup>1</sup>, Jont Allen<sup>1</sup>, Miriam Furst<sup>2</sup>

<sup>1</sup>University of Illinois, <sup>2</sup>Tel Aviv University

While there have been many experiments for detection thresholds of simple and complex tones (Fletcher, 1995; Hawkins and Stevens, 1950), there is relatively little on critical band speech detection thresholds. We report on 2 recent experiments that measure detection thresholds for bands of speech, less and greater than a critical band, in white masking noise.

The first experiment is for *narrow band speech thresholds* (NBST). Speech was presented at 2 center frequencies (CFs) [.65, 1.0] kHz and 3 bandwidths (BWs) [.85, .49, .26] oct. The stimuli were from LDC-2005S22. 4 CVs [ma, na, ba, da] by 4 talkers (2 male, 2 female) were used. The SNRs ranged from -14 to 8dB in 2dB steps, using the method of *constant stimuli*. The SNR was defined as the ratio of the 20 [ms] RMS peaks after filtering. The results are also calculated with respect to other measures, such as VU-level, and peaks using exponential windowing.

The second experiment was *talker identification*, a pitch discrimination task. The same stimuli were used. The first of 2 intervals had a CF of 1.1 kHz and a BW of .80 oct., at 20dB SNR. The second had a CF of .65 kHz, at BWs [.85, .49, .26] oct., and varied in SNR from -10 to 14dB in 2dB steps, using the method of *constant stimuli*. The subjects were asked if the talkers were the same or different (based on a gender cue).

These data may be used to verify speech perceptual models of the human auditory system (Al-GRAM). The Al-GRAM is a model designed to describe only parts of auditory stimuli that a human listener can detect, as related to phone scores (French and Steinberg, 1947). The Al-GRAM noise floor estimation is based on tone-in-noise thresholds. The NBST data will be used to analyze the validity of the noise floor estimation for narrow band speech.

(This work supported by a NSF Graduate Research Fellowship)

## 934 The Importance of Across-Frequency Timing Coincidences in the Perception of Some English Consonants in Noise

Marion Regnier<sup>1</sup>, Jont B. Allen<sup>1</sup>

<sup>1</sup>University of Illinois at Urbana-Champaign

Finding acoustic features to characterize basic speech sounds has been a hotly debated research area for many years, with important applications, including automatic speech recognition, telephone response, hearing aids and cochlear implants. After more than 50 years of work, the detailed characterization of phones remains unresolved. While human listeners can easily identify nonsense Consonant-Vowel (CV) sounds in significant noise (e.g., - 15 dB SNR), our understanding of human responses is extremely limited. The use of masking noise enables us to

reveal the confusion threshold of each utterance, unveiling large utterance heterogeneity. We use this heterogeneity to find the perceptually relevant cues in speech sounds. Correlating nonsense speech sounds confusion patterns and the acoustic cues available at a given signal-to-noise ratio (SNR), using model neurograms, is the key to this difficult problem. We will show that listeners use spectrotemporal across-frequency timing cues to discriminate sounds within confusion groups. For example, the recognition in noise of consonant /t/ critically depends on a ~20 ± 5 ms high frequency 3-8 kHz release burst. Masking or truncating the burst leads to the recognition of confusable competitors, typically /p/ or /k/. The addition of masking noise can remove such features, giving rise to morphing, where one sound is reliably heard as another. Most interesting is our analysis of nasals /ma/ and /na/ confusion patterns. In this case an across-frequency timing difference between high frequencies and mid-frequencies is responsible for the discrimination between /mA/ and /nA/. We will play audio examples of CVs, starting with fricatives /s/, /z/, plosives /p/, /t/, /k/ and nasals /m/ and /n/, followed by several vowels, where the primary spectrotemporal region for recognition of the consonant has been modified, leading to morphing. We argue that the identification of these "events" will lead to a new family of hearing aids.

#### 935 Speek Masking Release in Normal-Hearing Listeners: Effects of Masker Modulation Depth and Rate

**Dan Gnansia<sup>1,2</sup>**, Bernard Meyer<sup>3,4</sup>, Bruno Frachet<sup>4,5</sup>, Bertrand Philippon<sup>2,4</sup>, Vincent Jourdes<sup>4,6</sup>, Christian Lorenzi<sup>1</sup>

<sup>1</sup>LPP - FRE CNRS 2929, Univ. Paris 5, DEC, Ecole Normale Supérieure, and GRAEC GDR CNRS 2967, <sup>2</sup>MXM France, <sup>3</sup>Hôpital Saint-Antoine, Paris, <sup>4</sup>GRAEC GDR CNRS 2967, <sup>5</sup>Hôpital Avicenne, Bobigny, <sup>6</sup>MXM France, and Biomed I3S

In normal-hearing listeners, speech intelligibility is better in fluctuating than in steady-state backgrounds. This socalled "masking release (MR)" effect is reduced or abolished in hearing-impaired listeners and cochlear implantees. The current study attempts to clarify the different mechanisms involved in this MR effect. MR was assessed systematically as a function of masker modulation depth and rate in 8 normal-hearing listeners. Vowel-consonant-vowel logatomes were embedded in a steady-state or fluctuating speech-shaped noise masker and presented at a fixed signal-to-noise ratio yielding 50% correct identification in steady noise. Fluctuations in the masker was obtained by applying sinusoidal modulation to the amplitude of the noise. The masker modulation rate was fixed at 8 or 32 Hz. For each modulation rate, masker modulation depth was varied systematically between 0.6 and 1.0. The results show that for both masker modulation rates, MR (performance in fluctuating minus steady noise) increases as a function of masker modulation depth; however, MR increases more abruptly above a modulation depth of 0.5-0.6 and reaches 35% when modulation depth is 1.0. In a second experiment, the temporal fine structure of the stimuli encoded using 32 adjacent frequency bands was degraded to force listeners to identify the speech items using mainly temporal-envelope cues. The results show that MR increases slowly as a function of masker modulation depth and reaches about 15% when modulation depth is 1.0. Taken together, these results indicate that at least two different mechanisms are involved in the MR effect: A first mechanism using spectral (place) and/or envelope cues, and a second one based on fine structure cues. Most implant processors discard these fine structure cues and provide poor spectral information. These data provide therefore additional evidence that current implant processors should be modified to deliver place and fine structure cues in order to restore MR.

## 936 Effects of Amplitude Ramps on Continuity Illusion with Compressed Speech

**Deniz Baskent**<sup>1</sup>, Brent Edwards<sup>1</sup>, Cheryl Eiler<sup>1</sup>

<sup>1</sup>Starkey Hearing Research Center

In the simplest form, continuity illusion refers to the phenomenon where an interrupted tone sounds continuous, once the silence intervals are filled with a louder sound. A noise burst is commonly used for this purpose. Continuity illusion may also be beneficial for recognition of speech interrupted with silent intervals. Adding the loud noise bursts in the intervals facilitates phonemic restoration and 10-15% improvement is observed in recognition of sentences.

Previous research showed that continuity illusion is not as robust if falling or raising amplitude ramps are introduced on the tone preceding and following the noise bursts, respectively. When a softer sound accompanied by a louder one is compressed, release from compression would occur on the softer sound following the louder sound. Depending on the compression ratio and release time constant, and on the relative levels of the soft and loud sounds, the release from compression might produce a recovery trajectory, similar in shape to a raising amplitude ramp.

In the present study, it was explored if such fluctuations in the amplitude would affect phonemic restoration of compressed speech, similar to that observed with continuity illusion with tones. Ramps of varying durations were inserted before, after, and both before and after the noise bursts, and speech recognition by normal-hearing subjects was measured with interrupted and noise-filled speech. Results will be presented to show how the baseline benefit of filling the intervals with noise is affected by the presence of these accompanying amplitude fluctuations. The condition where the ramp is after the noise burst relates to possible effects that might occur due to release from compression, and the results are of importance for practical applications. The other conditions are related to how much phonemic restoration is generally affected by ramps of various durations and configurations, and are of importance for understanding this mechanism further.

## 937 Effects of Bandwidth Extension on Telephone Speech Recognition by Cochlear Implant Users

Chuping Liu<sup>1</sup>, Qian-Jie Fu<sup>2,3</sup>

<sup>1</sup>Dept. of Electrical Engineering, Univ. of Southern California, <sup>2</sup>Dept. of Auditory Implants and Perception, House Ear Institute, <sup>3</sup>Dept. of Biomedical Engineering, Univ. of Southern California

Previous studies have shown that cochlear implant (CI) users' speech recognition was significantly worse for telephone speech than for face-to-face conversation. The deficit in telephone speech recognition may be due to the limited bandwidth (i.e., 300-3400 Hz), elimination of visual cues and the reduced audibility of the telephone signal. The limited bandwidth may be particularly detrimental to those CI users who receive frequency information higher than this range. The present study investigated the effect of restoring the lost high frequency components to telephone speech signal on CI users' speech recognition performance. The lost high frequency information was recovered with a bandwidth extension technique. The wideband spectrum was estimated by minimizing the mean square error of feature pairs of narrowband and wideband speech. The wideband excitation was constructed from the narrowband excitation by spectral translation. The extended excitation was filtered by the extended spectrum, and then the high frequency of its output was extracted and extended to the original telephone signal to result in restored wideband speech. CI users' performance with restored wideband speech was evaluated using multi-talker IEEE sentence and consonant recognition tests. Preliminary results showed a significant improvement in the recognition of sentences with restored wideband speech, relative to performance with telephone speech. However, performance of consonant recognition was decreased with restored wideband speech than that of original telephone speech. Consonant confusion pattern was further analyzed and its implication on signal reconstruction was discussed. Although it is difficult to accomplish with such accuracy that a speech synthesis can be obtained without perceptual distortion to consonants, the present study indicated that CI users' speech recognition may still benefit from the restored high frequency information.

Research is supported by NIH-NIDCD.

## 938 Comparing the Neural Encoding and Psychoacoustics of Sinewave Speech: A Physiological Means to a Perceptual End

Jeremy Loebach<sup>1,2</sup>, Robert Wickesberg<sup>2</sup>

<sup>1</sup>Indiana University - Bloomington, <sup>2</sup>University of Illinois at Urbana-Champaign

Sinewave speech is a synthetic version of natural speech that contains just three time-varying sinusoids, and can be recognized relatively accurately (Remez *et al.*, 1981). Temporal cues in the ensemble responses of the auditory nerve have been shown to be important for the recognition of naturally-produced and noise-vocoded speech, and appear to be qualitatively similar to those observed for

sinewave speech (Loebach & Wickesberg, 2003). The goal of this study was to quantitatively assess temporal pattern similarity for naturally produced and sinewave speech tokens.

Normalized ensemble responses to the natural and sinewave tokens /b]/,  $/d\delta$ /,  $/p\delta$ / and /tu/ were computed from the responses of individual auditory nerve fibers recorded in ketamine-anesthetized chinchillas, and compared using dynamic time warping. The psychoacoustic recognizability of the sinewave tokens was determined in a larger study using 30 untrained, normal hearing subjects (Loebach & Wickesberg, 2006).

Dynamic time warping values for the ensemble responses to the sinewave tokens were plotted against the percent correct recognition scores for those tokens. A regression analysis revealed a linear relationship between the two variables and a significant negative correlation, indicating that the warping values comparing the physiological patterns decreased as perceptual accuracy increased.

The ensemble responses to the noise vocoded versions of these tokens were also obtained (Loebach & Wickesberg, 2006) and analyzed using the same procedures. The resulting warping values were plotted against the recognition scores for the noise vocoded versions of the tokens. A regression analysis revealed a linear relationship which accurately predicted the recognition scores for the sinewave tokens.

The correspondence between these two domains suggests a possible physiological substrate for psychoacoustic performance: stimuli that produce similar patterns in the peripheral auditory system can elicit a common percept.

### 939 Distance Estimation and Discrimination of Spoken Words

**Pierre Divenyi**<sup>1,2</sup>, Steven Greenberg<sup>3</sup>, JC Sander<sup>2</sup>

<sup>1</sup>VA Medical Center, <sup>2</sup>EBIRE, Martinez CA, <sup>3</sup>Silicon Speech, Santa Venetia, CA

Using impulse responses recorded at several distances in a medium-sized mildly reverberant room, series of spondee words were generated as if they were spoken at distances between 1 and 12 m from the listener, either at a 0° or a 45° right azimuth. In one experiment, normalhearing young listeners were asked to judge the apparent distance of a word, by moving a mouse to a point of the screen containing the photographic image of a straight footpath 13 m in length and two standing men to make the distance estimation more realistic. Similarly to other investigators (e.g., P. Zahorik, JASA 111, 1832-1846, [2002]), the results indicate a compression of the subjective distance scale, although to a lesser extent than previously reported. The compression was greater at the 45° azimuth as well as for words without fricatives. Justnoticeable distance increments at 2.5 m were smaller for the 45° than the 0° azimuth and for words containing fricatives. A tendency of clustering of estimates was observed at two regions on either side of about 5 m. In addition, distance perception of words containing highfrequency phonemes is better.

[Supported by an AFOSR STTR award and by the Veterans Affairs Medical Research.]

### 940 Time-Forward Speech Intelligibility in Time-Reversed Rooms

**Pavel Zahorik**<sup>1</sup>, Larica Longworth-Reed<sup>1</sup>, Eugene Brandewie<sup>1</sup>

<sup>1</sup>University of Louisville

This study examined the effect of time-reversed room acoustics on word recognition abilities using the HINT sentence corpus. Two acoustical conditions were tested. One in which room acoustics were simulated in a realistic time-forward fashion, and one in which the room acoustics were reversed in time, causing reverberation and acoustic reflections to precede the direct-path energy. auditory space (VAS) techniques were used to simulate the acoustics of a reverberant room with a broadband reverberation time of approximately 1.5 s. techniques also allowed for time-reversal of the room acoustics independent of the speech signals, which were presented in normal time-forward fashion. Dramatic decreases in speech intelligibility between the time-forward and time-reversed rooms were observed. This result is surprising given that standard methods for estimating speech intelligibility in rooms based on the modulation transfer function (MTF) of the room make nearly identical intelligibility predictions for the two conditions tested here. Intelligibility differences may instead be due to a differential degradation of onset information in the speech signals when room acoustics are time-reversed.

# 941 An Anatomically Precise Finite Element Model Predicts Current Flow in Labyrinths Implanted with a Multi-Channel Vestibular Prosthesis

**Russell Hayden**<sup>1</sup>, Susumu Mori<sup>1</sup>, Eric Frey<sup>1</sup>, Charles Della Santina<sup>1</sup>

<sup>1</sup>Johns Hopkins University

As is true for multi-channel cochlear implants, current spread beyond the intended target of a given electrode is a key factor determining the pattern of nerve stimulation by a multi-channel vestibular prosthesis. Ideally, different electrodes should independently stimulate each of the three ampullary nerves with high selectivity, minimizing stimulation of other ampullary nerves and the utricular, saccular, cochlear and facial nerves.

Our goal was to construct a robust, anatomically precise finite element model of current flow in the implanted labyrinth to better understand the biophysics of vestibular nerve stimulation and to facilitate rational design of electrode arrays with optimal selectivity. Model geometry was created through segmentation of high-resolution images of normal and implanted chinchilla (C. laniger) labyrinths. To individualize electrode position for each case, high-resolution microCT scans (36 µm voxels) of implanted animals were coregistered with microMRI data of a normal chinchilla obtained with an 11.7 Tesla magnet (47 µm voxels). We used Amira software for image segmentation and generation of a tetrahedral mesh, which was then analyzed under assumption of quasistatic conditions using finite element solvers in COMSOL Multiphysics. The model predicts relative current

intensities along the central axis of each ampullary nerve. We tested the finite element model by comparing its predictions against the axis of eye rotation we observed, using 3D binocular video-oculographic recording, for biphasic pulsatile stimuli across different electrode combinations.

The model's predicted axis aligned well with the actual axis of eye rotation, with misalignment of  $9.5\pm3.2$  degrees (mean  $\pm$  SD) for the 6 electrodes examined. By design, this procedure is partially automated and can be generalized to other species, including non-human primates and humans.

Supported by NIH/NIDCD K08 DC006216 (CCDS).

#### 942 Paired Linear Accelerometers Emulate Gyros to Reduce Power Consumption and Size for an Implantable Multi-Channel Vestibular Prosthesis

Russell Hayden<sup>1</sup>, Charles Della Santina<sup>1</sup>

<sup>1</sup>Johns Hopkins University

The current generation of the Johns Hopkins multi-channel vestibular prosthesis employs three mutually orthogonal gyro sensors to emulate the transduction of 3D head rotation velocity by the semicircular canals (SCC). The space and power required for each gyro sensor is small (150mm³ and ~30mW) and adequate for experimental applications in which the sensors are fixed to the skull but outside the head. However, transition to a fully implantable device for human use shall require sensors with smaller space and power requirements.

Compared to available gyros, linear accelerometers are smaller and consume less power. Our goal was to determine whether replacing the gyros with differentially amplified pairs of linear accelerometers can reduce prosthesis size and power consumption while still adequately emulating normal SCC function.

The new device computes angular accelerations from the difference signals of pairs of 3-axis accelerometers. A band-pass filter yields an estimate of angular velocity over 0.5-20Hz. Similar to the normal SCC frequency response, the output of this filter decreases as head rotation frequency approaches zero. The response of the circuit is also linearly dependent upon the distance between the linear accelerometers. Thus, low frequency response suffers as the size of the implant decreases. We tested this technique assuming an implantable device of 25 x 25 x 3 mm (comparable to cochlear implants and ~1/3 the current device thickness). We constructed a prototype using commercially available 3-axis accelerometers (ADXL330, Analog Devices). 3-axis sensing consumed 3 mW, 3.3% of that for 3 gyros. The device emulated a gyro down to rotations of 0.5Hz, 5 °/s with a signal-to-noise ratio of ≥12dB. If smooth pursuit and optokinetic nystagmus can be relied upon to augment gaze stabilization up to frequencies near 1 Hz, this approach may offer a viable alternative for a fully implantable vestibular prosthesis. Supported by NIH/NIDCD K08 DC006216 (CCDS).

## 943 Videooculography System for 3D Angular Eye Position Measurement in the Mouse

**Americo Migliaccio**<sup>1</sup>, Charles Della Santina<sup>1</sup> *Johns Hopkins School of Medicine* 

Recording of three-dimensional (3D) mouse eye movements is particularly challenging due to the small size and lack of iral striations on the mouse eye. Non-invasive pupil tracking video methods, which are the current state of the art, can only measure 2D (horizontal, vertical) eye positions in eye coordinates and 1D (horizontal) eye positions in head coordinates.

We report the first 3D measurements of mouse eve rotational position. We describe the changes necessary to adapt our existing video technique used in larger rodents to make it suitable for real-time measurement of binocular 3D eye position in mice. The method uses 130 Hz digital video cameras to track an array of three fluorescent markers affixed to each eye. The fluorescent marker is illuminated using UV light, and a UV cut filter in line with the camera lenses minimizes reflection artifacts, improving contrast and the signal to noise ratio of eye position data. When tested in vitro, the video-oculography (VOG) method had a <2.9% positional error (in each component of 3D eye position) for eye positions within 20° of center. Binocular three-dimensional eye position was measured in vivo in adult C57BL/6 mice (age 14 weeks). Eye movements during head rotation about the roll, pitch and yaw axes were conjugate: the average RMS velocity difference between the two eyes was ≤2.0% (in each component of 3D eye position). The yaw, pitch and roll VOR gains (eye velocity amplitude/head velocity amplitude) during 2Hz and 50°/s whole-body sinusoidal rotations, with the left and right eye data pooled, were  $0.79\pm0.04$ ,  $0.74\pm0.07$  and  $0.73\pm0.08$ , respectively. The yaw, pitch and roll VOR phases (positive indicates inverted eye leading head) during the same rotations were - $0.7\pm0.6^{\circ}$ ,  $-0.3\pm0.8^{\circ}$  and  $1.1\pm0.8^{\circ}$ , respectively. The mean yaw VOR gain was similar in value to those reported in other studies using 2D oculography.

#### 944 The 3-Dimensional Angular Vestibulo-Ocular Reflex Evoked by High-Acceleration Rotations in Normal Chinchilla is Conjugate, Nonlinear and Isotropic

Americo A. Migliaccio<sup>1</sup>, Lloyd B. Minor<sup>1</sup>, **Charles C. Della Santina**<sup>1</sup>

<sup>1</sup>Johns Hopkins Departments of Otolaryngology - Head & Neck Surgery and Biomedical Engineering

Our aim was to characterize the 3-dimensional angular vestibulo-ocular reflex (3D aVOR) of normal chinchillas (Chinchilla laniger) to create a basis for interpretation of responses in chinchillas treated with intratympanic gentamicin and prosthetic electrical stimulation of individual ampullary nerves with a multichannel vestibular prosthesis.

We characterized the 3D aVOR in response to yaw, pitch, roll, left-anterior/right-posterior (LARP) and right-anterior/left-posterior (RALP) head rotations in normal chinchillas. Eye movements were recorded using real-time

binocular 3D video-oculography (for 20-100°/s whole-body sinusoidal rotations at 0.01-2 Hz and for static rotational tilts) and the 3D scleral search coil technique (for 20-100°/s whole-body sinusoidal rotations at 0.05-15 Hz and for 3000°/s² acceleration steps to 150°/s) in darkness in 11 normal chinchillas.

As in humans and other frontal-eyed foveate-retina species, the 3D aVOR of chinchillas was partly compensatory over 0.05-15 Hz and fell in gain for frequencies <0.05 Hz. The chinchilla aVOR gain for steady state sinusoids was lower than that observed in humans and monkeys, ranging between 0.4-0.6. There was an increase in aVOR gain with peak head velocity, indicating nonlinearity in the system dynamics. Responses to acceleration steps were similar to that of primates, except that the aVOR latency during transient head rotations, which was the same across rotation planes, was longer 13.6±0.8 ms (mean±SD). In contrast to frontal-eyed, foveate-retina species, which have a lower 3D aVOR gain for roll head rotations than for yaw and pitch (presumably due to the lower adaptive drive induced by torsion of retinal images about the fovea), the aVOR gain in lateraleyed, afoveate-retina chinchillas was essentially isotropic, with similar magnitude for head rotations in all five planes of rotation. The chinchilla aVOR elicited conjugate eye rotations; however unlike in frontal eved animals, the gain isotropy yielded axes of eye rotation that closely aligned with the axis of head rotation regardless of starting orientation or rotation plane.

## 945 Effects of Vitamin E on AMPA-Induced Vestibulotoxicity in the Guinea Pig

Hiroaki Shimogori<sup>1</sup>, Kazuma Sugahara<sup>1</sup>, Takefumi Mikuriya<sup>1</sup>, Kenji Takeno<sup>1</sup>, Hiroshi Yamashita<sup>1</sup> <sup>1</sup>Yamaguchi University School of Medicine Ischemic injury is one of the major causes of inner ear diseases. The ischemic injury induced elevation of glutamate concentration in the cochlear perilymph. Glutamate is the most likely neurotransmitter between hair cells and primary afferents in the inner ear. But excessive glutamate also has toxic effects on the inner ear. We previously reported that local application of edaravone, one of the free radical scavengers clinically used in Japan, was useful to protect vestibular periphery from AMPAinduced peripheral vestubular disorder like ischemic injury. Another antioxidant, vitamin E, is popular and many people take vitamin E from supplementary diet. The aim of this study was to compare the effects of vitamin E between local application and systemic application on the acute peripheral vestibular disorder induced by topical application of AMPA.

A tiny hole was made adjacent to the round window in the guinea pig right ear, and 10 mM AMPA was infused through this hole by syringe pump at the rate of 0.6 ml/h for 5 minutes. In the local application group, vitamin E-soaked gelform was put on the round window membrane just after AMPA infusion. In the systemic application group, dietary vitamin E supplementation was given for a month before AMPA infusion. After surgery, we measured the frequency of spontaneous nystagmus in each animal as the number of quick phase beats per minute at 6, 9, 12, 15

and 18 h after surgery. We performed caloric tests 1 week after surgery by irrigating the external auditory meatus with 5 ml ice-cold water for 10 sec in the dark. Nystagmus was recorded on videotape with an infrared charge-coupled device camera, and caloric response time was measured. We calculated the time ratio as the ratio of the treated side response time (right) to the untreated side response time (left).

No significant difference was found both in the frequency of spontaneous nystagmus and the time ratio between two groups.

These data indicate the possibility that local or systemic application of vitamin E may no so useful in acute peripheral vestibular disorder induced glutamate excitotoxicity.

#### 946 Contribution of Hair Cell Bundles to Shear Stiffness of the Column Filament Layer in the Turtle Utricle

Julian Davis<sup>1</sup>, Wally Grant<sup>1</sup>

<sup>1</sup>Virginia Tech

The bullfrog saccule has been used to determine the contribution of hair cell bundles (HCB) to the shear stiffness of the column filament layer (CFL) (Benser et al. 1993). Once the otoconial layer was removed, stimulus to the remaining layers was provided though a flexible glass whisker. Finite element (FE) models of the Benser experiments were used to determine the modulus of the CFL and contribution of the HCB was included in the modulus evaluation (E=250 MPa) (Kondrachuk, 2000). Estimates of the HCB contribution to overall shear stiffness of the CFL ranged from 43 to 70% from the experimental work of Benser and the FE analysis of Kondrachuk.

Hair bundles in the utricle of the bullfrog (Baird, 1994) and in the red ear slider turtle (Xue & Peterson, 2006) are more varied in structure than in the saccule. Many hair bundles in the turtle utricle have a tall kinocilium and much shorter stereocilia resulting in relatively low bundle stiffness. In the current study, two sets of finite element models of the turtle utricle were utilized. The first incorporated the CFL modulus determined by Kondrachuk (2000) (which included the contribution of HCB). Then the model was modified and the CFL was replaced by only HCBs, which were represented with beams. These beams had stiffness values that reflected the experimental measurements of bundles across the surface of the epithelium. Results indicate that HCBs contribute approximately 5% or less to the total shear stiffness of the CFL in the turtle utricle. Support by NIH DC05063 and DC002290.

# 947 Experimental and Computational Analysis of Hair Bundle Mechanics at Different Macular Locations in the Turtel Utricle

Wally Grant<sup>1</sup>, **Corrie Spoon**<sup>1</sup>, Jong-Hoon Nam<sup>2</sup> <sup>1</sup>VA Tech, <sup>2</sup>Universtiy of Wisconsin-Madison

We present a combined experimental and finite element (FE) analysis of the mechanical behavior of hair bundles in the turtle utricle. Experimental measurements include the steady state bundle stiffness (K), Young's modulus of a

single kinocilium (E<sub>k</sub>), and reduction in bundle K after removal of different lateral links.

Bundle K was determined by measuring the bundle deflection when a known force was applied to the tip of the kinocilium in the excitatory direction. The bundle K in the striolar (S) and medial extrastriolar (MES) regions was 42  $\pm$  25 (n=28) and 10  $\pm$  0.9 (n=21)  $\mu$ N/m, respectively. The  $E_k$  was determined through a cantilever beam analysis. A glass probe was positioned against the kinocilium to fix the region between its apical insertion and the height of the tallest stereocilia. From kinocilium tip deflections under the action of a known force, diameter, and height above the tallest stereocilia the  $E_k$  was calculated as 10.6  $\pm$  0.9 MPa. Bundles were treated with BAPTA, which breaks tip, ankle, and kinocilium links, and K reduced by an average of 63%. Treatment with subtilisin, which breaks shaft and ankle links, reduced K by 60%.

Based on the measured data, a series of computational analyses identified the mechanical properties of the hair bundles structures. The Young's modulus of the stereocilia was 0.2 GPa, stiffness of the tip link was 2000  $\mu\text{N/m}$ , and the stiffness of lateral links was 20  $\mu\text{N/m}$  per micrometer. Using these mechanical properties, a series of stimuli that are equivalent to in vivo conditions were applied to the S and MES hair cell computer models. The results show that the S cell responses well to fast and small displacements while the MES cell response best to the slow and large displacements. This study showed that hair cell bundles in the turtle utricle have different mechanical properties in different macular regions.

(Supported by: NIH NIDCD R01 DC 05063 and NIH NIDCD R01 DC 002290-12.)

### 948 Coupling Between Hair Bundles and Otoconial Membrane in Turtle Utricle

Jingbing Xue<sup>1</sup>, lain Miller<sup>1</sup>, Ellengene Peterson<sup>1</sup>

<sup>1</sup>Department of Biological Sciences, Ohio University

To understand signaling by otoconial organs it is important to know how stimuli are delivered to hair bundles. Possible stimulus modes include forcing via endolymph flow over free-standing hair bundles or via an otoconial membrane (OM) attached to kinocilia, stereocilia, or both. Here we describe OM-bundle coupling in the utricle of a turtle, *T. scripta*, and its regional variation, using confocal

Bundles occupy lacunae in the column filament layer. Virtually all contact the overlying gel layer, but there are marked regional differences in these contacts. In the medial extrastriola (MES), kinocilia penetrate the thin (<3)

microscopy of utricular slices and wholemounts.

marked regional differences in these contacts. In the medial extrastriola (MES), kinocilia penetrate the thin (<3 m) gel layer; many extend into the otoconial layer (OL). We anticipate that displacement of MES bundles and the OL to which they are tethered, will be proportional to head acceleration. In the striola and adjacent lateral extrastriola, kinocilia extend ~1.5 m into the thick (7.7-11.1 m) gel layer where they appear attached to channel walls. A band of type II hair cells straddling the reversal line and adjacent type I hair cells supplying calretinin- positive calyces contact the OM via kinocilia and stereocilia. Our models suggest that direct coupling to the OM via the tallest stereocilia will increase the rise time of the hair cell transduction current. Finally, there are significant

differences in the height at which kinocilia of type II cells at different macular loci and type I cells supplying calretinin-positive and -negative calyces (probable all-calyx and dimorphic afferents, respectively) contact the OM. These differences in the height of the applied force correlate with previously documented differences in bundle structure. OM-bundle coupling adds to the constellation of features that distinguish hair bundles at different macular loci and suggest that subtypes of utricular hair cells will differ in their mechanical responses to head movement. Support by NIH DC05063.

# 949 Afferent Innervation Patterns of the Horizontal Crista Ampullaris Following Regeneration From Ototoxic Damage in Pigeons

**Zakir Mridha**<sup>1</sup>, Asim Haque<sup>1</sup>, J. David Dickman<sup>1</sup>
<sup>1</sup>Dept. of Anatomy and Neurobiology, Washington University, St. Louis, MO USA

Common to all animals, pigeon vestibular afferents innervate two types of sensory cells: type I and type II hair cells. There are three classes of afferents including calyx, bouton and dimorphic fibers. It has been known for long time that aminoglycoside antibiotics are ototoxic and produce stereocilia loss, hair cell death and denervation. It is also now established that in time regeneration of vestibular hair cells and their reinnervation, occurs after the cessation of ototoxic treatment. The primary objective of the present study is to determine, whether similar or vastly different afferent innervation patterns develop in semicircular canals of animals undergoing regeneration. Biotinylated Dextran Amine was injected into the vestibular nuclei of pigeons that had received complete loss of hair cells and denervated afferent via inralabyrinthine application of streptomycin 6-9 months earlier. Neural reconstructions of calyx, dimorph, and bouton afferenttypes were performed, and a unique 3-dimensional surface mapping of the organs was generated for both normal conditions and after long-term regenerative periods. Calyceal-bearing units occupied the central regions of the crista ampullaris whereas bouton-bearing units were found along the periphery. In general the hair cell distributions of the regenerated horizontal semicircular canal crsitae, as well as parent axon diameters, were not different from normal units. In both normal and regenerated cristae calyx afferents contained more type I hair cells than dimorphs. However, regenerated afferents were significantly less complex with smaller innervation terminal fields as compared to normal afferents.

This work was supported in part by NIDCD DC003286, DC006913, DC 007618  $\,$ 

## 950 Afferent Innervation and Central Projections of the Lagena Otolith Receptor in Homing Pigeons

V. Khoryevin<sup>1</sup>, David Huss<sup>1</sup>, **J. David Dickman<sup>1</sup>** 

<sup>1</sup>Washington University

We are interested in understanding lagena otolith system function in birds. In the present study, we examined the innervation patterns of afferent fibers and the central

projections into the brainstem and cerebellum. Afferents were labeled for retrograde transport using injections of biotin dextran amine (BDA) into the central vestibular nuclei. Central projections were labeled with BDA or with a fluorescent tracer (carbocyanine Dil) being selectively implanted into the neuroepithelium of the lagena. Calyx, dimorph, and bouton afferents were observed, with discrete topographic organizations of regional location. A central striola region was identified, with a high concentration of type I hair cells, calyx and dimorph afferents. Bouton afferents innervated the extrastriola, similar to the avian utricular macula. Central projections entered the vestibular nuclear complex (VNC) and bifurcated into ascending and descending branches. Lagena labeled terminals were found in all vestibular nuclei, but were concentrated in the lateral regions of the rostral and caudal VNC poles. Lagenar afferents terminated also in the n. cuneatus, descending trigeminal nucleus, locus coeruleus. No terminals were observed in the auditory nuclei, unless tracer had spread to the basilar papilla, when terminations were observed in the laterocaudal parts of n.magnocellularis. n.angularis and n.laminaris. The significance of lagenar innervation and projections to these brainstem structures is discussed in terms sensory function.

Supported in part by funds from NIH DC003286, DC006913, DC007618, NASA NNA04CC52G

# 951 Extracellular Recordings From Semicircular Canal Afferents in Mice that Lack the Alpha 9 Nicotinic Acetylcholine Receptor Subunit

**Gyu Han<sup>1</sup>**, David Lasker<sup>1</sup>, Douglas Vetter<sup>2</sup>, Lloyd Minor<sup>1</sup> Department of Otolaryngology - Head and Neck Surgery, Johns Hopkins University, <sup>2</sup>Department of Neuroscience, Tufts University

We recorded from 78 semicircular canal afferents in six adult mice (12-16 weeks) lacking the alpha 9 nACh receptor subunit. Background activity was recorded and the regularity of discharge rate was calculated based upon the normalized coefficient of variation (CV\*). Afferents were divided into regularly (CV\* < 0.1) and irregularly (CV\* > 0.1) discharging groups. CV\* ranged from 0.023 – 0.625 in the mutant mice, similar to the range in normal C57BL/6 mice (0.025 – 0.77). In the mutant mice, the average resting rate of regularly discharging afferents measured 57  $\pm$  18 sp/s versus 53  $\pm$  16 sp/s in C57BL/6 mice (p > 0.15, n = 55). The average resting rate from irregularly discharging afferents was 27  $\pm$  20 sp/s versus 37  $\pm$  18 sp/s measured in C57BL/6 mice. (p < 0.05, n =12).

Sensitivity ((sp/s)/(°/s)) and phase (°) re head velocity were measured for regularly and irregularly discharging afferents for rotations at 2 Hz. Sensitivity for regular afferents measured 0.17  $\pm$  0.05 and 0.14  $\pm$  0.06 for mutant and C57BL/6 mice, respectively (p > 0.05). Phase lead re velocity for these regular afferents measured 4.9  $\pm$  9.2° and 4.8  $\pm$  7.6° for mutant and C57BL/6 mice, respectively (p > 0.9). Response dynamics for irregular afferents were also similar for the mutant and C57BL/6 mice. Sensitivity for regular afferents measured 0.37  $\pm$  0.14 and 0.35  $\pm$  0.20

for mutant and C57BL/6 mice, respectively (p > 0.8). Phase lead re velocity for these afferents measured 23.2  $\pm$  11.7 and 22.2  $\pm$  11.7 for mutant and wild type mice, respectively (p > 0.9).

Although the resting rate, sensitivity, phase and range of CV\* were similar between the two populations of mice, the relative numbers of afferents with respect to CV\* was not similar. The proportion of afferents that were the most regularly discharging (CV\* < 0.05) was greater for the mutant (56 %) in comparison to the C57BL/6 (34 %) mice (p < 0.05). This distribution is in contrast to the bimodal distribution of afferents recorded in C57BL/6 mice of comparable age.

Supported by NIH R01 DC02390 (LM) and DC006258 (DEV)

## 952 A Comparison of the Synaptic Mechanisms Underlying Efferent Responses in Frog and Turtle

Joseph Holt1

<sup>1</sup>University of Texas Medical Branch (UTMB)

In vestibular organs, cholinergic efferent neurons can provide synaptic input to three targets: type II hair cells, bouton afferents, and afferent calyces. However, these efferent targets vary among vertebrates. In frog, efferents exclusively terminate on type II hair cells; in fish, efferents terminate on bouton afferents in addition to type II hair cells; and in turtle, birds, and mammals, all three types of efferent synapses can be found. Yet, efferent stimulation excites vestibular afferents in fish and mammals while it excites and inhibits vestibular afferents in frogs, turtles, and birds. So it seems that just knowing the efferent's target does little to explain this diverse panel of efferentmediated afferent responses. We propose that it is not the target per se, but the nature of the efferent receptor located on those targets. We have begun intracellular sharp-electrode recordings from afferents innervating the posterior crista of frog and turtles in order to compare the synaptic mechanisms underlying each afferent's response to efferent stimulation. Synaptic recordings have revealed that both frog and turtle crista afferents can respond to single efferent shocks. The electrophysiology and pharmacology of the inhibitory responses in both species are consistent with the activation of  $\alpha 9/\alpha 10$  nicotinic ACh receptors that subsequently activate small-conductance, calcium-dependent potassium channels (SK) in type II hair Efferent excitation in frog and turtle are both mediated by nAChRs that are pharmacologically distinct from  $\alpha 9/\alpha 10$ . These excitatory nAChRs are located on hair cells in the frog and on afferents in the turtle. Tests are under way to determine if they share the same pharmacology. Inhibitory responses in both turtle and frog are often truncated by a post-inhibitory excitation (PIE). In turtle, PIE is dependent on the hyperpolarization of type II hair cells driven by  $\alpha 9/\alpha 10$  and SK. Mechanisms of PIE in frog are being evaluated.

#### 953 Spatial Distribution of Utricular Hair Cell Morphologic Polarization Vectors: Role of Natural Stimuli

**Larry Hoffman**<sup>1</sup>, Carin Siegerman<sup>1</sup>, Diane Su<sup>1</sup>, Timothy Jones<sup>2</sup>

<sup>1</sup>Geffen School of Medicine at UCLA, <sup>2</sup>East Carolina University

As a component of a larger investigation of the development of afferent dendritic arbors, we have examined the spatial distribution of utricular hair cell morphologic polarization vectors (MPVs) in the mouse utricle. Though this distribution is critical to spatial coding of linear head movements, it is clear that the mechanisms by which hair cell MPVs develop and become organized reflect molecular and cellular pathways of planar cell polarity. However, it remains an open question whether these pathways within hair cells may be critically dependent upon activity modulation associated with natural stimulation. We have previously shown preliminary evidence suggesting that natural stimulation did not play a critical role in the spatial distribution of utricular hair cell MPVs. The present study represents an update of this investigation with more complete datasets and analyses. Utricles were obtained from adult mice in which otolitic membrane otoconia fail to develop (i.e. head tilt, het-Nox3; and tilted, tlt-Otop1), and in animals with in which otoconia develop normally (i.e. head-tilt and tilted heterozygotes, and wild type). These specimens were processed for optimal visualization of the stereocilia bundles and kinocilium location, and were systematically imaged via confocal microscopy. MPVs of individual hair cells were objectively measured relative to a standard orientation and coordinate reference frame. We developed a resampling statistical strategy to compare 95% confidence surfaces of hair cell MPVs in utricles of the five genotypes. We also investigated a measure of local MPV variability, termed These data indicate that the angular dispersion. distributions of utricular hair cell MPVs are similar in animals with and without otoconia, from which we conclude that the development and maintenance of these MPVs is independent of natural stimulation.

Supported by DC005776 to LFH and TAJ.

## 954 Spontaneous Discharge Patterns of Vestibular Neurons in the Otoconia-Deficient Mouse

**Timothy Jones**<sup>1</sup>, Sherri Jones<sup>1</sup>, Larry Hoffman<sup>2</sup>
<sup>1</sup>East Carolina University, <sup>2</sup>University of California Los Angeles

Vestibular primary afferents in the normal mammal are spontaneously active and discharge properties have been well characterized. Such discharge patterns are believed to be independent of stimulation and thought to depend on excitation by vestibular hair cells due to a stimulus-independent background release of synaptic neurotransmitter. In the case of otoconial sensory receptors, it is difficult to study spontaneous activity in the absence of natural tonic stimulation by gravity. We investigated discharge patterns of single primary afferent

neurons of the superior vestibular nerve in the absence of gravity stimulation using two mutant strains of mice that lack otoconia (head tilt. het-Nox3, and tilted, tlt-Otop1). Hair cells, primary afferents and synaptic apparatus were present in the maculae of these mutants. Spontaneous discharge activity was characterized in 201 neurons from anesthetized adult animals [neurons: het(-/-)n = 69; tlt(-/-)n = 47 and 85 neurons from control mice with normal otoconia het(+/-)]. The mean interval coefficient of variation (CVi = sd/mean) was similar for all groups and CVi values formed a bimodal distribution characteristic of the mammal. Mean discharge rates were significantly higher in otoconia-deficient strains for neurons wth CVi's < 0.4 [p < 0.02; rate in sp/s: het(-/-)=82.2 +/- 21.6(53); tlt(-/-)=82.2 +/- 21.6(53)= 84.5 +/- 22.9(36); het(+/-)= 73.4 +/- 22.9(51)]. These findings indicate that afferents in the superior vestibular nerve are spontaneously active and exhibit discharge rates higher than siblings with intact otoconia yet the distribution of CVi's appears to be normal. The vast majority of cells studied were unresponsive to rotational stimuli suggesting that a high percentage of cells innervated gravity receptors. The elevated rates are interesting in that they may reflect the presence of a functionally 'up-regulated' tonic excitatory process in the absence of natural sensory stimulation.

Supported by NIH-NIDCD 005776

## 955 Spike Measurement Distributions in Semicircular Canal Afferents Reflect Distributed Coding of Head Kinematic State

**Larry Hoffman**<sup>1</sup>, Dylan Hirsch-Shell<sup>1</sup>, Michael Paulin<sup>2</sup>
<sup>1</sup>Geffen School of Medicine at UCLA, <sup>2</sup>University of Otago The spike measurement distribution of a sensory neuron (SMD) has been defined as the conditional probability of stimulus-state at the occurrence of a spike (Pr(state|spike); Paulin MG, J. Neur. Eng. 2:S219-S234). We have previously shown that SMDs can be produced from the discharge of bullfrog semicircular canal afferents, and can be interpreted as the noisy measurement of angular head kinematic state that is asserted by each spike. In the present study we examined mammalian semicircular canal afferent SMDs, their relationship with afferent response dynamics, and how they represent distributed coding of head kinematic state. We recorded the spontaneous and stimulus-evoked discharge from horizontal and superior semicircular canal afferent neurons in barbiturateanesthetized chinchillas. Stimuli consisted of rotations having equal power across a limited frequency band (0.05 - 4.0 Hz) and values sampled from a Gaussian distribution. Discrete frequency sinusoids were also used for comparison to more classical characterization of response Afferent responses to the band-limited dynamics. Gaussian stimuli were well represented by time-domain models featuring a spontaneous discharge term, a sensitivity term, and a dynamic term in the form of a fractional-order differentiator. Models were verified across repeated trials with identical stimulus trajectories, as well as different stimulus trajectories having identical bandwidth and distribution. From the models we analytically determined afferent receptive fields (RFs) in angular head movement state (i.e. acceleration and velocity). SMDs

were generated from RFs by applying Bayes' Theorem, with the known stimulus distribution serving as a prior, and verified with the recorded spike trains. SMDs were systematically distributed across head kinematic state space. These data support a foundation for interpreting vestibular afferent dynamic discharge heterogeneity in the context of fundamental parameters of sensory neurophysiology.

Supported by DC005059 to LFH.

## 956 Information Analysis of Posterior Canal Afferent Responses in the Turtle, *Trachemys* (Pseudemys) Scripta

Michael Rowe<sup>1</sup>, Alexander Neiman<sup>2</sup>

<sup>1</sup>Dept. Biological Sciences and Neuroscience Program, Ohio University, <sup>2</sup>Dept. of Physics and Astronomy and Neuroscience Program, Ohio University

We used information metrics to characterize the responses of posterior canal afferents to Gaussian white noise (band limited to 10-50 Hz) and compared these to responses to single sine waves. Stimuli were delivered by mechanical indentation of the posterior duct via a small hole in the bony canal. Based on responses to efferent stimulation, afferents were identified as calyx-bearing (CD) or bouton, with the latter group subdivided according to location into those near the torus (BT), planum (BP), or middle (BM) of the hemicrista, using criteria developed by Brichta and Goldberg (2000).

A linear reconstruction technique was used to estimate the lower bound of the mutual information rate between stimulus and response. Information rates were highest for BT and CD units. Coherence functions between the spike train and stimulus were relatively flat for BT units, but tended to increase with frequency for CD units. For many units, the coherence function showed a broad minimum for frequencies near the mean firing rate. For frequencies below the mean firing rate, gain and phase measurements derived from the noise responses were similar to those obtained from sinusoidal stimuli.

A simple leaky integrate and fire model was used to simulate response properties of PC units to noise stimuli. The model was based on the afterhyperpolazation (AHP) model of Smith and Goldberg (1986) and included a slow negative feedback loop to mimic AHP current in addition to leak and synaptic currents. Parameters of the model were tuned to reproduce the spontaneous activity of regular and irregular units. Simulations indicated an increase in mutual information rate with increasing discharge regularity, confirming experimental data.

Supported by DC05468.

#### 957 Foxi1 is Required to Establish the Pre-Placodal Ectoderm Whereas Dlx3b-Dlx4b and Sox9a are Essential for Otic Induction

**Dong Liu<sup>1</sup>**, Monte Westerfield<sup>1</sup>

<sup>1</sup>University of Oregon

We have proposed that Fgfs from the developing hindbrain, together with Fgf-independent Foxi1 and Dlx3b-Dlx4b pathways, activate downstream effector genes such as Sox9a, to initiate otic development. By implanting Fgf-

coated beads into distinct ectodermal areas at midgastrula, which minimizes the drastic impact of global over expression of Fgfs, we have analyzed how ectodermal cells respond to ectopic Fgfs.

We find that about 40% of Fqf8 beads are able to generate ectopic ears when implanted into the ectodermal region that normally gives rise to most ectodermal placodes. Removing Dlx3b-Dlx4b function drastically reduces induction of ectopic ears (12%) by Fgf8 beads, whereas a loss of Foxi1 function does not affect ectopic induction in this region (42%). In contrast, more than 80% of Fgf8 beads implanted into belly ectoderm generate ectopic ears. Both hindbrain and pre-placode ectodermal (PPE) markers are induced around the beads implanted into belly regions, suggesting a sequential process of ectopic induction; Fgf8 induces ectopic neural ectoderm and an ectopic PPE, then ectopic ears form. In this region, loss of Foxi1 function, but not Dlx3b-Dlx4b, leads to a disorganized PPE and failure of ectopic ear induction, suggesting a role of Foxi1 in PPE specification.

Fgf8 beads induce ectopic sox9a in both placodal and belly ectoderm where Dxl3b is present, and loss of Sox9a function leads to a reduced ectopic induction in placodal precursor ectoderm (13%). Over expression of Sox9a activates Dlx3b and generates ectopic ears, even in the neural ectoderm. We suggest that Foxi1 is primarily responsible for specifying the PPE and that Fgf8 and Dlx3b initiate Sox9a expression in the PPE. Subsequently, Sox9a maintains expression or prevents degradation of Dlx3b to allow cells expressing both factors to adopt otic fates.

## 958 Sprouty1 and Sprouty2 Function in Morphogenesis of the Mouse Inner Ear Epithelium

Katherine Shim<sup>1</sup>. Gail Martin<sup>1</sup>

<sup>1</sup>University of California, San Francisco

The molecular rules governing how the inner ear epithelium achieves its complex three-dimensional structure from an initally simple, sac-like otocyst are mostly unclear. However, restricted gene expression domains within the unstructured otocyst suggest that regions of the otocyst are already specified to form specific cell-types and structures. Here we show that the Sprouty1 and Sprouty2 (Spry1 and Spry2) genes, which encode modulators of receptor tyrosine kinase signaling, are coexpressed in an anteroventral domain of the otocyst epithelium. While Spry2 is expressed in a broader domain, encompassing both the otic epithelium and adjacent mesenchyme, Spry1 expression is restricted to the otic epithelium. We find that Spry1-/-;Spry2-/- double mutants have a severe defect in early morphogenesis of the inner ear epithelium: the anterior semicircular canal does not close; the utricle, saccule, and anterior ampulla appear rudimentary and bulbous; and the cochlea is incompletely coiled. These phenotypes are uncovered only in the Spry1 /-;Spry2-/- double mutant combination, and are not observed in either the Spry1- or Spry2- single mutants alone. These data suggest that Spry1 and Spry2 may function redundantly in the epithelium of the otocyst to

control its morphogenesis. A molecular characterization of the patterning defects in the otocyst in *Spry1*<sup>-/-</sup>;*Spry2*<sup>-/-</sup> mutants will be presented.

## 959 Opposing Gradients of Gli Activator and Repressor Activities Mediate Shh Signaling Along the Dorsoventral Axis of the Inner Ear

**Jinwoong Bok**<sup>1</sup>, Diane K. Dolson<sup>2</sup>, Patrick Hill<sup>3</sup>, Ulrich Ruther<sup>3</sup>, Douglas J. Epstein<sup>2</sup>, Doris K. Wu<sup>1</sup>

<sup>1</sup>NIH/NIDCD, <sup>2</sup>University of Pennsylvania School of Medicine, <sup>3</sup>Heinrich-Heine University, Germany

Previously, we have shown that Sonic hedgehog (Shh) emanating from the floor plate or notochord is important for the proper formation of inner ear structures. Graded expression patterns of Shh target genes within the otocyst such as *Patched* and *Gli1*, indicate that otic tissues respond directly and differentially to Shh. To elucidate how Gli proteins, which mediate Shh signaling, function in the otic tissues, we examined the inner ears of mice with various combinations of mutant alleles for *Shh*, *Gli2*, and *Gli3*. We also examined the inner ears of *Gli3*∆699 mutants, in which only the truncated repressor form of the Gli3 protein is expressed.

Our results indicate that specific combinations of Gli activator (A) and repressor (R) activities are required for proper formation of different inner ear structures. The most ventral structure, the distal cochlear duct, fails to develop in *Gli2-/-;Gli3-/-* or *Gli3*△699 mutants, in which GliA functions are lacking or compromised. These results indicate that the distal cochlear duct, positioned closest to the sources of Shh, requires strong GliA function. Formation of the saccule and proximal region of the cochlear duct require less Shh signaling either to remove Gli3R or promote some degree of GliA function.

In *Gli3-/-* embryos, the dorsal inner ear structures such as the semicircular canals and the endolymphatic duct fail to develop properly. Similar dorsal phenotypes are observed in all the mutants that lack *Gli3* including, *Shh-/-;Gli3-/-* and *Gli2-/-;Gli3-/-*. In contrast, the dorsal inner ear structures are normal in *Gli3*∆699 and *Shh-/-;Gli3+/-* mutants. These results indicate that Gli3R is critical for the formation of dorsal inner ear structures. Taken together, our results suggest that opposing activity gradients of Gli3R and GliA mediate Shh signaling in the inner ear.

## 960 Sox2 Regulates Prox1 Expression and Inhibits Hair Cell Formation in the Mammalian Cochlea

**Alain Dabdoub**<sup>1</sup>, Chandrakala Puligilla<sup>1</sup>, Jennifer Jones<sup>1</sup>, Kathryn Cheah<sup>2</sup>, Matthew Kelley<sup>1</sup>

<sup>1</sup>NIDCD NIH, <sup>2</sup>University of Hong Kong

The mammalian cochlea develops from a pool of progenitor cells that undergo a well coordinated program of cell division, fate determination, and differentiation. One of the earliest transcription factors expressed in the cochlea is Sox2 (SRY-related HMG box), known to regulate various developmental processes. Expression at E12.5 marks the prospective organ of Corti, but by E16

Sox2 is down regulated in cells that will differentiate into hair cells and becomes restricted to support cells.

Expression of Sox2 in hair cell progenitors is followed by Atoh1, but as Atoh1 levels increase, Sox2 expression decreases leading to specification of the hair cell fate and indicating that Sox2 is upstream of Atoh1. Using electroporation, Sox2 over-expression in the sensory epithelium of cochlear explants at E13 inhibited hair cell formation indicating the necessity to reduce the levels of Sox2 in order for cells to differentiate as hair cells. We also double-transfected cells in Kolliker's organ with Sox2 and Atoh1 and these cells became Myosin6 positive demonstrating that Sox2 functions upstream of Atoh1.

Interestingly, over-expression of Sox2 consistently induced expression of Prox1 in both Kolliker's organ and the sensory epithelium, and Prox1 was absent from Sox2 mutant cochleae signifying that Sox2 is required for Prox1 expression. The expression of Prox1, a transcription factor, follows that of Sox2; at E14.5 Prox1 is expressed in all progenitor cells and by E18 it is down regulated in hair cells and becomes restricted to support cells. Using adenovirus containing Prox1 to infect cochlear cultures at E13, we show that over expression of Prox1 inhibits cells from differentiating into hair cells. Also, Prox1 induces p27kip1 in infected cells within the sensory epithelium.

Thus Sox2 regulates Prox1 and marks progenitor cells as they transition through states of developmental competence to generate the distinctly fated cell populations in the highly ordered mosaic of the cochlea.

# 961 In Vivo Electroporation of Mouse Atonal Homolog-1 Generates Supernumerary and Ectopic Hair Cells in the Developing Mouse Inner Ear

Samuel Gubbels<sup>1,2</sup>, David Woessner<sup>1,2</sup>, John Mitchell<sup>1,3</sup>, **John Brigande<sup>1,2</sup>** 

<sup>1</sup>Oregon Health & Science University, <sup>2</sup>Oregon Hearing Research Center, <sup>3</sup>School of Dentistry

Gain-of-function studies in the developing mammalian inner ear are essential to define the identity of and interactions among genes governing sensory organ specification. However, the inaccessibility of the postimplantation mouse embryo poses a formidable obstacle to gene misexpression studies. We have defined an approach to conduct gain-of-function studies in the developing mouse inner ear in utero. An expression plasmid consisting of the elongation factor 1-α promoter, an internal ribosome entry site, and enhanced green fluorescent protein (pEF1α-IRES-GFP), was introduced into the embryonic day 11.5 (E11.5) otocyst by transuterine microinjection. A square wave pulse train from lateral to medial was delivered across the injected otocyst by electrode placement on the flanking uterine walls. Electroporated embryos were allowed to mature in vivo and the inner ears were analyzed at E18.5. GFP expression was detected in hair cells and all types of supporting cells from the base to apex of the E18.5 organ of Corti. To validate this paradigm for gain-of-function studies, mouse atonal homolog 1 (Atoh1 or Math1), a

transcription factor essential for hair cell fate specification, was electroporated into the E11.5 otocyst with the expectation that its misexpression in otic epithelial progenitors would generate additional hair cells. E18.5 cochlear whole mount analysis of otocysts electroporated with Atoh1 (pEF1α-Atoh1-IRES-GFP) at E11.5 revealed myosin7a/GFP-positive supernumerary hair cells in the organ of Corti and ectopic hair cells in the nonsensory epithelium of the vestibule. Laser confocal and scanning electron microscopy identified immature stereocilliary bundles on the apical surfaces of these hair cells. Neurofilament immunostaining of cochlear whole mounts and retrograde labeling of nerve tracts in the cochlear nucleus suggest that the supernumerary hair cells are innervated by fibers projecting centrally. The postnatal survival and function of Atoh1-GFP-transfected cells will be discussed.

Supported by the NIH-NIDCD; the McKnight Endowment Fund for Neuroscience; the American Otological Society; and the Medical Research Foundation of Oregon.

## 962 The Ngn1-CreER<sup>T2</sup> BAC Transgenic Mouse: a Tool to Fate Map Cells in the Mouse Inner Ear.

**Edmund Koundakjian<sup>1,2</sup>**, Jessica Appler<sup>1,2</sup>, Lisa Goodrich<sup>1,3</sup>

<sup>1</sup>Harvard Medical School, <sup>2</sup>Program in Neurosciences,

<sup>3</sup>Department of Neurobiology

An essential first step in cochlear-vestibular ganglion development is the expression of the proneural transcription factor Neurogenin1 (Ngn1). Nan1 is expressed in presumptive neuroblasts within the otocyst prior to delamination, in the neuroblasts themselves, and in the early cochlear-vestibular ganglion. We used BACderived Ngn1 regulatory elements to drive expression of a tamoxifen-dependent Cre recombinase, CreER<sup>T2</sup>. expression exactly matches endogenous Ngn1 patterns. In the absence of tamoxifen, Cre recombinase activity is virtually silent. In the presence of tamoxifen,  $Cre \dot{E} R^{T2}$ induces recombination in many regions of the nervous system, including the brain, spinal cord, DRG, and the cochlear-vestibular ganglion. The degree of recombination is sensitive to the amount of tamoxifen provided, so low doses can be used to induce sparse labeling and visualize individual cells along their entire trajectory.

We used genetic fate mapping in the mouse to determine when cochlear neurons become distinct from vestibular neurons and to visualize the earliest steps in auditory circuit assembly. We found that *Ngn1*-positive progenitors produce vestibular and cochlear neurons during two temporally distinct waves of neurogenesis. Although hair cells in the utricle and saccule also arise from an Ngn1 population, we do not see evidence for a shared Ngn1positive progenitor for auditory hair cells and cochlear ganglion neurons. Since Ngn1 is expressed most strongly in delaminated cells, it is possible that common precursors for hair cells and neurons are present in the otic epithelium but produce low levels of Ngn1/Cre, a possibility we are currently testing. To follow the emergence of auditory circuits, individual cochlear ganglion neurons were genetically labeled and projections were traced from hair cells into the cochlear nuclei and down to the level of the endbulb of Held. We find that Type I and Type II cochlear ganglion neurons develop within common clusters and that central projections are tonotopically organized as early as E15.5. These results show that the auditory and vestibular systems diverge early in development and suggest that auditory precursors are programmed at early stages to make specific connections in the periphery and in the central nervous system.

## 963 The Primary Cilium in Planar Cell Polarity Signaling in the Organ of Corti

Chonnettia Jones<sup>1</sup>, Boglarka Banizs<sup>2</sup>, Dong Qian<sup>1</sup>,

Bradley Yoder<sup>2</sup>, Ping Chen<sup>1</sup>

<sup>1</sup>Emory University, <sup>2</sup>University of Alabama

The organ of Corti, the sensory organ of the mammalian ear, consists of four rows of precisely patterned sensory hair cells whose apical surfaces contain actin-filled stereocilia bundles. Each stereocilia bundle is invariably arranged in a V-shaped staircase formation with the vertex of each V uniformly pointing toward the abneural side of the sensory epithelium. This polarity of the stereocilia within the plane of the epithelium is called Planar Cell Polarity (PCP). The uniform orientation of stereocilia is regulated by a conserved genetic pathway, the PCP pathway, and coupled to convergent extension of the cochlea. During development, a single primary cilium, the kinocilium, is closely positioned at the vertex of each Vshaped bundle transiently and appears to lead the polarization of stereocilia. This observation has led to the model in which the kinocilium orients the stereocilia bundle in PCP signaling.

To test this model, we generated mice in which *Polaris*, an essential gene for ciliogenesis, has been conditionally knocked out (CKO) in the ear thus effectively disrupting kinocilia formation. While general inner ear development and hair cell differentiation appear normal in these mice, they exhibit shortened cochlear ducts with widened organ of Corti and defects in stereocilia orientation, characteristic of PCP signaling defects in convergent extension and planar polarization in the cochlea, respectively. We also detected a genetic interaction between *Polaris* and a known PCP gene in convergent extension of the cochlea and stereocilia orientation, confirming further a role for Polaris in PCP signaling.

A hallmark of PCP signaling involves directional cues that regulate the formation of polarized PCP complexes along the axis of planar polarization to direct cytoskeleton changes necessary to exhibit the morphological polarity. Next we examined the formation of polarized PCP complexes in *Polaris* CKO mice. Two PCP components displayed polarized subcellular localization in *Polaris* CKO mice similar to that in wild-type littermates, indicating that Polaris, or the kinocilium, is downstream of the formation of polarized PCP complexes in PCP signaling. We are undertaking additional experiments to dissect the molecular mechanism underlying the role of the kinocilium in PCP signaling in the cochlear epithelium.

### 964 Bardet-Biedl Syndrome: are the Answers in the Ear?

**Helen May-Simera**<sup>1</sup>, Andrew Forge<sup>1</sup>, Philip Beales<sup>1</sup>, Daniel Jagger<sup>1</sup>

<sup>1</sup>University College London

Bardet-Biedl syndrome is a rare heterogeneous condition, characterized by obesity, polydactyly, renal abnormalities, retinal dystrophy, and hearing impairment. To date 11 genes have been identified (BBS1-11), but their individual functions remain uncertain. As mutations in any of the BBS genes result in clinically indistinguishable phenotypes, it is likely that BBS proteins participate in common cellular processes. Several BBS genes have been associated with ciliary function and cognate proteins have been localized to the basal body of ciliated cells. Previous analysis of BBS protein expression has predominantly centered on in vitro cell culture systems. Given the limited extrapolation of cell lines to live organisms we have focused attention on whole organ systems, in particular the mammalian cochlea.

The developmental organization of the hair cell stereociliary bundle may be under control of the kinocilium (a primary cilium) and/or its basal body. Our prior studies have identified three BBS mouse mutants (Bbs1, 4 and 6) with bundle defects likely associated with perturbation of planar cell polarity. However, the extent of these defects is unlikely to explain the profound deafness exhibited by most null mice. Therefore, we have further investigated the involvement of BBS proteins in the organ of Corti. As expected, we observed a ubiquitous expression of Bbs6 in basal bodies of hair cells and supporting cells. However, there was strong but specific cytoskeletal expression of Bbs4 and Bbs2 in microtubule-rich supporting cells (pillar cells and Deiters' cells), in distinct spatio-temporal patterns. These data suggest that some but not all BBS proteins are tightly associated with microtubule function. We believe the inner ear presents an ideal organ for studying the developmental role of BBS proteins. Owing to their microtubular enrichment, supporting cells will be particularly useful to examine low abundance cytoskeletal proteins.

### 965 Longitudinal Effects on Pax2-Cre Mediated Rb1 Deletion in the Inner Ear

**Sonia M. Rocha-Sanchez<sup>1,2</sup>**, Lilian Calisto<sup>2</sup>, Bernd Fritzsch<sup>2</sup>, Kirk Beisel<sup>2</sup>

<sup>1</sup>Creighton University School of Dentistry, Department of Oral Biology, Omaha NE, 68178, USA, <sup>2</sup>Creighton University, Department of Biomedical Sciences, Omaha NE, 68178, USA

RB1 is a member of the pocket protein family, which includes p107 and p130 proteins. Cell cycle regulation in the OC depends on these pocket proteins, with *Rb1* being the major factor for hair cell cycle exit. Early in development, RB1 is highly expressed in HCs, but is also present in SCs. In the adult inner ear, *Rb1* expression in HCs follows a base to apex gradient. *Rb1* deletion in the mouse HCs was shown to cause an aberrant proliferation at early age, followed by a massive loss of HCs in the adults. The effects of *Rb1* ablation in the SCs, nonsensory cells and the inner ear neurons are not well

characterized. In our study, mice carrying floxed Rb1 and the Pax2-Cre transgenic were examined. Pax2 in embryonic mice is normally expressed in a wide variety of tissues including the developing otocyst. In postnatal (P) mice, Pax2 expression is limited to the kidney, testis and inner ear. The mice were viable and reached adulthood. They behaved normally and did not show signs of vestibular dysfunction. Whole mount confocal microscopic analysis of Pax2-Cre/floxed Rb1 P21 and P35 old mice already showed mild abnormalities, including disorganized OHCs and extra IHCs in the apex of the cochlea. Patches of lost OHCs were observed along the length of the cochlea, particularly concentrated in the basal turn, where RB1 expression is higher. Innervation pattern, as visualized by Dil labeling, revealed minor differences in pattern of radial fiber projections in the cochleae of Pax2-Crelfloxed Rb1 mice, as compared to wild type littermates. Pax2-Cre/floxed Rb1<sup>loxP/loxP</sup> mice showed a significant reduction in spiral ganglia neurons (SGN) and complete absence of type II fibers. Although preliminary, our results suggest a critical role of RB1 for the survival of inner ear type II afferent neurons and suggest an overlapping functional role of Rb1 and the remaining pocket proteins in the inner ear, which may have prevented the *Rb1* ablation effects to be more drastic.

## 966 Notch Signaling Regulates Supporting Cell Behavior During Hair Cell Regeneration in the Chicken Basilar Papilla

Nicolas Daudet<sup>1,2</sup>, Julian Lewis<sup>3</sup>, **Jennifer Stone<sup>4,5</sup>**<sup>1</sup>University College London, <sup>2</sup>UCL Ear Institute, <sup>3</sup>Cancer Research UK, <sup>4</sup>University of Washington, <sup>5</sup>VM Bloedel Hearing Research Center

Birds are the only warm-blooded vertebrates known to robustly regenerate hair cells (HCs) in maturity. In the chicken basilar papilla (BP), non-sensory supporting cells (SCs) serve as precursors to new HCs using two distinct Shortly after HC damage, some SCs mechanisms. undergo non-mitotic (direct) phenotypic conversion into HCs. Thereafter, additional SCs undergo mitotic division. forming new SCs and HCs. In this study, we investigated the role of signaling through the Notch receptor in regulating these two SC behaviors in the posthatch chicken BP. Using qRT-PCR and in situ hybridization, we examined expression of Notch1, Notch ligands (Serrate1, Serrate2, Delta1), Notch signaling regulators (Lunatic Fringe, Numb, MINT), and Notch effectors (Hairy1, Hes5.1, Hes5.3) in control BPs and in vivo Gentamicindamaged BPs. Expression of genes encoding negative regulators of Notch signaling, Numb and MINT, was decreased compared to controls at 1d post-Gentamicin (pG), while genes associated with Notch activation (Serrate1, Delta1, Notch1, Hairy1, Hes5.1, Hes5.3) showed a large increase by 4 days pG. At 4 days pG. highest levels of Notch activity occurred in the neural half of the BP, where SC division is heaviest. Treatment of Streptomycin-treated BPs in vitro with DAPT, an inhibitor of gamma-secretase (required for Notch activation), caused decreased Hes5.1 expression and increased Delta1 and Atoh1 expression, indicative of attenuated Notch activation. DAPT treatment also caused a dramatic

increase in SC-to-HC conversion in the neural BP, with substantial HC overproduction. This effect was not seen in regions with intact native HCs. DAPT appeared to have no direct effect on SC cell cycle entry, although cumulative SC proliferation was markedly decreased, presumably due to depletion of the SC progenitor pool during overconversion. Our findings suggest Notch activity prevents excess conversion of SCs into HCs, preserving SC progenitors for mitotic regeneration

967 Hair Cell Regeneration in the Zebrafish Lateral Line After Neomycin-Induced Damage Eva Y. Ma<sup>1</sup>, Edwin W. Rubel<sup>2,3</sup>, David W. Raible<sup>1,3</sup>

<sup>1</sup>Department of Biological Structure, <sup>2</sup>Department of Otolaryngology - HNS, <sup>3</sup>Virginia Merrill Bloedel Hearing Research Center, University of Washington Hair cell loss is irreversible in mammals, but in birds and other non-mammalian vertebrates, hair cells in the inner ear are able to regenerate after being damaged by noise or ototoxic drugs such as aminoglycoside antibiotics. As an aquatic vertebrate, zebrafish have hair cells located externally along the head and body within neuromasts of the lateral line system. Lateral line hair cells completely regenerate 72 hours after exposure to a high dose of the aminoglycoside antibiotic neomycin in animals 5 days post fertilization. Hair cell regeneration and its underlying mechanisms are not well characterized in zebrafish, but one hypothesis is that the initial hair cell loss triggers the proliferation and differentiation of the adjacent support cells, giving rise to new hair cells. Supporting this idea, we observe an increase in support cell proliferation after neomycin treatment, peaking at 15-18 hours post damage. Some of these dividing support cells then differentiate into new hair cells, forming the majority of the regenerated hair cells seen at 48 hours after damage. However, a subpopulation of hair cells do not arise from proliferating support cells. These cells are hypothesized to be both immature neomycin-resistant hair cells not killed at the time of treatment, and new hair cells that arose through a non-mitotic process such as direct differentiation from hair cell progenitors. Initial studies also reveal a role for Notch signaling in hair cell regeneration. Treatment with a Notch pathway inhibitor results in an increased number of regenerated hair cells after 48 hours of recovery. This increase is magnified at 72 hours and continues through 96 hours after neomycin damage. These excess hair cells are the result of an increased amount of support cell proliferation with Notch inhibition in neomycin-treated fish. However, no significant change is observed in hair cell numbers or support cell proliferation after Notch inhibition in animals not treated with neomycin. Our results suggest a model where interactions among hair cells and support cells regulate proliferation and regeneration.

## 968 Postnatal Development of Ionic Conductances in Vestibular Calyx Terminals Katherine Rennie<sup>1</sup>, Kenneth Anderson<sup>1</sup>

<sup>1</sup>University of Colorado Health Sciences Center Primary vestibular afferent neurons make synaptic contact with hair cells and have a resting discharge *in situ* that is modulated by hair bundle movement. Calyx neurons contacting type I vestibular hair cells have a discharge of action potentials distinct from neurons that make afferent synapses with type II hair cells. To investigate ionic conductances that shape action potential firing in calyces, whole cell patch-clamp recordings were made from calyceal terminals isolated with type I hair cells from the semicircular canals of Mongolian gerbils and Sprague Dawley rats. Since changes in afferent sensitivity to head movement occur concomitant with synaptogenesis and head growth, we also looked at calyx responses at different times during postnatal development.

In animals aged 3-12 weeks, a tetrodotoxin-sensitive inward Na<sup>+</sup> current preceded large outward K<sup>+</sup> currents at membrane potentials more depolarized than -40 mV as described previously (Rennie and Streeter *Neurophysiol.* 95:26-32, 2006). Three types of outward K<sup>+</sup> current were identified based on pharmacological and kinetic profiles. The first current was a rapidly activating, partially inactivating current blocked by 4-aminopyridine (0.5-2 mM, n = 15). The second more slowly activating current was present at membrane potentials depolarized to -40 mV and was sensitive to tetraethylammonium (30 mM, n = 11) and the KCNQ channel blocker linopirdine (20  $\mu$ M, n = 4). A third calcium-dependent component was blocked by removal of extracellular calcium.

At P10 and P11 most rat calyces expressed a Na $^{+}$  current with little evidence of outward K $^{+}$  currents. By the third postnatal week, large outward K $^{+}$  currents and miniature excitatory postsynaptic currents similar to those seen in adult animals were present in most cells.

Supported by DRF and NOHRF

### 969 A Biophysical Model of the Calyx Synapse of Type I Vestibular Hair Cells

**Imran Quraishi**<sup>1</sup>, Karen Hurley<sup>2</sup>, Robert Raphael<sup>1</sup>, Ruth Anne Eatock<sup>3</sup>

<sup>1</sup>Rice University, <sup>2</sup>University of Pennsylvania,

<sup>3</sup>Massachusetts Eye and Ear Infirmary

In the vestibular epithelia of mammals, birds, and reptiles, primary vestibular afferents form large calyx endings around the basolateral membranes of type I hair cells. The function of this unusual calvx geometry is not understood. No gap junctions have been seen. In rodent type I hair cells, an abundance of presynaptic ribbons shows that glutamate is released from synaptic vesicles, as it is at conventional hair cell synapses. But it has for many years been suggested that additional modes of transmission may occur—e.g., by K<sup>+</sup> accumulation in the synaptic cleft and/or ephaptic transmission from the flow of current across a high synaptic cleft resistance. We are modeling the synapse using a variant of the cable equation along with K<sup>+</sup> electrodiffusion in the cleft, simplified Hodgkin-Huxley-style ion currents, and stochastic vesicle release along an axisymmetric parametric surface representing the shape of the synapse. We make use of recent recordings of Na<sup>+</sup> and K<sup>+</sup> current kinetics from isolated calyx afferents. Both ephaptic transmission and K<sup>+</sup> accumulation are possible under certain conditions. The model will allow us to examine the frequency response, linearity, and delay

associated with Type I synapses and how these properties are influenced by such parameters as calyx morphology and ion channel distribution.

### 970 An Anatomical Model of Voltage-Gated Channels in the Rat Calyx Ending

**Anna Lysakowski**<sup>1</sup>, Sophie Gaboyard<sup>1</sup>, Shilpa Chitlani<sup>2</sup>, Jay M. Goldberg<sup>2</sup>, Ruth Anne Eatock<sup>3</sup>, Steven D. Price<sup>1</sup>

<sup>1</sup>Univ Illinois Chicago, <sup>2</sup>Univ Chicago, <sup>3</sup>Mass Eye Ear Infirm

Two questions are important in understanding the operation of calyx endings. 1) How do ionic currents spread from the inner face of the calyx, where synapses are located, to the outer face, where the spike-trigger site is presumably located? 2) Is the trigger site, in fact, located on the outer face? One possible solution to the first question is that synaptic currents are enhanced by voltage-activated currents. Recent physiological studies are consistent with this suggestion: synaptic potentials are enhanced by a persistent Na<sup>+</sup> current and are depressed by a persistent K<sup>+</sup> current (e.g., Holt et al., this meeting). To better understand the potential role of voltage-activated currents, we have studied their distribution, as well as that of accessory and scaffolding proteins, in the calyx ending. Sections and whole organs were stained with antibodies and viewed in a confocal microscope. Antibodies were obtained from Matthew Rasband (Na<sub>V</sub>1.6, Caspr1 and ankyrinG) and from Thomas Jentsch (KCNQ4); other antibodies were purchased from Chemicon. The several molecules differ in their distribution on the inner and outer faces. Na<sub>V</sub>1.6 is found in the hemi-node at the base of the calyx and, as such, could be involved in spike initiation. In contrast, Na<sub>V</sub>1.5 is located only on the inner face and could enhance synaptic transmission. ERG staining is uniform on the inner and outer faces, while KCNQ4 staining is more intense on the inner face, except in a circular region opposite the parent axon. When active, these K<sup>+</sup> channels could depress synaptic transmission. MIRP1, which can function as an accessory protein for either KCNQ or ERG channels, is found at the base of the calyx and may alter the properties of inner-face channels. Scaffolding proteins link ion channels to the cell membrane. Caspr1 and Caspr2 are found on the innerand outer-faces, respectively. AnkyrinG is at the heminode. The question remains: How do these elements fit together to determine the function of the calyx?

Supported by DC-02058, DC-02290, DC-02521.

## 971 What Lower Corner? Micromechanical vs. Afferent Adaptation in the Semicircular Canals *In Vivo*

Curtis King<sup>1</sup>, Richard Boyle<sup>2,3</sup>, Stephen M. Highstein<sup>3,4</sup>, **Richard Rabbitt<sup>1,3</sup>** 

<sup>1</sup>University of Utah, <sup>2</sup>NASA Ames, <sup>3</sup>Marine Biological Laboratory, <sup>4</sup>Washington University

A large percentage of semicircular canal afferents neurons are tuned to transmit angular head velocity to the brain over a broad range of angular motion frequencies and amplitudes. This simple behavior begins to break down for

stimuli below the "lower-corner" frequency where afferent sensitivity to head velocity declines. The decline is most easily seen for step velocity stimuli, where afferents initially increase their discharge rate followed by a period of adaptation back to their pre-stimulus resting rate. It has long been believed that this adaptation is due to elasticity of the cupula and the propensity of the deflected cupula to slowly recover back to its resting position over time. The relatively wide range of adaptation times associated with afferent nerve discharge however, led us to question the elasticity hypothesis. To investigate this we attached neutrally buoyant fluorescent microspheres to the cupula and recorded their motion using a triggered digital camera under direct microscopic observation in vivo. Afferent responses were recorded simultaneously, thus verifying health of the organ and providing direct comparisons between the micromechanics and the neural response. For a step stimulus of 50deg/sec, the peak cupula displacement was approximately 1.6 microns. Recovery of the cupula to its pre-stimulus position followed a dominant mechanical time constant of ~35s - an adaptation time constant that was much slower than a vast majority of semicircular canal afferent neurons. Only the most slowly adapting afferents approached the mechanical time constant. In general, results show that adaptation and the lower-corner frequency present in semicircular canal afferent responses are not dominated by the time constant of the cupula.

Supported by NIDCD R01 DC06685

### 972 Canal and Otolith Contributions to the Rvor in Pigeon (*Columba Livia*)

Kimberly L. McArthur<sup>1</sup>, J. David Dickman<sup>1</sup>

<sup>1</sup>Washington University in St. Louis

Previous studies of vestibular-related eye movements in pigeons have shown that otolith-driven eye movements in the dark compensate for actual head tilt relative to gravity during off-vertical axis rotation and apparent head tilt during earth-horizontal linear translation (Dickman & Angelaki 1999). Earth-horizontal axis rotation dynamically activates semicircular canals and otoliths, and evokes eye movements that compensate for actual head tilt (rVOR) (Dickman, Beyer & Hess 2000). However, the nature of the interaction between canal and otolith signals during rVOR has not been directly investigated. Furthermore, the three-dimensional organization of head movements in response to whole-body tilts has not been investigated in alert pigeons. In the current study, we record threedimensional eye and head movements during a "tilt/translation" stimulus protocol that allows us to compare behavior in the absence of dynamic canal signals ("translation-only"), in the absence of dynamic otolith signals ("tilt-translation"), and during combinations of dynamic canal and otolith signals ("tilt-only" and "tilt+translation"). We discuss our results in the context of pigeon gaze stabilization.

Support contributed by: NIH DC006913 and DC007618, NASA NNA 04CC52G, and T32 GM008151 Systems and Molecular Neurobiology Training Grant.

### 973 Ultra-High Frequency Vestibular-Evoked Ocular Reflexes

Daniel Merfeld<sup>1,2</sup>, Michael Saginaw<sup>2,3</sup>

<sup>1</sup>Harvard Medical School, <sup>2</sup>MEEI, <sup>3</sup>MIT

Reflexive responses can be evoked by sensory stimuli at surprisingly high frequencies. For example, the vestibuloocular reflex (VOR) has been shown to be compensatory for frequencies up to at least 25 Hz. The exceptional performance of the VOR occurs despite inertia and friction, both of which limit high-frequency motor performance. To investigate how the mammalian nervous system compensates for inertial and frictional effects, measured oscillatory eye movements evoked by electrically stimulating the neurons that innervate the vestibular system. Specifically, we applied biphasic current pulses to neurons that innervated a lateral canal; these current pulses were modulated on and off at frequencies between 1 Hz and 729 Hz. Horizontal eye movements were measured at the modulation frequency for frequencies exceeding 100 Hz, which is several times higher than the highest frequency VOR previously reported. The magnitude of the evoked eye responses over a very large frequency range - at least 1 Hz to 123 Hz - was relatively constant, ranging between 0.5 and 10 deg/sec. These variations of the response magnitude as a function of frequency were small especially in comparison to the oculomotor plant, which demonstrates more than a two hundred-fold response reduction over the same frequency range. This shows that the neural networks that evoke these reflexive eye responses, including those networks that compensate for the low-pass filter characteristics of the ocular globe, work surprisingly well even at frequencies that approach the maximal firing rate of neurons in the VOR neural network. These data were modeled using a simple model that: 1) includes a single free parameter, 2) includes an internal model of the oculomotor plant, and 3) is consistent with existing oculomotor models. These experimental and modeling findings provide new information that demonstrates both the exceptional performance of oculomotor compensation as well as its limits and may lead to new clinical tests of vestibular and oculomotor function.

Supported by NIH F31 DC006202 and R01 DC03066.

## 974 Incremental Adjustment of Velocity Error Signal Enhances VOR Adaptation

**Michael Schubert**<sup>1</sup>, Mark Shelhamer<sup>1</sup>, Charles C. Della Santina<sup>1</sup>

<sup>1</sup>Johns Hopkins University

Studies of the auditory and optokinetic systems provide compelling evidence that neural plasticity is enhanced when the error signal driving adaptation is adjusted incrementally throughout training. We sought to determine whether the same principle applies to adaptation of the angular vestibulo-ocular reflex (aVOR). We used the scleral search coil technique to measure horizontal aVOR gains before, during and after adaptation in 6 individuals with normal vestibular function exposed to an incremental error aVOR demand task (INCR) and a sudden X2 aVOR

demand task (X2). In each paradigm, the subject tried to fixate a visual target during active (self-generated) transient yaw head rotations. In the INCR paradigm, the target moved at a fraction of the head's velocity, and that fraction was incrementally adjusted upward. In the X2 paradigm, the target moved exactly opposite the head, effectively requiring a doubling of VOR gain to maintain target fixation over the same total number of training trials. Pre- and post-treatment aVOR gains were measured for both active and passive head rotations. Both paradigms elicited increases in aVOR gain for active head rotations compared with baseline after 20 minutes of training; however, the mean gain change for the INCR paradigm exhibited a trend for larger aVOR gain (16.6 ± 10.7% vs.  $4.3 \pm 12\%$ , p=0.09). Mean increase in aVOR gain for passive head rotations was significantly greater in the INCR group compared with the control (18.6  $\pm$  12% vs. 2.6 13%, p<0.05). Some individuals generated compensatory saccades that occurred in the same direction of the underpowered VOR. We conclude that incremental adjustment of a visual error signal provides a more potent adaptive stimulus for increasing aVOR gain than does immediate presentation of a X2 demand error, and that the resulting increase in aVOR is generalized across different contexts (active and passive) of head movement.

### 975 Improved Fluidmechanic Modelling of Canalithiasis

Stefan Hegemann<sup>1</sup>, Dominik Obrist<sup>2</sup>

<sup>1</sup>University Hospital Zurich, <sup>2</sup>ETH Zurich (Swiss Federal Institute of Technology)

In order to understand physiologic and pathophysiologic mechanisms of the vestibular organ a detailed knowledge of the flow field in the semicircular canals (SCC) is of great importance. Previous models were mostly based on the torsion pendulum equation due to Steinhausen (1933). Here we present a simple yet accurate solution for the flow field in the SCC based on the Navier-Stokes equations. Furthermore we have included a model for particle flow in the SCC which enables us to understand and calculate explicitly the effects observed in benign paroxysmal positioning vertigo (BPPV). This new model for BPPV provides deep insight into the underlying mechanisms of canalithiasis. It is amenable to a detailed mathematical analysis of the dynamics of canalithiasis and it is well suited for computer simulations of various configurations (e.g. different numbers and sizes of otoliths in the SCC). Early results show that 1) the maximum nystagmus slow phase velocity of BPPV is mainly depending on the total cross-section of the otoliths, 2) the latency decreases with the number and size of the particles and vanishes with many large particles and 3) the time from nystagmus onset to peak is independent of the number of particles. We measured eye movements in patients with BPPV using the three-dimensional search coil technique and were able to relate these measurements directly to our numerical simulations.

## 976 Long-Term Impact of Vestibular Rehabilitation After Gentamicin Therapy in the Outcome of Meniere's Disease

**Kim Gottshall**<sup>1,2</sup>, Michael Hoffer<sup>1,2</sup>, Robert Moore<sup>1</sup>
<sup>1</sup>Spatial Orientation Center, <sup>2</sup>Naval Medical Research Center

We have previously reported on the two year outcome of a cohort of individuals who underwent sustained release delivery of gentamicin in the treatment of Meniere's The twenty-five individuals in the study all received ten days of sustained release gentamicin for the treatment of Meniere's disease that had failed to respond to conservative medical therapy. This group of patients was divided into two study groups. Thirteen of the 25 individuals received vestibular rehabilitation whereas twelve of the individuals did not receive rehabilitation. The rehabilitation was composed of vestibulo-ocular reflex exercises, cervico-ocular exercises, depth perception exercises, somatosensory exercises, and aerobic conditioning. We now examine the long term outcome of this group of patients at five years after gentamicin treatment. We report on the following indices: vertigo control rate, dizziness handicap index (DHI), activities balance confidence scale (ABC), and dynamic gait index (DGI). We compare the outcome between the two groups. The results of this work have implications regarding the disease treatment of Meniere's especially transtympanic gentamicin treatment continues to gain in popularity. Understanding the short and long term impact of adjuvant vestibular rehabilitation therapy will provide improved outcome for patients.

#### **Author Index**

(Indexed by abstract number)

Aarnisalo, Antti 84 Abbas, Paul J. 354, 639 Abdala, Carolina 117, 520 Abe, Kousuke 427 Abraira, Victoria E, 561 Abrams, Daniel A. 699 Abrams, Kristina 918 Abskharoun, Mariam 107 Ackelson, Ashlee 440, 689 Ackley, Steven 174, 176 Acuna, Dora 704, 705 Adams, Joe 74, 564, 706, 777 Adams, Meredith E. 258 Adelstein, Robert 573 Adile, Eelam 93 Adler, Henry J. 30 Adunka, Oliver 447 Agee, D.A. 828 Aghaie, Asad 492 Agrawal, Smita 638 Agus, Trevor 932 Ahlstrom, Jayne B. 871, 872, 893 Ahmad, Shoeb 191, 193, 771, Ahmed, Zubair 200, 225, 490 Ahn, Joong Ho 595, 596, 843 Ahn, Kyung 326 Ahrens, Misha 395 Akeroyd, Michael 932 Akil, Omar 290, 784 Alagramam, Kumar 130, 274, Alain, Claude 913 Alam, Shaheen 110 Albert, Sébastien 197 Alexander, Joshua 891 Alexandrova, Olga 607 Alger, Heather 304 Ali, Dassan 881 Ali, Muhammed 190 Allak, Amir 185 Allen, Jont 655, 933, 934 Allen, Paul 751, 752, 822 Allen, Stanley 160 Alliston, Tamara 257 Almanza, Angélica 671 Aloor, Heather 312, 313 Altschuler, Richard 85, 827 Alvarez, Yolanda 319 Anandacoomaraswamy, Keith 277 Anderson, Charles 37, 785 Anderson, David 826 Anderson, James 490 Anderson, John 686 Anderson, Kenneth 968 Anderson, Lucy A. 406 Anderson, Malin 268 Anderson, Michael 428 Andersson, Gerhard 155 Andoni, Sari 836, 838 Andrews, Peter 270 Anteunis, Lucien 806 Antic, Dragana 574 Anvari, Bahman 48, 504 Aparicio, M. Auxiliadora 389 Appler, Jessica 556, 962 Arai, Tsuguyuki 794 Ardoint, Marine 919 Arehart, Kathryn 892 Arocena, Mariana 684 Arruda, Julie 128 Arts, H. Alexander 64 Asai, Yukako 316 Ashida, Go 427 Askew, Charles 571

Atal. Bishnu S. 441 Atlas Les 441 Atlas, Marcus 140, 277 Atzori, Marco 389 Auer, Manfred 237 Auner, Gregory 449, 450 Avan, Paul 492, 806 Avissar, Michael 111, 351 Avraham, Karen B. 254, 259, 489 Axelrod, Jeffrey 574 Axon, Patrick 646 Ayala, Marco A. 586 Baba, Kazuyasu 158 Babcock, Steve 911 Bach-y-Rita, Paul 187 Backes, Walter 691 Backhouse, Steven S. 275 Backus Bradford 508 Bae, Joon-ho 142 Baguley, David 646 Bahmad, Fayez 178 Bai, Jun-Ping 39 Bai, Lianhua 274 Bailey, Jasmine 400 Bailey, Peter J. 423 Bajo, Victoria 868 Bak, Matthew 755 Baker, Allison 440, 689 Baker, Kim 540 Balaban, Carey 584, 712, 801 Balaban, Evan 647 Balakrishnan, Veeramuthu 380 Balkany, Thomas 93, 581 Ballestero, Jimena 286 Baloh, Robert W. 663 Balough, Ben 129, 579 Banai, Karen 928 Bance, Manohar 123, 342 Banizs, Boglarka 963 Banks, Martin S. 3 Bao, Jianxin 276 Barald, Kate 554 Barbour, Dennis L. 115, 402, 890 Barkdull, Gregory 580 Barrett, Jessica 640 Barsz, Kathy 751, 752 Barta, Patrick E. 877 Bartels, Hilke 813 Bartles, James 105, 224, 491 Basappa, Johnvesly 292 Bashtanov, Mikhail E. 281 Baskent, Deniz 936 Basta Dietmar 631 695 Battey, Jim 216 Battmer, Rolf-Dieter 243 Batts, Shelley A. 83, 543 Baucom, Jessica 20 Baudoux, Sylvie 404 Baulande, Sylvain 781 Beales, Philip 964 Bechmann, Ralf 128 Bee Mark 912 Beineke, Andreas 127 Beisel, Kirk 303, 310, 739, Beitel, Ralph E. 397, 688, 693 Beltramello, Martina 775 Beltran-Parrazal, Luis 704, Belyantseva, Inna A. 226, 225, 298, 490 Bendett, Mark 356 Bendor, Daniel 410 Benitez, Raul 467

Benson, Jennifer M. 242 Benson Thane F 599 Ben-Tal, Nir 489, 492 Berecky, Ryan 766 Berend, Achim 260 Berg, Dana 63 Bergevin, Christopher 811 Bermingham-McDonogh. Olivia 309 Berninger, Erik 804 Bernstein, Leslie 15 Berrebi, Albert 327, 560, 606, 616 Berry, Elizabeth 218, 219 Berryman, Mark 664 Best, Virginia 437, 902, 909 Bettler, Bernhard 338 Beurg, Maryline 98 Beyer, Lisa A. 83, 86, 258 Beynon, Andy 25, 228 Bezerra, Roberta 178 Bian, Lin 510 Bianchi, Lynne 554 Biegner, Thorsten 54 Bielefeld, Eric 645 Bierer, Julie 629 Bierer, Steven 629 Biesecker, Leslie 321 Biesemeier, Deborah 12 Billings, Peter 339, 340 Bizaki, Argyro J. 564 Bizley, Jennifer 398, 403 Black, F. Owen 187 Blanks, Deidra 385 Bledsoe, Sanford C. 242, 373 Bleeck, Stefan 624, 646 Blevins, Nikolas 238, 472 Bloomberg, Jacob J. 188 Boatman, Dana 874 Boche, Jo Ellen 575 Boer, Egbert De 495 Boermans, Peter-Paul 453 Bogdanovic, Nenad 847 Bohne, Barbara A. 329, 330 Bok, Jinwoong 959 Bonham, Ben H. 397, 452, 635, 693 Booker, Emma 147 Bootz, Friedrich 135 Boppana, Suresh 262 Borina, Frank 922 Borkholder, David A. 585 Bortolozzi, Mario 775 Bose, Mitali 389 Botta, Luisa 676 Boyle, Patrick 453 Boyle, Richard 971 Bradley, Allan 227 Bradshaw, John 190 Braganza, Andrea 194 Bramer, Tobias 73 Bramhall, Naomi 199 Brandewie, Eugene 940 Brandon, Carlene S. 716 Bratt. Debbie 537 Brauer, Delia 257 Braun, Allen 870 Breshanhan, Glenn 826 Breuninger, Christian 526 Brewer, Carmen 317 Briaire, Jeroen 453 Brigande, John 961 Briley, Paul M. 423 Brill, Oliver J. 515 Brimijoin, Wm. Owen 394 Broman, K.W. 487 Brooks, Diane 609, 611

Brooks, Emma 140 Brors, Dominik 260, 264 Brose, Niels 357 Brough, Douglas E. 83, 540 Brown, Carolyn J. 639 Brown, Kevin 672 Brown, M. Christian 599, 605, 608 Brown, Mel 114 Brown, Steve D.M. 572, 746 Brownell, William 35, 36, 48, 504, 725, 726 Bruce, Ian 657 Brughera, Andrew 826 Buck, Tim 86 Bulankina, Anna 357 Burger, R. Michael 607, 721 Burgess, Barbara 74, 252 Burgess, Shawn M. 742 Burk. Robert 192 Burton, Joel R.A. 423 Buschermöhle, Michael 917 Buss, Emily 385, 414 Bussey, Rhiannon R. 362 Butcher, Kristin 257 Buytaert, Jan 529 Bystrom, Cory 228 Cai, Chun 65, 66 Cai, Hongxue 733 Cai, Qing 66 Cai, Shanqing 812, 819 Calisto, Lilian 965 Calzi, Daniela 551 Camalier, Corrie 409, 411 Camp, Guy Van 492 Campbell, Kathleen 709 Campbell, Sean 542 Camper, Sally 563 Campero, Andrea M. 558 Campos, Francisco Rodriguez Canlon, Barbara 333, 703, 707, 847 Cannavo, Justine 154 Cao, Juyang 196 Cao, Xiaojie 372 Cardona, Ana Caban 370 Carey, John 181, 185 Carey, Thomas E. 64 Carlile, Simon 902 Carlyon, Bob 914 Carlyon, Robert 646 Carn. Heloise 656 Carney, Laurel 378, 918, 920 Carr, Catherine 421 Carr. Suzanne 899 Carrera, Ximena 685 Carroll, Jeff 472 Carter, Olivia 913 Casalotti, Stefano O. 601 Caspary, Donald 756, 844, Castiglioni, Andrew 769 Castillo, Francisco Del 492 Cervantes, Sebastian 179 Cha, Chang II 137 Chabbert, Christian 296 Chadwick, Richard 499, 732 Chae, Sung Won 72, 141 Chaiet, Scott 35 Challagulla, Kavitha 554 Chan, Dylan 316 Chan, Eric 28 Chan, Kenny H. 160 Chan, Rebecca 312 Chang, Cheng C. 169 Chang, Jolie 257

Chang, Qing 190, 191, 193, Chang, Sun O. 768 Chang, Yi-ping 882 Chapman, Brittany J. 300 Chatlani, Shilpa 665, 666, 970 Chattaraj, Parna 490 Chatterjee, Monita 885 Chavez, Eduardo 553 Chays, André 189 Cheah, Kathryn 960 Cheatham, Mary Ann 37, 785 Chen Daniel 274 Chen, Fangyi 101, 501 Chen, Guang-Di 645, 710 Chen, Kejian 538, 591, 592 Chen, Lin 361 Chen, Max 348 Chen, Ping 771, 778, 963 Chen, Shibing 93, 581 Chen, Tsung-Yu 45 Chen, Wei 107, 270 Chen, Xiuwu 207 Chen, Zheng Yi 201, 545, 562 Chen. Zhiqiang 352 Cheng, Andrew 44 Cherian, Neil 179 Chertoff, Mark 112, 113 Cheung, Eunice 238 Cheung, Steven 397, 688, Chien. Wade 507, 528, 536 Chihara, Yasuhiro 677 Chiu, Lynn L 798 Cho, Cahng Gun 595 Cho. Catherine 683 Cho, Jae Hoon 72 Cho, Jae-Gu 141 Cho, Jang-Hyenon 505 Cho, Yang-Sun 803 Choi, Chul-Hee 592 Choi, Seong Jun 142, 301 Chon, Kyong-Myong 152 Chonnettia, Jones 771 Choski, Mulan 627 Choudhury, Niloy 501 Choung, Yun-Hoon 142, 301 Chowdhury, Farshad 445 Christensen, Barbara L. 278 Christensen-Dalsgaard, Jakob 421 Christianson, G. Bjorn 696 Chung, D. 884 Chung, Jong Hoon 142 Chung, Jong Woo 61, 595, 596, 597, 843 Chung, Won-Ho 803 Chung, Yong Won 795 Cioffi, Joseph 659, 660 Clark, Jason 672 Clark, Pascal 441 Clement, Ryan 630 Clendaniel, Richard 185 Cockayne, Debra A. 764 Coco, Anne 205, 462, 636 Coghill, Emma L. 746 Cohen, Adam 229 Cohen, Bernard 679, 680, 681, 683 Cohen, Helen 188 Cohen, Yale 440, 445, 484, 689 Colburn, H. Steven 430, 437, Coleman, Bryony 275 Coleman, John K. M. 586

Colesa, Deborah J. 242

Coling, Donald 348 Colletti, Vittorio 244 Collins, Leslie 457, 458 Converse, Connie 512, 513 Cook, James 184 Coomes, Diana 866 Corey, David P. 24, 97, 229, 289 Corrales, Eduardo 272 Cosgrove, Dominic 571 Cotanche, Douglas A. 23, 300, 541, 550, 737 Coticchia, James 149 Couderc, Remy 197, 781 Counter, Allen S. 73 Covey, Ellen 383 Cowan, Justin A. 146, 147 Cramer, Karina 364, 718 Crawley, Brianna 340 Crema, Matthew 628 Crenshaw, E. Bryan 326 Cristaudo, Salvatore 383 Crocetti, Andrea 157 Crone, Nathan 874 Crumling, Mark A. 83 Cui, Qi N. 905 Cui. Yilei 365, 827 Cullen, Kathleen E. 673 Cunningham, Lisa L 716 Cureoglu, Sebahattin 68 Cusack, Rhodri 914 Dabdoub, Alain 8, 317, 960 Dai, Chunfu 180 Dailey, Michael 850 Dallos, Peter 37, 785 D'Angelo, Egidio 676 D'Angelo, William 409, 411 Dangerfield, Katie 925 Daniel, Sam J. 522 Danilov, Yuri 186 Darr, Stacy 756 Darrow, Keith 759 Dasika, Vasant K. 463 Daudet, Nicolas 966 David, Stephen 869 Davids, Taryn 816 Davidson, Amy 726 Davis, Brianne 62 Davis, Julian 946 Davis. Kevin 388 Davis, Rickie 598 Davis, Robin L. 106, 107, 355 Dazert, Stefan 260, 264, 763 De Angelis, Martin Hrabe 255, 259, 489 De Aragaveytia, Teresa A. 684 De La Rochefoucauld, Ombeline 530, 531 De San Martín, Javier Zorrilla 286 Dean, Isabel 395, 418 Deans, Michael 574 Decraemer, Willem 122, 529, Deeks, John 646 Dees, Tasha 211 DeGagne, Jacqueline 133, 136 Delgutte, Bertrand 18 Deliano, Matthias 408 Deligeorges, Socrates 826 Delmaghani, Sedigheh 492 Delman, Bradley 63 Deng, Min 307 Denman, Daniel J. 91 Denoyelle, Françoise 197, 781 Denslow, Stewart 871 Dent, Michael 897, 909 Deo. Niranian 500

Devore, Sasha 18

Dhar, Sumit 698, 805

Diaz, Carmen 614 Diaz, Rodney 232 Dickerson, Ian M. 362 Dickman, J. David 949, 950, Dierking, Darcia M. 512, 513 Dijk, Pim Van 496, 691, 806, 813 Dillard, Karen 392 Dimitriadis, Emilios 499, 728 Dimitrijevic, Andrew 472 Dinda, Amit Kumar 817 Ding, Dalian 75, 77, 799, 800, Dinglasan, Judilee N. 291 Dirckx, Joris 138, 529, 531 Divenyi, Pierre 939 Dlugolenski, Keith 815 Dodson, Hilary 601 Dogheim, Yakout 164, 171 Doherty, Joni 261 Doi, Katsumi 158, 308 Doi, Takashi 619 Dolan, David 349, 563 Dolson, Diane K. 959 Dominguez, Elena 319 Donahue, Amy 216 Donato, Roberta 415 Dong, Wei 735 Donley, Lauren 462, 636 Dooling, Robert J. 30, 442 Dorman, Michael 853 Dormer, Kenneth 129, 538, Dosch, Hans Guenter 700 Doshi, Shachee 351 Doucet, John 600, 604 Drennan, Ward 465, 469, 637, 883 Drescher, Dennis G. 27, 31, 766 Drescher, Marian J. 31, 766 Drexl, Markus 498 Driver, Elizabeth Carroll 321 Dror, Amiel A. 259 D'Sa, Chrystal 555 D'Souza, Mary 345, 347, 753 Du, Li Lin 21, 201, 780 Du, Xiaoping 65 Dubno, Judy R. 641, 871, 872 893 Duggan, Anne 769 Duifhuis, Hendrikus 602 Duncan, Luke J. 300, 541 Duncan, R. Keith 287, 44, 563 Durham, Dianne 46, 368, 393, Durlach, Nathaniel I. 437 Dymecki, Susan 720 Dziorny, Adam C. 566 Easter, James 451 Eatock, Ruth Anne 40, 969, 970 Ebmeyer, Jorg 135 Eckert, Mark 871, 872 Economou, Androulla 318 Eddington, Donald 206 Eddins, David 153, 194, 642, 643, 644 Edge, Albert 266, 272, 273 Edge, Roxanne 37, 785 Edmiston, Sarah 660 Edmond, John 704, 705 Edsman, Katarina 73 Edwards, Brent 936 Eernisse, Rebecca 370, 600, 660 Eggermont, Jos 399 Egner, Alexander 282 Ehrlich, Garth 139 Ehrsson, Hans 53

Eiber, Albrecht 526

Eichhammer, Peter 166, 702

Eikelboom, Robert 140, 277 Eiler, Cheryl 936 Eisen, Ashley 438 Eisenberg, Laurie 144 Eisenberg, Michelle 442 Eisner, Frank 214 Ekborn, Andreas 73 Elgoyhen, Ana Belén 286, Elhilali, Mounya 401, 697 El-Kashlan, Hussam K. 64 Ellermeier, Wolfgang 432 Elliott, Stephen 493, 494 Englitz, Bernhard 626 Engmér, Cecilia 73 Epp, Bastian 431 Epp, Stephanie 205 Epstein, Douglas 9, 959 Erbe, Christy 660, 661, 662 Erenberg, Sheryl 466 Ernst, Arne 631, 695 Ernst, Stephan M.A. 878 Eron. Julia 679, 680 Esau, Katie 113 Escabi, Monty 386, 387 Eshraghi, Adrien 93, 581 Esmailzadegan, Arach 93 Espinosa-Jeffrey, Araceli 704 Euteneuer, Sara 553, 763 Evans, Michael 98 Eybalin, Michel 78, 297, 539, 760 Fairfield, Damon 94 Fairhall, Adrienne 621 Fallon, James 462, 636 Fang, Jie 99 Fang, Qing 563 Fanning, Alan 490 Farahbakhsh, Nasser 100 Fathke, Robert 829 Faulkner, Andrew 214 Fauser, Claudius 765 Fausti, Stephen 763 Fayad, Jose 49 Feeney, Patrick 118, 119 Fekete, Donna M. 12, 328, Feldmann, Delphine 197, 781 Felix, Richard A. 606 Feng, Albert S. 278 Feng, Feng 317, 612 Feng, Guoyin 196 Ferguson, Melanie A 147 Ferry, Robert 761 Fettiplace, Robert 98, 283 Feudel, Ulrike 917 Finco, Rebecca 815 Finlayson, Paul 824 Finley, Charles 447 Firestein, Gary S. 339 Fisher, Susan G. 64 Fishman, Yonatan 863 Fitzakerley, Janet 256 Fitzgerald, Tracy 514 Fitzgibbons, Peter 640 Fitzpatrick, Douglas 385, 414, 447 Flores, Brenda 62 Flores-Otero, Jacqueline 106 Floyd, Robert 592 Flynn, Eric 387 Foltz, Logan 385 Forge, Andrew 96, 490, 542, 601, 774, 964 Formby, Craig 154 Forsythe, Ian 369 Forti, Stella 157 Fowler, Karen 262 Frachet, Bruno 935 Fraenzer, Juergen-Theodor

Franklin, Alan 473 Franklin, S.R. 828 Freeman, Dennis M. 811 Freijd, Anders 155 French, Courntey 160 Frenz, Christopher 29 Frenz, Dorothy 320, 322, 797 Freund, Jan A. 917 Frey, Eric 941 Friderici, Karen H. 298 Friedland, David 370, 600 Friedman, Lilach M. 254 Friedman, Penelope 195, 490 Friedman, Thomas 26, 195, 200, 225, 226, 298, 490 Friedmann, David R. 738 Frijns, Johan 453 Frisch, Stefan 880 Frisina, Robert D. 194, 343, 344, 345, 347, 585, 642, 643, 644, 753, 754, 755 Frisina, Susan 194, 343, 344 Fritz, Jonathan 401, 407, 869 Fritzsch, Bernd 310, 317, 559, 569, 570, 612, 965 Froemke, Robert 851 Frolenkov, Gregory I. 225, 226, 298 Fu, Qian-Jie 215, 634, 882, . 887, 937 Fuchs, Helmut 255, 259, 489 Fuchs, Paul 231, 280, 286, Fujii, Masato 302, 568 Fujimoto, Yasuko 271 Fujioka, Masato 302 Fukuda, Takehiko 170 Funabiki, Kazuo 427 Funnell, W. Robert J. 522 Furlong, Cosme 534 Furman, Adam 111, 351 Furman, Joseph 183, 184, 678 Furness, David 283, 577 Furst, Miriam 615, 933 Furukawa, Shigeto 412, 429 Gabbard, Sandra A. 176 Gaboyard, Sophie 970 Gabriele, Mark 829 Gadzalla, Laura 228 Gaese, Bernhard 405 Gagnon, Patricia M. 749 Gahm, Caroline 53 Gai, Yan 378, 918 Galazyuk, Alexander 392 Gale, Jonathan 299, 717 Gale, Richard B. 746 Galindo-Leon, Edgar 867 Gallun, Frederick J. 437, 902, 909 Galvin, John 633, 634 Gan, Lin 307 Gan, Rong 524 Ganesh, Vidya 923 Gannon, Patrick 63 Gans, Donald 866 Gantz, Bruce 466 Gao, Hongxiang 363 Gao, Wei 557 Garabédian, Eréa-Noël 197, Garbern, James 149 Garcia, Jerel 291, 337 Garcia-Anoveros, Jaime 224, Garnier, Stephane 656 Gassmann, Martin 338 Gates, George 218, 220 Gaur, Ashmita 633 Ge. Xianxi 129 Gea, Stefan 122 Geisinger, Dario 685 Geleoc, Gwenaelle S.G. 32

Gellibolian, Robert 49, 69 Georgopoulos, Christina 785 Germiller John 554 Ghaheri, Bobak 136 Ghassemifar, Reza 140, 277 Giampoala, Matthew 234 Giancarlo, Zuliani 149 Gilbert, Daniel 630 Gilbert, Gaetan 656 Gill, Ruth M. 249 Gillespie, Peter G. 25, 228 Gilley, Phillip 853 Gilley, Reagan 80 Gioglio, Luciana 551 Giraud, Anne-Lise 846 Girod, Doug 368 Gittelman, Joshua 834, 835 Glass, Tiffany 248 Glavaski-Joksimovic, Aleksandra 268 Gleich, Otto 921 Glover, Joel 722 Glowatzki. Elisabeth 233. 266. 279 Gmitter, Christine 154 Gnansia, Dan 935 Gochee. Peter 46 Godar, Shelly P. 464 Goddard, John 267, 578 Goetze, Romy 695 Goh, Eui-Kyung 152 Gold, Susan 154 Goldberg, Jay M. 665, 666, 667, 668, 673, 970 Golding, N. L. 622 Gonzales, Oneximo 630 Goodrich, Lisa 311, 556, 561, 574, 723, 962 Goodyear, Richard 225, 299 Gopal, Kamakshi 860 Gordon, Karen 816 Gordon-Salant, Sandra 640 Gorga, Michael P. 512, 513 Gottshall, Kim 579, 976 Gourévitch, Boris 399 Goutman, Juan 233, 279 Govitrapong, Piyarat 601 Gow. Alexander 149 Grabosch, Christine 264 Grady, Brian 538 Grant, Lisa 280 Grant, Wally 946, 947 Gratton, Michael Anne 337, 476, 571, 762 Graves, Reid 93 Gray, Lincoln 439 Green, Gary 879 Green, Steven 90, 91, 92, 94, 110, 850 Greenberg, Steven 939 Greeson, Jennifer 34, 102 Greinwald, John 190 Grieco, Tina M. 464 Griest, Susan 156 Griffin, Sarah 15, 369 Griffith, Andrew J. 195, 225, 226, 317, 321 Griffiths, Timothy 875, 924 Grill, Warren M. 241 Grillet, Nicolas 32 Grosh, Karl 500 Gross, Gerhard 88 Gross, Guenter 860 Grothe, Benedikt 417, 607 Grover, Mary 108 Groves, Andrew 311, 324 Grube, Manon 924 Grushko, Julia 701, 797 Gu, Rende 544 Guan, Bing-Cai 58, 59, 60 Guan, Min-Xin 488 Guan, Zhenlong 374, 375, 449, 450

Francis, Howard W. 625

Gubbels, Samuel 961 Guerciolini, Roberto 545 Guidi, Jessica L. 300 Guimaraes, Patricia 643 Guinan, John J. 175, 519 Gull, Justin 896 Gumenyuk, Valia 701 Gunawan, David 650 Gunhanlar, Nilhan 50 Guo, Wei 325 Gürtler, Nicolas 782 Gustafsson, Jan-Åke 707 Guthrie, O'Neil 584 Haake, Scott 581 Hackett, Alyssa 557 Hackett, Troy 409, 411 Hackney, Carole 98, 283 Hadjab, Saïda 703, 847 Hagino, Tomotaka 900 Hahn, Hartmut 76 Hain, Timothy 805 Hajak, Goeran 166, 702 Hall, Susan 929 Halliday, Lorna F. 926 Hallworth, Richard 303, 506, 727, 739 Halpin, Chris 528 Halsey, Karin 349 Hammershøi, Dorte 517 Han, Demin 207 Han, Dongyi 196 Han, Gyu 951 Hancock, Kenneth E. 426 Hanke, Markus Sanchez 127 Hannon, Erin 913 Hansen, Anna 840, 841 Hansen, Laura 559 Hansen, Marlan 90, 110, 672 Hansen Stefan 260 264 Haque, Asim 949 Hara, Akira 95, 587 Harbidge, Donald 51, 52 Hardie, Natalie 251 Harding, Gary W. 329, 330 Harper, Elizabeth 129 Harper, Nicol S. 418 Harrington, Brian 148 Harrington, Ian A. 422, 425 Harris, Jeffrey 580 Harris, Julie A. 721 Harris, Kelly C. 641 Harrison, Robert 807, 816 Hartmann, Mitra J. 699 Hartmann, Rainer 461 Hartsock, Jared J. 56 Harvey, Margaret 285 Hasegawa, Jun 121 Hashimoto, Makoto 594, 589, 593. 794 Hashino, Eri 312, 313, 314 Hasson, Tama 489 Hatch, Ekaterina 315 Hatfield, James S. 766 Haulk, Devan 903 Häusler, Rudolf 782 Hawley, Monica 154 Hayashi, Toshinori 309 Hayden, Russell 941, 942 Hayes, Donald 153 He, David 325, 729, 770 He, Jiao 93 He, Lin 196 He, Wenxuan 502, 734 Heffner, Henry 393 Hegemann, Stefan 975 Heid, Silvia 461 Heil, Peter 114 Heiser, Marc 688 Hellberg, Victoria 53 Heller, Stefan 263 Helyer, Richard 265

Henderson, Donald 331, 332, 348, 645, 710 Henkel, C. 828, 829 Henkemeyer, Mark 364 Henry, James 156 Heo, Jeong-Hwa 768 Hernandez, Jeannie 85 Hernandez, Michelle 135 Hernández, Olga 831 Hernandez, Victor 775 Herrmann, Barbara S. 175 Hertzano, Ronna 489 Hess, Mailee 247 Hessner, Martin 659 Hiel, Hakim 295 Higgins, Nathan 845 Higgs, Matt 621 Highstein, Stephen M. 971 Higuchi, Hitomi 161, 162 Hill. Jennifer 521 Hill, Patrick 321, 959 Hind, Sally 925 Hinterwirth, Armin 730 Hiraumi, Harukazu 271, 708 Hiromichi, Kuriyama 82 Hirose, Keiko 67, 335 Hirose, Yoshinobu 589, 593, 594, 674 Hirsch-Shell, Dylan 955 Hirvu. Shizuko 900. 901 Ho, Edmund 667 Hoa, Michael 449 Hoesel, Richard van 638 Hof. Janny 806 Hoffer, Michael 579, 129, 976 Hoffman, Larry 284, 669, 670, 953, 954, 955 Hoffpauir Brian 603 Hofmann, Nicola 88 Holden, Timothy A. 249 Holdman, Jennifer 62 Holley, Matthew 265, 267 Holmstrom, Lars 833 Holt, Avril Genene 825, 827 Holt, J. Christopher 665, 666 Holt, Jeffrey R. 32 Holt, Joseph 952 Hondarrague, Yannick 580 Hong, Robert 468 Hong, Seok Min 137 Hong, Suling 134 Hong, Sung Hwa 803 Hoogduin, Hans 602 Hori, Ryusuke 22, 271 Hori, Shinya 168 Hori, Yoko 121, 125 Horii, Arata 308, 675 Hornstein, Eran 254 Horst, J. Wiebe 358 Horwitz, Amy R. 871, 872, 893 Hosoi, Hiroshi 170 Hosokawa, Tatsuro 901 Hossain, Amzad 847 Hossain, Waheeda 555 Hou, Zhou-hui 325 Housel, Nathaniel 822 Housley, Gary D. 32, 764 Howard, MacKenzie A. 721 Howard, Matthew 876 Howell, David 327, 560 Hradek, Gary 203, 204 Hseu, Anne 202 Hsu, Chi 540 Hu, Bohua 331, 332, 645 Hu, Rebecca 284, 669, 670 Hu, Yin-Yan 325 Huang, Jie 92, 110

Huang, Mingqian 562

Hubbard, Allyn 104, 826

Hudspeth, A. J. 20, 730

Huber, Alexander 526, 782

Hudspeth, James 316 Hughes, Larry 349, 709, 711, 756, 844, 856 Hultcrantz, Malou 138, 707, 767 Hume, Clifford 537, 542 Hur, Dong-Gu 768 Hurd, Elizabeth A. 258 Hurley, Karen 969 Huss, David 950 Husseman, Jacob 47 Hutson, Pete 856 Hwang, Chan Ho 323 Hwang, Soon-Jae 141 Idrizbegovic, Esma 155 Idrobo, Fabio 918 Ihlefeld, Antje 18, 437 lida. Koii 33 Ikeda, Katsuhisa 33 Im, Gi Jung 72, 141 Imig, Thomas 393, 818 Ingham, Neil 371 Ingraham, Michael 447 Irfan, Nashwa 620 Irvine, Dexter 114, 462, 636 Irving, Samuel 424 Isaacson, Jon 630 Isaradisaikul, Suwicha 176 Ishikawa, Kotaro 317 Ishiyama, Akira 663 Ishiyama, Gail 663 Ison, James 822 Ito, Juichi 22, 81, 265, 271, 582, 708 Ito, Ken 677 Ito, Yumi 168 Itoh, Kenji 873 Iwai, Koji 22 Iwaki, Takako 308 Iwasa, Kuni 99, 103, 728 Iwasaki. Shinichi 677 Izquierdo, Marco 830 Izzo, Agnella 109, 356, 446 Jabba, Sairam V. 51 Jaben, Korey 581 Jackson, Ronald L. 79, 129, 586, 591, 592 Jacques, Steven L. 501 Jagger, Daniel 774, 964 Jahnke, Klaus 132 Jajoo, Sarvesh 715 James, Adrian L. 807 Janky, Kristen 173 Jansen, E. Duco 356 Jaquish, Dawn 583 Järlebark, Leif 547 Jarng, Soon Suck 145 Jeng, Fuh-Cherng 639 Jenison, Rick 891 Jenkins, Herman A. 176, 451, 473 Jensen, Jamie 470 Jensen-Smith, Heather 506 Jeon, Sang-jun 273 Jero, Jussi 84 Jeschke, Marcus 408 Jesteadt, Walt 653 Jeung, Changmo 511 Jiang, Haiyan 75, 799, 800 Jiang, Hong-Yan 714 Jiang, Zhi-Gen 58, 59, 60, 294 Jin, Zhe 547 Joensuu, Joonas 84 Johansson, Peter 703 John, Earnest O. 160 John, M. Sasha 632 John, Padmore 681 Johnson, Dean G. 585 Johnson, Jacob 257

Johnson, Stuart 270, 296 Johnson, Tiffany A. 512, 513 Johnstone, Patti 438, 464 Jones, Chonnettia 963 Jones, Diane 74 Jones, Gary 434, 638 Jones, Jennifer 960 Jones, Linda 611 Jones, Sherri 954 Jones, Simon 692 Jones, Timothy 669, 670, 953, 954 Jongkamonwiwat, Nopporn Jonnard, Laurence 197, 781 Jonson, Kreg 832 Jordan, Craig 216 Joris. Philip 359, 384, 618 Joseph, Gert 243 Jost, Jürgen 626 Jourdes, Vincent 935 Jovic, Tina 503 Juhn, Steven 68 Juiz. Jose 614 Jung, Hak Hyun 72 Kaas, Jon 409, 411 Kachar, Bechara 230 Kada, Shinpei 271, 582 Kadner, Alexander 616 Kaga, Kimitaka 873 Kageyama, Ryoichiro 308 Kaiser, Christina L. 300 Kaiser-Moore, Simone 765 Kajikawa, Yoshi 409 Kallman, Jeremy 199, 487 Kalsoom, Saeeda 200 Kaltenbach, James 821, 824, 825 Kamien, Andrew 737 Kamijo, Tomoyuki 170 Kamiya, Kazusaku 21, 780 Kammerer, Bernd 54 Kanai, Rie 168 Kanda, Seiii 590 Kane, Daniel J. 43 Kaneko, Ken-ichi 168 Kang, Hun Hee 61, 595, 596, 597, 843 Kang, Robert 465 Kang, Sungook 301 Kang, Young-Jin 278 Kantardzhieva, Albena 562 Kanwal, Jagmeet 483 Kanzaki. Sho 131 Kappler, James 316 Karasawa, Takatoshi 789, Karavitaki, K. Domenica 97 Karimi, Kambiz 562 Karino, Shotaro 873 Karltorp, Eva 155 Karmody, Collin 126 Karnes, Hope 368 Karolat, Joerg 285 Kashio, Akinori 907 Kasic, James 451, 473 Kates, James 892 Kato, Toshihiko 161, 162 Katz, Eleonora 286 Kawai, Hideki 854 Kawamoto, Kouhei 158, 590 Kawasaki, Hiroto 876 Kawase, Tetsuaki 121, 125 Kazmierczak, Piotr 731 Keefe, Douglas 117, 520 Keirnes, Hannah 561 Keithley, Elizabeth 32, 339, 340, 580 Kelley, Matthew 8, 317, 321, 573, 960 Kelly, Jack B. 390 Kemp, David T. 515

Kempton, Beth 133, 136, 744, Kennedy, Elizabeth 512, 513 Kennedy, Kirin 351 Kenneth, Lee 190 Kent-Taylor, Anne 255 Kermany, Mohammad Habiby 65. 66 Kerschner, Joseph 139 Kershner, Bethany 118 Ketten, Darlene R. 127, 128 Khaddam, Samar 653 Khakh, Baljit S. 764 Khan, Khalid M. 766 Khan, Shaheen 200, 490 Khan, Shahid 200 Khanna, Shyam 531 Khimich, Darina 235, 357 Khoryevin, V. 950 Kidd, Gerald 436, 437 Kikkawa, Yayoi 743 Kikkawa, Yoshiaki 572 Kikuchi, Toshiaki 125 Kil. Jonathan 159, 544 Killian, Nathan J. 890 Kim, Ah Young 802 Kim. Ana H. 86 Kim, Beom-Gyu 61 Kim, Chong-Sun 768, 852 Kim. Duck 896 Kim, Hyung-Jong 61 Kim, Jang Ho 142 Kim, Ji Soo 182 Kim, Jin-Su 848 Kim, Jong Yang 165 Kim, Ki Ryung 803 Kim, Kyoung-Min 141 Kim, Seo Jin 72 Kim, So Young 595 Kim, SungHee 145 Kim, Yong-Bok 61 Kim, You Hyun 160 Kim, Young Ho 796 Kim, Young-Jin 843 Kimball, Kay T. 188 King, Andrew 19, 398, 403, 868 King, Curtis 503, 971 King, Kristin 62 King, W. M. 86 Kirby, Alana E. 471 Kishan, Amar 859 Kisley, Lauren 743 Kistler, Doris 435 Kita, Tomoko 22, 582 Kitahara, Tadashi 675 Kitajiri, Shin Ichiro 200, 490 Kite, Lisa 592 Kitterick, Pádraig T. 423, 906 Klapperich, Catherine 541 Klason, Tomas 73 Klein, Raymond 929 Kleine, Emile de 806, 813 Kleinjung, Tobias 166, 702 Klinge, Astrid 649 Klink, Karin B. 916 Kluender, Keith 7, 433, 891 Klug, Achim 607 Kluge, Kristina L. 330 Kluk, Karolina 632 Klump, Georg M. 418, 443, 649, 651, 916 Koay, Gim 393 Kobayashi, Toshimitsu 33, 121, 125, 788 Koch, Dawn Burton 456 Kocher, Brian 867 Koehler, Seth 373 Koehrn, Fred 583 Koeppl, Christine 350, 810 Kohei, Kawamoto 82 Kojima, Ken 265, 271

Johnson, Jamie 369

Johnson, Jane 311

Koka, Kanthaiah 416 Kokkinakis, Kostas 889 Kokuba, Hiroki 309 Kollmar, Richard 278, 316 Kommareddi, Pavan K. 64 Kondo, Kenji 553 Kondo, Takako 313, 314 Kong, Yunmi 899 Koo, Ja-Won 182, 768 Kopke, Richard 129, 538, 591, 592 Kopun, Judy G. 512, 513 Kössl, Manfred 405 Kotak, Vibhakar 849, 865 Kouike, Hiroko 568 Koundakjian, Edmund 311, 556, 962 Kouzaki, Hideaki 861 Kozlov, Andrei 730 Kral, Andrej 461 Krastins, Bryan 777 Kraus, Johanna 810 Kraus, Nina 5, 209, 210, 211, 699, 928 Krekeler, William 115 Krips, Ram 615 Krishnan, Ananthanarayan 382, 623 Kristiansen, Arthur G. 564 Kros, Corne 281, 293, 299 Krumbholz, Katrin 648 Ku, Emery 493, 494 Kubo, Takeshi 308, 675 Kucukoglu, M. Selin 458 Kudo, Koji 683 Kujawa, Sharon G. 175, 336, 352, 487, 706, 748 Kulesza, Randy 814 Kumagai, Izumi 33 Kumano, Shun 33 Kumar, Gagan 627 Kumar, Sukhbinder 875 Kumar, Vijay 64 Kumbla, Rekha 262 Kunin, Mikhail 681, 683 Kuriyama, Hiromichi 158, 590 Kurt, Simone 694, 855 Kwon, Bomjun 454 Labay, Valentina 195 Lacas-Gervais, Sandra 357 Ladrech, Sabine 549, 588 Laer, Lut Van 492 LaGasse, James 544 Lagziel, Ayala 26, 225, 490 Lahne, Manuela 717 Lalwani, Anil 257, 738 Lam, P. 884 Land, Susan 825 Lander, Arthur 719 Landgrebe, Michael 166 Lang, Hainan 267, 578 Langa, Francina 492 Langemann, Ulrike 443, 651 Langers, Dave 691, 813 Langguth, Berthold 166, 702 Lanting, Cris 813 Larky, Jannine 472 Larsen, Debra 709, 715 Larson, Charles 210 Larue, David 859 Las, Liora 420 Lasker, David 951 Lathrop, Mark 492 Lauer, Amanda 442 Laurell, Göran 53, 73 Lawson, Katherine 701 Lawton, Maxwell 577 Layne, Donna 809 Lazar, Ronit 854 Le, Chris 160 Leach-Berth, Tiffany 881 Leake, Patricia 203, 204

Leão, Pedro 78 Lebeau, Jason 229 Lechene, Claude 229 Lecluyse, Wendy 652 Lee, Adrian K.C. 911 Lee, Charles 859 Lee, Chen-Chung 422, 425 Lee, Chi-Kyou 803 Lee, Choong-Won 160 Lee, Daniel J. 599, 605 Lee, Dong Soo 848 Lee, Dong-Hoon 152 Lee, Haa-Yung 69 Lee, Heung-Man 141 Lee, Hyo-Jeong 846, 848 Lee, Il-Woo 152 Lee, Jae Sung 848 Lee, Jang-Hyeog 141 Lee, Jun Ho 768 Lee, Jung Ki 145 Lee, Kang-Jin 143 Lee, Kwang-Sun 165, 843 Lee, Kyu Yup 81, 271, 708 Lee, Linda 48 Lee, Sang Goo 545, 562 Lee, Sang Heun 271 Lee, Seunghwan 231 Lee, Steve C. 329 Lee, Suh-Kyung 913 Lee, Victoria 120 Lee, Yune-Sang 440 Lefebvre, Phillippe 29, 818 Legan, P. Kevin 225 Lehnerdt, Goetz 132 Leibold, Lori J. 653, 927 Leibovici, Michel 492 Leichtle, Anke 135 Lelli. Andrea 32 Lenarz, Minoo 243, 244, 448 Lenarz, Thomas 70, 88, 89, 243, 244, 448 Lenihan, Nicole 600, 604 Lenoir, Marc 549 Lerch-Gaggl, Alexandra 661, Letham, Benjamin 812, 819 Leu. Grace 191 Leuwer, Rudolf 122 Leveque, Marianne 189, 781 Levic, Snezana 548 Levin, Michelle 793 Levine, Jessica 608 Levine, Stephen 126 Levine, Steve 123 Lewis, Julian 966 Li, Boning 351 Li, Erica 306 Li, Lijun 320, 322 Li. Na 836, 838 Li, Peter 206 Li, Shengli 130 Li, Tianhao 215 Li, W. 884 Li, Yan 738 Li, Yongxin 207 Lian, Wei-Nan 45 Liang, Fenghe 269 Liang, Jin 742 Liang, Kevin 839 Liao, Amy 762 Liao, Bill 725 Liao, Zhijie 499 Liberman, M. Charles 252, 336, 338, 424, 487, 757, 758, 759 Lichtenhan, Jeffery 112, 113 Lies, Sarah M. 747 Lim, David J. 69 Lim, Hubert H. 70, 243, 244,

Lim, Ki Taek 142

Lim, Lynne 190

Lim, SangGyun 177 Limb, Charles 870 Limpach Aimee 310 Lin, Alice 446 Lin, Chia-Der 788 Lin, Feng 305 Lin, Hsin-Pin 537 Lin, Xi 190, 191, 193, 771, 778, 779 Linden, Jennifer F. 406, 696 Lineton, Ben 493 Ling, Lynne 856 Linthicum, Fred 49 Linville, Angela 719 Lister, Jennifer 880 Litovsky, Ruth 433, 434, 438, 464, 638 Littlefield. Philip 356 Litvak, Leonid 472 Liu, Chuping 937 Liu, Dong 957 Liu, Grace 465, 637 Liu, Haiying 726 Liu Jan-Jan 276 Liu, Jianzhong 79, 129, 591 Liu, Li Qian 44 Liu, Qing 355 Liu, Robert 482, 867 Liu, Wei 320, 322 Liu, Xue Zhong 21, 196, 201, 780 Liu, Ying-Peng 773 Lo, Tiffany 160 Lobarinas, Edward 71, 857, 862 Lobl, Thomas 70 Loebach, Jeremy 213, 938 Lohner, Andrea 765 Loizou, Philipos 889 Lomakin, Oleg 388 Lomax, Catherine 825 Long, Glenis R. 511 Longnion, Jeff 465, 469, 637 Longo-Guess, Chantal 780 Longworth-Reed, Larica 940 Lonsbury-Martin, Brenda 516 Lopez, Ivan A 663, 704, 705 Lorenzi, Christian 656, 919, 935 Losh, Joseph 850 Loundon, Natalie 197 Lowes, Christina 192 Lu, Shan 104 Lu, Tao 617 Lu, Yong 363 Lu, Yun-Gang 361 Luebke, Anne E. 362, 565, 566 Luisi, John 862 Luo, Xin 887 Lupo, Virginia 473 Lurie, Diana 609, 611 Lustig, Lawrence 150, 257. 290. 784 Ly, Derick 160 Lynch, Eric 159, 544 Lysakowski, Anna 667, 668, 970 Ma, Ellen 520 Ma, Eva Y. 967 Ma, Ling 401 Ma, Wei-Li 812, 819 Ma, Xuefei 573 MacArthur, Carol 133, 136 MacDonald, Glen 251 MacDougall, Hamish G. 187

Maganti, Rajanikanth J. 51 Magezi, David 648 Mahendran, Suresh 646 Mahendrasingam, Shanthini 283 Maier, Hannes 122 Maier, Julia K. 418 Maison, Stephane 338, 757. 758, 759 Maki, Katuhiro 412 Malbon, Craig 10 Malekpour, Mahdi 198 Malmierca, Manuel 383, 830, 831 Malmin, Boian 745 Mamassian, Pascal 919 Mammano, Fabio 775 Manaligod, Jose 306 Mangiardi, Dominic 300, 550 Manis, Paul 367, 377 Manley, Geoffrey 810 Mansour, Suzanne 315 Mapes, Frances 194 Marano, Robert 140 Marchetti, Gregory 183 Marcotti, Walter 270, 281, 296 Marcus, Daniel 51, 52, 479 Marietta, Chandler 642, 644 Mark Redfern 184 Marlin, Sandrine 197, 781 Marquardt, Torsten 904 Marrone, Nicole 436 Marshall, Grayson 257 Marshall, Sally 257 Martin, Brett 881 Martin, Danyelle 856 Martin, Donna M. 258 Martin Dusan 160 Martin, Gail 958 Martin, Glen 516 Martin, William 460 Martinez, Amy 144 Martinez-Galán, Juan R. 614 Martinez-Monedero, Rodrigo 266 Masahiko, Izumikawa 82 Masao, Yagi 82 Masaya, Konishi 82 Masetto, Sergio 676 Mason, Christine 436, 437 Masumura. Chisako 675 Mathers, Peter 327, 560 Mathews, P.J. 622 Matsui, Jonathan I. 300 Matsumoto, Masahiro 265, 271, 708 Matsunaga, Tatsuo 302, 568 Matsuo, Koichi 131 Matsuoka, Yoshinori 22 Matthews, Scott 501 May, Bradford J. 428, 625 Mayer-Pröschel, Margot 566 May-Simera, Helen 964 Mburu, Philomena 572 McAlpine, David 16, 395, 415, 418 McArthur, Kimberly L. 972 McCaffery, Sarah 706 McClaine, Elizabeth 897, 909 McCreery, Douglas 244 McCusker, Scott 497 McDermott, Brian 20 McDonald, Kent 237 McFadden, Dennis 809 McGee, JoAnn 358, 459, 575 McGettigan, Carolyn 214 McGinley, Matthew J 372 McGuire, Ryan M. 41 McHaffie, John 829 McKenna, Michael J. 535, McLaughlin, Katherine 784

McLaughlin, Myles 384 McMahon, Greg 229 McMillen, Debra 228 Mechaly, Ilana 296 Meddis, Ray 151, 652, 761 Meech, Robert 709 Meikle, Mary 156 Meinke, Deanna 516 Mellado, Marcia 498 Meltser, Inna 333, 707 Mendolia-Loffredo, Sabrina Merchant, Saumil N. 74, 178, 252, 507, 528, 532, 535, 536, 777 Merfeld, Daniel 973 Merkison, Marquitta 514 Merzenich, Michael M. 397, 693, 851 Mesgarani, Nima 869 Metherate, Raju 839, 854 Metz, Klaus Alfred 132 Meyer, Alexander C. 282 Meyer, Benjamin 312 Meyer, Bernard 935 Meyer, Lisa 659 Meyer, Thomas 580 Mhatre, Anand N. 738 Micco, Alan 202, 627 Michaels, Leslie 567 Michel, Vincent 492 Micheyl, Christophe 379, 401 Middlebrooks, John C. 240, 422, 425, 471 Migliaccio, Americo 185, 943 Mihaila, Camelia N. 566, 944 Mikiya, Asako 82 Miko, Ilona 364 Mikulec, Anthony A, 55 Mikuriya, Takefumi 589, 593, 594, 674, 794, 945 Milenkovic, Ivan 610 Millard, Rodney 462, 636 Miller, Charles 354, 639 Miller, Iain 664, 948 Miller, Josef 85, 89, 711 Miller, Katharine 37 Miller, Rebecca 295 Miller, Robert 274 Miller, Roger 217 Miller, Scott 433 Milligan, Ron 731 Millman, Rebecca 879 Mills, John H. 641 Minor, Lloyd B. 181, 673, 944, 951 Minter, Ricki 87 Mitani, Kenji 675 Mitchell, Diana 709 Mitchell, John 961 Miyao, Masumichi 339 Miyazawa, Toru 83 Mizutari, Kunio 302 Mlynski, Robert 260 Mohassel, Payam 291 Moiseff, Andrew 815, 896 Möller, Christoph 694, 855 Monfared, Ashkan 238 Montcouquiol, Mireille 489 Montemayor, Celina 305 Montey, Karen A. 367, 625 Moon, Sung K. 69 Moore, Brian C.J. 632, 656 Moore, David R. 146, 147, 424, 898, 925, 926 Moore, Harry 270 Moore, Robert 579, 976 Moore, Rosanna 648 Moore, Steven T. 187 Morefield, Kelly 62 Morell, Robert J. 26 Morest, D. Kent 555 Morgan, Warren 327, 560

Maeyama, Nobumichi 158

Maconochie, Mark 318, 319

MacPherson, Bret 159

422, 425

Madeo Anne 195

Mader, Sabrina 291

Macpherson, Ewan A. 14,

Mori, Susumu 941 Morizono, Tetsuo 161, 162 Morris, David P. 123, 163 Morris, Jackie 559 Morrow, Bernice 192 Mortenson, Curtis 392 Morton-Jones, Rachel T. 764 Moser, Tobias 235, 282, 357 Moska, Natalie 277 Moss, Cynthia 444 Motts, Susan D. 366 Mount, Richard J. 807 Mountain, David 104, 518, 550, 628, 826 Moushey, Jamie 176 Mridha, Zakir 949 Mu Karen J 45 Mueller, Ulrich 32, 731 Mugnaini, Enrico 105 Mukherjea, Debashree 715 Mulavara, Ajitkumar P. 188 Muldrow, Alaina 822 Mullen, Lina 28, 553 Mundi, Jagmet 356 Muniak, Michael A. 625 Murakoshi, Michio 33 Muralimanohar, Ramesh 892 Murashita, Hidekazu 587 Murata, Junko 308 Murphy, John 898 Murthy, Vidya 292 Musolino, Mark 682 Mustapha-Chaib, Mirna 563 Mutai, Hideki 568 Myers, Chris 217 Nabi, Hani 862 Nadol, Joseph B. 206, 777 Nagatani, Yoshiki 170 Nair Thankam S 64 Najmabadi, Hossein 198 Nakagawa, Takashi 161, 162 Nakagawa, Takayuki 22, 81, 271, 582, 708 Nakajima, Hideko Heidi 532 Nakamoto, Kyle 692, 858 Nakaya, Kazuhiro 51, 52 Nam, Jong-Hoon 947 Narayan, Rajiv 909 Narayan, Shyamla 733 Nardone, Heather 554 Narins, Peter 100, 288 Nathanson, Neil M. 757 Navaratnam, Dhasakumar 39 Navarrete, Francisco 671 Neef, Andreas 235 Neely, Stephen T. 512, 513 Neiman, Alexander 956 Nelken, Israel 420 Nelson, Brian 419 Nelson, Paul C. 918, 920 Ness, Lisa S. 787 Neubauer, Heinrich 114 Neuheiser, Anke 448 Neumann, Andreas 132 Newman, Dina 194 Ng, Philip 40 Nguyen, Jerry 160 Nguyen, Kimanh 181 Nicholl, Amanda 265 Nichols, Justin 389 Nichols, Michael 303 Nickel, Regina 774 Nicol, Trent 209, 699 Nicosia, Mark 160 Nicotera, Thomas 331 Nie, Kaibao 441, 463 Nie, Liping 45, 232, 291, 762 Nikjeh, Dee 880 Nishimura, Masato 158 Nishiyama, Toshimasa 590 Nobbe, Andrea 455

Nodal, Fernando 868

Nong, Xiaoyun 581 Nopp, Peter 455 Northrop, Clarinda 123, 126, 252 Norton, Susan J. 463 Nourski, Kirill V. 639 Nouvian, Regis 760 Novak, Zdenek 262 Noyes, Albert 315 Nutt, Robert C. 642, 644 Nuttall, Alfred L. 60, 101, 294, 334, 495, 500, 501, 502, Nymon, Amanda 110 Oas. John 179 Oba, Sandy 520 O'Beirne, Greg A. 57 Oberoi, Monica 446 Obrist, Dominik 975 O'Connell, Keri 787 Oda, Kiyoshi 788 O'Donoghue, Gerry 898 Oertel, Donata 372 Oesterle, Elizabeth 542 Ogawa, Kaoru 131, 302 Oghalai, John 40, 505 Ogita, Hideaki 81, 271 Ogura, Masaki 125 Oh, Seung-Ha 143, 792, 848, 852 Ohl, Frank W. 408 Ohlemiller, Kevin K. 749 Ohtsuka, Toshiyuki 308 Ohyama, Takahiro 324 Ok, Jeong-Hwan 152 Okano, Hideyuki 308 Okano, Takayuki 81, 271, 582, 708 Okoruwa, Remen 739 Okubo, Miki 158 Oliveira, Carlos 178 Oliver, Douglas 827, 830 Olivius, Petri 268 Olson, Elizabeth 530, 735 Olsynski, Patrycja 689 O'Malley, Jennifer 74, 128, 777 O'Mard, Lowel 116 O'Neil, Brock 344 O'Neill, William E. 905 Ono, Kazuya 708 Opanashuk, Lisa A. 565 Organ, Louise E. 34 Orita, Hiroshi 674 Orr, Lauren 445 Ortigoza, Eric B. 872 Osaki. Yasuhiro 683 Osberger, Mary Joe 456 O'Shea, K. Sue 85 Oshima, Kazuo 263 Oshima, Takeshi 121, 125, Osier, Michael 194 Osumi, Yasunori 590 Otake, Rika 907, 908 Ou, Henry 713, 798 Ouyang, Xiao Mei 21, 201, 780 Overath, Tobias 868 Owens, Kelly N. 787 Oxenham, Andrew J. 401, 519 Oya, Hiroyuki 876 Ozmeral, Erol 909 Paasche, Gerrit 88, 89 Pace, Edward 450 Paige, Gary D. 905 Pak, Kwang 28, 135, 553, 763 Palmer, Alan 400, 404, 692, 858

Palmer, Donna 40

Palmer-Toy, Darryl Erik 777

Paloski, William H. 187, 188

Pan, Huiqi 69 Pan, Ling 307 Pang, Jiaqing 334, 745 Pantano, Sergio 775 Paparella, Michael 68 Papsin, Blake 816 Pardo, Patricia 305 Park, Dong Choon 137 Park, HongJu 177 Park, Hun-Yi 301 Park, Jee Young 792 Park, Jung-Sub 142 Park, Keehyun 142, 301 Park, Min-Hyun 848 Park, Soo Chan 145 Park, Su-Kyoung 143 Park, Sunyoung 609 Park, Yong Ho 802 Parker, Andrew 746 Parker, Mark 23 Parody, Robert 194 Parrish, Jennifer 756, 844 Parrish, Todd 698 Parsons, Thomas 111, 234 Pasanen, Edward 809 Patel. Ankur 389 Patel, Chintan 44 Patel, Hiren 292 Patel Lina 815 Patel, Tejas 337 Patrick, James F. 243 Patuzzi. Robert B. 57 Paul. Asit 862 Paul, Isabella 423 Paulin, Michael 955 Pavco, Pamela 545 Pavlovich, Justin 335 Pawlowski, Karen 743 Peake, William T. 532 Peng, Shu-Chen 885, 886 Penmetsa, Amulya 753 Pereira, Frederick A. 35, 36, 40, 41, 304, 305, 505, 726 Pérez-González, David 383 Pergola, Nicholas 451 Pershouse, Mark 611 Pertegato, Vanessa 775 Pesch, Joerg 243 Peters, Theo 25, 228 Peterson, Ellengene 664, 948 Peterson, Kristen A. 43 Petit, Christine 197, 492, 781 Pettingill, Lisa 87 Pfannenstiel, Susanna 46, Pfingst, Bryan E. 239, 242 Pham, Tammy 160 Phansuwan-Pujito, Pansiri 601 Phatak, Sandeep 655 Philibert, Benedicte 397, 693 Philippon, Bertrand 935 Phillips. Dennis 929 Piazza, Valeria 229 Picton, Terence W. 632 Pienkowski. Martin 654 Pierce, Carol 159, 544 Pierce, Marsha 569, 570 Pietola, Laura 84 Pilcher, Connie 218 Pilipenko, Valentina 190, 783 Pillers, De-Ann M. 133, 136, 334, 745 Pillsbury, Harold 447 Pingault, Veronique 24, 289 Pinsky, Peter 525 Pirih, Primoz 235 Pisano, Dominic V. 877 Pisoni, David 213 Placek, Jill 509 Plack, Christopher 382

Pletcher, Scott D. 305 Plinkert, Peter K. 791 Plontke, Stefan 54 Plontke, Stefan K. 56, 249 Podgorski, Michael 38 Poeppel, David 486 Pogal-Sussman, Tracy 430 Pohl, Nina U. 651 Pollak, George 834, 835, 836, 837, 838 Polley, Daniel 690 Ponting, Sarah 648 Popel, Aleksander 504, 725 Popelka, Gerald 238 Popper, Arthur N. 742 Popper, Paul 370, 660, 661, Portfors, Christine 381, 832, 833 Post, Christopher 139 Powers, TuShun 741 Poytress, Bonnie 839 Praetorius, Mark 540, 791 Prahl, Susanne 127, 128 Prakash, S.R. 175 Prell, Colleen Le 349, 711 Prendergast, Garreth 879 Pressnitzer, Daniel 379 Price, Steven D. 970 Prieskorn, Diane 85 Prigioni, Ivo 551 Pritchard, Miranda 183 Procaccio, Vincent 781 Prolla, Tomas A. 346 Prosser, Haydn 227 Provenzano, Matthew 110 Pryor, Shannon 321 Puel, Jean-Luc 297, 539, 549, 588.760 Puligilla, Chandrakala 317, Pulli, Emily 345 Purdy, Kirstin 491 Puria, Sunil 250, 523, 525, 527, 736 Qazi, Taha 83 Qi, Li 522 Qi, Weidong 75, 77, 800 Qian, Dong 963 Qian, Feng 48 Qin, Wei 196 Qu, Yan 771, 778, 779 Quick, Andrew 456 Quinones, Herson 311 Quinones, Patricia 288 Quint, Elizabeth 255 Quraishi, Imran 478, 576, 969 Rabbitt, Richard 503, 971 Raft, Steven 311 Rahman, Anisur 138 Raible, David W. 713, 786, 787, 798, 967 Rajagopalan, Lavanya 35, 36, 726 Rakowiecki, Staci 9 Ralph, Heather 356 Ramakrishnan, Neelivath A. 27, 31 Ramesh, Arabandi 200 Ramkumar, Vickram 715 Ramon, Sesquile 194 Rampton, Marcus 347 Ramzan, Khushnooda 490 Ranatunga, Kishani 299 Ransohoff, Richard M. 335 Raphael, Robert M. 34, 41, 102, 237, 474, 478, 480, 576, 969<sup>°</sup> Raphael, Yehoash 83, 86, 258, 543, 796 Raphan, Theodore 679, 680, 681, 683 Rapson, Ian 248

Rask-Andersen, Helge 268 Ratnam, Rama 809, 895 Ratnanather, J. Tilak 877 Rau, Chistoph 42 Rauch, Steven 175, 218, 223 Ravicz, Michael 507, 534, 535 Ravindran, Rajan 842 Rawool, Vishakha 148 Ray, Bappaditya 817 Raz, Yael 557 Razavi, Babak 905 Read, Heather 386, 387, 690, Rebillard, Guy 539, 760 Rebscher, Stephen 203 Recio-Spinoso, Alberto 733 Redfern, Mark 682 Redmond, Sharon 140, 277 Rees, Adrian 831, 924 Reese, Zachary 347 Regnier, Marion 934 Reh, Thomas 309 Reich, Uta 448 Reim, Kerstin 357 Reinert, Thomas 610 Reiss, Lina 466 Remington, Melissa 64 Ren, Tianying 101, 501, 502, Renard, Nicole 78, 297 Renken, Remko 602 Rennie, Katherine 968 Reuschel, Emma 856 Reuter, Guenter 448 Reuter, Karen 517 Reynier, Pascal 781 Reynolds, Anna 32 Riazuddin, Saima 200, 225, 490 Riazuddin, Sheikh 200, 490 Ricci, Anthony 230 Riccomagno, Martin 9 Richardson, Guy 225, 299 Richter, Claus-Peter 42, 109, 202, 356, 446, 497, 627 Riffenburgh, Robert H. 586 Riley, Alison 147 Riquimaroux, Hiroshi 619, 900, 901 Risler, Thomas 730 Risley, Robert 805 Ritter, Steffen 700 Rivas, Alejandro 625 Rivoli, Peter 822 Rivolta, Marcelo N. 270 Roberts, Jason 414, 447 Roberts, Patrick 381, 832, 833 Roberts, William 353 Robinson, Barbara K. 354, 639 Robinson, Benjamin 395 Robinson, lan 42 Rocha-Sanchez, Sonia 310, 965 Roche, Joseph 660 Rodgers, Matthew 534 Roeder, Diane 149 Roehm, Pamela 90 Rogers, Brian 80 Roh, Yun-Sung 152 Roknic, Nicolas 782 Romand, Raymond 533 Romero, Rosario 572 Ron, Uri 489, 492 Roos, Matthew 428 Rorden, Chris 872 Rosen, Merri 864 Rosen, Stuart 214 Roska, Botond 605 Rosowski, John 507, 528, 532, 533, 534, 535, 536 Ross, Mike 827

Plazas, Paola V. 289

Ross, Shannon 262 Rowe, Michael 956 Roy, Tara Sankar 817 Rubel, Edwin W. 251, 546, 713, 721, 786, 787, 798, 967 Ruben, Robert 167 Rubinstein, Jav 441, 463. 465, 469, 637, 883 Rubio, Maria 360, 815 Rubsamen, Rudolf 610, 626 Ruel, Jerome 539, 588, 760 Ruffin, Chad 469, 637 Ruggero, Mario 733 Ruhland, Janet 894 Runge-Samuelson, Christina Rupp, André 700 Russ, Brian 440, 445, 689 Russell, Ian 498 Russo, Brianna 23 Russo, Giancarlo 551 Russo, Nicole M. 210, 211 Ruther, Ulrich 321, 959 Rutherford, Mark 353 Ryals, Brenda 439 Ryan, Allen F. 28, 32, 47, 135, 553, 763, 764 Rybak, Leonard 715 Ryugo, David 367, 625 Rzadzinska, Agnieszka 227, 255, 489 Sabin, Andrew T. 928, 930 Sabri, Firouzeh 728 Sadeghi, Soroush 673 Safarpour, Farzaneh 390 Safe, Theresa M. 565 Sage, Cyrille 24, 289 Saginaw, Michael 973 Sahani, Maneesh 395, 696 Sahara, Yoshinori 677 Sahlin, Lena 767 Sakaguchi, Takefumi 170 Sakai, Shuhei 95 Sakamoto, Tatsunori 22, 271 Saldana, Enrique 389 Salt, Alec N. 54, 55, 56, 218, 221, 245, 249 Salt, Miranda 43 Salvi, Richard J. 71, 75, 77, 799, 800, 823, 840, 841, 857. 862 Samanich, Joy 192 Samii, Amir 243 Samii, Madiid 243 Sams, David 664 Samson, James 842 Samuels, Tina 660, 661 Sanchez, Rhea 194 Sanchez-Hanke, Marcos 122 Sand, Philipp 166 Sander, J.C. 939 Sanes, Dan 849, 864, 865 Sanford, Chris A. 119 Sanjeevi, Divvya 739 Sanneman, Joel 51 Sanovich, Elena 30 Santi, Peter 245, 248 Santina, Charles C. Della 941, 942, 943, 944, 974 Santos, Felipe 786 Santos-Sacchi, Joseph 39, 236 Sappey-Marinier, Dominique 846 Sarracino, David 777 Sato, Eisuke 67 Sato, Toshinori 121 Satoh, Takunori 328 Saunders, James 111, 351 Savin, David 284 Saxon, Gene 247 Sayles, Mark 371, 379

Scarfone, Eric 547 Schachern, Patricia 68 Schacht, Jochen 76, 341, 714, 750 Schachtele, Scott 850 Scheffer, Deborah 24, 289 Scheich, Henning 694 Scheper, Verena 89 Schiller, Evelyn 417 Schilling, Thomas 719 Schimmang, Thomas 319 Schleich, Peter 455 Schloss, John 70 Schmiedt, Richard 267, 578 Schmuck, Nicholas 751, 752 Schneider, Richard 257 Schnitzer, Mark 238 Schnupp, Jan 398, 403 Schoenen, Jean 818 Schoernich, Sven 922 Schoffelen, Richard L. M. 496 Schofield, Brett R. 366 Scholes, Chris 404 Scholsem, Martin 818 Schor, Robert 678 Schreiner, Christoph E. 397, 688 693 851 Schrott-Fischer, Annelies 297 Schubert, Michael 185, 974 Schuck, Julie 80 Schuller, Gerd 922 Schulte, Bradley 267, 269, 475, 578 Schultz, Bruce 52 Schulze, Holger 694, 855 Schumacher, Kristopher 504 Schwab, Burkard 70 Schwander, Martin 32 Schwanke, Corbin 611 Schweizer, Felix E. 284, 288 Scott. L. L. 622 Scott, Matthew 574 Scott, Sophie K. 6, 214 Sczaniecka. Anna 32 Segar, Allyson 154 Segenhout, Johannes M. 496 Segil, Neil 311 Seidermann, Laurent 189 Seidman, Jonathan 178 Sekerkova, Gabriella 105 Sekimoto, Sotaro 873 Sekiya, Testuji 265 Semple, Malcolm 864 Sen, D. 650, 884 Sen, Kamal 909 Sendtner, Michael 260 Senn, Pascal 263 Senthilvelan, Manohar 842 Sequeira, Damien 526 Serrano, Elba E. 43, 740, 741 Sewell, William F. 352 Sfondouris, John 36 Sha. Su-Hua 341, 714, 750 Shabbir, Muhammad 200 Shaffer, Lauren 521 Shah Samit M 278 Shahin, Hashem 254, 259 Shalit, Ella 489 Shamma, Shihab 401, 407, 697, 869 Shannon, Robert 1, 244, 633 Shanske, Alan 192 Shanske, Sara 192 Shapira, Ayelet 420 Sharma, Alok 807 Sharma, Anu 853 Sharma, Saroj 817 Shatadal, Shalini 372 Sheeladevi, Rathinasamy 842

Shelhamer, Mark 974

Shepard, Neil 173

Shepherd, Robert 87, 205, 275, 462, 636 Shera, Christopher A. 519, 811 Sherlock, LaGuinn 154 Shi, Fuxin 272 Shi, Xiao-Rui 60, 334, 776 Shibata, Seiii 158, 590 Shick, Elizabeth 67, 335 Shilling, D.J. 487, 748 Shim, Dae Bo 177, 597 Shim, Hee-Yeon 803 Shim, Hyun Joon 596 Shim, Hyung Jun 145 Shim, Katherine 958 Shimada, Jun 69 Shimogori, Hiroaki 593, 594, 674, 794, 945 Shin, Dong Hoon 792 Shin, Grace Jung Eun 597 Shin, HyangAe 177 Shin, Jong Heon 145 Shin, June-Ho 276 Shin, Jung-Bum 25, 228 Shin, JungEun 177 Shin, Minyong 250, 527, 523 Shin, You Ree 142, 301 Shinn-Cunningham, Barbara G. 18, 437, 902, 909, 911, 915 Shiori, Yu 901 Shoemaker, Christopher 543 Shore, Susan 365, 373, 827 Shrivastav, Mini 212, 658 Shub, Daniel 899 Siebeneich, Wolfgang 661 Siebert, Ursula 127, 128 Siegel, Jonathan 120, 509 Siegerman, Carin 953 Sienknecht, Ulrike J. 12, 810 Silverstein, R.S. 748 Sim, Jae Hoon 250, 523, 527 Simmoneau, Lionel 549 Simmons, Richard 862 Simms, William 451 Simon, Jonathan 697 Simon, Julian 786 Simonoska, Rusana 767 Sinai, Alon 874 Singh, Ruchira 50 Sinha, Ghanshyam 728 Sininger, Yvonne 144 Sirjani, Davud B. 56 Siveke, Ida 417 Sivonen, Ville 432 Skinner, Kim 186 Sklare, Daniel 217 Skoe, Erika 209, 211 Skrzypiec, Anna 369 Slabbekoorn, Hans 651 Slabu, Lavinia 602 Slee, Sean 621 Sliwowska, Magdalena 695 Slonimsky, John 561 Smith, Michael 80 Smith, Peter 480 Smith, Richard 198, 200 Smith, Sonya 732 Smouha, Eric 63 Snyder, Joel 913 Snyder, Russell L. 240, 452, 635 Sobhy, Ossama 164 Sockalingam, Ravi 342 Sokolowski, Bernd 285 Somdas, Mehmet 206 Someya, Shinichi 346 Song, Dae Keun 145 Song, Jae-Jun 852 Song, Lei 236

Soto, Enrique 671 Soucek, Sava 567 Soukup, Garrett 569, 570 Spain, William 621 Spanjer, Genevieve 444 Spankovich, Christopher 150 Sparto, Patrick 184 Specht, Hans-Joachim 700 Spector, Alexander 504, 725 Spencer, Nathaniel 541 Spenger, Christian 73 Spirou, George 327, 560, 603 Spoon, Corrie 947 Srisailpathy, Srikumari 200 Staecker, Hinrich 46, 540, 791, 818 Stagner, Barden 516 Stakhovskaya, Olga 204, 452 Stallings, Valerie L. 187 Stankovic, Konstantina M. 564 Starlinger, Veronika 263 Starr, Arnold 472 Starr. Catherine 316 Stecker, G. Christopher 422, 910 Steel, Karen 227, 255, 489 Steele, Charles R. 250, 523, 527, 736 Stegemöller, Elizabeth 209 Steinschneider, Mitchell 863, 876 Stenberg, Annika 767 Stepanyan, Ruben 226 Stephan, Klaas 875 Sterbing-D'Angelo, Susanne J 409 411 Stewart, Barbara 156 Stewart, Lauren 875 Steyger, Peter 789, 790 Stick, Melissa 217 Stickney, Ginger 455 Stohl, Joshua 457, 458 Stolzberg, Daniel 840, 841, 857 Stone, Jennifer 966 Storace, Douglas 690 Stöver, Timo 70, 88, 89 Street, Sarah 367 Street, Valerie A. 199, 487, 748 Streijger, Femke 25, 228 Strenzke, Nicola 357 Strickland, Elizabeth 923 Strong, Darcy A. 176 Strutz, Juergen 166, 702, 921 Stupin, Laura 902 Sturm, Angela 726 Su, Diane 953 Suarez, Alejo 684, 685 Suarez, Hamlet 685 Suetake, Mitsuko 121 Sugahara, Kazuma 172, 589, 593, 594, 674, 794, 945 Sugamura, Mayumi 161, 162 Suh, Eul 109 Sul. Bora 103 Sultemeier, David R. 740 Summerfield, A. Quentin 423, 898.906 Sumner, Christian J. 404, 424 Sun, Genliu 342 Sun, Guangwei 568 Sun, Hanjun 196 Sun, Hongyu 391 Sun, Jian-he 325 Sun, Qing 196 Sun, Wei 71, 823, 840, 841, Sun, Xiao-Ming 808 Sussman, Elyse 701, 797 Suzuki, Mikio 820, 861 Suzuki, Mitsuya 907, 908

Swaminathan, Jayaganesh 623 Swiderski, Donald L. 83, 258 Tabata, Yasuhiko 708 Tabuchi, Keiji 95, 587 Tadros, Sherif F. 345, 347 Tahera, Yeasmin 333, 707, Takada, Yasunari 131 Takahashi, Terry 419 Takai, Yuko 158 Takebayashi, Shinji 22 Takemoto, Tsuyoshi 172, 593, 794 Takeno, Kenii 593, 674, 945 Takesian, Anne 849 Talaska, Andra E. 341 Taleb, Mona 716 Tamaki, Chizuko 174 Tamaki, Minao 861 Tamura, Manabu 308 Tan, Hongyang 513, 653 Tan, Joshua T. 489 Tan, Wen-Hann 23, 737 Tanaka, Kuniyoshi 594 Tang, Louisa 304 Tang, Qing 467, 472 Tang, Wenxue 193, 771, 778, Tang, Yezhong 421 Tang, Zheng-Quan 361 Tanksley, John 368 Tanokura, Masaru 346 Tao, Ran 196 Tarantino, Lisa M. 32 Tardif. Suzette 809 Tasneem, Saba 200 Tavares, Maria Amélia 78 Taylor, Jenny L. 926 Taylor, Jessica 466 Taylor, Ruth 96, 542 Teixido, Michael 253 Telian, Steven A. 64 Telischi, Fred 93 Tempel, Bruce L. 336, 487, 747, 748 Tenne, Tamar 489 Teo, Dawn Tju Wei 263 Ter-Mikaelian, Maria 864 Terry, Caitlin E. 300 Teudt, Ingo 497 Theunissen, Frederic 689 Thompson, Ann 613 Thompson, Christopher K. Thompson, Sarah 914 Thorne, Peter R. 764 Throckmorton, Chandra 457, 458 Tiede, LeAnn 303 Tillein, Jochen 461 Tinling, Steven P. 337 Tirko, Natasha 630 Tjan, Bosco 2 Todd, N. Wendell 124 Todt, Ingo 631 Toga, Arthur 246 Tokunaga, Akinori 308 Tollin, Daniel J. 17, 413, 416 Tolman, Andrew 381 Tolnai, Sandra 626 Tong, Ling 827 Tong, Mingjie 287 Tong, Yi-Cai 130 Toren, Ginat 254 Toshio, Yamashita 82 Tourtillott, Brandon 113 Townsend, Stuart 572 Trachte, George 256 Trahiotis, Constantine 15 Tran, Huy 544 Triffo, William 237

Songer, Jocelyn 507

Sørensen, Mads 252

Trigueiros-Cunha, Nuno 78 Tristano, Jenny 108 Trujillo-Provencio, Casilda 740, 741 Trune, Dennis R. 133, 136, 218, 222, 334, 744, 745, Trussell, Larry 360, 380, 617 Truy, Eric 846 Tsai, Jeffrey J. 413 Tsai, Ming-Jer 505 Tsumoto, Kouhei 33 Tsuprun, Vladimir 68 Tucci, Debara 373 Tucker, Andrew 561 Tuck-Lee, James 250, 525 Turcan, Sevin 292 Turner, Christopher 466, 468 Turner, J. Bradley 896 Turner, Jeremy 756, 844, 856 Turner, Joyce 321 Tyler, Mitchell E. 187 Tzounopoulos, Thanos 360 Uehara, Ken 820, 861 Uemaetomari, Isao 95, 587 Ueno. Tetsuko 161, 162 Ulppenkamp, Stefan 878 Ulfendahl, Mats 547 Ulmer, Erik 189 Unge, Magnus Von 138 Uno, Atsuhiko 158, 675 Upile, Tao 567 Uppunda, Ajith 698 Urness, Lisa 315 Urquidi, Lina 43 Ursick, Joseph 818 Vajda, Viktor 826 Vakhtin, Andrei B. 43 Valero, Jerome 816 Valero, Michelle 809 Valkenier. Kenneth 123 Vallurupalli, Mounica 64 Van De Sande, Bram 384 Van De Water. Thomas 93. 581 Van Der Heijden, Marcel 359, 384, 618 Van Der Zee, Catharina E.E.M. 25 Van Netten, Sietse M. 293 Vanpoucke, Filiep 453 Vargeese, Chandra 545 Vasilyeva, Olga 343, 344 Vasquez, Angelica 538, 592 Vazquez, Ana E. 45, 291, 337 Vega, Rosario 671 Velkey, Matt 85 Venail, Frederic 539 Vendrell, Victor 319 Verduzco, Esteban 337 Verhey, Jesko 431, 878 Verrall, Aimee 199 Vetter, Douglas 292, 758, 951 Viberg, Agneta 707, 847 Vicente-Torres, M. Angeles 341 Vieira, Mauricio 278 Viemeister, Neal F. 920 Vinuela, Antonio 389 Visosky, Ann Marie 505 Vlajkovic, Srdjan M. 764 Voie, Arne 247, 248 Volk, Matthew 35 Volkenstein, Stefan 260 Vollmer, Maike 203, 397, 688, 693 Von Der Behrens, Wolfger 405 Voytenko, Sergiy 392 Vu, Annette 554 Wackym, P. Ashley 470, 659, 660, 661, 662 Wada, Hiroshi 33

Wadhwa, Shashi 817 Waguespack, Jessica 230 Wahlfors, Jarmo 84 Walczak, Adam 871 Walker, Kerry 398, 403, 929 Wallace, Mark 400 Wallimann, Theo 228 Walsh, Edward 358, 575 Walsh, Joseph T. 109, 356 Walsh, Kimberly 895 Walton, Joseph 394, 751, 752 Wang, Dali 915 Wang, Haobing 252 Wang, Hongning 856 Wang, Jian 342 Wang, Jing 539, 549, 588 Wang, Lulu 737 Wang, Qi 789, 790 Wang, Qiong 91 Wang, Soo-Geun 152 Wang, Xiang 770 Wang, Xiaofen 315 Wang, Xiaoqin 410, 485 Wang, Xuelin 524 Wang, Yong 377 Wang, Yuan 546 Wangemann, Philine 50, 51, 52, 481 Warchol, Mark 552 Warnecke, Athanasia 88 Warner, Margaret 707 Warr, W. Bruce 575 Warren, Jason 875 Warrier, Catherine 209 Wassel, Richard 129 Wassel, Ronald 538 Wasserman, Stephen 135 Watanabe, Yoshiaki 900, 901 Watkins, Paul V. 402, 890 Watson, Bracie 217 Watts, Kelly 510 Webb, Jim 356 Webber, Audra 801 Webber, Douglas 704 Weber, Christopher 290, 784 Weeks, Daniel 306 Wei, Dongguang 547 Wei, Lei 71, 823 Wei, Weigi 888 Weik, Verena N. 916 Weikhardt, Heike 765 Weil, Dominique 492 Weinberger, Norman 839 Weindruch, Richard 346 Welch, Thomas 897 Wenstrup, Jeffrey 376, 866 Wenzel, Gentiana I. 70 Werner, Hauke 357 Werner, Lynne 463, 927 Wesolwoski, Karolina 85 Wess, Jürgen 757 Wester, Derin 579 Westerfield, Monte 957 Weston, Michael 569, 570, Wheeler, Bruce C. 278 Wheeler, David A. 305 White, Denise 783 White. Richard 719 White, Stephen 38 Whiten, Darren 206 Whitlon, Donna 108 Whitney, Susan 183, 184 Whittaker, Charlie 741 Whitworth, Craig 715

Wickesberg, Robert 938

Wightman, Frederic 435

Wijhe, Rene Van 123, 163

Wiersinga-Post, J. Esther C.

Wiegrebe, Lutz 922

602

Wile, Daryl 647

Wilson, Roselyn M. 931 Wilson-Kubalek, Elisabeth Wiltshire, Tim 32 Windsor, Alanna 605 Winer, Jeffery 859 Winkler, John 662 Winter, Ian 371, 379, 624, 646 Wissel, Kirsten 88 Witte, Mirko 610 Woessner, David 961 Wojtczak, Magdalena 920 Wolf, Fred 235 Won, Jong Ho 637, 883 Wong, Gerard 491 Wong, Nelson Pak Hung 904 Wong, Patrick 211, 698 Woo, Jeong-Im 69 Woo, Jung-Su 141 Wood, Melissa L. 336, 533 Wood, Scott J. 187 Woods, Will 879 Woodson, Erika 90 Wool, Lauren 445 Woolf, Nigel 583 Wooltorton, Julian 40 Wright, Anthony 567 Wright, Beverly A. 928, 930, Wright, Charles 743 Wright, Tracy 315 Wu, Doris K. 323, 959 Wu, Shu Hui 391, 620 Wu, Tao 51, 294 Wys, Noel 85 Xia, Anping 40, 505 Xiang, Juanjuan 697 Xiang, Yongqing 681 Xiao, Ming 537 Xie, Ruili 834, 835, 837 Xie, Xiaoling 307 Xu, Han 865 Xu. Li 207, 208, 888 Xu, Ningyong 90, 110 Xue, Jingbing 948 Xu-Friedman, Matthew 823 Yagi, Masao 590 Yakushin, Sergei B. 679, 680, 681 Yamaguchi, Terry 13 Yamamoto, Norio 22, 573 Yamano, Takafumi 161, 162 Yamasaki, Aigo 172 Yamashita, Hiroshi 172, 589, 593, 594, 674, 794, 945 Yamashita, Tetsuji 38 Yamashita, Toshio 590 Yamasoba, Tatsuya 346, 908 Yamauchi, Daisuke 788 Yamoah, Ebenezer N. 45, 232, 291, 477, 548, 762 Yan, Denise 21, 196, 201, 780 Yan, Jun 396 Yan, Kai 30 Yan, Li 28 Yang, Guang 857 Yang, Kuo-Hsiung 763 Yang, Shiguang 217 Yang, Shi-ming 325 Yang, Shuzhi 196 Yang, Wei-Ping 332, 645 Yang, Weiyan 196 Yang, Xiao 325 Yang, Yu-Qin 60 Yao, William 669 Yapa, Nadeeka 933 Yarin, Yuri 282

Yerukhimovich, Michael 274 Yi, Eunyoung 266 Yin, Pingbo 401, 407 Yin, Shankai 342 Yin, Tom C.T. 17, 894 Ying, Yu-Lan Mary 712 Yoder, Bradley 963 Yonekawa, Hiromichi 572 Yoo, Tai June 65, 66 Yoon, Sang Won 596 Yoon, Yang-Soo 655 Yoon, Yong-Jin 736 Yoshida, Naohiro 121 Young, Eric D. 687, 812, 819 Young, Sue J. 746 Yu, Gonggiang 464 Yu, Heping 130, 743, 780 Yu, Ning 325, 724, 772 Yu, Wei-Ping 45 Yu, Zhiping 342 Yuan, Huijun 196 Yueh, Bevan 465 Yumoto, Masato 873 Zaccolo, Manuela 775 Zahorik, Pavel 903, 940 Zalewski, Christopher 317 Zander, Kaitlin 110 Zecker, Steven G. 699 Zelarayan, Laura 319 Zeng, Fan-Gang 4, 467, 472 Zettel, Martha L. 753 Zhang, Duan-Sun 229 Zhang, Fawen 354 Zhang, Huiming 390, 620 Zhang, Jinsheng 374, 375, 449, 450 Zhang, Ji-shuai 325 Zhang, Kui 262 Zhang, Liyan 840, 841 Zhang, Mei 793 Zhang, Ming 62 Zhang, Xuedong 518 Zhang, Yongkui 867 Zhang, Yunfeng 396 Zhang, Yuzhou 198 Zhao, Hong-Bo 773, 724, 772 Zhao, Xiaoyan 207 Zheng, Jiefu 500, 101, 495, Zheng, Jing 37, 224 Zheng, Lili 105, 224, 491 Zheng, Qing 130, 743, 780 Zheng, Yi 386 Zhou, Bin 65, 66 Zhou, Jianxun 365 Zhou, Ning 207, 208 Zhu, Jun 232, 762 Zhu, Mei 298 Zhu, Xiaoxia 343, 344, 345, 347, 585, 753, 754, 755 Zierhofer, Clemens 455 Zilany, Muhammad 657 Zoheir, Malak 171 Zokoll, Melanie A. 443 Zopf, David 313 Zou. Yimin 11 Zou, Yuan 101, 500, 501 Zuiderveld, Loren 756, 844 Zuo. Jian 38 Zwart, Jon 160

Yavuzoglu, Asuman 376

Yee, Stephanie 822

Yeo, Seung Geun 137